KAISER–HILL
COMPANY

ACTINIDE MIGRATION EVALUATION PATHWAY ANALYSIS REPORT

TECHNICAL APPENDIX

April 2002

Environmental Media Management
Rocky Flats Environmental Technology Site

Classification Exemption #CEX-105-01

SEP 2002
RECEIVED
DOCUMENT CENTER

1/685

ADMIN RECORD
SW-A-004547

ACTINIDE MIGRATION EVALUATION PATHWAY ANALYSIS REPORT TECHNICAL APPENDIX

TABLE OF CONTENTS

Introduction and Background	Section TA-1
Measured Actinide Concentrations in the Environment at RFETS	Section TA-2
Plutonium, Americium and Uranium Geochemical Transport Processes	Section TA-3
Actinide Transport Pathways Analysis - Based on Measured RFETS Actinide Concentrations	Section TA-4
Actinide Transport Pathways Analysis - Based on Measured and Modeled RFETS Actinide Concentrations	Section TA-5
Actinide Transport Pathways Analysis - Based on Modeled Data for Extreme Conditions	Section TA-6
Summary and Conclusions	Section TA-7

Attachments

Attachment A Sum-of-Ratios Data Plots

Attachment B Uranium Usage and Potential Uranium Contamination in Buildings

List of Acronyms and Basic Nomenclature

SECTION TA-1 - TABLE OF CONTENTS

TA-1 INTRODUCTION AND BACKGROUND 1-1

TA-1.1 Purpose of the Pathway Report 1-1

TA-1.2 Report Organization 1-1

TA-1.3 Actinide Migration Evaluation Program 1-2

TA-1.4 Conceptual Model for Actinide Transport 1-3

TA-1.5 Regulatory Framework 1-4

TA-1.6 Background Site Description 1-5

TA-1.6.1 General Site Description 1-5

TA-1.6.2 Climate 1-6

TA-1.6.3 Geology 1-10

TA-1.6.4 Hydrogeology and Geochemistry 1-16

TA-1.6.5 Surface Water Features 1-27

TA-1.6.6 Biological and Ecological Resources 1-31

TA-1.6.7 Microbiology 1-35

TA-1.7 Technical Appendix Section TA-1 References 1-38

SECTION TA-1 TABLES

Table TA-1-1. NOAA Precipitation Stations Used to Compare with RFETS Data 1-8

Table TA-1-2. Hydraulic Conductivity of UHSU Units 1-17

3

SECTION TA-1 FIGURES

Figure TA-1-1. Potential Actinide Transport Pathways at RFETS – Conceptual Model Diagram. 1-41
Figure TA-1-2. Site Map 1-42
Figure TA-1-3. Monthly Average Precipitation at RFETS 1-43
Figure TA-1-4. Correlation of RFETS Monthly Precipitation with Regional Data - for Water Years 1997 - 1999 1-43
Figure TA-1-5. Precipitation at Boulder Station 50848 – Cumulative Departure of Water Years 1997 – 1997 from Monthly Normals 1-44
Figure TA-1-6. Mean Wind Speed and Direction Distribution at RFETS (1999) 1-44
Figure TA-1-7. RFETS Soils Map 1-45
Figure TA-1-8. RFETS Geologic Map 1-46
Figure TA- 1-9. Generalized Stratigraphic Column for the RFETS Area 1-47
Figure TA-1-10. Generalized Geologic Cross-Section of the Front Range and the RFETS Area 1-48
Figure TA-1-11. Potentiometric Surface Map of Unconsolidated Surficial Deposits 1-49
Figure TA-1-12. Rock Creek Flow Path – Major Ion Concentrations in UHSU Groundwater 1-50
Figure TA-1-13. Industrial Area Flow Path – Major Ion Concentrations in UHSU Groundwater 1-51
Figure TA-1-14. Woman Creek Flow Path – Major Ion Concentrations in UHSU Groundwater 1-52
Figure TA-1-15. Southern Area Flow Path – Major Ion Concentrations in UHSU Groundwater 1-53
Figure TA-1-16. RFETS Vegetation Map 1-54

4

TA-1 INTRODUCTION AND BACKGROUND

TA-1.1 PURPOSE OF THE PATHWAY REPORT

The purpose of the Actinide Migration Evaluation (AME) Pathway Report is to provide a quantified analysis of the processes that impact movement of actinides in the environment at the Rocky Flats Environmental Technology Site (RFETS or Site). Actinides, for the purposes of this study, refer to plutonium (Pu), americium (Am) and uranium (U).

Evaluation of remedial alternatives for actinide contamination at RFETS must consider migration and mobility along available environmental pathways. Major transport pathways addressed in this study include air, surface water, groundwater and biota. The analysis investigates the physical and chemical interactions between the pathways as well as processes involving surrounding environmental media, including surface soils, sub-surface soils and sediments. The ultimate objective of the study is to quantitatively compare and rank the various pathways in terms of total actinide loads transported off-Site for a given time period.

This report expands upon the pathway analysis work addressed by the AME Conceptual Model document written in 1998 (Kaiser-Hill, 1998; see Section TA-1.4). The Conceptual Model was developed to address the AME goals outlined in Section TA-1.3 with the understanding it would be revised and formally updated as new data are obtained by the AME Group.

TA-1.2 REPORT ORGANIZATION

The Pathway Report is presented in two documents, a Summary Report and a Technical Appendix. The Summary Report provides a condensed review of the major topics and findings presented in the Technical Appendix. The Technical Appendix presents detailed discussions, calculations and literature references to support subjects addressed in the Summary Report.

Technical Appendix headings, table and figure numbers are all preceded with a "TA" to clarify the organization of the Pathway Report. The Technical Appendix is organized in the following manner:

- Section TA-1 presents background information on the development of the Pathway Report, pertinent regulatory issues and general information on the physical characteristics of the Site;
- Section TA-2 presents measured actinide data for RFETS environmental media. Data are presented on related "background" actinide levels in the environment and regulatory limits for different media. Section TA-2 is a presentation of measured Site data without interpretation;
- Section TA-3 addresses Pu, Am and U geochemical transport processes;
- Section TA-4 provides an analysis of actinide transport pathways using measured data *only*;
- Section TA-5 provides an analysis of actinide transport pathways using measured data combined with modeled data. Models provide data for actinide transport pathways where measured data are not available;
- Section TA-6 provides model results of actinide transport for hypothetical extreme environmental conditions;
- Section TA-7 presents the summary, conclusions and implications for Site closure.

TA-1.3 ACTINIDE MIGRATION EVALUATION PROGRAM

The AME group was established in 1996 to provide guidance at RFETS on issues of actinide behavior and mobility in surface water, groundwater, air, soil and biota (Kaiser-Hill, 2000a). The AME activity at RFETS brings together investigations, management and external advisory personnel to facilitate integration and review of RFETS remediation, D&D, monitoring and

project planning. Where appropriate, the external advisory team identifies research, techniques and approaches that can be used to solve short- and long-term issues. The external advisory team covers a broad range of relevant expertise and the advisors are explicitly independent of RFETS-funded projects on AME. Knowledge garnered by the AME group is used to help characterize current RFETS environmental conditions and to recommend a path forward for long-term protection of surface water quality during and after Site closure. Long-term protection of surface water quality at the Site is specified in the Rocky Flats Cleanup Agreement (RFCA)(see Section TA-1.5). Specifically, the goals of the AME are to answer the following questions in the order of urgency shown (Kaiser-Hill, 2000a):

- Urgent: What are the important actinide migration sources and migration processes that account for surface water quality standard exceedances?
- Near-term: What would be the impacts of planned remedial actions on actinide migration? To what level do sources need to be remediated to protect surface water from exceeding action levels for actinides?
- Long-term: How will actinide residual contamination and migration affect surface water quality and Site stewardship after closure?

TA-1.4 CONCEPTUAL MODEL FOR ACTINIDE TRANSPORT

The *Conceptual Model for Actinide Migration Studies at the Rocky Flats Environmental Technology Site* report was written as an initial effort to provide a qualitative understanding of the relationship between actinide sources and transport pathways at RFETS (Kaiser-Hill, 1998). Physical aspects of the Site, including surface and subsurface geology, soils, hydrology and meteorology were discussed in terms of their impact on actinide fate and transport.

7

As noted in the Conceptual Model report, the transport of actinides in the environment involves complex chemical and physical processes dependent on the type and source of the actinide as well as the influence of the surrounding environmental media. To facilitate understanding the potential routes for actinide transport at RFETS, a graphic depiction of the multiple potential actinide transport pathways was included in the Conceptual Model Diagram (see Figure TA-1-1). Further detail on suspected major and minor pathways and their variability with different actinides was also diagrammed in the Conceptual Model. These more detailed conceptual pathway schematics are presented in Section TA-4. They provide an initial model to be tested and expanded upon by the pathway analysis described in this report.

TA-1.5 REGULATORY FRAMEWORK

The RFCA Action Level Framework (ALF) sets forth standards and action levels for environmental media (DOE, 1996). These standards and action levels incorporate the RFCA vision and land- and water-use controls in the RFETS cleanup. Surface water action levels for Point of Evaluation (POE) monitoring locations and standards for Point of Compliance (POC) monitoring locations, are 0.15 picoCuries per liter (pCi/L) for both Pu and Am. These standards and action levels are based upon human health risk based on ingestion of surface water over a 30-year period.

The Site's surface water quality standard for total U is currently set at 10 pCi/L for Walnut Creek and 11 pCi/L for Woman Creek based on ambient levels in Site surface waters. In comparison, the Environmental Protection Agency (EPA) promulgated a total U Maximum Contaminant Level (MCL) of 30 micrograms per liter (µg/L) for drinking water on December 7, 2000 (Federal Register, 2000). The ruling noted that treating drinking water to below 20 µg/L was not considered feasible. Converting mass to activity, the 30 µg/L total U MCL corresponds to a total U activity of approximately 20 pCi/L using the isotopic proportions typically found in surface water at RFETS. Measured total U concentrations in surface water at RFETS from Water Years

8

1997 through 1999, at POE and POC monitoring stations, averaged approximately 2 to 5 μg/L or roughly one order of magnitude less than the recently established MCL for drinking water.

The RFCA soil action levels (Section TA-3.3.2) do not take into account the transport of soil containing actinides to surface water. This is because it was assumed, when the soil action levels were calculated, that there would be no consumption of groundwater or surface water (Rocky Mountain Remediation Services [RMRS], 1997). The soil radionuclide action levels must be assessed for long-term protectiveness of surface water. The RFCA states "protection of surface water uses with respect to the long-term Site condition will be the basis for making soil and groundwater remediation and management decisions and that additional groundwater or soil remediation or management may be required for the protection of surface water quality or ecological resources (DOE, 1996)."

TA-1.6 BACKGROUND SITE DESCRIPTION

TA-1.6.1 General Site Description

RFETS is located 16 miles northwest of Denver in Jefferson County, Colorado. Owned by the United States Department of Energy (DOE), the former nuclear weapons facility encompasses approximately 6,550 acres of federally owned land (Figure TA-1-2). Major plant structures, including all former production buildings, are located within a centralized 385-acre Industrial Area that is surrounded by a 6,165-acre Buffer Zone (EG&G, 1993a). From its first construction in 1951, the Site evolved into a complex of over 440 permanent and temporary structures used as manufacturing, chemical processing, laboratory, support and administrative facilities (DOE, 1995). Production operations occurred from 1952 until 1989, at which time RFETS was added to the Comprehensive Environmental Response, Compensation and Liability Act (CERCLA) National Priorities List for environmental cleanup. Site-specific regulatory requirements for remediation and closure were established in 1995 when RFCA was signed by the DOE, EPA and Colorado Department of Public Health and Environment (CDPHE) (DOE, 1996).

9

The plant produced components for nuclear weapons made from Pu, U, beryllium and stainless steel. Other production activities included chemical recovery and purification of recyclable transuranic radionuclides, metal fabrication and assembly and related quality control functions. The plant conducted research and development programs in metallurgy, machining, nondestructive testing, coatings, remote engineering, chemistry and physics. Parts manufactured at the Site were shipped to other locations for final assembly.

Site operations generated solid and liquid nonhazardous, hazardous, radioactive and mixed (hazardous and radioactive) waste streams. These wastes have been handled and disposed of in a variety of ways. Solid nonhazardous and nonradioactive wastes are recycled, stored on Site, or shipped off Site for recycling, treatment or disposal.

TA-1.6.2 Climate

Basic climatological information, including general descriptions of precipitation, temperature and wind patterns, is pertinent to understanding the hydrologic setting and actinide migration potential of environmental media at RFETS (RMRS, 1997). For example, precipitation amount, frequency, intensity and seasonality (combined with air temperatures, humidity and wind conditions) influence the erosion potential due to wind and water, groundwater recharge and evapotranspiration.

The RFETS climate is temperate and semiarid, characteristic of Colorado's Front Range. The dry atmosphere of the Site at 1,830 meters (m) (6,000 foot [ft]) elevation above mean sea level (MSL) often causes wide temperature fluctuations between daytime and nighttime. Summer high temperatures are typically in the upper-20 degrees Centigrade (°C)(equivalent to mid-80 degrees Fahrenheit [°F]), with nighttime lows falling to approximately 16°C (60°F) (EG&G, 1993b). During the winter, temperatures typically range from 4°C to 7°C (40°F to 45°F) during the day and -9°C to -4°C (15°F to 25°F) at night. Arctic and Siberian air masses occasionally

10

bring frigid air during the winter when low temperatures may drop to between -21°C and -24°C (-5°F and -12°F) (EG&G, 1993b).

Precipitation

The average annual precipitation based on 30 years of record is approximately 368 millimeters (mm) (14.5 inches [in]) (DOE, 1995). Roughly half of the precipitation occurs as rain and half as snow, with precipitation falling primarily as snow from late October through early April and as rain during the remaining months (RMRS, 1997). Annual snowfall averages approximately 1,778 mm (70 in), with the highest monthly snowfall average (approximately 406 mm [16 in]) occurring in March (EG&G, 1993b). Rainfall is highest from April through June, with nearly 42 % of the average annual precipitation occurring during those months (EG&G, 1993b). The average monthly distribution of precipitation, based on data collected at the Site 61-meter meteorological tower from 1993 through 1999, is shown in Figure TA-1-3.

These precipitation data cover the time frame, from Water Year 1997 through 1999 (October 1996 through September 1999), during which the surface water actinide data presented in Section TA-2 were collected. This precipitation record was also used to calculate estimated erosion rates, presented in Section TA-5, to predict actinide transport in surface water runoff.

Analysis of Precipitation for Water Years 1997 Through 1999

Surface water actinide data from Water Years 1997 through 1999 are analyzed later in this report because similar sampling protocols were used at multiple locations throughout the Site during this time frame. This allowed for reasonable comparison of data from different sampling locations. To determine whether this three-year period of study was relatively wet or dry compared to normal, an analysis was performed to compare RFETS precipitation data with other precipitation gages in the region that have longer historical precipitation records.

11

Monthly total precipitation data were obtained from two sources, the Colorado Climate Center (CCC) and the National Climate Data Center (NCDC), for five National Oceanic and Atmospheric Administration (NOAA) monitoring stations (CCC, 2001 and NCDC, 2001). These stations, their NOAA station numbers and their data sources are listed in Table TA-1-1. These stations were chosen based on their proximity to RFETS, the available period of record and, in the case of the Fort Collins station, because previous RFETS studies had used the station for comparison.

Table TA-1-1. NOAA Precipitation Stations Used to Compare with RFETS Data

Station	NOAA Station #	Data Source
Boulder	50848	Colorado Climate Center
Denver	52220	National Climate Data Center
Fort Collins	53005	National Climate Data Center
Lakewood	54762	National Climate Data Center
Ralston	56816	Colorado Climate Center

Monthly precipitation records from each of the stations for Water Years 1997 through 1999 were plotted against the corresponding monthly precipitation depth measured at RFETS (Figure TA-1-4). The Boulder station has the best correlation with the RFETS data ($R^2 = 0.79$), followed by the Ralston Reservoir and Lakewood stations. During Water Years 1997 through 1999, the Boulder, Lakewood and Fort Collins stations contain a complete data set, while the Ralston Reservoir and Denver stations have missing months in their data sets.

The Boulder station was used as the reference to compare with the RFETS record because it had the best correlation with the RFETS precipitation data. The difference in monthly precipitation for Water Years 1997 through 1999 with the normal precipitation at the Boulder station was plotted (Figure TA-1-5). Normal monthly precipitation depths for the Boulder station are based

12

on a period of record from 1961-1990. Both the Boulder and RFETS stations followed the same trend with Water Year 1999 having the greatest amount of precipitation followed by Water Years 1997 and 1998. Precipitation at the Boulder station for Water Years 1997-1999 exceeded the normal by approximately 490 mm (19.3 in) over the three-year period as shown in Figure TA-1-5. The Boulder station record provides a better historical basis than the more limited RFETS record to indicate that the three-year period of study, from Water Years 1997 through 1999, received above-normal precipitation.

Evapotranspiration

Evapotranspiration averages over 400 mm (16 in) per year, creating a water deficit in most years (Wright Water Engineers, Inc. [WWE], 1995). Much of the runoff feeding the Site's drainages occurs rapidly, originating from the mainly impervious Industrial Area surfaces (RMRS, 1998). RFETS is located in a semi-arid environment. For perspective, evapotranspiration in a humid environment, such as Florida, can average over 890 mm (35 in) per year (Hanson et al., 1991).

Winds

Winds at RFETS are predominantly from the northwest toward the southeast. This wind pattern reflects the influence of local terrain combined with prevailing winds from west to east. Winds at RFETS average approximately 4 meters per second (m/s) (9 miles per hour [mph]), with a range from zero (calm) to sustained winds over 18 m/s (40 mph), with gusts to over 45 m/s (100 mph). Figure TA-1-6 shows the joint wind speed and direction distribution (wind rose) for 1999. Wind speed data for 1997, 1998 and 1999 were used to develop models, presented in Section TA-5 that forecast actinide transport via the air pathway.

RFETS is noted for the periodic occurrence of strong, gusty winds, which can be an important factor in the resuspension of soil and actinides. Higher wind speeds may be associated with thunderstorms and the passage of weather fronts, while the highest wind speeds typically occur with storms from the west called Chinooks (EG&G, 1993b). These windstorms occur from late

November into April, but reach their height around January in most years. Chinook winds occur when air masses are forced over the Continental Divide. The air masses warm and dry out, as they compress on the eastern side of the mountains. The steep-sided canyons along the Front Range tend to channel the airflow, which also contributes to high wind speeds.

Other flow patterns also occur at RFETS. Moderately strong winds from the north or from the south are common in winter and summer, respectively. During periods of atmospheric stability, when regional flow patterns are weak, thermally driven upslope and downslope flow predominates, with downslope flow at night and upslope during the day. Winds from the east can also occur following frontal passages. These upslope events may be associated with heavy snowfall or other precipitation. A more detailed summary of the climatology and meteorology at the Site is provided in the *RFETS Historical Data Summary* (Aerovironment, 1995).

TA-1.6.3 Geology

The Site is situated approximately two miles east of the Front Range of Colorado, on the western margin of the Colorado Piedmont section of the Great Plains Physiographic Province (Spencer, 1961). Geologic units at RFETS can be grouped into two general categories: unconsolidated surficial deposits and underlying consolidated bedrock (RMRS, 1999a). The surficial geologic unit has a relatively shallow agricultural soil horizon that developed by *in situ* weathering processes and/or erosion of the geologic units. Soils information is important for understanding actinide transport based on microbiologic processes, water balances, vegetation, erosion, infiltration and runoff all of which impact actinide transport and vary with different soil environments. An understanding of the Site geology is necessary when discussing contaminant transport because of the sub-surface pathways that may exist. General descriptions of the soils and major geologic units at RFETS are provided in the following sections.

14

Soils

The United States Department of Agriculture (USDA) Soil Conservation Service (SCS) developed map unit models on aerial photographs to reasonably predict the types of soils that have formed near the surface on the geologic units in the area. The boundaries of the soil map units were refined and the map unit models were tested by digging test pits and recording the characteristics of the soil profiles (EG&G, 1995b). A soils map for the Site is presented in Figure TA-1-7.

The RFETS geologic map units are described in the *Geologic Characterization Report for the Rocky Flats Environmental Technology Site, Final Report, Volume I of the Sitewide Geoscience Characterization Study* (EG&G, 1995b). The geologic map units are shown in Figure TA-1-8. A comparison between the agricultural soils map (Figure TA-1-7) and the geologic map (Figure TA-1-8) illustrates the relationship between agricultural soils and geologic map units. Generally, there are four agricultural soil types at RFETS that are associated with the geologic units as follows:

- Pediment (flat upland areas) soils are located on the broad, dissected, eastward-sloping pediment surface in the western portion of the Site. These soils are associated with the Rocky Flats Alluvium (Qrf) geologic map unit;

- Valley slope soils are located in the stream-cut valleys of the intermittent Rock Creek, Walnut Creek and Woman Creek drainages. These are associated with the Laramie Formation (Kl), Arapahoe Formation (Ka) and Landslide (Qls) geologic map units;

- Hilltop soils of the eastern third of RFETS are similar to valley slope soils and are associated with the Laramie (Kl) and Arapahoe (Ka) Formations. Localized areas on hill summits are associated with Terrace Alluvium (Qta); and

- Drainage bottom soils form in recent alluvium (Qa) along drainage bottoms.

Unconsolidated Surficial Deposits

Approximately 99 % of the Site is covered with surficial deposits that include artificial fill, colluvial, landslide and alluvial deposits. A generalized stratigraphic cross-section, including unconsolidated and consolidated layers, shows the vertical sequence of geologic units (Figure TA- 1-9).

Surficial deposits range in thickness from zero to 30.5 meters (0 to 100 feet) (EG&G, 1995b). The unconsolidated surficial deposits, combined with the weathered portion of subcropping bedrock formations, have the greatest importance regarding groundwater flow and contaminant transport at the Site (Rocky Mountain Remediation Services [RMRS], 1999). Further detail on the various types of surficial deposits found at RFETS is provided below.

Artificial Fill Materials

These materials are present across the Site including road and railroad embankments, earth dams and other engineered fills, as well as compacted and uncompacted landfills and spoil piles along some of the irrigation ditches. The artificial deposits are commonly less than 3.05 meters (10 feet) thick, although some of the earth dams and landfills are greater than 9.1 meters (30 feet) thick. Most of these deposits are relatively impermeable and restrict groundwater flow (EG&G, 1995c).

Colluvial Deposits

This material covers the steep hill slopes in the incised stream drainages (EG&G, 1995b). These middle Pleistocene to Holocene deposits were derived from older alluvial units and bedrock and were deposited by sheet wash and soil creep. Colluvial deposits range in thickness from 0.9 to 4.6 meters (3 to 15 feet). Lithologically, the colluvium consists of silty sand, sandy silt, clayey silt and silty clay with pebbles and cobbles. These deposits are typically poorly sorted and

116

poorly stratified. Colluvial deposits are variably saturated and colluvial groundwater tends to flow downslope following paleogullies developed on the bedrock surface.

Landslide Deposits

These deposits are present along the steep hill slopes in the incised drainages (EG&G, 1995c). These middle Pleistocene to Holocene deposits include earth flows, earth slumps, debris flows, debris slumps, rock-block slides and complex landslides. These deposits range in thickness from 3 to 30.5 meters (10 to 100 feet). Landslide scarps are present in all of the drainages in the map area and are most numerous in the Rock Creek drainage (EG&G, 1995b). Landslides are commonly located downgradient from alluvial or bedrock groundwater discharge areas. Groundwater discharge increases the saturation within downgradient soils, leading to failure of the material.

Alluvial Deposits

Alluvial deposits have been mapped in floodplains, stream channels and terraces along the drainages across the Site and include valley-fill alluvium, undifferentiated alluvium and Rocky Flats Alluvium. Valley-fill alluvium includes the Pleistocene Louviers, Broadway and pre-Piney Creek Alluvium and the Holocene Piney Creek and post-Piney Creek alluvial units. Valley-fill alluvium consists of channel and terrace deposits in and along most of the ephemeral streams that cross the Site (EG&G, 1995b).

Valley-fill alluvium ranges in thickness from 3 to 12.2 meters (10 to 40 feet) and is variably saturated. The valley-fill alluvium is permeable and may provide preferential pathways for groundwater migration. Undifferentiated alluvial deposits include the Pleistocene Slocum Alluvium and Verdos Alluvium of Shroba and Carrara (1994). These units form small remnants of pediment or terrace deposits primarily in the southeastern portion of the RFETS. The undifferentiated alluvial deposits range in thickness from 1.5 to 6.1 meters (5 to 20 feet), but this unit is not a significant component of the hydrologic system on the Site (EG&G, 1995c).

17

The Rocky Flats Alluvium caps the pediment at the Site. These Pleistocene sediments were deposited as alluvial fans along the eastern edge of the Front Range. The deposit diminishes from west to east with thicknesses ranging from approximately 30.5 to less than 0.3 meters (100 to less than 1 foot). In the central portion of the Site the deposit is approximately 35.1 to 7.6 meters (15 to 25 feet) thick (RMRS, 1999). Thicker deposits correspond to paleoscours and thinner deposits occur along the crests of paleoridges. Groundwater flow within the Rocky Flats Alluvium is influenced by the topography of the underlying bedrock surface (paleotopography), the geometry and lithology of alluvial lithofacies and the regional hydraulic gradient.

Consolidated Bedrock Deposits

Bedrock from the Arapahoe, Laramie, Fox Hills and uppermost Cretaceous Pierre Formations are present at RFETS (Figure TA- 1-9) (EG&G, 1995c). Further detail on these bedrock deposits is provided below.

Arapahoe Formation

The Arapahoe Formation is composed of claystone and silty claystone with lenticular sandstone in the basal portion of the formation. The Arapahoe Formation is generally less than 7.6 meters (25 feet) thick at the Site, occurring as erosional remnants of fine-grained sandstone above the Laramie Formation at various locations on the Site (EG&G, 1995c). This basal Arapahoe Formation sandstone, which is currently defined as the No. 1 Sandstone, is of concern as a potential contamination pathway, especially where it subcrops beneath the alluvial/bedrock unconformity.

Laramie and Fox Hills Sandstone Formations

The Laramie Formation is approximately 180 to 245 meters (590 to 800 feet) thick and is composed of a lower sandstone/claystone/coal interval and an upper, thick claystone interval. Within the upper claystone interval, thin, lenticular sandstone lenses occur (EG&G, 1991). The discontinuous nature of these sandstone lenses coupled with the large claystone layer that

18

encloses them mitigates their potential for transmitting groundwater contamination in both horizontal and vertical directions.

The Fox Hills sandstone is primarily fine-grained sandstone with thin siltstone and claystone interbeds and an approximate thickness of between 20 and 40 meters (65 and 130 feet) contamination (Figure TA- 1-9). The Fox Hills sandstone crops out and subcrops along a narrow, north-south trending pattern in the extreme western part of the Site, upgradient from known sources of (EG&G, 1995b).

The regionally-important Laramie-Fox Hills aquifer is composed of the permeable lower unit of the Laramie Formation and the underlying Fox Hills Sandstone (Robson, 1983). This aquifer system is an important water source in the South Platte River Basin and is the sole water supply for some residents in the RFETS area (Rocky Mountain Remediation Services, 1999a). This aquifer lies approximately 180 to 275 meters (590 to 900 feet) below the Industrial Area and is protected from Site contamination by the intervening Laramie Formation claystones (EG&G, 1995b).

Pierre Formation

The Pierre Formation is a 7,500-foot thick, dark gray, silty bentonitic shale that acts as a lower confining layer for the Laramie-Fox Hills aquifer in the Denver Basin. This thick marine shale unit subcrops only in the extreme western part of the Site (RMRS, 1999).

Structural Features

The Site is located along the western margin of the Denver Basin, an asymmetric basin with a steeply east-dipping western flank and a gentle eastern flank. The interpretation of the subsurface structure is generalized in the west-east generalized geological cross section of the Site area presented in Figure TA-1-10. A monoclinal fold limb exposed west of the Site is the most significant surficial structural feature in the Site area. Along the west limb of the fold, an

angular unconformity exists between the Upper Cretaceous bedrock and the base of the Quaternary Rocky Flats Alluvium.

No active faults have been identified at the Site. Several high-angle bedrock faults have been inferred to exist in the Industrial Area based on various stratigraphic and borehole correlation criteria. These faults appear to have only a limited hydrologic significance with regard to vertical groundwater movement and contaminant transport (RMRS, 1996).

TA-1.6.4 Hydrogeology and Geochemistry

Hydrostratigraphy and Hydraulic Conductivities

Shallow groundwater flow systems at RFETS have been categorized into two hydrostratigraphic units based on contrasts observed between groundwater geochemistry, core logging and hydraulic conductivity determinations (EG&G, 1995b). These are generally referred to as the upper hydrostratigraphic unit (UHSU) and lower hydrostratigraphic unit (LHSU) and are described in detail in the Hydrogeologic Characterization Report for RFETS (EG&G, 1995b). General descriptions of the UHSU and LHSU are provided in the following subsections.

Upper Hydrostratigraphic Unit

UHSU Hydrostratigraphy. The UHSU has many subunits, of which two are primarily important: the surficial deposits (unconsolidated materials) and the weathered bedrock in hydraulic connection with the overlying unconsolidated surficial deposits or with the ground surface. The degree of hydraulic communication between the UHSU subunits varies with the permeability of the units. The relative amount of hydraulic communication between the UHSU subunits is much greater than that between the UHSU and LHSU, which is the basis for including portions of the weathered bedrock in the UHSU (EG&G, 1995b).

The UHSU is comprised of several distinct lithostratigraphic units. These include the alluvium (including Rocky Flats Alluvium), colluvium and landslide deposits; weathered portions of the

20

Cretaceous Arapahoe and Laramie Formations; and all sandstones within the Arapahoe and Laramie Formations that are in hydraulic connection with the overlying, surficial deposits or the ground surface (EG&G, 1995c). On the west side of the Site, the UHSU may also include weathered portions of the Cretaceous Pierre Shale and Fox Hills Sandstone.

UHSU Hydraulic Conductivities. The UHSU at the Site has a relatively low to moderate hydraulic conductivity that typically yields small amounts of water to groundwater monitoring wells. The UHSU exhibits a wide range of hydraulic conductivities because of the diverse nature of the individual geologic units that comprise this unit.

The relative ranking of individual UHSU units are listed in Table TA-1-2 in order of decreasing geometric mean hydraulic conductivity (RMRS, 1999):

Table TA-1-2. Hydraulic Conductivity of UHSU Units

UHSU Unit	Hydraulic Conductivity in centimeters per second (cm/sec)	Hydraulic Conductivity in meters per year (m/year)
Valley-fill Alluvium	2.5×10^{-3}	789
Arapahoe No. 1 Sandstone	7.9×10^{-4}	249
Rocky Flats Alluvium	2.1×10^{-4}	66
Colluvium	93×10^{-5}	29
Weathered Laramie	3.9×10^{-5}	12
Weathered Laramie	8.8×10^{-7}	0.3

Lower Hydrostratigraphic Unit

LHSU Hydrostratigraphy. The LHSU is comprised of all lithostratigraphic units in the unweathered portions of the Arapahoe and upper Laramie Formations, except for subcropping sandstones at the alluvial/bedrock unconformity (EG&G, 1995b). In general, saturated

21

sandstones that lie within unweathered claystones and siltstones of the Arapahoe or Laramie Formations are confined units. These sandstone units are not interpreted as being directly interconnected and each may act as an isolated hydrostratigraphic unit. In addition, recharge to these units occurs through the confining claystone and siltstone units. Therefore, all unweathered bedrock is considered part of the LHSU (EG&G, 1994 and 1995b). The LHSU forms a thick (over 100 meters (several hundred feet)), regionally extensive confining layer that serves to isolate shallow groundwater from the underlying Laramie-Fox Hills aquifer (RMRS, 1996).

LHSU Hydraulic Conductivities. Hydraulic conductivities for LHSU materials are generally significantly lower than those of the overlying unit with geometric mean values for individual lithologic groups ranging from 1.6×10^{-7} to 5.8×10^{-7} cm/sec (EG&G, 1995c). The low permeability and +180-meter (+590-foot) thickness of the upper Laramie Formation claystones act as effective aquitards that restrict downward vertical groundwater flow and contaminant transport to the Laramie-Fox Hills aquifer (RMRS, 1999).

Groundwater Occurrence and Flow Conditions

Groundwater Occurrence

The Site is located in a regional groundwater recharge area (EG&G, 1991). Groundwater is found in all geologic units present at RFETS, although not always in predictable amounts and availability. Groundwater recharge occurs from the infiltration of precipitation and from stream, ditch and pond seepage. Much of the groundwater that discharges from the UHSU to streams and seeps evaporates as it is being discharged. Limited investigation of the former Operable Unit 2 (OU 2) area during the period of July through October 1993 indicated that the precipitation component of recharge was lost to evapotranspiration demands (EG&G, 1993c).

In the western part of the Site, where the thickness of the Rocky Flats Alluvium reaches 30.5 meters (100 feet), the depth to the water table is 15 to 21 meters (50 to 70 feet) below the

22

surface. The depth to water generally becomes shallower from west to east, as the alluvial material thins and the confining claystones are closer to the ground surface. At the head of stream drainages and along valley sides, seeps are common at the base of the Rocky Flats Alluvium where it is in contact with claystones of the Arapahoe/Laramie Formations and where the Arapahoe Formation sandstone crops out. In general, the unconsolidated surficial materials are thicker in the western, higher elevations at the Site. Accordingly, the saturated thickness of these materials also thins eastward. The potentiometric surface of groundwater in unconsolidated surficial deposits was mapped and is shown in Figure TA-1-11 for the second quarter of 1998, a time of year when static water levels are expected to be high. Areas of unsaturated and seasonally unsaturated alluvium and colluvium are indicated east and northeast of the Industrial Area.

Groundwater in the Arapahoe Formation sandstone units, which subcrop beneath the alluvial material, is not confined when in contact with the surficial materials. In this setting, a hydraulic connection exists between the bedrock sandstone and the alluvial material allowing the bedrock groundwater to exist under unconfined conditions as part of the UHSU. The subcropping Arapahoe Formation No. 1 sandstone, located in the eastern portion of the Industrial Area and in the area between South Walnut Creek and Woman Creek, is part of the UHSU (EG&G 1991). The upper discontinuous sandstones of the Laramie Formation also subcrop beneath alluvium and colluvium but in limited areas in the valleys and along valley slopes. Groundwater in the lenticular sandstone units of the Laramie Formation occurs under confined conditions over scattered areas of the Site.

Groundwater levels in UHSU wells fluctuate in response to seasonal recharge events. Approximately 15 % of the groundwater monitoring wells are commonly dry during at least one of the quarterly sampling events. Of the remaining wells, approximately half cannot yield sufficient water volume (4.5 gallons) necessary for a full suite of laboratory samples. Sampling crews must return later, after wells have recovered, to obtain additional sample volumes.

The Arapahoe aquifer is one of the primary aquifers in the Denver Basin east of the Site. Existing evidence indicates that the Arapahoe Formation at RFETS is not in communication with the regional Arapahoe aquifer in the Denver Basin (EG&G, 1995b).

The Arapahoe Formation is present only at the top of the Rocky Flats pediment and is breached by modern streams along the valley slopes. Consequently, the channel deposits within the formation are cut off and do not extend eastward into the Denver Basin. The groundwater within the channel deposits discharge via springs and seeps along the hillsides. Therefore, the sandstones of the Arapahoe Formation are not considered primary pathways for off-Site groundwater migration. A thorough discussion of the hydrogeologic characteristics of the UHSU is included in the *Hydrogeologic Characterization Report* (EG&G, 1995d).

The Laramie/Fox Hills aquifer is present at greater depth (approximately 180 to 275 meters (590 to 900 feet)) below the Site (Robson, 1983). This deeper hydrostratigraphic unit is composed of the lower unit of the Laramie Formation and the underlying Fox Hills Sandstone. These units subcrop beneath the Rocky Flats alluvium and are locally exposed in gravel quarries near the western boundary of the Site. Recharge to the aquifer occurs along this subcrop zone. Claystones of the Laramie Formation have very low hydraulic conductivities. In a study of Site hydrology, the United States Geological Survey (USGS) concluded the low hydraulic conductivities in the Laramie Formation would prevent Site operations from impacting the underlying Laramie-Fox Hills aquifer (Hurr, 1976).

Groundwater Flow Conditions

A conceptual description of unconfined groundwater flow was developed for the Site as part of the *Well Evaluation Report* (EG&G, 1994). That report described three general zones where the characteristics of groundwater flow are distinctive. These zones occupy the western, central and eastern portions of the Site.

24

A relatively unbroken topographic slope formed on the Rocky Flats Alluvium characterizes the western zone. In this zone, alluvial thickness is greatest, water-level fluctuations are minor and the alluvium is rarely, if ever, completely unsaturated. Groundwater in the UHSU flows generally east, with slight variations in flow direction occurring along the top of the bedrock surface. The predominantly claystone bedrock impedes downward vertical migration of groundwater and directs flow laterally.

The central zone has a gently eastward-sloping topographic surface that is incised by east-west-trending drainages. Topographic highs are capped by thick alluvial deposits and flanked by colluvium. Water flowing through the capping alluvium follows the bedrock surface and emerges at seeps, drains into hillside colluvium, or migrates vertically into lower lithostratigraphic units (weathered or unweathered bedrock). The potentiometric surface of groundwater in the UHSU generally resembles the ground surface and paleotopographic (bedrock) surface. The potentiometric surface slopes gently to the east and more steeply north-northeast and south-southeast along hillslopes of the incised drainage valleys. Groundwater flows from broad areas of recharge located upgradient and on nearby topographic highs, toward the erosional limit of alluvium and then directly toward creeks in incised drainages. Groundwater and surface water are in direct connection at seeps and in some alluvial deposits along these drainages. In areas of relatively steep topography, baseflow to creeks may occur. The paleotopographic surface also plays a role in directing groundwater flow and in the development of unsaturated zones in unconsolidated surficial deposits. Channels and depressions on the top-of-bedrock surface may act as conduits, or even small basins, for groundwater. Surficial deposits on either side of these channels can be drained, or dewatered, by flow toward the channel.

The eastern zone is characterized by relatively flat surface topography, the absence of thick alluvial deposits (Rocky Flats Alluvium) and more widespread valley-fill deposits. Thin deposits of colluvium generally cover the ground surface. The hydraulic gradients are relatively low and groundwater in unconsolidated deposits may not flow directly toward the axes of stream

valleys. Baseflow to creeks is probably also diminished relative to the central zone because of the lower hydraulic gradients.

In summary, the direction of groundwater flow in the UHSU is largely controlled by the topography of the ground surface and bedrock surface. Both surfaces slope gently to the east and are incised by stream valleys. Groundwater generally flows from west to east across the Site following the regional topography. The incised valleys in the central area of the Site have formed east-west-trending ridges and east-draining valleys. Groundwater in the UHSU generally flows to the east along the ridge tops, flows north and south along the valley sides and flows east in the valley bottoms (EG&G, 1994 and EG&G, 1995d). The permeability of bedrock units, composed primarily of claystone with lesser amounts of siltstone and sandstone, is typically several orders of magnitude less than for unconsolidated surficial deposits. The 180+ meters (590+ feet) of unweathered bedrock between the shallow groundwater flow system and deep regional Laramie-Fox Hills aquifer provide an effective barrier to vertical groundwater and contaminant movement.

Groundwater Interaction With Surface Waters and Soils

The pattern of seep distribution confirms that seep occurrence is controlled by local geologic conditions. Hillside seeps at RFETS are common along the eastern extent of the Rocky Flats Alluvium at the contact between the Rocky Flats Alluvium and underlying claystone subcrops. In general, seeps occur in greater number and areal extent along the north side of the pediment ridges, as observed along South Walnut Creek and Rock Creek. Most seeps are ephemeral in nature and only discharge at the ground surface in the spring. Perennial seeps are relatively rare, with most located in the Rock Creek drainage. Groundwater seepage also occurs along segments of Woman Creek's stream channel, particularly above the Woman Creek's stream diversion structure at Pond C-2, as determined from a stream gain/loss study (Fedors and Warner, 1993). The stream channels of North and South Walnut Creeks are so extensively interrupted by impoundments that channel seepage measurements have not been made (RMRS, 1997).

26

Seep flow data are generally unavailable due to difficulties inherent with measuring broad, diffuse sources of discharge. The results of an incomplete seepage inventory conducted after the 1995 spring recharge event in portions of the Woman, Walnut and Rock Creek's watersheds revealed that, of over 200 potential seep areas indicated by wetland vegetation, only 32 had a measurable flow and, of these, 14 had flows of one gallon per minute or less (EG&G, 1995d and RMRS, 1997). The remaining sites were moist to wet at the ground surface with little or no evidence of surface flow. Given the magnitude of the spring recharge event as reflected by Site-wide high water table conditions, it is likely that seep flows measured during this time were at or near maximum levels. It was commonly observed during this survey that surface flow from many ephemeral hillside seeps percolate back into the soil below the discharge point before entering a surface water body. Direct contact with surface water may occur during exceptionally wet periods because of increased seep flow caused by abnormal water table rises or by mixing with surface runoff.

The most common type of seep develops at the contact between the Rocky Flats Alluvium and underlying bedrock claystones. These seeps are thought to be related to preferential flow channels in bedrock surface topography and/or alluvial stratigraphy (high hydraulic conductivity zones) (EG&G, 1995b). In the 903 Pad and East Trenches areas, some seep occurrences have been attributed to discharge from the subcropping Arapahoe Formation sandstone, which receives recharge from the overlying surficial deposits (EG&G, 1995b). The most notable sandstone seeps in this area include a grouping of seeps situated above the B-1 pond in the South Walnut Creek drainage and the 903 Pad hillside seep (Figure TA-1-2).

Along the north slope of Woman Creek from the 903 Pad eastward to Indiana Street, evidence of present-day seep activity is limited primarily to the 903 Pad hillside seep and potentially a few scattered small seeps. Periodic activation of a series of presumably old seepage sites located east of the 903 Pad have occurred from historic spray evaporation operations conducted at the South Spray field; however, these sites have since returned to a dry state following cessation of spray field operations. Sites for groundwater interaction with surficial soils and surface water are both

27

limited in extent and predictable based on the high degree of hydrologic control exerted by the local geology (RMRS, 1997).

Groundwater discharge to surface water is presumed to occur along major stream channels, although relatively little information is available to evaluate the significance of this interaction. Stream gain/loss studies conducted along Woman Creek (EG&G, 1995d) have indicated that the flow regime in the upper reaches of the creek (west of the confluence with Antelope Springs Creek) tend to be predominantly gaining, while the lower reaches (east of Antelope Springs Creek) tend to be predominantly losing. The presence of gaining segments found just upstream of Ponds C-1 and C-2 suggests that these impoundments exert a local influence on groundwater discharge to surface water in the alluvium. Similar relationships are suspected to occur in the Walnut Creek drainage but to an unknown degree because gain/loss stream flow data are lacking in this area. It can be assumed, however, that groundwater/surface water interactions are potentially more complex in North and South Walnut Creeks because of the influence of plant discharges and a more extensive pond system and other stream channel modifications. These interactions are potentially meaningful in terms of actinide transport, though it is important to recognize the interactions involve only the upper hydrostratigraphic unit and surface water. Hydraulic communication from the upper to the lower hydrostratigraphic units is limited (EG&G, 1995d).

Groundwater Geochemistry

A comprehensive evaluation of groundwater geochemistry at the Site is presented in the *Groundwater Geochemistry Report* (EG&G, 1995c). The study identified four probable groundwater flow paths after a review of the potentiometric surface contours for the UHSU (EG&G, 1995c). Selection of each flow path was made with the assumption that groundwater flow is perpendicular to the contours of the potentiometric surface. Major cations and anions in the UHSU groundwater are presented using stiff diagrams, based on data collected from 1990 through 1994, for the Rock Creek flow path (Figure TA-1-12), Industrial Area flow path (Figure

28

TA-1-13), Woman Creek flow path (Figure TA-1-14) and the Southern Area flow path (Figure TA-1-15). The four flow paths selected, from northernmost to southernmost and the distinguishing geochemical characteristics of each path are summarized below.

Rock Creek Flow Path – The Rock Creek Drainage covers the northern portion of the Site's Buffer Zone. This northern Buffer Zone flow path begins northwest of the Industrial Area and flows northeast along Rock Creek to the northern boundary of the Site. The flow path length is approximately 5 kilometers (km) (3 miles (mi)). Flat areas to the west, several small stock ponds within the creek bed and multiple steep gullies and stream channels to the east characterize the drainage channel. This basin is hydrologically isolated from the developed areas.

The Rock Creek flow path is considered to be largely unaffected by historic activities at the Site and clearly shows the results of water/rock interaction (EG&G, 1995c). Bicarbonate is the dominant ion in groundwater along this path. Wells along the Rock Creek flow path exhibit the least amount of variability in major ion chemistry (i.e., exhibit the tightest clustering of points of the four flow paths). Major ion concentrations at the upstream wells range from approximately 10 milligrams per liter (mg/L) or less for sulfate, chloride, calcium and sodium up to 100 mg/L for bicarbonate. From flow path beginning to end, the concentrations of many major ions increase by approximately one order of magnitude. Total Dissolved Solids (TDS) concentrations vary from 144 mg/L at the initial well to approximately 1160 mg/L at the most downgradient well on the path.

Industrial Area Flow Path – The Industrial Area flow path begins in the West Spray Fields, directly west of the Industrial Area and flows eastward through the center of the Industrial Area, down South Walnut Creek through the B-Series ponds and on to the Site boundary at Indiana Street. The flow path length is approximately 7 km (4 mi). Major ion concentrations at the upstream wells range from approximately 10 mg/L or less for sulfate, chloride, calcium and sodium up to 100 mg/L for bicarbonate. Similar to Rock Creek, the magnitude of overall increase in elemental concentrations is approximately one order of magnitude from the initial to

the final wells. Groundwater within the central Industrial Area shows increases in the concentrations of some major ions for certain wells. However, groundwater samples from the beginning to end of the Industrial Area flow path indicate only equal or less of an increase in ion concentrations than were observed along the shorter Rock Creek flow path (EG&G, 1995c).

The major-ion composition of UHSU groundwater also undergoes a change along this flow path. Groundwater changes from a calcium-bicarbonate water within the Industrial Area to a mixed sodium-bicarbonate/sodium-sulfate water along South Walnut Creek. At the end of the Industrial Area flow path, the groundwater is again a calcium-bicarbonate water. The observed major-ion variations thus have a limited extent and may reflect inputs from contaminant sources in the Industrial Area or along Walnut Creek (EG&G, 1995c). TDS shows the highest variability within and immediately downgradient of the Industrial Area and varies from 138 mg/L at the initial well to approximately 455 mg/L at the most downgradient well on the path.

Woman Creek Flow Path – The regional Woman Creek flow path extends eastward from the base of the foothills near Coal Creek Canyon to Standley Lake. On-Site, Woman Creek flows through the southwest Buffer Zone, through Pond C-1, to the Site boundary at Indiana Street. The flow path length is approximately 6 km (4 mi). Similar to the Industrial Area flow path, groundwater along the Industrial Area and Woman Creek flow paths shows local increases in the relative proportions of chloride and sulfate. Major ion concentrations at the upstream wells range from approximately 10 mg/L or less for sulfate, chloride, calcium and sodium up to approximately 60 mg/L for bicarbonate. Major ion concentrations show an upgradient-to-downgradient increase of approximately one order of magnitude. This is similar to the increases observed in the Industrial and Rock Creek flow paths. The impact of Site activities is potentially suggested in wells located along Woman Creek on the southeast corner of the Industrial Area (EG&G, 1995c). TDS concentrations vary from 140 mg/L at the initial well to approximately 500 mg/L at the most downgradient well on the path.

30

Southern Flow Path – The southern flow path begins in the south Buffer Zone just east of Rocky Flats Lake. It continues eastward to the ponds in the southeast corner of the Site and on to the Site boundary. The flow path length is approximately 7 km (4 mi). Similar to the Rock Creek flow path, bicarbonate is the dominant ion in groundwater along the southern flow path. Major ion concentrations at the upstream wells range from approximately 10 mg/L or less for sulfate, chloride and sodium up to approximately 100 mg/L for calcium and bicarbonate. Major ion concentrations show an upgradient-to-downgradient one order of magnitude increase similar to that observed in the Industrial and Rock Creek flow paths. TDS concentrations vary from 331 mg/L at the initial well to approximately 500 mg/L at the most downgradient well on the path.

As noted in the *Groundwater Geochemistry Report*, the major-ion chemistry of the UHSU and LHSU groundwater generally supports the current definition of the two hydrostratigraphic units. The major-ion composition of groundwater is much less variable in the UHSU than in the LHSU. Groundwater in the UHSU is generally distinct in composition from groundwater in the LHSU, although groundwater in the two hydrostratigraphic units can be similar. These observations are consistent with hydrologic evidence for two distinct hydrostratigraphic units that have only limited hydraulic communication with each other (EG&G, 1995c).

TA-1.6.5 Surface Water Features

Streams and seeps at RFETS are largely ephemeral, with stream reaches gaining or losing flow, depending on the season and precipitation amounts. Surface water flow across RFETS is primarily from west to east, with three major drainages traversing the Site. A total of 14 detention ponds (plus several small stock ponds) collect surface water runoff, although only ten ponds are actively managed. The Site drainages and detention ponds, including their respective interest to this report, are described below and shown in Figure TA-1-2.

Walnut Creek

Walnut Creek drains the central third of RFETS, including the majority of the Industrial Area. It consists of several tributaries (North Walnut Creek, South Walnut Creek and No Name Gulch) that join prior to Walnut Creek flowing off RFETS at the eastern boundary (Indiana Street). East of Indiana Street, Walnut Creek is diverted by the Broomfield Diversion Ditch to the south of Great Western Reservoir and into Big Dry Creek. The Walnut Creek tributaries, from north to south, are described below.

McKay Ditch

The McKay Ditch was formerly a tributary to Walnut Creek within the RFETS boundaries but was diverted in July 1999 into a new pipeline to keep McKay Ditch water from co-mingling with RFETS water in Walnut Creek. Although no longer a contributor to Walnut Creek, the McKay Ditch drainage is described here to clarify water routing at the Site. The new configuration allows the City of Broomfield to transport water from the South Boulder Diversion Canal, across the northern RFETS Buffer Zone and directly into Great Western Reservoir (east of the Site) without contacting Walnut Creek water from the Site's stormwater detention ponds.

No-Name Gulch

This drainage is located downstream from the former Site landfill. Runoff from the Industrial Area does not flow into this basin.

North Walnut Creek

Runoff from the northern portion of the Industrial Area flows into this drainage, which has four detention ponds (Ponds A-1, A-2, A-3 and A-4). The combined capacity of the A-series ponds is approximately 197,000 cubic meters (m^3) (50 million gallons [160 acre-feet]). Ponds A-1 and A-2 are kept off-line and maintained for emergency spill control; evaporation or transfer controls water levels in these ponds. Pond A-1 also receives water pumped from the Landfill Pond

32

roughly once per year. North Walnut Creek flow is diverted around Ponds A-1 and A-2 to Pond A-3, where water is held and settling of solids occurs. Pond A-3 is transferred in batches to the A-series "terminal pond," Pond A-4. After filling to a predesignated level (typically approximately 50 % of capacity). Pond A-4 water is isolated, sampled and released if water quality standards are met. These off-Site discharges, each averaging approximately 63,000 m^3 (17 million gallons [50 acre-feet]), typically occur 2 to 4 times per year.

The average annual discharge to North Walnut Creek at the east perimeter of the Industrial Area (at station SW093) is approximately 148,000 m^3 (40 million gallons [120 acre-feet]). The average mean daily flow rate at station SW093, from October 1992 through April 1997, was 0.005 cubic meters per second (m^3/s) (0.16 cubic feet per second [cfs]). The maximum mean daily flow rate during this period was approximately 0.25 m^3/s (9 cfs).

South Walnut Creek

Runoff from the central portion of the Industrial Area flows into this drainage, which has five detention ponds (Ponds B-1, B-2, B-3, B-4 and B-5). The combined capacity of the South Walnut Creek detention ponds (B-series ponds) is approximately 102,000 m^3 (30 million gallons [85 acre-feet]). Ponds B-1 and B-2 are kept off-line and maintained for emergency spill control; evaporation or transfer controls water levels in these ponds. Pond B-3 receives effluent from the Site's wastewater treatment plant (WWTP) and flows into Pond B-4. South Walnut Creek flow is diverted around Ponds B-1, B-2 and B-3, into Pond B-4, which flows continuously into "terminal pond" Pond B-5. After filling to a pre-designated level, Pond B-5 is released in batches of approximately 54,000 m^3 (15 million gallons [45 acre-feet]) to South Walnut Creek. Pond B-5 discharges typically occur 6 to 8 times per year.

The average annual discharge to South Walnut Creek, including effluent from the Site's WWTP, is approximately 318,000 m^3 (85 million gallons [260 acre-feet]). The average mean daily flow rate measured in South Walnut Creek (at station GS10), from October 1992 through April 1997,

was 0.003 m^3/s (0.12 cfs) and the maximum mean daily flow rate during this period was approximately 0.142 m^3/s (5 cfs).

South Interceptor Ditch

South of the Industrial Area is the South Interceptor Ditch (SID)/Woman Creek system. Although it is tributary to Woman Creek, the SID warrants more thorough discussion than other comparable tributaries at the Site because it captures runoff from the southern portion of the Industrial Area, a drainage basin that includes the 903 Pad. The 903 Pad, located on the southeast corner of the Industrial Area, has some of the highest known levels of actinides in surface soils on the Site as shown in Section TA-3.

Surface water runoff from the southern portion of the Industrial Area is captured by the SID, which flows from west to east into Pond C-2. Water from Pond C-2 is sampled and, if surface water quality criteria are met, pump discharged into Woman Creek that flows to the Woman Creek Reservoir. Off-Site discharges from Pond C-2, averaging approximately 46,900 m^3 (13 million gallons [40 acre-feet]), typically occur once per year.

There is frequently no flow in the SID. The average mean daily flow rate (at station SW027), from October 1994 through April 1997 and including the periods of no flow, was 0.001 m^3/s (0.05 cfs). The maximum mean daily flow rate during this period was approximately 0.170 m^3/s (6 cfs).

Woman Creek

South of the SID is Woman Creek, which flows through Pond C-1 and off-Site at Indiana Street. The Woman Creek drainage basin extends eastward from the base of the foothills, near Coal Creek Canyon, to Standley Lake. Woman Creek currently flows into the Woman Creek Reservoir, where it is held until it is pump transferred to Big Dry Creek. The average annual yield of the basin is approximately 420,000 m^3 (110 million gallons [340 acre-feet]). The

34

average mean daily flow rate in Woman Creek (at Indiana Street) was 0.010 m^3/s (0.47 cfs) and the maximum mean daily flow rate during this period was approximately 2.150 m^3/s (76 cfs).

Other Drainages

The largest major drainage at the Site, other than Walnut and Woman Creeks, is Rock Creek. The Rock Creek drainage covers the northern portion of the Site's Buffer Zone. Flat areas to the west, several small stock ponds within the creek bed and multiple steep gullies and stream channels to the east characterize the drainage channel. This basin is hydrologically-isolated from the developed areas. It receives no runoff from the Industrial Area and contaminant transport by surface (or subsurface) processes is not indicated or suspected based on data presented in the *Background Geochemical Characterization Report* (EG&G, 1993a). Analytical data for Rock Creek are not presented in this report.

Smart Ditch, located south of Woman Creek, is also hydrologically-isolated from the RFETS Industrial Area. The D-series Ponds (D-1 and D-2) are located on Smart Ditch. This drainage and these ponds are not discussed in this report.

TA-1.6.6 Biological and Ecological Resources

The Buffer Zone provides habitat for a wide range of plant and animal species. Background information on the plants and wildlife found at the Site is provided below as a reference for the biological transport pathway analysis presented later in this report.

Vegetation

The topography and close proximity of the Site to the mountains provides for a diverse mixture of prairie and foothills plant communities in the Site's Buffer Zone. Currently, over 585 species of plants are reported to exist at the Site (Kaiser-Hill, 2000b). Plant communities at RFETS range from xeric (dry) grassland communities to more hydric (wet) communities, such as wet meadows and marshes. The plant communities of greatest ecological significance on Site are the

xeric tallgrass prairie, the Great Plains riparian community, the tall upland shrubland community and wetlands (Kaiser-Hill, 1996) (Figure TA-1-16).

The xeric tallgrass prairie occurs on the cobbly alluvium found on pediments and ridges at the Site and is a part of what is classified as xeric mixed grassland. This prairie is distinguished by such tallgrass plant species as big bluestem (*Andropogon gerardii*), little bluestem (*Andropogon scoparius*), prairie dropseed (*Sporobolus heterolepis*) and switchgrass (*Panicum virgatum*).

The Great Plains riparian community is found along streams at the Site. Examples of this community are found in the Rock Creek, Walnut Creek, Woman Creek and Smart Ditch drainages (Figure TA-1-2). Cottonwood trees and willows predominate in this community. Another unusual shrub community, dominated by leadplant, is also often found in association with the Great Plains riparian community at the Site. These communities provide important habitat for many of the bird and mammal species found here, including the Preble's meadow jumping mouse (*Zapus hudsonius preblei*).

The tall upland shrubland community is found on north-facing slopes primarily in the Rock Creek drainage and commonly occurs just above wetlands and seeps. The dominant tall shrubs are hawthorne and chokecherry, which are associated with other shrubs and plants common in the foothills to the west of the Site. This community is used by many animals throughout the year for cover, including several rare bird species during the breeding season and is used preferentially during the spring by mule deer for fawning areas.

Wildlife

RFETS provides habitat for a large variety of wildlife, ranging from big-game species to small mammals, bird species, fish and reptiles. Descriptions of commonly observed animal species, with information on their preferred habitat at the Site, is provided here as a reference for understanding potential actinide transport mechanisms related to wildlife. Details on wildlife observed at the Site can be found in the *2000 Annual Wildlife Report for the Rocky Flats*

Environmental Technology Site (Kaiser-Hill, 2001). Information is provided on data collection and analysis methods, survey results, species density analysis and other survey data.

At the end of the 2000 field season, 253 terrestrial vertebrate species had been verified as using the Site's ecosystems. This compares to the 322 terrestrial vertebrate species found at the Rocky Mountain National Park, an area 98 % larger than RFETS. The Site's diversity includes 189 species of birds, 20 of which are raptors; 3 big game species; 12 species of carnivores; 3 lagomorphs (rabbits and hares); 6 large rodents; 19 small mammal species, including the federally listed Preble's meadow jumping mouse; 6 bats, 11 reptiles; and 7 amphibians recorded since 1991 (Kaiser-Hill, 2001).

The dominant big game species at the Site is the mule deer (*Odocoileus hemionus*). The current population at the Site is estimated to be 130 to 150 individuals (Murdock, 2002). White-tailed deer (*Odocoileus virginianus*) numbers have increased and it is probable that more than a dozen of this species regularly use the Site. Elk (*Cervas elephas*) continue to be in the vicinity during spring and, during spring 2001, a herd of 80 to 100 elk has been observed in the grasslands west of the Site. South-facing mesic hillsides are used extensively by deer as feeding areas during the late fall, winter and spring. Shrublands, particularly tall upland shrublands are critical areas for mule deer fawning in spring and as wind-break sites during the winter months. Tall upland shrubland and Great Plains riparian habitats are heavily used for shade cover during the summer. Xeric mixed grassland, which is found on the flat uplands, is important to the deer during the breeding season, second only to mesic mixed grasslands of the hillsides. Mountain lions (*Felis concolor*) are uncommon visitors to the Site, but are reported in various habitats every year (Kaiser-Hill, 1996).

The most frequently observed carnivore species at the Site is the coyote (*Canis latrans*) and the next is the raccoon (*Procyon lotor*). Coyotes, which are active both diurnally and nocturnally, were found in all habitats. Both species are common in most habitats, with coyotes favoring grasslands and raccoons preferring areas around ponds and creeks.

Muskrats (*Ondatra zibethicus*) have been recorded in ponds in the Woman Creek, Walnut Creek and Rock Creek drainages. They are also present in the SID. Physical signs continue to confirm the occasional presence of striped skunks (*Mephitis mephitis*) around water and badgers (*Taxidea taxus*) in grasslands, though neither species is abundant at the Site. Bobcats (*Lynx rufus*) and red fox (*Vulpes vulpes*) are seldom seen but have been recorded at the Site. Beavers have been observed sporadically.

Small game mammals include desert cottontail rabbits (*Sylvilagus audubonii*), two species of jackrabbits (*Lepus californicus* and *Lepus townsendii*) and fox squirrels (*Sciurus niger*). The rabbits inhabit disturbed areas, scrap storage areas, riprap areas and other areas affording cover. Fox squirrels are usually found in shrublands and woodlands, although they have been recorded in the developed areas of the Site as well. Other large rodents include black-tailed prairie dogs (*Cynomys ludovicianus*) and porcupines (*Erethizon dorsatum*). Porcupines prefer tall upland shrubland habitat and the scattered ponderosa pines on the Site. Long-tailed weasels (*Mustela frunata*) are recorded infrequently, usually around heavy shrub cover, or along creeks. Gray fox (*Urocyon cinereoargenteus*) and mink (*Mustela vison*) have been observed once each since 1991. Preble's meadow jumping mice (*Zapus hudsonius preblei*) live in the riparian areas and around ponds. This species is seldom found far from tall vegetation and water (Kaiser-Hill, 1996).

During 2000, 85 bird species were recorded on migratory bird surveys alone. This compares to 153 species that have been recorded along bird survey transects at the Site since bird surveys were initiated in 1991. Trends over the last seven years indicate bird diversity in wetlands appears to be gradually increasing in winter while diversity appears to be steadily decreasing in grasslands in spring. No other trends are discernible (Kaiser-Hill, 2001).

Songbird density and diversity numbers indicate little change in songbird use of all habitats at the Site over the past decade. Completing an accurate census of migratory waterfowl is more difficult, but surveys conducted in 2000 indicate these species continue to be observed in

36

numbers similar to past years (Kaiser-Hill, 2001). Raptor species exhibited their normal species richness and seasonal species assemblages. As in past years, red-tailed hawks (*Buteo jamaicensis*), Swainson's hawks (*Buteo swainsoni*), American kestrels (*Falco sparverius*) and Great Horned Owls (*Bubo virginianus*) nested at the Site, demonstrating that the habitat continues to provide the necessary resources for these raptors.

TA-1.6.7 Microbiology

Microbial Ecology of Contaminated Sites

Microbial ecology is the relationship between microbial populations and their biotic and abiotic environments. Because microorganisms can tolerate, adsorb, reduce (or oxidize) and precipitate metals, microbial populations potentially can modify trace metal geochemistry. Conversely, microbial population structure and dynamics (species, abundance, diversity and activity) may be subject to environmental changes in metal chemistry. Thus, the geochemical and microbial characteristics of contaminated sites are interrelated and interdependent. Moreover, it is only recently that the interactions between indigenous microbial populations and metal contaminants have been investigated adequately. Part of the problem has been the lack of accurate tools to assess the species, numbers, diversity and activity of an indigenous population. Recent applications of molecular tools, such as polymerase chain reaction (PCR) amplification and advanced DNA sequencing techniques have advanced our understanding of native microbial populations. In the past few years, dozens of new microbial kingdoms have been identified, attesting to our past lack of understanding of native microbial populations.

It is possible, however, to make a few general statements taken from past studies about the interdependency of microorganisms and contaminants. The effects of toxic metals on microbial ecology vary with several environmental parameters such as nutrients, temperature, pH, salinity, water, light and oxygen. It is believed that only a subset of the organisms present in the environment has the ability to adapt to environments highly modified by metal pollution. Toxic

metal contaminants are believed to reduce cell abundance and species diversity by selecting for metal resistant subsets of the population (Duxbury, 1986; Babich, 1985). In general, prokaryotes (e.g., bacteria) are more sensitive than eukaryotes (fungi, algae, etc.) to heavy metal pollution in soils, due perhaps to their higher surface area per unit volume than other life forms. Finally, it is widely recognized that Gram negative bacteria are more metal-tolerant than are gram positive microorganisms (the Gram reaction divides microorganisms into categories based on their cell wall characteristics).

It can be difficult to separate the effects from metals from the effects of other environmental components. However, the microbial ecology of high U environments has been studied using both traditional microbiological and newer molecular techniques (Suzuki; Bafield, 1999). Generally, these studies reveal the presence of microorganisms in these contaminated environments. For example, 16S-rRNA gene sequencing methods were used by Puers and Selensks-Pobell (Puers, 1998). To assess bacterial diversity in a U mining waste pile having elevated U concentrations up to 58 mg/L revealed that microorganisms related to *Proteobacteria* (24 %), green-non-sulfur bacteria (41 %) and *Fibrio/Acidobacteria* subdivisions (19 %) were the most prevalent. Only 5 % of the clones were Gram-positive, confirming the dominance of Gram negative species over Gram positive with respect of metal tolerance.

Microbial Ecology and Geomicrobiology at RFETS

Unfortunately, Site-specific data on the microbial ecology of RFETS do not exist, nor have studies been performed detailing specific geomicrobiological processes in the surface soils, subsurface material or surface waters. While it is tempting to extrapolate this information from studies conducted at nearby locations along the Front Range (e.g., Pawnee National Grasslands), such attempts would provide little in the way of irrefutable and defensible evidence regarding the role of microorganisms in actinide transport. Certainly, to develop a more complete description of transport pathways, a fundamental need of this program will be to perform a minimum assessment of the microbial ecology in both contaminated and uncontaminated locations at the

40

Site. The recent merging of molecular biology with microbial ecology has provided new and exciting techniques to probe the microbial complexity of soil and aquatic environments. They are now being used with ever increasing resolution to understand the relatedness of contaminants and indigenous populations.

241

TA-1.7 TECHNICAL APPENDIX SECTION TA-1 REFERENCES

Aerovironment. 1995. Rocky Flats Environmental Technology Site Historical Data Summary, Volume 1. Monrovia, CA: Aerovironment.

Babich, H. and G. Stotzky. 1985. Heavy Metal Toxicity to Microbe-mediated Ecologic Processes: a review and potential application to regulatory policies. Environ. Res. Vol. 36, p. 111.

Colorado Climate Center (CCC). 2001. Colorado Climate Center website. http://ccc.atmos.colostate.edu. Data queried on January 12, 2001.

Department of Energy (DOE). 1995. Rocky Flats Environmental Technology Site Environmental Report for 1994. Golden, CO: U.S. Department of Energy.

DOE. 1996. Rocky Flats Cleanup Agreement, Final. July 1996. Golden, CO: U.S. Department of Energy.

Duxbury, T. 1985. Ecological Aspects of Heavy Metal Responses in Microorganisms, in, Advances in Microbial Ecology. Vol. 8, pp. 185-235. Marshall, K. C. Eds. Plenum Press, New York.

EG&G Rocky Flats, Inc. (EG&G). 1991. Final Geologic Characterization Report for the U.S. Department of Energy Rocky Flats Plant. Golden, CO: EG&G Rocky Flats, Inc.

EG&G. 1993a. Background Geochemical Characterization Report. Rocky Flats Environmental Technology Site. Golden, CO.

EG&G. 1993b. Site Environmental Report for 1993, Rocky Flats Environmental Technology Site. Golden, CO: EG&G Rocky Flats, Inc.

EG&G. 1993c. Groundwater Recharge Study, Final Interim Report, Rocky Flats Plant. Golden, CO: EG&G Rocky Flats, Inc.

EG&G. 1994. Final Well Evaluation Report. Golden, CO: EG&G Rocky Flats, Inc.

EG&G. 1995a. Geochemical Characterization of Background Soils: Background Soils Characterization Program. Golden, CO: EG&G Rocky Flats, Inc.

EG&G. 1995b. Geologic Characterization Report for the Rocky Flats Environmental Technology Site, Final Report, Vol. I of the Sitewide Geoscience Characterization Study. Golden, CO: EG&G Rocky Flats, Inc.

42

EG&G. 1995c. Groundwater Geochemistry Report for the Rocky Flats Environmental Technology Site, Final Report, Vol. III of the Sitewide Geoscience Characterization Study. Golden, CO: EG&G Rocky Flats, Inc.

EG&G. 1995d. Hydrogeologic Characterization Report for the Rocky Flats Environmental Technology Site, Sitewide Geoscience Characterization Study, Vol. II. Golden, CO: EG&G Rocky Flats, Inc.

Federal Register. 2000. Federal Register, 2000, National Primary Drinking Water Regulations, Radionuclides; Final Rule, 40 CFR Parts 9, 141 and 142, Vol. 65, No. 236, pp. 766707 - 76753, December 7, 2000.

Fedors, R. and J.W. Warner. 1993. Characterization of Physical and Hydraulic Properties of Surficial Materials and Groundwater/Surface Water Interaction Study at Rocky Flats Plant. Golden, Colorado. Fort Collins, CO: Colorado State University.

Fetter, C.W. 1988. Applied Hydrogeology. Columbus, OH: Merrill Publishing Company.

Hanson, R.L. 1991. Evapotranspiration and Droughts. In Paulson, R.W., Chase, E.B., Roberts, R.S. and Moody, D.W., Compilers, National Water Summary 1988 – 89 – Hydrologic Events and Droughts: U.S. Geological Survey Water-Supply Paper 2375, pp. 99-104.

Hurr, R.T. 1976. Hydrology of a Nuclear-Processing Plant Site, Rocky Flats, Jefferson County, Colorado. U.S. Geological Survey Open-File Report 76-268. Denver, CO: U.S. Geological Survey.

Kaiser-Hill. 1996. Summaries of Natural Resource Protection and Management Issues at Rocky Flats Environmental Technology Site, Golden, CO. Golden, CO: Kaiser-Hill.

Kaiser-Hill. 1998. Conceptual Model for Actinide Migration Studies at the Rocky Flats Environmental Technology Site, Golden, CO. Golden, CO: Kaiser-Hill.

Kaiser-Hill. 1999. Rocky Flats Closure Project, Project Management Plan, Rev. 3. Golden, CO: Kaiser-Hill.

Kaiser-Hill. 2000a. Actinide Migration Evaluation for the Rocky Flats Environmental Technology Site, Fiscal Year 2001 Activities. Golden, CO: Kaiser-Hill.

Kaiser-Hill. 2000b. 1999. Annual Vegetation Report for the Rocky Flats Environmental Technology Site, Golden, CO. Golden, CO: Kaiser-Hill.

Kaiser-Hill. 2001. 2000. Annual Wildlife Survey for the Rocky Flats Environmental Technology Site, Golden, CO, June 2001. Golden, CO: Kaiser-Hill.

Murdock, M. 2002. Personal communication with Marcia Murdock, Rocky Flats Environmental Technology Site Biologist, February 21, 2002.

National Climate Data Center (NCDC). 2001. National Climate Data Center website. http://www.ncdc.noaa.gov. Data queried on January 4, 2001.

Robson, S.G. 1983. Alluvial and Bedrock Aquifers of the Denver Basin: Eastern Colorado's Dual Groundwater Resource: U.S. Geological Survey Water Supply Paper 2302.

Rocky Mountain Remediation Services (RMRS). 1996. Analysis of Vertical Contaminant Migration Potential, Final Report. RF-ER-96-0040.UN. Golden, CO: RMRS.

RMRS. 1997. Summary of Existing Data on Actinide Migration at the Rocky Flats Environmental Technology Site. RF/RMRS-97-074.UN. Golden, CO: Rocky Mountain Remediation Services.

RMRS. 1998. Loading Analysis for the Actinide Migration Studies at the Rocky Flats Environmental Technology Site. Golden, CO: Rocky Mountain Remediation Services.

RMRS. 1999. 1998. Annual Rocky Flats Cleanup Agreement (RFCA) Groundwater Monitoring Report for the Rocky Flats Environmental Technology Site. RF/RMRS-99-433.UN. Golden, CO: Rocky Mountain Remediation Services.

Puers, C. and S. Selenska-Pobell. 1998. Investigation of Bacterial Diversity in a Soil Sample of Depleted Uranium Mining area nearby Johanngeorgenstadt, Saxonia, via 16S-RDNA-Sequence Analysis/ Abstracts of Euroconference on Bacteria-Metal/ Radionuclide Interaction: Basic Research and Biorem.

Spencer, F.D. 1961. Bedrock Geology of the Lousiville Quadrangle, Colorado. USGS. Geological Quadrangle Map GQ-151. Denver, CO: U.S. Geological Survey.

Shroba, R.R. and P.E. Carrara. 1994. Preliminary Surficial Geologic Map of the Rocky Flats Plant and Vicinity, Jefferson and Boulder Counties, Colorado. USGS Open File Report 94-162. Denver, CO: U.S. Geological Survey.

Suzuki, Y. and J.F. Banfield. 1999. Geomicrobiology of Uranium. In: Uranium: Mineralogy, Geochemistry and the Environment. P. C. Burns and R. Finch, eds. Mineralogical Society of America, Wash. D.C. pp. 393-432.

Wright Water Engineers (WWE). 1995. Site-Wide Water Balance Study Task 8, Final Deliverable Technical Guidance Relating to Water Rights. Rocky Flats Environmental Technology Site, Golden, CO.

44

Figure TA-1-1. Potential Actinide Transport Pathways at RFETS – Conceptual Model Diagram.

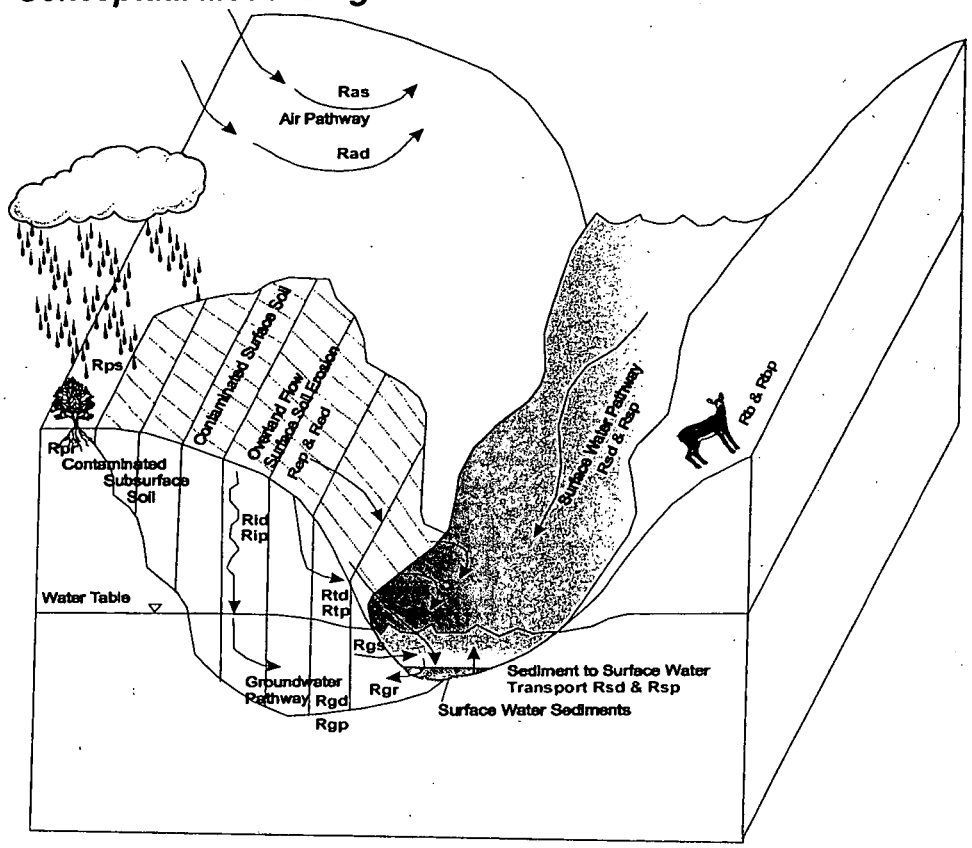

Actinide Transport Rate Coefficients:

(Source: Kaiser-Hill, 1998)

R =	rate of actinide transport in medium (subscripts indicate transport mechanism)
Ras =	air suspension
Rad =	air deposition
Rb =	bio-uptake
Rbp =	biotransport (including bioturbation and biopedal transport)
Rep =	soil erosion and overland flow particulate/colloid transport
Red =	soil erosion and overland flow dissolved transport
Rip =	infiltration particulate/colloid transport
Rgd =	groundwater dissolved transport
Rgp =	groundwater particulate / colloid transport
Rgs =	groundwater discharge
Rgr =	groundwater recharge
Rpr =	vegetation root uptake
Rps =	raindrop splash
Rsp =	surface water particulate / colloid transport
Rsd =	sediment to surface water dissolved transport
Rtp =	particulate vadose zone transport (subsurface storm flow)
Rtd =	dissolved vadose zone transport (subsurface storm flow)

45

Figure TA-1-3. Monthly Average Precipitation at RFETS

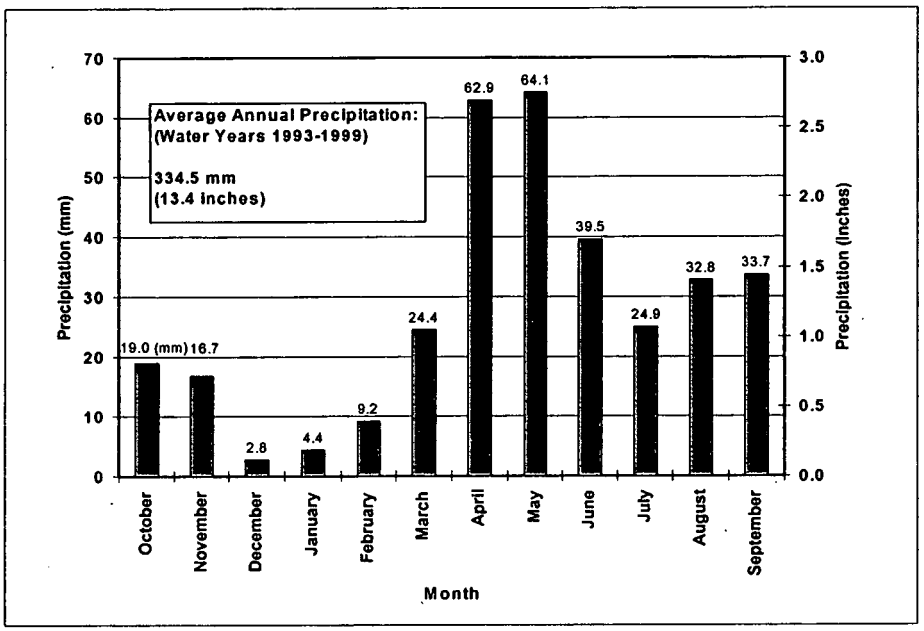

Figure TA-1-4. Correlation of RFETS Monthly Precipitation with Regional Data - for Water Years 1997 - 1999

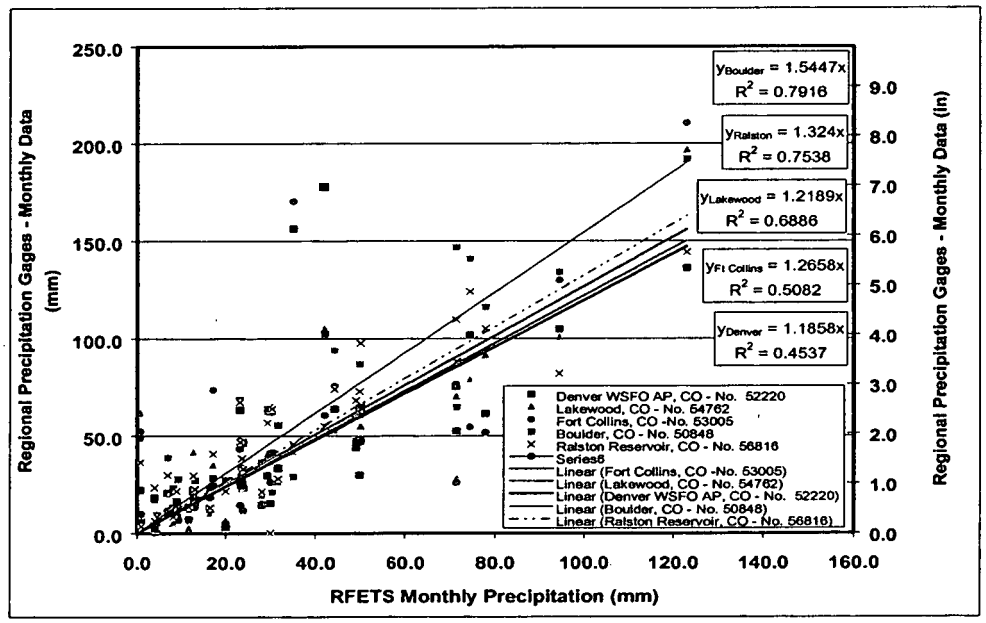

47

Figure TA-1-5. Precipitation at Boulder Station 50848 – Cumulative Departure of Water Years 1997 – 1997 from Monthly Normals

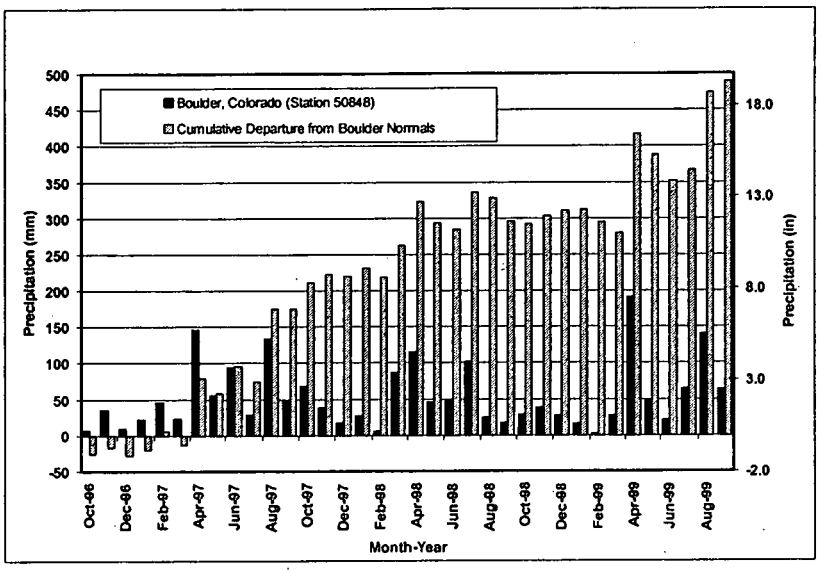

Figure TA-1-6. Mean Wind Speed and Direction Distribution at RFETS (1999)

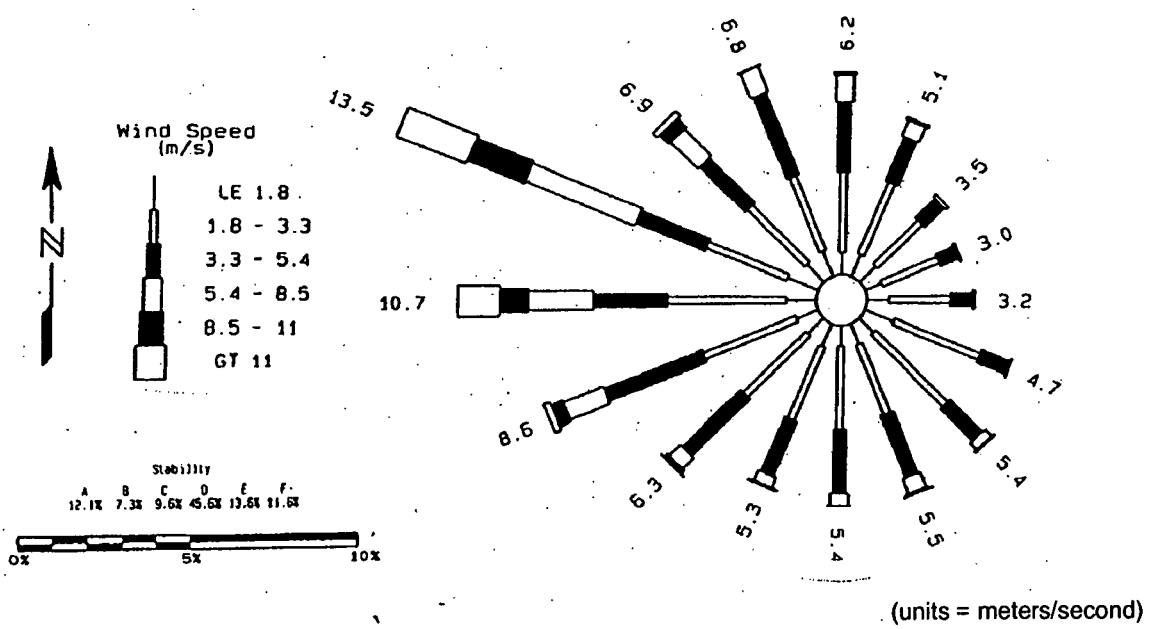

48

Figure TA- 1-9. Generalized Stratigraphic Column for the RFETS Area

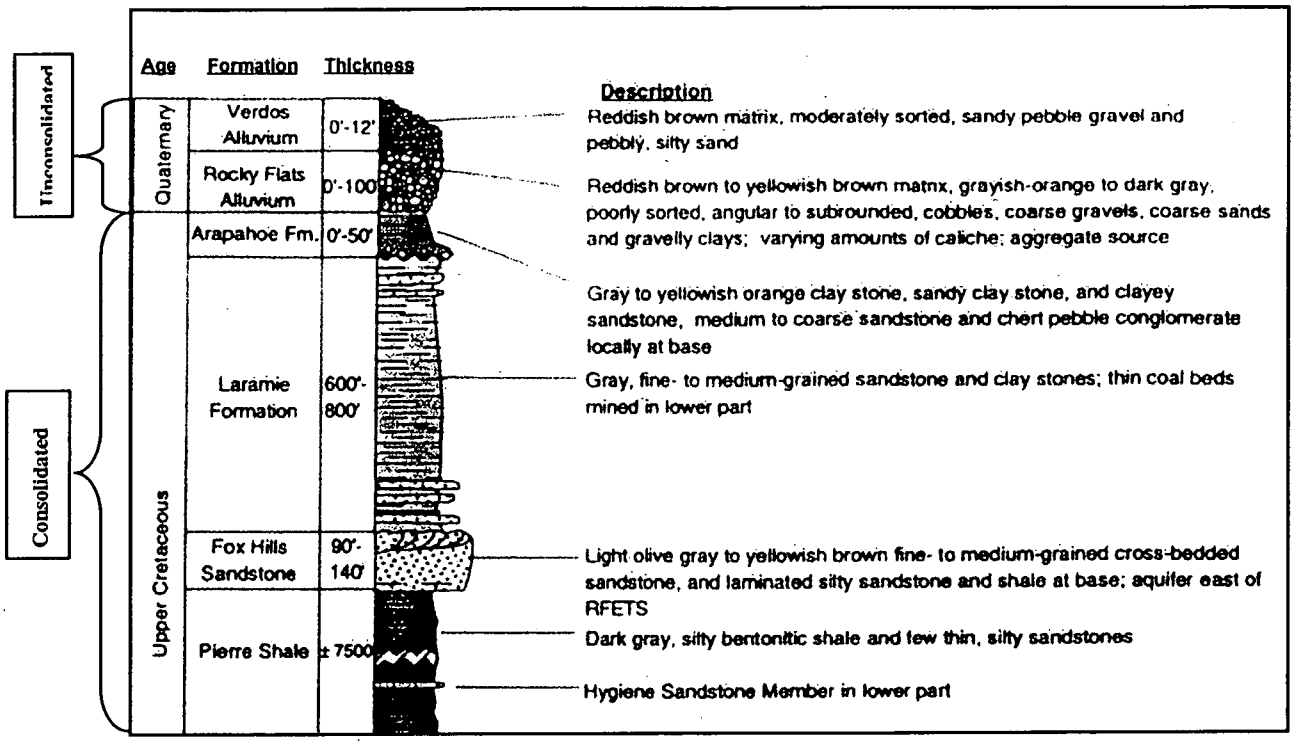

Source: Geologic Characterization Report for the RFETS, Volume 1, March 1995 (EG&G, 1995b)

51

Figure TA-1-10. Generalized Geologic Cross-Section of the Front Range and the RFETS Area

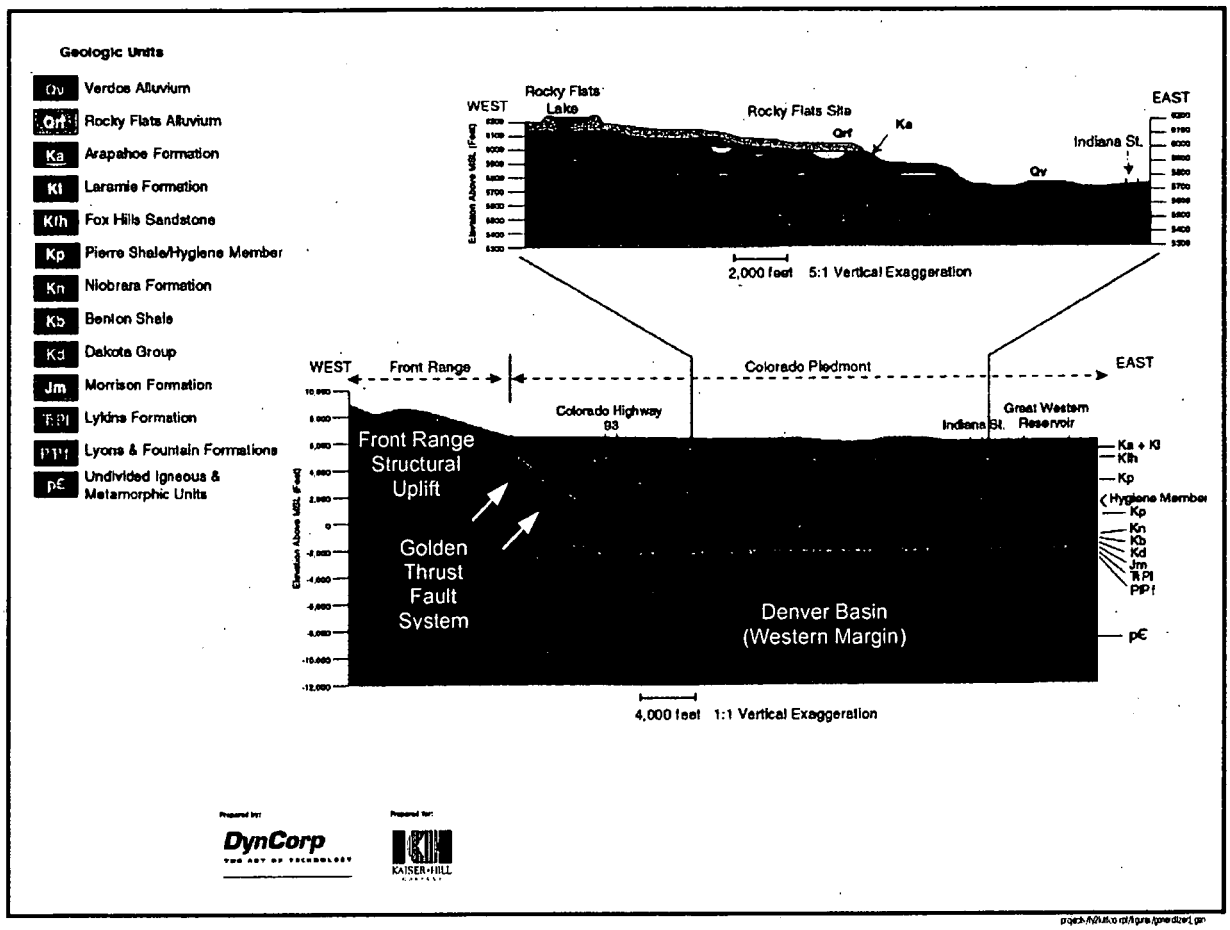

Source: Geologic Characterization Report for the RFETS, Volume 1, March 1995 (EG&G, 1995b)

52

SECTION TA-2 - TABLE OF CONTENTS

TA-2 MEASURED ACTINIDE CONCENTRATIONS IN THE ENVIRONMENT AT RFETS 2-1

TA-2.1 RFETS Actinide Data Sources 2-2
TA-2.1.1 Background Actinide Concentrations 2-2
TA-2.1.2 Soil and Water Database Actinide Data 2-4
TA-2.1.3 Other Actinide Data Not Stored in the Soil and Water Database 2-6

TA-2.2 Locations of Actinide Sources 2-8
TA-2.2.1 Process Used To Identify Actinide Sources 2-8
TA-2.2.2 Actinide Source Maps 2-21

TA-2.3 Surface Soil Actinide Concentrations 2-21
TA-2.3.1 Background Surface Soil Actinide Concentrations 2-21
TA-2.3.2 RFCA Action Levels 2-22
TA-2.3.3 RFETS Surface Soil Actinide Figures 2-23
TA-2.3.4 Surface Soil Data Query Process 2-25
TA-2.3.5 Surface Soil Data Description 2-25
TA-2.3.6 Geostatistical Analyses of Surface Soil Samples 2-27

TA-2.4 Sub-Surface Soil Actinide Concentrations 2-37
TA-2.4.1 Background Sub-Surface Soil Actinide Concentrations 2-37
TA-2.4.2 RFCA Action Levels for Sub-Surface Soils 2-37
TA-2.4.3 RFETS Sub-Surface Soil Actinide Figures 2-38
TA-2.4.4 Sub-Surface Soil Data Query Process 2-39
TA-2.4.5 Sub-Surface Soil Data Description 2-40

TA-2.5 Sediment Actinide Concentrations 2-41
TA-2.5.1 Background Sediment Actinide Concentrations 2-41
TA-2.5.2 RFCA Action Levels 2-42
TA-2.5.3 RFETS Sediment Actinide Figures 2-42

TA-2.5.4 Sediment Data Query Process 2-43
TA-2.5.5 Sediment Data Description 2-44

TA-2.6 Building Material Actinide Concentrations 2-45
TA-2.6.1 Background Building Material Actinide Concentrations 2-45
TA-2.6.2 Underground Building Contamination Analysis 2-48

TA-2.7 Surface Water Actinide Concentrations 2-51
TA-2.7.1 Background Surface Water Actinide Concentrations 2-51
TA-2.7.2 RFCA Action Levels 2-52
TA-2.7.3 RFETS Surface Water Actinide Figures 2-52
TA-2.7.4 Surface Water Data Query Process 2-54
TA-2.7.5 Surface Water Data Description 2-55

TA-2.8 Ground Water Actinide Concentrations 2-60
TA-2.8.1 Background Groundwater Actinide Concentrations 2-60
TA-2.8.2 RFCA Action Levels 2-62
TA-2.8.3 RFETS Groundwater Actinide Figures 2-63
TA-2.8.4 Groundwater Data Query and Refinement Process 2-64
TA-2.8.5 Groundwater Data Description 2-65

TA-2.9 Air Actinide Concentrations 2-71
TA-2.9.1 Background and Baseline Air Actinide Concentrations 2-71
TA-2.9.2 Air Regulatory Standards 2-76
TA-2.9.3 Air Data Acquisition Figures 2-78
TA-2.9.4 Air Data Acquisition Process 2-78

TA-2.10 Biota Actinide Concentrations 2-79
TA-2.10.1General Observations in Biota 2-79

TA-2.11 Technical Appendix Section TA-2 References 2-81

SECTION TA-2 TABLES

Table TA-2-1. Analytical Data Verification and Validation Qualifiers 2-6
Table TA-2-2. Table of Actinide Sources 2-11
Table TA-2-3. Actinide Source Locations With Associated Surface and Sub-Surface Soil Data (Sample Page) 2-20
Table TA-2-4. Background Surface Soil Actinide Concentrations 2-22
Table TA-2-5. RFCA Surface Soil Action Levels 2-23
Table TA-2-6. Summary Statistics for Surface Soil Data Set 2-26
Table TA-2-7. Selected Variogram Models 2-32
Table TA-2-8. Estimated Areas for Actinide Concentrations in Surface Soils – Based on Kriging Analysis 2-36
Table TA-2-9. Background Sub-Surface Soil Actinide Concentrations 2-37
Table TA-2-10. RFCA Sub-Surface Soil Action Levels 2-38
Table TA-2-11. Table of Sub-Surface Soil Maps 2-39
Table TA-2-12. Summary Statistics for Sub-Surface Soil Data Set 2-41
Table TA-2-13. Background Sediment Actinide Concentrations 2-41
Table TA-2-14. RFCA Sediment Action Levels 2-42
Table TA-2-15. Summary Statistics for Sediment Data Set 2-44
Table TA-2-16. Combined Total Surface Activity Data Summary 2-46
Table TA-2-17. Building 771 UBC Sampling Specifications and Rationale 2-49
Table TA-2-18. Building 771 UBC, Soil Sampling Results 2-50
Table TA-2-19. Building 771 UBC, Groundwater Sampling Results 2-50
Table TA-2-20. Background Surface Water Actinide Concentrations 2-51
Table TA-2-21. RFCA Surface Water Action Levels 2-52
Table TA-2-22. Summary Statistics for Surface Water Actinide Data Set 2-56
Table TA-2-23. Alpha Spectrometry and ICP/MS Detection Limit Range 2-61
Table TA-2-24. Background Groundwater Actinide Concentrations 2-62
Table TA-2-25. RFCA Groundwater Action Levels 2-63
Table TA-2-26. Summary Statistics for Groundwater Actinide Data (1991-1999) 2-67

61

Table TA-2-27. Average Annual Air Concentrations, Pu-239/240 and Am-241 2-74
Table TA-2-28. Average Annual Air Concentrations, U-234, U-235 and U-238 2-75
Table TA-2-29. Boundary Values of Annual Average Ambient Air Concentrations, 1997-1999 2-76
Table TA-2-30. Compliance Concentration Levels from 40 CFR 61, Table 2 2-77

SECTION TA-2 FIGURES

Figure TA-2-1. Actinide Sources – Entire Site 2-85
Figure TA-2-2. Actinide Sources – Industrial Area 2-86
Figure TA-2-3. Pu-239/240 Activity in Surface Soils 2-87
Figure TA-2-4. Am-241 Activity in Surface Soils 2-88
Figure TA-2-5. U-233/234 Activity in Surface Soils 2-89
Figure TA-2-6. U-235 Activity in Surface Soils 2-90
Figure TA-2-7. U-238 Activity in Surface Soils 2-91
Figure TA-2-8. Pu-239/240 Activity in Surface Soils, Kriged Isoplot 2-92
Figure TA-2-9. Am-241 Activity in Surface Soils, Kriged Isoplot 2-93
Figure TA-2-10. U-233/234 Activity in Surface Soils, Kriged Isoplot 2-94
Figure TA-2-11. U-235 Activity in Surface Soils, Kriged Isoplot 2-95
Figure TA-2-12. U-238 Activity in Surface Soils, Kriged Isoplot 2-96
Figure TA-2-13. Site Area Variograms for Pu-239/240 2-97
Figure TA-2-14. Site Area Variograms for Am-241 2-98
Figure TA-2-15. Site Area Variograms for U-233/234 2-99
Figure TA-2-16. Site Area Variograms for U-235 2-100
Figure TA-2-17. Site Area Variograms for U-238 2-101
Figure TA-2-18. Pu-239/240 Activity in Subsurface Soils, Depth 0.5 to 2 Feet 2-102
Figure TA-2-19. Pu-239/240 Activity in Subsurface Soils, Depth 2 to 4 Feet 2-103
Figure TA-2-20. Pu-239/240 Activity in Subsurface Soils, Depth 4 to 6 Feet 2-104
Figure TA-2-21. Pu-239/240 Activity in Subsurface Soils, Depth 6 to 8 Feet 2-105

Figure TA-2-22. Pu-239/240 Activity in Subsurface Soils, Depth 8 to 10 Feet 2-106
Figure TA-2-23. Pu-239/240 Activity in Subsurface Soils, Depth Greater Than 10 Feet 2-107
Figure TA-2-24. Am-241 Activity in Subsurface Soils, Depth 0.5 to 2 Feet 2-108
Figure TA-2-25. Am-241 Activity in Subsurface Soils, Depth 2 to 4 Feet 2-109
Figure TA-2-26. Am-241 Activity in Subsurface Soils, Depth 4 to 6 Feet 2-110
Figure TA-2-27. Am-241 Activity in Subsurface Soils, Depth 6 to 8 Feet 2-111
Figure TA-2-28. Am-241 Activity in Subsurface Soils, Depth 8 to 10 Feet 2-112
Figure TA-2-29. Am-241 Activity in Subsurface Soils, Depth Greater Than 10 Feet 2-113
Figure TA-2-30. U-233/234 Activity in Subsurface Soils, Depth 0.5 to 2 Feet 2-114
Figure TA-2-31. U-233/234 Activity in Subsurface Soils, Depth 2 to 4 Feet 2-115
Figure TA-2-32. U-233/234 Activity in Subsurface Soils, Depth 4 to 6 Feet 2-116
Figure TA-2-33. U-233/234 Activity in Subsurface Soils, Depth 6 to 8 Feet 2-117
Figure TA-2-34. U-233/234 Activity in Subsurface Soils, Depth 8 to 10 Feet 2-118
Figure TA-2-35. U-233/234 Activity in Subsurface Soils, Depth Greater Than 10 Feet 2-119
Figure TA-2-36. U-235 Activity in Subsurface Soils, Depth 0.5 to 2 Feet 2-120
Figure TA-2-37. U-235 Activity in Subsurface Soils, Depth 2 to 4 Feet 2-121
Figure TA-2-38. U-235 Activity in Subsurface Soils, Depth 4 to 6 Feet 2-122
Figure TA-2-39. U-235 Activity in Subsurface Soils, Depth 6 to 8 Feet 2-123
Figure TA-2-40. U-235 Activity in Subsurface Soils, Depth 8 to 10 Feet 2-124
Figure TA-2-41. U-235 Activity in Subsurface Soils, Depth Greater Than 10 Feet 2-125
Figure TA-2-42. U-238 Activity in Subsurface Soils, Depth 0.5 to 2 Feet 2-126
Figure TA-2-43. U-238 Activity in Subsurface Soils, Depth 2 to 4 Feet 2-127
Figure TA-2-44. U-238 Activity in Subsurface Soils, Depth 4 to 6 Feet 2-128
Figure TA-2-45. U-238 Activity in Subsurface Soils, Depth 6 to 8 Feet 2-129
Figure TA-2-46. U-238 Activity in Subsurface Soils, Depth 8 to 10 Feet 2-130
Figure TA-2-47. U-238 Activity in Subsurface Soils, Depth Greater Than 10 Feet 2-131
Figure TA-2-48. Pu-239/240 Activity in Sediments 2-132
Figure TA-2-49. Am-241 Activity in Sediments 2-133
Figure TA-2-50. U-233/234 Activity in Sediments 2-134
Figure TA-2-51. U-235 Activity in Sediments 2-135

63

Figure TA-2-52. U-238 Activity in Sediments 2-136
Figure TA-2-53. Pu-239/240 Activity in Surface Water -
Pu-239/240 Load, Water Yield and Pu-239/240 Concentrations 2-137
Figure TA-2-54. Am-241 Activity in Surface Water -
Am-241 Load, Water Yield and Am-241 Concentrations 2-138
Figure TA-2-55. U-233/234 Activity in Surface Water -
U-233/234 Load, Water Yield and U-233/234 Concentrations 2-139
Figure TA-2-56. U-235 Activity in Surface Water -
U-235 Load, Water Yield and U-235 Concentrations 2-140
Figure TA-2-57. U-238 Activity in Surface Water -
U-238 Load, Water Yield and U-238 Concentrations 2-141
Figure TA-2-58. Monitoring Station GS10 2-142
Figure TA-2-59. Example of Hydrograph Showing Rising-Limb Flow-Paced Composite
Sampling 2-143
Figure TA-2-60. Unfiltered UHSU Pu-239/240 in Groundwater, 1991-1999 (Average) 2-144
Figure TA-2-61. Unfiltered UHSU Pu-239/240 in Groundwater, 1991-1999 (Average) 2-145
Figure TA-2-62. Unfiltered UHSU Am-241 in Groundwater, 1991-1999 (Average) 2-146
Figure TA-2-63. Unfiltered UHSU Am-241 in Groundwater, 1991-1999 (Average) 2-147
Figure TA-2-64. Filtered UHSU U-233/234 in Groundwater, 1991-1999 (Average) 2-148
Figure TA-2-65. Filtered UHSU U-233/234 in Groundwater, 1991-1999 (Average) 2-149
Figure TA-2-66. Filtered UHSU U-235 in Groundwater, 1991-1999 (Average) 2-150
Figure TA-2-67. Filtered UHSU U-235 in Groundwater, 1991-1999 (Average) 2-151
Figure TA-2-68. Filtered UHSU U-233/234 in Groundwater, 1991-1999 (Average) 2-152
Figure TA-2-69. Filtered UHSU U-238 in Groundwater, 1991-1999 (Average) 2-153
Figure TA-2-70. Unfiltered LHSU Pu-239/240 in Groundwater, 1991-1999 (Average) 2-154
Figure TA-2-71. Unfiltered LHSU Am-241 in Groundwater, 1991-1999 (Average) 2-155
Figure TA-2-72. Filtered LHSU U-233/234 in Groundwater, 1991-1999 (Average) 2-156
Figure TA-2-73. Filtered LHSU U-235 in Groundwater, 1991-1999 (Average) 2-157
Figure TA-2-74. Filtered LHSU U-238 in Groundwater, 1991-1999 (Average) 2-158
Figure TA-2-75. Groundwater Basins and Divides for Permeable Units of the UHSU 2-159

64

Figure TA-2-76. Groundwater Basins and Divides for Permeable Units of the UHSU (Industrial Area) 2-160
Figure TA-2-77. RAAMP Sampler Locations 2-161
Figure TA-2-78. Average Actinide Concentrations in Air at RFETS Perimeter, 1997 –1999 2-162
Figure TA-2-79. Expanded View of RAAMP Sampler 2-163
Figure TA-2-80. RAAMP Sampler (foreground) Near 903 Pad 2-164

65

This page intentionally left blank.

66

TA-2 MEASURED ACTINIDE CONCENTRATIONS IN THE ENVIRONMENT AT RFETS

This section presents actinide data measured in environmental media at RFETS. For each media, measured data are presented for Pu-239/240, Am-241, U-233/234, U-235 and U-238. The media include:

- Surface soil;
- Sub-surface soil;
- Sediments;
- Building materials (exposed to the environment);
- Surface water;
- Groundwater;
- Air; and
- Biota.

Actinides occur in the environment at RFETS as either "background" material, or as material released during operations at the Site. Pu and Am background concentrations exist because of global fallout from historic atmospheric nuclear testing. In the case of U, background quantities also occur naturally in the soil and underlying geologic material. Therefore, background levels of actinides for each of the environmental media studied in this report provide an important reference to distinguish between actinides present in the environment at RFETS because of historic Site operations versus actinides that exist because of sources *not* related to historic Site operations.

The bulk of information on actinides measured in environmental media at RFETS is presented in the Figures at the end of Section TA-2. Text supporting these data compilation is organized in the following manner:

- Section TA-2.1 provides descriptions of the actinide data sources. Subjects addressed include background actinide levels for environmental media at RFETS, the RFETS Soil and Water Database (SWD) and environmental actinide data not stored in the SWD;

- Section TA-2.2 summarizes actinide source data at RFETS. The data were obtained from a review of the collection of Historical Release Report (HRR) documents (DOE, 1992; DOE, 1993; DOE, 1994; DOE, 1995a; Kaiser-Hill, 1996; Kaiser-Hill, 1997; Kaiser-Hill, 1998a; Kaiser-Hill, 1999). The actinide sources are shown in a table and on two maps. Surface water drainage basins and surface water monitoring stations are shown on the actinide source maps to facilitate data analyses presented in later sections of this report. A third table relates individual actinide sources with actinide concentrations in surface and sub-surface soil sampling locations associated with the source;

- Sections TA-2.3 through TA-2.7 present media-specific actinide data measurements and information compiled from the SWD. Each section contains a summary of the sample collection methods used and a discussion of the electronic queries applied to the SWD. For surface soil, sub-surface soil and sediments, data are portrayed in a series of media-specific Site figures which show the location, concentration and frequency distribution of data gathered plus background actinide levels and RFCA Tier I and Tier II Action Levels for reference; and

- Surface water data are presented as actinide concentrations, water yields and the resulting actinide loads at eight RFCA monitoring stations located at the Site. Surface water drainage basins and surface water monitoring stations are delineated on all actinide data figures to facilitate the surface water actinide transport analysis presented later in this report.

TA-2.1 RFETS ACTINIDE DATA SOURCES

TA-2.1.1 Background Actinide Concentrations

The Background Geochemical Characterization Program was conducted from 1989 to 1993 to assess the chemistry of environmental materials in areas near RFETS that remained undisturbed

68

by historic Site operations (EG&G, 1993). The *Background Geochemical Characterization Report* (EG&G, 1993) and the *Geochemical Characterization of Background Surface Soils: Background Soils Characterization Program* report (EG&G, 1995) were the main sources of background data referenced for this actinide pathway study.

The *Background Geochemical Characterization Report* addresses five environmental media, including: surface soil; sub-surface soil (or borehole material); stream sediment; surface water and, groundwater (EG&G, 1993). The *Geochemical Characterization of Background Surface Soils: Background Soils Characterization Program* report specifically addresses surface soils (EG&G, 1995).

Background locations were characterized by analyzing environmental media collected at a number of sampling sites. The resulting chemical data were statistically summarized to provide a basis for comparison with chemical results from non-background areas at RFETS. As described in the *Background Geochemical Characterization Report,* an independent subcontractor validated the laboratory analysis data. Quality control checks were run routinely during the data-entry process to ensure data reliability (EG&G, 1993). Quality control data such as rinsates, blanks and spikes were excluded from the working data set. All rejected data were excluded from statistical and geochemical analyses.

Non-detects greater than two times the minimum reporting limits were omitted from statistical analysis and the remaining non-detects were replaced with one-half the detection limit. Details of the statistical analyses are provided in the *Background Geochemical Characterization Report* (EG&G, 1993).

With respect to specific media, the geochemical data were categorized into subgroups by the geologic unit, flow system, or location. Groundwater and geologic material (borehole) samples were collected and grouped into geologic units: Rocky Flats alluvium (RFA), valley-fill alluvium (VFA), colluvium (COL), weathered claystone of upper Arapahoe/Laramie Formations (WCS) and unweathered, undifferentiated Arapahoe/Laramie Formation (KAR). These data were grouped into upper (RFA+VFA+COL+WCS) and lower (KAR) flow systems for chemical

69

comparison. The upper flow system is largely a calcium bicarbonate type and the mean concentrations of the radionuclides and water quality parameters showed significant differences among the geologic units (EG&G, 1993).

Background data for each media are provided in Sections TA-2.3 through TA-2.10.

TA-2.1.2 Soil and Water Database Actinide Data

The majority of the data presented in this report are stored in the RFETS SWD. Data used in this report and not stored in SWD are described in Section TA-2.1.3. SWD contains over three million environmental data records for surface soil, sub-surface soil, sediment, groundwater and surface water samples collected since approximately 1990 (Kaiser-Hill, 2000a). SWD also contains results of some waste container and tank sampling at RFETS well as data generated as part of non-environmental sampling programs.

All analytical data generated in accordance with the Standard Services and Radiochemistry Parameter Specific Analytical (PSA) Modules contained in a contracted laboratory's Statement of Work are subject to data assessment (Kaiser-Hill, 2000a). Data assessment is a generic term for a quality assurance evaluation of analytical chemistry data. This assessment involves:

- An initial review of the data package by the contracted laboratory performing the analysis;
- A cursory examination of the data by RFETS Analytical Services Division (ASD) personnel prior to customer release of preliminary data;
- Verification that ranges from a cursory completeness check and quality control verification of the Data Review Checklist to a more thorough check of the data; and
- Validation by ASD or subcontractor personnel of the hard-copy deliverable for results of sample analyses, otherwise known as the data package.

The nature and extent of the verification and validation activities are based upon program and customer specifications and ASD requirements to evaluate contractor laboratory performance

70

against the laboratory's Statement of Work. Verification is a graded assessment process to ensure that data meet certain specified criteria. It involves assessing both the compliance of the data package with the Statement of Work and acceptability of the data, using PSA Module verification and validation guidelines. Verification ranges from a cursory check of the Data Review Checklist to a more thorough review of the data, up to and including the assignment of data qualifiers. Verification may indicate that the data package requires validation (Kaiser-Hill, 2000a).

Validation is a more thorough assessment process than verification. Validation criteria for isotopic analyses of actinides are based on specifications detailed in the contracted laboratory's Statement of Work. Validation involves the inspection of data package contents for compliance with the contracted analytical laboratory's Statement of Work and validity of the data, using PSA Module verification and validation guidelines. Validation usually includes examination of raw data and calculations.

Descriptions of the validation criteria applied to determine data acceptance for inclusion in this report are provided in the relevant sub-sections for the different environmental media. Verification and validation qualifier nomenclature is presented in Table TA-2-1. More detailed information on verification and validation of RFETS isotopic actinide analytical data are dependent on the analytical method used. For alpha spectrometry, the analytical method used for much of the data presented in this report, the data assessment guidelines are contained in the Site procedure *Statement of Work for Analytical Measurements, Isotopic Determinations by Alpha Spectrometry* (Kaiser-Hill, 1998b).

11

Table TA-2-1. Analytical Data Verification and Validation Qualifiers

Data Qualifier	Description
V	Problems with the data were not observed at the indicated review level. All data that meet validation criteria ("V" data) are assigned a Validation Reason Code that provides further information on data quality issues, if any, raised during the validation process.
J	The associated value is an estimated quantity.
JB	Result qualified due to blank contamination for results below the RDL.
U	The associated value is considered undetected at an elevated level of detection.
NJ	The associated value is presumptively estimated.
UJ	The associated value is considered estimated at an elevated level of detection.
R	The data are unusable (Note: analyte may or may not be present).

Source: Kaiser-Hill, 2000a.

TA-2.1.3 Other Actinide Data Not Stored in the Soil and Water Database

The majority of environmental media data presented in this report were extracted directly from the SWD described above in the fall of 2000. However, the data sets described below are presented in this report but were not archived in SWD at the time the data queries were performed. Since these data did not come directly from the SWD, they are included on the CD-ROM at the back of this Technical Appendix.

12

Sediment data in lower Walnut Creek, east of the detention pond system and west of the Site boundary at Indiana Street, were not stored in SWD when the sediment data queries were made (September, 2000). These data, presented in Section TA-2.5, were previously reported in *Progress Report #2 to the Source Evaluation and Preliminary Mitigation Plan for Walnut Creek* (Rocky Mountain Remediation Services [RMRS], 1998). The process to add these data to the SWD has since been initiated (Dunstan, 2000).

- Results from individual surface water samples, including composited samples described in Section TA-2.7.4, are stored in SWD. Average annual actinide concentrations, actinide loads and water yields presented in Section TA-2.7 are not stored in SWD. These values were calculated from data sets stored and maintained by the Kaiser-Hill Environmental Media Management organization;

- Sum-of-Ratios data reflect the combined total activity of Pu-239/240, Am-241, U-2333/234, U-235 and U-238 and their relationship to RFCA surface soil Action Levels discussed. The Sum-of-Ratios data were calculated from the same SWD data sub-sets used to produce the surface soil actinide maps described in TA-2.3.3. Sum-of Ratios maps and text were contributed to this report later than other data sets and are therefore described and presented as an attachment to this Technical Appendix (Attachment A). Future versions of this Technical Appendix will integrate the Sum-of-Ratios data and maps into the main body of the document; and

- Detailed information on uses of U within Site buildings is presented in Attachment B to this Technical Appendix. The U information was contributed to this report later than other data sets. Future versions of this Technical Appendix may integrate this specific U data into the main body of the document.

It should be recognized that the data described in Sections TA-2.1.2 and TA-2.1.3 are from multiple, previously established Site data sets and from other data sets compiled for the purposes of this study. These data sets were not all created using the same criteria for data acceptability.

If standardized data sets are ultimately established and accepted for each of the environmental media at the Site, then future versions of this report would utilize these data.

TA-2.2 LOCATIONS OF ACTINIDE SOURCES

TA-2.2.1 Process Used To Identify Actinide Sources

Formal efforts to document the extent of Site contamination were established with the signing of the Interagency Agreement (IAG) in 1991. At that time, Solid Waste Management Units (SWMUs), initially identified in 1985 by the DOE Los Alamos Operations Office, were re-named as Individual Hazardous Substance Sites (IHSSs) (Kaiser-Hill, 2000b). IHSS is a term defined under CERCLA and the IAG as "locations associated with a release or threat of release of hazardous substances that may cause harm to human health/or the environment." It should be noted that the IHSS locations involve a wide range of contaminants that are *not* limited to actinides and, therefore, the actinide sources are a subset of all the sources identified on the Site.

In accordance with the IAG, a Historical Release Report (HRR) was developed. The original intent of the HRR was to capture existing information on historical incidents and plant practices involving hazardous substances at RFETS. Additionally, the IAG required that the HRR reporting process continue quarterly for reporting of new or newly identified releases of hazardous substances to the environment (now identified as Potential Areas of Concern or PACs) (Kaiser-Hill, 2000b). Following the signing of RFCA in 1996, the earlier IAG requirements for updating the HRR were continued. However, it was agreed that reporting would be required on an annual basis instead of quarterly.

For purposes of the HRR process and mapping clarity, original IHSSs were designated a unique "PAC Area" prefix number based on the location within 14 geographic sub-divisions at the Site. For example, IHSS 123.1, located in the 700 Area of the Site, is designated as PAC 700-123.1. An area where there has been a post-1992 release or finding of a hazardous substance in the environment is also assigned a PAC area prefix number followed by the next numerically higher PAC reference number for that area. The areas referred to as PACs are equivalent to IHSSs in

14

terms of being CERCLA sites requiring management through the HRR and CERCLA reporting process. Large PAC areas (i.e., PACS which cross geographic PAC boundaries) such as the Original Process Waste Lines (OPWL; PAC#000-121) have been assigned a 000 prefix due to their boundary extent (Kaiser-Hill, 2000b).

In addition to the IHSSs, potential Under Building Contamination (UBC) sites were also discussed in the original HRR (DOE, 1992). UBC location designations were necessary due to the potential contamination under specific buildings from broken process waste lines or other potential sources related to the historic operations in a particular building (Kaiser-Hill, 2000b).

A subset of the sites identified in the HRR was developed for this report that contains actinide sources only. The HRR documents and corresponding maps dating from 1992 through 1999 were carefully reviewed to identify potential actinide sources (DOE, 1992; DOE, 1993; DOE, 1994; DOE, 1995a; Kaiser-Hill, 1996; Kaiser-Hill, 1997; Kaiser-Hill, 1998a; Kaiser-Hill, 1999). Personnel from the Kaiser-Hill Environmental Remediation organization were consulted during the data review process to confirm that the appropriate resources for Site information were being utilized. Data from the review was entered into a Microsoft® Excel spreadsheet. The spreadsheet contains columns for the IHSS, Operable Unit (OU) and PAC designations (Table TA-2-2) and continues with the source description (unit name), actinide type and the HRR in which the source was originally identified. Finally, the status of each IHSS, including update information from the HRR and Proposed No Further Action (NFA) or Recommended NFA designation was entered. References in the HRR were double-checked to ensure all the sources were accounted for and entered correctly into the database. The spreadsheet (Table TA-2-2) was sorted into the following five categories:

- Active actinide sites. Site in this category are under consideration for future remedial action, which might include a further action determination;
- UBC locations;
- Proposed NFA sites;

15

- Potential Incidents of Concern (PIC); PIC locations, which were referenced in the earlier versions of the HRR and included in the database, are not included in the table. PICs were locations determined by DOE and the regulatory agencies in the mid-1990's to not warrant further action; and

- Recommended NFA sites. NFA sites are those locations where no further remedial action is warranted as determined by DOE and the regulatory agencies. However, final, approved NFA status cannot be granted until the Final Record of Decision for the Site is approved. NFA determinations are documented in the HRR.

An additional table was created to link SWD actinide data from surface soils and sub-surface soils, presented later in Section TA-2, to IHSS and UBC locations. A sample page from the table is shown in Table TA-2-3. Actinide concentration values in the table are color-coded according to the color scheme used on the figures. The complete color-coded table with all of the source locations and all of the environmental media actinide data associated with the sources is approximately 70 pages long. The entire color-coded table is on the CD-ROM included with this Technical Appendix.

Table TA-2-2. Table of Actinide Sources

IHSS	OU	PAC	Description (Unit Name)	Actinide Type	Info. Source	Updated	Proposed NFA	Recommen. NFA
Active Source Locations								
101	IA	000-101	207 Solar Evaporation Ponds	Pu, U	HRR	Quarterly 9, Quarterly 11, Annual 1998	N/A	N/A
116.1	IA	400-116.1	West Loading Dock, Building 447 (IAG Name: West Loading Dock Area)	U235, U238	HRR		N/A	N/A
116.2	IA	400-116.2	South Loading Dock, Building 444 (IAG Name: South Loading Dock Area)	U235, U238	HRR		N/A	N/A
117.1	IA	500-117.1	North Site Chemical Storage	U	HRR		N/A	N/A
120.1	IA	600-120.1	Fiberglassing Area North of Building 664	Pu, Am, U	HRR		N/A	N/A
120.2	IA	600-120.2	Fiberglassing Area West of Building 664	Am, U, Pu	HRR		N/A	N/A
121	IA	000-121	Original Process Waste Lines (Includes Tanks T-2, T-3, T-10, T-14, T-16, T-40)	Am, Pu-238, 239,240, 241, 242 U-234, 235, 238	HRR	Annual 1996, Annual 1998 (UBC 123)	N/A	N/A
122	IA	400-122	Underground Concrete Tank	U	HRR	Annual 1996 (000-121)	N/A	N/A
123.2	IA	700-123.2	Valve Vault West of Building 707	Pu, U	HRR		N/A	N/A
124.1	IA	700-124.1	30,000 Gallon Tank (Tank #68)	Pu, U	HRR	Annual 1996 (000-121)	N/A	N/A
124.2	IA	700-124.2	14,000 Gallon Tank (Tank #66)	Pu, U	HRR	Annual 1996 (000-121)	N/A	N/A
124.3	IA	700-124.3	14,000 Gallon Tank (Tank #67)	Pu, U	HRR	Annual 1996 (000-121)	N/A	N/A
125	IA	700-125	Holding Tank (Tank #66)	Pu, U	HRR		N/A	N/A
126.1	IA	700-126.1	Westernmost Out-of-Service Waste Tank	Pu, U	HRR		N/A	N/A
126.2	IA	700-126.2	Easternmost Out-of-Service Waste Tank	Pu, U	HRR		N/A	N/A
127	IA	700-127	Low-Level Radioactive Waste Leak	Pu	HRR		N/A	N/A
128	IA	300-128	Oil Burn Pit No. 1	U238	HRR		N/A	N/A
131	IA	700-131	Radioactive Site - 700 Area Site #1	Pu	HRR		N/A	N/A
132	IA	700-132	Radioactive Site - 700 Area Site #4	U234/235/238, Pu238/239/240, Pu241/242, Am241	HRR	Annual 1996 (000-121), Annual 1997	N/A	N/A

Table – page 1 of 9

17

Table TA-2-2. Table of Actinide Sources (continued)

IHSS	OU	PAC	Description (Unit Name)	Actinide Type	Info. Source	Updated	Proposed NFA	Recommen. NFA
136.1	IA	400-136.1	Cooling Tower Pond West of Building 444 (IAG Name: Cooling Tower Pond Northeast Corner of Building 460)	U238	HRR		N/A	N/A
136.2	IA	400-136.2	Cooling Tower Pond East of Building 444 (IAG Name: Cooling Tower Pond West of Building 460)	U238	HRR		N/A	N/A
138	IA	700-138	Cooling Tower Blowdown Building 779		HRR		N/A	N/A
143	IA	700-143	Bldg. 771 Outfall (IAG Name: Old Outfall)	Pu	HRR	Annual 1997	N/A	N/A
144	IA	700-144(N)	Sewer Line Overflow (IAG Name: Sewer Line Break)	Pu	HRR		N/A	N/A
144	IA	700-144(S)	Sewer Line Overflow (IAG Name: Sewer Line Break)		HRR		N/A	N/A
146.1	IA	700-146.1	Concrete Process Waste Tanks 7,500 Gallon Tank (31)	Pu, U	HRR		N/A	N/A
146.2	IA	700-146.2	Concrete Process Waste Tanks 7,500 Gallon Tank (32)	Pu, U	HRR		N/A	N/A
146.3	IA	700-146.3	Concrete Process Waste Tanks 7,500 Gallon Tank (34W)	Pu, U	HRR		N/A	N/A
146.4	IA	700-146.4	Concrete Process Waste Tanks 7,500 Gallon Tank (34E)	Pu, U	HRR		N/A	N/A
146.5	IA	700-146.5	Concrete Process Waste Tanks 3,750 Gallon Tank (30)	Pu, U	HRR		N/A	N/A
146.6	IA	700-146.6	Concrete Process Waste Tanks 3,750 Gallon Tank (33)	Pu, U	HRR		N/A	N/A
147.1	IA	700-147.1	Process Waste Line Leaks (IAG Name: Maas Area)	Pu, U	HRR		N/A	N/A
148	IA	100-148	Waste Spills		HRR	Annual 1998 (UBC 123)	N/A	N/A
149.1	IA	700-149.1	Effluent Pipe (North Lines to Solar Ponds)	Pu	HRR		N/A	N/A
149.2	IA	700-149.2	Effluent Pipe (South Lines to Solar Ponds)	Pu	HRR		N/A	N/A
150.1	IA	700-150.1	Radioactive Site North of Building 771 (IAG Name: Radioactive Leak North of Building 771)	Pu, Am	HRR		N/A	N/A
150.2	IA	700-150.2	Radioactive Site West of Buildings 771 and 776 (IAG Name: Radioactive Leak West of Building 771)	Pu	HRR		N/A	N/A
150.3	IA	700-150.3	Radioactive Site Between Buildings 771 & 774 (IAG Name: Radioactive Leak Between Buildings 771 & 774)	Pu	HRR		N/A	N/A
150.4	IA	700-150.4	Radioactive Site Northwest of Building 750 (IAG Name: Radioactive Leak East of Building 750)	Pu	HRR		N/A	N/A

Table – page 2 of 9

78

Table TA-2-2. Table of Actinide Sources (continued)

IHSS	OU	PAC	Description (Unit Name)	Actinide Type	Info. Source	Updated	Proposed NFA	Recommen NFA
150.6	IA	700-150.6	Radioactive Site South of Building 779 (IAG Name: Radioactive Leak South of Building 779)		HRR		N/A	N/A
150.7	IA	700-150.7	Radioactive Site South of Building 776 (IAG Name: Radioactive Leak South of Building 776)	Pu	HRR		N/A	N/A
150.8	IA	700-150.8	Radioactive Site Northeast of Building 779 (IAG Name: Radioactive Leak Northeast of Building 779)		HRR		N/A	N/A
152, 157.1, 172	IA	600-1004	Central Avenue Ditch Cleaning Incident (formerly identified as 400-820)		Quarterly 6	Quarterly 7	N/A	N/A
153	IA	900-153	Oil Burn Pit No. 2	U	HRR	Annual 1999	N/A	N/A
157.1	IA	400-157.1	Radioactive Site North Area	U235, U238	HRR		N/A	N/A
157.2	IA	400-157.2	Radioactive Site South Area	U235, U238	HRR		N/A	N/A
158	IA	500-158	Radioactive Site – Building 551	U	HRR		N/A	N/A
159	IA	500-159	Radioactive Site – Building 559	Pu, U	HRR		N/A	N/A
160	IA	600-160	Radioactive Site Building 444 Parking Lot	Pu, U	HRR		N/A	N/A
161	IA	600-161	Radioactive Site - Building 664	Pu, Am, U	HRR		N/A	N/A
162	IA	000-162	Radioactive Site - 700 Area Site # 2	unknown	HRR		N/A	N/A
163.1	IA	700-163.1	Radioactive Site 700 Area Site No.3 Wash Area		HRR		N/A	N/A
163.2	IA	700-163.2	Radioactive Site 700 Area Site No.3 Buried Slab	Am	HRR		N/A	N/A
164.2	IA	800-164.2	Radioactive Site 800 Area Site #2, Building 886 Spills	U	HRR		N/A	N/A
164.3	IA	800-164.3	Radioactive Site 800 Area Site #2, Building 889 Storage Pad	U	HRR		N/A	N/A
172	IA	500-907	Tanker Truck Release of Hazardous Waste From Tank 231B		Quarterly 9		N/A	N/A
173	IA	900-173	South Dock - Building 991 (IAG Name: Radioactive Site - 900 Area)	Pu, U	HRR		N/A	N/A
176	IA	900-176	S&W Contractor Storage Yard		HRR	Quarterly 11	N/A	N/A
182	IA	400-182	Building 444/453 Drum Storage Area	U	HRR		N/A	N/A
184	IA	900-184	Building 991 Steam Cleaning Area	Pu, U235, U238	HRR		N/A	N/A
186	IA	300-186	Valve Vault 12	U238	HRR		N/A	N/A
196	IA	SW-196	Water Treatment Plant Backwash Pond	unknown - S. of Bldg. 124	HRR		N/A	N/A
207	IA	400-207	Inactive 444 Acid Dumpster	U, Am	HRR		N/A	N/A
213	IA	900-213	Unit 15, 904 Pad Pondcrete Stor.	Pu, U	HRR		N/A	N/A
214	IA	700-214	750 Pad Pondcrete & Saltcrete Storage, Unit 25	U	HRR		N/A	N/A
NA	IA	000-500	Sanitary Sewer System (not shown on Plate 3)	Pu	HRR		N/A	N/A
NA	IA	000-504	New Process Waste Lines	Pu, Am, U	Annual 1999		N/A	N/A

Table – page 3 of 9

79

Table TA-2-2. Table of Actinide Sources (continued)

IHSS	OU	PAC	Description (Unit Name)	Actinide Type	Info. Source	Updated	Proposed NFA	Recommen. NFA
NA	IA	000-505	Storm Drains	U238	Annual 1999		N/A	N/A
NA	IA	100-602	Building 123 Process Waste Line Break	U	HRR		N/A	N/A
NA	IA	400-802	Storage Area, South of Building 334	U	HRR		N/A	N/A
NA	IA	400-804	Road North of Building 460	unknown	HRR		N/A	N/A
NA	IA	400-810	Beryllium Fire - Building 444	U	HRR		N/A	N/A
NA	IA	400-815	RCRA Tank Leak in Building 460	U	Quarterly 8		N/A	N/A
NA	IA	600-1001	Temporary Waste Storage Building 663		HRR	Annual 1997	N/A	N/A
NA	IA	700-1100	French Drain North of Building 776/777	Pu	HRR		N/A	N/A
NA	IA	700-1101	Laundry Tank Overflow - Building 732		HRR		N/A	N/A
NA	IA	700-1106	Process Waste Spill - Portal 1	Pu, Am, U	HRR		N/A	N/A
NA	IA	700-1108	771/774 Footing Drain Pond	Pu	HRR	Annual 1999	N/A	N/A
NA	IA	800-1200	Valve Vault 2	U238	HRR		N/A	N/A
NA	IA	800-1201	Radioactive Site S. of Building 883	Pu, U235	HRR		N/A	N/A
NA	IA	800-1204	Building 866 Spills	U	HRR		N/A	N/A
NA	IA	800-1205	Building 881, East Dock	Pu, U	HRR		N/A	N/A
NA	IA	800-1212	Building 866 Sump Spill		Quarterly 5		N/A	N/A
NA	IA	900-1301	Building 991 Enclosed Area	U235, U238	HRR		N/A	N/A
NA	IA	900-1307	Explosive Bonding Pit	U	HRR	Annual 1999	N/A	N/A
111.2	BZ	NE-111.2	Trench T-5	Pu, U	HRR		N/A	N/A
111.3	BZ	NE-111.3	Trench T-6	Pu, U	HRR		N/A	N/A
111.4	BZ	NE-111.4	Trench T-7	Pu, U	HRR		N/A	N/A
111.5	BZ	NE-111.5	Trench T-8	Pu, U	HRR		N/A	N/A
111.6	BZ	NE-111.6	Trench T-9	Pu, U	HRR		N/A	N/A
111.7	BZ	NE-111.7	Trench T-10	Pu, U	HRR		N/A	N/A
111.8	BZ	NE-111.8	Trench T-11	Pu, U	HRR		N/A	N/A
112	BZ	900-112	903 Pad (IAG Name: 903 Drum Storage Area)	Pu, U	HRR	Annual 1997, 1998, 1999	N/A	N/A

Table – page 4 of 9

80

Table TA-2-2. Table of Actinide Sources (continued)

IHSS	OU	PAC	Description (Unit Name)	Actinide Type	Info. Source	Updated	Proposed NFA	Recommen. NFA
155	BZ	SE-1602	East Firing Range	U238	Annual 1999		N/A	N/A
155	BZ	900-155	903 Lip Area	Pu239	HRR	Annual 1997, 1998, 1999	N/A	N/A
174A	BZ	NW-174A	PU&D Yard Container Storage Area	unknown	HRR	Annual 1997, Annual 1998	N/A	N/A
177	BZ	800-177	Building 885 Drum Storage and Paint Storage (IAG Name: Building 885 Drum Storage Area)	U235	HRR		N/A	N/A
NA	BZ	NE-1412	Trench T-12 Located in OU-2 East Trenches	Pu, U	Quarterly 10		N/A	N/A
NA	BZ	NE-1413	Trench T-13 Located in OU-2 East Trenches	Pu, U	Quarterly 10		N/A	N/A
NA	BZ	SW-1702	Recently Identified Ash Pit (also referred to as TDEM-2)	U235, U238	Quarterly 9		N/A	N/A
114	7	NW-114	Present Landfill	U, Pu	HRR		N/A	N/A
165	6	900-165	Triangle Area	Pu	HRR		N/A	N/A
115	5	SW-115	Original Landfill	U-238	HRR		N/A	N/A
133.1	5	SW-133.1	Ash Pit 1	U-238	HRR		N/A	N/A
133.2	5	SW-133.2	Ash Pit 2	U-238	HRR		N/A	N/A
133.3	5	SW-133.3	Ash Pit 3	U-238	HRR		N/A	N/A
133.4	5	SW-133.4	Ash Pit 4	U-238	HRR		N/A	N/A
119.1	1	900-119.1	West Scrap Metal Storage and Solvent Spill Area (CAD/ROD Specifies Maintenance/D&D Tasks to Close IHSS 119.1) i.e., Deferred Status	U	HRR	Annual 1996, Annual 1997, Annual 1998	N/A	N/A
Under Building Contamination (UBC)								
NA	IA	UBC-122	Building 122 (UBC-122)		HRR		N/A	N/A
NA	IA	UBC-123	Building 123 (UBC-123)		HRR	Annual 1998	N/A	N/A
NA	IA	UBC-125	Building 125 (UBC-125)		HRR		N/A	N/A
NA	IA	UBC-331	Building 331 (UBC-331)		HRR		N/A	N/A
NA	IA	UBC-371	Building 371 (UBC-371)	Pu	HRR		N/A	N/A
NA	IA	UBC-374	Building 374 (UBC-374)		HRR		N/A	N/A
NA	IA	UBC-439	Building 439 (UBC-439)	U	HRR		N/A	N/A
NA	IA	UBC-440	Building 440 (UBC-440)	U	HRR		N/A	N/A

Table – page 5 of 9

81

Table TA-2-2. Table of Actinide Sources (continued)

IHSS	OU	PAC	Description (Unit Name)	Actinide Type	Info. Source	Updated	Proposed NFA	Recommen. NFA
155	BZ	SE-1602	East Firing Range	U238	Annual 1999		N/A	N/A
NA	IA	UBC-441	Building 441 UBC-441)		HRR		N/A	N/A
NA	IA	UBC-442	Building 442 (UBC-442)	U	HRR		N/A	N/A
NA	IA	UBC-444	Building 444 (UBC-444)		HRR		N/A	N/A
NA	IA	UBC-447	Building 447 (UBC-447)		HRR		N/A	N/A
NA	IA	UBC-528	Building 528 (UBC-528)		HRR		N/A	N/A
NA	IA	UBC-559	Building 559 (UBC-559)	Pu	HRR		N/A	N/A
NA	IA	UBC-701	Building 701 (UBC-701)		HRR		N/A	N/A
NA	IA	UBC-707	Building 707 (UBC-707)	Pu	HRR		N/A	N/A
NA	IA	UBC-731	Building 731 (UBC-731)		HRR		N/A	N/A
NA	IA	UBC-770	Building 770 UBC-770)		HRR		N/A	N/A
NA	IA	UBC-771	Building 771(UBC-771)	Pu, Am	HRR		N/A	N/A
NA	IA	UBC-774	Building 774 (UBC-774)		HRR		N/A	N/A
NA	IA	UBC-776	Building 776 (UBC-776)	Pu	HRR		N/A	N/A
NA	IA	UBC-777	Building 777 (UBC-777)		HRR		N/A	N/A
NA	IA	UBC-778	Building 778 (UBC-778)		HRR		N/A	N/A
NA	IA	UBC-779	Building 779 (UBC-779)	Pu	HRR		N/A	N/A
NA	IA	UBC-865	Building 865 (UBC-865)		HRR		N/A	N/A
NA	IA	UBC-881	Building 881 (UBC-881)	U	HRR		N/A	N/A
NA	IA	UBC-883	Building 883 (UBC-883)		HRR		N/A	N/A
NA	IA	UBC-886	Building 886 (UBC-886)		HRR		N/A	N/A
NA	IA	UBC-887	Building 887 (UBC-887)		HRR		N/A	N/A
NA	IA	UBC-889	Building 889 (UBC-889)		HRR		N/A	N/A
NA	IA	UBC-991	Building 991 (UBC-991)	Pu, U	HRR		N/A	N/A

Table – page 6 of 9

82

Table TA-2-2. Table of Actinide Sources (continued)

IHSS	OU	PAC	Description (Unit Name)	Actinide Type	Info. Source	Updated	Proposed NFA	Recommen. NFA
Proposed No Further Action (NFA)								
101	IA	900-1314	Solar Evaporation Pond 207B Sludge Release		Quarterly 9		Quarterly 9	N/A
108	IA	900-108	Trench T-1	U	HRR	Annual 1997, 98	Annual 1999	N/A
117.3	IA	600-117.3	Chemical Storage – South Site	Pu	HRR	Annual 1997	Annual 1997	N/A
123.1	IA	700-123.1	Valve Vault 7	U	HRR	Annual 1997	Annual 1997	N/A
147.2	IA	800-147.2	Bldg. Conversion Activity Contamination Area (IAG Name: Owen Area)	U235, U238	HRR	Annual 1997	Annual 1997	N/A
150.5	IA	700-150.5	Radioactive Site West of Building 707 (IAG Name: Radioactive Leak West of Building 707)	U	HRR	Annual 1998	Annual 1998	N/A
156.1	IA	300-156.1	Building 371 Parking Lot (2 locations designated on Plate #2)	Pu, U	HRR	Annual 1997	Annual 1997	N/A
164.1	IA	600-164.1	Radioactive Slab from Bldg. 776	Pu	HRR	Annual 1997	Annual 1997	N/A
181	IA	300-181	Building 334 Cargo Container Area		HRR	Annual 1997	Annual 1997	N/A
192	IA	900-1313	Seep Area Near OU-2 Influent	Pu239/241, Am241, U235	Quarterly 9	Annual 1999	Annual 1999	N/A
212	IA	300-212	Building 371 Drum Storage Area, Unit 63 (deferred to Part VIII of the RFETS RCRA Mixed Residues Modification; see Annual 1997)	U	HRR	Annual 1997	Annual 1997	N/A
NA	IA	000-503	Solar Pond Water Spill Along Central Avenue		Quarterly 7		Quarterly 7	N/A
NA	IA	400-811	Transformer 443-2, Building 443	Pu, Am, U	Quarterly 2	Quarterly 3, Annual 1998	Annual 1998	N/A
NA	IA	600-1002	Transformer Storage - West of Building 666	Pu	HRR	Annual 1996	Annual 1996	N/A
NA	IA	900-1311	Septic Tank East of Building 991	Pu239/241, Am241, U235	Quarterly 7	Annual 1999	Annual 1999	N/A
NA	IA	900-1312	OU-2 Water Spill	Pu239/241, Am241	Quarterly 7	Annual 1999	Annual 1999	N/A
NA	IA	900-1315	Tanker Truck Release on East Patrol Road, North of Spruce Ave.		Quarterly 10	Quarterly 11	Quarterly 11	N/A
109	BZ	900-109	Trench T-2 - Ryan's Pit	Pu, U	HRR	Annual 1996, Annual 1997	Annual 1997	N/A
110	BZ	NE-110	Trench T-3	Pu, U	HRR	Annual 1996, Annual 1997	Annual 1997	N/A
111.1	BZ	NE-111.1	Trench T-4	Pu, U	HRR	Annual 1996, Annual 1997	Annual 1997	N/A
113	BZ	900-113	Mound Area	Pu, U235, U238	HRR	Annual 1997	Annual 1997	N/A
140	BZ	900-140	Hazardous Disposal Site (IAG Name: Reactive Metal Destruction Site)	Pu239/240, Am241, U233/234/235/238	HRR	Annual 1997, Annual 1998	Annual 1998	N/A
170	BZ	NW-170	PU&D Storage Yard - Waste Spills	unknown	HRR	Annual 1997, Annual 1998	Annual 1998, Annual 1999	N/A
174B	BZ	NW-174B	PU&D Container Storage Facilities	unknown	HRR	Annual 1997, Annual 1998	Annual 1998, Annual 1999	N/A
183	BZ	900-183	Gas Detoxification Area	Pu	HRR	Annual 1997	Annual 1997	N/A
216.2	BZ	NE-216.2	East Spray Field - Center Area	Pu, Am	HRR	Annual 1997	Annual 1997	N/A

Table – page 7 of 9

83

Table TA-2-2. Table of Actinide Sources (continued)

IHSS	OU	PAC	Description (Unit Name)	Actinide Type	Info. Source	Updated	Proposed NFA	Recommen NFA
216.3	BZ	NE-216.3	East Spray Field - South Area	Pu, Am, U	HRR	Annual 1997	Annual 1997	N/A
NA	BZ	NE-1406	771 Hillside Sludge Release	unknown	Quarterly 4	Annual 1998	Annual 1998	N/A
NA	BZ	SW-1701	Recently Identified Ash Pit (also referred to as TDEM-1)	U235, U238	Quarterly 9	Annual 1997	Annual 1997	N/A
179	15	800-179	Building 865 Drum Storage Area (defer to D&D and UBC 447; refer to OU 15 CAD/ROD)	U	HRR	Annual 1996	Annual 1996	N/A
180	15	800-180	Building 883 Drum Storage Area (defer to D&D and UBC 447; refer to OU 15 CAD/ROD)	U	HRR	Annual 1996	Annual 1996	N/A
204	15	400-204	Original U Chip Roaster (deferred to D&D and UBC 447; see OU 15 CAD/ROD)	U	HRR	Annual 1996	Annual 1996	N/A
167.2	7	NE-167.2	Pond Area Spray Field (Center Area)	Pu, Am	HRR	Annual 1996	Annual 1996	N/A
167.3	7	NE-167.3	South Area Spray Field	Pu, Am	HRR	Annual 1996	Annual 1996	N/A
203	7	NW-203	Inactive Hazardous Waste Storage Area		HRR	Annual 1996, Annual 1998	Annual 1998	N/A
141	6	900-141	Sludge Disposal	Pu	HRR	Annual 1997	Annual 1997	N/A
142.1	6	NE-142.1	Pond A-1	Pu	HRR	Annual 1997	Annual 1997	N/A
142.12	6	NE-142.12	Flume Pond (IAG Name: Newly Identified Pond A-5) (Off-scale of Plate #2)	Pu	HRR	Annual 1996	Annual 1996	N/A
142.2	6	NE-142.2	Pond A-2	Pu	HRR	Annual 1997	Annual 1997	N/A
142.3	6	NE-142.3	Pond A-3	Pu	HRR	Annual 1997	Annual 1997	N/A
142.4	6	NE-142.4	Pond A-4	Pu	HRR	Annual 1997	Annual 1997	N/A
142.5	6	NE-142.5	Pond B-1	Pu	HRR	Annual 1997	Annual 1997	N/A
142.6	6	NE-142.6	Pond B-2	Pu	HRR	Annual 1997	Annual 1997	N/A
142.7	6	NE-142.7	Pond B-3	Pu	HRR	Annual 1997	Annual 1997	N/A
142.8	6	NE-142.8	Pond B-4	Pu	HRR	Annual 1997	Annual 1997	N/A
142.9	6	NE-142.9	Pond B-5	Pu	HRR	Annual 1997	Annual 1997	N/A
156.2	6	NE-156.2	Soil Dump Area (between the A and B Series Drainages)	Pu	HRR	Annual 1997	Annual 1997	N/A
166.1	6	NE-166.1	Trench A	U	HRR	Annual 1996	Annual 1996	N/A
166.2	6	NE-166.2	Trench B	U	HRR	Annual 1996	Annual 1996	N/A
166.3	6	NE-166.3	Trench C (2 areas designated on Plate #2)	U	HRR	Annual 1996	Annual 1996	N/A
167.1	6	NE-167.1	Landfill North Area Spray Field	Pu, Am	HRR	Annual 1997	Annual 1997	N/A
216.1	6	NE-216.1	East Spray Fields - North Area	Pu, Am	HRR	Annual 1996	Annual 1996	N/A
133.5	5	SW-133.5	Incinerator Facility	U238	HRR	Annual 1997	Annual 1997	N/A
133.6	5	SW-133.6	Concrete Wash Pad	unknown - incinerator ash	HRR	Annual 1997	Annual 1997	N/A
142.10	5	SE-142.10	Retention Pond C-1	Am, Pu, U	HRR	Annual 1997	Annual 1997	N/A
142.11	5	SE-142.11	Retention Pond C-2	Am, Pu, U	HRR	Annual 1997	Annual 1997	N/A
Recommended No Further Action (NFA)								
172	IA	000-172	Central Avenue Ditch	Pu, U	HRR	Annual 1998	Annual 1998	OU 11 CAD/ROD
197	IA	500-197	Scrap Metal Sites		HRR			To Be Completed in July 1992
NA	IA	700-1109	U Incident - Building 778	U238	HRR			EPA, 1992

Table – page 8 of 9

84

Table TA-2-2. Table of Actinide Sources (continued)

IHSS	OU	PAC	Description (Unit Name)	Actinide Type	Info. Source	Updated	Proposed NFA	Recommen NFA
NA	IA	700-1117	Building 701 Water Line, Soil Put-back	Pu239/240, Am241	Annual 1998		Annual 1998	CDPHE 1998
NA	IA	900-1300	RO Plant Sludge Drying Beds		HRR			EPA, 1992
NA	BZ	SE-1600	Pond 7 – Steam Condensate Releases	unknown - from Bldg. 881	HRR			EPA, 1992
NA	BZ	000-501	Roadway Spraying	Pu, U	HRR			EPA, 1992
178	15	800-178	Building 881 Drum Storage Area	U235	HRR	Annual 1996		OU 15 CAD/ROD
211	15	800-211	Building 881 Drum Storage, Unit 26	U	HRR	Annual 1996		OU 15 CAD/ROD
168	11	000-168	West Spray Field	Pu, Am	HRR	Annual 1996		OU 11 CAD/ROD
199	3	OFF-SITE AREA 1	Off-Site Area 1	Pu	HRR	Annual 1997		OU 3 CAD/ROD
200	3	OFF-SITE AREA 2	Great Western Reservoir	Pu	HRR	Annual 1997		OU 3 CAD/ROD
201	3	OFF-SITE AREA 3	Standley Lake	Pu	HRR	Annual 1997		OU 3 CAD/ROD
202	3	OFF-SITE AREA 4	Mower Reservoir	Pu	HRR	Annual 1997		OU 3 CAD/ROD
102	1	800-102	Oil Sludge Pit		HRR	Annual 1997		OU 1 CAD/ROD
104	1	800-104	Liquid Dumping	Unknown	HRR	Annual 1997		OU 1 CAD/ROD
106	1	800-106	Bldg. 881, Outfall	Pu, Am	HRR	Annual 1997		OU 1 CAD/ROD
107	1	800-107	Bldg. 881, Hillside Oil Leak	Pu	HRR	Annual 1997		OU 1 CAD/ROD
119.2	1	900-119.2	East Scrap Metal Storage Area and Solvent Spill	U	HRR	Annual 1996 Annual 1997		OU 1 CAD/ROD
130	1	900-130	Contaminated Soil Disposal Area East of Bldg. 881	Pu	HRR	Annual 1997		OU 1 CAD/ROD
145	1	800-145	Sanitary Waste Line Leak		HRR	Annual 1997		OU 1 CAD/ROD

Table – page 9 of 9

85

Table TA-2-3. Actinide Source Locations With Associated Surface and Sub-Surface Soil Data (Sample Page)

					Actinide Concentrations (pCi/g)				
NORTHING	EASTING	DEPTH FT	JHSS NUMBER	PAC NUMBER	Pu	Am	U233/U234	U235	U238
751261.00	2084127.00	0.5-2	101	700-1108	1.48000	0.33000	1.2400		0.9180
751250.00	2084087.00	0.5-2	101	700-1108	0.32000	0.18000	0.8250	0.1080	0.7560
751245.00	2084067.00	0.5-2	101	700-1108	1.87000	1.47000	1.2900	0.0480	1.6900
751245.00	2084067.00	2-4	101	700-1108	0.65200	0.46100	0.9440	0.0500	1.4900
751234.00	2084057.00	0.5-2	101	700-1108	0.35300	0.28100	0.9840	0.0330	1.1600
751232.00	2084082.00	0.5-2	101	700-1108	0.00700		1.0300	0.0180	1.1600
751232.00	2084082.00	2-4	101	700-1108	0.00800	-0.05500	0.9450	0.0330	0.9410
751230.00	2084066.00	0.5-2	101	700-1108	0.26200	0.13900	0.7210	0.0180	0.9400
751230.00	2084066.00	2-4	101	700-1108			1.0300		1.0300
751219.00	2084060.00	0	101	700-1108	2.68400				
750897.00	2085228.00	2-4	101	900-1310	2.90000	2.10000	1.9000		1.4000
750897.00	2085228.00	8-10	101	900-1310	0.01300		1.2000	0.0410	1.0000
750484.00	2085230.00	0	101	900-1314	0.42100	0.83200			
750483.57	2085224.67	0	101	900-1314			1.1700		1.2200
750463.00	2085223.00	2-4	101	900-1314	0.04800	1.80000	0.7800	0.0170	0.8300
750463.00	2085223.00	8-10	101	900-1314	0.00291	0.00447	0.5887	0.0241	0.6124
751280.00	2084141.00	0.5-2	101	NA	0.31000	0.16000	1.0700	0.0320	0.8740
751279.00	2084200.00	0.5-2	101	NA	0.16600	0.20200	0.7640		0.9110
751270.18	2084238.37	0	101	NA			0.9283	0.0463	0.8559
751270.00	2084240.00	0	101	NA	0.82440	0.70540			
751251.00	2084510.00	0	101	NA	0.46000	0.20000			
751250.87	2084513.00	0	101	NA			3.3000	0.1700	2.3000
751250.00	2084164.00	0.5-2	101	NA	0.28300		0.9910	0.1080	0.8550
751250.00	2084164.00	2-4	101	NA	0.02600	0.00700	0.8300		0.9760
751249.00	2084128.00	0.5-2	101	NA	0.01800		1.2100	0.0170	1.3400
751249.00	2084128.00	2-4	101	NA	0.01500	-0.01600	1.4900		1.1700
751221.48	2084513.79	0	101	NA			2.9000	0.5100	1.9000
751221.00	2084510.00	0	101	NA	0.16000	0.16000			
751219.41	2084858.45	0	101	NA				0.1900	4.1000
751219.00	2084860.00	0	101	NA	1.20000	0.58000			
751177.43	2084894.75	0	101	NA			5.0000	0.1800	3.3000
751177.00	2084900.00	0	101	NA	0.50000	0.45000			
751154.00	2084649.00	0	101	NA			2.7000	0.0190	1.2000
751154.00	2084650.00	0	101	NA	0.31000	0.34000			
751139.25	2084916.37	0	101	NA					3.5740
751139.03	2084528.41	0	101	NA			2.4000	0.1800	2.3000
751139.00	2084530.00	0	101	NA	4.90000	1.50000			
751139.00	2084920.00	0	101	NA	0.19070	0.21580			
751137.12	2084568.87	0	101	NA			1.2840	0.1145	0.7418
751137.00	2084570.00	0	101	NA	3.07700	0.97830			
751089.00	2084627.00	2-4	101	NA			1.5000		1.2000
751089.00	2084627.00	6-8	101	NA			1.3000		1.1000
751089.00	2084627.00	>10	101	NA			1.2000		1.3000
751078.00	2085100.00	0	101	NA		1.50000	1.1000		0.7000
751078.00	2085100.00	2-4	101	NA			0.5180	0.0091	0.4270
751075.00	2084920.00	0	101	NA					
751074.87	2084916.50	0	101	NA				2.3000	
751064.12	2084581.75	0	101	NA			2.1000		2.0000
751064.00	2084580.00	0	101	NA	2.10000	0.93000			
751047.00	2085182.00	0.5-2	101	NA	0.28000	0.35000	1.3000	0.0380	1.2000
751044.21	2084873.76	0	101	NA			2.4000		0.8900
751044.00	2084870.00	0	101	NA	3.40000	4.50000			
751030.00	2085260.00	0	101	NA		2.78300			
751029.68	2085260.00	0	101	NA			2.8720		1.4730
751008.31	2084395.00	0	101	NA			3.1650	0.1309	1.4280
751008.00	2084400.00	0	101	NA		1.38100			
750993.31	2084865.00	0	101	NA				0.3000	4.7000
750993.00	2084870.00	0	101	NA					
750983.00	2084540.00	0	101	NA		0.46000			
750983.00	2084544.00	0	101	NA			0.9500		0.6600
750983.00	2084544.00	2-4	101	NA	1.30000	0.27000	1.5380		0.8473
750962.00	2084436.00	2-4	101	NA	1.60000	0.25000	2.7000	0.0350	1.7000
750962.00	2084436.00	6-8	101	NA	0.03900	0.04200	1.2000	0.0410	0.8700

Table - page 1 of 1 (Complete table on CD-ROM with report)

86

TA-2.2.2 Actinide Source Maps

Two maps, at different scales, were created to show the actinide source locations identified by the review of HRR records. Figure TA-2-1 shows the actinide source locations for the entire Site. Figure TA-2-2 provides a smaller scale map near the Industrial Area, where the majority of the sources are located. This map includes the detention pond system. Both maps depict "active" actinide locations (including process waste line systems), UBC sites, proposed NFA sites and recommended NFA sites. Numbers associated with the different source locations correspond with the source identification numbers listed in Table TA-2-2. The numbering system used to denote the different sources was described in Section TA-2.2.1.

The actinide source maps, similar to other maps presented in this section, have surface water drainage basins delineated to identify the drainage in which each source is located.

TA-2.3 SURFACE SOIL ACTINIDE CONCENTRATIONS

TA-2.3.1 Background Surface Soil Actinide Concentrations

Surface soil, as defined in RFCA, is the upper six inches of soil (DOE, 2000). Background values for actinide activities in surface soil come from the *Geochemical Characterization of Background Surface Soils: Background Soils Characterization Program* report (EG&G, 1995). These levels are presented in Table TA-2-4. Background activity for the U isotopes is associated with naturally-occurring U in the soils and underlying geologic formations whereas background Pu and Am is associated with global fallout from historic nuclear testing.

Table TA-2-4. Background Surface Soil Actinide Concentrations

Analyte	# of samples	Maximum (pCi/g)	Minimum (pCi/g)	Std. Deviation (pCi/g)	Mean (pCi/g)
Pu-239/240	50	0.07	0.02	0.01	0.04
Am-241	50	0.03	0.00	0.01	0.01
U-233/234	20	3.10	0.60	0.58	1.10
U-235	20	0.11	0.03	0.02	0.05
U-238	20	2.60	0.74	0.46	1.09

TA-2.3.2 RFCA Action Levels

RFCA surface soil action levels are defined in Attachment 5 of RFCA (DOE, 2000) and presented in Table TA-2-5. The surface soil action levels have been calculated using a two-tier approach based on protection of appropriate human exposure. Tier II Action Levels are more restrictive than Tier I Action Levels.

Tier I surface soil action levels for radionuclides are the more conservative of:

- An annual radiation dose of 15 millirem (mrem) per year for the appropriate land use receptor; or
- An annual radiation dose of 85 mrem for a hypothetical future resident assuming failure of passive control measure.

  The total dose from multiple radionuclides will be accounted for by applying the sum-of-ratios method (DOE, 2000).

Tier II surface soil Action Levels are based on:

- An annual radiation dose of 15 mrem to a hypothetical future resident.

88

The total dose from multiple radionuclides will be accounted for by applying the sum-of-ratios method (DOE, 2000).

RFCA also specifies that surface soil may need to be remediated or managed to protect surface water quality via runoff or ecological resources. The amount of soil and the protective remediation levels and/or management technique will be determined on a case-by-case basis (DOE, 2000).

Table TA-2-5. RFCA Surface Soil Action Levels

Analyte	Tier I		Tier II [c]
	Industrial Use [a] (pCi/g)	Open Space Use [b] (pCi/g)	(pCi/g)
Pu-239/240	1088	1429	252
Am-241	209	215	38
U-234	1627	1738	307
U-235	113	135	24
U-238	506	586	103

Notes:

[a] Based on annual dose limit of 15 mrem to an office worker.

[b] Based on an annual dose limit of 85 mrem to a hypothetical future resident.

[c] Based on an annual dose limit of 15 mrem to a hypothetical future resident.

These values apply to single radionuclides only. In order to account for the total dose from multiple radionuclides, sum-of-ratios calculations will be applied to all radionuclides that are present above background. Actual values that trigger actions will therefore likely be lower than the values listed in this table (DOE, 2000).

TA-2.3.3 RFETS Surface Soil Actinide Figures

Figure TA-2-3 through Figure TA-2-7 present results of surface soil sampling for Pu-239/240, Am-241, U-233/234, U-235 and U-238 at discrete locations. Surface water drainage sub-basins are delineated to indicate the drainage basin in which specific surface soil samples were collected. For the surface soil figures, as well as the sub-surface soil and sediment figures presented in later sub-sections, the following ten categories of actinide concentrations (pCi/g) were established for the data presentation:

- Less than 0.01;
- 0.01 to 0.05;
- 0.05 to 0.1;
- 0.1 to 0.5;
- 0.5 to 1.0;
- 1.0 to 5.0;
- 5.0 to 10;
- 10 to 100;
- 100 to 1000; and
- greater than 1000.

The distribution of surface soil sample results for each actinide is displayed in a histogram in the legend of each actinide-specific surface soil map. Each histogram shows the relationship of measured actinide concentrations to the:

- Analytical Required Detection Limit (RDL);
- Background concentrations in surface soil for the actinide data displayed; and
- RFCA Tier I and Tier II Action Levels.

Figure TA-2-8 through Figure TA-2-12 depict estimated spatial concentrations of Pu-239/240, Am-241, U-233/234, U-235 and U-238, respectively, in surface soil at RFETS that were calculated by a geostatistical analysis process, called kriging, using the discrete data points. For these maps, the Site is divided into individual "blocks" of 75 feet by 75 feet that are shaded with colors representing the estimated average concentration over each block area. Section TA-2.3.5 provides a description of the geostatistical analysis process used to generate the values plotted in the maps.

TA-2.3.4 Surface Soil Data Query Process

Surface soil sample data presented in this report were originally compiled into data sets for two other, independent projects. The first data set, for Pu and Am surface soil data, was queried from SWD in the fall of 1999 for the development of an RFETS erosion and sediment transport model (Kaiser-Hill, 2000d). The second data set, for U isotopic surface soil data, was queried from SWD in the fall of 2000 by Kaiser-Hill Media Management for the Site-wide Dose Assessment project (Kaiser-Hill, 2001a). Data quality criteria applied to these data sets are described below.

Sample results with a rejected data qualifier, indicating a rejected analytical result, were excluded from both the Pu/Am and the U data sets (see Table TA-2-1). All of the remaining non-rejected samples were included in both of the data sets. Where multiple sample results existed for one location, the sample with the maximum activity was used for that location.

Further details on the methodologies used to collect surface soil data and geostatistical analyses of these data are discussed in the following sub-sections.

TA-2.3.5 Surface Soil Data Description

A total of 2,468 Pu-239/240, 2,262 Am-241 and 1,182 U-233/234, U-235 and U-238 surface soil samples met the acceptance criteria discussed in TA-2.3.4 and were used to evaluate actinide concentrations across the Site. The data sets include samples dating from June 1991 through September 1999 and incorporate samples analyzed by both laboratory and, in the case of certain Am-241 samples, field High Purity Germanium (HPGe) spectrometry techniques. Pu-239/240 estimated activities were derived from the Am-241 values in those locations where the HPGe spectrometery technique was used (RMRS, 1999). Summary statistics for the Site surface soil sample data set are shown in Table TA-2-6.

Table TA-2-6. Summary Statistics for Surface Soil Data Set

Statistic	Actinide				
	Pu-239/240 (pCi/g)	Am-241 (pCi/g)	U-233/234 (pCi/g)	U-235 (pCi/g)	U-238 (pCi/g)
Number of Sample Data	2468	2262	1,182	1,182	1,182
Minimum	Non-Detect	Non-Detect	Non-Detect	Non-Detect	Non-Detect
Maximum	152,260	31,670	2,800	670	38,000
Mean	145.8	27.7	4.2	0.74	37.7
Std. Deviation	3146	677	82	19.6	1108
Median	1092	227	0.94	0.049	0.978

Note: Minimum Detected Activities (MDAs) vary for each sample

In summary, the surface soil data sets do not include sample results with a rejected data qualifier. All of the remaining non-rejected samples were utilized, including those sample results that were not validated. In cases where multiple sample results existed for one location, the sample with the maximum activity was used for display on the figure.

Types of Surface Soil Sample Data

The data used in the Site-wide surface soil analysis represent several sampling events and sample types. Sample types include the following:

- Discrete grab samples;
- Rocky Flats method (composite);
- Colorado Department of Public Health and the Environment (CDPHE) method (composite); and
- HPGe spectrometry (for Pu and Am only).

92

For the composite samples, two different methods were used (DOE, 1995b). The first, known as the Rocky Flats method, involved removing soil in a 10 by 10-cm square to a depth of 5-cm. Five such square areas were combined to create a composite sample representative of the center of the sampling grid. Similarly, the CDPHE method took 25 six by five-cm rectangles 0.64-cm deep and composited them to form a sample. HPGe spectrometry data, used to measure Am-241 and, by correlation, to estimate Pu-239/240 activities, represent surface soil surveys of actinide concentrations over a 10-meter (m) diameter circular area (RMRS, 1999).

TA-2.3.6 Geostatistical Analyses of Surface Soil Samples

Geostatistical analyses were performed on the Pu-239/240, Am-241, U-233/234, U-235 and U-238 sample data for surface soil concentrations at RFETS. Geostatistical analyses, including the techniques of variograms and kriging, are commonly used approaches when sample data exist in a large spatial area, such as the RFETS (Myers, 1997). Spatial data require special analytical techniques in order to extract the maximum amount of information available from the data and to minimize the uncertainty associated with concentration estimates and contaminant distribution maps. Geostatistical techniques have proved to be especially appropriate in the analysis of spatial data and in the assessment of uncertainty.

Variability of Surface Soil Sample Data

Sample Data Variability Due to Sample Support. As described above, sample data were composed of differing physical sizes (areas or volumes). The physical size, shape and orientation of a sample are referred to as the sample support (Pitard, 1993; Myers, 1997). Typically, samples with larger support have less variability than samples with smaller support. This support-related characteristic was observed in the three data types. Grab samples exhibited the greatest variability, composite samples showed less variability and HPGe samples had the least variability. The variability of the various sample supports is also related to the spatial location of the differently-sized supports. This spatial relationship is described in the next paragraph.

93

Spatial Variability of Sample Data. The distribution of the actinide concentrations in surface soils at the Site is relatively consistent in many areas, but highly variable in others. In addition, the variability is dependent on the specific actinide.

For Pu and Am, variability is especially high in areas known to be sources, such as the 903 Pad. In locations quite distant or upwind from the source areas, variability is relatively low. Because of this spatial variability, the Pu and Am data were separated into different spatial areas, called domains, for the geostatistical analysis.

The first domain for the Pu and Am data are the 903 Pad and Site locations generally to the east and south of the Pad. The northern boundary of this domain runs approximately parallel to Central Avenue, with the southern boundary running approximately west to east just south of the SID. The eastern boundary is Indiana Street. Sample data in this domain show Pu-239/240 concentrations above 10 pCi/g for much of the area from the 903 Pad eastward to within 1,000 ft (305 meters [m]) of Indiana Street. Am-241 concentrations range between 1 and 5 pCi/g over much of the same area. Extreme actinide concentrations and concentration variability are exhibited at and around the 903 Pad, with generally decreasing concentrations to the east.

The second data analysis domain for Pu and Am is the region outside of the 903 Pad domain. This area away from the 903 Pad contains sample concentrations mostly below 10 pCi/g with lower spatial variability than the 903 Pad region.

In the case of the U isotopes, source areas include the 903 Pad as well as the Old Landfill and Ash Pits southwest of the Industrial Area. Site-wide, the U isotopes showed a broad trend, with generally higher concentrations to the west and gradually diminishing concentrations to the east. One notable anomaly to this trend is the southeast corner of the Site, where some concentrations were more similar to those observed in the western areas.

The Site-wide actinide data indicated a highly-skewed, lognormal-type distribution. These attributes are typical of environmental contaminant data, with a large number of the data

showing low concentrations and a small number showing higher concentrations combined with a few extreme values. Actinide data span approximately eight orders of magnitude.

For all of the actinides, this wide variation in the data range is primarily the result of mixing sample populations at the Site (i.e., background activity samples combined with Site-influenced samples). Over much of the Site, actinide concentrations are quite low and may well be thought of as background concentrations. However, Site activities appear to have introduced additional actinides into Site soils, particularly in the original Landfill, Ash Pits, the 903 Pad area and around buildings where actinides were used or stored. Non-anthropogenic sources (background) do not exhibit actinide concentrations that approach the Tier 2 action levels, with these concentrations typically falling one to four orders of magnitude below the Tier 2 action levels. Actinide concentrations that approach Tier 2 action levels are associated with anthropogenic activities.

Surface Soil Sample Variogram Analysis

Variogram analysis, or variography, is a fundamental step in a geostatistical analysis to quantify the degree of spatial variability of the contamination. Because significant spatial variation is exhibited by the sample data, variographic analysis was performed on the RFETS surface soil data for each of the actinides. It has been widely documented in the earth and environmental sciences that nearby samples generally have concentrations more similar than samples that are further apart (Matheron, 1965; David, 1977; Isaaks and Srivastava, 1987; Litaor, 1995; Myers, 1997). In statistical terms, this means that the samples are correlated. Correlation is useful information that can be captured and used to minimize estimation errors of contaminant concentrations. Variogram analysis performs the task of capturing correlation information by comparing sample data at different distance intervals. Generally, as the distance between samples increases, the variability also increases, with a corresponding decrease in the correlation. Eventually, at some distance, the variability reaches a maximum, indicating that correlation between samples no longer exists and that samples are independent.

For Pu and Am, variography was performed on the data in the Site and plume domains separately. The reason for this is the substantial difference in the spatial data variability between the two domains as well as the various sample supports. Because the HPGe data are less prone to sampling and sub-sampling errors due to the larger sample support size (Pitard, 1993), only the HPGe data were used in the Pu-239/240 variogram analysis for the plume area. Due to lower Am-241 concentrations and lower variability, data from the 903 Pad as well as the HPGe data were used for the Am-241 variograms.

For the U isotope data, variography was performed on a Site-wide basis. The relatively small, localized areas exhibiting U concentrations considerably above background and/or greater than Tier 2 levels (Landfill, Ash Pits and 903 Pad) did not contain sufficient data to justify separate variographic analysis.

For each actinide, five different directions were analyzed: north-south, northeast-southwest, east-west, northwest-southeast and an omni-directional variogram (all directions simultaneously). Experience has shown that the spatial variability can differ dramatically in different directions; thus, it is appropriate to investigate several directions during the variogram analysis. Situations where the variability is equal in all directions produce variograms that are said to be isotropic and the spatial continuity can be visualized as circular. Situations where variability is not equal in all directions produce anisotropic variograms, with a short and long axis of spatial continuity and can be visualized as elliptical in nature. Anisotropic variograms were found for both Pu-239/240 and Am-241 data in both domains and for each of the U isotopes in the one domain analyzed for U.

Due to the high variability in the data in some areas, several types of variogram analyses were also performed. Different types of variogram analyses can often mitigate the influence of the high variability of the sample data values. For data in the Site and plume domains, variograms for untransformed data were analyzed. In addition, general relative variograms, local relative variograms and logarithmic variograms were also run in the Site and plume domains. The variogram graphs indicated that the best results were for the untransformed data. Variogram

graphs for the Site-wide analysis appear in Figure TA-2-13 through Figure TA-2-17 for Pu-239/240, Am-241, U-233/234, U-235 and U-238, respectively.

For Pu and Am, variogram graphs in the plume domain exhibit structure similar to that found at other environmental sites where there is a small, concentrated contaminant source and where wind is a significant dispersion mechanism. For example, lead smelters typically show very high concentrations close to the smelter, combined with down-wind contamination dispersion. In such cases, the variogram graphs tend to rise very quickly from the origin for a short distance, then rise more gradually for a longer distance (Myers, 1985). This type of feature was observed in the Pu and Am plume domain variography. For the U isotopes, variogram graphs for each isotope exhibit similar structural aspects. Each isotope displayed a more continuous spatial structure in the north-south direction as compared to the east-west direction. Because isotopic ratios vary considerably, each isotope has a unique variogram anisotropy. Mathematical models were fit to the long and short axes of spatial continuity on the variogram graphs for each isotope. The mathematical model describes the variability and correlation of the sample data as the distance between samples increases.

The correlation modeled during the variographic analysis is used in the kriging process. Numerous types of mathematical equations are available for variogram modeling. For the Site and plume variograms, the commonly used spherical model was selected to represent the graphs. Table TA-2-7 lists the variogram models selected for the long and short axes of spatial continuity and the direction of these axes for each isotope. The equation for the spherical model appears below:

$$\gamma(h) = C_o + C\left[\frac{3}{2}\frac{h}{a} - \frac{1}{2}\frac{h^3}{a^3}\right]$$

where:

$\gamma(h)$ = variance at distance h

C_o = nugget effect

97

C = spherical component

a = range of influence

Sill = $C_o + C$

Table TA-2-7. Selected Variogram Models

Actinide	Domain	Variogram Parameters							
		C_o	C	a_{min} (ft)	a_{min} (m)	Direction	a_{max} (ft)	a_{max} (m)	Direction
Pu-239/240	Site	0.20	1.55	500	152	E-W	700	213	N-S
	Plume	0.0	7000	125	38	N-S	175	53	E-W
Am-241	Site	0.0	5.8	175	53	NW-SE	275	84	NE-SW
	Plume	25	70	250	76	N-S	375	114	E-W
U-233/234	Site	0.15	0.40	400	122	E-W	1000	305	N-S
U-235	Site	0.016	0.003	250	76	E-W	900	274	N-S
U-238	Site	0.25	0.62	400	122	E-W	600	183	N-S

The nugget effect indicates that there is variability even at a distance of zero, demonstrating that extreme variability may occur over very sort distances. It is also an indication of sampling and analytical error. No nugget effect was observed for the Pu-239/240 plume data set and a relatively small nugget effect (approximately 10 to 25 % of the sill value) was observed for the Pu-239/240 Site data set. For Am-241, no nugget effect was observed for the Site data set and a relatively small effect was observed for the plume data set. Significant nugget effects, ranging from approximately 25 to 40 %, were observed for each of the U isotopes.

In summary, both Pu-239/240 and Am-241 data produced variograms exhibiting significant spatial correlation in both the Site and plume domains. The raw, untransformed data were used to produce the variograms and logarithmic transformation was not necessary. The U-233/234,

98

U-235 and U-238 data produced variograms exhibiting significant spatial correlation for the Site-wide domain (as previously noted, a plume domain was not produced for the U data). The raw, untransformed data were used to produce the variograms, with each of the isotopes exhibiting significant nugget effects and anisotropies.

Surface Soil Data Kriging

Kriging Process

Because it is not practical to sample the surface soil of every square meter at the Site, existing sample data must be used to estimate the concentrations of Pu-239/240, Am-241, U-233/234, U-235 and U-238 at locations that have not been sampled. Various computerized estimation techniques have been developed for this purpose. The geostatistical technique known as kriging was selected to perform the estimation of the sample data at the RFETS.

Kriging offers many advantages over other estimators. Among these is the fact that kriging is a best linear unbiased estimator (BLUE). A BLUE estimator simply means that the estimation is done with the minimum amount of error. Other BLUE estimators exist in statistical analysis, including the well-known linear regression equation. Kriging is a BLUE that has been specially adapted to handle spatial data estimation. As indicated, kriging is also unbiased, meaning that the technique does not systematically over- or under-estimate the soils contaminant concentrations.

Kriging uses variogram models, such as those in Table TA-2-7, to optimize the estimation and to minimize the estimation errors. During the kriging process, the kriging program searches for samples that are closest to the unsampled area being estimated. Kriging recognizes that samples closest to the area being estimated should be given more weight than samples further away. The kriging program calculates the optimal weighting system for the available samples and derives an optimal estimate of the actinide concentration at the unsampled location.

Models created with any interpolator, including kriging, are subject to certain problems. One such problem is variable sample density. In areas of abundant data, interpolating systems

99

generally perform well. More difficulties are experienced, however, in areas of sparse sampling. In such areas, available samples are often extrapolated great distances in order to create a complete model. This creates uncertainty in the model where sampling is sparse. This problem exists in the RFETS Pu, Am and U isotope data sets, with large areas outside the Industrial Area that are sparsely sampled.

Another problem situation occurs when zones of high concentration and/or high variability samples are not well bounded by other samples. This situation occurs in several areas at the RFETS. Therefore, in the case of Pu-239/240 and Am-241, several kriging domains were established. The major domain areas, the Site and the plume, were retained but were further subdivided. Within the Site domain, an area to the north and west of the 903 Pad was defined for kriging. The impact of Pu-239/240 and Am-241 contamination in this area is thought to be significantly less than in the areas to the east of the 903 Pad. This domain was kriged by using samples in the Site domain, but not samples from the plume area, which had Pu-239/240 and Am-241 concentrations orders of magnitudes higher. The remainder of the Site area was kriged as a single unit. The Site variogram models for Pu-239/240 and Am-241 were used in kriging.

Within the plume domain for Pu-239/240 and Am-241, the 903 Pad was defined as a separate domain for kriging. The concentrations and variability of the sample data on the Pad are more extreme than at any other portion of the Site. As such, the 903 Pad was kriged using sample data exclusively from the 903 Pad area and a limited number of samples from the Site domain. The Trench 1 area, also within the plume domain and located north and east of the 903 Pad, has undergone remediation and resurfacing. No actual kriging was performed in the Trench 1 area because these soils were remediated and assigned a background concentration value. The remainder of the plume domain was kriged using the sample data from the plume domain. Both the 903 Pad and plume domains were kriged using the plume variogram models for Pu-239/240 and Am-241.

With the U isotopes, the highest concentrations are found in the Landfill and Ash Pit areas. At least one high concentration sample in each of these areas is on the edge of the sample cluster. As such, this high sample value could be extrapolated hundreds of feet beyond the boundary of

100

the facility. A more likely scenario is that these samples represent localized high concentrations resulting from anthropogenic activities, such as placing wastes in these locations and that the high-level contamination does not extend outside the boundaries of these facilities.

To mitigate the problem of excessive extrapolation or inappropriate extension of data beyond reasonable areas of influence, discrete limiting boundaries were placed around the landfill, ash pit and 903 Pad areas for the U data. High concentration sample data within these boundaries were restricted from being used for estimation beyond the boundaries. These high concentration samples were used, however, to estimate areas inside the facility boundaries.

The kriging performed in each of the five domains of the Site (for Pu-239/240 and Am-241) and the three domains (for the three U isotopes) was done using ordinary kriging of block areas. Block kriging integrates the estimate of the U isotope concentration over the area of the block. Blocks used for kriging measured 22.8 m x 22.8 (75 x 75 ft) in all areas of the Site. Each block represents 523 square meters (m^2) (5625 [ft^2]) in area, or approximately 0.05 hectares (ha) (0.15 acres [ac]). The concentration estimated for each block represents the average expected activity level for the particular U isotope over the entire block.

Kriging Results

Some notable artifacts exist in the maps of the kriged surface soil actinide activities at RFETS (Figure TA-2-8 through Figure TA-2-12), which are related to the sampling density and sampling pattern used at the Site. For Pu-239/240, an area of approximately 202 ha (500 ac) on the west side of the Site exhibits concentrations between 0.1 and 1.0 pCi/g. This feature is the result of limited sampling in the area. Approximately four samples are responsible for this artifact. These samples are located along the road running north then northeast from the Raw Water Reservoir. No other samples exist between these samples and the Site boundary on the west. As such, the concentrations of these samples have a greater influence on the kriged-estimated activity to the west.

Similarly, large areas south of the RFETS facility exhibit Pu-239/240 concentrations between 0.1 and 5.0 pCi/g. These areas were estimated using approximately 10 to 20 samples. A line of four

samples running east-west exists approximately 915 m (3,000 ft) north of the southern Site boundary and a single sample exists south of the boundary. These five samples are highly influential in the estimated concentrations shown on the map, representing approximately 200 ha (500 ac). For Am-241, a smaller area of elevated activity representing approximately 40 ha (100 ac) exists south of the Industrial Area (Figure TA-2-9). This artifact results for the same reason as described for Pu-239/240.

For the U isotopes, the Site domain is generally characterized by relatively low concentrations. Exceptions to this appear near the Original Landfill, Ash Pits and 903 Pad. Table TA-2-8 lists the estimated areas covered by varying concentrations of the different actinides corresponding to the kriged maps.

Table TA-2-8. Estimated Areas for Actinide Concentrations in Surface Soils – Based on Kriging Analysis

Surface Soil Actinide Concentration (pCi/g)	Estimated Area (Hectares)					Estimated Area (Acres)				
	Pu-239/240	Am-241	U-233/234	U-235	U-238	Pu-239/240	Am-241	U-233/234	U-235	U-238
< = 0.01	12.1	88.5	0.0	111.0	0.0	29.8	218.7	0.0	274.3	0.0
0.01 to <= 0.05	105.8	1302.8	0.0	1022.4	0.0	261.4	3219.3	0.0	2526.3	0.0
0.05 to <= 0.1	839.6	383.9	0.0	897.3	0.0	2074.7	948.7	0.0	2217.1	0.0
0.1 to <= 0.5	754.6	434.7	12.7	430.4	30.3	1864.5	1074.2	31.4	1063.4	74.8
0.5 to <= 1.0	201.9	110.7	918.3	46.5	767.7	499.0	273.6	2269.2	114.8	1896.9
1.0 to <= 5.0	382.7	165.9	1572.3	1.4	1706.1	945.7	410.0	3885.1	3.5	4215.8
5.0 to <= 10.0	74.8	10.2	3.1	0.3	2.5	184.8	25.2	7.6	0.6	6.1
10.0 to <= 100.0	7	10.8	2.9	0.8	1.7	323.0	26.6	7.2	2.1	4.1
100.0 to <= 1000.0	6.3	2.1	0.6	0.2	1.3	15.6	5.3	1.4	0.5	3.2
> 1000.0	1.7	0.5	0.2	0.0	0.7	4.1	1.2	0.5	0.0	1.7
Total Area	2510.2	2510.2	2510.2	2510.2	2510.2	6202.6	6202.6	6202.6	6202.6	6202.6

102

TA-2.4 SUB-SURFACE SOIL ACTINIDE CONCENTRATIONS

TA-2.4.1 Background Sub-Surface Soil Actinide Concentrations

Sub-surface soils, as defined in RFCA, are those soils deeper than six inches below the ground surface (DOE, 2000). Background levels of actinide activity in sub-surface soil come from the *Background Geochemical Characterization Report* (EG&G, 1993). These levels are presented in Table TA-2-9. The upper flow system, or UHSU, average background data were used as a comparison with sub-surface soils data. The majority of sub-surface soil samples were collected within or near the Industrial Area that is situated on the Rocky Flats Alluvium.

Table TA-2-9. Background Sub-Surface Soil Actinide Concentrations

Analyte	# of samples	Maximum (pCi/g)	Minimum (pCi/g)	Std. Deviation (pCi/g)	Mean (pCi/g)
Pu-239/240	99	0.03	-0.01	0.01	0.00
Am-241	28	0.01	-0.02	0.01	0.00
U-233/234	99	8.90	0.20	0.93	0.78
U-235	99	0.20	0.00	0.05	0.02
U-238	99	3.20	0.20	0.38	0.73

Note: Negative values due to instrument calibration.

TA-2.4.2 RFCA Action Levels for Sub-Surface Soils

RFCA Tier I and Tier II Action levels for radionuclides in sub-surface soils are equivalent to the corresponding values for surface soil described in TA-2.3.2. To maintain a consistent format for each of the environmental media, values for these Action Levels are presented again in Table TA-2-10.

Table TA-2-10. RFCA Sub-Surface Soil Action Levels

Analyte	Tier I		Tier II [c]
	Industrial Use [a] (pCi/g)	Open Space Use [b] (pCi/g)	(pCi/g)
Pu-239/240	1088	1429	252
Am-241	209	215	38
U-234	1627	1738	307
U-235	113	135	24
U-238	506	586	103

Note: Values for radionuclides in sub-surface soils are equal to the corresponding values in surface soils:

[a] Based on annual dose limit of 15 mrem to an office worker.

[b] Based on an annual dose limit of 85 mrem to a hypothetical future resident.

[c] Based on an annual dose limit of 15 mrem to a hypothetical future resident.

These values apply to single radionuclides only. In order to account for the total dose from multiple radionuclides, sum-of-ratios calculations will be applied to all radionuclides that are present above background. Actual values that trigger actions will therefore likely be lower than the values listed in this table (DOE, 2000).

TA-2.4.3 RFETS Sub-Surface Soil Actinide Figures

Sub-surface soil data are presented in figures that represent horizontal "slices" at six different depth intervals. The intervals are:

- 0.5 to 2 feet;
- 2 to 4 feet;
- 4 to 6 feet;
- 6 to 8 feet;
- 8 to 10 feet; and
- greater than 10 feet.

Therefore, six sub-surface soil figures were created each for Pu-239/240, Am-241, U-233/234, U-235 and U-238 (Figure TA-2-11 and Figure TA-2-47). The multiple figure approach was taken because no pattern was identified in the sub-surface soil data that allowed a simpler data presentation without first analyzing or interpreting the data. At locations where more than one

sample result existed within the same depth interval, the highest sample result was the one displayed on the figure. Table TA-2-11 lists the depth interval and the corresponding figure number for each respective actinide. A more detailed interpretation is provided in TA-4.3.

Table TA-2-11. Table of Sub-Surface Soil Maps

	Depth Interval (feet)					
Actinide	**0.5 - 2**	**2 – 4**	**4 - 6**	**6 - 8**	**8 - 10**	**> 10**
Pu–239/240	Figure TA-2-18	Figure TA-2-19	Figure TA-2-20	Figure TA-2-21	Figure TA-2-22	Figure TA-2-23
Am–241	Figure TA-2-24	Figure TA-2-25	Figure TA-2-26	Figure TA-2-27	Figure TA-2-28	Figure TA-2-29
U–233/234	Figure TA-2-30	Figure TA-2-31	Figure TA-2-32	Figure TA-2-33	Figure TA-2-34	Figure TA-2-35
U–235	Figure TA-2-36	Figure TA-2-37	Figure TA-2-38	Figure TA-2-39	Figure TA-2-40	Figure TA-2-41
U–238	Figure TA-2-42	Figure TA-2-42	Figure TA-2-43	Figure TA-2-44	Figure TA-2-45	Figure TA-2-46

Note: All Figures at back of Section TA-2.

The sub-surface soil figures show the surface water drainage sub-basins and the surface water monitoring stations to facilitate analysis of the surface water actinide transport pathway. All of the sub-surface soil figures have a histogram in the legend that shows the actinide-concentration distribution of sub-surface soil sample results displayed in the figure. Reference values are provided for the analytical Required Detection Limit (RDL) and relevant background concentrations in sub-surface soil.

A description of the database query process used to gather and generate the sub-surface soil data set is presented in Section TA-2.4.4.

TA-2.4.4 Sub-Surface Soil Data Query Process

A Site-wide sub-surface soil data set was created specifically for this report. It was developed from data archived in SWD using multiple queries that are briefly summarized below. The Structured Query Language (SQL) code written to perform the queries is contained on the CD-ROM included with this Technical Appendix.

Initial queries were performed to link SWD sub-surface sample locations, analytical results and sample event information. Sub-surface samples were defined as those collected at depths of 152 mm (6 in) or greater. These initial queries created a preliminary sub-surface soil data set.

Sample results with a data qualifier code of "R", indicating a rejected analytical result, were excluded from the data set (see Table TA-2-1). Subsequent queries were performed on the remaining, non-rejected data set to eliminate laboratory quality assurance sample results, such as rinsates and blanks. Sample results with analytical units inconsistent with soil samples were also eliminated from the data set. For example, a sub-surface soil sample result with units of pCi/L indicated a water sample was pulled from the sub-surface sampling location. Such a result was eliminated during the query process.

All sub-surface soil records in the SWD location table are in pairs with a record at a given location for top depth of the sample and a record for bottom depth. The average depth for each of these sample pairs was calculated and stored in a new field of the data set for this report.

Six queries were run to create separate tables for Pu-239/240, Am-241, U-233/U234, U-235, U-238 and Total U. Review of the new tables revealed some records with the same x-y coordinates and within the same depth interval. In these cases, the sample with the highest concentration was selected for display on the applicable figure. A final table was developed to merge the sample locations and analytical results for all the accepted actinide data. This table was used to generate the sub-surface soil figures (Figure TA-2-18 through Figure TA-2-47).

TA-2.4.5 Sub-Surface Soil Data Description

A total of 972 Pu-239/240, 971 Am-241, 991 U-233/234, 988 U-235 and 991 U-238 sub-surface soil samples met the acceptance criteria discussed in TA-2.4.4 and were used to evaluate sub-surface soil actinide concentrations across the Site. Summary statistics for the sub-surface soil sample data set are shown in Table TA-2-12.

106

Table TA-2-12. Summary Statistics for Sub-Surface Soil Data Set

Statistic	Actinide				
	Pu-239/240 (pCi/g)	Am-241 (pCi/g)	U-233/234 (pCi/g)	U-235 (pCi/g)	U-238 (pCi/g)
Number of Sample Data	972	971	991	988	991
Minimum	-0.014	-0.055	0.021	-0.019	0.000
Maximum	1744.000	208.700	971.000	67.610	1210.000
Mean	3.373	0.648	3.787	0.266	7.672
Std. Deviation	60.049	8.354	34.996	2.684	70.435
Median	0.010	0.008	0.934	0.047	0.963

Note: Negative results due to instrument calibration

In summary, the sub-surface soil data sets do not include sample results with a rejected data qualifier. The remaining non-rejected samples were utilized, including those sample results that were not validated. In cases where multiple samples had the same x-y coordinates and were within the same depth interval, the sample result with the highest concentration was selected for display on the figure.

TA-2.5 SEDIMENT ACTINIDE CONCENTRATIONS

TA-2.5.1 Background Sediment Actinide Concentrations

Background values for actinide activities in sediments are from the *Background Geochemical Characterization Report* (EG&G, 1993). These values are presented in Table TA-2-13.

Table TA-2-13. Background Sediment Actinide Concentrations

Analyte	# of samples	Maximum (pCi/g)	Minimum (pCi/g)	Std. Deviation (pCi/g)	Mean (pCi/g)
Pu-239/240	42	2.36	0.00	0.59	0.17
Am-241	35	0.82	-0.01	0.19	0.07
U-233/234	47	4.50	0.14	1.15	1.68
U-235	49	0.19	0.00	0.05	0.06
U-238	36	3.82	0.13	1.03	1.40

Note: Negative values due to instrument calibration.

107

TA-2.5.2 RFCA Action Levels

RFCA Tier I and Tier II Action Levels for radionuclides in sediments are equal to the corresponding values for surface soil described in TA-2.3.2. To maintain a consistent format for each of the environmental media, values for these Action Levels are presented again in Table TA-2-14.

Table TA-2-14. RFCA Sediment Action Levels

Analyte	Tier I		Tier II [c]
	Industrial Use [a] (pCi/g)	Open Space Use [b] (pCi/g)	(pCi/g)
Pu-239/240	1088	1429	252
Am-241	209	215	38
U-234	1627	1738	307
U-235	113	135	24
U-238	506	586	103

Notes:

Values for radionuclides in sediments are equal to the corresponding values in surface soil:

[a] Based on annual dose limit of 15 mrem to an office worker.

[b] Based on an annual dose limit of 85 mrem to a hypothetical future resident.

[c] Based on an annual dose limit of 15 mrem to a hypothetical future resident.

These values apply to single radionuclides only. In order to account for the total dose from multiple radionuclides, sum-of-ratios calculations will be applied to all radionuclides that are present above background. Actual values that trigger actions will therefore likely be lower than the values listed in this table.

TA-2.5.3 RFETS Sediment Actinide Figures

Figure TA-2-48 through Figure TA-2-52 display results of sediment sampling for Pu-239/240, Am-241, U-233/234, U-235 and U-238, respectively. The sediment figures show the surface water drainage sub-basins and the surface water monitoring stations to facilitate analysis of the surface water actinide transport pathway. All of the sediment figures have a histogram in the legend that shows the actinide-concentration distribution of sediment sample results displayed.

Reference values for each actinide are provided for background concentrations in sediment, analytical Required Detection Limit (RDL) and RFCA Tier I and Tier II Action Levels.

A description of the query process used to generate the sediment data set is presented in Section TA-2.5.4.

TA-2.5.4 Sediment Data Query Process

A Site-wide sediment data set was created specifically for this report. It was developed from data archived in SWD using multiple queries that are briefly summarized below. The Structured Query Language (SQL) code written to perform the queries is contained on the CD-ROM included with this Technical Appendix.

Initial queries were performed to link SWD sediment sample locations, analytical results and sample event information. This created a preliminary sediment data set. Sample results with a data qualifier code of "R", indicating a rejected analytical result, were excluded from the data set (see Table TA-2-1). Subsequent queries were performed on the remaining, non-rejected data set to eliminate laboratory quality assurance sample results, such as rinsates and blanks. Sample results with analytical units inconsistent with soil samples were also eliminated from the data set. For example, a soil sample result with units of pCi/L indicated a water sample was pulled from the sub-surface sampling location. Such a result was eliminated during the query process.

Non-validated sediment data were not used, even if not rejected, because the ratio of rejected to validated data was quite high, nearly 28 %, thereby diminishing the confidence in non-validated sediment results. Therefore only validated data, as designated by a "V" data qualifier code (see Table TA-2-1), were accepted for further consideration. However, validated results with problems, as denoted in the Validation Reason Codes field of the database where validated data are further qualified, were also excluded from the data set. Following these queries, the resulting records included only validated samples that met the acceptance criteria for this sediment data set.

The remaining sediment data contained several locations where multiple samples were collected at different times. The sample with the maximum actinide concentration was used for display on the figure in these cases. A regression analysis was run on all sediment sampling locations where three or more Pu-239/240 samples were collected to evaluate if temporal trends were evident at any of these locations. Of the eighteen locations where more than three samples were collected at different times, three passed a two-sided student's t-test (alpha of 95 % with the hypothesis of x coeffcient <> 0). These three locations showed a small increase in Pu-239/240 concentration over time. The remaining 15 locations did not display a meaningful trend in Pu-239/240 concentration, either increasing or decreasing, over time.

TA-2.5.5 Sediment Data Description

A total of 143 Pu-239/240, 137 Am-241, 132 U-233/234, 131 U-235 and 132 U-238 sediment samples met the acceptance criteria discussed in TA-2.5.4 and were used to evaluate sediment actinide concentrations across the Site. Summary statistics for the sediment sample data set are shown in Table TA-2-15.

Table TA-2-15. Summary Statistics for Sediment Data Set

Statistic	Actinide				
	Pu-239/240 (pCi/g)	Am-241 (pCi/g)	U-233/234 (pCi/g)	U-235 (pCi/g)	U-238 (pCi/g)
Number of Sample Data	143	137	132	131	132
Minimum	-0.008	0.000	0.380	-0.013	0.310
Maximum	643.400	389.400	25.220	1.302	43.090
Mean	20.228	9.408	2.326	0.127	3.226
Std. Deviation	85.991	41.986	3.498	0.210	5.804
Median	0.19	0.07	1.19	0.06	1.29

Note: Negative results reported due to calibration

110

In summary, the sediment data sets do not include sample results with a rejected data qualifier. Non-rejected sediment data that were not validated were also not used. Validated results with problems, as denoted in the Validation Reason Codes field of the SWD database, were also excluded from the data set. In cases where multiple samples had the same x-y coordinates and were collected at different times, the sample result with the highest concentration was selected for display on the applicable figure.

TA-2.6 BUILDING MATERIAL ACTINIDE CONCENTRATIONS

TA-2.6.1 Background Building Material Actinide Concentrations

The amount of anthropogenic radioactivity is an essential factor in characterizing, classifying and demolishing facilities and making unrestricted release decisions (Kaiser-Hill, 2002). A 2002 Site study compiled data on building materials for the purpose of collecting radiological background measurement in locations not impacted by RFETS activities (Kaiser-Hill, 2002). These areas have been established and qualified by an initial examination process and include on-Site and off-Site locations with no histories of radiological contamination or impact due to radiological operations. The background reference areas analyzed have been approved by the *Radiological Background Determination Plan*, April 2000 (Kaiser-Hill, 2002).

Background alpha activities for six different building materials are presented in Table TA-2-16 below. On-Site and off-Site sampling results are presented collectively.

Generally, thirty or more data points are accepted when defining statistical distribution characteristics, and therefore it is recommended that background values be derived from data sets containing 30 or more measurements. Ultimately, the results indicate on-Site distributions are lower than off-Site distributions, thus there is no positive bias due to anthropogenic activity (Kaiser-Hill, 2002).

Table TA-2-16. Combined Total Surface Activity Data Summary

Location	On-Site or Off-Site	Year of Construction	Number of Measurements	Mean (pCi/100cm^2) (alpha)	Standard Deviation (pCi/100cm^2) (alpha)
Asphalt and Tar					
Building 334	On-Site	1953	30	23.7	7.2
National Wind Technology Center	Off-Site	1981	15	1.9	3.8
National Renewable Energy Laboratories	Off-Site	1984	15	25.6	8.2
Asphalt Shingle					
Building 130	On-Site	1985	30	25.5	7.9
Brick					
Building 131	On-Site	1987	30	9.3	4.5
Federal Center 25	Off-Site	1941	15	19.4	5.9
Ceramic Tile					
Building 112	On-Site	1953	15	18.7	5.0
Building 130	On-Site	1985	15	22.9	8.2
National Wind Technology Center	Off-Site	1981	15	7.1	5.5
National Renewable Energy Laboratories	Off-Site	1984	15	8.8	6.8
Federal Center 25	Off-Site	1941	15	29.9	5.9
Cinder Block (Bare)					
National Wind Technology Center	Off-Site	1981	30	13.7	5.7
National Renewable Energy Laboratories	Off-Site	1984	15	1.1	2.6
Federal Center 25	Off-Site	1941	15	15.5	4.8

Table – Page 1 of 3

112

Table TA-2-16. Combined Total Surface Activity Data Summary (continued)

Location	On-Site or Off-Site	Year of Construction	Number of Measurements	Mean (pCi/100cm^2) (alpha)	Standard Deviation (pCi/100cm^2) (alpha)
Cinder Block (Bare)					
National Wind Technology Center	Off-Site	1981	30	13.7	5.7
Building 112	On-Site	1953	15	2.7	4.7
Building 121	On-Site	1983	30	11.9	4.3
Building 130	On-Site	1985	15	5.1	5.6
National Wind Technology Center	Off-Site	1981	30	10.0	8.0
National Renewable Energy Laboratories	Off-Site	1984	15	4.8	5.3
Federal Center 25	Off-Site	1941	15	3.6	3.3
City of Arvada Purchasing/ Receiving Bldg.	Off-Site	1956	30	7.5	5.7
Concrete (Bare)					
Building 060	On-Site	1988	15	15.9	5.3
Building 120	On-Site	1986	15	19.0	5.2
Building 131	On-Site	1987	15	5.4	3.5
Building 335	On-Site	1970	15	5.8	5.0
National Renewable Energy Laboratories	Off-Site	1984	30	7.7	6.8
Federal Center 25	Off-Site	1941	15	16.4	10.9
City of Arvada Purchasing/ Receiving Bldg.	Off-Site	1956	30	19.9	6.1

Table – Page 2 of 3

Table TA-2-16. Combined Total Surface Activity Data Summary (continued)

Location	On-Site or Off-Site	Year of Construction	Number of Measurements	Mean (pCi/100cm^2) (alpha)	Standard Deviation (pCi/100cm^2) (alpha)
Concrete (Painted)					
Building 111	On-Site	1953	15	7.3	5.3
Building 334	On-Site	1953	30	4.2	5.7
Building 864	On-Site	1953	15	2.6	3.6
National Wind Technology Center	Off-Site	1981	15	1.3	3.4
National Renewable Energy Laboratories	Off-Site	1984	15	4.0	4.1
Federal Center 25	Off-Site	1941	15	1.3	2.2

Source: Kaiser-Hill, 2002

Table – Page 3 of 3

TA-2.6.2 Underground Building Contamination Analysis

UBC data are not as comprehensive as other actinide data presented in this report. A preliminary characterization of the potential UBC near and inside Building 771 is provided in the soil and groundwater analytical results. (RFETS, 2001).

Building 771 was selected to present UBC data based on its historical building operations. In 1953, operations included machining processes, coating inspections, radiography, residue and metal recovery, chemistry and metallurgy research and development and laboratory analysis. Building 771 potential for UBC contamination is based upon HRRs and Annual Update documents. These data sources were used to select biased sample location inside Building 771 and identify potential contaminants for sample analysis in support of UBC characterization. Soil samples were collected beneath the foundation slab and from 13 locations along the inside perimeter of the building and three locations were sampled inside the building. The sixteen sample locations are specified in Table TA-2-17.

114

Table TA-2-17. Building 771 UBC Sampling Specifications and Rationale

Location	Relative Location Description**	Sampling Purpose	Sampling Technique	Sample Depth Intervals (Each Location)*	Comments
1	SE corner, Bldg. 771	Inside Perimeter Characteri-zation	Manual Soil Auger	1) 0 to 2.0 ft. 2) 2.0 to 4.0 ft.	Room 181A; Fire/Spill related releases
2	SE corner, Bldg. 771				Corridor E; Area flooded during Building 776 fire and water line break, located near building sump
3	SE corner, Bldg. 771				Room 182; Fire/Spill related releases
4	S.-side, center Bldg. 771				Room 182; Fire/Spill related releases
5	SW corner, Bldg. 771				Room 182A; Flood area from Building 776 fire
6	SW corner, Bldg. 771				Building 776/771 tunnel airlock; Conduit for Building 776 fire and water line break
7	SW corner, Bldg. 771				Room 184; Former storage vault
8	NW corner, Bldg. 771				Room 187; Former storage vault
9	NW corner, Bldg. 771				Room 188; Former SNM storage vault, early releases
10	NW corner, Bldg. 771	Interior Building Characteri-zation			Room 165; Wall and foundation contaminated by 1957 fire
11	SE corner, Bldg. 771				Room 149; Void space beneath building slab
12	NE corner, Bldg. 771				Room 114; West side of infinity room, multiple spills of Pu and Pu/beryllium
13	NE corner, Bldg. 771	Inside Perimeter Characteri-zation			Room 146B; Multiple nitric acid spills
14	NE corner, Bldg. 771				Room 146C; Multiple nitric acid spills
15	NW corner, Bldg. 771				Corridor H; Near Plenum Deluge Catch Tank
16	NE corner, Bldg. 771				Corridor G; East of Room 141/Elevator shaft

Source: Kaiser-Hill, 2001b.

*With the exception of locations, 4 and 6 as noted in Section 3.1 of Kaiser-Hill, 2001b.
**Sample locations on southern half of Building 771.

115

Alpha spectrometry was used for soil and groundwater radiological analysis. Background soil and groundwater sampling results are included in Table TA-2-18 and Table TA-2-19 below. Groundwater samples were taken at locations 3, 6, 14 and 16.

Table TA-2-18. Building 771 UBC, Soil Sampling Results

Analyte	Mean	Min	Max	S.D.	Bkgd	Tier I Action Level	Tier I I Action Level	# of samples	# of non-detects	# of detects	Units
Radionuclides											
Pu-239/240	4.98	0	157	27.74	0.02	1429	252	32	19	13	pCi/g
Am-241	0.42	0	12.8	2.26	0.02	215	38	32	25	7	pCi/g
U-233,234	1.28	0.68	2.1	0.38	2.64	1738	307	32	0	32	pCi/g
U-235	0.03	0	0.5	0.1	0.12	135	24	32	27	5	pCi/g
U-238	1.11	0.64	1.9	0.28	1.49	586	103	32	0	32	pCi/g

Table TA-2-19. Building 771 UBC, Groundwater Sampling Results

Analyte	Mean	Min	Max	S.D.	Tier I Action Level	Tier I I Action Level	# of samples	# of non-detects	# of detects	Units
Radionuclides										
Pu-239/240	0.283	0	0.535	0.27	15.1	0.151	4	1	3	pCi/L
Am-241	0.1285	0	0.309	0.15	14.5	0.145	4	2	2	pCi/L
U-233,234	5.35	2.08	8.85	3.78	106	1.06	4	0	4	pCi/L
U-235	0.2597	0	0.467	0.24	101	1.01	4	1	3	pCi/L
U-238	4.0675	1.21	7.35	3.06	76.8	0.768	4	0	4	pCi/L

Shaded result exceeds Tier II Action level for Groundwater.

116

The soil sample results did not exceed the RFCA Tier I Action Levels for subsurface soil. Action Levels do not exist specifically for building materials such as contaminated floor slabs or foundations. Groundwater sampling results indicate Pu-239/240, Am-241, U-233/234, U-235 and U-238 were detected above Tier II Action Levels at locations 6 and 16. U-233/234 and U-238 were detected above the Tier II Action Levels in locations 3 and 14. Generally, the highest frequency of actinide exceedances occurred at location 16. Findings imply the locations and depths of the contaminants do not suggest a definitive point source of contamination or a potential source location because the Tier II exceedances observed in groundwater are from locations where surrounding soils and below action levels. Additionally, there is no apparent correlation between groundwater contaminant location, type or magnitude with any soil contaminant location, type or magnitude (RFETS, 2001).

TA-2.7 SURFACE WATER ACTINIDE CONCENTRATIONS

TA-2.7.1 Background Surface Water Actinide Concentrations

Background levels for actinide activity in surface water are from the *Background Geochemical Characterization Report* (EG&G, 1993). These levels are presented in Table TA-2-20.

Table TA-2-20. Background Surface Water Actinide Concentrations

Analyte	# of samples	Maximum (pCi/L)	Minimum (pCi/L)	Std. Deviation (pCi/L)	Mean (pCi/L)
Pu-239/240	105	0.05	-0.02	0.01	0.00
Am-241	106	0.04	-0.02	0.01	0.00
U-233/234	79	3.21	-0.01	0.55	0.49
U-235	75	0.38	-0.03	0.07	0.05
U-238	55	1.82	0.00	0.43	0.36

Note: Negative values due to instrument calibration.

117

TA-2.7.2 RFCA Action Levels

RFCA Action Levels are defined in Attachment 5 of RFCA (DOE, 2000). For Pu and Am, the surface water Action Levels are based on a 1.0 x 10^{-6} increased carcinogenic risk to human health from direct exposure including consumption. For U, the Action Level is the Site-specific standard found in Table 2 of 5, Colorado Code of Regulations (CCR) 1002-8, §3.8.0. It should be noted that, in contrast to soils the action level for U in surface water is not isotope-specific, but rather is for total U.

Table TA-2-21. RFCA Surface Water Action Levels

Analyte	Woman Creek [a] pCi/L	Walnut Creek [a] pCi/L	Temporary Modifications	Basis
Pu-239/240	0.15	0.15	[b]	BS
Am-241	0.15	0.15	[b]	BS
U, Total	11	10		SS

Notes:

[a] The values in this table reflect the classifications and standards approved by the WQCC effective March 2, 1997. Radiologic parameters are distinguished by drainage basin in Table 2 of 5 CCR 1002-38. All values apply as standards in Segments 4a and 4b and as Action Levels in Segment 5.

[b] The narrative temporary modification for Am and Pu in Segment 5 of Walnut Creek is that concentration that is consistent with attaining the numerical water quality standards in segment 4(b) of Big Dry Creek. These temporary modifications are effective June 30, 1999 and expire December 31, 2000.

ACRONYMS: BS=Basic Standard; SS=Site-Specific Standard

TA-2.7.3 RFETS Surface Water Actinide Figures

For each of the actinides of interest, data are presented from Water Years 1997 through 1999. A Water Year is defined as October of the previous year through September. For example, Water Year 1997 runs from October 1, 1996 through September 30, 1997. Data were plotted to represent the spatial and temporal variability of the different actinides in surface water at RFETS. A unique surface water figure was created for Pu-239/240, Am-241, U-233/234, U-235 and U-238 (Figure TA-2-53 through Figure TA-2-57, respectively).

118

The actinide load at a particular surface water monitoring station is a function of both the actinide concentration in the water and the volume of water (yield) at the station. For example, a station with low actinide concentration can transport a greater actinide load than another station with higher concentration if the first station has a greater water yield. Even fallout background concentrations in the eroded soil and transported sediment can result in elevated surface water actinide activity if there is significant enrichment or if the sediment loads in transport increase. This illustrates why both the actinide loads and water yields must be compared simultaneously to evaluate the transport of actinides through the Site watersheds. Therefore, for each actinide and at each monitoring location, data are presented for actinide load, water yield and actinide concentration in the surface water.

The surface water figures present data for eight different surface water monitoring locations. These include:

- Three POE monitoring stations located east of the Industrial Area but upstream from the detention ponds (SW093, GS10 and SW027);
- Three POC monitoring stations located downstream from the detention ponds (GS11, GS08 and GS31); and
- Two POC monitoring stations located at the RFETS eastern boundary along Indiana Street (GS01 and GS03).

For each surface water monitoring location, a pair of charts displays the surface water actinide data. Surface water actinide load data are located on the upper chart of each pair. Water yield and surface water actinide concentration data are located on the lower chart of each pair. Further details on these three types of surface water data, presented for each actinide and for each monitoring location, are provided below:

- Actinide loads (measured in pCi) are calculated using a water-volume weighted methodology and presented in graphs for each Water Year from 1997 through 1999. An average of the actinide loads from Water Years 1997 through 1999 is also depicted by a gray arrow at each

monitoring station site. The arrows are sized proportionately to the size of the average annual actinide load. Hence, a large arrow indicates a greater average annual actinide load than a smaller arrow. At locations where the average annual actinide load is relatively low, the arrow may be so small that it is barely visible. Annual actinide loads for Water Years 1997 through 1999 are presented in the corresponding yellow bar charts for each monitoring location. Further detail on the surface water data collection methods and the computation of actinide loads is presented in TA-2.7.4;

- Average annual actinide concentrations in surface water (measured in pCi/L) are plotted in bar graphs for each Water Year from 1997 through 1999. In addition, an average actinide concentration in surface water for Water Years 1997 through 1999 is also included on each of the bar graphs. All of the actinide concentration data for surface water is shown as a green bar that references the right-hand vertical axis. This data are on the bottom chart for each of the surface water monitoring locations; and

- Annual water yields (measured in liters) are plotted in bar graphs for each Water Year from 1997 through 1999. In addition, an average of the annual water yields for Water Years 1997 through 1999 is also included on the bar graph. All of the water yield data are shown as a blue bar that references the left-hand vertical axis. These data are on the bottom chart for each of the surface water monitoring locations.

A description of RFETS surface water sampling methods and protocols is provided in Section TA-2.7.5.

TA-2.7.4 Surface Water Data Query Process

Surface water sample data for Water Years 1997 through 1999 that are presented in this report were retrieved from a preliminary data set stored and maintained by the Kaiser-Hill Environmental Media Management organization and simultaneously archived in SWD. A reconciliation process to confirm that the preliminary data set matches the SWD data set is being

120

conducted by the Kaiser-Hill Media Management organization. Data quality criteria applied to the surface water data presented in this report are described below.

Sample results with a data qualifier code of "R", indicating a rejected analytical result, were excluded from the data set (see Table TA-2-1). Subsequent queries were performed on the remaining, non-rejected data set to eliminate laboratory quality assurance sample results, such as rinsates and blanks. The remaining non-rejected samples were included in the data set, of which approximately 25 % were validated. Additional samples were validated in those cases where the result was used to calculate reportable RFCA 30-day moving average values.

With the accepted data, any field duplicate or re-run, laboratory results were averaged with the original sample result. When the accepted result was reported as a negative value, due to instrument calibration, a value of 0.0 pCi/L was used for actinide load calculations. In certain instances, the surface water actinide load at a specific location and for a specific time period was estimated by the Kaiser-Hill Media Management organization. Examples of these cases were when an insufficient sample quantity was collected because of automated sampler malfunction or when a sample was analyzed but rejected in the analytical quality control process.

Further details on the methodology used to collect surface water data presented in this report are discussed in Section TA-2.7.5.

TA-2.7.5 Surface Water Data Description

Only continuous flow-paced samples at POE and POC monitoring locations were used to evaluate Site-wide surface-water actinide transport in this section of the report. These stations are GS01, GS03, GS11, GS08, GS31, SW027, SW093 and GS10 (Figure TA-1-1). These data were selected because all of the samples were collected using the same continuous flow-paced sampling protocol throughout the year. Therefore, they are the most appropriate data available for comparing "apples to apples" in terms of actinide and water yields at different monitoring locations. Data collected prior to 1997 for non-RFCA monitoring programs are still considered

121

valid, valuable information, but are less suitable for estimating actinide loads because different sampling protocols were used.

A total of 537 Pu-239/240, 537 Am-241 and 348 U-233/234, U-235 and U-238 surface water samples from eight monitoring locations met the acceptance criteria discussed in TA-2.7.4. These samples were used to evaluate surface water actinide concentrations and loading at RFCA POE and POC monitoring stations across the Site. Summary statistics for the surface water sample data set are shown in Table TA-2-22.

Table TA-2-22. Summary Statistics for Surface Water Actinide Data Set

Statistic	Actinide				
	Pu-239/240 (pCi/L)	Am-241 (pCi/L)	U-233/234 (pCi/L)	U-235 (pCi/L)	U-238 (pCi/L)
Number of Sample Data	537	537	348	348	348
Minimum	0.000	0.000	0.045	0.000	0.039
Maximum	1.910	2.210	2.900	0.235	3.960
Mean	0.049	0.041	1.232	0.054	1.329
Std. Deviation	0.147	0.150	0.581	0.034	0.678
Median	0.009	0.009	1.148	0.050	1.195

In summary, the surface-water data sets do not include sample results with a rejected data qualifier. The remaining non-rejected samples were utilized, including those sample results that were not validated.

Description of Surface Water Monitoring Programs

RFETS surface-water monitoring data are collected by the Site's automated surface-water monitoring program for implementation of the *Rocky Flats Cleanup Agreement* (DOE, 2000) in accordance with the *RFETS Integrated Monitoring Plan (IMP) Background Document* (Kaiser-Hill, 2000c). The IMP provides a framework for monitoring in support of activities at the Site.

122

This framework includes implementation of a high-resolution surface-water monitoring program that supports data-driven decisions determined by the IMP Data Quality Objectives (DQO) process.

This monitoring program is intended to provide:

- Monitoring of multiple parameters for the safe and effective operation of the Site detention ponds;
- Monitoring of flows and contaminant levels in sub-drainages to allow for the location of contaminant sources;
- Monitoring of various surface-water parameters at various locations on an Ad Hoc basis in support of special projects and/or building operations;
- Monitoring of Pu and Total Suspended Solids (TSS) values at various locations to determine a correlation between Pu and TSS;
- Detection of a release of contaminants from specific high-risk projects within the Industrial Area;
- Detection of statistically significant increases of contaminants in runoff from within the Industrial Area in general;
- Detection of contaminants exceeding RFCA Action Levels in discharges entering Stream Segment 5 and the Site detention ponds;
- Detection of contaminants exceeding RFCA Standards in discharges entering Stream Segment 4;
- Monitoring of indicator parameters in discharges leaving the Site boundary as a prudent management action; and

- Monitoring of flows and water-quality in the Buffer Zone for ecological and water rights issues, as well as supporting studies into the interaction between media.

Each surface water monitoring location is equipped with automated instrumentation capable of satisfying the location-specific data collection requirements. Precipitation data are collected at additional locations as a prudent management practice. At POC and POE monitoring locations, continuously recording water-quality probes also collect water-quality parameter data, such as temperature, pH, conductivity, turbidity and nitrate concentration.

Water-Quality Sample Collection

Continuous Flow-Paced Composite Samples. The automated monitoring equipment includes continuously recording flow meters linked to automatic water samplers. Gaging station GS10, which measures flow and collects samples from Industrial Area runoff on South Walnut Creek, is shown in Figure TA-2-58. The flow meters measure the stage (i.e., depth) of the stream water in/on a measurement device such as a flume or weir. The flow meter converts the measured stage into a discharge value (e.g., cubic feet per second).

The samplers are programmed to collect 200-mL grab samples at specified intervals of flow. Thus the samples are weighted by the flow or are "flow-paced." The sampler composites the grab samples in a 15- or 22-Liter Nalgene™ carboy container. In other words, one grab sample is collected in the carboy each time a specified volume of stream discharge is measured by the flow meter. Figure TA-2-59 displays an example of flow-paced grab samples collected for every 4,390 cubic feet of stream discharge for a continuous flow-pacing sampling event. The chosen flow pace depends on expected stream discharge, the composite volume desired and the desired composite sampling time period.[1] The flow-pacing is changed consistent with seasonally changing hydrologic conditions. At each monitoring station, the automatic sampler collects the

[1] The Site IMP specifies the targeted composite sample collection frequency for each monitoring location.

grab samples by pumping the stream water through an intake that is installed in a fixed position at a location where the stream is appears to be well-mixed.

Continuous flow-paced composite samples are collected during all flow conditions, every day, throughout the year. When a composite sample is removed from the sampler for analysis, the next carboy container is placed in the sampling unit to begin collecting composite samples immediately.

Ideally, by flow-pacing composite samples and effectively collecting more frequent grabs during higher flow rates, an analytical result (concentration [e.g., mg/L] or activity [e.g., pCi/L]) that is representative of the entire sampling period is obtained. This result can then be used with the corresponding discharge volume to calculate a constituent load. This sampling protocol is currently used for many different purposes, including POCs and POEs. For this report, data from POCs and POEs are evaluated to identify actinide transport in Site surface waters.

Storm-Event Rising-Limb Flow- or Time- Paced Composite Samples. Storm-event, rising-limb, flow- and time- paced samples are composite samples collected during the initial "first flush" conditions during a direct runoff event or during the entire runoff event.[2] The storm-event samplers are programmed to wait for direct runoff conditions at all times year-round. When the flow meter measures a predetermined increase in stream stage (manually set as the sampler "enable level")[3], the sampler begins collecting grab samples. Although the samplers are programmed to collect composite samples for all runoff events, only selected composite samples are retained for analysis. Professional judgement is used to select representative samples for analysis.[4] When a composite sample is removed from the sampler to be submitted for analysis

---

[2] For locations that have flow measurement capabilities, flow-paced composite samples are collected. Locations without flow measurement collect time-paced composite samples.

[3] The enable level is chosen based on professional judgment, considering the seasonal runoff conditions expected for a particular location. The intent is to begin sampling at the first indication of direct runoff. This can either be some level above normal baseflow, or when an ephemeral location first measures runoff.

(or to be discarded), a clean sample container is installed and the sampler is reset to wait for the next runoff event.

A composite sample generally consists of 15 grab samples[5], which are flow-, or time- paced. In other words, one grab sample is collected in the sample bottle each time a specified volume of stream discharge is measured by the flow meter or at uniform time intervals. Figure TA-2-59 shows a hydrograph during a rising-limb storm-event sample that received a grab sample for every 200 cubic feet of stream discharge. The chosen flow- or time- pace depends on expected stream discharge during the rising limb of the hydrograph, such that all the 15 grab samples are collected during the rising limb.

TA-2.8 GROUND WATER ACTINIDE CONCENTRATIONS

TA-2.8.1 Background Groundwater Actinide Concentrations

Background actinide activity-concentrations have been determined for groundwater in two documents, the *Background Geochemical Characterization Report* (EG&G, 1993) and the *Draft Background Comparison for Radionuclides in Groundwater* (RMRS, 1996). The difference between these mean background values lies mainly with the well sets used for the calculations. The EG&G data use a flow system approach (UHSU and LHSU) and the RMRS data use a geologic unit approach (UHSU alluvium only). RMRS (1996) reevaluated groundwater radionuclide data from the period 1990 to 1995 in response to CDPHE concerns that the original EG&G UHSU U isotope background values were unrepresentative of alluvial groundwater quality. For this analysis, wells completed in the weathered bedrock component of the UHSU

---

[4] The intent is to collect samples according to the sampling frequencies targeted by the IMP. For many of the current locations, this frequency is one per month. Samples are also selected for analysis with the intent to sample a range of rising-limb runoff rates, extreme events (i.e., very large precipitation events) and events where samplers at multiple locations enabled for the same runoff event.

[5] Current grab sample volume for storm-event rising limb flow-paced composite samples is 500-1000mL. This location-specific volume is chosen to obtain the required volume of sample based on the location-specific analyte suites.

were omitted from the data set and new values were calculated for UHSU alluvium only. This reanalysis produced similar U background values compared to those calculated by EG&G. The RMRS values are currently used in favor of the EG&G values for comparisons involving UHSU groundwater. Table TA-2-24 contains the results of calculations for background actinide concentrations presented in both reports.

There are two primary techniques practiced for measuring isotopic ratios; alpha spectrometry and ICP/MS. The ICP/MS analytical method is more accurate in determining U species than the standard alpha spectrometry analysis done at RFETS. ICP/MS calculates an isotopic mass as opposed to an activity, which is measured by alpha spectrometry. Count time and masking effects likely influence the alpha spectrometry results. ICP/MS allows for the differentiation between anthropogenic U sources and natural-occurring, background U. Additionally, detection limit ranges for the two techniques are noticeably different. Table TA-2-23 provides a comparison.

Table TA-2-23. Alpha Spectrometry and ICP/MS Detection Limit Range

U Isotope	Alpha Spectrometry Required Detection Limit Range (pCi/L)	ICP/MS Instrument Detection Limit Range (µg/L)
U-234	1.0	0.000015 – 0.000033
U-235	1.0	0.000030 – 0.000031
U-236	- -	0.0000035 – 0.0000071
U-238	1.0	0.00095 – 0.00135

Sample and data collection followed *the Rocky Flats ER Program Standard Operating Procedures* (Rockwell International, 1989a) and the *ER Program Quality Assurance (QA)/QC Plan* (Rockwell International, 1989b). The Environmental Management Department (EMD) Standard Operating Procedures (EG&G, 1991a) and the Rocky Flats Plant Site-Wide QA Project

127

Plan (EG&G, 1991b) superceded those documents. It is assumed the filter technique followed a Site-wide standard using a 0.45-micron filter. Table TA-2-24 present filter and unfiltered data.

Table TA-2-24. Background Groundwater Actinide Concentrations

Analyte[3]	Unit	# of samples	Maximum (pCi/L)	Minimum (pCi/L)	Std. Deviation (pCi/L)	Mean (pCi/L)
Pu-239/240, unfiltered[1]	UHSU	194	0.22	-0.01	0.02	0.00
Am-241, unfiltered[1]	UHSU	183	0.10	-0.01	0.01	0.01
U-233/234, 0.45-µm filtered[1]	UHSU	205	199.5	-0.02	23.94	6.23
U-235, 0.45-µm filtered[1]	UHSU	207	4.80	-0.04	0.64	0.20
U-238, 0.45-µm filtered[1]	UHSU	176	135.60	-0.04	17.71	4.77
Pu-239/240, unfiltered[2]	UHSU Alluvium	289	0.224	-0.005	0.021	0.005
Am-241, unfiltered[2]	UHSU Alluvium	275	0.19	-0.02	0.015	0.006
U-233/234, 0.45-µm filtered[2]	UHSU Alluvium	287	199.5	-0.078	27.1	6.55
U-235, 0.45 µm filtered[2]	UHSU Alluvium	288	5.353	-0.035	0.780	0.0233
U-238, 0.45-µm filtered[2]	UHSU Alluvium	286	135.6	-0.04	18.6	4.60
Pu-239/240, unfiltered[1]	LHSU	48	0.05	-0.00	0.01	0.00
Am-241, unfiltered[1]	LHSU	43	0.10	-0.00	0.02	0.01
U-233/234, 0.45-µm filtered[1]	LHSU	57	15.33	-0.01	2.85	1.64
U-235, 0.45-µm filtered[1]	LHSU	57	0.23	-0.04	0.06	0.03
U-238, 0.45-µm filtered[1]	LHSU	54	8.01	-0.18	1.53	0.77

Note: Negative values due to instrument calibration.

[1] Background Geochemical Characterization Report (EG&G, 1993)

[2] Draft Background Comparison of Radionuclides in Groundwater (RMRS, 1996)

[3] Laboratory analysis performed using alpha spectrometry.

TA-2.8.2 RFCA Action Levels

RFCA Action Levels for Pu-239/240, Am-241, U-233/234, U-235 and U-238 are defined in Attachment 5 of RFCA (DOE, 2000) and are presented in Table TA-2-25. A dual tier system of action levels is specified with the intention of preventing contamination of surface water by

128

applying Preliminary Programmatic Remediation Goals (PPRGs) for residential groundwater ingestion as groundwater action levels. Tier I action levels are equal to a value that is a hundred times the PPRG value. These action levels are used to identify areas that have high concentrations of groundwater contamination that should be addressed through an accelerated action. Tier II action levels are equal to the PPRG value and are used for triggering groundwater management actions that may be required to prevent surface water from exceeding surface water Action Levels. Each well in the groundwater-monitoring network is given a designation that determines the function of the well. The well function determines what decisions are to be made if contaminant concentrations exceed action levels or other specifications given by the DQO process.

Table TA-2-25. RFCA Groundwater Action Levels

Analyte	Tier I pCi/L	Tier II pCi/L
Am-241	14.5	0.145
Pu-239/240	15.1	0.151
U-233/234	106	1.06
U-235	101	1.01
U-238	76.8	0.768

TA-2.8.3 RFETS Groundwater Actinide Figures

Figure TA-2-60 through Figure TA-2-69 display results of groundwater sampling for UHSU unfiltered Pu-239/240, unfiltered Am-241, filtered U-233/234, filtered U-235 and filtered U-238, respectively. A similar series of figures (Figure TA-2-70 through Figure TA-2-74) display results of groundwater sampling for LHSU wells. Figure TA-2-75 and Figure TA-2-76 shows the location of groundwater basin and divide boundaries to facilitate analysis of the groundwater actinide transport pathway. The UHSU U isotope figures depict the lateral extent of areas where activity-concentrations exceed the Tier II action level and background values of each actinide. These areas are not specifically meant to represent groundwater contaminant plumes, although

129

some areas, such as the Solar Ponds, coincide with the approximate extent of known plumes. The results of special ICP/MS U isotope sampling used for source identification are also shown in these figures. Similar patterns for Pu-239/240, Am-241 and LHSU U isotopes were not presented because of the uncertainty associated with the representativeness of the data (Pu-239/240 and Am-241) and concerns about depicting lateral extent in a predominantly vertical groundwater flow field (LHSU U isotopes). Reference values for each actinide are provided for background mean plus two standard deviation concentrations in groundwater, used for IMP decisions involving selected well categories and the RFCA Tier II Action Level, which is used for other selected IMP well categories.

A description of the query process used to generate the groundwater data set is presented in Section TA-2.8.4.

TA-2.8.4 Groundwater Data Query and Refinement Process

The bulk of groundwater actinide data used and presented in this report were retrieved from SWD, an environmental database that stores raw analytical data from groundwater sampling activities from 1986 to present. Groundwater data retrieved from SWD consisted of all actinide results reported for monitoring well samples for the period 1991 to 1999. The pre-1991 groundwater data were excluded from the data set because of data quality and consistency concerns compared to later data. For completeness, additional groundwater actinide data from a small subset of well samples collected in 1996, 1997 and 1998 by the Groundwater Operations program were incorporated with the SWD data to provide a full data set for evaluation and interpretation. These data consist of a SWD residual data entry backlog that is currently stored by Kaiser-Hill Environmental Media Management in a preliminary data set maintained by the Groundwater Operations program. These data have also been presented with the SWD data in various Annual and Quarterly RFCA Groundwater Monitoring Reports, which are available from the RFETS Environmental Data Dynamic Information Exchange (EDDIE) web site.

All actinide data for groundwater samples reported for the search period were retrieved, compiled and cleansed to remove rejected, duplicate and spurious records. Sample results with

an "R" data qualifier code, indicating a rejected analytical result, were excluded from the data set (see Table TA-2-1). Subsequent queries were performed on the remaining, non-rejected data set to eliminate laboratory quality assurance sample results, such as rinsates and blanks. Sample rerun and duplicate analyses were retained in favor of the original result if the alternate result was reported at a higher concentration and/or was reported with a higher-quality laboratory data qualifier code. Analytical results with spurious location codes were compared against an existing well alias list and reconciled, where possible, to provide a complete sampling record of the affected locations. Most non-reconciled records appeared to be associated with tank, incidental water, or similar type of grab water samples; only a small number of records contained numeric codes suggestive of a monitoring well location. All non-reconciled results were rejected and excluded from the data set.

After the final data set was assembled, the data were further sorted to differentiate unfiltered and filtered samples by hydrostratigraphic unit (UHSU and LHSU) for final use. Mean values for each analyte were then calculated for constructing the concentration maps described and presented in Section TA-2.8.3.

TA-2.8.5 Groundwater Data Description

Groundwater actinide data were compiled as a result of the acceptance process described in Section TA-2.8.4 and consist of 17,609 individual records. Most of these data were collected for UHSU wells, which monitor the shallowest and most susceptible flow system to contaminant releases and subsequent transport to surface water. Significant amounts of data are also available from LHSU wells used for characterizing vertical contaminant migration, especially in areas of known UHSU groundwater contamination. Generally, most wells have, at various times, been part of routine groundwater sampling operations and have been sampled more than once. Table TA-2-26 presents a statistical summary of all groundwater actinide data used in this report.

The largest quantity of data for individual actinides exist for unfiltered Pu-239/240, unfiltered Am-241 and filtered U-233/234, U-235 and U-238, which reflect the sampling approach adopted based on the expected transport behavior of these contaminants (see discussion of actinide

geochemistry in Section 3). Unfiltered Pu-239/240 and Am-241 samples are normally collected because these contaminants are not naturally-occurring, have a low aqueous solubility, are strongly sorbed to geologic media and have a potential to migrate via colloid-facilitated transport. Filtered Pu-239/240 and Am-241 data are available from over 100 wells and serve to document actinide phase association as a basis for unfiltered sampling. U samples are normally field filtered (0.45 μm) because U is considerably more soluble than Pu and Am and, consequently, transport is expected to occur mainly in the dissolved phase. Although U is more soluble than Pu and Am, it is relatively insoluble. In addition, total suspended solids derived from the local geologic media contain significant concentrations of natural U that can contaminate groundwater samples and lead to erroneously high analytical results.

Table TA-2-26. Summary Statistics for Groundwater Actinide Data (1991-1999)

Actinide[1]	Unit	No. of Wells	No. of Samples	Min. (pCi/L)	Max. (pCi/L)	Mean (pCi/L)	Std. Dev. (pCi/L)	Median (pCi/L)
Pu-239/240, unfiltered	UHSU	402	3147	-0.054	218.4	0.416	6.946	0.003
Pu-239/240, filtered	UHSU	135	464	-0.022	1.999	0.016	0.130	0.001
Am-241, unfiltered	UHSU	405	3009	-0.15	40.27	0.063	1.008	0.005
Am-241, filtered	UHSU	131	464	-0.029	21.31	0.073	1.076	0.003
U-233/234, filtered	UHSU	481	3918	-0.521	491.625	8.639	21.992	2.591
U-235, filtered	UHSU	481	3919	-0.11	35.725	0.349	1.086	0.102
U-238, filtered	UHSU	481	3918	-0.183	324.646	6.086	14.107	1.7
Pu-239/240, unfiltered	LHSU	50	432	-0.018	10.32	0.038	0.502	0.007
Pu-239/240, filtered	LHSU	13	74	-0.003	0.015	0.002	0.003	0.001
Am-241, unfiltered	LHSU	48	399	-0.061	0.47	0.008	0.027	0.004
Am-241, filtered	LHSU	12	69	-0.003	0.018	0.003	0.003	0.003
U-233/234, filtered	LHSU	63	572	-0.031	26.0	1.881	2.022	1.353
U-235, filtered	LHSU	62	571	-0.099	1.3	0.085	0.135	0.043
U-238, filtered	LHSU	62	571	-0.059	29.0	0.848	1.449	0.61

[1] Filtered samples were collected using a 0.45-µm membrane filter.

In addition to these data, analyses of U isotope ratios from selected groundwater samples using ICP/MS analytical techniques have been performed in recent years. This technique is capable of

providing highly accurate U concentrations for interpretation of potential U sources. Samples were collected from over 50 wells in areas with high U groundwater activity-concentrations to help differentiate whether the elevated U levels were caused by Site operations or by natural sources. The samples were analyzed for U-234, U-235, U-236 and U-238 concentrations and U-235/U-238 and U-236/U-238 ratios. The source of the U (i.e., natural, depleted, or enriched U) is indicated by a comparison of the sample U isotope ratios to natural U isotope ratios. The significance of these data will be discussed later in Section 4. The data are presented in the 1999 Annual RFCA Groundwater Monitoring Report (Kaiser-Hill, 2000e).

Description of Groundwater Monitoring Programs

RFETS groundwater monitoring data are collected by Kaiser-Hill Environmental Media Management Groundwater Operations program for implementation of the *Rocky Flats Cleanup Agreement* (DOE, 2000) requirements related to groundwater. The monitoring program is implemented in accordance with the *RFETS Integrated Monitoring Plan (IMP)* (Kaiser-Hill, 2000c), which describes and specifies program goals and objectives, compliance monitoring and reporting requirements, quality assurance/quality control criteria and other key components of the program. Incorporated into the IMP are the routine groundwater monitoring requirements of the Resource Conservation and Recovery Act (RCRA), CERCLA, Industrial Area Interim Measure/Interim Remedial Action (IM/IRA) Decision Document, DOE Order 5400.1 and other governing documents. Decisions related to groundwater monitoring, the IMP DQO process that uses a well classification system for specifying well monitoring function and administrative actions determines data.

As defined in the IMP, the objectives of the RFETS groundwater monitoring program are to:

- Protect surface water quality;
- Demonstrate compliance with regulations;
- Minimize the chances of further degradation of the UHSU; and

- Support the design and selection of remedial measures and assess the effect of any future remedial actions.

Groundwater monitoring is an essential function of surface water protection at the Site, since the majority of groundwater becomes surface water within the Site boundaries. The overall objective is to identify contaminated groundwater and associated pathways to surface water and protect those resources from further or potential damage. A network of over 1,000 monitoring wells has historically been used to characterize groundwater flow and quality within the boundaries of the Site.

Elements of the current program include measurement of radionuclide concentrations in groundwater, determination of hydraulic gradient and direction of groundwater flow and assessment of the nature and extent of any contaminant plumes in the UHSU within Site boundaries. The monitoring network is designed to monitor areas of known or suspected groundwater contamination based on groundwater plume information and OU specific source characterization activities. Earlier groundwater monitoring activities (pre-IMP) focused more heavily on the characterization of former OUs, establishment of background groundwater concentrations and LHSU flow system groundwater quality.

The current monitoring network comprises the following monitoring components (Kaiser-Hill, 2000e):

- A network of 148 wells sampled on a semiannual basis;
- A network of 28 wells and seeps sampled quarterly;
- Monthly measurement of water elevations at 73 wells;
- Quarterly measurement of water elevations at 147 wells;
- Semiannual measurement of water elevations at 85 wells;
- Continuous measurement of water elevations in 33 wells;

- A program for updating and proposing changes to the groundwater monitoring program;
- Annual evaluation and reporting to the appropriate regulatory and community agencies;
- Quarterly reporting of groundwater data that exceed action limits; and
- Other special projects pertinent to groundwater assessment.

Monitoring wells are classified into seven categories that determine a decision or action that is prompted when specified criteria is met. These categories include plume definition, plume extent, drainage, boundary, performance, D&D, RCRA and plume degradation (organic constituents), which are described in more detail in the IMP.

Groundwater Sample Collection

Groundwater samples are collected from all wells after the wells have been properly purged to remove stagnant water from the well casing. Purging consists of removing a minimum volume of water (at least three casing volumes) and measuring the discharge water at regular intervals for stabilization of temperature, pH, electrical conductivity and turbidity. Due to low well yields and prolonged water level recovery times, most wells are purged and sampled using a bailer. In wells capable of sustained yields, dedicated bladder pumps are used in combination with low-flow rate sampling methods. Dry well conditions are a frequent occurrence in RFETS wells located in the eastern half of the Site because of seasonal desaturation effects, especially near the margin of the Rocky Flats Alluvium and along hillsides where groundwater is scarce. Under the current monitoring program, bailed and pumped samples for Pu and Am are processed unfiltered to prevent loss of suspended actinide-contaminated particles on the filter. U isotope samples are field filtered using a 0.45-μm filter capsule.

Groundwater samples are collected at substantially longer time intervals (quarterly to semiannually) compared to surface water samples because groundwater flow velocities are several orders of magnitude slower that surface water flow rates. Consequently, changes in contaminant concentrations are very slow, thus allowing for a remedial response before the

136

contamination reaches a surface water body. The current groundwater monitoring well network is designed so that detection of contaminant migration along groundwater flow pathways leaving the Site are adequately monitored to protect surface water quality.

TA-2.9 AIR ACTINIDE CONCENTRATIONS

TA-2.9.1 Background and Baseline Air Actinide Concentrations

Background concentrations of actinides in ambient air, i.e., those naturally-occurring and man-made actinides present in the global atmosphere due to fallout from weapons testing, resuspension of isotopes in soils and other ubiquitous sources, are difficult to quantify. The scientific literature provides a range of Pu concentrations that show seasonal periodicity and fluctuate due to weapons testing events. Data are rarely provided on background levels of Am-241. Background levels of U isotopes are strongly influenced by natural sources. Additionally, non-ubiquitous sources of actinides such as the RFETS have biased local measurements of background.

Background Pu-239/240 and Am-241

Data from Pan and Stevenson (1996) show that fallout of Pu-239/240 from nuclear testing during the 1950s through 1970s decreased with time following the last atmospheric test in 1980. After 1984, fallout as measured at various locations in the U.S., had leveled off, indicating that an equilibrium condition had been reached. Fallout levels of Pu-239/240 are now though to be due to resuspension of material in the lower atmosphere; during and for a few years after atmospheric testing, fallout was instead controlled by the amount of stratospheric Pu-239/240 that was exchanged with the troposphere and subsequently deposited at the surface.

The following concentrations of Pu-239/240 in air were measured by the EPA Environmental Radiation Ambient Monitoring System (ERAMS) between 1984 and 1992 in locations without localized sources:

- Chicago, IL. 4.0×10^{-7} pCi/m^3;

137

- New York, NY 3.0×10^{-7} pCi/m^3;
- Denver, CO 5.1×10^{-7} pCi/m^3; and
- Portland, OR 3.0×10^{-7} pCi/m^3.

These values are in general agreement with the overall magnitude of Pu-239/240 in air seen in other locations globally during similar time periods (Pan and Stevenson, 1996).

Fallout of Pu-239/240 is expected to vary between locations due to latitude and climatology, primarily the annual precipitation. Consequently, it is desirable to have more localized estimates of fallout Pu-239/240 levels to apply to the Site environment. Samplers located in communities surrounding Rocky Flats and at some distance from the Site fenceline provide another set of data points. The Community Radiation Monitoring (COMRAD) program operates five monitors to the east of the Site that collect particulate matter on filters that are analyzed for Pu-239/240 on a monthly basis. The Northglenn station is the most distant from the Site and is therefore the least likely to show Site influence. Airborne Pu-239/240 concentrations at that station averaged 4.1×10^{-7} pCi/m^3 for the most recent 18 month period, within the range of concentrations reported for U.S. cities by pan and Stevenson (1996).

Two other monitoring locations were examined. The Site operated an ambient air sampler in Boulder in the early 1990s that collected samples that were analyzed for Pu-239/240 on a monthly basis. The average Pu-239/240 recorded at that location between 1990 and 1994 was 3.6×10^{-7} pCi/m^3. Finally, a sampler was installed at a distance of approximately 5.8 km to the north of the Site in late 1998, making it the most distant of the Site's perimeter samplers. In 1999, the average annual airborne Pu-239/240 concentrations from that sampler totaled 4.35×10^{-7} pCi/m^3.

The results of these comparisons suggest that local background levels of Pu-239/240 in air due to fallout are somewhere between the concentrations reported by Pan and Stevenson (1996) for Denver (5.1×10^{-7} pCi/m^3) and those reported for New York and Chicago (3.0×10^{-7} pCi/m^3).

Am (Am-241) background concentrations are more difficult to define due to the dearth of studies on the topic. One approach, using the ratio of Am-241 to Pu-239/240 found in Colorado surface soils at some distance from RFETS, would estimate the background concentration of Am-241 to be in the range of 1.1×10^{-7} pCi/m^3 to 1.8×10^{-7} pCi/m^3, based on the previously presented Pu-239/240 data (Hulse et al., 1999).

Background Uranium

Global background air concentrations of naturally-occurring U (U-233/234, U-235 and U-238) result primarily from resuspension soil and sediment, since U is a common component of the earth's crust. The Rocky Mountain region has a high incidence of naturally-occurring U in its soil and bedrock, so local background is likely higher than other regions. In general, it can be assumed that the majority of the U isotopes measured at Site samplers represent natural background concentrations. This conclusion is because measured ratios of U-233/234 to U-238 are characteristic of naturally-occurring U and do not show noticeable Site influence.

Baseline Actinide Concentrations

Baseline concentrations of air actinides, i.e., the typical air actinide concentrations measured around the Site in the current configuration, are also difficult to quantify with a high degree of certainty. Because actinide air concentrations are a function of the resuspension and deposition rates of dust-bound actinide particles, they vary with wind speed, soil moisture, snow cover and other meteorological factors. However, given the large number of ambient dust samples collected at RFETS over the years using the Radioactive Ambient Air Monitoring Program (RAAMP) sampler network, reasonable upper and lower bounds for baseline air actinide concentrations for the current Site configuration can be defined.

Table TA-2-27 summarizes the annual average concentrations of Pu-239/240 and Am-241 in ambient air at RAAMP samplers arrayed around the Site perimeter. Table TA-2-28 presents the same information for U isotopes. Figure TA-2-77 illustrates the locations of these samplers. These samplers are used to evaluate compliance with the National Emission Standards for

139

Emissions of Radionuclides Other Than Radon From Department of Energy Facilities (Rad NESHAP), as codified in Subpart H of Title 40, Part 61 of the Code of Federal Regulations (40 CFR 61, Subpart H). This standard is discussed further in TA-2.9.2.

Table TA-2-27. Average Annual Air Concentrations, Pu-239/240 and Am-241

Sampler	Pu-239 (pCi/m^3)			Am-241 (pCi/m^3)		
	1997	1998	1999	1997	1998	1999
S-131	3.95E^{-07}	1.58 E^{-06}	1.10 E^{-06}	n/a	7.45 E^{-07}	1.46E^{-06}
S-132	3.10E^{-07}	1.69 E^{-06}	4.40E^{-06}	n/a	5.06 E^{-07}	1.23E^{-06}
S-134	3.86E^{-07}	1.36 E^{-06}	5.81E^{-07}	n/a	4.76 E^{-07}	2.60E^{-07}
S-135	n/a	n/a	9.03E^{-07}	n/a	n/a	7.64E^{-07}
S-136	2.16E^{-07}	1.05 E^{-06}	1.72E^{-06}	n/a	1.25 E^{-06}	4.21E^{-07}
S-137	2.98E^{-07}	2.31 E^{-06}	2.26 E^{-06}	n/a	1.03 E^{-06}	4.56E^{-07}
S-138	9.22E^{-07}	1.85 E^{-06}	1.38 E^{-06}	n/a	4.84 E^{-07}	3.19E^{-07}
S-139	n/a	n/a	8.88E^{-07}	n/a	n/a	5.73E^{-07}
S-140	3.23E^{-07}	1.88 E^{-06}	4.65E^{-07}	n/a	9.06 E^{-07}	4.82E^{-07}
S-141	2.15E^{-07}	1.67 E^{-06}	1.59E^{-06}	n/a	3.10 E^{-07}	2.58E^{-07}
S-142	1.36E^{-07}	1.05 E^{-06}	4.58E^{-07}	n/a	7.20 E^{-07}	4.68E^{-07}
S-201	3.60E^{-07}	1.68 E^{-06}	1.24E^{-06}	n/a	1.41 E^{-06}	5.81E^{-07}
S-207	4.19E^{-07}	1.08 E^{-06}	1.09E^{-06}	n/a	6.21 E^{-07}	2.77E^{-07}
S-209	2.06E^{-07}	9.83 E^{-07}	5.62E^{-07}	n/a	5.31 E^{-07}	4.15E^{-08}
S-254	n/a	n/a	4.35E^{-07}	n/a	n/a	4.39E^{-07}

Notes: E# = x 10; #n/a = data not available; pCi/m^3= picocuries per cubic meter

140

Table TA-2-28. Average Annual Air Concentrations, U-234, U-235 and U-238

Sampler	U-234 (pCi/m^3)			U-235 (pCi/m^3)			U-238 (pCi/m^3)		
	1997	1998	1999	1997	1998	1999	1997	1998	1999
S-131	7.92E^{-06}	3.21 E^{-05}	3.16 E^{-05}	2.24E^{-07}	1.57 E^{-06}	2.02E^{-06}	8.02E^{-06}	3.24 E^{-05}	2.90E^{-05}
S-132	1.15E^{-05}	4.85 E^{-05}	4.33 E^{-05}	5.94E^{-07}	2.04 E^{-06}	2.14E^{-06}	1.16E^{-05}	4.87 E^{-05}	4.38E^{-05}
S-134	4.07E^{-06}	2.13 E^{-05}	1.95E^{-05}	8.36E^{-08}	1.76 E^{-06}	1.31E^{-06}	3.86E^{-06}	1.87 E^{-05}	1.75E^{-05}
S-135	n/a	n/a	3.60E^{-05}	n/a	n/a	2.31E^{-06}	n/a	n/a	3.59E^{-05}
S-136	4.92E^{-06}	1.92 E^{-05}	2.13E^{-05}	2.32E^{-07}	1.12 E^{-06}	1.18E^{-06}	4.41E^{-06}	1.86 E^{-05}	1.90E^{-05}
S-137	5.68E^{-06}	2.63 E^{-05}	2.36 E^{-05}	1.60E^{-07}	1.08 E^{-06}	1.15E^{-06}	5.18E^{-06}	2.54 E^{-05}	2.45E^{-05}
S-138	4.75E^{-06}	2.25 E^{-05}	2.19 E^{-05}	3.27E^{-07}	9.12 E^{-07}	1.79E^{-06}	5.61E^{-06}	2.06 E^{-05}	2.00E^{-05}
S-139	n/a	n/a	2.87E^{-05}	n/a	n/a	1.31E^{-06}	n/a	n/a	2.74E^{-05}
S-140	1.27E^{-05}	4.78 E^{-05}	5.19E^{-05}	6.34E^{-07}	2.25 E^{-06}	2.74E^{-06}	1.32E^{-05}	4.60 E^{-05}	5.25E^{-05}
S-141	5.39E^{-06}	2.25 E^{-05}	2.31E^{-05}	3.15E^{-07}	1.05 E^{-06}	1.52E^{-06}	5.09E^{-06}	2.38 E^{-05}	2.46E^{-05}
S-142	5.30E^{-06}	2.44 E^{-05}	2.36E^{-05}	1.50E^{-07}	2.16 E^{-06}	1.66E^{-06}	5.31E^{-06}	2.07 E^{-05}	2.45E^{-05}
S-201	6.30E^{-06}	2.68 E^{-05}	2.96E^{-05}	2.53E^{-07}	1.26 E^{-06}	1.59E^{-06}	5.33E^{-06}	2.46 E^{-05}	2.76E^{-05}
S-207	7.07E^{-06}	2.66 E^{-05}	3.06E^{-05}	1.84E^{-07}	1.65 E^{-06}	1.67E^{-06}	6.95E^{-06}	2.78 E^{-05}	2.77E^{-05}
S-209	5.97E^{-06}	2.52 E^{-05}	2.90E^{-05}	1.70E^{-07}	1.29 E^{-06}	1.64E^{-06}	5.83E^{-06}	2.21 E^{-05}	3.14E^{-05}
S-254	n/a	n/a	2.32E^{-05}	n/a	n/a	1.65E^{-06}	n/a	n/a	2.90E^{-05}

Notes: E# = x 10; #n/a = data not available; pCi/m^3= picocuries per cubic meter

Table TA-2-29 summarizes the highest, lowest and median concentrations of U-234, U-235, U-238, Pu-239/240 and Am-241 measured in ambient air between January 1997 and December 1999. These values are illustrative of the range of airborne concentrations of actinides observed at RFETS and provide reasonable boundaries on ambient background concentrations for actinides in air for the current Site configuration and activities.

141

Table TA-2-29. Boundary Values of Annual Average Ambient Air Concentrations, 1997-1999

	Am-241	Pu-239/240	U-234	U-235	U-238
Maximum, pCi/m^3	1.46E^{-06}	4.40E^{-06}	5.19E^{-05}	2.74E^{-06}	5.25E^{-05}
Minimum, pCi/m^3	4.15E^{-08}	1.36E^{-07}	4.07E^{-06}	8.36E^{-08}	3.86E^{-06}
Median, pCi/m^3	4.56E^{-07}	4.47E^{-07}	1.27E^{-05}	1.18E^{-06}	1.90E^{-05}

A range of typical air actinide concentrations describes the atmospheric actinide concentration better than would a single background value because about 73 % of all airborne actinides in the RFETS environment in recent years have been resuspended from Site soils (versus 26 % from remediation projects and 1 % from building emissions) and soil resuspension rates are dependent on complex relationships between wind speed, soil moisture, vegetative cover and other environmental variables. The minimum and maximum values presented are the highest and lowest annual average, as opposed to the highest or lowest single monthly result. Therefore, these values provide a reasonable range of expected values but not absolute bounds on the range of background actinide concentrations in ambient air at the Site perimeter under current conditions.

TA-2.9.2 Air Regulatory Standards

The National Emission Standard for Hazardous Air Pollutants (NESHAP) for radionuclide emissions from DOE facilities, 40 CFR 61, Subpart H and Colorado Air Quality Control Commission Regulation No. 8, Part A, Subpart H, requires the radiation dose to the public from RFETS be determined annually and reported to EPA and CDPHE. These regulations limit the air pathway dose from Site activities to any member of the public to an annual effective dose equivalent (EDE) of 10 millirem (mrem). For comparison, the average annual EDE for residents of the Denver area from all sources of radiation is approximately 420 mrem, over 80 % of which is due to natural background radiation (Roberts, 1998).

142

Compliance with the 10-mrem standard has been determined by comparing environmental radionuclide air concentrations at critical receptor locations, sampled with RAAMP samplers, with the "Concentration Levels for Environmental Compliance" listed in Table 2 of Appendix E to 40 CFR 61, in accordance with an alternative compliance demonstration method approved by EPA and CDPHE (DOE, 1997; DOE, 1998). Compliance is demonstrated when each measured radionuclide air concentration is less than its corresponding compliance level in Appendix E, Table 2 and when the "fractional sum" of all radionuclides is less than one. The fractional sum is calculated by dividing the actual annual average concentration of each isotope by the compliance limit, then summing these ratios for all isotopes of interest. Figure TA-2-78 shows the three-year average concentrations of each isotope at each compliance sampler, along with the corresponding percentage of the 10-mrem standard that each fractional sum represents.

Table TA-2-30 details the Table 2 compliance levels for the isotopes of interests at RFETS. A comparison of the maximum annual averages to the compliance concentrations shown in Figure TA-2-78 shows that in recent years, ambient airborne actinide concentrations have been orders-of-magnitude lower than the allowable limits.

Table TA-2-30. Compliance Concentration Levels from 40 CFR 61, Table 2

	Pu-239/240 (pCi/m^3)	Am-241 (pCi/m^3)	U-233/234 (pCi/m^3)	U-235 (pCi/m^3)	U-238 (pCi/m^3)
Allowable Annual Average Concentration	$2.0\ E^{-03}$	$1.9\ E^{-03}$	$7.1/7.7\ E^{-03}$	$7.1\ E^{-03}$	$8.3\ E^{-03}$

RAAMP radionuclide concentrations have been dominated by naturally-occurring U isotopes. At the RAAMP samplers with the largest fractional sums, for example, U isotopes characteristic of naturally-occurring U have represented an order-of-magnitude larger dose than that contributed by non-U isotopes. In addition, the locations where the highest total radionuclide levels were measured during 1997 - 1999 (northwest and southeast of the Site) were influenced by off-Site activities that generated dust, such as traffic or quarrying operations. The

143

resuspension of naturally-occurring radioisotopes by such activities has dwarfed Site impacts on the air pathway in recent years.

TA-2.9.3 Air Data Acquisition Figures

Figure TA-2-77 shows the locations of the all RAAMP samplers, including the fourteen RAAMP samplers used to assess compliance with Rad NESHAP (these are located at the Site perimeter and identified by sampler number in Table TA-2-27 and Table TA-2-28). The compliance samplers are arrayed such that any wind sector where potential receptors reside or work contains a compliance RAAMP sampler. Additional samplers may need to be installed in the future, as the communities surrounding RFETS grow toward the Site. The remaining samplers in Figure TA-2-77 are used to monitor Site projects or to sample a potential plume in case of an emergency.

TA-2.9.4 Air Data Acquisition Process

The baseline actinide air concentration data presented here were obtained through the Radioactive Ambient Air Monitoring Program. Sample data presented in this report were originally compiled to assess compliance with Rad NESHAP, in accordance with the alternative compliance demonstration method approved by EPA and CDPHE (DOE, 1997; DOE, 1998) and to comply with DOE Order requirements for environmental surveillance.

The RAAMP samplers are size-partitioning, high-volume (HVOL) ambient air samplers that collect fine atmospheric dust on 8-inch by 10-inch glass fiber filters and coarse dust on oiled paper impactor pads. Figure TA-2-79 provides an expanded view of the sampler design. The nominal size cut of the RAAMP samplers is 10 micrometers (μm) aerodynamic equivalent diameter (AED). This size class of particles is commonly referred to as PM_{10} and includes all particles that are inhalable or respirable by humans. The particles that collect on the oiled impactor pads are 10- to 30-μm AED and provide additional information about transport and deposition of actinide-contaminated particles from the Site.

144

Though only the inhalable particle sizes (PM_{10}) contribute to inhalation dose effects, the RAAMP sampler network results are always reported with both PM_{10} and larger size particles included. This provides a conservative approach to assessing compliance with EPA and state standards and accounts for actinide migration among non-inhalable size fractions. Figure TA-2-80 illustrates an actual field installation of the RAAMP sampler design.

TA-2.10 BIOTA ACTINIDE CONCENTRATIONS

TA-2.10.1 General Observations in Biota

General observations of actinide concentrations in biota at the Site are discussed here. More detailed information on actinide concentrations and movement via different biological transport mechanisms is provided in Section TA-4.6.

In general, investigations on biota in the most studied location, the 903 Pad and Lip area, showed that Pu concentrations in biota were significantly lower than in soils. As summarized by Setlock and Blaha (1986), arthropods and small mammals had Pu concentrations 100 times lower than soil, with no significant differences in seven tissue types analyzed. The concentration hierarchy followed a downward trend from dead plant litter to fresh vegetation to animal compartments that were analyzed (Little et al., 1980; Setlock and Blaha, 1986). The higher values for plant litter are expected since the litter is more closely associated with the soil surface and prone to the accumulation of soil particulate matter.

In a study of actinides in the environment, Watters, et al. (1983) reviewed actinide behavior with emphasis on chemical, physical and biological factors that influence actinide mobility. Their general conclusion was that sources of actinide in the environment, with few exceptions, have resulted in very low transfer of these elements into food webs, regardless of transport process.

In a "White Paper" written to assess the biological mobility of environmental Pu, Higley and Whicker (1999) observed that Pu is not a biologically essential element, nor does it serve as an

analogue for any other essential element. They further stated that because of its insoluble nature (most forms of Pu are insoluble), the passage of Pu through biological membranes and any uptake into plant and animal tissues is normally very minor. After reviewing and summarizing results of Rocky Flats studies, Higley and Whicker (1999) concluded that the majority of Pu measured in plant material was associated with surficial dust particles and that transport of Pu into plants is decreasing over time. They also observed that although concentrations in vegetation and litter strongly correlated with soil concentrations, those in small mammal tissues did not, but instead appeared to be independent. This led them to conclude that the small amount of Pu in small mammal tissues may result from the generally-distributed global fallout. Considering the variable soil concentrations often mentioned in these papers and in light of the mobility of even small mammals, it is likely that the small mammals were variably exposed to differing soil concentrations of contaminants throughout their home ranges and over their life spans. The closer correlation of vegetation concentrations to soil concentrations in a specific location is reasonable, given that plants remain rooted in the same soil throughout their lifetimes.

Higley and Whicker (1999) further concluded that although the nature and source of a Pu release is important in its distribution, environmental processes could alter the composition and distribution over time. Soils and sediments have been found to become the ultimate repository for the majority of Pu. A tiny fraction of the Pu inventory is soluble and therefore bioavailable. They found that while Pu is incorporated into plant, animal and human tissues, the concentrations are typically orders of magnitude less than soil and sediment concentrations. Biomagnification – the concentration of a chemical or compound from one trophic level to the next – does not appear to occur with Pu. Their review found that although biological processes can redistribute Pu in the soil profile, the impact is essentially local.

146

SECTION TA-2 REFERENCES

Brackett, W.A. etal. 1983. Colorado Energy Balance-1981. Colorado Geological Survey Department of Natural Resources Denver, Colorado. Plate 3: Uranium, Oil Shale and Geothermal Production, Movement and Consumption, Resource Series, No.26.

David, M. 1977. Geostatistical Ore Reserve Estimation. Dordrecht: Elsevier Scientific Publishing.

Department of Energy (DOE). 1992. Historical Release Report for the Rocky Flats Plant, Rocky Flats Plant, Golden, CO.

DOE. 1993. Quarterly Updates 1 – 4, Historical Release Report for the Rocky Flats Plant, Rocky Flats Plant, Golden, CO.

DOE. 1994. Quarterly Updates 5 – 8, Historical Release Report for the Rocky Flats Plant, Rocky Flats Plant, Golden, CO.

DOE. 1995a. Quarterly Updates 9 – 12, Historical Release Report for the Rocky Flats Plant, U.S. Department of Energy, Rocky Flats Plant, Golden, CO.

DOE. 1995b. Final Phase II RFI/RI Report, 903 Pad, Mound, East Trenched Area, Operable Unit No. 2, RF/ER-95-0079.UN, U.S. Department of Energy, Rocky Flats Plant, Golden, CO.

DOE. 1997. Proposal to Use Environmental Sampling for Demonstrating Compliance with 40 CFR 61, Subpart H. Rocky Flats Field Office, Golden, CO. July, 1997.

DOE. 1998. Addendum to the Proposal to Use Environmental Sampling for Demonstrating Compliance with 40 CFR 61, Subpart H. Rocky Flats Field Office, Golden, CO. December, 1998.

DOE. 2000. Rocky Flats Cleanup Agreement, Final, Revised. U.S. Department of Energy, Golden, CO. March 21, 2000.

DOE. 2001. Building 771 Phase 1 Under Building Contamination Characterization Sampling Report, Rocky Flats Environmental Technology Site, Golden, CO. September 21, 2001.

Dunstan, L. 2000. Personal communication with Leslie Dunstan, Rocky Mountain Remediation Services. December 29, 2000.

147

EG&G Rocky Flats Inc. (EG&G) 1991a. EMD Operating Procedure Manual, Rocky Flats Plant, Vols. I-IV. EG&G, 5-21000-OPS.

EG&G. 1991b. Rocky Flats Plant Site-Wide Quality Assurance Project Plan for CERCLA RI/FS and RFI/CMS Activities. EG&G. May 7, 1991.

EG&G. 1993. Background Geochemical Characterization Report. Rocky Flats Environmental Technology Site, Golden, CO.

EG&G. 1995. Geochemical Characterization of Background Surface Soils: Background Soils Characterization Program.

Higley, K. and F.W. Whicker. 1999. Biological Mobility of Environmental Plutonium. "White Paper". Kathryn Higley, Oregon State University, and F. Ward Whicker, Colorado State University. October 16, 1999.

Hulse, S.E., S.A. Ibrahim, F.W. Whicker, and P.L. Chapman. 1999. Comparison of 241A,. 239/240 Pu and 137 Cs Concentrations in Soil around Rocky Flats. Health Physics, Vol.76, No. 3.

Isaaks, E.H. and R.M. Srivastava. 1987. An Introduction to Applied Geostatistics. New York: Oxford University Press.

Kaiser-Hill Company, L.L.C. (Kaiser-Hill) 1996. Annual Update for the Historical Release Report, Rocky Flats Environmental Technology Site, Golden, CO.

Kaiser-Hill. 1997. Annual Update for the Historical Release Report, Rocky Flats Environmental Technology Site, Golden, CO.

Kaiser-Hill. 1998a. Annual Update for the Historical Release Report, Rocky Flats Environmental Technology Site, Golden, CO.

Kaiser-Hill. 1998b. Statement of Work for Analytical Measurements, Isotopic Determinations by Alpha Spectrometry, Module RC01-B.3, Rocky Flats Environmental Technology Site, Golden, CO. April 24, 1998.

Kaiser-Hill. 1999. Annual Update for the Historical Release Report, Rocky Flats Environmental Technology Site, Golden, CO.

Kaiser-Hill. 2000a. Rocky Flats Environmental Technology Site Analytical Services website (http://rfetshp/Analytic_Services.gov), Rocky Flats Environmental Technology Site, Golden, CO. December 28, 2000.

Kaiser-Hill. 2000b. Annual Update for the Historical Release Report, Rocky Flats Environmental Technology Site, Golden, CO.

148

Kaiser-Hill. 2000c. Integrated Monitoring Plan (IMP) Background Document, Rocky Flats Environmental Technology Site, Golden, CO.

Kaiser-Hill. 2000d. Report on Soil Erosion and Surface Water Sediment Transport Modeling for the Actinide Migration Evaluation at the Rocky Flats Environmental Technology Site, Rocky Flats Environmental Technology Site, Golden, CO.

Kaiser-Hill. 2000e. 1999 Annual RFCA Groundwater Monitoring Report. Rocky Flats Environmental Technology Site, Golden, CO.

Kaiser-Hill. 2001a. Correspondence from Mark Wood, Kaiser-Hill Media Management, , Rocky Flats Environmental Technology Site, Golden, CO. February 26, 2001.

Kaiser-Hill. 2001b. Building 771 Phase 1 Under Building Contamination Characterization Sampling Report. Rocky Flats Environmental Technology Site, Golden, CO.

Kaiser-Hill. 2002. Technical Basis Document DRAFT Technical Justification for Determining Radiological Backgrounds and their use at the RFETS, Golden, CO.

Little, et al. 1980. Plutonium in Grassland Ecosystem at Rocky Flats. Journal of Environmental Quality, Vol. 9, No. 3.

Litaor, M.I. 1995. Spatial Analysis of Plutonium-239+240 and Americium-241 in Soils around Rocky Flats, Colorado. Journal of Environmental Quality. Madison, Wisconsin.

Matheron, G. 1965. The Theory of Regionalized Variables and Their Applications. Paris: Editions Masson.

Myers, J.C. 1985. Geostatistical Analysis of Lead Contamination around Industrial Smelters. Masters Thesis, Colorado School of Mines.

Myers, J.C. 1997. Geostatistical Error Management (GEM): Quantifying Uncertainty For Environmental Sampling and Mapping. New York, NY. John Wiley & Sons.

Pan, V. and K.A. Stevenson. 1996. Temporal Variation Analysis of Plutonium Baseline Concentration in Surface Air from Selected Sites in the Continental United States. Environmental Measurements Laboratory, U.S. Department of Energy, New York, NY.

Pitard, F.F. 1993. Pierre Gy's Sampling Theory and Practice. Boca Raton: CRC Press.

Radian. 2001. Environmental Air Monitoring Quality Assurance Plan. Radian International, Denver, Colorado. January, 2001.

Rocky Mountain Remediation Services (RMRS). 1996. Draft Background Comparison for Radionuclides in Groundwater. Rocky Flats Environmental Technology Site, Golden, CO.

149

RMRS. 1998. Progress Report #2 to the Source Evaluation and Preliminary Mitigation Plan for Walnut Creek.

RMRS. 1999. Characterization Report for the 903 Drum Storage Area, 903 Lip Area, and Americium Zone, Rocky Flats Environmental Technology Site, Golden, CO.

Roberts, R. 1998. Personal Communication with Rick Roberts of Kaiser-Hill Company L.L.C. June 16, 1998.

Rockwell International. 1989a. Standard Operating Procedures. Environmental Restoration Program, Rocky Flats Plant. Rockwell International. January, 1989.

Rockwell International. 1989b. ER Program Quality Assurance/Quality Control Plan. Rockwell International. January, 1989.

Scott. 2001. Building 771 Phase 1 Under Building Contamination Characterization Sampling Report. Rocky Flats Environmental Technology Site, Golden, CO.

Setlock, G.H. and F.J. Blaha. 1986. Rocky Flats Plant Radioecology and Airborne Pathway Summary Report. Environmental Management , Rockwell International. Rocky Flats Plant, Golden, CO.

Snedecor, G. W., and W. G. Cochran. 1967. Statistical Methods, Sixth Edition. The Iowa State University Press. Ames, Iowa.

Watters, et al. 1983. The Behavior of Actinides in the Environments. R.L. Watters, T.E. Hankonson, and L.J. Lane. Radiochimica Acta, Vol. 32, pp. 89-103.

Figure TA-2-13. Site Area Variograms for Pu-239/240

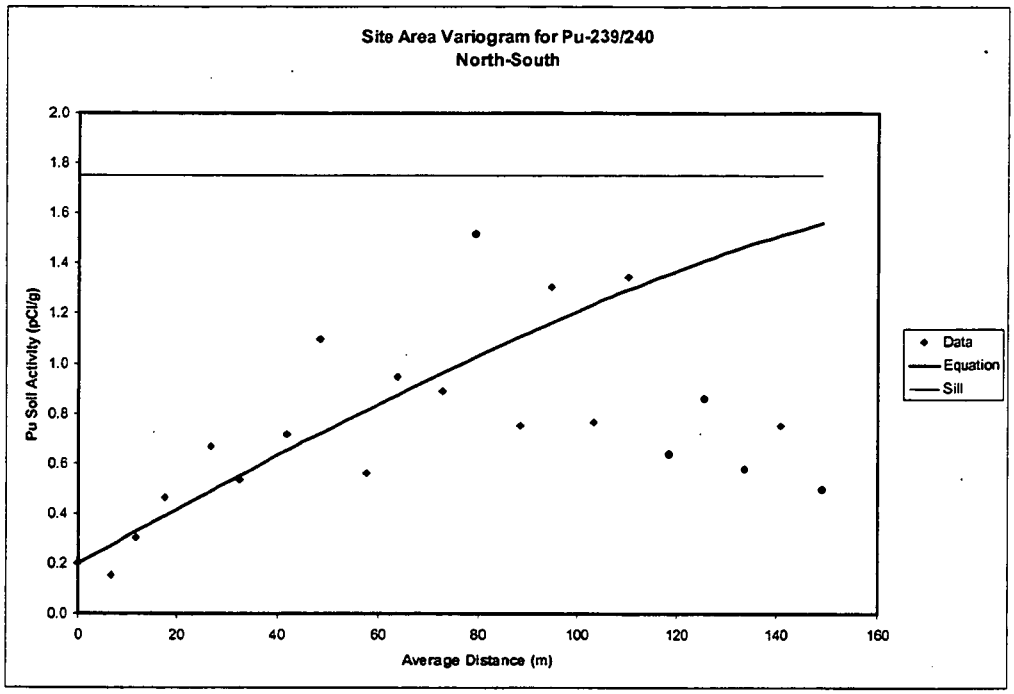

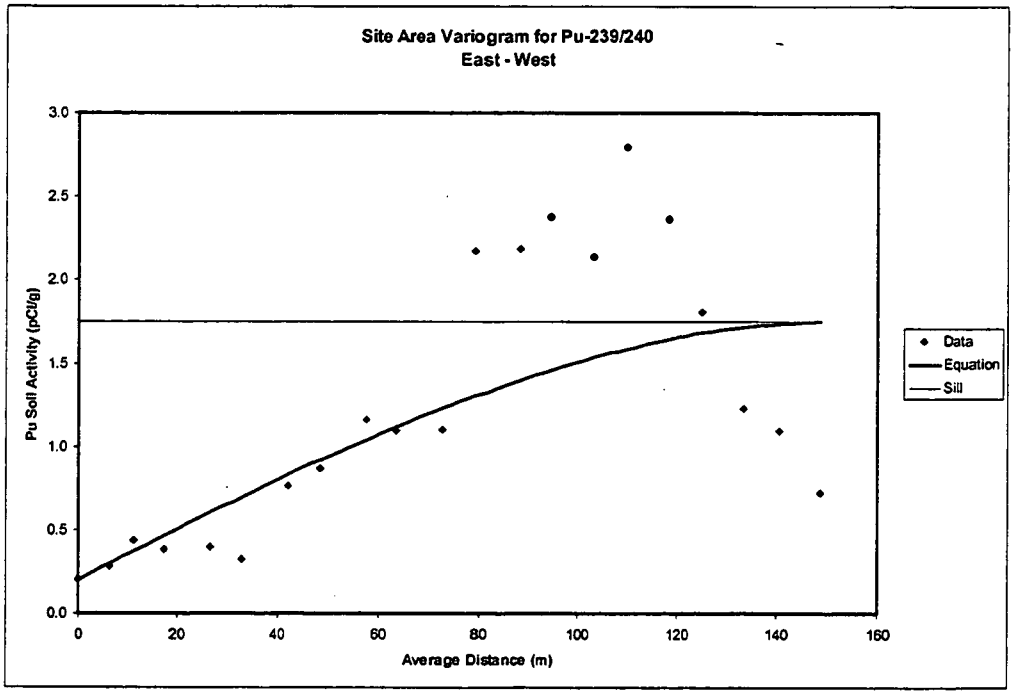

163

Figure TA-2-14. Site Area Variograms for Am-241

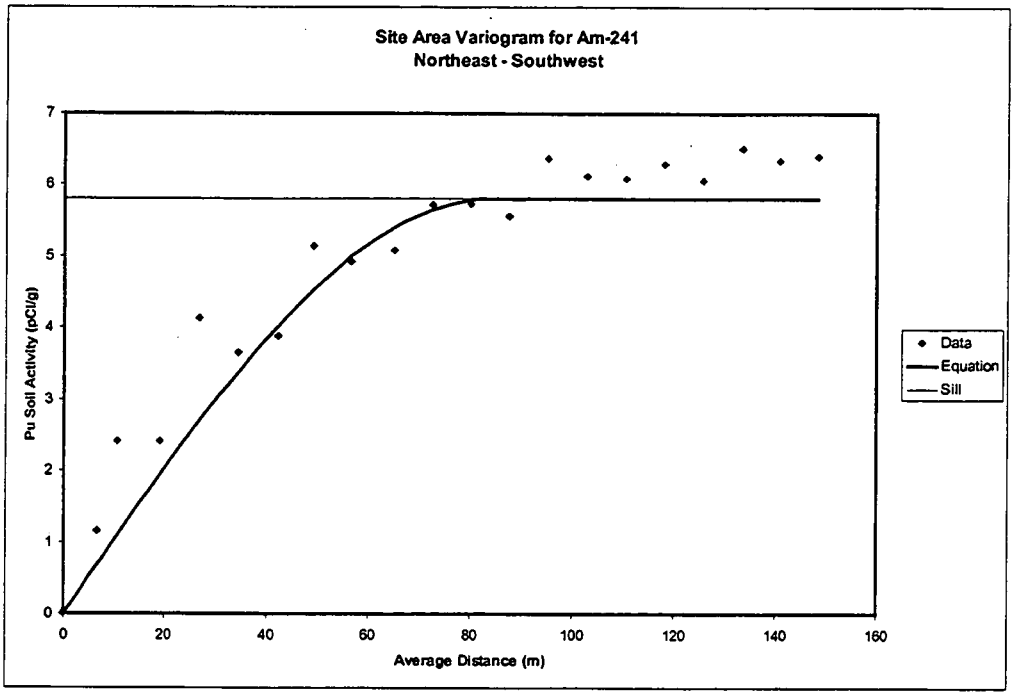

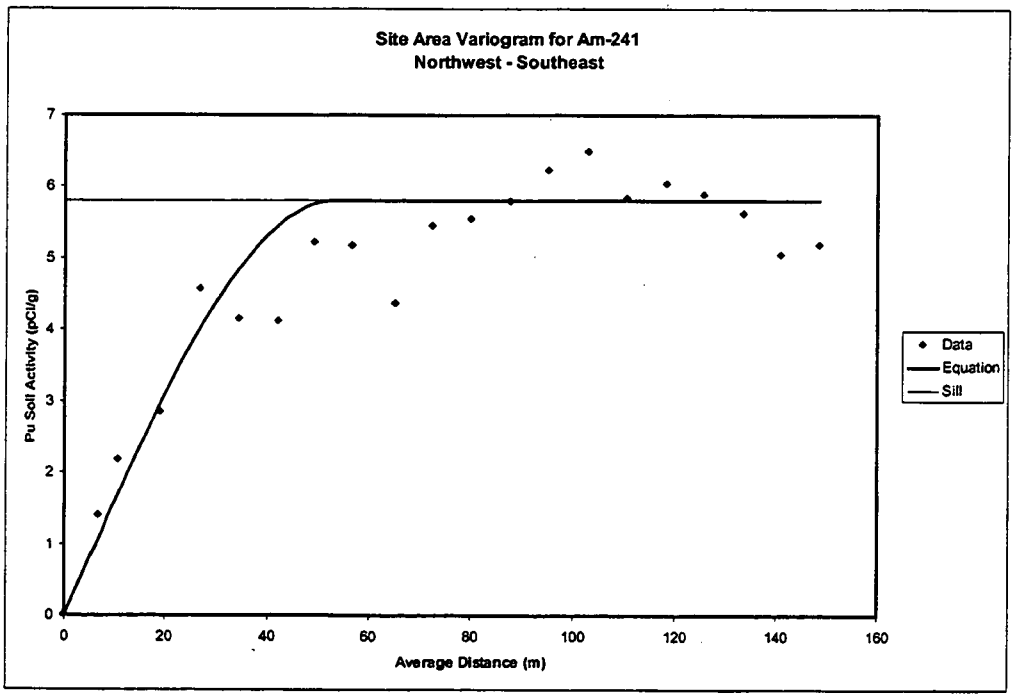

164

Figure TA-2-15. Site Area Variograms for U-233/234

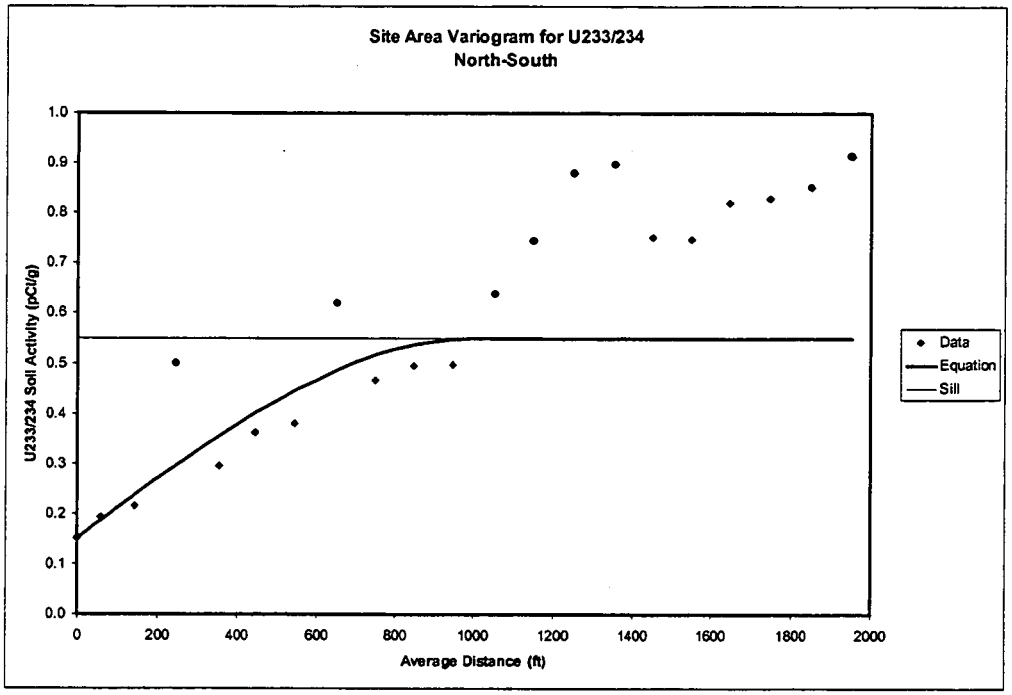

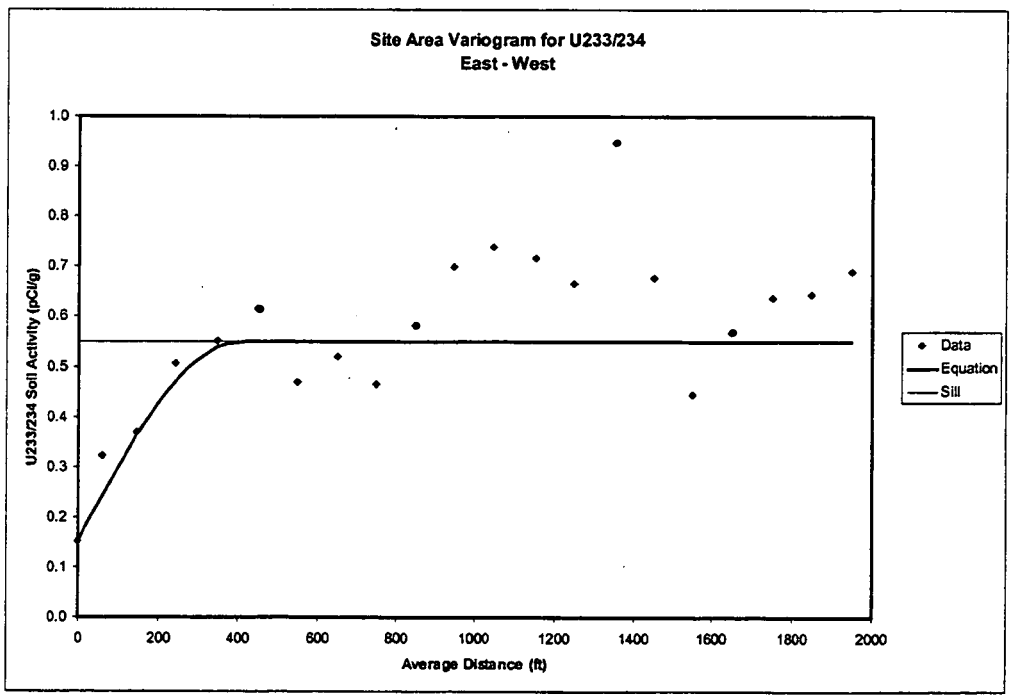

165

Figure TA-2-16. Site Area Variograms for U-235

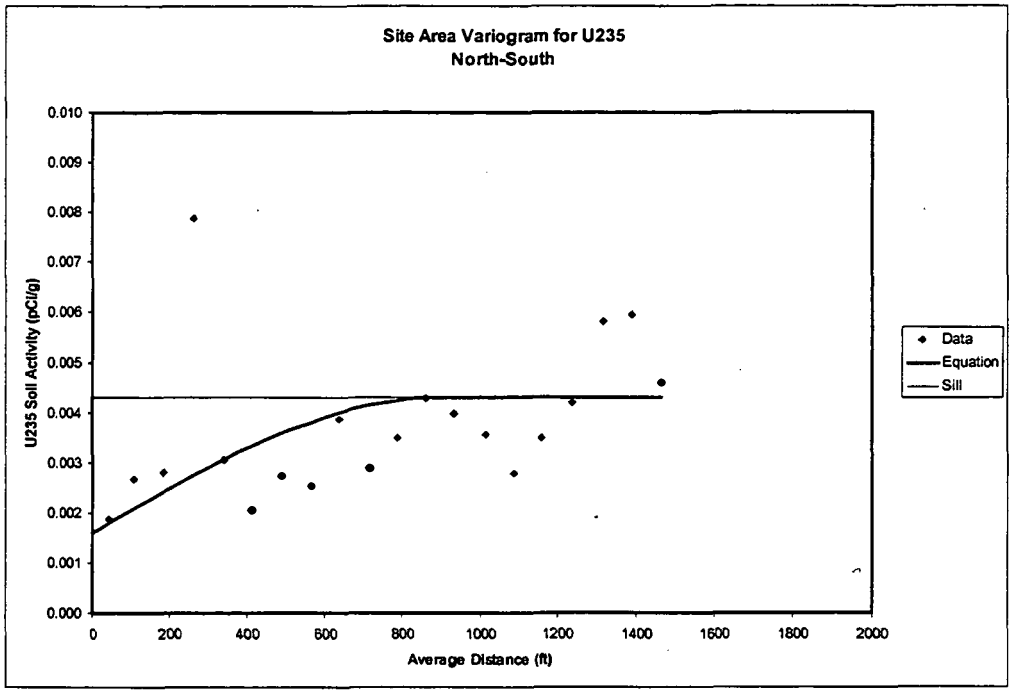

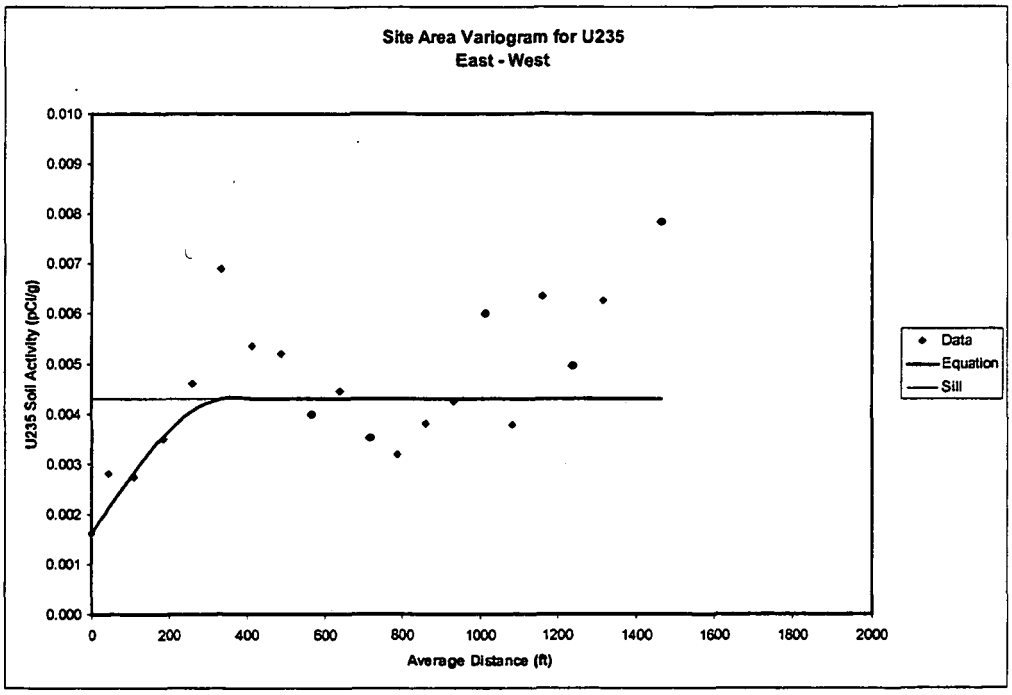

166

Figure TA-2-17. Site Area Variograms for U-238

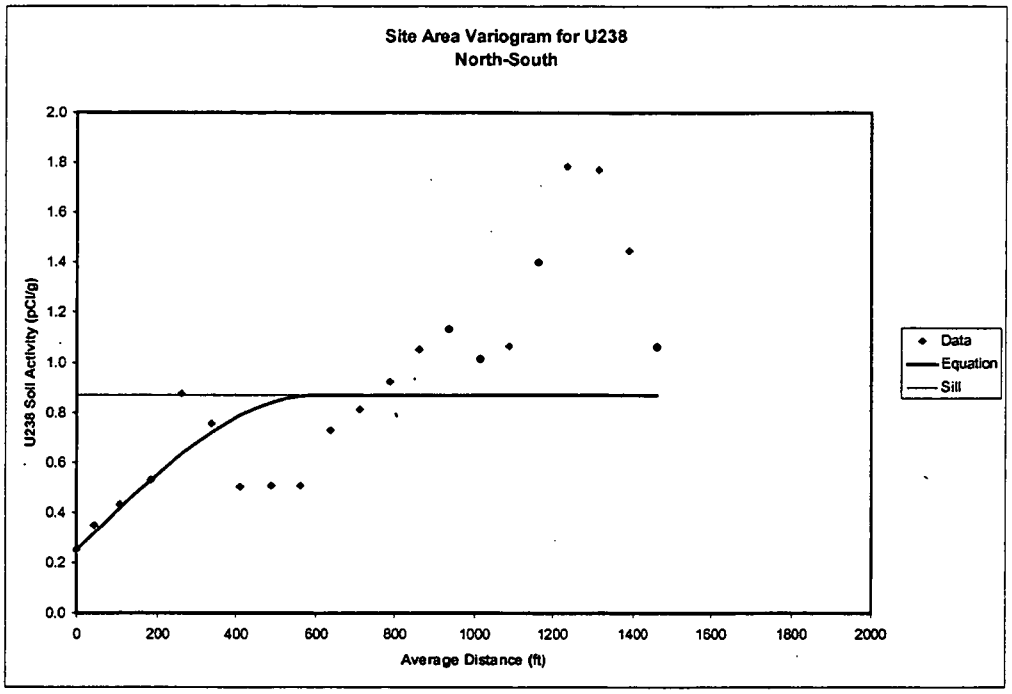

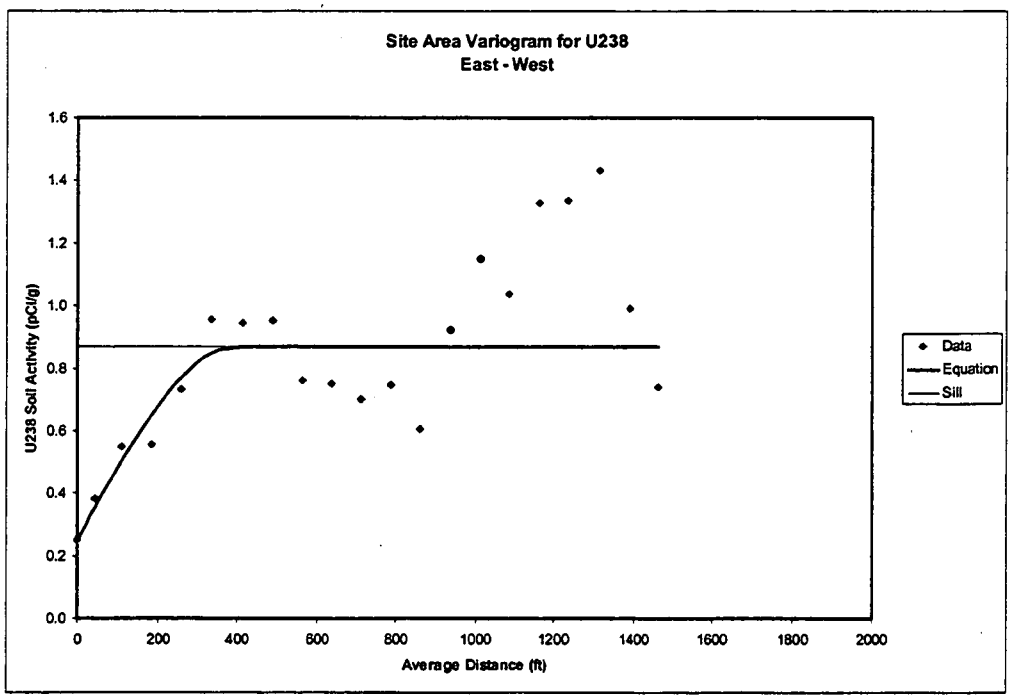

167

Figure TA-2-58. Monitoring Station GS10.

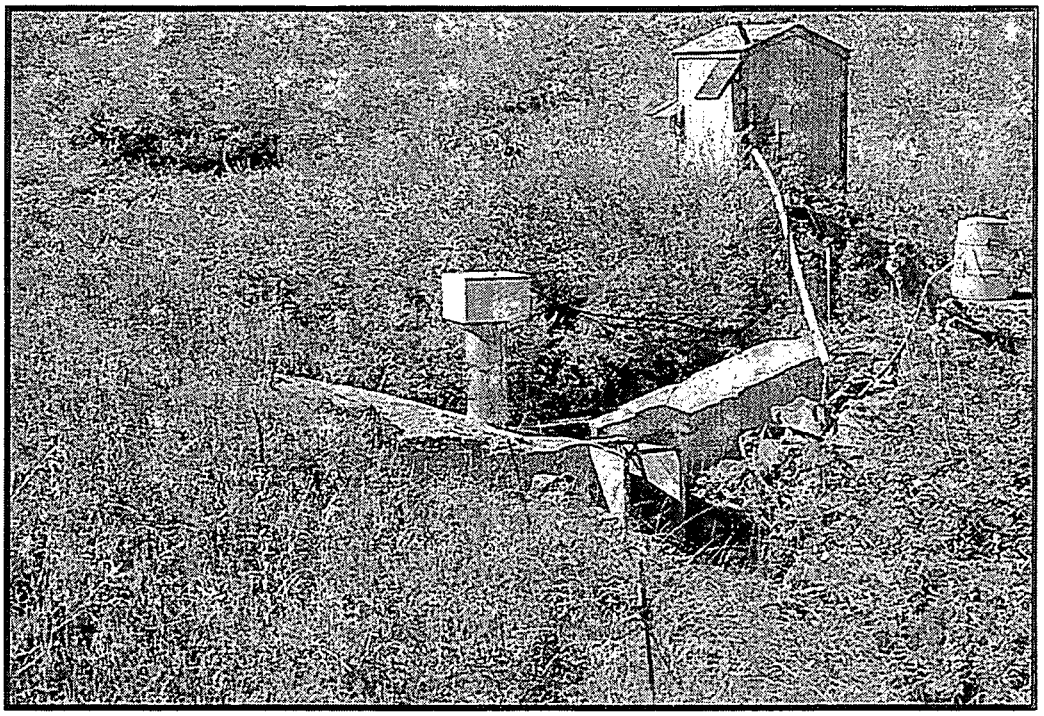

207

Figure TA-2-59. Example of Hydrograph Showing Rising-Limb Flow-Paced Composite Sampling.

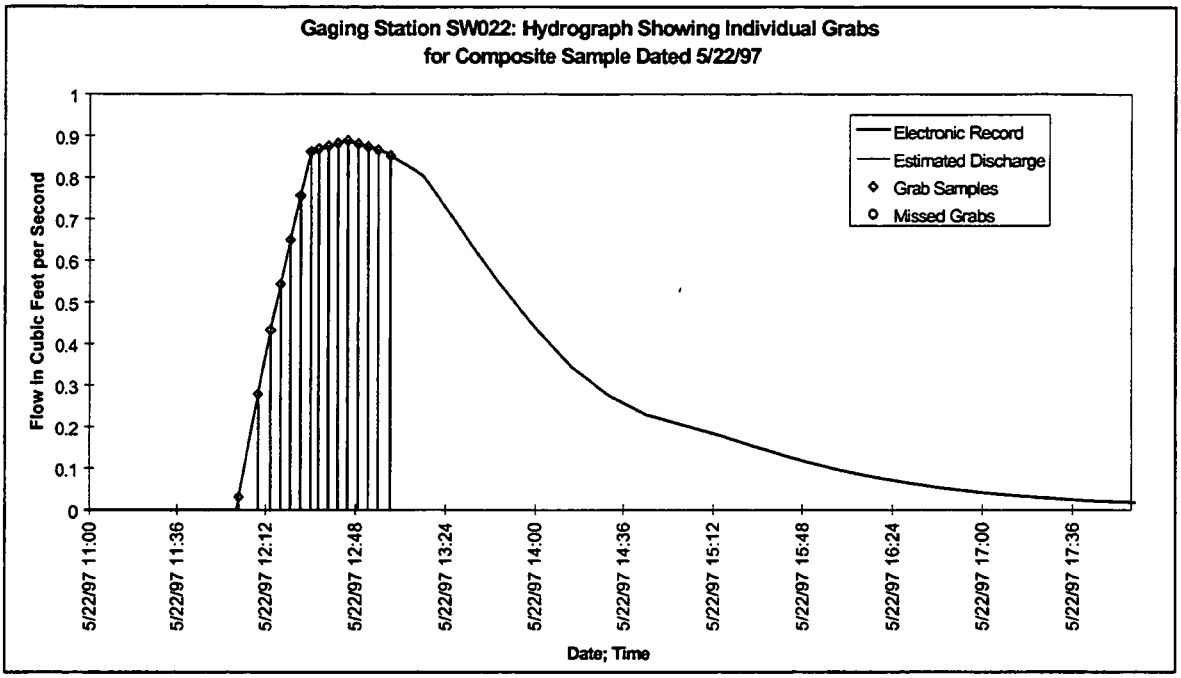

Figure TA-2-78. Average Actinide Concentrations in Air at RFETS Perimeter, 1997 –1999

(Total dose as a fraction of the 10-mrem standard converted using 40 CFR 61, Subpart H, Table 2)

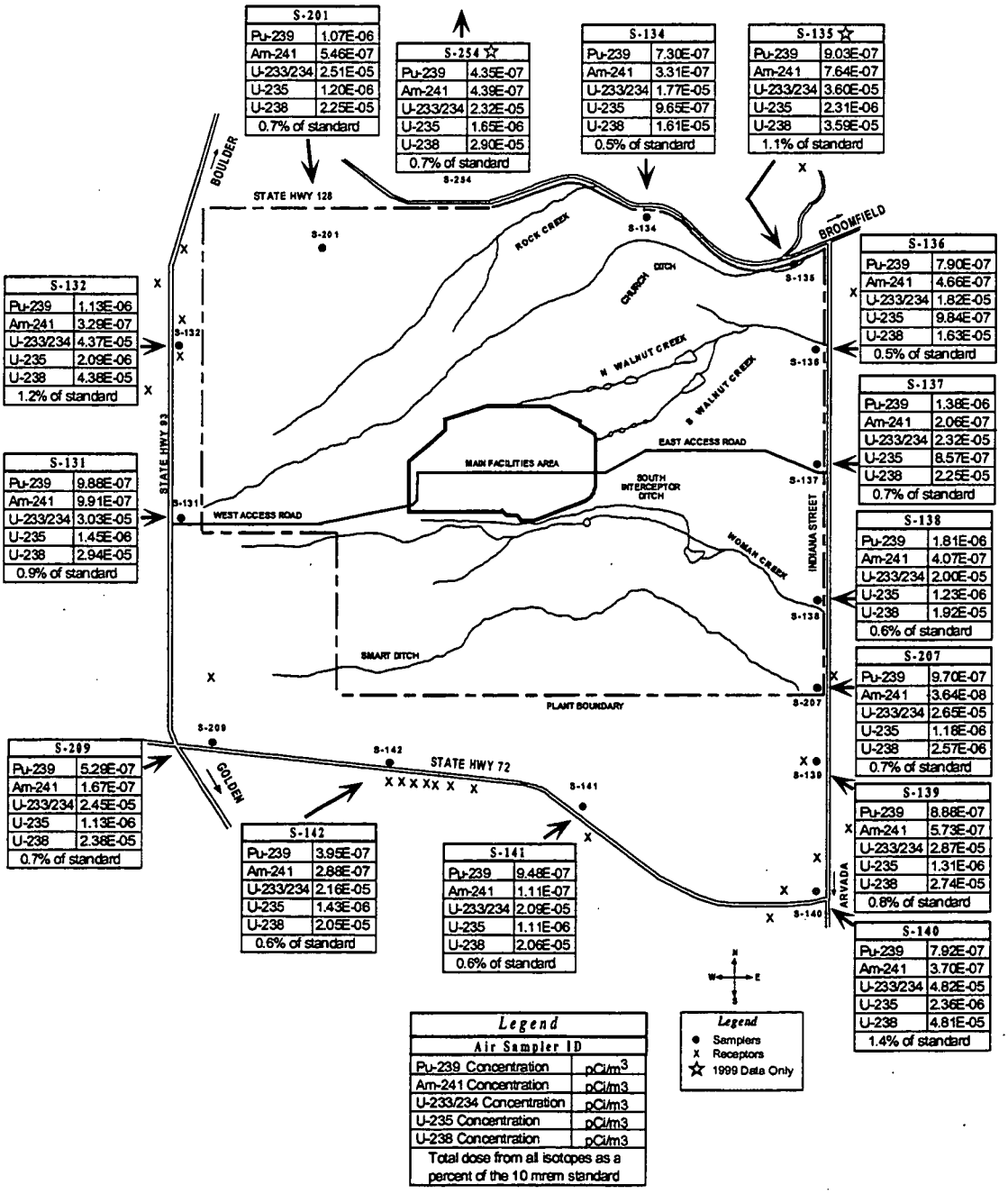

227

Figure TA-2-79. Expanded View of RAAMP Sampler

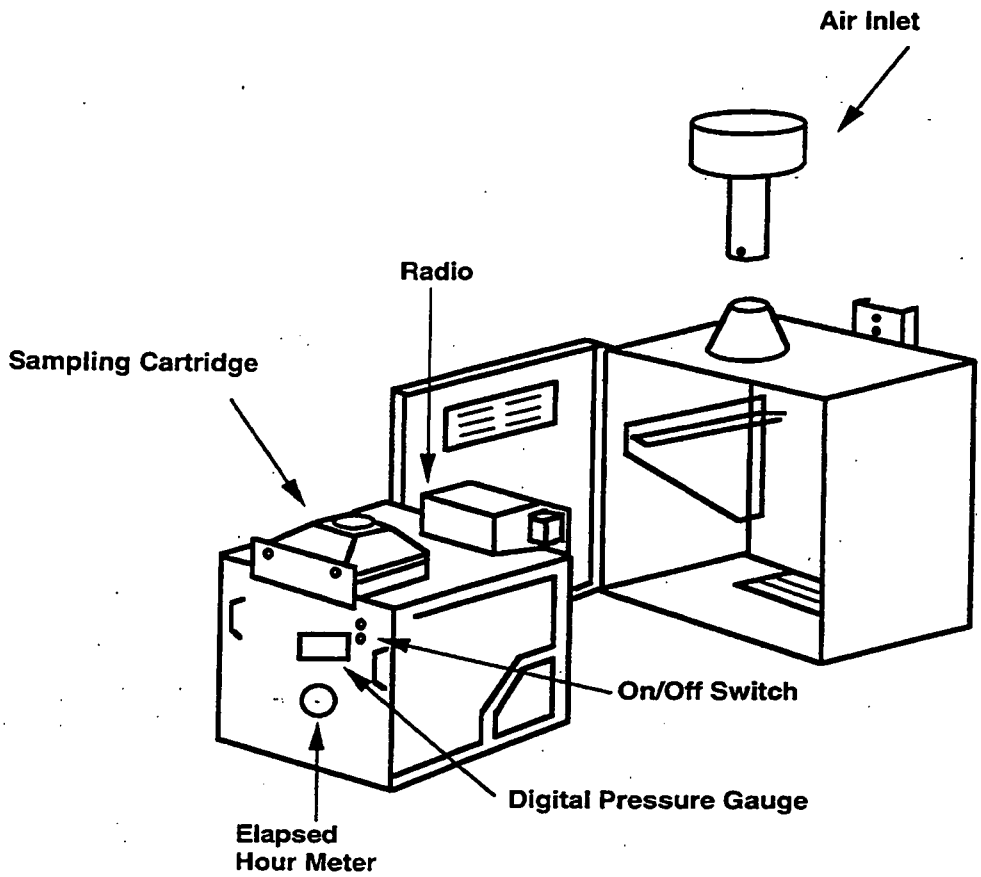

Figure TA-2-80. RAAMP Sampler (foreground) Near 903 Pad

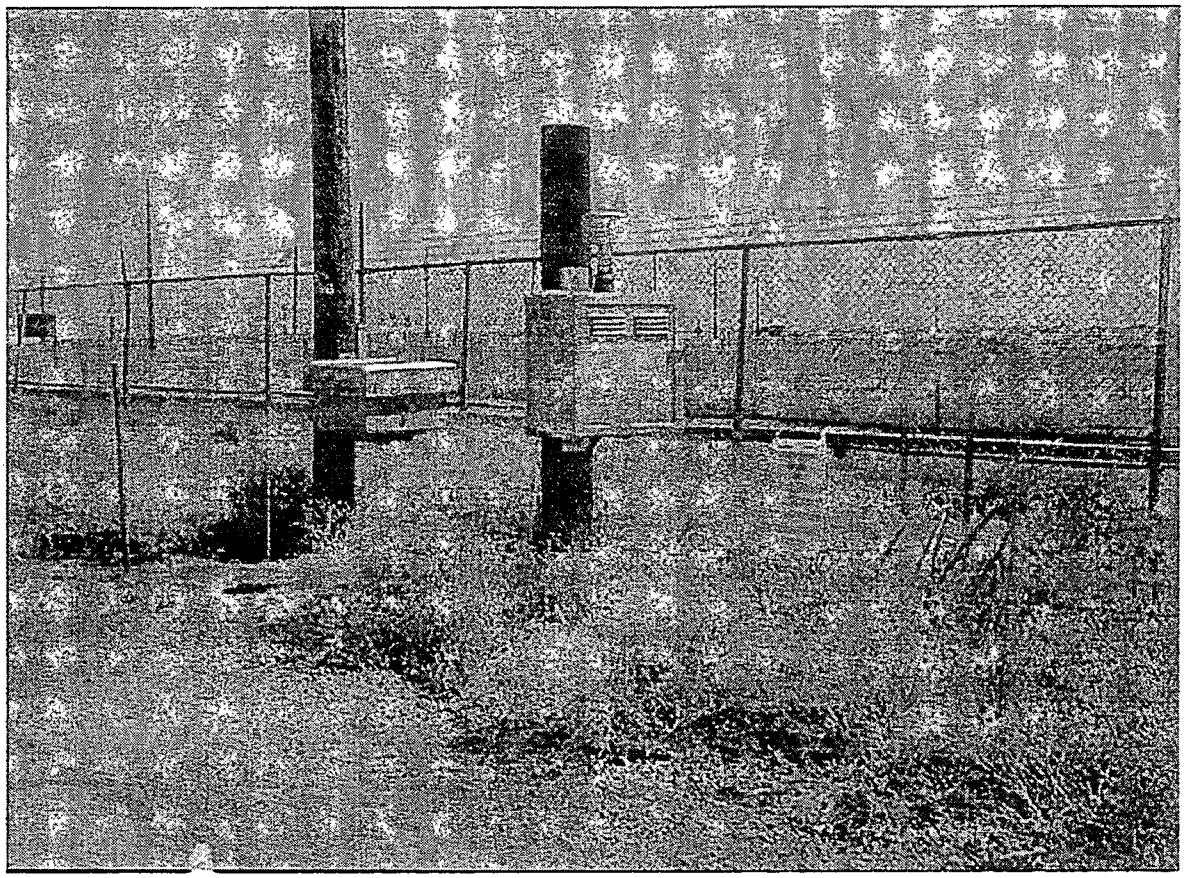

229

SECTION TA-3 – TABLE OF CONTENTS

TA - 3 PLUTONIUM, AMERICIUM AND URANIUM GEOCHEMICAL TRANSPORT PROCESSES 3-1

TA-3.1 Chapter Organization 3-1

TA-3.2 Summary of Initial Observations 3-2

TA-3.3 Summary of Actinide Elements: Plutonium, Americium and Uranium 3-7

TA - 3.3.1 Plutonium and Americium 3-11

TA - 3.3.2 Uranium 3-13

TA-3.4 Plutonium Geochemistry 3-14

TA - 3.4.1 Origin and Occurrence of Plutonium 3-14

TA - 3.4.2 Plutonium at RFETS 3-16

TA - 3.4.3 Aqueous Speciation 3-17

TA - 3.4.4 Dissolution, Precipitation and Coprecipitation of Plutonium 3-25

TA - 3.4.5 Sorption/Desorption of Plutonium 3-29

TA-3.5 Americium Geochemistry 3-31

TA - 3.5.1 Origin and Occurrence of Americium 3-32

TA - 3.5.2 Aqueous Speciation of Americium 3-33

TA - 3.5.3 Dissolution, Precipitation and Coprecipitation of Americium 3-35

TA - 3.5.4 Sorption/Desorption of Americium 3-37

TA-3.6 Uranium Geochemistry 3-38

TA - 3.6.1 Origin and Occurrence of Uranium 3-38

TA - 3.6.2 Aqueous Speciation of Uranium 3-42

TA - 3.6.3 Dissolution, Precipitation and Coprecipitation of Uranium 3-49

TA - 3.6.4 Sorption/Desorption of Uranium 3-50

TA-3.7 Colloid formation, Aggregation and Aqueous Particle Size distribution 3-52

TA - 3.7.1 Introduction 3-52

230

TA - 3.7.2 Colloid Definitions 3-54
TA - 3.7.3 Environmental Behavior of Colloids 3-57
TA - 3.7.4 Non-RFETS Data Concerning Colloid-Facilitated Transport of Actinides 3-65
TA - 3.7.5 Current RFETS Data on Colloid-Associated Actinides 3-66
TA - 3.7.6 Summary of Colloid-Facilitated Actinide Transport 3-70

TA-3.8 Applicability of Empirical Partition Coefficient, K_d, Values for Modeling Actinide Transport in Soils and Groundwater at RFETS 3-73
TA - 3.8.1 Introduction 3-73
TA - 3.8.2 Definitions and Concepts 3-73
TA - 3.8.3 Actinide Empirical K_d Values From the Literature 3-93
TA - 3.8.4 Recommendation on the Use of Empirical K_d values at RFETS. 3-113

TA-3.9 Biogeochemistry 3-115
TA - 3.9.1 Microbial Effects on Actinide Transport in the Environment 3-115
TA - 3.9.2 Microbiological Transformations 3-130
TA - 3.9.3 Biogeochemistry Conclusions 3-138

TA-3.10 Technical Appendix Section TA-3 References 3-139

SECTION TA-3 TABLES

Table TA-3-1. Isotopic Ratios in Potential Sources of Uranium at RFETS 3-40
Table TA-3-2. Literature Relevant to Actinide Association with Colloids at RFETS 3-71
Table TA-3-3. Empirical K_d Values for Uranium at Non-RFETS Locations 3-99
Table TA-3-4. Empirical K_d Values for Uranium at RFETS 3-102
Table TA-3-5. Empirical K_d Values for Plutonium-239/240 at Non-RFETS Locations 3-106
Table TA-3-6. Empirical K_d Values for Plutonium-239/240 at RFETS 3-109
Table TA-3-7. Empirical K_d Values for Am-241 at Non-RFETS Locations 3-111
Table TA-3-8. Empirical K_d Values for Am-241 at RFETS 3-112
Table TA-3-9. Functional Groups and Complexing Compounds Produced by Microorganisms 3-116

231

Table TA-3-10. Reduction Potentials (pH 7, $Mn^+(aq)$ = 10-6 M) for Selected Metal Oxyhydroxides 3-131

SECTION TA-3 FIGURES

Figure TA-3-1. Periodic Table of the Elements 3-8
Figure TA-3-2. Pourbaix Diagram for Plutonium 3-11
Figure TA-3-3. Computer simulation of Pu aqueous speciation as a function of pH using the MINTEQA2 program 3-24
Figure TA-3-4. Calculated pCO_2–pH predominance diagram for the system Am(III)/CO_2/H_2O 3-34
Figure TA-3-5. Fractional distribution of Am(III) complexes as a function of pH 3-36
Figure TA-3-6. Calculated Pourbaix predominance diagram for aqueous species in the U-O_2-CO_2-H_2O system 3-43
Figure TA-3-7. Calculated distribution of U(VI) hydrolysis species as a function of pH 3-45
Figure TA-3-8. Calculated distribution of U(VI) aqueous species as a function of pH 3-45
Figure TA-3-9. Physical processes that cause particle collisions in surface water that can also lead to aggregation 3-60
Figure TA-3-10. Simulation results obtained by Filella and Buffle (1993) that illustrate the development of volume-based particle size distributions in surface water starting from an initially uniform size distribution 3-60
Figure TA-3-11. Processes occurring in porous media, which control colloid and particle transport in groundwater 3-62
Figure TA-3-12. Computed affect of diameter on the degree of transport of colloids and particles in groundwater 3-64
Figure TA-3-13. Diagram illustrating predicted and typical experimental breakthrough curves for trace metals adsorbed on an elution column 3-77

232

Figure TA-3-14. Uranium literature K_d values versus pH 3-94
Figure TA-3-15. Dissolved speciation of U(VI) at a total concentration of 10^{-6} M and ionic strength = 0.1 3-95
Figure TA-3-16. Radionuclide Transport: Interactions with Microorganisms 3-115
Figure TA-3-17. DFB Chelated Iron (Fedes) and Non-Chelated Iron (Fe) Unsaturated Transport through Crushed Tuff 3-119
Figure TA-3-18. Structures of DFE Free Ligand and Metal Complexes 3-133
Figure TA-3-19. Structures of the exopolymers produced by B. licheniformis (left) and R. erythropolis (right, proposed), respectively 3-134

TA - 3 PLUTONIUM, AMERICIUM AND URANIUM GEOCHEMICAL TRANSPORT PROCESSES

TA-3.1 CHAPTER ORGANIZATION

Chapter TA-3 reviews chemical reactions that potentially affect Pu, Am and U mobility in the environment. The major subsections address the following subjects:

- Section TA-3.2 summarizes observations drawn from a review of available actinide transport data;

- Section TA-3.3 provides an overview of some fundamentals of actinide chemistry, colloid and actinide mobility and a comparison of world-wide and RFETS-specific K_d values;

- Sections TA-3.4, TA-3.5 and TA-3.6 review in more detail the fundamentals and current state of knowledge of Pu, Am and U chemistry. This information is helpful in estimating the environmental behavior of these actinides and critically reviewing the reasonableness and limitations of transport analyses and computer model predictions. These sections also contain data concerning chemical properties of Pu, Am and U that are essential for transport evaluations and include references that clarify the conditions under which the data were collected;

- Section TA-3.7 provides a discussion of the environmental behavior of colloids. Colloid-facilitated movement of actinides can be a potentially significant actinide transport mechanism; and

- Section TA-3.8 discusses the limitations and usefulness of the distribution coefficient, K_d, as an indicator of actinide environmental mobility, including the difficulty of defining the term "dissolved" when colloids are present. K_d represents the measured concentration of a compound associated with solid materials divided by its concentration dissolved in water that is in contact with the solid materials. For example, if $K_d = 10^3$ mL/g for a compound, then the concentration of that compound in solid forms (precipitated solids or sorbed to solid

234

surfaces) is 1,000 times greater than its dissolved concentration. For comparison, most K_d values for Pu measured at RFETS lie between about 10^4 mL/g and 10^5 mL/g. The K_d parameter is useful for calculating a *retardation factor,* which is used for predicting the rate of movement, relative to groundwater velocity, of *soluble* contaminants in a soil environment where surface sorption is the main retarding process. A K_d value of 10^3 or greater indicates that the contaminant is essentially immobile in the soil. Because of the many environmental factors that can affect K_d, field-measured values are always very Site-specific. Section TA-3.8 also summarizes measured values of K_d at RFETS and other locations world-wide, including data concerning many of the environmental factors that influence measured K_d values.

TA-3.2 SUMMARY OF INITIAL OBSERVATIONS

(The following observations are derived from data presented in Chapter TA-3. References for this Section are given in the more complete discussions of Sections TA-3.3 through TA-3.8.)

- Pu and Am at RFETS are almost entirely (around 99 %) in solid forms, either bound to soil and sediment particles or precipitated as oxides and hydroxides. This percentage is essentially the same as that found world-wide. These findings are consistent with the fact that the large values of K_d reported for Pu and Am at RFETS (between about 10^3 and 10^5 mL/g) lie within the range of all world-wide K_ds identified so far for these actinides. However, it must be recognized that a K_d interpretation may be invalid because mobility of Pu and Am at RFETS may not involve chemical sorption reactions.

- There are background levels for Pu, Am and U at RFETS that arise from non-RFETS activities. Fallout from atmospheric weapons testing contributes to Pu and Am concentrations in surface soils and leaching from U minerals contributes to U groundwater and subsurface soil concentrations. Because Pu, Am and U used at RFETS have isotopic signatures that can be distinguished from fallout and natural abundances, measurements of the isotope abundances of these actinides are useful for identifying the RFETS contribution to on-Site concentrations. It should be noted that the isotopic content of a given actinide

236

does not influence its environmental mobility, although it is important for a risk assessment because the different isotopes have different half-lives, specific activities and decay particle energies.

- Recent measurements of Pu in RFETS soils in the Buffer Zone support many earlier studies indicating that Pu at RFETS is almost entirely present as PuO_2, generally accepted to be immobile in the subsurface, except for potential colloid-facilitated movement. See Section TA-3.7 for a discussion of colloids.

- Nearly all the Pu and Am radioactivity in RFETS soils is confined to the top 20 centimeters (about 90 % in the top 12 centimeters) and has been stable in that configuration with no significant movement below this depth for about 30 years.

- The solubility of Pu and Am solids under the oxidizing environmental conditions most common at RFETS is very low, around 10^{-15} moles/liter. Although reducing conditions are likely to exist in the treatment ponds and in landfill locations, there is evidence that reducing conditions do not increase Pu mobility at RFETS.

- A result of the observations above is that subsurface mobility of Pu and Am is expected to be very low. Measurements at RFETS support this conclusion. Measured Pu and Am concentrations in groundwater below the Industrial Area and near the 903 Pad range from below the analytical detection limit (about 0.01 to 0.02 pCi/L) to about 0.1 pCi/L. In contrast, soil levels (3 to 4 inches below original grade) within the 903 Pad and Lip Area ranged between 0.8 to 152, 260 pCi/g for Pu and 0.2 to 31,670 pCi/g for Am (RMRS, 2000). At present, it cannot be stated with certainty whether detections of Pu and Am in groundwater arise from surface contamination carried downward by well-drilling activities, from subsurface water transport of colloids carrying sorbed Pu and Am or from both processes. These possibilities are presently being studied with a series of wells drilled under "aseptic" conditions.

236

- Am and Pu have generally similar spatial distributions in RFETS soil and the Pu/Am activity ratio remains relatively constant at different locations. This might be expected since dispersal mechanisms are similar for both elements and because a substantial fraction of the Am-241 at RFETS results from radioactive decay of Pu-241 (half-life = 14.4 years), both before and after release to the environment. Since the similar spatial distributions have been in place for about two half-lives of Pu-241, it can be concluded that the important distribution mechanisms are physical rather than chemical. This means that surface particulate and/or colloid erosion mechanisms are dominant for Pu and Am at RFETS and that transport of soluble species of Pu and Am through the subsurface plays a very minor and so far undetectable, role. These conclusions do not apply to U, which undergoes significant subsurface transport.

- Since K_d models are intended for predicting movement of *soluble* contaminants in an environment where soluble transport is significant and surface sorption is the main retarding process, K_d models will not accurately predict Pu and Am migration at RFETS. Although K_d modeling is not valid for RFETS Pu and Am mobility, evaluations of *empirical* K_ds have two valid functions at RFETS. (1) They may be useful for worst-case scenarios of subsurface transport. (2) Their high values predict that Pu and Am will be almost entirely associated with solids and, therefore, that particulate transport mechanisms for Pu and Am are dominant at RFETS.

- Studies at RFETS suggest that appropriate empirical K_ds at RFETS would lie in the 10^4 to 10^5 mL/g range for Pu and in the 10^3 to 10^8 range for Am. K_ds of 10^3 mL/g or greater indicate immobilized actinides and support the conclusion that subsurface transport of soluble species from the 903 Pad area and other RFETS locations should be a negligible pathway for Pu and Am transport.

- Measurements of actinide movement caused by wind and storm runoff show that the observed mobility of Pu and Am at RFETS is largely controlled by soil surface erosion processes and is essentially the same as the mobility of the surface soils and stream sediments.

231

- Although transport by erosion of surface soil particulates is the predominant mechanism for Pu and Am movement at RFETS, the smaller potential for Pu and Am migration downward and laterally through the soil subsurface should be addressed. Pu and Am are known to associate with colloid-sized solids small enough to be carried by water movement through the soil matrix. Pu and Am are also known to form ionic species of increased solubility through complexation and hydrolytic processes involving environmental anions such as hydroxide and carbonate to form positively or negatively charged ions. Such charged complexes often have greater solubility than the uncomplexed solids. The positively charged ions generally have high sorptivity, while negatively charged ions generally have low sorptivity. The significance of complex-facilitated transport of Pu and Am at RFETS is not quantified at this time.

- The oxidation state of actinides has a controlling effect on their environmental behavior. Oxidation states, in turn, are determined by each actinide's unique electronic structure and the geochemical conditions of surrounding soil and water. The actinide oxidation states of environmental interest are III, IV, V and VI. Different oxidation states can form various molecular complexes, each with a characteristic solubility and chemical reactivity. Actinides in the lower oxidation states (III and IV) tend to form complexes with very low solubilities and the strongest sorption to mineral and rock surfaces. Actinides in the higher oxidation states (V and VI) tend to form complexes with much higher solubilities and the weakest sorption to mineral and rock surfaces.

- Because of oxidation state differences, the environmental behavior of U is very different from that of Pu and Am. Whereas Pu and Am tend to be in the lower oxidation states III (Am) and IV (Pu) under environmental conditions, U can be present in the two oxidation states IV and VI. Because U(VI) forms compounds of much greater solubility than do Pu(IV) or Am(III), U exhibits a much greater tendency to be in dissolved forms than do Pu or Am.

- World-wide K_d values for U show greater variability than for Pu and Am. World-wide U K_ds vary from less than unity to around 10^4 mL/g, with typical values between about 10 and

1,000 mL/g. The EPA (1999) recommends that the best way to model the concentration of U may be with solubility constants rather than a K_d approach.

- U occurs naturally at much higher concentrations than are measured for Pu and Am. Leaching of U from mineral deposits and sediments derived from U-containing rocks contributes to the overall U concentrations measured at RFETS. Some of the U used at RFETS was depleted in U-234 and U-235 and some was enriched, relative to naturally-occurring U. These isotopic differences have been used to confirm that most of the sampled wells contain natural U along with anthropogenic U originating from RFETS activities. However, studies so far are not yet complete enough to determine relative contributions from natural and RFETS sources.

- Unlike Pu and Am, environmental U species can undergo significant subsurface transport. However, except in the immediate vicinity of source terms, measured levels of U at RFETS are difficult to distinguish from background. Data concerning the historical distribution of natural U will be useful for predicting the movement of anthropogenic U, since U from RFETS sources will be subject to similar conditions of geochemistry and dispersal mechanisms as background U.

- In many instances, K_d models have been shown to predict geochemical behavior that is contrary to field measurements. If the basic K_d approach is refined by including data concerning the effects on K_d of various environmental parameters, its predictive capabilities improve. However, the K_d approach will still combine multiple disparate processes and chemical reactions into a simplified parameter so that an empirical component will always be present.

- The complexity and spatial heterogeneity of the subsurface soil/water matrix makes an important contribution to restrictions on using empirical K_ds for predicting contaminant mobility. The restrictive conditions imposed on a K_d value indicate that its application will always be highly Site-specific, especially when precise and single-valued K_ds are required. For extremely low-solubility elements (e.g. Pu and Am), mechanical/physical processes will

totally dominate transport mechanisms and will negate the use of chemical approaches such as K_d and/or equilibrium/complexation models.

- Both the K_d and chemical equilibrium/complexation approaches assume conditions of system equilibrium and reversibility. Neither approach can deal convincingly with kinetically controlled and open non-conservative) systems. Nevertheless, both modeling approaches can use literature data to compare mobility predictions with known transport behavior at RFETS. Such comparisons indicate that, even with extensive Site-specific K_d data, such modeling approaches will not provide useful predictive capabilities for decision support with respect to Pu and Am transport, although they might be of value for U.

TA-3.3 SUMMARY OF ACTINIDE ELEMENTS: PLUTONIUM, AMERICIUM AND URANIUM

Pu, Am and U are members of the actinide group of elements, those fourteen elements with atomic numbers 90 to 103 that follow actinium in the Periodic Table (Figure TA-3-1). The actinide elements occupy their unique position at the bottom of the Periodic Table and they all contain 5*f* electrons in their valence shell.

A common characteristic of the actinide elements is that their electronic structures minimize chemical differences among them and results in similar chemical behavior within a given period as well as within a given group of the periodic table. This behavior can be explained by similarities in atomic radii and ionization energies and is in contrast to the main group (non-transition) elements, where chemical similarities occur mainly within a periodic table group and chemical properties change markedly across a given period. Because chemical differences among the actinides are small, systematic and largely predictable, it is frequently possible to estimate chemical properties of less well-known actinides from observations on more studied members of the group. In fact, some properties of the heavier members of the actinides were predicted prior to discovery (Seaborg and Loveland, 1990).

Figure TA-3-1. Periodic Table of the Elements

1 1A																	18 8A
1 **H** 1.008	2 2A											13 3A	14 4A	15 5A	16 6A	17 7A	2 **He** 4.003
3 **Li** 6.941	4 **Be** 9.012											5 **B** 10.81	6 **C** 12.01	7 **N** 14.01	8 **O** 16.00	9 **F** 19.00	10 **Ne** 20.18
11 **Na** 22.99	12 **Mg** 24.31	3 3B	4 4B	5 5B	6 6B	7 7B	8 8B	9 8B	10 8B	11 1B	12 2B	13 **Al** 26.98	14 **Si** 28.09	15 **P** 30.97	16 **S** 32.07	17 **Cl** 35.45	18 **Ar** 39.95
19 **K** 39.10	20 **Ca** 40.08	21 **Sc** 44.96	22 **Ti** 47.88	23 **V** 50.94	24 **Cr** 52.00	25 **Mn** 54.94	26 **Fe** 55.85	27 **Co** 58.93	28 **Ni** 58.70	29 **Cu** 63.55	30 **Zn** 65.38	31 **Ga** 69.72	32 **Ge** 72.59	33 **As** 74.92	34 **Se** 78.96	35 **Br** 79.90	36 **Kr** 83.80
37 **Rb** 85.47	38 **Sr** 87.62	39 **Y** 88.91	40 **Zr** 91.22	41 **Nb** 92.91	42 **Mo** 95.94	43 **Tc** (98)	44 **Ru** 101.1	45 **Rh** 102.9	46 **Pd** 106.4	47 **Ag** 107.9	48 **Cd** 112.4	49 **In** 114.8	50 **Sn** 118.7	51 **Sb** 121.8	52 **Te** 127.6	53 **I** 126.9	54 **Xe** 131.3
55 **Cs** 132.9	56 **Ba** 137.3	57 ***La** 138.9	72 **Hf** 178.5	73 **Ta** 180.9	74 **W** 183.9	75 **Re** 186.2	76 **Os** 190.2	77 **Ir** 192.2	78 **Pt** 195.1	79 **Au** 197.0	80 **Hg** 200.6	81 **Tl** 204.4	82 **Pb** 207.2	83 **Bi** 209.0	84 **Po** (209)	85 **At** (210)	86 **Rn** (222)
87 **Fr** (223)	88 **Ra** 226.0	89 **#Ac** 227.0	104 **Rf** (261)	105 **Db** (262)	106 **Sg** (263)	107 **Bh** (262)	108 **Hs** (265)	109 **Mt** (266)									

*Lanthanide series	58 **Ce** 140.1	59 **Pr** 140.9	60 **Nd** 144.2	61 **Pm** (145)	62 **Sm** 150.4	63 **Eu** 152.0	64 **Gd** 157.3	65 **Tb** 159.0	66 **Dy** 162.5	67 **Ho** 164.9	68 **Er** 167.3	69 **Tm** 168.9	70 **Yb** 173.0	71 **Lu** 175.0
# Actinide series	90 **Th** 232.0	91 **Pa** 231.0	92 **U** 238.0	93 **Np** 237.0	94 **Pu** (244)	95 **Am** (243)	96 **Cm** (247)	97 **Bk** (247)	98 **Cf** (251)	99 **Es** (252)	100 **Fm** (257)	101 **Md** (258)	102 **No** (259)	103 **Lr** (260)

All actinides undergo the characteristic chemical reactions of reduction/oxidation, acid-base changes in speciation, precipitation and coprecipitation, formation of aqueous complexes, sorption and formation of finely divided particles (true colloids and pseudocolloids; see Section TA-3.7) (Allard and Rydberg, 1983, Choppin, 1988, Dozol and Hagemann, 1993, Silva and

241

Nitsche, 1995). Because actinide environmental behavior is so complex, the environmental fate of actinides can differ markedly at different sites due to differing geochemical conditions.

Environmental properties of actinides are controlled largely by their oxidation state. Oxidation states, in turn, are determined by each actinide's unique (although similar) electronic structure and the geochemical conditions of surrounding soil and water. The actinide oxidation states of environmental interest are III, IV, V and VI. Different oxidation states can form various molecular complexes, each with a characteristic solubility and chemical reactivity. Actinides in the lower oxidation states (III and IV) hydrolyze readily and form complexes with very low solubilities and the strongest sorption to mineral and rock surfaces. Actinides in the higher oxidation states (V and VI) can form complexes that have much higher solubilities and the weakest sorption to mineral and rock surfaces. Because of differences in electronic structure, each actinide exhibits different oxidation states for any given set of solution conditions.

Within the actinides, the stability of the higher oxidation states (V and VI) decreases with increasing atomic number and there is a corresponding increase in the stability of, first the IV state and then the III state. Thus, the VI state is more important for U (atomic number 92) than for Pu (atomic number 94) or Am (atomic number 95). The most stable state for Pu is IV and for Am, it is III.

The most common way to display the dependence of oxidation state on solution conditions is with a plot that shows oxidation states as a function of pH and redox potential (E_h). Such plots are called Pourbaix diagrams, E_h-pH diagrams or "predominance-area" diagrams (because they show the predominant redox species within different E_h/pH ranges). Figure TA-3-2 shows a Pourbaix diagram for aqueous Pu species (ΣPu(aq) = 10^{-8} M) in water containing Pu, hydroxide, carbonate and fluoride ions. It shows which oxidation states and chemical species are predominant under different conditions of pH and redox (E_h) potential. Other less abundant species and oxidation states may be present at the same time under the same conditions.

The ranges over which different oxidation states are most stable are bounded by solid straight lines. The exact position of the oxidation state boundaries depends also on the total Pu

242

concentration and the solution ionic strength. In general, the more dilute the solution, the larger the predominance areas for soluble species. Pure acid-base equilibria between different oxidation states are indicated by vertical boundaries and pure redox equilibria by horizontal boundaries. Combination equilibria involving both redox potential and pH produce diagonal boundaries. Diagonal boundaries generally slope downward from left to right because basic solutions tend to favor the more oxidized species.

Of particular interest is the range of E_h/pH values found in natural waters (seawater, rainwater and groundwater), bounded by the grayed area in Figure TA-3-2 (Wulfsberg, 1987). The figure shows that, in natural waters and Pu concentration of 10^{-8} M, dissolved Pu may exist in oxidation states III, IV and V depending on the actual geochemical (pH, Eh, etc.) conditions. Note that the stability zone for solid PuO_2(c) overlaps nearly all of the E_h/pH range on natural waters. The three solid dots are triple points, where Pu can exist simultaneously in three different oxidation states. Disproportionation reactions can occur at and near these points. See Katz et al. (1986), Choppin et al. (1995) and Cooper (2000) for discussions of actinide solution chemistry.

Although different actinides in the same oxidation state have similar chemical properties, the overall environmental chemistry of the actinides, especially Pu, is complex because of the potential to have multiple oxidation states in solution, to undergo extensive hydrolysis and to undergo hydrolytic polymerization (Coughtrey et al., 1984; Katz et al., 1986; Seaborg and Loveland, 1990; Choppin et al., 1995). In addition to oxidation state, actinide speciation in dissolved and solid phases, as well as sorption/desorption behavior, can also depend on:

- pH;
- presence of organic and inorganic complexing ligands;
- formation of polymers and colloids; and
- nature of solid surfaces.

A summary of important points from Sections TA-3.4 through TA-3.7, related to actinide mobility of Pu, Am and U in the environment is presented in Sections TA-3.3.1 and TA-3.3.2.

243

Figure TA-3-2. Pourbaix Diagram for Plutonium

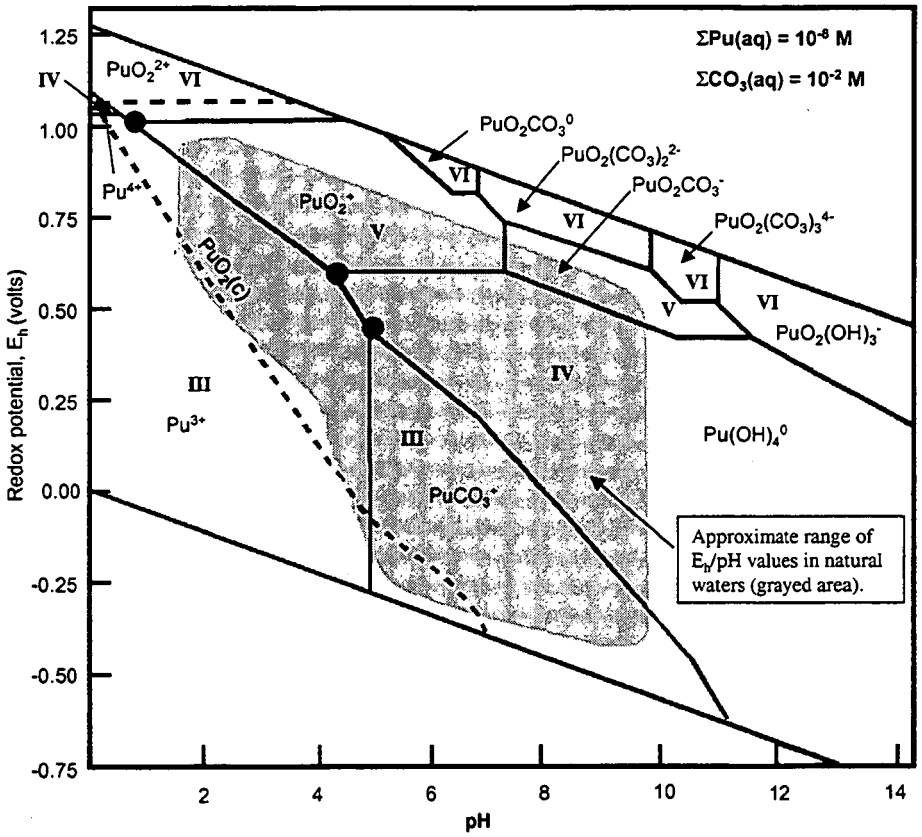

E_h vs. pH diagram showing the stability fields of predominant aqueous species calculated for the system $Pu/O_2/CO_2/H_2O$ at 25°C and 1 bar total pressure. The diagram is calculated for a total dissolved Pu [ΣPu(aq)] concentration of 10^{-8} M and a total dissolved carbonate [ΣCO_3(aq)] concentration of 10^{-2} M. Roman numerals indicate predominant Pu oxidation states. The approximate range of E_h/pH values found in natural waters is found within the gray zone. The dashed lines show the stability field of highly insoluble PuO_2(c), which overlaps most of the diagram and limits the maximum concentration of Pu in the overlapped regions to about 10^{-8} M. The three solid dots are triple points, where Pu can exist in three different oxidation states. The slanted lines that are upper and lower bounds to the diagram define the area of water stability. Above the upper line, water is thermodynamically unstable and is oxidized to elemental oxygen gas and hydrogen ions; below the lower line, hydrogen ions in water are reduced to elemental hydrogen gas (adapted from Langmuir, 1997).

TA - 3.3.1 Plutonium and Americium

Pu and Am often behave similarly in the environment, differing from U due to differences in environmentally stable oxidation states. Natural background concentrations for Pu and Am are very low, arising primarily from past atmospheric nuclear weapons testing.

244

The environmental species of Pu and Am are often similar in that they both are relatively insoluble. In natural waters, Pu and Am solubility is generally limited by the formation of amorphous hydroxides or oxides. Sorption of hydrolyzed Pu(IV) or Am(III) in natural water on mineral surfaces and surfaces coated with organic material is often accountable for the very low observed concentrations of dissolved Pu and Am. The strong tendency of the hydroxides to sorb onto surfaces is a dominant and often controlling feature in Pu and Am geochemistry. Therefore, both Pu and Am are generally transported with soil particles or colloids, carried by wind and water movement. A result of the environmental predominance of solid phases is that environmental K_d values for Pu and Am are large (10^3 to 10^5 mL/g).

The main processes by which Pu and Am become associated with solids are by:

- Adsorption of dissolved Pu and Am to solid surfaces of soils, sediments and colloids;
- Ion exchange of dissolved Pu and Am to charged sites on clay and mineral surfaces and humic material;
- Precipitation of hydrolyzed Pu and Am as polyhydroxides and oxides;
- Coprecipitation and occlusion of dissolved Pu and Am with other precipitating minerals, such as oxides of aluminum, iron and manganese; and
- Polymerization of Pu ions into colloidal solids with molecular weights up to about 10,000 Daltons.

Pu and Am tend to be in the least soluble lower oxidation states III (Am) and IV (Pu) under environmental conditions common at RFETS. Pu(IV) and Am(III) hydrolyze readily to form hydrolytic species with the general formulas:

$$Pu(OH)_m^{(4-m)+} \ (m = 1,2,3,4) \qquad \text{and} \qquad Am(OH)_n^{(3-n)+} \ (n = 1,2,3)$$

245

For m = 1, 2 or 3, Pu forms the cations $Pu(OH)^{3+}$, $Pu(OH)_2^{2+}$ and $Pu(OH)_3^{+}$, which can contribute significantly to the overall solubility of Pu(IV). However, the case of m = 4 leads to amorphous $Pu(OH)_4(s)$, which has very low solubility. Am behaves similarly, hydrolyzing to form the soluble cations $Am(OH)^{2+}$ and $Am(OH)_2^{+}$ for n = 1 and 2, but producing the much less soluble $Am(OH)_3(s)$ for n = 3. When the solid hydrolysis products $Pu(OH)_4(s)$ and $Am(OH)_3(s)$ are present, their solubilities tend to limit the overall actinide solubility of systems that also contain the cationic hydrolysis products.

Amorphous $Pu(OH)_4$ polymerizes during aging by losing protons and forming oxygen bridges between adjacent molecules, aging toward the still less soluble form of polycrystalline $PuO_2(c)$. The estimated solubility of amorphous $Pu(OH)_4$ is around $10^{-9(\pm 2)}$ M and that of $PuO_2(c)$ around $10^{-15(\pm 3)}$ M (Knopp, 1999). The solubilities of the solid forms of Pu impose an upper limit on the total amount of dissolved Pu that can be present, even if Pu(V) or Pu(VI) are the more stable dissolved forms. In Figure TA-3-2, the stability fields of $Pu(OH)_4$ (not shown) and $PuO_2(c)$ (shown) overlap most of the E_h/pH range of natural waters. When $Pu(OH)_4(am)$ and $PuO_2(c)$ are present, they limit the concentrations of soluble Pu species to about 10^{-8} M (Langmuir, 1997).

However, in addition to hydrolysis, Pu and Am can form aqueous complexes with carbonate and other anionic species, as well as with humic substances. Complex formation can influence solubility and sorption characteristics. In a worst-case scenario, solubility may be increased and sorption inhibited, resulting in increased mobility.

TA - 3.3.2 Uranium

U must be treated apart from Pu and Am; it occurs naturally, has a higher natural background arising primarily from U-bearing mineral deposits and, because of oxidation state differences, the environmental behavior of U is very different from that of Pu and Am. U is stable in the two oxidation states IV and VI. Because U(VI) forms compounds of much greater solubility than do Pu(IV) or Am(III), U exhibits a much greater tendency to be in dissolved forms than do Pu or Am. In general, U is slightly soluble under RFETS environmental conditions, as compared to the insolubility of Pu and Am.

246

- U is the most abundant actinide occurring naturally in the environment. U activity in Colorado surface soils averages around 1.2 pCi/g. U is ubiquitous in the Colorado Front Range and background measurements of U activity in wells west of RFETS (generally upgradient and upwind of the Industrial Area) have been measured as high as 1,200 pCi/L.

- Because of its greater solubility under environmental conditions, aqueous dissolved transport of U must be recognized as a potentially important pathway.

- U, generally, is least mobile in reducing (anaerobic) environments with low concentrations of complexing anions and most mobile in oxidizing (aerobic) environments with high concentrations of complexing anions.

The EPA (1999) suggests that, because precipitation reactions often regulate the levels of dissolved U more effectively than sorption processes, in some cases the use of solubility constants may be a better way to model U mobility than the K_d concept. Langmuir (1997), however, states that trace levels of U (and other actinides) in the subsurface equilibrate with sorption sites. At pH>5 and concentrations below the solid/dissolved equilibrium, dissolved U partitions between water and solid surfaces such that more than 99 % is associated with surfaces and less than 1 % is in the mobile dissolved form.

TA-3.4 PLUTONIUM GEOCHEMISTRY

TA - 3.4.1 Origin and Occurrence of Plutonium

General Literature Background

Pu (atomic number 94) has 15 known isotopes, all radioactive, 5 of which are of environmental concern due to their abundances and long half-lives: Pu-238 ($t_{1/2}$ = 87.7 y), Pu-239 ($t_{1/2} = 2.4 \times 10^4$ y), Pu-240 ($t_{1/2} = 6.5 \times 10^3$ y), Pu-241 ($t_{1/2}$ = 14.4 y) and Pu-242 ($t_{1/2} = 3.8 \times 10^5$ y) (Lide, 1990). The use of Pu-239 as a basic fuel or source of fuel for release of nuclear energy is well known. Because of the large amount of heat released during its radioactive decay, Pu-238 is used to

247

provide energy for small thermoelectric power units such as those used in NASA's space program.

As with all transuranium elements, Pu is a product of nuclear reactions that only rarely occur naturally (Katz et al., 1986; Seaborg and Loveland, 1990; Choppin et al., 1995). Pu is produced when U nuclei in fissioning U fuel capture neutrons. Therefore, Pu is almost entirely a product of the nuclear industry and is not associated in more than ultratrace concentrations with ore bodies or other geological formations. Pu has been produced in larger quantities than any other transuranic element and has been the subject of extensive ecological and biological research.

Pu enters the environment as waste material, through accidental releases or disposal of wastes generated during fuel processing and by the production and detonation of nuclear weapons (Warner and Harrison, 1993, Chapter 1; Watters et al., 1983). Pu in the environment exists mostly as precipitated oxides and in a strongly sorbed state to the organic and oxide fractions of surface soils and sediments (Livens et al., 1986). Pu dissolved in environmental waters tends to be progressively eliminated from the water as it encounters surfaces to which it can sorb and conditions that result in precipitation. Over 99 % of Pu released to arid environments ends up in soil and sediments (Warner and Harrison, 1993, Chapter 4; Watters et al., 1983).

The global average activity of Pu in soils is between 5×10^{-4} and 2×10^{-2} pCi/g, with most of the Pu being near the soil surface (top 10 to 15 cm) (Guillaumont and Adloff, 1992, Seaborg and Loveland, 1990). The physical transport of Pu-bearing solids is primarily due to wind and surface water movement (Federov et al., 1986; Little et al., 1980; Little and Whicker, 1977; McLeod et al., 1980; Pinder et al., 1990; Watters et al., 1980; Whicker and Schultz, 1982). Because higher Pu concentrations can be strongly related to smaller soil particle sizes, there is a potential for concentration enrichment of Pu in sediments derived from eroding soil (Warner and Harrison, 1993, Chapter 4). This potential for enrichment can influence the eventual redistribution of Pu and its transport by air and water pathways.

Several studies of Pu released to relatively shallow aquatic ecosystems (such as Lake Michigan and the Irish Sea) show that around 95 % or greater of aquatic Pu ends up in sediments

(Edgington and Robbins, 1976, Heatherington, 1978, Livingston and Bowen, 1976, Pillai and Mathew, 1976). In lake waters, the average concentration of Pu is about 10^{-4} pCi/L, while lake sediments contain about 0.1 pCi/g (Guillaumont and Adloff, 1992). In surface and groundwaters, a significant part of sorbed Pu is attracted by electrical charge forces to colloidal-size solids (0.001 to 2.0 μm) and may be mobilized in this form by water flow until coagulation, flocculation and soil sorption processes cause settling and immobilization. In aquatic sediments, there is some translocation of Pu to the sediment surface due to the activities of benthic biota. Less than one percent (and perhaps closer to 0.1 %) of all Pu in the environment ends up in the biota (Watters et al., 1983). The percentage of all Pu found in vegetation ranges from 10^{-5} to 2 %, in ground surface litter from 10^{-4} to 2 % and in animals from 10^{-8} to 1 % (Watters et al., 1983). When judging the significance of percent distributions, it should be kept in mind that, as stated above, the global average activity of Pu in soils is between 5×10^{-4} and 2×10^{-2} pCi/g.

The distribution of fallout Pu from testing nuclear weapons is not uniform across the earth's surface. Geographic and meteorologic variability have produced spatial differences in fallout levels. Hardy et al. (1973) studied the distribution of fallout Pu and measured the isotopic ratios in soil samples collected from around the world. They determined that the heaviest fallout of Pu-239 and Pu-240 lies in the temperate latitudes of the Northern Hemisphere, whereas, concentrations of Pu-238 are greatest in the temperate latitudes of the Southern Hemisphere (Hardy et al., 1973). Purtymun et al. (1990) studied the deposition and distribution of Pu from world-wide fallout and concluded that variations in Pu concentrations and isotope ratios can be attributed to regional and local weather patterns, unequal distribution by physical transport and variability in Pu particle size.

TA - 3.4.2 Plutonium at RFETS

"Weapons grade" Pu was used exclusively at Rocky Flats. The abundances of the Pu isotopes of concern in weapons grade Pu are: Pu-238, 0.01 wt. %; Pu-239, 93.79 wt. %; Pu-240, 5.8 wt. %; Pu-241, 0.36 wt. %; Pu-242, 0.03 wt. % (DOE, 1997).

249

Pu and other actinides entered the RFETS environment primarily as reactive metal, oxide or in solution (DOE, 1997). Acidic Pu-containing solutions, commonly nitric acid, were used at the site in the Pu recovery processes and solvents and oils were used for machining Pu metal. The behavior of actinides of RFETS origin, therefore, potentially contrasts in many respects with that of actinides deposited following thermonuclear explosions or deposited in the form of refractory wastes resistant to nitric, hydrofluoric and hydrochloric acid digestion. Nevertheless, measurements at RFETS (Little, 1977, Little, 1980, Tamura, 1977, Langer, 1986) are similar to world-wide measurements, showing that about 99 % of Pu at that site is associated with soil particles.

TA - 3.4.3 Aqueous Speciation

General Literature Background

In the normal range of environmental pH and redox conditions, Pu can exist in four oxidation states: III, IV, V and VI (Allard and Rydberg, 1983; Choppin et al., 1997). A fifth oxidation state, Pu(VII), is also known to exist (Krot and Gelman, 1967) but only under extremely oxidizing conditions rarely found in nature and not relevant to this report. In a discussion of long-term behavior of constructed actinide mobility barriers, Kim (2000) offered a few general guidelines to actinide geochemistry under reducing conditions, (*An* refers to any actinide element):

- Under reducing conditions, which are common for deep aquifers, actinides in oxidation states An(V) and An(VI) are reduced to An(III) or An(IV);
- Actinides of An(III) and An(IV) are sparingly soluble in water at neutral pH; and
- These anoxic chemical properties lead to the strong tendency of actinides in the subsurface to sorb to native colloids, forming so-called pseudo-colloids.

The behavior of Pu in its different oxidation states is influenced by factors such as: concentration, the presence of complexing, oxidizing and reducing agents, pH and extent of

hydrolysis (Choppin, 1983; EPA, 1999). Under reducing conditions, Pu(III) species are dominant up to pH values of about 8.5 to 10; above this pH range Pu(IV) species are dominant. (See Figure TA-3-2). However, under oxidizing conditions and at pH values greater than 4.0, Pu can exist in IV, V and VI oxidation states (Clark et al., 1994; Keeney-Kennicutt and Morse, 1985). The Pu(III) and Pu(IV) oxidation states are notably more sorptive and less soluble than the higher states because of the high net charge on their aquo-ions (Duff et al., 1999). The higher states, Pu(V) and Pu(VI), are less charged because their aquo-ions exist as dioxo cations: $Pu(V)O_2^+$ and $Pu(VI)O_2^{2+}$ (Choppin et al., 1997; Duff et al., 1999 and included references).

Reilly et al. (2000) investigated the solubility and speciation of the Pu(VI)/carbonate system under carefully controlled laboratory conditions. These authors found that Pu(VI) in low ionic strength carbonate solutions is reduced to Pu(IV) within hours to days, while highly concentrated NaCl appears to stabilize the Pu(VI) state.

Pu(V) ions will disproportionate to Pu(IV) and Pu(VI). The condition under which this disproportionation reaction occurs is highly sensitive to pH and metal ion concentration. At low Pu concentrations (less than about 10^{-6} M) and neutral pH, the stability of Pu(V) is enhanced, making Pu(V) the dominant form of soluble Pu found in seawater (Choppin et al., 1997; Nitsche et al., 1994; Rai et al., 1980b). Under high actinide concentrations, such as those found in laboratory experiments, radiolytic decomposition of water from the radioactivity of dissolved Pu can generate strong redox reagents such as the short-lived radicals •H, •OH and •O as well as the radical recombination products H_2, O_2 and H_2O_2. The result is that radiolysis tends to initiate disproportionation of Pu(V) to Pu(IV) and Pu(VI) and further, to reduce Pu(VI) and Pu(V) to the Pu(IV) and Pu(III) states (Clark, 2000; Runde, 2000).

The environmental behavior of Pu is also influenced significantly by its tendency to form aqueous complexes with hydroxyl (hydrolysis), carbonate and other anionic species, as well as with humic substances (complexation). Nelson et al (1987) and Choppin and Morse (1987) have shown that the oxidation state of dissolved Pu under natural conditions can also be influenced by the colloidal organic carbon content of the system.

251

Hydrolysis

In near-neutral pH surface and ground waters, actinide speciation is dominated by hydrolysis processes (reactions with water to form complexes of H_2O, OH^- and O^{2-}), with lesser influence from complexation with dissolved organic matter and inorganic anions such as carbonate and phosphate (Clark et al., 1995). Actinide hydrolysis yields soluble hydroxide or oxide complexes, as well as precipitates of hydroxides, oxides or basic salts. Hydrolysis reactions are significant for all actinide ions at pH values found in natural waters, with the exception of Pu(V). Both Pu(IV) ions have high charge-to-size ratios and form hydrolysis products even in acidic solutions, as low as pH = 0. (Clark, et al., 1995) Pu(V) has the lowest tendency to hydrolyze and form complexes with ligands (Choppin, 1983) while Pu(IV) hydrolyzes more readily than all other redox species of Pu (Allard, 1982; Knopp et al., 1999). The order of hydrolysis of Pu redox species follows the sequence Pu(IV) > Pu(III) > Pu(VI) > Pu(V) (Choppin, 1983).

Pu tends to be in the least soluble lower oxidation state, Pu(IV), under environmental conditions common at RFETS. Pu(IV) hydrolyzes readily to form hydrolytic species with the general formula, $Pu(OH)_m^{(4-m)+}$ (m = 1, 2, 3, 4). For m = 1, 2 or 3, Pu forms the cations $Pu(OH)^{3+}$, $Pu(OH)_2^{2+}$ and $Pu(OH)_3^{+}$, which can contribute significantly to the overall solubility of Pu. However, the case of m = 4 leads to amorphous $Pu(OH)_4(s)$, which has very low solubility.

With four hydroxyl groups attached to $Pu(IV)(OH)_4$, there is a tendency to polymerize beyond simple dimers or trimers and form extensive polymeric networks, which can reach colloidal dimensions and exists as colloidal suspensions. These species are metastable and will ultimately condense with loss of water to form oxo-bridged polymers [$Pu(OH)_4(am)$ or $PuO_2 \cdot 2H_2O$)] of various molecular weights, as high as 10^4 au (atomic units) (Cleveland, 1979; Toth et al., 1983). Shortly after forming, these polymers can be decomposed by acidification or oxidation. As the polymers age, however, protons are lost, oxygen bridges increase in abundance and the polymerization process becomes increasingly irreversible. As aging develops, the polymeric material begins to develop a crystalline structure, which increasingly resists dissolution even in concentrated nitric acid (Toth et al., 1983; Choppin, 1983). These positively charged solid

252

polymer particles are mixtures of $Pu(OH)_4(am)$ and polycrystalline $PuO_2(c)$ and are of colloidal dimensions (Triay, 1991; Thiyagarajan, 1990). The degree of crystallinity of its solid compounds is the second most important factor affecting the solubility of Pu, the first being its oxidation state; amorphous solids in the same oxidation state being more soluble than the corresponding polycrystalline solids. As the transformation is kinetically slow, it may take up to several years for amorphous $Pu(OH)_4(s)$ to change to polycrystalline $PuO_2(c)$. When the hydrolysis product $Pu(OH)_4(s)$ is present, its solubility tends to limit the overall Pu solubility of systems that also contain the cationic Pu hydrolysis products.

The estimated solubility of amorphous $Pu(OH)_4$ is around $10^{-9(\pm 2)}$ M and that of $PuO_2(c)$ around $10^{-15(\pm 3)}$ M. The solubilities of the solid forms of Pu impose an upper limit on the total amount of dissolved Pu that can be present, even if Pu(V) or Pu(VI) are the more stable dissolved states. In Figure TA-3-2, the stability fields of $Pu(OH)_4(am)$ (not shown) and $PuO_2(c)$ (shown) overlap most of the E_h/pH range of natural waters. When $Pu(OH)_4(am)$ and $PuO_2(c)$ are present, they limit the concentrations of soluble Pu species to about 10^{-8} M to 10^{-10} M (Langmuir, 1997; Rai et al., 1980a and Delegard, 1987). In a study of the speciation of neptunium and Pu in Yucca Mountain waters reported by Efurd (1998), 99 % of the soluble Pu was calculated to be in the IV state as $Pu(OH)_4(aq)$. When using $Pu(OH)_4(s)$ as the solubility-limiting solid in their geochemical models, the dissolved Pu concentration was predicted to be about 10^{-9} M, based on thermodynamic data available in the open literature. In this study, experimental data indicated Pu concentrations that are larger by one to two orders of magnitude, presumably because Pu solubility is actually controlled by amorphous oxide/hydroxides or colloidal forms of Pu(IV). Runde notes that if crystalline $PuO_2(s)$ were the solubility-limiting solid, Pu(IV) solubility would be about 10^{-17} M, well below the Pu(IV) hydroxide solubility range.

Nelson et al. (1987) found that Pu precipitation occurred if the solution concentration exceeded 10^{-7} M. The formation of insoluble Pu/oxygen polymers may render invalid simple solubility constants (K_{sp}) calculated for solid Pu hydroxides (Choppin, 1983) and can influence the measured values of empirical distribution coefficients (K_d) for systems containing Pu hydroxides (EPA, 1999).

253

Complexation

Dissolved Pu is known to form complexes with naturally-occurring oxygen- and nitrogen-donor organic and inorganic ligands (Cleveland, 1979). Common inorganic ligands include hydroxyl (discussed in the Hydrolysis section), carbonate, nitrate, sulfate, phosphate, chloride, bromide and fluoride. Organic ligands include acetate, citrate, formate, fulvate, humate, lactate, oxalate, tartrate and dissolved natural organic matter (humic and fulvic material). Two synthetic organic ligands known to complex Pu are EDTA and 8-hydroxyquinoline derivatives; it is likely that there are many more.

The tendency of Pu in various oxidation states to form complexes depends on the ionic potential, defined as the ratio (z/r) of the formal charge (z) divided by the ionic radius (r) of an ion. Among Pu redox species, Pu(IV) exhibits the highest ionic potential and, therefore, forms the strongest complexes with various ligands. Because the ionic radii of the four common oxidation states are of similar magnitude, the stability of Pu complexes parallels the overall charge of the central Pu ion:

$$Pu^{4+} > Pu^{3+} \approx PuO_2^{2+} > PuO_2^{+}.$$

Pu^{4+} forms the strongest complexes and PuO_2^{+} forms the weakest. Clark (2000) points out that the actinyl cations (cations where an actinide atom is covalently bonded to two oxygen atoms), PuO_2^{+} and PuO_2^{2+}, form complexes that are stronger than would be expected when compared with monovalent and divalent cations of lighter elements.

Pu ions have relatively large ionic radii, so that many ligands can fit around them. They also can exhibit high oxidation states and have a large number of valence shell orbitals available for bonding. Therefore, many donor atoms will bond to the central Pu ion and so coordination numbers of 8 and 9 appear to be very common in Pu complexes (Clark, 2000). Ligands, such as chloride and nitrate, form weak complexes with Pu, whereas fluoride, sulfate, phosphate, citrate and oxalate form stronger complexes. Carbonate and bicarbonate anions are found in significant

254

concentrations in many natural waters and are exceptionally strong Pu-complexing agents. It has been shown for dilute Pu(VI)/carbonate solutions, that actinyl species of composition $PuO_2(CO_3)$, $PuO_2(CO_3)_2^{2-}$ and $PuO_2(CO_3)_3^{4-}$ can all exist under the appropriate solution conditions (Clark et al., 1995). Pu ionic species that normally exhibit very low solubilities in near-neutral solutions can become much more soluble through the formation of anionic carbonate complexes (Clark, 2000).

Also included among the strongest complexes of Pu are the hydroxy-carbonate mixed ligand complexes (e.g., $Pu(OH)_2(CO_3)_2^{2-}$), formed when carbonate complexation competes with hydrolysis (Runde, 2000; Clark, 2000, Tait et al., 1995; Yamaguchi et al., 1994; Kim et al., 1983). Additionally, dissolved fulvic and humic material may also form complexes with Pu. Although the nature of humic complexes of Pu and their stability constants have not been fully characterized, it is believed that they may be the dominant soluble species in natural environments at pH below 5 to 6 (Allard and Rydberg, 1983). Recent studies using lanthanide field tracers (McCarthy et al., 1998) have shown, by analogy, that complexation with naturally-occurring organic matter can facilitate the mobility of Pu and other actinides.

The EPA (1999) modeled the aqueous speciation of dissolved Pu as a function of pH, under redox conditions characteristic of typical river water, to predict the most probable dominant Pu aqueous species. The variables included redox state as well as the pH and composition of the water. The calculation employed the MINTEQA2 computer code using water properties of river water with a world mean composition from Hem (1985) and a total dissolved Pu concentration of 3.2×10^{-10} mg/L (1.36×10^{-15} M). This Pu concentration is based on the maximum activity of Pu-239/240 measured by Simpson et al. (1984) in 33 water samples taken from the highly alkaline Mono Lake in California.

The MINTEQA2 computer code is generally used with a thermodynamic database to calculate complex chemical equilibria among aqueous species, gases and solids and between dissolved and adsorbed states. It was originally constructed by combining the mathematical structure of the MINEQL code (Westall et al., 1976) with the thermodynamic database and geochemical

255

attributes of the WATEQ3 code (Ball et al., 1981). See Allison et al. (1991) for a description of MINTEQA2.

The species distribution was calculated assuming multiple Pu oxidation states might be present based on thermodynamic equilibrium considerations. The redox conditions used were based on an experimentally determined pH/E_h relationship described by Lindsay (1979) for suspensions of sandy loam and distilled water. Thermodynamic data for aqueous species considered in the calculation were taken primarily from Lemire and Tremaine (1980) and other secondary sources, with database modifications described by Krupka and Serne (1998).

Results are plotted as a species distribution diagram in Figure TA-3-3, reproduced from EPA (1999). The calculations predict that, within the pH range of about 3.0 - 3.5, PuF_2^{2+} and PuO_2^+ are the dominant species of Pu. The free ionic species, PuO_2^+ is the dominant form at pH from 4 to 5. Within the pH range of 5.5 to 6.5, the main species of Pu are PuO_2^+ and $Pu(OH)_2(CO_3)_2^{2-}$ accompanied by minor amounts of the neutral hydrolytic species $Pu(OH)_4^0(aq)$ and the phosphate complex $Pu(HPO_4)_4^{4-}$. At pH values exceeding 6.5, the dominant dissolved Pu form (about 90 %) is $Pu(OH)_2(CO_3)_2^{2-}$ with a minor percentage of $Pu(OH)_4^0(aq)$. Such illustrative computations indicate that, in the example water and under pH conditions typical of surface and ground waters (>6.5), the dominant form of dissolved Pu is expected to be the tetravalent complex species, $Pu(OH)_2(CO_3)_2^{2-}$. It is important to note that the speciation of Pu can change significantly with changing redox conditions, pH, types and total solution concentrations of complexing ligands and major cationic constituents.

Figure TA-3-3. Computer simulation of Pu aqueous speciation as a function of pH using the MINTEQA2 program

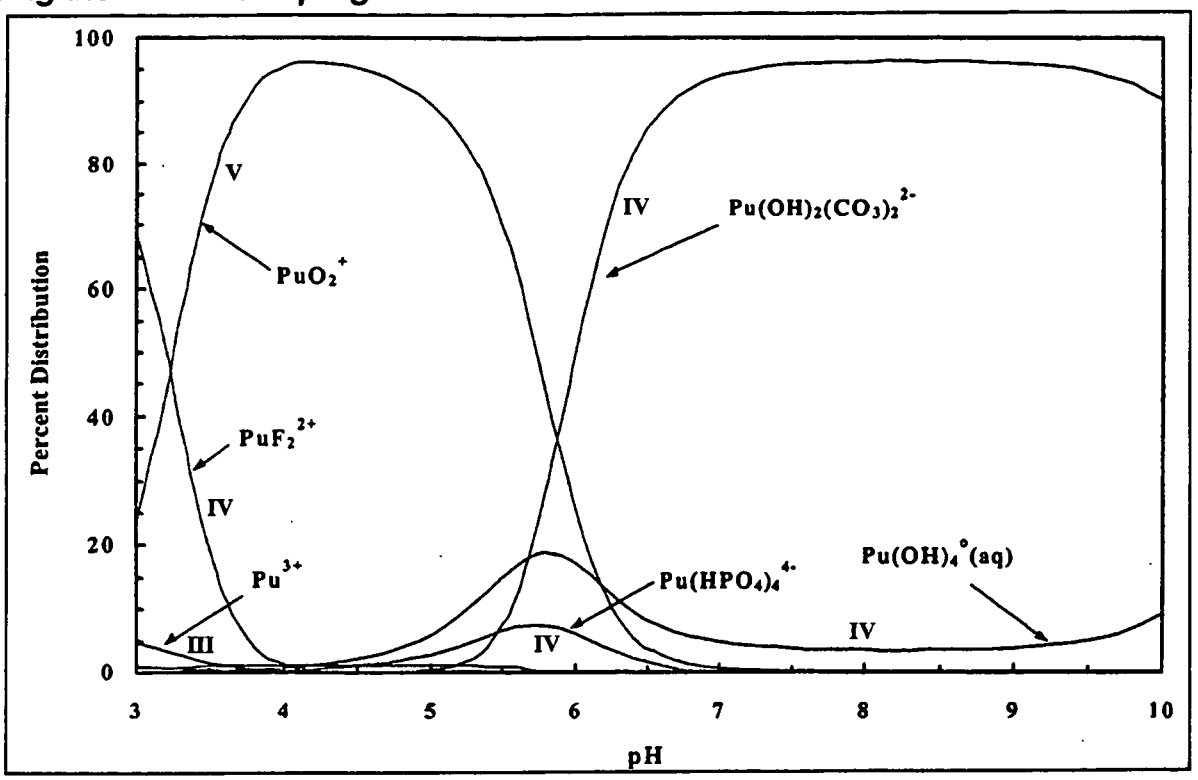

Redox conditions were based on an experimentally determined pH/E_h relationship described by Lindsay (1979) for suspensions of sandy loam and distilled water. The model assumed a water composition equivalent to world mean parameter values for river water as determined by Hem (1985) and a total dissolved Pu concentration of 3.2×10^{-10} mg/L (1.36×10^{-15} M). Roman numerals have been added to indicate the Pu oxidation states (Adapted from EPA 1999).

These results are consistent with the work of Sanchez et al. (1985), who found that at pH 8.6 increasing the total carbonate concentration beyond 100 milliequivalent per liter (meq/L) greatly decreased the adsorption of both Pu(IV) and Pu(V) to goethite. As the concentration of carbonate approached 1,000 meq/L, practically no adsorption occurred. Because goethite at pH 8.6 contains mainly negatively charged sorption sites that would not attract anionic species, the essentially complete suppression of Pu(IV) and Pu(V) adsorption was attributed to the presence of anionic Pu-hydroxy-carbonate species in solution. This work indicates that the pH-of-zero-charge for the soils and sediments with which Pu solutions interact can be an important parameter affecting mobility.

257

Aqueous Speciation of Plutonium at RFETS

The background discussion of aqueous speciation will be generally applicable to RFETS. Measurements of Pu in RFETS soils, wells and surface waters indicate that hydrolysis reactions have led to polymerized precipitates in the forms of Pu oxides sorbed to soil and sediment particles and as colloid-sized oxide particles (Cleveland, 1976, McDowell and Whicker, 1978, Higley, 1992; Runde et al., 2000).

It is known that calcium carbonate can be a common constituent of RFETS soils (BNFL, 1998). Therefore, carbonate complexation could potentially influence Pu speciation at RFETS. Because nearly 99 % of RFETS Pu is associated with solids in soils and sediments, it appears that complexation and parameters such as pH and redox potential, which potentially could influence Pu speciation at RFETS, do not significantly affect Pu solubility on the Site. In sequential extraction experiments, Litaor and Ibrahim (1996) found that only 1 to 7 % of Pu in soils taken from a location about 250 meters east of the 903 Pad were associated or bound with carbonate minerals, based on phase speciation studies. These authors found no clear relationship between the Pu and carbonate contents of the soil and the amount of Pu associated with carbonates but attributed the lack of correlation to experimental difficulties.

TA - 3.4.4 Dissolution, Precipitation and Coprecipitation of Plutonium

General Literature Background

The presence of amorphous and partly crystallized $PuO_2\ xH_2O$ in near surface soils appears to limit soluble Pu concentrations to around 10^{-8} M to 10^{-10} M, when dissolved carbonate species are absent (Rai et al., 1980a; Delegard, 1987; Yamaguchi et al., 1994; Efurd et al., 1998). However, under controlled laboratory conditions with artificially high dissolved carbonate concentrations, dissolved Pu concentrations may increase to micromolar levels. Efurd et al. note that their studies do not exclude the possibility that small-sized Pu colloids might be included in their filtrates, so that their solubility data should be regarded as an upper bound to the "real" solid-liquid phase equilibria in soils. The same caution is likely to apply to the other cited solubility studies.

Allard and Rydberg (1983) showed that the aqueous concentrations of Pu in nature might be controlled by the solubility of the solid phase $PuO_2\ xH_2O$. Calculations by Allard and Rydberg (1983) based on available thermodynamic data at the time, showed that, under reducing conditions, the solubility of dissolved Pu is limited by solid phase PuO_2 at pH values greater than 8 and by solid phase $Pu_2(CO_3)_3$ of trivalent Pu at lower pH values.

Laboratory studies conducted by Delegard (1987) and Yamaguchi et al. (1994) indicate that a *freshly precipitated* amorphous $PuO_2{\cdot}xH_2O$ phase controls the equilibrium solubility of Pu to around 10^{-8} M. Solubility measurements on *aged precipitates* by Rai et al. (1980a) and Delegard (1987) showed that the equilibrium Pu concentration of partially crystallized $PuO_2{\cdot}xH_2O$ phase is lowered to around 10^{-10} M, but still about 100 times greater than the solubility of amorphous $PuO_2{\cdot}xH_2O$. Efurd et al. (1998) found that Pu solubility in a Yucca Mountain groundwater was controlled by the formation of Pu hydroxides and/or Pu colloids, which aged towards $PuO_2{\cdot}xH_2O$. The dominant species in dissolved Pu was $Pu(OH)_4(aq)$. Efurd et al. (1998) found that different crystallinities of Pu(IV) colloidal material (possibly caused by different aging times or growth in different ionic strength solutions) result in a range of solubilities. They suggest that amorphous materials could be the reason for some reported Pu solubility discrepancies.

For over 50 years it has been widely held that the Pu(IV) oxide, PuO_2, is the most stable oxide and that higher oxidation state oxides, such as PuO_3, are unstable (Katz et al., 1986; Seaborg and Loveland, 1990; Choppin et al., 1995). Haschke et al. (2000) have recently shown that PuO_2 slowly reacts with adsorbed H_2O to form PuO_{2+x} and H_2 via a non-radiolytic chemical reaction. From considerations of valence and from some older X-ray photoelectron spectroscopy (XPS) data, the authors proposed that O^{2-} and a small percentage of Pu(VI) accumulates in the oxide over time during exposure to humid air. The authors speculated that the purported Pu(VI) in this oxide could dissolve and be transported more easily than previously estimated for PuO_2 alone.

The identification by Haschke et al. (2000) of some amount of a higher oxide in the $PuO_2(c)$ lattice does not alter the observed and experimentally well-known fact that Pu oxide is very *insoluble* in water. In reality, the solubility of Pu dioxide is so low that it has always been subject to experimental ambiguities regarding the true identity of the solid and solution phases.

259

Decades of study reveal a range of solubility centered around 10^{-11} M for PuO_2 in water at near-neutral pH (Knopp et al., 1999). If this higher oxide indeed proves to be present, then dozens of measurements, performed all over the world during a period of many decades, inherently include the influence of this higher oxide on solubility.

Moreover, upon speculating that the formation of Pu(VI) in PuO_{2+x} might increase the solubility of Pu, the authors failed to consider the influence of environmental factors such as pH, E_h etc. Even if the presence of Pu(VI) in a PuO_2 matrix were to increase the rate of dissolution, the chemical condition (pH, E_h, mineral chemistry, etc.) will determine the stability of Pu oxidation states in the aqueous phase and the overall Pu mobility. It is well established that Pu(VI) is unstable under environmental conditions and, once in solution, it is generally reduced to lower oxidation states that are prone to precipitation as $Pu(OH)_4(s)$ or $PuO_2(s)$.

The relative stability of Pu(IV) under environmental conditions has recently been demonstrated by Runde et al. (2000), who studied the solubility of Pu as a function of pH, E_h and electrolyte concentration (NaCl) in carbonate-containing groundwaters from the Yucca Mountain Site. In such waters, X-ray absorption measurements have shown that the presence of amorphous Pu(IV) solids control Pu solubility (Rai et al., 1980a; Delegard, 1987; Yamaguchi et al., 1994; Efurd et al., 1998). Geochemical modeling supported the prediction that Pu(IV) would dominate at E_h (solution redox potential) < 300 mV. As the redox potential was increased above this value, Pu(V) was observed. Maintaining E_h at an oxidizing potential (500 mV) while raising the pH subsequently produced Pu(VI). The observed Pu(VI) was found to be unstable and converted back to Pu(IV) at low pH and low NaCl concentrations, even in the carbonate-containing groundwaters of the Yucca Mountain Site. Runde et al. did observe that Pu(VI) was stabilized at higher pH (pH > 9) and higher NaCl concentrations. At the carbonate concentrations common for natural waters, Pu(VI) is calculated to be stable only at pH above 9. Runde et al. also studied the speciation of Pu in contaminated soils from RFETS. The data from X-ray absorption spectroscopy (XANES, EXAFS) indicated that Pu was present in the Pu(IV) state as expected and was structurally similar to the highly stable and immobile PuO_2.

260

Another dominant factor influencing Pu dissolution (or apparent dissolution due to association with colloids) is the presence of dissolved/colloidal organic carbon (COC), mainly humic substances (Berry et al., 1991; Choppin, 1988). Many observations show that Pu associated with soils and particulate organic matter is present in the Pu(IV) oxidation state (Choppin and Morse, 1987; Nelson and Lovett, 1980; Nelson et al., 1987; Silver, 1983). Data from laboratory experiments (Nelson et al., 1987) showing K_d values as a function of concentration of COC indicate clearly that there is a critical concentration of COC above which K_d decreases significantly (2 to 3 orders of magnitude). The critical COC ranges from about 0.1 mg/L to about 3 mg/L, depending on water composition.

In a recent study of forest soils within the 30-km zone around Chernobyl (Muramatsu et al., 2000) it was found that Pu activity was divided about equally between the uppermost organic soil horizon and the underlying mineral layer. This may indicate that, when Pu was initially deposited from the atmosphere, it became associated with organic colloidal material near the surface and was subsequently carried by colloid movement in percolating water to greater depths. Sampling depths below the soil surface were not reported.

COC also appears to influence the redox behavior of Pu, possibly by acting as a reducing agent. Field and laboratory studies (Nelson et al., 1987) indicate that the concentration of oxidized Pu is influenced by the concentration of COC. For concentrations up to about 10 mg/L of COC, the effects on total Pu sorption caused by complexation of Pu(III,IV) and reduction of Pu(V,VI) seem to cancel each other out, so that dissolved levels of total Pu and, thus, K_d remain more or less constant. Above 10 mg/L of COC, dissolved Pu(V,VI) has all but disappeared and Pu(III,IV) complexation dominates, decreasing the K_d for total Pu markedly.

Dissolution, Precipitation and Coprecipitation of Plutonium at RFETS

The water extractability (solubility) of Pu (and other actinides) from RFETS soil has been found to be pH dependent and is lowest (0 to 2 %) between pH 3 to 6 (Higley, 1992). Honeyman et al. (1999) found no evidence that reducing conditions at RFETS enhanced Pu-239/240 solubility (defined as Pu-239/240 activity released from soils to an aqueous phase that passed a 0.45-μm

261

filter). These results might indicate that the dissolution of soil components under reducing conditions, such as iron and manganese oxides, is not associated with the release of Pu at RFETS. As stated before, Runde et al. (2000) found that Pu in RFETS soils was present as Pu(IV) and was structurally similar to the stable and immobile PuO_2.

As described above, high concentrations of dissolved carbonate may result in dissolved Pu concentrations at micromolar levels. This might potentially be significant for RFETS soils in which calcium bicarbonate can be a common constituent (BNFL, 1998). However, evidence of carbonate complexation with Pu was not noted in recent spectroscopic measurements of Pu speciation and distribution in soil samples from the Site (Neu et al., 1999). Because Pu concentrations were generally low, only the most concentrated samples yielded useful results. In these, Pu was found to be in the stable and immobile solid form of PuO_2, to be not highly associated with elements other than oxygen and to be most concentrated in the 0.01- to 0.02-inch size fractions.

TA - 3.4.5 Sorption/Desorption of Plutonium

General Literature Background

Pu sorbs to soil components such as clays, oxides, hydroxides, oxyhydroxides, aluminosilicates and organic matter and to construction material such as cement and concrete (BNFL, 1998). The empirical K_ds for Pu adsorption can vary from low (11 mL/g for pH ~2-3 on quartz) to extremely high (300,000 mL/g for pH ~7 on clays and soils with low carbonate concentrations), depending on the pH, the properties of the substrate and the composition of the solution (Allard and Beall, 1981; Baes and Sharp, 1983; Coughtrey et al., 1985; Thibault et al., 1990). A number of studies indicate that iron hydroxides adsorb and reduce penta- and hexavalent Pu to the tetravalent state on the solid surface (e.g., Bunzl et al., 1995). Tetra- and pentavalent Pu aqueous species oxidize to the hexavalent form upon adsorption onto manganese dioxide surfaces, whereas pentavalent Pu adsorbed on goethite disproportionates into tetra and hexavalent forms (Keeney-Kennicutt and Morse, 1985). Subsequently, the hexavalent form of Pu is reduced to the tetravalent state.

Additionally, these reactions were found to occur faster under light conditions than under dark conditions, suggesting photochemical catalysis of some adsorbed Pu redox reactions.

Duff et al. (1999) found that Pu(V) sorption on a natural zeolitic tuff was primarily at manganese oxide and smectite surfaces, with subsequent heterogeneity in the Pu oxidation state. They observed that Pu was not sorbed strongly to iron oxides on the natural tuff surface. The preferential sorption of Pu to negatively charged sites on manganese oxides suggested that the sorbing Pu species were positively charged. Duff et al. (1999) concluded from this that the calculated equilibrium speciation for dissolved Pu species is not representative of the distribution of sorbed Pu species on the surface and cannot provide conclusive interpretations about the redox behavior of sorbed Pu.

Some laboratory studies indicate that increasing carbonate concentrations decreased adsorption of tetra- and pentavalent Pu on goethite surfaces (Sanchez et al., 1985). Similar behavior has also been observed for other actinides known to form strong hydroxy-carbonate mixed ligand aqueous species. These data suggest that Pu would be most mobile in high pH and carbonate-rich groundwaters. See Figure TA-3-3 and associated text.

It has been observed that the mass of Pu retarded by soil may not be easily desorbed from soil mineral components. For example, Bunzl et al. (1995) studied the association of Pu-239/240 from global fallout with various soil components. They determined which fractions of Pu were present as readily exchangeable and which were bound to carbonates, iron and manganese oxides, organic matter and residual minerals. For soils at their study site in Germany, the results indicated that 30-40 years after deposition the readily exchangeable fraction of Pu was less than 1 %. More than 57 % of the Pu was sorbed to organic matter and a considerable mass was sorbed to oxide and mineral fractions.

Sorption/Desorption of Plutonium at RFETS

Studies at RFETS related to the mobility of dissolved/colloidal Pu do not provide much information about sorption/desorption processes. Litaor et al. (1996 and 1998) collected infiltrating water from natural and simulated precipitation and snowmelt. They found that the

263

majority of the activity did not move with the infiltrating water. From 0.02 % to 0.07 % of the Pu and Am in the surface soil was mobilized, with 83 % to 97 % of the mobile Pu associated with particulates greater than 0.45-mm in diameter. An increase in the flux of infiltrating water by several orders of magnitude at the deeper sampling levels (40-70 centimeters [cm]) did not increase the flux of Pu or Am. This was interpreted as indicating that Pu and Am were immobilized by the soil matrix as the water percolated through it. These results are consistent with depth distributions of actinides measured for the OU 2, (RCRA Facility Investigation/Remedial Investigation [RFI/RI] [DOE 1995b]), which showed that approximately 90 % of the Pu and Am in contaminated soil near the 903 Pad was in the top 12 cm of soil more than 20 years after release.

Sediments in the A-, B- and C-Series ponds are contaminated with actinides (RFETS, 1998). Research on sediments from the ponds has shown that, in the normal environmental pH range of 6 to 9, Pu and Am are highly insoluble and remain associated with the solid phase (Johnson et al., 1974 and Cleveland et al., 1976). Cleveland (1976) found that Pu- and Am-contaminated pond sediments extracted with pond water at pH values of 7 and 8 released only between 0.00084 % and 0.0015 % of the Pu.

Honeyman and Santschi (1997) leached soil isolates from a region southeast of the 903 Pad and found that 0.04 to 0.09 % of soil-associated Pu was "exchangeable." Based on this "exchangeable fraction they determined upper-bounding Pu K_d values for these soils under oxic conditions to be between about 10^4 and 10^5 mL/g. Honeyman (1998) and Honeyman et al. (1999) varied the redox potential and found that, for oxic and mildly reducing conditions, less that 0.18 % of soil Pu was released to solution or colloids.

TA-3.5 AMERICIUM GEOCHEMISTRY

The geochemical behavior of Am in the environment is similar to that of Pu; in the absence of complexing ligands, particularly carbonate, both actinides tend to be strongly adsorbed to the solid phase under neutral to alkaline and oxidizing conditions.

264

TA - 3.5.1 Origin and Occurrence of Americium

General Literature Background

Am (Am, atomic number 95) has 15 known isotopes, all radioactive, including all mass numbers between Am-232 and Am-247. Most Am isotopes have short half-lives ($t_{1/2}$) (between 0.9 minutes and 50.9 hours) except for Am-241 ($t_{1/2}$ = 432.2 y), Am-242 ($t_{1/2}$ = 141 y) and Am-243 ($t_{1/2}$ = 7.4×10^3 y) (Lide 1990). The most important isotope of Am is Am-241, which is formed by radioactive decay of relatively short-lived Pu-241 ($t_{1/2}$ = 14.4 y). Processing reactor-generated Pu produces kilogram quantities of Am-241. The most common use of Am is as an ionization source in household smoke detectors[1], which use most of the several kilograms of Am, produced each year. Am mixed with beryllium is also used as a neutron source for nondestructive testing of metal machinery parts, oil well flow measurements, thickness gauges and certain medical diagnoses (Grayson and Eckroth, 1985).

As with Pu, naturally-occurring Am is not found in significant quantities, but a world-wide background exists as a result of bomb tests. Am has been detected around waste disposal sites, operating power plants and in world-wide atmospheric fallout.

Americium at RFETS

Am at RFETS primarily arises as a radioactive decay product of Pu-241 ($t_{1/2}$ = 14.4 y) contained within weapons Pu. Am also was purified at RFETS by means of a molten salt extraction process and sold for commercial applications. Am oxide was sent as a chemical product to Oak Ridge National Laboratory (DOE, 1997).

---

[1] The Australian Radiation Laboratory conducted tests on radiation sources used in 25 brands of smoke detectors available in Australia. These tests showed that each detector contained less than 10^6 pCi of Am-241 or about 2×10^{-4} g, as required by Australian Standard AS3786 (Uranium Information Centre Ltd 1997).

265

TA - 3.5.2 Aqueous Speciation of Americium

General Literature Background

Am can exist in multiple oxidation states (III, IV, V, VI) but is invariably in the Am(III) state in aerated waters, in the absence of oxidants other than atmospheric oxygen (Bondietti et al., 1977; Nelson and Orlandini, 1986). The major reactions influencing the environmental fate of Am are formation of complexes with anions and natural organic matter (controlled by pH and strength of complexing anions), precipitation (controlled by solution composition) and sorption (controlled by solution composition and the nature of solid phases). Am also may form pseudo and true colloids, which could potentially migrate through groundwater in colloidal form, although evidence for such migration is equivocal (Silva and Nitsche, 1995). A critical review of the chemical thermodynamics of Am has been compiled by Silva et al. 1995.

Because actinides in the same oxidation state exhibit the same general chemical behavior, Am(III), the only state of Am common under environmental conditions (Bondietti et al., 1977; Nelson and Orlandini, 1986), is expected to behave in much the same manner as Pu(III). For example, Am(III) forms strong hydroxyl and carbonate complexes, as does Pu(III). Figure TA-3-4 shows a pCO_2–pH predominance diagram for the Am(III)/CO_2/H_2O system. Am-carbonate complexes dominate as pH increases above a value that depends on the carbonate concentration. Anionic carbonate complexes can form above pH 7 and can markedly increase Am solubility (Penrose et al., 1990; Silva, 1995).

2616

Figure TA-3-4. Calculated pCO_2–pH predominance diagram for the system $Am(III)/CO_2/H_2O$

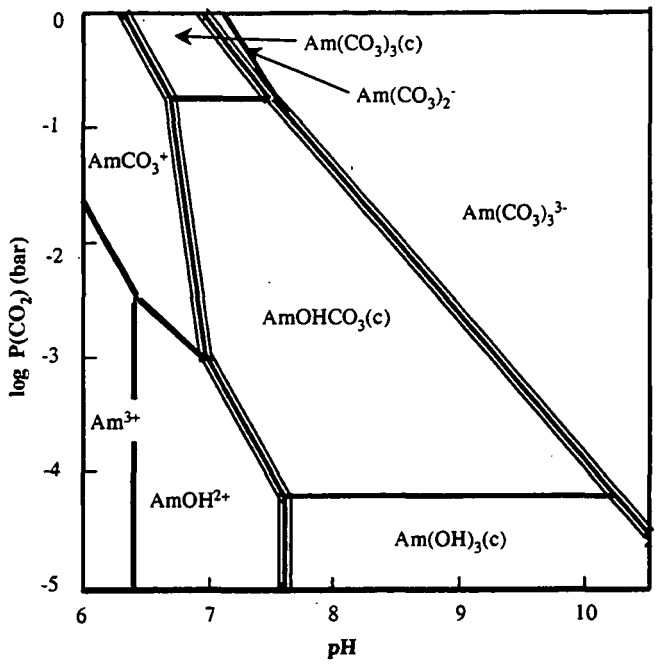

Ionic strength = 0, ΣAm(III)(aq) = 10^{-6} M and T = 25°C. Tripled lines indicate solid/aqueous boundaries (Figure adapted from Langmuir, 1997).

Aqueous Speciation of Americium at RFETS

Although Fowler and Essington (1978) found that environmental Am might be more soluble than Pu, Litaor et al. (1996) found no evidence for this at the Site. Am and Pu have generally similar spatial distributions and dispersal mechanisms at RFETS (Litaor and Allen, 1996). This might be expected since it is believed that nearly all the Am-241 activity in soil on the Site results from radioactive decay of Pu-241 ($t_{1/2}$ = 14.4 y) to Am-241 (Litaor et al., 1996). Since the similar spatial distributions have been in place for about two half-lives of Pu-241, it can be concluded that the important distribution mechanisms are physical (which would distribute both Pu and Am in the same way) rather than chemical. If a chemical process were operative, one might expect differing chemical behaviors to result in the Am and Pu to separate over time. The observation

267

that they remain associated indicates that surface particulate erosion mechanisms are dominant and that transport of soluble species plays a minor role, if any.

TA - 3.5.3 Dissolution, Precipitation and Coprecipitation of Americium

General Literature Background

The most likely redox state of Am in soils is Am(III) (Bondietti et al., 1977; Nelson and Orlandini, 1986), which forms relatively insoluble oxides and hydroxides. Am hydroxide, resulting from rapid hydrolysis of Am in solution, is insoluble in both fresh and marine waters, precipitating as particulate matter or sorbing to suspended particulates (Warner and Harrison, 1993, Chapter 1). The association of Am with particulate matter and sediments controls its behavior and distribution in the aquatic environment. In sediments, the highest Am concentrations are generally associated with the smallest particle sizes.

In freshwater and marine environments, it has been found that the soluble fraction of Am is not in the form of cations but in the form of negatively charged complexes (Warner and Harrison, 1993). Note the negatively charged carbonate complexes of Am in Figure TA-3-4 and Figure TA-3-5. Soluble complexes with organic ligands serve to maintain Am in solution. Nelson and Orlandi (1986) have shown that Am(III) is complexed by dissolved/colloidal organic carbon (COC) in much the same manner as Pu(III,IV). In a lake in northern Scotland that received waste discharges from a reactor plant, all the dissolved actinides measured, including Am-241, were found mainly associated with the colloidal fraction (Orlandini et al., 1990).

Figure TA-3-5. Fractional distribution of Am(III) complexes as a function of pH

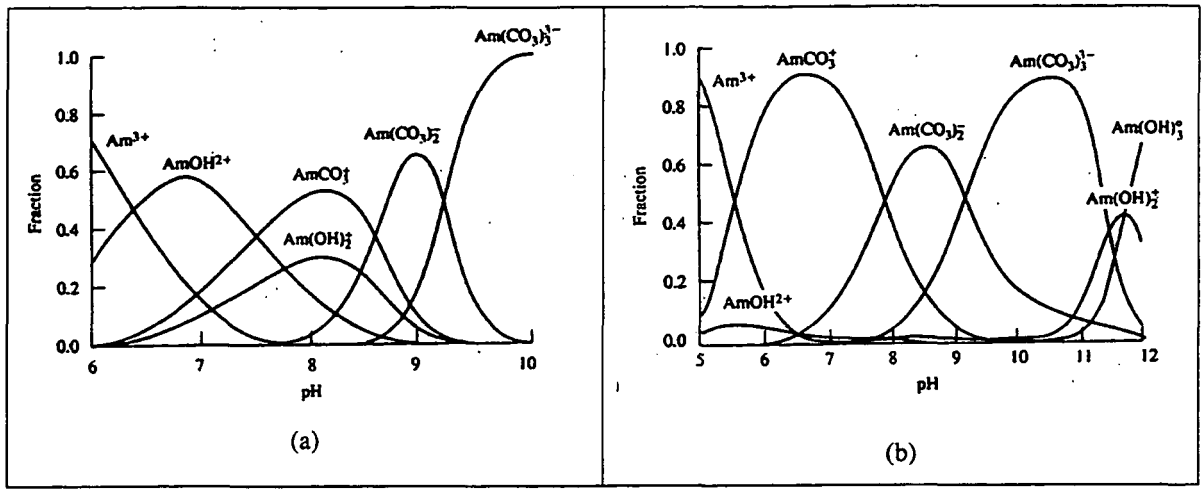

(From Silva et al., 1995)
(a) $pCO_2 = 10^{-3.5}$ atm; $\Sigma Am(III)(aq) = 10^{-6}$ M
(b) Total carbonate = 0.01 M; $\Sigma Am(III)(aq) = 10^{-6}$ M

Dissolution, Precipitation and Coprecipitation of Americium at RFETS

No research related specifically to dissolution, precipitation and coprecipitation of Am at RFETS has been found so far. Since most of the Am-241 activity in soil on the Site results from radioactive decay of Pu-241, most of the Am is associated with Pu in solid particles. Therefore, it is likely that the processes of dissolution, precipitation and coprecipitation of Am are not continuously occurring in RFETS soils, sediments and surface waters.

As stated above, Am and Pu have generally similar spatial distributions and dispersal mechanisms at RFETS (Litaor and Allen, 1996). This might imply that differences in the environmental chemistry of Am(III) and Pu(IV) are not large and that dissolution, precipitation and coprecipitation of these two actinides are similar at RFETS.

269

TA - 3.5.4 Sorption/Desorption of Americium

General Literature Background

In a study of the mobility of Pu and Am through a shallow aquifer in Mortandad Canyon at Los Alamos, Penrose et al. (1990) reported that Am appeared to behave quite differently from Pu for reasons not clearly identified in their paper. Although measured Pu concentrations decreased almost exponentially with distance, Am concentrations remained relatively constant. This resulted in empirical K_d values for Pu that were relatively constant with distance from a historical waste outfall (the distance to the farthest well was about 3,500 meters), while K_ds for Am decreased systematically over the same distance. The authors noted that the Am behavior was unexpected for an element generally considered to be strongly adsorbed to particles. They speculated that the fraction of Am not associated with colloids appears to be a stable, anionic complex of unknown composition. However, data from Penrose et al. (1990) have been shown by Marty et al. (1997) to be consistent with surface water transport, which would invalidate many of Penrose et al.'s conclusions.

However, the conclusion of Penrose et al. (1990) of stable, anionic complexes of Am is consistent with the more recent work by Warner and Harrison (1993), where it was found that the soluble fraction of Am in freshwater was in the form of negatively charged complexes. Since surface adsorption sites on soils and minerals are usually negatively charged under normal environmental conditions (Weiner, 2000, Chapter 4), sorption of negatively charged complex species will be strongly diminished.

Sorption/Desorption of Americium at RFETS

Little research related specifically to sorption/desorption at RFETS has been found so far. At the Site, Harnish et al. (1996) concluded that most of the Am, as well as U from Well 1587 and surface water sites SW-51 and SW-53, were present in an anionic form not associated with fulvic acid. Honeyman (1998) leached Am from soil obtained near the 903 Pad (1998) while varying the redox potential between oxic and mildly reducing conditions over the "normal" range of

RFETS environmental conditions. He found that less than 0.38 % of soil Am was released to solution.

Litaor et al. (1996 and 1998) collected infiltrating water from natural and simulated precipitation and snowmelt. They found that a large majority of the activity did not move with the infiltrating water. About 0.07 % of the Am in the surface soil was mobilized. An increase in the flux of infiltrating water by several orders of magnitude at the deeper sampling levels (40-70 cm) did not increase the flux of Am. This was interpreted as indicating that Am was immobilized by the soil matrix as water percolated through it. These results are consistent with depth distributions of actinides measured for the OU 2, RFI/RI (DOE 1995b), which showed that approximately 90 % of the Am in contaminated soil near the 903 Pad was in the top 12 cm of soil more than 20 years after release.

Cleveland (1976) found that Pu- and Am-contaminated pond sediments extracted with pond water at pH values of 7 and 8 released only between 0.0011 % to 0.0028 % of the Am present in the sediments.

TA-3.6 URANIUM GEOCHEMISTRY

TA - 3.6.1 Origin and Occurrence of Uranium

General Literature Background

U (atomic number 92) has 18 isotopes, all radioactive, with atomic masses ranging from 222 to 242. Naturally-occurring U typically contains 99.275 wt. % U-238 ($t_{1/2} = 4.5 \times 10^9$ y), 0.719 wt. % U-235 ($t_{1/2} = 7.1 \times 10^8$ y) and 0.0057 wt. % U-234 ($t_{1/2} = 2.47 \times 10^5$ y) (Langmuir 1997). The mass differences among the U isotopes are small and the isotopes do not normally fractionate through natural physical or chemical processes (Faure, 1977). U exists in U(III), U(IV), U(V) and U(VI) oxidation states, of which the U(IV) and U(VI) states are most commonly found in the environment.

U occurs naturally in the earth's crust with an average concentration of around 2.3 mg/kg (Langmuir, 1997). The mineralogy of U-containing minerals is described by Frondel (1958). U

is a lithophilic element which is most abundant in granites (averaging 5 mg/kg) and shales (averaging 3.5 mg/kg) (Krauskopf, 1979). Myrick et al. (1983) evaluated the concentrations of U-238 in surface soils across the United States to determine background levels. U activity in surface soils of Colorado was found to range from 0.47 to 3.0 pCi/g, with a mean of 1.2 pCi/g and a standard deviation of 0.91 pCi/g..

U(IV) and U(VI) exist in a variety of primary and secondary minerals. Important U(IV) minerals include uraninite (UO_2 through $UO_{2.25}$) and coffinite ($USiO_4$) (Langmuir, 1978; Clark et al., 1997). Aqueous U(IV) is inclined to form sparingly soluble precipitates, adsorb strongly to mineral surfaces and partition to organic matter, thereby reducing its mobility in groundwater. Important U(VI) minerals include carnotite [$K_2(UO_2)_2(VO_4)_2$], schoepite ($UO_3 \cdot 2H_2O$), rutherfordine (UO_2CO_3), tyuyamunite [$Ca(UO_2)_2(VO_4)_2$], autunite [$Ca(UO_2)_2(PO_4)_2$], potassium autunite [$K_2(UO_2)_2(PO_4)_2$] and uranophane [$Ca(UO_2)_2(SiO_3OH)_2$] (Langmuir, 1978; Clark et al., 1997). Some of these are secondary phases, which may form when sufficient U leaches from contaminated wastes or a disposal system and migrates downstream. Commercially-recoverable concentrations of U are also found in phosphate rock and lignite. In the presence of lignite and other sedimentary carbonaceous substances, U enrichment is believed to be the result of U reduction to form insoluble precipitates, such as uraninite.

Uranium at RFETS

Natural U is ubiquitous in the Front Range of Colorado and complicates studies of U contamination at RFETS. High U granites occur throughout the Front Range and U ore (utilized by the Schwartzwalder mine near Ralston Reservoir) is located in the headwaters of Ralston Creek within 10 miles of RFETS. High U concentrations have also been reported in domestic wells in the Coal Creek watershed (Moody and Morse, 1992). Total U concentrations in 33 domestic wells in Coal Creek Canyon ranged from 1.3 to 1,200 pCi/L, with a mean and standard deviation of 174.9 and 33.1 pCi/L, respectively.

The natural alkaline and oxidizing environment in near-subsurface water mobilizes U in groundwater and "...higher U concentrations in water samples...are probably due to leaching of

272

uraniferous strata in the Pierre and Laramie formations..."The South Platte River is "...anomalously rich in U compared to most other rivers of its size" (Bolivar et al., 1978).

Isotopic abundances (by weight) in some of the U used at RFETS, given in Table TA-3-1, differ significantly from natural values (DOE, 1997) and this may be useful in determining which fraction of U on the Site represents RFETS contamination. Some of the U used at RFETS for manufacture of nuclear weapons components was enriched in U-234 and U-235 and some was depleted in U-234 and U-235 (EG&G, 1988). Using appropriate techniques, the isotopic signatures of both types of contamination can be differentiated from natural U. Most samples collected from RFETS have been analyzed by alpha-spectroscopy, which provides only an estimation of U isotope ratios.

Table TA-3-1. Isotopic Ratios in Potential Sources of Uranium at RFETS

Percent by Mass			
Uranium Isotope	**Natural U***	**Depleted U****	**Highly-Enriched U****
U-238	99.27 %	99.75 %	5 %
U-235	0.72 %	0.25 %	95 %
Activity Ratios			
Isotope / Isotopeo	**Natural U***	**Depleted U****	**Highly-Enriched U****
U-233/234	0.005	0.0005	Not determined
U-234/U-238	1.06	0.09	>>5.74

Source: DOE, 1997
*Naturally found in soils at RFETS.
** Contributed from industrial activities at RFETS.

Efurd et al. (1993a) used thermal ionization mass spectrometry (TIMS) to measure U-234, -235, -236 and -238 in RFETS sediment and water samples, a technique that is more accurate than alpha-spectroscopy and provides more certain isotopic ratios. On the basis of these data, the authors concluded that the "...largest source of radioactivity in the terminal ponds was naturally-occurring U and its decay product, radium," and that the "...largest source of anthropogenic radioactivity in the terminal ponds was depleted U." Approximately half the U present in Ponds A-4 and C-2 and approximately 20 % of the U present in Pond B-5 apparently originated as depleted U. These results are significant because they show that U contributed by RFETS activities can be differentiated from naturally-occurring background U.

U-236 is produced by neutron capture on U-235 in nuclear reactors or atomic explosions and does not occur naturally or in U that has not been in a reactor. Therefore, according to Efurd et al. (1993a), U-236 would not be expected to be present in the natural U background at RFETS. Efurd et al. however, detected U-236 in some samples and concluded that "...the presence of U-236 in the surface water samples collected at the RFP and the variable U-238/U-235 atom ratios detected in water samples collected from the holding ponds prove that anthropogenic U is present." U-236 is also produced by alpha decay of Pu-240 ($t_{1/2}$ = 6,537 y), so it is clear that some part of U-236 at RFETS will result from Pu-240 decay. However, three-isotope U plots of 236/238 and 235/238 will have three end members, natural, enriched and depleted. Anthropogenic U should fall within this boundary. Any U-236 that is derived from Pu-240 decay would tend to plot outside of this region with a fourth component.

U-238/U-235 ratios for dissolved U in RFETS groundwater, from which non-detects have been excluded, show wide scatter. According to DOE (1977), this could be due to lack of a systematic treatment of sampling and analytical counting errors or real variability in isotopic ratios. The most likely explanation is unpropagated error, because background wells show high variability in isotopic ratios that cannot be otherwise explained.

The equilibrium among abundances of daughter radioisotopes, if all isotopes remain at the location where they are formed by radioactive decay, is called *secular equilibrium.* Under conditions of secular equilibrium, the kinetics of radioisotope decay requires that the isotope radioactivities are all equal. Therefore, the U-234/U-238 activity ratio can be used to distinguish among natural, enriched and depleted U (Table TA-3-1). The counting ratio should be 1.0 at secular equilibrium, but the measured ratios ranged from <1.0 to >2.5 for RFETS background areas (DOE, 1993). If secular equilibrium were expected at the sites measured, these results would indicate that unexpected factors affected U-234/U-238 activity ratios, limiting their usefulness in distinguishing between natural and RFETS U. Note that, in addition to an invalid assumption of secular equilibrium, errors can be introduced into this procedure by counting time and masking effects.

DOE (1993) reported a range of 1.19 to 2.43 for U-234/U-238 activity ratios in filtered background groundwater and stream water and DOE (1995) reported U-234/U-238 activity ratios ranging from 0.34 to 18.5 for groundwater in the upper hydrostratigraphic unit at the Solar Ponds (formerly known as OU 4). However, DOE (1997) observes that neither report dealt systematically with analytical counting errors; the results, therefore, are of limited value.

The most recent effort to measure U isotope ratios for identifying anthropogenic U at RFETS is by ICP/MS (inductively-coupled plasma/mass spectrometry), reported in the soon-to-be released 1999 Annual RFCA, Groundwater Monitoring Report. This study appears to have sufficient accuracy for showing a clear distinction between natural and anthropogenic U. Groundwater sampling locations were chosen to be at areas with high U concentrations, the boundary wells along Indiana Avenue and upgradient from the Industrial Area. Data reported so far indicate that natural U is present in the majority of wells and that some wells contain anthropogenic U.

TA - 3.6.2 Aqueous Speciation of Uranium

General Literature Background

Because of its importance in nuclear chemistry and technology, a great deal is known about the aqueous chemistry of U (reviewed by Baes and Mesmer [1976], Langmuir [1978], Grenthe et al. [1992] and Palmer and Nguyen-Trung [1995]). U is more soluble in natural waters than Pu or Am. Although all of the positive oxidation states of U from III to VI are observed, dissolved U(III) readily oxidizes to U(IV) under most environmental conditions and the U(V) aqueous species (UO_2^+) readily disproportionates to U(IV) and U(VI). Consequently, U(IV) and U(VI) are the most common oxidation states of U in natural waters and soils.

U ions in aqueous solution can give very complex species. In addition to having four oxidation states, U undergoes complexing reactions with virtually all anions as well as hydrolytic reactions leading to polymeric ions (Clark et al., 1997; Cotton et al., 1999). Anions, such as carbonate, nitrate, chloride, fulvic acid, humic acid and EDTA, form complexes with both U(IV) and U(VI), increasing the amount of U that can remain in solution and, thereby, increasing the overall mobility of U. Generally, U is least mobile in reducing (anaerobic) environments free of

275

complexing anions and most mobile in oxidizing (aerobic) environments with high concentrations of complexing anions.

Figure TA-3-6. Calculated Pourbaix predominance diagram for aqueous species in the U-O_2-CO_2-H_2O system

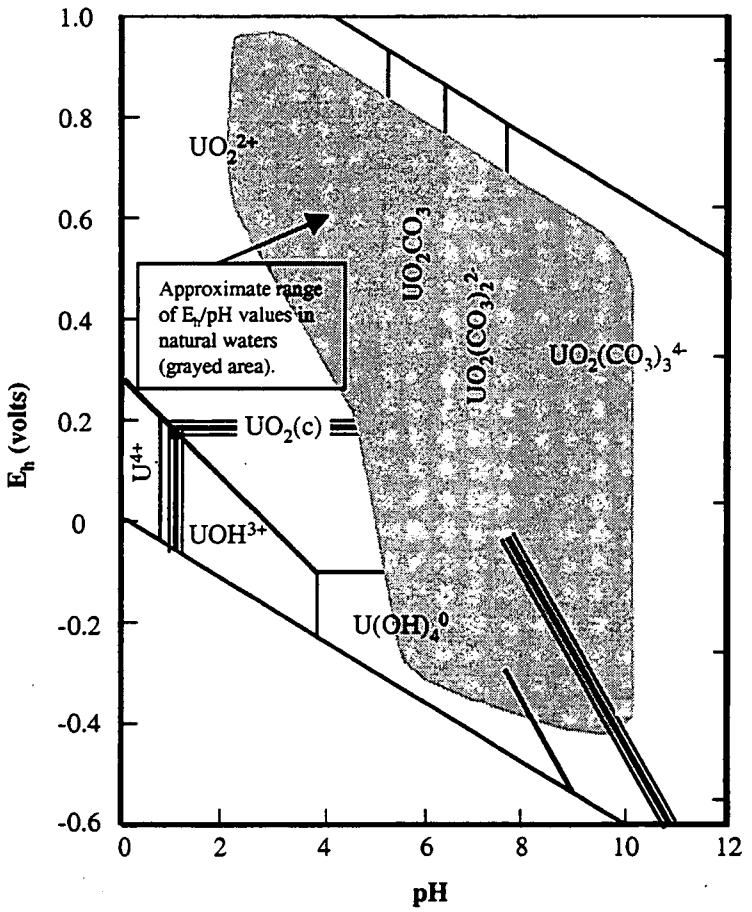

Conditions are pure water at 25°C, 1 bar total pressure, $\Sigma U = 10^{-8}$ M and $p(CO_2) = 0.01$ bar. The $UO_2(c)$ solid/solution boundary for $\Sigma U = 10^{-8}$ M is shown as a tripled line overlay. The approximate range of E_h/pH values found in natural waters is shown within the grayed area. (Adapted from Langmuir, 1997.)

U(VI) species dominate in oxidizing environments, where U(VI) retention by soils and rocks in alkaline conditions is poor because of the predominance of neutral or negatively charged species above pH 5. This is one of the main differences between U behavior and Pu behavior and this fact is emphasized by comparison of the predominance diagrams for U shown here and for Pu

276

shown on page x. An increase in CO_2 pressure in soil solutions can further reduce U(VI) adsorption by promoting the formation of poorly sorbing carbonate complexes. Dissolved U(VI) hydrolyzes to form a number of aqueous species. The calculated distribution of U(VI) hydrolysis and carbonate complexing species is shown in Figure TA-3-7 and Figure TA-3-8.

Because dissolved uranyl(VI) ions (species containing U in the VI oxidation state) can be present as polynuclear (containing more than one cation) hydroxyl complexes, the hydrolysis of uranyl ions under oxic conditions is dependent on the concentration of total dissolved U. To demonstrate this aspect of U chemistry, two concentrations of total dissolved U (0.1 and 1,000 μg/L), are shown in Figure TA-3-7. Hem (1985, p. 148) gives 0.1 to 10 μg/L as the range for dissolved U in most natural waters. For waters associated with U ore deposits, Hem states that the U concentrations may be greater than 1,000 μg/L.

In a U(VI)-water system, the dominant species were UO_2^{2+} at pH values less than 5, $UO_2(OH)_2^0$(aq) at pH values between 5 and 9 and $UO_2(OH)_3^-$ at pH values between 9 and 10. This was true for both U concentrations, 0.1 μg/l (Figure TA-3-7) and 1,000 μg/l dissolved U(VI) (Figure TA-3-8). At 1,000 μg/l dissolved U, some polynuclear species, $(UO_2)_3(OH)_5^+$ and $(UO_2)_2(OH)_2^{2+}$, were calculated to exist between pH 5 and 6. Morris et al. (1994) provided additional proof using spectroscopic techniques that an increasing number of polynuclear species formed in systems containing higher concentrations of dissolved U.

A large number of additional U(VI) species will exist in a chemically more complicated system containing inorganic complexing ligands and a U(VI) concentration of 1,000 μg/L, as shown in Figure TA-3-8. See EPA (1999) for details of the water composition. At pH values less than 5 the UO_2F^+ species dominates the system, whereas at pH values greater than 5 carbonate complexes [$UO_2CO_3^0$(aq), $UO_2(CO_3)_2^{2-}$, $UO_2(CO_3)_3^{4-}$] dominate the system. These calculations clearly show the importance of carbonate chemistry on U(VI) speciation. For this water composition, complexes with chloride, sulfate and phosphate were relatively less important.

277

Figure TA-3-7. Calculated distribution of U(VI) hydrolysis species as a function of pH

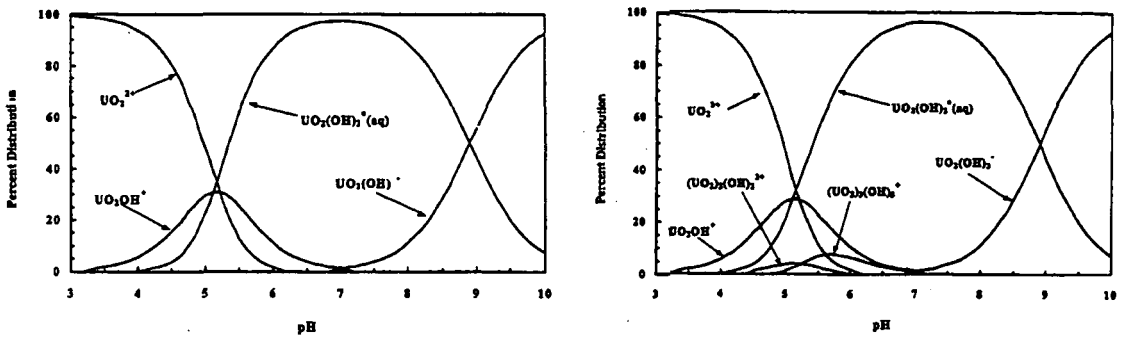

(a) (b)

Uses thermodynamic data from Grenthe et al., 1993. The distribution of uranyl species was calculated using the MINTEQA2 code (from EPA, 1999).
(a) U(VI) concentration = 0.1 μg/L.; (b) U(VI) concentration = 1,000 μg/L

Figure TA-3-8. Calculated distribution of U(VI) aqueous species as a function of pH

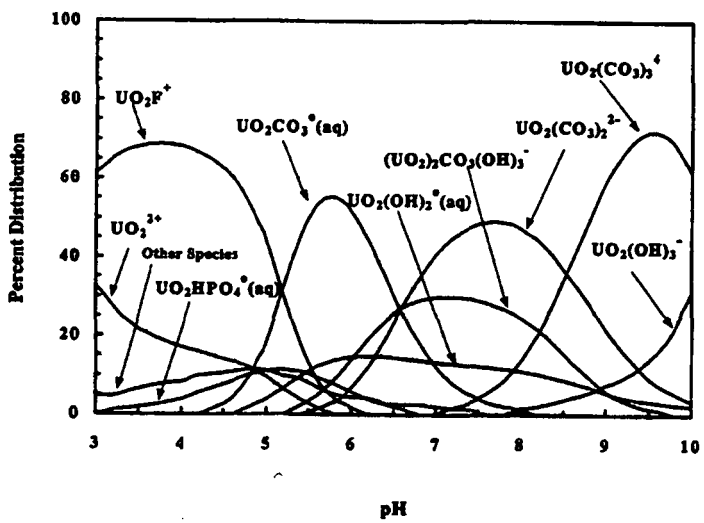

Water containing inorganic complexing ligands and a U(VI) concentration of 1,000 μg/L. The distribution of U(VI) species was calculated using the MINTEQA2 code using thermodynamic data from Grenthe et al. (1993). Figure TA-3-8 reproduced from EPA (1999).

278

Consistent with the results in Figure TA-3-8, Langmuir (1978) concluded that the U(VI) complexes with chloride, phosphate and sulfate were not important in a typical groundwater. The species distribution illustrated in Figure TA-3-8 changes slightly at pH values greater than six if the concentration of total dissolved U is decreased from 1,000 to 1 μg/l. At the lower concentration of dissolved U, the species $(UO_2)_2CO_3(OH)_3^-$ is no longer present as a significant aqueous species.

Sandino and Bruno (1992) showed that UO_2^{2+}-phosphate complexes [$UO_2HPO_4^0$(aq) and $UO_2PO_4^-$] could be important in aqueous systems with a pH between 6 and 9 when the total concentration ratio, PO_4(total)/CO_3(total), is greater than 0.1. Complexes with sulfate, fluoride and possibly chloride are potentially important U(VI) species where concentrations of these anions are high. However, their stability is considerably less than the carbonate and phosphate complexes (Grenthe et al., 1993). Organic complexes are also important to U aqueous chemistry. The uncomplexed U(VI) ion has a greater tendency to form complexes with fulvic and humic acids than many other metals with a +2 valence (Kim, 1986, Shanbhag and Choppin, 1981). Kim (1986) concluded that, in general, VI actinides, including U(VI), would have approximately the same tendency to form humic- or fulvic-acid complexes as to hydrolyze or form carbonate complexes. This suggests that the dominant reaction of the uranyl ion depends on the relative concentrations of hydroxide, carbonate and organic materials. Importantly, U(VI) can form stable organic complexes, thereby increasing its solubility and mobility. Shanbhag and Choppin (1981) suggest that the simplest interpretation of their studies of humic complexation would be that U and Am bind to the carboxylate sites in humic acids.

The total U(IV) concentration in solution is generally quite low (between 3 and 30 μg/L), because of the low solubility of U(IV) solid phases (Bruno et al., 1988; Bruno et al., 1991). U(IV) species dominate in reducing environments. U(IV) tends to hydrolyze and form strong hydrolytic complexes. U(IV) also tends to form sparingly soluble precipitates that are the main control of U(IV) concentrations in groundwaters. U(IV) forms strong complexes with naturally-occurring organic materials, which may increase U(IV) solubility in areas where there are high concentrations of dissolved organic materials. Other important environmental parameters

279

affecting U migration include redox state, pH, ligand concentrations (carbonate, fluoride, sulfate, phosphate and dissolved carbon), aluminum- and iron oxide mineral concentrations and U concentration.

As with all actinides, the U(IV) oxidation state hydrolyzes, precipitates easily, undergoes strong specific sorption reactions and is preferred over other cations in ion exchange reactions. These reactions render U(IV) largely immobile in the environment despite highly stable complexes with inorganic and organic ligands. The more oxidized U(VI) is more soluble, undergoes weaker specific sorption and tends to be more mobile (Salomons and Foerstner, 1984).

U(IV) also hydrolyzes readily. The U^{4+} ion is more readily hydrolyzed than UO_2^{2+}, as expected from its higher ionic charge. Langmuir (1978) calculated U(IV) speciation in a system containing typical natural water concentrations of chloride (10 mg/L), fluoride (0.2 mg/L), phosphate (0.1 mg/L) and sulfate (100 mg/L). Below pH 3, UF_2^{2+} was the dominant U species. Speciation of dissolved U(IV) at pH > 3 is dominated by hydrolytic species such as $U(OH)_3^+$ and $U(OH)_4^0$ (aq). Complexes with chloride, fluoride, phosphate and sulfate were unimportant above pH 3. See Palmer and Nguyen-Trung (1995) for a recent discussion of U hydrolysis.

Aqueous Speciation of Uranium at RFETS

Most of the Site-specific speciation studies at RFETS have been concerned with Pu and Am. Only three studies that contain U speciation information (Litaor ,1995; Honeyman and Santschi. 1997; Ball, 2000) have been found to date and the earlier two of these dealt with U speciation only incidentally. However, the general discussion of U speciation above will apply to RFETS. In the oxidizing and neutral pH conditions of RFETS surface soils (DOE, 1997), U is expected to be in both the U(IV) and U(VI) states. As described above, U(VI) species are more soluble than U(IV) species and do not sorb strongly to soils under neutral pH because of the predominance of neutral or negatively charged species. As a result, U(VI) is expected to be transported by water as a soluble species.

Ball (2000) reported on results of computer modeling U speciation in groundwater using a chemical speciation code (WATEQ4F) for natural waters. The model used the most recent

complete data sets selected from analyses of 950 well water samples collected from the Solar Ponds Plume area. The data were analyzed to determine saturation indices for major ions and to identify solubility controls for dissolved groundwater constituents. Predominant dissolved species were not plotted as a function of pH. The model indicated that:

- U is migrating as a dissolved component of the groundwater plume;
- Above pH 6, all dissolved U species are undersaturated with respect to U minerals in the subsurface. This implies that, under the pH and redox conditions studied, there are no obvious solubility controls on mobility of U in the groundwater of the Solar Ponds Plume;
- The dissolved U plume has not migrated as far from the Solar Ponds source area as has the dissolved nitrate plume. However, the extent that this is due to retardation of the U plume is not known at present. Dates of nitrate disposal are not known and may be distributed in time somewhat differently than U disposal. In addition, it is possible that other factors such as differing dispersivities of U and nitrate and selective microbial reduction of U play a role; and
- The interpretation that dissolved U species are undersaturated suggests that any transport retardation that may occur is due to sorption processes.

Litaor (1995) found that the spatial distribution of U in RFETS soil did not follow the west-to-east plume observed for Pu and Am, with most of the observed U activity well within the natural range of U background levels in Colorado soils. U activity was highest (between about 800 and 7,700 pCi/kg) near the 903 Pad and the former storage site of U-contaminated waste oils but dropped sharply to around Colorado background range (between about 500 to 3,000 pCi/kg) within about 500 meters of that site. Litaor explained these findings as due to the greater solubility of U(VI) over Pu species, especially when complexed by carbonates. Insoluble Pu solids are transported easterly from the 903 Pad area by wind and water surface erosion, while U is mobilized predominantly by water, dissolving in rainfall and migrating downward through the soil column.

Litaor's conclusion is supported by Honeyman and Santschi (1997) who found K_d values ranging between about 30 to 170 mL/g for U(VI) interactions with Solar Pond core isolates under oxidizing conditions. A steady decrease in K_d with depth reflected changes in the core composition and is possibly due to a down-core decrease in the ratio of sand to clay.

TA - 3.6.3 Dissolution, Precipitation and Coprecipitation of Uranium

General Literature Background

Dissolution, precipitation and coprecipitation have a much greater effect on the concentrations of U(IV) than on the concentration of U(VI) in groundwaters, because of the lower solubility of U(IV) compounds. Nevertheless, in low carbonate waters where aqueous U(VI) is in contact with the lower solubility phosphate and vanadate uranyl minerals (note the minerals listed in Section 2.6.1), uranyl solution-mineral equilibria can impose some additional precipitation control on U migration (Clark et al., 1997; Langmuir, 1997).

However, at low dissolved uranyl concentrations under oxidizing conditions, as in oxygenated groundwaters far from a U source, solution-mineral equilibria will not limit the concentration of U(VI). Near a U source where concentrations are higher or in reduced environments, these processes become increasingly important and several coprecipitates may form, depending on the environmental conditions (Falck, 1991, Frondel, 1958). Reducing conditions may exist in deep aquifers, marsh areas, landfills or engineered barriers that can cause U(IV) to precipitate.

Dissolution, Precipitation and Coprecipitation of Uranium at RFETS

As pointed out above, on-Site studies of U geochemistry at RFETS are sparse. The modeling study by Ball (2000) indicated that dissolved U species in the vicinity of the Solar Pond Plume are well undersaturated and that retardation of U mobility in the subsurface should not be significantly influenced by the solubility of U mineral phases.

The reports by Ball (2000), Litaor (1995) and Honeyman and Santschi (1997) all indicate that U is present primarily as soluble U(VI) species that move downward in the soil column, with percolating water to the water table and then laterally with the groundwater at a slightly retarded

velocity. Precipitation and coprecipitation do not appear to be important processes near the Solar Ponds Plume. This suggests that other processes such as sorption may be important in U retardation.

TA - 3.6.4 Sorption/Desorption of Uranium

General Literature Background

In low ionic strength solutions with low U(VI) concentrations, dissolved uranyl concentrations are likely to be controlled by cation exchange and adsorption processes. The uranyl ion and its complexes adsorb onto clays (Ames et al., 1982; Chisholm-Brause et al., 1994), organics (Borovec et al., 1979; Read et al., 1993; Shanbhag and Choppin, 1981) and oxides (Hsi and Langmuir, 1985; Waite et al., 1994). As the ionic strength of an oxidized solution increases, other ions, mainly Ca^{2+}, Mg^{2+} and K^{+}, displace the uranyl ion from soil exchange sites, forcing it into solution. For this reason, the uranyl ion is particularly mobile in high ionic-strength solutions. Not only do other cations dominate over the uranyl ion in competition for exchange sites but carbonate ions form strong soluble complexes with the uranyl ion, increasing the total amount of U in solution (Yeh and Tripathi, 1991).

Some of the uranyl sorption processes are not completely reversible. Sorption onto iron and manganese oxides can be a major process for extraction of U from solution (Hsi and Langmuir, 1985; Waite et al., 1994). These oxide phases act as a relatively irreversible sink for U in soils. U bound in these phases is not generally in isotopic equilibrium with dissolved U in the same system, suggesting that the reaction rate mediating the transfer of the metal between the two phases is slow.

Moyes et al. (2000) used X-ray absorption spectroscopy to show that dissolved U uptake by different minerals can proceed by different mechanisms. On the iron hydroxides goethite and lepidocrocite, uptake occurred by surface complexation and ceased when the surface became saturated. On the silicate mineral muscovite, the surface did not saturate and uptake increased linearly with U concentration, which was interpreted as the formation of a precipitated U phase on the surface. U uptake by the iron sulfide mackinawite was more complicated, suggesting

initial complex formation at sites that have become oxidized, followed by coupled reduction of U and surface oxidation. This appeared to result in surface precipitation of a U oxide phase at high U concentrations.

Naturally-occurring organic matter is another possible sink for U(VI) in soils and sediments. The mechanisms by which U is sequestered by organic matter have not been worked out in detail (EPA, 1999). A possible process involves adsorption of U to humic substances through rapid ion-exchange and complexation with carboxylic and other acidic functional groups (Boggs et al., 1985; Borovec et al., 1979; Idiz et al., 1986; Shanbhag and Choppin, 1981; Szalay, 1964). These groups can coordinate with the uranyl ion, displacing waters of hydration, to form stable complexes. This could account for a significant fraction of the organically bound U in surface and subsurface soils.

Alternatively, sedimentary organic matter may act to reduce dissolved U(VI) species to U(IV) (Nash et al., 1981). U sorption to iron oxide minerals and smectite clay has been shown to be extensive in the absence of dissolved carbonate (Ames et al., 1982; Hsi and Langmuir, 1985; Kent et al., 1988). However, in the presence of carbonate and organic complexing agents, sorption has been shown to be substantially reduced (Hsi and Langmuir, 1985; Kent et al., 1988).

Water pH has little effect on U(VI) sorption to solids between about pH 5 and 8 (See Figure TA-3-14). Below pH 5 and above pH 8 there is a marked decrease in U K_ds indication a corresponding decrease in sorptivity. This behavior is attributed to the pH-dependent surface charge properties of the substrates and complexation of dissolved U(VI) with carbonates above pH 7 (EPA, 1999). The K_d maximum occurs in the pH range where the dominant U aqueous species change from cations to anions, as pH increases (Figure TA-3-7 and Figure TA-3-8).

Sorption/Desorption of Uranium at RFETS

U sorption experiments on RFETS soils, completed by the Colorado School of Mines in 1997 (Honeyman and Santschi, 1997), indicate that from 0.5 to 3.2 % of added U remained in solution in the aqueous phase. Samples with higher clay content had less U remaining in solution. These results give an upper-bound estimate of potential U release from RFETS sediments because they

284

are based on sorption rather than release of contamination; contact between sediment particles and water is much greater in the laboratory than at the bottom of a pond. Morphological differences between soils and sediments may also influence release.

TA-3.7 COLLOID FORMATION, AGGREGATION AND AQUEOUS PARTICLE SIZE DISTRIBUTION

TA - 3.7.1 Introduction

One potential mechanism for actinide migration in the environment is facilitated transport by colloids. Colloids are naturally-occurring particles, defined as ranging in size from 0.1 to 0.001 μm. They are found in nearly all surface water and groundwater and are formed because of the weathering of rocks, soils and decomposing plant materials. Colloids are naturally-occurring, sub-micron-sized particles that, due to their small size, have the potential to be transported by groundwater. Colloids consist of organic and inorganic material. Because radionclides can sorb to colloids, they can facilitate transport of contaminants, including actinides. Though the importance of colloid-facilitated transport is dependent on local geologic and hydrogeologic conditions, a number of generalizations can be made that will be further elaborated in the following discussion.

Conditions at RFETS are conducive to the association of actinides with colloids and mobility of actinide-colloids in surface water has been shown to occur at RFETS. Some measurements have also shown that small amounts of actinide colloids are present in RFETS groundwater. Subsurface transport of colloidal actinides at other sites has been indicated by studies at the Nevada Test Site and Los Alamos National Laboratory (see "Colloids—Carriers of Actinides into the Environment", in Cooper, 2000, Volume II, page 490).

Therefore, there is a potential for colloid-facilitated movement of actinides at RFETS. However, the likelihood and potential importance of subsurface mobility of actinide-colloids at RFETS is yet to be determined.

285

The relative importance of colloids for the transport of actinides in surface and groundwater at RFETS depends on the following factors:

- The low solubility of actinides, which greatly reduces the extent of dissolved transport;
- The strong tendency of actinides to sorb to colloids, as demonstrated by the high K_d values of actinides;
- The potential for "hot particles" of colloidal size to form; and
- The abundance of natural colloids (clays, organic matter, etc.) in the RFETS soils and sediments that are potentially capable of sorbing and transporting actinides.

Actinides in the environment can become associated with colloids by:

- Directly polymerizing and precipitating as colloid-sized particles because of hydrolysis, redox and pH reactions;
- Sorbing from the dissolved state to the surface of inorganic and organic colloids that are already present; and
- Co-precipitating with other metal compounds (metal oxides, carbonates, etc.).

The low aqueous solubility of actinides is discussed in the previous sections on actinide geochemistry (TA-3.4, TA-3.5 and TA 2.6). The partitioning behavior of actinides and the K_d model are discussed in Section TA-3.8. In this section, the evidence for colloid-facilitated transport of actinides at off-Site locations, the available data on colloid association of actinides at RFETS and the mechanisms that will most likely control colloidal actinide behavior at RFETS are discussed.

For practical purposes, a colloidal actinide is actinide radioactivity associated with a particle of colloidal dimensions. Actinides can associate to some extent with any of the colloidal materials present in the soils and waters at RFETS. Some examples could be: an actinide ion complexed

286

to a colloidal natural organic ligand, an actinide ion sorbed directly to a clay mineral particle or an ion sorbed to or co-precipitated with a metal (e.g. Fe, Mn and Al) oxide particle. In the radiochemistry literature, these would be termed "pseudo-colloids" in order to differentiate them from what is defined as "true" or "intrinsic" colloids. This latter term is used to describe an oxide or hydroxide of the actinide having colloidal dimensions [e.g., polymers or crystals of $Pu(OH)_4(am)$ or PuO_2]. These different forms of colloidal actinides may have differences in their chemical behavior, but for many considerations, such as environmental transport, their exact chemical form may be less important than their physical properties, such as size (Weiner 2000, Chapter 4). The presence of "hot" particles creates an additional complication to understanding actinide migration at RFETS (McDowell and Whicker, 1978). Behavior of actinides associated with other colloidal phases, such as clays or organic matter, should be governed by sorption/complexation reactions. Thus, their behavior might be in part predictable if and when the needed equilibrium-binding constants are known. However, colloids composed of actinide oxides or hydroxides are not necessarily in thermodynamic equilibrium with either the solution or the aquifer matrix and are, therefore, governed only by hydrologic transport and colloid processes such as aggregation (EPA, 1999, McCarthey and Zachara, 1989).

TA - 3.7.2 Colloid Definitions

The following discussion of colloids and colloidal behavior draws on a number of general references (Buffle and Leppard, 1995, Ranville and Schmiermund, 1999, Ryan and Elimelech, 1996, Stumm and Morgan, 1996).

A colloidal system is rigorously described as a two-phase system in which one phase is uniformly and permanently distributed or dispersed in a second phase. This is in contrast to both a true solute/solvent system, which comprises a single phase and a suspended-particle/solvent system, which is a two-phase system but is typically not uniform and never permanent. Long-term kinetic stability as a uniform suspension fundamentally defines a colloidal system. For environmental systems, a more practical set of definitions based on size (or mass) or, perhaps more importantly, on environmental behavior, is more useful.

Colloid Definition Based on Particle Size

Chemical species present in natural waters occur over an essentially continuous range of sizes, referred to as the solute/colloid/suspended-sediment size continuum. While the end member sizes are easily conceptualized as dissolved ions or molecules and macroscopic particles, the term colloid collectively identifies the intermediate continuum of sizes. The size cutoffs are a matter of varying definition. Generally, the size of colloids is defined as simply being sub-micrometer or, more specifically, ranging from 0.001 to 1.0 μm (1 to 1000 nm). A slightly larger lower size limit is used by some, while others extend the upper range from 2 to 5 μm for agreement with the classical clay-silt boundary; still others further extend this range to 10 μm (Stumm and Morgan, 1996). Some workers use the 0.45 μm cutoff, traditionally used to differentiate between "dissolved" and "particulate," as the upper limit of the colloidal range. However, it is understood that colloids exist well below the 0.45 μm cutoff and are not in the dissolved phase. Therefore, when referencing work where a 0.45 μm definition is used, caution must be exercised to not misinterpret or over-interpret the data. As is generally the case when describing a continuum, intermediate limits and bounds are somewhat arbitrary.

Colloid Definition Based on Environmental Behavior

Size-based definitions as described above can be arbitrary; especially those based on filters such as the 0.45 μm cutoff. However, some of these size-based cutoffs do have a direct connection to environmental behavior. For example, one of the most significant properties of colloids is their relatively high degree of mobility in aquatic systems. As implied in their definition, colloids do not settle in surface waters. The slow settling rates of 1 to 2 μm soil mineral particles, on the order of less than a few tens-of-cm/day, makes these sizes a reasonable cutoff between colloids and suspended sediments (Buffle and Leppard, 1995). Furthermore, as presented in a subsequent discussion, a 1 to 2 μm upper limit for colloids is consistent with the predicted upper limit for particle transport in aquifers and other porous media (Ryan and Elimelech, 1996). The lower colloid-size limit, separating colloids from dissolved molecules, is perhaps adequately defined by considering whether or not a surface exists.

Colloidal particles in natural waters may be composed of a variety of natural and synthetic materials, ranging from macromolecules (molecular weight >1000) to oxides and phyllosilicates. There are two main groups of colloids: hydrophilic and hydrophobic. For hydrophobic solids, permanent dispersion or suspension is maintained by the random thermal activity of water molecules (Brownian movement). Normally, uncharged hydrophobic particles tend to aggregate in water solutions. Because colloids tend to be negatively charged under environmental conditions, coulombic repulsion between particles maintains dispersion and allows attractive interactions with water molecule dipoles, making the colloids effectively more hydrophilic. In contrast, inherently hydrophilic macromolecules, which more closely approach true solute behavior, maintain their colloidal stability via interactions between charged functional groups and water molecule dipoles.

The relative abundance of various kinds of colloids will vary with the environment of the water. In groundwater, for example, clay minerals, humic substances and iron and aluminum oxides derived from the soils may be the most abundant colloids. In biologically productive surface water, such as the RFETS ponds, living microorganisms and nonliving organic materials can also contribute significantly to the colloid population.

Colloids originate in at least three ways:

- They are acquired from the surrounding environment by the process of disaggregation or dissolution and entrainment (e.g., suspension of primary or authigenic clays, acquisition of atmospheric dust by rain, weathering of framework silicates, suspension of oxides and oxyhydroxides, dissolution of fulvic acids in soil profiles, erosion of mineral and rock fragments from soil profiles);

- As a result of in-situ aqueous phase precipitation due to changing chemical or physical conditions (e.g., precipitation of calcite due to pH changes, precipitation of iron oxides and/or sulfides due to redox changes, formation of complex phosphate mineral suspensions at chemical interfaces in lakes and polymerization of dissolved silica due to pH changes); and

- Because of biological activity (e.g., growth and death of microbes, production of fibrils, organic skeletons and protein-rich cell fragments [Leppard, 1992], biologically-mediated precipitation or dissolution).

TA - 3.7.3 Environmental Behavior of Colloids

The ability to evaluate and predict the role of colloid-facilitated transport for actinides at RFETS may require computer models that incorporate colloids into transport calculations for both groundwater and surface water pathways. However, direct measurements of colloid-associated actinides, which are needed for verifying modeling results, are often inconclusive (e.g., Buffle et al., 1992; EPA, 1999).

In order to build a conceptual model for actinide transport that includes colloids, it is necessary to evaluate the important processes that control both the mobility of colloids and the association of actinides with colloids. Colloid mobility is discussed in this section. The association of actinides with colloids is closely related to the tendency of the actinides to adhere or adsorb to the various natural colloids present in the soils and sediments at RFETS and is discussed in Section 2.8.

Hydrodynamic and chemical forces govern interaction of colloids with one another and with macroscopic solid phases (O'Melia, 1987). Hydrodynamic forces tend to bring colloids into contact with each other and with other surfaces such as larger mineral grains in porous media. The frequency of these contacts is directly related to particle size and temperature. Stability of colloids refers to their ability to remain dispersed in surface or groundwater by avoiding aggregation during particle contacts; it does not imply chemical stability. Colloid stability depends on the nature of the colloid surfaces and solution composition.

Collision of two particles can have two outcomes: either the particles adhere to each other or they do not. The stability, W, of a colloidal suspension is related inversely to the collision efficiency factor, α, which is defined as the fraction of collisions that result in sticking or aggregation (O'Melia, 1987, Stumm and Morgan, 1996).

$$\alpha = \frac{N_s}{N_t} = \frac{\text{rate at which particles attach}}{\text{rate at which particles collide}} = \frac{1}{W}$$

The value of W, and hence the colloid stability, increases as N_s decreases. Interfacial electrostatic forces, as previously described, govern the value of α. As two similar, like-charged, hydrophobic particles approach each other, they begin to experience electrostatic repulsion as the gap between them closes. As particle separation decreases, repulsive forces increase and more energy is required to continue the approach. If the separation becomes sufficiently small, van der Waal's attractive forces come into play and ultimately overwhelm the repulsive forces, allowing aggregation to occur. The maximum net repulsive force must be overcome to achieve aggregation. The thickness of the diffuse charge layer surrounding the particle controls the distance of approach and this thickness is decreased by the presence of ions in the aqueous media (i.e., ionic strength). As ionic strength increases, aggregation is more likely. Divalent (Ca^{2+}, Mg^{2+}) and trivalent cations (Al^{3+}, Fe^{3+}) can reduce the net negative charge and form bridges between two negatively charged colloids. Such cations can be very effective at causing flocculation of colloids. Replacement of polyvalent cations by monovalent cations (Na^+, K^+) by cation exchange increases the degree of dispersion of colloids.

Organic compounds play a critical and complex role in aggregation in natural waters, both stabilizing and destabilizing colloids. Humic substances are considered to be low molecular weight compounds containing acidic functional groups that result in a net negative charge on the molecules. Humic substances have been shown to sorb strongly to oxides, which results both in the formation of a negative surface charge (Tipping and Cooke, 1982) and in an increase in the stability of the colloidal oxides (Tipping and Higgins, 1982; Wilkinson et al., 1997). Since colloidal clay minerals, organic matter and humic-coated oxides all have a net negative charge at most environmental pHs, their colloids can be reasonably stable in aquatic environments.

Many microorganisms and algae produce high molecular weight carbohydrates that can form strong bonds to particle surfaces. Because of their high molecular weight, these materials can form bridges between particles and thus are very effective at promoting aggregation (Wilkinson et al. 1997). Thus, organic matter can either decrease (humics) or increase (carbohydrates) the

291

value of α. Humic substances are most likely introduced into surface waters from the soil, whereas most carbohydrates are probably produced within the water body by aquatic organisms. The composition of sewage effluents may play an important role in the behavior of colloids and particles in the RFETS ponds.

Colloidal Processes Occurring in Surface Waters

Particles larger than a few microns can be effectively removed from lakes by settling. During this process smaller particles and colloids can also be removed by gravitational aggregation, as illustrated in Figure TA-3-9. The aggregation of colloids in lakes, as previously described, is dependent on both particle stability and initial particle size (Ali et al., 1985). Smaller colloids have higher diffusion coefficients and are thus subject to a greater frequency of collisions. If their α value is high, then perikinetic aggregation occurs (Figure TA-3-9). Currents or other differential fluid velocities can also cause colloid collisions and subsequent aggregation (orthokinetic aggregation). Aggregated colloids are then subject to sedimentation, which may act to transport adsorbed metals from the water column to the sediments (Sigg, 1985). The bulk chemical properties between settling colloidal aggregates and non-settling colloids and particles can be very different, especially in respect to their organic matter and trace metal content (Ranville et al., 1991).

The net result of these processes is that particle size distributions in surface waters are dominated by colloids near 1 micron in size (Filella and Buffle, 1993). This colloid behavior is illustrated by computer simulations performed by Filella and Buffle (1993). An example of their results is reproduced in Figure TA-3-10. The simulation was performed by starting with equal numbers of colloids and particles ranging in size from 0.001 to 100 microns. After 10 days, the combined effects of settling and aggregation resulted in a size distribution of particles having an average size of about 1 to 2 microns. Thus, we might expect to observe in the ponds a loss of actinides associated with both rapidly settling particles and very small colloids. The simulation was performed with all particle sizes having the same α value. This may not be true in reality and, thus, observations at RFETS may differ from the picture presented by the simulations.

Figure TA-3-9. Physical processes that cause particle collisions in surface water that can also lead to aggregation

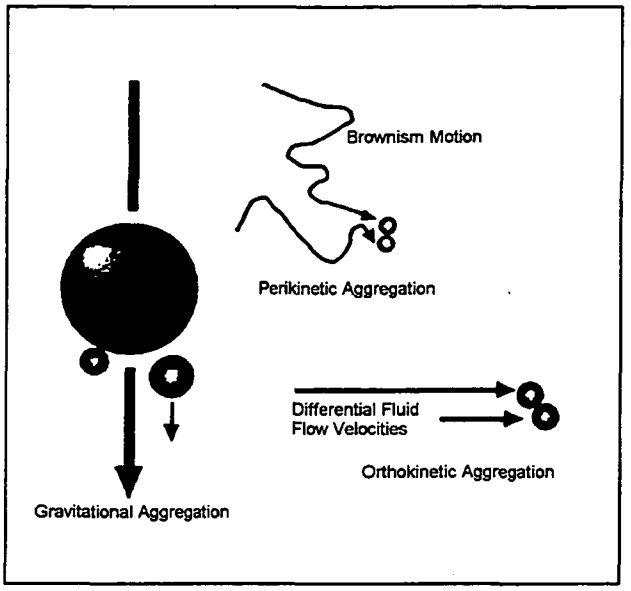

Figure TA-3-10. Simulation results obtained by Filella and Buffle (1993) that illustrate the development of volume-based particle size distributions in surface water starting from an initially uniform size distribution

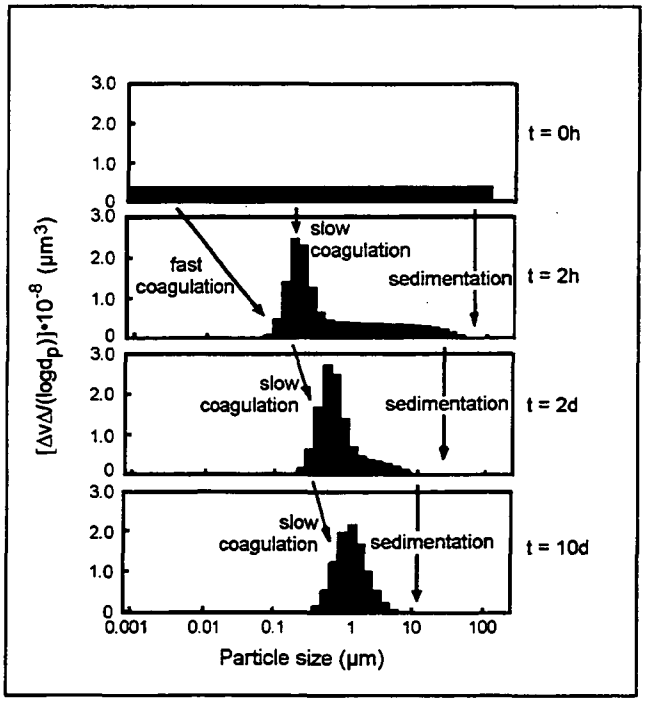

293

Colloidal Processes in Groundwater

The abundance of colloids in groundwater is a function of the source area and/or in-situ processes. Weathering and disaggregation result in the generation or release of colloids from mineral grain surfaces. Behavior of colloids in porous media, such as a groundwater aquifer, involves all the mechanisms of surface water transport with the added complications of finite pore sizes, complex flow paths and higher solid-to-liquid ratios that allow abundant opportunity for interactions with the solid aquifer matrix. These processes are illustrated in Figure TA-3-11. They are described in detail by McDowell-Boyer et al. (1986) and summarized. The ratio of particle diameter to media diameter (d_p/d_m) is greater than 0.1 and particles are normally excluded from a porous media and form external filter cakes, assuming spherical suspended particles and matrix grains. Larger particles entering the porous media are subject to gravitational settling and filter straining. Filter straining appears to be most important when $0.1 > d_p/d_m > 0.05$ and be relatively ineffective below 0.05. Significant losses of porosity may occur due to filter straining and the mechanism itself may become important with either increasing d_p due to particle agglomeration and/or decreasing d_m due to changes in lithology. Gravitational settling is strongly dependent on particle density.

294

Figure TA-3-11. Processes occurring in porous media, which control colloid and particle transport in groundwater

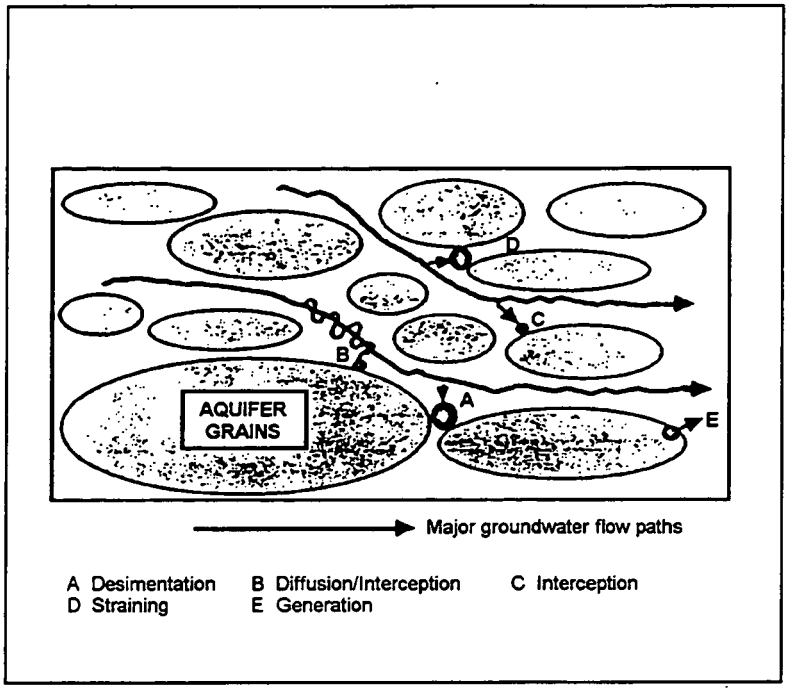

The combination of these mechanisms probably controls the upper size limit for suspended and/or mobile particles in porous media. Even the largest colloids (1 μm diameter) could easily enter a fine sand aquifer with uniform spherical grain sizes of 0.1 mm. Assuming clay-sized (0.001 mm) aquifer grains, colloids up to 50 nm could potentially move through the available pore spaces. These conservative estimates do not take into account irregular grain shapes and packing, which would reduce the maximum size of transportable particles. The presence of soil macropores may significantly increase the amount of colloids that can be transported (Ryan et al., 1998).

For particles small enough to penetrate a porous media, the probability that they remain suspended or entrained in the prevailing flow depends in large measure on particle-media interactions. McDowell-Boyer et al. (op. cit.) regards the process as physical-chemical filtration comprised of the initial collision and subsequent attachment mechanisms. Settling of larger suspended particles may result in collisions with the matrix surfaces. For particles moving with the groundwater, the trajectory of the flow lines may result in direct interception of particles by

295

the surface. For smaller particles and perhaps all colloids, Brownian motion is the predominant collision mechanism. Brownian motion allows colloids to diffuse from the principal flow region between grains and closely approach the aquifer grains where attachment may occur. Attachment is determined by the complex nature of the electrified interface and is a balance between attractive and repulsive forces as previously described. Attractive forces are dependent upon the nature of the particles, whereas repulsive forces, due to charge on the surface, are also dependent upon water chemistry. Water chemistry parameters of importance include pH (Kita et al., 1987), ionic strength (Cerda, 1987, McDowell-Boyer, 1992) and solution composition.

The consequence of these processes, which remove both large and small particles, is an optimum particle size for transport in porous media (Yao et al., 1971). This is illustrated in Figure TA-3-12 taken from Harvey and Garabedian (1991), where calculations were performed for microorganisms of nearly neutral density. The graph illustrates the relationship between particle size and the single collector efficiency η. The parameter η is the rate at which the particle/colloid collides with the surface divided by the rate at which the particle/colloid travels towards the surface. If α is the same for all particle sizes, then η also represents the probability that the particle/colloid will be captured by the porous media. Thus, the greatest mobility occurs for colloids of about one micron in diameter.

These processes have been most clearly demonstrated by the work of Harvey et al. (1989) with various tracer tests which were conducted between monitoring wells in a glacial aquifer on Cape Cod, Massachusetts under conditions of natural and induced flow gradients. Chloride and bromide were used as conservative tracers and fluorescent-labeled bacteria and submicron latex spheres were used to study the mobility of particles. The tests demonstrated that micron and submicron particles could easily migrate in porous media, as shown by the similarity of the arrival times in the second well. The average velocities of the particles also can exceed conservative solutes. This is because size exclusion of the particles from the smaller pores reduces the flow path tortuousity that the particles experience as compared to the conservative solutes. Their results also indicated that submicron particles travel more slowly than micron-sized particles, as predicted by filtration theory. The chemical functionality of the sphere

surfaces (carboxyl, carbonyl, uncharged) also affected retention and retardation. The transport of these spheres was successfully modeled by colloid filtration theory (Harvey and Garabedian, 1991).

Figure TA-3-12. Computed affect of diameter on the degree of transport of colloids and particles in groundwater

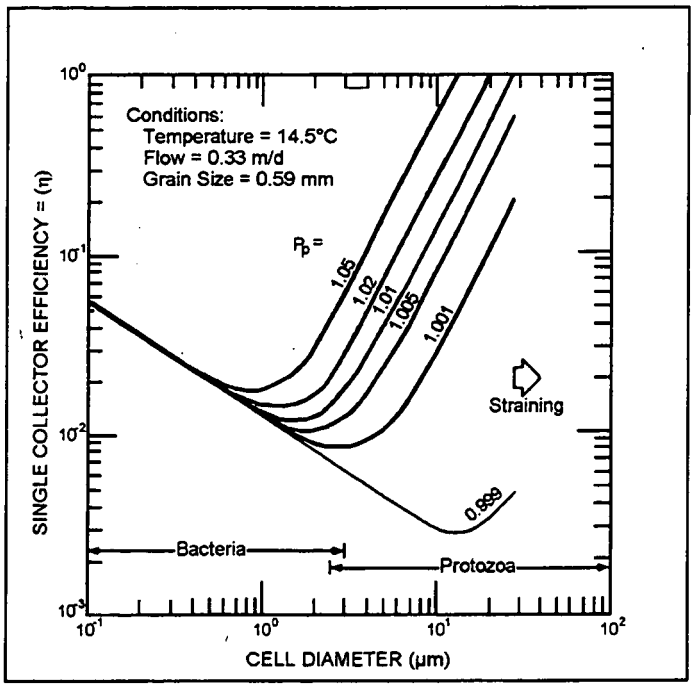

An illustration of the relationship between particle size and the single collector efficiency η. η equals the collision frequency of a particle/colloid with a surface, divided by the particle/colloid velocity towards the surface. If α, the fraction of sticky collisions, is the same for all particle sizes, then η also represents the probability that the particle/colloid will be captured by the porous media. The greatest mobility occurs for colloids of about one micron in diameter. Reproduced from Harvey and Garabedian (1991).

Additional research reveals the potential impact of colloids on adsorbed contaminant transport in a porous media (Puls and Powell, 1992). These authors compared the mobility of arsenic associated with iron oxide colloidal particles to truly dissolved arsenic in laboratory columns of natural aquifer material. Tritium was used as conservative tracer. They reported the following:

- Iron oxide colloids moved very easily through the columns, as shown by the similarity of the tritium and colloid elution times;

297

- Colloid-associated arsenic was transported through the columns 21 times faster than dissolved arsenic; and
- Colloid velocity was a function of size and the ionic composition of the solutions.

TA - 3.7.4 Non-RFETS Data Concerning Colloid-Facilitated Transport of Actinides

A number of studies at sites other than RFETS have shown an association between natural colloids and actinides in groundwater (Kaplan et al., 1994; Kim et al., 1992; Nagasaki et al., 1997) and surface water (Orlandini et al., 1990). Other studies have demonstrated the importance of intrinsic actinide colloid formation (Kim, 1991; Knopp et al., 1999; Leiser et al., 1992; Nagaski et al., 1994). Some studies have also suggested that colloids have been able to increase the degree of transport of actinides under some situations (Baek and Pitt, 1996; Satmark, 1994; Smith and Degueldre, 1996; Tanaka and Nagasaki, 1997; Totok et al., 1990). Dissolved and colloidal organic matter, in particular, can increase actinide transport (McCarthy, 1998; Marley et al., 1993). Fewer studies have attempted to incorporate colloids into transport models (Luhrmann, 1998; Schuessler et al., 2000).

At the Nevada Test Site (NTS), Kersting et al., (1999) found that Pu and other radionuclides detected in two different aquifers originated from an underground nuclear test conducted 1.3 km upgradient. The Pu was associated with the colloidal fraction of the groundwater. The underground tests were conducted beneath the groundwater table in fractured volcanic rock. This geologic condition is different from RFETS and it is not yet known if transport conditions at the NTS function at the RFETS.

Penrose et al., (1990) work at Los Alamos National Laboratory, indicating groundwater transport of actinides under conditions more similar to RFETS, were reinterpreted to suggest groundwater well contamination may have resulted from surface water transport of colloidal actinides (Marty et al., 1997). Although conditions at Los Alamos National Laboratory are more similar to RFETS than NTS, it remains unclear whether these conditions apply to RFETS. Due to the implications of these studies and previously discussed field and laboratory examples of colloid-

facilitated contaminant transport, it is important to determine the conditions that facilitate this type of transport exist at RFETS.

TA - 3.7.5 Current RFETS Data on Colloid-Associated Actinides

A variety of different methods has been used to examine the amount of actinide activity associated with colloidal particles at RFETS. Most of these studies are listed in Table TA-3-2.

McDowell and Whicker (1978) and Povetko and Higley (2000) directly identified colloidal particles containing actinides using autoradiographic methods, in which radioactive soil particles are brought into contact with a plastic detector film. The alpha particle emitters in the soil produce tracks in the detector that can be observed after etching the film with a basic solution.

McDowell and Whicker (1978) observed a relatively minor contribution by Pu oxide colloids to the total activity from Pu (12 to 31 %) in a surface soil collected 200 meters southeast of the 903 Pad area. They found that the average size of the Pu oxide particles was about 0.25 micron, although a number of large (> 1.5 micron) particles were observed. A single 6.86 micron particle accounted for 7 % of the average activity in one gram of surface soil. Because only about one gram of soil was investigated, there is considerable uncertainty about the importance of large Pu oxide particles. The presence of small numbers of large "hot" particles could explain the sample variability in Pu content seen in some other studies (Little, 1976; Higley, 1992).

Another autoradiographic study by Povetko and Higley (2000) demonstrated a much greater contribution by Pu oxide colloids to the Pu activity of a surface soil collected from the Buffer Zone. Their size distribution was very similar to that of McDowell and Whicker (1978), with an average Pu oxide colloid size of 0.15 micron. Povetko and Higley (2000) also found one especially large particle having an equivalent Pu oxide diameter of about 6 microns, which contributed 94 % of the total soil Pu activity. This particle was believed to consist of an aggregate of colloidal Pu oxide residing within a larger 500-micron soil aggregate. Of the remaining 6 % of sample activity, 89 % was attributed to PuO_2.

Most colloid studies at RFETS have used fractionation methods such as tangential-flow filtration (TFF), sedimentation or centrifugation to separate various size fractions for analysis of actinide size distributions. Gravitational settling using established soil analysis techniques is capable of providing a size separation as small as 2 micron. This size cut provides differentiation between a particulate fraction and a colloidal/dissolved fraction, which is useful for indicating changes in environmental mobility that occur at about this size. By substituting centrifugation for gravity settling, size fractionations can be made at smaller sizes. This allows differentiation of colloids within the submicron range and can provide an operational definition of "dissolved" versus colloidal. Both centrifugation and gravity settling depend on the buoyant density of the colloids and, thus, are actually mass-based, versus size-based, separations. Not by substituting centrifugation for gravity settling, but using both methods you can differentiate between particle size (> 2 microns), colloids and dissolved. Unfortunately, this method is difficult to apply to large volumes. For this reason, most colloid studies at RFETS have used TFF.

The TFF method has the advantage of being able to process large volumes of fluids. It uses an ultrafilter with a large surface area. The sample travels parallel to the surface of the filter at a high flow rate and is recirculated, while a portion of the sample diffuses through the filter at a much slower flow rate. This flow pattern uses hydrodynamic shear to prevent filter plugging during sample processing. The combination of high filter surface area and continuous washing of the filter allows the processing of large volumes of sample (in some cases hundreds of liters) that are often required in order to fractionate and concentrate enough sample for radiochemical analysis. Care must be taken to avoid clogging of the filters. Filter pore size can range from a few thousand Daltons (a few nanometers) to about 0.6 micron. Thus, TFF can be used to differentiate "dissolved" from colloidal species. Several studies have shown that other factors, such as charge repulsion between the sample and the filter surface, surface aggregation and filter plugging, may make the actual size cutoffs much different than the manufacturer-stated pore size cutoffs (Buffle et al., 1992).

A number of studies have used size-fractionation methods to determine the distribution of actinides in soil particles of different size ranges. In studies by Ranville et al. (1998) and RMRS

300

(1998a), 18 samples were suspended in de-ionized water and size-fractionated using settling to obtain Pu and Am concentrations in the < 2 micron size fraction. Since the solubility of Pu and Am is very low, this fraction can be considered to primarily represent the colloidal fraction of actinides in these samples. The Pu and Am abundances were in the colloidal fraction ranged from 0.6 to 6.6 % and 1.0 to 5.1 %, respectively. The relatively small amount of actinides present in the <2 micron size is due to the formation of soil aggregates.

A more recent study by Ranville et al. (2000), investigated the influence of soil aggregation on the size distribution of Pu in two soil samples. The <2 micron fraction was further separated using TFF into coarse colloidal (2 to 0.45 micron), fine colloidal (0.45 micron to 10K Dalton) and "dissolved" (<10K Dalton) fractions. Different dispersion methods were used to determine the relative strength of the aggregates and what materials were most responsible for binding the aggregates. When the soils were dispersed in water, only about 5 to 9 % of the total Pu was in the <2 micron fraction. Mechanical disruption of the aggregates increased the amount of Pu in the <2 micron fraction to 14 to 19 % of the total. Chemical dispersion using hexametaphosphate, destruction of organic matter by hydrogen peroxide and dissolution of iron oxides by citrate-dithionite-bicarbonate increased the amount of Pu in the colloid fraction to 45 to 48 %, 35 % and 50 %, respectively. In most cases, the bulk of the Pu was in the coarse colloid fraction (2 to 0.45 micron). For the hydrogen peroxide and citrate-dithionite-bicarbonate treatments, some Pu was found in the fine colloid (0.45-micron to 10K-Dalton size) and "dissolved" (<10K-Dalton size) fractions. Overall, recoveries of Pu for this study ranged from 90 to 127 %. The overall results suggest that a considerable amount of colloid Pu exists in the soils but that the bulk of this material is held in larger aggregates. The role of organic matter in binding aggregates was especially significant. Thus, aggregation is an important process in limiting colloidal transport of actinides in the surface soils.

A similar study of the effect of soil aggregation on soil particle size distributions of Pu was performed by Tamura (1977). In this study, soil was dispersed in de-ionized water and in a chemical solution that destroyed the organic matter and dispersed the soil particles. These samples were also ultrasonically treated to mechanically break up any aggregates not dispersed

301

by the chemical treatment. Samples were sieved to remove the sand fraction, then centrifuged to obtain a separation at 5 microns. When only de-ionized water was used, the amount of Pu in the <5 micron fraction ranged from 14.7 to 51.3 % of the total. After the aggressive disaggregation treatment, this amount increased to 67.7 to 89.2 %. Percent recovery of Pu was not determined.

Harnish et al. (1996) determined the amount of colloidal actinides present in two surface water seeps (SW-51, SW-53) located 100 to 300 meters from the 903 Pad. Unfiltered Pu 239/240 activities were 1.45 and 4.14 pCi/L for SW51 and SW53, respectively. In this case, either 5.0 or 0.45 micron filtration could be used to differentiate particulate from colloidal. The 5.0 micron filter was chosen for distinguishing between the two, because of the greater relevance to environmental behavior of the larger size cutoff. The distribution of Pu and Am among particulate, colloidal and dissolved fractions was determined both by direct analysis of the filter retentates and by calculation using each of the serial filtrate values. Results differed between the two methods. The activities of Pu-239/240 in particulate, colloidal and dissolved fractions for SW-51 were 1.16, 0.23 and 0.06 pCi/L when computed by filtrate analysis. From retentate analysis, the Pu activities were 0.015 and 0.72 pCi/L for particulate and colloidal fractions, respectively. For SW-53, the Pu activities were 3.28, 0.83, 0.03 pCi/L from filtrate analysis and 0.675 and 0.226 pCi/L by retentate analysis. The percent Pu distributions are given in Table TA-3-2.

The size distribution of Pu in the C-2 pond was examined by Polzer and Essington (1992) using TFF. Total measured Pu was 0.0196 pCi/L. However, the particulate/colloid differentiation was made using a 0.45-micron filter, so comparison with other studies using different definitions of colloid size is difficult. The Pu distribution was determined by analysis of the retentates. About 30 % of the Pu was not recovered. The Pu activities in the particulate, colloidal and dissolved fractions were 0.0081, 0.0013 and 0.0043 pCi/L, respectively.

Recent surface water investigations (Santschi, 1998; Santschi et al., 1999 and 2000) have used TFF to examine colloidal size fractions of Pu and Am. The reported size distributions for Pu are given in Table TA-3-1.

302

Two studies (Harnish et al., 1993 and 1996) have directly measured the size distribution of actinides in a single groundwater well at RFETS using TFF to fractionate the samples. Filter sizes used were 5.0 micron, 0.45 micron, 100KDalton and 10KDalton. The percent Pu distribution was computed both from retentate and filtrate data. The results have a large degree of uncertainty due to the very low actinide activities present in the groundwater. Total Pu activities for well 1587 were 0.0235 and 0.26 pCi/L in 1991 and 1992, respectively. The percent Pu distributions are given in Table TA-3-2.

TA - 3.7.6 Summary of Colloid-Facilitated Actinide Transport

Research indicates that colloid-facilitated transport is possible for actinides in the III and IV oxidation states. The importance of colloid-facilitated actinide transport will depend strongly on Site-specific conditions. Although field and laboratory experiments have identified many of the important parameters governing the mobility of actinides associated with colloids (Cooper, 2000, vol. 2), the application of this knowledge to specific sites so far remains largely qualitative. Colloid transport through the subsurface is likely to occur mostly in fractures since the movement of colloids through the soil column is expected to be impeded by sorption and filtration processes. At RFETS, movement of Pu and Am occurs primarily by wind and water surface erosion processes that are expected to include colloid movement (Santschi et al., 2000).

303

Table TA-3-2. Literature Relevant to Actinide Association with Colloids at RFETS

Reference	Authors	Comments	Observations
Soil			
(1978) Size characteristics of Pu particles in Rocky Flats soils, Health Physics, 35, p. 293-299.	McDowell, L.M. and Whicker, F.W.	Used autoradiography to determine size of Pu oxide particles in soil. Soil was taken from very near the 903 Pad and had very high total activity (1486 pCi Pu-239/240 per g).	Colloidal PuO_2 accounted for 12-31 % of the total activity. Average PuO_2 diameter was 0.2 micron, although particles up to 6.86 micron were observed. Later work by Hayden showed the large particle to be an agglomerate of submicron particles.
(1977) Effect of pretreatment on the size distribution of Pu in surface soil from Rocky Flats, In, Transuranics in Desert Ecosystems, Nevada Applied Ecology Group. NVO-1871 UC-11, p 173-186	Tamura, T.	Used sieving and centrifugation to examine Pu size distributions in three size fractions of 8 soils. Compared mild dispersion (water) to aggresive dispersion (sodium acetate, peroxide, sodium carbonate). Total Pu ranged from 0.08-2.5 pCi/g.	For water dispersed soils, the amount of Pu in the <5 micron fraction averaged 28 %. After aggressive dispersion the amount of Pu in the <5 micron fraction averaged 78 % of the total.
(1992)Vertical movement of actinide contaminated soil particles, CSU dissertation	Higley, K.A.	Used centrifugation and filtration to differentiate 2-0.45, <0.45 µm actinides in three soils at 4 depths. Soil Pu activities were approximately 81 pCi/g.	Approximately 14 ± 9 % and 8 ± 3 % of total Pu was found in 2-0.45 and <0.45 micron fractions, respectively.
(RMRS 1998a) Actinide content and aggregate size analyses for surface soil in the Walnut Creek and Woman Creek watershed at the Rocky Flats Environmental Technology Site, RF/RMRS-98-281.UN	RMRS	Used gravitational settling to determine the amount of actinides present in the <2 micrometer fractions of 18 surface soils after water dispersion. Total Pu activities ranged from 0.07-34 pCi/g (plus one sample having a total activity of 397 pCi/g).	About 1-7 % of the total Pu occurred in the <2 micron (colloid plus dissolved) fraction.
(2000) Soil aggregation and its influence on Pu particle-size distributions of soils collected from Rocky Flats, CO, Final Report to EPA Region VIII	Ranville, J. F.; Harnish, R.A.; Winkler, S.; and Honeyman, B.D.	Used settling and Tangential flow filtration (TFF) to determine Pu size distributions in colloidal fractions of soil subject to different dispersion methods. Examined three soil samples from a hillslope about 0.7 km from the 903 Pad. Also examined one runoff sample. Bulk soil Pu-239/240 ativities ranged from 3 to 35 pCi/g and runoff activity was about 1.5 pCi/L.	Dispersion with water showed less than 5 % of the total soil Pu to be in colloidal and dissolved fractions. In the runoff sample nearly 80 % of the total Pu was in the colloidal and dissolved forms. Most Pu <2 µm was found in the 2-0.45 µm fraction for surface soils and in the <10 kDa fraction for the runoff sample. Chemical dispersion increased the amount of Pu in the <2 µm soil fraction to nearly 50 %.
(2000) Study of particles of actinides in soil samples using nuclear track detectors. Poster presented at Health Physics Society Meeting, Denver, CO.	Povetko, O.G. and Higley, K. A.	Used autoradiography to determine size distribution of Pu oxide particles in a single 15 cm soil profile. Sample was collected near the 903 Pad area and contained high activity (730 pCi Pu-239/240 per g)	Average size was 0.13-0.23 micron, however 94 % of the total activity occurred in a single 500 µm soil aggregate. This aggregate contained a single >6 µm PuO_2 particle that was itself composed of smaller PuO_2 colloids.
Vadose Zone			
The hydrogeochemistry of actinides in the soil of Rocky	Litaor, M.I.; Barth, G.; and Litus, G.	TFF was used to determine the amount of actinides	The % of the total Pu activity in each size fraction

304

Reference	Authors	Comments	Observations
Flats, Colorado (unpublished report)		associated with colloids in soil interstitial water. Site was very near the 903 Pad and total Pu in the soil intersitial waters ranged from 650-12,000 pCi/L.	averaged: 0.45 µm: 48 ± 22 % 0.45-0.001 µm: 40 ± 19 % <0.001 µm: 12 ± 8 %
Surface Water			
(1992) The physical and chemical characterization of radionuclides in the surface waters at Rocky Flats Plant. LA-UR-92-1812	Polzer, W.L. and Essington, E.H.	TFF was used to determine the amount of actinides associated with colloids in 2 surface water samples from pond C-2. Total Pu activities were about 0.02 pCi/L.	Pu percent distribution was Particulate 41 Colloid 7 Dissolved 22 Not recovered 30
(1996) Particulate, colloidal and dissolved phase associations of Pu and Am in a water sample from Well 1587 and Surface Water Sites SW-51 and Sw-53 at the Rocky Flats Plant, Colorado, WRI 96-4067	Harnish, R.A.; McKnight, D.M.; Ranville, J.F.; Stephens, V.C.; and Orem, W.H.	TFF was used to determine the amount of actinides associated with particles and colloids in groundwater and two surface water samples. A 5-micron filter was used o distinguish particulate from colloidal. Total Pu activities in the surface waters ranged from 1.45-4.14 pCi /L.	From analysis of filtrate data the percent Pu distribution was: SW-51 SW-53 Particulate 80 80 Colloid 16 20 Dissolved 4 < 1 From retentate data Particulate 28 73 Colloid 39 24 Dissolved 33 3
(1998) Final report on phase speciation of Pu and Am for "actinide migration studies at the Rocky Flats Environmental Technology Site." 15 October 1998	Santschi, P.H.	TFF was used to determine the amount of actinides associated with suspended sediments and colloids in surface water samples. Total Pu activity was 0.0035 pCi/L.	Most Pu (82 %) was in the >5 micron fraction. The distribution in the colloid and dissolved fractions was: 5-0.45 µm: 8 % 0.45-0.1 µm: 3.5 % 0.1 µm-100 kDa: 1.5 % <100 kDa: 5 %
(1999) Final report on phase speciation of Pu and Am for "actinide migration studies at the Rocky Flats Environmental Technology Site." 28 September 1999.	Santschi, P.H.; Roberts, K. and Guo, L.	TFF was used to determine the amount of actinides associated with suspended sediments and colloids in two surface water samples. Total Pu activity was 0.0263 and 0.1373 before and during a storm event, respectively.	Very similar size distributions for approximate percent of the total Pu were seen for both samples. >20 µm 25 % 20-0.5 µm 15 % 0.5µm –100 kDa 15 % 100–3 kDa 25 % <3 kDa 20 %
Groundwater			
(1993) Particulate, colloidal and dissolved phase associations of Pu and Am in a water sample from Well 1587 at the Rocky Flats Plant, Colorado, WRI 93-4175	Harnish, R.A.; McKnight, D.M.; and Ranville, J.F.	TFF was used to determine the amount of actinides associated with colloids in a groundwater sample. Groundwater activities in well 1587 were low, 0.02 pCi Pu/L, leading to significant uncertinties in the size distributions.	Analysis of TFF retentates found most Pu is in <10 kDa fraction wheras analysis of the filtrates showed 22 % >5 micron, 43 % 5 micron 10 kDa and 35 % <10 kDa.
(1996) Particulate, colloidal and dissolved phase associations of Pu and Am in a water sample from Well 1587 and Surface Water Sites SW-51 and Sw-53 at the Rocky Flats Plant, Colorado, WRI 96-4067	Harnish, R.A.; McKnight, D.M.; Ranville, J.F., Stephens, V.C. and Orem, W.H.	TFF was used to determine the amount of actinides associated with colloids in groundwater and surface water samples. Total Pu activity was 0.26 pCi/L in well 1587.	Analysis of TFF filtrates suggested nearly all Pu activity was in particles >5 microns

305

TA-3.8 APPLICABILITY OF EMPIRICAL PARTITION COEFFICIENT, K_d, VALUES FOR MODELING ACTINIDE TRANSPORT IN SOILS AND GROUNDWATER AT RFETS

TA - 3.8.1 Introduction

Assessment of chemical risk due to subsurface contaminants and the cost of remediation depends critically on the models that predict contaminant breakthrough times and concentrations to specific targets: drinking water wells, surface water bodies and/or geographical boundaries to a contaminated site. For systems where contaminant partitioning is dominated by chemical equilibria, a rigorous approach to surface and solution speciation (based on sound chemical thermodynamic principles) will provide a reliable description of contaminant chemistry (Grenthe and Puigdomenech, 1997).

For systems where equilibrium conditions exist, a variety of adsorption models, from simple distribution coefficients (K_d) to more sophisticated electrostatic adsorption models have been used for contaminant transport modeling. The most commonly used adsorption model in contaminant transport calculations is the distribution coefficient or K_d model. In large part, this reflects the simplicity of including a K_d value in a transport calculation. As with any model, the simple K_d model has a set of well-defined boundary conditions under which it can be used properly. The conditions and assumptions that go into a K_d model will be described in the sections that follow, along with recommendations regarding the use of K_ds for U, Pu and Am at the RFETS.

TA - 3.8.2 Definitions and Concepts

The tendency of a contaminant to move from one phase to another is often quantified by the use of a partition coefficient, also called a distribution coefficient. Partition coefficients are contaminant and medium specific. They can be measured directly *in situ*, by laboratory experiments or, in some cases, estimated from other properties of the contaminant. Although it may be possible to assign some theoretical significance to partition coefficients, based on their

response to system changes, they nevertheless are empirical quantities which often lump together many different factors, both known and unknown.

The simplest form of a partition coefficient is the ratio of contaminant concentration in phase 1 to its concentration in phase 2:

$$K_{1,2} = \frac{\text{concentration in phase 1}}{\text{concentration in phase 2}} \qquad (3.8\text{-}1)$$

For this report, the contaminants of interest are U, Pu and Am and the phases of interest are water and the solid constituents of soil. The partition coefficient that describes the tendency for a contaminant to become sorbed to soil from its dissolved state in water is called K_d, the soil-water partition coefficient. K_d is dependent on the chemical but not the isotopic composition of the contaminant. The simplest form of K_d is defined as:

$$K_d = \frac{C_s}{C_w} \qquad (3.8\text{-}2)$$

where:

C_s = concentration (mg/kg) of contaminant (adsorbate) adsorbed on the solid at equilibrium and

C_w = concentration (mg/L) of contaminant dissolved in water in contact with the soil at equilibrium.

The units of K_d are volume divided by mass or, using the above concentration units, L/kg (or its equivalent, mL/g). In the case of radioisotopes, concentrations may be expressed in terms of activity instead of mass, so that C_s becomes pCi/kg or Bq/kg and C_w becomes pCi/L or Bq/L. The units of K_d do not change when activities are used.

307

This simplest definition of K_d assumes that the linear relation $C_s = K_d C_w$ exists between the concentrations of contaminant sorbed on soil and dissolved in water. This generally will be true only if sorption/desorption reactions are reversible, equilibrium is achieved and the number of available sorption sites is much larger than the number of dissolved species competing for them (i.e., at a *relatively* low contaminant concentration).

An important example of the limitation of Equation 3.8-2 under field conditions is its incorrect prediction that sufficient water flushing will completely remove sorbed heavy metal and organic contaminants from soils. In fact, effluent from such treatment consistently contains a slowly diminishing but persistent residual "tail" of contaminant, which can remain of regulatory concern long after the time when a K_d model would have predicted "zero" concentration (Bethke and Brady, 2000 and accompanying references).

At least two non-exclusive explanations have been proposed for this behavior (Alexander, 1995; Brusseau, 1994; Doty and Davis, 1991; Fetter, 1993; Weiner, 2000):

- In heterogeneous soils, there are sorption sites with different attractive forces for the sorbed species; and
- The speciation and location of sorbed species can change (age) over time, to surface locations and chemical forms from which desorption is increasingly less likely.

Because the simple K_d model overestimates dissolved contaminant mobility (Bethke and Brady, 2000), it is considered by some to be a conservative approach for radionuclides having significant solubility and, therefore, protective of human health. This is true for short-term scenarios, where K_d models may predict initially higher rates of transport than would a complexation model. However, the K_d model predicts the eventual depletion of the contaminant source and continual migration of radionuclides, with steady dispersion and dilution along the path. Models that include surface complexation predict less initial mobility, but they also predict, more accurately, that a slowly diminishing residual concentration of contaminant will remain (Figure TA-3-13) (Bethke and Brady, 2000).

For these reasons, K_d models should not be used to design long-term remediation methods, but they can be useful for modeling conservative transport calculations with certain assumptions. Figure TA-3-13 shows that, with a K_d model, the initial breakthrough concentration of contaminant that elutes from a column is the highest concentration that is ever predicted to elute. The concentration curve eventually drops back to background when the contaminant is completely removed from the column. If the contaminant source were infinite, the predicted concentration curve would remain at the breakthrough level as long as there is water flow.

This means that when a K_d model is used to predict actinide transport, the concentration of actinide that initially reaches a target population is the concentration predicted to be highest that will ever occur. This conclusion assumes that primary sources have been removed or controlled and that further concentration of secondary sources does not occur. More refined models may predict more accurately how the concentration at the target location will change with time but, if the initial concentration predicted by a K_d model using a conservative value of K_d is considered an acceptable risk level, then more detailed calculations are not necessary.

309

Figure TA-3-13. Diagram illustrating predicted and typical experimental breakthrough curves for trace metals adsorbed on an elution column

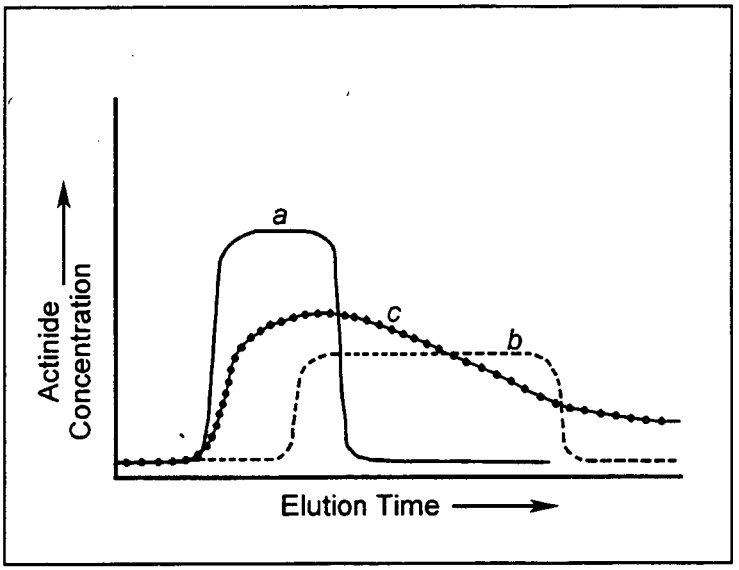

Curves a and b: Predicted curves for a K_d model where $K_d(a) < K_d(b)$.
Curve c: Illustration of a typical experimental curve, showing a slowly diminishing residual concentration of actinide and incomplete desorption, not predicted by K_d models.

In addition to the above limitations, a K_d value is valid for a particular contaminant only under the same conditions of temperature, contaminant concentration, chemical speciation (e.g., oxidation state and kinds and extent of complexation), nature of soil matrix and water solution parameters (e.g., pH, ionic strength, chemical composition and redox potential) at which it was measured. A consequence of this specificity is that environmental K_d values, measured for the same contaminant travelling along two different pathways in the same region of the same site, can differ by orders of magnitude (Little, 1980; Little et al., 1980). This can occur because of differences in flow rate (affecting the attainment of sorption equilibrium), nature of the soil matrix, presence of other ions and the presence of complexing agents.

The restrictive conditions imposed on a K_d value indicate that its application will always be highly Site-specific. Laboratory determinations of K_d almost never satisfactorily replicate the desired field conditions, although they are sometimes useful for identifying some of the

310

important Site-specific environmental variables. The use of empirical K_d values for estimating radionuclide mobility through terrestrial and aquatic pathways is reviewed in *Radioecology after Chernobyl* (Warner and Harrison, 1993). The EPA (1999) has published a thorough examination of limitations on the use of K_d partition coefficients for predicting contaminant mobility in the environment and Bethke and Brady (2000) discuss the failure of K_d models to accurately predict the transport of trace metals in groundwater.

The reality is that modeling contaminant mobility in the subsurface requires some sort of quantifiable parameter that assigns a velocity to contaminant movement. Because K_d lends itself to a convenient calculation of retardation factors for dissolved contaminants (relative to the velocity of the transporting water), K_d values have become an integral part of most contaminant fate and transport models. When used in a transport-modeling program, K_d need only allow a meaningful estimate of dissolved contaminant mobility; the precise theoretical significance of K_d is unnecessary. For example, there are several empirical methods for estimating K_d values where Site-specific values are not available (ANL, 1993), none of which is based on purely sorption/desorption reactions. Such approaches include:

- A groundwater concentration method, based on the elapsed time between contaminant release and measured groundwater concentration at a distant site;
- A solubility limit method, based on the contaminant solubility constant and stability diagrams;
- A leach rate method, based on a sorption/desorption and ion-exchange leaching model; and
- A plant/soil concentration method based on a strong correlation between the plant/soil concentration ratio and the contaminated zone K_d value.

By using any of these approaches, the modeler has abandoned the interpretation of K_d as a measure of only sorption/desorption reactions and accepts an empirical definition that is valuable insofar as it allows useful predictions of Site-specific contaminant mobility. In practice, modelers generally attempt to identify and measure the Site variables that are most important for

influencing the values of K_d and then generate data tables or equations that give values of K_d as a function of these variables.

However, there is little assurance that the variables identified as controlling parameters in a transport model are the ones actually controlling contaminant movement on the Site. The K_d approach is complicated by several factors:

- The spatial heterogeneity of most sites limits the region over which any K_d value is applicable. Most models divide sites into cells within which the important variables are assumed to be constant. Efurd et al. (1993b) emphasized the importance of obtaining measurements of actinide concentration inhomogeneity at RFETS. When they analyzed three, 2 L aliquots of water from a single larger sample taken from pond C-2, they found a 16 % coefficient of variation in the results. Little and coworkers (Little, 1980; Little et al., 1980) reported large variability in Pu activity in soil measured in like samples (same depth and particle size range) at RFETS. They also reported large spatial variability, citing one instance where the Pu concentrations in aliquots taken less than 15 cm apart varied by nearly three orders of magnitude;

- It may be difficult or impossible to measure all the important variables on a fine enough scale to obtain the best results from a simulation model. This often determines the degree of uncertainty in the model's predictions and the extent of field calibrations required;

- The important variables are often different from site to site. Thus, each site must be assessed individually for these parameters;

- The contaminant may be present simultaneously in several chemical and physical forms, which differ in important characteristics, such as oxidation number, nature and degree of complexation, association with colloidal solids, ionic charge, molecular diameter, solubility etc. Thus, different fractions of the contaminant may have different K_d values in the same soil environment; and

312

- As stated earlier, where important transport mechanisms involve movement of solid particulate matter, a transport model altogether different from the K_d approach is necessary, such as water and wind erosion models.

In practice, an environmental K_d should be regarded as an empirical parameter that contains within it a site-specific set of variables, many of which are likely to be unknown. As stated earlier, an environmental K_d used in transport modeling can be regarded as the ratio of immobile to dissolved/mobile forms of a radionuclide in the subsurface, i.e.:

$$K_{d,environmental} = \frac{\text{Concentration of Immobile Radionuclide}}{\text{Concentration of Mobile Radionuclide}}$$

Because the forms of the mobile fraction (dissolved, complexed, colloidal, etc.) are not necessarily known, it cannot be assumed that the retardation of all components of the mobile fraction is the same, relative to the velocity of carrying water fraction. It may be necessary to introduce additional retardation factors.

Every modeling program brings its own set of compromises to fate and transport calculations. As computational ability improves for including more variables on a finer scale, the modeling results become more robust and scientifically defensible. To the extent that uncertainty is present in modeling results, K_ds should be chosen to yield conservative estimates. If a K_d can be confidently shown a maximal or minimal possible value, such calculations can provide bounding or conservative information on Pu transport. The bounding minimum K_d approach has become standard in the modeling of radionuclide transport (Meijer, 1992).

K_d Models

Constant Kd Model

The chief difficulty with a constant K_d as defined by Equation 2.8-2 is that it contains no information concerning which system variables have a significant influence on its value. Consequently, there is no guidance for which variables to control in laboratory measurements or where to anticipate Site-specific variations in value due to different conditions.

313

Where environmental releases have occurred, deliberately or accidentally, site-specific K_ds can sometimes be measured in the field. Enough measurements must be made at different locations to assure that local variability is adequately accounted for in subsequent modeling programs.

Where field data are not available, batch or column laboratory measurements must be made. These typically use soil from the Site and actual or simulated groundwater to which a characteristic concentration of contaminant has been added. Laboratory experiments seldom attempt to duplicate the flow heterogeneity that often exists in the Site environment where soil fractures, animal burrows, root systems, utility lines and construction sites may establish preferred pathways for water flow. In addition, laboratory and field measurements share a common difficulty of obtaining enough samples from varying locations to assure that the Site has been adequately characterized.

The EPA (1999) gives examples of the sensitivity of the constant K_d model to changes in key system variables, where reports by Delegard and Barney (1983), Kaplan and Serne (1995), Kaplan et al. (1998), Sheppard et al. (1976), Thibault et al. (1990) and others are referenced. In laboratory tests, Am K_d values changed by a factor of 200 when aqueous phase chemistry was varied, by a factor of 7 when slightly different sediments were used and by a factor of 350 when similar aqueous phases but diverse soils were used. K_ds for U varied by a factor of 10^6 and for Pu by a factor of 10^4, depending on the experimental conditions.

Parametric K_d Model

An obvious approach for improving the constant K_d model is to introduce important aqueous and solid-phase variables into its definition. Then K_d can vary as a function of empirically derived relationships among the variable parameters. Such a parametric K_d model is more robust and removes the burden of making separate K_d measurements for each environmental condition. It does, however, introduce a new set of requirements; the essential site-specific variables must be identified and their spatial variability determined. A major advantage of the parametric K_d model is that it can be calibrated to the Site by using statistical regression methods to fit certain

314

locations where K_d and values of the variables are known. The resulting empirical K_d equations may be either linear or polynomial expressions.

An example of this approach is given by EPA (1999, Vol. II, Appendix G), where Pu K_d values (ranging between 5 mL/g and 3,130 mL/g) for 17 soil samples from 9 different sites were used, as determined by Glover et al. (1976). The data set was the most extensive available in terms of soil properties. Soil properties measured included conductivity, pH and soluble carbonate in soil extracts, inorganic and organic carbon content, CEC and soil texture (weight, percent of sand, silt and clay). Soil textures varied from clay to fine sand.

This example demonstrates that Site conditions can sometimes be greatly simplified and still yield useful predictions. Although the Glover et al. (1976) data showed that K_ds were affected by several different variables, careful statistical analysis showed that just two soil variables were the most significant for predicting K_d values. These were concentration of dissolved carbonate in soil extracts and the percentage of clay in the soil. It was important to restrict the initial Pu concentration to 2.4×10^{-3} mg/L to avoid complications from the formation of Pu precipitates. Using only these two variable parameters, a two-part linear regression equation for K_d was developed with a coefficient of determination of $R^2 = 0.9730$ (EPA, 1999, Vol. II, Appendix G).

The dependence on carbonate suggests that Pu complexation with carbonate was a dominant process in the Glover et al. (1976) studies. Although carbonate is one of the most common groundwater constituents, it must be remembered that carbonate complexation might be relatively unimportant in systems of low alkalinity. At other sites, complexation with different species might be more important. Sposito (1989) estimated that groundwater could contain 100 to 200 different soluble species, many of which are complexed metals. The most common anions for forming soluble metal complexes in groundwater are HCO_3^-/CO_3^{2-}, Cl^-, SO_4^{2-} and dissolved organic carbon (humic materials), any one of which might be dominant at a given site. The influence on K_ds for Pu and other trace metals of the concentration of dissolved organic matter has been reported by Berry et al. (1991), Choppin (1988, 1992), Moulin et al. (1992) and Lenhart (1997), among others.

)315

The dependence on clay content indicates those sorption sites on constituents of the Glover et al. soils larger than clay sizes were in relatively low abundance. However, in a soil with high organic carbon and low clay content, K_d could depend on the concentration of organic carbon more strongly than clay.

Although pH, ionic strength (electrical conductivity) and redox potential were not the major controlling variables in the Glover et al. (1976) determinations of Pu K_d values, many other researchers have found them to be very important (e.g., Barney, 1992; Billon, 1982; Bondietti et al., 1975; Choppin and Morse, 1987; Nelson et al., 1987; Ticknor, 1993). Thus, the results of the EPA (1999, Vol. II, Appendix G) analysis of the Glover et al. data should not be assumed useful for other sites.

Thermodynamic K_d Model

An elaboration of the parametric approach is to include calculations of interactions among important parameters in the transport model, such as pH, carbonate concentration, redox potential and the presence of competitive complexing agents (Turner et al., 1991). This is similar to the K_d "unfolding" approach of Brendler (1999). When sufficient thermodynamic data are available, this modification allows the use of modeling codes, such as MINTEQA2 (Brendler, 1999; Allison et al., 1991), for predicting radionuclide speciation and solubility under solution conditions that have not been measured directly. For example, a simple parametric model might bracket expected conditions at the Site by measuring K_d values for three or four groundwater compositions. However, by including a procedure for calculating interactions among the important parameters, the model allows the interpolation of K_d values between these bracketing groundwaters as well as extrapolation to other potentially unexpected groundwater compositions.

Isotherm Adsorption K_d Model

A plot of dissolved concentration versus adsorbed concentration for a contaminant, other parameters being held constant, is called an adsorption isotherm. It is often observed that, as dissolved concentration increases, a level is reached where the concentration of adsorbed

contaminant no longer increases in direct proportion to the concentration of dissolved contaminant and the adsorption isotherm becomes nonlinear. Therefore, in the region of nonlinearity, the value of K_d calculated by Equation 2.8-2 decreases as the concentration of dissolved contaminant species increases. It is generally accepted that the most common reason for this behavior is the soil becomes saturated with adsorbate, as the number of available adsorption sites becomes limited relative to the number of dissolved species competing for them (EPA, 1999, Vol. I).

Much effort has been spent on interpreting the shape of adsorption isotherms in terms of adsorption mechanisms (e.g., Dubinin and Radushkevich, 1947; Freundlich, 1926; Giles et al., 1974; Langmuir, 1918; Rai and Zachara, 1984; Salter et al., 1981b; Sposito, 1984). It appears that this might be possible for well-defined and relatively simple systems. However, in a complex system, such as a natural soil/water environment, it is unlikely that the shape of an adsorption isotherm gives any dependable or useful information concerning the mechanism of the adsorption process.

Present subsurface transport models cannot quantitatively incorporate all of the physical-chemical complexity inherent in natural systems. An adsorption isotherm approach bypasses the need for identifying all the variables needed for a parametric K_d approach and, at some sites, an adsorption isotherm model might be more suitable than a K_d model. In general, one should view the shape of an adsorption isotherm only as an empirical result related to the specific site. However, since isotherm equations have one or more empirically derived constants, an empirical adsorption isotherm is easily incorporated into many contaminant transport models. Because adsorption isotherms include one measured variable (contaminant concentration) and one or two empirical constants obtained by calibration at the Site, they represent an improvement over the linear K_d of Equation 2.8-2. In terms of producing robust and scientifically defensible results when used in transport models, adsorption isotherms lie between linear K_ds and parametric K_ds.

The three mathematical forms of adsorption isotherms in common use are the Langmuir (1918), Freundlich (1926) and Dubinin-Radushkevich (1947) models. Sposito (1984) and Salter et al. (1981a, b) cite several instances where the Langmuir isotherm has successfully been fitted to

317

trace adsorption by natural substrates. They describe modifications allowing interactions between two different adsorbates competing for two different kinds of substrate sites. The Freundlich isotherm has been found to fit nonlinear adsorption behavior better than the Langmuir isotherm for many radionuclides (Sposito, 1984). The more recent Dubinin-Radushkevich isotherm was designed for use with adsorption of trace amounts of adsorbates onto heterogeneous substrates containing sites of different attractive strengths. It cannot be used near sorption saturation of the substrate. Ames et al. (1982) used the Dubinin-Radushkevich isotherm to successfully model the adsorption of U onto basalt and its weathering products.

Developing Empirical K_d Values

In a laboratory under controlled experimental conditions, the concentration of a chemical sorbed to a well-defined solid surface, divided by its concentration dissolved in water in contact with the solid, may, under equilibrium conditions, be interpreted as an adsorption partition coefficient, K_d. However, in a natural environmental setting, such as where a chemical is transported by groundwater movement through a soil matrix, a similar measurement must be interpreted less mechanistically because a variety of different processes, both known and unknown, may be at work. An environmental K_d reflects the response of a chemical to all of the variables that affect its interactions with the solid and aqueous phases with which it is in contact. The relative concentrations of the chemical associated with the dissolved and solid states can be influenced by, for example:

- The formation of compounds of low solubility, resulting in precipitation;
- The formation of complexes that increase the number of soluble species;
- The presence of other dissolved chemicals competing for adsorption sites;
- The presence of several different types of surface sites with different attraction potentials;
- Multiple speciation of the dissolved chemical because of pH and/or redox conditions, where each species can have a different K_d value;

- Variability of solid surface charge with changes in pH;
- Association of the chemical with colloidal solids, which may increase or decrease the apparent dissolved concentration, depending on the separation process (filtration or centrifugation);
- The degree to which reaction equilibrium has been attained; and
- The presence of preferred pathways for water flow within the soil matrix. This not only influences the extent of reaction equilibrium attained, it may result in anomalous measured K_d values and retardation factors. Bundt et al. (2000) found that activities of atmospherically deposited radionuclides, including Pu and Am, were enriched in preferential flow paths in the vadose zone by a factor of up to 3.5. Litaor et al. (1994) found evidence that small amounts of radionuclides could move down the soil column through a network of macropores formed by decayed root channels and other biological processes.

It is clear that environmental K_d values can reflect more than only sorption reactions and may be expected to be very Site-specific. The most typical situation is one where there is too little information about the physicochemical conditions and their spatial distribution at the Site to allow complete understanding of the factors influencing a measured K_d value. In this case, K_d is best viewed only as a measured parameter that can be correlated with contaminant movement within a limited region at a given site. At best, the influence on K_d of a few important soil and water variables will have been measured, making the transport model less dependent on a thorough statistical coverage of measured site contaminant mobility.

Runde (2000) notes that the solubility of an actinide species establishes an upper limit to the actinide concentration in solution and may be considered as the first barrier to the transport of dissolved actinides. The sorption of dissolved actinides to surrounding rock and mineral surfaces may be expected to act as a secondary barrier. The K_d parameter serves as an indicator of the effectiveness of this secondary barrier in that it furnishes a convenient method of calculating a retardation factor for dissolved contaminant mobility in the soil subsurface. Dissolved actinides

319

with high values of K_d (>300 mL/g) under specified circumstances show little movement through subsurface soils but have a high potential for resuspension at the soil surface (the movement by water or wind mediated erosion of actinides adsorbed to solids), whereas those with low K_d values (<30 mL/g) show greater movement in subsurface soils and have a lower potential for resuspension. Inclusion of resuspension in modeling is important because higher actinide concentrations are often related to smaller soil particle sizes, leading to a potential for enriching actinides in eroding soil. This potential for enrichment can affect the long-term redistribution of actinides and their relative transport by wind and surface/ground water movement.

Part of the concern over the use of K_d values for transport modeling arises because K_d is often used to indicate an adsorption coefficient, although it also is used as a partition coefficient and/or distribution coefficient. In transport modeling, K_d is most appropriately called a distribution coefficient, describing the distribution of a radionuclide between immobile and mobile forms, without necessarily defining the physicochemical nature of these forms. Perhaps another symbol, such as R_p, as used by Santschi et al. (1999) to define a phase-partitioning coefficient, would be preferable in order to emphasize the empirical meaning of an environmental K_d coefficient. Whatever symbol or model is used, K_d always becomes a summarizing value for the underlying assumptions used to calculate a net retardation factor. Obviously, the modeling results must be thoroughly tested against field data to assure reliability.

In this regard, Davis (2001) suggests that surface complexation modeling of radionuclide adsorption should be given wider recognition in transport and performance assessment modeling. Surface Complexation Modeling offers a more scientifically defensible means of linking the selection of K_d values for performance assessment to existing knowledge and thermodynamic date for radionuclide speciation in aqueous systems.

The conclusion of this K_d discussion is that there can be multiple stages of K_d development, each more detailed with respect to incorporation of additional variables:

- The isotherm K_d model, which determines an empirical graphical relation between dissolved and adsorbed concentrations of a contaminant to a solid substrate. Although the shape of the

320

adsorption isotherm may contain information about the adsorption mechanism, the method is sometimes useful without any mechanistic interpretation at locations where there is little variability across the Site;

- The simple constant adsorption K_d model with no variables (see Equation 2.8-2), which can accurately describe adsorption/desorption behavior for low concentrations of a single dissolved chemical species to a uniform solid surface; and

- The parametric K_d model, which allows adjustment of K_d values to fit Site-specific differences in several variables identified as important by laboratory or field experiments. K_d adjustments can be made by the use of tables that include ranges of variables that bracket site conditions or by including the variables into polynomial equations for calculating K_ds.

The thermodynamic K_d model, which includes calculations, based on thermodynamic data, of how surface interactions (both electrostatic and non-electrostatic) among important parameters (such as pH, carbonate concentration, redox potential and the presence of competitive complexing agents) influence the speciation of contaminants and their transport properties. This approach is the most robust because it allows the interpolation and extrapolation of K_d values beyond the limited number of measured values. However, this approach requires the greatest theoretical and practical understanding of Site conditions.

Use of Empirical K_ds in Chemical Reaction Models

As emphasized in previous sections, K_d values can be very site specific. No tasks related to using K_d values in chemical reaction models are more important than:

- Identifying those contaminants for which the K_d approach is appropriate; and

- Determining what K_ds are appropriate for a given site.

Choices of K_d must be based on Site measurements, good science and computer verification. If literature-derived K_ds are to be used for modeling contaminant transport at a given site, it is

324

important to understand the conditions under which the literature values were obtained and whether or not they are applicable to the site under study.

Even when look-up tables or parametric equations are used to calculate K_ds as a function of controlling variables, the transport modeler must have site-specific evidence that the literature variables are appropriate for the site to be modeled. No single set of variables, such as dissolved carbonate and clay content, are suitable for all sites. Look-up tables and parametric equations typically include only a few variables determined by experiment to be the most important for the study in question. Another site might require that additional variables or even a completely different set of variables, be included for sufficient accuracy.

For example, Multimedia Environmental Contaminant Assessment System (MEPAS) is a human health risks model (Buck et al., 1995) which has been used by Strenge and Peterson (1989) to create a look-up table for U K_ds. MEPAS uses pH and soil texture as the controlling variables. It is shown in EPA (1999) that, by including the additional parameter of oxidation state into the MEPAS variable set, appreciably greater accuracy is obtained for K_d values. The reduced form of U, U(IV), has a much larger apparent K_d than U(VI) at all values of pH, because U(IV) is known to precipitate from solution at the concentrations used.

Summary of Issues and Limitations of the Empirical K_d Approach

First, the empirical K_d approach is not appropriate for contaminants of very low solubility, whose mobility is significantly influenced by processes different from sorption/desorption mechanisms, such as water and wind erosion of soil particulates. For dissolved contaminants, the complexity and spatial heterogeneity of the subsurface soil/water matrix is the cause of important restrictions to the use of empirical K_ds for predicting contaminant mobility. Unfortunately for the transport modeler, the measured value of K_d can be very sensitive to subtle changes in subsurface conditions. For example, a pore water pH change not only affects the chemical speciation of the dissolved contaminant; it can also affect the soil components by altering the magnitude and, possibly, the sign of surface charge, the amount and nature of precipitates, the activity of

microbes and the mobility of colloids. A change in any of these parameters may affect the value of K_d.

As another example (EPA, 1999), small changes in soil properties with depth from the surface can change K_d markedly. At a South Carolina site, a coating of organic matter on surface soils, comprising only 1 % by weight, completely masked the sorption properties of the underlying mineral surfaces (Kaplan et al., 1993) and yielded larger K_ds than expected from the mineral content of the soil. Just below the organic-coated soils, soil particles were coated with iron oxides, creating a region dominated by pH-dependent surface charges.

The sensitivity of K_ds to site conditions imposes a responsibility on the transport modeler to address the issues presented in the following sections.

Limitations of K_d Values From Laboratory Experiments.

Laboratory K_d measurements, whether batch or column type, often are performed on relatively simple systems. Soils may be represented by well-defined phases such as montmorillonite, quartz or goethite. Groundwater may be approximated by a synthesized solution containing, for example, only carbonate, chloride, sodium and calcium. Such simplified experiments are important because they can produce useful information about solute-surface interactions that could not be obtained otherwise. However, it should not be assumed that K_d values from such experiments could be applied to a specific site, even if it is believed that site conditions are similar.

Laboratory K_d experiments generally start with a well-characterized soluble form of a radionuclide and measure how much of this soluble form sorbs to a selected solid matrix. When determining an *in situ* K_d value, the measurement involves determining the amount of radionuclide removed from solution by a combination of all possible mechanisms (sorption, precipitation, etc.). *In situ* radionuclides may be present in several different forms, including relatively insoluble forms such as oxides (e.g., PuO_2). In such a case, the K_d determination is limited by the intrinsic solubility of low solubility material, which for PuO_2 is of the order of 10^{-15} M. Thus, the K_d value determined under such conditions is frequently controlled by the

323

presence of compounds of low solubility and is likely to be very large (i.e., $K_d = 10^4$ to 10^5 L/kg). For these reasons, an *in situ* K_d will often differ substantially from a K_d measured in the laboratory.

For Site-specific calculations from laboratory data, experiments should utilize soils and groundwater from the site (Cleveland et al., 1983). It is important to have an idea of which site parameters have a significant influence on K_d (from simplified experiments) so that the site can be sampled in a representative fashion.

Ideally, on-Site contamination, from either accidental or purposeful releases, can be used to calculate K_ds from measurements of contaminant phase distributions at specific locations. By measuring as many additional chemical and physical properties as practicable, it might be possible to identify the most important site parameters and use them to calibrate the model at other locations.

Spatial Variability at the Site

Measurements of the subsurface soil/water matrix are always made on a limited number of samples. The required sampling density at a site depends on how variable subsurface conditions are across the site. The modeler should seek evidence that the site has been adequately sampled to accurately represent the spatial variability of subsurface conditions.

Soil texture and stratigraphy may be available from well-log data. Where necessary, hydrological and chemical properties sometimes can be deduced from soil texture information (Peterson et al., 1996), but it is better to measure important parameters such as pH, ion-exchange capacity, redox potential and carbonate/bicarbonate concentration at the site. There always is a trade-off between comprehensive data collection and time and costs. Therefore, the effort expended in determining the most important parameters is generally well spent.

Colloid Transport

Colloid transport, as it relates to RFETS, is discussed in more detail in Section 2.7. Since colloids are solids in the form of small particles, they can interact with radionuclides through

324

sorption interactions. Because of their small size, colloidal solids are potentially mobile when present in water flowing through a soil matrix. Radionuclides may become associated with colloids because dissolved species have precipitated as colloidal-sized particles, have sorbed to colloidal solids present in the soil matrix or have been irreversibly bound as an integral part of the colloid structure. Although sorption to the soil matrix always retards the movement of radionuclides, sorption to colloidal solids can either retard or enhance their mobility. If the colloid sorbs to or is filtered by the stationary part of the soil matrix, associated radionuclide mobility will be retarded. If the colloid is carried along freely by water movement, associated radionuclide mobility will be enhanced.

The presence of colloids can also influence the measured value of K_d. Because a determination of K_d requires a measurement of the dissolved and sorbed phases of a chemical, the separation of the sample into aqueous and solid phases is an essential part of the measurement. Separation of aqueous and solid phases is commonly accomplished by filtration and/or centrifugation. Both methods present difficulties:

- With filtration, the filter material may sorb solute species. This can be a significant source of error if the solute of interest is in low concentration. If filtration does not remove all the colloidal material, radionuclides associated with the unfiltered colloids will be measured as part of the dissolved contaminant concentration; and

- With centrifugation, some colloidal material may remain suspended and be counted as part of the liquid.

No matter what method is used for separation, it operationally determines how large a particle must be before it is considered to be dissolved (part of the aqueous phase) and is no longer associated with the solid phase. If initially dissolved contaminants become sorbed to colloid-sized particles that pass through a filter or remain suspended after centrifugation, they will be incorrectly assigned to the dissolved phase, C_w. This will result in a K_d value that is too low if the colloids are less mobile in the environment than dissolved species and too large if the colloids are more mobile. In an early report, Cleveland et al. (1976) dealt with the colloid issue

325

by using the term "solubilization" to mean any dispersal of a solid in water, whether the mechanism be true dissolution, colloid peptization or formation of a fine suspension. These authors state: "Only that concentration (of Pu and Am) filterable through 0.2 micron filters can be present in true solution and a large portion of this fraction is undoubtedly present as smaller colloids." If colloid-enhanced transport of contaminants is an important process, transport models should be adapted to include this mechanism; see, for example, Reible et al. (1991).

TA - 3.8.3 Actinide Empirical K_d Values From the Literature

Uranium Empirical K_d Values

The EPA (1999) concludes that the best way to model the concentration of U is not with the K_d construct but with solubility constants. Nevertheless, they have analyzed a large number of literature K_d values for U for developing a look-up table for modeling input parameters. The following discussion utilizes many of their conclusions.

Effects of pH

Figure TA-3-14 from EPA (1999) shows U K_ds for a wide variety of solution and substrate conditions plotted against pH. Despite the wide scatter in the data (which illustrates the importance of other parameters), certain general trends are evident for all environmental and laboratory conditions:

- K_d (U) is small (<10 mL/g) for pH <3;
- K_d (U) increases rapidly from pH 3 to 5;
- K_d (U) reaches a broad maximum between pH 5 to 8; and
- K_d (U) decreases as pH increases above 8.

This behavior is attributed to the pH-dependent surface charge properties of the substrates and complexation of dissolved U(VI) with carbonates in the range pH >7. The pH maximum occurs where the dominant U aqueous species change from cations to anions as pH increases.

Figure TA-3-14. Uranium literature K_d values versus pH

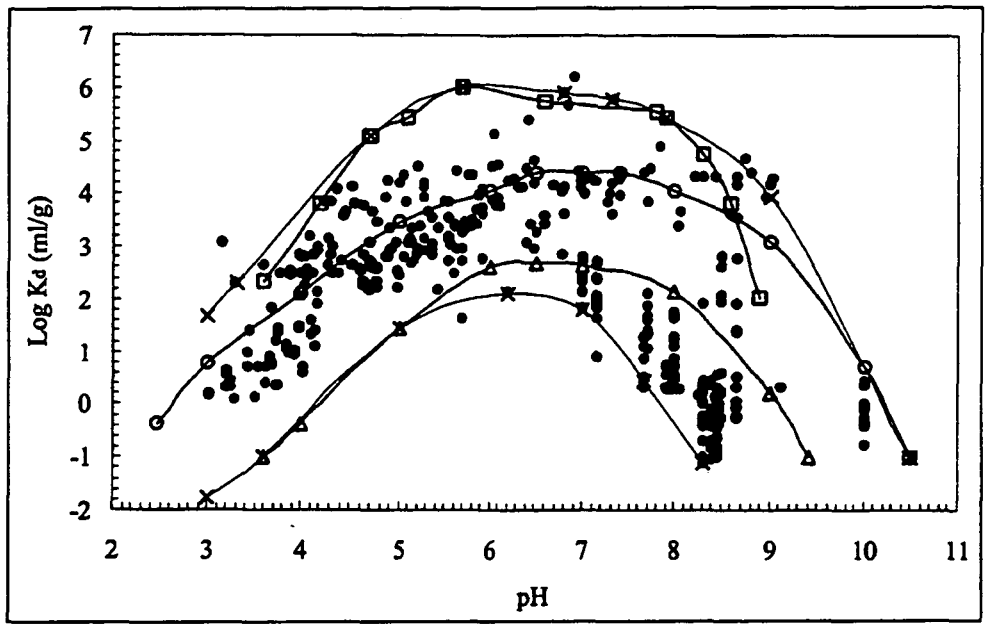

Source: EPA (1999)

Effects of Mineralogy

The data scatter in Figure TA-3-14 shows other parameters besides pH can have an important influence on U K_d values. A part of the scatter is caused by heterogeneity in the soil mineralogy. Soils containing larger percentages of iron oxide minerals and mineral coatings and/or clay minerals exhibit higher sorption characteristics than soils dominated by quartz and feldspar minerals. This variability in U adsorption with respect to mineralogy is evident in U K_d values versus pH calculated from adsorption measurements on ferrihydrite, kaolinite and quartz by Waite et al. (1992). The difference in the maximum and minimum K_d values for these minerals is nearly 3 orders of magnitude at any fixed pH value in the pH range from 3 to 9.5.

Effects of Dissolved Carbonate Species

Many researchers have noted that dissolved carbonate/bicarbonate has a significant effect on the aqueous chemistry and solubility of dissolved U(VI) through the formation of strong anionic carbonate and bicarbonate complexes at alkaline pH conditions. See, for example, Tripathi (1984); Hsi and Langmuir (1985) et al. (1992 1994), McKinley et al. (1995); Duff and Amrheim

327

(1996); and Turner et al. (1996). Figure TA-3-16 (Waite et al., 1994) shows how the dissolved speciation of U(VI) varies with pH, for a solution at 25°C with total U(VI) = 10^{-6} M, (a) in equilibrium with atmospheric carbon dioxide ($pCO_2 = 10^{-3.5}$ atm) and (b) at a typical groundwater concentration for carbon dioxide ($pCO_2 = 10^{-2}$ atm). As with Pu (see Figure TA-3-3), carbonate complexes are predominant above about pH 6, greatly increasing the solubility and mobility of U minerals. Figure TA-3-16 shows that differences in the partial pressure of CO_2 can have a major affect on U speciation.

Figure TA-3-15. Dissolved speciation of U(VI) at a total concentration of 10^{-6} M and ionic strength = 0.1

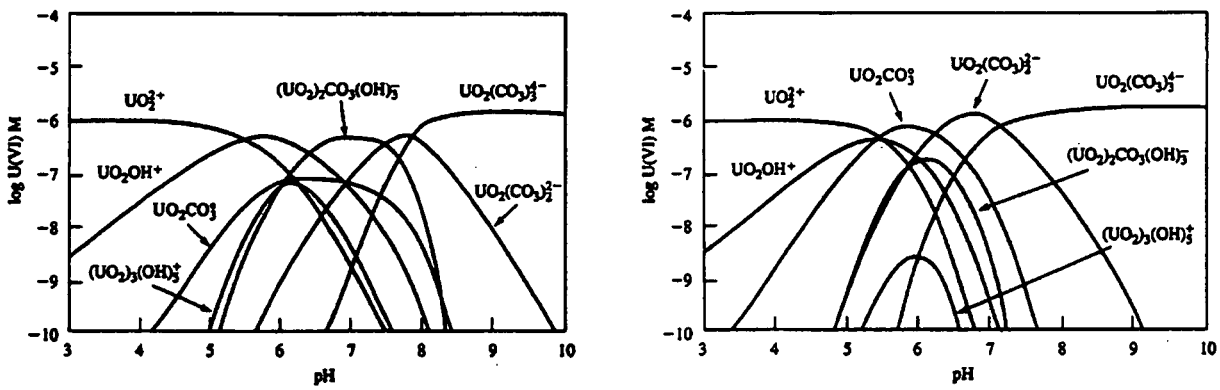

(a) In an open system equilibrated with carbon dioxide at a partial pressure of $10^{-3.5}$ atm.
(b) In a system equilibrated with carbon dioxide at a partial pressure of $10^{-3.5}$ atm, typical of many groundwaters. Calculations were made with the equilibrium speciation computer code HYDRAQL (Papelis et al., 1988). Adapted from Waite et al. (1994).

Waite et al. (1994) show that the percent of U(VI) adsorbed onto ferrihydrite decreases from approximately 97 to 38 % when CO_2 is increased from ambient 0.03 % to an elevated 1 % partial pressure. Soil pore space gases may contain up to 10 % of CO_2 generated by decomposition of organic matter and, therefore, can exert a strong influence on U mobility.

Adsorption studies conducted in a CO_2-free atmosphere (see references above for complex formation) show that, in the absence of dissolved carbonate, U maintains a maximum adsorption with increasing pH above seven. Although carbonate-free systems are not relevant to natural soil/groundwater systems, they are important to understanding the reaction mechanisms affecting

328

the aqueous and adsorption geochemistry of U. It should be expected that the adsorption of U will decrease rapidly, possibly to very low values, at pH values greater than 8 for waters in contact with CO_2 or carbonate minerals. Where complexation of U by carbonates or other species is an important parameter, it might be necessary to include surface complexation modeling techniques into the transport model.

The EPA (1999) describes the use of electrostatic surface complexation models in chemical reaction codes, such as EPA's MINTEQA2, to derive K_d values for some radionuclides as a function of key geochemical parameters, such as pH and carbonate concentrations. The EPA (1999) states that the current state of knowledge regarding surface complexation constants for U adsorption onto important soil minerals, such as iron oxides and development of a mechanistic understanding of these reactions is probably as advanced as for any other trace metal. In the absence of site-specific K_d values for the geochemical conditions of interest, EPA encourages the use of surface complexation models to predict bounding U K_d values and their dependence on important geochemical parameters. Brendler (1999) gives details of a similar approach for including complexation models in the developing of K_d as a summation vector representing multiple parameters.

Effects of Clay Content and CEC

Studies on the effects of clay concentration and CEC on U K_ds are limited. Serkiz and Johnson (1994) found no correlation between their *in-situ* U K_d values and the clay content or CEC of their soils over a pH range from 3 to 7. However, others (Chisholm-Brause, 1994; Morris et al., 1994; McKinley et al., 1995; Turner et al., 1996), found that U adsorption to clay minerals is complicated and involves multiple binding sites, including exchange and edge-coordination sites. Kovalevski (1967) observed that the U content of western Siberian non-cultivated soils increased with their clay content and that clay soils contained at least 3 times more U than sands.

Literature Values for Uranium Empirical K_ds

Empirical K_d values for U at non-RFETS locations, obtained from a review of available literature, are presented in Table TA-3-3. Empirical K_d values for U at the Site, obtained from a review of available reports and literature, are presented in Table TA-3-4.

Summary of Uranium Empirical K_d Values

Table TA-3-4 includes the only reported values, found so far, for U empirical K_ds specific to RFETS. The values range from essentially 0 – 1000 mL/g. These values are certainly within the range of K_ds reported for U world-wide.

Initial U movement from any source at RFETS is mostly vertical through the subsurface toward the groundwater; wind and surface runoff transport of U are minor pathways (Litaor, 1995). Soil levels of U drop rapidly from higher-than-background near the primary sources at the 903 Pad, to background range only a few hundred meters downgradient (Litaor, 1995). Litaor also notes that U mobility is greatly retarded below the *A* soil horizon, where high clay content greatly reduces hydraulic conductivity. Seed et al. (1971) found hot spots below the asphalt cap placed over the former storage area from which they retrieved >31 kg of U, showing that U will concentrate at zones of lower hydraulic conductivity. Anthropogenic U that eventually reaches the groundwater will join any background U that might be present and move with groundwater flow, with possible retardation. Some groundwater returns to the surface east of the Industrial Area and contributes to the treatment pond system, thereby introducing U to those surface water bodies.

Data from an elaborate system of monitoring wells were used to determine the distribution of U at RFETS (RMRS, 1998b). All but one well contained U below established background levels. An exceedance of background level was defined as more than two standard deviations above the mean background established for that location. One well, 07391, at Ryan's Pit near the 903 Pad showed an increasing trend in U concentration during 1998, culminating in a measurement exceeding the background criterion. The causes of this anomaly are being studied.

From the above studies, it appears that the only observed significant RFETS contribution to U in groundwater is in the immediate vicinity of the primary sources. This contrasts with Pu and Am, where wind and stormwater transport have established a region of secondary contaminant sources east of the Industrial Area.

At the time of this report, the source terms for U are not as well identified as those for Pu. When the distribution of natural and anthropogenic U at RFETS is better defined, it seems possible that data concerning the historical distribution of natural U might be useful predicting the movement of anthropogenic U, since U from RFETS sources will be subject to similar conditions of geochemistry and dispersal mechanisms as background U.

An important influence on both natural and anthropogenic U movement introduced by RFETS activities are associated with potential concentration of U isotopes, as in the treatment pond sediments. Some groundwater U background levels already exceed state drinking water standards (Moody and Morse, 1992) and a large portion of groundwater at RFETS feeds into the surface treatment pond system. Data described in Chapters TA-2 and TA-3 show that, unlike Pu and Am, U is not significantly retained in the pond sediments. Thus, pond discharge water may introduce U into surface waters that otherwise might have remained in groundwater.

Table TA-3-3. Empirical K_d Values for Uranium at Non-RFETS Locations

Reference	Location/ Substrate	K_d Range (mL/g)	Controlled Variables	Notes
Erickson, 1980	Iron-rich abyssal red clay	200 at pH=2.8 7.9×10^5 at pH=7.1	pH	
Giblin, 1980	Kaolinite	$211 - 3.8 \times 10^4$	pH	K_d was <1,000 at pH < 4.8, rose to ~3.8×10^4 between pH 4.8 and 6.9 and then decreased to 1.4×10^4 at pH 9.9.
Borovec, 1981	Kaolinite, illite and montmorillonite	50–1,000	U conc., substrate minerals	K_d increases with decreasing U conc. K_d(kaolinite) < K_d(illite) < K_d(montmorillonite).
Salter et al., 1981	Columbia R. basalts	0.4–2.8 at pH 10 2.2–16 at pH 8 23°C and oxidizing conditions	T, P, solution composition, redox pot.	Hanford groundwater. Batch studies at 23 and 60°C under oxidizing and reducing conditions.
Andersson et al., 1982	Igneous rocks and related single mineral phases	$2–6.5 \times 10^4$	pH, substrate minerals	On quartz, K_d increased from ~2 at pH 3.5 to ~1.5×10^4 at pH 9. On biotite, K_d increased from ~27 at pH 3.4 to ~1.7×10^4 at pH 7.3, then fell to ~ 8×10^3 at pH 9. On apatite, K_d increased from ~200 at pH 3.3 to ~1.4×10^5 at pH 6. On attapulgite, K_d increased from ~460 at pH 3.6 to ~6.5×10^5 at pH 7.3, then fell to ~ 4.6×10^4 at pH 8.7. On montmorillonite, K_d increased from ~1.2×10^3 at pH 3.2 to ~2×10^4 at pH 9.
Ames et al., 1982	Columbia R. basalts	0.19–127 pH = 7.65–8.48 CEC = 1.5–4.8 meq/100g (one sample at 72 meq/100g)	U conc., T, pH, CEC, basalt source, surface area, contact time	Synthetic groundwaters to simulate Hanford site groundwater.
Ames et al., 1983a,b	Silicate minerals	0.6–3,500 pH = 7–8.65 CEC = 0.95–140.2 meq/100g	U conc., T, substrate type, surface area, solution composition, contact time	Batch experiments under oxidizing conditions.

332

Table TA-3-3. Empirical K_d Values for Uranium at Non-RFETS Locations (continued)

Reference	Location/ Substrate	K_d Range (mL/g)	Controlled Variables	Notes
Ames et al., 1983c	Amorphous ferric hydroxide	$0.4x10^4$–$3x10^4$ in 0.01 M $NaHCO_3$ $0.5x10^6$–$2x10^6$ in 0.01 M NaCl	U conc., T, pH, solution composition	Batch experiments under oxidizing conditions. K_d values reflect high adsorptive capacity of ferric hydroxides.
Bell and Bates, 1988	Glacial till clay, sand, low sorptive coarse deposits	46–2,200	pH, T, solution composition, contact time	Used Site borehole water. For low sorptive soils, K_d doubled when T increased 5°C. K_ds showed maxima near pH 6 and 10 for sand and clays.
Baes and Sharp, 1983	Characteristic agricultural soils	10.5–4,400	Based on lit. review	pH range 4.5–9. Suggested a default K_d = 45 mL/g for agricultural soils based on literature review.
Looney et al., 1987	Characteristic of waste sites at Savannah River Plant, SC	0.1 - 10^6	Based on lit. review	Give a recommended value of K_d = 39.8 mL/g that is specific for Savannah River Plant Site. See later work by Serkiz and Johnson (1994).
Sheppard and Thibault, 1988	3 peat soils typical of Canadian Precambrian Shield	700–18,600	Soil type	In situ and batch analyses. Reducing conditions. K_d did not vary with porewater concentration.
Thibault et al., 1990	Wide range of soils; see notes	0.03–2,200: sand 0.2–4,500: loam 46–$4x10^5$: clay 33–7,350: organic	Soil type	Compilation of K_ds from other sources for soils appropriate for assessing a Canadian geologic repository for spent nuclear fuel.
Erikson et al., 1993	Soil from Aberdeen (silt loam) and Yuma (sandy loam) Proving Grounds	328–4,360: Aberdeen soil 44–54: Yuma soil	pH	Low K_d for Yuma soil attributed to carbonate complexation.
McKinley and Scholtis, 1993	Wide range of substrates, both freshwater and marine; see notes	0.02–5,000 (clays, fresh and marine sediments) 4–5,000 (crystalline rocks) 20–1,700 (soils)	Sorbing material	Reviewed international databases for data appropriate for nuclear waste repositories.
Serne et al., 1993	Sediments from Hanford site	1.7–79.3	CEC, soil type	Used Hanford groundwater, pH = 8.3.
Warneke et al., 1986 Warneke and Hild, 1988	Former Konrad iron ore mine	2.6 – 20	Fresh and saline waters	

333

Table TA-3-3. Empirical K_d Values for Uranium at Non-RFETS Location (continued)

Reference	Location/ Substrate	K_d Range (mL/g)	Controlled Variables	Notes
Warneke et al., 1984,1986,1994; Warneke and Hild 1988	Gorleben Salt Dome sand	0.3–1,400	Fresh and saline waters, soil type	pH varied from 6 to 9.
Zachara et al., 1992	Clay-mineral separates from 3 DOA sites	176–43,700	pH, soil type, ionic strength, carbonate complexation	Glovebox with CO_2-free atmosphere, used to eliminate effects from complexation of U(VI) by dissolved carbonate.
Serkiz and Johnson, 1994 and Johnson et al., 1994	Soils from Savannah River site, SC	$1.2–3.4 \times 10^3$ pH 3–6.7	pH	Field derived K_d values. K_d increases from ~1.2 at pH pH 3 to a maximum of ~3.4×10^3 at pH 5.2.
Lindemeier et al., 1995	<2-mm sediments from Trench 8 at Hanford	0.5–2.7	Degree of column saturation	CEC = 5.2 meq/100g, 87 % sand, 7 % silt, 6 % clay. Groundwater from Site. K_d decreased with less column saturation, from ~2 at 100 % saturation to 0.6 at 29 % saturation.
Kaplan and Serne, 1995	Loamy sand from Trench 8 at Hanford	0.08–2.8: pH 8.3	pH	Unsaturated column tests, neutral to high pH, low organic carbon, low ionic strength.
Kaplan et al., 1996	Four different Hanford soils	0.1–3.5	pH, ionic strength, soil moisture, contact time, U conc., soil type	U(VI) K_ds increased with increased contact time and with pH between 8 and 10. Ppt occurred above pH 10. K_d increased with moisture content for coarse grained soils, but decreased for fine grained soils; attributed to changes in tortuousity and effective porosity. K_d was constant for U(VI) concentrations between 3.3–100 µg/L.
Kaplan et al., 1998	Carbonate-containing sediment from Hanford site	1.07–2.12 For pH = 8.17–9.31 (higher apparent K_ds, >400 mL/g, accompanied ppt above pH=10.3)	pH, ionic strength, U conc., soil type	U(VI) adsorption was constant for U conc. between 3.3–100 µg/L and ionic strengths up to 14 mM $NaClO_4$. Ppt. of U(VI) occurred at pH>10.3 (only if sediment present; possibly co-ppt with $CaCO_3$), yielding apparent K_ds > 400 mL/g.

Table TA-3-4. Empirical K_d Values for Uranium at RFETS

Reference	Location/ Substrate	K_d Range (mL/g)	Controlled Variables	Notes
DOE, 1996	OU3	$0–4.4x10^3$		Representative value of $K_d = 1.55x10^3$ for U-234.
Honeyman and Santschi, 1997	903 Pad core isolates	30-170	Soil content, depth below surface redox state [U(VI)].	K_d decreased with depth below surface, probably because of decrease in sand/clay ratio.

335

Plutonium Empirical K_d Values

A 1990 literature review of Pu K_d values (Thibault et al., 1990) shows a range over 4 orders of magnitude, a result that illustrates the importance of:

- Determining whether the K_d approach is even appropriate for modeling Pu at a given site; and
- Identifying the site-specific parameters that have a significant influence on K_d.

The EPA (1999) has summarized a number of parameters that are known to influence the sorption behavior of Pu:

- Because Pu in nature can exist in multiple oxidation states (III, IV, V and VI), the soil redox potential will influence the Pu redox state and its adsorption to soils. K_d data from studies where the oxidation state of Pu in solution was not determined or controlled cannot, in general, be applied to other investigations;
- In natural systems with organic carbon concentrations exceeding about 10 mg/kg, Pu exists mainly in trivalent and tetravalent redox states. If initial Pu concentrations exceed about 10^{-7} M, the measured K_d values reflect mainly precipitation reactions and not sorption reactions;
- Sorption data show that the presence of ligands influences Pu sorption onto soils. Increasing the concentration of ligands decreases Pu sorption;
- If no complexing ligands are present, Pu sorption increases with increasing pH (between 5.5 and 9.0); and
- Pu is known to sorb to soil components such as aluminum and iron oxides, hydroxides, oxyhydroxides and clay minerals. However, the relationship between the amounts of these components in soils and the measured sorption of Pu has not been quantified.

Studies conducted by Nelson et al. (1987) and Choppin and Morse (1987) indicate that the oxidation state of dissolved Pu under natural conditions can depend on the colloidal organic

336

carbon content in the system. Additionally, Nelson et al. (1987) also showed that Pu precipitation occurred if the solution concentration exceeded 10^{-7} M. The importance of the Pu redox status on adsorption was demonstrated in early studies by Bondietti et al. (1975) who reported about 2 orders of magnitude difference in K_d values between hexavalent (250 mL/g) and tetravalent (21,000 mL/g) Pu species sorbing to montmorillonite.

Bondietti et al. (1975) also demonstrated that natural dissolved organic matter (fulvic acid) reduces Pu from a hexavalent to a tetravalent state, thus potentially affecting Pu adsorption in natural systems. Still earlier adsorption experiments also demonstrated that complexation of Pu by various ligands significantly influences its adsorption behavior. Increasing concentrations of acetate (Rhodes, 1957) and oxalate (Bensen, 1960) ligands resulted in decreasing adsorption of Pu. Sorption experiments conducted more recently (Sanchez et al., 1985) indicate that increasing concentrations of carbonate ligand also depress the Pu sorption on various mineral surfaces.

Literature Values for Plutonium Empirical K_d Values

Empirical K_d values for Pu at non-RFETS locations, obtained from a review of available literature, are presented in Table TA-3-5. Empirical K_d values for Pu at the Site, obtained from a review of available reports and literature, are presented in Table TA-3-6.

Summary of Plutonium Empirical K_d Values

Table TA-3-6 lists reported values for empirical Pu K_ds measured at RFETS. Data related to soil, wells and seeps from around the 903 Pad area indicate a range for K_d of about 10^4 to $3x10^5$ mL/g. K_ds from pond sediments, pond discharges, storm runoff and OU3 are more variable but are mainly grouped in the same range. Pu K_d values measured at RFETS lie well within the range of world-wide K_ds presented in Table TA-3-5 and are more narrowly distributed, reflecting a more restricted range of significant environmental variables.

K_ds greater than 10^3 mL/g indicate immobilized Pu and support the conclusion that subsurface transport from the 903 Pad area and other RFETS locations should be a negligible pathway for actinide transport. Recent measurements by Litaor and Ibrahim (1996), Neu et al. (1999) and

337

Runde et al. (2000) support many earlier studies indicating that Pu at RFETS is almost entirely present as PuO_2, generally accepted to be immobile in the subsurface except for potential colloid-facilitated movement.

The studies at RFETS to the date of this report suggest that a conservative empirical K_d for Pu at RFETS would lie in the 10^4 to 10^5 mL/g range. However, since these same studies indicate that Pu movement occurs by water and wind erosion mechanisms and is not influenced significantly by mechanisms involving sorption of dissolved species, K_d is not an appropriate parameter for use in transport modeling.

Table TA-3-5. Empirical K_d Values for Plutonium-239/240 at Non-RFETS Locations

Reference	Location/ Substrate	K_d Range (mL/g)	Controlled Variables	Notes
Dahlman et al., 1976	Miami silt loam clay	$3x10^5$: Pu(IV)	Oxid. State	Pu(VI) was reduced to Pu(IV) on sorption.
Rodgers, 1976	Clay and silt fractions from DOE's Mound Facility, Ohio	$50–1.7x10^5$	PH	Soil was glacial till. Highest K_d at pH = 5 to 6.
Glover et al., 1976	Soils from 9 sites in USA, including 7 DOE sites.	$35–1.4x10^4$ (Using only lower Pu concentration of $2.4x10^{-3}$ mg/L to limit precipitation, range was $5–3.1x10^3$.)	pH, pore water properties, soil texture	Properties measured were: conductivity, pH and soluble carbonate in soil extracts, inorganic and organic carbon content, CEC and soil texture (wt. % of sand, silt and clay). Soil textures varied from clay to fine sand. Most significant soil variables for predicting K_d values were concentration of dissolved carbonate in soil extracts, clay and sand content and CEC. EPA (1999, Vol. II, Appendix G) used concentration of dissolved carbonate in soil extracts and % clay as the 2 most important variables to develop a parametric K_d equation with R^2 = 0.9730.
Relyea and Brown, 1978	Sand (Fuquay from SC), loamy sand (Burbank from WA), silt loam (Muscatine from IL)	316 (sand), $6x10^4$ (loamy sand), $8x10^4$ (silt loam)	EDTA, DTPA, oxid. state	With chelating agent EDTA at 10^{-3} M: 120 (sand), 94.5 (loamy sand), 338 (silt loam) With chelating agent DTPA at 10^{-3} M: 0.12 (sand), 1.06 (loamy sand), 0.24 (silt loam)
Nelson and Lovett, 1978	Irish Sea sediments	$3.4x10^5–6x10^6$: Pu(III + IV) $6x10^3–2.8x10^4$: Pu(V + VI)	Oxid. state	Pu on sediments was in reduced state. Pu in interstitial water was mostly reduced.
Nelson et al., 1987	Lake and oceanic particulates	$3x10^3–4x10^5$: lake sediments $1x10^5–4x10^5$: ocean sediments	TDS, colloidal org. carbon, oxid. state	In sea water, Pu oxidized states (V, VI) have $K_d \sim 2.5x10^3$; reduced states (III, IV) have $K_d \sim 2.8x10^6$. K_d fell from around 10^5-10^6 at 0.1 mg/L colloidal organic carbon to around 10^3-10^4 at 100 mg/L colloidal organic carbon.

Table TA-3-5. Empirical K_d Values for Plutonium-239/240 at Non-RFETS Locations (continued)

Reference	Location/ Substrate	K_d Range (mL/g)	Controlled Variables	Notes
Edgington, 1981	Freshwater and marine sites around the world	$0.6x10^4$–$60x10^4$		In situ measurements. K_ds within 1 to 2 orders of magnitude over a wide geographical range.
Nelson et al., 1987	Lake and oceanic particulates	$3x10^3$–$4x10^5$: lake sediments $1x10^5$– $4x10^5$: ocean sediments	TDS, colloidal org. carbon, oxid. state	In sea water, Pu oxidized states (V, VI) have $K_d \sim 2.5x10^3$; reduced states (III, IV) have $K_d \sim 2.8x10^6$. K_d fell from around 10^5-10^6 at 0.1 mg/L colloidal organic carbon to around 10^3-10^4 at 100 mg/L colloidal organic carbon.
Edgington, 1981	Freshwater and marine sites around the world	$0.6x10^4$–$60x10^4$		In situ measurements. K_ds within 1 to 2 orders of magnitude over a wide geographical range.
Billon, 1982	Bentonite, attapulgite	$3.2x10^4$–$32x10^4$ for Pu(IV) 100–$6.3x10^4$ for Pu(VI)	pH = 3.1–7.5, oxid. state	High initial conc. of Pu ($1.7x10^{-6}$ to $4x10^{-6}$ M) of Pu(IV) makes precipitation likely, causing high K_d values. Precipitation occurs for [Pu] > 10^{-7} M.
Barney, 1984	Basalt from Hanford site	~500	---	Low value may be from high carbonate (215 mg/L) in water.
Barney, 1992	Shallow sediment from Hanford site	$2.1x10^3$–$11.6x10^3$: Pu(IV) $2.7x10^3$–$4.6x10^3$: Pu(V) $1x10^3$–$4.6x10^3$: Pu(VI)	Oxid. state	Pu(V) and Pu(VI) reduced to Pu(IV) when sorbed.
Bell and Bates, 1988	Clay to sand range from Sellafield and Driggs sites, England	32–$7.6x10^3$	pH, soil texture	Maximum sorption at pH ~ 6.
Penrose et al., 1990	Soil from Mortandand Canyon, Los Alamos and Lake Michigan	$2x10^4$–$2x10^6$	DOC	Experiments indicated that Pu was irreversibly associated with colloids. Decrease in K_d with distance from sources suggests that colloids mobile in the subsurface were gradually filtered out. Evidence for this is not conclusive.

340

Table TA-3-5. Empirical K_d Values for Plutonium-239/240 at Non-RFETS Locations (continued)

Reference	Location/ Substrate	K_d Range (mL/g)	Controlled Variables	Notes
IAEA, 1991	Agricultural soils	5.5×10^2 (sand); 1.2×10^3 (loam) 4.9×10^3 (clay); 1.8×10^3 (org. soil)		Selected representative K_d values.
Ticknor, 1993	Goethite, hematite	0.17×10^3–1.4×10^3	High TDS, low HCO_3^-	pH = 7.5
Hursthouse and Livens, 1993	Soil and interstitial water	1.9×10^5–9.0×10^5		
Fisher et al., 1999	Surface sediments in Arctic waters N of Russia	8×10^4–1.5×10^5		In situ. Values are about the same as for temperate seawaters.

Table TA-3-6. Empirical K_d Values for Plutonium-239/240 at RFETS

Reference	Location/ Substrate	K_d Range (mL/g)	Controlled Variables	Notes
Jakubic, 1976	Partially saturated loamy soil	$5x10^3$		pH = 6
Cleveland et al., 1976	Pond sediments	$0.36x10^5$ - $2.4x10^5$ pH 6 - 8	pH, equil. time	Samples not filtered, but centrifuged. Thus, K_ds includes suspended sediments with the aqueous phase and represents lower bounds.
Harnish et al., 1996	Water from Well 1587 and seeps SW51 and SWSW53 at 903 Pad area	$8.2x10^5$–$1.9x10^3$ (Calc. by Chromec 1999 from Harnish data.)	suspended sediment	65 % of Pu in aqueous phase was colloidal. Filtered at 0.45 μm and 10,000 daltons; high K_ds are for 10,000 daltons filtrate due to removal of colloids. Data seems to be at upper bound for empirical K_ds for groundwater.
DOE, 1996	OU3	0.4–$8.7x10^6$		Representative value of $K_d = 4.5x10^3$.
Litaor et al., 1998	Soil pits E of 903 Pad at 0-20 cm	$2.1x10^5$ - $3.1x10^5$		In situ.
Honeyman, 1997	Surface soil from 903 Pad area	$9.8x10^3$–$1.4x10^5$	Pu conc.	0.45 μm filtrate
Honeyman, 1998	Surface soil from 903 Pad area	$2.2x10^4$–$4.3x10^4$		Extracted with KNO_3 to determine "exchangeable" Pu; 0.45 μm filtrate; K_ds are lower bound because of high ionic strength of extracting solution.
Honeyman, 1999	Surface soil from 903 Pad area	$5.0x10^4$–$2.8x10^4$	E_h	E_h varied between +800 mV and –90 mV; K_ds higher at lower E_H.
Santschi et al., 1999	Pond Discharge (Walnut Creek)	$1.7x10^4$ (R_p)		Used phase partitioning coefficient, R_p, instead of K_d, because of colloid separation. $R_p = \frac{\text{activity concentration in particles} \geq 0.5\ \mu\text{m}}{\text{activity concentration in phases passing a } 0.5\ \mu\text{m filter}}$ Measured colloid fraction.
Santschi et al., 1999	Storm Runoff (GS10)	$4.1x10^3$ (R_p)		Ditto

Americium Empirical K_d Values

Literature Values for Americium Empirical K_ds

Empirical K_d values for Am at non-RFETS locations, obtained from a review of available literature, are presented in Table TA-3-7. Empirical K_d values for Am at the Site, obtained from a review of available reports and literature, are presented in Table TA-3-8.

Summary of Americium Empirical K_d values.

Table TA-3-8 includes all the reported values found so far for empirical Am K_ds measured at RFETS. The K_d values are generally similar to that for Pu, but extend to lower and higher values. Because the data set is small, the significance of high and low extremes is unknown.

The studies at RFETS to the date of this report suggest that a conservative empirical K_d for Am at RFETS would lie in the 10^2 to 10^3 mL/g range. As with Pu, these same studies indicate that Am movement occurs by water and wind erosion mechanisms and is not influenced significantly by mechanisms involving sorption of dissolved species. Therefore, K_d is not an appropriate parameter for use in Am transport modeling.

Table TA-3-7. Empirical K_d Values for Am-241 at Non-RFETS Locations

Reference	Location/ Substrate	K_d Range (mL/g)	Controlled Variables	Notes
Routson et al. 1975	Eastern Washington	$> 1.2 \times 10^3$	Ca, Na	*Not affected by cation concentrations.*
Glover et al. 1976	Soils from 9 RCRA sites in USA	$82–1.0 \times 10^4$	pH, pore water properties, soil texture	Properties measured were: conductivity, pH and soluble carbonate in soil extracts, inorganic and organic carbon content, CEC and soil texture (wt. % of sand, silt and clay). Soil textures varied from clay to fine sand. Most significant soil variables for predicting K_d values were concentration of dissolved carbonate in soil extracts, clay and sand content and CEC.
Penrose et al. 1990	Soil from Mortandand Canyon, Los Alamos and Lake Michigan	$\sim 10^2$–$\sim 10^4$	DOC	Experiments indicated that Am was irreversibly associated with colloids. Decrease in K_d with distance from sources suggests that mobile colloids were gradually filtered out.
IAEA 1991	Agricultural soils	2.0×10^2 (sand); 9.9×10^3 (loam); 8.1×10^3 (clay); 1.1×10^5 (org. soil)		Selected representative K_d values.
Hursthouse and Livens 1993	Soil and interstitial water	11×10^5–39×10^5		
Fisher et al. 1999	Surface sediments in Arctic waters north of Russia	1.4×10^6–3×10^6		*In situ.* Values are about the same as for temperate sea waters.

Table TA-3-8. Empirical K_d Values for Am-241 at RFETS

Reference	Location/ Substrate	K_d Range (mL/g)	Controlled Variables	Notes
Cleveland et al. 1976	Pond sediments	0.21×10^5 - 2.0×10^5 pH 6 - 8	pH, equil. time	Samples not filtered but centrifuged. Thus, K_ds includes suspended sediments with the aqueous phase and represents lower bounds.
DOE 1996	OU3	0–4.7×10^4	---	Representative value of K_d = 700.
Litaor et al. 1998	Soil pits E of 903 Pad at 0-20 cm	1.4×10^5–3.0×10^5	---	In situ.
Honeyman 1999	Surface soil from 903 Pad area	2.3×10^4–1.5×10^8	E_h	E_h varied between +800 mV and –90 mV; no correlation of K_ds with E_h because Am(III) was the only state present.
Santschi et al. 1999	Pond Discharge (Walnut Creek)	7.9×10^3 (R_p)	---	Used phase partitioning coefficient, R_p, instead of K_d, because of colloid separation. Measured colloid fraction. $R_p = \frac{\text{activity concentration in particles} \geq 0.5\ \mu\text{m}}{\text{activity concentration in phases passing a } 0.5\ \mu\text{m filter}}$
Santschi et al. 1999	Storm Runoff (GS10)	7.9×10^3 (R_p)	---	Ditto

TA - 3.8.4 Recommendation on the Use of Empirical K_d values at RFETS.

Uranium

The data compiled from the literature and from the AME studies are consistent with our expectations of U chemical behavior in the RFETS environment. The data indicate that U from both natural and anthropogenic sources can form soluble complexes and move in the RFETS environment. Therefore, U has a significant probability of aqueous dissolved transport and dissolved species transport calculations that employ a K_d approach may be useful for risk assessment of U contamination at the Site. A thorough understanding of the U geochemistry, the U source-term and the overall water balance at the Site are of great importance with respect to such U transport calculations. In view of the relatively high natural background of U, it seems likely data concerning the historical distribution of natural U at RFETS might be useful for predicting the movement of anthropogenic U, since U from RFETS sources will be subject to similar conditions of geochemistry and dispersal mechanisms as background U.

For U therefore, both the application of K_d models for risk assessment and the application of more sophisticated geochemical models are useful and scientifically defensible. The U K_d data for the Site are extremely limited and span a range from 30 to 1000 mL/g. Recognizing that the bounding minimum K_d approach has become standard in the modeling of radionuclide transport (Meijer 1992), this range of K_d values seems to be a conservative range in the absence of more definitive Site-specific date.

Plutonium and Americium

The data compiled from the literature and from the AME studies are consistent with our expectations of Pu and Am chemical behavior in the environment. The data indicate that Pu and Am in RFETS surface waters have extremely low concentrations, in the femtomolar (10^{-15} M) range, similar to global fallout. Site-specific studies at RFETS indicate that reducing conditions do not remobilize Pu or Am and that the bulk of Pu and Am is associated with small (<2 μm) colloidal particles that readily settle in pond water. Moreover, the Pu/Am ratio remains

relatively constant throughout the Site, indicating that these two elements have not segregated as a result of chemical reactions. These results are consistent with the known chemical behavior of Pu(IV) and Am(III). Extended X-ray Absorption Fine Structure (EXAFS) studies show unambiguously that Pu in soils taken from the 903 Pad is in oxidation state IV, in the chemical form (speciation) of insoluble PuO_2. The identification of Pu(IV) in the chemical form of PuO_2 is consistent with the observed insolubility of Pu in RFETS surface waters. Furthermore, the data clearly indicate that physical (particulate and/or colloid) transport is the dominant mechanism for Pu and Am migration at RFETS. The observed environmental behavior of Pu and Am at RFETS, coupled with an understanding of the boundary conditions under which a K_d value may be applied, clearly indicates that transport models based on the K_d approach (which assumes dissolved Pu and Am species) are inappropriate and not scientifically defensible. Therefore, no K_d value for either Pu or Am is recommended. Instead, it is recommended that Pu and Am environmental behavior at RFETS be modeled using a particulate or colloid transport approach.

TA-3.9 BIOGEOCHEMISTRY

TA - 3.9.1 Microbial Effects on Actinide Transport in the Environment

In general, actinides will participate in sorption/desorption reactions with the minerals on the surface of the matrix; and microorganisms can affect this interaction several ways, as can be seen in Figure TA-3-16.

Figure TA-3-16. Radionuclide Transport: Interactions with Microorganisms

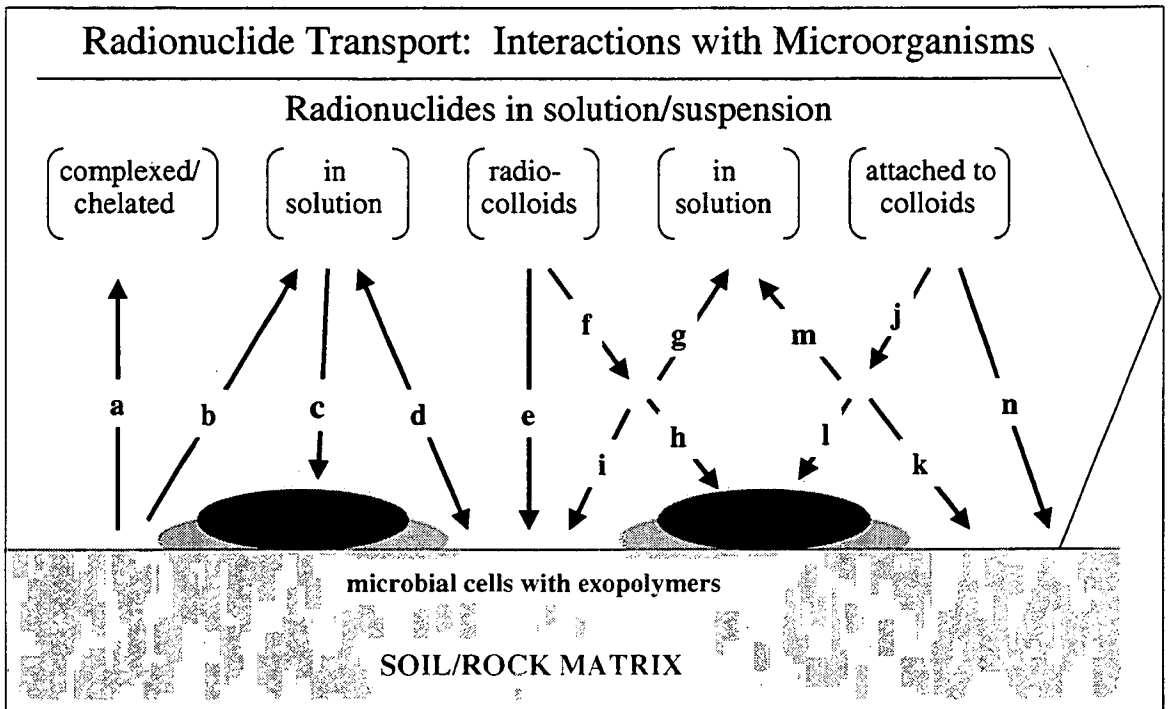

Interactions between radionuclides in solution/suspension and indigenous microorganisms, where: (a) adsorbed radionuclides are complexed/chelated; (b) dissolution occurs; (c) radionuclides are sorbed by microorganisms; (d) various redox reactions result in solubilization or precipitation; (e and n) agglomeration of colloids; dissolution of (f) radiocolloids or (j) radionuclides attached to colloids, leading to (g and m) solubilization, (h and l) sorption, or (i and k) adsorption/precipitation.

It is important to stress that some or all of these processes are occurring currently at RFETS, as is true at all actinide contaminated locations. Suffice to say, microorganisms and actinides, present in the same environment, will interact. Briefly then, the categories in Figure TA-3-16 are discussed in the following section.

348

Complexation/chelation (a). A very important interaction between soluble radionuclides and microorganisms is complexation/chelation. A radionuclide complexed or chelated to an organic ligand would not participate in sorption/desorption reactions as readily as an uncomplexed metal and would, therefore, have a higher transport rate. Microorganisms produce a myriad of extracellular compounds, containing a variety of functional groups that complex strongly with metals (Table TA-3-9).

Table TA-3-9. Functional Groups and Complexing Compounds Produced by Microorganisms

(Adapted from Birch and Bachofen, 1990)

Functional Groups	
Basic	**Acidic**
$-NH_2$ (amino)	$-CO_2H$ (carboxylic)
=NH (imino)	$-SO_3H$ (sulphonic)
-N= (tert. Acyclic or Heterocyclic nitrogen)	$-PO(OH)_2$ (phosphonic)
=CO (carbonyl)	-OH (enolic, phenolic)
-O- (ether)	=N-OH (oxime)
-OH (alcohol)	-SH (phioenolic & thiophenolic)
-S- (thioether)	
$-PR_2$ (substituted phosphine)	
$-AsR_2$ (substituted arsine)	
Complexing Compounds Produced by Microorganisms	
Tricarboxylic acids	Humic acids
Catachol	Fulvic acids
Hydroxamate	
Organic Acids (e.g., oxalate, salicylate, acetate, lactate, pyruvate, citrate and polypeptides)	
Uncharacterized, low molecular weight anions, ions and organic ligands	

When a compound attaches to a metal with two or more functional groups, forming a ring structure, then this complexation is called chelation (from the Greek "chele" meaning lobster' claws) (Birch, 1990; Dwyer, 1964). In soil systems Birch and Bachofen described two groups of microbial compounds which are considered complexing agents:

349

- By-products of microbial metabolism and degradation, such as simple organic compounds (low molecular weight organic acids and alcohols) and macromolecular humic and fulvic acids; and

- Microbial exudates induced by metals ions. These include iron binding siderophores produced in response to low iron concentrations and toxic-metal binding proteins.

By-Products of Microbial Metabolism. Francis found low molecular organic acids and alcohols in the leachate from shallow land burial sites of radionuclides (Francis, 1982). As a rule, the original organic materials present will dictate the types of organic compounds, which will be produced by microorganisms. Although various organic acids released by microorganisms have been investigated for metal complexation ability, it is difficult to evaluate the complexation capabilities of the metabolic products, as their production is dependent on environmental conditions. The degree of relative metabolic activity in the vadose zone will determine the amount of small molecular weight complexing agents.

The metal binding effects of large macromolecular humates (collectively humic and fulvic acids) is well documented in the literature. The following is a brief example of their interactions with metals:

- Humates alter the adsorption onto particulates bioavailability and toxicity of some heavy metals (Davis, 1978 Giesy, 1977);

- Humates also reduce the radionuclides Np(V), Pu(V) and Pu(VI) and(Nash, 1981 Bondietti, 1976); and

- Humates can solubilize Am-241 and Th (Sibley, 1984; Miekeley, 1987; Nash, 1980).

With organic matter present in the RFETS soils, one would anticipate organic matter/actinide interactions.

Microbial Exudates - Siderophores. Microorganisms, as do all life forms, have an essential requirement for Fe (a small group of homolactic fermenting bacteria, the lactic streptococci, are

the only exception). Fe is used for DNA synthesis, electron transfer proteins and nitrogen fixation. However, iron suffers from an extreme insolubility in aerobic environments at physiological pH; consequently, aerobic and facultative anaerobic microorganisms have developed a high affinity system for Fe(III) acquisition. In 1981 Neilands stated that "Siderophores are viewed as the evolutionary response to the appearance of O_2 in the atmosphere, the concomitant oxidation of Fe(II) to Fe(III) and the precipitation of the latter as ferric hydroxide, Ks = $<10^{-38}$" (Neilands, 1981).

Siderophores are low molecular mass, ferric-specific ligands that are induced at low iron concentrations for the purpose of biological assimilation of Fe(III). Over 200 siderophores have been isolated, of which several score have been fully characterized, with most being classified chemically as either catechols or hydroxamates. Siderophores have a very strong binding affinity for Fe(III), with complex formation constants in the range of 10 or higher (Gadd, 1990). An effective ligand of Fe(III) chelation has a molecular mass of 500 to 1000 Daltons; however, such a molecular size exceeds the free diffusion limit of the outer membrane of microorganisms. In order to compensate, microorganisms have specialized surface proteins (receptors) and associated internal enzymes and proteins that transport the siderophore-Fe(III) complex to the sites of physiological utilization (Inouye, 1979).

The most common siderophores contain the hydroxamic acid functional group, -R-CO-N(OH)-R', which forms a five membered chelate ring with Fe(III) through the two oxygen atoms, with the hydroxyl proton being displaced. Frequently three hydroxamate groups are found on a single siderophore molecule and thus supply six oxygen ligands to satisfy the preferred hexacoordinate octahedral geometry of Fe(III). Other bidentate ligand moieties (e.g., catechol, α-hydroxy acid, 2-(2-hydroxyphenyl)-oxazoline and a fluorescent chromophore) also are found in siderophores (Bossier, 1988). Like the hydroxamates, catechols can occur in triplicate as the only unit in a siderophore molecule (e.g., the siderophore enterobactin). It is also common to find siderophores that contain a mixture of functional moieties, such as pseudobactin, which contains a hydroxamate, an α-hydroxy acid and a fluorescent chromophore.

351

Although the common characteristic of all siderophores is that they are virtually ferric specific, with some reported to have 1:1 complex formation constants with Fe(III) that exceed 10, Neilands and Raymond et al believe that because Fe(III) and Pu(IV) are similar in their charge/ionic radius ratio (4.6 and 4.2, respectively), Pu(IV) and other (IV) actinides may serve as analogs to Fe(III) and could therefore be chelated by siderophores (Neilands, 1981; Raymond et al., 1984). Indeed Hersman et al. reported that a siderophore purified from a *Pseudomonas* sp. formed complexes with Pu-239(IV) (Hersman, 1993). Additionally, the same siderophore was found to increase, significantly, the transport of Fe(III) through an unsaturated column of crushed tuff (Story, 1996). Transport of Fe-DFO resulted in fractional Fe recoveries of up to 27 % with a peak concentration occurring at 1.9 to 2.3 effective pore volumes, which agreed with the retardation factor predicted from batch sorption experiments (Figure TA-3-17). Conversely, the unchelated Fe transport in the absence of DFB resulted in extremely low equilibrium concentrations and low recoveries of Fe (1.9 %).

Figure TA-3-17. DFB Chelated Iron (Fedes) and Non-Chelated Iron (Fe) Unsaturated Transport through Crushed Tuff

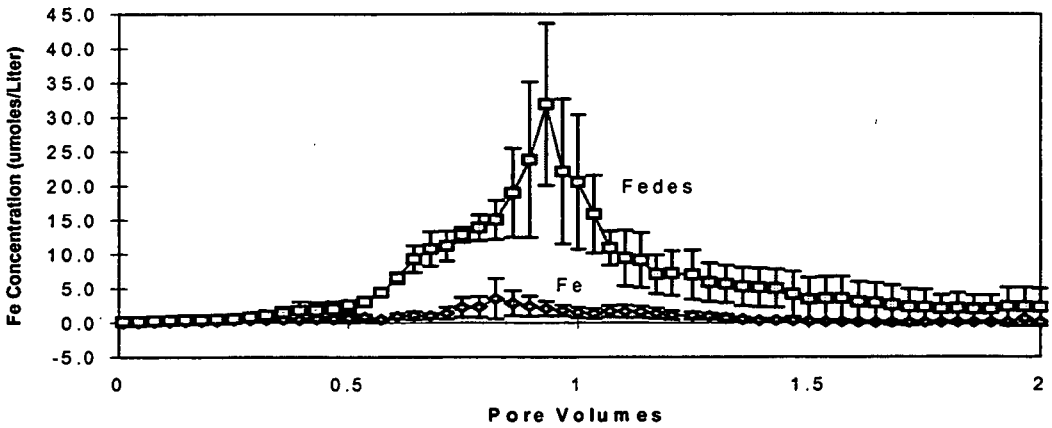

It is possible that radionuclides could be transported in the environment via the siderophore/iron transport system. Thus, it is assumed that microbially produced siderophores such as desferal can increase drastically mobile concentrations of Fe in solution.

Complexation/chelation would increase the amount of radionuclides in solution, thereby increasing their availability for transport.

Biodegradation of complexing agents (reverse of a). The microbial metabolites and naturally-occurring organics that can complex/chelate radionuclides were discussed earlier. Complexed/chelated radionuclides would therefore be transported to a new region of the vadose zone and would become subject to microbial degradation. All of the microbial metabolites that complex/chelate radionuclides are subject to microbial degradation, particularly in an environment of limited nutrients. Low molecular weight organic acids, alcohols and siderophores could all serve as nutrients for indigenous microbial populations. Unfortunately there have been relatively few studies on the degradation of ligands complexed to radionuclides. Francis and Dodge have investigated the biodegradation of iron-citrate complexes (Francis, 1993). They found that the rates of degradation varied, depending on the structure of the complex formed between the metal and the citric acid. For example, when ferric iron formed a bidentate complex with citric acid, the complex was degraded rapidly. However, when ferrous iron formed a tridentate complex with citrate, biodegradation did not occur until it underwent oxidation and hydrolysis conversion to a ferric citrate tridentate complex.

Generally, the biodegradation of metal complexing agents may result in precipitation of the released ion as water insoluble hydroxides, oxides or salts, thus retarding transport (Figure TA-3-16). The stability of naturally-occurring and microbially-synthesized radionuclide complexing agents is critical for understanding the mobility of radionuclides in a natural environment (Francis, 1990).

Dissolution (b). Microbial-enhanced dissolution reactions will affect the stability of radionuclides in radiocolloids and radionuclides attached (either sorbed or precipitated) to natural colloidal particles, to the matrix surface or to the surfaces of microorganisms.

As discussed earlier, there is a chemical similarity between Fe(III) and the (IV) actinide metals. Secondly, when analyzing well water Harnish et al (Harnish, 1994) documented that 65 % of Pu-239 and Pu-240 was associated with particulate and largest colloidal fractions. Further analysis revealed that the particulate and colloidal phases contained Fe oxyhydroxides and clay minerals,

both of which serve as Fe sources for microorganisms. Thus, to better understand how microorganisms can affect the solubility of radionuclides, it is useful, therefore, to review the dissolution of Fe oxides. For the Fe oxides there are three general categories of dissolution: 1) proton promoted, 2) ligand-promoted and 3) reductive dissolution. For each of these, the first step involves the formation of a surface complex by fast adsorption of protons, ligands, electron donors or a combination of these. This leads to a polarizing and thereby a weakening of the Fe-O bond and then to the detachment of the Fe atom into solution. In dissolving a Fe(III)(hydr) oxide complex the coordinative environment of Fe(III) changes. The Fe(III) in the crystalline structure replaces its O^{2-} or OH^- by water or another ligand. In reductive dissolution, it also changes its oxidation state to Fe(II) (Stumm, 1992).

Microorganisms are known to participate in dissolution processes. Due to the similarities between Fe and Mn and radionuclides, there is mounting evidence that microorganisms affect the dissolution rates of radionuclides. The long-term adsorption/precipitation of radionuclides on the surface of the rock matrix or the stability of radiocolloids would be affected by microorganisms. Therefore, the overall result of enhanced dissolution is difficult to predict. On one hand, a portion of the radionuclides removed from the surface of the rock matrix would be in solution and therefore available to be complexed or chelated by microbial metabolites (another portion would precipitate onto or be reabsorbed by the matrix), thereby increasing the migration rate of radionuclides. Alternatively, the removal of adsorbed/precipitated radionuclides from the surface of natural colloids or the dissolution of radiocolloids, both of which have the potential to be very mobile, would have a net negative affect on the transport rate; because, before dissolution all of the colloidal radionuclides were potentially mobile, whereas after dissolution only the complexed/chelated portion would remain in solution.

Microbial sorption, accumulation and bioprecipitation (c, h and l). Bioaccumulation, precipitation, biosorption and mineral formation are essential processes involved in actinide immobilization and metals in general (Francis, 1998; Ledin, 2000). In general, bioaccumulation is an active process whereby metals are accumulated internally in living cells through complexation with metal-binding metabolites or by precipitation. Biosorption is a chemical

process where the cell surface binds metals by ligand interaction or by ion exchange. Finally, microorganisms also catalyze both the precipitation of metals and secondary mineral formation.

Metal biosorption/bioaccumulation by microorganisms has been discussed extensively in the literature (see Beveridge and Doyle; Macaskie et al.; and Fowle et al. and references therein) (Beveridge, 1989; Macaskie, 2000; Fowle, 2000). Relative to their effects on actinide transport, the attached microbial population would occupy a percentage of the total matrix surface area, with both cells and exopolymers. This combination of cells and exopolymers would have different sorption characteristics than the bare surface of the matrix. The outer cellular membrane of microorganisms has a net negative charge and generally is regarded as being active in binding heavy metal cations. For gram positive bacteria, carboxyl groups of the glutamic acid of peptidoglycan is a major site of metal deposition, as are teichoic and teichuronic acids. Gram negative bacteria tend to collect metals at the polar head groups of the constituent membrane bilayers of the envelope or along the peptidoglycan layer between the bilayers in the periplasmic space (Gadd, 1990). Likewise, the carboxyl residues in exopolysaccharides and the uronic acids in extracellular capsules serve as electron donor groups that form bonds with metals, are very efficient metal binding agents and are of major importance in metal removal from solution (Geesey, 1981). Finally, Macaskie et al has detailed the accumulation of uranyl ion via precipitation with phosphate ligand liberated by phosphatase activity (Macaskie, 2000).

Microorganisms sorb a variety of metals as a way of protection against the metals' toxic effects. Generally, metals are only toxic when they have activity as ions. By removing metals from solution, microorganisms reduce the activity of a metal, thereby reducing its toxicity. The simplest mechanism used by microorganisms is to deposit metals on its outer surface. The binding of the metal to the outer surface is specific; the charge, ionic radius and coordination geometry are the predominant factors. The deposition of the metal is facilitated by the activities of membrane-associated sulfate-reductases or through the biosynthesis of oxidizing agents such as oxygen or hydrogen peroxide. By depositing metals, internally or externally, microorganisms are not only protecting themselves from the toxic effects of the metal ions but are also, in effect, concentrating the metal on the matrix surface to an extent greater than would be done by the matrix alone.

Overall, one would anticipate that biosorption/bioaccumulation by those microorganisms attached to mineral surfaces would decrease the aqueous phase concentration of actinides, thereby reducing actinide transport. However, sorption by unattached microorganisms (either in soils, in surface or ground waters) would increase actinide mobility, due to the mobility of these microorganisms.

Redox reactions (d). Radionuclide speciation, which includes 1) the identification of the radionuclide, 2) its oxidation state and 3) the formula and molecular structure of the ionic and/or solid complex (i.e., the stoichiometry and structure of the metal ion as complexed by ions and/or ligands), is fundamentally important to the determination of radionuclide solubility (Clark, 1994). Hence, the solubility of a radionuclide is related to its oxidation state. For example, Pu(IV) is the least soluble oxidation state for all the Pu valences and U(III) is less soluble than the more oxidized states of U. If microorganisms affect the redox chemistry of radionuclides, they would also affect the solubility of the radionuclides.

An enormous area of research, rich in publications, is metal redox reactions that are mediated by microorganisms. The cycling of metals in the geosphere by microorganisms is the foundation for the disciplines of Biogeochemistry and Geomicrobiology. Microorganisms are able to both directly and indirectly affect redox changes in metals (Erlich, 1990; Nealson, 1983; Nealson, 1993). Examples of direct effects are:

- the oxidation of a metal as a source of energy and electrons; and
- the use of a metal as a terminal electron acceptor for respiration, thereby reducing the metal.

Examples of indirect effects are:

- the non specific oxidation of metals at the outer surface of the bacterial envelope; and
- reductions of secondary metals caused by the presence of a microbially reduced primary metal, such as the reduction of Fe(III) to Fe(II) via respiration and the subsequent reduction of surrounding metals by Fe(II).

Pedersen and Karlsson presented an excellent review of specific microbially mediated metal redox reactions, where they discuss the oxidation of iron, manganese, hydrogen, ammonia, sulfur and carbon; and, the reduction of iron, manganese, nitrate, sulfate and carbon (Pedersen, 1995). Although these discussions and others common in the literature provide mainly circumstantial evidence, there is some evidence of microbial involvement in radionuclide redox reactions. Although direct reduction was not confirmed, their results implicate the involvement of metal reducing bacteria in the reduction of a radionuclide.

It is less likely that microorganisms could derive energy directly from the oxidation of radionuclides, particularly at neutral pH. However, indirect oxidation of radionuclides by microorganisms is very probable, given the reactive nature of the cell wall's surface. Metal oxides, such as Fe oxides, are readily deposited on the surfaces of several microbial species, most notably sheathed bacteria. Although the evidence for enzymatic oxidation is equivocal, it is recognized that these bacteria do accumulate large amounts of Fe oxides (Erlich, 1990).

Perhaps the indirect mechanism with the most potential for affecting the redox state of radionuclides is the effects of microbially produced oxidized or reduced metals. For example, Mn(III), an intermediate in the microbial reduction of Mn(IV) to Mn(II) or in the microbial oxidation of Mn(II) is a strong oxidant (having a reduction potential close to molecular oxygen). Several studies have discussed the potential importance of dissolved Mn(III) as an environmental oxidant in marine and freshwater sediments(Burdige, 1993; Davidson, 1993; Luther, 1994; Kosta, 1995). The inter relatedness of Mn and Fe as environmental redox mediators has been discussed in detail by Nealson and Myers (Nealson, 1992). The oxidized and reduced state of these metals, as a function of biological activity, affect the oxidation state of each other and other metals in the surrounding environment.

Because the effect of redox on solubility varies with each radionuclide, the overall effect of microbially mediated redox reaction would have varying effects on radionuclide solubility.

Colloidal agglomeration (e and n). Colloidal dispersion has long been implicated as a means of transporting radionuclides through soil and rock systems (Sposito, 1989). In fact much of the mobile Pu inventory at RFETS is believed to be colloidal in nature (Harnish, 1994). When

357

irreversibly attached to a colloid, these radionuclides are unable to participate in sorption/desorption reactions with the soil or rock matrix. As a consequence, radionuclides can potentially move at an accelerated rate with the colloids through the soil or rock matrix. If, however, colloids become attached to one another to form agglomerates, then the colloids would no longer be available to participate in colloidal dispersion processes because their increased size would exclude them from movement through the small pores or because their increase in size would result in an accelerated sedimentation rate. Obviously, the net result would be an overall decrease in the transport of metals and wastes. Hence, increasing colloidal stability (agglomeration) at RFETS would reduce actinide transport. Thus, it is import to understand the role that microorganisms play in colloidal processes, either as colloids themselves or interacting with mineral colloids and pseudocolloids formed during actinide hydrolysis.

Within the literature there is a substantial body of information regarding the interactions between microorganisms and solid surfaces (including colloidal particles) and the affects of microbial adhesion to colloids. These interactions include the attraction processes, adhesion, adsorption and flocculation.

Attraction of Bacteria to Solid Surface. Many natural habitats have a low nutrient status, therefore solid surfaces are potential sites for concentrating nutrients (as ions and macromolecules) and, consequently, for promoting intensified microbial activity. The movement of water across a surface provides increased opportunities for microorganisms to approach solid-liquid interfaces. In addition, there are many physico-chemical and biological attraction mechanisms operative in the immediate vicinity of interfaces:

Chemotaxis. Mobile bacteria are capable of a chemotactic response to low concentrations of nutrients introduced into a normally nutrient-deficient system. Chemotaxis, of course, cannot account for the attraction of non-motile bacteria to solid-liquid or other interfaces.

Brownian motion. Although more of a collision process, Brownian motion (colloidal particles in a state of continual random motion caused by the chaotic thermal motion of molecules) can cause molecules to collide with each other and with particles suspended in the liquid.

Electrostatic attraction. The interaction of negatively charged surfaces of bacteria with solid surfaces probably depends on the properties of the surface in question. Because most surfaces in nature are negatively charged, it is unlikely that electrostatic phenomena are involved directly in the attraction of bacteria to such surfaces, where electrostatic repulsion would dominate. It should be emphasized, however, that solids in natural environments often acquire different surface properties through sorption of macromolecular compounds to the surface. Therefore, the surface, as "seen" by the bacteria, may be very different from the original surface.

van der Waals interaction. "This interaction involves weak bonding between polar units, either permanent (like OH and C=O) or induced by the presence of neighboring molecules. The induced van der Waals interaction is the result of correlation between fluctuating polarizations created in the electron configurations of two nearby nonpolar molecules. Although the time-averaged polarization induced in each molecule is zero (otherwise it would not be a nonpolar molecule), the correlation between the two induced polarizations do not average to zero. These correlations produce a net attractive interaction between the two molecules"(Buddemeier, 1988). Although the van der Waals interaction between just two molecules is very weak, the van der Waals component is additive and strong when many molecules or larger surface areas interact simultaneously.

Electrical double layer effects. When two negatively charged bodies are in close association, they may be held close to each other by a connecting bridge of cations in solution, called the double layer. The strength of the bonding between the two particles, through the double layer, depends on the thickness of the interacting aqueous double layers, which in turn, is dependent on the concentration and the valence of the electrolyte (cations). For example, an increase in the cation concentration or valence will decrease the double-layer thickness.

Cell-surface hydrophobicity. The role of hydrophobic interaction has been detailed eloquently by Rosenberg and Kjelleberg in their 1986 review (Rosenberg, 1988). Although there are exceptions, it is quite reasonable to assume that part or all, of the outer surface of some bacteria is hydrophobic. It is, therefore, reasonable to consider that such bacteria are "rejected" from the aqueous phase and attracted towards hydrophobic solid surfaces.

359

As stated earlier, surfaces are the potential sites of nutrient concentration and consequently of increased microbial activity. Adsorption of organic substrates on soils depends on the nature of the particulate matter, the organization of the fabric, the clay types, the cationic status of the soils and on the concentration and molecular structure of the substrate. Hence, the availability of substrates to soil microorganisms may be enhanced or reduced by the presence of particulates. If substrates were concentrated at the surface of clay minerals, then these minerals would become populated with microorganisms utilizing those substrates, thereby increasing the potential for interactions between microorganisms and clay particles. Such interactions often lead to formation of multiple bacterial, colloidal particle agglomerates, which then result in the removal of the colloids from suspension. The first step in this process is adhesion.

Adhesion. The adhesion of bacteria to inanimate surfaces is widely recognized as having enormous ecological significance. Adhesion of microorganisms is involved in certain diseases of humans and animals, in dental plaque formation, in industrial processes, in fouling of man-made surfaces, in microbial influenced corrosion and in syntrophic and other community interactions between microorganisms in natural habitats. Most aquatic bacteria appear to adhere to surfaces by means of surface polymers, including lipopolysaccharides, extracellular polymers and capsules, pili, fimbriae, flagella and more specialized structures such as appendages and prosthecae. Although these surface components play a role in the initial, reversible adhesion, they often serve to anchor the bacterium at an interface by polymeric bridging.

The composition and quantity of bacterial cell surface polymers vary considerably and are strongly influenced by growth and environmental conditions. Although extracellular polysaccharides have been reported as being responsible for irreversible adhesion, this is not always true. For example, Brown and coworkers demonstrated adhesion in mixed, carbon-limited populations despite no evidence of extracellular polymer production (Brown, 1977). In addition, a nitrogen-limited culture resulted in poor adhesion, although large extracellular polymer production was observed. It should always be kept in mind that polymers present between the cell and the substratum but not observed in light or scanning electron microscopy could be responsible for the adhesion. It appears with respect to inanimate surfaces, there is a subtle balance of cell surface components {extracellular polysaccharides or lipopolysaccharides

360

(LPS)} that may reduce or promote (fibriae) adhesion to inanimate surfaces. Jonsson and Wadstrom observed that an encapsulated *Staphylococcus aureus* strain did not bind to hydrophobic octyl-Sepharose gel, whereas a noncapsulated variant showed binding capabilities (Jonsson, 1982). In fact, polyanionic extracellular carbohydrate material may not be of primary concern with the initial adhesion processes, but rather with development of subsequent bacterial film(Pringle, 1983). The presence of LPS reduces cell surface hydrophobicity and decreases adhesion to the air-water interface of *Salmonella typhimurium* (Hermansson, 1983).

Adsorption to Colloidal Particles. The adsorption of colloidal clays to bacterial surfaces has been studied by Lahav and Marshall (Lahav, 1962; Marshall, 1969). Lahav suggested that clay platelets may be oriented in a number of ways at the bacterial surface, as a consequence of the net negative charge on clay platelets and the existence of some positive charges on broken edges of platelets (Lahav, 1962). Marshall reported that a species of Rhizobium with a carboxyl type ionogenic surface sorb more Na+-illite per cell than do species with a carboxyl-amino ionogenic surface(Marshall, 1969). Using sodium hexametaphosphate (HMP) to suppress positive charges on platelet edges, Marshall[51] found that the HMP-clay did not sorb to a carboxyl type bacteria, whereas a limited amount of this clay sorbed to carboxyl-amino type bacteria. He interpreted these results in terms of the electrostatic attraction between the platelets and the bacterial cell surfaces. Normal sodium montmorillonite particles sorb in an edge-to-face manner to carboxyl type bacterial surfaces, with positive charged edges of the clay attracted to the negative charged bacterial surface. Sorption in this manner is prevented by neutralization of positive edge charges of the clay by HMP.

Microbial Enhanced Flocculation. Several processes have been patented for the flocculation of clays, particularly clays derived from phosphate benefaction. Microbial polysaccharides from such organisms as *Pullularia, Xanthomonas, Arthrobacter, Cryptococcus, Hansenula and Plectania* were found to flocculate finely divided inorganic solids in an aqueous medium (Goren, 1968). In another application, the use of alkaline-treated microbial nucleoprotein is described for flocculating organic and inorganic wastes (Bomstein, 1972). Used in this process were nucleoproteins from the microbes *Polangium, Myxococcus, Sorangium, Flavobacterium, Leuconostoc, Micrococcus* and *Alcaligenes*. Nucleoprotein derived from these organisms was

361

treated with any one of a variety of alkaline compounds, including $Ca(OH)_2$, KOH, NaOH, NH_3, Na_3PO_4 and quaternary ammonium compounds, which would raise the pH to the point where the microbial material would lyse and form a Sol. Flocculation of suspended waste resulted when the concentration of alkaline-treated microbial material was present in concentrations of 1 to 500 parts per million (ppm) (Bomstein, 1972). Floc deterioration can result from biological factors as well as physical factors. Synthetic and natural polymers used for flocculation of colloids may be subject to degradation by microorganisms, which could result in floc destabilization (Brown, 1979; Obayashi, 1973). Finally, Hersman has demonstrated that both microbial cells and their metabolites enhanced the agglomeration rates of bentonite particles (Hersman, 1986).

Although the overall results of colloidal/radionuclide transport is not completely understood, in general microbial mediated colloidal agglomeration will retard the transport of radionuclides as colloids. However, bacteria acting as colloids (e.g., biocolloids) would enhance actinide transport.

Summary of Microbial Effects on Actinide Transport in the Environment

The processes presented in Figure TA-3-16 and discussed above, there are numerous potential interactions between indigenous microorganisms and actinide metals, some or all being operative at contaminated sites. Thus, all transport pathways will include microbial components, contributing to either the retardation or mobility of actinides or both simultaneously. This participation could range between levels that are below detection to contributions that dominate the overall retardation or mobility. Thus, the transport pathways for the actinides present at RFETS currently contain a microbial component.

Furthermore, by changing the chemical and/or physical constraints of the environment, it is possible not only to alter the type of microbial participation (sorption, reduction, etc.) but also to alter the percent of the total contribution attributable to microbial activity. It is now widely accepted that through directed control of specific microbial metabolic activity, alterations of either the retardation or mobility of actinide elements can be effected for specific sites – i.e., the basis of bioremediation. While it is beyond the scope of this document to discuss

bioremediation, it is important to emphasize that prior to development of a bioremediation strategy, it is first essential to fully characterize a candidate site, microbiologically.

TA - 3.9.2 Microbiological Transformations

Plutonium

Biosorption and Bioaccumulation

It has been known for some time that microorganisms take up Pu. For example, Giesy and Paine demonstrated that Pu was taken up by Aeromonas hydrophila (Giesy, 1977). Later, Hersman investigated the sorption of Pu239(IV) by a *Pseudomonas* sp (Hersman, 1986). Perhaps the most outstanding feature of the data is the strong sorption of the Pu by the bacteria, which concentrated Pu239(IV) to nearly 10,000 times greater than did the sterile control (one gram of sterile, crushed tuff, 75 to 200 mesh). Sorption onto the cell also appeared to be related to the physiological state of the bacteria. On a per-gram, dry-weight basis, the 3 hour culture sorbed the most Pu, followed closely by the 6 hour culture. The lowest sorption was observed for the 12 hour and 24 hour cultures followed by a slight increase in sorption by the 48 hour culture. Many other researchers have also detailed the sorption of radioactive elements by microorganisms (Shumate, 1978; Faison, - Treen-Sears, 1984; Wildung, 1982).

In more recent studies, Francis et al.determined that a mixed culture of halophilic bacteria isolated from the Waste Isolation Pilot Plant (WIPP) associated with dissolved actinides as follows (calculated as moles $cell^{-1}$): Th, 10^{-12}; U, 10^{-15}-10^{-18}; Np, 10^{-15}-10^{-19}; Pu, 10^{-18}-10^{-21}; and Am, 10^{-18}-10^{-19} (Francis, 1998). Variations in accumulation with the cultures were noted and differences in association were attributed to the extent of bioaccumulation and biosorption by the bacteria, pH, the composition of the brine and the speciation and bioavailability of the actinides.

Other studies confirm biosorption and bioaccumulation of Pu. For example, Gillow et al (Gillow, 2000). Demonstrated Pu uptake by Acetobacterium sp. isolated from the Grimsel Test Site (GTS) varied from 30 to 145 per gram of Pu mg^{-1} cell dry weight. Finally, Keith-Roach et al. (Keith-Roach, 2000). Measured porewater concentrations of Np, Pu and Am at a salt march in west Cumbria, UK. Changes in Pu and Am concentrations between April and September were

363

related to changes in the microbial community and suggest that these elements were taken up in biosorption processes.

Reduction

Like iron, the radionuclides are redox active metals, therefore their dissolution should be enhanced by redox reactions mediated by microorganisms. Listed in Table TA-3-10 are the reduction potentials for several metal oxyhydroxides.

Table TA-3-10. Reduction Potentials (pH 7, $Mn^+(aq) = 10\text{-}6$ M) for Selected Metal Oxyhydroxides

Reaction	E'(v)
$UO_2^{2+} + 2e^- = UO_2(s)$	0.94
$1/2\text{-}MnO_2(s) + 2H^+ + e^- = 1/2Mn^{2+} + H_2O$	0.64
$\alpha\text{-}FeOOH(s) + 3H^+ + e^- = Fe^{2+} + 2H_2O$	-0.22
$PuO_{2\gamma}(H_2O)(s) + 4H^+ + e^- = Pu^{3+} + (O + 2)H_2O$	-0.27

(Adapted from Rusin et al., 1994)

Because the reduction potentials of hydrous PuO_2 and goethite (α-FeOOH) are similar, one would suspect that microorganisms capable of reducing goethite may be able to reduce Pu(IV) oxyhydroxides (Ksp approx. = 10^{-57}) to Pu(III) hydroxide (Ksp = $10^{-22.6}$), thus increasing its solubility significantly (Kim, 1989; Morse, 1986).

Solubilization

Unfortunately, there are few quantitative discussions in the literature regarding microbially mediated dissolution of radionuclides. One notable exception is the recent work of Rusin et al (Rusin, 1994). In this experiment, several iron-reducing Bacillus species were observed to promote the dissolution of hydrous PuO_2. Furthermore, this effect was enhanced by the presence of nitrilotriacedic acid (NTA), which was added to the reaction vessels to stabilize the soluble Pu(III). Although circumstantial, the authors suggested that the Bacilli reduced Pu(IV) to Pu(III), which in turn was complexed and spontaneously oxidized by NTA. Fortunately, Pu(IV)-NTA complex remained in solution and could be quantified using liquid scintillation techniques.

364

We have demonstrated modest $Pu(OH)_4$ dissolution by the siderophore DFE (desferrioxamine E) compared to EDTA (Neu et al., 1999). Surprisingly, the siderophores desferrioxamine E and B (DFE and DFB) are 100 times slower than EDTA (0.02 μM/day, reaching only 3-4 μM Pu in the same time, despite having significantly higher solution complex formation constants with Pu(IV) (log β DFE = 32; DFB = 30, EDTA = 26).

Chelation and Complexation

As part of the DOE/NABIR Program, Neu and Hersman made the following observations regarding the interactions of microbially-produced siderophores, exopolymers and whole cells with Pu:

- **Siderophores can form complexes with Pu that have similarities to Fe complexes.** We have determined the complex structure of Pu(IV)-DFE and compared that structure to those of DFE and Fe(III)-DFE (Figure TA-3-18)(Neu et al., 2000a). The Pu(IV)-DFE complex is nine coordinate, tricapped trigonal prismatic with the DFE bound in approximately one hemisphere and three waters in the other. The conformation is cis-cis, the same as Fe(III)-DFE and it has a nearly identical 'molecular footprint';

365

Figure TA-3-18. Structures of DFE Free Ligand and Metal Complexes

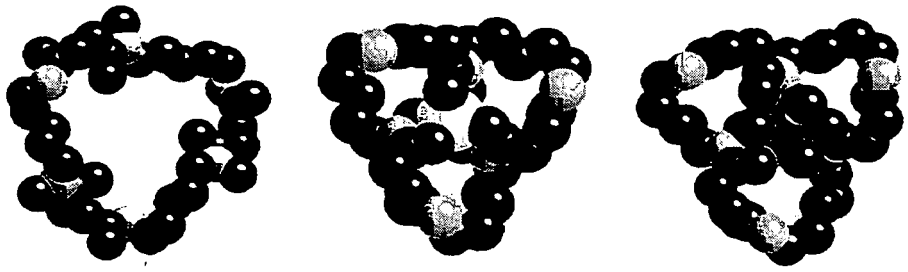

Metal Free DFE	*Fe(III) DFE Complex*	*Pu(IV) DFE Complex*
(Hossain et al., 1983)	(van der Helm and Poling, 1976)	(Neu et al., 2000b)

- **Desferrioxamine siderophores stabilize the Pu(IV) and U(VI).** If Pu(III) is mixed with DFB or DFE in air, the Pu(IV) complex quickly forms. DFE and DFB also rapidly and irreversible reduce Pu(VI) to Pu(V) and eventually to Pu(IV). Up to 12 equivalents of Pu(VI) can be reduced to Pu(V) per DFE/DFB instantly, so long as there is greater than 1 equivalent DFO per six equivalents Pu. (Under environmental, iron-starved conditions for microorganisms, the concentration of siderophore will generally be greater than the concentration of actinide contaminant.) At pH greater than 6, the reduction of Pu(VI) directly to Pu(IV) is instantaneous. Aqueous U(IV, V) is instantaneously oxidized to U(VI) in the presence of DFO;

- **Siderophore – Pu(IV) complexes can be taken up by microorganisms, but U(VI) siderophore complexes cannot.** Uptake of Pu and U mediated by DFB has been studied for the common soil aerobe *Microbacterium flavescens* (JG-9). *Microbacterium flavescens* does not bind or take up U(VI)-DFB or nitrilotriacetic acid (NTA) complexes of U(VI), Fe(III) or Pu(IV), but does accumulate Fe(III)-DFB and Pu(IV)-DFB. Pu(IV) and Fe(III) accumulation are similar: Only living and metabolically active cells take up the metal-DFB complexes. The Fe(III)-DFB and Pu(IV)-DFB complexes mutually

inhibit uptake of the other, indicating that they compete for shared binding sites or uptake proteins (Neu, et al., 1999); and

- **Exopolymers bind significant quantities of U and Pu.** The exopolymer produced by *B. licheniformis*, γ-polyglutamic acid (PGA), has been isolated and characterized (Figure TA-3-19) and we have investigated the structural, chemical and U(VI) and Pu(IV) binding properties of PGA. At the highest concentration of metal added, every mg of polymer binds 108 μg of Pu of the 156 μg added (70 % binding efficiency), 20 μg of the 36 μg Fe(III) added (56 % binding efficiency) and 63 μg of the 246 μg U(VI) added (30 % binding). These values correspond to 0.30 μmol, 0.36 μmol and 0.45 μmol of U(VI), Fe(III) and Pu(IV), respectively, bound per mg of exopolymer. The Fe(III) value is in excellent agreement with that reported by McLean *et al* (Mclean, 1990). The metal binding strength of the polymer was estimated by competition experiments. When tiron or NTA is titrated into the metal PGA complex solution (pH=4 with a ratio of 1:100 metal to Glu residue), Fe(III), Pu(IV) and U(VI) all form metal tiron or NTA complexes, suggesting that the actinide polymer complex has a binding constant *log* $K_i < 10$. This is consistent with the binding strength of other exopolymers, humic and fulvic acids (Lester, 1995; Chen, 1995; Neu, et al., 1999).

Figure TA-3-19. Structures of the exopolymers produced by* B. licheniformis *(left) and* R. erythropolis *(right, proposed), respectively

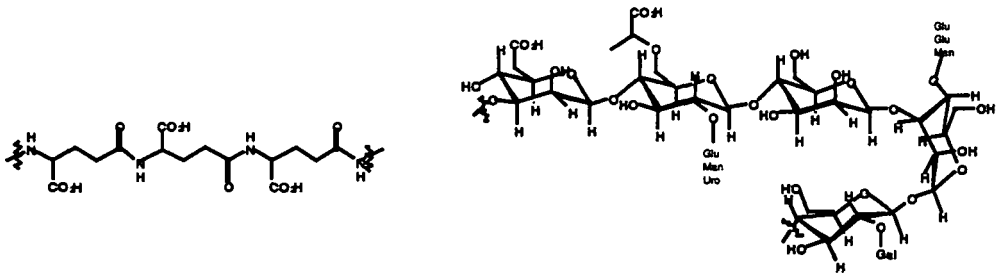

367

- **Whole cells can bind more Fe and Actinide than isolated exopolymer.** When Fe(III) and Pu(IV) were added to whole cells of *B. licheniformis* at pH=6 in saline, greater than 90 % of the metal added was bound by the cell and polymer. Only 60 to 75 % of the U(VI) was bound by the cell and polymer, this decrease may be due to the structural binding constraints of the 'dioxo' uranyl ion. The amount of metal bound by the whole cells (including exopolymer) was much greater on a per mass basis than that of the isolated exopolymer, for Pu those amounts were approximately 0.7 mg/mg whole cells vs 0.45 mg/mg exopolymer.

Americium

Compared to Pu and U, very little microbial work has been done on Am. It is known that microbes biosorb and bioaccumulate Am (Francis, 1998). Bacterial uptake of Am has been reported to be primarily sorption onto the cell's surface; sorption was reversible and was dependent upon nutrients, pH, physiological state of the cell and the presence of bacterial exometabolites (Wurtz, 1986).

Uranium

A significant amount of information is available on U geomicrobiology, largely because of the commercial use of microorganisms to leach this metal from low-grade ores. Also fundamental research on microbial abilities to limit the release of U and other metals has become increasingly important, from a bioremediation standpoint (for an excellent review of U geomicrobiology see Suzuki and Banfield and references therein)(Suzuki, 1999).

Solubilization

Garcia Junior investigated a bacterial leaching process to leach U from Brazilian ore deposits (Junior, 1993). Under laboratory conditions, 60 % of the U was leached in samples inoculated with *Thiobacillus ferrooxidans*, as compared to 30 % in the uninoculated controls. Francis et al. reported that the predominant mechanism of dissolution of U from ores is oxidation (Francis, 1991). The oxidant Fe(III) is produced from Fe(II) in the ore by *T. ferrooxidans*, which then oxidizes UO_2 to UO_2^{2+} (Abdelouas et al. and references therein) (Abdelouas, 1999).

368

Reduction

U reduction has been reported by several investigators, as a mechanism of immobilization (i.e, to retard a U contaminant plume). Lovley and coworkers and Gorby and Lovley have investigated the reduction of U by a variety of bacteria and have demonstrated that dissimilatory iron reducing bacteria were also able to obtain energy for growth by electron transport to U(VI) (Lovley, 1991; Lovley, 1992; Gorby, 1992; Lovley, 1993). Sulfate reducing bacteria have also been shown to reduce U(VI) with rates comparable to iron reducing bacteria (Lovley, 1991). In a later study, the importance of cytochrome C_3 in the reduction was determined, thereby demonstrating that the reduction of U was enzymatic and not indirect (Lovley, 1993). Francis et al. have also confirmed enzymatic reduction of U by a *Clostridium* sp.; and, suggested that direct U reduction should occur in the sequence Mn(IV) > U(VI) > Fe(IV) based upon the free energies of reduction: -83.4, -63.3 and -27.2 kcal mol^{-1} CH_2O for Mn, U and Fe, respectively (Francis, 1994).

Tebo and Obraztsova described the first sulfate-reducing bacterium that can grow on U(VI) (and other metals) as the sole electron acceptor (Tebo, 1997). It shares properties with both other sulfate and metal reducing microorganisms. U(VI) reduction kinetics have been detailed by Truex et al. (Truex, 1997). The organism, *Shewanella alga*, reduces U(VI) at a rate the is 30 % of its Fe(III) reduction rate.

Interestingly, Robinson et al. demonstrated that while bacterial reduction of U(VI) complexed to acetate, oxalate, citrate and tiron occurred, the rate of reduction varied (Robinson, 1998). Acetate complexed U was fastest while citrate complexed U was slowest, indicating that differences in the functional groups involved in complexation may affect the rate of U(VI) reduction. In addition, it appeared that precipitation of reduced U was limited by the ligand concentration, indicating that for successful precipitation (as a bioremediation process) it may be necessary to simultaneously degrade selected ligands from solution.

More recent U reduction studies have been performed by Xu et al and Francis et al (Xu et al, 2000 Francis, 2000). Furthermore, U reduction has emerged as a very important technology and is being investigated rigorously by scientists associated with the Department of Energy, Natural

361

and Accelerated Bioremediation (NABIR) program. For example, Fredrickson et al. have discussed the reduction of U(VI) in goethite [α-$FeOOH_{(s)}$] suspensions by dissimilatory metal-reducing bacteria (DMRB). These findings are important because of the common occurrence of the Fe-bearing mineral goethite in soil environments and therefore DMRB could reduce soluble U(VI) to insoluble U(IV) in the presence of solid Fe mineral phases (Fredrickson, 2000). In a second paper, Fredrickson and coworkers discuss the reduction of U(VI) and other metals by the radiation-resistant microorganism, *Deinococcus radiodurans*. *D. radiodurans* is capable of surviving acute exposures of ionizing radiation doses of 15,000 Gy (Fredrickson, 2000). This recent reported ability to reduce U now only serves to increase potential utility of this microorganism for the bioremediation of U contaminated sites.

Biosorption and Bioaccumulation

There are numerous reports in the literature of biosorption of U by microorganisms (e.g., Francis)(Francis, 1998). Macaskie and coworkers have detailed the enzymatic bioprecipitation of U by bacteria (Macaskie, 2000). They attribute this to phosphatase ligand liberated by phosphatase activity. Furthermore, both rate and onset of deposition were promoted by NH_4^+, forming $NH_4UO_2PO_4$. Panak et al. have demonstrated that both vegetative cells and spores of several *Bacillus* species accumulate high amounts of U(VI) in the concentration range of 11-214 mg/L (Panak et al., 2000). Hu et al. noted that even though U binding to *Pseudomonas aeruginosa* occurred, Fe(III) was a strong inhibitor of binding, suggesting that the Fe(III) and U may share the same binding sites on biomass (Hu et al., 1996). Finally, Suzuki and Banfield provide an excellent review of U biosorption and bioaccumulation (Banfield, 1999).

Biodegradation

Biodegradation of U - ligand complexes has been investigated extensively by Francis and coworkers (e.g., Francis) (Francis, 1998). For example, Francis and his group have reported that although citrate is commonly metabolized by bacteria, several species were unable to biodegrade the uranyl-citrate complex. Furthermore, this complex was not transported into the cells. As anticipated from the above results, the metal reducing bacteria *Clostridium sphenoides* was able to reduce U in the uranyl-citrate complex only when supplied glucose or uncomplexed citrate as

an electron donor. Francis and coworkers have concluded, "complexed U is readily accessible for microorganisms as an electron acceptor, despite their ability to metabolize the organic ligand complexed to the actinide" (Francis, 1998).

TA - 3.9.3 Biogeochemistry Conclusions

Microorganisms inhabit soil environments and could be considered to do so preferentially. Furthermore, the soil microbial population should be regarded as being stable and this stability becomes an important parameter when developing performance evaluations for the migration of radionuclides. Because of its stability, the soil community will be in place and metabolically active, however diminutive, for the entire time frame under consideration. Given the time frame required, the potential for significant microbial effects on transport are increased and therefore the metabolic process performed by microorganisms when interacting with radionuclides must become part of performance assessment. As discussed, microbial metabolic processes affecting radionuclide solubility are significant and varied. These processes include, but are not limited to, sorption/precipitation, complexation/chelation, biodegradation of complexed actinides, dissolution, oxidation/reduction reactions and colloidal agglomeration. Additionally, microorganisms create microenvironments of nutrient and chemical gradients, capable of altering radionuclide solubilities. Although no site-specific geomicrobiological data exists, one can safely assume that many or all of the geomicrobiological processes discussed herein are in place and operative at RFETS. These processes are important to understand, not only to provide a more complete understanding of ongoing and potential actinide transport pathways, but also for potential development and expansion as part of a Site remediation program.

371

TA-3.10 TECHNICAL APPENDIX SECTION TA-3 REFERENCES

Geochemistry References (Sections TA-3.1 through TA-3.8)

(References for Biogeochemistry, Section TA-3.9, follow in separate listing).

Allard, B. 1982. Solubilities of Actinides in Neutral or Basic Solutions. In Actinides in Perspective, ed. N. Edelstein. pp. 553-580. New York: Pergamon Press.

Allard, B. and G.W. Beall. 1981. Management of Alpha-Contaminated Wastes. Vienna, Austria: International Atomic Energy Committee.

Allard, B. and J. Rydberg. 1983. Behavior of Plutonium in Natural Waters. In Plutonium Chemistry, eds. W.T. Carnall and G.R. Choppin. pp. 275-295. Washington, DC: American Chemical Society.

Alexander, M. 1995. How Toxic Are Toxic Chemicals in Soil? Environmental Science and Technology. Vol. 29, No. 11, pp. 2713-2717.

Ali, W., C.R. O'Melia and J.K. Edzald. 1985. Colloidal Stability of Particles in Lakes-Measurements and Significance. Water Science and Technology Vol. 17, pp. 701-712.

Allison, J.D., D.S. Brown and K.J. Novo-Gradac. 1991. MINTEQA2/PRODEFA2, A Geochemical Assessment Model for Environmental Systems: Version 3.0 User's Manual. EPA/600/3-91/021. Athens, GA: U.S. Environmental Protection Agency.

Actinide Migration Evaluation (AME). 1998. Actinide Migration Evaluation Advisory Group Summary. October 1998. Golden, CO: Rocky Flats Environmental Technology Site.

AME. 1999. Actinide Migration Evaluation Advisory Group Summary. October 1999. Golden, CO: Rocky Flats Environmental Technology Site.

Ames, L.L., J.E. McGarrah, B.A. Walker and P.F. Salter. 1982. Sorption of Uranium and Cesium by Hanford Basalts and Associated Secondary Smectites. Chemical Geology Vol. 35, pp. 205-225.

Argonne National Laboratory (ANL). 1993. Manual for Implementing Residual Radioactive Material Guidelines Using RESRAD, Version 5.0, Working Draft for Comment. ANL/EAD/LD-2. Argonne, IL: Environmental Assessment Division, Argonne National Laboratory.

Aston, S.R. 1980. Evaluation of Chemical Forms of Plutonium in Seawater. Marine Chemistry Vol. 8, pp. 317-326.

372

Baek, I. and W.W. Pitt, Jr. 1996. Colloid-Facilitated Radionuclide Transport in Fractured Porous Rock. Waste Management Vol. 16, No. 313.

Baes, C.F., Jr. and R.E. Mesmer. 1976. The Hydrolysis of Cations. New York: John Wiley and Sons.

Baes, C.F. and R.D. Sharp. 1983. A Proposal for Estimation of Soil Leaching Constants for Use in Assessment Models. Journal of Environmental Quality Vol. 12, pp. 17-28.

Ball, J.W. 2000. Geochemical Modeling of Solar Ponds Plume Groundwater at the Rocky Flats Environmental Technology Site, Part I: Ion Plots and Speciation Modeling. Golden, CO: U.S. Geological Survey, forthcoming.

Ball, J.W., E.A. Jenne and M.W. Cantrell. 1981. WATEQ3: A Geochemical Model With Uranium Added. Open-File Report 81-1183. Menlo, Park, CA: U.S. Geological Survey.

Barney, G.S. 1992. Adsorption of Plutonium on Shallow Sediments at the Hanford Site, WHC-SA-1516-fp. Westinghouse Hanford Company, Richland, WA.

Berry, J.A., K.A. Bond, D.R. Ferguson and N.J. Pilkington. 1991. Experimental Studies of the Effects of Organic Materials on the Sorption of Uranium and Plutonium. Radiochimica Acta, Vol. 52/53, pp. 201-209.

Bethke, C.M. and P.V. Brady. 2000. How the Kd Approach Undermines Ground Water Cleanup. Groundwater Vol. 38, No. 3, pp. 435-443.

Billon, A. 1982. Fixation D'elements Transuraniens a Differents Degres D'oxydation Sur Les Argiles. In Migration in the Terrestrial Environment of Long-lived Radionuclides from the Nuclear Cycle. IAEA-SM-257/32. Vienna, Austria: International Atomic Energy Agency. pp. 167-176.

British Nuclear Fuel Limited, Inc. (BNFL). 1998. A Literature Review on the Behavior of Buried Contaminated Concrete Over Time and Relevance to Plutonium, Americium and Uranium Contamination at The Rocky Flats Environmental Technology Site. Englewood, CO.

Boggs, Jr., S., D. Livermore and M.G. Seitz. 1985. Humic Substances in Natural Waters and Their Complexation with Trace Metals and Radionuclides: A Review. ANL-84-78. Argonne, IL: Argonne National Laboratory.

Bolivar, S.L., Broxton, D.E. and Olsen, C.E. 1978. Uranium Hydrogeochemical and Stream Sediment Reconnaissance of the Denver and Greeley NTMS Quadrangles, CO. LANL Informal Report LA-7177-MS. Los Alamos, NM: Los Alamos National Laboratory.

373

Bondietti, E.A., S.A. Reynolds and M.H. Shanks. 1975. Interaction of Plutonium with Complexing Substances in Soils and Natural Waters. In Transuranium Nuclides in the Environment, pp. 273-287, IAEA-SM-199/51. Vienna, Austria: International Atomic Energy Agency.

Bondietti, E.A., S.H. Sweeton and H. Fox. 1977. Transuranic Speciation in the Environment. In Transuranics in Natural Environments, eds. M.G. White and P.B. Dunaway, NVO-178, U.S. Energy Research and Development Administration. Springfield, VA: NTIS.

Bondietti, E.A. and J.R. Trabalka. 1980. Evidence for Plutonium(V) in an Alkaline, Freshwater Pond. Radioanalytical Letters ,Vol. 43, pp. 169-176.

Borovec, Z., B. Kribek and V. Tolar. 1979. Sorption of Uranyl by Humic Acids. Chemical Geology, Vol. 27, pp. 39-46.

Brendler, Vinzenz. 1999. Physico-Chemical Phenomena Governing the Behaviour of Radioactive Substances. State-of-the-Art Description, Restoration Strategies for Radioactively Contaminated Sites and their Close Surroundings. RESTRAT - WP2, Forschungszentrum Rossendorf, Institute of Radiochemistry, P.O.Box 51 01 19, D-01314, Dresden, Germany.

Bruno, J., I. Casas and I. Puigdomenech. 1988. The Kinetics of Dissolution of OU2 Under Reducing Conditions. Radiochimica Acta, Vol. 11, pp. 44-55.

Bruno, J., I. Casas and I. Puigdomenech. 1988a. The Kinetics of Dissolution of OU2 Under Reducing Conditions and the Influence of an Oxidizing Surface Layer (UO2+x). Geochimica et Cosmochimica Acta, Vol. 55, pp. 647-658.

Brusseau, M.L. 1994. Transport of Reactive Contaminants in Heterogeneous Porous Media. Review of Geophysics, Vol. 32, No. 3, pp. 285-313.

Buck, J.W., G. Whelan, J.G. Droppo, D. L. Strenge, K.J. Castleton, J.P. McDonald, C. Sato and G.P. Streile. 1995. Multimedia Environmental Pollutant Assessment System (MEPAS) Application Guidance, Guidelines for Evaluating MEPAS Input Parameters for Version 3.1. Report PNL-10395. Richland, WA: Pacific Northwest Laboratory.

Buffle, J., D. Perret and M. Neuman. 1992. The Use of Filtration and Ultrafiltration for Size Fractionation of Aquatic Particles, Colloids and Macromolecules. In Environmental Particles: Vol. 1, eds. J. Buffle and H. P. van Leeuwen. Boca Raton, FL: Lewis Publishers, pp. 231-290.

Buffle, J. and G.G. Leppard. 1995. Characterization of Aquatic Colloids and Macromolecules. 1. Structure and Behavior of Colloidal Material. Environmental Science and Technology, Vol. 29, pp. 2169-2175.

374

Bundt, M., A. Albrecht, P. Froidevaux, P. Blaser and H. Fluhler. 2000. Impact of Preferential Flow on Radionuclide Distribution in Soil. Environmental Science and Technology, Vol. 34, pp. 3895-3899.

Bunzl, K., H. Flessa, W. Kracke and W. Schimmack. 1995. Association of Fallout 239+240Pu and 241Am With Various Soil Components in Successive Layers of a Grassland Soil. Environmental Science and Technology, Vol. 29, No. 2513-2518.

Cerda, C.M. 1987. Mobilization of Kaolinite Fines in Porous Media. Colloids and Surfaces, Vol. 27, No. 1-3, pp. 219-241.

Chisholm-Brause, C., S.D. Conradson, C.T. Buscher, P.G. Eller and D.E. Morris. 1994. Speciation of Uranyl Sorbed at Multiple Binding Sites on Montmorillonite. Geochimica et Cosmochimica Acta, Vol. 58, pp. 3625-2631.

Choppin, G.R. 1983. Aspects of Plutonium Solution Chemistry. In Plutonium Chemistry, eds. W.T. Carnall and G.R. Choppin. Washington, DC: American Chemical Society, pp. 213-230.

Choppin, G.R. and J.W. Morse. 1987. Laboratory Studies of Actinides in Marine Systems. In Environmental Research on Actinide Elements, eds. J.E. Pinder, J.J. Alberts, K.W. McLeod and R. Gene Schreckhise, CONF-841142. Washington, DC: Office of Scientific and Technical Information, U.S. Department of Energy, pp. 49-72.

Choppin, G.R. 1988. Humics and Radionuclide Migration. Radiochimica Acta Vol. 44/45, pp. 23-28.

Choppin, G.R. 1992. The Role of of Natural Organics in Radionuclide Migration in Natural Aquifer Systems. Radiochimica Acta, Vol. 58/59, pp. 113-120.

Choppin, G.R, J.O. Liljenzin and J. Rydberg. 1995. Radiochemistry and Nuclear Chemistry, 2nd Ed. Buttersworth-Heinenmann, Oxford.

Choppin, G.R., A.H. Bond and P.M. Hromadka. 1997. Redox Speciation of Plutonium. Journal of Radioanalytical and Nuclear Chemistry, Vol. 219, No. 2, pp. 203-210.

Clark, D.L. 2000. The Chemical Complexities of Plutonium. In Challenges in Plutonium Science, Volume 2, Editor, Necia Grant Cooper, Los Alamos Science, Number 26, LA-UR-00-4100, Los Alamos National Laboratory, Los Alamos, NM. www.lanl.gov/external/science/lascience/index.html

Clark, D.L., S.A. Ekberg, D.E. Morris, P.D. Palmer and C.D. Tait. 1994. Actinide(IV) and Actinide (VI) Carbonate Speciation Studies by PAS and NMR Spectroscopies, Yucca Mountain Project. Milestone Report 3031-WBS 1.2.3.4.1.3.1, LA-12820-MS. Los Alamos, NM: Los Alamos National Laboratory.

375

Clark, D.L., D.E. Hobart and M.P. Neu. 1995. Actinide Carbonate Complexes and their Role in Actinide Environmental Chemistry. Chemical Reviews. 95. p. 25.

Clark, D.L., D.W. Keough, M.P. Neu and W. Runde. 1997. Uranium and Uranium Compounds. Kirk-Othmer Encyclopedia of Chemical Technology, 4th Ed. Wiley Interscience, New York, Vol. 24. pp. 638-694.

Clark, D.L. and D.R. Janecky. 1997. Private communication to Christine Davis, Kaiser-Hill Company, LLC. Golden, CO: RFETS.

Cleveland, J.M., T.F. Rees and W.C. Gottschall. 1976. Factors Affecting Solubilization of Plutonium and Americium from Pond Sediments at the Rocky-Flats Facility. Report ES-376-76-196. Golden, CO: Rockwell International, Rocky Flats Plant.

Cleveland, J.M., T.F. Rees and K.L. Nash. 1983. Ground-water Composition and Its Relationship to Plutonium Transport Processes. In Plutonium Chemistry, eds. W.T. Carnall and G. R. Choppin. Washington, DC: American Chemical Society, pp. 235-245.

Cleveland, J. M. 1979. The Chemistry of Plutonium. LaGrange Park, IL: American Nuclear Society.

Cooper, Necia Grant, Editor, 2000, Challenges in Plutonium Science, Volumes 1 and 2, Los Alamos Science, Number 26, LA-UR-00-4100, Los Alamos National Laboratory, Los Alamos, NM. www.lanl.gov/external/science/lascience/index.html

Cotton, F.A., G. Wilkinson, C.A. Murillo and M. Bochmann. 1999. Advanced Inorganic Chemistry. Wiley-Interscience Publishers. New York, NY.

Coughtrey, P.J., D. Jackson, C.H. Jones, P. Kane and M.C. Thorne. 1984. Radionuclide Distribution and Transport in Terrestrial and Aquatic Ecosystems; A Compendium of Data. Boston, MA: A. A. Balkema.

Dahlman, R.C., E.A. Bondietti and L.D. Eyman. 1976. Biological Pathways and Chemical Behavior of Plutonium and Other Actinides in the Environment. In Actinides in the Environment, ed. A.M. Friedman, Washington, DC: American Chemical Society, pp. 47-80.

Delegard, C.H. and G.S. Barney. 1983. Effects of Hanford High-Level Waste Compounds on Sorption of Cobalt, Strontium, Neptunium, Plutonium and Americium of Hanford Sediments. RHO-RE-ST-1 P. Richland, WA: Rockwell Hanford Operations.

Delegard, C.H. 1987. Solubility of PuO2·xH2O in Alkaline Hanford High-Level Waste Solution. Radiochimica Acta, Vol. 41, pp. 11-21.

Department of Energy (DOE). 1993. Background Geochemical Characterization Report for the Rocky Flats Plant. Golden, CO: Rocky Flats Plant.

DOE. 1995-1994. Annual RCRA Groundwater Monitoring Report for Regulated Units at the Rocky Flats Plant, CO. Golden, CO: Rocky Flats Environmental Technology Site.

DOE. 1997. Summary of Existing Data on Actinide Migration at the Rocky Flats Environmental Technology Site. RF/RMRS-97-074.UN. Golden, CO: U.S. Department of Energy, Rocky Flats Environmental Technology Site.

Doty, C.B. and C.C. Davis. 1991. The Effectiveness of Groundwater Pumping as a Restoration Technology. ORNL/TM-11866. Oak Ridge, TN: Oak Ridge National Laboratory.

Dubinin, M.M. and L.V. Radushkavich. 1947. Equation of the Characteristic Curve of Activated Charcoal. Proceedings of the Academy of Sciences, Physical Chemistry Section, U.S.S.R., Vol. 55, pp. 331-333.

Duff, M.C. and C. Amrhein. 1996. Uranium(VI) Adsorption on Goethite and Soil in Carbonate Solutions. Soil Science Society of America Journal, Vol. 60, No. 5, pp. 1393-1400.

Duff, M.C., D.B. Hunter, I.R. Triay, P.M. Bertsch, D.T. Reed, S.R. Sutton, G. Shea-McCarthy, J. Kitten, P. Eng, S.J. Chipera and D.T. Vaniman. 1999. Mineral Associations and Average Oxidation States of Sorbed Pu on Tuff. Environmental Science and Technology, Vol. 33, pp. 2163-2169.

Edgington, D.N. and J.A. Robbins. 1976. The Behavior of Plutonium and Other Long-Lived Radionuclides in Lake Michigan, II: Patterns in Sediments. In Impacts of Nuclear Releases into the Aquatic Environment, STI/PUB/406. Vienna, Austria: International Atomic Energy Agency.

Efurd, D.W., D.J. Rokop and R.E. Perrin. 1993a. Characterization of the Radioactivity in Surface-Waters and Sediments Collected at the Rocky Flats Facility. LANL Report LA-UR-93-4373. Los Alamos, NM: Los Alamos National Laboratory.

Efurd, D.W., D.J. Rokop and R.E. Perrin. 1993b. Actinide Determination and Analytical Support for Water Characterization and Treatment Studies at Rocky Flats, Task Element A, Final Report, Radiochemical Analyses, Radionuclide Characterization and Radionuclide Treatment of Rocky Flats Pond Waters. LATO-EG&G-91-022. Los Alamos, NM: Los Alamos National Laboratory.

Efurd, D.W., W. Runde, J.C. Banar, D.R. Janecky, J.P. Kaszuba, P.D. Palmer, F.R. Roensch and C.D. Tait. 1998. Neptunium and Plutonium Solubilities in a Yucca Mountain Groundwater. Environmental Science and Technology, Vol. 32, pp. 3893-3900.

EG&G Rocky Flats Inc. (EG&G). 1988. Health Physics Manual of Good Practices for Uranium Facilities. NTIS DE88-013620. Springfield, VA: NTIS.

Eisenbud, M. 1987. Environmental Radioactivity. New York: Academic Press, Inc.

377

Environmental Protection Agency (EPA). 1999. Understanding Variation in Partition Coefficient, Kd, Values. Vol. I EPA 402-R-004A and Vol. II EPA 402-R-004B. Washington, DC: Office of Radiation and Indoor Air, Office of Solid Waste and Emergency Response and Office of Environmental Restoration.

Falck, W.E. 1991. CHEMVAL Project. Critical Evaluation of the CHEMVAL Thermodynamic Database with Respect to its Contents and Relevance to Radioactive Waste Disposal at Sellafield and Dounreay. DoE/HMIP/RR/92.064. London, England: Department of Environment, Her Majesty's Stationary Office.

Faure, G. 1977. Principles of Isotope Geology. New York: John Wiley and Sons.

Federov, Y.E., A.S. Bakurov, M.N. Fedorova and F. Rasulev. 1986. Behavior of Plutonium in the Soil and its Entry into Plants. Agrokhimiya, Vol. 12, pp. 83-88.

Fetter, C.W. 1993. Contaminant Hydrogeology. New York: Macmillan.

Filella, M. and J. Buffle. 1993. Factors Controlling the Stability of Submicron Colloids in Natural Waters. Colloids and Surfaces A, Physicochemical and Engineering Aspects, Vol. 73, pp. 255-273.

Fisher, N.S., S.W. Fowler, F. Boisson, J. Carroll, K. Rissanen, B. Salbu, T.G. Sazykina and K. Sjoeblom. 1999. Radionuclide Bioconcentration Factors and Sediment Partition Coefficients in Arctic Seas Subject to Contamination from Dumped Nuclear Wastes: Environmental Science and Technology, Vol. 33, pp. 1979-1982.

Fowler, E.B. and E.H. Essington. 1974. Soils Element Activities, October 1972–September 1973. In The Dynamics of Plutonium in Desert Environments, eds. P.B. Dunnaway and M.G. White, NVO-142, 7-16. s.l.: Nevada Applied Ecology Group, U.S. Energy Research & Development Administration.

Freundlich, H. 1926. Colloid and Capillary Chemistry. London, England: Methuen.

Frondel, C. 1958. Systematic Mineralogy of Uranium and Thorium. Geological Survey Bulletin 1064. Washington, DC: U.S. Geological Survey.

Giles, C.H., D. Smith and A. Huitson. 1974. A General Treatment and Classification of the Solute Adsorption Isotherm. I. Theoretical. Journal of Colloid and Interface Science, Vol. 47, pp. 755-765.

Glover, P.A., F.J. Miner and W.O. Polzer. 1976. Plutonium and Americium Behavior in the Soil/Water Environment. I. Sorption of Plutonium and Americium by Soils. In Proceedings of Actinide-Sediment Reactions Working Meeting, Seattle WA. Richland, WA: Battelle Pacific Northwest Laboratories. BNWL 2117, pp. 225-254.

Grayson, M and D. Eckroth, Eds. 1985. Kirk-Othmer Concise Encyclopedia of Chemical Technology. New York: Wiley-Interscience.

Grenthe, I., J. Fuger, R. J. M. Konings, R. J. Lemire, A. B. Muller, C. Nguyen-Trung, H. Wanner, review team. 1993. Chemical Thermodynamics of Uranium. Volume 1 of Chemical Thermodynamics Series. H. Wanner and I. Forest (eds.). Elsevier Science Publishing Company, Inc., New York, New York.

Grenthe, I. and I. Puigdomenech, Eds., 1997, "Modeling in Aquatic Chemistry", Nuclear Energy Agency, OECD-OCDE.

Guillaumont, R. and J.P. Adloff. 1992. Behaviour of Environmental Plutonium at Very Low Concentration. Radiochimica Acta, Vol. 58/59, pp. 53-60.

Hardy, E.P., P.W. Krey and V.L. Volchok. 1973. Global Inventory and Distribution of Fallout Plutonium. Nature, Vol. 241, pp. 444-445.

Harnish, R.A, D.M. McKnight and J.F. Ranville. 1993. Particulate, Colloidal and Dissolved Phase Associations of Plutonium and Americium in a Water Sample From Well 1587 at the Rocky Flats Plant, CO. Water Resources Investigations Report 93-4175. Golden,CO: U.S. Geological Survey.

Harnish, R.A., D.M. McKnight, J.F. Ranville, V.C. Stephens and W.H. Orem. 1996. Particulate, Colloidal and Dissolved-Phase Associations of Plutonium, Americium and Uranium in Water Samples from Well 1587 and Surface-Water Sites SW-51 and SW-53 at the Rocky Flats Plant, Colorado. Water Resources Investigations Report 96-4067. Denver, CO: U.S. Geological Survey.

Harvey, R.W. and S. Garabedian. 1991. Use of Colloid Filtration Theory in Modeling the Movement of Bacteria Through a Contaminated Sandy Aquifer. Environmental Science and Technology, Vol. 25, pp. 178-185.

Harvey, R.W., L.H. George, R.L. Smith and D.R. Leblanc. 1989. Transport of Microspheres and Indigenous Bacteria Through a Sandy Aquifer: Results of Natural and Forced Gradient Tracer Tests. Environmental Science and Technology, Vol. 23, pp. 51-56.

Haschke, J.M., T.H. Allen and L. Morales. 2000. Reaction of Plutonium Dioxide with Water: Formation and Properties of PuO2+x. Science, Vol. 287, pp. 285-287.

Haschke, J.M. and T.E. Ricketts. 1997. Adsorption of Water on Plutonium Dioxide. Journal of Alloys and Compounds, Vol. 252, 148p.

Hem, J.D. 1985. Study and Interpretation of the Chemical Characteristics of Natural Water. U.S. Geological Survey Water Supply Paper 2254. Alexandria, VA: U.S. Geological Survey.

Heatherington, J.A. 1978. The Uptake of Plutonium Nuclides in Marine Sediments. Marine Science Communications Vol. 4, No. 3, 239p.

Higley, K.A. 1992. Vertical Movement of Actinide Contaminated Soil Particles. Ph.D. Dissertation, Dept. of Radiological Health Sciences, Colorado State University.

Honeyman, B.D. and P.H. Santschi. 1997. Actinide Migration Studies at the Rocky Flats Environmental Technology Site, Final Report. Golden, CO: Colorado School of Mines.

Honeyman, B.D., R. Harnish, T. McKibben, J. Spear and S. Winkler. 1999. Actinide Migration Studies at the Rocky Flats Technology Site: The Effect of Soil-Water Redox Potential on 239,240Pu Solubility. Final Report to Kaiser-Hill on Contract KH800022MW (Fiscal Year 1999). Golden, CO: Rocky Flats Environmental Technology Site.

Hsi, C-K. D. and D. Langmuir. 1985. Adsorption of Uranyl Onto Ferric Oxyhydroxides: Application of the Surface Complexation Site-Binding Model. Geochimica et Cosmochimica Acta, Vol. 49, pp. 1931-1941.

Idiz, E.F., D. Carlisle and I.R. Kaplan. 1986. Interaction Between Organic Matter and Trace Metals in a Uranium Rich Bog, Kern County, California, USA. Applied Geochemistry, Vol. 1, pp. 573-590.

Johnson, J.E., S. Svalberg and D. Paine. 1974. Study of Plutonium in Aquatic Systems of the Rocky Flays Environs, Final Technical Report from the Department of Animal Sciences and Radiology and Radiation Biology. Colorado State University for Dow Chemical Co. Golden, CO.

Kaplan, D.I., P.M. Bertsch, D.C. Adriano and W.P. Miller. 1993. Soil-Borne Mobile Colloids as Influenced by Water Flow and Organic Carbon. Environmental Science and Technology , Vol. 27, pp. 1193-1200.

Kaplan, D.I., P.M. Bertsch and K.A. Orlandini. 1994. Actinide Association With Groundwater Colloids in a Coastal Plain Aquifer. Radiochimica Acta, Vol. 66/67, 181p.

Kaplan, D.I. and R.J. Serne. 1995. Distribution Coefficient Values Describing Iodine, Neptunium, Selenium, Technetium and Uranium Sorption to Hanford Sediments. PNL-10379, Supplement 1. Richland, WA: Pacific Northwest Laboratory.

Kaplan, D.I., T.L. Gervais and K.M. Krupka. 1998. Uranium(VI) Sorption to Sediments Under High pH and Ionic Strength Conditions. Radiochimica Acta, Vol. 80, pp. 201-211.

Katz, J.J., G.T. Seaborg and L.R. Morss. 1986. The Chemistry of the Actinide Elements. Chapman and Hall, London

Keeney-Kennicutt, W.L. and J.W. Morse. 1985. The Redox Chemistry of Pu(V)O2+ Interaction with Common Mineral Surfaces in Dilute Solutions and Seawater. Geochimica Cosmochimica Acta, Vol. 49, pp. 2577-2588.

Kersting, A.B., D.W. Efurd, D.L. Finnegan, D.K. Rokop, D.K. Smith and J.L. Thompson. 1999. Migration of Plutonium in Groundwater at the Nevada Test Site. Nature, Vol. 397, pp. 56-59.

Kim, J.J., Ch. Lierse and F. Baumgartner. 1983. Complexation of the Plutonium(IV) Ion in Carbonate-Bicarbonate Solutions. In Plutonium Chemistry, eds. Carnall, W.T. and Choppin, G.R.. Washington, DC: American Chemical Society, pp. 317-333.

Kim, J.J. 1986. Chemical Behavior of Transuranic Elements in Aquatic Systems. In Handbook on the Physics and Chemistry of the Actinides, eds. A.J. Freeman and C. Keller. Amsterdam, Netherlands: Elsevier Science Publishers, pp. 413-455.

Kim, J.I. 1991. Actinide Colloid Generation in Groundwater. Radiochimica Acta, Vol. 52/53, 71p..

Kim, J.I., P. Zeh and B. Delakowitz. 1992. Chemical Interactions of Actinide Ions With Groundwater Colloids in Gorleben Aquifer Systems. Radiochimica Acta, Vol. 58/59, 145p.

Kim, J.J. 2000. Aquatic Chemistry of Actinides: Is a Thermodynamic Approach Appropriate to Describe Natural Dynamic Systems. In Plutonium Futures–The Science, Conference Transactions, eds. K.K.S. Pillay and K.C. Kim. Santa Fe, NM: American Institute of Physics.

Kita, S.F., H.S. Folger and M.G. Reed. 1987. Effect of pH on Colloidally Induced Fines Migration. Journal of Colloid and Interface Science, Vol. 118, pp. 158-168.

Knopp, R., V. Neck and J.I. Kim. 1999. Solubility, Hydrolysis and Colloid Formation of Plutonium (IV). Radiochimica Acta, No. 86, pp. 101-108.

Kovalevskii, A.L. 1967. Dependence of the Content of Some Trace Elements on the Clayiness of Soils. In Mikroelem. Biosfere Ikh Primen. Scl. Khoz. Med. Sib. Dal'nego Vostoka, Dokl. Sib. Knof. Ulan-Ude, USSR.:V. Makew. Buryat. Khizhn. lzd.

Krauskopf, K. 1979. Introduction to Geochemistry. New York: McGraw-Hill.

Krot, N.N. and A.D. Gel'man. 1967. Doklady Akademii Nauk SSSR, Vol. 177, No. 1, 124p.

Krupka, K.M. and R.J. Serne. 1998. Effects on Radionuclide Concentrations by Cement/Ground-Water Interactions to Support Performance Assessment of Low-Level Radioactive Waste Disposal Facilities. NUREG/CR-6377. Richland, WA: Pacific Northwest National Laboratory.

Langer, G. 1986. Dust Transport–Wind Blown and Mechanical Resupension, July 1983 to December 1984, Report RFP-3914. Golden, CO: Rockwell International, Rocky Flats Plant.

Langmuir, I. 1918. The Adsorption of Gases on Plane Surfaces of Glass, Mica and Platinum. Journal of the American Chemical Society, Vol. 40, pp. 1361-1403.

Langmuir, D. 1978. Uranium Solution-Mineral Equilibria at Low Temperatures with Applications to Sedimentary Ore Deposits. Geochimica et Cosmochimica Acta, Vol. 42, pp. 547-569.

Langmuir, D. 1997. Aqueous Environmental Chemistry. Upper Saddle River, NJ: Prentice Hall.

Lemire, R.J. and P.R. Tremaine. 1980. Uranium and Plutonium Equilibria in Aqueous Solutions to 200EC. Journal of Chemical Engineering Data, Vol. 25, pp. 361-370.

Leppard, G.G. 1992. Evaluation of Electron Microscope Techniques for the Description of Aquatic Colloids. In Environmental Particles, Vol. 1, eds. J. Buffle and H. P. van Leeuwen. Boca Raton, FL: Lewis Publishers, pp. 231-290.

Lieser, K.H. and R. Hill. 1992. Hydrolysis and Colloid Formation of Thorium in Water and Consequences for its Migration Behavior, Comparison With Uranium. Radiochimica Acta, Vol. 56, 37p.

Lide, David R., ed. 1990. CRC Handbook of Chemistry and Physics. Boca Raton, FL: CRC Press.

Lindsay, W.L. 1979. Chemical Equilibria in Soils. New York: J. Wiley and Sons.

Litaor, M.I., M.L. Thompson, G.R Barth and P.C. Molzer. 1994. Plutonium 239 + 240 and Americium-241 in Soils East of Rocky Flats. Journal of Environmental Quality, Vol. 23, pp. 1231-1239.

Litaor, M.I. 1995. Uranium Isotopes Distribution in Soils at the Rocky Flats Plant, Colorado. Journal of Environmental Quality, Vol. 24, pp. 314-323.

Litaor, M.I. and L. Allen. 1996. Comprehensive Appraisal of Am-241 in Soils of Colorado, Colorado. Health Physics, Vol. 70, pp. 1213-1233.

Litaor, M.I. and S.A. Ibrahim. 1996. Plutonium Association with Selected Solid Phases in Soils of Rocky Flats, Colorado, Using Sequential Extraction Technique. Journal of Environmental Quality, Vol. 25, pp. 1144-1152.

Litaor, M.I., G.R Barth and E.M. Zika. 1996. Fate and Transport of Plutonium -239,240 and Americium-241 in the Soil of Rocky Flats, Colorado. Journal of Environmental Quality Vol. 25, pp. 671-683.

Litaor, M.I., G.R Barth, E.M. Zika, G. Litus, J. Moffitt and H. Daniels. 1998. The Behavior of Radionuclides in the Soil of Rocky Flats, Colorado. Journal of Environmental Radioactivity, Vol. 38, No. 1, pp. 17-46.

Little, C.A. 1980. Plutonium in a Grassland Ecosystem. In Transuranic Elements in the Environment, ed. W.C. Hanson. Washington DC: Technical Information Center/U.S. Department of Energy.

Little, C.A. and F.W. Whicker. 1977. Plutonium Distribution in Rocky Flats Soil. Health Physics, Vol. 34, pp. 451-457.

Little, C.A., F.W. Whicker and T.F. Winsor. 1980. Plutonium in a Grassland Ecosystem at Rocky Flats. Journal of Environmental Quality, Vol. 9, No. 3, pp. 350-354.

Livens, F.R., M.S. Baxter and S.E. Allen. 1986. Physico-chemical Associations of Plutonium in Cumbrium Soils. In Speciation of Fission and Activation Products in the Environment, eds. R.A. Bulman and J.R. Cooper. Amsterdam, Netherlands: Elsevier, pp.143-150.

Livingston, H.L. and V.T. Bowen. 1976. Americium in the Marine Environment: Relationships to Plutonium. In Environmental Toxicity of Aquatic Radionuclides: Models and Mechanisms, eds. M.W. Miller and J.N. Stannard. Ann Arbor, MI: Ann Arbor Science Publishers.

Luhrmann, I., U. Noseck and C. Trix. 1998. Model of Contaminant Transport in Porous Media in the Presence of Colloids Applied to Actinide Migration in Column Experiments. Water Resources Research, Vol. 34, pp.421.

Madic, C. 2000. Toward the End of PuO2's Supremacy. Science, Vol. 287, pp. 243-244.

Marley, N.A., J.S. Gaffney, K.A. Orlandini, K.A. and M.M. Cunningham. 1993. Evidence For Radionuclide Transport and Mobilization in a Shallow, Sandy Aquifer. Environmental Science and Technology, Vol. 27, pp. 2456-2461.

Marty, R.C., D. Bennet and P. Tullen, P. 1997. Mechanism of Plutonium Transport in a Shallow Aquifer in Mortandad Canyon, Los Alamos National Laboratory, New Mexico. Environmental Science and Technolgy, Vol. 31, pp. 2020.

McCarthy, J.F. and J.M. Zachara. 1989. Subsurface Transport of Contaminants. Environmental Science and Technology, Vol. 23, pp. 496-502.

McCarthy, J.F. 1998. Colloid-Facilitated Transport of Contaminants in Groundwater: Mobilization of Transuranic Radionuclides From Disposal Trenches by Natural Organic Matter. Physics and Chemistry of the Earth, Vol. 23, p.171.

383

McCarthy, J.F., W.E. Sanford and P.L. Stafford. 1998. Lanthanide Field Tracers Demonstrate Enhanced Transport of Transuranic Radionuclides by Natural Organic Matter. Environmental Science and Technology, Vol. 32, pp. 3901-3906.

McDowell, L.M. and F.W. Whicker. 1978. Size Characteristics of Plutonium Particles in Rocky Flats Soils. Health Physics, Vol. 35, No. 293-299.

McDowell-Boyer, L.M., J.R. Hunt and N. Sitar. 1986. Particle Transport Through Porous Media. Water Resources Research, Vol. 22, pp. 1901-1921.

McDowell-Boyer, L.M. 1992. Chemical Mobilization of Micron-Sized Particles in Saturated Porous Media Under Steady Flow Conditions. Environmental Science and Technology, Vol. 26, pp. 586-593.

McLeod, K.W., D.C. Adriano, A.L. Boni, J.C. Corey, J.H. Horton, D. Paine and J.E. Pinder III. 1980. Influence of a Nuclear Fuel Chemical Separations Facility on the Plutonium Contents of a Wheat Crop. Journal of Environmental Quality, Vol. 9, No. 2, pp. 306-315.

McKinley, J.P., J.M. Zachara, S.C. Smith and G.D. Turner. 1995. The Influence of Uranyl Hydrolysis and Multiple Site-Binding Reactions on Adsorption of U(VI) to Montmorillonite. Clays and Clay Minerals, Vol. 43, No. (5), pp. 586-598.

Meijer, A. 1992. The Yucca Mountain Project Far-field Sorption Studies and Data Needs. Los Alamos National Laboratory Report, LA-11671-MS. Los Alamos, NM: Los Alamos National Laboratory.

Moody, J.S. and J.L. Morse. 1992. Final Report for the State Indoor Radon Grant, Jefferson County Health Department, CO. Golden, CO: Jefferson County Health Department.

Morris, D.E., C.J. Chisholm-Brause, M.E. Barr, S.D. Conradson and P.G. Eller. 1994. Optical Spectroscopic Studies of the Sorption of UO22+ Species on a Reference Smectite. Geochimica et Cosmochimica Acta, Vol. 58, pp. 3613-3623.

Moulin, V., J. Tits and G. Ouzounian. 1992. Actinide Speciation in the Presence of Humic Substances in Natural Water Conditions. Radiochimica Acta, Vol. 58/59, pp. 179-190.

Moyes, L.N., R.H. Parkman, J.M. Charnock, D.J. Vaughan, F.R. Livens, C.R. Hughes and A. Braithwaite. 2000. Uranium Uptake from Aqueous Solution by Interaction with Goethite, Lepidocrocite, Muscovite and Mackinawite: An X-ray Absorption Spectroscopy Study. Environmental Science and Technology, Vol. 34, pp. 1062-1068.

Muramatsu, Y., W. Rühm, S. Yoshida, K. Tagami, S. Uchida and E. Wirth. 2000. Concentrations of 239Pu and 240Pu and Their Isotopic Ratios Determined by ICP-MS in Soils Collected from the Chernobyl 30-km Zone. Environmental Science and Technology, Vol. 34, pp. 2913-2917.

Myrick, T.E., B.A. Berven and F.F. Haywood. 1983. Determination of Concentration of Selected Radionuclides in Surface Soil in the U.S. Health Physics, Vol. 45, No. 3, pp. 631-641.

Nagasaki, S., S. Tanaka and A. Suzuki. 1994. Colloid Formation and Sorption of Americium in the Water/Bentonite System. Radiochimica Acta, Vol. 66/67, 207p.

Nagasaki, S., S. Tanaka and A. Suzuki 1997, Interfacial Behavior of Actinides with Colloids in the Geosphere. Journal of Nuclear Materials, Vol. 248, pp.323.

Nash, K., S. Fried, A.M. Freidman and J.C. Sullivan 1981, Redox Behavior, Complexing and Adsorption of Hexavalent Actinides by Humic Acid and Selected Clays. Environmental Science and Technology, Vol. 15, pp. 834-837.

Nelson D.M. and K.A. Orlandini. 1979. Identification of Pu(V) in Natural Waters. ANL-79-65. Argonne, IL: Argonne National Laboratory.

Nelson D.M. and K.A. Orlandini. 1986. The Role of Natural Dissolved Organic Compounds in Determining the Concentrations of Americium in Natural Waters. In Speciation of Fission and Activation Products in the Environment, eds. R.A. Bulman and J.R. Cooper. Amsterdam, Netherlands: Elsevier, pp. 262-268.

Nelson, D.M. and M.B. Lovett. 1980. Measurements of the Oxidation State and Concentration of Plutonium in Interstitial Waters in the Irish Sea. In Impacts of Radionuclide Releases into the Marine Environment, ed. IAEA Staff, 105-118. Vienna, Austria: International Atomic Energy Agency.

Nelson, D.M., R.P. Larson and W.R. Penrose. 1987. Chemical Speciation of Plutonium in Natural Waters. In Environmental Research on Actinide Elements, eds. J.E. Pinder, J.J. Alberts, K.W. McLeod and R. Gene Schreckhise. Washington, DC: Office of Scientific and Technical Information, U.S. Department of Energy, pp. 27-48.

Neretnieks, I. 1982. Prediction of Radionuclide Migration in the Geosphere: Is the Porous-flow Model Adequate? In The Environmental Migration of Long-lived Radionuclides, Proceedings of an International Symposium on Migration in the Terrestrial Environment of Long-Lived Radionuclides From the Nuclear Fuel Cycle Organized by the International Atomic Energy Agency, the CEC and the Organisation for Economic Co-operation and Development Nuclear Energy Agency and Held in Knoxville, TN, 27-31 July 1981. Vienna, Austria: International Atomic Energy Agency, pp. 635-657.

Neu, M., W. Runde, M.A. Lin, D.M. Smith, S.D. Conradson and A. Wong. 1999. Plutonium Speciation and Distribution in Soil Samples from the Rocky Flats Environmental Test Site. Los Alamos, NM: Los Alamos National Laboratory.

Nitsche, H., K. Roberts, T. Prussin, A. Muller, K. Becraft, D. Keeney, S.A. Carpenter and R.C. Gatti. 1994. Measured Solubilities and Speciations from Oversaturation Experiments of Neptunium, Plutonium and Americium in UE-25p #1 Well Water from the Yucca Mountain Region, Milestone Report. LA-12563-MS. Los Alamos, NM: Los Alamos Nuclear Laboratory.

Organisation for Economic Co-operation and Development Nuclear Energy Agency (OECD/NEA). 1981. The Environmental and Biological Behavior of Plutonium and Some Other Transuranium Elements. Paris: OECD Nuclear Energy Agency.

O'Melia, C.R. 1987. Particle-particle Interactions. In Aquatic Surface Chemistry, ed. W. Stumm. New York: John Wiley and Sons, pp. 385-403.

Orlandini, K.A., W.R. Penrose, B.R. Harvey, M.B. Lovett and M.W. Findlay. 1990. Colloidal Behavior of Actinides in an Oligotrophic Lake. Environmental Science and Technology, Vol. 24, pp. 706-712.

Palmer, D.A and C. Nguyen-Trung. 1995. Journal of Solution Chemistry, Vol. 24, No. 12, pp. 1281-1291.

Penrose, W.R., W.L. Polzer, E.H. Essington, D.M. Nelson and K.A. Orlandi. 1990. Mobility of Plutonium and Americium Through a Shallow Aquifer in a Semiarid Region. Environmental Science and Technology, Vol. 24, pp. 228-234.

Pillai, K.C. and E. Mathew. 1976. Plutonium in the Aquatic Environment: Its Behavior, Distribution and Significance. In Transuranium Nuclides in the Environment, STI/PUB/410. Vienna, Austriaa: International Atomic Energy Agency (IAEA).

Pinder, J.E. III, K.W. McLeod, D.C. Adriano, J.C. Corey and A.L. Boni. 1990. Atmospheric Deposition, Resuspension and Root Uptake of Pu in Corn and Other Grain-Producing Agroecosystems Near a Nuclear Fuel Facility. Health Physics, Vol. 59, No. (6), pp. 853-867.

Polzer, W.L. and E.H. Essington. 1992. The Physical and Chemical Characterization of Radionuclides in the Surface Waters at Rocky Flats Plant. LA-UR-92-1812. Los Alamos, NM: Los Alamos Nuclear Laboratory.

Povetko, O.G. and K.A. Higley. 2000. Study of Particles of Actinides in Soil Samples Using Nuclear Track Detectors. Poster presented at Health Physics Society Meeting, Denver, CO. McLean, VA: Health Physics Society.

Puls, R. and R. Powell. 1992. Transport of Inorganic Colloids Through Natural Aquifer Material: Implications For Contaminant Transport. Environmental Science and Technology, Vol. 26, pp. 614-621.

Purtymun, W.D., R.J. Peters and M.N. Maes. 1990. Plutonium Deposition and Distribution from Worldwide Fallout in Northern New Mexico and Southern Colorado. LANL Report LA-11794-MS. Los Alamos, NM: Los Alamos National Laboratory.

Rai, D., R.J. Serne and D.A. Moore. 1980a. Solubility of Plutonium Compounds and Their Behavior in Soils. Soil Science Society of America Journal, Vol. 44, pp. 490-495.

Rai D., R.J. Serne and J.L. Swanson. 1980b. Solution Species of Plutonium in the Environment. Journal of Environmental Quality, Vol. 9, pp. 417-420.

Rai, D. and J.M. Zachara. 1984. Chemical Attenuation Rates, Coefficients and Constants in Leachate Migration. Volume 1: A Critical Review. EPRI EA-3356, Volume 1. Palo Alto, CA: Electric Power Research Institute.

Ranville, J.F. and Schmiermund. 1999. General Aspects of Aquatic Colloids in Environmental Geochemistry. In Geochemisty of Mineral Deposits, ed. G. Plumblee, Volume 6. Littleton, CO: Society of Economic Geologists.

Ranville, J.F., R.A. Harnish and D.M. McKnight. 1991. Particulate and Colloidal Organic Matter in Pueblo Reservoir, Colorado: Influence of Autochthonous Source on Chemical Compositon. In Organic Substances and Sediments in Water Vol. 1, ed. R. Baker. Chelsea, MI: Lewis Publishers, pp. 47-74.

Ranville, J.F., R.A. Harnish, S. Winkler and B. D. Honeyman. 2000. Soil Aggregation and Its Influence on Pu Particle-Size Distributions of Soils Collected From Rocky Flats, CO, Final Report to EPA Region VIII. Denver, CO: Environmental Protection Agency.

Read, D., T.A. Lawless, R.J. Sims and K.R. Butter. 1993. Uranium Migration Through Intact Sandstone Cores. Journal of Contaminant Hydrology, Vol. 13, pp. 277-289.

Reible, D.D., K.T. Valsara and L.J. Thibodeaux. 1991. Chemodynamic Models for Transport of Contaminants From Sediment Beds. In The Handbook of Environmental Chemistry, Vol. 2, Part F, Reactions and Processes, ed. O. Hutzinger. New York: Springer-Verlag, pp. 185-228.

Reilly, S.D., M.P. Neu and W. Runde. 2000. Solubility and Speciation of Plutonium (VI) Carbonates and Hydroxides. In Plutonium Futures, The Science, Conference Transactions, eds. K.K.S. Pillay and K.C. Kim. College Park, MD: American Institute of Physics.

Rocky Flats Environmental Technology Site (RFETS). 1998. Conceptual Model for Actinide Migration Studies at the Rocky Flats Environmental Technology Site. Golden, CO: Rocky Flats Environmental Technology Site.

387

Rocky Mountain Remediation Services (RMRS). 1998a. Actinide Content and Aggregate Size Analyses for Surface Soil in the Walnut Creek and Woman Creek Watershed at the Rocky Flats Environmental Technology Site. RF/RMRS-98-281.UN. Golden, CO: Rocky Flats Environmental Technology Site.

RMRS. 1998b. 1998 Annual Rocky Flats Cleanup Agreement (RFCA) Groundwater Monitoring Report for the Rocky Flats Environmental Technology Site. RF/RMRS-99-433.UN. Golden, CO: Rocky Flats Environmental Technology Site.

RMRS. 2000. Characterization Report for the 903 Drum Storage Area, Lip Area and Americium Zone. RF/RMRS-99-427.UN Rev. 1. June 26, 2000. Final. Golden, CO: Rocky Flats Environmental Technology Site.

Runde, W. 2000. The Chemical Interactions of Actinides in the Environment. In Challenges in Plutonium Science, Volume 2, Editor, Necia Grant Cooper, Los Alamos Science, Number 26, LA-UR-00-4100, Los Alamos National Laboratory, Los Alamos, NM. www.lanl.gov/external/science/lascience/index.html

Runde, W., D. Efurd, M.P. Neu, S.D. Reilly, C. VanPelt and S.D. Conradson. 2000. Plutonium in the Environment: Speciation, Solubility and the Relevance of Pu(VI). In Plutonium Futures, The Science, Conference Transactions, eds. K.K.S. Pillay and K.C. Kim. College Park, MD: American Institute of Physics.

Ryan, J.N. and M. Elimelech. 1996. Colloid Mobilization and Transport in Groundwater. Colloids and Surfaces A, Physicochemical and Engineering Aspects, Vol. 107, pp. 1-56.

Ryan, J.N., T.H. Illangasekare, M.I. Litaor and R. Shannon. 1998. Particle and Plutonium Mobilization in Macroporous Soils During Rainfall Simulations. Environmental Science and Technology, Vol. 32, pp. 476-482.

Salomons, W. and W. Foerstner. 1984. Metals in the Hydrocycle. New York: Springer-Verlag.

Salter, P.F., L.L. Ames and J.E. McGarrah. 1981a. The Sorption Behavior of Selected Radionuclides on Columbia River Basalts. RHO-BWI-LD-48. Richland, WA: Rockwell Hanford Operations.

Salter, P.F., L.L. Ames and J.E. McGarrah. 1981b. Sorption of Selected Radionuclides on Secondary Minerals Associated with the Columbia River Basalts. RHO-BWI-LD-43. Richland, WA: Rockwell Hanford Operations.

Sanchez, A.L., J.W. Murray and T.H. Sibley. 1985. The Adsorption of Pu(IV) and Pu(V) on Goethite. Geochimica et Cosmochimica Acta, Vol. 49, pp. 2297-2307.

Sandino, A. and J. Bruno. 1992. The Solubility of $(UO_2)_3(PO_4)_2 \cdot 4H_2O(s)$ and the Formation of U(VI) Phosphate Complexes: Their Influence on Uranium Speciation in Natural Waters. Geochimica et Cosmochimica Acta, Vol. 56, pp. 4135-4145.

Santschi, P.H. 1998. Final Report on Phase Speciation of Pu and Am for "Actinide Migration Studies at the Rocky Flats Environmental Technology Site. Golden, CO: Rocky Flats Environmental Technology Site.

Santschi, P.H., K. Roberts and L. Guo. 1999. Final Report on Phase Speciation of Pu and Am for Actinide Migration Studies at the Rocky Flats Environmental Technology Site. Galveston, TX: Texas A&M University.

Santschi, P.H., K. Roberts and L. Guo. 2000. Final Report on Phase Speciation of Pu and Am for Actinide Migration Studies at the Rocky Flats Environmental Technology Site. Galveston, TX: Texas A&M University.

Satmark, B.A., Y. Albinsson and L. Liang. 1996. Chemical Effects of Goethite Colloid on the Transport of Radionuclides Through a Quartz-Packed Column. Journal of Contaminant Hydrology, Vol. 21, 231p.

Schuessler, W., R. Artinger and J. Kim. 2000. Conceptual Modeling of the Humic Colloid-Borne Americium (III) Migration by a Kinetic Approach. Environmental Science and Technology, Vol. 34, pp. 2608-2611.

Schwantes, J.M. and B. Batchelor. 2000. Equilibrium, Kinetic and Reactive Transport Models for Pu: Employing Numerical Methods to Uncover the Nature of the Intrinsic Colloid. In Plutonium Futures, The Science, Conference Transactions, eds. K.K.S. Pillay and K.C. Kim. College Park, MD: American Institute of Physics.

Seaborg, Glenn T. 1958. The Transuranium Elements. New Haven, NJ: Yale University Press.

Seaborg, Glenn and Walter Loveland. 1990. The Elements Beyond Uranium. New York: John Wiley.

Seed, J.R., K.W. Calkins, C.T. Illsley, F.J. Miner and J.B. Owen. 1971. Committee Evaluation of Pu Levels in Soils Within and Surrounding USAEC Installation at Rocky Flats, Colorado. RFP-INV-1. Golden, CO: DOW Chemical Company.

Serkiz, S. M. and W. H. Johnson. 1994. Uranium Geochemistry in Soil and Groundwater at the F and H Seepage Basins (U). EPD-SGS-94-307. Aiken, SC: Westinghouse Savannah River Company, Savannah River Site.

Shanbhag, P.M. and G.R. Choppin. 1981. Binding of Uranyl by Humic Acid. Journal of Inorganic Nuclear Chemistry, Vol. 43, pp. 3369-3372.

Sheppard, J.C., J.A. Kittrick and T.L. Hart. 1976. Determination of Distribution Ratios and Diffusion Coefficients of Neptunium, Americium and Curium in Soil-Aquatic Environments. RTO-221-T-12-2. Richland, WA: Rockwell Hanford Operations.

Sigg, L. 1985. Metal Transfer Mechanisms in Lakes-Role of Settling Particles. In Chemical Processes in Lakes, W. Stumm, ed. New York: John Wiley and Sons, pp. 283-310.

Silva, R.J., G. Bidoglio, M.H. Rand, P.B. Robouch, H. Wanner, I. Puigdomenech. 1995. Chemical Thermodynamics of Americium. Elsevier Publishing Co. Amsterdam, Netherlands.

Silva, R.J. and H. Nitsche. 1995. Actinide Environmental Chemistry. Radiochimica Acta, Vol. 70/71, pp. 377-396.

Silver, G.L. 1983. Comment on the Behavior of the Chemical Forms of Plutonium in Seawater and Other Aqueous Solutions. Marine Chemistry, Vol. 12, pp. 91-96.

Simpson. H.J., R.M. Trier, Y.H. Li, R.F. Anderson and A.L. Herczeg. 1984. Field Experiment Determinations of Distribution Coefficient of Actinide Elements in Alkaline Lake Environments. NUREG/CR-3940. Palisades, NY: Columbia University.

Smith, P.A. and C. Degueldre. 1996. Colloid-Facilitated Radionuclide Transport in Fractured Porous Rock. Waste Management, Vol. 16, 313p.

Sposito, G. 1984. The Surface Chemistry of Soils. New York: Oxford University Press.

Sposito, G. 1989. The Chemistry of Soils. New York: Oxford University Press.

Stakebake, J.L., D.T. Larsen and J.M. Haschke. 1993. Characterization of the Plutonium-water Reaction II: Formation of a Binary Oxide Containing Pu(VI). Journal of Alloys and Compounds, Vol. 202, pp. 251-263.

Strenge, D.L. and S.R. Peterson. 1989. Chemical Databases for the Multimedia Environmental Pollutant Assessment System. PNL-7145. Richland,WA: Pacific Northwest Laboratory.

Stumm, W. and J.J. Morgan. 1996. Aquatic Chemistry. New York: Wiley-Interscience.

Szalay, A. 1964. Cation Exchange Properties of Humic Acids and their Importance in the Geochemical Enrichment of UO22+ and Other Cations. Geochimica et Cosmochimica Acta, Vol. 28, pp. 1605-1614.

Tait, C.D., S.A. Ekberg, P.D. Palmer and D.E. Morris. 1995. Plutonium Carbonate Speciation Changes as Measured in Dilute Solutions with Photoacoustic Spectroscopy. LA-12886-MS. Los Alamos, NM: Los Alamos National Laboratory.

Tamura, T. 1977. Effect of Pretreatment on the Size Distribution of Plutonium in Surface Soil from Rocky Flats. In Transuranics in Desert Systems, NVO-1871 UC-11. Las Vegas, NV: Nevada Applied Ecology Group, pp. 173-186.

Tanka, S. and S. Nagasaki. 1997. Impact of Colloid Generation on Actinide Migration in High-Level Radioactive Waste Disposal: Overview and Laboratory Analysis. Nuclear Technology, Vol. 118, p. 58.

Thibault, D.H., M.I. Sheppard and P.A. Smith. 1990. A Critical Compilation and Review of Default Soil Solid/Liquid Partition Coefficients, Kd, for Use in Environmental Assessments. AECL-10125. Pinawa, Canada: Whiteshell Nuclear Research Establishment, Atomic Energy of Canada Limited.

Ticknor, K.V. 1993. Actinide Sorption by Fracture-Filling Minerals. Radiochimica Acta, Vol. 60, pp. 33-42.

Tipping, E. and D. Cooke. 1982. The Effects of Adsorbed Humic Substances in the Surface Charge of Goethite (a-FeOOH) in Freshwaters. Geochimica et Cosmochimica Acta, Vol. 46, pp. 75-80.

Tipping, E. and D.C. Higgins. 1982. The Effect of Adsorbed Humic Substances on the Colloid Stability of Hematite Particles. Colloids and Surfaces, Vol. 5, pp. 85-92.

Torok, J., L.P. Buckley and B.L. Woods. 1990. The Separation of Radionuclide Migration by Solution and Particle Transport in LLRW Repository Buffer Material. Journal of Contaminant Hydrology,

Torok, J., L.P. Buckley and B.L. Woods. 1990. The Separation of Radionuclide Migration by Solution and Particle Transport in Soil. Journal of Contaminant Hydrology, Vol. 6, No. 2, pp. 185.

Toth, L.M., Friedman, H.A. and M.M. Osborne. 1983. Aspects of Plutonium(IV) Hydrous Polymer Chemistry. In Plutonium Chemistry, eds. W.T. Carnall and G.R. Choppin. Washington, DC: American Chemical Society, pp. 231-240.

Tripathi, V.S. 1984. Uranium(VI) Transport Modeling: Geochemical Data and Submodels. Ph.D. Dissertation, Stanford University, Stanford, CA.

Turner, D.R., S. Knox, F. Penedo, J.G. Titley, J. Hamilton-Taylor, M. Kelley and G. Williams. 1991. Surface Complexation Modelling of Plutonium Absorption on Sediments of the Esk Estuary, Cumbria. In Radionuclides in the Study of Marine Processes, eds. P.J. Kershaw and D.S. Woodhead. London: Elsevier, pp. 165-174.

Turner, G.D., J.M. Zachara, J.P. McKinley and S.C. Smith. 1996. Surface-Charge Properties and UO22+ Adsorption of a Subsurface Smectite. Geochimica et Cosmochimica Acta, Vol. 60, No. 18, pp. 3399-3414.

Uranium Information Centre Ltd. 1997. Smoke Detectors and Americium. Nuclear Issues Briefing Paper 35. Melbourne, Australia: Uranium Information Centre Ltd.

391

Waite, T.D., T.E. Payne, J.A. Davis and K. Sekine. 1992. Alligators Rivers Analogue Project, Final Report Volume 13, Uranium Sorption.

Waite, T.D., J.A. Davis, T.E. Payne, G.A. Waychunas and N. Xu. 1994. Uranium(VI) Adsorption to Ferrihydrite: Application of a Surface Complexation Model. Geochimica et Cosmochimica Acta, Vol. 58, No. 24, pp. 5465-5478.

Warner, F. and R.M. Harrison, eds. 1993. Radioecology After Chernobyl. New York: John Wiley & Sons.

Watters, R.L., D.N. Edgington, T.E. Hakonson, W.C. Hanson, M.H. Smith, F.W. Whicker and R.E. Wildung. 1980. Synthesis of the Research Literature, In Transuranic Elements in the Environment, ed. W.C. Hanson, DOE/TIC-228000. Washington, DC: U.S. Department of Energy, National Technical Information Service.

Watters, R.L., T.E. Hakonson and L.J. Lane. 1983. The Behavior of Actinides in the Environments. Radiochimica Acta, Vol. 22, pp. 89-103.

Weiner, E.R.. 2000. Applications of Environmental Chemistry: A Practical Guide for Environmental Professionals. Boca Raton, FL: Lewis Publishers.

Westall, J. C., J. L. Zachary and F. M. M. Morel. 1976. MINEQL, A Computer Program for the Calculation of Chemical Equilibrium Composition of Aqueous Systems. Technical Note 18, Department of Civil Engineering. Cambridge, MA: Massachusetts Institute of Technology.

Whicker, F.W. and V. Schultz. 1982. Radioecology: Nuclear Energy and the Environment", Vol. 1 and 2. Boca Raton, FL: CRC Press, Inc.

Wilkinson, K.J., A. Joz-Roland and J. Buffle. 1997. Different Roles of Pedogenic Fulvic Acids and Aquagenic Biopolymers on Colloid Aggregation and Stability in Freshwaters. Limnology and Oceanography, Vol. 42, pp. 1714-1724.

Wulfsberg, Gary. 1987. Principles of Descriptive Inorganic Chemistry. Brooks/Cole Publishing Co. Monterey, CA. 461p.

Yamaguchi, T., Y. Sakamoto and T. Ohnuki. 1994. Effect of the Complexation on Solubility of Pu(IV) in Aqueous Carbonate System. Radiochimica Acta, Vol. 66/67, pp. 9-14.

Yao, K., M.T. Habibian and C.R. O'Melia. 1971. Water and Wastewater Filtration-Concepts and Applications. Environmental Science and Technology, Vol. 5, pp. 1105-112.

Yeh, G. and V.S. Tripathi. 1991. A Model for Simulating Transport of Reactive Multispecies Components: Model Development and Demonstration. Water Resources Research, Vol. 27, pp. 3075-3094.

Biogeochemistry References (Section TA-3.9)

Abdelouas, A., W. Lutze and H. E. Nuttall. 1999. Uranium Contamination on the Subsurface: Characteriation and Remediation. In: Uranium: Mineralogy, Geochemistry and the Environment. P. C. Burns and R. Finch, eds. Mineralogical Society of America, Wash. DC. pp. 433-473.

Babich, H. and G. Stotzky. 1985. Heavy Metal Toxicity to Microbe-mediated Ecologic Processes: a Review and Potential Application to Regulatory Policies. Environ. Resources, Vol. 36, p. 111.

Beveridge, T. J. and R.J. Doyle. 1989. Metal Ions and Bacteria, John Wiley and Sons, New York, NY.

Birch, L. and R. Bachofen. 1990. Complexing Agents from Microorganisms, Experientia, Vol. 46, p.827.

Bomstein, R. A. 1972. Waste Treatment with Microbial Nucleoprotein Flocculating Agent. U.S. Patent No. 3, Vol. 684, p. 706.

Bondietti, E. A., S.A. Reynolds and M.H. Shanks. 1976. Interaction of Plutonium with Complexing Organics in Soils and Natural Waters, in Transuranium Nuclides in the Environment. I.A.E.A. Vienna, Austria.

Bossier, P., M. Hofte and W. Verstraete. 1988. Ecological Significance of Siderophores in Soil. Adv. Microbiol. Ecol., Vol. 10, p. 385.

Brown, C. M., D.C. Ellwood and J.R. Hunter. 1977. Growth of Bacteria at Surfaces: Influence of Nutrient Limitations. FEMS Microbiol. Lett., Vol. 1, p. 163.

Brown, M. J. and J.N. Lester. 1979. Metal Removal in Activated Sludge: The Role of Extra-cellular Polymers. Water Research, Vol. 13, p. 817.

Buddemeier, R. W. and J.R. Hunt. 1988. Transport of Colloidal Contaminants in Groundwater: Radionuclide Migration at the Nevada Test Site, Appl. Geochem., Vol. 3, p. 535.

Burdige, D. J. 1993. The Biogeochemistry of Manganese and Iron Reduction in Marine Sediments. Earth Sci. Rev., Vol. 35, p. 249.

Chen, J. -H., D.R. Czajka, L.W. Lion, M.L. Shuler and W.C. Ghiorse. 1995. Trace Metal Metabolization in Soil by Bacterial Polymers. Environ. Health. Persp., Vol. 103, pp. 53-58.

Clark, D. L., Watkin, J. G., D.E. Morris. and J.M. Berg. 1990. Molecular Models for Actinide Speciation, Los Alamos National Laboratory Report, LA-12780-MS, UC-802.

393

Davidson, W. 1993. Iron and Manganese in Lakes. Earth Sci. Rev., Vol. 34, No. 119.

Davis, J. A. and J. Leckie. 1978. Effects of Adsorbed Complexing Ligands on Trace Metal Uptake by Hydrousoxides. Environ. Sci. Tech., Vol. 12, p. 1309.

Duxbury, T. 1985. Ecological Aspects of Heavy Metal Responses in Microorganisms. In, Advances in Microbial Ecology. Marshall, K. C. Eds. Plenum Press, New York, NY., Vol. 8, pp. 185-235.

Dwyer, F. P. and D.P. Mellor. 1964. Chelating Agents and Metal Chelates, Academic Press, New York, NY.

Erlich, H. L. 1990. Geomicrobiology. Marcel Dekker, Inc. New York, NY.

Faison, B. D., C.A. Cancel, S.N. Lewis and H.I. Adler. 1996. Binding of Dissolved Strontium by Micrococcus Luteus. Appl. Environ. Microbiol., Vol. 56, p. 3649.

Fowle, D. A., J. B. Fein and A. M. Martin. 2000. Experimental Study of Uranyl Adsorption onto Bacillus subtilis. Environ. Sci. Technol., Vol. 34, p. 3737.

Francis, A. J. 1982. Microbial Transformation of Low-level Radioactive Waste, in Environmental Migration of Long-Lived Radionuclides. I.A.E.A. Report. SM-257/72.

Francis, A. J. 1990. Characteristics of Nuclear and Fossil Energy Wastes. Experientia, Vol. 46, p. 794.

Francis, A. J. 1998. Biotransformation of Uranium and Other Actinides in Radioactive Wastes. J. Alloys and Compounds. Vol. 71-73, p. 78.

Francis, A. J. and C.J. Dodge. 1993. Influence of Complex Structures on the Biodegradation of Iron-citrate Complexes. Appl. Environ. Microbiol., Vol. 59, p. 109.

Francis, A. J., C. J. Dodge, J. B. Gillow and H. W. Papenguth. 2000. Biotransformation of Uranium Compounds in High Ionic Strength Brine by a Halophilic Bacterium Under Denitrifying Conditions. Environ. Sci. Technol. Vol. 34, p. 2311.

Francis, A. J., C. J. Dodge, J. B. Gillow and J. E. Cline. 1991. Microbial Transfromations of Uranium in Wastes. Radiochim Acta., Vol. 52, p. 311.

Francis, A. J., C.J. Dodge, F. Lu, G.P. Halada and C.R. Clayton. 1994. XPS and XANES Studies of Uranium Reduction by Clostridium Sp. Environ. Sci. Technol., Vol. 28, p. 636.

Francis, A. J., J. B. Gillow, C. J. Dodge, M. Dunn, K. Mantione, B. A. Strietelmeier, M. E, Pansoy-Hjelvik and H. W. Papenguth. 1998. Role of Bacteria as Biocolloids in the Transport of Actinides from a Deep Underground Radioactive Waster Repository. Radiochim. Acta., Vol. 82, p. 347.

394

Fredrickson, J. K., H. M. Kostandarithes, S. W. Li, A. E. Plymale and M. J. Daly. 2000. Reduction of Fe(III), Cr(VI), U(VI) and Tc(VII) by Deinococcus Radiodurans R1. Appl. Environ. Microbiol., Vol. 66, p. 2006.

Fredrickson, J., K., J. M. Zachara, D. W. Kennedy, M. C. Duff, Y. A. Gorby, S-M. Li and K. M. Krupka. 2000. Reduction of U(VI) in Goethite (α-FeOOH) Suspensions by a Dissimilatory Metal-reducing Bacterium. Geochim. Cosmochim. Acta. Vol. 64, p. 3085.

Gadd, G. M. 1990. Heavy Metal Accumulation by Bacteria and Other Microorganisms. Experientia, Vol. 46, p. 834.

Garcia Junior, O. 1993. Bacterial Leaching of Uranium Ore from Figueira-PR, Brazil, at Laboratory and Pilot Scale. FEMS Microbiol. Rev., Vol. 11, p. 237.

Geesey, G. G. and L. Jang. 1981. Interactions Between Metal Ions and Capsular Polymers. Metal Ions and Bacteria, Beveridge, T. J. and Doyle, R. J., Eds, John Wiley and Sons, New York, NY, p. 325.

Giesy, J. P. and D. Paine. 1977. Appl. Environ. Microbiol., Vol. 33, p. 89.

Giesy, J. P., G.T. Leversee and D.R. Williams. 1977. Effects of Naturally Occurring Aquatic Fractions of Cadmium Toxicity to Simomcephalus Serrulatus (Daphnidae) and Ambusia Affinis (Poecilliidae), Water Res., Vol. 11, p. 1013.

Gillow, J. B., M. Dunn, A. J. Francis, D. A. Lucero and H. W. Papenguth. 2000. The Potential of Subterranean Microbes in Facilitating Actinide Migration at the Grimsel Test Site and Waste Isolation Pilot Plant. Radiochim. Acta., Vol. 88, p. 769.

Gorby, Y. A. and D.R. Lovley. 1992. Enzymatic Uranium Precipitation, Environ. Sci. Technol., Vol. 26, p. 205.

Goren, M. B. 1968. Process for Flocculating Finely Divided Solids Suspended in an Aqueous Medium with a Microbial Polysaccharide, U.S. Patent No. 3,406,114.

Harnish, R. A., D. M. McKnight and J. F. Ranville. 1994. Particulate, Colloidal and Dissolved-phase Association of Plutonium and Americium in a Water Sample from Well 1587 at the Rocky Flats Plant, Colorado. U.S. Geological Survey, Water-Resources Investigations Report 93-4175.

He, L., M.P. Neu, L.A. Venderberg. 2000. Bacillus Licheniformis Gamma-Glutamyl Exopolymer Physiochemical Characterization and U(IV) Interaction. Environmental Science and Technology. Vol. 34(9), p. 1694.

Hermansson, M., S. Kjelleberg, T.K. Korhonen and T.A. Stenstrom. 1983. Hydrophobic and Electrostatic Characterization of Surface Structures of Bacteria and Its Relationship to Adhesion at an Air/Water Surface, Arch. Microbiol., Vol. 131, p. 308.

Hersman, L. E. 1986. Sorption of 239Pu by a Pseudomonas Species. Abstracts of the Annual Meeting of the American Society for Microbiology, Vol. 258.

Hersman, L. E. 1995. Microbial effects on colloidal agglomeration, Los Alamos National Laboratory Report, La-12972-MS, Los Alamos.

Hersman, L. E., P.D. Palmer and D.E. Hobart. 1993. The Role of Siderophores in the Transport of Radionuclides. Materials Research Society Proceedings. Vol. 294, p. 765.

Hossain, M.B., D. Van der Helm amd M. Poling. 1983. Acta Cryst. B., Vol. 39: pp. 258-263.

Hu, M. Z.-C., J. M. Norman, B. D. Faison and M. E. Reeves. 1996. Biosorption of Uranium by Pseudomonas Aeruginosa Strain CSU: Characterization and Comparison Studies. Biotech. Bioengineer. Vol. 51, p. 237.

Inouye, M. 1979. Bacterial Outer Membranes, John Wiley and Sons, New York.

Jonsson, P. and T. Wadstorm. 1983. High Surface Hydrophobicity of Staphylococcus Aureus as Revealed By Hydrophobic Interaction Chromatography, Curr. Microbiol., Vol. 8, p. 347.

Keith-Roach, M. J., J. P. Day, L. K. Fifield, N. D. Bryan and F. R. Livens. 2000. Seasonal Variations in Interstitial Water Transuranium Element Concentrations. Eviron. Sci. Technol., Vol. 34, p. 4273.

Kim, J. I. and B. Kanellakopulos. 1989. Solubility Products of Plutonium(IV) Oxide and Hydroxide, Radiochim. Acta, Vol. 79, p. 26.

Kostka, J. E., G.W. Luther and K.H. Nealson. 1995. Chemical and Biological Reduction of Mn(III)-pyrophosphate Complexes: Potential Importance of Dissolved Mn(III) and an Environmental Oxidant, Geochim. Cosmochim. Acta, Vol. 59, p. 885.

Lahav, N. 1962. Adsorption of Sodium Bentonite Particles on Bacillus Subtilis, Plant and Soil, Vol. 17, p. 191.

Ledin, M. 2000. Accumulation of Metals by Microorganisms - Processes and Importance in Soil Systems. Earth-Science Reviews. Vol. 51, p. 1.

Lester, J.N., R.M. Sterritt and T. Rudd. 1984. Formation and Conditional Stability Constants of Complexes Formed between Heavy Metals and Bacterial Extracellular Polymers. Water Res., Vol. 18, pp. 379-384.

Lovley, D. R. and E.J.P. Phillips. 1992. Reduction of Uranium by Desulfovibrio Desulfuricans. Appl. Environ. Microbiol., Vol. 58, p. 850.

Lovley, D. R., E.J.P. Phillips, Y.A. Gorby and E.R. Landa. 1991. Microbial Reduction of Uranium, Nature, Vol. 350, p. 413.

396

Lovley, D. R., P.K. Widman, J.C. Woodward and E.J.P. Phillips. 1993. Reduction of Uranium by Cytochrome C3 of Desulfovibrio Vulgaris, Appl. Environ. Microbiol., Vol. 59, p. 3572.

Luther, G. W., D.B. Nuzzio and J. Wu. 1994. Speciation of Manganese in Chesapeake Bay Waters by Voltammetric Methods. Anal. Chem. Acta, Vol. 284, p. 473.

Macaskie, L.E., K. M. Bonthrone, P. Yong and D.T. Goddard. 2000. Enzyically Mediated Bioprecipitation of Uranium by a Citrobacter sp.: A Concerted Role of Exocellular Lipopolysaccharide and Associated Phosphatase in Biomineral Formation. Microbiology, Vol. 146, p. 1855.

Marshall, K. C. 1968. Interaction between Colloidal Montmorillonite and Cells of Rhizobium Species with Difference Ionogenic Surfaces. Biochem. Biophys. Acta, Vol. 156, p. 179.

Marshall, K. C. 1969. Orientation of Clay Particles Sorbed on Bacteria Possessing Different Ionogenic Surfaces. Biochem. Biophys. Acta, Vol. 193, p. 472.

Marshall, K. C. 1969. Studies by Microelectrophoretic and Microscopic Techniques of the Sorption of Illite and Montmorillonite to Rhizobia. J. Gen. Microbiol., Vol. 56, p. 301.

McLean, R.J.C., D. Beauchemin, L. Chepman, T.L. Beveridge. 1990. Metal Binding Characteristics of the Gamma-Glutamyl Ploymer of Bacilus Lecheniformis ATCC 9945. Applied Environmental Microbiology, Vol. 5, p. 3671.

Miekeley, N. and Kuchler, I. L. 1987. Interactions Between Thorium and Humic Compounds on Surface Waters. Inorgan.Chim. Acta, Vol. 140, p. 315.

Morse, L. R. 1986. Thermodynamic Properties, in The Chemistry of the Actinide Elements, 2nd ed., Seaborg, G. and Morse, T., Eds., Chapman and Hall. New York, NY. p. 1289.

Nash, K. and G. Choppin. 1980. Interaction of Humic and Fulvic Acids with Th(IV). J. Inorgan. Nucl. Chem., Vol. 42, p. 045.

Nash, K., F. Sherman, A.M. Fiedman and J.C. Sullivan. 1981. Redox Behavior, Complexing and Adsorption of Hexavalent Actinides by Humic Acid and Selected Clays. Environ. Sci. Technol., Vol. 15, p. 834.

Nealson, K. H. 1983. The Microbial Manganese Cycle, in Microbial Geochemistry, Krumbein, W. E., Eds., Blackwell Scientific Publications, Oxford, p. 191.

Nealson, K. H. 1983. The Microbial Iron Cycle, in Microbial Geochemistry, Krumbein, W. E., Eds., Blackwell Scientific Publications, Oxford, p. 159.

Nealson, K. H. and C.R. Myers. 1992. Microbial Teduction of Manganese and Iron: New Approaches to Carbon Cycling. Appl. Environ. Microbiol., Vol. 58, p. 439.

397

Neilands, J. B. 1981. Microbial Iron Compounds. Ann. Rev.Biochem., Vol. 50, p. 715.

Neu, M.P. and C.E. Ruggiero. In Press. Inorganic Chemistry.

Neu, M.P., J.H. Matonic, C.E. Ruggiero, B.L. Scott. 2000a. The First Structural Characterization of Plutonium (IV) Complexed by a Sidephore: Single Crystal Structure of Pu Desferrioxamine E. Angew. Chemie. Int. Ed. 2000, Vol. 39(8), p. 1442.

Neu, M.P., J.H. Matonic, C.E. Ruggiero, B.L. Scott. 2000b. The First Structural Characterization of Plutonium Complexed by a Biomolecule and Comparison of single Crystal Structures of the Siderphore Desferrioxamine E and the Fe(III) and Pu(IV) Comlexes. Angew. Chemie. Int. Ed. 2000, vol. 112(8), p. 1501.

Obayashi, A. W. and A.F. Gaudy. 1973. Aerobic Digestion of Extracellular Microbial Polysaccharides. J. Water Poll.Contr. Fed., Vol. 45, p. 1584.

Panak, P. J., J Raff, S. Selenska-Pobell, G. Geipel, G. Bernhard and H. Nitche. 2000. Complex Formation of U(VI) with Bacillus-Isolates from a Uranium Mining Waste Pile. Radiochim. Acta., Vol. 88, p. 71.

Pedersen, K. and F. Karlsson. 1995. Investigations of Subterranean Microorganisms: Their Importance for Performance Assessment of Radioactive Waste Disposal. SKB Technical Report 95-10, Swedish Nuclear Fuel and Waste Management Co., Stockholm, Sweden. p. 168.

Pringle, J. H., M. Fletcher and D.C. Ellwood. 1983. Selection of Attachment Mutants During the Continuous Culture of Pseudomonas Fluorescens and Relationship Between Attachment Ability and Surface Composition, J. Gen. Microbiol., Vol. 129, p. 2557.

Puers, C. and S. Selenska-Pobell. 1998. Investigation of Bacterial Diversity in a Soil Sample of Depleted Uranium Mining Area Nearby Johanngeorgenstadt, Saxonia, via 16S-RDNA-Sequence Analysis/ Abstracts of Euroconference on Bacteria-Metal/ Radionuclide Interaction: Basic Research and Bioremediation, p. 85.

Raymond K. N., G. Muller and B.F. Matzanke. 1984. Complexation of Iron by Siderophores: A Review of Their Solution and Structural Chemistry and Biological Function. Current Chem., Vol. 123, p. 49.

Robinson, K.G., R. Ganesh and G.D. Reed. 1998. Impact of Organic Ligands on Uranium Removal During Anaerobic Biological Treatment. Wat. Sci. Tech. Vol. 37, No. 8, pp. 73-80.

Rosenberg, M. and S. Kjelleberg. 1988. Hydrophobic Interactions: Role in Bacterial Adhesion, in Adv.Microbial Ecol., Marshall, K. C., Ed., Plenum Press, New York. Vol. 9, pp. 353.

Rusin, P. A., L. Quintana, L., J.R. Brainard, B.A. Strietelmeier, C.D. Tait, S.A. Elkerg, P.D. Palmer, T.W. Newton and D.L. Clark. 1994. Solubilization of Plutonium Hydrous Oxide by Iron- reducing Bacteria. Environ. Sci. Technol., Vol. 28, p. 1686.

Shumate, S. E., G.W. Strandberg and J.R. Parrot. 1978. Biological Removal of Metal Ions from Aqueous Process Streams, in Biotechnology in Energy Production, Conservation Biotechnology and Bioengineering Symposium, No. 8, Scott, C. D. , Eds., John Wiley and Sons, New York, p. 13.

Sibley, T. H., J.R. Clayton, E.A. Wurtz, A.L. Sanchez and J.J. Alberts. 1984. Effects of Dissolved Organic Compounds on the Adsorption of Transuranic Elements. Dev. Biochem., Vol. 1, p. 289.

Sposito, G. 1989. The Chemistry of Soils, Oxford University Press, New York, Vol. 57, p. 68.

Story, S., L. Hersman, M. Martinez and M. Aldrich. 1996. Unpublished Data.

Stumm W. and B. Sulzberger. 1992. The Cycling of Iron in Natural Environments: Considerations Based on Laboratory Studies of Heterogeneous Redox Processes. Geochem. Cosmochim. Acta., Vol. 56, p. 3233.

Suzuki, Y. and J. F. Banfield. 1999. Geomicrobiology of Uranium. In: Uranium: Mineralogy, Geochemistry and the Environment. P. C. Burns and R. Finch, eds. Mineralogical Society of America, Wash. DC. pp 393-432.

Tebo, B. M. and A. Y. Obraztosova. 1997. Sulfate-reducing Bacterium Grow with Cr(VI), U(VI), Mn(IV) and Fe(III) and Electron Acceptors. FEMS Microbiol. Letters. Vol. 162, p. 193.

Treen-Sears, M. E., B. Volesky and R. Neufeld. 1984. Ion Exchange/Complexation of the Uranyl ion by Rhizopus Biosorbant. Biotechnol. Bioenginer., Vol. 26, p. 1323.

Truex, M. J., B. M. Peyton, N. B. Valentine and Y. A. Gorby. 1997. Kinetics of U(VI) Reduction by a Dissimilatory Fe(III)-reducing Bacterium Under Non-growth Conditions. Biotech. Bioengineer. Vol. 55, p. 490.

Van der Helm, D. M. and Poling. 1976. J. Am. Chem. Soc., Vol. 98, pp. 82-86

Wildung, R. E. and T.R. Garland. 1982. Effects of Plutonium on Soil Microorganisms, Appl. Environ. Microbiol., Vol. 43, p. 418.

Wurtz, E. A., T. H. Sibley and W. R. Schell. 1986. Health Phys. Vol. 50, p. 79.

Xu, H., L. L. Barton, P. Zhang and Y. Wang. 2000. TEM Investigation of U6+ and Re7+ Reduction by Desulfovibrio Desulfuricans, a Sulfate-reducing Bacterium. Mat. Res. Symp. Proc., Vol. 608, p. 299.

399

Section TA-3 Figures are embedded in the text.

SECTION TA-4 - TABLE OF CONTENTS

TA-4 ACTINIDE TRANSPORT PATHWAYS ANALYSIS - BASED ON MEASURED RFETS ACTINIDE CONCENTRATIONS 4-1

TA-4.1 The Conceptual Model Compared with Quantified Analyses 4-1

TA-4.2 Introduction to Actinide Transport Pathways Analysis 4-3

TA-4.3 Analysis of Surface and Sub-Surface Soil Data 4-3

TA-4.3.1 Source Locations Linked with Surface and Sub-Surface Soil Data 4-3

TA-4.3.2 Pu and U-238 Surface and Subsurface Soil Data Analysis 4-6

TA-4.4 Surface Water Pathway Analysis 4-9

TA-4.4.1 Methodology Used for Surface Water Pathway Analysis 4-9

TA-4.4.2 General Patterns of Surface Water Actinide Transport at RFETS 4-11

TA-4.4.3 Description and Purpose of Mass Balance Analyses 4-16

TA-4.4.4 Channels Selected for Analysis 4-17

TA-4.4.5 Lower Walnut Creek Analysis 4-20

TA-4.4.6 A- and B-Series Ponds Analysis 4-24

TA-4.4.7 South Interceptor Ditch Analysis 4-31

TA-4.4.8 Summary of Surface Water Pathway Analysis 4-34

TA-4.5 Groundwater Pathway Analysis 4-38

TA-4.5.1 Methodology Used for Groundwater Pathway Analyses 4-38

TA-4.5.2 General Patterns of Groundwater Actinide Transport at RFETS 4-38

TA-4.5.3 Plutonium and Americium Transport Patterns for Unsaturated Groundwater 4-39

TA-4.5.4 Plutonium and Americium Transport Patterns for Saturated Zone Groundwater 4-44

TA-4.5.5 Uranium Transport Patterns for Unsaturated Zone Groundwater 4-52

TA-4.5.6 Uranium Transport Patterns for Saturated Zone Groundwater 4-53

TA-4.5.7 Site-Wide LHSU Groundwater 4-58

401

TA-4.5.8 Actinide Drilling-Artifact Contamination Investigation 4-60
TA-4.5.9 Summary of Groundwater Pathway Analysis 4-63

TA-4.6 Air Pathway Analysis 4-65
TA-4.6.1 Sources of Airborne Actinides at RFETS 4-65
TA-4.6.2 General Patterns of Airborne Actinide Transport At RFETS 4-68
TA-4.6.3 Description of Air Pathway Analysis Methodology for Measured Data 4-70
TA-4.6.4 Results of Air Pathway Analysis Using Measured Data 4-78

TA-4.7 Biological Pathway Analysis 4-81
TA-4.7.1 Introduction 4-81
TA-4.7.2 Terrestrial Studies 4-81
TA-4.7.3 Aquatic Studies 4-88
TA-4.7.4 Conclusions 4-89

TA-4.8 Technical Appendix Section TA-4 References 4-91

SECTION TA-4 TABLES

Table TA-4-1. Actinide Source Locations - Summary of Surface and Sub-Surface Soil Samples (Sample Page) 4-5
Table TA-4-2. Lower Walnut Creek Study Area – Monitoring Stations 4-18
Table TA-4-3. A- and B-Series Ponds Study Area – Monitoring Stations 4-19
Table TA-4-4. South Interceptor Ditch Study Area – Monitoring Stations 4-20
Table TA-4-5. Lower Walnut Creek, Pu Mass Balance Results – Measured Load Data Only, Average for Water Years 1997 - 1999 4-20
Table TA-4-6. Summary of Lower Walnut Creek Pu Loading Analysis 4-21
Table TA-4-7. A- and B-Series Ponds, Pu Mass Balance Results – Measured Load Data Only, Average for Water Years 1997 - 1999 4-24
Table TA-4-8. Summary of A- and B-Series Ponds Pu Loading Analysis 4-25
Table TA-4-9. A- and B-Series Ponds, U-238 Mass Balance Results – Measured Load Data Only, Average for Water Years 1997 - 1999 4-28

402

Table TA-4-10. Summary of A- and B-Series Ponds U-238 Loading Analysis 4-29
Table TA-4-11. South Interceptor Ditch, Pu Mass Balance Results – Measured Load Data Only, Average for Water Years 1997 - 1999 4-31
Table TA-4-12. Summary of South Interceptor Ditch Pu Loading Analysis 4-32
Table TA-4-13. Selected UHSU and LHSU Bedrock Wells with Detectable Pu-239/240 4-51
Table TA-4-14. Annual Off-Site Actinide Transport Calculated Using Measured Data[a] 4-79

SECTION TA-4 FIGURES

Figure TA-4-1. Conceptual Model Schematic Diagram for Pu and Am Transport at RFETS 4-98
Figure TA-4-2. Conceptual Model Schematic Diagram for U Transport at RFETS 4-99
Figure TA-4-3. Actinide Sources and Sample Locations 4-100
Figure TA-4-4. Actinide Source Areas and Pu in Surface Soils Above Background Activity 4-101
Figure TA-4-5. Actinide Source Areas and Pu in Surface Soils Above Tier II Activity 4-102
Figure TA-4-6. Actinide Source Areas and Pu in Sub-Surface Soils Above Background Activity 4-103
Figure TA-4-7. Actinide Source Areas and Pu in Sub-Surface Soils Above Tier II Activity 4-104
Figure TA-4-8. Actinide Source Areas and U-238 in Surface Soils Above Background Activity 4-105
Figure TA-4-9. Actinide Source Areas and U-238 in Surface Soils Above Tier II Activity 4-106
Figure TA-4-10. Actinide Source Areas and U-238 in Sub-Surface Soils Above Background Activity 4-107
Figure TA-4-11. Actinide Source Areas and U-238 in Sub-Surface Soils Above Tier II Activity 4-108
Figure TA-4-12. Lower Walnut Creek Study Area – Schematic Diagram 4-109

403

Figure TA-4-13. A- and B-Series Ponds Study Area – Schematic Diagram 4-109
Figure TA-4-14. South Interceptor Ditch Study Area – Schematic Diagram 4-110
Figure TA-4-15. Lower Walnut Creek, Pu Loading Profile – Measured Load Data Only 4-111
Figure TA-4-16. A- and B-Series Ponds, Pu Loading Profile - Measured Load Data Only 4-112
Figure TA-4-17. A- and B-Series Ponds, U-238 Loading Profile - Measured Load Data Only 4-112
Figure TA-4-18. South Interceptor Ditch, Pu Loading Profile- Measured Load Data Only 4-113
Figure TA-4-19. Site-Wide Vertical Distribution of Pu-239/240 in Groundwater 4-114
Figure TA-4-20. UHSU Groundwater Uranium-238 Trend for RFETS Background Areas 4-114
Figure TA-4-21. Site-Wide Vertical Distribution of U-238 in Groundwater 4-115
Figure TA-4-22. UHSU Groundwater Uranium-238 Trend for the Woman Creek Groundwater Basin 4-115
Figure TA-4-23. UHSU Groundwater Uranium-238 Trend for the Walnut Creek Groundwater Basin 4-116
Figure TA-4-24. Air Box Model Figure 4-117

404

TA-4 ACTINIDE TRANSPORT PATHWAYS ANALYSIS - BASED ON MEASURED RFETS ACTINIDE CONCENTRATIONS

TA-4.1 THE CONCEPTUAL MODEL COMPARED WITH QUANTIFIED ANALYSES

The *Conceptual Model for Actinide Studies at the Rocky Flats Environmental Technology Site* report, introduced in Section TA-1.4, provides a qualitative understanding of the relationships between actinide sources and transport pathways at RFETS (RMRS, 1998). Differences in the chemistry and behavior of the predominant actinide species found in the environment at RFETS, specifically the insoluble nature of Pu(IV) and Am(III) and the relatively soluble nature of U(VI), were primary considerations in the development of the conceptual model. The marked difference in environmental behavior between insoluble and soluble actinide species resulted in the development of separate qualitative models for Pu/Am and U. These models are summarized in schematic diagrams depicting the relative importance of the multiple pathways by which actinides move in the environment. The conceptual model Pu/Am transport diagram is shown in Figure TA-4-1 and the U transport diagram is shown in Figure TA-4-2.

The objective of Sections TA-4 through TA-6 is to quantify the relative importance of alternative pathways, for Pu, Am and U, as presented in the conceptual model. This summary below of the pathways discussed in conceptual model provides perspective for the quantified analyses that follow in subsequent sections.

Conceptual Model - Plutonium/Americium Transport Pathways

- Surface Water - Major pathways for input loads are overland erosion transport of particulate or colloidal Pu/Am and sediment resuspension. The major pathway for output loads is sediment deposition. Minor pathways for input loads include airborne deposition, groundwater discharge and overland erosion transport of dissolved Pu/Am. Groundwater recharge is a minor pathway for output loads.

- Groundwater – No major pathways were identified for Pu and Am. Minor pathways include infiltration, sub-surface storm flow and recharge from surface water for input loads and discharge to surface water for output loads.

405

- Air – No major pathways were identified for Pu and Am. Minor pathways include surface soil suspension and flora to air transport for input loads and deposition to soil, flora and surface water for output loads.

- Biota - No major pathways were identified for Pu and Am. Minor input pathways include soil-to-fauna, soil-to-flora from raindrop splash and airborne deposition to flora. Minor output pathways include flora-to-air, fauna-to-soil and flora to fauna.

Conceptual Model - Uranium Transport Pathways

- Surface Water – Major pathways are groundwater discharge and sediment resuspension for input loads and sediment deposition for output loads. Minor input pathways include airborne deposition, overland erosion transport of particulate, colloidal or dissolved U and sub-surface storm flows. The minor output pathway identified was surface water recharge to groundwater.

- Groundwater – Major pathways for input loads are infiltration and vadose zone transport from soil. Discharge to surface water is a major pathway for output loads. A minor pathway for input loads is sub-surface storm flow.

- Air – The relative pathway importance identified that impact air is the same for U and Pu/Am. No major air pathways were identified for U. Minor pathways include surface soil suspension and flora to air transport for input loads and deposition to soil, flora and surface water for output loads.

- Biota - The relative importance of pathways that impact biota are the same for U as for Pu/Am. No major biota pathways were identified for U. Minor input pathways include soil-to-fauna, soil-to-flora from raindrop splash and airborne deposition to flora. Minor output pathways include flora-to-air, fauna-to-soil and flora to fauna.

406

TA-4.2 INTRODUCTION TO ACTINIDE TRANSPORT PATHWAYS ANALYSIS

Section TA-4 is the first of three sections that present analyses of actinide transport for the surface water, groundwater, air and biological transport pathways. The type of data organizes these sections, either measured or modeled, being analyzed. The pathway analysis sections and data types used in each section are listed below:

- Section TA-4 – Pathway analysis using measured data only;
- Section TA-5 – Pathway analysis using measured data presented in Section TA-4 coupled with modeled data for pathways where measured data are unavailable; and
- Section TA-6 – Pathway analysis using modeled data only for extreme climatic conditions.

Within Section TA-4, five main sub-sections follow this introduction. First, Section TA-4.3 provides analysis of surface and sub-surface soil actinide data presented in Section TA-2 to better understand the connections between different sources and actinide transport pathways. Next, Sections TA-4.4 through TA-4.6.4 address the surface water, groundwater, air and biological pathway analyses, respectively.

TA-4.3 ANALYSIS OF SURFACE AND SUB-SURFACE SOIL DATA

TA-4.3.1 Source Locations Linked with Surface and Sub-Surface Soil Data

Surface and sub-surface soil data presented in Section TA-2 were analyzed and organized to facilitate analysis of specific actinide transport pathways. A total of 215 actinide source locations designated as active IHSS, UBC, NFA or Recommended NFA were included in the evaluation. These locations were reviewed to determine which had sample data that met the acceptance criteria discussed in Section TA-2 and whether or not sample results indicated actinides above background or RDL levels. Actinide source locations with data above background or RDL levels for a specific actinide were labeled with a "Y" in the corresponding column. Locations with data below background or RDL levels were identified with an "N" in the corresponding column. Locations without data were identified with a "NO DATA" label.

407

Over 50 % of the locations, 120 out of 215 total, had "NO DATA" for all of the actinides, using the data acceptance criteria used for this report. Source locations with actinide data were crosschecked with the Historical Release Reports and summary comments were written regarding the sample results. A sample page from the table is presented in Table TA-4-1. The complete table is on the CD-ROM included with this Technical Appendix.

In addition to the data evaluation compiled in Table TA-4-1, surface and sub-surface soil sampling locations were plotted along with the boundaries of the actinide source areas (Figure TA-4-3). This figure graphically displays the actinide source areas that have been sampled and those source areas that have not been sampled.

408

Table TA-4-1. Actinide Source Locations - Summary of Surface and Sub-Surface Soil Samples (Sample Page)

(Complete table available on CD-ROM)

IHSS	Description	Actinide type reported in HRR	Surface soil samples for all actinides (Y/N?)	Sub-Surface Soil Samples for all actinides (Y/N?)	Pu-239/240		Am-241		U-233/234		U-235		U-238		Flag	Comments
					> Bgrd (Y/N)	> RDL (Y/N)	> Bgrd (Y/N)	> RDL (Y/N)	> Bgrd (Y/N)	> RDL (Y/N)	> Bgrd (Y/N)	> RDL (Y/N)	> Bgrd (Y/N)	> RDL (Y/N)		
101	207 Solar Evaporation Ponds	Pu, U	Y	Y	Y	Y	Y	Y	Y	Y	Y	Y	Y	Y	Y	One Am sample above Tier II, one U235 sample above RDL, Reported as 101,138 & 101,149.1 & 101,149.2 & 101,150.6 & 101,150.8 & 101,163.1
111.2	Trench T-5	Pu, U	Y	Y	Y	Y	Y	Y	Y	Y	Y	N	Y	Y		Pu, Am, U conc. decrease with depth
111.3	Trench T-6	Pu, U	N	Y	Y	N	Y	N	Y	Y	Y	N	Y	Y		Pu/Am either high or low, U less variable in trenches
111.4	Trench T-7	Pu, U	N	Y	Y	Y	Y	Y	Y	Y	Y	N	Y	Y		Some U samples below bkgrd., one Pu/Am sample high toward surface and rest w.in RDL, U more uniform distribution over depth
111.5	Trench T-8	Pu, U	No Data	No Data	No Data	No Data	No Data	No Data	No Data	No Data	No Data	No Data	No Data	No Data		N/A
111.6	Trench T-9	Pu, U	Y	Y	Y	Y	Y	Y	Y	Y	Y	N	Y	Y		Many samples below bkgrd.
111.7	Trench T-10	Pu, U	N	Y	Y	Y	Y	Y	Y	Y	Y	N	Y	Y		One sample very high for all actinides, most near bkgrd. & within R.D.L.
111.8	Trench T-11	Pu, U	N	Y	Y	N	Y	N	Y	N	Y	N	Y	Y		Actinide samples slightly above/below bkgrd. levels

Table page 1 of 1

TA-4.3.2 Pu and U-238 Surface and Subsurface Soil Data Analysis

Surface and sub-surface soil data for Pu and U-238 presented in Section TA-2 were investigated to link known source locations with the soil data to better understand relationships between specific sources and transport pathways. Am-241 was not investigated in this manner because its environmental behavior, as discussed in Section TA-3, resembles that of Pu. Similarly, U-233/234 and U-235 were not included in this analysis because their patterns of transport resemble U-238.

Plutonium Surface and Sub-Surface Soil Data

Plutonium Surface Soil Data

A Pu surface soil data set was created which all sample results equal to or less than background activities were removed. Background surface soil activity for Pu, discussed in Section TA-2, is 0.04 pCi/g (EG&G, 1995). These data were mapped along with boundaries of the actinide source areas (Figure TA-4-4).

Pu surface soil data were further screened by mapping only those known sample results exceeding the RFCA Tier II Action Level of 252.0 pCi/g. These data are shown in . The contrast in number of samples with results above background activity above Tier II activity is clear. Pu sample results that exceed Tier II levels are limited to the 903 Pad and Lip Area vicinity southeast of the Industrial Area, whereas sample results that exceed background are widely distributed throughout the Industrial Area and beyond.

Plutonium Sub-Surface Soil Data

Similar to the surface soil analysis, a figure was created for Pu sub-surface soil data in which sub-surface sample results equal to or less than background levels were removed from the data set. Sub-surface soil samples from all depths were included in this sorting process. Background sub-surface soil activity, discussed in Section TA-2, is 0.00 pCi/g for Pu. These above-background data were mapped along with the boundaries of the actinide source areas (Figure TA-4-6).

The second step in the Pu sub-surface soil data evaluation process involved mapping only those sub-surface results that exceed the RFCA Tier II Action Level of 103.0 pCi/g for Pu. These data are shown in Figure TA-4-7. Two Pu sub-surface soil sample results exceed Tier II Action Levels. These samples were collected within or near IHSS 111.4 – a former burial trench located in the SID drainage basin approximately 460 m (1500 ft) east of the eastern Industrial Area fence.

Plutonium – Analysis of Surface and Sub-Surface Soil Figures

When viewed collectively, the Pu surface and sub-surface soil figures display a distinctive trend in terms of transport. Data shown in for sub-surface samples show that Pu, with few exceptions, was not detected below the surface at concentrations that exceed Tier II. The two samples where Pu was measured above Tier II activity were both associated with locations where the Pu source was buried. Therefore, despite the widespread existence of Pu detected on the surface soils (Figure TA-4-4) and the presence of Pu on surface soils near the 903 Pad that exceed Tier II concentrations (Figure TA-4-5), Pu does not display an obvious pattern of vertical downward migration into the sub-surface soil. This is in agreement with previous findings regarding the presence of Pu occurring mainly in the surface soils (Hakonson, 1981; Hartmann, et al, 1989). The tendency of Pu to remain near the surface is further supported by the kriged Pu surface soil data (Figure TA-2-8) that show an obvious west to east pattern of airborne transport originating from the 903 Pad Pu source.

Uranium-238 Surface and Sub-Surface Soil Data

Uranium-238 Surface Soil Data

Using the same method applied to Pu, a figure was created for U-238 surface soil data in which all sample results equal to or less than background levels were removed. Background surface soil activity is 1.09 pCi/g for U-238. These data were mapped along with the boundaries of the actinide source areas (Figure TA-4-8).

411

U-238 surface soil data were further evaluated by mapping only those sample results exceeding the RFCA Tier II Action Level of 103.0 pCi/g. These data are shown in Figure TA-4-9 for U-238. U-238 sample results that exceed Tier II activity are less common than for Pu. Sites with U-238 that exceed Tier II are limited to the Original Landfill and Ash Pits areas southwest of the Industrial Area and within the 903 Pad boundary southeast of the Industrial Area.

U-238 Sub-Surface Soil Data

A figure was created for U-238 sub-surface soil data in which sub-surface sample results equal to or less than background levels were removed from the data set. Sub-surface soil samples from all depths were included in this sorting process. Background sub-surface soil activity, as presented in Section TA-2, is 0.73 pCi/g for U-238. These above-background data were mapped along with the boundaries of the actinide source areas (Figure TA-4-10).

The second step in the U-238 sub-surface soil data evaluation process involved mapping only those sample results that exceed the RFCA Tier II Action Level. Tier II Action Levels for sub-surface soil are the same as for surface soil, 103.0 pCi/g U-238. These data are shown in Figure TA-4-11. Sub-surface soil samples for U-238 that exceed the RFCA Tier II Action Level are confined to the Ash Pits southwest of the Industrial Area and one location southwest of the 903 Pad.

Uranium-238 – Analysis of Surface and Sub-Surface Soil Figures

The pattern of U-238 migration in the surface and sub-surface soil data does not reflect the surface erosion transport processes and associated plumes that were discussed regarding Pu. Because few surface soil sample locations exist with U-238 activity above the Tier II level (Figure TA-4-9), sub-surface U-238 activities would not be expected to exceed Tier II, unless the sources of U-238 were buried. Therefore, it is not surprising that Figure TA-4-11 shows few sub-surface samples that exceed Tier II. However, it is noteworthy that the sub-surface U-238 data in Figure TA-4-10 are generally of the same

concentration, slightly above the regional background level, as the overlying surface soil samples presented in Figure TA-4-8.

Based on the similar levels of activity observed in the surface and sub-surface soils, it might be inferred that the majority of U-238, at and below the surface, is from natural sources with activities slightly above the regional background level. Alternatively, the U-238 detected above background in sub-surface soils could be from downward migration into the soil of anthropogenic U-238 from the surface. In either case, U-238 surface soil data do not indicate the same type of distribution, with a large source area and widespread surface soil plumes, as does Pu. Instead, aside from background concentrations, higher U-238 concentrations are present both at and below the ground surface in spotty locations associated with specific sources.

Determining whether the U-238 is naturally-occurring or from anthropogenic sources can be accomplished by examining U isotopic abundance ratios. The natural U-235/U-238 ratio is approximately 0.045. A U-235/U-238 ratio analysis for RFETS soils performed by Litaor was confounded by large analytical error associated with the alpha spectroscopy determination of U-235 in soils. This made interpretation of the U235/U-238 ratio difficult (Litaor, 1995). The U-234/U-238 ratio, approximately 1.0 with naturally-occurring soils, was also analyzed by Litaor and found to be well within the naturally-occurring range of variation. The U-234/U-238 ratio study indicates that, other than in localized point sources with elevated activity, the existence of anthropogenic U sources in surface soil appears to be limited.

TA-4.4 SURFACE WATER PATHWAY ANALYSIS

TA-4.4.1 Methodology Used for Surface Water Pathway Analysis

A two-tiered approach is used in Section TA-4.4 to analyze, interpret and present measured surface water actinide transport data. First, in Section TA-4.4.2, general surface water actinide transport patterns at the Site are discussed. Distinctions are made between different actinide species and the effects that physical features of the Site, such

413

as detention ponds, have on their behavior. Surface water impacts from varying concentrations of actinides, in different environmental media, are also addressed. This general overview of surface water actinide transport patterns provides a basis for interpreting the more detailed second tier of analysis described below.

The second tier of surface water actinide transport analysis, presented in Sections TA-4.4.5 through TA-4.4.7, involves detailed study of three distinct channel reaches each having unique characteristics in terms of channel geometry and actinide sources. Discussion regarding these study area characteristics follows in the "Channels Selected for Analysis" text. Mass balance calculations are performed for each reach, using measured surface water actinide data, to quantify actinide loads flowing in and out of each study area. Results of the mass balances are analyzed and discussed in terms of the factors that affect actinide transport within each reach. In this section, where measured data only are studied, observations are noted and briefly discussed. Later, when modeled data are introduced in Section TA-5, more detailed discussion regarding the factors that can influence actinide migration is provided. These factors include, but are not limited to, actinide concentrations in soils and sediments, channel geometry and other watershed characteristics such as vegetation and soil types. Differences among the characteristics of the three study areas and the differences in actinide transport within each are reviewed and discussed.

In summary, the objective of Section TA-4.4.2 is to present a broad overview of surface water actinide transport at the Site. It is followed by a discussion of the mass balance analyses in Section TA-4.4.3 and a description of the three study channel reaches selected in Section TA-4.4.4. The mass balance analyses are presented in Sections TA-4.4.5 through TA-4.4.7, using measured data only. Modeled data are introduced in Section TA-5 to estimate actinide transport via those pathways where measured data are not available.

TA-4.4.2 General Patterns of Surface Water Actinide Transport at RFETS

General characteristics of actinide transport observed in surface water at RFETS, as displayed in data presented in Section TA-2, are discussed in this section. Recognizing patterns of actinide transport observed in surface water provides a basis for understanding and interpreting mass balance evaluations presented in later sub-sections. Pu and Am, which share similar environmental transport characteristics, are discussed separately from U, which displays different patterns of transport in surface water.

Two types of actinide transport metrics are addressed in this discussion. The first is actinide concentration in surface water, measured as activity per volume of water, typically in units of pCi/L.

The second metric is actinide load, measured as total activity transported per unit time, presented in this report in units of pCi/year. Actinide load for a particular surface water monitoring station is calculated by multiplying the actinide concentration in the water by the volume of water yielded at the station over the same period. A location with low actinide concentration can have a greater load than a location with high concentration if the first station has a greater water yield. This illustrates why both the actinide concentration and load need to be addressed when examining surface water transport. A more thorough explanation of the process used to collect samples and calculate actinide loads in RFETS surface water is provided in Section TA-2.7.

Plutonium and Americium Transport Patterns in Surface Water

Actinide transport patterns in surface water are discussed with respect to data presented in Section TA-2 for Water Years 1997 through 1999 for RFCA POE and POC monitoring stations. The analysis herein focuses on Pu but applies generally to Am because it, like Pu, is relatively insoluble and both actinides exhibit similar transport patterns in surface water.

415

Industrial Area Runoff - Plutonium and Americium

Annual average concentrations of Pu in surface water vary by roughly two orders of magnitude, from 10^{-1} to 10^{-3} pCi/L, at monitoring stations across the Site. The highest surface water Pu concentration and the largest Pu load measured at the Site are from central Industrial Area runoff measured at monitoring station GS10, located immediately upstream from the B-Series ponds on South Walnut Creek (see Figure TA-2-53). This is noteworthy because the largest area with elevated surface and sub-surface soil concentrations of Pu is not located in the GS10 drainage basin, but rather in the SID/station SW027 drainage basin.

The average surface water concentration of Pu at GS10 (0.196 pCi/L) was more than twice the average concentration measured at SW027 (0.082 pCi/L). This compares with the RFCA Action Level for POE and POC locations of 0.15 pCi/L based on a 30-day moving average. Station GS10 has an average annual water yield of 151 million liters (122.4 acre-feet) which is roughly four times the water yield measured at SW027. The combined effect of higher Pu concentration and higher water yield resulted in the average annual Pu load measured at GS10 (28.8 μCi), to be nearly nine times the average annual load measured at station SW027 (3.3 μCi). The higher load at GS10 occurs despite the fact that the SW027 basin is roughly 25 % larger than the GS10 basin and largest Pu source areas with the highest Pu concentrations are SW027.

This indicates that watershed characteristics of the GS10 drainage basin provide preferential transport efficiencies for Pu when compared with the SW027 watershed. Both of the basins are approximately the same size, 167 acres for GS10 and 214 acres for SW027. However, the GS10 basin is all within the Industrial Area and is approximately 47 % impervious combined with some disturbed pervious areas. The SW027 basin, in contrast, is approximately 14 % impervious with the majority of the watershed comprised of the vegetated hillslope that borders the north side of the SID.

Two factors suspected to contribute to the higher relative mobility of Pu in the GS10 basin, when compared with the SW027 basin, are the proportion of impervious surfaces

416

and the type of soil in each basin. First, the higher percentage of impervious surfaces in the GS10 basin causes increased runoff, which promotes erosion of Pu-bearing soils and channel sediments from unpaved areas. Second, the GS10 basin contains more exposed soil areas that are devoid of vegetation and with apparent reduced amounts of organic matter in the soil. It is recognized and discussed in Section TA-3-6, that micro-organisms in the soil can effectively sorb actinides. Hersman found a *Pseudomonas* bacteria species to concentrate Pu-239(IV) nearly 10,000 times more than a sterile control of crushed tuff, 75 to 200 mesh (Hersman, 1986).

The Pu concentrations measured at GS10 above the RFCA Action Level occur predominantly during periods of increased stormwater runoff in the spring and summer (RMRS, 1999; Santschi, 2000). RFCA-reportable levels of Pu and Am in the spring of 1999 prompted a Pu and Am source investigation study. Extensive analysis of multiple factors, including review of actinide sources, Site operations and comparison with water quality parameters, did not find any discrete sources of Pu and Am that caused the elevated 30-day moving average results (RMRS, 1999). Instead, the investigators concluded that diffuse soil and sediment contamination was the source of actinides that caused the reportable values.

RFETS Ponds - Plutonium and Americium

The RFETS ponds effectively reduce the Pu load in surface water. This likely indicates that the predominant form of Pu in the surface water at RFETS settles or sorbs to particles that will settle in the ponds. When viewed as a whole, the A- and B-Series ponds in North and South Walnut Creek removed approximately 75 % of their input Pu load from Water Year 1997 through 1999. Pond C-2, which receives the discharge from the SID, removed approximately 70 % of its input Pu load during the same time frame. These data are consistent with previous Site findings dating back to the 1970's regarding the pond removal efficiencies for Pu (Paine, 1970; Thompson, 1975).

The mechanism for removal of Pu from the ponds has not been thoroughly quantified. Although the removal process is suspected to be largely caused by settling of Pu adsorbed

417

to inorganic particulate matter, other biological transport vectors such as seston and zooplankton have been measured that can remove Pu from the water column (Johnson, 1974). Santschi et al. found that roughly 10 % of the Pu in Site runoff is bound with colloidal-size particles that are not effectively settled in the ponds (Santschi et al., 2000). This corroborates earlier research that found approximately 10 to 20 % of the Pu in the B-series ponds to be associated with particles less than 0.42 microns (Johnson, 1974). These findings provide an explanation for the fraction of Pu in the ponds that is not removed by settling. The colloidal material that Santschi found with Pu was composed primarily of clay and significant amounts of organic detritus, organism parts and other natural organic materials. Paine also found Pu to be preferentially-associated with clay in RFETS sediments (Paine, 1970).

Downstream from the RFETS Ponds - Plutonium and Americium

Lower Walnut Creek below the A-series ponds and upstream from station GS03 (at Indiana Street) was a gaining reach in Water Years 1997 and 1998 and a losing reach in Water Year 1999 in terms of Pu load. The annual average of these three years was a Pu load approximately 30 % greater on the downstream end of the channel than on the upstream end. In other words, a greater Pu load was measured flowing out of this section of Walnut Creek than was measured flowing in. This reach has recently been thoroughly studied, including extensive sediment sampling, although no conclusive findings were made regarding localized Pu sources that could cause elevated concentrations at the downstream end of the channel reach (RMRS, 1998). Thompson calculated in the mid-1970's that the Pu inventory in the sediments of this channel reach was approximately 0.2 mCi. It was determined that a substantial portion of the inventory was introduced to the channel when excavation work in the ponds caused large areas of disturbed, contaminated soil to be mobilized (Thompson, 1975). Sediments in lower Walnut Creek remain as a source term that is suspected to be a significant contributor to the Pu loads measured downstream end.

Similar to the lower Walnut Creek channel, the reach between Pond C-2 and station GS01 in the Woman Creek watershed gains Pu load at the downstream end. The average

annual Pu load increases between station GS31 (below Pond C-2) and Station GS01 (at Indiana Street) by more than a factor of three.

To put the off-Site Pu loads in perspective, the average annual load measured at Station GS01 (3.6 μCi/yr) is approximately one quarter of that at Station GS03 (on Walnut Creek at Indiana Street). The average GS01 Pu concentration during the study period was less than 0.01 pCi/L and the water quality comply with the RFCA 0.15 pCi/L Action Level from 1997 through 1999.

Uranium Transport Patterns in Surface Water

Industrial Area Runoff - Uranium

In contrast with Pu, the concentrations for each of the U isotopes are largely uniform in surface water across the Site. The differences in U concentrations, regardless of isotope, are much less from location to location than the spatial differences observed for Pu and Am. Therefore, the U load from one station to the next is largely a function of the water yield at each station.

It is notable that the largest average annual surface water U load from Industrial Area runoff occurs on North Walnut Creek at station SW093. Similar to Pu and Am, the surface and sub-surface soils with the highest U concentrations occur largely in the SID drainage monitored by station SW027. Despite the presence of sources with elevated U activity, the isotopic surface water U concentrations measured at station SW027 are comparable with the rest of the Site. Because of the low flows at SW027, the average annual U loads at SW027 are lower than at other monitoring locations and are roughly one order of magnitude less than the load measured at station SW093.

RFETS Ponds - Uranium

Based on isotopic U data presented in Section TA-2, the ponds are relatively ineffective in removing the U load in surface water. Although U concentrations immediately below the A- and B-Series ponds are slightly lower than in the inflow to the ponds, this could be attributed to inflows from the treated WWTP effluent that dilute the U concentrations in

the pond system. The A- and B-Series ponds also gain groundwater in wet years that could potentially add a U load. The groundwater pathway is addressed with modeled data in Section TA-5.

Pond C-2 outflows have average annual loads of U-233/234, U-235 and U-238 that are approximately 65, 50 and 45 % higher, respectively, than the pond inflow loads measured at station SW027. The increased outflow loads are a combination of two factors. First, average U concentrations below Pond C-2 are 20 to 40 % higher for the different isotopes than the average concentrations measured in the inflow at station SW027. Second, the average annual water volume flowing out of Pond C-2 is roughly 50 % higher than the inflow water volume measured at SW027. The higher outflow volume is caused by runoff from the basin surrounding Pond C-2 that is not measured at station SW027. The combination of higher water yield and increased U concentrations results in the increased U loads measured below Pond C-2.

Downstream from the RFETS Ponds - Uranium

Interpretation of surface water U transport patterns for the entire Site is obscured by the absence of data at the stations along the Site boundary at Indiana Street. RFETS boundary stations at Walnut Creek (GS03) and Woman Creek (GS01) do not have isotopic U data from Water Year 1997 through 1999. The absence of data at the Indiana Street stations is due to the fact there has historically not been a problem at the Site with U standard compliance. RFCA POC monitoring for U is performed at the terminal pond monitoring locations.

TA-4.4.3 Description and Purpose of Mass Balance Analyses

Mass balance calculations are performed for specific channel reaches, using measured surface water actinide data, to quantify actinide loads flowing in and out of each study area. The purpose of this effort is to better characterize the movement of different actinides in surface water at different locations. When coupled with information regarding watershed characteristics and actinide sources, impacts of the variables that affect actinide transport in surface water can be better understood. The analyses address

Pu and U-238 only because the environmental behavior and occurrence of Am is closely related to Pu and U-238 reflects the behavior and general occurrence of U-233/234 and U-235. Uncertainties associated with actinide loads in surface water from measured data are addressed in Section TA-5.

TA-4.4.4 Channels Selected for Analysis

Three channel segments, each with unique characteristics in terms of channel geometry and actinide sources, were selected for mass balance analysis. These channel reaches and the reason for their selection, are described below:

Lower Walnut Creek

The Lower Walnut Creek study area is bounded on the upstream end by monitoring stations GS11 and GS08 and on the downstream end by station GS03 (Figure TA-4-12). This reach is of interest because the average annual Pu load flowing out of the reach from Water Year 1997 through 1999 was approximately 30 % more than the Pu load flowing into the reach (Section TA-2). The surface soils immediately surrounding the reach have relatively low activity, with approximately 0.5 pCi/g or less of Pu and other Pu sources that could cause an increased load from upstream to downstream are not readily apparent. Further analysis is therefore warranted, particularly because water flowing from this study area flows directly off-Site.

Three tributaries to the Lower Walnut Creek study area are included in the mass balance analysis. These are No Name Gulch (station GS33) and McKay Ditch (station GS35) on the north side of Walnut Creek and an unnamed tributary (station GS41) on the south side of Walnut Creek (Figure TA-4-12).

A summary of surface water monitoring stations in the Lower Walnut Creek study area is presented in Table TA-4-2.

Table TA-4-2. Lower Walnut Creek Study Area – Monitoring Stations

Surface Water Station Number	Description of Water Monitored	Type of Load for Study Area
GS11	Pond A-4 Outfall	Inflow from Upstream
GS08	Pond B-5 Outfall	Inflow from Upstream
GS33	No Name Gulch	Tributary Inflow
GS35	McKay Ditch	Tributary Inflow
GS41	Unnamed Tributary S. of Walnut Creek	Tributary Inflow
GS03	Walnut Creek Near Site Boundary	Outflow

A- and B-Series Ponds

The A- and B-Series Ponds study area is bounded on the upstream end by monitoring stations SW093 and GS10 and on the downstream end by stations GS11 and GS08 (Figure TA-4-13). This study area, encompassing both North and South Walnut Creeks, was selected for three reasons. First, these drainages receive the majority of Industrial Area runoff. Second, flows from station GS10 contain the highest Pu and Am loads on the Site (Section TA-2). Third, study of the detention ponds is necessary to analyze their efficiency in removing different types of actinides from the water column.

Analysis of the A- and B-Series Ponds independent of one another was not feasible because of multiple transfers of water between the two systems during the period of study from Water Years 1997 through 1999. The two drainages were therefore grouped together as one study area for this mass balance analysis.

Two tributaries to the A- and B-Series Ponds study area are included in this investigation. These are an unnamed Industrial Area drainage that joins North Walnut Creek upstream from the ponds (station SW091) and the Site Waste Water Treatment Plant (WWTP) effluent that discharges into Pond B-3 in South Walnut Creek).

A summary of surface water monitoring stations in the A- and B-Series Ponds study area is presented in Table TA-4-3.

422

Table TA-4-3. A- and B-Series Ponds Study Area – Monitoring Stations

Surface Water Station Number	Description of Water Monitored	Type of Load for Study Area
SW093	North Industrial Area Runoff	Inflow from Upstream
GS10	Central Industrial Area runoff	Inflow from Upstream
SW091	Northeast Industrial Area runoff	Tributary Inflow
WWTP	Wastewater Treatment Plant Effluent	Tributary Inflow
GS11	Pond A-4 Outfall	Outflow
GS08	Pond B-5 Outfall	Outflow

South Interceptor Ditch

The SID study area does not have a surface water monitoring station to form its upstream boundary in the same manner that the other study areas are bounded. Instead, the upstream SID study area boundary is formed by the western end of the channel. The downstream boundary is formed by surface water monitoring station SW027 (Figure TA-4-14). The shortcoming of not having a measured input load at the upstream end of the study area is apparent because only the easternmost, or most downstream, portion of the SID has measured data for input actinide loads. This shortcoming is addressed later in Section TA-5, when modeled data for hillslope runoff are introduced and the entire length of the SID is accounted for in the mass balance. This section, however, will deal strictly with measured data only.

The SID study area was selected for two reasons. First, it receives the remaining Industrial Area runoff that is not addressed by the A- and B-Series Ponds mass balance analysis. Second, much of the runoff from the area surrounding the 903 Pad, with the highest concentrations of Pu and Am in surface soil at the Site, flows into the SID (Section TA-2).

One tributary to the SID study area is included in this analysis (station GS42). This is an unnamed drainage swale that joins the SID immediately west (upstream) of the study area's downstream boundary (Figure TA-4-14).

423

Surface water monitoring stations in the SID study area are listed in Table TA-4-4.

Table TA-4-4. South Interceptor Ditch Study Area – Monitoring Stations

Surface Water Station #	Description of Water Monitored	Type of Load for Study Area
GS42	Drainage Swale North of SID	Tributary Inflow
SW027	SID Outfall	Outflow

TA-4.4.5 Lower Walnut Creek Analysis

Lower Walnut Creek – Plutonium Mass Balance

Results from the Pu mass balance analysis for Lower Walnut Creek, using measured data only, are presented in Table TA-4-5. The data represent average annual Pu loads in Water Years 1997 through 1999 at all monitoring stations in the study area. Net gain or loss in outflow load compared to inflow load is presented at the bottom of the table.

Table TA-4-5. Lower Walnut Creek, Pu Mass Balance Results – Measured Load Data Only, Average for Water Years 1997 - 1999

Pu-239/240 Inputs

Measured Inputs

Input	Description	Load (pCi)
GS11	Pond A-4 Out	2.48E+06
GS08	Pond B-5 Out	6.95E+06
GS33	Tributary	3.71E+05
GS35	Tributary	7.79E+05
GS41	Tributary	9.15E+03
Total Measured Inputs		1.06E+07

Lower Walnut Creek
Study Area

Pu-239/240 Outputs

Measured Outputs

Output	Description	Load (pCi)
GS03	Walnut Ck	1.40E+07
Total Measured Outputs		1.40E+07

Gain (+) or Loss (-) of Pu in Study Area

Variables	Delta (pCi)	Change from Input	Remarks
Measured Data (Out - In)	3.41E+06	32%	Approx. 30% gain in Pu load

Table TA-4-6 contains information on Pu concentrations, Pu loads and drainage sub-basin characteristics for each of the lower Walnut Creek monitoring stations. The

424

rightmost column of the table contains the estimated average annual Pu load yielded per square meter of the sub-basin, calculated by dividing the average annual Pu load measured at a given station by the respective sub-basin area.

Pu surface water load data for lower Walnut Creek are plotted by year from Water Year 1997 through 1999 (Figure TA-4-15). Positive values in the bar graphs represent input loads of Pu and negative values represent output loads. This graph provides perspective on the annual variation of loads contributed by different sub-basins. Uncertainty with these data is addressed in Section TA-5.

Table TA-4-6. Summary of Lower Walnut Creek Pu Loading Analysis

Monitoring Location	Basin Description	Sub-Basin Size		Approx. % Impervious	Water Yield (Annual Average)		Pu Concen. (Annual Average)	Pu Load (Annual Average)	% of Total Input Load	Pu Yield per Unit Area (Annual Average)
		(Hectares)	(Acres)	(%)	(Liters)	(Acre-Feet)	(pCi/L)	(pCi)	(%)	(pCi/m²-Yr)
Input Loads										
GS11 (Measured)	North Industrial Area Runoff Thru Pond A-4	178.6	441.3	16%	4.0E+08	321.5	0.006	2.5E+06	23.4%	1.4
GS08 (Measured)	South Industrial Area Runoff Thru Pond B-5	105.3	260.2	31%	2.1E+08	170.8	0.033	6.9E+06	65.6%	6.6
GS33 (Measured)	No Name Gulch	99.6	246.2	0%	4.1E+07	33.3	0.009	3.7E+05	3.5%	0.4
GS35 (Measured)	McKay Ditch	225.8	557.9	5%	1.5E+08	119.6	0.005	7.8E+05	7.4%	0.3
GS41 (Measured)	Unnamed tributary south of Walnut Creek	5.5	13.6	0%	5.7E+05	0.5	0.016	9.2E+03	0.1%	0.2
				Totals	8.0E+08	645.6	-	1.1E+07	100%	-
Measured Output Loads										
GS03 (Measured)	Entire Walnut Creek watershed	960.7	2374.0	10%	7.8E+08	628.7	0.018	1.4E+07	100.0%	1.5
				Totals	7.8E+08	6.3E+02	-	1.4E+07	100%	-

Analysis of Lower Walnut Creek Plutonium Mass Balance Results

The Water Year 1997 through 1999 data indicate the average annual Pu load conveyed by the flow out of the study area, measured at GS03, was approximately 30 % higher than the load measured flowing into the reach. Because of this general loading pattern, station GS03, located on Walnut Creek and Indiana Street, has the second highest Pu load of any monitoring station at the Site. However, review of the loading profile for each year

425

shows that lower Walnut Creek was a gaining reach only in Water Years 1997 and 1998 (Figure TA-4-15). In Water Year 1999, however, the trend of the previous two years was reversed when the measured inflow load (2E+07 pCi) was approximately twice as large as the outflow load measured at GS03 (1E+07).

The primary factor in the 1999 loading pattern, where inflow load exceeded outflow, was the large inflow load caused by one flow-paced composite sample collected at station GS08 from 6/23/99 to 8/5/99. This particular sample had measured Pu activity of 0.603 pCi/L, or approximately 50 times more than the mean activity of the other twelve samples collected at GS08 that year (0.012 pCi/L). The water associated with the 6/23/99 to 8/5/99 composite sample accounted for roughly 83 % of the Water Year 1999 Pu load, even though the water volume was only 8 % of the total GS08 yield for the year. If the 6/23/99 to 8/5/99 sample result been equal to the mean Pu activity of the other samples collected at GS08 in Water Year 1998, then the 1999 Pu loading pattern would have been more comparable to Water Years 1997 and 1998. In this hypothetical case the Pu load flowing out of the reach would have exceeded the inflow load by roughly 4E+06 pCi or 60 %.

It is noteworthy that when the 0.603 pCi/L Pond B-5 discharge sample was collected, there was not a corresponding level of Pu activity observed in the water downstream at station GS03. The sample container started on the same day at GS03 had a result of 0.005 pCi/L Pu, roughly two orders of magnitude less than that measured upstream at GS08. There was not a delayed rise in Pu observed at GS03 later that year either - the Water Year 1999 Pu load was less than in the prior two years. These results raise the question whether or not the 6/23/99 GS08 sample container result was representative of the water volume from which the sample was collected. The presence of a "hot particle" in a sample container that could result in misrepresentation of overall water quality has been addressed in previous Site surface water investigations, though the concept was never proved or disproved (RMRS, 1997).

Thus, the lower Walnut Creek data indicate the channel reach can generate a substantial Pu load, from sediment resuspension, hillslope erosion or other mechanism, in some

4Dd6

years. In other years, the reach can lose Pu load, from a mechanism such as sediment deposition. Other mechanisms that can impact the loading in the channel are addressed in Section TA-5 when modeled and measured data are combined.

The Lower Walnut Creek study area is characterized by two types of sub-basins. The first type monitored by stations GS08 and GS11, captures Industrial Area runoff that is routed through the A- and B-Series ponds. Despite the efficiency of the ponds upstream of GS11 and GS08 in removing Pu, these two outfalls contribute roughly 90 % of the total measured Pu load to lower Walnut Creek. The estimated average annual Pu load yielded per square meter was 1.4 and 6.6 pCi/m^2/year for GS11 and GS08, respectively.

Station GS08, at the outfall of Pond B-5, warrants further discussion because flows at this station have the highest Pu concentration (0.033 pCi/L), average annual load (6.9E+06 pCi/year) and load per square meter (6.6 pCi/m^2/year) of any sub-basin in the lower Walnut Creek study area. The GS08 sub-basin constitutes approximately 65 % of the Pu load for all of lower Walnut Creek and the load per square meter is up to 30 times that observed at the less disturbed, well-vegetated basins. GS08 is downstream from station GS10, which receives runoff from the central Industrial Area, with multiple concentrated Pu sources and has the highest average annual Pu load measured at the Site. The GS10 drainage is discussed further in TA-4.4.6.

The second type of sub-basin in the lower Walnut Creek study area, in contrast to those described above that receive Industrial Area runoff, is characterized by predominantly undisturbed, well-vegetated terrain. These drainages, monitored by stations GS33, GS35 and GS41, are roughly 15 % larger in combined size than the GS11 and GS08 basins together, but supply only about 10 % of the Pu load contributed by GS11 and GS08. No identified Pu sources, other than relatively low concentrations of diffuse surface soil and sediment contamination, exist in the GS33, GS35 and GS41 sub-basins. The estimated average annual Pu load yielded per square meter was comparable for each of these stations, with values of 0.4, 0.3 and 0.2 pCi/m^2/year for GS33, GS35 and GS41, respectively. Consequently, measured loads from the tributary channels that feed lower Walnut Creek do not provide an explanation for the increased loads observed at the

downstream end of the lower Walnut Creek study area.

Lower Walnut Creek – Uranium-238 Mass Balance

A U-238 mass balance was not calculated for Lower Walnut Creek using measured data only. Measured data were unavailable for Water Years 1997 through 1999 for tributary stations GS33, GS35 and GS41 or for the downstream boundary station GS03. Analysis of U-238 in this reach is performed in Section TA-5 using measured and modeled data combined.

TA-4.4.6 A- and B-Series Ponds Analysis

Mass balance analyses for the A- and B-series ponds study areas were performed for Pu and for U-238. These analyses are described separately below.

A- and B-Series Ponds Plutonium Mass Balance

Results from the Pu mass balance analysis for the A- and B-Series ponds, using measured data only, are presented in Table TA-4-7. The data represent average annual Pu loads in Water Years 1997 through 1999 at all monitoring stations in the study area. Net gain or loss in outflow load compared to inflow load is presented at the bottom of the table.

Table TA-4-7. A- and B-Series Ponds, Pu Mass Balance Results – Measured Load Data Only, Average for Water Years 1997 - 1999

Pu-239/240 Inputs

Measured Inputs

Input	Description	Load (pCi)
SW093	N. Walnut In	8.7E+06
GS10	S. Walnut In	2.9E+07
SW091	Tributary	1.7E+05
WWTP	Tributary	1.1E+06
Total Measured Inputs		3.9E+07

A- and B- Series Ponds Study Area

Pu-239/240 Outputs

Measured Outputs

Input	Description	Load (pCi)
GS11	N. Walnut Out	2.5E+06
GS08	S. Walnut Out	6.9E+06
Total Measured Outputs		9.4E+06

Gain (+) or Loss (-) of Pu in Study Area

Variables	Delta (pCi)	Change from Input Load	Remarks
Measured Data (Out - In)	-2.9E+07	-76%	76% of inflow Pu stays in reach

428

Table TA-4-8 contains information on Pu concentrations, Pu loads and drainage sub-basin characteristics for each of the monitoring stations in the A- and B-Series ponds study area. The rightmost column of the table contains the estimated average annual Pu load yielded per square meter of the sub-basin.

Pu surface water load data for the A- and B-Series ponds are plotted by year from Water Year 1997 through 1999 (Figure TA-4-16). Positive values in the bar graphs represent input loads of Pu and negative values represent output loads. This graph provides perspective on the annual variation of loads contributed by different sub-basins. Uncertainty with these data is addressed in Section TA-5.

Table TA-4-8. Summary of A- and B-Series Ponds Pu Loading Analysis

Monitoring Location	Basin Description	Sub-Basin Size		Approx. % Impervious	Water Yield (Annual Average)		Pu Concen. (Annual Average)	Pu Load (Annual Average)	% of Total Input Load	Pu Yield per Unit Area (Annual Average)
		(Hectares)	(Acres)	(%)	(Liters)	(Acre-Feet)	(pCi/L)	(pCi)	(%)	(pCi/m^2-Yr)
Input Loads										
SW093 (Measured)	North Industrial Area Runoff	98.0	242.3	28%	2.2E+08	178.5	0.040	8.7E+06	22.5%	8.9
GS10 (Measured)	Central Industrial Area Runoff	67.7	167.4	47%	1.5E+08	122.3	0.191	2.9E+07	74.3%	42.5
SW091 (Measured)	Northeast Industrial Area Runoff	4.4	10.8	5%	7.5E+05	0.6	0.226	1.7E+05	0.4%	3.8
WWTP (Measured)	WWTP Treated Effluent to Pond B-3	N/A	N/A	N/A	2.5E+08	205.5	0.004	1.1E+06	2.8%	N/A
				Totals	6.3E+08	506.9	-	3.9E+07	100%	-
Output Loads										
GS11 (Measured)	North Industrial Area Runoff Thru Pond A-4	178.6	441.3	16%	4.0E+08	321.5	0.006	2.5E+06	26.3%	1.4
GS08 (Measured)	South Industrial Area Runoff Thru Pond B-5	105.3	260.2	31%	2.1E+08	170.8	0.033	6.9E+06	73.7%	6.6
				Totals	6.1E+08	492.2	-	9.4E+06	100%	-

Analysis of A- and B-Series Ponds Plutonium Mass Balance Results

Water Year 1997 through 1999 data indicate the average annual Pu load conveyed by the flow out of the study area, measured at stations GS11 and GS08, was approximately 76 % less than the load measured flowing into the reach. Review of the loading profile for each year (Figure TA-4-16) shows that the A- and B-Series ponds were a Pu "sink" every year from Water Year 1997 through 1999. However, while the ponds had a Pu load

429

removal efficiency of 92 % and 88 %, respectively, in Water Years 1997 and 1998, the removal efficiency in Water Year 1999 was only 37 %.

The reduced Pu removal efficiency by the ponds in Water 1999 can be directly attributed to the flow-paced composite sample collected from 6/23/99 to 8/5/99 at the Pond B-5 outfall on the downstream boundary of the study area. The 0.603 pCi/L sample result, addressed in the discussion on the lower Walnut Creek reach, had nearly 50 times the mean Pu activity of the other GS08 samples that year (0.012 pCi/L) and accounted for approximately 83 % of the GS08 Water Year 1999 load. If the 6/23/99 to 8/5/99 composite sample result been equal to the mean result of the other 12 flow-paced samples collected at GS08 that year, then the Water Year 1999 Pu load flowing out of Pond B-5 would have been much lower, 3E+06 pCi, instead of the measured 2E+07 pCi. In this hypothetical case, the efficiency of the A- and B-Series ponds for removing Pu from the water column would have been 83 % – comparable to that observed in Water Years 1997 and 1999.

Santschi et al. found that roughly 90 % of the Pu in Site runoff, measured at station GS10, is bound with particulate-size material (greater than 5 microns in diameter) (Santschi, 2000). The majority of the remaining 10 % of Pu was colloidal, that is, it passed through a 5 micron filter and was filtered out only by 100 kiloDalton or 3 kiloDalton ultrafilters using cross-flow filtration (Santschi, 2000). The observed colloidal fraction is consistent with the 92 and 88 % Pu load removal efficiencies observed in the ponds in Water Years 1997 and 1998. It is not consistent with the 37 % removal efficiency observed in Water Year 1999. However, as addressed above, the removal efficiency for Water Year 1999 would increase to 83 % if the 6/23/99 result was consistent with the other flow-paced, multiple-grab samples collected at GS08 that year.

The A- and B-Series ponds have two general types of measured inflows. The first type, Industrial Area runoff, is monitored by stations GS10, SW093 and SW091. The second type, treated WWTP effluent routed to Pond B-3, is monitored at the WWTP outfall. The sub-basins that capture Industrial Area runoff will be discussed first.

1/30

The two largest Industrial Area sub-basins, GS10 (68 hectares [167 acres]) and SW093 (98 hectares [242 acres]), contribute the vast majority, 74 % and 22 %, respectively, of the average annual Pu load flowing into the A- and B-Series ponds. Central Industrial Area runoff, monitored by Station GS10, has the largest Pu load of any sub-basin at the Site. The average annual Pu load per square meter, 42.5 pCi/m^2, exceeds the basin with the next highest area-normalized load, the station SW093 basin, by a factor of five. The high amount of Pu in GS10 surface water relative to other sub-basins does not correspond with the relative amount of Pu observed in the surface soil. Although the GS10 basin has multiple Pu IHSSs, it does not have the highest Pu surface soil concentrations at the Site and has no surface soil sample results above the RFCA Tier II Action Level. The GS10 sub-basin is approximately 47 % impervious and is characterized by large areas of pavement mixed with areas of poorly vegetated exposed soil.

The SW093 sub-basin collects runoff from the northern Industrial Area, but has only 28 % impervious surfaces compared with 47 % in the GS10 basin. As noted earlier, the average annual Pu load per square meter from the SW093 basin, 8.9 pCi/m^2, is approximately one fifth that of the GS10 basin, but still the second highest on the Site. The average annual Pu load measured at the SW093 basin, 8.7E+06 pCi/year, is the third largest at the Site behind stations GS10 and GS03, with loads of 2.9E+07 pCi/year and 1.4E+07 pCi/year, respectively.

The other Industrial Area sub-basin that contributes to the A- and B-Series ponds, monitored by station SW091 (4 hectares [11 acres]), is much smaller than the GS10 and SW093 sub-basins. The SW091 sub-basin, which collects runoff from the northwest corner of the Industrial Area, includes a documented Pu surface soil source (IHSS 141 – a former Pu sludge disposal area). However, the basin has only 5 % impervious area and, consequently, has little runoff. The resulting average annual Pu load delivered from the sub-basin, less than 1 % of that discharged to the ponds, is relatively small. The average annual Pu load per square meter for the SW091 drainage sub-basin is 3.8 pCi/m^2, or approximately one tenth of the Pu load delivered per square meter by the GS10 sub-basin.

The WWTP treated effluent, which discharges into Pond B-5, is the single largest measured source of water flowing into the A- and B-Series ponds. The WWTP contributes an annual average of approximately 2.5E+08 L (205 acre-feet), or 40 % of the measured discharges to the ponds. Although the relative volume of water contributed by the WWTP is large, the average Pu activity in the WWTP effluent, 0.004 pCi/L, is low. The resulting average load contributed by the WWTP therefore constitutes roughly only 3 % of the load discharged annually to the ponds.

A and B-Series Ponds Uranium-238 Mass Balance

Results from the U-238 mass balance analysis for the A- and B-Series ponds, using measured data only, are presented in Table TA-4-9. The data represent average annual U-238 loads in Water Years 1997 through 1999 at all monitoring stations in the study area. Net gain or loss in outflow load compared to inflow load is presented at the bottom of the table.

Table TA-4-9. A- and B-Series Ponds, U-238 Mass Balance Results – Measured Load Data Only, Average for Water Years 1997 - 1999

U-238 Inputs

Measured Inputs

Input	Description	Load (pCi)
SW093	N. Walnut In	2.6E+08
GS10	S. Walnut In	2.0E+08
SW091	Tributary	1.4E+06
WWTP	Tributary	9.4E+07
Total Measured Inputs		5.6E+08

A- and B- Series Ponds
Study Area

U-238 Outputs

Measured Outputs

Input	Description	Load (pCi)
GS11	N. Walnut Out	3.8E+08
GS08	S. Walnut Out	1.8E+08
Total Measured Outputs		5.6E+08

Gain (+) or Loss (-) of U-238 in Study Area

Variables	Delta (pCi)	Change from Input Load	Remarks
Measured Data (Out - In)	2.9E+05	0.1%	Little change of U-238 in reach

Table TA-4-10 contains information on U-238 concentrations, U-238 loads and drainage sub-basin characteristics for each of the monitoring stations in the A- and B-Series ponds study area. The rightmost column of the table contains the estimated average annual U-238 load yielded per square meter of the sub-basin.

432

U-238 surface water load data for the A- and B-Series ponds are plotted by year from Water Year 1997 through 1999 (Figure TA-4-17). Positive values in the bar graphs represent input loads of U-238 and negative values represent output loads. This graph provides perspective on the annual variation of loads contributed by different sub-basins. Uncertainty with these data is addressed in Section TA-5.

Table TA-4-10. Summary of A- and B-Series Ponds U-238 Loading Analysis

Monitoring Location	Basin Description	Sub-Basin Size		Approx. % Impervious	Water Yield (Annual Average)		U-238 Concen. (Annual Average)	U-238 Load (Annual Average)	% of Total Input Load	U-238 Yield per Unit Area (Annual Average)
		(Hectares)	(Acres)	(%)	(Liters)	(Acre-Feet)	(pCi/L)	(pCi)	(%)	(pCi/m^2-Yr)
Input Loads										
SW093 (Measured)	North Industrial Area Runoff	98.0	242.3	28%	2.2E+08	178.5	1.172	2.6E+08	46.4%	263.2
GS10 (Measured)	Central Industrial Area Runoff	67.7	167.4	47%	1.5E+08	122.3	1.346	2.0E+08	36.5%	299.5
SW091 (Measured)	Northeast Industrial Area Runoff	4.4	10.8	5%	7.5E+05	0.6	1.901	1.4E+06	0.3%	32.4
WWTP (Measured)	WWTP Treated Effluent to Pond B-3	N/A	N/A	N/A	2.5E+08	205.5	0.369	9.4E+07	16.8%	N/A
				Totals	6.3E+08	506.9	-	5.6E+08	100%	-
Output Loads										
GS11 (Measured)	North Industrial Area Runoff Thru Pond A-4	178.6	441.3	16%	4.0E+08	321.5	0.950	3.8E+08	67.7%	210.8
GS08 (Measured)	South Industrial Area Runoff Thru Pond B-5	105.3	260.2	31%	2.1E+08	170.8	0.853	1.8E+08	32.3%	170.6
				Totals	6.1E+08	492.2	-	5.6E+08	100%	-

Analysis of A- and B-Series Ponds U-238 Mass Balance Results

An important pattern of U-238 surface water transport in the A- and B-Series ponds study area is that surface water concentrations of U-238 do not vary much from location to location. The one exception is the WWTP effluent stream that had roughly one fourth of the U-238 concentration measured at the storm water monitoring locations. Average annual U-238 concentrations at the storm water locations within the study area ranged from approximately 1.0 to 2.0 pCi/L, which is consistent with the pattern observed across the Site. This pattern contrasts with average Pu concentrations that vary by up to a factor of 30 from one location to another. Because of the relatively similar concentrations, the

433

variation of U-238 loads flowing from one location to another is largely a function of water volume.

Water Year 1997 through 1999 data indicate the average annual U-238 load conveyed by the flow out of the study area, measured at stations GS11 and GS08, was essentially the same as the load measured flowing into the reach. Review of the loading profile for each year (Figure TA-4-17) shows that the A- and B- ponds were a U-238 "sink" in Water Year 1997, with approximately 13 % of the inflow load removed. In Water Years 1998 and 1999, the ponds were a U-238 "source", when a gain of roughly 8 % and 2 % compared to the inflow load, was observed. The average of the three years of loading data was that inflow and outflow loads were roughly equal.

The northern Industrial Area basin, measured by station SW093, contributes the largest single fraction, approximately 45 %, of the total input U-238 load to the ponds. Central Industrial Area runoff, measured by station GS10, contributes approximately 35 % of the total input U-238 load. As discussed earlier, the proportion of loads delivered by these major Industrial Area sub-basins is largely a function of water volume because the U-238 surface water concentrations for the two sub-basins are comparable. The average annual U-238 concentration for station SW093 is 1.2 pCi/L and for station GS10 is 1.3 pCi/L. Similarly, the U-238 load delivered per square meter is also comparable for these basins, 263 pCi/m^2 for SW093 and 299 pCi/m^2 for GS10.

The sub-basin with the highest concentration of U-238 in the runoff is the northeast Industrial Area sub-basin, monitored by SW091, with an annual average concentration of 1.9 pCi/L. However, as addressed in the Pu mass balance analysis, the SW091 sub-basin has only 5 % impervious surface area. Consequently, there is little runoff from this drainage and the resulting U-238 load delivered per square meter, 32.4 pCi/m^2, is roughly one tenth of that delivered by the more impervious SW093 and GS10 basins. This aspect of U-238 transport in the A- and B-Series ponds study area is consistent with the patterns observed in the Pu loading analysis. Drainages with relatively higher percentages of impervious surfaces, such as the SW093 and GS10 sub-basins, deliver up to 10 times the actinide load to downstream receiving waters as basins with minimal impervious area.

TA-4.4.7 South Interceptor Ditch Analysis

South Interceptor Ditch Plutonium Mass Balance

Results from the Pu mass balance analysis for the SID, using measured data only, are presented in Table TA-4-11. The data represent average annual Pu loads in Water Years 1997 through 1999 at all monitoring stations in the study area. Net gain or loss in outflow load compared to inflow load is presented at the bottom of the table.

Table TA-4-11. South Interceptor Ditch, Pu Mass Balance Results – Measured Load Data Only, Average for Water Years 1997 - 1999

Pu-239/240 Inputs

Measured Inputs

Input	Description	Load (pCi)
GS42	Tributary	1.3E+05
Total Measured Inputs		1.3E+05

South Interceptor Ditch
Study Area

Pu-239/240 Outputs

Measured Outputs

Output	Description	Load (pCi)
SW027	SID Out	3.3E+06
Total Measured Outputs		3.3E+06

Gain (+) or Loss (-) of Pu in Study Area

Variables	Delta (pCi)	Change from Input Load	Remarks
Measured Data (Out - In)	3.2E+06	2366%	GS42 Does Not Reflect All Inputs

Table TA-4-12 contains information on Pu concentrations, Pu loads and drainage sub-basin characteristics for each of the monitoring stations in the SID study area. The rightmost column of the table contains the estimated average annual Pu load yielded per square meter of the sub-basin.

Pu surface water load data for the SID are plotted by year from Water Year 1997 through 1999 (Figure TA-4-18). Positive values in the bar graphs represent input loads of Pu and negative values represent output loads. This graph provides perspective on the annual variation of loads contributed by different sub-basins. Uncertainty with these data is addressed in Section TA-5.

435

Table TA-4-12. Summary of South Interceptor Ditch Pu Loading Analysis

Monitoring Location	Basin Description	Sub-Basin Size		Approx. % Impervious	Water Yield (Annual Average)		Pu Concen. (Annual Average)	Pu Load (Annual Average)	% of Total Input Load	Pu Yield per Unit Area (Annual Average)
		(Hectares)	(Acres)	(%)	(Liters)	(Acre-Feet)	(pCi/L)	(pCi)	(%)	(pCi/m^2-Yr)
Input Loads										
GS42 (Measured)	Tributary flow to SID (vegetated hillsope)	18.2	45.0	3%	1.2E+05	0.1	1.104	1.3E+05	100.0%	0.7
				Totals	1.2E+05	0.1	-	1.3E+05	100%	-
Output Load										
SW027 (Measured)	Entire SID Basin	86.7	214.2	14%	3.7E+07	29.7	0.090	3.3E+06	100.0%	3.8
				Totals	3.7E+07	29.7	-	3.3E+06	100%	-

Analysis of South Interceptor Ditch Plutonium Mass Balance Results

A mass balance analysis for the SID drainage basin, using measured data only, is not practical given the lack of measured inflow data to the study area in Water Years 1997 through 1999. However, review of the data for the two monitoring stations for which there are measurements does provide some insight into Pu transport patterns in the study area.

The sub-basin monitored by station GS42, 18 hectares (45 acres), comprises approximately 20 % of the SID basin area and is located southeast of the 903 Pad. The GS42 sub-basin consists primarily of a well-vegetated hillslope, with only a 3 % impervious area. The GS42 drainage has a documented Pu surface soil source, IHSS 216.3, within the sub-basin boundaries and has Pu soil activity, ranging from 10 to 100 pCi/g, which is relatively high compared with the rest of the Site. Despite the presence of the Pu surface soil sources, the annual Pu load delivered per square meter, 0.7 pCi/m^2, is relatively low. For comparison sake, the GS42 sub-basin load per square meter is approximately two percent of the load measured per square meter for the central Industrial Area runoff at station GS10. The GS42 average annual load constitutes only about 4 % of the load measured flowing out of the SID at station SW027. The remainder of the input load to station SW027 in comprised of the southern Industrial Area runoff,

hillslope runoff and other input variables addressed in Section TA-5 where measured and modeled data are combined.

Station SW027, which forms the downstream boundary of the SID drainage basin, receives runoff from the areas with the highest surface soil Pu concentrations at the Site. Several Pu IHSSs, including 109, 140 and 183, are located within the boundaries of the SW027 basin along with a widespread plume of elevated Pu soil activity that is not included within an IHSS boundary (see Figure TA-4-4 and Figure TA-4-5). The SW027 sub-basin has the only surface soil sample results at the Site, in the vicinity of the 903 Pad, that exceed the RFCA Tier II Action Level for Pu. Average annual concentrations of Pu in the surface water at SW027 (0.090 pCi/L) are less than at central Industrial Area station GS10. The 87 hectare (214 acre) SW027 basin is characterized by well-vegetated slopes, with only 14 % impervious area. Compared with the central Industrial Area, the SID drainage has approximately one fifth of the runoff volume per unit area. The Pu load per square meter, 3.8 pCi/m^2, is roughly one tenth of that observed for the central Industrial Area basin.

For perspective, the Site's surface water quality standard for total U, as noted in Section TA-1, is currently set at 10 pCi/L for Walnut Creek and 11 pCi/L for Woman Creek. In comparison, the EPA promulgated a total U MCL of 30 μg/L for drinking water on 12/7/00 (Federal Register, 2000). Converting mass to activity, the 30 μg/L total U MCL corresponds to a total U activity of approximately 20 pCi/L using the isotopic proportions typically found in RFETS surface water. Total U concentrations from Water Years 1997 through 1999, at RFETS POE and POC monitoring stations, averaged approximately 2 to 5 μg/L or roughly one order of magnitude less than the recently established MCL for drinking water.

South Interceptor Ditch Uranium-238 Mass Balance

A U-238 mass balance was not calculated for the SID using measured data only. Measured data were unavailable for Water Years 1997 through 1999 for tributary station GS42. Therefore, the only measured U-238 surface water data available are for

downstream boundary station SW027. Analysis of U-238 for the SID is performed in Section TA-5 using measured and modeled data combined.

TA-4.4.8 Summary of Surface Water Pathway Analysis

Key findings from the surface water pathway analysis using only measured, not modeled, data are summarized in this section. These findings are compared with the pathways qualitatively described in the conceptual model report and summarized in Section TA-4.1. The measured data indicate an actinide transport patterns that fully supports the transport mechanisms identified in the conceptual model.

- **The central Industrial Area is the largest source of surface water Pu load at the Site, although it is *not* the area with the highest Pu concentrations in surface soil.** Central Industrial Area runoff, monitored by Station GS10, has the largest Pu load of any sub-basin. The average annual Pu load delivered per square meter at GS10, 42.5 pCi/m^2, exceeds the next highest major sub-basin by nearly a factor of five, which is northern Industrial Area runoff monitored at station SW093. The GS10 sub-basin does not have the highest Pu surface soil concentrations at the Site and has no surface soil sample results above the RFCA Tier II Action Level. The 68-hectare (167-acre) GS10 sub-basin, approximately 47 % impervious, is characterized by large areas of pavement mixed with areas of poorly vegetated exposed soil.

  Large impervious areas increase runoff, which in turn, increases erosion processes on hillslopes and in channels that are unpaved. The high relative Pu load from the central Industrial Area supports the conceptual model postulation that overland erosion is a dominant transport mechanism for Pu at RFETS.

- **High Pu concentration in the surface soil does not necessarily correspond with a high relative Pu load delivered to surface water.** The sub-basin with the highest surface soil Pu concentrations at the Site is the SID drainage, monitored by station SW027. The SW027 sub-basin has the only surface soil sample results at the Site, in the vicinity of the 903 Pad, that exceed the RFCA Tier II Action Level for Pu.

Average annual concentrations of Pu in the surface water at SW027 (0.090 pCi/L) are less than at station GS10 (0.191 pCi/L). The 87 hectare (214 acre) SW027 basin is roughly 30 % larger than the GS10 basin and has much different hydrologic conditions than the GS10 sub-basin. Instead of large impervious surfaces, the SW027 basin is characterized by well-vegetated slopes, with only 14 % impervious area. Therefore, The SID drainage has less runoff per unit area than the central Industrial Area and the Pu load per square meter is roughly one tenth of that observed in the GS10 sub-basin.

As discussed above, large impervious areas increase runoff and corresponding erosion processes in areas without pavement. Areas with high Pu surface soil activity, if not prone to erosion, would not be expected to contribute as high a Pu load as expected from a watershed that is prone to erosion.

- **A high percentage of pervious area in a drainage basin appears to substantially reduce the quantity of Pu delivered, per unit area, to surface water.** The SW091 sub-basin, which collects runoff from the northwest corner of the Industrial Area, has a Pu delivery pattern similar to the SID (SW027) basin. This is the case although the SW091 basin size (4 hectares [11 acres]) is only 5 % of the SW027 drainage area. The SW091 sub-basin has a Pu surface soil source (IHSS 141) and has a low percentage of impervious surfaces. Also similar to the SID drainage, SW091 has average Pu surface water concentrations that are higher than other basins without Pu sources. However, because the basin has a low percentage of impervious area, there is little runoff and the resulting average annual Pu load delivered from the sub-basin is relatively small. The average annual Pu load per square meter for the SW091 drainage sub-basin is 3.8 pCi/m^2 - the same measured in the SW027 (SID) basin. This is approximately one tenth of the Pu load delivered per square meter by the impervious GS10 sub-basin. Reduced runoff from the SW091 basin results in reduced erosion and less movement of Pu in the surface water.

- **The detention ponds generally remove 80 to 90 % of the annual inflow Pu load.** Loading data indicate that the A- and B-Series ponds were a Pu "sink" every year

from Water Year 1997 through 1999. However, while the ponds had a Pu load removal efficiency of 92 % and 88 % in Water Years 1997 and 1998, respectively, the removal efficiency in Water Year 1999 was only 37 %. The reduced Pu trapping efficiency in Water Year 1999 is linked to one flow-paced composite sample at the outfall of Pond B-5, collected from 6/23/99 to 8/5/99, that had Pu activity 50 times greater than the average measured that year. Although no increase in Pu load was measured downstream from the ponds during this period, the sample altered the Pu loading pattern calculated for that year.

The efficiency of the ponds removing inflow Pu load reflects Site studies that show approximately 90 % of Pu flowing into the ponds is bound to particulate-sized particles that will settle out of the water column.

- **Lower Walnut Creek generally has a larger outflow Pu load than inflow load.** Data for Water Years 1997 through 1999 indicate the average annual Pu load moving out of lower Walnut Creek, measured at GS03, was approximately 30 % higher than the load measured moving into the reach. Water Years 1997 and 1998 were consistent with this pattern, with outflow loads exceeding inflow loads. Water Year 1999 reversed this trend when the inflow Pu load exceeded outflow by approximately 50 %. The Water Year 1999 Pu loading pattern reversed the trend of the prior two years when a large Pu load was measured out of Pond B-5, a direct consequence of the high activity sample, discussed above, collected from 6/23/99 to 8/5/99. Because no increase in Pu load was measured downstream during that time frame, the calculated Water Year 1999 loading pattern indicated a deposition of Pu to the channel. The tributary channels that feed lower Walnut Creek do not provide an explanation to the increased loads measured at the downstream end. Therefore, some other Pu source, such as the channel sediments, supplies the Pu that increases the Pu load at the downstream end of the channel.

  Resuspension of channel sediments is a major Pu transport pathway in the conceptual model. The measured data indicate that another Pu transport mechanism, such as channel sediment resuspension, is contributing to the Pu load in lower Walnut Creek.

- **There is little variation in the relative abundance of different U isotopes measured from one location to another across the Site.** The U transport pattern contrasts with average Pu concentrations that vary by up to a factor of 30 from one location to another. Because of the relatively similar concentrations, the variation of U loads flowing from one location to another is largely a function of water volume. For perspective, from Water Years 1997 through 1999, total U concentrations at RFETS POE and POC monitoring stations averaged roughly one order of magnitude less activity than the recently established 30 μg/L MCL for drinking water.

  U concentrations in surface soils for individual isotopes throughout the Site are generally at background levels except in a limited number of specific source locations. Plumes of surficial U contamination do not exist in the same fashion as for Pu and Am. This is evident when reviewing the figures with kriged surface soil data (Figure-TA-2-8 through Figure-TA-2-12). The absence of surficial U plumes supports the conceptual model that identifies downward infiltration as the dominant transport pathway for U.

- **Drainage basins with a high percentage of impervious area deliver measurably higher U loads, per unit area, than basins with minimal impervious area.** This aspect of U transport is consistent with patterns observed in Pu loading patterns. Drainages with higher percentages of impervious surfaces, such as the SW093 and GS10 Industrial Area sub-basins, deliver up to 10 times the U load to downstream receiving waters compared to basins with minimal impervious area.

441

TA-4.5 GROUNDWATER PATHWAY ANALYSIS

TA-4.5.1 Methodology Used for Groundwater Pathway Analyses

The general overview of groundwater actinide contaminant extent and transport patterns presented in this section serves to provide a basis for developing and interpreting the groundwater pathway analysis performed in Section TA-5.3. Unlike the Section TA-4 discussions for surface water and air pathway transport analyses, groundwater pathway analyses based on measured data will be limited to discussions of actinide contaminant extent and transport patterns only. This approach is being taken because direct measurements of groundwater flux required for loading calculations are unavailable and must be calculated for most areas of the Site. Measurements of linear groundwater fluxes are available from data collected at groundwater collection and treatment systems (i.e., East Trenches, Mound and Solar Ponds Plume), but these measurements are only applicable to limited reaches of stream and cannot reliably be extrapolated across the rest of the Site. Groundwater actinide loading to streams will be quantitatively evaluated in Section TA-5.2 using groundwater flux estimates provided by the Site-Wide Water Balance Model.

TA-4.5.2 General Patterns of Groundwater Actinide Transport at RFETS

Extensive hydrogeologic investigations and monitoring activities involving groundwater movement and actinide transport in the saturated zone and, to a lesser extent, unsaturated zone have been conducted at RFETS to identify and understand the relationship between contaminant occurrence, extent and fate. This subsection presents a Site-wide analysis of groundwater actinide characteristics and patterns for the data presented in Section TA-2 and other sources as a basis for performing actinide loading calculations presented in later subsections. To facilitate discussions, the groundwater pathway has been divided into unsaturated zone and saturated zone components, each of which affect actinide transport in different ways.

442

Given the similar, non-conservative geochemical behavior of Pu and Am in the aquatic environment (see Section TA-3), these actinides are considered jointly in transport analyses, with emphasis placed on Pu transport because of its greater historical use and abundance at RFETS. U transport patterns are considered separately because of its greater solubility and mobility in groundwater compared to that of Pu and Am. For practical purposes, the U discussion will focus on U-238 since the geochemical behavior of the individual U isotopes U-233/234, U-235 and U-238 are indistinguishable.

TA-4.5.3 Plutonium and Americium Transport Patterns for Unsaturated Groundwater

Pu and Am transport through the unsaturated zone to the saturated zone at RFETS is hypothesized to involve three basic pathways: migration of Pu-239/240 and Am-241 from subsurface releases related to process waste line, process waste holding tank and/or UBC:

- Infiltration of incident precipitation and runoff through contaminated soils and sediments resulting in the leaching or entrainment of Pu-239/240 and Am-241 as dissolved and/or colloidal phases, possibly due to preferential flow in macropores; and

- Cross-contamination from drilling and well installation activities conducted in areas of surficial soil and sediment contamination.

The occurrence and vertical distribution of actinide contaminants in soils (specifically Pu and Am at the 903 Pad, Lip and outlying areas) have been a subject of study at RFETS for a period of over 30 years (Krey and Hardy, 1970; Little, 1976; Krey et al., 1977; Webb, 1992; Webb et al., 1993; Schierman, 1994; Ibrahim et al., 1996; Litaor et al., 1994). Pu and Am movement from surface to shallow subsurface soils (one meter depth) have been observed in all test trench and pit investigations conducted in surficially-contaminated soil areas at RFETS, irrespective of soil type and surface soil activity-concentration. The main mechanism for downward movement of Pu and Am in the soil

appears to be infiltration of contaminated water through macropores. With the exception of groundwater sample results, data on Pu and Am migration through the soil below a depth of one meter are generally unavailable. The removal and disposal of Pu-contaminated soil associated with historical process waste line (e.g., B559) and tank (e.g., B774) repairs (Stewart, 1973) underscore the potential for Pu and Am migration near these facilities.

Krey and Hardy (1970) found detectable amounts of Pu at a depth of 20 cm just two or three years after wind-blown Pu was suspected of being released from the 903 Pad. This result was subsequently confirmed by Little (1976) who reported measurable amounts of Pu at a depth of 21 cm within five to six years (1972 to 1974) after the release. These data indicate that Pu initially moved rapidly through the uppermost soil horizon, but was effectively attenuated by the deeper layers.

In 1977, Krey et al. sampled soils to a 40 cm depth to more closely examine Pu migration rates and relate the results to reductions in the mean annual air concentration observed at sampling stations. They found that maximum Pu concentrations no longer existed at the soil surface, but had translocated to the 2 to 6 cm depth interval depending upon soil conditions. The vertical profile of Pu contamination was otherwise identical to the earlier Krey and Hardy study. Using a simple diffusion model fit to measured data, they estimated fractional transfer rates ranging from 25 %/yr cm to 65 %/yr cm for the uppermost soil layer. The model results agreed reasonably well with observed values to a depth of 20 cm, but underestimated Pu concentrations below that depth. They also concluded, based on Am-241/Pu-239/240 ratio data, that Am-241 appeared to have a slightly greater mobility in soil.

Webb (1992) and Webb et al. (1993) examined the Pu depth profile and concentration gradients presented by Little (1976) and Little and Whicker (1978) compared to similar data collected by the authors in 1989 and concluded that, with the exception of the 0 to 3 cm depth, no significant differences could be discerned from the data. A similar comparison was undertaken by Schierman (1994) and Ibrahim et al. (1996) who compared their Pu depth profiles with those of Webb and Little and found no significant

444

differences. These authors concluded that the stability of the soil Pu depth profile and Am-241/(Pu-239/240) ratios over a 25-year period provided an indication of the low mobility of these actinides in the soil environment.

Further information on the vertical distribution of Pu-239/240 and Am-241 in RFETS soils and pedological properties that potentially control their transport was provided by Litaor et al. (1994). In 23 of the 25 soil pits sampled and analyzed, they observed an exponential decrease in actinide activity with depth similar to that reported by other RFETS investigators. The pattern was consistent regardless of soil characteristics, level of contamination, distance or direction from the 903 Pad. In soils close to the 903 Pad (Area A) they found that actinides may have been transported to greater depths than previously reported as a result of coarser soil textures and higher hydraulic conductivity values in this area. Biological activity (earthworms) was implicated as an upward actinide transport mechanism at one sampling pit (Pit 8) and evidence of intense earthworm activity was observed at other locations. Extensive macroporosity networks caused by decayed root channels were documented in the soil pits, but these networks were not observed at depths greater than 120 cm. Samples collected from decayed root channel macropores showed higher Pu-239/240 activity compared to the surrounding soil matrix (7.0 Bq/kg and 5.9 Bq/kg macropore compared to 0.03 Bq/kg matrix at 90 cm in Pit 3 and 8.5 Bq/kg macropore compared to 1.5 Bq/kg and 0.7 Bq/kg matrix at 70 cm and 96 cm, respectively, in Pit 4). Based on this data, Litaor et al. (1994) concluded that preferential flow along macropores was a viable actinide transport mechanism; however, direct macropore transport to the saturated zone was unlikely considering that the depth of the macropore network was limited to the upper 120 cm of soil.

Until 1996, direct evidence of actinide transport in percolating soil waters at the Site was unavailable. Litaor et al. (1996) conducted a series of field experiments that evaluated water and actinide movement through *in situ* unsaturated soils east of the 903 Pad. Five heavily instrumented trenches (Pits 1 through 5) equipped with a series of zero tension samplers and tension lysimeters installed at three depth increments (0 to 20 cm, 20 to 40 cm and 40 to 70 cm) were used to collect percolating water for actinide analysis. These

samplers were purposely installed to intercept macropores where they were evident in the trench wall. Percolation water was created using an automated rainfall simulator to apply simulated rainfall events for recurrence intervals ranging from 10 to 100 years. The study revealed a depth pattern of Pu-239/240 activity-concentration in soil interstitial waters that mimicked the Pu-239/240 soil distribution reported in earlier papers. Soil water Pu-239/240 activity-concentrations were highest in the zero to 20 cm depth interval with mean values ranging from 0.71 Bq/L (19.17 pCi/L) to 2.57 Bq/L (69.39 pCi/L) depending on simulated rainfall amounts. At the 40 to 70 cm depth increment, mean Pu-239/240 activity-concentrations ranged from 0.07 Bq/L (1.89 pCi/L) to 0.16 Bq/L (4.32 pCi/L), with the highest values reported for the 100 year rainfall event. These results, combined with evidence from the vertical distribution of volume flux and various edaphic conditions described for trench soils, led Litaor et al. (1996) to hypothesize that "the translocation of actinides to deeper soil horizons may be constrained by macropores too small to accommodate the transport of the discrete particles". They also concluded that the observed short duration of macropore flow and presumed small soil volume associated with this type of flow would further minimize the movement of Pu-contaminated particles in the soil. Given the biased nature of the sampling approach (trenches located at hillside sites containing lateral soil discontinuities, extreme rainfall events and experimental artifacts caused by soil disturbances during sampler installation and macropore truncation), these results should be viewed as providing a worst case assessment for actinide transport to saturated zone groundwater.

Litaor et al. (1998), expanding on the earlier work of Litaor et al. (1996), performed additional rainfall simulation experiments (100 year rainfall only), monitored natural precipitation events and characterized the fractionation of Pu-239/240 and Am-241 among particulate, colloidal and dissolved phases in selected soil interstitial water samples. The small water fluxes measured in the deepest samplers (40 to 70 cm) during natural rain and snowmelt events (all <25 year recurrence interval) indicated that only a minimal potential exists for actinide transport to groundwater under these conditions. The extreme rainfall simulation events indicated that actinides were not mobilized downward into the soil column in large amounts, although large rainfall amounts may be

important in translocating small amounts of actinides downward to groundwater. The amount of Pu-239/240 and Am-241 remobilized from the top, most contaminated sampling depth (0 to 20 cm) was estimated to range from 0.002 to 0.07 % of the total inventory, respectively. This result is consistent with the limited penetration of these actinides observed in the soil and soil water depth profiles at these locations. The authors suggest that the Pu and Am fluxes calculated for the 40 to 70 cm depth interval for the large rain event experiments may indicate potential transport to groundwater under extremely wet conditions.

To assess actinide phase associations in soil waters, Litaor et al. (1998) collected seven soil water samples during rain simulations. These samples were fractionated into particle size ranges of >5 μm (particulate), >0.45 μm to 5 μm (colloids), >10 kDa to 0.45 μm (colloids) and <10 kDa (dissolved) and analyzed for Pu-239/240 and Am-241 content. Litaor et al. (1998) determined that greater that 80 % of the Pu-239/240 and Am-241 in all samples were associated with the >5 μm size fraction and between 83 and 97 % of these actinides were associated with the >0.45 μm size fraction, regardless of sampling depth or sample activity. From these results, the authors conclude that actinide mobility through soils should be limited and will depend on the spatial arrangement and continuity of the macropore network. They cautioned that deep, well-developed macropores, such as those formed by the Canadian Thistle, have the greatest potential to transport suspended particles and, hence, actinides to shallow groundwater.

Additional information about particle and Pu mobilization in soils at RFETS is provided by Ryan et al. (1998). Using the soil monitoring system described by Litaor et al. (1998), Ryan et al. (1998) conducted additional rainfall simulations that investigated the effects of macropore flow on particle generation and movement. Ryan et al. (1998) observed a three order of magnitude decrease in soil water Pu-239/240 activity from the shallowest (0 to 20 cm) to the deepest (40 to 70 cm) zero tension lysimeter intervals in Pit 4. They concluded that Pu transport by infiltrating rainfall is significantly attenuated by the upper soil horizons. The authors found a lack of correlation between particle concentration,

particle size, infiltration velocity and soil type, which they conclude could be caused by flow through macropores.

In summary, multiple studies conducted on Pu movement through soils at RFETS demonstrate that Pu and Am transport is mainly limited to the upper soil horizons. Pu and Am are strongly associated with colloids and particles whose movement through the soil controls the distribution of these actinides in the unsaturated zone. Macropores are implicated as the most likely pathway for Pu and Am transport to deeper soil horizons (to 70 cm). Transport of Pu and Am below a depth of 96 cm is expected to be small, based on available information.

TA-4.5.4 Plutonium and Americium Transport Patterns for Saturated Zone Groundwater

Figures TA-2-60 through TA-2-63 present the unfiltered mean Pu-239/240 and Am-241 activity-concentrations, respectively, for RFETS monitoring wells. The following discussion will focus primarily on Pu-239/240 transport patterns given the similarities in transport behavior between these two actinides in the groundwater environment. Delineation of groundwater Pu and Am plumes has not been attempted on these figures considering that the mode of transport to groundwater (drilling-induced versus natural) has not been conclusively resolved.

Background

With rare exception (see Section TA-3), Pu and Am do not occur naturally in the environment, hence their presence in groundwater is necessarily indicative of an anthropogenic release. Groundwater Pu-239/240 and Am-241 activities measured from background UHSU wells at the Site are generally low, with averages of 0.005 pCi/L for unfiltered Pu-239/240 and 0.006 pCi/L for unfiltered Am-241. These activities provide a baseline for comparison to the industrialized and disturbed areas of the Site. Concentration gradient characteristics of naturally-occurring elements, such as described for U in Section TA-4.5.2, are not expected to be an important factor for interpreting Pu and Am groundwater data.

Woman Creek Groundwater Basin

Wells containing appreciable Pu-239/240 and Am-241 contamination in the Woman Creek basin are found around the 903 Pad and associated surface soil contaminated area and the Original Landfill. In the Woman Creek basin portion of the 903 Pad area, nine UHSU wells (0171, 0271, 1587, 00191, 00291, 07191, 09091, 09691 and 11791) contain mean unfiltered Pu-239/240 activity-concentrations that exceed the groundwater Tier II action level of 0.15 pCi/L. The Pu-239/240 in these wells undoubtedly originates from surface soil contamination, although the mechanism of transport, natural versus drilling-induced, has been the subject of uncertainty for almost a decade. RMRS (1998) reviewed the available data for the 903 Pad and surrounding area wells and concluded that cross-contamination introduced by drilling and well installation through contaminated surface soils was the most likely cause of the elevated Pu and Am activity-concentrations in these wells. A more detailed discussion of recent field investigations designed to evaluate the drilling artifact contamination pathway is presented in Section TA-4.5.8.

Well 59493 located in the Original Landfill contains a mean unfiltered Pu-239/240 value of 0.21 pCi/L, with activity-concentrations ranging from below detection to 1.037 pCi/L. The repeated detection of Pu-239/240 in this well indicates that some Pu contamination may be present in the Landfill, although the absence of Pu in other nearby and downgradient landfill wells tend to preclude a large or widespread source.

Aside from the well data presented in Figures TA-2-60 through TA-2-63 and described above, additional unpublished saturated zone Pu-239/240 and Am-241 data was collected at the 903 Hillside Soil Study area during a period of unusually high groundwater levels in 1995 (Litaor et al., 1999). The study area is located in a hillside setting within a bedrock groundwater discharge area that became flooded from an extended period of subsurface discharge to the overlying colluvial material. Field observations of completely saturated soils occurring in a seepage area with a subsurface discharge source indicate that upwelling and subsequent lateral flow of groundwater through the colluvial soil cover may contribute to Pu and Am transport, at least for seepage areas located in soil contamination areas. Under these conditions, an increase in Pu and Am flux related

to lateral groundwater flow, especially through the upper, more permeable and contaminated soil horizons, is plausible, although the magnitude, extent and mechanism for this mode of actinide transport have been the subject of recent dispute. Litaor et al. (1999) reported that as much as 24.2 MBq (0.65 mCi) Pu-239/240 and 4.3 MBq (0.12 mCi) Am-241 were transported across the down-gradient boundary of the soil study area during a 65 day period of saturation.

These results have revived concerns among the public and regulatory agencies that Pu and Am migration in groundwater may pose a greater long-term off-Site threat to water supplies than previously thought possible and, in large part, were the impetus for the current AME program. Accordingly, the study results have been carefully reviewed resulting in many questions about the validity of the analysis and proposed actinide mobilization mechanism. It is generally accepted that the potential for lateral actinide transport in shallow contaminated surface soils is increased when fully saturated from below; however, the magnitude and fate of the resulting actinide flux is uncertain. With regard to the calculated fluxes, several aspects of the sampling methodology deserve scrutiny. For example, the functionality of zero tension samplers (ZTSs) designed to collect gravitationally-flowing water (downward vertical flow) in the unsaturated zone, when submerged, has not been addressed. Localized particle mobilization (up to 9,800 mg/L) has been inferred for ZTSs at RFETS during unsaturated zone infiltration experiments (Ryan et al., 1998). It therefore seems reasonable that flow perturbations caused by sampler operation will affect particle mobilization under saturated conditions, especially since water pressure (hydraulic head) at the soil/sampler interface will be significantly greater than experienced under unsaturated conditions. Furthermore, given that soil macropores are implicated as an important pathway for vertical actinide transport (i.e., vertical K > horizontal K), it is reasonable to infer that a significant fraction of vertical flow and actinide flux was collected by the ZTSs. Consequently, the ability of these devices to provide samples representative of lateral actinide transport remains suspect and should be viewed only as a worst case scenario.

The mechanism of Pu and Am transport at the 903 Hillside Soil Study area has also been the subject of controversy. Litaor et al. (1999) hypothesized that redox changes in flooded soils, from aerobic to anaerobic, were responsible for the dissolution of sesquioxides and release of Pu colloids into soil interstitial waters. Subsequent experimentation by Honeyman et al. (1999), who investigated the effect of redox potential on Pu solubility in RFETS soil-waters, found no evidence for Pu mobilization under changing redox conditions. Considering the hydrologic setting and conditions observed in the field, Pu mobilization via physical particle detachment from soil macropores may have been initiated from upward flowing groundwater, similar to the way a filter is backflushed. The absence of Pu in down-gradient wells (00491 and 1487; also see 90099 and 90399 in Section TA-4.5.3) provides evidence that groundwater transport in deeper, perennially saturated colluvial material is minimal. At the soil study area, episodic transport of actinides during infrequent, high water table conditions may be locally significant for emergent seepage water and subsurface flow through the uppermost soil layers, but the magnitude of this process has likely been overestimated with the available data because of experimental artifacts. In any event, any actinide flux associated with shallow subsurface flow that migrates toward Woman Creek will be intercepted by the SID, which extends well below the base of the uppermost Pu contaminated soil horizons.

Walnut Creek Groundwater Basin

The Walnut Creek groundwater basin contains all of the major Pu and Am processing buildings, much of the process waste line and holding tank systems, the Solar Evaporation Ponds, the northern portion of the 903 Pad and Lip areas, the A- and B-series ponds, the former Present Landfill and other potential areal actinide source areas. Consequently, this basin contains perhaps the greatest potential for Pu and Am transport to surface water. Historical Pu-239/240 and Am-241 groundwater data is somewhat sparse within the PA, except for the Solar Ponds area. The lack of monitoring wells in critical areas, such as the PA, is currently being addressed by the implementation of D&D

monitoring well networks around key buildings, including, but not limited to, Buildings 371, 559, 771, 707, 776/777, 779 and 991.

Groundwater Pu-239/240 and Am-241 activity-concentrations elevated above Tier II action levels are found in eighteen wells in the Walnut Creek groundwater basin. Eight of the eighteen wells (wells 00191, 06591, 06691, 06891, 06991, 08891, 13191 and 13491) are located in the northern portion of the 903 Pad area. The source of Pu and Am in these wells is identical to the southern portion; hence, the previous discussion of transport mechanisms applies to this basin as well. The main difference with the Woman Creek basin is that surface soil contamination at seepage areas in the Walnut Creek basin is less widespread and lower in activity, which lessens the potential for significant lateral Pu and Am transport through the uppermost soil horizons. In the Industrial Area, Pu contamination was also detected in well P313489 near former B663 and B668 storage areas; well 5671 at B122; well 3686 in South Walnut Creek above Pond B-1; and in Solar Pond wells 2286 and P209189. The contamination in these wells is thought to result from inadequate precautions taken during drilling and well installation to prevent contaminated soil from entering the well intake zone. The same transport mechanism is probably responsible for the Pu-239/240 contamination found in former well 1286 located above Pond A3 and boundary well 41691. The Pu contamination detected in former Present Landfill wells 6387, 72093 and 72393 is possibly related to low-level radioactive wastes buried early in the history of the Landfill.

East Drainages Groundwater Basin

As shown in Figure TA-2-70, the East Drainages groundwater basin is located east of the Industrial Area in an area that is hydrologically isolated from most Site activities. Historical Site impacts to this basin are mainly related to operation of the former South Spray Field, which temporarily reactivated spring and seep sites at the rim of the plateau and wind-blown actinide contamination (principally Pu and Am) from the 903 Pad. Because of it's isolation and absence of significant actinide source areas, the basin has received little attention except at the Site east boundary, where groundwater monitoring has been conducted to verify compliance with RFCA.

452

Examination of the East Drainages basin well data given in Figures TA-2-60 through TA-2-63 indicate that Pu-239/240 and Am-241 occur at background levels. In consideration of this information and its hydrologic isolation from potential source areas, the basin is not viewed as a significant pathway of concern for long-term off-Site migration of Pu or Am.

Site-Wide LHSU Groundwater

The lateral distribution of Pu-239/240 and Am-241 in LHSU groundwater is shown in Figures TA-2-65 and TA-2-66. These figures are supplemented by a table showing the Site-wide vertical distribution of Pu-239/240 with depth (Table TA-4-13). These figures demonstrate that Pu-239/240 and Am-241 activity-concentrations in LHSU groundwater are generally below detection. Wells with detectable Pu-239/240 and Am-241 are rare and tend to occur in areas with known surface soil contamination. Seven wells contain mean Pu-239/240 activity-concentrations above 0.05 pCi/L; these are 1687, 46692, 46792, 46892, 22193, B204189 and B217789. There appears to be no correlation between well and fault location for any of the wells listed above.

RMRS (1996) attributed Pu-239/240 and Am-241 detections in LHSU wells to drilling-artifact contamination based on consideration of well locations, drilling methodology and trend plot interpretation. An additional approach to understanding the vertical distribution of Pu-239/240 in groundwater shown in Table TA-4-13 involves an interpretation of the environmental isotope data collected at RFETS during the early 1990s. Environmental isotopes consist of various naturally-occurring, light stable and radioactive isotopes which, depending on the isotope and application, are capable of providing information about the history and/or source of water or solutes. In hydrologic studies, the most commonly employed environmental isotopes for tracing water movement are the rarer, heavier isotopes of oxygen and hydrogen, specifically oxygen-18 (O-18), deuterium (H-2 or D) and tritium (H-3 or T), that comprise a minor fraction of oxygen and hydrogen isotopes in water. Interpretation of stable O-18 and D data is dependent upon small but significant variations in isotopic content that are created by temperature-dependent fractionation processes, including evaporation and condensation.

These variations are transmitted in recharge water to groundwater where they are essentially preserved until discharged again as surface water. Under normal groundwater temperatures (< 80 degrees C), O-18 and D are not affected by reactions with geologic materials, thus they behave as conservative tracers of water movement through an aquifer or confining layer (Fontes, 1981). In recent years, the vertical O-18 and/or D distribution in confining layer groundwater has been utilized by some researchers as a low-resolution indicator of paleoclimate change (Remenda et al., 1994).

This information, considered with the vertical distribution of Pu-239/240 shown in Figure TA-4-19 and tabulated in Table TA-4-13, strongly implies that vertical Pu transport into and through the LHSU is highly unlikely. For Pu transport to occur in bedrock, it would be expected that the associated groundwater would also contain detectable amounts of H-3 and an UHSU-type O-18 signature. Table TA-4-13 indicates that LHSU wells containing detectable Pu-239/240 are untritiated and isotopically heavier than UHSU groundwater, thus another mode of transport, such as drilling artifact contamination or analytical problems are implicated as the likely cause of Pu (and Am) contamination in these wells. Some analyses from many of these wells are clearly problematic. For example in almost every LHSU well, single spurious results account for the high mean values in these wells compared to other LHSU wells. With the exception of wells 22193 and B204189, all of the LHSU bedrock wells were drilled in areas of known Pu soil contamination without utilizing surface soil isolation techniques (isolation techniques were used in well 22193). The problem of potential cross-contamination in these wells is therefore identical to that of the UHSU wells described in Section TA-4.5.3.

454

Table TA-4-13. Selected UHSU and LHSU Bedrock Wells with Detectable Pu-239/240

Well	Hydrostratigraphic Unit	Screen Midpoint Depth Relative to Bedrock, ft	Total Number of Samples (1991-1999)	Number of Samples >0.05 pCi/L	Minimum Pu-239/240, pCi/L	Maximum Pu-239/240, pCi/L	Mean Pu-239/240, pCi/L	$\delta^{18}O$, per mil (VSMOW)[1]	Tritium, T.U.[1]
11791	UHSU	4.3	20	13	-0.003	13.36	2.497	-14.61	N/D
13191	UHSU	5.3	13	12	0.058	5.024	1.247	-14.6	22.9
09691	UHSU	6.9	9	8	0.0483	1.1	0.319	-14.82	20.1
P209189	UHSU	13.9	11	11	0.0834	0.51	0.307	-13.29	N/D
06591	UHSU	25.1	12	12	0.7779	2.9	1.505	-13.83	1.4
25093	UHSU	30.4	2	1	0.008	0.2	0.104	N/D	N/D
02991	UHSU	31.2	11	2	0.002	0.8	0.112	-14.63	23.2
24993	UHSU	31.2	2	1	0.009	0.21	0.110	N/D	N/D
00291	UHSU	33.0	12	11	0.042	0.78	0.241	-13.74	<0.8
22193	LHSU Bedrock	44.5	9	1	-0.001	0.4154	0.049	-13.67	<0.8
B217789	LHSU Bedrock	54.3	2	1	0.0064	0.1438	0.075	-11.94	<0.8
46692	LHSU Bedrock	55.0	11	3	0	0.9696	0.103	-12.53	<0.8
46792	LHSU Bedrock	79.8	3	1	0	0.53	0.189	-11.79	<0.8
B204189	LHSU Bedrock	84.7	6	1	-0.0008	10.32	1.721	-11.865	<0.8
1687	LHSU Bedrock	90.3	13	5	0.0074	0.42	0.087	-12.07	<0.8
46892	LHSU Bedrock	129.9	6	2	0.001	0.48	0.097	-12.48	<0.8

N/D = not determined
[1] Analyses performed by the University of Waterloo Environmental Isotope Lab

455

TA-4.5.5 Uranium Transport Patterns for Unsaturated Zone Groundwater

U transport patterns in unsaturated zone groundwater have received relatively little attention compared to Pu and Am at RFETS. This situation exists partly because U occurs naturally, partly because the fate of U in soils is better understood than the other two actinides and partly because the health risks associated with U are lower than with Pu or Am. In addition, most potential U sources are buried and, outside of the Solar Ponds, have produced only limited indications of contamination in the underlying saturated zone. It is worth noting that elevated U detections in groundwater are usually associated with source areas where liquid wastes were released to the subsurface; elevated groundwater U is not normally seen in source areas containing buried solid U wastes, including as the Ash Pits and East Trenches.

Physical and chemical data for unsaturated zone geologic materials and pore waters have been collected by DOE (1994) at the Solar Evaporation Ponds (SEPs). Among the investigations performed were soil sample analyses for U isotopes (U-233/234, U-235 and U-238) and the installation and sampling of 15 single and/or dual lysimeters inside and around the perimeter of the ponds. The highest soil U concentrations were found immediately beneath the SEPs in the 0 to 6 foot interval. Maximum concentrations detected were 21 pCi/g U-233/U-234, 0.87 pCi/g U-235 and 11.46 pCi/g U-238, with most analyses exceeding their respective calculated background values (n = 134). Pore water samples were collected from the lysimeter network for a six-month period. All three U isotopes were detected at both the upper and lower lysimeters. In general, unfiltered pore water U concentrations were highest beneath or adjacent to the SEPs. Maximum unfiltered U isotope concentrations detected in the upper lysimeters were 733 pCi/L U-233/U-234; 47 pCi/L U-235; and 671 pCi/L U-238. In the lower lysimeters, the maximum unfiltered U isotope concentrations were 3,400 pCi/L U-233/U-234; 120 pCi/L U-235; and 3,700 pCi/L U-238. Unfortunately, these concentrations cannot be directly compared to the saturated zone results presented in the next section because of differences in sample preparation (lysimeter samples were unfiltered, well samples were filtered).

456

TA-4.5.6 Uranium Transport Patterns for Saturated Zone Groundwater

Background

Relatively high concentrations of the U isotopes U-233/234, U-235 and U-238 have been found in groundwater in disturbed and undisturbed areas of the Site. As described in Section 3.6, high groundwater U concentrations are not uncommon for the region and, given the relative mobility of U in the subsurface environment, have the greatest potential of the actinides considered in this report to affect surface water quality on Site. Gaining an understanding of natural background U concentrations is critical for evaluating the distribution of anthropogenic U in groundwater at RFETS. To this end, special background and ICP/MS isotope ratio analytical studies have been undertaken by RFETS over the last decade to address the issue of differentiating anthropogenic from natural U.

Background areas for groundwater U data comprise the Rock Creek and Lower Smart Ditch basins and the South Woman Creek sub-basin. These basins are delineated mainly based on physical hydrology and the absence of historical plant activities that could have released radionuclides to groundwater. As a result, background data are only available for areas that are up-gradient or cross-gradient of the Industrial Area; no pre-plant background data are known to exist for the Industrial Area and down-gradient lower Woman Creek and Walnut Creek groundwater basins.

As presented in Section 2.8.1, mean background concentrations for U isotopes have been determined for the UHSU and LHSU flow systems (EG&G, 1993) and UHSU alluvium (RMRS, 1996). These values provide an initial benchmark for assessing the U isotope contents of non-background groundwater, but fail to account for natural concentration gradients that exist for U as groundwater flows eastward across the Site. This phenomenon was first reported for selected groundwater flow paths by EG&G (1995) and follows a general trend of increasing concentration for most major and minor non-radioactive, inorganic constituents. The presence of a Site-wide, background groundwater U gradient has important implications for facility compliance with RFCA, as ambient U concentrations at the east boundary are projected to exceed the current, mean background action levels.

Figure TA-4-20 illustrates the horizontal Site-wide pattern of filtered U-238 for UHSU background wells plotted as a function of distance from the west boundary (state plane easting coordinates). This approach is based on consideration of regional groundwater flow patterns, which indicate a prevailing eastward flow direction through the Site. The trend in U-238 concentration is indicated with a moving average (n=5) that show U-238 increasing by over an order of magnitude from west to east. This trend suggests that most of the U in UHSU groundwater near the east boundary probably results from natural rock-water interactions. Consideration of the vertical Site-wide distribution of U-238 (Figure TA-4-21) indicates that groundwater interaction with bedrock materials, coupled with a general decrease in saturated thickness and extent from west to east, may be an important factor in controlling the UHSU U concentration gradient across the Site.

ICP/MS U isotope ratios were determined for ten background wells (B405489, B302089, B302789, B305389, 10294, 11294, B102289, B200589, B201589 and B205589) located in the Woman Creek, Lower Smart Ditch and Rock Creek basins. As expected, all U-235/U-238 and U-236/U-238 ratios from these wells fall within the ranges expected for natural U (U-235/U-238 = 0.0072 and U-236/U-238 = 0), thus demonstrating that relatively high U concentrations (above 10 pCi/L) occur naturally within the Site, especially near the downgradient (north and east) boundaries.

The filtered mean U-233/234, U-235 and U-238 background concentration patterns presented in Figures TA-2-64 through TA-2-69, respectively, indicate that below Tier II concentrations generally occur in the western third of the Site in areas dominated by the Rocky Flats Alluvium. Areas of higher background U concentrations tend to be found in the valley bottoms after groundwater from the upland areas has had an opportunity to interact with underlying permeable bedrock sandstones or UHSU bedrock materials contained within hillslope colluvial deposits. Compared to the background portion of the Woman Creek basin, the relatively low U concentrations observed in stream valley alluvium wells in the lower Rock Creek basin (i.e., B202489 and B202589) probably reflect the greater amount of spring discharges, which issue from the base of the Rocky Flats Alluvium. In many cases, spring flow discharges directly to the creek as surface water, thus directly recharging the stream valley alluvium. Furthermore,

groundwater flow paths from the Rocky Flats Alluvium to valley bottom materials in the Rock Creek basin tend to be shorter than in the background portion of Woman Creek.

Woman Creek Groundwater Basin

Further subdivision of the non-background well data by major groundwater basins provides additional information about the UHSU U groundwater distribution at the Site. The Woman Creek groundwater basin contains the southernmost portion of the Industrial Area, including the 400 and 800 building complexes, IHSS 119.1, Original Land Fill, Ash Pits, Ryan's Pit, southern part of the 903 Pad, South Spray Field and C-series ponds. Portions of the original process waste line and tank system associated with Buildings 444, 881 and 883 are also located within the basin. As shown in Figure TA-2-62, numerous wells have been installed and monitored on hillsides and drainage reaches below potential source areas, thus providing a fairly comprehensive picture of U distribution in potentially affected areas of the basin.

Figure TA-4-22 illustrates the trend of non-background wells present in the Woman Creek groundwater basin. Above-background concentration peaks are observed in the trend line in the vicinity of Industrial Area facilities, such as the Original Land Fill and Building 881 (also see Figure TA-2-64); however, the general trend is consistent with the background trend. Perhaps significantly, groundwater U concentrations in the vicinity of the Building 400 complex, a well-known U processing area, do not appear to be elevated, although the building foundation drain and sump system may restrict or contain groundwater movement beneath the building. The flattening of U-238 concentrations evident in the lower Woman Creek basin area (below the C-2 pond) may reflect the influence of sampling bias, as all wells in this area are located near the stream. Woman Creek originates off-Site and is expected to contain lower U contents than the surrounding colluvial groundwater. ICP/MS ratios for two stream valley alluvial wells (00193 and 10394) indicate a natural signature for groundwater U associated with this segment of the stream/hydrogeologic system for the lower Woman Creek basin.

On the basis of ICP/MS U isotope ratio testing, anthropogenic (depleted) U has been detected in groundwater associated with the Original Land Fill (well 61093) and Ryan's Pit (well 07391). The extent of anthropogenic U in the Original Land Fill appears to be limited, as the ICP/MS

ratios from two wells (59393 and 59793) within the >5 pCi/L isoconcentration contour exhibit natural ratios. The largest area of elevated Industrial Area groundwater U, that associated with Building 881, appears to be entirely natural based on the ICP/MS results from six wells (0487, 5387, 10592, 37791, 36391 and 37991). A natural U isotope signature is also reported for well 04991, located down-gradient of the former South Spray Field. A small, isolated area of greater than 5 pCi/L U-238 is also delineated by wells 2987, 01291 and 23196 on the 903 Pad Hillside south of the old firing range. This information demonstrates that the distribution of groundwater anthropogenic U in the Woman Creek basin is limited and coincides mainly with buried sources. Additional ICP/MS testing in areas of other potential sources, specifically the Ash Pits and 903 Pad, would be required to more fully define the extent of anthropogenic U in this basin.

Walnut Creek Groundwater Basin

The Walnut Creek groundwater basin contains the largest concentration of potential Industrial Area and Buffer Zone anthropogenic U sources, including numerous production and support buildings, the Solar Evaporation Ponds, 903 Pad, the Mound and East Trench sites, the Present Landfill and the A- and B-series ponds. Active groundwater remediation for U is currently underway for the Solar Ponds Plume and underground releases of radionuclides are known to have occurred from process waste line leaks and breaks. Accordingly, a significant amount of groundwater investigation has been and continues to be conducted for this area of the Site, including current efforts involving the D&D groundwater monitoring of individual production buildings and complexes. Figure TA-2-75 illustrates the approximate boundaries of this basin.

Figure TA-4-23 illustrates the U-238 concentration trend with distance of non-background wells present in the Walnut Creek groundwater basin. As might be expected, the most prominent U-238 concentration peak in the moving average trend line (n=5) coincides with the Solar Ponds. From the west boundary to mid-Industrial Area, the trend line is relatively flat or slightly rising reflecting the influence of the thicker saturated portion of the Rocky Flats Alluvium flow system in this part of the basin. U-238 concentrations rise and fall sharply in the eastern half of the Industrial Area, mainly as a result of Solar Ponds influence and resume a general increasing trend that approximates the background groundwater U trend. The trend line starts to flatten out at the easting 2089000 coordinate and shows a declining trend eastward to the east boundary.

The significance of this decline is thought to be related to the Pond A-4 and B-5 dams, which, by design, cutoff alluvial and shallow bedrock groundwater flow and cause mixing of groundwater with surface water. A portion of the water discharged from the pond, which contains a significant fraction of imported water with low U contents (average U-238 concentration of 0.51 pCi/L (DOE, 1995), infiltrates into the streambed and recharges the alluvial groundwater system (lower Walnut Creek is primarily a losing stream reach). Neglecting the influence of any future anthropogenic U transport in the lower Walnut Creek basin, it is expected that U concentrations will eventually rise to original background levels following the cessation of water importation at closure.

Groundwater U ICP/MS ratios were determined for selected wells located within the Solar Ponds Plume, East Trenches area, Building 886 and along the drainage courses of North and South Walnut Creeks east of the Industrial Area. Anthropogenic U signatures were reported for wells P209189 and P209489 (depleted) and P209589 and 42993 (enriched) in the Solar Ponds Plume; well 07991 (depleted) in the East Trenches area; and well 41691 (possibly depleted) at the east boundary. Normal background ratios were reported for six other Solar Pond Plume wells (1586, P207689, B208689, P209889, B210489 and 43993); all drainage wells (except 41691) located below the Industrial Area and Present Landfill; well 03991 located down-gradient from the East Trenches and North Spray Field; and Well 22996 located down-gradient of B886. This information indicates that, despite its relative mobility in groundwater, U transport tends to remain relatively localized near source areas at RFETS. This observation may also hold true for the potential anthropogenic U signature at well 41691, which has historically contained above-background concentrations of Pu-239/240 and Am-241 and appears to be located within the footprint of a former pond shown on an early RFETS map.

Additional areas showing >5 pCi/L U-238 in the Walnut Creek basin include well P219189 (mean U-238 = 42.28 pCi/L) located down-gradient of B774. The available U isotope data from Industrial Area monitoring wells indicate that any U releases from the process waste line system were probably minor or of limited extent, as large areas of elevated U are not evident in Figures TA-2-64 through TA-2-69. However, additional U data from down-gradient areas of the Eighth

4e1

Street utility corridor and selected Protected Area buildings, including the process waste line breaks reported at B559, are needed to verify these preliminary conclusions.

East Drainages Groundwater Basin

Due to its limited basin length and low well density, East Drainages basin U-238 data have not been plotted against distance to examine concentration trends. Mean U-238 concentrations for boundary wells 0286, 0386, 41591 and 06491 range from 6.99 to 18.51 pCi/L and fall within the expected concentration range for groundwater at this locality based on comparison to the background U-238 concentration trend. U ICP/MS ratios for all wells tested in the basin (wells 06291, 0286, 0386 and 06491) and well 04991, located just outside of the basin down-gradient of the South Spray field, exhibit a natural U signature. Consequently, there appears to be no evidence that Site operations have contributed appreciable amounts of anthropogenic U to groundwater in the basin.

TA-4.5.7 Site-Wide LHSU Groundwater

An understanding of U concentrations in LHSU groundwater is relevant to evaluating U transport potential to the underlying Laramie-Fox Hills Aquifer. Analysis of vertical contaminant migration potential at the Site has previously been performed for dense, non-aqueous phase liquids (DNAPLs) and resulting volatile organic contaminants, but U transport was not specifically addressed (RMRS, 1996). Nevertheless, much of the previous analysis is applicable to U because of its presence in the dissolved phase, vertical migration through LHSU materials and dissimilar geochemical behavior in oxic and anoxic aqueous environments. The reader is referred to the original analysis for more details on analysis methods and assumptions, LHSU lithologic and hydraulic properties and discussion of results.

The lateral distribution of U isotopes in LHSU groundwater is shown in Figures TA-2-72 through TA-2-74. These figures, together with the vertical distribution of U-238 provided in Figure TA-4-21, indicate that U concentrations are significantly lower in LHSU groundwater compared to UHSU groundwater. This decline in concentration with depth seems to coincide with the transition from weathered to unweathered bedrock, which averages about 40 feet below

462

the bedrock surface. None of the wells located near inferred bedrock faults show evidence of elevated U concentrations that might indicate enhanced vertical migration. It is not known conclusively, however, whether the wells are completed close enough to fracture zones to monitor their effect, if any, on downward contaminant migration (RMRS, 1996). To date, U ICP/MS ratios have not been tested for any LHSU wells primarily because none of the wells indicate concentrations that are suggestive of a potential contamination problem.

Factors that affect the vertical U distribution in groundwater at RFETS include the rate of vertical groundwater flow and U fluxes and retardation mechanisms, such as solubility, precipitation and sorption. Considering the absence of environmental tritium in groundwater samples presented earlier in Table TA-4-13, it seems likely that a low vertical groundwater flux is the main reason why U concentrations have remained low in the LHSU. The decline in U concentration with depth below the weathered bedrock surface (about 40 feet below bedrock surface) is potentially controlled by transition of soluble U(VI) to relatively insoluble U(IV), as dissolved oxygen in the groundwater is consumed by carbonaceous matter as it moves vertically deeper into the flow system. RMRS (1996) has postulated that carbonaceous matter (1.03 %) contained within the claystone confining layer would have a significant role in attenuating organic contaminants as a result of increased sorptive capacity and dissolved oxygen consumption (abiotic degradation facilitation). Similar processes are expected to control U transport through the LHSU, insomuch that oxygen consumption will lower the Eh resulting in a decrease in U solubility. Consequently, any increased concentrations of anthropogenic U found in the overlying UHSU flow system (e.g., Solar Ponds) which migrate into the LHSU are expected to be attenuated to a significant degree by solubility limitations set by local redox conditions. Additional geochemical modeling of U speciation and transport beyond that conducted by Ball (2000) would be necessary to investigate whether this explanation is a viable attenuation mechanism for U removal from groundwater, should transport be detected in monitoring wells.

463

TA-4.5.8 Actinide Drilling-Artifact Contamination Investigation

Background

The potential migration of Pu-239/240 and Am-241 from surface soils to groundwater at RFETS is being considered as part of the long-term remedial strategy currently under evaluation for Site closure implementation by DOE, the Kaiser-Hill Team and the Actinide Migration Evaluation Group. Existing data on actinide migration at RFETS was summarized for the development of a conceptual model designed to gain an understanding of actinide transport pathways active at the Site (DOE, 1997). Over 30 monitoring wells at RFETS were found to contain mean groundwater Pu-239/240 and Am-241 activity-concentrations that exceeded RFCA Tier II action levels (0.15 pCi/L and 0.145 pCi/L, respectively) for these contaminants (DOE, 1997). Groundwater interactions with surface water are inevitable as virtually all shallow groundwater on Site flows toward the major stream drainages and is eventually discharged to surface water via streams or reservoirs. Consequently, groundwater was characterized as representing a potential long-term threat to surface water based on a preliminary review of the available data.

The presence of Pu-239/240 and Am-241 in groundwater samples at RFETS has been the subject of much speculation and study (DOE, 1997; EG&G, 1995; CDPHE, 1996; Harnish et al., 1994 and 1996; Litaor, et al., 1996). These contaminants are usually considered relatively immobile in the soil and groundwater environment due to their low aqueous solubility and tendency to strongly sorb on soil media (Cleveland et al., 1976; Honeyman and Santschi, 1997). Most wells with exceedances are located near potential source areas, such as the 903 Pad, but some are located at great distances from sources, including monitoring wells located at the east Site boundary along Walnut Creek. Colloid facilitated-transport of radionuclides in groundwater has been reported in the literature as being a potentially important mechanism for increased radionuclide mobility in the subsurface. Alternatively, it has been speculated that well completion zones may have been cross-contaminated when drilling through radionuclide-bearing surface soils or sediments found near source areas.

Because a significant disparity exists between observed versus expected Pu-239/240 and Am-241 groundwater contaminant distributions, further evaluation of historical groundwater Pu-

464

239/240 and Am-241 data and potential transport pathways was undertaken in 1998 to assess the significance of groundwater action level exceedances reported for RFETS monitoring wells (RMRS, 1998). This analysis concluded that much of the Pu-239/240 and Am-241 contamination detected in groundwater probably occurs from residual surface soil contamination introduced to the borehole during drilling and well installation operations (drilling-artifact contamination). Groundwater samples collected from these wells using historical RFETS sampling techniques (i.e., bailing) have the unavoidable effect of suspending contaminated drilling-artifact soil materials, thus creating artificially high contaminant levels. Under these circumstances, existing groundwater sampling results are unreliable indicators of groundwater contaminant concentration and transport.

Well drilling and installation using special surface-casing techniques offer a means to minimize or eliminate drilling-artifact contamination as a source for Pu-239/240 and Am-241 detections in groundwater samples. When paired with existing monitoring wells containing Pu-239/240 and Am-241, monitoring wells installed with special surface-casing techniques can 1) provide a basis for assessing the effects, if any, of drilling-artifact contamination on groundwater sample quality; and 2) allow for the collection of groundwater samples that more accurately represent contaminant concentrations and transport conditions. Non-paired, specially-cased monitoring wells were installed in 1994 to evaluate elevated Pu-239/240 and Am-241 activity-concentrations in the lower Walnut Creek drainage and to upgrade boundary monitoring well integrity in other RFETS drainages (EG&G, 1995). No Pu-239/240 and Am-241 contamination above Tier II groundwater action levels was detected in any of the wells installed under this program. Until 1999, monitoring wells installed with special surface-casing techniques were not paired with existing monitoring wells to validate or invalidate radionuclide detections found in the original well.

Type and Extent of Contamination

Soils

Actinide transport to groundwater from contaminated surficial soils is a primary concern at RFETS. As shown in Figure TA-2-8, widespread areas of the Buffer Zone and localized areas in

the Industrial Area have received windblown Pu-239/240 surface soil contamination. Vertical soil profiles of Pu-239/240 activity-concentrations for the uppermost 96 cm (3 feet) of RFETS soils presented in RMRS (1998) and Litaor et al. (1994) indicate that Pu movement is mainly restricted to the top 20 to 25 cm of soil. Pu-239/240 activity-concentrations exponentially decline below a depth of about 12 cm (Litaor et al., 1994) to less than 1 pCi/g at 72 cm. Elevated Pu activity-concentrations were detected in soil macropores (i.e., root channels) compared to the surrounding soil matrix, but extensive macropore development was not observed below a depth of 120 cm (4.0 feet) (Litaor et al., 1994). This depth roughly corresponds with the average depth of most RFETS grass and forb root systems as reported in Weaver (1920). According to Weaver (1920), many grassland plants have root systems that can exceed a depth of 5 feet and some can attain maximum depths in excess of 10 feet. This information suggests that deep soil macropores may be present at RFETS, but these macropores should be relatively unimportant as a source medium for drilling-artifact contamination.

Groundwater

Figures TA-2-60 and TA-2-61 illustrate that wells containing unfiltered Pu-239/240 contamination (colored dots) are generally associated with surface soil contamination areas (color-shaded contours). The highest groundwater unfiltered Pu-239/240 activity-concentrations are found in alluvial wells at and east of the 903 Pad. Elevated unfiltered Pu-239/240 activity-concentrations are also found in certain bedrock wells in this area, including well 11791, as described in RMRS (1998).

Activity-concentration plots of unfiltered Pu-239/240 and Am-241 for wells 1587, 06991, 11791 and P313489 presented in RMRS (1998) indicate that, with the exception of well 1587, Pu-239/240 and Am-241 activity-concentrations have generally declined with time. The reason for this decline is thought to result from the flushing of contaminants in the borehole disturbed zone caused by routine sampling activities.

4666

TA-4.5.9 Summary of Groundwater Pathway Analysis

- **Pu-239/240 and Am-241 are relatively immobile in unsaturated soils.** Soil profile data collected at the 903 Pad over the past three decades demonstrate that movement is limited mainly to the uppermost 20 cm of soil. Small amounts of these actinides have penetrated deeper into soil presumably via macropores, which occur to a depth of about 100 cm below ground surface. Considering that over three decades have passed since these actinides were first released to 903 Pad area soils, the low activity-concentrations (<1 pCi/g) in soil and soils waters at and below 70 cm indicate that the flux of these actinides to shallow groundwater is expected to be small.

- **Pu-239/240 and Am-241 are found in low activity-concentrations (<0.15 pCi/L) in UHSU wells usually associated with surface and near-surface soil contamination areas.** Pu-239/240 and Am-241 groundwater contamination is generally not found in areas outside of surface soil contamination areas, including the RFETS Industrial Area. This situation indicates that widespread contamination from potential underground Industrial Area actinide sources, such as process waste lines and buildings, is not present in the UHSU. The only contamination found that was not attributable to surface soil contamination occurs at the Present Landfill, where low level radioactive wastes were buried soon after landfilling operations began. Additional areas of local-scale contamination may still be discovered as D&D monitoring programs for individual building closures are implemented over the next few years.

  Recent sampling results from the actinide drilling-artifact contamination investigation confirm that trace activity-concentrations of these actinides are found in UHSU groundwater associated with surface-contaminated soils. These results are generally below Tier II action levels and are significantly lower than activity-concentrations previously reported for older companion monitoring wells. The significance of these detections is still subject to uncertainty until analytical and/or sampling variations are better quantified and understood. Consequently, further investigation may be necessary to refine analytical and sampling techniques for the reliable measurement of low activity-concentrations of these actinides.

467

- **Vertical migration of Pu-239/240 and Am-241 from surficial hydrostratigraphic units to the Laramie-Fox Hills Aquifer is not implicated as a significant transport pathway.** For LHSU groundwater to be contaminated, it follows that the overlying UHSU groundwater must also be contaminated. Until the source and concentration levels of Pu-239/240 and Am-241 in the UHSU are confidently established, the issue of contamination in the LHSU can not be completely addressed. Nevertheless, the available LHSU hydrogeologic and environmental isotope data indicate that Pu-239/240 and Am-241 should not have been transported deep into the groundwater flow system beneath the Site, except possibly by cross-contamination of surficial soils during drilling and well installation. The lack of consistent and repeatable detections of these actinides in LHSU wells showing contamination is further reason to doubt their presence in deep groundwater.

- **On the basis of U isotope ICP/MS analyses, anthropogenic U contamination associated with Site activities has been detected in UHSU groundwater at various areas in the Industrial Area; however, it is erroneous to equate high U activity-concentrations with contamination.** Background U activity-concentrations are observed to increase approximately an order of magnitude from the west boundary to the east boundary. This trend indicates that a natural concentration gradient exists across the Site, which must be considered when evaluating groundwater U data. Other than anthropogenic U isotope levels in the Solar Pond Plume, the highest U isotope activity-concentrations on Site occur in background areas. It is difficult to detect anthropogenic groundwater U contamination in the UHSU except in a few Industrial Area localities.

TA-4.6 AIR PATHWAY ANALYSIS

TA-4.6.1 Sources of Airborne Actinides at RFETS

The Site has been a source of airborne actinides throughout its history. Over time, small amounts of Pu, Am and other actinides have been deposited on or mixed with surface soils at the Site. Wind or mechanical disturbance of the contaminated soil can result in actinide-laden soil particles becoming airborne. These resuspended particles, along with particles emitted from building stacks and vents, are transported some distance downwind before being deposited on the ground or in water by a variety of mechanisms that remove particles from the air, such as rainout or dry deposition. As a result, airborne migration is one of several transport pathways that redistribute actinides in the environment in the vicinity of the Site.

Current sources of airborne actinide emissions at the Site include stack emissions, wind erosion of contaminated soils and projects that disturb contaminated soil or handle other contaminated materials. Tritium has historically been the only gaseous radionuclide of interest at the Site and it is no longer emitted on a routine basis. Other airborne radionuclides are released as particles. Stack emissions are a small component of total emissions because most are vented through high efficiency particulate air (HEPA) filters, which results in very low particulate emissions. Stack emissions typically account for 1 % or less of the annual airborne dose from the Site (Radian, 2000).

Actinide resuspension due to natural phenomena at the Site is episodic in nature and influenced primarily by meteorological variables (wind speed and rainfall); soil properties (moisture level and particle size and density); and surface characteristics (density and type of vegetative growth and presence or absence of snow cover). Given the density of vegetation growing on the contaminated soil areas of the Site, a primary source of contaminated soil resuspension is likely to be the dust-laden vegetation and litter, with less potential for direct resuspension from soil surfaces except during high wind events or after disturbances. Wind erosion of contaminated soil occurs mainly outside of the Industrial Area because of the large amount of surface area within the Industrial Area that is covered by buildings, roads and parking lots.

469

Wind erosion is generally a function of wind speed raised to a power—therefore, as the wind speed increases, soil and actinide emissions increase in a nonlinear fashion. Some types of surfaces have been shown to have a definite threshold for initiation of wind erosion; significant wind erosion does not occur until winds exceed this threshold velocity. Wind tunnel studies at RFETS, however, have not demonstrated a definite threshold for wind erosion, although erosion has been shown to increase rapidly when winds at 10 meters height increase above approximately 40 miles per hour (mph) (MRI, 2001). Below those speeds, resuspension of soil occurs but at a very low rate. This lack of a definite threshold for initiation of wind erosion occurs because there are multiple contributors to wind generated particulate matter emissions: 1) bulk soil; 2) settled surface dust trapped by vegetation; and 3) the vegetation itself. The particle releases from these reservoirs are all driven by different mechanisms, each with different wind speed dependence.

Wind erosion also varies seasonally because of differences in soil moisture levels, changes in vegetation cover and variations in wind speed. Moist soil and snow covers are effective in limiting resuspension. Growing vegetation cover may have a more complicated effect by decreasing erosion from the soil surface, while providing an enhanced reservoir of erodible particles on the leaf surfaces.

Higher winds are more effective in causing resuspension of particles; however, it is important to note that total airborne soil and actinide emissions are ultimately limited by the available reservoir of erodible particles on the soil or leaves. A high wind event will rapidly deplete the erodible particles. The first few minutes of high winds may result in significant airborne emissions but the emission rate will decrease with time as fewer and fewer erodible particles remain. Sustained windy periods will not result in further emissions until the erosion potential is replenished by deposition or by other factors that generate erodible particles (such as freeze/thaw cycles, rainsplash, animal activity, etc.).

The most significant soil contamination areas contributing to airborne actinides at the Site are the 903 Pad and the adjacent "Lip" area. During the 1950s and 1960s, the 903 Pad was contaminated with Pu-laden cutting oil that leaked from metal drums into the soil beneath the

drums. Removal of the drums in the late 1960s and associated cleanup activities resulted in dispersion of contaminated soil to the east and south of the 903 Pad, much of it through the air pathway. The storage pad was covered with asphalt in 1969 and is no longer a source of resuspendable actinides. However, the initial spread of the contaminated soil prior to the installation of the asphalt pad resulted in a plume of actinides in the surface soils extending to the east and southeast from the 903 Pad itself. These areas of contaminated surface soils continue to result in low levels of actinide resuspension on an ongoing basis.

Other spills and releases have resulted in smaller areas at the Site where the surface soils are contaminated with Pu and other actinides (such as U isotopes). In addition, naturally-occurring U deposits may also result in areas of elevated surface soil U concentrations. Actinide concentrations in surface soils at the Site have been sampled and mapped and are shown in Figure TA-2-3 through Figure TA-2-7 in Section TA-2.3. These soils, including soils deposited on vegetation surfaces, constitute the primary source for airborne actinide emissions from the Site.

Prior to 1989, the Site fabricated nuclear weapons components from Pu, U, beryllium and stainless steel. Weapons operations were curtailed at the Site in 1989 due to safety concerns and in February 1992, the Site's weapons production mission was discontinued. Between 1989 and 1995, resuspension of actinide-containing soils and transport through the air pathway occurred primarily due to natural processes, such as wind erosion. Remediation of contaminated soils and waste disposal areas at the Site and building decommissioning activities began in 1995. Such activities can disturb contaminated soils or contamination on building or equipment surfaces and result in additional airborne actinides.

Project-related actinide emissions vary from year to year and depend on the type of activity and the actinide content of the soil or other materials handled. Some years they have represented a significant source of airborne dose at the Site, while in most years, wind erosion has been the major source. Future resuspension of actinide-containing material will occur due to both natural and anthropogenic activities.

471

Following Site closure, emissions of actinides will result from wind-driven resuspension of any remaining contaminated surface soils. Wind erosion of undisturbed, vegetated areas will occur at a low rate. However, any activity that disturbs the soil or removes the covering vegetation would increase emissions for a period of time. Such activities might include excavation or fires; the magnitude of the increase would depend on the frequency of disturbance and whether or not the disturbance is followed by high winds before the soil crusts or the vegetation is restored.

TA-4.6.2 General Patterns of Airborne Actinide Transport At RFETS

Once released into the air, actinide particles or particles of soil with attached actinides are transported away from source areas by the wind (*dispersion*). Concentrations of airborne actinides will generally be higher closer to the source areas; the concentrations become diluted as they are transported downwind. During transport, particles are brought down to the surface through the combined processes of turbulent diffusion and gravitational settling. Once near the surface, they may be removed from the atmosphere and deposited on soil or water surfaces (*deposition*).

The distance a particle travels before being deposited depends on the particle's size and density. Larger, denser particles are deposited closer in to the source, while very small particles may remain suspended and carried much farther downwind.

The concentration and deposition of actinides in the Site environment depends on the local patterns of wind flow over the Site. Figure TA-1-6 shows a joint frequency distribution of wind speed and direction (wind rose) for 1999, a representative year. The figure shows that prevailing winds occur from the northwest quadrant, but that winds from other directions also occur, with reduced frequency.

More importantly, the figure shows that higher speed winds occur almost exclusively from the northwest quadrant. This is significant because wind erosion emissions are a function of wind speed; larger amounts of soil are resuspended by high winds than by lower speed winds. The higher speed winds are also more effective at transporting particles away from source areas (further downwind), where many of these particles will be redeposited as wind speeds decrease.

Finally, wind speed influences the range of particle sizes emitted and transported. Higher speed winds are capable of resuspending and transporting larger particles than lighter winds.

As previously discussed, the main source area of resuspended actinides at the Site is the area surrounding the 903 Pad. The Pu particles in the cutting oil that leaked at the 903 Pad were small (<3 micrometers [μm] diameter). Once in contact with the soil, however, the Pu particles became attached to soil particles. Experimental data from the Site (Langer, 1986) and elsewhere (Shinn, 1999) indicate that most of the airborne Pu activity is carried by the >15 μm diameter size fraction. Many of these larger particles are aggregates made up of varying size soil particles held together by binding agents (e.g., organic matter). Lesser amounts of Pu may be attached to smaller, primary clay- and silt-sized particles. Because of its attachment affinity, the airborne transport of Pu is dependent on the soil or aggregate particle properties and not the properties of the individual Pu particles.

Am-241 in the 903 Pad area and other areas of the Site is due, in part, to Am ingrowth from decaying weapons-grade Pu (Am-241 is formed by radioactive decay of Pu-241 atoms). Consequently, Am-241 contamination due to Site sources is expected to be distributed in the soil matrix in a similar manner as Pu-239/240. Past research at the Site has shown that coarse particles (>15 μm) also carry most of the U activity in windblown dust (Langer, 1987). Therefore, the activity distribution among various particle size categories was assumed to be the same for each of these isotopes for purposes of estimating airborne transport.

The present surface soil contamination patterns of Pu-239/240 and Am-241 are largely the result of windblown suspension and subsequent deposition of soil that was contaminated by leaking drums at the 903 Pad, with some additional spread due to surface runoff from the contaminated area. In addition, suspension occurs more readily from recently disturbed soil, so the particular wind speeds and directions coincident with disturbances during the initial 903 Pad remediation sequence would have a strong influence on the resulting surface soil contamination patterns.

TA-4.6.3 Description of Air Pathway Analysis Methodology for Measured Data

Concentrations of Pu-239/240, Am-241, U-233/234, U-235 and U-238 are routinely measured at various locations on and around the Site using the RAAMP sampling network, described in Section TA-2.9. Data for 1997 through 1999 are presented in Tables TA-2-27 and TA-2-28. These concentrations are reflective of current actinide levels in air around the Site perimeter. Airborne actinides result from emissions due to wind erosion of contaminated soils, with small additional contributions from project and stack emissions in most years. Pu-239/240 and Am-241 in the air at the Site also result from fallout from atmospheric testing of nuclear weapons in the 1960s and 1970s (see Section TA-2.9 for additional discussion).

In the case of the U isotopes, naturally-occurring U is also a major contributor to airborne actinides in the environment of the Site. U-233/234 and U-238 measured by the RAAMP network in recent years is almost entirely due to naturally-occurring isotopes, rather than emissions from Site activities.

To calculate net off-Site transport of actinides through the air pathway under current conditions, an analysis was performed using the data presented in Tables TA-2-27 and TA-2-28 for two possible scenarios regarding the source of the measured actinides. For the first scenario, all the actinides measured at the perimeter sampler were assumed to originate on Site, largely through wind erosion of contaminated soil. This is an overestimation, particularly for the U isotopes that occur naturally in the surrounding soils. However, this first set of calculations bias the off-Site transport calculations on the high side.

For the second scenario, an assumed background concentration of each actinide was first subtracted from each measured actinide concentration (see discussion of background concentrations in Section TA-2.9). The off-Site transport was then calculated based on the remaining material. This is likely to be a more realistic portrayal of the off-Site transport of Site-derived actinides than the first method but it depends heavily on an accurate portrayal of the average airborne background actinide concentrations, data that are not readily and reliably available for the Site. For purposes of estimating non-fallout transport, a value of 4.1×10^{-7} pCi/m^3 Pu-239/240 was attributed to fallout. Am-241 in fallout was estimated from the Pu-

239/240 fallout value, based on a ratio of Am-241 to Pu-239/240 activity found in soil at sites in Colorado that are distant from RFETS (Hulse et al., 1999).

Determination of background values to use for the U isotopes present an even larger problem, because U occurs naturally in the local rocks and soils. Past examination of the activity ratios of various U isotopes in RAAMP data show that the measured U at the perimeter of the Site cannot be distinguished from naturally-occurring U. Consequently, it is possible that nearly everything that is measured is actually background U. Therefore, the second scenario was not evaluated for the U isotopes, since it is impossible to accurately partition the measured data between background and airborne concentrations that result from Site contamination.

For Pu-239/240 and Am-241, the difference between off-Site transport calculated using the first method and the second served as an estimate of apparent off-Site transport of "background" actinides—those concentrations that occur ubiquitously in the regional air and that do not originate from Site contamination or stack emissions. (In fact, background airborne actinides that do not originate on Site should have no **net** off-Site transport since winds will simultaneously move material both on and off the Site.)

Calculation Methodology

Off-Site transport of actinides through the air pathway was estimated using a simple dispersion formulation called a "box model", combined with the RAAMP data presented previously. A box model assumes that a parcel of air can be described from three dimensions—length (along the axis of the wind), width (crosswind) and height. Air pollutants are assumed to be uniformly dispersed throughout the resulting volume. Flow of pollutants out of the box for a given period of time can then be calculated based on the area of the "end" of the box (height x width, in square meters, m^2), multiplied by the average wind speed through the box in meters per second to estimate the mass flow rate of air out of the box in cubic meters per second. If the concentration of a pollutant in the air within the box is known or can be estimated (in units of mass or activity per cubic meter, the rate of pollutant transport can be estimated (e.g., pCi/m^3 x m^3/s = pCi/s). Figure TA-4-24 illustrates this concept.

An average wind speed must be estimated for each time step. The resulting rate of pollutant loss from the box can be multiplied by the total number of seconds in a time step, then the individual time step transport amounts summed to give a total annual mass or activity loss from the box.

For the situation discussed here, the major source areas for actinides are located in the interior of the Site. Actinides are transported off-Site through the air pathway in all directions over the course of a year, although more transport occurs in some directions than in others because wind speeds and directions are not uniformly distributed among compass directions (Figure TA-1-6). A total of 16 "boxes" were defined, one located at the distance of the Site fenceline in each of 16 compass sectors. The area of the end of each box was defined by a height of 195 m (discussed below) and a crosswind distance equal to the length of a 22.5° arc of a circle located at the sector-specific fenceline distance from the center of the Site. Each box was assumed to be 1 m in length. Derivation of actinide concentrations within each box and of the sector average wind speed for each time step are described below.

Estimation of Average Monthly Actinide Concentrations within Each Box

To estimate off-Site transport, monthly RAAMP data for 1997 through 1999 for Pu-239/240, Am-241, U-233/234, U-235 and U-238 were obtained for each perimeter sampling location. Because the samplers are all located at different distances from the Site center and from source areas such as the 903 Pad, a screening level dispersion model (SCREEN3; EPA, 1995a) was used to calculate scaling factors to adjust measured concentrations for each sampler to the distance of the Site fenceline along a line from the center of the Site to each sampler. The equivalent fenceline concentrations were then assigned to a sector. In some cases, concentrations from two samplers were averaged if both were located within the same sector or if a sampler was located on a boundary between sectors. A sector-specific fenceline distance was calculated in the same way.

The measured data represent actinide concentrations at RAAMP inlet height, about 2 m above the ground. While these concentrations are representative of what a person located at the fenceline would be likely to inhale, use of these concentrations directly to calculate the amount of airborne actinide moving off-Site on an annual basis would be incorrect. Because most

476

actinides released from the Site originate from ground-level area sources, the concentrations at any point downwind would generally be highest near the ground and would decrease with height. Based on past research into the way that air pollutants disperse from a source, the pattern of concentrations with height would be expected to follow a Gaussian or bell-shaped distribution (Turner, 1970), with the ground-level concentration representing the middle of the "bell" or the highest value in the distribution.

An essential parameter in describing the Gaussian curve (or Gaussian plume, as it is referred to with respect to air quality) is the standard deviation, which describes the degree of "spread" around the center. Turner (1970) gives values of the vertical standard deviation of the Gaussian distribution (called σ_z) based on stability and distance downwind from an air pollutant source. Stability is a measure of the tendency toward vertical motion or turbulence in the atmosphere. On an annual average basis, the stability at the Site is neutral (stability class D). For the average fenceline distance from the center of the Site (around 2,800 m) and D stability, σ_z is around 65 m.

Nearly all of the values in the Gaussian distribution (i.e., all of the mass in the plume) will be contained within three standard deviations of the center of the distribution (Snedecor and Cochran, 1967). Consequently, for use in calculating off-Site transport of airborne actinides, the region from the ground to approximately 195 m height is of interest and 195 m was chosen as the height of each "box" (Figure TA-4-24). Turner (1970) gives the following equation for

$$y = \frac{1}{\sqrt{2\pi}\,\sigma_z} \exp\left[-\frac{1}{2}\left(\frac{x-\bar{x}}{\sigma_z}\right)^2\right]$$

calculating the ordinate values (height) of the Gaussian distribution:

where:

y is the ordinate value or height of the curve (in this case, a relative concentration)
σ_z, as previously defined, is the vertical standard deviation (= 65 m)
x is the distance from the center of the distribution (i.e., height above ground level)
$\bar{x}$ is the expected value of the x coordinate (in this case, 0 m, ground level)

Using this formula, a relative concentration was calculated at 1 m intervals from ground level to 195 m. These values were then normalized to 2 m, the height of the RAAMP data. The normalized concentration values were then summed and averaged, giving a multiplier that could be applied to a given RAAMP value to estimate the average concentration at that distance downwind from the Site center, from ground level through 195 m.

Estimation of Average Actinide Concentrations for Each Time Step

A problem arises in using measured airborne actinide concentrations directly because the time scale is relatively coarse compared to the wind gusts that drive the wind erosion process. While emission and transport dynamics may vary from minute to minute, the RAAMP data are available as monthly average concentrations. Capturing the dynamics of transport are important, because both the volume of air moved off-Site in a given period of time and the actinide concentration carried by the wind are a function of wind speed (assuming that the major emission source is wind erosion of contaminated soil). So higher speed winds not only entrain larger quantities of material than lighter winds, they also move more cubic meters of air over the fenceline in a time step.

To capture the dynamics of the process, a 15-minute time step was used for the calculations. Wind tunnel studies of wind erosion performed at the Site in 2000 showed that the amount of erodible material present on undisturbed Site surfaces varied with wind speed (MRI, 2000a, MRI, 2000b). The studies also showed that the erodible material would be rapidly depleted at a given wind speed, usually within 10 to 15 minutes or less. Consequently, a 15-minute time step was appropriate to the calculations. (Erodible material is renewed on an ongoing basis through deposition and small-scale disturbances, so depletion of the erodible material is temporary.)

Meteorological data are measured at a 61-m tower located in the northwest Buffer Zone that is instrumented at several levels. Meteorological data were obtained for 1997 through 1999 at a level of 10 m above the ground. Fifteen-minute average wind data were used in the box model calculation described previously. The calculations were performed on a month-by-month basis, consistent with the sampling periods, then the monthly transport totals were summed to estimate

478

annual transport amounts. A method was derived to estimate 15-minute actinide concentration data in each box from monthly measured average concentrations, as described below:

- For each 15-minute period, the measured 10-m wind direction was assigned to one of 16 directions (boxes) and monthly arrays of 0:1 multipliers were created (number of 15-minute periods in a sampling month by 16 directions). This was necessary to isolate the time steps during which assumed Site emissions contributed to each measured actinide concentration in a given direction;

- A generic weighting factor was calculated for each 15-minute period in the sampling month. The weighting factor (discussed below) accounted for the fact that the airborne actinide concentration in a box in any given time step would be a function of the emission rate of the actinide, the spread of the plume at the downwind distance of the sampler and the volume of air that the emitted actinide was introduced into;

- The generic weighting factors were multiplied by the 0:1 multiplier array to produce an array of "relative concentration" values. These were divided by the monthly sum of the relative concentrations for a given wind direction to calculate the fraction of the totaled sampled actinide activity that should be assigned to each time step in the sampling month;

- For each actinide, the activity measured in each direction over each sampling month was calculated by multiplying the measured average monthly actinide concentration for each direction by the volume of air that was sampled for a specific month. The total sampled activity was partitioned among the time steps based on the fractions calculated from the relative concentration values; and

- For each actinide, the activity assigned to each time step and box was divided by the volume of air that was sampled in a 15-minute period, calculated by dividing the monthly sample volume by the number of 15-minute time steps in the sampling month. The result of this calculation was an array of 15-minute concentration values for each box and actinide, for each sampling month in the three-year period.

479

The weighting factor used to assign portions of total measured activity in a sampling month to individual 15-minute time steps was derived using a portion of the formula for the Gaussian plume. The standard Gaussian plume equation relates ambient concentrations at a given downwind location to the emission rate of a pollutant, meteorological conditions such as wind speed and stability and the location of the receptor relative to the centerline of the plume and to the emission height of the source. The key factors that influence measured actinide concentrations at the Site perimeter, assuming that windblown dust originating in the interior of the Site is the major emission source, are the emission rate (a function of wind speed), the spread of the plume (a function of wind speed and stability) and the volume of air the emissions are introduced into in a time step (also a function of wind speed). Eliminating portions of the Guassian plume equation that deal with off-centerline and elevated concentrations, source configurations with elevated emissions and geometry factors that would be the same for each time step resulted in the weighting factor shown below:

$$WF = Q / (\sigma_y \times \sigma_z \times u)$$

WF functions as a time-step weighting factor and Q is a particulate matter emission rate for the contaminated soil areas at the Site in grams per second (g/s). Q is a function of wind speed and is based on recent wind tunnel studies at the Site; σ_y and σ_z are horizontal and vertical dispersion coefficients for the Gaussian plume equation at an average downwind fenceline distance of 2,800 m. Coefficient u is the measured, 15-minute average wind speed (m/s) at 10-m height.

The dispersion coefficients were calculated from the 10-m wind speed and the standard deviation of wind direction measured during each 15-minute time step at the Site's meteorological tower (10-m level). Formulas and values for estimating the dispersion coefficients σ_y and σ_z from stability classes and wind speed were taken from the *ISCST3 User's Guide, Volume II* (EPA, 1995b). Calculation of the stability classes from the standard deviation of wind direction was derived from formulas and tables in EPA's *Meteorological Monitoring Guidance for Regulatory Modeling Applications* (EPA, 2000).

The emission rate, Q, was calculated from an equation for estimating erosion potential from undisturbed portions of the Site that was based on the wind tunnel studies performed in 2000

(MRI, 2000). The resulting erosion potential equation, as a function of 10-m wind speed in meters per second, is:

$$EP = 3.933 \times 10^{-6} (u^{2.516})$$

where:

EP is the total suspended particulate (TSP) erosion potential per 15-minute period in grams per square meter (g/m^2); and u is the 15-minute average, 10-m wind speed (m/s).

The erosion potential was converted to an emission rate in grams per second (g/s) by multiplying by an assumed source area and dividing by the number of seconds in 15 minutes. An assumed source area of 5×10^6 m^2 was used, which represents an area large enough to encompass the area of the Site where the surface soil is contaminated with Pu-239/240 above a level of 2-3 pCi/g.

Meteorological Data

To calculate the movement of airborne actinides off-Site, the flow of air must be estimated moving off-Site in each sector in each 15-minute time step. As noted previously, airflow was calculated as the area of the end of each sector-specific box, multiplied by a 15-minute wind speed. The wind speed in each box was calculated as described below.

The 15-minute wind data used for this analysis were taken from the 10-m level of the Site meteorological tower. As with concentrations, average conditions in the layer between ground level and 195 m in height above the ground were needed to complete the box model formulation. Wind speed typically increases with height and the rate of increase varies with stability. Using a power law formula from the *ISCST3 User's Guide, Volume II* (EPA, 1995b) for the increase in wind speed with height, a multiplier was developed that could be applied to 10 m wind speeds to convert them to 0 to 195 m average wind speeds.

Calculation of Off-Site Transport

To complete the calculation of off-Site transport, each 15-minute actinide concentration (pCi/m^3), in each box, was multiplied by the 15-minute, 10-m wind speed projected throughout

the height of the box (m/s) and by the area of the end of the box (m^2). The resulting pCi/s value for each box, actinide and time step was multiplied by the number of seconds in a time step to estimate the amount of each actinide transported off-Site in a time step.

The activity transported off-Site in each 15-minute time step was summed for each actinide to calculate the total off-Site transport in a year. Three years of data were used in the calculations (1997 through 1999). The amount of apparent off-Site transport thought to be due to airborne background concentrations was calculated for Pu-239/240 and Am-241 as the difference between the off-Site transport amounts calculated for the two emission scenarios.

TA-4.6.4 Results of Air Pathway Analysis Using Measured Data

The calculated annual average off-Site air transport calculations for each actinide and scenario are shown in Table TA-4-14. As noted previously, background actinides would have no net off-Site transport because wind would move material both on and off the Site simultaneously. This is particularly true for the U isotopes, which occur naturally in area soils. Much of the U measured over the Site is due to these naturally-occurring sources, rather than Site contamination. Am-241 concentrations shown in Table TA-4-14 appear to be somewhat overestimated relative to the Pu-239/240 concentrations. As noted previously, Am-241 at the Site occurs, in part, due to ingrowth from weapons grade Pu, which contains a number of Pu isotopes. Generally, Am-241 activity due to ingrowth would be about 15 % of the activity measured for Pu-239/240, the most prevalent isotope in weapons grade Pu. The concentrations of Am-241 in Table TA-4-14 are higher, partly because only positive concentration values were used in the analysis, consistent with the manner in which radionuclide concentrations are reported at the Site for regulatory compliance purposes. (The higher ratio of Am-241 to Pu-239/240 in fallout compared to ingrowth probably also contributes to relatively higher Am-241 transport figures.)

482

Table TA-4-14. Annual Off-Site Actinide Transport Calculated Using Measured Data[a]

Actinide	Total Off-Site Transport (Ci/yr)	Off-Site Transport: Site Component (Ci/yr)	Off-Site Transport: Background (Ci/yr)
Pu-239/240	0.00071	0.00054	0.00017
Am-241	0.00041	0.00035	0.00006
U-233/234[b]	0.0145	NA	NA
U-235[b]	0.00095	NA	NA
U-238[b]	0.0140	NA	NA

[a] An increase in transport of up to 20 % may be warranted due to undercollection by RAAMP samplers.
[b] Partition between Site component and background component cannot be accurately determined.

Exposed filters from RAAMP samplers are "corrected" by subtracting the radioactivity measured in a population of blank (unexposed) filters to account for the presence of small amounts of radioactivity in the filters themselves. The resulting "blank-corrected" concentrations may be negative. For the analyses presented here, negative concentrations were treated as zero values, since negative values indicate that the actual concentrations in the air were very small, not necessarily different from zero. Because airborne Am-241 is present at lower concentrations than Pu-239/140, the Am-241 data contain values that are more negative. Consequently, use of "positive only" values tends to inflate the Am-241 concentrations **relative to** Pu-239/240 values in a comparable data set; this bias in the Am-241 data has been carried through the calculations reported in this section.

Sources of Uncertainty

As is apparent from the above discussion, the estimation of off-Site transport using measured data relies on a number of assumptions, most of which could bias the result either high or low. Two factors that lead to potential underestimation are discussed below.

RAAMP samplers measure particles in two size fractions—up to approximately 10 μm aerodynamic equivalent diameter and between 10 μm and approximately 30 μm (see Section TA-2.9 for further discussion of the RAAMP methodology). While these size fractions capture most of the particles capable of being resuspended and transported over substantial distances, they do not capture 100 % of such particles. Particles up to approximately 100 μm diameter may be resuspended during high (100 mph +) winds but the larger the particles, the shorter the downwind distance before they are redeposited. Consequently, wind erosion of large particles from the more highly contaminated portions of the Site is not expected to move a substantial amount of material past the Site fenceline in an annual time frame. Because a restricted size class was used in the transport calculations, the off-Site transport values given in Table TA-4-14 represent the majority but not the totality of off-Site transport through the air pathway. The inhalable portion of the values in Table TA-4-14 is around 50 % or less of the total.

In addition, no ambient sampler is 100 % efficient; some under-collection also would be expected. Based on limited testing by EPA of the sampler design in use at the Site, it is expected that this under-collection is relatively small, less than 20 %. While small, under-collection by the sampler would lead to an expected underestimation of off-Site actinide transport of a similar magnitude.

484

TA-4.7 BIOLOGICAL PATHWAY ANALYSIS

TA-4.7.1 Introduction

From the 1960s through the early 1990s, an extensive series of radioecology studies were carried out by the Department of Radiology and Radiation Biology at Colorado State University (CSU) in Fort Collins, Colorado. These studies generally concentrated on areas contaminated with Pu and other actinides and largely ignored areas of low to background concentrations. The lead investigator was Dr. F. Ward Whicker, who was assisted by several other CSU staff, in oversight of a number of students performing original research on various ecological compartments of the RFETS ecosystem. A series of progress reports presented study results written by various students as partial completion of thesis work. Additionally, all involved researchers published other progress reports and peer-reviewed papers. Several different journal articles present results from the same studies. These reports provide considerable data and summary findings for macro-biological studies at RFETS. Studies from other locations have also been reviewed for this compilation, but most were not directly applicable to the Site and are not cited.

TA-4.7.2 Terrestrial Studies

Terrestrial Vegetation

A study of Pu uptake by RFETS vegetation and other biotic media was conducted in the early 1970s (Little et al., 1980). In this study, unwashed vegetation and litter were analyzed for Pu concentrations. Results showed a soil concentration to vegetation concentration ratio of 1:3.4 x 10^{-2}. Little, citing the Arthur study (1977), stated that ultrasonic washing of vegetation had demonstrated that much of the Pu associated with the vegetation was soil adhering to the plant surface. He surmised that his own data probably reflected Pu in soil particles adhering to vegetation surfaces, as well as actual Pu uptake in vegetation.

In 1976-77, Arthur and Alldredge (1982) collected grassland and streamside vegetation and experimented with ultrasonic washing to determine how much of the Pu associated with vegetation might actually be the result of soil particles adhering to vegetation. They concluded that Pu adhering to the surface of the vegetation was a major contributor to the total Pu

associated with plants. This study demonstrated that washed versus unwashed vegetation could show significant differences in associated Pu. In their study the mean vegetation concentration of 0.70 pCi/g, compared to the mean concentration of 28.6 pCi/g in an earlier study (Little, 1976).

The conclusion that adhering soil particles can strongly influence the total Pu concentration associated with plant material was further corroborated by Dreicer, et al. (1984) who found that rainsplash contributed significantly in transporting Pu to plant surfaces. They found that about four times as much Pu was associated with vegetation samples collected within 20 cm of the ground surface as with samples collected above 20 cm from the surface.

Whicker and Ibrahim (1991) found that the mean vegetation uptake ratio and the concentration ratio (soil to vegetation) values were generally low and ranged from 10^{-3} to 10^{-5}. Data from this study indicated there was a decrease in the bioavailability of Pu for plant uptake and accumulation over time, after results were compared with the Little study (1976). When compared to values presented by Little, et al. (1980), Pu soil values documented by Whicker and Ibrahim (1991) were also lower.

In the findings of his study on RFETS vegetation, Webb (1992) stated that by 1989 vegetation and litter concentrations had decreased to less than 16 % of those reported in the earlier Little study (1980). Webb found that the isotopic ratios of Pu-239/Pu-238 remained unchanged over the intervening 15 years. Although present day (2001) data are unavailable for these locations, a CDPHE study that included soil samples collected 11 different years between 1970 and 1989 showed a steady decline in concentrations of Pu in soil (Terry, 1991). Given these data, it is probable that the concentrations have continued to decline. Webb's study identified surficial contamination of vegetation with Pu as at least as important as internal accumulation of Pu in plant tissues. Most of the authors have alluded to wind and water transport, as well as downward migration through the soil profile, as reasons for the declining Pu concentrations in the soil.

486

Terrestrial Fauna

General Observations in Biota

In general, investigations on biota in the most studied location, the 903 Pad and Lip area, showed that Pu concentrations in biota were significantly lower than in soils. As summarized by Setlock and Blaha (1989), arthropods and small mammals had Pu concentrations 100 times lower than soil, with no significant differences in seven tissue types analyzed. The concentration hierarchy followed a downward trend from dead plant litter to fresh vegetation to animal compartments that were analyzed (Little et al., 1980; Setlock and Blaha, 1989). The higher values for plant litter are expected since the litter is more closely associated with the soil surface and prone to the accumulation of soil particulate matter.

In a study of actinides in the environment, Watters, et al. (1983) reviewed actinide behavior with emphasis on chemical, physical and biological factors that influence actinide mobility. Their general conclusion was that sources of actinide in the environment, with few exceptions, have resulted in very low transfer of these elements into food webs, regardless of transport process.

In a "White Paper" written to assess the biological mobility of environmental Pu, Higley and Whicker (1999) observed that Pu is not a biologically essential element, nor does it serve as an analogue for any other essential element. They further stated that because of its insoluble nature (most forms of Pu are insoluble), the passage of Pu through biological membranes and any uptake into plant and animal tissues is normally very minor. After reviewing and summarizing results of RFETS studies, Higley and Whicker (1999) concluded that the majority of Pu measured in plant material was associated with surficial dust particles and that transport of Pu into plants is decreasing over time. They also observed that although concentrations in vegetation and litter strongly correlated with soil concentrations, those in small mammal tissues did not, but instead appeared to be independent. This led them to conclude that the small amount of Pu in small mammal tissues may result from the generally-distributed global fallout. Considering the variable soil concentrations often mentioned in these papers and in light of the mobility of even small mammals, it is likely that the small mammals were variably exposed to differing soil concentrations of contaminants throughout their home ranges and over their life

spans. The closer correlation of vegetation concentrations to soil concentrations in a specific location is reasonable, given that plants remain rooted in the same soil throughout their lifetimes.

Higley and Whicker (1999) further concluded that, although the nature and source of a Pu release is important in its distribution, environmental processes can alter the composition and distribution over time. Soils and sediments have been found to become the ultimate repository for the majority of Pu. A tiny fraction of the Pu inventory is soluble and therefore bioavailable. They found that while Pu is incorporated into plant, animal and human tissues, the concentrations are typically orders of magnitude less than soil and sediment concentrations. Biomagnification – the concentration of a chemical or compound from one trophic level to the next – does not appear to occur with Pu. Their review found that although biological processes can redistribute Pu in the soil profile, the impact is essentially local.

Arthropods

Arthropods were studied as part of the comprehensive long-term investigations performed at RFETS by staff and students at CSU. This group was selected due to their mobility and rapid population turnover rate. The Bly and Whicker study (1979) found that although the concentrations of Pu in soil and arthropods were closely correlated the ratio of activity in arthropods: soil was on the order of 10^{-2} to 10^{-3}. Although arthropod biomass is considerably higher than that of small mammals, the Pu concentration in the arthropod compartment was found no greater than 10^{-8} of the Pu inventory in the ecosystem (Bly and Whicker, 1979). The authors noted that it was difficult to ensure that additional soil was not collected with the ground-dwelling arthropods during capture. No attempt was made to scrub the arthropods, therefore all clinging soil would have been analyzed as part of the contaminant load of this biotic compartment. Because ground-dwelling arthropods do not generally move substantial distances during their life spans, there is little potential for mass transport of Pu by this group; however flying insects such as bees could contribute to some transport of contamination (Bly and Whicker, 1979).

Small Mammals

Few of the small mammal samples taken during the Whicker and Ibrahim (1991) study showed Pu above detection limits. After earlier studies encountered problems with instrumental detection limits, tissue samples were pooled by Whicker and Ibrahim (1992) to increase the Pu concentration of the total sample to detectable levels. These findings were consistent with Little (1976), who concluded that a very small portion of the total Pu in the Site ecosystem was associated with small mammal tissues. Animal hide samples contained the majority of Pu found in small mammal tissues. This is expected since soil particles can adhere to the pelt and there is no description of an attempt to remove soil from hides. Reported concentrations of Pu-239 in tissues ranged from 1.0×10^{-1} Bq/g in hide to a low of -1.2×10^{-2} Bq/g in lung tissue (Whicker and Ibrahim, 1992, Antonio, et al., 1992). The negative values reported for this study apparently reflect readings below the reliable detection limits of the instrumentation at that time. No significant differences were found between results of this study and those of Little (1976; 1980).

A study in "Macroplot 1", a 0.75 ha plot located approximately 140 meters southeast of the 903 Pad, found that northern pocket gophers (*Thomomys talpoides*) do contribute to the redistribution of Pu in soils, but that the redistribution was largely vertical, through the soil profile (Winsor and Whicker, 1980). Burrow activity reported for pocket gophers during this study far exceeds present observations (pers. obs. M. Murdock, 2001). Therefore, the estimated 0.5 % of the soil Pu that pocket gophers may cast to the surface in a decade might overstate average conditions. Small mammal populations are well known to exhibit cyclic maximums and minimums and the 1975 population may have represented a periodic maximum. The authors concluded that the long-term impact of these animals may be a more uniform vertical distribution of Pu in the soil, coupled with a small amount of horizontal dispersion (Winsor and Whicker, 1980). In considering this study, it should be noted that cumulative studies in the area evaluated indicated that 99 % of the Pu inventory was in the top 21 cm of soil and that approximately half that is in the top 3 cm. This condition would make transport to depth more likely than transport of more Pu to the surface (Setlock and Blaha, 1986).

Snakes

Geiger and Winsor (1977) evaluated Pu-239 concentrations in snakes at RFETS and found that they had the lowest Pu-239 concentrations of any biota studied at the Site. They concluded their data suggested that snakes are not important organisms in the redistribution of Pu-239.

Mule Deer

A radiotelemetry study conducted by CSU on mule deer (*Odocoileus hemionus*) from 1990 through 1991 allowed researchers to radio collar or radio eartag 138 deer for the purpose of tracking movements. This study also estimated a summer deer population of approximately 161 individuals and a winter deer population of approximately 199 individuals (Symonds 1992). Analysis of deer tissues during the 1990-91 telemetry study did not detect measurable Pu or Am and Symonds (1992) speculated that because of the sedentary nature of the RFETS deer herd, deer had a low potential for transporting contamination off-Site. She also postulated that deer represented a minimal pathway for contamination of humans.

Whicker (1979) found that most of the Pu ingested by deer grazing in contaminated areas is redeposited on-Site in the form of fecal pellets. These pellets are randomly distributed as the deer travel around the Site, with greater deposition expected in areas of higher deer use. Over time, areas most frequented by deer have been found the more heavily vegetated hillside grasslands, shrublands and woodlands (K-H 1998; 1999), which provide greater erosion protection than disturbed or sparsely vegetated areas. Once the fecal pellets have been deposited in these areas, further redistribution over a wide area would be restricted by the limited erosion potential.

Symonds (1992) found that does seldom moved farther than 0.05 km from the Site. Either of these types of off-Site movement could provide a pathway (through fecal deposition or death and decomposition) for Pu that was consumed in forage before the deer left the Site. Symonds (1992) reported use of "contaminated" areas by deer during her study, but the assignment of the term "contaminated" in context of this study appears to broadly include any area where an IHSS may have been tentatively identified, regardless of potential contaminant (e.g., radiological or

490

chemical). In other studies the area identified as "contaminated" was more specific to Macroplot 1 used in numerous CSU-sponsored studies, or included the 903 Pad and Lip area (Whicker, et al., 1990; Winsor and Whicker, 1980; Little, et al., 1980; Arthur and Alldredge, 1982).

Mule deer have been studied as a biological pathway for actinide movement because of their mobility, amount of soil consumption and the size of the herd. Quantifying off-Site transport of actinides by mule deer provides a reference for comparing the effects of the overall biological transport pathway. The methodology for calculating estimated actinide transport by mule deer is presented in Section TA-5 because the analysis is based exclusively on modeled data.

Cattle

In 1973, cattle that had been grazing on what is the present day northeast Buffer Zone of RFETS were analyzed for uptake of Pu-239, Am and U-238 (Smith and Black, 1975). These cattle (five adults and five calves of the year) had been grazing and drinking water from streams flowing through the Site. The adults had been grazed six months per year for eight years and the calves spent their entire lives on RFETS pasture before slaughter. Cattle from other radiologically contaminated sites were also studied, but results of RFETS cattle are discussed here.

Smith and Black (1975) found that the cattle held Pu concentrations that were statistically equivalent to those found in other herds grazing in areas where Pu in soil was above the U.S. average level. Concentrations of Am were about 0.25 to 0.5 of the Pu-239 concentrations in the same tissues. The U-238 concentrations were above average and the authors concluded this reflected the higher natural environmental levels on the eastern slope of the Rocky Mountains. Smith and Black (1975) reported that the levels of Pu-239 found in the cattle were comparable to those found in the general U.S. population from fallout. Unlike deer, the location of fecal deposition by cattle of forage remnants from the Site could be controlled, if there were actual concern about actinide contamination or redistribution by this route.

Other Highly Mobile Biota

Several other mobile species undoubtedly transport some small quantity of actinide off-Site. Species such as waterfowl and other birds, coyotes and insects could transport actinides off-Site. However, data for these species are not available and would be very difficult and in some cases logistically impossible to obtain. Using the deer data and normalizing by the biomass of deer, it is estimated that off-Site transport by other selected terrestrial species is comparable to transport by deer or probably lower.

TA-4.7.3 Aquatic Studies

A study of the existing pond system, initiated in 1971 and concluded in June 1974, provides the bulk of information on Pu movement in a freshwater system. This study also included a pilot study on an analytical procedure that allowed analysis of a large number of samples at reasonable cost (Johnson, et al., 1974). Not surprisingly, this study found that a greater percentage of the Pu was associated with the root system than was associated with aerial plant parts (the opposite of the findings in studies of terrestrial plants). This is because particulate actinides will settle to the bottom of a water body, which is closer to the roots than the aerial plant parts. Rainsplash is not a redistribution mechanism in an aquatic system and rain tends to wash dust from emergent vegetation in terrestrial systems.

Limited studies are available on the fate of Pu in the aquatic ecosystem. Two segments of this aquatic study concluded that Pu in water depended largely on the amount of suspended material in the samples (Johnson, et al. 1974; Paine, 1980). Paine's study showed that "seston" (floating organic material including phytoplankton and plant fragments) samples accumulated Pu at a higher rate than other aquatic organisms, but methods described may have allowed inorganic particles (i.e., clay) to be sampled along with organic samples. Paine observed that clay sediments showed an extremely high affinity for Pu and if left undisturbed, appear to be an excellent reservoir for Pu in the aquatic system. When collecting and preparing seston samples for this study, the methods described may not have allowed suspended sediment to be effectively separated from the seston, allowing the possibility that suspended sediment was sampled as part of the seston. This might have given a conservatively high value for Pu in seston.

492

Other findings of this study (Paine, 1980) were that an increase in trophic level concentration of Pu did not occur, there appeared to be a selective mechanism which discriminated against Pu at the phytoplankton to zooplankton level. The highest concentration in crawfish was found in the exoskeleton. Whole fish had detectable activity, but fish flesh showed none.

Biological transport of Pu through the aquatic ecosystem is probably minimal because of the limited development of the RFETS aquatic ecosystem. The intermittent and ephemeral stream system supports a very limited population of aquatic organisms outside of the impoundments on the Site. Certain waterfowl do consume small fish and other aquatic organisms, but there is apparently little Pu available in the food items that would be consumed and transported off-Site. Transport by abiotic (i.e., physical or mechanical) means is discussed elsewhere in the main report and is not the subject of speculation here.

TA-4.7.4 Conclusions

Since the 1960s, extensive research has been conducted in actinide-contaminated areas of RFETS to evaluate the uptake and biological transport potential for Pu. Most of the research has estimated that greater than 99 % of the Pu inventory is in soil and sediment. In the terrestrial communities, vegetation studies from the early 1970s through the early 1990s have concluded that much of the Pu associated with plant material adheres as particles, rather than as Pu incorporated into plant tissues. These studies have shown that Pu has low bioavailability, due to its insolubility and that uptake into plant and animal tissues is minor. Data have shown a decrease in plant uptake and accumulation over time. Results from these studies suggest that as Pu availability and uptake by plants has declined over time, the amounts available to primary consumers have also decreased and thus the potential for redistribution has declined.

Studies of animals, including arthropods, small mammals, snakes and mule deer have demonstrated little accumulation of Pu in the tissues of these species. Biomagnification through the trophic levels does not appear to occur. Results of studies on soil redistribution by wildlife suggest that redistribution of Pu through burrowing is a limited-area phenomenon and this process has only local effect. Although several studies assumed that mule deer have the greatest potential to redistribute Pu, because of their greater mobility and greater intake of soil, results of

these studies indicate they redistribute approximately 10^{-7} of the soil actinide inventory. Deer are estimated to transport approximately 10^{-11} of the actinide inventory off-Site. Other terrestrial or semi-aquatic (e.g., ducks) species are estimated to transport less actinides than the deer to off-Site areas, but no data are available for more accurate quantification.

The limited aquatic studies that were done at RFETS have not indicated a significant potential for aquatic biota to redistribute Pu in these systems.

This review has found evidence from past studies of insignificant biouptake, bioavailability or biological transport of actinides. The potential for biological actinide redistribution off the Site is minimal.

One data gap identified during this review is the lack of recent vegetation contamination data for the "Macroplot 1" study area. Since the last studies were performed, the plant association in that area has changed somewhat. The uptake and adherence potentials of the unevaluated plant species may be different from those previously studied, therefore evaluation of transport potential by present vegetation may be warranted.

494

TA-4.8 TECHNICAL APPENDIX SECTION TA-4 REFERENCES

Surface Water Pathway References (TA-4.1 through TA-4.4)

EG&G Rocky Flats, Inc. (EG&G). 1995. Geochemical Characterization of Background Surface Soils: Background Soils Characterization Program. Rocky Flats Environmental Technology Site, Golden , CO.

Hartmann G., Thom C. and K. Bachmann. 1989. Sources for Pu in Near Surface Air, Health Physics, Vol. 56, No. 1, pp. 55-69.

Hakonson T., R. Watters and W. Hanson. 1981. The Transport of Plutonium in Terrestrial Ecosystems, Health Physics, Vol. 40, No. 1, pp. 63-69.

Hersman L. E. 1986. Sorption of 239Pu by a Pseudomonas species. Abstracts of the Annual Meeting of the American Society for Microbiology, Vol. 258, p. 1986.

Johnson J., S. Svalberg and D. Paine. 1974. The Study of Plutonium in Aquatic Systems of the Rocky Flats Environs. Department of Animal Sciences and the Department of Radiology and Radiation Biology. Colorado State University. Prepared for Dow Chemical Company. Rocky Flats. Golden, CO.

Paine D., 1974. Plutonium in Rocky Flats Freshwater Systems. Transuranic Elements in the Environment. Technical Information Center. United States Department of Energy, pp. 644-658.

Litaor M. I. 1995. Uranium Isotopes Distribution in Soils at the Rocky Flats Plant, Colorado. Journal of Environmental Quality, Vol. 24, No. 2, pp. 314-323.

Rocky Mountain Remediation Services (RMRS). 1997. Progress Report #1 to the Source Evaluation and Preliminary Mitigation Plan for Walnut Creek. Report RF/RMRS-97-089.UN. Revison 0. Rocky Flats Environmental Technology Site, Golden, CO.

RMRS. 1998. Final Report to the Source Evaluation and Mitigation Actions Plan for Walnut Creek. Report RF/RMRS-98-234.UN. Rocky Flats Environmental Technology Site, Golden, CO.

RMRS. 1999. Source Evaluation Report for Point of Evaluation GS10. Report RF/RMRS-99-376.UN. Rocky Flats Environmental Technology Site, Golden, CO.

Santschi P., K. Roberts and L. Guo. 2000. Final Report on Phase Speciation of Pu and Am for Actinide Migration Studies at the Rocky Flats Environmental Technology Site. Texas A&M University, Galveston, Texas. September 29, 2000.

Thompson M. 1975. Plutonium in the Aquatic Environment around the Rocky Flats Facility. Dow Chemical Company. Rocky Flats Division, Golden, CO.

Groundwater References (Section TA-4.5)

Ball, J. W. 2000. Geochemical Modeling of Solar Ponds Plume Groundwater at the Rocky Flats Environmental Technology Site, Part 1: Ion Plots and Speciation Modeling, Golden, CO, U. S. Geological Survey, (forthcoming).

Colorado Department of Public Health and Environment (CDPHE). 1996. Ground Water Plutonium239,240 Data in Walnut Creek Alluvium East of the Terminal Ponds of Rocky Flats Environmental Technology Site to Great Western Reservoir. Technical Status Report. February 15, 1996.

Cleveland, J. M., T. F. Rees and W. C. Gottschall. 1976, Factors Affecting Solubilization of Plutonium and Americium from Pond Sediments at the Rocky-Flats Facility, ES-376-76-196, Rockwell International, Rocky Flats Plant. December 29, 1976.

Department of Energy (DOE). 1994. OU4 Solar Evaporation Ponds Interim Measure/Interim Remedial Action Environmental Assessment Decision Document, Part II, Volume 1, Revision: Proposed. February, 1994.

DOE. 1995. Rocky Flats Environmental Technology Site, Site Environmental Report for 1994. RFP-ENV-94.

DOE. 1997a. Summary of Existing Data on Actinide Migration at the Rocky Flats Environmental Technology Site. RF/RMRS-97-074.UN, September, 1997.

DOE. 1997b. Sampling and Analysis Plan for the Site Characterization of the 903 Drum Storage Area (IHSS 112), 903 Lip Area (IHSS 155) and Americium Zone. RF/RMRS-97-084. December 15, 1997.

DOE. 1999. Sampling and Analysis Plan for Groundwater Investigations Involving Actinide Drilling-Artifact Contamination, the Industrial Area VOC Plume East Boundary and Solar Ponds Plume Well Installations, Final. RF/RMRS-99-347. July, 1999.

EG&G. 1995. 1994 Well Abandonment and Replacement Program Final Report, Rocky Flats Environmental Technology Site. March.

Fontes. 1981. Paleowaters. In: Stable Isotope Hydrology – Deuterium and Oxygen-18 in the Water Cycle. IAEA, Vienna, Austria. Technical Report Series, No. 210, pp.273-302.

Harnish, R. A., D. M. McKnight and J. F. Ranville. 1994. Particulate, Collodial and Dissolved-Phase Associations of Plutonium and Americium in a Water Sample from Well 1587 at the Rocky Flats Plant, Colorado. U.S.G.S. Water-Resources Investigations Report 93-4175.

496

Harnish, R. A., D. M. McKnight, J. F. Ranville, V. C. Stephens and W. Orem. 1996. Particulate, Collodial and Dissolved-Phase Associations of Plutonium and Americium in Water Samples from Well 1587, Surface Water SW051 and Surface Water SW053 at the Rocky Flats Plant, Colorado. U.S.G.S. Water-Resources Investigations Report 96-4067.

Honeyman, B. D. and P. H. Santschi. 1997. Actinide Migration Studies at the Rocky Flats Environmental Technology Site, Final Report. December 15, 1997.

Honeyman, B. D., R. Harnish, T. McKibben, J. Spear and S. Winkler. 1999. Actinide Migration Studies at the Rocky Flats Environmental Technology Site: The Effect of Soil-Water Redox Potential on 239,240Pu Solubility. Final Report to Kaiser-Hill on Contract KH800022MW. Golden, CO.

Ibrahim, S. A., M. J. Schierman and F. W. Whicker. 1996. Comparative Distribution of 241Am and 239,240Pu in Soils Around the Rocky Flats Environmental Technology Site, Health Physics, Vol. 70, No. 4, pp. 520-526.

Krey, P. W. and E. P. Hardy. 1970. Plutonium in Soil Around the Rocky Flats Plant. U.S.A.E.C-Health and Safety Laboratory, HASL-235. August, 1970.

Krey, P. W., E. P. Hardy and L. E. Toonkel. 1977. The Distribution of Plutonium and Americium with Depth in Soil at Rocky Flats. U.S.E.R.D.A-Health and Safety Laboratory, HASL-318. April, 1977.

Litaor, M.I., M.L. Thompson, G.R. Barth and P.C. Molzer. 1994. Plutonium-239+240 and Americium-241 in Soils East of Rocky Flats, Colorado. Journal of Environmental Quality, Vol. 23, pp. 1231-1239.

Litaor, M.I., G.R. Barth and E.M. Zika. 1996. Fate and Transport of Plutonium-239+240 and Americium-241 in the Soil of Rocky Flats, Colorado. Journal of Environmental Quality, Vol. 25, pp: 671-683.

Litaor, M.I. and S.A. Ibrahim. 1996. Plutonium Association with Selected Solid Phases in Soils of Rocky Flats, Colorado, using Sequential Extraction Techniques. Journal of Environmental Quality, Vol. 25 pp. 1144-1152.

Litaor, M. I., G. R. Barth, E. M. Zika, G. Litus, J. Moffitt and H. Daniels. 1998. The Behavior of Radionuclides in the Soils of Rocky Flats, Colorado. Journal of Environmental Radioactivity, Vol. 38, No. 1, pp. 17-46.

Litaor, M. I., G. Barth and G. Litus. 1999. The Hydro-geochemistry of Actinides in the Soil of Rocky Flats, Colorado. unpublished manuscript.

Little, C. A. 1976. Plutonium in a Grassland Ecosystem (Dissertation), Colorado State University.

497

Little, C. A. and F. W. Whicker. 1978. Plutonium Distribution in Rocky Flats Soil. Health Physics, Vol. 34, pp. 451-457.

McCarthy, J. F. and J. M. Zachara. 1989. Subsurface Transport of Contaminants: Environmental Science and Technology, Vol. 23, pp. 496-502.

Remenda, V. H., J. A. Cherry and T. W. D. Edwards. 1994. Isotopic Composition of Old Groundwater from Lake Agassiz: Implication for Late Pleistocene Climate. Science, Vol. 266, pp. 1975-1978.

RMRS. 1996. Analysis of Vertical Contaminant Migration Potential. RF/ER-96-0040.UN. August, 1996.

RMRS. 1998. Evaluation of Plutonium and Americium in Groundwater at the Rocky Flats Environmental Technology Site (Draft). RF/RMRS-98-229.UN. March 19, 1998.

RMRS. 1999. Sampling and Analysis Plan for Groundwater Investigations Involving Actinide Drilling-Artifact Contamination, the Industrial Area VOC Plume East Boundary and Solar Ponds Plume Well Installations. RF/RMRS-99-347. July, 1999.

Ryan, J. N., T. H. Illangasekare, M. I. Litaor and R. Shannon. 1998. Particle and Plutonium Mobilization in a Macroporous Soil during Rainfall Smiulations. Environmental Science and Technology, Vol. 32, pp. 476-482.

Schierman, M. J. 1994. Characterization of Americium and Plutonium Concentrations in Soil Profiles at the Rocky Flats Plant. Thesis. Colorado State University, Ft. Collins, CO.

Stewart. L. M. 1973. Areas of Concern at Rocky Flats: Soil Contamination and Related Incidents, Part 1: Plutonium. Product and Health Physics Research HPR-317-381-138, June 29, 1973.

Weaver, J. E. 1920. Root Development in the Grassland Formation: A Correlation of Root Systems of Native Vegetation and Crop Plants. Carnegie Institution of Washington, Washington DC.

Webb, S. B. 1992. A Study of Plutonium in Soil and Vegetation at the Rocky Flats Plant. Thesis. Colorado State University, Ft. Collins, Colorado.

Webb, S. B., S. A. Ibrahim and F. W. Whicker. 1993. A Study of Soil and Vegetation at the Rocky Flats Plant, In: Kathren, R. L., et al., eds. Environmental Health Physics, Richland, Washington, pp. 611-623.

Air Pathway References (Section TA-4.6)

Environmental Protection Agency (EPA). 1995a. Screen3 Model User's Guide. U.S. Environmental Protection Agency, Office of Air Quality Planning and Standards, Emissions, Monitoring and Analysis Division, Research Triangle Park, North Carolina. September, 1995.

EPA. 1995b. User's Guide for the Industrial Source Complex (ISC30 Dispersion Models, Volume I and II (EPA-454/B-95-003a) U.S. Environmental Protection Agency, Office of Air Quality Planning and Standards, Emissions, Monitoring and Analysis Division, Research Triangle Park, North Carolina. September, 1995.

Hulse, S.E., S.A. Ibrahim, F.W. Whicker and P.L. Chapman. 1999. Comparison of 241A,. 239/240 Pu and 137 Cs Concentrations in Soil Around Rocky Flats. Health Physics Vol. 76, No. 3.

Langer. G. 1986. Dust Transport-Wind blown and Mechanical Resuspension, July 1983 to December 1984 (RFP-3914). Rockwell International, Golden, CO. September, 1986.

Langer. G., 1987. Dust Transport-Wind blown and Mechanical Resuspension. HS & E Applications Technology Semiannual Progress Report. May, 1987. p. 16.

Midwest Research Institue (MRI). 2001. Effect of Controlled Burning on Soil Erodibility by Wind. Revised Draft Test Report. Midwest Research Institute, Kansas City, MO.

Radian. 2000. Air Transport and Deposition of Actinides for the Actinide Migration Evaluation at the Rocky Flats Environmental Technology Site. Radian International, Denver, CO.

Shinn. J. 1999. Personal Communicaton with Joseph Shinn. April, 1999.

Biological Pathway References (Section TA-4.7)

Arthur, W.J. 1977. Plutonium Intake by Mule Deer at Rocky Flats Colorado. M.S. Thesis. Colorado State University, Fort Collins, Co. 1077.

Arthur and Alldredge. 1982. Importance of Plutonium Contamination on Vegetation Surfaces at Rocky Flats, Colorado. Environmental and Experimental Botany, Vol. 22, No. 1, pp. 33-38.

Antonio, et al. 1992. The Distribution of and Concentration of Plutonium in Small Mammals Residing on a Contaminated Soil Site; Progress Report. Agreement ASC 83749AM. Colorado State University, Ft. Collins, CO. February, 1992.

Bly and Whicker. 1979. Plutonium Concentrations in Arthropods at a Nuclear Facility. Health Physics, Pergamon Press. Vol. 37, pp. 331-336.

Dreicer et al. 1984. Rainsplash as a Mechanism for Soil Contamination of Plant Surfaces. Health Physics, Vol 46, No 1, pp 177-187. January, 1984.

Geiger, R.G. and T.F. Winsor. 1977. 239Pu Contamination in Snakes Inhabiting the Rocky Flats Plant Site. Health Physics, Pergamon Press, Vol. 33, pp. 145-148. August, 1977.

Higley, K. and F.W. Whicker. 1999. Biological Mobility of Environmental Plutonium. "White Paper". Kathryn Higley, Oregon State University and F. Ward Whicker, Colorado State University. October 16, 1999.

Kaiser-Hill Company, L.L.C. (Kaiser-Hill). 1998. 1997 Annual Wildlife Survey Report, Natural Resource Compliance and Protection Program. Kaiser-Hill Company, Rocky Flats Environmental Technology Site, Golden, CO. May, 1998.

Kaiser-Hill. 1999. 1998 Annual Wildlife Report for Rocky Flats Environmental Technology Site. Prepared by Exponent for Kaiser-Hill Company, LLC. Rocky Flats Environmental Technology Site, Golden, CO. June, 1999.

Johnson, et al. 1974. The Study of Plutonium in Aquatic Systems of the Rocky Flats Environs. Colorado State University, Ft. Collins, CO. June 1, 1974.

Little. 1976. Plutonium in a Grassland Ecosystem. C.A. Little. Colorado State University, Ft. Collins, CO. Dissertation.

Little, et al. 1980. Plutonium in a Grassland Eecosystem at Rocky Flats. Journal of Environmental Quality. Vol. 9, No. 3, pp. 350-354.

Murdock, M. 2001. Kaiser-Hill Ecology Group, Rocky Flats Environmental Technology Site. Golden, Co. Personal Observations by Marcia Murdock made during Ecological Monitoring Field Work.

Paine, D. 1980. Plutonium in Rocky Flats Freshwater Systems. In Transuranic Elements in the Environment; A Summary of Environmental Research on Transuranium Radionuclides funded by the U.S. Department of Energy through Calendar Year 1979. W.C. Hanson, Editor. DOE/TIC-22800. Technical Information Center. U.S. Department of Energy.

Setlock, G.H. and F.J. Blaha. 1986. Rocky Flats Plant Radioecology and Airborne Pathway Summary Report. Environmental Management , Rockwell International. Rocky Flats Plant. Golden CO. December, 1986.

Smith, D.D. and S.C. Black. 1975. Actinide Concentrations in Tissues from Cattle Grazing near Rocky Flats Plant. National Environmental Research Center. EPA, Las Vegas, NV. February, 1975.

Symonds, K.K. and A. W. Alldredge. 1992. Deer Ecology Studies at Rocky Flats, Colorado; 1992-1992 progress report. Agreement ASC 49074 and ASC 77313AM. Colorado State University, Ft. Collins, CO. Summer, 1992.

500

Terry. 1991. Contamination of Surface Soil in Colorado by Plutonium, 1970-1989: Summary and Comparison of Plutonium Concentrations in Soil in the Rocky Flats Plant Vicinity and eastern Colorado. Presented at the Central Rocky Mountain Chapter, Health Physics Society annual Technical Meeting. April 22, 1991.

Watters, et al. 1983. The Behavior of Actinides in the Environments. Radiochimica Acta, Vol. 32, pp. 89-103.

Webb, et al. 1992. A Study of Plutonium in Soil and Vegetation at the Rocky Flats Plant; Progress Report. Agreement ASC 83749AM. Colorado State University, Ft. Collins, CO. April, 1992.

Winsor, T.F. and F.W. Whicker. 1980. Pocket Gophers and Redistribution of Plutonium in Soil. Health Physics, Vol. 39, pp. 257-262.

Whicker, F.W. et al. 1973. Plutonium Behavior in the Terrestrial Environs of the Rocky Flats Installation. Proceedings from IAEA Symposium on Environmental Surveillance around Nuclear Installations. Colorado State University. Ft. Collins, CO.

Whicker, F.W. 1979. Radioecology of Natural Systems; Final report for the period May 1, 1962-October 31, 1979. Contract No. EY-76-S-02-1156 (COO-1156-117). Colorado State University, Fort Collins, CO.

Whicker, F.W. et al. 1990. Progress Report on Radiological Investigations at Rocky Flats. Agreement ASC 49074 WS. Colorado State University, Ft. Collins, CO. September 15, 1990.

Whicker, F.W. et al. 1992. Progress Report on Radiological Investigations at Rocky Flats. Agreement ASC 83749AM. Colorado State University, Ft. Collins, CO. January, 1992.

Whicker, F.W. and S.A. Ibrahim. 1991. Progress Report on Radiological Investigations at Rocky Flats. Agreement ASC 83749AM. Colorado State University, Ft. Collins, CO. June 24, 1991.

Figure TA-4-1. Conceptual Model Schematic Diagram for Pu and Am Transport at RFETS

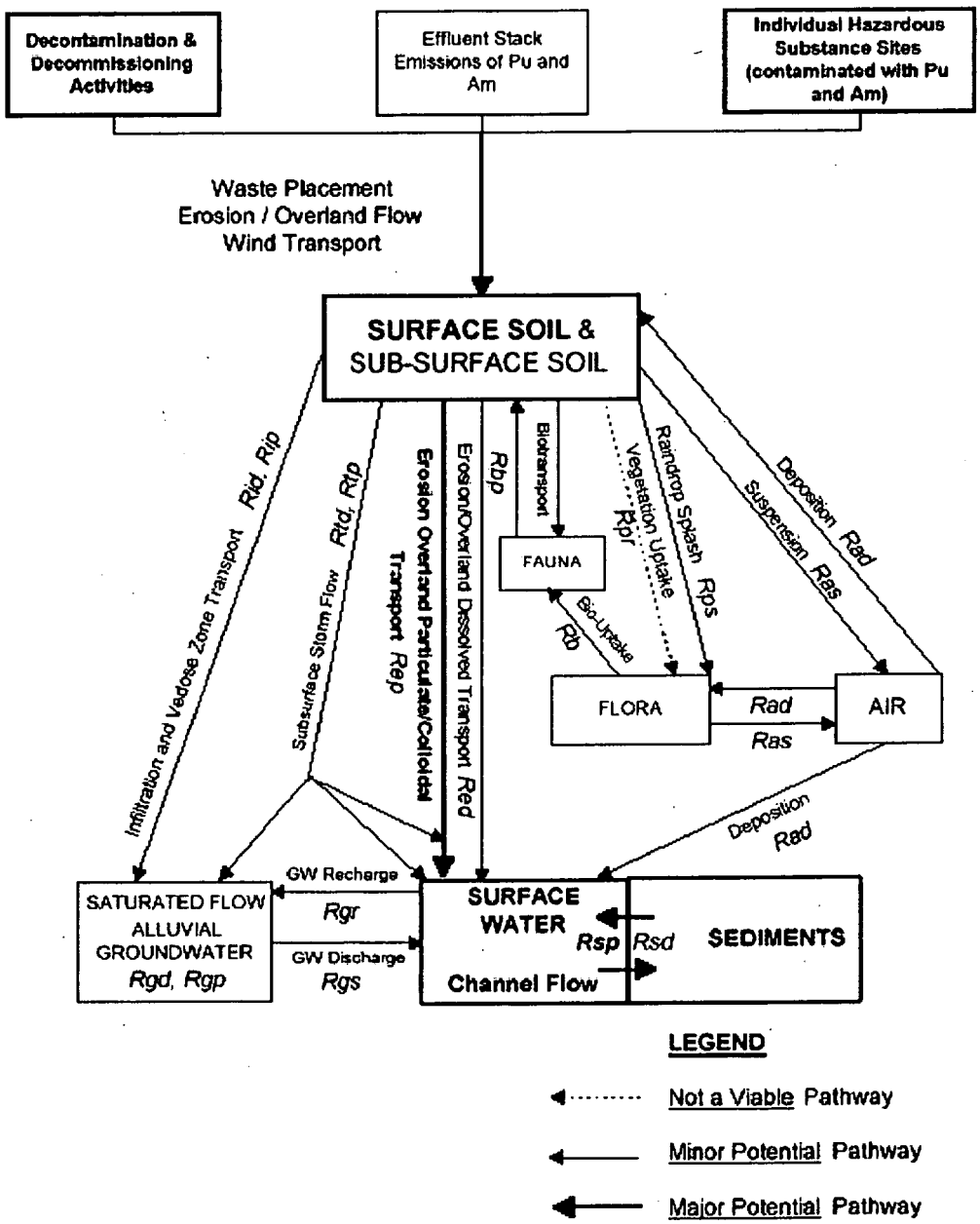

502

Figure TA-4-2. Conceptual Model Schematic Diagram for U Transport at RFETS

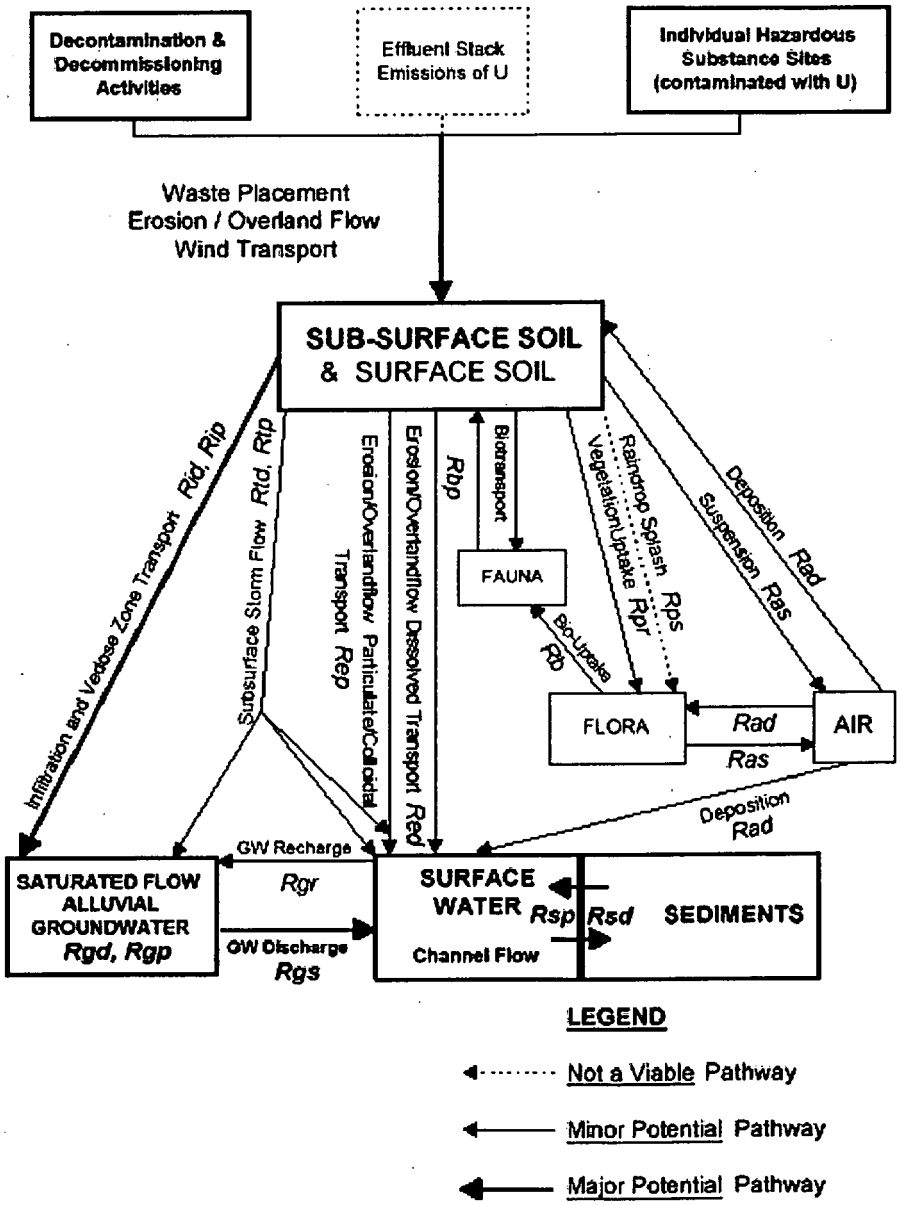

503

Figure TA-4-12. Lower Walnut Creek Study Area – Schematic Diagram

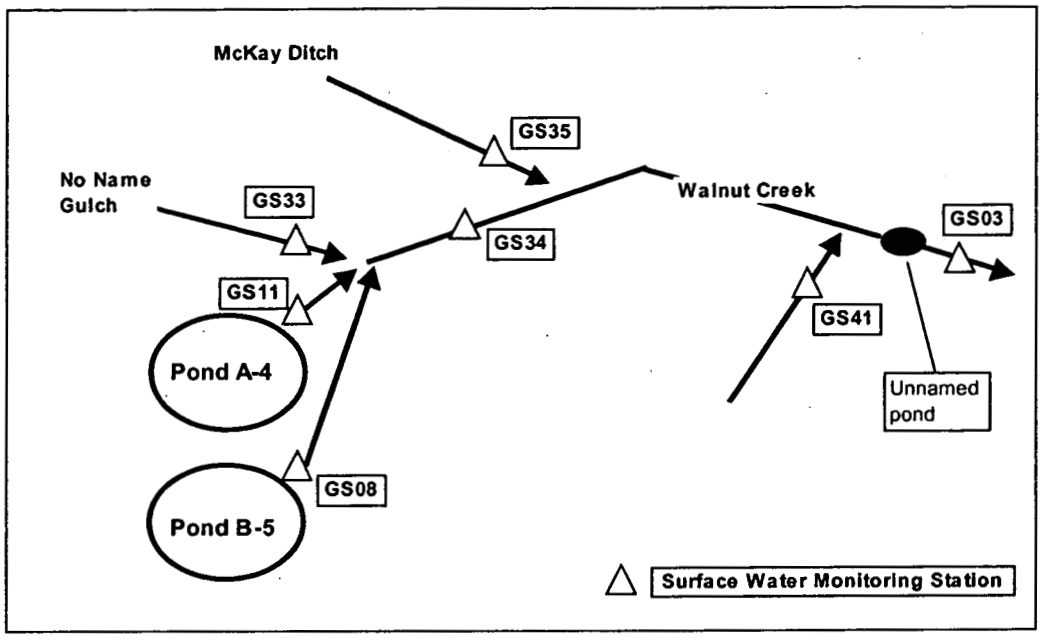

Figure TA-4-13. A- and B-Series Ponds Study Area – Schematic Diagram

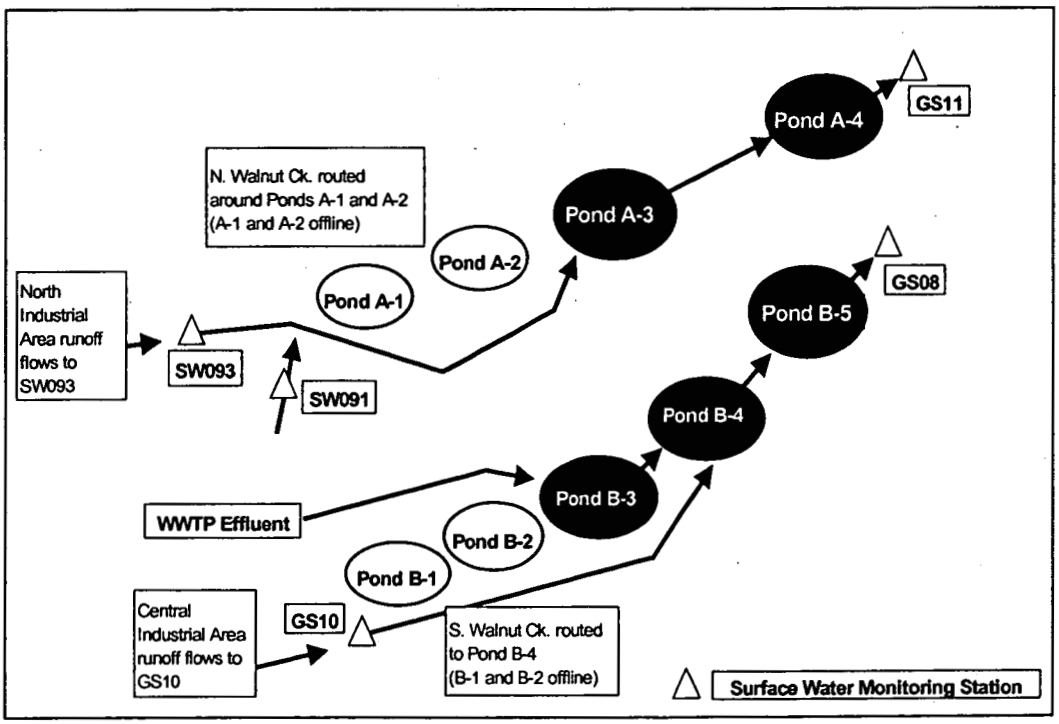

513

Figure TA-4-14. South Interceptor Ditch Study Area – Schematic Diagram

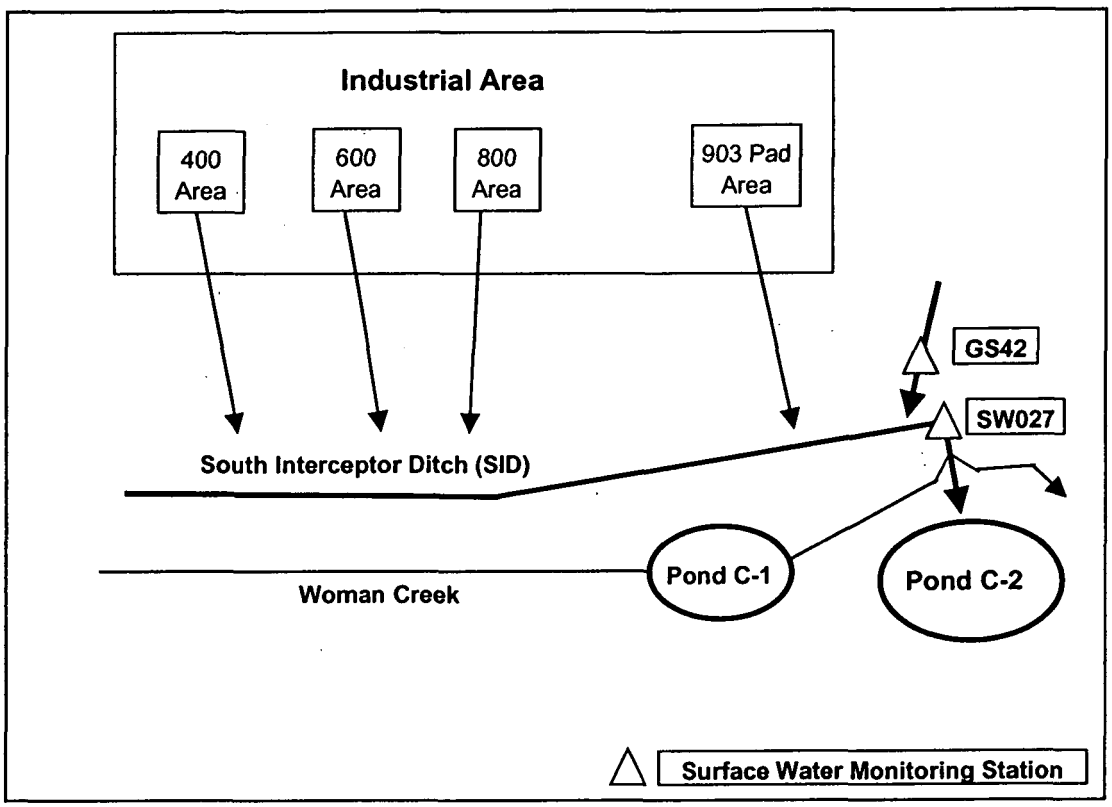

514

Figure TA-4-15. Lower Walnut Creek, Pu Loading Profile – Measured Load Data Only

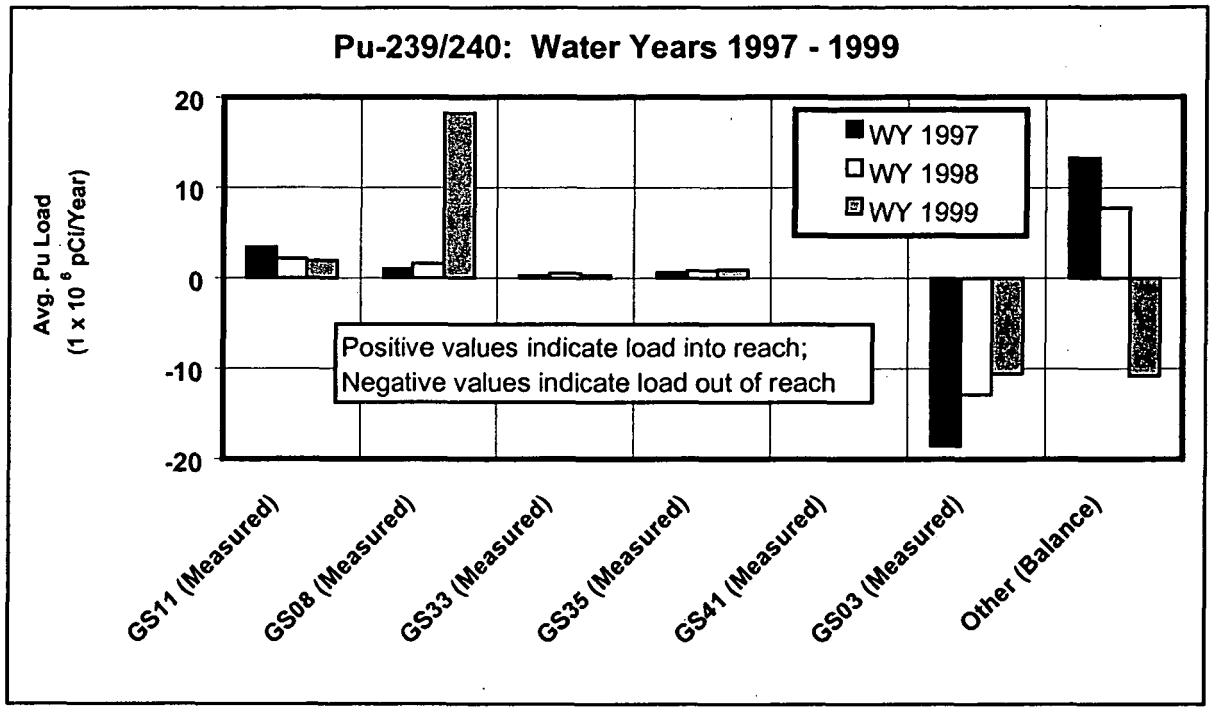

515

Figure TA-4-16. A- and B-Series Ponds, Pu Loading Profile - Measured Load Data Only

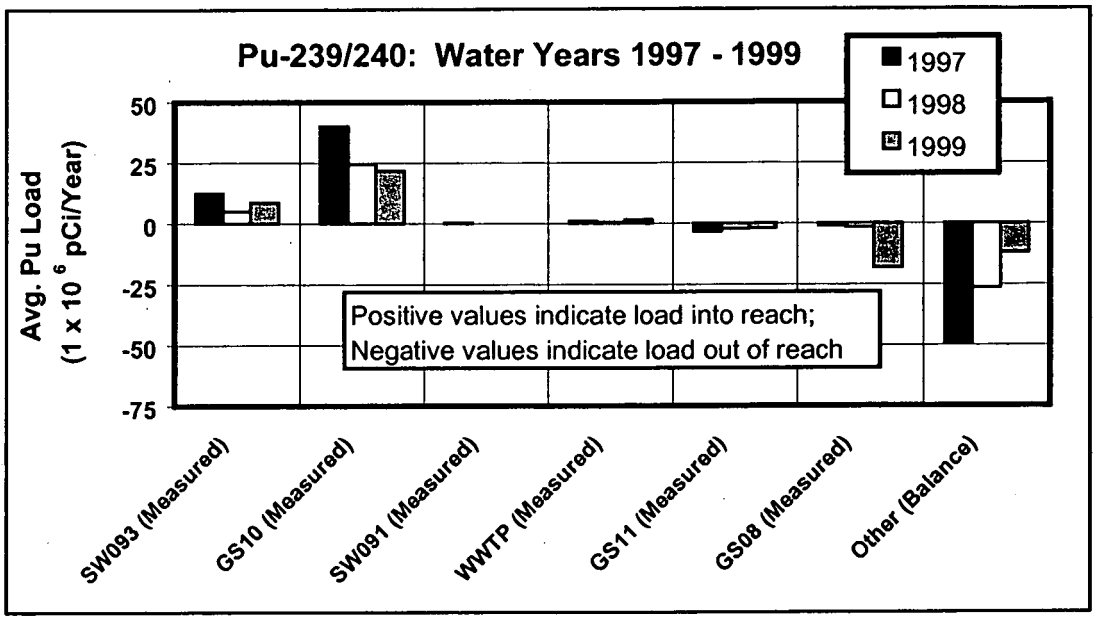

Figure TA-4-17. A- and B-Series Ponds, U-238 Loading Profile - Measured Load Data Only

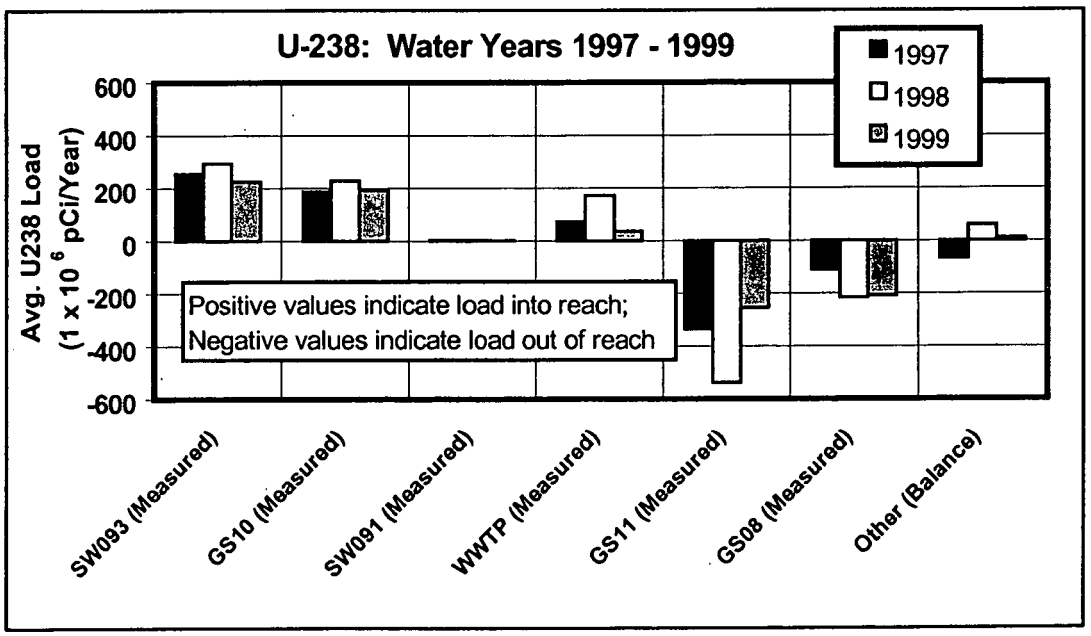

516

Figure TA-4-18. South Interceptor Ditch, Pu Loading Profile-Measured Load Data Only

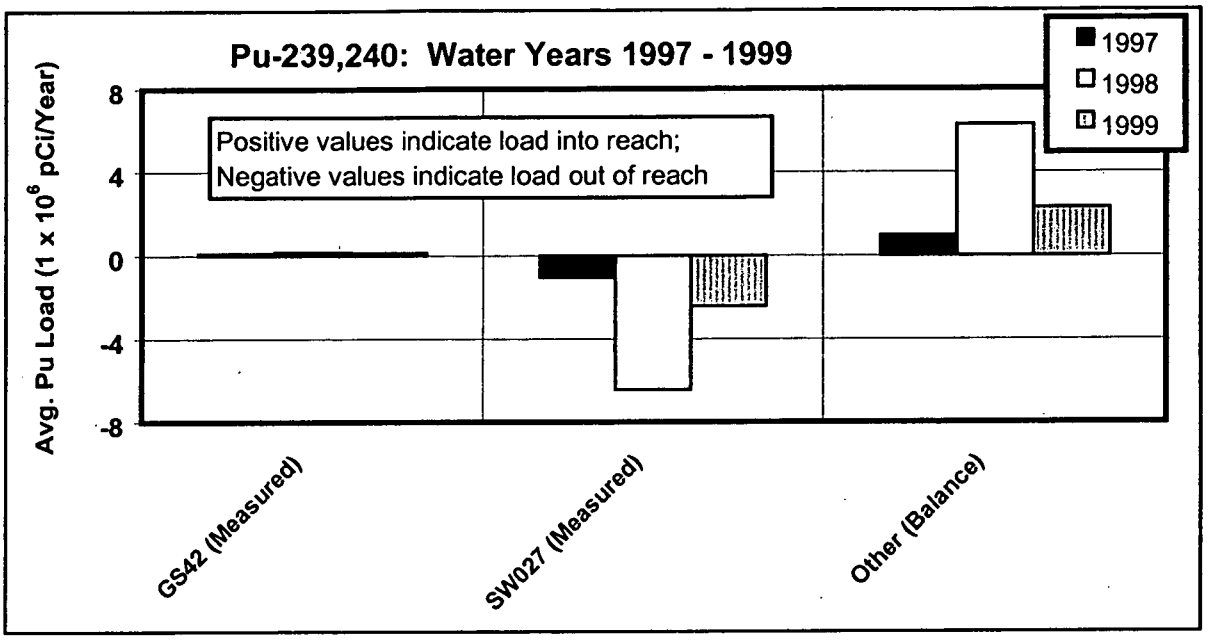

Figure TA-4-19. Site-Wide Vertical Distribution of Pu-239/240 in Groundwater

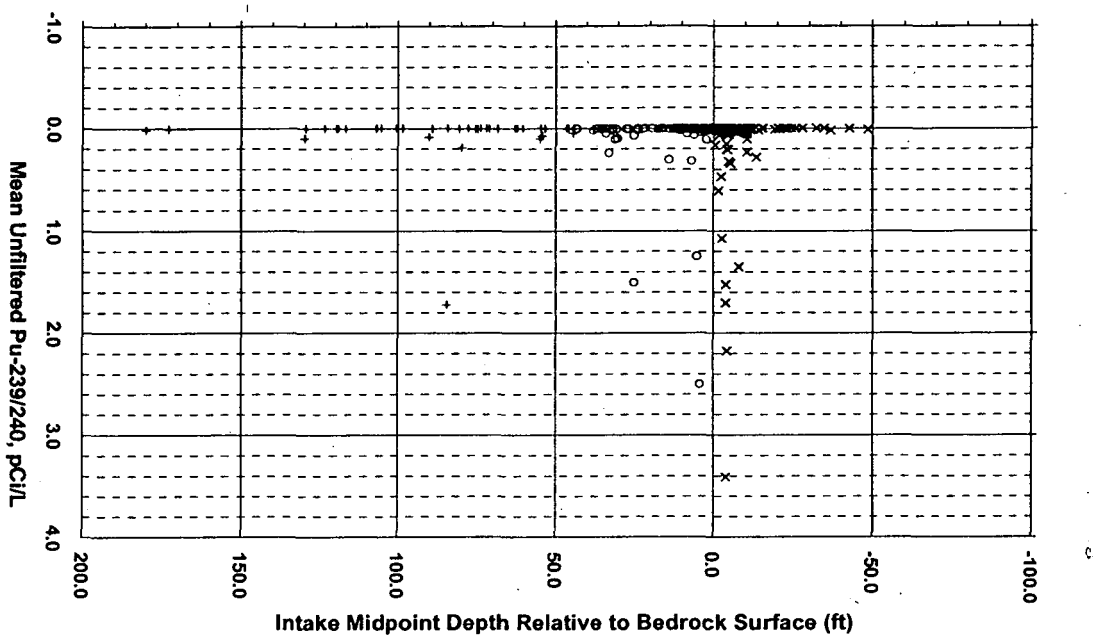

Figure TA-4-20. UHSU Groundwater Uranium-238 Trend for RFETS Background Areas

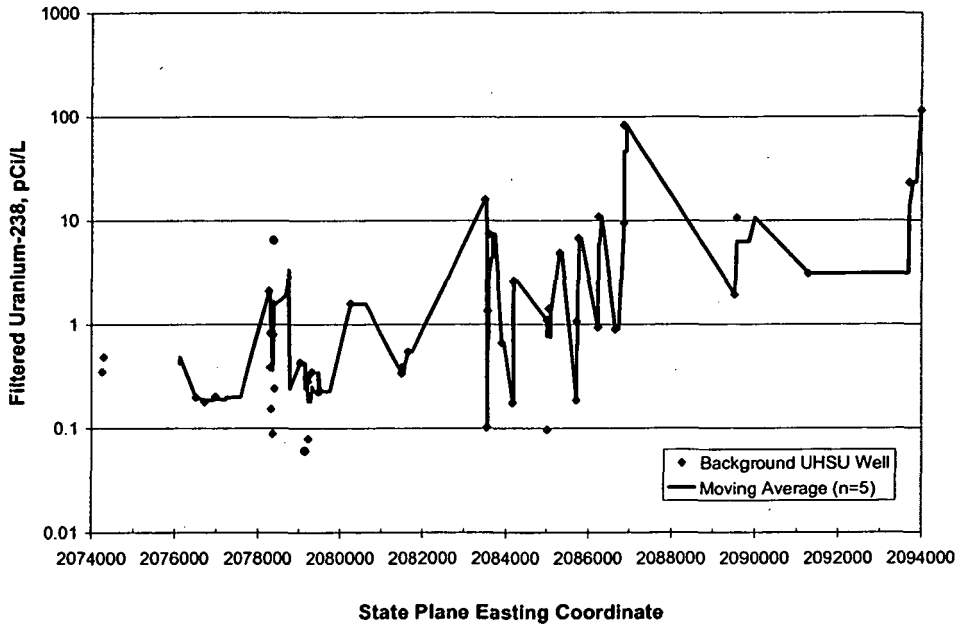

518

Figure TA-4-21. Site-Wide Vertical Distribution of U-238 in Groundwater

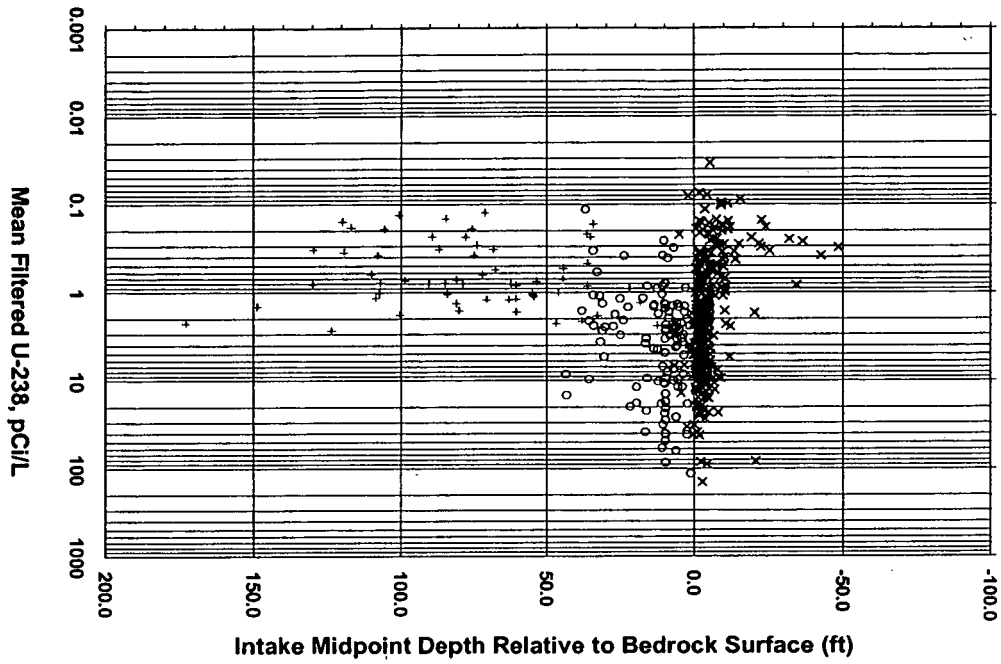

Figure TA-4-22. UHSU Groundwater Uranium-238 Trend for the Woman Creek Groundwater Basin

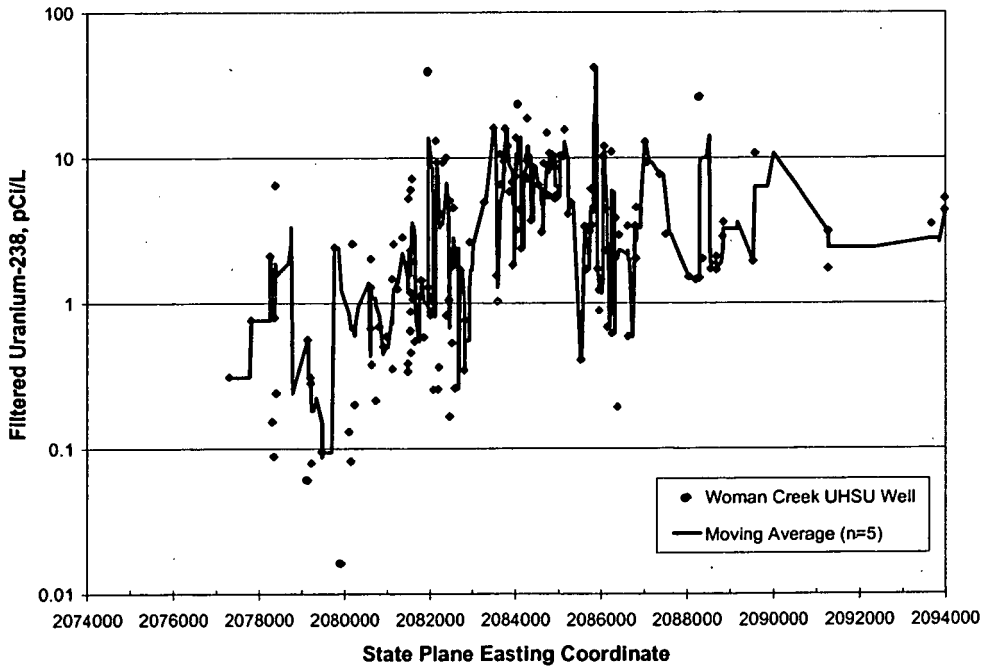

519

Figure TA-4-23. UHSU Groundwater Uranium-238 Trend for the Walnut Creek Groundwater Basin

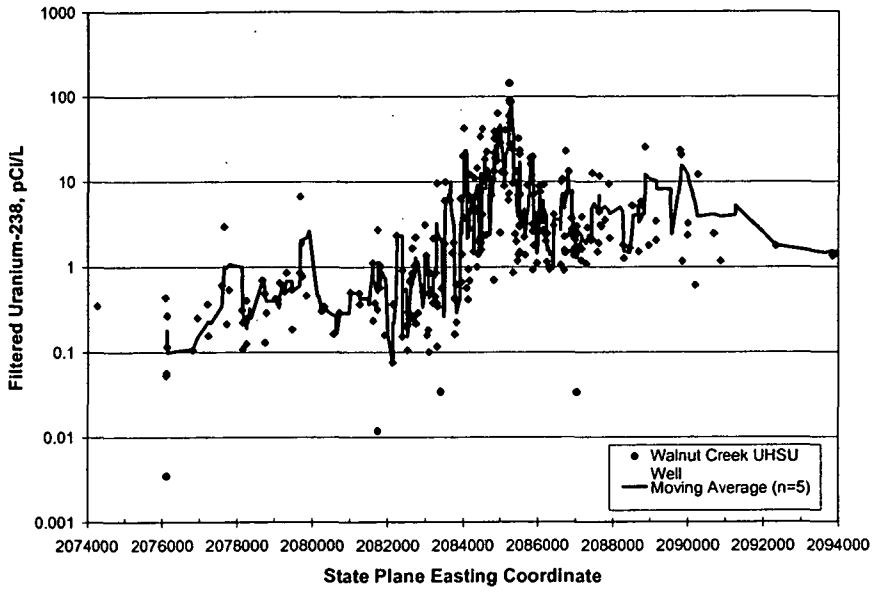

520

Figure TA-4-24. Air Box Model Figure

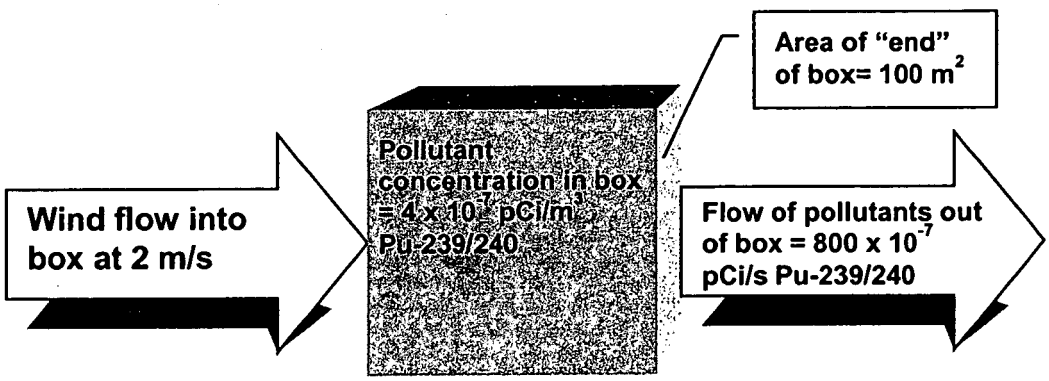

524

SECTION TA-5 - TABLE OF CONTENTS

TA-5 ACTINIDE TRANSPORT PATHWAYS ANALYSIS - BASED ON MEASURED AND MODELED RFETS ACTINIDE CONCENTRATIONS 5-1

TA-5.1 Further Comparison With the Conceptual Model 5-1

TA-5.2 Surface Water Pathway Analysis 5-1

TA-5.2.1 Mass Balance Methodology Using Measured and Modeled Data 5-1

TA-5.2.2 Uncertainty Analysis 5-7

TA-5.2.3 Lower Walnut Creek Mass Balance Analysis 5-12

TA-5.2.4 A- and B-Series Ponds Mass Balance Analyses 5-21

TA-5.2.5 SID Mass Balance Analysis 5-29

TA-5.2.6 Summary of the Surface Water Pathway Analysis - Using Measured and Modeled Data Combined 5-37

TA-5.3 GroundWater Pathway Analysis 5-39

TA-5.3.1 Introduction 5-39

TA-5.3.2 Description of Methodology to Calculate Shallow Groundwater Actinide Transport 5-40

TA-5.3.3 Estimated Actinide Transport Off-Site 5-41

TA-5.3.4 Summary of the Shallow Groundwater Pathway Analysis 5-42

TA-5.4 Air Pathway Analysis 5-43

TA-5.4.1 Emission Estimation 5-43

TA-5.4.2 Modeling Methods 5-49

TA-5.4.3 Calculation of Off-Site Transport 5-51

TA-5.4.4 Air Pathway Analysis – Modeled Data 5-51

TA-5.5 Biological Pathway Analysis 5-52

TA-5.5.1 Introduction 5-52

TA-5.5.2 Calculation Methodology 5-52

TA-5.5.3 Estimated Actinide Transport Off-Site 5-53

TA-5.5.4 Summary of Biological Pathway Analysis—Modeled Data 5-54

TA-5.6 Technical Appendix Section TA-5 References 5-55

SECTION TA-5 TABLES

Table TA-5-1. Input and Output Variables Used in Water Balance for Each Study Area 5-5

Table TA-5-2. Shallow Groundwater Well Results Used for Mass Balance Analyses 5-6

Table TA-5-3. Lower Walnut Creek, Pu Mass Balance Results –
Measured and Modeled Data Combined, Average for Water Years 1997 - 1999 5-12

Table TA-5-4. Summary of Lower Walnut Creek Pu Loading Analysis 5-13

Table TA-5-5. Uncertainty Analysis Summary – Lower Walnut Creek Pu Mass Balance 5-14

Table TA-5-6. Lower Walnut Creek, U-238 Mass Balance Results –
Measured and Modeled Data Combined, Average for Water Years 1997 - 1999 5-17

Table TA-5-7. Summary of Lower Walnut Creek U-238 Loading Analysis 5-18

Table TA-5-8. Uncertainty Analysis Summary –
Lower Walnut Creek U-238 Mass Balance 5-19

Table TA-5-9. A- and B-Series Ponds, Pu Mass Balance Results –
Measured and Modeled Data Combined, Average for Water Years 1997 – 1999 5-21

Table TA-5-10. Summary of A- and B-Series Ponds Pu Loading Analysis 5-22

Table TA-5-11. Uncertainty Analysis Summary –
A- and B-Series Ponds Pu Mass Balance 5-23

Table TA-5-12. A- and B-Series Ponds, U-238 Mass Balance Results –
Measured and Modeled Data Combined, Average for Water Years 1997 – 1999 5-25

Table TA-5-13. Summary of A- and B-Series Ponds U-238 Loading Analysis 5-26

Table TA-5-14. Uncertainty Analysis Summary –
A- and B-Series Ponds U-238 Mass Balance 5-27

Table TA-5-15. SID, Pu Mass Balance Results –
Measured and Modeled Data Combined, Average for Water Years 1997 – 1999 5-29

Table TA-5-16. Summary of SID Pu Loading Analysis 5-30

523

Table TA-5-17. Uncertainty Analysis Summary – SID Pu Mass Balance 5-31
Table TA-5-18. SID, U-238 Mass Balance Results –
Measured and Modeled Data Combined, Average for Water Years 1997 – 1999 5-33
Table TA-5-19. Summary of SID U-238 Loading Analysis 5-34
Table TA-5-20. Uncertainty Analysis Summary –
SID U-238 Mass Balance 5-35
Table TA-5-21. Model-Estimated Shallow Groundwater Off-Site Flux for the
Walnut Creek and Woman Creek Groundwater Basins 5-40
Table TA-5-22. Shallow Groundwater Actinide Activities 5-41
Table TA-5-23. Particle Size Distribution Data Used for Dispersion Modeling 5-50
Table TA-5-24. Results of Air Pathway Analysis ISCST3 Modeling 5-52
Table TA-5-25. Biological Off-Site Actinide Transport 5-54

SECTION TA-5 FIGURES

Figure TA-5-1. Lower Walnut Creek, Pu Loading Profile –
Measured and Modeled Data Combined 5-59
Figure TA-5-2. Lower Walnut Creek, Pu Mass Balance Uncertainty Analysis 5-59
Figure TA-5-3. Lower Walnut Creek, Pu Analysis Figure 5-60
Figure TA-5-4. Lower Walnut Creek, U-238 Loading Profile –
Measured and Modeled Data Combined 5-61
Figure TA-5-5. Lower Walnut Creek, U-238 Mass Balance Uncertainty 5-61
Figure TA-5-6. Lower Walnut Creek, U-238 Analysis Figure 5-62
Figure TA-5-7. A- and B-Series Ponds, Pu Loading Profile
Measured and Modeled Data Combined 5-63
Figure TA-5-8. A- and B-Series Ponds, Pu Mass Balance Uncertainty 5-63
Figure TA-5-9. A- and B-Series Ponds, Pu Analysis Figure 5-64
Figure TA-5-10. A- and B-Series Ponds, U-238 Loading Profile Measured and
Modeled Data Combined 5-65

524

Figure TA-5-11. A- and B-Series Ponds, U-238 Mass Balance Uncertainty 5-65
Figure TA-5-12. A- and B-Series Ponds, U-238 Analysis Figure 5-66
Figure TA-5-13. SID, Pu Loading Profile –
Measured and Modeled Data Combined 5-67
Figure TA-5-14. SID, Pu Mass Balance Uncertainty 5-67
Figure TA-5-15. SID, Pu-239/240 Analysis Figure 5-68
Figure TA-5-16. SID, U-238 Loading Profile Measured and
Modeled Data Combined 5-69
Figure TA-5-17. SID, U-238 Mass Balance Uncertainty 5-69
Figure TA-5-18. SID, U-238 Analysis Figure 5-70
Figure TA-5-19. Shallow Groundwater Off-Site Actinide Load 5-71
Figure TA-5-20. Pu-239 Surface Soil Isopleths for Air Model 5-72
Figure TA-5-21. Am-241 Surface Soil Isopleths for Air Model 5-73
Figure TA-5-22. U-233/234 Surface Soil Isopleths for Air Model 5-74
Figure TA-5-23. U-235 Surface Soil Isopleths for Air Model 5-75
Figure TA-5-24. U-238 Surface Soil Isopleths for Air Model 5-76
Figure TA-5-25. Biological Model Method 1 Results 5-77
Figure TA-5-26. Biological Model Method 2 Results 5-77

525

TA-5 ACTINIDE TRANSPORT PATHWAYS ANALYSIS - BASED ON MEASURED AND MODELED RFETS ACTINIDE CONCENTRATIONS

TA-5.1 FURTHER COMPARISON WITH THE CONCEPTUAL MODEL

In Section TA-4, measured data were used to verify the relative importance of different transport pathways, for different actinides, presented in the conceptual model. Measured values, versus model results, are the preferred data source for such a comparison. However, not all of the actinide transport terms of the conceptual model can be measured or have measured data available, to permit this type of verification. Examples of terms from the conceptual model without available measured data include airborne deposition and transport, shallow groundwater transport and overland transport caused by hillslope erosion. Modeled data are introduced in this section to provide quantified estimates of specific unmeasured transport pathways, thereby allowing further verification of the conceptual model than could be accomplished using measured data alone.

TA-5.2 SURFACE WATER PATHWAY ANALYSIS

TA-5.2.1 Mass Balance Methodology Using Measured and Modeled Data

Surface water pathway study areas in this section are identical to those analyzed in Section TA-4, where only measured data were discussed. Modeled estimates for actinide transport to surface water were developed for hillslope erosion (for Pu), airborne deposition of actinides on to surface water and shallow groundwater recharge and discharge. The measured data presented in this section, for reference, are the same data presented in Section TA-4. Sources of modeled data presented in this section are discussed below.

Modeled Data Sources

Hillslope Erosion to Surface Water

A hillslope erosion model was used to estimate the water volume and quantity of Pu-239/240 running off hillslopes that do not flow to one of the tributary channels monitored by Site gaging

stations. The Water Erosion Prediction Project (WEPP) model has been calibrated to Site conditions to estimate erosion from overland flow processes (RMRS, 2000). Details about the modeling techniques are documented in the *Report on Soil Erosion and Surface-Water Sediment Transport for the Actinide Migration Evaluation at the RFETS* (RMRS, 2000). The model application and calibration for RFETS were reviewed and approved by Dr. Leonard Lane, a nationally recognized authority on erosion and use of the WEPP model (RMRS, 2000). The WEPP model and its application to the mass balances are discussed below.

Predicted hillslope erosion rates from WEPP output are distributed spatially on a grid for each hillslope using a Triangular Integrated Networks (TIN) technique. The resulting erosion grid is mapped using Geographic Information Systems (GIS) software and is overlaid with kriged Pu-239/240 surface soil grids (see Section TA-2). The erosion and Pu-239/240 surface soil grids are combined to create Pu-239/240 mobility maps that predict where Pu-239/240 movement will occur due to overland runoff and erosion processes. The actinide mobility grid is used in a subsequent algorithm using a GIS program to estimate quantities of Pu-239/240 delivered to stream channels at the bottoms of the hillslopes. Calibrated model output for estimated runoff and sediment yields are considered accurate to within one order of magnitude for the Site hillslopes (RMRS, 2000).

For the mass balance analyses in this section, the WEPP model was used in the continuous simulation mode for the calendar year 1997-1999 period, using climate data from the Site's 61-meter meteorological tower. WEPP output was processed for the three surface water pathway study areas. Erosion and actinide mobility grids were created for the three-year average annual erosion for the 1997-1999 period. Annual Pu-239/240 loads delivered to the channels were calculated by using WEPP-predicted annual runoff values to calculate a runoff-weighted annual Pu-239/240 load for each hillslope for Water Years 1997 through 1999.

An acknowledged shortcoming of the RFETS erosion and sediment transport model is that it does not account for channel erosion or sediment resuspension. The model is being expanded in 2001 to account for these processes, though these changes were not incorporated into the model used to estimate erosion rates for this report.

527

Air Deposition on Surface Water

Transport of airborne particulate matter with associated actinides was modeled to estimate loads of Pu-239/240 and U-238 deposited on the water surface in channels and ponds in the different study areas. Site wind data from 1997 through 1999 were used in conjunction with measured airborne actinide concentrations to estimate the airborne deposition loads to surface water. A brief summary of the air transport model is provided below.

The ISCST3 Version 98356 model was used to perform refined dispersion and deposition modeling for the air pathway study. ISCST3 is described in detail in the User's Guide for the Industrial Source Complex (ISC3) Dispersion Models, Volumes I and II (EPA, 1995a).

The ISCST3 model was developed and is supported by EPA to predict air concentrations and deposition resulting from multiple source types, including stacks, areas of fugitive emissions, equipment operation and open pits. This is an essential feature for simulating the types of activities that the actinide migration study is most concerned. ISCST3 is a Gaussian plume model, where plume spread in both the vertical and horizontal dimensions can be represented by a Gaussian (i.e., bell-shaped) distribution of pollutant mass. The plume spread depends on distance downwind from the release area (source) and various meteorological factors such as wind speed and stability. The time resolution in the short-term model is one hour and averaging periods up to several years can be calculated. The model is suitable for calculating concentration or deposition in simple to somewhat complex terrain at distances up to 50 km from the source (Radian, 1999).

Gaussian plume models, in general, offer a trade-off between precision and ease of use. The model inputs, including meteorological data, are generally available and the model set up can be easily modified to simulate different scenarios. However, the results may be considered to have an uncertainty that ranges from a factor of two to over an order of magnitude (EPA, 1995b). Longer-term averages (i.e., annual) have less uncertainty than short-term results (i.e., 1 hour) and patterns of concentration/deposition are more reliable than a single-point prediction. The large uncertainty with this type of model is recognized in the uncertainty analysis presented for each mass balance calculation.

528

Shallow Groundwater Loads to and from Surface Water

The actinide load from shallow groundwater conveyed to surface water or, in the case of a losing reach, from surface water to shallow groundwater, was estimated for each study area. Natural waters typically contain suspended colloids, sub-micron-sized particles formed as a result of the weathering of rocks, plants and soils. Colloids are of concern in terms of shallow groundwater actinide transport because radionuclides can sorb strongly to the suspended tuff colloids and form actinide-bearing pseudocolloids that can move via the shallow groundwater pathway (Eckhardt et al, 2000).

Estimation of the shallow groundwater load interactions with surface water involved calculating: 1) the water balance for each study area, in order to estimate shallow groundwater contributions to each reach; and 2) the average actinide concentration in each study area. Methodologies for estimating these variables are described below.

Water Balance

Estimating the shallow groundwater yield to surface water or the surface water recharge to shallow groundwater for each study area involved subtracting the input water yields from the output water yields as shown in Equation (1).

$$SGW = (YIELD_{OUT} + EVAP + STOR) - (YIELD_{IN} + TRIB_{IN} + HILL_{IN} + TRANS_{IN}) \quad (1)$$

where:

SGW:	Shallow groundwater yield to surface water (+); Recharge to shallow groundwater (-);
$YIELD_{OUT}$:	Surface water yield output;
EVAP:	Evaporative losses (applied to study area with ponds);
STOR:	Change in pond volume storage (+ equals increased storage);
$YIELD_{IN}$:	Surface water yield input;
$TRIB_{IN}$:	Tributary surface water yield input;

529

$HILL_{IN}$: Hillslope water yield input (from WEPP model); and

$TRANS_{IN}$: Transfer of water from the other drainages to the A-Series ponds (transfers of Landfill Pond water to Pond A-3, for example).

Data sources for each of the variables in Equation 1 are shown in Table TA-5-1.

Table TA-5-1. Input and Output Variables Used in Water Balance for Each Study Area

Water Yield Input / Output	Variable	Data Source (Measured or Modeled)
Input	Channel Inflow	Surface Water Monitoring Network (Measured)
	Tributary Inflow	Surface Water Monitoring Network (Measured)
	Hillslope Runoff (Not captured by tributary)	WEPP Runoff / Erosion Model (Model)
	Pond Storage Volume – Net Decrease Over Time	Archived RFETS Pond Level Data and Stage/Storage Relationships (Model)
	Pond Transfers (Pond study area only)	Archived RFETS pond transfer volume data
Output	Evaporation (Pond study area only)	RMRS 1999 Evaporation Study (Model)
	Pond Storage Volume – Net Increase Over Time	Archived RFETS Pond Level Data and Stage/Storage Relationships (Model)

Shallow Groundwater Quality

Shallow groundwater wells selected to be representative of shallow groundwater quality in each study area were reviewed with Site personnel knowledgeable in RFETS shallow groundwater and well characteristics. Wells used to evaluate shallow groundwater actinide concentrations were: 1) alluvial wells in connection with surface water; or 2) wells in outcropping sandstone formations that issue shallow groundwater to the surface. Shallow groundwater wells used and actinide data from Water Years 1997 through 1999 are presented in Table TA-5-2.

530

Table TA-5-2. Shallow Groundwater Well Results Used for Mass Balance Analyses

Channel Reach	Well #	Location Description	Time Sampled (Mean or only result in gray)	Analytical Results (pCi/L) Pu-239/240	Am-241	U-233/234	U-235	U-238
Lower Walnut Creek	10794	Between No Name & McKay	Mean: 2/96 to 10/96	0.0003	0.0047			
	10894	Between McKay & GS03	Mean: 12/94 to 10/96	0.0157	0.0067	2.6318	0.0916	2.2659
A- and B-Ponds	1786	Between SW093 and A-1	1997/Q4	0.0020	0.0000	35.5000	1.1900	24.8000
			1998/Q2	0.0163	0.0008	40.7418	1.4601	28.6724
			1998/Q4	0.0000	0.0000	33.2000	0.9010	26.6000
			1999/Q2	0.0097	0.0204	33.7918	1.1271	27.4020
			Mean	0.0070	0.0053	35.8084	1.1696	26.8686
	1386	Between well 1786 and A-1	1997/Q4	0.0050	0.0020	9.5700	0.5010	9.4900
			1998/Q2	0.0139	0.0601	8.9367	0.4919	7.0840
			1998/Q4	0.0000	0.0030	7.0100	0.2640	6.9000
			Mean	0.0063	0.0217	8.5056	0.4190	7.8247
	75992	Just upstream from B-1	1997/Q3	0.0000	0.0000	9.7500	0.3960	8.5400
			1997/Q4	0.0370	0.0000	8.2400	0.3680	6.7900
			1998/Q3	0.0000	0.0097	10.4647	0.5046	8.1705
			1999/Q1	0.0070	0.0515	11.6554	0.3646	9.4137
			1999/Q3	0.0099	0.0076	8.4590	0.2955	8.4572
			Mean	0.0108	0.0138	9.7138	0.3857	8.2743
	03991	South of B-4	1997/Q1	0.0002	0.0017	1.884	0.1067	1.324
			1997/Q2	0.0050	0.0000	0.0310	0.0380	0.0460
			1997/Q4	0.0020	0.0020	1.5800	0.0460	1.2000
			Mean	0.0024	0.0012	1.1650	0.0638	0.8567
South Inter. Ditch	6486	500 ft upstream from C-1	1997/Q3	-	-	5.8800	0.1320	4.0600
			1998/Q1	-	-	5.0500	0.1690	3.1600
			1998/Q3	-	-	7.6092	0.3063	4.1884
			Mean	-	-	6.1797	0.2024	3.8028
	23096		1997/Q3	0.0000	0.0130	2.4000	0.1380	2.4800
	6586		1997/Q2	0.009	0.005	2.41	0.148	2.13
			1997/Q4	0.006	0.011	3.49	0.149	3.16
			Mean	0.0075	0.0080	2.9500	0.1485	2.6450
GS10 Basin	75992	Just upstream from GS10	1997/Q3	0.0000	0.0000	9.7500	0.3960	8.5400
			1997/Q4	0.0370	0.0000	8.2400	0.3680	6.7900
			1998/Q3	0.0000	0.0097	10.4647	0.5046	8.1705
			1999/Q1	0.0070	0.0515	11.6554	0.3646	9.4137
			1999/Q3	0.0099	0.0076	8.4590	0.2955	8.4572
			Mean	0.0108	0.0138	9.7138	0.3857	8.2743
	3586	500 ft west of well 75992	1997/Q1	0.0004	0.0031	2.5810	0.1651	1.8080
			1997/Q3	0.0060	0.0110	2.5500	0.0660	2.3900
			Mean	0.0032	0.0070	2.5655	0.1156	2.0990
	22996	N.E. of Bldg. 886	1997/Q2	0.014	0.017	2.61	0.123	1.92

Calculation of Shallow Groundwater Loads

Shallow groundwater actinide loads were calculated for each study area and for each year from Water Year 1997 through 1999. The loads were calculated by multiplying the water balance result by the shallow groundwater well actinide concentration. Channel reaches that gained shallow groundwater gained actinide load. Accordingly, reaches that lost shallow groundwater lost actinide load to the shallow groundwater.

531

TA-5.2.2 Uncertainty Analysis

Mass Balance Uncertainty

There is considerable uncertainty associated with the quantification of the concentration and mobility of trace constituents in the environment, largely due to sampling and monitoring techniques and the limitations of chemical analysis methods and instruments. The mass balance analysis in this report is based on two fundamental components for each media: 1) the quantity of actinide in the soil, air and water; and 2) the rate of movement of the actinide bearing material in each media. There is an amount of quantifiable uncertainty associated with the measurement of each of these components, but there are also elements of uncertainty which are known to exist but are very difficult to quantify.

Uncertainty Based on Measured Data

Accurate surface-water flow measurement largely depends upon the type and condition of flow-measurement devices such as flumes and weirs, which have an inherent uncertainty of between 5 to 10 % (USBR, 1998). Additional error is associated with continuous measurement of water level (stage) in the device using an electronic flow meter (Grant and Dawson, 1995). For this analysis, a standard 10 % error was conservatively applied to the flow measurement data and this error was assumed one standard deviation from the true flow. Therefore, the square root of the error term is the variance for the number of liters of measured stream flow. The example given below illustrates how the error terms are calculated for the flow component of the actinide load estimates.

The actinide water samples are analyzed by alpha spectrometry for Pu, Am and U isotopes and each analysis is reported with a counting error term that is based on background radiation hitting the detector, detector efficiency and other factors. Data analysis indicates higher counting errors are typically associated with lower actinide concentrations. In other words, the uncertainty in the radiochemical analyses decreases when there is more radionuclide present to detect.

The counting error is based on the Poisson distribution, which is commonly used for counted data, such as the number of disintegrations of actinide atoms per unit time (Iman and Conover, 1983 and

532

Kaiser Hill, 2000). The counting errors reported with the analytical results are two standard deviations (2σ error) from the mean background activity. For this analysis, the 2σ error for each sample analysis was divided by two to obtain the standard deviation (1σ error) for the radiochemical analysis.

Example:

Consider a Pu-239/240 analysis with a result of 0.05 pCi/L and a 2σ error = +/- 0.04 pCi/L collected over a flow of 26,520 m^3 (87,008 cubic feet).

Example Flow Measurement:

$$87{,}008\ ft^3 = 2{,}464{,}067\ Liters$$

$$Error = Ten\ percent\ of\ flow$$

$$= 0.10 \times 2{,}464{,}067\ Liters$$

$$= 246{,}407\ Liters$$

From the radiochemical analysis:

$$2\sigma\ error = 0.04$$

$$1\sigma\ error = 0.02$$

Next, compute the actinide load by multiplying the flow by the actinide concentration as follows.

$$Pu\ Load = 0.05\ pCi/L \times 2{,}464{,}067\ Liters = 123{,}203\ pCi$$

The 1σ error is converted to a percentage of the analytical result to obtain the relative standard deviation for the analysis.

533

$$\textit{Analytical Relative Standard Deviation (\%)} = (1\sigma \textit{ error / result}) \times 100$$

$$\textit{Per the example:} \quad (0.04/0.05) \times 100 = 80\%$$

The 1σ error for the flow measurement is 10 %. Because the flow is multiplied by the concentration to obtain the load, the standard deviation of the estimate is calculated as follows (Skoog and West, 1980).

$$\textit{Load Relative Standard Deviation} = ((\textit{Flow Relative Std. Dev.})^2 + (\textit{Analytical Relative Std. Dev.})^2)^{0.5}$$

Per the example: $\textit{Load Relative Standard Deviation} = ((0.10)^2 + (0.80)^2)^{0.5} = 0.81$

The absolute load standard deviation is computed by multiplying the load relative standard deviation by the load as follows.

$$\textit{Absolute Standard Deviation} = (\textit{Pu Load}) \times (\textit{Load Relative Standard Deviation})$$

Thus per the example: $\textit{Absolute Standard Deviation} = 123{,}203 \text{ pCi} \times (0.81) = 99{,}794 \text{ pCi}.$

Squaring the absolute standard deviation gives the variance:

$$var_1 = (99{,}794 \text{ pCi})^2 = 9{,}958{,}928{,}259 \text{ pCi}^2$$

This example shows how the variance for a single measured actinide load is computed. To obtain the annual average standard deviation on the average annual load, the square root of the sum of the variances is computed for all of the measurements in a water year.

$$\textit{Annual Average Standard Deviation} = (\Sigma(var_1, var_2, \ldots var_n))^{0.5}$$

Finally, the coefficient of variation (C.V.) is computed by dividing the annual average standard deviation by the annual mean load and converted to a percentage as shown.

$$C.V._{annual}\,(\%) = (\textit{Annual Mean Load (pCi)} / \textit{Annual Average Standard Deviation (pCi)}) \times 100$$

534

This methodology was used to estimate the uncertainties associated with the measured annual Pu and U-238 loads in the Walnut Creek and SID study reaches. Lower Walnut Creek uncertainty analysis results are shown in Table TA-5-5 and Table TA-5-8 for Pu and U-238, respectively. The A- and B-Series ponds uncertainty analysis results are shown in Table TA-5-11 and Table TA-5-17 for Pu and U-238, respectively. Finally, SID uncertainty analysis results are shown in Table TA-5-17 and Table TA-5-20 for Pu and U-238, respectively. The results of the analysis indicate that the coefficients of variation for estimation of actinide loads at surface-water gaging and sampling stations ranges from less than 10 % to as high as 2,528 %.

Estimated Uncertainty for Models

Modeled results were also used to evaluate the actinide mass balance, but quantification of the uncertainty of the modeled results is not as straight forward. The erosion / sediment transport and air transport models estimate actinide movement believed to be accurate within an order of magnitude (factor of 10 or 1,000 %). The runoff quantities estimated by the erosion and sediment transport models are believed to be accurate to within 0.5 orders of magnitude (factor of 5 or 500 %). The uncertainties of the models are based on comparison of predicted results with measured data.

The shallow groundwater component of the mass balance was estimated by computing a flow mass balance between the gaging stations per the flow records measured at each station. Therefore, the uncertainty associated with the shallow groundwater flow was estimated by computing the sum of squared standard deviations for flow for each gaging station in each study reach. The uncertainty associated with the actinide transport in shallow groundwater is computed as follows.

Shallow Groundwater Loading Uncertainty =

$$((\textit{Relative Flow Standard Deviation})^2 + (\textit{Relative Load Standard Deviantion})^2)^{0.5}$$

For this analysis, the 2σ errors for each analysis were not available in the shallow groundwater data set. Therefore, the standard deviations for station GS11 were assumed to be representative for the shallow groundwater load because of the low concentrations at GS11, which are similar to the

535

shallow groundwater concentrations. The volume-weighted average relative analytical standard deviation at GS11 is approximately 62 % for Pu and 14 % for U-238. Similar assumptions were made when data were not available for quantifying the uncertainty of the loading estimates for other selected gaging stations. These assumptions are noted at the bottom of the tables quantifying uncertainty for the different surface water study areas.

Qualitative Uncertainties

There are many sources of uncertainty in the monitoring data and models that can be identified, but not necessarily quantified. Sources of error are associated with sampling methodology, sample preparation and sample analysis, to name a few.

For example, surface-water samples collected for actinide analysis are obtained using automatic water samplers with fixed-position intakes in the streams. The fixed position in the water column might not accurately represent average water-quality conditions, especially for high flows. This sampling uncertainty has not been quantified for Site water monitoring stations. However, the AME intends to estimate this element of sampling error through data collection in 2001.

Another example of uncertainty is in sample preparation. The sample preparation protocols can introduce uncertainty due to the particulate nature of actinides in the environment. In the field, composite water samples are collected in 15 to 22-Liter plastic containers (carboys), but only four liters are containerized for radiochemical analysis. The water is acidified and homogenized as much as possible in the carboys before pouring off the four liters, but particle-associated actinides are likely not always dissolved by the acid nor appropriately homogenized and represented in the water samples submitted for analysis.

There are no standard methods for radiochemical analysis that ensure comparable results from different laboratories. Each lab has slightly different methods of sample preparation and analysis and thus introduces uncertainty that is not quantified.

530

TA-5.2.3 Lower Walnut Creek Mass Balance Analysis

Lower Walnut Creek Pu Mass Balance

Results from the Pu mass balance analysis for lower Walnut Creek, using measured and modeled data combined for Water Years 1997 through 1999, are presented in Table TA-5-3. The data represent average annual Pu loads in Water Years 1997 through 1999 for all input and output loads measured or estimated for the study area. Net gain or loss in the outflow load compared to inflow load is presented at the bottom of the table.

Table TA-5-3. Lower Walnut Creek, Pu Mass Balance Results – Measured and Modeled Data Combined, Average for Water Years 1997 - 1999

Pu-239/240 Inputs

Measured Inputs

Input	Description	Load (pCi)
GS11	Pond A-4 Out	2.5E+06
GS08	Pond B-5 Out	6.9E+06
GS33	Tributary	3.7E+05
GS35	Tributary	7.8E+05
GS41	Tributary	9.2E+03
	Subtotal	1.1E+07

Modeled Inputs

Hill Erosion	Diffuse Input	4.3E+05
Air Depo.	Diffuse Input	3.5E+03
	Subtotal	4.3E+05
	Total Inputs	1.1E+07

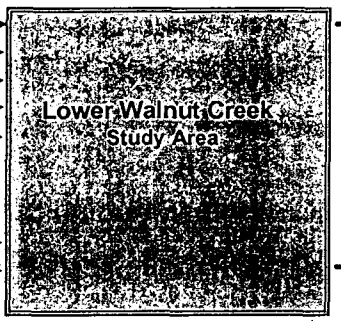

Pu-239/240 Outputs

Measured Outputs

Input	Description	Load (pCi)
GS03	Walnut Ck	1.4E+07
	Subtotal	1.4E+07

Modeled Outputs

Groundwater	Diffuse Output	1.8E+05
	Subtotal	1.8E+05
	Total Outputs	1.4E+07

Gain (+) or Loss (-) of Pu in Study Area

Variables	Delta (pCi)	Change from Input Load	Remarks
Measured Data Only (Out - In)	3.4E+06	32%	Approx. 30% gain in Pu load
Measured + Modeled (Out - In)	3.2E+06	29%	Approx. 30% gain in Pu load

Table TA-5-4 contains summary information for each of the input and output loads, measured and modeled, in this mass balance analysis. Information includes sub-basin characteristics including size, percent impervious surface, average annual water yield, average surface water concentration of Pu, annual Pu load, the fraction that each load represents of the total input or output and the Pu

537

load delivered per square meter of the drainage basin. The same characteristics are presented for the modeled hillslope erosion. Modeled Pu loads conveyed by air deposition and shallow groundwater transport are also included in Table TA-5-4 for comparison purposes.

Table TA-5-4. Summary of Lower Walnut Creek Pu Loading Analysis

Monitoring Location	Basin Description	Sub-Basin Size		Approx. % Impervious	Water Yield (Annual Average)		Pu Concen (Annual Average)	Pu Load (Annual Average)	% of Total Input Load	Pu Yield per Unit Area (Annual Average)
		(Hectares)	(Acres)	(%)	(Liters)	(Acre-Feet)	(pCi/L)	(pCi)	(%)	(pCi/m²-Yr)
Input Loads										
GS11 (Measured)	North Industrial Area Runoff Thru Pond A-4	178.6	441.3	16%	4.0E+08	321.5	0.006	2.5E+06	22.5%	1.4
GS08 (Measured)	South Industrial Area Runoff Thru Pond B-5	105.3	260.2	31%	2.1E+08	170.8	0.033	6.9E+06	63.0%	6.6
GS33 (Measured)	No Name Gulch	99.6	246.2	0%	4.1E+07	33.3	0.009	3.7E+05	3.4%	0.4
GS35 (Measured)	McKay Ditch	225.8	557.9	5%	1.5E+08	119.6	0.005	7.8E+05	7.1%	0.3
GS41 (Measured)	Unnamed tributary south of Walnut Creek	5.5	13.6	0%	4.1E+05	0.3	0.023	9.2E+03	0.1%	0.2
Hill Erosion (Model)	Hillslope runoff (other than measured tribs)	345.9	854.8	2%	2.2E+06	1.8	0.194	4.3E+05	3.9%	0.1
Air Depo. (Model)	N/A	N/A	N/A	N/A	N/A	N/A	N/A	3.5E+03	0.03%	N/A
				Totals	8.0E+08	647.3	N/A	1.1E+07	100%	N/A
Output Loads										
GS03 (Measured)	Entire Walnut Creek watershed	960.7	2374.0	10%	7.8E+08	628.7	0.018	1.4E+07	98.7%	1.5
Groundwater (Model)	N/A	N/A	N/A	N/A	2.3E+07	18.6	0.008	1.8E+05	1.3%	N/A
				Totals	8.0E+08	647.3	-	1.4E+07	100%	-

Pu load data for lower Walnut Creek are plotted by year from Water Year 1997 through 1999 (Figure TA-5-1). Positive values in the bar graphs represent input loads of Pu and negative values represent output loads. This graph provides perspective on the annual variation of loads contributed by different sub-basins.

A summary of the uncertainty analysis for the input and output loads, both measured and modeled, is presented in Table TA-5-5. Plots with error bars reflecting the uncertainty associated with the measured and modeled loads are presented in Figure TA-5-2.

538

Table TA-5-5. Uncertainty Analysis Summary – Lower Walnut Creek Pu Mass Balance

Load	Data Source	Flow Gaging Device	Water Yield (Annual Avg) [Liters]	Water Yield Uncertainty (1 sigma) [Liters]	Pu Load (Annual Avg) [pCi]	Pu Load 1 Std. Dev. [pCi]	Pu Load 2 Std. Dev. [pCi]	Pu Load Lower Range (Load - 1 Std. Dev.) [pCi]	Pu Load Upper Range (Load + 1 Std. Dev.) [pCi]	C.V.
Input Loads										
Surface Water (Measured Loads)	GS11	2' Parshall Flume	4.0E+08	9.9E+06	2.5E+06	5.0E+05	1.0E+06	2.0E+06	3.0E+06	20%
	GS08	2' Parshall Flume	2.1E+08	7.5E+06	6.9E+06	1.4E+06	2.7E+06	5.6E+06	8.3E+06	20%
	GS33	9.5" Parshall Flume	4.1E+07	2.2E+06	3.7E+05	1.8E+05	3.5E+05	2.0E+05	5.5E+05	47%
	GS35	36" contracted rectangular thin-plate weir	1.5E+08	6.9E+06	7.8E+05	4.6E+05	9.3E+05	3.2E+05	1.2E+06	60%
	GS41	0.5' H-Flume	4.1E+05	2.1E+04	9.2E+03	2.6E+03	5.2E+03	6.6E+03	1.2E+04	28%
Erosion (Model)	WEPP/ HEC6T/ Pu Transport Model	N/A	2.2E+06	1.1E+07	3.5E+03	3.5E+04	6.9E+04	0.0E+00	3.8E+04	1000%
Air Deposition (Model)	N/A	N/A	N/A	NA	3.5E+03	3.5E+04	6.9E+04	0.0E+00	3.8E+04	1000%
Output Loads										
Surface Water (Measured Load)	GS03	6" and 36" Parshall Flume	7.8E+08	1.7E+07	1.4E+07	1.9E+06	3.8E+06	1.2E+07	1.6E+07	14%
Groundwater (Model)	Calculated	N/A	2.3E+07	2.5E+07	1.8E+05	2.3E+05	4.6E+05	0.0E+00	4.1E+05	126%

Notes:

The runoff volume uncertainty for erosion model results is 0.5 orders of magnitude and for actinide loads is 1 order of magnitude based on conclusions of AME Erosion and Sediment Transport Modeling Study.

Reference regarding flow measurement uncertainty:

Parshall flumes - Techniques of Water Resources Investigations of the United States Geological Survey. Use of Flumes in Measuring Discharge. Book 3, Chapter A14. p. 13.

Figure TA-5-3 provides a compilation of Pu surface soil and sediment concentrations, actinide source locations, vegetation type, soil type and shallow groundwater potentiometric surface

539

information for the lower Walnut Creek study area. This provides a general reference for the mass balance discussion.

Analysis of Lower Walnut Creek Pu Mass Balance Results

Analysis of measured data only for the lower Walnut Creek Pu mass balance is contained in Section TA-4.3.5. This analysis included discussion of the large load measured at station GS08 in Water year 1999 which was attributed to one flow-paced composite sample collected from June 23, 1999 to August 5, 1999. This sample was 50 times higher than the mean concentration of the other Water Year 1999 samples at that location. No increased Pu loads were observed downstream in Water Year 1999.

The mass balance shows that approximately 4 % of the total Pu input to the reach is estimated to come from erosion caused by overland runoff and 0.03 % is estimated to be caused by airborne deposition of Pu. Losses to shallow groundwater are estimated to account for approximately 2 % of the total Pu load out of the channel reach. Comparison of the measured and modeled Pu load input and output in this reach indicates that roughly one fourth of the average annual load gained in the reach could be accounted for by streambed sediment resuspension and channel erosion.

The hillslope and channel erosion and deposition processes that move the Site's Pu inventory in the soil are an ongoing process. Foster and Hakonson (1984) used modeling techniques and measured data to estimate Pu mobility due to erosion and sediment transport on a broad, regional scale. They concluded that about 9 to 48 % of the originally deposited Pu in U.S. soils will remain after 1,000 years. Accordingly, the soil and streambed erosion process is expected to move Pu through the Site watersheds for a long time. The impacts of hillslope erosion and sediment transport on actinide migration are detailed in the Report on Soil Erosion, Surface-Water Sediment Transport at the RFETS (RMRS, 2000).

The contribution of actinides to surface water by airborne deposition is relatively small compared to other pathways; primarily because the surface area of the stream channels and ponds is small compared to the entire watershed. However, the airborne pathway provides a nearly constant source of actinide transport. Langer showed that Pu concentrations in air just east of the 903 Pad

540

were approximately 20 to 30 times background concentrations during the period 1970-1977, but the time trend mirrored background concentrations that were affected by atmospheric nuclear testing (Langer, 1980). Emission rates for Pu in airborne soil particles are derived in the Air Transport and Deposition of Actinides report (Radian, 2000).

The estimated loss to shallow groundwater, approximately only one percent of the outflow load in this analysis, is more logical for U than for Pu and Am because of the relatively higher solubility of U (see Section TA-3). The shallow groundwater transport process is not as likely to occur for Pu and Am, which are adsorbed to particulate phases. However, Kersting et al. (1999) demonstrated that colloidal Pu can move extended distances in the subsurface and Santschi et al. (1998-2000) showed that approximately 10 % of the Pu in surface water at the Site is in a colloidal form. Therefore, it is realistic to assume that there is some colloidal transport of Pu and Am in Site shallow groundwater associated with the loss of surface water to the alluvial systems.

The biological pathway was not considered in this pathway analysis. Thompson (1975) and Paine (1990) found Pu in multiple vectors in the aquatic system, include fish, crayfish, zooplankton and seston. The annual off-site transport of actinides via this pathway is small and thus not incorporated in predictive models (Whicker, 2000). However, approximately 1×10^{-7} of the Site plutonium inventory is estimated to be redistributed by a major biological vector, mule deer, on an annual basis (Whicker, 1979). More detailed discussion of biological transport mechanisms is provided in Section TA-5.4.

Lower Walnut Creek U-238 Mass Balance

Results from the U-238 mass balance analysis for lower Walnut Creek, using measured and modeled data combined for Water Years 1997 through 1999, are presented in Table TA-5-6. The data represent average annual U-238 loads in Water Years 1997 through 1999 for all input and output loads measured or estimated for the study area. Net gain or loss in the outflow load compared to inflow load is presented at the bottom of the table.

Table TA-5-6. Lower Walnut Creek, U-238 Mass Balance Results – Measured and Modeled Data Combined, Average for Water Years 1997 - 1999

U-238 Inputs

Measured Inputs

Input	Description	Load (pCi)
GS11	Pond A-4 Out	3.8E+08
GS08	Pond B-5 Out	1.8E+08
	Subtotal	5.6E+08

Modeled Inputs

GS33	Tributary	1.3E+08
GS35	Tributary	2.1E+08
GS41	Tributary	5.7E+05
Air Depo.	Diffuse Input	6.6E+04
	Subtotal	3.4E+08
	Total Inputs	8.9E+08

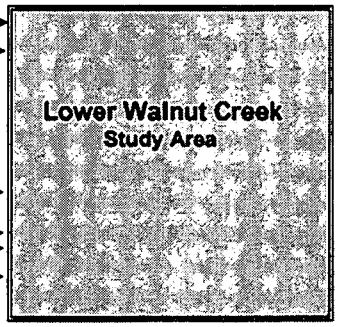

U-238 Outputs

Modeled Outputs

Input	Description	Load (pCi)
GS03	Walnut Ck	6.7E+08
Groundwater	Diffuse Output	5.2E+07
	Subtotal	7.2E+08
	Total Outputs	7.2E+08

Gain (+) or Loss (-) of U-238 in Study Area

Variables	Delta (pCi)	Change from Input Load	Remarks
Measured + Modeled (Out - In)	-1.7E+08	-19%	Approx. 20% removal of U-238 load

Table TA-5-7 contains summary information for each of the input and output loads, measured and modeled, in this mass balance analysis. Information includes sub-basin characteristics including size, percent impervious surface, average annual water yield, average surface water concentration of U-238, annual U-238 load, the fraction that each load represents of the total input or output and the U-238 load delivered per square meter of the drainage basin. The same characteristics are

542

presented for the modeled hillslope erosion. Modeled U-238 loads conveyed by air deposition and shallow groundwater transport are also included in Table TA-5-7 for comparison purposes.

Table TA-5-7. Summary of Lower Walnut Creek U-238 Loading Analysis

Monitoring Location	Basin Description	Sub-Basin Size		Approx. % Impervious	Water Yield (Annual Average)		U-238 Concen. (Annual Average)	U-238 Load (Annual Average)	% of Total Input Load	U-238 Yield per Unit Area (Annual Average)
		(Hectares)	(Acres)	(%)	(Liters)	(Acre-Feet)	(pCi/L)	(pCi)	(%)	(pCi/m^2-Yr)
Input Loads										
GS11 (Measured)	North Industrial Area Runoff Thru Pond A-4	178.6	441.3	16%	4.0E+08	321.5	0.950	3.8E+08	42.1%	210.8
GS08 (Measured)	South Industrial Area Runoff Thru Pond B-5	105.3	260.2	31%	2.1E+08	170.8	0.853	1.8E+08	20.1%	170.6
GS33 (Model)	No Name Gulch	99.6	246.2	0%	4.1E+07	33.3	3.170	1.3E+08	14.6%	130.7
GS35 (Model)	McKay Ditch	225.8	557.9	5%	1.5E+08	119.6	1.400	2.1E+08	23.1%	91.5
GS41 (Model)	Unnamed tributary south of Walnut Creek	5.5	13.6	0%	4.1E+05	0.3	1.400	5.7E+05	0.1%	10.4
Air Depo. (Model)	N/A	N/A	N/A	N/A	N/A	N/A	N/A	6.6E+04	0.01%	N/A
				Totals	8.0E+08	645.5	N/A	8.9E+08	100%	N/A
Output Loads										
GS03 (Model)	Entire Walnut Creek watershed	960.7	2374.0	10%	7.8E+08	628.7	0.863	6.7E+08	92.8%	69.6
Groundwater (Model)	N/A	N/A	N/A	N/A	2.3E+07	18.6	2.252	5.2E+07	7.2%	N/A
				Totals	8.0E+08	647.3	-	7.2E+08	100%	-

U-238 load data for lower Walnut Creek are plotted by year from Water Year 1997 through 1999 (Figure TA-5-4). Positive values in the bar graphs represent input loads of U-238 and negative values represent output loads. This graph provides perspective on the annual variation of loads contributed by different sub-basins.

A summary of the uncertainty analysis for the input and output loads, both measured and modeled, is presented in Table TA-5-8. Plots with error bars reflecting the uncertainty associated with the measured and modeled loads are presented in Figure TA-5-5.

543

Table TA-5-8. Uncertainty Analysis Summary – Lower Walnut Creek U-238 Mass Balance

Load	Data Source	Flow Gaging Device	Water Yield (Annual Avg) [Liters]	Water Yield Uncertainty (1 sigma) [Liters]	U-238 Load (Annual Avg) [pCi]	U-238 Load 1 Std. Dev. [pCi]	U-238 Load 2 Std. Dev. [pCi]	U-238 Load Lower Range (Load - 1 Std. Dev.) [pCi]	U-238 Load Upper Range (Load + 1 Std. Dev.) [pCi]	C.V.
Input Loads										
Surface Water (Measured Loads)	GS11	2' Parshall Flume	4.0E+08	9.9E+06	3.8E+08	1.3E+07	2.7E+07	3.6E+08	3.9E+08	4%
	GS08	2' Parshall Flume	2.1E+08	7.5E+06	1.8E+08	1.2E+07	2.3E+07	1.7E+08	1.9E+08	6%
Surface Water (Modeled Loads)	GS33	9.5" Parshall Flume	4.1E+07	2.2E+06	1.3E+08	6.8E+06	1.4E+07	1.2E+08	1.4E+08	5%
	GS35	36" contracted rectangular thin-plate weir	1.5E+08	6.9E+06	2.1E+08	9.5E+06	1.9E+07	2.0E+08	2.2E+08	5%
	GS41	0.5' H-Flume	4.1E+05	2.1E+04	5.7E+05	2.9E+04	5.8E+04	5.4E+05	6.0E+05	5%
Erosion (Model)	WEPP/ HEC6T/ Pu Transport Model	N/A	2.2E+06	1.1E+07	-	-	-	-	-	-
Air Deposition (Model)	N/A	N/A	N/A	NA	6.6E+04	6.6E+05	1.3E+06	0.0E+00	7.3E+05	1000%
Output Loads										
Surface Water (Model)	GS03	6" and 36" Parshall	7.8E+08	1.7E+07	6.7E+08	1.5E+07	3.0E+07	6.5E+08	6.8E+08	2%
Groundwater (Model)	Calculated	N/A	2.3E+07	2.5E+07	5.E+07	5.7E+07	1.1E+08	0.0E+00	1.1E+08	110%

Notes:
The runoff volume uncertainty for erosion model results is 0.5 orders of magnitude and for actinide loads is 1 order of magnitude based on conclusions of AME Erosion and Sediment Transport Modeling Study. Model data not available for U-238 load from hillslope erosion.
Reference regarding flow measurement uncertainty:
Parshall flumes - Techniques of Water Resources Investigations of the United States Geological Survey. Use of Flumes in Measuring Discharge. Book 3, Chapter A14. p. 13.
U-238 not measured at GS33, GS35, GS41. U-238 load at these stations estimated using average concentration from historical sample data multiplied by measured water yield.
U-238 not measured at GS03. U-238 load at GS03 estimate based on volume-weighted concentrations from upstream stations contributing to GS03.
U-238 load uncertainties at GS33, GS35, GS41 and GS03 are estimated to be proportional to flow measurement uncertainty.

Figure TA-5-6 provides a compilation of U-238 surface soil and sediment concentrations, actinide source locations, vegetation type, soil type and shallow groundwater potentiometric surface information for the lower Walnut Creek study area. This provides a general reference for the mass balance discussion.

Analysis of Lower Walnut Creek U-238 Mass Balance Results

In contrast with Pu, which acquires additional load in lower Walnut Creek, the mass balance for U-238 estimates that approximately 20 % of the input U-238 load will "drop out" in the reach. The

544

lack of U-238 data in Water Years 1997 through 1999 made necessary the estimation of U-238 concentrations for the GS33, GS35 and GS41 sub-basins using historic samples from those locations. The estimated concentration of 3.2 pCi/L, based on one sample collected in 1990, is relatively high compared with the consistently measured U-238 concentrations across the Site of approximately 1 to 2 pCi/L. Therefore, the predicted inflow load of U-238 from station GS33 could be overestimated.

The 2.3-pCi/L U-238 concentration in shallow groundwater is based on sample results from two wells in Lower Walnut Creek (Figure TA-5-6). This compares with the mean background concentration of U-238 in alluvial, shallow groundwater of 4.60 pCi/L (RMRS, 1996).

As noted in Section TA-4, the total U concentrations from Water Years 1997 through 1999, at RFETS POE and POC monitoring stations, averaged, after converting activity to mass, approximately 2 to 5 μg/L. This is roughly one order of magnitude less than the recently established 30 μg /L MCL for drinking water.

545

TA-5.2.4 A- and B-Series Ponds Mass Balance Analyses

A- and B-Series Ponds Pu Mass Balance

Results from the Pu mass balance analysis for the A- and B-Series ponds, using measured and modeled data combined for Water Years 1997 through 1999, are presented in Table TA-5-9. The data represent average annual Pu loads in Water Years 1997 through 1999 for all input and output loads measured or estimated for the study area. Net gain or loss in the outflow load compared to inflow load is presented at the bottom of the table.

Table TA-5-9. A- and B-Series Ponds, Pu Mass Balance Results – Measured and Modeled Data Combined, Average for Water Years 1997 – 1999

Pu Inputs

Measured Inputs

Input	Description	Load (pCi)
SW093	N. Walnut In	8.7E+06
GS10	S. Walnut In	2.9E+07
SW091	Tributary	1.7E+05
WWTP	Tributary	1.1E+06
	Subtotal	3.9E+07

Modeled Inputs

Erosion	Diffuse Input	8.2E+06
Groundwater	Diffuse Input	1.2E+05
Air Deposition	Diffuse Input	6.5E+06
	Subtotal	1.5E+07
	Total Inputs	5.4E+07

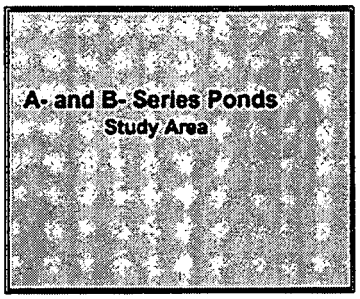

Pu Outputs

Measured Outputs

Input	Description	Load (pCi)
GS11	N. Walnut Out	2.5E+06
GS08	S. Walnut Out	6.9E+06
	Subtotal	9.4E+06
	Total Outputs	9.4E+06

Gain (+) or Loss (-) of Pu in Study Area

Variables	Delta (pCi)	Change from Input	Remarks
Measured Data Only (Out - In)	-2.9E+07	-76%	76% of inflow Pu accumulates
Measured + Modeled (Out - In)	-4.4E+07	-82%	82% of inflow Pu accumulates

Table TA-5-10 contains summary information for each of the input and output loads, measured and modeled, in this mass balance analysis. Information includes sub-basin characteristics including size, percent impervious surface, average annual water yield, average surface water concentration of Pu, annual Pu load, the fraction that each load represents of the total input or output and the Pu load delivered per square meter of the drainage basin. The same characteristics

546

are presented for the modeled hillslope erosion. Modeled Pu loads conveyed by air deposition and shallow groundwater transport are also included in Table TA-5-10 for comparison purposes.

Table TA-5-10. Summary of A- and B-Series Ponds Pu Loading Analysis

Monitoring Location	Basin Description	Sub-Basin Size		Approx. % Impervious	Water Yield (Annual Average)		Pu Concen. (Annual Average)	Pu Load (Annual Average)	% of Total Input Load	Pu Yield per Unit Area (Annual Average)
		(Hectares)	(Acres)	(%)	(Liters)	(Acre-Feet)	(pCi/L)	(pCi)	(%)	(pCi/m²-Yr)
Input Loads										
SW093 (Measured)	North Industrial Area Runoff	98.0	242.3	28%	2.2E+08	178.5	0.040	8.7E+06	16.3%	8.9
GS10 (Measured)	Central Industrial Area Runoff	67.7	167.4	47%	1.5E+08	122.3	0.191	2.9E+07	53.8%	42.5
SW091 (Measured)	Northeast Industrial Area Runoff	4.4	10.8	5%	7.5E+05	0.6	0.226	1.7E+05	0.3%	3.8
WWTP (Measured)	WWTP Treated Effluent to Pond B-3	N/A	N/A	N/A	2.5E+08	205.5	0.004	1.1E+06	2.0%	N/A
Hill Erosion (Model)	Hillslope runoff (other than measured trib)	113.7	281.0	1%	5.1E+06	4.1	1.598	8.2E+06	15.2%	7.2
Groundwater (Model)	N/A	N/A	N/A	N/A	1.2E+07	9.5	0.010	1.2E+05	0.2%	N/A
Air Depo. (Model)	N/A	N/A	N/A	N/A	N/A	N/A	N/A	6.5E+06	12.18%	N/A
				Totals	6.4E+08	520.5	N/A	5.4E+07	100%	N/A
Output Loads										
GS11 (Measured)	North Industrial Area Runoff Thru Pond A-4	178.6	441.3	16%	4.0E+08	321.5	0.006	2.5E+06	26.3%	1.4
GS08 (Measured)	South Industrial Area Runoff Thru Pond B-5	105.3	260.2	31%	2.1E+08	170.8	0.033	6.9E+06	73.7%	6.6
				Totals	6.1E+08	492.2	-	9.4E+06	100%	-

Note: Water yield input does not equal output because of evaporative losses in ponds.

Pu load data for the A- and B-Series ponds are plotted by year from Water Year 1997 through 1999 (Figure TA-5-7). Positive values in the bar graphs represent input loads of Pu and negative values represent output loads. This graph provides perspective on the annual variation of loads contributed by different sub-basins.

A summary of the uncertainty analysis for the input and output loads, both measured and modeled, is presented in Table TA-5-11. Plots with error bars reflecting the uncertainty associated with the measured and modeled loads are presented in Figure TA-5-8.

547

Table TA-5-11. Uncertainty Analysis Summary – A- and B-Series Ponds Pu Mass Balance

Load	Data Source	Flow Gaging Device	Water Yield (Annual Avg) [Liters]	Water Yield Uncertainty (1 sigma) [Liters]	Pu Load (Annual Avg) [pCi]	Pu Load 1 Std. Dev. [pCi]	Pu Load 2 Std. Dev. [pCi]	Pu Load Lower Range (Load - 1 Std. Dev.) [pCi]	Pu Load Upper Range (Load + 1 Std. Dev.) [pCi]	C.V.
Input Loads										
Surface Water (Measured Loads)	SW093	3' Parshall Flume with 3' Rectangular Weir Insert	2.2E+08	4.8E+06	8.7E+06	8.1E+05	1.6E+06	7.9E+06	9.5E+06	9%
	GS10	9" Parshall Flume	1.5E+08	3.2E+06	2.9E+07	1.7E+06	3.4E+06	2.7E+07	3.1E+07	6%
	SW091	6" Cutthroat Flume	7.5E+05	1.8E+05	1.7E+05	1.6E+04	3.2E+04	1.5E+05	1.8E+05	10%
	WWTP*	60° V-notch Weir	2.5E+08	7.4E+06	1.1E+06	1.4E+06	2.7E+06	0.0E+00	2.4E+06	127%
Erosion (Model)**	WEPP/ HEC6T/ Pu Transport Model	N/A	5.1E+06	2.6E+07	8.2E+06	8.2E+07	1.6E+08	0.0E+00	9.0E+07	1000%
Groundwater (Model)	Estimated	N/A	1.2E+07	2.8E+07	1.2E+05	2.9E+05	5.7E+05	0.0E+00	4.1E+05	243%
Air Deposition (Model)	N/A	N/A	N/A	NA	6.5E+06	6.5E+07	1.3E+08	0.0E+00	7.2E+07	1000%
Output Loads										
Surface Water (Measured Loads)	GS11	2' Parshall Flume	4.0E+08	9.9E+04	2.5E+06	5.0E+05	1.0E+06	2.0E+06	3.0E+06	20%
	GS08	2' Parshall Flume	2.1E+08	7.5E+06	6.9E+06	1.4E+06	2.7E+06	5.6E+06	8.3E+06	20%

Notes:
*Uncertainty for Pu load at WWTP is assumed to be equal to uncertainty at GS08
**The runoff volume uncertainty for erosion model results is 0.5 orders of magnitude and for actinide loads is 1 order of magnitude based on conclusions of AME Erosion and Sediment Transport Modeling Study.
Reference regarding flow measurement uncertainty:
Parshall flumes - Techniques of Water Resources Investigations of the United States Geological Survey. Use of Flumes in Measuring Discharge. Book 3, Chapter A14. p. 13.

Figure TA-5-9 provides a compilation of Pu surface soil and sediment concentrations, actinide source locations, vegetation type, soil type and shallow groundwater potentiometric surface information for the ponds study area. This provides a general reference for the mass balance discussion.

548

Analysis of A- and B-Series Ponds Pu Mass Balance Results

The mass balance using measured data only showed Pu removal efficiency in the A- and B-Series ponds of approximately 76 % of the input load. This ratio of inflow load "trapping" and its consistency with historic measurements, is discussed in Section TA-4.3.6.

The increased Pu removal by the ponds in the mass balance analysis using measured and modeled data combined is due to the additional load accounted for in the hillslope erosion, airborne deposition and shallow groundwater models.

Calculation of the Pu mass balance for the A- and B-Series ponds (Figure TA-5-8) shows that about 83 % of the Pu input to the ponds is removed from the surface-water column within the reach. The Pu removal is dominated by physical settling of Pu associated with particles. Santschi et al used measurements of Thorium(IV), as an analogue of Pu(IV), in dissolved, particulate and total fractions of Pond B-5 water to estimate the time, approximately one day, required for a four-valent ion to be sorbed to particulate material and removed from the water (Santschi, 2000). The terminal ponds discharge approximately every 45 to 60 days; allowing ample settling time for settleable solids. However, Santschi et al (2000) also showed that about 10 % of the Pu in Site runoff is associated with colloidal-size particles which will not settle from the water column because they are kept in suspension due to their surface charge and Brownian motion. These findings are consistent with the monitoring data shown in the mass balance.

Air deposition accounts for approximately 12 % of the Pu input to the A- and B-series ponds, which is comparable to the estimated 15 % erosion pathway contribution. Although the air deposition and hillslope erosion models may overestimate by up to one order of magnitude, it is notable that they exceed the estimated tributary surface water load input of 2 %. The airborne transport pathway for Pu in the A- and B-Series ponds is substantial due to the close proximity of the ponds to the Industrial Area and the relatively large surface area of the ponds compared to stream channel surface areas in other reaches. Most of the transport through the reach is driven by surface water runoff from the highly impervious Industrial Area.

549

The mass balance in Figure TA-5-8 shows that this reach is gaining water from the shallow groundwater, which has relatively low Pu concentration (0.01 pCi/L). The estimated shallow groundwater contribution is less than one percent of the Pu to the reach. Whether this quantity of Pu would actually reach the surface water is debatable due to the colloidal nature of Pu in shallow groundwater and the retardation of colloidal material by the interstices of the subsurface.

A- and B-Series Ponds U-238 Mass Balance

Results from the U-238 mass balance analysis for the A- and B-Series ponds, using measured and modeled data combined for Water Years 1997 through 1999, are presented in Table TA-5-12. The data represent average annual U-238 loads in Water Years 1997 through 1999 for all input and output loads measured or estimated for the study area. Net gain or loss in the outflow load compared to inflow load is presented at the bottom of the table.

Table TA-5-12. A- and B-Series Ponds, U-238 Mass Balance Results – Measured and Modeled Data Combined, Average for Water Years 1997 – 1999

U-238 Inputs

Measured Inputs

Input	Description	Load (pCi)
SW093	N. Walnut In	2.6E+08
GS10	S. Walnut In	2.0E+08
SW091	Tributary	1.4E+06
WWTP	Tributary	9.4E+07
	Subtotal	5.6E+08

Modeled Inputs

Groundwate	Diffuse Input	1.9E+08
Air	Diffuse Input	2.7E+06
	Subtotal	2.0E+08

Total Inputs	7.5E+08

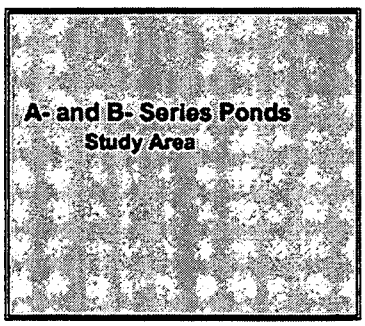

U-238 Outputs

Measured Outputs

Input	Description	Load (pCi)
GS11	N. Walnut Out	3.8E+08
GS08	S. Walnut Out	1.8E+08
	Subtotal	5.6E+08

Total Outputs	5.6E+08

Gain (+) or Loss (-) of U-238 in Study Area

Variables	Delta (pCi)	Change from Input	Remarks
Measured Data (Out - In)	2.9E+05	0.1%	Little change of U-238 in reach
Meas. + Modeled (Out - In)	-2.0E+08	-26%	26% of inflow U-238 accum. in reach

550

Table TA-5-13 contains summary information for each of the input and output loads, measured and modeled, in this mass balance analysis. Information includes sub-basin characteristics including size, percent impervious surface, average annual water yield, average surface water concentration of U-238, annual U-238 load, the fraction that each load represents of the total input or output and the U-238 load delivered per square meter of the drainage basin. The same characteristics are presented for the modeled hillslope erosion. Modeled U-238 loads conveyed by air deposition and shallow groundwater transport are also included in Table TA-5-13 for comparison purposes.

Table TA-5-13. Summary of A- and B-Series Ponds U-238 Loading Analysis

Monitoring Location	Basin Description	Sub-Basin Size		Approx. % Impervious	Water Yield (Annual Average)		U-238 Concen. (Annual Average)	U-238 Load (Annual Average)	% of Total Input Load	U-238 Yield per Unit Area (Annual Average)
		(Hectares)	(Acres)	(%)	(Liters)	(Acre-Feet)	(pCi/L)	(pCi)	(%)	(pCi/m^2-Yr)
Input Loads										
SW093 (Measured)	North Industrial Area Runoff	98.0	242.3	28%	2.2E+08	178.5	1.172	2.6E+08	34.3%	263.2
GS10 (Measured)	Central Industrial Area Runoff	67.7	167.4	47%	1.5E+08	122.3	1.346	2.0E+08	26.9%	299.5
SW091 (Measured)	Northeast Industrial Area Runoff	4.4	10.8	5%	7.5E+05	0.6	1.901	1.4E+06	0.2%	32.4
WWTP (Measured)	WWTP Treated Effluent to Pond B-3	N/A	N/A	N/A	2.5E+08	205.5	0.369	9.4E+07	12.4%	N/A
Groundwater (Model)	N/A	N/A	N/A	N/A	1.2E+07	9.5	16.574	1.9E+08	25.8%	N/A
Air Depo. (Model)	N/A	N/A	N/A	N/A	N/A	N/A	N/A	2.7E+06	0.36%	N/A
				Totals	6.4E+08	516.4	N/A	7.5E+08	100%	N/A
Output Loads										
GS11 (Measured)	North Industrial Area Runoff Thru Pond A-4	178.6	441.3	16%	4.0E+08	321.5	0.950	3.8E+08	67.7%	210.8
GS08 (Measured)	South Industrial Area Runoff Thru Pond B-5	105.3	260.2	31%	2.1E+08	170.8	0.853	1.8E+08	32.3%	170.6
				Totals	6.1E+08	492.2	-	5.6E+08	100%	-

Note: Water yield input does not equal output because of evaporative losses in ponds.

U-238 load data for the A- and B-Series ponds are plotted by year from Water Year 1997 through 1999 (Figure TA-5-10). Positive values in the bar graphs represent input loads of U-238 and

551

negative values represent output loads. This graph provides perspective on the annual variation of loads contributed by different sub-basins.

A summary of the uncertainty analysis for the input and output loads, both measured and modeled, is presented in Table TA-5-14. Plots with error bars reflecting the uncertainty associated with the measured and modeled loads are presented in Figure TA-5-11.

Table TA-5-14. Uncertainty Analysis Summary – A- and B-Series Ponds U-238 Mass Balance

Load	Data Source	Flow Gaging Device	Water Yield (Annual Avg) [Liters]	Water Yield Uncertainty (1 sigma) [Liters]	U-238 Load (Annual Avg) [pCi]	U-238 Load + 1 Std. Dev. [pCi]	U-238 Load + 2 Std. Dev. [pCi]	U-238 Load Lower Range (Load - 1 Std. Dev.) [pCi]	U-238 Load Upper Range (Load + 1 Std. Dev.) [pCi]	CV
Input Loads										
Surface Water (Measured Loads)	SW093	3' Parshall Flume with 3' Rectangular Weir Insert	2.2E+08	4.8E+06	2.6E+08	7.0E+06	1.4E+07	2.5E+08	2.7E+08	3%
	GS10	9" Parshall Flume	1.5E+08	3.2E+06	2.0E+08	5.8E+06	1.2E+07	2.0E+08	2.1E+08	3%
	SW091	6" Cutthroat Flume	7.5E+05	1.8E+05	1.4E+06	1.0E+05	2.1E+05	1.3E+06	1.5E+06	7%
	WWTP	60° V-notch Weir	2.5E+08	7.4E+06	9.4E+07	1.8E+07	3.7E+07	7.5E+07	1.1E+08	20%
Erosion (Model)**	WEPP/ HEC6T/ Pu Transport Model	N/A	5.1E+06	2.6E+07	-	-	-	-	-	-
Groundwater (Model)	Calculated	N/A	1.2E+07	2.8E+07	1.9E+08	4.6E+08	9.2E+08	0.0E+00	6.5E+08	235%
Air Deposition (Model)	N/A	N/A	N/A	NA	2.7E+06	2.7E+07	5.4E+07	0.0E+00	3.0E+07	1000%
Output Loads										
Surface Water	GS11	2' Parshall Flume	4.0E+08	9.9E+04	3.8E+08	1.3E+07	2.7E+07	3.6E+08	3.9E+08	4%
	GS08	2' Parshall Flume	2.1E+08	7.5E+06	1.8E+08	1.2E+07	2.3E+07	1.7E+08	1.9E+08	6%

Notes:
**The runoff volume uncertainty for erosion model results is 0.5 orders of magnitude and for actinide loads is 1 order of magnitude based on conclusions of AME Erosion and Sediment Transport Modeling Study. Model data not available for U-238 load from hillslope erosion.
Reference regarding flow measurement uncertainty:
Parshall flumes - Techniques of Water Resources Investigations of the United States Geological Survey. Use of Flumes in Measuring Discharge. Book 3, Chapter A14. p. 13.

552

Figure TA-5-12 provides a compilation of U-238 surface soil and sediment concentrations, actinide source locations, vegetation type, soil type and shallow groundwater potentiometric surface information for the ponds study area. This provides a general reference for the mass balance discussion.

Analysis of A- and B-Series Ponds U-238 Mass Balance Results

The mass balance for U-238 in the A- and B-series ponds (Figure TA-5-11) is markedly different from the balance for Pu, owing to the differences in solubility of these actinides (Section 3). The U-238 mass balance shows that U-238 input and output in surface-water are equal in this reach, but there is U-238 input from shallow groundwater and airborne U-238 contribution to the reach as well. The result of the mass balance is a net 26 % of the U input accumulating in the reach. This result is consistent with the findings of Efurd et al (1993), who concluded that the largest source of anthropogenic radioactivity in the terminal ponds is from depleted U. Efurd et al. further states that approximately half of the U in Ponds A-4 and C-2 and 20 % of the U in Pond B-5 originated as depleted U. Contrasting the U daughter isotopes with the Pu activities in the pond sediments, Efurd et al point out that there is 70 to 450 times more alpha activity resulting from the decay of naturally-occurring Radium (Ra) than alpha activity from Pu.

The mechanisms for the estimated U removal and/or transport retardation in the A- and B- series ponds is not completely understood, but it is well-known that reducing environments can cause the precipitation of U mineral phases (see Section TA-3). Honeyman et al. found that the pond bottom sediments are reducing environments with micro-organisms that can create strongly reducing conditions (Honeyman et al, 1999). Ponds that become stagnant, such as Pond C-2, can thermally stratify and thus create reducing environments at depth in the water column and in bottom sediments (RMRS, 1996). Therefore, there is a strong body of evidence that the ponds are removing U from the water column through reduction of U-VI to U-IV through natural occurring anoxic conditions, which are created and/or enhanced by microorganisms. Settling of particulate U in the ponds is also likely occurring, but data that specifically address this process are difficult to quantify due to the reactive transport of U in water.

TA-5.2.5 SID Mass Balance Analysis

SID Pu Mass Balance

Results from the Pu mass balance analysis for the SID, using measured and modeled data combined for Water Years 1997 through 1999 are presented in Table TA-5-15. The data represent average annual Pu loads in Water Years 1997 through 1999 for all input and output loads measured or estimated for the study area. Net gain or loss in the outflow load compared to inflow load is presented at the bottom of the table.

Table TA-5-15. SID, Pu Mass Balance Results – Measured and Modeled Data Combined, Average for Water Years 1997 – 1999

Pu-239/240 Inputs

Measured Inputs

Input	Description	Load (pCi)
GS42	Tributary	1.3E+05
	Subtotal	1.3E+05

Modeled Inputs

400 Area	Tributary	1.2E+05
600 Area	Tributary	1.0E+05
800 Area	Tributary	2.9E+05
Hill Erosion	Diffuse Input	8.7E+07
Groundwate	Diffuse Input	6.8E+04
Air	Diffuse Input	3.1E+05
	Subtotal	8.8E+07

Total Inputs	8.8E+07

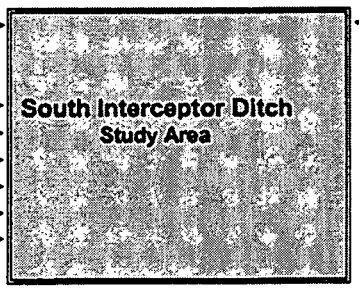

Pu-239/240 Outputs

Measured Outputs

Output	Description	Load (pCi)
SW027	SID Out	3.3E+06
	Subtotal	3.3E+06

Total Outputs	3.3E+06

Gain (+) or Loss (-) of Pu in Study Area

Variables	Delta (pCi)	Change from Input Load	Remarks
Measured Data (Out - In)	3.2E+06	2366%	GS42 Does Not Reflect All Inputs
Measured + Modeled (Out	-8.5E+07	-96%	Majority of eroded Pu accum. in reach

Table TA-5-16 contains summary information for each of the input and output loads, measured and modeled, in this mass balance analysis. Information includes sub-basin characteristics including size, percent impervious surface, average annual water yield, average surface water concentration of Pu, annual Pu load, the fraction that each load represents of the total input or output and the Pu load delivered per square meter of the drainage basin. The same characteristics

554

are presented for the modeled hillslope erosion. Modeled Pu loads conveyed by air deposition and shallow groundwater transport are also included in Table TA-5-16 for comparison purposes.

Table TA-5-16. Summary of SID Pu Loading Analysis

Monitoring Location	Basin Description	Sub-Basin Size		Approx. % Impervious	Water Yield (Annual Average)		Pu Concen. (Annual Average)	Pu Load (Annual Average)	% of Total Input or Output Load	Pu Yield per Unit Area (Annual Average)
		(Hectares)	(Acres)	(%)	(Liters)	(Acre-Feet)	(pCi/L)	(pCi)	(%)	(pCi/m^2-Yr)
Input Loads										
GS42 (Measured)	Tributary runoff to SID (vegetated hillsope)	18.2	45.0	3%	1.2E+05	0.1	1.104	1.3E+05	0.15%	0.7
400 Area (Model)	Indus. Area runoff from 400 Area to SID	7.0	17.2	82%	1.2E+07	9.5	0.010	1.2E+05	0.13%	1.7
600 Area (Model)	Indus. Area runoff from 600 Area to SID	1.3	3.2	46%	3.5E+06	2.8	0.030	1.0E+05	0.12%	7.9
800 Area (Model)	Indus. Area runoff from 800 Area to SID	4.1	10.2	54%	5.5E+06	4.5	0.053	2.9E+05	0.33%	7.0
Hill Erosion (Model)	Hillslope runoff (other than GS42 basin)	56.1	138.6	5%	4.1E+06	3.3	21.240	8.7E+07	98.84%	155.2
Groundwater (Model)	N/A	N/A	N/A	N/A	1.2E+07	9.6	0.006	6.8E+04	0.08%	N/A
Air Depo. (Model)	N/A	N/A	N/A	N/A	N/A	N/A	N/A	3.1E+05	0.4%	N/A
				Totals	3.7E+07	29.9	N/A	8.8E+07	100%	N/A
Output Load										
SW027 (Model)	Entire SID Basin	86.7	214.2	14%	3.7E+07	29.7	0.090	3.3E+06	100.0%	3.8
				Totals	3.7E+07	29.7	N/A	3.3E+06	100%	N/A

Pu load data for the SID are plotted by year from Water Year 1997 through 1999 (Figure TA-5-13). Positive values in the bar graphs represent input loads of Pu and negative values represent output loads. This graph provides perspective on the annual variation of loads contributed by different sub-basins.

A summary of the uncertainty analysis for the input and output loads, both measured and modeled, is presented in Table TA-5-17. Plots with error bars reflecting the uncertainty associated with the measured and modeled loads are presented in Figure TA-5-14.

555

Table TA-5-17. Uncertainty Analysis Summary – SID Pu Mass Balance

Load	Data Source	Flow Gaging Device	Water Yield (Annual Avg) [Liters]	Water Yield Uncertainty (1 sigma) [Liters]	Pu Load (Annual Avg) [pCi]	Pu Load 1 Std. Dev. [pCi]	Pu Load 2 Std. Dev. [pCi]	Pu Load Lower Range (Load - 1 Std. Dev.) [pCi]	Pu Load Upper Range (Load + 1 Std. Dev.) [pCi]	C.V.
Input Loads										
Surface Water (Measured Loads)	GS42	3" Parshall Flume	1.2E+05	8.6E+03	1.3E+05	1.3E+04	2.6E+04	1.2E+05	1.5E+05	10%
Surface Water (Modeled Loads)*	400 Area (Model)*	2' H-Flume	1.2E+07	1.8E+05	1.2E+05	1.6E+04	3.2E+04	1.0E+05	1.3E+05	14%
	600 Area (Model)*	3" Cutthroat Flume	3.5E+06	1.8E+05	1.0E+05	1.6E+04	3.2E+04	8.7E+04	1.2E+05	16%
	800 Area (Model)*	0.5' and 1.0' H-Flumes	5.5E+06	1.8E+05	2.9E+05	1.6E+04	3.2E+04	2.7E+05	3.1E+05	6%
Erosion (Model)**	Hill Erosion (Model)	N/A	4.1E+06	2.1E+07	8.7E+07	8.7E+08	1.7E+09	0.0E+00	9.6E+08	1000%
Groundwater (Model)	Groundwater (Model)	N/A	1.2E+07	2.1E+07	6.8E+04	1.2E+05	2.5E+05	0.0E+00	1.9E+05	182%
Air Deposition (Model)	Air Depo. (Model)	N/A	N/A	NA	3.1E+05	3.1E+05	6.2E+05	0.0E+00	6.2E+05	100%
Output Loads										
Surface Water	SW027	Twin, 120° V notch Weirs	3.7E+07	1.3E+06	3.3E+06	3.3E+05	6.5E+05	3.0E+06	3.6E+06	10%

*Flow and Load Uncertainties for 400, 600, and 800 Area runoff is assumed to be the same as calculated for SW091 in Walnut Creek due to drainage similarities.
**The runoff volume uncertainty for erosion model results is 0.5 orders of magnitude and for actinide loads is 1 order of magnitude based on conclusions of AME Erosion and Sediment Transport Modeling Study.
Reference regarding flow measurement uncertainty:
Parshall flumes - Techniques of Water Resources Investigations of the United States Geological Survey. Use of Flumes in Measuring Discharge. Book 3, Chapter A14. p. 13.

Figure TA-5-15 provides a compilation of Pu surface soil and sediment concentrations, actinide source locations, vegetation type, soil type and shallow groundwater potentiometric surface information for the ponds study area. This provides a general reference for the mass balance discussion.

Analysis of SID Pu Mass Balance Results

The mass balance for Pu in the SID watershed provides a good example how Pu transport is retarded by settling of particulates from the water column. The mass balance in Figure TA-5-14 shows that 96 % of the Pu input to the SID is lost from transport in the water column in the SID

556

channel. Only 3 % of the surface-water load can be accounted for by possible movement to the shallow groundwater. Settling of particulate actinides in the SID channel is consistent with the erosion and sediment transport models and the fact that the SID sediments contain about one pCi/g Pu (RMRS, 2000). This SID channel has many sections with abundant marsh vegetation such as cattails, cottonwood and willows, which commonly filter out particles from the surface flow (Walton-Day, 1996) (Figure TA-5-15). The channel has a shallow grade, which slows water velocity and promotes settling. The actinides deposited in the stream channel are available for resuspension by high-flow events such as intense rain storms that cause flooding (Section TA-6).

The estimated soil and stream channel erosion from overland runoff in the SID watershed accounts for about 99 % of the predicted Pu transport in the SID. However, the erosion model uncertainty is estimated to be about one order of magnitude. Only slightly more than one percent of the Pu input to the SID comes from Industrial Area runoff that comes from the 400, 600 and 800 areas. These estimates are based on historic surface water Pu concentrations from samples collected at outfalls for these Industrial Area basins. The estimated Pu load per square meter for the 600 and 800 areas (7.9 and 7.0 pCi/m^2/year), respectively, is consistent with that measured in the northern Industrial Area at SW093, but less than the 42.5 pCi/m^2/year, measured at GS10. The Pu load per square meter for the 400 area (1.7 pCi/m^2/year) is less than that observed for other Industrial Area sub-basins with a relatively high percentage of impervious surface area.

Air deposition of Pu in the SID channel accounts for less than one percent of the Pu input to the SID. Extending the SID Pu mass balance to the outfall of Pond C-2 (i.e. gaging station GS31) indicates that nearly all of the Pu transported in the SID is removed from the surface-water prior to flowing into Woman Creek for normal hydrologic conditions. However, some colloidal Pu is likely discharged from Pond C-2. The particle-size distribution of the Pu in GS31 water has not been measured.

SID U-238 Mass Balance

Results from the U-238 mass balance analysis for the SID, using measured and modeled data combined for Water Years 1997 through 1999 are presented in Table TA-5-18. The data represent

557

average annual U-238 loads in Water Years 1997 through 1999 for all input and output loads measured or estimated for the study area. Net gain or loss in the outflow load compared to inflow load is presented at the bottom of the table.

Table TA-5-18. SID, U-238 Mass Balance Results – Measured and Modeled Data Combined, Average for Water Years 1997 – 1999

U-238 Inputs

Measured Inputs

Input	Description	Load (pCi)
GS42	Tributary	1.1E+05
	Subtotal	1.1E+05

Modeled Inputs

400 Area	Tributary	3.8E+06
600 Area	Tributary	1.6E+06
800 Area	Tributary	2.8E+06
Groundwate	Diffuse Input	4.0E+07
Air	Diffuse Input	1.3E+05
	Subtotal	4.9E+07

Total Inputs	4.9E+07

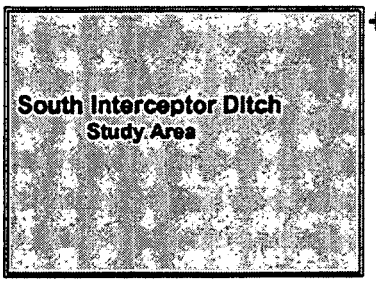

U-238 Outputs

Measured Outputs

Output	Description	Load (pCi)
SW027	SID Out	4.8E+07
	Subtotal	4.8E+07

Total Outputs	4.8E+07

Gain (+) or Loss (-) of Pu in Study Area

Variables	Delta (pCi)	Change from Input Load	Remarks
Measured Data (Out - In)	4.8E+07	43139%	GS42 Does Not Reflect All Inputs
Measured + Modeled (Out - In	-4.8E+05	-1%	Near Balance of Inputs/Outputs

Table TA-5-19 contains summary information for each of the input and output loads, measured and modeled, in this mass balance analysis. Information includes sub-basin characteristics including size, percent impervious surface, average annual water yield, average surface water concentration of U-238, annual U-238 load, the fraction that each load represents of the total input or output and the U-238 load delivered per square meter of the drainage basin. The same characteristics are presented for the modeled hillslope erosion. Modeled U-238 loads conveyed by air deposition and shallow groundwater transport are also included in Table TA-5-19 for comparison purposes.

558

Table TA-5-19. Summary of SID U-238 Loading Analysis

Monitoring Location	Basin Description	Sub-Basin Size		Approx. % Impervious	Water Yield (Annual Average)		U-238 Concen. (Annual Average)	U-238 Load (Annual Average)	% of Total Input Load	U-238 Yield per Unit Area (Annual Average)
		(Hectares)	(Acres)	(%)	(Liters)	(Acre-Feet)	(pCi/L)	(pCi)	(%)	(pCi/m²-Yr)
Input Loads										
GS42 (Measured)	Tributary runoff to SID (vegetated hillsope)	18.2	45.0	3%	1.2E+05	0.1	0.918	1.1E+05	0.23%	0.6
400 Area (Model)	Indus. Area runoff from 400 Area to SID	7.0	17.2	82%	1.2E+07	9.5	0.320	3.8E+06	7.72%	54.1
600 Area (Model)	Indus. Area runoff from 600 Area to SID	1.3	3.2	46%	3.5E+06	2.8	0.450	1.6E+06	3.19%	119.2
800 Area (Model)	Indus. Area runoff from 800 Area to SID	4.1	10.2	54%	5.5E+06	4.5	0.507	2.8E+06	5.75%	67.9
Groundwater (Model)	N/A	N/A	N/A	N/A	1.2E+07	9.6	3.399	4.0E+07	82.85%	N/A
Air Depo. (Model)	N/A	N/A	N/A	N/A	N/A	N/A	N/A	1.3E+05	0.3%	N/A
				Totals	3.3E+07	26.6	N/A	4.9E+07	100%	N/A
Output Load										
SW027 (Model)	Entire SID Basin	86.7	214.2	14%	3.7E+07	29.7	1.318	4.8E+07	100.0%	55.7
				Totals	3.7E+07	29.7	N/A	4.8E+07	100%	N/A

Note: Water yield input does not equal output because the estimated hillslope runoff water volume (input – 0.04E+06 Liters, as shown on Pu loading analysis), is accounted for in the shallow groundwater volume, but the hillslope runoff volume is not shown in this loading analysis. The hillslope erosion model is for Pu and Am only, hence the runoff and load is only shown in the Pu analysis.

U-238 load data for the SID are plotted by year from Water Year 1997 through 1999 (Figure TA-5-16). Positive values in the bar graphs represent input loads of U-238 and negative values represent output loads. This graph provides perspective on the annual variation of loads contributed by different sub-basins.

A summary of the uncertainty analysis for the input and output loads, both measured and modeled, is presented in Table TA-5-20. Plots with error bars reflecting the uncertainty associated with the measured and modeled loads are presented in Figure TA-5-17.

559

Table TA-5-20. Uncertainty Analysis Summary – SID U-238 Mass Balance

Load	Data Source	Flow Gaging Device	Water Yield (Annual Avg) [Liters]	Water Yield Uncertainty (1 sigma) [Liters]	U-238 Load (Annual Avg) [pCi]	U-238 Load 1 Std. Dev. [pCi]	U-238 Load 2 Std. Dev. [pCi]	U-238 Load Lower Range (Load - 1 Std. Dev.) [pCi]	U-238 Load Upper Range (Load + 1 Std. Dev.) [pCi]	C.V.
Input Loads										
Surface Water (Measured Loads)	GS42*	3" Parshall Flume	1.2E+05	8.6E+03	1.E+05	2.E+04	3.5E+04	9.4E+04	1.5E+05	16%
	400 Area (Model)	2' H-Flume	1.2E+07	1.8E+05	3.8E+06	1.0E+05	2.1E+05	3.7E+06	4.0E+06	3%
	600 Area (Model)	3" Cutthroat Flume	3.5E+06	1.8E+05	1.6E+06	1.0E+05	2.1E+05	1.4E+06	1.8E+06	7%
	800 Area (Model)	0.5' and 1.0' H-Flumes	5.5E+06	1.8E+05	2.8E+06	1.0E+05	2.1E+05	2.7E+06	3.0E+06	4%
Erosion (Model)***	Hill Erosion (Model)	N/A	4.1E+06	2.1E+07	-	-	-	-	-	-
Groundwater (Model)	Groundwater (Model)	N/A	1.2E+07	2.1E+07	4.0E+07	6.9E+07	1.4E+08	0.0E+00	1.1E+08	172%
Air Deposition (Model)	Air Depo. (Model)	N/A	N/A	NA	1.3E+05	1.3E+06	2.6E+06	0.0E+00	1.4E+06	1000%
Output Loads										
Surface Water	SW027	Twin, 120° V-notch Weirs	3.7E+07	1.3E+06	5.E+07	3.E+06	5.6E+06	4.5E+07	5.1E+07	6%

Notes:
*Uncertainty for U load at GS42 is assumed to be equal to uncertainty at SW027.
**Flow and Load Uncertainties for 400, 600, and 800 Area runoff is assumed to be the same as calculated for SW091 in Walnut Creek due to drainage similarities.
***The runoff volume uncertainty for erosion model results is 0.5 orders of magnitude and for actinide loads is 1 order of magnitude based on conclusions of AME Erosion and Sediment Transport Modeling Study. Model data not available for U-238 load from hillslope erosion.
Reference regarding flow measurement uncertainty:
Parshall flumes - Techniques of Water Resources Investigations of the United States Geological Survey. Use of Flumes in Measuring Discharge. Book 3, Chapter A14. p. 13.

Figure TA-5-18 provides a compilation of U-238 surface soil and sediment concentrations, actinide source locations, vegetation type, soil type and shallow groundwater potentiometric surface information for the ponds study area. This provides a general reference for the mass balance discussion.

560

Analysis of SID U-238 Mass Balance Results

The U-238 mass balance for the SID basin indicates that input U-238 loads area approximately equal to output loads. The dominant mechanism in this U-238 model, in sharp contrast to the Pu model for the same reach, is shallow groundwater transport. The estimated U-238 concentration of shallow groundwater (3.4 pCi/L) is based on the average of three wells located along the SID (see Table TA-5-2 and Figure TA-5-18). This compares with the estimated mean background concentrations for filtered (4.6 pCi/L) and unfiltered (10.5 pCi/L) alluvial shallow groundwater (RMRS, 1996).

The U-238 surface water loads estimated for the 400, 600 and 800 Areas are based on limited data from samples collected prior to Water Years 1997 to 1999. These limited data have less than half of the U-238 activity observed in the general Site-wide trend from Water Year 1997 through 1999 when U-238 concentrations were approximately one pCi/L. Underestimation of U-238 loads from the southern Industrial Area would partially account for inordinately large percentage of input load from shallow groundwater. Regardless, taking the uncertainties of estimated loads into consideration, the role of shallow groundwater in U transport, when compared with Pu, is substantial.

561

TA-5.2.6 Summary of the Surface Water Pathway Analysis - Using Measured and Modeled Data Combined

Key findings from the mass balances presented in Section TA-5, that utilize a combination of measured and modeled data combined, are summarized in this section. These findings are compared with the pathways qualitatively described in the conceptual model. The measured and modeled data combined indicate an actinide transport pattern that supports the transport mechanisms addressed in the conceptual model, with an exception being modeled airborne transport of Pu to the ponds. Modeled estimates indicate this pathway represents more than a negligible fraction of the input Pu load. This unique case, discussed further below, is counter to the conceptual model, which identifies the air-to-surface water pathway as minor.

- **Deposition of airborne Pu and U to surface water contributes a negligible input to surface water loads in most cases.** Model estimates for the airborne transport of Pu and U-238 to surface water indicate a relatively minor input load, less than one percent of the total, for all actinides in all study areas, with one exception. In the case of the A- and B-Series ponds, the modeled deposition of airborne Pu accounts for 12 % of the total input load. The large surface area of the ponds and the existence of a large source for airborne Pu nearby, the 903 Pad area, causes the ponds to be impacted more by airborne Pu deposition than other surface water channels at the Site.

  In general, the role of airborne transport for Pu, versus U, is made evident by the obvious wind-driven plume of Pu in the surface soil apparent in the kriged surface soil data (Figure TA-2-8).

- **Shallow groundwater is a minor pathway of Pu transport to or from surface water.** The estimated average annual load of Pu conveyed in shallow groundwater comprises one percent or less of the total input or output load for any of the areas studied. The potential for colloidal Pu to be transported in the shallow groundwater is acknowledged and assumed to be the mechanism by which shallow groundwater Pu transport would most likely occur. Shallow

562

groundwater transport of particulate Pu via a sub-surface channel is also recognized as a potential transport mechanism but was not identified in this study.

- **Shallow groundwater is a major pathway of U transport to or from surface water.** Model estimates for U-238 in shallow groundwater ranged from 7 % of the output load in lower Walnut Creek to 83 % of the input load in the SID basin. This is in contrast to shallow groundwater transport of Pu, for which one percent or less of the total input or output load was estimated in all study areas.

- **The Pu transport processes in the area of highest soil contamination are dominated by hillslope erosion and deposition in the SID.** The SID sub-basin has areas, near the 903 Pad, with the highest Pu surface soil contamination at the Site. Model predictions indicate that hillslope erosion accounts for approximately 99 % of the input load to the SID. However, approximately 96 % of the estimated Pu load moved from the hillslopes and tributaries never reaches monitoring station SW027 at the downstream end of the SID. The erosion model overpredicts either the amount of Pu moved off the vegetated hillslopes or the Pu bound to eroded material settles out in the channel. In either case, the net effect is that the measured Pu load delivered per square meter of drainage basin is 3.8 pCi/m^2/year in the SID basin. This is roughly one tenth of the Pu load delivered per square meter delivered to surface water in the central Industrial Area at station GS10.

563

TA-5.3 GROUNDWATER PATHWAY ANALYSIS

TA-5.3.1 Introduction

Shallow groundwater represents another pathway by which actinides can potentially be transported. This study focuses on "shallow" groundwater because geologic conditions at RFETS limit the depth of groundwater potentially impacted by Site contamination. Shallow groundwater refers to water flowing in the Site's alluvium and weathered bedrock geologic units and is found from just below the ground surface to depths of approximately 30 meters (100 feet).

Shallow groundwater and surface water are inextricably linked. Water from stream channels infiltrates downward, recharging the shallow groundwater. Seeps discharge shallow groundwater to the surface. Therefore, it is not surprising that an actinide's solubility, which controls actinide transport in surface water, also dictates actinide transport in shallow groundwater. Insoluble actinides, such as Pu, Am and U in the IV oxidation state, are generally considered to be relatively immobile in the soil and shallow groundwater environment due to their low aqueous solubility and tendency to strongly sorb on soil media (Cleveland et al., 1976 and Honeyman and Santschi, 1997). However, work at RFETS as well as studies in the literature have shown that insoluble actinides can sorb to natural, sub-micrometer sized colloid particles that can potentially facilitate actinide movement (Santschi, 2000). Another transport process similar to surface water involves more soluble actinides, such as U in the VI oxidation state, that can move in solution with the shallow groundwater flow.

Beneath where shallow groundwater flows in the alluvium and weathered bedrock geologic units is a thick, highly impermeable, unweathered bedrock layer that prevents downward groundwater flow. Because the shallow groundwater is prevented from flowing vertically downward, it moves laterally along the unweathered bedrock surface and generally flows from west to east. The shallow groundwater flow is directed toward streams, where it either discharges as baseflow into the stream, evapotranspires to the atmosphere or continues as shallow groundwater flowing downstream within the more permeable valley fill alluvium material just below the ground surface. Below the unweathered bedrock is the regional Laramie-Fox Hills aquifer, approximately 200 to

564

300 meters below the Site. A U.S. Geological Survey study indicates this aquifer will not be impacted by Site activities because of the intervening unweathered bedrock layer, specifically the Laramie Formation, that has claystones with low hydraulic conductivities (Hurr, 1976).

TA-5.3.2 Description of Methodology to Calculate Shallow Groundwater Actinide Transport

Calculating actinide quantities transported off-Site each year in shallow groundwater requires quantifying: 1) the volume or flux, of shallow groundwater flowing off-Site; and 2) concentrations of different actinides in the shallow groundwater. The following sub-sections discuss the methods used to develop estimates for these variables.

Estimation of Shallow Groundwater Flux

The volume of shallow groundwater flowing off-Site or shallow groundwater flux, is calculated using the SWWB model that uses the "Mike SHE" code. This integrated hydrologic model simulates all of the significant hydrologic flow processes including overland flow, channel flow and sub-surface flow in the saturated and unsaturated zones. Lateral shallow groundwater flow off the Site is computed for saturated flow within the unconsolidated alluvial and weathered bedrock material. For actinide transport analysis, off-Site shallow groundwater flux volumes were estimated for Water Year 2000 (from October 1999 through September 2000) for the Walnut Creek and Woman Creek groundwater basins, those most likely impacted by RFETS activities. Model results for estimated shallow groundwater flux, comprising the flow through the alluvial materials and unweathered bedrock, are shown in Table TA-5-21.

Table TA-5-21. Model-Estimated Shallow Groundwater Off-Site Flux for the Walnut Creek and Woman Creek Groundwater Basins

Walnut Creek Model Estimated Groundwater Off-Site Flux (L/year)	Woman Creek Model Estimated Groundwater Off-Site Flux (L/year)	Total (L/year)
5.47×10^6	2.26×10^6	7.73×10^6

565

Shallow Groundwater Actinide Activity

Shallow groundwater actinide measurements, collected from alluvial wells located near where Walnut and Woman Creeks intersect the eastern Site boundary, were used to determine the concentration of actinides in shallow groundwater flowing off the Site. The estimated annual shallow groundwater flux volumes for the Walnut and Woman Creek basins were multiplied by the average shallow groundwater actinide concentrations within each basin to estimate the actinide loads transported off-Site.

Table TA-5-22 provides the mean and the mean 1σ error for two wells from the Walnut Creek groundwater basin and two wells from the Woman Creek groundwater basin.

Table TA-5-22. Shallow Groundwater Actinide Activities

Actinide	Walnut Creek G.W. Basin (Wells 41691 and 0486)		Woman Creek G.W. Basin (Wells 41491 and 0186)	
	Mean (pCi/L)	Mean 1σ Error	Mean (pCi/L)	Mean 1σ Error
Pu239/240	0.035	0.018	0.003	0.004
Am241	0.018	0.011	0.006	0.008
U233/234	1.748	0.522	2.665	0.961
U235	0.101	0.123	0.703	0.393
U238	1.589	0.480	2.037	0.824

TA-5.3.3 Estimated Actinide Transport Off-Site

Shallow groundwater actinide loads transported off-Site in the Walnut and Woman Creek groundwater basins are summarized in Figure TA-5-19.

5646

TA-5.3.4 Summary of the Shallow Groundwater Pathway Analysis

Pu and Am in shallow groundwater. Determination of Pu and Am levels in shallow groundwater at the Site is complicated by residual surface soil contamination potentially introduced down boreholes during drilling and well installation operations. Shallow groundwater samples collected using traditional bailing techniques may suspend these contaminated drilling-artifact soil materials, thereby producing shallow groundwater samples with artificially high Pu or Am concentrations. Because of potential well construction and sampling biases, new clean or "aseptic wells" were drilled and efforts to improve sampling protocols undertaken. This work is currently ongoing. Therefore, Pu and Am concentrations in alluvial wells used in this analysis may represent a "worst case" scenario. Mean Pu activities in alluvial wells at the Site boundary were 0.035 pCi/L (+/- 0.018 pCi/L) in the Walnut Creek groundwater basin and 0.003 pCi/L (+/- 0.004 pCi/L) in the Woman Creek groundwater basin.

U in shallow groundwater. U-233/234 and U-238 isotopes are the dominant actinides found in shallow groundwater in terms of total activity because of their natural abundance in shallow groundwater, particularly in the Rocky Flats region. Though U activity in shallow groundwater at RFETS is within the range of natural levels, shallow groundwater flowing from RFETS can have contributions from anthropogenic (man-made) U sources. Special high resolution analytical techniques, such as ICP/MS, must be utilized to study isotopic ratios in the shallow groundwater and determine whether any of the U in the shallow groundwater has origins from anthropogenic sources. For natural U, the ratio of U-235/U-238, by mass, is approximately 0.0072. A ratio less than 0.0072 indicates the presence of anthropogenic U-238 or "depleted" U, whereas a ratio greater than 0.0072 indicates the presence of anthropogenic U-235 or "enriched" U. Additionally, ICP/MS analysis can detect the presence of U-236, a fission product that is not found in natural U.

Samples collected at Site wells from July 1999 to August 2000 were analyzed using ICP/MS. Most samples analyzed indicate U from natural sources. This is the case for samples collected in the Woman Creek groundwater basin at the Site boundary (RMRS, 2000). However, Walnut Creek basin groundwater samples collected near the Site boundary, though having total U concentrations within the natural range, had a U-235/U-238 mass ratio of 0.006408. This indicates that an

567

anthropogenic "depleted U" source is contributing to the U load in the Walnut Creek groundwater basin. In addition, the same Walnut Creek boundary location had detectable levels of U-236, an isotope that comes only from an anthropogenic U source.

TA-5.4 AIR PATHWAY ANALYSIS

During fiscal years 1999 and 2000 (FY99 and FY00), a Site-specific emission estimating method was developed that allowed calculation of actinide emissions due to resuspension of contaminated soil particles by wind. The estimating method was based on wind speed, size of the contaminated areas and surface soil concentrations of actinides within each contaminated area. A Site-specific implementation of the EPA's Industrial Source Complex Short-Term dispersion and deposition model (ISCST3; EPA 1995b) was developed, which incorporated one year of on-Site meteorological data. The emission estimating technique and model were extensively revised in FY01, based on wind tunnel investigations on the Site in FY00 (MRI, 2001).

For this report, the emission estimating and modeling techniques developed through previous work were used to calculate the difference between actinide resuspension from the Site and deposition of actinides back onto the Site. These differences were used as estimates of the annual off-Site transport of actinides through the air pathway based on modeling. As discussed in Section TA-4.6, although wind erosion does not account for all the airborne emissions of actinides from the Site, it does account for the majority of emissions in recent years.

TA-5.4.1 Emission Estimation

A significant amount of research in particle and actinide resuspension has occurred over the years (Radian, 1999). This research emphasizes the need to customize any approach to the particular location of interest. Unique meteorological, soil and surface characteristics must be taken into account to produce a reliable emission estimating approach for a given area.

568

Past wind tunnel experiments on Site relate wind erosion of particulate matter to ambient wind speed. In FY99, a method was developed to estimate emissions of actinides from vegetated surfaces as a function of wind speed based on wind tunnel data taken in OU3 (located just east of Indiana Street) in June 1993 (EG&G, 1994).

Wind tunnel tests conducted at the Site in April, May and June 2000 primarily focused on emissions from burned areas of grassland. However, for comparison, wind erosion emissions were also measured from adjacent, unburned areas in April and June. The unburned area data were used to revise the emission estimating technique developed in FY99.

A power function was fitted to the combined April and June unburned area wind tunnel data (R^2 = 0.88). The resulting erosion potential equation, as a function of 10-meter wind speed, is:

$$EP = 3.933 \times 10^{-6} (u^{2.516})$$

where:

EP is the TSP erosion potential per 15-minute period in grams per square meter (g/m^2); and u is the 15-minute average, 10-m wind speed (m/s).

Estimates of particle resuspension provided the basis for predicting airborne radioactivity concentrations and activity deposition on ground or water surfaces. Soil isopleth maps showing the distribution of actinide activity in surface soils have been developed previously from soil sampling conducted on Site. These maps provided the spatial "source strength" that form the basis for the emission estimates. Figure TA-5-20 and Figure TA-5-21 show the simplified versions of these distributions that were used to estimate Pu-239/240 and Am-241 emissions. The particulate (wind erosion) emissions calculated using the above equation were combined with the data shown in Figure TA-5-20 through Figure TA-5-24 to yield actinide emission rates for input to a dispersion and deposition model. (Because little ambient airborne U is derived from Site contamination, only Pu and Am were modeled for this exercise.)

569

Application of the Wind Erosion Emission Equation

The emission estimating technique described above has been used to evaluate the movement of airborne particulate matter and associated actinides in the Site environment (URS, 2001). The process used to calculate and model wind erosion emissions at the Site is described below.

Meteorological data collected at the Site in 1996 were processed into 15-minute averages (1996 data have been used previously for dispersion modeling baseline studies). The emission equation described above was applied to each 15-minute average, 10-m wind speed, assuming the erosion potential for a given wind speed will be exhausted within a 15-minute time step. A sequential file of *potential* emissions of particulate matter from undisturbed areas of the Site (g/m^2/15-minutes) was generated for the year. Wind tunnel data showed the potential emissions to be exhausted within two to four minutes typically, depending on windspeed.

However, wind erosion emissions are not a function of wind speed alone. Emissions are also dependent on mechanisms such as periodic disturbances that act to renew the erosion potential of the surface. If erosion potential is not renewed following an erosive event, additional emissions will not occur. Consequently, *actual* wind erosion emissions will be a function of potential emissions, coupled with the amount of erodible particulate matter present on Site surfaces during any given time period. If potential emissions exceed the amount of erodible material, actual emissions will be limited to the mass of particles that constitute the erodible material "reservoir".

How frequently and to what extent is Site erosion potential renewed by disturbances? In most of the Site Buffer Zone, large-scale disturbances (i.e., excavations, traffic) are rare and isolated. Small-scale disturbances, in contrast, occur frequently due to freeze/thaw action, burrowing animals, movement of large animals such as deer over the surface, splashing caused by raindrops, disturbance of surface crusts by vegetation growth and turbulence caused by dust devils and thunderstorm convective activity. These frequent small disturbances renew erosion potential to some extent, but no measurements of this phenomenon are available for the Site.

570

Erosion potential is also renewed by deposition of airborne particulate matter. Particulate matter in the air over the Site is constantly being deposited on Site soil and vegetation surfaces. Deposition rates vary with wind speed and other conditions. As with small-scale generation of erosion potential, the dynamic nature of deposition has not been measured at the Site.

In the absence of specific data regarding the rate and dynamics of deposition and erosion potential generation by small-scale disturbances, the emission estimating procedure assumed that both phenomena occur at a relatively constant rate over the year. This allowed the amount of erodible material to be tracked over time as the erodible material reservoir was renewed by deposition and small-scale disturbances and depleted by resuspension. For each 15-minute period of the year-long data set, the mass of particles in the erodible material reservoir was compared with the potential particulate matter emissions defined by the emission equation derived from the wind tunnel studies. Actual particulate matter emissions were calculated as the lesser of the potential emissions or the amount of material available for resuspension at the appropriate wind speed. "Leftover", non-resuspended material was carried forward to the next 15-minute period, so that during periods of low wind speeds, the "available material" reservoir was built up and during windy periods it was depleted. A computer code was written to track these dynamics.

Effects of Precipitation and Snow Cover

It was assumed that no wind erosion emissions would occur while there was snow cover. The presence or absence of snow cover was determined from solar reflectance (albedo) data; the information was applied in the emission-tracking program so that no emissions were calculated for periods when snow cover was present. Deposition and small-scale erosion potential generation were assumed to continue during snow cover periods.

The effect of precipitation was also considered. Tests performed on soil samples from the wind tunnel test areas showed that moisture is very effective in limiting erosion potential. Consequently, no wind erosion emissions were expected to occur from soil surfaces during precipitation events and for a short period thereafter as the soil was drying. The extent of the period following a precipitation event during which wind erosion emissions were eliminated was

based on the amount of precipitation and on soil temperature, both of which were obtained from Site 1996 meteorological data records (higher soil temperatures were assumed to speed the restitution of erosion potential by increasing moisture evaporation rate). This information was used by the tracking program to determine whether emissions would occur for a given 15-minute period. As with snow cover, deposition and small-scale generation of erosion potential were assumed to continue during periods of no emissions due to precipitation effects.

Renewal of Erosion Potential

The renewal of erosion potential through deposition of particulate matter was estimated using monitoring data. TSP concentrations are monitored at various locations around the Site perimeter. Monthly average TSP concentrations from four of the locations were averaged for each month in 1996. Particulate matter deposition was calculated by multiplying the average monthly concentration of TSP by a deposition velocity to yield deposition estimates (in g/m^2/15-minute period) for each month. Deposition velocities were calculated using an algorithm contained in the *User's Guide for the Industrial Source Complex Dispersion Models* (EPA, 1995) and 1996 meteorological data for the Site.

The rate of ongoing erosion potential renewal through small-scale disturbances was estimated indirectly. In 2001, a calculation was performed to determine the net loss of Pu-239/240 and Am-241 from the Site each year through the air pathway, based on previous simulation modeling. By excluding regional background concentrations, these net loss calculations should represent the off-Site movement of *Site-generated* actinide emissions through the air pathway.

The net loss estimates were used as an initial estimate of the rate at which erosion potential is renewed by small-scale disturbances. An assumption was made that an ongoing actinide loss from the Site through the air pathway can only be sustained by the corresponding generation of new, erodible actinide-containing material in at least equal amounts. The total annual net loss of Pu-239/240 and Am-241 from the Site was partitioned among various actinide-contaminated soil areas based on their size and soil activity levels. A loss rate was calculated for each contaminated soil area. The estimated actinide loss rate was used to calculate a rate of generation of particulate

572

matter erosion potential by factoring out the soil activity concentration levels. These values were converted to particulate matter generation per 15-minute time step, assuming that erosion potential renewal is constant throughout the year. (The erosion potential renewal rate initially estimated was later adjusted downward by 40 % to calibrate model results to measured actinide data.)

Calculation of Actinide Emissions

To model actinide emissions, estimated particulate matter emissions for each 15-minute period were combined with information regarding the activity concentration of the available particulate matter to yield estimated actinide emissions (in pCi/m^2/15-minute period). This required tracking additional information for each contaminated soil source area.

While particulate matter emissions were assumed uniform across undisturbed areas of the Site, actinide emissions vary by source area. The renewal of erosion potential by small-scale disturbances will generate erodible material that will reflect the actinide concentration levels in the underlying surface soil. The renewal of erodible material by deposition, in contrast, will generate erodible material that will reflect the actinide concentration levels in the air over the Site.

To calculate the rate of activity deposition, average airborne Pu-239/240 and Am-241 concentrations were estimated over each of the contaminated soil source areas. Data from the RAAMP samplers were used to produce annual average air concentration isopleths over the Site for Pu-239/240 and Am-241. The air concentration patterns were mapped to the contaminated soil source areas. As with particulate matter, deposition of actinides was estimated by multiplying an average air concentration by a deposition velocity to calculate deposition of Pu-239/240 and Am-241 (in pCi/m^2/15-minute period). Deposition velocities were calculated as for particulate matter using 1996 meteorological data for the Site and Site-specific information on actinide distribution in various size fractions of airborne dust. Rates of erosion potential renewal by actinide deposition were tracked separately for each contaminated soil source area.

The ongoing generation of actinide erosion potential through small-scale disturbances was described previously. As with deposition, the period-by-period renewal of erosion potential through this mechanism was tracked separately for each contaminated soil source area.

For each 15-minute period, the increase in available erodible activity was calculated due to deposition and small-scale disturbances for each actinide and source area and added to the erodible activity remaining from the previous time step. The activity concentration of the available erodible material was calculated by dividing the total pCi/m^2 for each actinide and source area by the total available particulate matter (in g/m^2) for each time step. The resulting pCi/g value determined for each actinide and source area was then multiplied by the calculated particulate matter emissions for each time step to determine actinide emissions. A computer code was written to track these dynamics and to produce a variable emission rate file for each contaminated soil source area for input to ISCST3.

TA-5.4.2 Modeling Methods

A dispersion and deposition model (ISCST3) was used to simulate the transport of pollutants from the locations of emission to other locations of interest (termed receptors). The model requires the input of detailed source characteristic information, meteorological data and desired locations of model predictions (i.e., receptors). The essential inputs used are described below.

An ISCST3 meteorological input file was created using the EPA Meteorological Processor for Regulatory Models (MPRM). Surface meteorological parameters that were measured at the Site in 1996 were combined with concurrent upper-air and cloud cover data from the National Weather Service (NWS) station in Denver. The output from MPRM was an hourly meteorological input file. The 1996 meteorological data file was described more fully in the FY99 air pathway report (Radian, 1999).

Surface soil activity isopleths were used to generate actinide emission rates for each source area as previously described. Figure TA-5-19 and Figure TA-5-20 show the digitized contours that defined source areas within the model. Actinide emissions varied for each source area and time

574

step. The actinide sources were modeled as area sources, with release heights at the ground surface.

To account for dry deposition, particle size categories must be defined for each source. Associated with each particle size category is a mass (or actinide activity) fraction, a particle density and a particle diameter. Deposition is calculated as the product of a near ground-level concentration and a deposition velocity that is estimated by the model.

Particle size category bounds were chosen based on available Site-specific joint particle size/actinide activity data (Langer, 1986) and are shown in Table TA-5-23. To model the deposition of resuspended actinides, the activity fractions shown in Table TA-5-23 were input for the mass fractions of both Pu-239/240 and Am-241.

Table TA-5-23. Particle Size Distribution Data Used for Dispersion Modeling

Particle Size Category	Lower-Upper Bound for Particle Size Category (μm)	Mean Diameter for Particle Size Category (μm)	Particle Density (g/cm^3)[a]	Pu Activity Fraction[b]
1	1-3	2.15	2.65	0.04
2	3-15	10.15	2.65	0.19
3	15-30	23.23	1.8	0.77

[a] Foster et al., 1985.
[b] Values at the measurement height of 1 meter (Langer, 1987).
Notes: μm = micrometers
g/cm^3 = grams per cubic centimeter

Modeling receptors included a Cartesian receptor grid with 200-m receptor spacing that encompassed the Site and extended approximately 400 meters to 500 meters beyond the Site boundary in selected directions.

To verify model performance, wind erosion emissions of Pu-239/240 and Am-241 from undisturbed areas of the Site were modeled with ISCST3 and compared to measured ambient air concentrations at various locations around the Site. The annual average concentrations of Pu-

575

239/240 and Am-241 predicted by the model, when added to regional background concentrations, provided a good fit to measured data at all sampler locations.

TA-5.4.3 Calculation of Off-Site Transport

To estimate the net annual loss of actinides, wind erosion of actinides from pre-closure, contaminated soil areas and their deposition back onto the Site were calculated. Actinide resuspension was calculated from the 15-minute wind erosion estimates described previously. For a given isopleth area, the estimated activity flux for each time step was multiplied by the area associated with the isopleth level (consistent with source areas used in dispersion modeling) and then summed over all time steps in the year to produce the total amount of Pu-239/240 or Am-241 resuspended in pCi/yr.

Actinide deposition was estimated using the ISCST3 model. The same spatial areas used in the wind erosion calculations were modeled as emission sources for each actinide. The ISCST3 model was executed to predict annual deposition in units of pCi/m^2/yr for each receptor. This rate was converted to a total activity by multiplying by the area associated with each receptor. The annual net loss for each actinide was then determined as the difference between total activity resuspended and total activity redeposited on Site.

TA-5.4.4 Air Pathway Analysis – Modeled Data

Table TA-5-24 shows the results of the off-Site transport calculations using modeled data. While the off-Site transport values shown in Table TA-5-24 are not specific as to direction, it can be assumed that most off-Site transport of actinides through the air pathway occurs from the eastern boundary of the Site based on the patterns of concentration and deposition seen in the base modeling.

Table TA-5-24. Results of Air Pathway Analysis ISCST3 Modeling

Actinide	Annual Transport Off-Site Through the Air Pathway[a] (Ci)
Pu-239/240	7.9E-5
Am-241	1.2E-5

[a] Represents off-Site transport of Site-derived actinides only (i.e., excluding background concentrations).

TA-5.5 BIOLOGICAL PATHWAY ANALYSIS

TA-5.5.1 Introduction

Estimating off-Site transport of actinides by mule deer provides a framework for quantifying the overall macro-biological transport pathway. The following section describes two different methods used to develop estimates of off-Site actinide transport by mule deer.

TA-5.5.2 Calculation Methodology

Method 1

The first estimation method is based on the Whicker (1979) calculation of the Pu quantity moved by deer on the Site. Whicker, et al. (1990) documented the fact that adult does migrate on- and off-Site, but they did not appear to leave permanently. Whicker (1979) calculated that deer move less than 10^{-7} of the Site Pu inventory in the soil annually. Using the average mule deer population, 140, in conjunction with telemetry data that indicate approximately 5 % of the deer leave the Site annually (Symonds and Alldredge, 1992), an estimate was developed for the number of individual deer that leave the Site each year. On-Site soil is deposited off-Site during the time it takes a deer to cycle forage through its system. It is estimated to take approximately 48 hours for a deer to completely cycle forage it consumes before its bowel is empty (Alldredge and Reeder, 1972). Multiplying all of these factors yields the total fraction of on-Site Pu that is deposited off-Site.

517

The estimated off-Site transport is 2.8 x 10^{-11} of the on-Site Pu inventory that is potentially distributed off-Site by deer annually. Krey (1976) estimated the on-Site soil inventory of Pu is approximately 8 Ci and Little (1980) estimated that greater than 99 % of the total Site Pu inventory is contained in the soil. Using these data, an amount of Pu deposited off-Site annually was calculated. Average soil activities were calculated for each actinide, based on an area-weighting calculation using the kriged surface soil activities presented in Section TA-2. The mean soil activities were used to estimate the amount of soil transported off-Site by mule deer, which were used to estimate the amounts of the other actinides off-Site. Results for this method are presented in Table TA-5-25 and Figure TA-5-25.

Method 2

The second method used to estimate off-Site actinide transport is based on the amount of soil consumed by deer. This method used the number of deer at RFETS, the number of deer that leave the Site, the amount of soil consumed daily (Arthur et al., 1982) and the time needed for deer to cycle the forage through their digestive system (Alldredge et al., 1972). The quantity, by mass, of on-Site soil deposited off-Site annually was calculated. Average soil activities were calculated for each actinide, based on an area-weighting calculation using the kriged surface soil activities presented in Section TA-2. The average soil activities for each actinide were multiplied by the calculated quantity of soil consumed on-Site and deposited off-Site. The calculated daily soil consumption mass resulted in a standard deviation (σ) +/- 12 g/d. Results are presented in Table TA-5-25 and Figure TA-5-26.

TA-5.5.3 Estimated Actinide Transport Off-Site

Table TA-5-25 summarizes the estimated biological actinide transport off-Site using Methods 1 and 2.

Table TA-5-25. Biological Off-Site Actinide Transport

Actinide	*Method 1* Off-Site Transport (Ci/year)	*Method 2* Off-Site Transport (Ci/year)
Pu-239/240	2×10^{-10}	1×10^{-9}
Am-241	5×10^{-11}	3×10^{-10}
U-233/234	9×10^{-11}	6×10^{-10}
U-235	6×10^{-12}	4×10^{-11}
U-238	1×10^{-10}	7×10^{-10}

TA-5.5.4 Summary of Biological Pathway Analysis—Modeled Data

Method 1 uses calculations based on mule deer studies conducted by Whicker (1979). In light of studies on rainsplash redistribution of soil particles on plants (Dreicer et al., 1984), it is possible that the Whicker (1979) estimate of transport is overly conservative (i.e., overestimates actinide transport). Although the 1979 paper does not provide detail on the estimation assumptions, if it was based on total Pu load on vegetation clipped to ground level, the estimate would have accounted for plant parts that deer were less likely to consume. Studies of deer food habits (Wallmo, 1981) indicate that deer select food items on the basis of best available nutrition, which normally are the vigorously growing new shoots and flower heads. These plant parts would be younger (i.e., early spring growth has less time to accumulate soil from rainsplash before it is consumed) and for part of the season would be farther from the soil surface (i.e., new growth is typically at the tips and farther from the soil surface, permitting less accumulation of particulates from rainsplash mechanisms). Older growth and plant parts closer to the soil surface have greater opportunity to accumulate soil from wind and rainsplash deposition. Since rainsplash studies indicate the greatest accumulation of soil on vegetation less than 20 cm from the soil surface (Dreicer et al. 1984), new growth on taller plants would have less contamination. Therefore, deer would be expected to selectively consume less than the total available contaminant load on vegetation. Intentional, direct soil consumption by mule deer has been documented, however, so soil content in fecal pellets can sometimes be relatively high (Arthur, 1977).

579

TA-5.6 TECHNICAL APPENDIX SECTION TA-5 REFERENCES

Surface Water Pathway References (Section TA-5.2)

Eckhardt, et al. 2000. Colloids, Carriers of Actinides into the Environment, Challenges in Plutonium Science, Los Alamos Science, Los Alamos National Laboratory Vol. II, No. 26, pp. 490-491.

Environmental Protection Agency (EPA). 1995a. User's Guide for the Industrial Source Complex (ISC3) Dispersion Models, Volume I and II (EPA-454/B-95-003a). EPA Office of Air Quality Planning and Standards, Emissions, Monitoring and Analysis Division. Research Triangle Park, North Carolina.

EPA. 1995b. Guideline on Air Quality Models, (Revised), (EPA-450/2-78-027-R-C) EPA Office of Air and Radiation. Office of Air Quality Planning and Standards, Emissions, Monitoring and Analysis Division. Research Triangle Park, North Carolina.

Foster, G.R. and Hakonson, T.E. 1984. Predicted Erosion and Sediment Delivery of Fallout Plutonium. J. Environmental Quality, Vol. 13, No. 4, pp 595-602.

Honeyman, B.D. 1999. The Affect of Soil Water Redox Potential on Pu-239,240 Solubility, Actinide Migration Studies at the Rocky Flats Environmental Technology Site. Colorado School of Mines, Golden, CO. October 7, 1999.

Kersting, A.B., Efurd, D.W., Finnegan, D.L., Rokop, D.J., Smith, D.K. and Thompson, J.L., 1999, Migration of Plutonium in Groundwater at the Nevada Test Site. Nature, No. 397, pp. 56-59.

Langer, G. 1980. Dust Measurements from Windblown Resuspension, in Rocky Flats Report RFP-3115, Rocky Flats Plant, Golden, CO.

Radian. 1999. Air Transport and Deposition of Actinides at the Rocky Flats Environmental Technology Site, FY99 Report. Prepared for Kaiser-Hill Company, Rocky Flats Environmental Technology Site, Golden, Colorado.

Rocky Mountain Remediation Services (RMRS). 2000. Report on Soil Erosion and Surface Water Sediment Transport Modeling for the Actinide Migration Evaluation at the Rocky Flats Environmental Technology Site. Report 00-RF-01823. Prepared for Kaiser-Hill Company, Rocky Flats Environmental Technology Site, Golden, Colorado.

RMRS. 1996. Draft – Background Comparison for Radionuclides in Groundwater. Rocky Flats Environmental Technology Site, Golden, CO.

580

Santschi, P.H. 1998. Final Report on Phase Speciation of Pu and Am for Actinide Migration Studies at the Rocky Flats Environmental Technology Site. Texas A&M University, Galveston, TX.

Santschi, P.H. Roberts, K. and Guo, L. 1999. Final Report on Phase Speciation of Pu and Am for Actinide Migration Studies at the Rocky Flats Environmental Technology Site. Texas A&M University, Galveston, TX. September 28, 1999.

Santschi, P.H. Roberts, K. and Guo, L. 2000. Final Report on Phase Speciation of Pu and Am for Actinide Migration Studies at the Rocky Flats Environmental Technology Site. Texas A&M University, Galveston, TX. September 29, 2000.

Spence, S.D. 1993. Some Physical Characteristics of C-2 Sediments, EG&G Rocky Flats Internal Report. Environmental Technologies Group, Rocky Flats Environmental Technology Site, Golden, CO. 14p.

Walton-Day, Katherine. 1996. Geochemistry of the Processes that Attenuate Acid Mine Drainage in Wetlands, in Plumlee, G.S, Logsdon, M.J. and Lesher, C.M., eds., Reviews in Economic Geology, Vol. 6A, The Environmental Geochemistry of Mineral Deposits, Part A: Processes, Techniques and Health Issues, Chapter 10, Society of Economic Geologists.

Whicker, F.W. 1979. Radioecology of Natural Systems Final Report, Plutonium Behavior in a Grassland Ecosystem. Report to U. S. Department of Energy, Rocky Flats Plant, Golden, CO.

Whicker, F.W. 2000. Biologically-Mediated Mechanisms of Actinide Migration, Abstracts of Papers Presented at The 45th Annual Meeting of The Heath Physics Society, Denver, CO. (Supplement to Health Physics, Lippencott, Williams and Wilkins, p. S159), Vol. 78, No. 6, June, 2000

Groundwater Pathway References (Section TA-5.3)

Cleveland, J.M., TlF. Rees and W.C. Gottschall. 1976. Factors affecting Solubilization of Plutonium and Americium from Pond sediment at the Rocky-Flats Facility. Report ES-376-76-196. Rockwell International, Rocky Flats Plant, Golden, CO.

Honeyman, B. D. and P. H. Santschi. 1997. Actinide Migration Studies at the Rocky Flats Environmental Technology Site, Golden, CO. Final Report. December 15, 1997.

Hurr, R.T. 1976. Hydrology Of A Nuclear-Processing Plant Site, Rocky Flats, Jefferson County, Colorado. U.S. Geological Survey Open-File Report 76-268. U.S. Geological Survey. Denver, CO.

Santschi, P.H., K. Roberts and L. Guo. 2000. Final Report on Phase Speciation of Pu and Am for Actinide Migration Studies at the Rocky Flats Environmental Technology Site. Texas A&M University. Galveston, TX. September 29, 2000.

Air Pathway References (Section TA-5.4)

EG & G. 1994. OU3 Wind Tunnel Study, volume I: Test Report, Volume II: Field Data Sheets. DOE Prime Contract No. DE-AC04-90DP62349, Subcontract No.ASC218973GG, MRI Project No. 3155-M. Golden, Colorado. January, 1994.

EPA. 1999 . Revised Risk Assessment for the Air Characteristic Study, Volume I, Overview (EPA 530-R-99-019a). Office of Solid Waste, Washington, DC.

Langer, G. 1986. Dust Transport-Wind Blown and Mechanical Resuspension, July 1983 to December 1984 (RFP-3914). Rockwell International, Golden, Colorado. September, 1986.

Langer. G. 1987. Dust Transport-Wind blown and Mechanical Resuspension, HS & E Applications Technology Semiannual Progress Report. p. 16. May, 1987.

MRI. 2001. Effect of Controlled Burning on Soil Erodibility by Wind. Revised Draft Test Report. Midwest Research Institute, Kansas City, MO.

Biological Pathway References (Section TA-5.5)

Arthur III, W.J. and A.W. Alldredge. 1982. Soil Ingestion by Mule Deer in Northcentral Colorado, Journal of Range Mgmt.

Alldredge and Reeder. 1972. Gastrointestinal Retention of Ingesta in Mule Deer and Domestic Sheep. A.W. Alldredge and D.E. Reeder. Radioecology of Some Natural Organisms and Systems in Colorado. Tenth Annual Progress to USAEC, pp. 18-22.

Dreicer et al. 1984. Rainsplash as a Mechanism for Soil Contamination of Plant Surfaces. Health Physics, Vol 46, No 1, pp 177-187. January, 1984.

Krey, Philip W. 1976. Remote Plutonium Contamination and Total Inventories from Rocky Flats. Health Physics Pergamon Press. Vol 30, pp. 209-214.

Little, et al. 1980. Plutonium in a Grassland Ecosystem at Rocky Flats. Journal of Environmental Quality. Vol 9, No. 3, pp. 350-354.

582

Symonds, K.K. and A.W. Alldredge. 1992. Deer Ecology Studies at Rocky Flats, Colorado; 1992-1992 progress report. Agreement ASC 49074 and ASC 77313AM. Colorado State University, Ft. Collins, CO. Summer, 1992.

Wallmo, O.C. 1981. Mule and Black-tailed Deer of North America. University of Nebraska Press, Lincoln.

Whicker, F.W. 1979. Radioecology of Natural Systems; Final Report for the Period May 1, 1962-October 31, 1979. Contract No. EY-76-S-02-1156 (COO-1156-117). Colorado State University, Fort Collins, CO.

Whicker, F.W. et al. 1990. Progress Report on Radiological Investigations at Rocky Flats. Agreement ASC 49074 WS. Colorado State University, Ft. Collins, CO. September 15, 1990.

Figure TA-5-1. Lower Walnut Creek, Pu Loading Profile – Measured and Modeled Data Combined

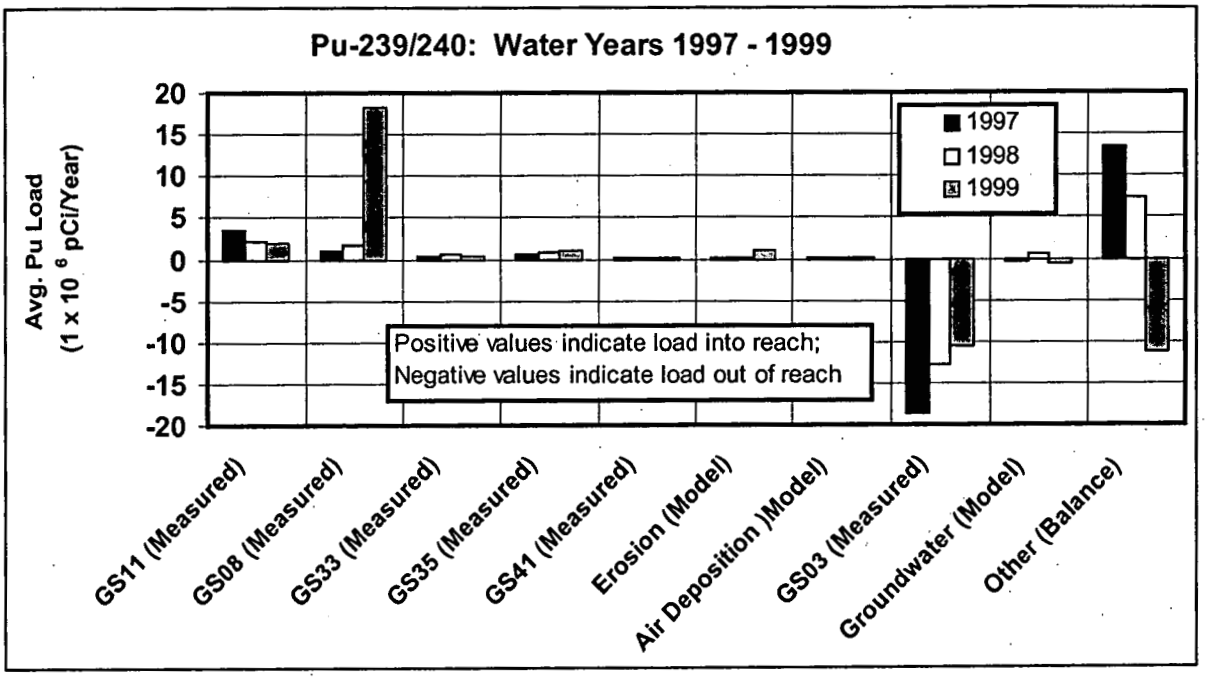

Figure TA-5-2. Lower Walnut Creek, Pu Mass Balance Uncertainty Analysis

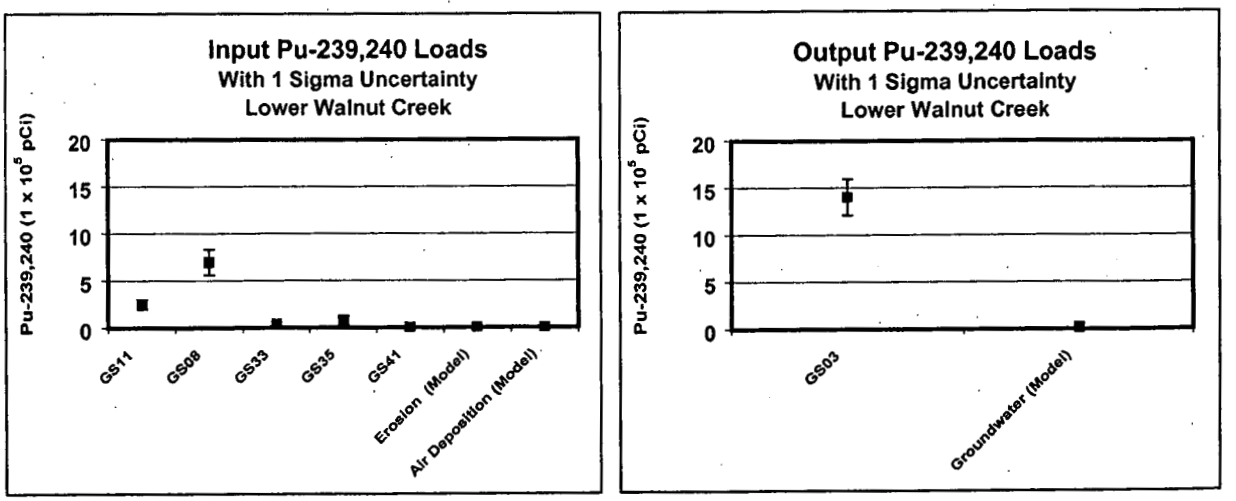

584

Figure TA-5-4. Lower Walnut Creek, U-238 Loading Profile – Measured and Modeled Data Combined

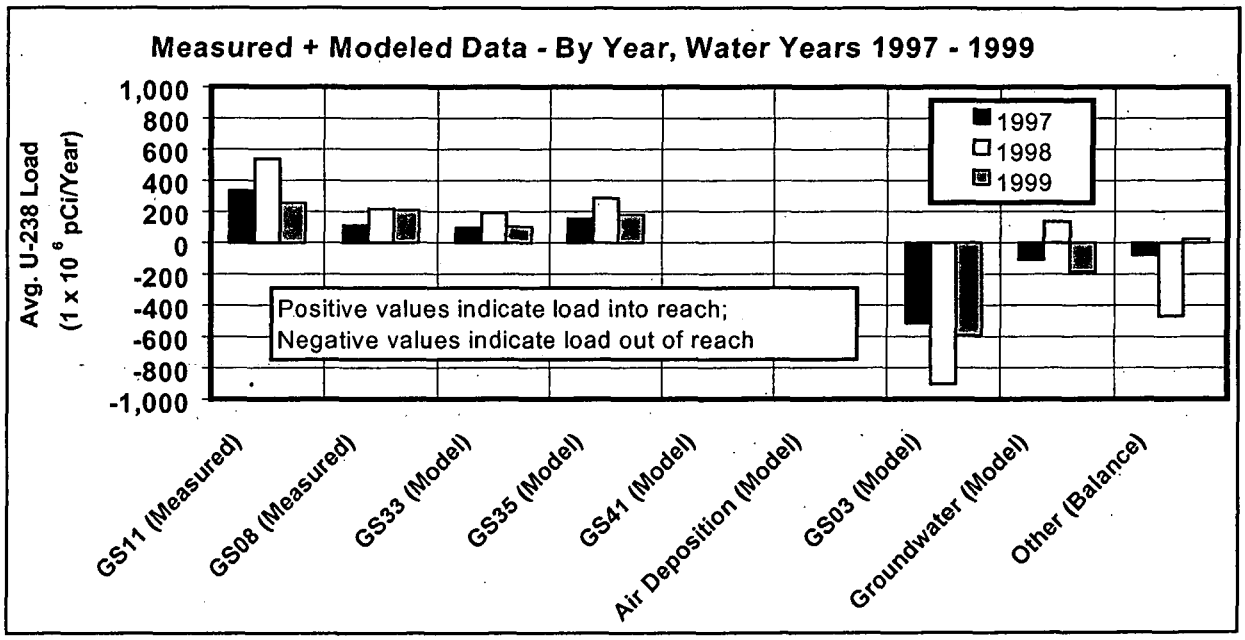

Figure TA-5-5. Lower Walnut Creek, U-238 Mass Balance Uncertainty

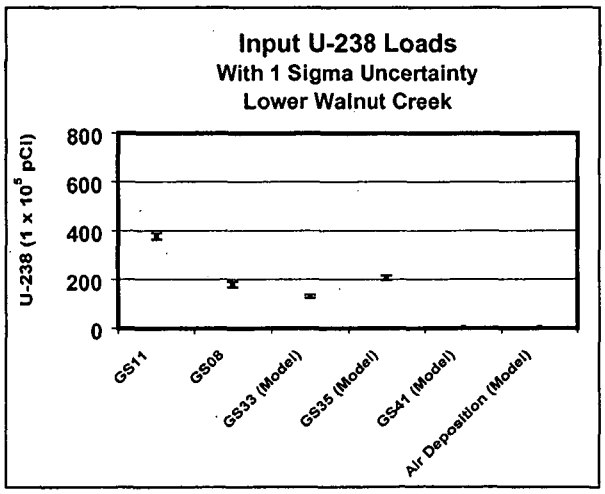

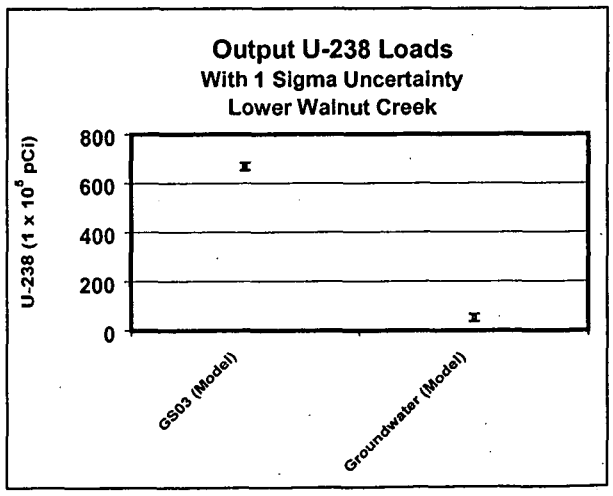

586

Figure TA-5-7. A- and B-Series Ponds, Pu Loading Profile Measured and Modeled Data Combined

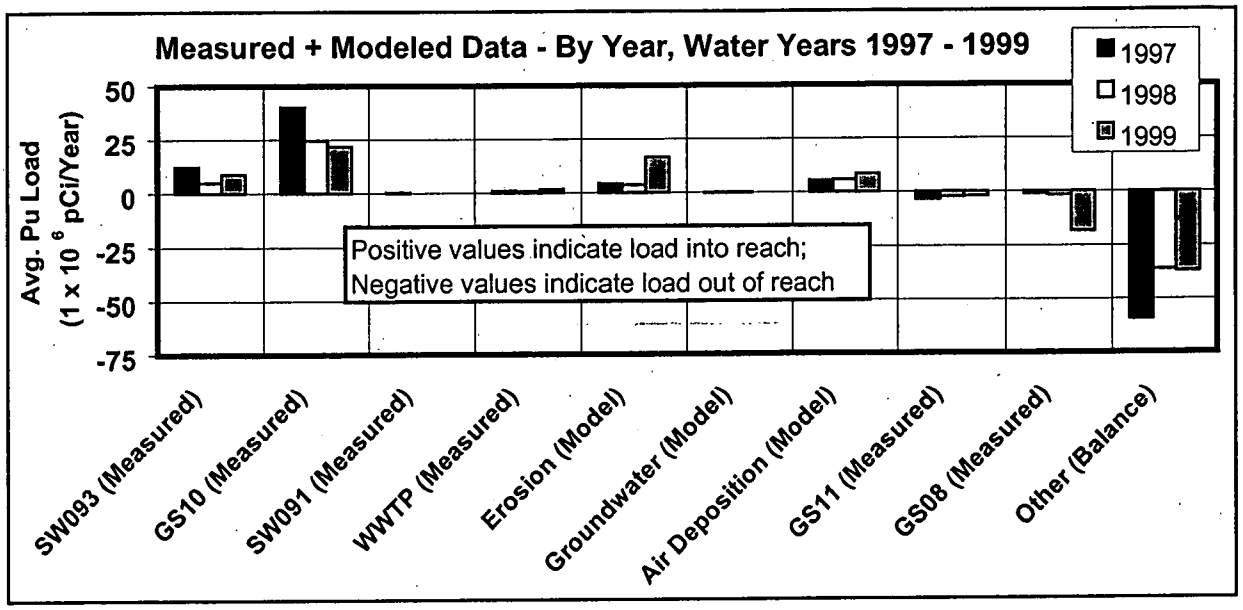

Figure TA-5-8. A- and B-Series Ponds, Pu Mass Balance Uncertainty

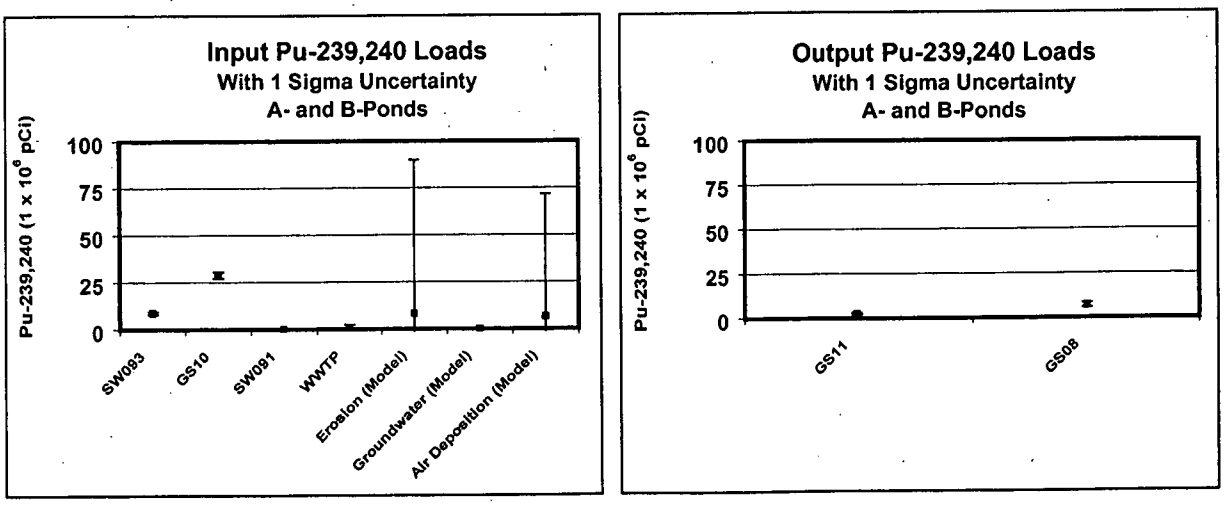

588

Figure TA-5-10. A- and B-Series Ponds, U-238 Loading Profile Measured and Modeled Data Combined

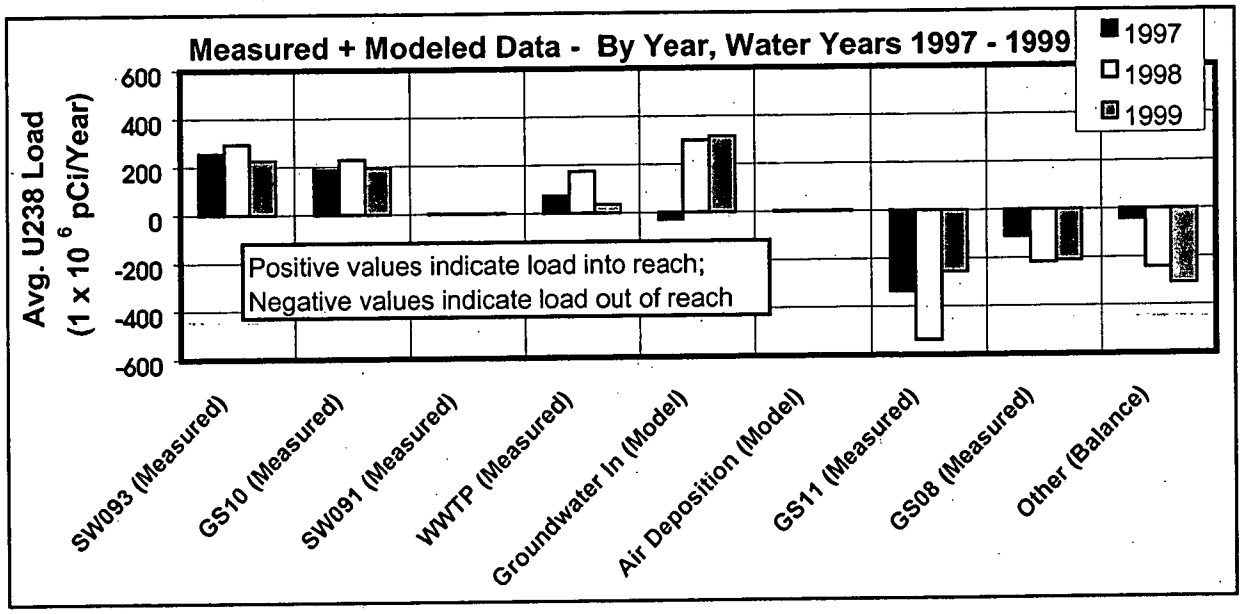

Figure TA-5-11. A- and B-Series Ponds, U-238 Mass Balance Uncertainty

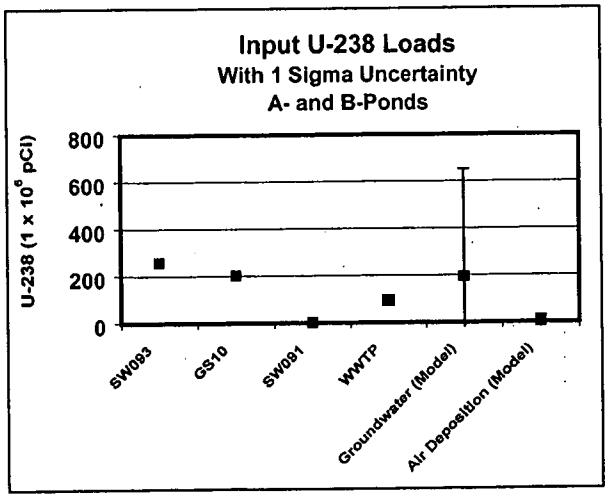

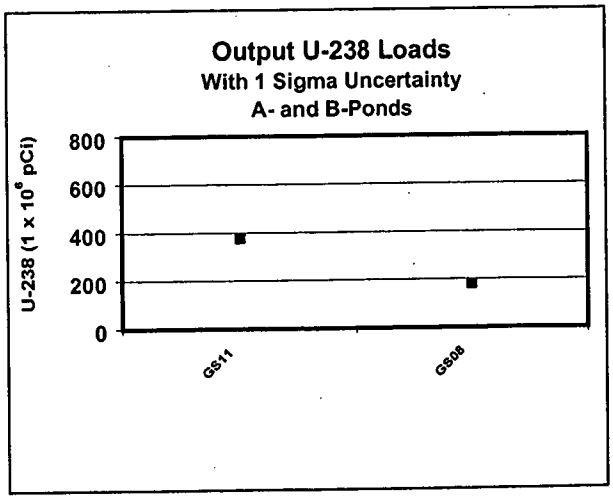

590

Figure TA-5-13. SID, Pu Loading Profile – Measured and Modeled Data Combined

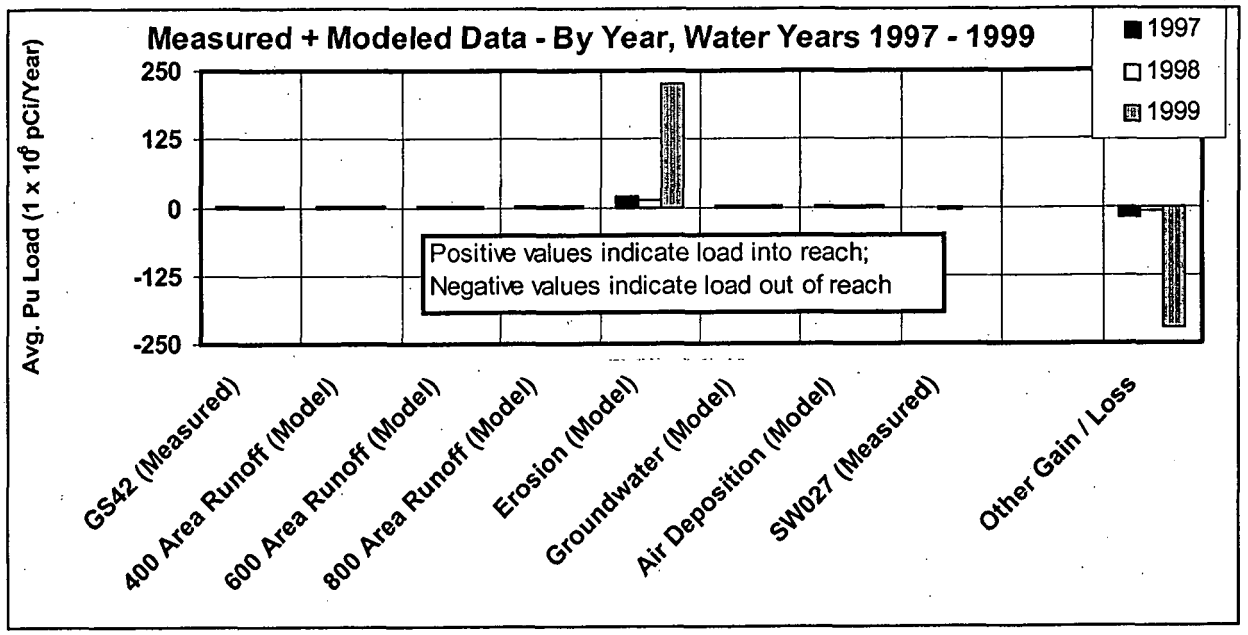

Figure TA-5-14. SID, Pu Mass Balance Uncertainty

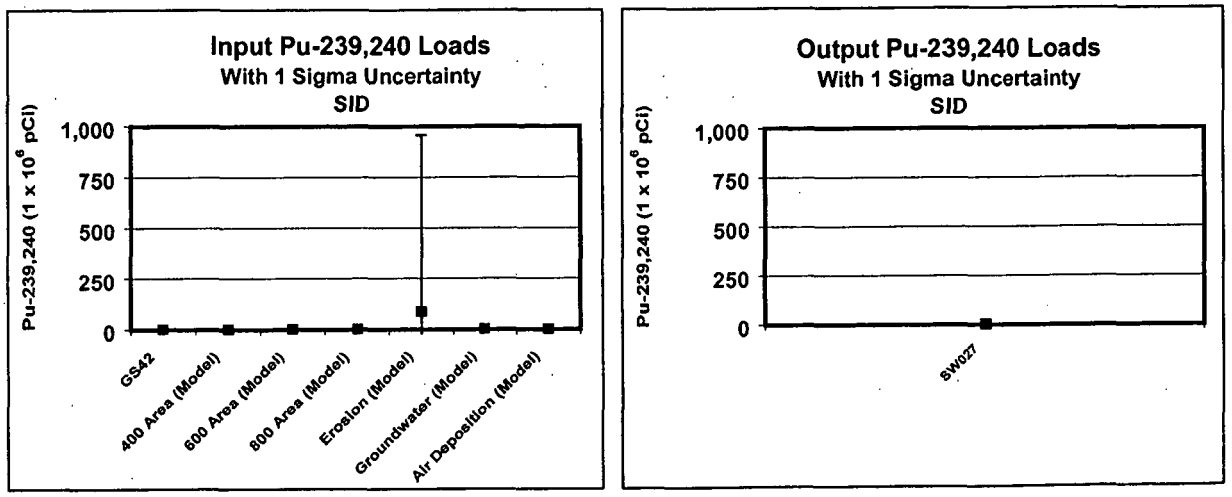

592

Figure TA-5-16. SID, U-238 Loading Profile Measured and Modeled Data Combined

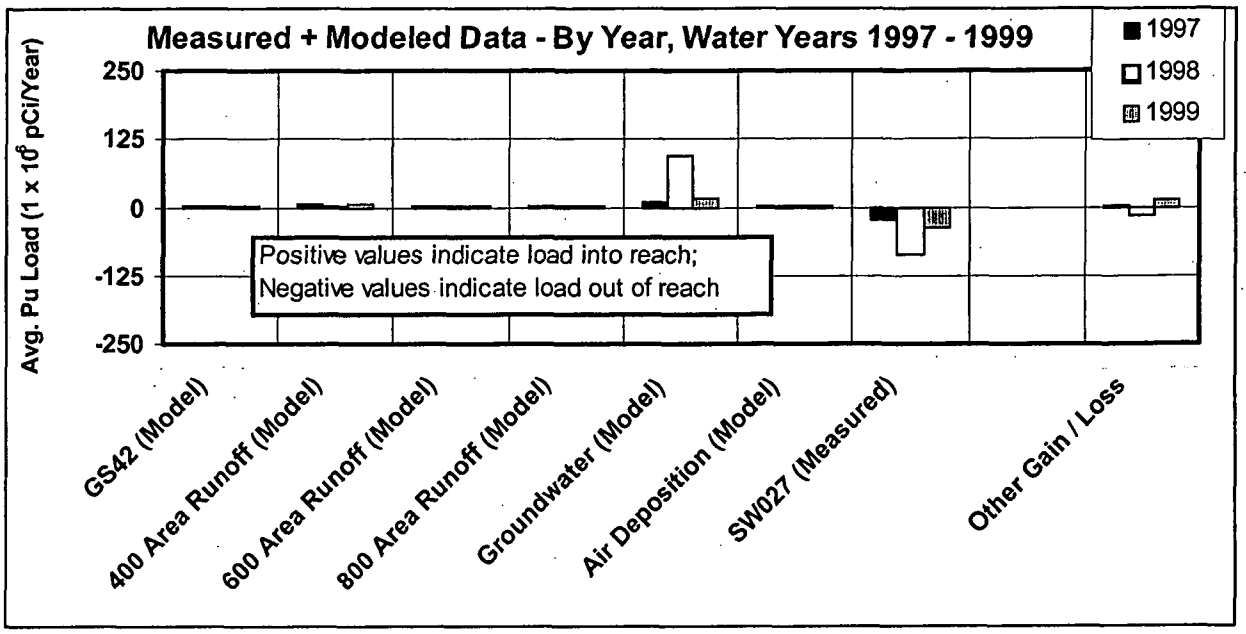

Figure TA-5-17. SID, U-238 Mass Balance Uncertainty

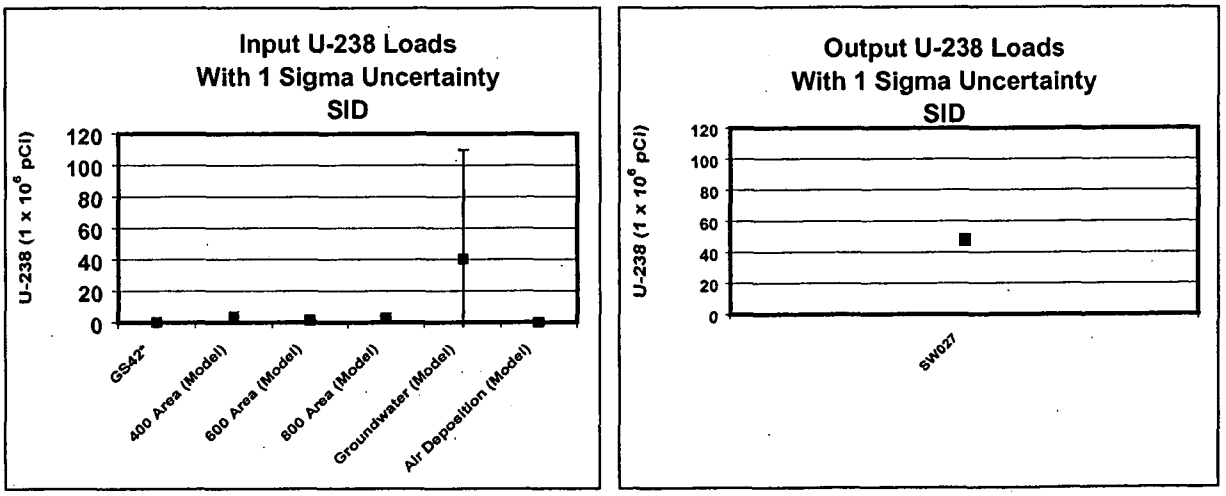

594

Figure TA-5-19. Shallow Groundwater Off-Site Actinide Load

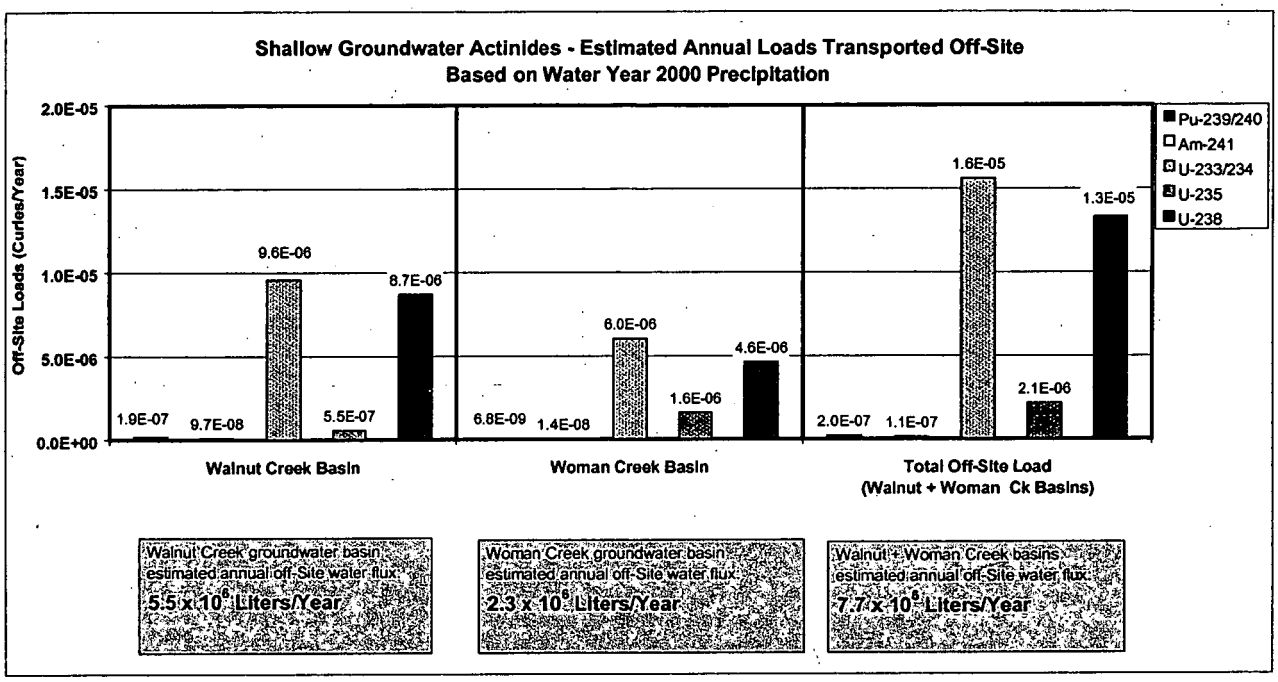

596

Figure TA-5-20. Pu-239 Surface Soil Isopleths for Air Model

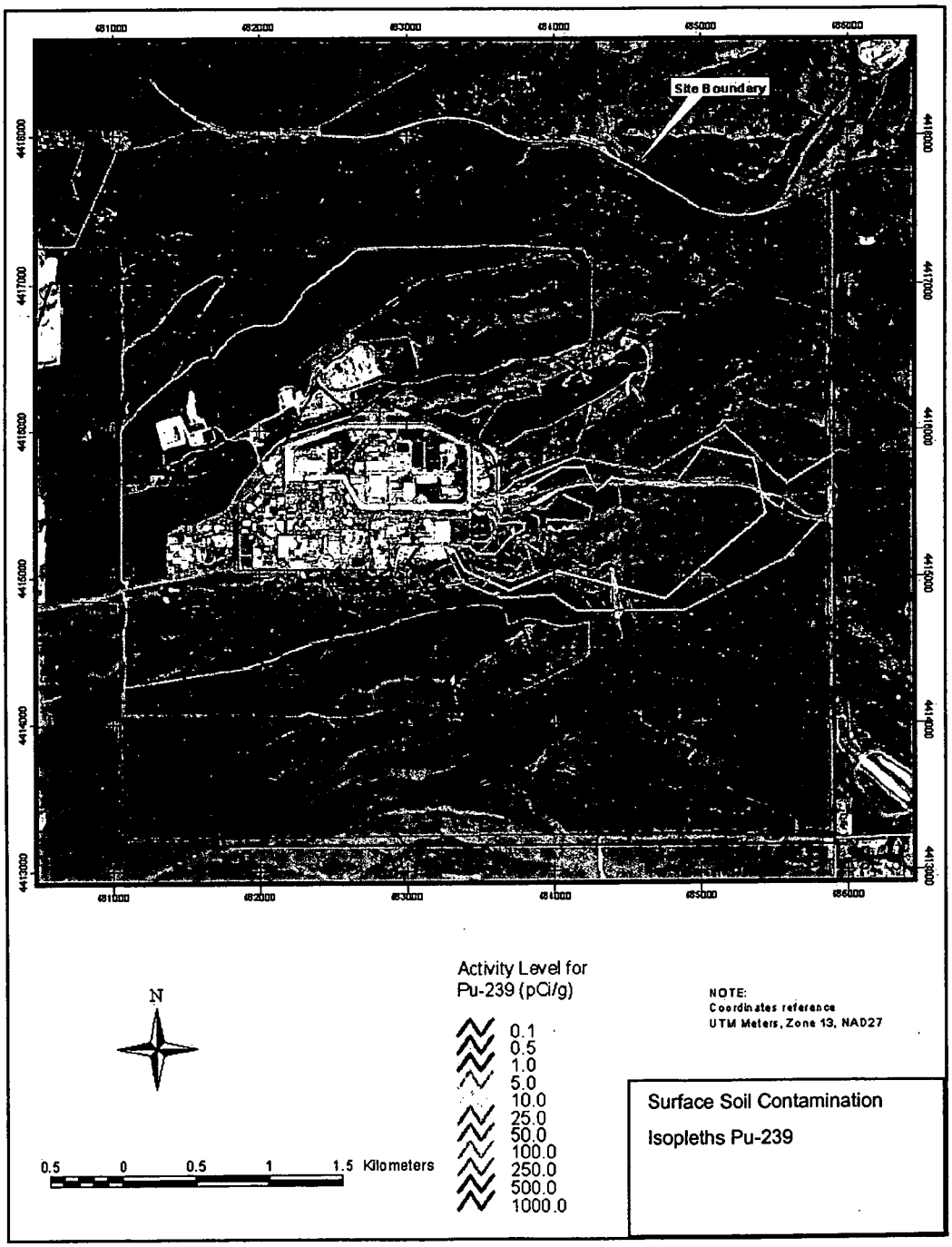

597

Figure TA-5-21. Am-241 Surface Soil Isopleths for Air Model

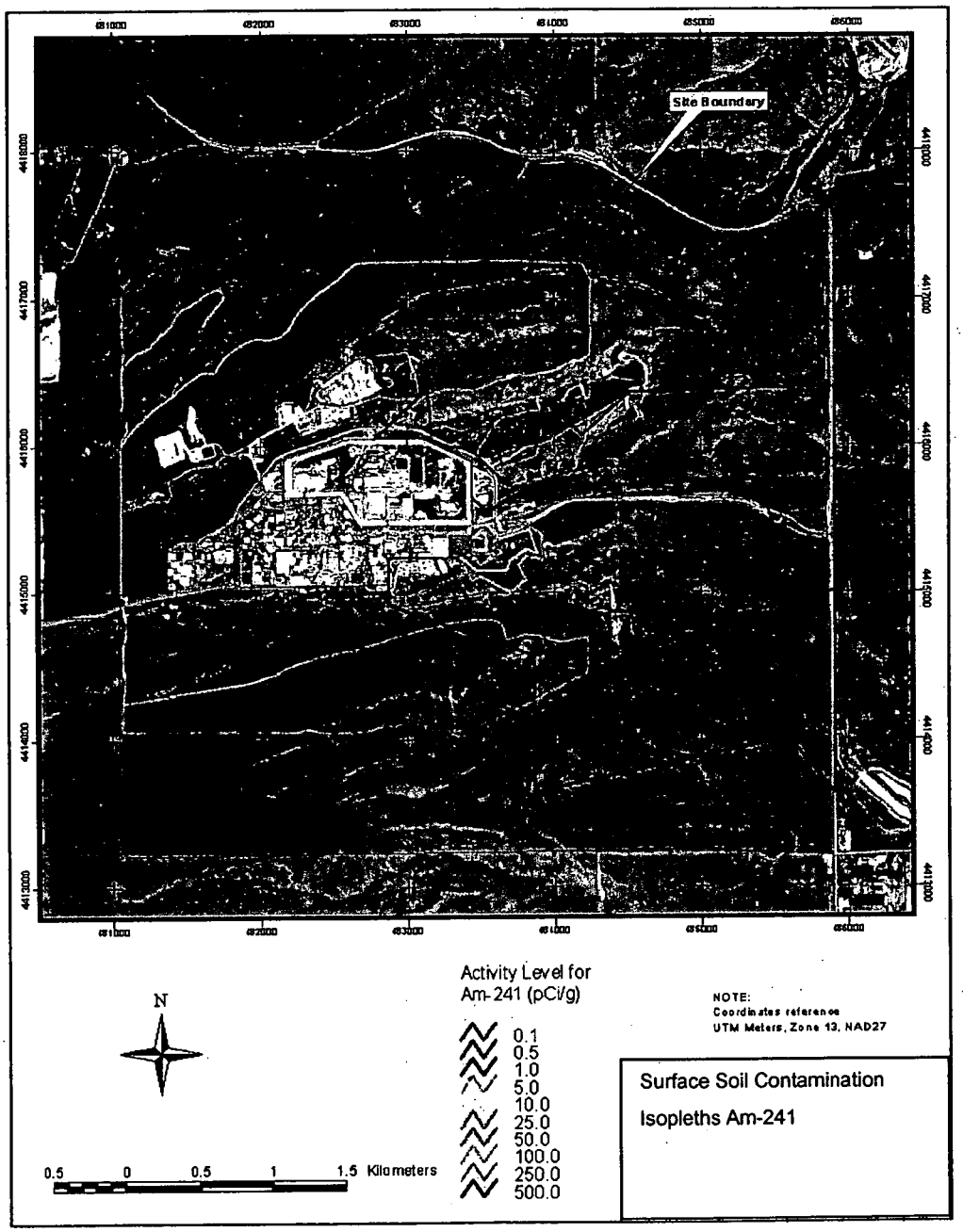

598

Figure TA-5-22. U-233/234 Surface Soil Isopleths for Air Model

599

Figure TA-5-23. U-235 Surface Soil Isopleths for Air Model

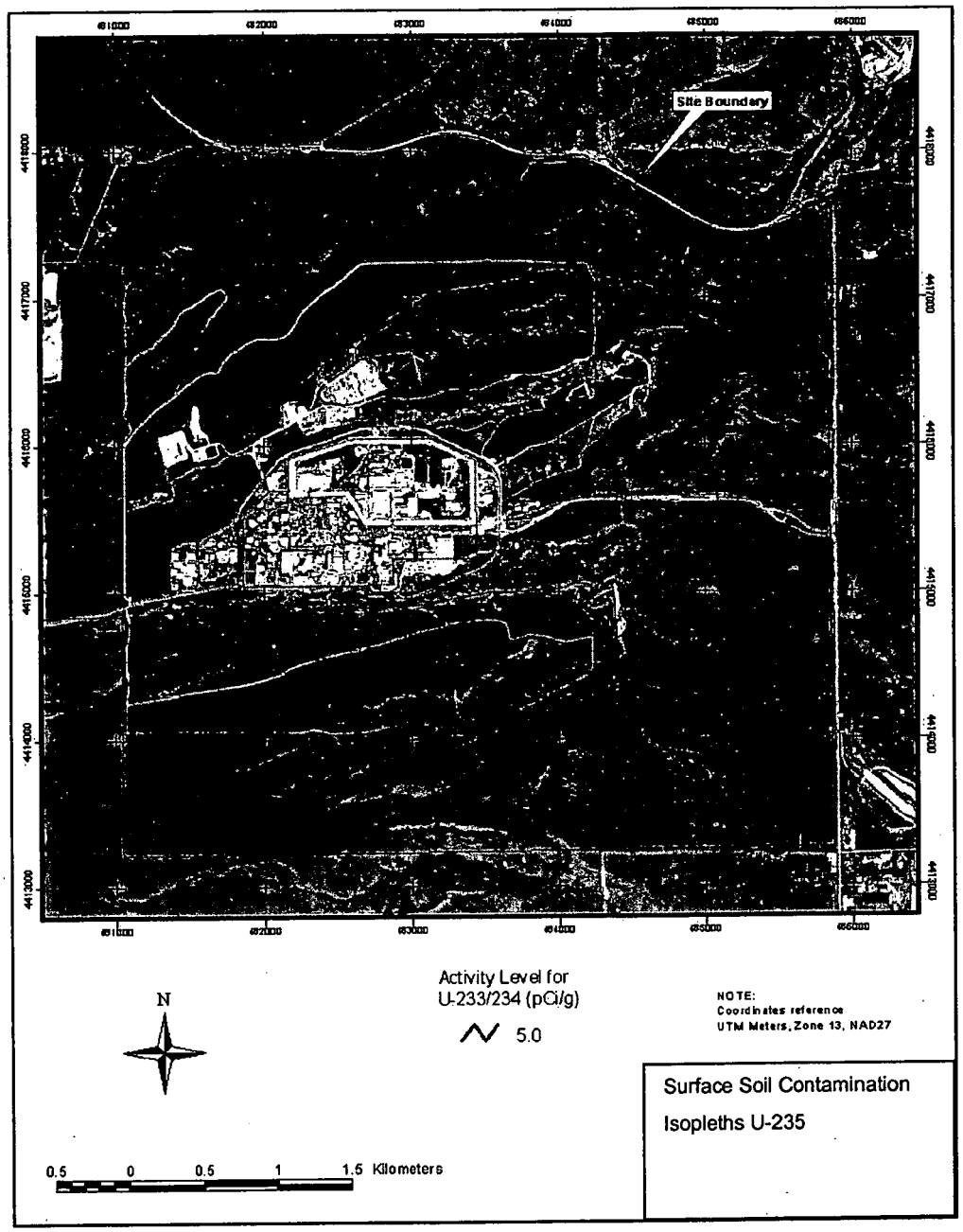

600

Figure TA-5-24. U-238 Surface Soil Isopleths for Air Model

601

Figure TA-5-25. Biological Model Method 1 Results

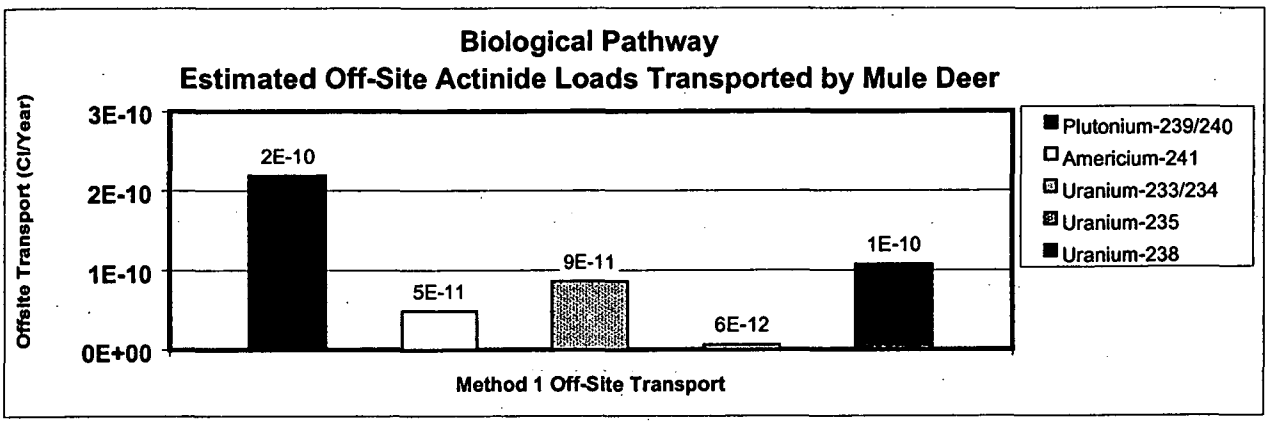

Figure TA-5-26. Biological Model Method 2 Results

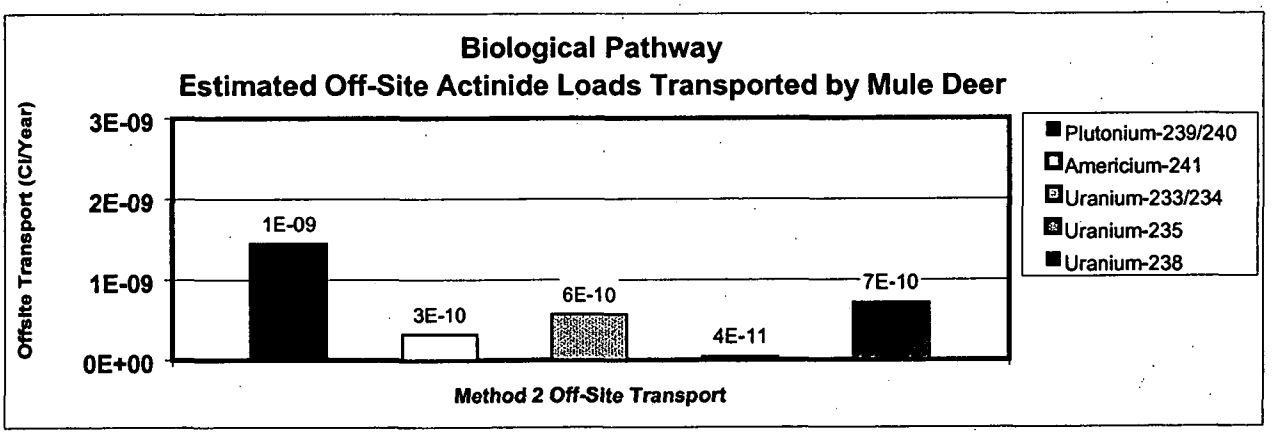

602

SECTION TA-6 - TABLE OF CONTENTS

TA-6 ACTINIDE TRANSPORT PATHWAYS ANALYSIS - BASED ON MODELED DATA FOR EXTREME CONDITIONS 6-1

TA-6.1 Introduction 6-1

TA-6.2 Surface Water Pathway – Extreme Conditions Analysis 6-1

TA-6.2.1 Extreme Conditions Modeled 6-1

TA-6.2.2 Lower Walnut Creek Extreme Event Analyses 6-3

TA-6.2.3 A- and B- Series Ponds Extreme Event Analyses 6-5

TA-6.2.4 SID Extreme Event Analyses 6-7

TA-6.2.5 Summary of the Surface Water Pathway Extreme Events Analyses 6-10

TA-6.3 Groundwater Pathway – Extreme Conditions Analysis 6-11

TA-6.4 Air Pathway – Extreme Conditions Analysis 6-12

TA-6.4.1 Air Pathway Analysis - Extreme Events and Alternative Scenarios 6-12

TA-6.5 Biological Pathway – Extreme Conditions Analysis 6-17

TA-6.6 Technical Appendix Section TA-6 References 6-18

SECTION TA-6 TABLES

Table TA-6-1. Lower Walnut Creek – Pu Mass Balance Results – 10-Year, 6-Hour Storm 6-3

Table TA-6-2. Lower Walnut Creek – Pu Mass Balance Results – 100-Year, 6-Hour Storm 6-4

Table TA-6-3. A- and B-Series Ponds – Pu Mass Balance Results – 10-Year, 6-Hour Storm 6-5

Table TA-6-4. A- and B-Series Ponds – Pu Mass Balance Results – 100-Year, 6-Hour Storm 6-6

1003

Table TA-6-5. SID – Pu Mass Balance Results –
10-Year, 6-Hour Storm 6-7
Table TA-6-6. SID – Pu Mass Balance Results –
100-Year, 6-Hour Storm 6-8

SECTION TA-6 FIGURES

Figure TA-6-1. Lower Walnut Creek – Pu Loading Profile for
Water Year 1997 – 1999 Average Compared with Extreme Events 6-19
Figure TA-6-2. A- and B-Series Ponds – Pu Loading Profile for
Water Year 1997 – 1999 Average Compared with Extreme Events 6-19
Figure TA-6-3. SID –Pu Loading Profile for Water Year 1997 – 1999 Average
Compared with Extreme Events 6-20
Figure TA-6-4. Model-Estimated Off-Site Groundwater Flux for Walnut Creek
Groundwater Basin – Wet Conditions Compared with Normal 6-21
Figure TA-6-5. Model-Estimated Off-Site Groundwater Flux for Woman Creek
Groundwater Basin – Wet Year Compared with Normal 6-21

604

TA-6 ACTINIDE TRANSPORT PATHWAYS ANALYSIS - BASED ON MODELED DATA FOR EXTREME CONDITIONS

TA-6.1 INTRODUCTION

Extreme events were modeled for the surface water, groundwater and air transport pathways for comparison with "normal" meteorological conditions, discussed in Section TA-1, that were used as a basis for analysis in Sections TA-4 and TA-5. Models used to generate the estimated extreme event actinide loads are the same as those identified and discussed in Section TA-5. Extreme event model results are compared with pathways described in the conceptual model to assess whether extreme conditions modify the relative importance of different migration pathways when compared with non-extreme conditions.

TA-6.2 SURFACE WATER PATHWAY – EXTREME CONDITIONS ANALYSIS

TA-6.2.1 Extreme Conditions Modeled

Evaluation of runoff and erosion for six design storms of varying intensity, duration and return interval was performed and presented in the *Soil Erosion and Sediment Transport Modeling of Hydrologic Scenarios for the Actinide Migration Evaluations at the Rocky flats Environmental Technology Site* (Kaiser-Hill, 2002). Modeling results from the following two design storms are presented in this report to provide perspective on surface water transport of Pu related to storm events:

- A 62.3-mm, 10-year, 6-hour event; and
- A 97.1-mm, 100-year, 6-hour event.

Pu loads transported by these storms in Walnut Creek and the SID were estimated using the WEPP hillslope erosion model coupled with the HEC-6T sediment transport model and integrated with Pu soil data. A thorough discussion of how the WEPP and HEC-6T models are integrated for predicting Pu transport in surface water is presented in the *Report on Erosion and*

605

Surface Water Sediment Transport Modeling for the Rocky Flats Environmental Technology Site (Kaiser-Hill, 2000).

The design-storm precipitation distributions were obtained from the RFETS Plant Drainage and Flood Control Master Plan (EG&G, 1992). The rainfall distributions are derived from the Colorado Urban Hydrograph Procedure (EG&G, 1992). The design storms were selected to represent specific return periods to assign a probability of occurrence to the erosion and sediment yields associated with each storm. The reciprocal of the return interval is the probability that the event will occur in any year (e.g., the annual probability of the 100-year event is 1 %).

Model results for storm events account for erosion and sediment transport of Pu in the stormwater runoff. The models are based on "worst-case" scenarios in terms of the ponds being full at the onset of the storm events, thereby minimizing the effective capacity of the ponds to settle actinide-bearing particles. The extreme event models simulate Pu transport only. Other transport mechanisms, such as groundwater transport and airborne deposition, were not considered in these surface water pathway mass balance analyses. The time duration required for those other mechanisms to have an impact on a watershed is much longer than the short duration of the extreme precipitation storm events.

TA-6.2.2 Lower Walnut Creek Extreme Event Analyses

10-Year, 6-Hour Storm

Results from the Pu mass balance analysis for lower Walnut Creek, using modeled data for the 10-year, 6-hour storm (62.3 mm), are presented in Table TA-6-1. Net gain or loss with the outflow load compared to inflow load is presented at the bottom of the table.

Table TA-6-1. Lower Walnut Creek – Pu Mass Balance Results – 10-Year, 6-Hour Storm

Pu-239/240 Inputs

Modeled Inputs

Input	Description	Load (pCi)
GS11	Pond A-4 Out	7.4E+06
GS08	Pond B-5 Out	1.6E+07
GS33	Tributary	2.8E+05
GS35	Tributary	6.2E+03
GS41	Tributary	5.5E+05
Total Modeled Inputs		2.5E+07

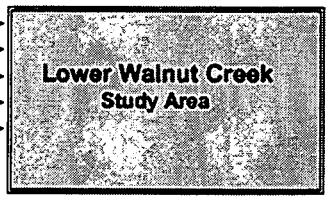

Pu-239/240 Outputs

Modeled Outputs

Output	Description	Load (pCi)
GS03	Walnut Ck	9.0E+07
Total Modeled Outputs		9.0E+07

Gain (+) or Loss (-) of Pu in Study Area

Variables	Delta (pCi)	Change from Input	Remarks
Modeled Data (Out - In)	6.5E+07	264%	Over 250% gain in Pu load in reach

607

100-Year, 6-Hour Storm

Results from the Pu mass balance analysis for lower Walnut Creek, using modeled data for the 100-year, 6-hour storm (97.1 mm), are presented in Table TA-6-2. Net gain or loss with the outflow load compared to inflow load is presented at the bottom of the table.

Table TA-6-2. Lower Walnut Creek – Pu Mass Balance Results – 100-Year, 6-Hour Storm

Pu-239/240 Inputs

Modeled Inputs

Input	Description	Load (pCi)
GS11	Pond A-4 Out	1.3E+07
GS08	Pond B-5 Out	3.4E+07
GS33	Tributary	2.1E+06
GS35	Tributary	2.9E+05
GS41	Tributary	1.3E+06
Total Modeled Inputs		5.1E+07

Lower Walnut Creek
Study Area

Pu-239/240 Outputs

Modeled Outputs

Output	Description	Load (pCi)
GS03	Walnut Ck	1.6E+08
Total Modeled Outputs		1.6E+08

Gain (+) or Loss (-) of Pu in Study Area

Variables	Delta (pCi)	Change from Input	Remarks
Modeled Data (Out - In)	1.1E+08	216%	Approx. 200% gain in Pu load in reach

Analysis of Lower Walnut Creek Extreme Event Modeling Results

Analysis of extreme event loads were compared with average annual loads for water years 1997 through 1999 in the lower Walnut Creek reach (Figure TA-6-1). Results presented in Figure TA-6-1 show that the model for the 10-year event, with the ponds in a full or "worst-case" condition at the onset of the storm, predicts approximately 6 times the Pu load off-Site past station GS03 compared with the average annual load based on 1997 – 1999 data. The 100-year event, also with the ponds full before the storm, is predicted to move approximately 11 times more Pu off-Site than the average annual load. If additional pond storage capacity is available before the onset of a storm, additional removal of Pu by the ponds will occur through the settling process and will therefore reduce the load entering the lower Walnut Creek study area.

TA-6.2.3 A- and B- Series Ponds Extreme Event Analyses

Results from the Pu mass balance analysis for the A- and B-Series Ponds, using modeled data for the 10-year, 6-hour storm, are presented in Table TA-6-3. Net gain or loss with the outflow load compared to inflow load is presented at the bottom of the table.

10-Year, 6-Hour Storm

Table TA-6-3. A- and B-Series Ponds – Pu Mass Balance Results – 10-Year, 6-Hour Storm

Pu-239/240 Inputs

Modeled Inputs

Input	Description	Load (pCi)
SW093	N. Walnut In	2.7E+06
GS10	S. Walnut In	2.9E+06
SW091	Tributary	2.1E+04
Total Modeled Inputs		5.6E+06

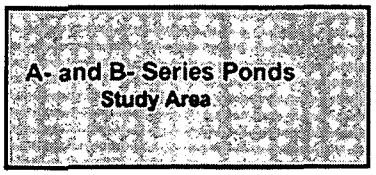

Pu-239/240 Outputs

Modeled Outputs

Input	Description	Load (pCi)
GS11	N. Walnut Out	7.4E+06
GS08	S. Walnut Out	1.6E+07
Total Modeled Outputs		2.4E+07

Gain (+) or Loss (-) of Pu in Study Area

Variables			
Modeled Data (Out - In)	Delta (pCi)	Change from Input Load	Remarks
	1.8E+07	323%	Over 300% gain in load

609

100-Year, 6-Hour Storm

Results from the Pu mass balance analysis for the A- and B-Series Ponds, using modeled data for the 100-year, 6-hour storm, are presented in Table TA-6-4. Net gain or loss with the outflow load compared to inflow load is presented at the bottom of the table.

Table TA-6-4. A- and B-Series Ponds – Pu Mass Balance Results – 100-Year, 6-Hour Storm

Pu-239/240 Inputs

Modeled Inputs		
Input	Description	Load (pCi)
SW093	N. Walnut In	8.2E+06
GS10	S. Walnut In	4.5E+06
SW091	Tributary	4.9E+04
Total Modeled Inputs		1.3E+07

→ **A- and B- Series Ponds**
Study Area →

Pu-239/240 Outputs

Modeled Outputs		
Input	Description	Load (pCi)
GS11	N. Walnut Out	1.3E+07
GS08	S. Walnut Out	3.4E+07
Total Modeled Outputs		4.7E+07

Gain (+) or Loss (-) of Pu in Study Area

Variables			
Modeled Data (Out - In)	Delta (pCi)	Change from Input Load	Remarks
	3.4E+07	269%	Over 250% gain in load

Analysis of A- and B-Series Ponds Extreme Event Modeling Results

Analyses of extreme event loads were compared with average annual loads for water years 1997 through 1999 for the A- and B-series ponds (Figure TA-6-2). Results presented in Figure TA-6-2 show that the model for the 10-year event, with the ponds full prior to the storm, predicts more than 2 times the Pu load transport past the ponds than the average annual load based on 1997 – 1999 data. The 100-year event, also with the ponds full before the storm, is predicted to move approximately 5 times more Pu past the ponds than the average annual load. Again, an important implication of the model results is that if the ponds are full at the onset of a storm, there is diminished time for settling and removal of Pu as typically occurs during normal precipitation conditions. Additional storage capacity in the ponds allows for increased detention time and more effective settling of Pu.

610

TA-6.2.4 SID Extreme Event Analyses

10-Year, 6-Hour Storm

Results from the Pu mass balance analysis for the SID, using modeled data for the 10-year, 6-hour storm, are presented in Table TA-6-5. Net gain or loss with the outflow load compared to inflow load is presented at the bottom of the table.

Table TA-6-5. SID – Pu Mass Balance Results – 10-Year, 6-Hour Storm

Pu-239/240 Inputs

Modeled Inputs

Input	Description	Load (pCi)
GS42	Tributary	1.6E+07
400 Area Runoff	Tributary	2.7E+04
600 Area Runoff	Tributary	2.2E+04
800 Area Runoff	Tributary	7.9E+04
Hillslope Erosion	Tributary	2.7E+08
	Subtotal	2.8E+08

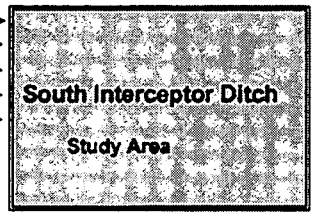

Pu-239/240 Outputs

Modeled Outputs

Output	Description	Load (pCi)
SW027	SID Out	3.3E+06
	Subtotal	3.3E+06

Total Inputs	2.8E+08

Total Outputs	3.3E+06

Gain (+) or Loss (-) of Pu in Study Area

Variables	Delta (pCi)	Change from Input Load	Remarks
Modeled Data (Out - In)	-2.8E+08	-99%	Large load accumulation in channel

611

100-Year, 6-Hour Storm

Results from the Pu mass balance analysis for the SID, using modeled data for the 10-year, 6-hour storm, are presented in Table TA-6-6. Net gain or loss with the outflow load compared to inflow load is presented at the bottom of the table.

Table TA-6-6. SID – Pu Mass Balance Results – 100-Year, 6-Hour Storm

Pu-239/240 Inputs

Modeled Inputs

Input	Description	Load (pCi)
GS42	Tributary	2.5E+07
400 Area Runoff	Tributary	3.5E+04
600 Area Runoff	Tributary	2.9E+04
800 Area Runoff	Tributary	1.0E+05
Hillslope Erosion	Tributary	5.1E+08
	Subtotal	5.4E+08
	Total Inputs	5.4E+08

South Interceptor Ditch

Study Area

Pu-239/240 Outputs

Modeled Outputs

Output	Description	Load (pCi)
SW027	SID Out	5.7E+08
	Subtotal	5.7E+08
	Total Outputs	5.7E+08

Gain (+) or Loss (-) of Pu in Study Area

Variables	Delta (pCi)	Change from Input Load	Remarks
Modeled Data (Out - In)	3.9E+07	7%	Approx. 7% gain in Pu load

Analysis of SID Extreme Event Modeling Results

Analyses of extreme event loads were compared with average annual loads for water years 1997 through 1999 in the SID (Figure TA-6-3). Modeling results indicate that for both the 10-year and 100-year storm events, hillslope erosion is the main source of actinide loading to the SID channel. This is expected based on the elevated concentrations of Pu in the SID watershed surface soils. For the 10-year, 6-hour storm, it is notable that nearly all of the Pu delivered from the hillslopes is predicted to settle out in the SID channel prior to reaching station SW027 at the downstream end of the SID. In contrast, for the 100-year event, 6-hour storm, there is not predicted accumulation of Pu in the channel. The Pu eroded from the hillslopes for the larger storm is all predicted to reach station SW027, plus additional Pu from sediment erosion.

612

Comparison of Figure TA-6-1, Figure TA-6-2 and Figure TA-6-3 indicates that the Pu load in surface water during extreme events is greater at the downstream end of the SID than at the downstream ends of lower Walnut Creek or the A- and B-Series ponds. The Pu load delivered to the end of the SID from a 10-year, 6-hour storm is approximately 2 times larger than the load delivered off-Site in Walnut Creek for the same storm. Similarly, the Pu load delivered to the end of the SID from a 100-year, 6-hour storm is approximately 4 times larger than the load delivered off-Site in lower Walnut Creek for the same storm. It is important to re-state that model predictions for Walnut Creek are based on "worst-case" scenarios where the detention ponds are full at the onset of the modeled storms and particle-settling processes in the ponds are therefore minimized.

The eastern SID watershed soils are the most contaminated soils on-Site. Overland flow and erosion on undisturbed soils in the SID watershed occurs only during larger storm events. However, when a large event does generate runoff and erosion, a large inventory of Pu currently exists in the SID watershed surface soil that can be mobilized and transported into surface water. Therefore, it is not surprising that the model estimates indicate more Pu transport for extreme events in the SID than in Walnut Creek. It is important to recognize an important distinction between Pu transport in the SID versus lower Walnut Creek. In the current Site configuration, actinide loads in the SID are not routed off-Site but rather are directed into Pond C-2 and detained, thereby allowing time for particle settling before later being released off-Site in a controlled manner. Remediation of Pu contamination in 903 Pad area soils will reduce Pu loads in the SID watershed during normal precipitation conditions as well as during extreme events.

613

TA-6.2.5 Summary of the Surface Water Pathway Extreme Events Analyses

Key findings from mass balances, calculated using model-predicted Pu transport in surface water resulting from hillslope erosion and sediment transport during extreme events, are summarized in this section. Model results support transport mechanisms identified in the conceptual model.

- **The Pu load delivered off-Site from Walnut Creek in a 100-year storm is roughly one order of magnitude greater than the load delivered off-Site in an average year.** The 100-year event is estimated to move approximately 11 times the average annual Pu load measured flowing off-Site in Walnut Creek, past station GS03 at Indiana Street. For the 10-year event, model results indicate an off-Site Pu load that is approximately 3 times larger than the amount of Pu discharged off-Site during an average year.

- **The Pu load estimated to be transported past the A- and B-Series ponds is larger for the 10- and 100-year storm events than during an average year, based on a "worst-case" scenario where the ponds are full at the onset of the storm.** Model results indicate the 10-year and 100-year events would transport approximately 2 and 5 times more Pu past the ponds, respectively, than in an average year. Less water held in the ponds prior to the storm will result in increased storage capacity and particle removal efficiency of the ponds during the storm.

- **The Pu load delivered to the end of the SID during extreme events is larger relative to other watersheds.** The Pu load delivered from the 100-year event to station SW027, at the downstream end of the SID, is approximately 4 times larger than the load delivered off-Site in Walnut Creek for the same storm. This is opposite to the trend observed for normal hydrologic conditions, where Walnut Creek yields roughly 4 times the average annual Pu load observed at the end of the SID. The eastern SID watershed soils have the highest levels of Pu contamination on Site, but model predictions indicate overland flow and erosion (and associated Pu transport) is markedly increased on these well-vegetated soils only during extreme events. Remediation of 903 Pad area soils will reduce Pu loads in the SID watershed for all storms events that generate runoff and erosion.

CEM

TA-6.3 GROUNDWATER PATHWAY – EXTREME CONDITIONS ANALYSIS

Using the MIKE SHE integrated flow system model discussed in Section TA-5, shallow groundwater flux off-Site was estimated for above-normal precipitation conditions using precipitation data for January through May of 1995. During this period, approximately 340 mm (13.5 in) or roughly twice the average amount of precipitation was measured at the Site. Model results provide insight into the increase in shallow groundwater flows during wet conditions. Figure TA-6-4 and Figure TA-6-5 present model-estimated monthly off-Site shallow groundwater flux volumes for Walnut and Woman Creeks, respectively, for Water Year 2000 (relatively normal precipitation conditions) with the first five months of Water Year 1995 (wet conditions). Model estimates of increased groundwater flux during wet precipitation conditions were most notable for May 1995, when 194 mm (7.65 in) of precipitation occurred or roughly three times the May norm. The estimated shallow groundwater off-Site flux in May 1995 increased by approximately 100 % in the Walnut Creek drainage and approximately 50 % in the Woman Creek drainage compared with Water Year 2000. The Woman Creek groundwater basin model also includes shallow groundwater flux associated with the Mower Ditch region, similar to model results presented in Section TA-5.

Modeling Water Year 1995 provides insight into the magnitude of increased shallow groundwater flux off-Site that can be expected during wet conditions. Changes in shallow groundwater actinide concentrations during wet conditions, including potentially reduced concentrations resulting from dilution effects, were not modeled. Assuming the concentration of actinides in shallow groundwater remained constant during wet conditions, the increase in off-Site groundwater flux would cause a corresponding relative increase in off-Site actinide transport.

615

TA-6.4 AIR PATHWAY – EXTREME CONDITIONS ANALYSIS

During FY00 and FY01, the model described in Section TA-5.4.2 was used to estimate actinide concentrations and deposition due to remediation, decommissioning and fire-related scenarios.

The FY01work also estimated the airborne actinide concentrations and deposition that would result from normal resuspension processes following Site closure, assuming an absence of significant soil disturbance (consistent with wildlife refuge uses). The potential effect of periodic disturbances on resuspension following Site closure was reviewed in the FY00 work (Radian, 2000; URS, 2001)

The FY00 and FY01 air pathway work was designed to investigate emission scenarios and events that may be of interest with regard to actinide migration during and after Site closure. The scenarios were not intended to provide definitive data regarding specific remediation or decommissioning projects because many pertinent details of those actions are still undergoing review and refinement. Instead, the modeling was intended to provide reasonable upper bounds for the expected impacts of closure activities and post-closure Site configurations.

The conclusions reached from the FY00 and FY01 scenario modeling effort are summarized in below:

TA-6.4.1 Air Pathway Analysis - Extreme Events and Alternative Scenarios

Modeling conducted in FY00 examined the effects that a variety of events and emission scenarios would have on airborne actinide concentrations. Because off-Site transport of actinides though the air pathway will be related to concentrations, the effect of such events on off-Site transport can be inferred, to some extent, from the modeling results. The revised emission methodology and modeling conducted in FY01 reexamined impacts from post-fire and post-closure scenarios. The scenarios modeled and conclusions drawn are summarized below:

- **Post-closure wind erosion impacts.** Wind erosion from undisturbed vegetated surfaces at the Site under current conditions results in small airborne actinide concentrations and modest amounts of deposition. Post-closure impacts and off-Site transport through the air pathway

6116

may increase somewhat with removal of paved areas and buildings, which would expose larger areas to wind erosion. Comparison of maximum impacts for pre-closure wind erosion and post-closure wind erosion scenarios (assuming cleanup of Site soils to RFCA Tier I levels [DOE et al., 1996]) predicted airborne concentrations of Pu-239/240 and Am-241 over the center of the Site that were approximately double those estimated for wind resuspension under current conditions (URS, 2001), while fenceline concentrations were predicted to increase by approximately 10 % or less. It should be noted that in all cases the resulting maximum concentrations were predicted to be well below EPA standard limitations. The increase in airborne concentrations following Site closure would be expected to result in a similar increase in off-Site transport;

- **Periodic disturbances.** Periodic disturbances of soil or vegetation would increase airborne concentrations in proportion to their frequency and the amount of surface area involved. Off-Site transport would also be expected to increase consequently;

- **Remediation.** Remediation would result in short-term increases in actinide concentrations in air and in off-Site transport. The scenario modeled in FY00 (Radian, 2000), which assumed cleanup of the 903 Pad area to RFCA Tier I levels using minimal emission controls, did not predict actinide concentrations that would exceed federal or Colorado standards. Maximum off-Site annual average concentrations of Pu-239/240 and Am-241 would increase during remediation but the increase would be less than a factor of two. Off-Site transport would be expected to increase by similar amounts. U impacts from remediation of the 903 Pad area would be considerably less than the contribution from naturally-occurring U due to wind blown dust. The inclusion of additional particulate matter controls could lower impacts further, while cleanup to more restrictive standards would increase impacts and off-Site transport. A high wind event occurring during remediation would increase emissions from disturbed ground areas and from storage piles. Excavation activities and traffic would cease, however, which would limit emission increases. Over a 24-hour wind event, off-Site concentrations of Pu-239/240 and Am-241 would be expected to increase by a factor of two or less, with off-Site transport showing similar increases. Consequently, high winds during a

617

remediation project would be expected to show effects on off-Site transport of actinides that are similar to those of other remediation activities that generate particulate matter emissions, such as excavation and traffic. Following remediation, disturbed areas would be subject to increased rates of wind erosion until a growing cycle was complete and a new layer of thatch was laid down. Worst-case increases in erosion potential are discussed below in relation to the effects of a wildfire. Revegetation activities involving protective mulch and fast-growing plants would minimize this effect;

- **Decommissioning**. The release of an unexpected "pocket" of contaminated concrete during decommissioning could result in relatively high but very short-lived impacts that would increase overall actinide transport off Site by insignificant amounts. Maximum impacts would occur very near the point of release, within Site boundaries and impacts at the fenceline would be several orders of magnitude lower. On an annual average basis, off-Site transport would be minimally-impacted because of the short duration of the increased concentrations;

- **Wildfire.** A wildfire could result in high, short-term particulate matter concentrations (for example, PM_{10} concentrations within the plume were estimated to be several hundred times the normal PM_{10} concentrations at RFETS and such levels could persist for the duration of the fire). The significance of the impacts depends both on the size of the burned area and the weather conditions during the fire. Light winds and stable conditions would contribute to higher pollution levels at the ground than windy conditions, although a wildfire is likely to burn a much larger area under high winds. Airborne actinide concentrations would vary depending on where on the Site the fire occurs;

- **Post-fire.** Post-fire wind erosion would increase from the burned areas. Wind erosion following a fire in the 903 Pad area was predicted to cause as much as a 5- to 13-fold increase in annual actinide concentrations when compared to unburned conditions. Particulate matter concentrations were predicted to increase by smaller amounts. The increases in particulate matter and actinide concentrations associated with the aftereffects of a wildfire would vary with the location of the fire and with the time of the year that the fire

Vol 8

occurred. A fall fire would cause greater concentration increases than a spring fire because vegetation would recover more slowly over the winter months than during the spring and summer. For example, the post-fire resuspension scenarios modeled in FY01 predicted that, over the course of a year, recovery from a spring fire near the 903 Pad would result in a 5- to 8-fold increase in actinide impacts from the burned area. In contrast, a fall fire in the same location, representing a reasonable worst-case vegetation recovery scenario, would increase actinide impacts from the burned area 9- to 13-fold. The post-closure vegetative recovery scenarios showed somewhat higher concentrations than the pre-closure scenarios. The reason is that the area of the 903 Pad itself would become a source subject to wind erosion after the asphalt covering is removed. To put these results in perspective, the worst-case, pre-closure fire was predicted to result in an annual Pu-239/240 effective dose equivalent (EDE) of approximately 7.5 millirem (mrem) and an Am-241 EDE of 3.05 mrem. These concentrations represent a receptor located within the burned area itself. At the Site fenceline, predicted worst-case, post-fire concentrations totaled 0.038 mrem Pu-239/240 and 0.011 mrem Am-241.

- **Post-Closure.** Post-closure impacts would be somewhat higher for a fire in the same location; a total of 10.5 mrem Pu-239/240 and 3.16 mrem Am-241 for a receptor located within the burned area and 0.055 mrem Pu-239/240 and 0.013 mrem Am-241 for a fenceline receptor. For comparison, the EPA NESHAP standard limits emissions of radionuclides from DOE facilities to amounts that would result in annual off-Site impacts of no more than 10 mrem. The increased wind erosion that would follow a fire would also increase off-Site transport, but the increase would be highly dependent on the distance from the burned area to the fenceline. The increased emissions would only apply to the actual area burned; adjacent, unburned areas would be unaffected. Wind erosion rates would generally be expected to return to a pre-burn state within a year or so; the effect would not be ongoing after a new layer of thatch has been developed. Although a fire would remove the vegetation and thatch that provides erosion protection for the soil, increases in emissions would be limited by the tendency of the soil to crust and by the remaining roughness elements, such as rocks, large soil particles and burned vegetation clumps, that also limit wind resuspension. As with

619

unburned conditions, total erosion is limited by the fact that there is a limited supply of particles available for erosion. Wind events would temporarily deplete this reservoir on the burned area, just as they would an unburned area; and

- **High winds.** High winds can resuspend much larger amounts of particulate matter and actinides than lower wind speeds, with resulting increases in downwind concentrations and off-Site transport. The effect of increasing wind speed on emissions is particularly pronounced if the ground surface has been disturbed by traffic or excavation or any other natural or man-induced event that renews the erosion-prone surface layer of soil. As noted above, however, the effect is temporary because the supply of particles available for erosion is rapidly depleted by high winds. Consequently, increased emissions and off-Site transport may only increase for a few minutes to a few hours, at most, during windy periods at the Site. Resuspension after a wind event will actually decrease for a period until additional particles are deposited or otherwise generated.

620

TA-6.5 BIOLOGICAL PATHWAY – EXTREME CONDITIONS ANALYSIS

Extreme conditions were not evaluated for the biological actinide transport pathway. However, an estimation of the potential impact to biological actinide transport from a hypothetical extreme event, such as a flood or range fire, can be made based on results presented in Section TA-5. In the estimation approach presented in Section TA-5, approximately 5 % of the mule deer were estimated to leave the Site annually based on radio-telemetry tracking data (Symonds and Alldredge, 1992). If an extreme event caused 100 % of the mule deer to leave the Site, then the estimates for off-Site actinide transport by mule deer presented in Section TA-5 could be increased by a factor of 20.

C621

TA-6.6 TECHNICAL APPENDIX SECTION TA-6 REFERENCES

DOE, EPA and CDPHE. 1996. Final Rocky Flats Cleanup Agreement. July, 1996.

EG&G. 1992. Rocky Flats Plant Drainage and Flood Control Master Plan, Rocky Flats Plant, Golden, CO.

Kaiser-Hill. 2000. Report on Erosion and Surface Water Sediment Transport Modeling for the Rocky Flats Environmental Technology Site, Golden, CO. August, 2000.

Kaiser-Hill. 2002. Soil Erosion and Sediment Transport Modeling of Hydrologic Scenarios for the Actinide Migration Evaluations at the Rocky Flats Environmental Technology Site, Golden, CO. April, 2002.

Radian. 2000. Air Transport and Deposition of Actinides for the Actinide Migration Evaluation at the Rocky Flats Environmental Technology Site. Radian International, Denver, CO.

Rocky Mountain Remediation Services (RMRS). 2000. Report on Soil Erosion and Surface Water Sediment Transport Modeling for the Actinide Migration Evaluation at the Rocky Flats Environmental Technology Site. Report 00-RF-01823. Prepared for Kaiser-Hill Company, Rocky Flats Environmental Technology Site, Golden, Colorado.

Symonds, K.K. and A.W. Alldredge. 1992. Deer Ecology Studies at Rocky Flats, Colorado; 1992-1992 Progress Report. Agreement ASC 49074 and ASC 77313AM. Colorado State University, Ft. Collins, CO. Summer, 1992.

6022

Figure TA-6-1. Lower Walnut Creek – Pu Loading Profile for Water Year 1997 – 1999 Average Compared with Extreme Events

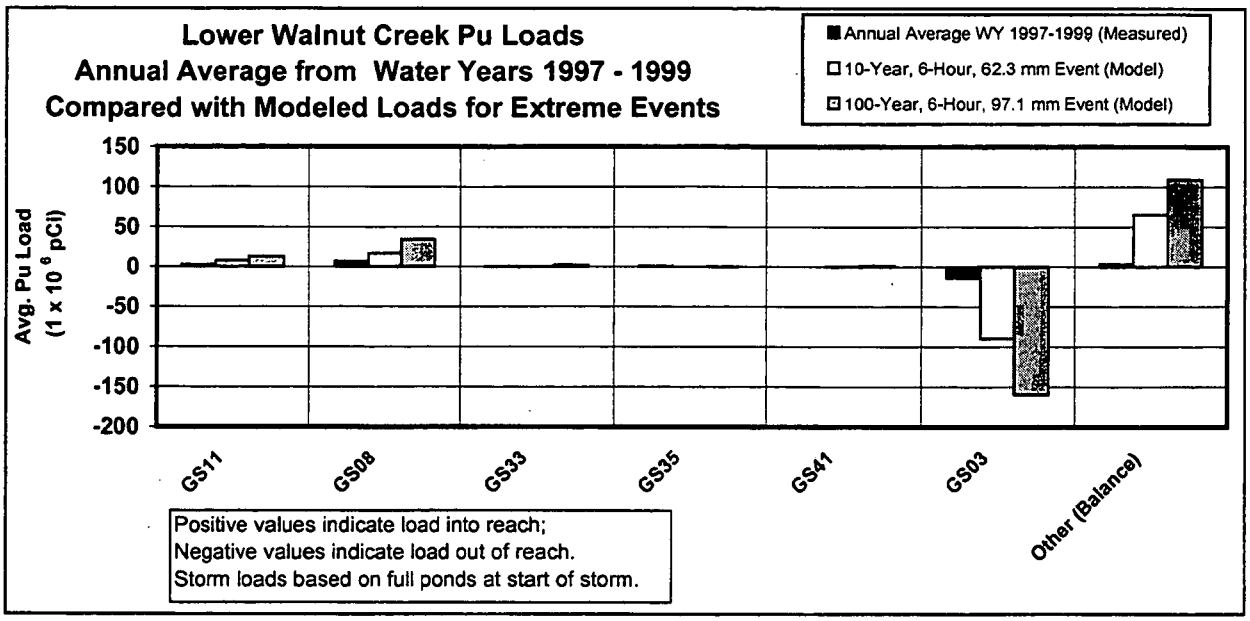

Figure TA-6-2. A- and B-Series Ponds – Pu Loading Profile for Water Year 1997 – 1999 Average Compared with Extreme Events

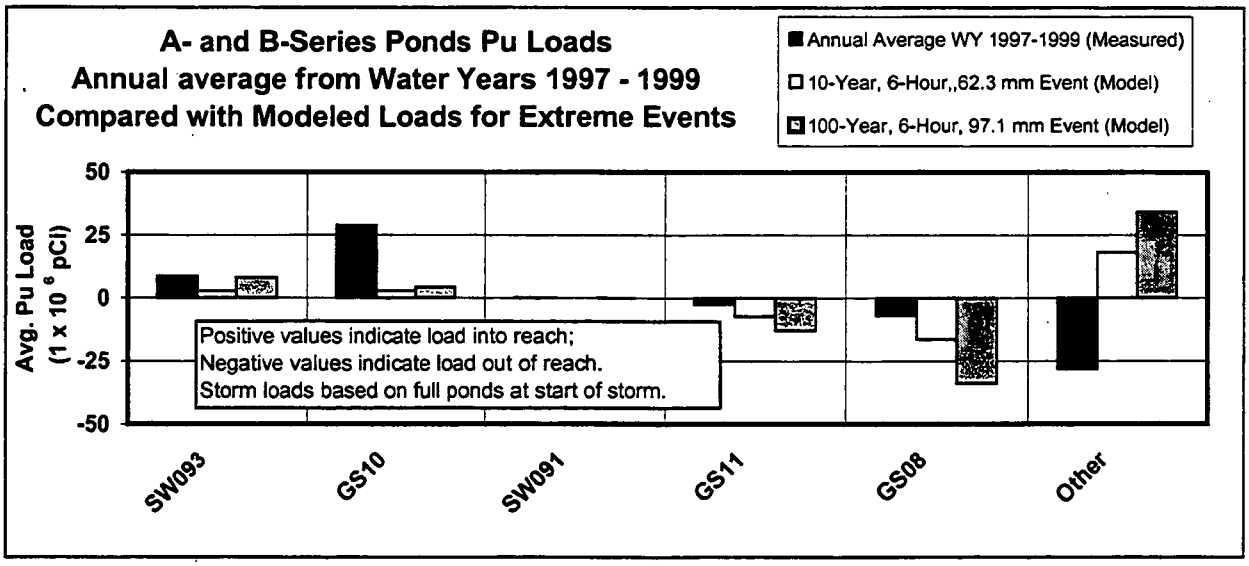

423

Figure TA-6-3. SID –Pu Loading Profile for Water Year 1997 – 1999 Average Compared with Extreme Events

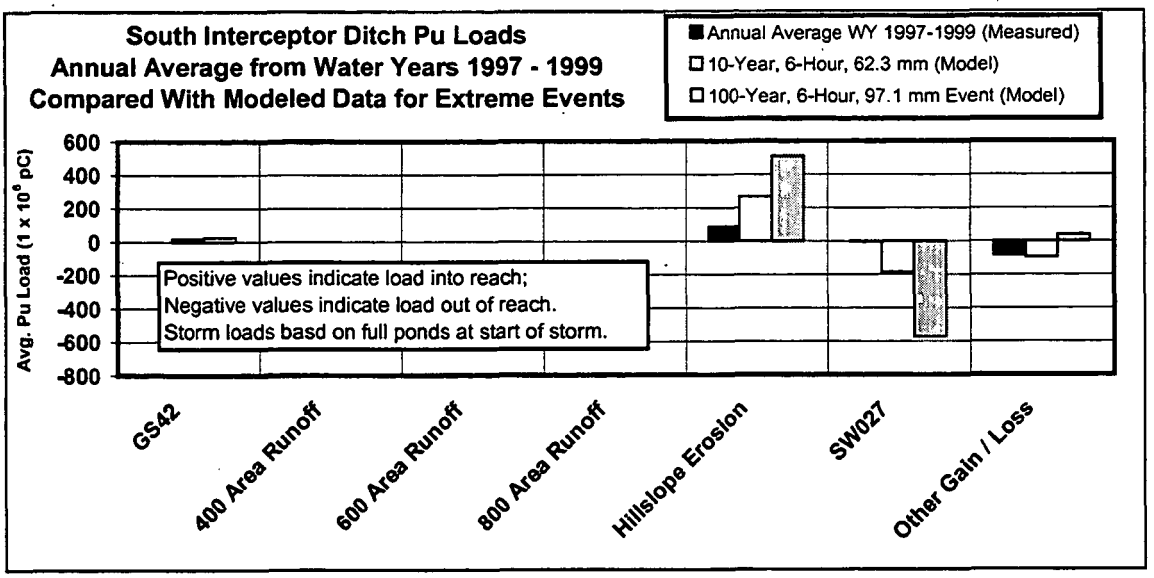

624

Figure TA-6-4. Model-Estimated Off-Site Groundwater Flux for Walnut Creek Groundwater Basin – Wet Conditions Compared with Normal

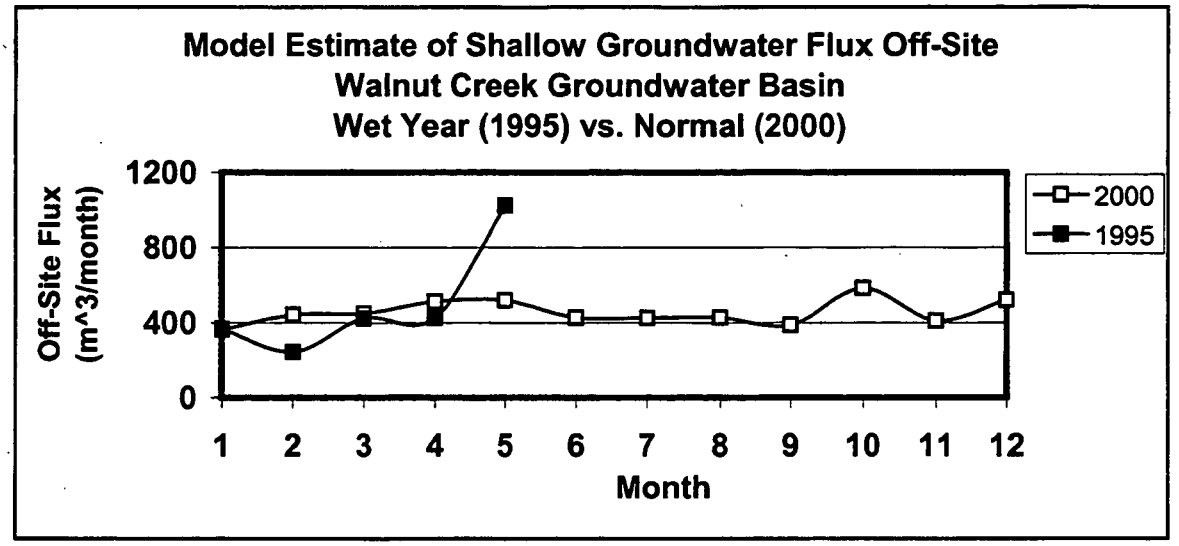

Figure TA-6-5. Model-Estimated Off-Site Groundwater Flux for Woman Creek Groundwater Basin – Wet Year Compared with Normal

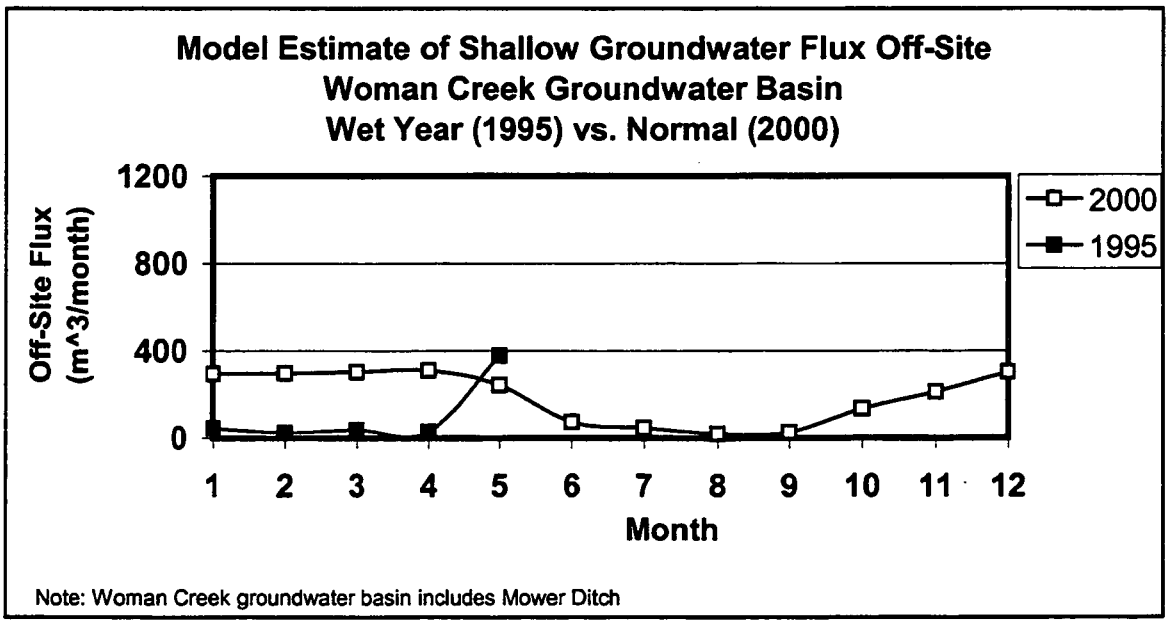

625

SECTION TA-7 - TABLE OF CONTENTS

TA-7 SUMMARY AND CONCLUSIONS 7-1

TA-7.1 Summaries of Major Topics 7-1

TA-7.1.1 Actinide Sources 7-1

TA-7.1.2 Pu, Am and U Geochemistry 7-2

TA-7.1.3 Surface Water Actinide Transport 7-3

TA-7.1.4 Groundwater Actinide Transport 7-5

TA-7.1.5 Airborne Actinide Transport 7-6

TA-7.1.6 Biological Actinide Transport 7-8

TA-7.1.7 Summary of Identified Data Gaps 7-10

TA-7.1.8 Pathway Comparison 7-11

TA-7.1.9 Evolution of the Conceptual Model 7-12

TA-7.2 Conclusions 7-13

SECTION TA-7 FIGURES

Figure TA-7-1. Estimated Off-Site Annual Actinide Loads (Logarithmic-Scale) 7-14

Figure TA-7-2. Modified Conceptual Model for Pu and Am Transport 7-15

426

This page intentionally blank

W27

TA-7 SUMMARY AND CONCLUSIONS

TA-7.1 SUMMARIES OF MAJOR TOPICS

Major subjects addressed in the Technical Appendix are summarized below. Findings that support or are different than actinide transport pathways identified in the conceptual model are noted as appropriate.

TA-7.1.1 Actinide Sources

There are background levels for Pu and Am at RFETS that arise from non-RFETS activities. Global fallout from atmospheric weapons testing dispersed low levels of Pu and Am to surface soil around the world. This causes a "background level" of Pu and Am to be transported by the surface water, air and biological pathways.

A significant natural U background exists at RFETS that complicates the determination of how much U at the Site has been contributed by RFETS activities. U occurs naturally in the earth's crust, particularly in the Front Range near RFETS. The natural abundance of U causes a background level to be transported by the surface water, air, groundwater and biological pathways. Progress is being made on differentiating natural from anthropogenic U using characteristic differences in isotopic abundances. Studies indicate that the only easily detectable RFETS contribution to U in soil and groundwater is in the immediate vicinity of the primary sources. Beyond the immediate vicinity of the sources, specialized isotopic ratio analyses are required to distinguish anthropogenic U from background activity.

Species of very low solubility, which are predominantly those containing Pu and Am, have remained largely at and near the location of their initial release over approximately a 30 year period. Approximately 90 % of the Pu and Am measured in soil is in the top 12 centimeters and nearly all is confined to the top 20 centimeters of the soil surface. These effectively insoluble actinides are mostly (greater than 99 %) associated with solids, either strongly sorbed to soil particles or precipitated as oxides and hydroxides. Transport of Pu and

628

Am solid species at RFETS is chiefly by wind, soil and pond sediment erosion processes. Transport by dissolution into groundwater is not significant.

Over 50 % of the actinide source locations identified in the Historical Release Report did not have surface or sub-surface soil data for Pu, Am and U. Using the data acceptance criteria used for this report, 120 out of 215 total actinide source locations had no data for the three actinides studied in this investigation. Source locations designated as active IHSS, UBC, NFA or Recommended NFA were included in the evaluation.

TA-7.1.2 Pu, Am and U Geochemistry

Transport mechanisms are controlled by solubilities. Chapter TA-3 of the Technical Appendix presents the geochemical transport processes for Pu, Am and U species resulting from actinide releases to the environment. These transport mechanisms are based on extensive review of experimental and theoretical literature. On-Site studies at RFETS, which are in agreement with the conceptual model, indicate that the main transport mechanisms for Pu, Am and U are controlled by the solubilities of the actinide chemical species formed under environmental conditions at the RFETS.

Oxidation state of the actinide effects solubility. The oxidation state of actinides has a controlling effect on their environmental behavior. Oxidation states, in turn, are determined by each actinide's unique electron structure and the chemical conditions of surrounding soil and water. The actinide oxidation states of environmental interest are III, IV, V and VI. Different oxidation states can form various molecular complexes, each with a characteristic solubility and chemical reactivity. Actinides in the lower oxidation states (III and IV) tend to form complexes with very low solubilities and the strongest sorption to mineral and rock surfaces. Actinides in the higher oxidation states (V and VI) tend to form complexes with much higher solubilities and the weakest sorption to mineral and rock surfaces.

Because of oxidation state differences, the environmental behavior of Pu and Am is very different from that of U. Whereas Pu and Am tend to be in the lower oxidation states III (Am) and IV (Pu) under environmental conditions, U is most stable in the IV and VI oxidation states.

629

Because U(VI) forms compounds of much greater solubility than do Pu(IV) or Am(III), U exhibits a much greater tendency to be in soluble forms than do Pu or Am.

Mobility of Pu and Am at RFETS is largely controlled by soil surface erosion processes. Measurements of actinide movement caused by wind and surface water runoff show that the observed mobility of Pu and Am at RFETS is largely controlled by soil surface erosion processes and is essentially the same as the mobility of the surface soils and stream sediments.

Unlike Pu and Am, environmental U species can undergo significant subsurface transport, although measured levels of U at RFETS are difficult to distinguish from background. Except in the immediate vicinity of source terms, data concerning the historical distribution of natural U will be useful for predicting the movement of anthropogenic U, since U from RFETS sources will be subject to the same geochemistry and dispersal mechanisms as background U.

TA-7.1.3 Surface Water Actinide Transport

Analysis of measured and modeled Site data indicate actinide transport patterns that almost fully support the transport mechanisms addressed in the conceptual model. An exception is that modeled data indicate airborne transport of Pu to surface water may, in the case of the ponds, be more significant than expected in the conceptual model.

Pu activity concentrations in surface water vary by up to a factor of 40 from drainage to drainage. Average Pu activity concentrations measured in surface water range from 0.191 pCi/L, for central Industrial Area runoff monitored at station GS10, to 0.005 pCi/L for Woman Creek at station GS01 located near Indiana Street.

U activity concentrations in surface water are relatively uniform across the Site. Due to similar U concentrations, U load delivered by one basin or another is largely a function of each basin's water yield. Though surface water across the Site has U concentrations well below the MCL standard for drinking water, high resolution analytical techniques are planned to definitively determine whether any U from anthropogenic sources is impacting Site surface water.

630

The central Industrial Area has the highest Pu loads in surface water per square meter of drainage area, although it is *not* the area with the highest Pu concentrations in surface soil. Central Industrial Area runoff, monitored by Station GS10 on South Walnut Creek, has the largest Pu load of any sub-basin (2.9E+07 pCi/year). The average annual Pu load delivered per square meter at GS10, (42.5 pCi/m^2/year) exceeds the next highest major sub-basin by nearly a factor of five. However, the GS10 sub-basin does not have the highest Pu surface soil concentrations at the Site. Nearly half of this basin is composed of impervious Industrial Area surfaces that generate large volumes of runoff during storms. The higher runoff causes erosion and actinide loading in surface water. In contrast, the SID drainage has areas near the 903 Pad with the highest known levels of Pu activity in soil at the Site, but the basin is largely well-vegetated and therefore, under normal precipitation conditions, much less runoff is generated that can cause erosion and transport actinides. The surface water Pu load discharged per square meter of the SID basin (3.8 pCi/m^2/year) is roughly one tenth of the load per square meter of watershed measured in the central Industrial Area runoff.

For extreme conditions, the SID may yield proportionately higher actinide loads. Model results indicate a hypothetical 100-year, 6-hour storm event (97.1 mm) would cause erosion in the SID basin and result in Pu loads to the channel that are two to three orders of magnitude higher than observed in the Walnut Creek basin. Remediation of soils within the SID watershed will reduce actinide loads transported in extreme events.

The detention ponds on North and South Walnut Creeks serve to settle out particulates and generally remove 80 % to 90 % of the annual Pu and Am load that flows into the ponds. This corresponds with Site research that demonstrates approximately 10 % of the Pu and Am flowing into the ponds is sorbed to colloid particles that are not likely to settle in the ponds. Another important observation regarding Pu transport involves the lower section of Walnut Creek. The average annual Pu load measured in Walnut Creek near the Site boundary is approximately 30 % greater than the Pu load measured upstream, below the detention ponds. Site investigations indicate the Pu source in this area is diffuse, low-level legacy contamination in soils and sediments (RMRS, 1998).

Deposition of airborne Pu and U to surface water contributes a negligible input to surface water loads in most cases. Model estimates for the airborne transport of Pu and U-238 to surface water indicate a relatively minor input load, less than one percent of the total, for all actinides in all study areas, with one exception. In the case of the A- and B-Series ponds, the modeled deposition of airborne Pu accounts for 12 % of the total input load. The large surface area of the ponds causes them to be impacted more by airborne actinide deposition than channel reaches without ponds. This unique case is counter to the conceptual model, which identifies the air-to-surface water pathway as minor.

Groundwater is a minor pathway of Pu and Am transport to or from surface water. The estimated average annual load of Pu conveyed in groundwater comprises one percent or less of the total input or output load for any of the areas studied. The potential for colloidal Pu to be transported in the groundwater is acknowledged and assumed to be the mechanism by which groundwater Pu transport would most likely occur.

Groundwater is a major pathway of U transport to or from surface water. Model estimates for U-238 in groundwater ranged from 7 % of the output load in lower Walnut Creek to 83 % of the input load in the SID basin. This is in contrast to groundwater transport of Pu, for which 1 % or less of the total input or output load was estimated in all study areas.

TA-7.1.4 Groundwater Actinide Transport

At RFETS, potential groundwater actinide transport involves lateral, shallow groundwater flow in the alluvium and weathered bedrock geologic units. Shallow groundwater at the Site does not percolate down toward the regional Laramie-Fox Hills aquifer. A thick, intervening layer of impermeable claystones in the Laramie Formation prevents vertical movement from the shallow groundwater down to the regional aquifer.

Shallow groundwater and surface water are inextricably linked. Similar to surface water, an actinide's solubility dictates its transport in shallow groundwater. Pu and Am are relatively immobile in the soil and groundwater because of their low solubility and tendency to sorb onto soil. However, work at RFETS and studies in the literature have shown that insoluble actinides

632

can sorb to natural, sub-micrometer-sized colloid particles that can potentially facilitate actinide movement. In addition to colloidal transport, sub-surface actinide transport can also occur when more soluble actinides, such as U in the VI oxidation state, move in solution with the groundwater.

Determination of Pu and Am levels in shallow groundwater is complicated by residual surface soil contamination potentially introduced down boreholes during drilling and well installation operations. Low levels of Pu and Am have been detected in shallow groundwater wells at the eastern Site boundary. However, determination of Pu and Am levels in shallow groundwater is complicated by residual surface soil contamination potentially introduced down boreholes during the well installation process. New clean or "aseptic wells" were drilled and efforts to improve sampling protocols are currently ongoing. For this analysis, Pu and Am activity measured in shallow groundwater wells may represent activities higher than what actually exists in the shallow groundwater.

U-233/234 and U-238 isotopes are the dominant actinides found in shallow groundwater in terms of total activity because of their natural abundance. U in RFETS shallow groundwater is generally within the range of U detected naturally. Data from high-resolution ICP/MS analyses indicate that U in most areas of the Site is from natural sources. However, shallow groundwater samples at the Site boundary in the Walnut and Woman Creek groundwater basins have a U-235/U-238 ratio that is slightly less than found naturally. Though potentially related to analytical uncertainty, these results indicate that the alluvial groundwater in these basins has a signature indicating a small fraction of the uranium is "depleted" U.

TA-7.1.5 Airborne Actinide Transport

Transport of actinides through the air occurs largely by wind erosion of actinide-containing particulate matter from Site soil and dust-laden vegetation. The general direction of airborne actinide transport follows the prevailing winds, from the northwest to the southeast. More importantly, higher winds, which transport exponentially larger loads than lower winds, occur almost exclusively from the northwest quadrant.

633

The amount of activity from airborne U-238 and U-234 is nearly 100 times the amount measured from airborne Pu at the Site as a result of the natural U inventory in the soil. Airborne U is primarily from wind erosion of soils that contain natural-occurring U. Airborne loads of Pu and Am are primarily caused by wind erosion of contaminated soils near and east of the 903 Pad area. The perimeter air monitoring location with the highest total airborne actinide concentration from 1997 through 1999 was station S-140 beside Indiana Street in the southeast corner of the Site. This location had airborne actinide concentrations totaling approximately 1.4 % of the 10 millirem regulatory standard governing airborne radionuclide concentrations at DOE facilities.

Wind erosion has been determined to represent the majority of air emissions transported from the Site during recent years. Off-Site transport was calculated for Pu-239/240 and Am-241 as the difference between annual wind erosion emissions from the Site and deposition of actinides back onto the Site. Off-Site transport through the air pathway was estimated using measured data and emission deposition model results from the FY01 air pathway modeling.

Any activity that disturbs the soil, whether natural or anthropogenic, will increase the potential for wind resuspension for some period of time. As discussed in Section TA-6, various hypothetical events and activities analyzed through modeling would produce higher rates of off-Site transport than occur under current Site conditions. Post-closure emissions could be somewhat higher than current emissions from undisturbed areas because removal of buildings and roads will expose more surface area to wind resuspension. High winds result in higher rates of emission than calm or breezy conditions but the effect may be temporary as erodible particles are rapidly depleted. Closure activities such as decommissioning may also temporarily increase emissions and off-Site transport. Generally, decommissioning activities have a low probability for significant actinide emissions to air because building surfaces will be decontaminated prior to demolition. However, release from an unexpected pocket of contamination could result in elevated emissions for a very short period.

634

Remediation activities have a higher potential for emissions of actinides bound to soil particles because, in addition to particulate matter emissions that will occur during earth moving activities such as excavation, disturbance of the soil increases the reservoir of erodible particles. Two practices that are routinely employed at the Site during such activities greatly limit this potential cessation of outside work during high winds and revegetation efforts when soil disturbance has ceased.

Model results for a hypothetical rangeland fire indicate a 5- to 13-fold increase in airborne annual actinide concentrations would be expected for a wildfire in the vicinity of the 903 Pad for the first year following a fire. A wildfire at the Site would result in temporary increases in emissions of particulate matter from the smoke plume. The amount of actinide emissions would depend on where the fire occurred. Post-fire resuspension would increase until vegetation and thatch was restored. Emission estimation and modeling based on recent wind tunnel studies at the Site indicated a 5- to 13-fold increase in annual actinide concentrations would be expected for a wildfire in the vicinity of the 903 Pad for the first year following a fire.

TA-7.1.6 Biological Actinide Transport

RFETS-specific studies and other scientific literature indicate that Pu has low bioavailability, due to its insolubility and uptake into plant and animal tissues is minor. There is little accumulation of Pu in the tissues of arthropods, small mammals, snakes and mule deer and biomagnification through the trophic levels does not appear to occur. In the terrestrial communities, vegetation studies from the early 1970s through the early 1990s have concluded that much of the Pu associated with plant material adheres to the surface, rather than as Pu incorporated into plant tissues. Results from these studies suggest that as Pu availability and uptake by plants has declined over time, the amounts available to primary consumers have also decreased and thus the potential for redistribution has declined. Additionally, Pu-contaminated soil redistribution through burrowing is a limited-area phenomenon and this process has only local effect. Other terrestrial or semi-aquatic (e.g., ducks) species are estimated to transport less actinides than the deer to off-Site areas, but no data are available for more accurate quantification.

635

Limited aquatic studies at RFETS indicate an insignificant potential for biota to redistribute Pu in aquatic systems. Paine (1980) found that an increase in trophic level concentration of Pu did not occur. There appeared to be a selective mechanism, which discriminated against Pu at the phytoplankton to zooplankton level. The highest concentration in crawfish was found in the exoskeleton. Whole fish had detectable activity, but fish flesh showed none. These results point to low bioavailability of the Pu due its chemical partitioning to solid particles.

The estimated Pu load transported off-Site annually by deer movement is approximately 5 to 6 orders of magnitude less than transported by the surface water and air pathways. The Pu activity transported off-Site by deer movement is estimated to be approximately 200 to 1000 pCi annually. This estimated off-Site transport load is approximately 5 to 6 orders of magnitude less than the off-Site loads estimated for the surface water pathways. Mule deer have been studied as the most probable biological pathway for off-Site actinide movement because of their mobility, amount of soil intake and size of the herd.

Microbial metabolic processes affecting radionuclide solubility are significant and varied. Given the time frame required, the potential for significant microbial effects on transport are increased and therefore the metabolic process performed by microorganisms when interacting with radionuclides must become part of performance assessment. These processes include, but are not limited to, sorption/precipitation, complexation/chelation and biodegradation of complexed actinides, dissolution, oxidation/reduction reactions and colloidal agglomeration. Additionally, microorganisms create microenvironments of nutrient and chemical gradients, capable of altering radionuclide solubilities. Although no Site-specific geomicrobiological data exists, one can safely assume that many or all of the geomicrobiological processes discussed herein are in place and operative at RFETS. These processes are important to understand, not only to provide a more complete understanding of ongoing and potential actinide transport pathways, but also for potential development and expansion as part of a site remediation program.

636

The soil microbial population should be regarded as being stable and this stability becomes an important parameter when developing performance evaluations for the migration of radionuclides. Because of its stability, the soil community will be in place and metabolically active, however diminutive, for the entire time frame under consideration.

TA-7.1.7 Summary of Identified Data Gaps

Data gaps identified in the AME Pathway Report are summarized below in order of perceived importance to Site closure:

- Some buried sources with potential actinide contamination, such as Process Waste Lines, have not been characterized. Process Waste Lines are known to have contained high concentrations of actinides and represent potentially significant actinide sources. It is recognized that extensive further characterization of the Industrial Area is planned;

- Actinide data exist for all environmental media at approximately one half of actinide source areas identified in the HRR, including IHSS, UBC and Proposed NFA sites. These data are potentially important depending on the nature and location of the actinide source;

- Surface water isotopic U data are not collected at boundary monitoring stations GS01, on Woman Creek or GS03, on Walnut Creek. The current RFCA POC locations for total U in surface water are at the terminal pond outfalls upstream from stations GS01 and GS03. Although U data at the Site boundary would be of interest, U concentrations in surface water have historically not been a compliance issue and are believed to be largely natural U. ICP/MS analysis is planned to determine where surface water at the Site contains anthropogenic U.

- Models have not been developed for hillslope runoff of U. Again, U concentrations in surface water have not been an issue in terms of compliance with water quality regulations;

- Recent actinide data do not exist for vegetation in the Macroplot 1 study area and surface contamination of vegetation effects all pathways, either directly or indirectly. However, the

631

analysis and conclusions of previous studies in this area are believed to still be relevant to current Site conditions;

- Historic biological studies addressed Pu, not U. Although the Pu results can reasonably be inferred to resemble the biological transport patterns expected for Am, there is an absence of information regarding biological transport of U. However, data indicate the biological transport pathway is relatively minor and U transport via biota is not considered to be significant; and

- Microbiological soil profile data do not exist. Although the soil microbe populations have not been characterized at RFETS, the microbes will remain in existence following Site closure. Therefore, although obtaining soil profile data may prove interesting, addressing this data gap would not necessarily lead to any changes being implemented during the Site closure process.

TA-7.1.8 Pathway Comparison

Estimates of average annual actinide loads transported off-Site by each of the major pathways addressed in this report are summarized and compared in this section. In cases where more than one method was used to estimate off-Site loads for a specific pathway, the method yielding the highest estimated off-Site load was used for the comparison. Because quantities of actinides transported off-Site vary by several orders of magnitude depending on the actinide and transport pathway, a logarithmic scale is used to display the results (Figure TA-7-1). Therefore, each horizontal line represents an actinide load that is larger, by a factor of 10, than the line below. Actinide transport pathways are compared in terms of orders of magnitude due to the uncertainties associated with analytical measurements and model estimation results.

For all actinides, air and surface water are the dominant transport mechanisms. For Pu, the estimated annual airborne load transported off-Site exceeds the surface water load by roughly a factor of 40. For Am, the trend of the results is the same, which is logical because both Pu and Am are transported in a similar manner.

638

For shallow groundwater, estimated Pu and Am loads are approximately 2 orders of magnitude less, or 1/100th, of the load conveyed in surface water. These shallow groundwater loads are, however, potentially biased high because of residual low-level surface soil contamination introduced down boreholes during drilling and well installation operations. The difference between the surface water and groundwater off-Site Pu and Am loads reflects approximately the same difference in water yields between surface water and shallow groundwater flux.

The biological pathway is also minor relative to the air and surface water pathways. It is estimated to transport approximately five orders of magnitude less, or 1/100,000, of the Pu load compared with the surface water pathway.

TA-7.1.9 Evolution of the Conceptual Model

The following findings from the quantified analysis of Site measured and modeled data indicate the conceptual model for actinide transport at the Site, first introduced in Section TA-1, should be modified accordingly.

Pu and Am

- The surface soil-to-air and air-to-soil pathways, both for resuspension for Pu and Am, including suspension and deposition, should be identified as major, not minor pathways.
- The air deposition-to-surface water pathway for Pu and Am should be identified as a major, not minor pathway, when a large surface area, such as a pond, is impacted.
- The flora-to-air interface pathways for Pu and Am, including suspension and deposition, were not modified to major pathways, mainly because this transfer mechanism is not fully understood.

The modified Pu and Am conceptual model diagram is shown in Figure TA-7-2.

U

- Data indicate no reason to modify the U transport pathways in the conceptual model.

639

TA-7.2 CONCLUSIONS

Quantified analyses of RFETS actinide pathways generally support the conceptual model that identified soil and sediment transport processes as the primary mechanisms for Pu and Am transport. Measured and modeled data confirm that wind and water erosion are the dominant Pu and Am transport pathways, though the relative magnitude of airborne transport is more significant than previously suggested in the qualitative conceptual model study.

Modeled data also support the conceptual model in terms of shallow groundwater transport being a relatively minor pathway for Pu and Am. This behavior is a function of the low solubility and strong soil sorption characteristics of these actinides. Data also support the conceptual model regarding the importance of sub-surface U transport, due to its higher solubility, though isotopic ratio analyses indicate most of the U in shallow groundwater is from natural sources. U loads transported off-Site in shallow groundwater are small compared to surface water. However, mass balance analyses indicate that discharges of shallow groundwater to the surface contribute a major fraction of the surface water U load in specific stream channels.

For the biological pathway, Site-specific research indicates there is little accumulation of Pu in the tissues of arthropods, small mammals, snakes and mule deer. Calculations for estimated off-Site actinide transport by mule deer reflect that the biological pathway is a relatively minor actinide transport mechanism. Microorganisms in the soil and water can both facilitate and inhibit mobility of actinides in the environment. In general, soils rich with organic material tend to inhibit the mobilization of radionuclides.

640

SECTION TA-7 FIGURES

Figure TA-7-1. Estimated Off-Site Annual Actinide Loads (Logarithmic-Scale)

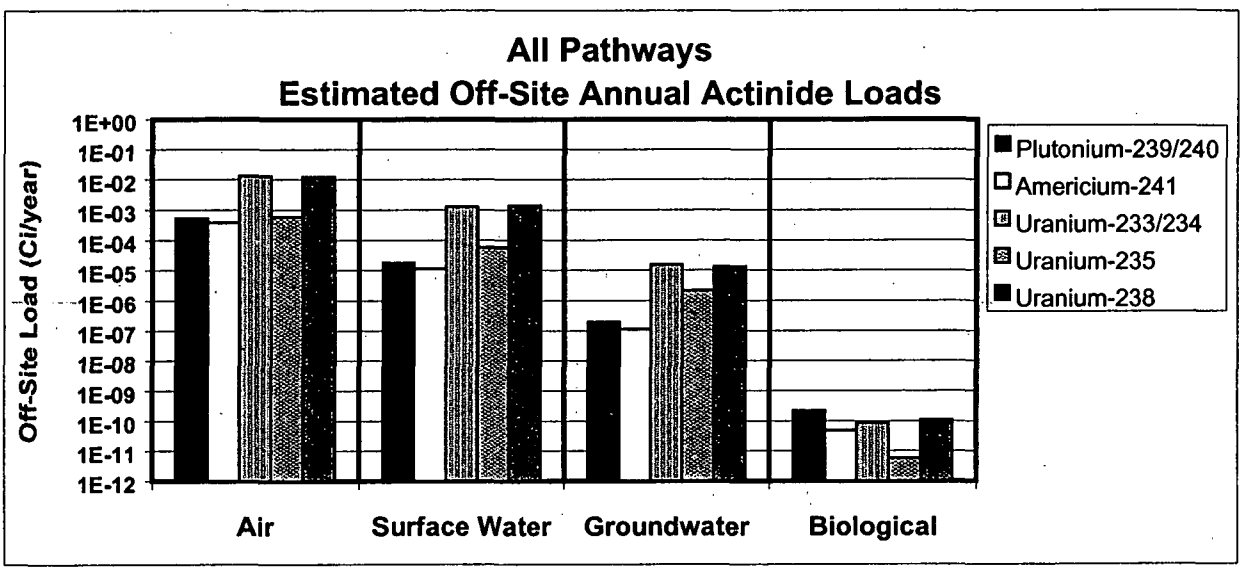

641

Figure TA-7-2. Modified Conceptual Model for Pu and Am Transport

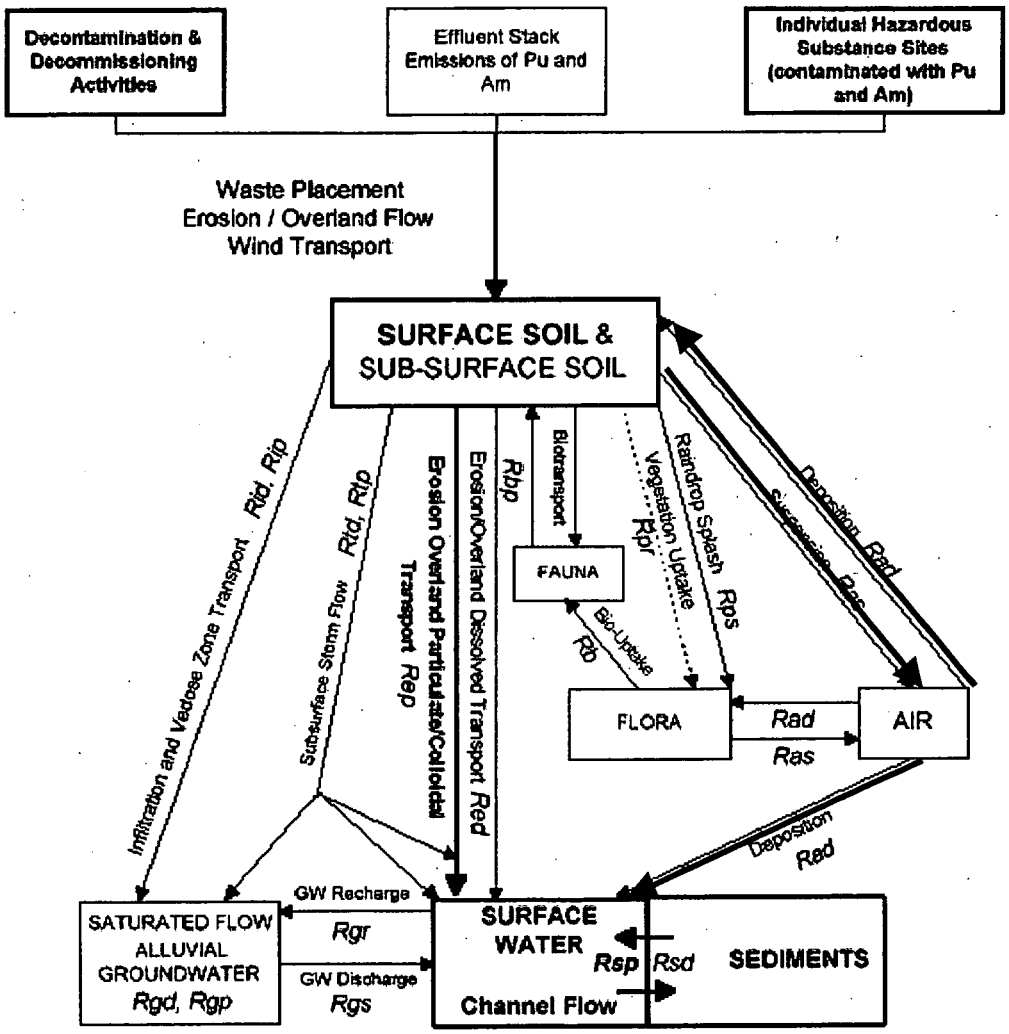

Notes:
1) Boldness indicates relative importance of pathways/processes for actinide migration.

2) R = Rate of actinide transport (subscripts indicate transport pathways in Figure 2).

LEGEND

- Not a Viable Pathway
- Minor Potential Pathway
- Major Potential Pathway

642

1.0 OVERVIEW – ANALYSIS OF Pu/Am RATIO: SURFACE SOIL DATA

Geostatistical analyses were performed on the ratio of Pu-239/240 to Am-241 sample data (Pu/Am) for surface soils at the RFETS. A total of 473 ratio values based on surface soil samples were used to evaluate the ratio variability across the Site. The data sets include samples dating from June 1991 to the present. Pu/Am ratios used in the study ranged from 0.06 to over 22.6. However, more than 1700 results with Pu or Am values below 0.04 pCi/g (approximately natural background) were excluded from the analysis.

2.0 DATA ANALYSIS

2.1 Types of Sample Data

The data used in the site-wide analysis represent several sampling events and sample types. The first type of samples was discrete grab samples. The second type of samples was composite samples. Two different methods of composite samples were used. The first method, known as the Rocky Flats method, removed soil in a 10 by 10-cm square to a depth of five-cm. Five such square areas were combined to create a composite sample that represented the center of a sampling grid. Similarly, CDPHE method took 25 six by five-cm rectangles 0.64 cm deep and composited them to form a sample. The third type of samples are HPGE samples. These samples represent surface soil actinide concentrations over a circular area with a 10-m diameter.

2.2 Reduction of the Data Set

The Pu-239/240 and Am-241 sample data from 2,186 locations were used to calculate the Pu/Am ratio. The ratio values are unitless. The ratio data set of 2186 values contained ratios from approximately 0.005 to over 22.6. The final data set used for the geostatistical analysis was significantly smaller than the starting ratio data set. Individual Pu-239/240 or Am-241 values below 0.04 pCi/g were deleted from the data set as these represent soil activities below natural background and therefore do not provide meaningful insight regarding the Pu/Am ratio. The final data set contained 473 ratio values.

2.3 Spatial Variability of Sample Data

The distribution of actinide concentrations in surface soils at the Site is relatively consistent in many areas, but highly variable in others. Values in the Protected Area and areas just to the east generally exhibit low ratios, indicating Am-241 enrichment. However, some high ratios are also present, indicating localized Pu-239/240 enrichment. In contrast, the 903 pad and areas to the east and south generally contain relatively high ratios, indicating enrichment by Pu-239/240. Locations and ratio values can be seen in Figure TA-A-2 below (Note: Figure TA-A-1 is a map at the end of this attachment).

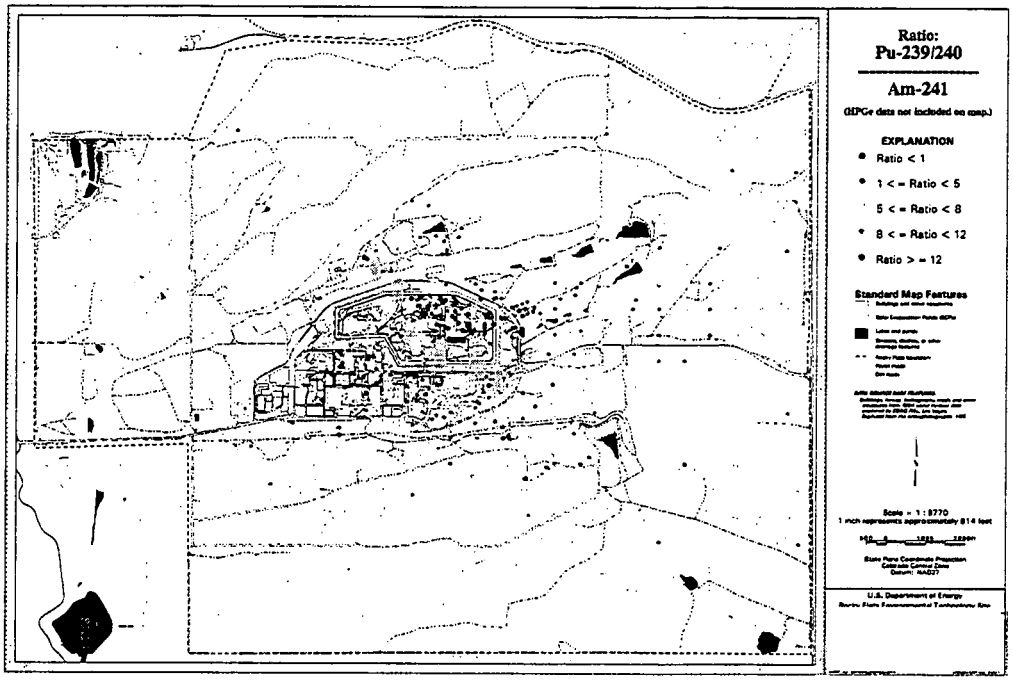

Figure TA-A-2
Location Map of Pu/Am Ratio Data

2.4 Statistical Analysis of Data

The two data domains, NW and SE, were analyzed for statistical parameters. The histograms for the NW and SE data can be seen in Figures TA-A-3 and TA-A-4 respectively. The NW histogram shows a left-skewed histogram, with a few relatively high ratio values. This type of skewness is typical of environmental data. The SE data create a histogram that is more symmetrical, similar to a normal distribution, but with some relatively high ratio values.

Probability plots of the NW and SE ratio data are shown in Figures TA-A-5 and TA-A-6. The NW area ratio data show distinct departure from normality throughout the curve, confirming the histogram results (a straight line indicates normality). The SE area ratio data show a relatively high degree of linearity (normality) in the lower 90 % of the distribution. Above 90 %, the observed outliers cause the line to deviate from normality. Results of the statistical analysis are summarized in Table TA-A-1.

644

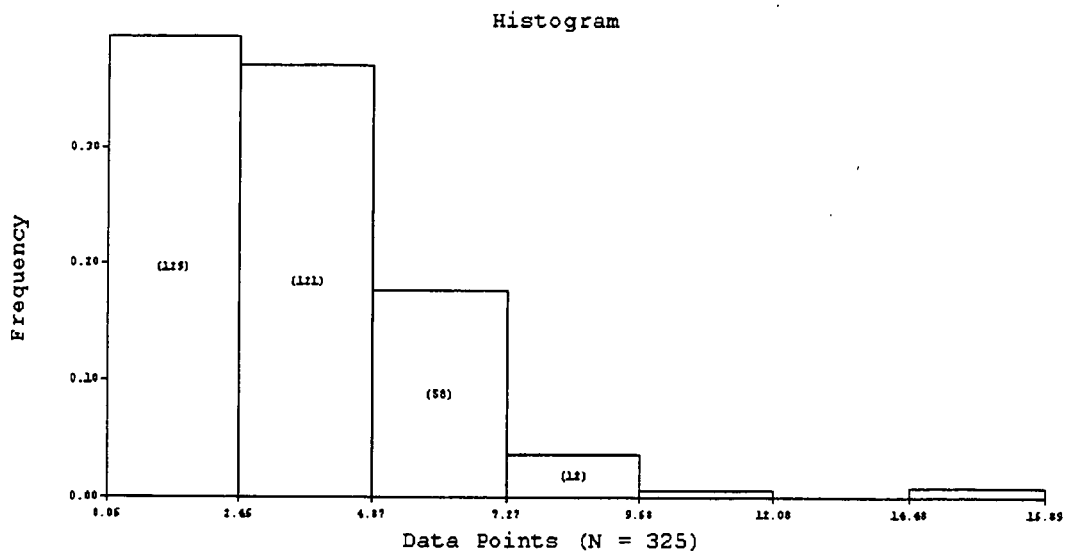

Figure TA-A-3
Histogram of NW Area Ratio Data

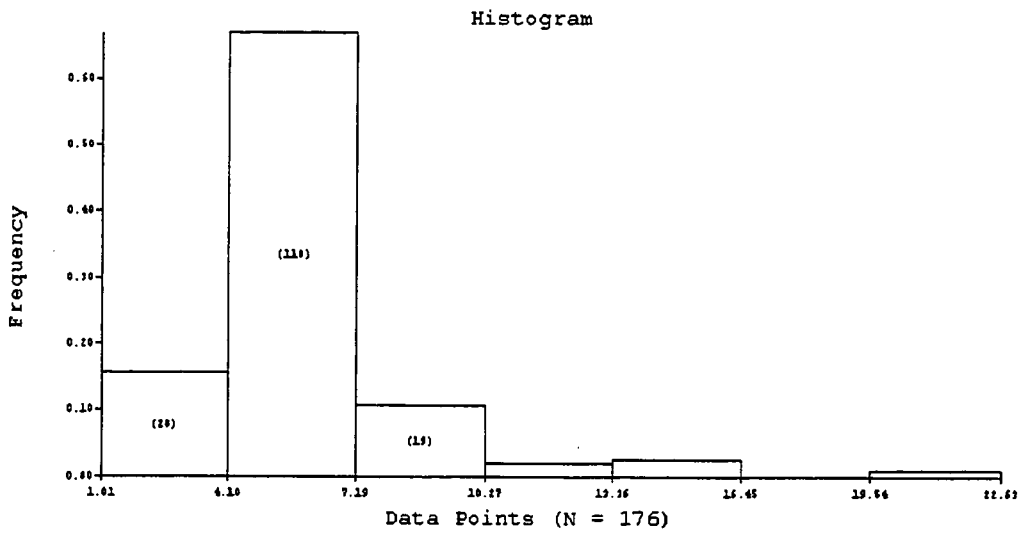

Figure TA-A-4
Histogram of SE Area Ratio Data

C45

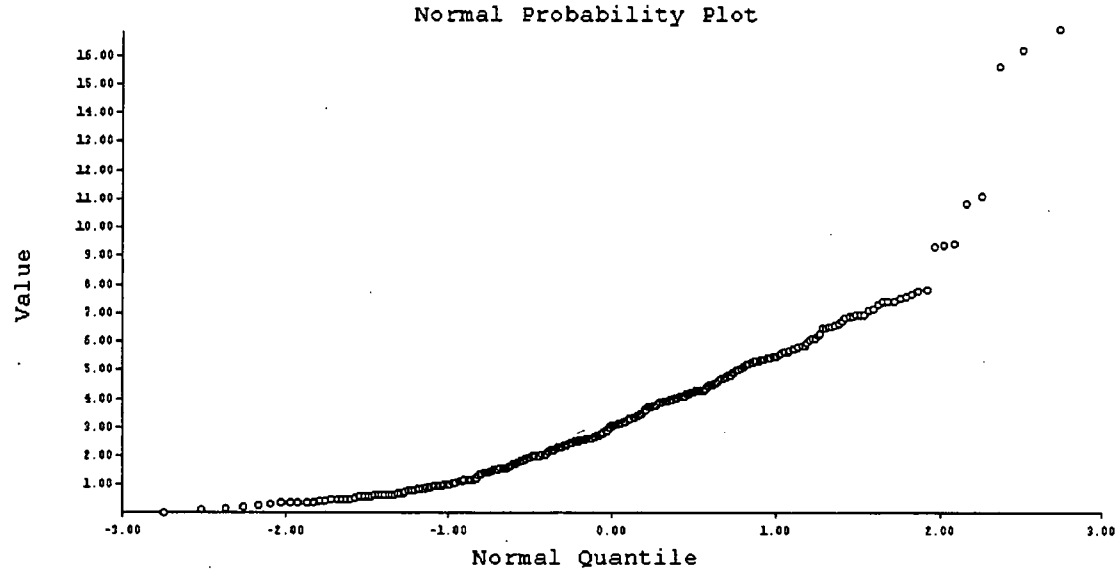

Figure TA-A-5
Cumulative Frequency Plot of NW Area Ratio Data

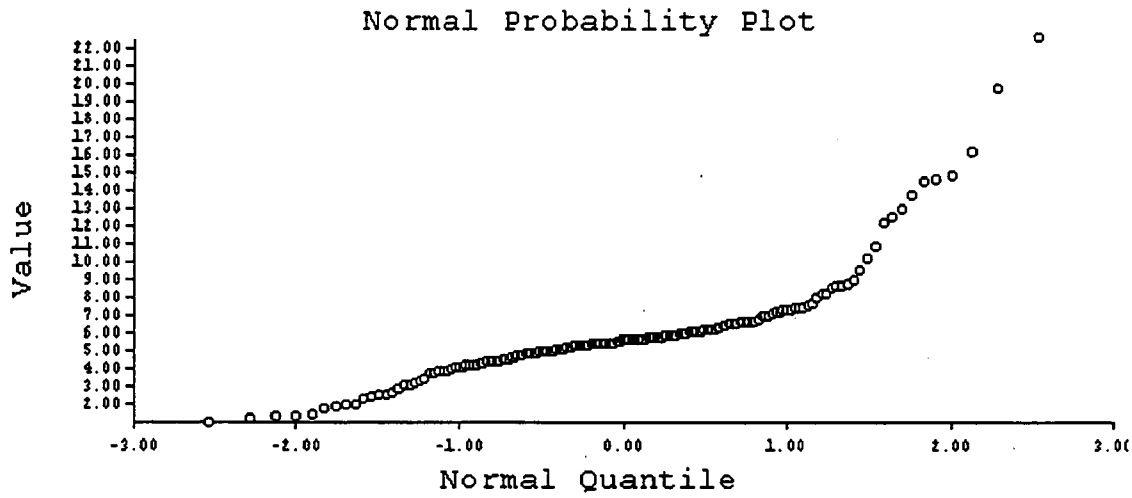

Figure TA-A-6
Cumulative Frequency Plot of SE Area Ratio Data

646

Statistic	Contaminant	
	NW Area (ratio)	SE Area (ratio)
Minimum	0.061	1.007
Maximum	16.9	22.6
Mean	3.40	5.96
Variance	5.94	8.74
Standard Deviation	2.44	2.96
Number of Samples	325	176
Median	3.02	5.59
Coefficient of Variation	0.72	0.50

Table TA-A-1

3.0 VARIOGRAM ANALYSIS

Variography was performed on the data in the NW and SE domains separately. The reason for this is the substantial difference in the spatial data variability noted between the two domains as well as the differing statistical distributions. Within each area (NW and SE), five different directions were analyzed: North-south, northeast-southwest, east-west, northwest-southeast, and an omni-directional variogram (all directions simultaneously). The spatial variability in these five directions was analyzed for the ratio of Pu-239/240 to Am-241.

Several types of variograms were calculated during the variography study. Different types of variogram analyses can often mitigate the influence of the high variability of the sample data values. Variograms calculated and studied during the variography analysis were absolute variograms, general relative variograms, local relative variograms, and logarithmic variograms. Variogram graphs for the NW area appear in Figures TA-A-7 and TA-A-8 for the Pu/Am ratio data. Variogram graphs for the SE area appear in Figures TA-A-9 through TA-A-10. Variogram graphs in both the NW and SE areas exhibit good structure.

Once the variogram graphs were obtained, mathematical models were fit to each directional variogram graph (Figures TA-A-7 through TA-A-10). The mathematical model describes the variability and correlation of the sample data as the distance between samples increases. This correlation is used in the kriging process. Numerous types of

647

mathematical equations are available for variogram modeling. For the site and plume variograms, the commonly used spherical model was selected to represent the graphs. Table TA-A-2 lists the variogram models selected for the long and short axes of spatial continuity and the direction of these axes. The equation for the spherical model appears below:

$$\gamma(h) = C_o + C\left[\frac{3}{2}\frac{h}{a} - \frac{1}{2}\frac{h^3}{a^3}\right]$$

where

$\gamma(h)$	= variance at distance h
C_o	= nugget effect
C	= spherical component
a	= range of influence
Sill	= $C_o + C$

Variogram graphs in the NW area were modeled using a general relative variogram. Variogram graphs in the SE area were modeled using an absolute variogram.

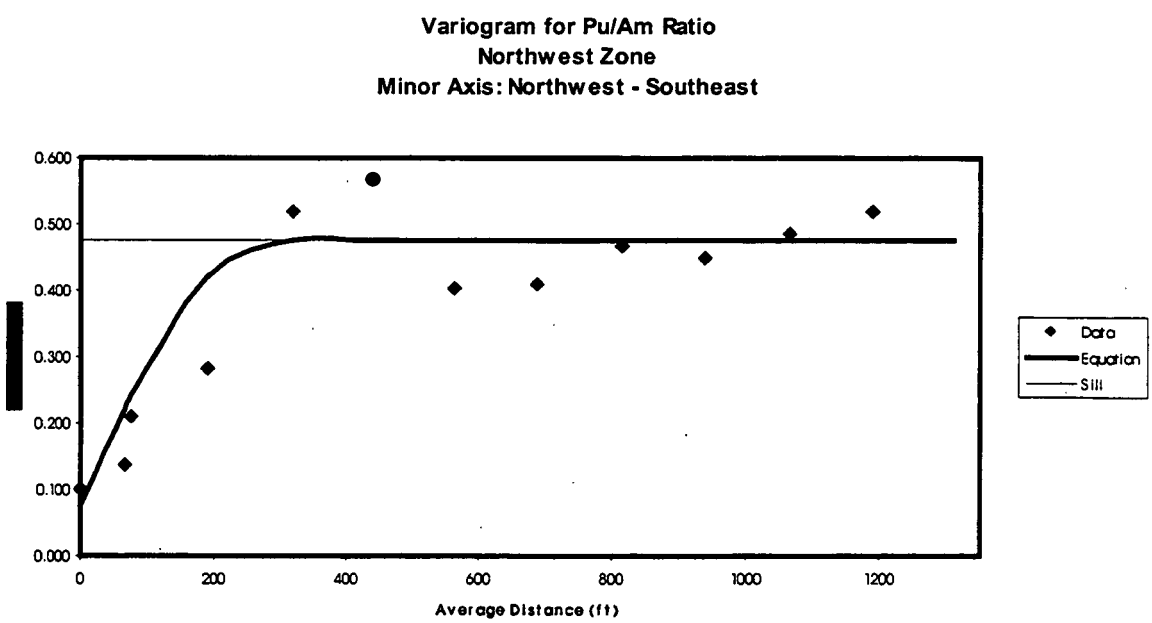

Figure TA-A-7
Variogram Graph of NW Area Ratio Data: Minor Axis (NW-SE)

6048

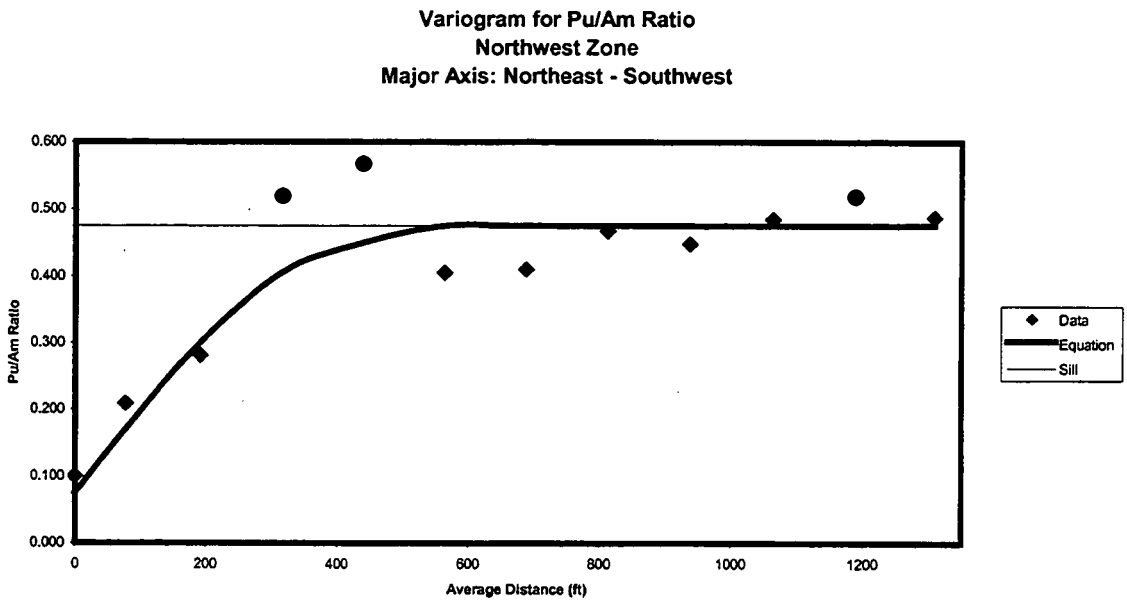

Figure TA-A-8
Variogram Graph of NW Area Ratio Data: Major Axis (NE-SW)

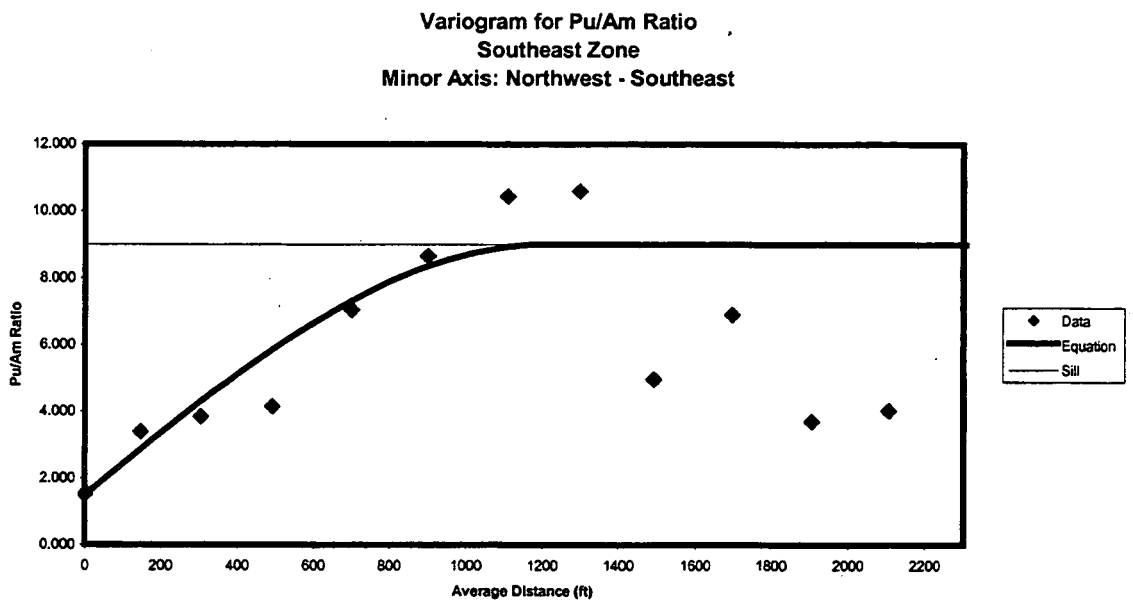

Figure TA-A-9
Variogram Graph of SE Area Ratio Data: Minor Axis (NW-SE)

C649

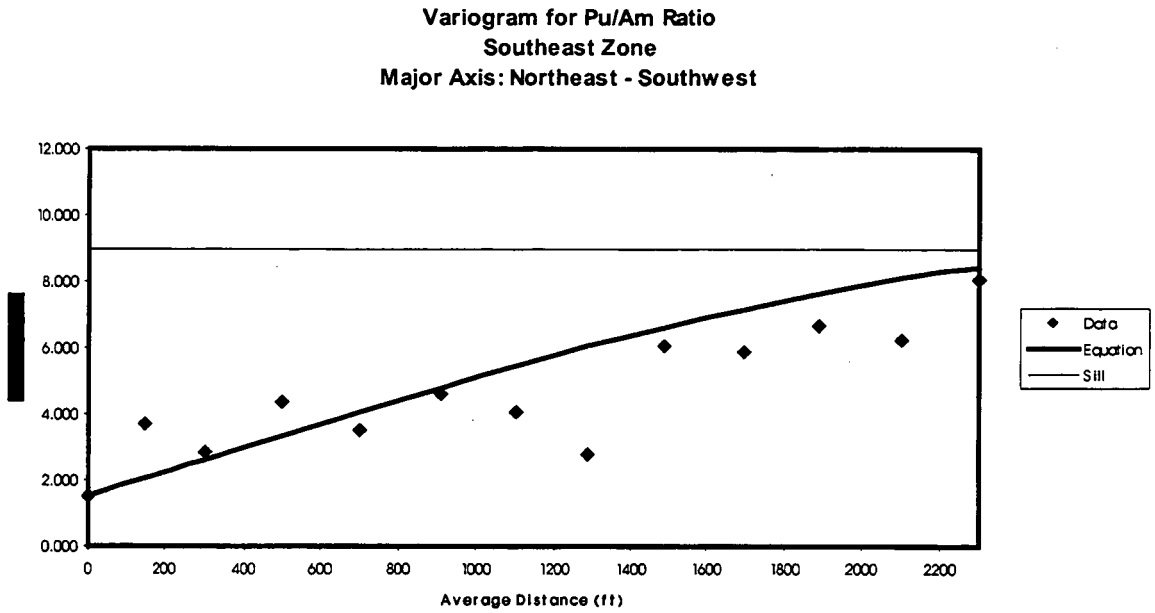

Figure TA-A-10
Variogram Graph of SE Area Ratio Data: Major Axis (NE_SW)

Pu/Am Ratio Study	Variogram Parameters					
	C_o	C	a_{min}	Direction	a_{max}	Direction
NW Area	0.075	0.375	250'	NW-SE	450'	NE-SW
SE Area	1.5	7.5	1200"	NE-SW	3000'	NW-SE

Table TA-A-2

The nugget effect indicates that there is variability even at a distance of zero, demonstrating that extreme variability may occur over very short distances. The nugget effect is also an indication of sampling and analytical error. Nugget effects were observed in both the NW and SE variogram results for the Pu/Am ratio. The nugget

650

effects were relatively small for both data sets and were approximately 15 % of the sill value.

KRIGING

As with the variogram analysis, kriging performed separately in the two different domains (NW and SE) using ordinary block kriging. Block kriging integrates the estimate of the actinide concentration over the area of the block. Blocks used for kriging measured 75 x 75 ft in both Site domains. Each block represents a 5625 square ft area, or approximately 0.13 acres.

Visual representations of the block kriging estimates for Pu239/240 are shown in Figure TA-A-1 at the end of this Section. Each block has been shaded with a color representing the estimated average concentration over the block area. Five Pu/Am ratio categories (pCi/g) have been established for the map display: Less than 1, 1 to 5, 5 to 8, 8 to 12, and greater than 12. Ratios below approximately 5 indicate areas of Am-241 enrichment, whereas areas with ratios above approximately 8 indicate zones of Pu-239/240 enrichment.

RESULTS

The block map shown in Figure TA-A-1 shows some distinct features. A zone of Am-241 enrichment exists on the east side of the Protected Area. This zone extends slightly to the east and north. Three primary zones of Pu-239/240 enrichment exist. The first is to the east of the 903 Pad. This zone results from a cluster of three samples exhibiting Pu/Am ratios above 12. The second zone of Pu-239/240 enrichment is approximately 2500 to 3000 ft east of the 903 Pad and is just to the north of the Site access road. This enriched zone is based on a single elevated sample location. The third zone of Pu-239/240 soil is located approximately 2500 ft to the southeast of the 903 Pad. This is the largest zone, however, it is based on a single sample value. This sample point is isolated from other sample locations in the area. Thus, the enriched location is shown to influence a relatively large area. Large areas to the east and south of the 903 Pad are shown to be between 5 and 8 in Figure TA-A-1. These ratios are considered "typical" for Pu/Am at the Site. Large areas to the north and west of the 903 Pad exhibit ratios of 5 and below. This feature is largely the result of a very few data points in these areas, most of which exhibit ratios of 5 or less.

SECTION TA-B - TABLE OF CONTENTS

TA-B Uranium Usage and Potential Uranium Contamination in Buildings.....B-1

Scope B-1

Methodology.....B-1

SECTION TA-B TABLES

Table TA-B-1. Uranium Usage and Potential Uranium Contamination in Buildings.....B-3

Table TA-B-2. References.....B-20

SECTION TA-B FIGURES

Figure TA-B-1. Uranium Usage and Potential Uranium Contamination in Buildings B-22

(U,NU)
REVIEWED FOR CLASSIFICATION/UCNI
By J.T. Mathiasmeier, Sr. Classifier
Date 04-12-01 Analyst
Approved for Public Release

653

TA-B URANIUM USAGE AND POTENTIAL CONTAMINATION IN BUILDINGS

Purpose

The objective of the study is to provide a qualitative depiction of the extent of uranium usage at the Rocky Flats Environmental Technology Site (RFETS). Documentation of uranium usage by uranium isotope (e.g., uranium-233, uranium-235, and uranium-238) was initiated in response to qualitative questions raised during the Actinide Migration Evaluation uranium geochemical modeling activities during 1999 and 2000. Results of this qualitative study will provide a general understanding of the potential building sources of uranium contamination. In addition, the building-oriented results will assist in determining groundwater-monitoring requirements for specific uranium isotopes during building decommissioning.

The following presents the compilation of historical process knowledge pertaining to uranium usage and potential sources of uranium contamination in buildings in tabular and pictorial formats. As a qualitative compilation, waste volumes and concentrations representative of short periods of time are provided for a general understanding of uranium usage and waste production at RFETS. This compilation is designed to complement the published environmental remediation documentation with production-related information. Therefore, the compilation does not repeat the information included in RFETS remedial investigations, technical memoranda, other Rocky Flats Cleanup Agreement decision documents, or the Historical Release Report.

Methodology

The methodology for researching information included the following:

- Review of documents; and
- Interviews of personnel.

654

The compiled information is presented as follows:

- Table TA-B-1 presents a written summary by building of the uranium usage at RFETS.
  - Uranium usage is identified qualitatively based on production and waste operations present in the specific buildings. (Note: Specific information regarding known environmental contamination is available in the RFETS environmental restoration and remediation documentation and reports referenced earlier in this section.)
  - Buildings with potential uranium contamination are identified, even if contamination is unlikely (e.g., cooling towers associated with buildings that processed uranium are unlikely to be contaminated with uranium unless the closed systems were breached).
  - Sources of information are referenced by number, e.g., (1)
- Table TA-B-2 presents the references reviewed and identified on Table TA-B-1.
- Figure TA-B-1 depicts which buildings at RFETS used uranium in production or waste operations.
  - Usage of uranium-233, uranium-235 (enriched uranium or EU), and uranium-238 (depleted uranium or DU) is depicted through color on the figure.
  - The location of the Original Process Waste Lines are identified to provide a spatial understanding of the uranium solution transfer pathways that may be areas of potential uranium contamination onsite.
  - The Original Process Waste Lines transferred aqueous wastes to 771/774, the Solar Evaporation Ponds, the Sewage Treatment Plant, and to several outfalls. Except for Buildings 707 and 776/777 organic TRU waste, organic waste was transferred between buildings and to the trenches and burn pits onsite (1950s through 1960s) in containers.
  - Buildings with no known uranium operations or potential uranium contamination have not been included on the figure.

655

	Table TA-B-1		Uranium Usage and Potential Contamination at RFETS							
Building No.	Building Description	Uranium (U) Usage	Primary Form of U, that could have been released/ Comments	Secondary Form of U that could have been released/Comments	Operation Size: Volume of Liquid Wastes	Operation Size: Radiologic Activity in Liquids	Disposition of liquid waste (process waste lines)	Other Radionuclides	OPWL Installed (piping) (6)	OPWL Abandoned (piping) (6)
122	Occupational Health - Medical	Decontamination solutions from personnel contamination incidents (1)	Aqueous -- depleted uranium (DU) and enriched uranium (EU) in personnel decontamination solutions, in general solutions quite dilute		Infrequent: 300-400 gallons per transfer (25)					
123	Health Physics Laboratory -- Building DEMOLISHED -- slab and subsurface sumps and piping still in-place	Environmental and biological radioassay analyses. Analytical laboratory, dosimetry and instrument calibration activities. R&D on a small scale in support of nuclear weapons production. (12) In 1975 and 1976, U-236 present in MBA for environmental and health sample analysis. (14, 16)	Aqueous -- DU and EU -- through OPWL and current Process Waste Line, from scrubbers located on outside of building	Particulate	Generally 5000 gallons per weekly transfer, range between 500 to 6000 gallons (25)	1.0E+02 to 1.5E+03 d/m/l Total Alpha	Solar Evaporation Ponds 207A in 1981	Sealed sources of numerous radioactive isotopes. Plutonium and americium. Cesium. Tritium. Curium also listed as a contaminant of concern in Original Process Waste Lines beneath and leading from 123. Releases to soil from the OPWL have been documented. Radioactive isotopes used as spikes and standards in sample analysis included the following: Am-241, Cs-137, Sr-90, H-3, U-234, U-235, U-235, U-236, U-238, Pb-210, Be-133, Cf-250, Gd-148, Ni-63, Cm-244, Pu-238, Pu-239, Pu-240, Pu-240, Pu-241, Pu-242 (12)	1952, 1968	6/82
125	Standards Lab	Prepared standards containing U (1)	Aqueous -- primarily DU							
126	Source Calibration and Storage Building		Aqueous -- DU							
207	Untreated Waste Storage Tank, aka Tank 198 (NE of 777)	Currently contains groundwater from the Solar Evaporation Ponds and other areas onsite; previously used for storage of 774 laundry and treated aqueous waste that did not meet Solar Evaporation Ponds or Walnut Creek discharge limits	Aqueous -- primarily groundwater with DU							
207 Clarifier	Clarifier Tank (east of 788) - Tank REMOVED	Solar Evaporation Pond sludge solidification process; adjacent to and identified as part of the Solar Evaporation Ponds IHSS	Aqueous -- DU and EU							
Pond 2 and Auxiliary Pond	Original Solar Evaporation Ponds (Pond No. 2 also known as "High Nitrate Pond")	Completed in November 1953 (20 -- 11/6/53) Placed in service in December 1953. Abandoned in August 1956. (22, 23) Primary radionuclide in waste solutions was uranium. (23) IHSS no. 101 (3)	Aqueous -- solutions containing U-233, U-235, U-238 from original production buildings, e.g., 881, 771/774							
207 A, B-C, B-N, B-S, C	Solar Evaporator Ponds OU-4	1961-1970. Received enriched U-contaminated waste from Coors. (1) Received aqueous wastes. Pond 207A placed into service in August 1956, Pond 207B in June 1960. Started using Nigrosine dye in ponds to enhance evaporation in February 1968. Pond 207C placed into service in December 1970. Nitrate "catch" trenches installed from October 1971 through April 1974. French drain system installed in May 1972 to capture runoff from the solar evaporation ponds. (22) IHSS no. 101 (3)	Aqueous -- DU and EU							

656

	Table TA-B-1		Uranium Usage and Potential Contamination at RFETS							
Building No.	Building Description	Uranium (U) Usage	Primary Form of U, that could have been released/ Comments	Secondary Form of U that could have been released/Comments	Operation Size: Volume of Liquid Wastes	Operation Size: Radiologic Activity in Liquids	Disposition of liquid waste (process waste lines)	Other Radionuclides	OPWL Installed (piping) (6)	OPWL Abandoned (piping) (6)
208	Sanitary Sewer Lines	Early 1950's untreated laundry waste from 881, and in Mid 1950's through mid 1960's laundry waste from 442 was transferred through sanitary sewer lines to Sewage Treatment Plant for treatment.	Aqueous -- DU and EU							
209	Storm Drain System 10,150 GPD	Routine activities provide no source for uranium contamination unless contaminated through air releases or spills from other sources.	Aqueous -- U may be present in sediments							
215D	Evaporation Distillated Storage Tank (910) (aka Tank 142)		Aqueous -- DU and low concentration of EU; primarily Solar Evaporation Ponds water							
219	Solids Waste Landfill	1968-1990s. ~1000 kg sanitary sewage treatment sludge with 800-8000 dpm activity buried between 1968-1970. (1) IHSS no. 114 (3)	Solid							
226	NaCl Brine Tank - 3800 Gal. B910 (Reverse Osmosis Underground Concrete Tank - not in use)		Aqueous -- DU, primarily Solar Ponds water today							
228A	Drying Bed	Potential low-concentration uranium contamination of sewage sludge	Particulate	Aqueous -- percolation of liquids into soils prior to late 1960s when drying beds were not covered with roofs						
228B	Drying Bed	Potential low-concentration uranium contamination of sewage sludge	Particulate	Aqueous -- percolation of liquids into soils prior to late 1960s when drying beds were not covered with roofs						
231	Process Waste Pump House - Low Level	Potential low-concentration uranium-contaminated groundwater	Aqueous -- DU and low concentration of EU; groundwater and Solar Evaporation Ponds water; sump water from 444 and other buildings							
231A	Waste Storage Tank - Low Level	Potential low-concentration uranium-contaminated groundwater	Aqueous -- DU and low concentration of EU; groundwater and Solar Evaporation Ponds water; sump water from 444 and other buildings							
231B	Waste Storage Tank - Low Level	Potential low-concentration uranium-contaminated groundwater	Aqueous -- DU and low concentration of EU; groundwater and Solar Evaporation Ponds water; sump water from 444 and other buildings							
308B	Modular Storage Tank Pump House	Groundwater containing U from Solar Ponds interceptor trench system	Aqueous -- DU and EU							
308B-A	Modular Storage Tank, aka Tank 341	Groundwater containing U from Solar Ponds interceptor trench system	Aqueous -- DU and EU							
308B-B	Modular Storage Tank, aka Tank 343	Groundwater containing U from Solar Ponds interceptor trench system	Aqueous -- DU and EU							
308B-C	Modular Storage Tank, aka Tank 344	Groundwater containing U from Solar Ponds interceptor trench system	Aqueous -- DU and EU							

657

	Table TA-B-1		Uranium Usage and Potential Contamination at RFETS							
Building No.	Building Description	Uranium (U) Usage	Primary Form of U, that could have been released/ Comments	Secondary Form of U that could have been released/Comments	Operation Size: Volume of Liquid Wastes	Operation Size: Radiologic Activity in Liquids	Disposition of liquid waste (process waste lines)	Other Radionuclides	OPWL Installed (piping) (6)	OPWL Abandoned (piping) (6)
308D	Central Sump Pump House (Quonset Hut-northeast of B761)	Groundwater containing U from Solar Ponds interceptor trench system	Aqueous – DU and EU							
308E	Treatment Cell (southeast of Modular Tanks)	Groundwater containing U from Solar Ponds interceptor trench system	Aqueous – DU and EU							
331	Plant Garage	Some R&D on rolling of enriched U foil (1964), and depleted and enriched U casting techniques. (1)	Particulate	Organic liquids						
334	Maintenance Facility	Depleted U Sheared in maintenance shop (1)	Particulate	Organic liquids				Thorium sheared (1)		
367	Waste Stabilization and Storage									
371	Pu Recovery	During early 1980s ran pilot tests with materials that may have contained U. (1) Laboratory analyzed samples containing U. Standards labs created U-containing standards. (1, 2, 10) Beginning in 1982, U-235 present in MBAs for pyrochemical operations, Pu recovery, analytical labs, NDA, residue repack, and container storage. U-238 present in MBAs for pyrochemical operations and container storage. In 1991, the current inventory of U-233 was identified as 8 grams located in 5 drums – each with less than or equal to 3 grams of U-233. (14, 16)	Aqueous – primarily nitric acid solutions and caustic scrubber solutions. Brines and solutions transferred to Solar Evaporation Ponds in response to upset conditions.	U detected in Recon Char sampling in one of 3 samples in Set V, Rooms 3801 and 3803 (10)				Pilot americium and plutonium recovery operations in mid-1980s. (1)		
373	Cooling Tower - B374	None unless contaminated through air releases from other sources or by cross-over in Building process and cooling water systems.								
374	Liquid Process Waste Treatment - Low Level Pu	1978 brought online. (2) Waste water treatment of U-contaminated solutions (1, 2, 14)	Aqueous – primarily nitric acid solutions	Organic – low-level contaminated oils used in equipment				Received wastes include americium, plutonium, tritium,		
376	Chem Recovery									
378	Waste Collection Pump House									
428	Waste Collection Pump House Low Level - Unit 40	Process waste from 122, 123, 444/447, 460 (1)	Aqueous – DU							
429	Process Waste Pit & Tank (B441 UST 36) aka Tank 077		Aqueous							
440	Waste Storage	1971 through mid 1990s non-radioactive building. Currently LL and TRU waste storage facility. (1)	Particulate							

658

	Table TA-B-1		Uranium Usage and Potential Contamination at RFETS							
Building No.	Building Description	Uranium (U) Usage	Primary Form of U, that could have been released/ Comments	Secondary Form of U that could have been released/Comments	Operation Size: Volume of Liquid Wastes	Operation Size: Radiologic Activity in Liquids	Disposition of liquid waste (process waste lines)	Other Radionuclides	OPWL Installed (piping) (6)	OPWL Abandoned (piping) (6)
441		Original health physics laboratory (1)	Aqueous -- DU		Transfers ranging from 5,400 to 34,400 gallons between 1957 and 1963; Generally 23,000 to 39,000 gallons per monthly transfer in 1963 (20)	Range 8.3E-11 to 9.1E-09 Curies/l and 1,800 to 20,200 d/m/l total alpha between 1957 and 1963 (20)	Original Solar Evaporation Ponds 2, 2A and 2B between 1957 and 1963; 774 in 1963 ((20)	Abandoned OPWL tank behind 441, IHSS 122 (6)	1952	6/82
442		Laundered 444's laundry (1)	Aqueous -- DU and EU; Primarily U-238 and beryllium. 1964 laundry received that was impregnated with U-235 from Building 883. (4)		Transfers ranging from 65,100 to 220,100 gallons on an apparent monthly basis from December 1956 through December 1963 (20)	Range 7.2E-10 to 1.8E-08 Curies/l (20)	Sanitary Waste (Building 995) (25)			
443/ Steam condenset e	Steam Plant	Oil-fired boilers. Generally non-radioactive building. Steam circulated throughout RFETS. Steam condensate supplemented by 374 evaporator condensate.	Aqueous		Two transfers of 3,500 and 6,700 gallons between December 22, 1980 and June 3, 1981. (25)	6.2E+02 and 6.0E+02 d/m/l total alpha (25)	374 (25)			
444	Manufacturing Building Depleted U Ops	1953-1989 depleted U foundry, casting, melting, fabrication, machining, cleaning, and assembly. 1989 U foundry shut down. Fabrication of depleted U parts. (1, 2, 17) 1974 U-235 present in MBA for production control-fabrication. 1967 to 1968 produced U-molybdenum alloys. (1) 1970 several fires involving depleted U. Acidic plating wastes may have been contaminated with U. (2) In 1974, U-235 present in MBA for production control - fabrication. After 1972, U-238 present in MBAs for R&D, metallurgy, foundry, fabrication, and NDT. (14) IHSS no. 116.2, south loading dock (3)	Aqueous -- primarily DU, 1974 = EU also, mostly acidic, nitric acid solutions (1, 2) Liquid wastes were transferred through OPWL, then current process waste lines to Building 774 and the Solar Evaporation Ponds for treatment (17) 1966, a broken process waste line to north of Building 444 resulted in possible soil infiltration. Open ingot (uranium) storage area east of Building 444 and a metal storage area to the south may have resulted in "low-level infiltration" into the soil. (4)	Organic -- oils and solvents for machining. Machining oils and organics were burned in open burn pits (3, 19) DU machining chips buried in drums in trenches onsite. (3, 19)	Aqueous transfers ranging from 1,000 to 17,200 gallons between September 1957 and May 1963 (20); 400 to 36,000 gallons weekly between December 22, 1980 and June 3, 1981 (25)	Range 3.2E-10 to 5.9E-9 Curies/l and 700 to 12,700 d/m/l total alpha (20); 4.7E+01 to 7.3E+04 d/m/l total alpha (25)	Original Solar Evaporation Ponds 2, 2A and 2B between 1957 and 1963 (20): 374 and Solar Evaporation Pond 207C (25)	Depleted U-niobium alloys production in arc furnace in 1970's. Alloying began in 1966 using electron beam furnace. (1)	1952	4/81
447	Depleted U Manufacturing Building	Depleted U manufacturing operations (welding, chemical milling, casting of U and alloys) (1) 1957 U chip roaster (for DU and EU) and cementation operations began. Late 1960's, full scale use of the vacuum arc furnace produced U-niobium and U-zirconium alloys. Final cleaning of all War Reserve production parts produced in 444 and 447 in Oakite NST detergent and distilled water. (2) IHSS no. 116.1, west loading dock (3)	Aqueous -- caustic and acidic, aqueous detergent (containing Oakite NST and Mariko) containing DU	Organic -- oils and solvents for machining and cleaning Particulate -- potential from chip roaster. May 1980 a vacuum collector fire resulted in approximately 44 uCi U-238 on the roof. December 1962 uranium/beryllium release from an unfiltered hood was noted. 1953 high winds resulted in release of uranium from drums resulting in direct count of 7500 dpm/100 cm2 and removable count as high as 350 dpm. (4)	Aqueous transfers included in 444 transfers					
448	Shipping and U Material Storage	Shipped materials and waste generated in 444/447 (1)	Particulate -- DU							
450	Filter Plenum Building (south of 444) for B444 Zone 1	HEPA filtration of building effluent air	Particulate -- DU							
451	Filter Plenum Building (south of 447) for B447 Zone 2	HEPA filtration of building effluent air	Particulate -- DU							
454	Cooling Tower - B444 - 800 Tons	None unless contaminated through air releases from other sources or by cross-over in Building process and cooling water systems.	Aqueous -- overspray -- DU							

659

	Table TA-B-1		Uranium Usage and Potential Contamination at RFETS							
Building No.	Building Description	Uranium (U) Usage	Primary Form of U, that could have been released/ Comments	Secondary Form of U that could have been released/Comments	Operation Size: Volume of Liquid Wastes	Operation Size: Radiologic Activity in Liquids	Disposition of liquid waste (process waste lines)	Other Radionuclides	OPWL Installed (piping) (6)	OPWL Abandoned (piping) (6)
455	Filter Plenum (444 Plating Lab) Hepa-for 444 Zone 2	HEPA filtration of building effluent air	Particulate -- DU							
457	Cooling Tower - B447 - 400 Tons	None unless contaminated through air releases from other sources or by cross-over in Building process and cooling water systems.	Aqueous -- overspray -- DU							
528	Process Waste Pit (B559) Low Level Liquid	Received liquid wastes from sample analyses conducted in 559 that most likely contained U. (1)	Aqueous -- DU and EU		Aqueous transfers included in 559 transfers					
551	General Warehouse and Empty Waste Containers	Empty drums contaminated with U were received at 551 between 1959 and 1970. PAC 500-158 (3)	Particulate -- DU	All ten biased floor paint samples taken for Recon Char measured greater than MDA for U-233/234 and U-238. One of 10 samples measured greater than MDA for U-235.						
551 Pad	Waste Storage Pad (RCRA Unit 18.03)	IDM waste storage	Particulate DU and EU unlikely -- container storage	Containerized solid environmental media (e.g., soil)						
559	Plutonium Analytical Lab	Analysis of samples containing U-233/234, U-235, U-238 (1, 14) Preparation of standards containing U. (14) 1970-1983, U-233 was most likely present in the analytical laboratories. (15, 16)	Aqueous primarily nitric and hydrochloric acid solutions containing DU and EU. Pyrex glass process waste lines (part of the Original Process Waste Line) which transferred waste from 559 to tanks 528 broke. Soil was excavated, leaving the soil under the line which was subsequently covered with fill dirt (24)					Some analytical samples of plutonium contained americium. Other radionuclides include plutonium, tritium. (1) Multiple releases from OPWL pipelines between 559 and 528, IHSS 159 (6)	1968	7/82
559-TUN	559-561 Tunnel	Tunnel through which process waste lines and plenum ductwork run	Aqueous -- DU and EU	Aqueous -- depleted and enriched U						
560	Cooling Tower - B559	None unless contaminated through air releases from other sources or by cross-over in Building process and cooling water systems.	Aqueous -- overspray							
561	Filter Plenum - B559	HEPA filtration of building effluent air	Particulate -- DU and EU							
563	Cooling Tower - B559	None unless contaminated through air releases from other sources or by cross-over in Building process and cooling water systems.	Aqueous -- overspray -- DU and EU							
569	Crate Counter	Low level radioactive waste storage facility. 1989-present U-235 present in MBA for NDA-crate counter. In 1980, U-238 present in MBA for lab support. (14) Routine activities provide no source for uranium contamination unless contaminated through air releases or spills from other sources or from containers being stored/counted.	Particulate -- DU and EU	Containerized solid low level and TRU waste						
570	Filter Plenum - B569	HEPA filtration of building effluent air	Particulate -- DU and EU							
664	Waste Storage and Shipping	Containerized TRU waste storage facility. U-235 present in MBA for waste storage and shipment. (14) Routine activities provide no source for uranium contamination unless contaminated through air releases from other sources or spills from containers.	Particulate -- DU and EU	Containerized solid low level and TRU waste						

660

	Table TA-B-1		Uranium Usage and Potential Contamination at RFETS							
Building No.	Building Description	Uranium (U) Usage	Primary Form of U, that could have been released/ Comments	Secondary Form of U that could have been released/Comments	Operation Size: Volume of Liquid Wastes	Operation Size: Radiologic Activity in Liquids	Disposition of liquid waste (process waste lines)	Other Radionuclides	OPWL Installed (piping) (6)	OPWL Abandoned (piping) (6)
666	Storage	Container storage of non-radioactive and radioactive PCB waste. Routine activities provide no source for uranium contamination unless contaminated through air releases from other sources or spills from containers.	Particulate -- DU and EU	Containerized liquid and solid waste						
702	Pump House - Tower 712	None unless contaminated through air releases from other sources or by cross-over in Building process and cooling water systems.	Aqueous -- overspray							
703	Pump House - Cooling Tower 713	None unless contaminated through air releases from other sources or by cross-over in Building process and cooling water systems.	Aqueous -- overspray							
705	Coatings Lab	In 1977, U-238 present in MBA for coatings. (14)	Organic -- DU							
707	Plutonium Ops Manufacturing	After 1969 fire in 776, final assembly operations moved to 707 in 1972. Assembly operations include enriched and depleted U components. (1,2) After 1972, U-235 present in MBAs for metal fabrication (including machining and casting) and for storage. U-238 present in MBAs for NDT, metal fabrication, machining, casting and oxide brushing, radiography, and container storage. (14) 1997, an electrolytic decontamination process to remove Pu contamination from EU parts was initiated. (17) During construction of 707 a section of the original process waste line was removed, residual materials are likely to be in residence. (4)	Organic -- TCE then TCA wash of EU parts	Aqueous -- wastes from building operations -- DU and EU; recently sodium nitrate solutions used in electrolytic decontamination process to remove surficial Pu contamination from EU parts	Transfers of aqueous waste: 1,200 to 1,300 gallons twice per month from December 22, 1980 through March 18, 1981; Transfers of organic and solvent waste: <1000 gallons (25)	Aqueous range 3.5E+02 to 2.2E+06 d/m/l total alpha (25)	Aqueous to Solar Evaporation Pond 207A; Aqueous and organic to 774 (25)	Americium present in small percentages in Pu-241 as a decay product. Plutonium fabrication operations. Tritium from assembly operations. (1) OPWL original valve vault no. 7 west of 707 removed in 3/73, IHSS 123.2 (6)	1968	3/84
709	Cooling Tower - B707 - 4000 Tons (out of service)	None unless contaminated through air releases from other sources or by cross-over in Building process and cooling water systems.	Aqueous -- overspray -- DU and EU	All ten biased concrete floor samples taken for Recon Char measured greater than MDA for U-233/234 and U-238. Nine of 10 samples measured greater than MDA for U-235. Pre-survey sediment sample indicates a maximum total beta contamination of 2055 dpm/100cm2, and removal beta contamination of less than 200. These results are above instrument MDC but below contamination limits prescribed in DOE Order 5400.5. (9)	Currently out-of-service					
711	Cooling Tower B707	None unless contaminated through air releases from other sources or by cross-over in Building process and cooling water systems.	Aqueous -- overspray -- DU and EU							
712	Cooling Tower for B776/777/779A	None unless contaminated through air releases from other sources or by cross-over in Building process and cooling water systems.	Aqueous -- overspray -- DU and EU							

6.6.1

	Table TA-B-1		Uranium Usage and Potential Contamination at RFETS							
Building No.	Building Description	Uranium (U) Usage	Primary Form of U, that could have been released/ Comments	Secondary Form of U that could have been released/Comments	Operation Size: Volume of Liquid Wastes	Operation Size: Radiologic Activity in Liquids	Disposition of liquid waste (process waste lines)	Other Radionuclides	OPWL Installed (piping) (6)	OPWL Abandoned (piping) (6)
713	Cooling Tower for B776/777/779A	None unless contaminated through air releases from other sources or by cross-over in Building process and cooling water systems.	Aqueous -- overspray -- DU and EU							
713A	Valve Pit (east of 713)		Aqueous -- DU and EU							
718	Pump House - Cooling Tower 711	None unless contaminated through air releases from other sources or by cross-over in Building process and cooling water systems.	Aqueous -- overspray -- DU and EU							
728	Process Waste Pit - B771		Aqueous -- DU and EU		Included in 771 transfers			2 abandoned OPWL tanks in 728, IHSS 126 (8)		
730	Process Waste Pit - B 776		Aqueous -- DU and EU		Included in 776 transfers			Laundry waste pit tanks. 4 abandoned OPWL tanks in 730, IHSS 132 (8)		
731	Process Waste Pit B707 Plenum Deluge		Aqueous -- DU and EU		Included in 707 transfers					
732	Laundry Waste Pit - B776		Aqueous -- basic solutions, primarily DU		Included in 776 transfers					
750 Pad	Pondcrete Storage Pad (Tent #'s 2, 3, 4, 5, 6 and 12)	Containerized waste storage facility. Routine activities provide no source for uranium contamination unless contaminated through air releases from other sources or spills from containers.	Aqueous -- precipitation runoff from spill areas -- DU and EU	Containerized solids and liquids -- solidified Solar Ponds sludge.						
750-DP	750 Decon Pad	Decontamination of equipment and vehicles	Aqueous -- overspray -- DU and EU							
750HAZ	Main Hazardous Storage Area (Unit 1, Unit 2205) (Cargo containers)	Containerized waste storage facility. Routine activities provide no source for uranium contamination unless contaminated through air releases from other sources or spills from containers.	Particulate	Aqueous -- precipitation runoff from spill areas; stores solid and liquid low level wastes						
765A	Emergency Pump									

662

	Table TA-B-1		Uranium Usage and Potential Contamination at RFETS							
Building No.	Building Description	Uranium (U) Usage	Primary Form of U, that could have been released/ Comments	Secondary Form of U that could have been released/Comments	Operation Size: Volume of Liquid Wastes	Operation Size: Radiologic Activity in Liquids	Disposition of liquid waste (process waste lines)	Other Radionuclides	OPWL Installed (piping) (6)	OPWL Abandoned (piping) (6)
771	Plutonium Recovery Facility	Oralloy leaching of surface impurities from enriched U parts. 1967 to 1968 U-molybdenum alloy was alloyed with plutonium. Early days contained its own laundry facilities. U-233 was aqueously processed, cast and machined from 1950s to 1970s. U-233 and U-238 were separated on a lab scale. (1) Recovery operations for enriched U were conducted on a limited basis from 1964-1989. (2) Acid dissolution of U from parts. Solvent extraction of U from acidic solutions. U impurities in parts and recovery feed solutions were removed by anion exchange processes. Process simulation lab used for R&D work. (8) After 1972, U-235 present in MBAs for chemical separations and special recovery operations (alloy, aqueous, volatile fluoride). Oralloy leach, foundry operations, metallurgy, residue processing, standards lab, NDA, and storage. U-238 present in MBAs for R&D chemistry, physical metallurgy, Pu fabrications, analytical laboratories, chemicals standards lab, special recovery - metals and alloys, aqueous recovery, container and tank storage. (14) 1965 -1983, U-233 present in MBAs for aqueous process chemistry, metallurgy, special recovery -- aqueous and alloys, analytical labs, metal machining, and container storage. R&D personnel used hot plates or small muffle furnaces to burn combustible waste contaminated with U-233. Some wastes containing low-levels of U-233 were likely burned in the Building 771 production incinerator. (15, 16) IHSS nos. 143, 150.1,.2,.3 (3)	Aqueous -- DU and EU; A mixture of sulfuric acid and nitric acid were used in the Oralloy leaching process. U and plutonium were precipitated from the acid solution by sparging gaseous ammonia through the solution. The 1959 fire in 771 was doused with water resulting in soils, process and sanitary drains becoming contaminated. These drains were later sealed. Residual contamination from the 1969 fire in 776 which was doused with water is anticipated in the tunnel area. (8) October 1956 process waste tanks overflowed resulting in "minor environmental infiltration". September 1957 the 771 fire and fire extinguishing efforts resulted in "some environmental infiltration." April 1958 soil infiltration measured at 17,400 dpm/g at the laundry outfall -- Building 773. May 1968 sewer line break resulted in sewage lift station tank overflowing to Building 773 outfall. May 1970 soil samples from Building 773 outfall measured 100,000 dpm/g -- 149 drums of soil were removed for off-site disposal. (4)	Organic. Particulate -- 1956 fire and contamination incident in fabrication line resulting from a burning briquet, 1957 peroxide explosion and contamination incident, 1957 fire and contamination incident relating to a filter system, 1963 fire and contamination incident in the skull line, 1969 fire in 776 771 tunnel (21)	Aqueous laundry waste transfers ranging from 143,250 to 353,500 gallons to Walnut Creek from May 1969 to September 1954; 7000 to 359,700 gallons to Original Solar Evaporation Ponds from January 1954 to February 1957; one transfer of 7,500 gallons to the Outlet below 995 in February 1954; 12,300 to 328,500 gallons to Pond A-1 from April 1955 to September 1957; 15,350 to 347,350 gallons to Pond B-2 from July 1957 to April 1964 (20); transfers from 3,200 to 7,000 gallons transferred to Storage from December 22, 1981 through June 3, 1981 (25)	5.1E-11 to 2.0E-10 Curies/l and 191 to 446 d/m/l total alpha to Walnut Creek; 3.1E-10 to 1.1E-09 Curies/l and 690 to 2419 d/m/l total alpha to the Original Solar Evaporation Ponds; 1.8E-10 Curies/l and 389 d/m/l total alpha to the Outlet below 995; 1.5E-10 to 5.3E-10 Curies/l and 350 to 1,200 d/m/l total alpha to Pond A-1; 1.4E-10 to 3.8E-10 Curies/l and 300 to 850 d/m/l total alpha (20); 1.9E+03 to 2.2E+05 d/m/l to Storage (25)	Walnut Creek, Original Solar Ponds, Outlet below 995, Pond A-1 (previously Pond 6), Pond B-2 (previously Pond 3) (20); Storage (25)	Curium reprocessing, Neptunium and Cerium usage - curium, neptunium, and cerium used as tracers. Neptunium used in uranium and plutonium (1,4,5) Americium recovery operations began in 1957. Plutonium recovery, purification, and component manufacturing operations began in 1953. Plutonium recovery operations may have been contaminated with tritium. Incinerator used for Pu recovery from 1958 through 1988. Few kilograms of natural thorium were used in special projects. (1) Laundry operation were located in the NW corner of the building. (2)	1966, 1968, 1969,	5/82
771-S	771 Stack	HEPA filtration of building effluent air	Particulate							
771-TUN	771-776 Tunnel		Aqueous -- firewater infiltration from 776 fire in 1969							

663

	Table TA-B-1		Uranium Usage and Potential Contamination at RFETS							
Building No.	Building Description	Uranium (U) Usage	Primary Form of U, that could have been released/ Comments	Secondary Form of U that could have been released/Comments	Operation Size: Volume of Liquid Wastes	Operation Size: Radiologic Activity in Liquids	Disposition of liquid waste (process waste lines)	Other Radionuclides	OPWL Installed (piping) (6)	OPWL Abandoned (piping) (6)
774	Liquid Waste Treatment Plant - 771 Plutonium Ops	Treatment of radioactive waste through pH adjustment, precipitation, vacuum filtration and evaporation. (1) Treatment of organic wastes (TCE then TCA) containing enriched U. (1) U-235 and U-238 present in MBA for aqueous and organic waste treatment. (14) 1965 -1968, and 1973 - 1983, U-233 was most likely present in 774. (15)	Aqueous -- DU and EU; primarily nitric acid solutions. Liquids meeting acceptance criteria were shipped to 374 or Solar Evaporation Ponds. March 1972 approximately 500 gallons of plutonium waste (approximately 350,000 dpm/l) released from 774 tanks. (4)		Treated aqueous waste transfers of 12,250 to 208,750 gallons per month to Original Solar Evaporation Ponds between December 1953 and April 1964; 14,300 to 74,500 gallons per month to the Outlet below 995 from October 1953 to September 1954; 10,625 to 242,450 gallons per month to Pond B-2 from April 1955 through April 1964 (20); between December 22, 1980 and June 3, 1991, transfers ranging between 9,000 and 16,000 gallons to Sanitary, and 8,000 to 16,000 gallons to Solar Evaporation Pond 207A and 207C (25)	9.0E-11 to 1.0E-8 Curies/l and 200 to 22,000 d/m/l total alpha to Original Solar Evaporation Ponds; 1.2E-10 to 3.1E-10 Curies/l to the Outlet below 995; 1.1E-10 to 7.5E-10 Curies/l and 250 to 1,600 d/m/l total alpha to Pond B-2 (20); <100 to 4.0E+02 d/m/l total alpha to Sanitary, and 1.0E-04 to 8.4E+04 d/m/l total alpha and 5.4E-04 to 1.1E+06 total beta to the Solar Evaporation Ponds (25)	Original Solar Evaporation Ponds, Outlet below 995, Pond B-2 (previously Pond 3) (20), Sanitary, current Solar Evaporation Ponds 207A and 207C (25)	Aqueous wastes received for processes contained americium, plutonium, tritium. 3 abandoned OPWL tanks east of 774, IHSS 124.1, 124.2, 124.3. OPWL pipeline between 774 and 995 broken during construction activities near 774, IHSS 127. 6 removed process waste tanks beneath south wing of 774, IHSS 146.1-146.6. Multiple releases from OPWL between 774 and 400/800 areas, IHSS 147.1. OPWL pipeline between 774 and Solar Evaporation Ponds leaked in 7/80, IHSS 149. (8)	1952, 1968	1972, 3/84, Active?
774A	Waste Treatment Plant RCA Tank (nw of 774T)									
774B	Waste Treatment Plant Non RCA (nw of 774T)									
775	Sewage Lift Station									
776	Manufacturing and Utilities Low Level and TRU Solid	1957-1969 Product assembly and disassembly included U components. 1967 to 1968 U-molybdenum-plutonium alloys were sealed within stainless steel envelopes. U-233 was aqueously processed, cast and machined from 1950s to 1970s. R&D personnel used hot plates or small muffle furnaces to burn combustible waste contaminated with U-233. (1, 15) After 1972, U-235 present in MBAs for assembly operations, recovery operations, the pilot incinerator and the fluidized bed incinerator, residue processing and repacking, machining, and container storage. U-238 present in MBAs for assembly engineering, advanced size reduction facility, and metal fabrication - machining. In 1976, U-233 present in MBA for quality acceptance. (14)	Aqueous -- acid and caustic solutions -- DU and EU	Organic solutions -- TCE and TCA with DU and EU Particulate -- June 1964 explosion in a glovebox resulted in release of plutonium to the interior and some to the exterior of the north side of building. (4) 1965 explosion and contamination incident at chip washing operations, 1965 contamination from a plutonium fire incident, 1969 major fire in 776 and 777. (21) TRU organic wastes were transferred to 774 for solidification.	Aqueous transfers from 9,300 to 134,100 gallons to Original Solar Evaporation Ponds from September 1957 through July 1961; 19,000 to 542,400 gallons to Pond B-2 (20); 8400 to 38,000 gallons to 774 from April 1963 to September 1963; Transfers of organic and solvent waste: <1000 gallons (25)	7.8E-11 to 1.7E-09 Curies/l and 200 to 3700 d/m/l total alpha to the Solar Evaporation Ponds; 7.0E-11 to 8.4E-10 Curies/l and 200 to 2,000 d/m/l total alpha to Pond B-2 (20); (no activities identified for 1963) (25)	Solar Evaporation Ponds; Pond B-2 (previously Pond 3); Aqueous and organic to 774 (25)	Plutonium research and production activities. Waste management activities, including size reduction, may have generated small quantities from any radiological area onsite.	1957	12/82

664

	Table TA-B-1		Uranium Usage and Potential Contamination at RFETS							
Building No.	Building Description	Uranium (U) Usage	Primary Form of U, that could have been released/ Comments	Secondary Form of U that could have been released/Comments	Operation Size: Volume of Liquid Wastes	Operation Size: Radiologic Activity in Liquids	Disposition of liquid waste (process waste lines)	Other Radionuclides	OPWL Installed (piping) (6)	OPWL Abandoned (piping) (6)
782	Filter Plenum B779 (Zone 2) HEPA Filters	HEPA filtration of building effluent air	Particulate							
783	Pump House Tower Water - Building 779	None unless contaminated through air releases from other sources or by cross-over in Building process and cooling water systems.	Aqueous							
790	Radiation Calibration Labs									
827	Emergency Generator B865/875/883/886									
828	Process Waste Pit B886 Low Level Inactive	Received process wastewater from Building 886	Aqueous -- EU							
865	Materials and Process Development Lab	R&D for U metalworking processes including casting, metallography (including nitric acid etch), grit blasting. (1) After 1972, U-238 present in MBAs for metallurgy and production control. (14)	Aqueous -- DU and EU, nitric acid used for chemical etching. Liquid wastes were transferred through OPWL, then current process waste lines to Buildings 374 and 774 for treatment (17)		Transfers ranging from 1,700 to 3,000 gallons to Solar Evaporation Pond 207A; 2,000 gallon transfers to 774 for treatment from December 22, 1980 through June 3, 1981 (25)	2.7E+00 to 3.0E+04 d/m/l total alpha to Solar Evaporation Pond 207A; 3.2E+04 to 3.4E+04 d/m/l total alpha to 774 for treatment	Solar Evaporation Pond 207A; 774		1968	5/82
866	Process Waste Transfer B865	Receives process waste from B865 and 889 including depleted U.	Aqueous -- DU and EU							
867	Filter Plenum (west of B865) Zone 1	HEPA filtration of building effluent air	Particulate							
868	Filter Plenum (east of B865) Zone 2	HEPA filtration of building effluent air	Particulate							
875	Filter Plenum B886 Zone 1	HEPA filtration of building effluent air. Filter Plenum building for 886 (1)	Particulate -- EU and DU; high contamination areas (HCA) (13)							
879	Filter Plenum B883 Zone 1	HEPA filtration of building effluent air	Particulate							
880	Storage Shed	Stored radioactively contaminated waste and materials used for studies in 886 (13)	Particulate -- EU and DU; interior contains contamination areas (CAs) (13)							

	Table TA-B-1		Uranium Usage and Potential Contamination at RFETS							
Building No.	Building Description	Uranium (U) Usage	Primary Form of U, that could have been released/ Comments	Secondary Form of U that could have been released/Comments	Operation Size: Volume of Liquid Wastes	Operation Size: Radiologic Activity in Liquids	Disposition of liquid waste (process waste lines)	Other Radionuclides	OPWL Installed (piping) (6)	OPWL Abandoned (piping) (6)
777	Assembly Building Plutonium Manufacturing Ops	1958-1960s Product assembly including enriched U components, 1958 -1989 Disassembly of Site Returns including enriched and depleted U components (1,2) 1988 "hot laundry" facility began operation in 777. (2) After 1972, U-235 present in MBAs for systems development, R&D lab chemistry - metal, disassembly, laser fusion, aqueous processing, NDT, and container storage. U-238 present in MBAs for systems development, physical metallurgy, NDT, joining technology, coatings, metal fabrication, disassembly, residue treatment, special assembly, and vault storage. (14) 1965 -1968, and 1977 - 1983, U-233 present in MBAs for assembly, and disassembly. R&D personnel used hot plates or small muffle furnaces to burn combustible waste contaminated with U-233. (15, 16)	Aqueous -- DU and EU	Organic solutions -- DU and EU, TRU organic wastes were transferred to 774 for solidification.	Included in 776 transfer description			Some disassembled parts of weapon components are processed via molten salt extraction to remove americium. Tritium gettering system. Other radionuclides include plutonium, thorium in small quantities. (1)	1957	10/82
778	Service/ Contaminated Clothing Laundry	Laundry remaining from enriched U operations in 881 were laundered in 778 in Mid-1960s. In 1976 began cleaning laundry for entire site. (1)	Aqueous -- primarily DU, DU and EU	Particulate -- lint from dryers	Transfers from 1650 to 22,000 gallons from December 22, 1980 through June 3, 1981 (25)	3.7E-02 to 1.0E+04 d/m/l total alpha (25)	Solar Evaporation Pond 207C (25)	1958 became laundry facility for plutonium related operations. (1)	1957	1978
779 and 779A	Plutonium Process Development Building -- DEMOLISHED	U-233 was aqueously processed, cast and machined from 1950s to 1970s. (1) Operations were separated into five areas: Process Chemistry Technology, Physical Metallurgy, Machining and Gaging, Joining Technology, and Hydriding Operations. After 1972, U-235 present in MBAs for assembly, residue processing, R&D disablement, vacuum melting, physical metallurgy, and hydriding operations. U-238 present in MBAs for product physical chemistry, R&D disablement, aqueous residue processing development, chemical technology, vacuum melting, metallurgy, joining and coating technologies, hydride operations, R&D machining, and storage. (14) 1976 -1982, U-233 present in MBA for R&D machining. R&D personnel used hot plates or small muffle furnaces to burn combustible waste contaminated with U-233. (15)	Aqueous -- DU and EU, acid cleaning and rinsing of parts. Coatings laboratory coated U with other metals. (11) Building constructed over the site of one of the original solar evaporation ponds. During excavation in September 1962 levels of radioactivity ranging from 11 to 75 dpm/g were noted, and later pools of water in these excavations had levels to 150 dpm/l. The radioactive material was primarily uranium. (4)	Particulate					Some disassembled parts of weapon components are processed via molten salt extraction to remove americium. Other radionuclides include americium, cobalt, plutonium, strontium, thorium in small quantities, and tritium contamination from hydriding operations. (1, 11)		
779OT	779-777 Overhead Tunnel -DEMOLISHED		Particulate							
779-TUN	779-782 Tunnel - DEMOLISHED		Particulate							
780A	Metal Storage									
781	Compressor Building - 777 (Helium Pumps)									

	Table TA-B-1		Uranium Usage and Potential Contamination at RFETS							
Building No.	Building Description	Uranium (U) Usage	Primary Form of U, that could have been released/ Comments	Secondary Form of U that could have been released/Comments	Operation Size: Volume of Liquid Wastes	Operation Size: Radiologic Activity in Liquids	Disposition of liquid waste (process waste lines)	Other Radionuclides	OPWL Installed (piping) (6)	OPWL Abandoned (piping) (6)
883	U Rolling and Forming Facility	Rolling and forming operations for EU from 1957-1968, and rolling and forming operations for DU from 1957 to 1989. These manufacturing operations included casting, cleaning, and heating of the U. (1, 2, 17) Nitric acid pickling processes. Manufactured depleted U calorimeter plates, and other depleted U products as special projects. (1) In 1977 and 1986, U-235 present in MBA for metal fabrication - rolling. U-238 present in MBAs for metal fabrication - rolling, and storage. (14) 1965 -1968, U-233 was most likely present in 883. R&D personnel used hot plates or small muffle furnaces to burn combustible waste contaminated with U-233. (15)	Aqueous -- primarily DU, primarily nitric acid solutions. Liquid wastes were transferred through OPWL, then current process waste lines to Building 774 for treatment (17)	TCE and PCE solvent use for cleaning was discontinued, and replaced with Oakite in 1985 or 1986. Use of freon and other CFCs was discontinued in 1988. Spent nitric acid solutions with pH 1-2, water from quench tanks, and other routine building operations contained enriched and depleted U. (2) Spent cleaning (degreasing) solutions drummed and transferred to Building 774 for solidification. (17) Particulate -- EU combustible waste incinerated. (17)	Transfers of aqueous waste ranging from 700 to 11,324 gallons to the Original Solar Evaporation Ponds from April 1957 through September 1963 (20); 650 to 700 gallons to the current Solar Evaporation Ponds; 300 to 1,300 gallons to 774 for treatment from December 22, 1980 through June 3, 1981 (25)	1.9E-8 to 3.9E-07 Curies/l total alpha and 42,200 to 868,000 d/m/l total alpha to the Original Solar Evaporation Ponds; 1.1E+03 to 2.1E+03 d/m/l total alpha to the current Solar Evaporation Ponds; 1.7E+04 to 1.2E+08 d/m/l total alpha to 774 for treatment	Original Solar Evaporation Ponds; current Solar Evaporation Ponds; 774		1957	3/84
883C	Cooling Tower 8883 - 4,000 Tons	None unless contaminated through air releases from other sources or by cross-over in Building process and cooling water systems.	Aqueous -- overspray							
884	Warehouse - Low Level Waste RCRA Unit 13	Containerized storage of radioactive waste. Routine activities provide no source for uranium contamination unless contaminated through air releases from other sources or spills from containers.	Particulate	Aqueous -- precipitation runoff from areas where spills occurred.						
886	Nuclear Safety Criticality Lab	From 1965 - 1989, nuclear criticality safety experiments using enriched uranyl nitrate, Oralloy metal and oxides. (1, 17) After 1972, U-235 present in MBAs for EU solutions, EU metal, low EU oxide, and holdup. U-238 present in MBAs for EU solutions, and metal. (14)	Aqueous -- primarily EU; uranyl nitrate (EU) solutions used. Experiments using liquid, powder, and metal forms of U. High Contamination Areas (HCAs) Several spills of uranyl nitrate solution with volumes up to 60 gallons have been documented. (13)	Particulate -- an accumulation of uranyl nitrate salt was identified in the filter plenum. (13)				Plutonium critical mass experiments using liquid, powder, and metal forms. (1) Principal isotopes of concern U-234, U-235, U-238, Pu-239, Am-241. (13)		
887	Sewage & Process Waste Lift Station	Documented releases of 881 waste from process waste tanks.	Aqueous -- DU and EU					Plutonium, and other radionuclides used during manufacturing and laboratory operations.		
889	Waste Storage and Treatment Building	Equipment decontamination facility (drums, forklifts, etc.); Low level waste baler and waste storage.	Aqueous -- DU and EU; overspray when decontaminating equipment, infiltration through concrete sump walls or process waste piping	Particulate	Transfers 100 to 1,800 gallons to Building 374 or to the current Solar Evaporation Pond 207A from February 8, 1981 through December 23, 1982	9.5E+00 to 2.1E+04 d/m/l total alpha	Solar Evaporation Pond 207A or 374	Plutonium	1968	5/82
890	Cooling Tower Pump House - 881, 883	None unless contaminated through air releases from other sources or by cross-over in Building process and cooling water systems.	Aqueous -- overspray							
890 Pad	Cooling Tower Equipment Storage	None unless contaminated through air releases from other sources or by cross-over in Building process and cooling water systems.	Aqueous -- overspray							
891	Ground Water Treatment Facility OU-1	Groundwater treatment facility	Aqueous -- spills and overflow of groundwater prior to treatment							
902 Pad	Sludge Waste Storage Pad (Tent 7)	Containerized storage of radioactive waste. Routine activities provide no source for uranium contamination unless contaminated through air releases from other sources or spills from containers.	Particulate	Aqueous -- potentially, precipitation runoff from areas where spills occurred						

	Table TA-B-1		Uranium Usage and Potential Contamination at RFETS							
Building No.	Building Description	Uranium (U) Usage	Primary Form of U, that could have been released/ Comments	Secondary Form of U that could have been released/Comments	Operation Size: Volume of Liquid Wastes	Operation Size: Radiologic Activity in Liquids	Disposition of liquid waste (process waste lines)	Other Radionuclides	OPWL Installed (piping) (6)	OPWL Abandoned (piping) (6)
881	Manufacturing and General Support Building	1952-1968 EU foundry, machining manufacturing (casting, rolling, forming, cleaning), recovery and purification. (1, 2, 17) Some EU metalworking continued into 1970s. U-233 was refined and machined from 1950s to 1970s. Oralloy leaching of site returns. Laundry facilities in original building. Analytical laboratories for inorganic, organic, and radionuclide analyses. (1, 17) U recovery operations on parts received from Oak Ridge discontinued in mid-1970's. A special recovery process involved dissolving several thousand beryllium-coated U fuel rods. EU artillery pieces were coated with cadmium and then machined. (2) After 1972, U-235 and U-238 present in MBAs for chemistry instrumentation, analytical services lab, chemical standards lab, and laser fusion. (14, 16) 1965 -1973, U-233 present in MBAs for chemistry implementation, and laboratory analytical services. R&D personnel used hot plates or small muffle furnaces to burn combustible waste contaminated with U-233. (15) Laundry wastes below 10,000 d/m/l discharged to sanitary system based on management of effluent from lower pond remaining between 10-25% of drinking water tolerance. (20-11/6/53)	Aqueous -- DU and EU; solvent extraction processes (using nitric acid, peroxide, dibutylcarbitol, anhydrous hydrogen fluoride, potassium hydroxide) for EU in 1950's. Nitric acid used to scrub "heels" of the stills - EU and DU. Nitric acid used in Oralloy leaching operation (EU). TCE and PCE used to clean enriched U parts. Spent acid, caustic, and HF scrubber solutions were recycled through the U recovery process. Twice during 1964 and 1969, natural thorium was used for "thorium strikes" to remove Th-228 from U-233 metal. Thorium production in 1950s through 1960s. (1,2) Ductwork upstream of filter plenums, process cooling water tanks, hydrofluoric acid and caustic scrubber systems, floors, walls and ceilings have had documented contamination from EU and DU and plutonium. (2) U-233 liquid wastes were transferred through the OPWL to 774 for treatment (16) Waste solutions from primary solvent extraction and secondary extraction of EU from uranyl nitrate transferred through OPWL to the Solar Evaporation Ponds. Liquid wastes generated during EU processing activities transferred to 774 through OPWL for treatment. (17) Laundry wastes below 10,000 d/m/l discharged to sanitary system. (20-11/6/53)	Particulate -- EU combustible waste incinerated. (17) U-233 casting skulls and machining chips were burned to oxide. (18) Organic -- Machining oils and organics were burned in open burn pits. (19) Spent lathe coolant was collected in drums and shipped to 774 for solidification or went to the burning pits based on U concentration. (17) 1958-1959 spread of contamination resulting from an Oralloy (U-235) fire (21)	Aqueous laundry waste transfers ranging from 5,400 to 38,230 gallons to Sanitary Waste 995 from January 1954 through September 1955; 9,600 to 21,600 gallons to Pond B-2 from April to May 1955; 2,700 to 107,400 gallons to Original Solar Evaporation Ponds from April 1957 to April 1964 (20)	3.7E-10 to 3.8E-09 Curies/l and 8,214 to 8,450 d/m/l total alpha to Sanitary Sewer 995; 3.2E-10 to 2.9E-10 Curies/l and 6,440 to 7,193 d/m/l total alpha to Pond B-2 (previously Pond 3); 2.8E-09 to 6.9E-08 Curies/l and 6,200 to 153,000 d/m/l total alpha to Original Solar Evaporation Ponds (20); <100 to 4.0E+02 d/m/l total alpha to Sanitary, and 1.0E-04 to 8.4E+04 d/m/l total alpha and 5.4E-04 to 1.1E+06 total beta to the Solar Evaporation Ponds (25)	Sanitary Sewer; Pond B-2 (previously Pond 3); Original Solar Evaporation Ponds; current Solar Evaporation Ponds	Neptunium, curium, and cerium used as tracers in the metal alloys. Thorium-containing components were manufactured from 1950s to 1960s. Trace materials were kept separate from regulator production operations. Dissolution and recovery of special waste streams was conducted in a separate area of the building. (2)	1952, 1957	12/80
881C	Cooling Tower B881 - 900 Tons	None unless contaminated through air releases from other sources or by cross-over in Building process and cooling water systems.	Aqueous -- overspray							
881F	Filter Plenum (881 roof) Zone 1	HEPA filtration of building effluent air	Particulate							
881G	Emergency Generator Facility-B881	None unless contaminated through air releases from other sources								
881H	Electrical Equipment Building	None unless contaminated through air releases from other sources								
881-S1	881-883 Stack (north of 881, west stack)	HEPA filtration of building effluent air	Particulate							
881-S2	881-883 Stack (north of 881, east stack)	HEPA filtration of building effluent air	Particulate							
881-S3	881-883 Stack (south of 881)	HEPA filtration of building effluent air	Particulate							
881-TUN	881-883 Tunnel	DU and EU parts and waste were transferred through tunnel.	Aqueous -- EU and DU; infiltration of groundwater into potentially contaminated areas.							

	Table TA-B-1		Uranium Usage and Potential Contamination at RFETS							
Building No.	Building Description	Uranium (U) Usage	Primary Form of U, that could have been released/ Comments	Secondary Form of U that could have been released/Comments	Operation Size: Volume of Liquid Wastes	Operation Size: Radiologic Activity in Liquids	Disposition of liquid waste (process waste lines)	Other Radionuclides	OPWL Installed (piping) (6)	OPWL Abandoned (piping) (6)
973	Sewage Treatment Sludge Drying Bed 3 (995)	Potential low-concentration uranium contamination of sewage sludge	Particulate	Aqueous -- percolation of liquids into soils prior to late 1960s when drying beds were not covered with roofs						
974	Sewage Treatment Sludge Drying Bed 4 (995)	Potential low-concentration uranium contamination of sewage sludge	Particulate	Aqueous -- percolation of liquids into soils prior to late 1960s when drying beds were not covered with roofs						
975	Sewage Treatment Sludge Drying Bed 5 (995)	Potential low-concentration uranium contamination of sewage sludge	Particulate	Aqueous -- percolation of liquids into soils prior to late 1960s when drying beds were not covered with roofs						
976	Sewage Treatment Sludge Drying Bed 6 (995)	Potential low-concentration uranium contamination of sewage sludge	Particulate	Aqueous -- percolation of liquids into soils prior to late 1960s when drying beds were not covered with roofs						
977	Sewage Treatment Sludge Drying Bed 7 (995)	Potential low-concentration uranium contamination of sewage sludge	Particulate	Aqueous -- percolation of liquids into soils prior to late 1960s when drying beds were not covered with roofs						
984	Shipping Container Storage Facility		Particulate							
985	Filter Plenum 8998/997/999	HEPA filtration of building effluent air	Particulate							
987	Storage Vault (WSI Plant Protection) Bunker (vacant)	Recently stored smoke grenades and seals								
990	Pre-Aeration Building									
990A	Waste Water Treatment									
991	Product Warehouse	1952-1957 Product Assembly (including enriched and depleted U components.) Early days contained its own laundry facilities. (1) 1966 - 1974 explosives forming project. (2) Shipping and receiving. Currently TRU waste storage. After 1972, U-235 and U-238 present in MBAs for container storage. (14)	Particulate	Organic -- product assembly operation used TCE and acetone on wipes for wipe-down of parts prior to assembly. (2)						
991TUN	Tunnels Between 991 Cluster Buildings	Transfer of weapon components, parts, and waste between 991 and vaults	Particulate	Groundwater -- potential contamination of groundwater through percolation of groundwater into and out of hallways between vaults.						
993	Security Storage Vault (WSI)	1965-1968, explosive bonding experiments using U, stainless steel, and dynamite (1)	Particulate							
995	Sewage Treatment Facility Low Level -- Including aeration basins, clarifiers, digesters, effluent cells, dryer beds	1954-1968 low level sewage sludge buried in east trenches. In 1968 sent to Present Sanitary Landfill.	Particulate	Aqueous infiltration from concrete. The original process waste line outfall from Building 774 was located just west of the Building 995 and the Building 995 outfall. In 1972 this outfall was rerouted through the sanitary sewer lines into Building 995. The abandoned/capped line was still in place in 1974. (4)						

	Table TA-B-1		Uranium Usage and Potential Contamination at RFETS							
Building No.	Building Description	Uranium (U) Usage	Primary Form of U, that could have been released/ Comments	Secondary Form of U that could have been released/Comments	Operation Size: Volume of Liquid Wastes	Operation Size: Radiologic Activity in Liquids	Disposition of liquid waste (process waste lines)	Other Radionuclides	OPWL Installed (piping) (6)	OPWL Abandoned (piping) (6)
903	Contamination Barrier - East and West Trenches									
903 Pad	Contamination Barrier/Pad									
903A	Main Decontamination Facility (MDF) including storage pad and tanks	Decontamination of equipment and vehicles	Aqueous – overspray							
904 Pad	LL Mixed Waste Storage Pad (Tents 8,9,10,11) (RCRA Unit 15A-Cargo Containers)	Tent 10 Permacon was used for pondcrete/saltcrete repack operations. (9)	Aqueous – precipitation runoff from areas where spills have occurred	Historical release of pondcrete or saltcrete possible. Tent 10 and Tent 11 Recon Char sampling results are above instrument MDC but below contamination limits prescribed in DOE Order 5400.5. Particulate – permacon is posted as a CA. (9)						
906	Central Waste Storage	Containerized storage of radioactive waste	Particulate	Aqueous – precipitation runoff from areas where spills occurred.						
910	Solar Pond Evaporator Building	1977 constructed for Reverse Osmosis treatment of solar evaporation pond liquids	Aqueous – DU and EU	Aqueous. All 30 paint samples exceeded the MDC for U-238. 29 samples exceeded the MDC for U-234/235. Six samples exceeded the MDC for U-235. These results are above instrument MDC but below contamination limits prescribed in DOE Order 5400.5. (9)						
928	Fire Water Pump House									
960	Contractor Storage Area, south of 964 (no longer used)	Windblown contamination from the Solar Evaporation Ponds containing U	Aqueous – overspray							
964	Waste Drum Storage RCRA Unit 24 Low Level Hazardous	Windblown contamination from the Solar Evaporation Ponds containing U	Aqueous – overspray							
966	PA Decontamination Pad (aka 964P)	Decontamination of equipment and vehicles	Aqueous – overspray							
971	Sewage Treatment Sludge Drying Bed 1 (995)	Potential low-concentration uranium contamination of sewage sludge	Particulate	Aqueous – percolation of liquids into soils prior to late 1960s when drying beds were not covered with roofs						
972	Sewage Treatment Sludge Drying Bed 2 (995)	Potential low-concentration uranium contamination of sewage sludge	Particulate	Aqueous – percolation of liquids into soils prior to late 1960s when drying beds were not covered with roofs						

	Table TA-B-1		Uranium Usage and Potential Contamination at RFETS							
Building No.	Building Description	Uranium (U) Usage	Primary Form of U, that could have been released/ Comments	Secondary Form of U that could have been released/Comments	Operation Size: Volume of Liquid Wastes	Operation Size: Radiologic Activity in Liquids	Disposition of liquid waste (process waste lines)	Other Radionuclides	OPWL Installed (piping) (6)	OPWL Abandoned (piping) (6)
996	Storage Vault - Building 991	Storage of weapon components, parts, waste	Particulate -- Routine surveys prior to 1974 indicate that some infiltration of uranium may be present. (4)	Groundwater -- potential contamination of groundwater through percolation of groundwater into and out of hallways between vaults.						
997	Storage Vault - Building 991	Storage of weapon components, parts, waste	Particulate	Groundwater -- potential contamination of groundwater through percolation of groundwater into and out of hallways between vaults.						
998	Storage Vault - Building 991	Storage of weapon components, parts, waste	Particulate	Groundwater -- potential contamination of groundwater through percolation of groundwater into and out of hallways between vaults.						
999	Storage Vault - Building 991	Storage of weapon components, parts, waste	Particulate	Groundwater -- potential contamination of groundwater through percolation of groundwater into and out of hallways between vaults.						
C865	Cooling Tower (865)	None unless contaminated through air releases from other sources or by cross-over in Building process and cooling water systems.								
VV001	Process Waste Valve Vault (west of 881)	Receives waste from 881 (7)	Aqueous -- DU and EU		See individual buildings for transfer information					
VV002	Process Waste Valve Vault (west of 883)	Receives waste from 881 and 883 (7)	Aqueous -- DU and EU		See individual buildings for transfer information					
VV003	Process Waste Valve Vault (northwest of 889)	Receives waste from 881, 883, 889, 865 (7)	Aqueous -- DU and EU		See individual buildings for transfer information					
VV004	Process Waste Valve Vault (northwest of 889)	Receives waste from 889, 865 (7)	Aqueous -- DU and EU		See individual buildings for transfer information					
VV005	Process Waste Valve Vault (northeast of 889)	Receives waste from 865 (7)	Aqueous		See individual buildings for transfer information					
VV006	Process Waste Valve Vault (east of 889)	Receives waste from 865 (7)	Aqueous		See individual buildings for transfer information					
VV007	Process Waste Valve Vault (southwest 707)	Receives waste from 881, 883, 889, 865 (7)	Aqueous -- DU and EU		See individual buildings for transfer information					
VV008	Process Waste Valve Vault (west of 707)	Receives waste from 707, 774, 778, 881, 883, 889, 865 (7)	Aqueous -- DU and EU		See individual buildings for transfer information					
VV009	Process Waste Valve Vault (west of 778)	Receives waste from 707, 774, 778 (7)	Aqueous -- DU and EU		See individual buildings for transfer information					
VV010	Process Waste Valve Vault (south of 528)	Receives waste from 559, 707, 774, 778, 881, 883, 889, 865 (7)	Aqueous -- DU and EU		See individual buildings for transfer information					
VV011	Process Waste Valve Vault (east of 549)	Receives waste from 559, 707, 774, 778, 881, 883, 889, 865 (7)	Aqueous -- DU and EU		See individual buildings for transfer information					

671

	Table TA-B-1		Uranium Usage and Potential Contamination at RFETS							
Building No.	Building Description	Uranium (U) Usage	Primary Form of U, that could have been released/ Comments	Secondary Form of U that could have been released/Comments	Operation Size: Volume of Liquid Wastes	Operation Size: Radiologic Activity in Liquids	Disposition of liquid waste (process waste lines)	Other Radionuclides	OPWL Installed (piping) (6)	OPWL Abandoned (piping) (6)
VV012	Process Waste Valve Vault (southeast of 231)	Receives waste from 559, 707, 774, 778, 881, 883, 889, 865, Pump Station 231 (7)	Aqueous -- DU and EU		See individual buildings for transfer information					
VV013	Process Waste Valve Vault (west of 231)	Receives waste from 122, 123, 443, 444, 460, 559, 707, 774, 778, 881, 883, 889, 865, Pump Station 231 (7)	Aqueous -- DU and EU		See individual buildings for transfer information					
VV014	Process Waste Valve Vault (south of 372A)	Receives waste from 122, 123, 443, 460 (7)	Aqueous -- DU and EU		See individual buildings for transfer information					
VV015	Process Waste Valve Vault (west of 334)	Receives waste from 122, 123, 443, 460 (7)	Aqueous -- DU and EU		See individual buildings for transfer information					
VV016	Process Waste Valve Vault (east of 443)	Receives waste from 122, 123, 443, 460 (7)	Aqueous -- DU and EU		See individual buildings for transfer information					
VV017	Process Waste Valve Vault (southeast of 443)	Receives waste from 122, 123, 460 (7)	Aqueous -- DU and EU		See individual buildings for transfer information					
VV018	Process Waste Valve Vault (north of 460)	Receives waste from 122, 123, 460 (7)	Aqueous -- DU and EU		See individual buildings for transfer information					
VV019	Process Waste Valve Vault (southwest of 452)	Receives waste from 444 (7)	Aqueous -- primarily DU, 1974 = EU also		See individual buildings for transfer information					
VV020	Process Waste Valve Vault (west of 452)	Receives waste from 444 (7)	Aqueous -- primarily DU, 1974 = EU also		See individual buildings for transfer information					

672 A

	Table TA-B-2 References
Ref #	**Reference/Description**
1	Reconstruction of Historical Rocky Flats Operations & Identification of Release Points, Phase 1: Historical Public Exposures, Project Tasks 3 & 4, Final Draft Report, prepared by ChemRisk for CDPHE, August 1992
2	Building Histories, for Buildings 371, 444, 460, 707, 771, 776/777, 881, 883, and 991, Historical Release Report (HRR), EG&G Rocky Flats, Inc. November 1994
3	Historical Release Report for the Rocky Flats Plant, U.S. Department of Energy, June 1992
4	Environmental Inventory, A Historical Summation of Environmental Incidents Affecting Soils at or Near the U.S. AEC Rocky Flats Plant, Rocky Flats Division Dow Chemical U.S.A., January 29, 1974
5	Draft Final Technical Memorandum 1, Volume II, Pipelines , Addendum to Phase I RFI/RI Work Plan, Field Sampling Plan, Volume IIA - Text and Appendices, Rocky Flats Environmental Technology Site, Original Process Waste Lines (Operable Unit 9), US Department of Energy, November 1994
6	Final Phase I RFI/RI Work Plan, Rocky Flats Plant Original Process Waste Lines, OU-9, U.S. Department of Energy, February 1992
7	Valve Vault maps from procedure WO-3016, dated April 27, 1990
8	Building 771/774 Cluster Closure Project, Reconnaissance Level Characterization Report, Revision 2, August 8, 1998
9	Reconnaissance-Level Characterization Report (RLCR), Group A Facilities, Revision 2, June 14, 2000
10	Reconnaissance Level Characterization Report (RLCR), Building 371 Cluster, Revision 0, August 28, 2000
11	Reconnaissance Level Characterization Report for the 779 Cluster, December 1997
12	Reconnaissance Level Characterization Report for Building 123, August 1997
13	Reconnaissance Level Characterization Report for the 886 Cluster Decommissioning Project, Revision 1, December 24, 1997
14	Historical Material Balance Area (MBA) Designator Usage, and Isotope Inventory Review for: Uranium 235 (235 U) and 238 (238 U), Plutonium 238 (238 U), Neptunium 237 (237 Np), Californium 252 (252 Cf), Curium 244 (244 Cm), Thorium (Th), RS-090-065, prepared by The IT Group, August 31, 1999
15	History of Uranium-233 (233 U) Processing at Rocky Flats Plant, In Support of the RFETS Acceptable Knowledge Program, RS-090-056, prepared by ICF Kaiser Engineers, Inc., April 1, 1999
16	Disposition of Uranium-233 (233 U) in Plutonium Metal and Oxide at the Rocky Flats Environmental Technology Site, prepared by The IT Corporation, March 1, 2000
17	Draft Report of the Flow of Recycled Uranium at the Rocky Flats Plan, 1953-1993, March 30, 2000
18	Report on the Flow of Recycled Uranium at the Department of Energy's Rocky Flats Plant, 1953-1993, June 30, 2000

673

	Table TA-B-2 References
Ref #	**Reference/Description**
19	Recycled Uranium, The Flow and Characteristics of Recycled Uranium Throughout the DOE Complex, 1952-1999, Volume I, DOE Complex-Wide Draft Summary Report (Rev 1), US Department of Energy, February 2001
20	Monthly History Reports and Progress reports contained in Memoranda from the Waste Disposal Coordinating Group or the Process Waste Disposal Group, authored by E.S. Ryan and E. F. Johnston, 1953 through 1964. (Record review did not include every History or Progress Report)
21	Report on Reference Material in Reply to Summary of Known Incidents at Rocky Flats, Report from J. G. Stearns to B.W. Colston, Area Manager, November 1, 1973
22	History of 207 Solar Evaporation Ponds and Nitrate in Walnut Creek, J. B. Owen to E. W. Bean, April 10, 1974
23	Attachment I, Rocky Flats Plant Past Disposal Sites from RFP Revised Part A Permit Application, Form 3 Item V, August 7, 1989
24	Areas of Concern at Rocky Flats: Soil Contamination and Related Incidents, Part I: Plutonium, Product and Health Physics Research HPR-317-381-138, L.M. Steward, June 29, 1973
25	774's Building Waste Transfer Log Book, December 22, 1981 through June 7, 1985 (Original Logbook located in 774 control room); Concentrations and volumes referenced for dates December 22, 1980 through June 3, 1981 for all buildings noted except 889 (December 20, 1980 through December 23, 1982)
	Documents Reviewed but not Referenced
	Reconnaissance-Level Characterization Report (RLCR), Building 111 and Building 333, Revision 0, January 15, 2001
	Reconnaissance Level Characterization Report for Trailer 112B (T112B), (Survey Unit 112B), Revision 0, April 3, 2000
	Reconnaissance Level Characterization Report for Trailer T112A and Trailer T112C, Revision 1, September 30, 1999
	Reconnaissance-Level Characterization Report (RLCR), Group B Facilities, Revision 0, August 2, 2000 -- trailers
	Reconnaissance Level Characterization Report (RLCR), Group C Facilities, Revision 0, August 9, 2000
	Reconnaissance Level Characterization Report for the T690 Complex Office Trailer Removal, May 22, 1997
	Reconnaissance-Level Characterization Report (RLCR), Building 575, Revision 0, June 26, 2000
	Reconnaissance-Level Characterization Report (RLCR), Building 707 Cluster, Revision 1, August 1, 2000 -- NOTE: no U-235 referenced for EU decon or production part cleaning, Tank V-100; no U-238 contamination identified in 778 laundry
	Reconnaissance Level Characterization Report (RLCR) Supplement, 771 Closure Project, Revision 0, November 3, 2000
	Reconnaissance Level Characterization Report (RLCR), Type 1 Facilities, Building 771 Closure Project, Revision 0, December 19, 2000

674

LIST OF ACRONYMS AND BASIC NOMENCLATURE

$\gamma(h)$	Variance at distance h
°C	Centigrade
°F	Fahrenheit
a	Range of influence
ac	Acre(s)
AED	Aerodynamic Equivalent Diameter
AL	Action Levels
Al	Elemental Aluminum
ALF	Action Level Framework
Am	Elemental Americium
am	Amorphous phase
AME	Actinide Migration Evaluation
aq	Aqueous phase
ASD	Analytical Services Division
atm	Atmospheres used as a unit of pressure measurement
au	Atomic Unit
BLUE	Best Linear Unbiased Estimator
Bq	Becquerel(s)
BZ	Buffer Zone
C	Spherical component
C	Elemental Carbon
c	Crystalline phase

Ce76

Ca	Elemental Calcium
CCC	Colorado Climate Center
CCR	Colorado Code of Regulations
CDPHE	Colorado Department of Public Health and Environment
CERCLA	Comprehensive Environmental Response, Compensation and Liability Act
CFR	Code of Federal Regulations
cfs	Cubic meters per second
Ci/L	Curie(s) per Liter
cm/sec	Centimeter(s) per second
cm^2	Centimeter(s) squared
CO	Colorado
C_o	Nugget effect
COC	Colloidal Organic Carbon
COL	Colluvium
COMRAD	Community Radiation Monitoring
CSU	Colorado State University
CUHP	Colorado Urban Hydrograph Procedure
D&D	Decommission and Demolish
d	Day(s)
Da	Dalton(s)
DFB	Desferrioxamine B
DFE	Desferrioxamine E
DFO	Desferrioxamine O
DNA	Deoxyribonucleic Acid

677

DNAPL	Dense, Non-Aqueous Phase Liquids
DOE	United States Department of Energy
d_p/d_m	Particle Diameter to Media Diameter
DQO	Data Quality Objectives
DMRB	Dissimilatory Metal-Reducing Bacteria
E	1E+06 is equivalent to 1×10^6 (Scientific Notation)
EDDIE	Environmental Data Dynamic Information Exchange
EDE	Effective Dose Equivalent
EDTA	Ethylene Diamine Tetraacetic Acid
EG&G	EG&G, Inc. formerly Edgerton, Germeshausen and Grier, Inc.
E_h	Reduction-Oxidation Potential expressed in volts
EP	Erosion Potential of the total suspended particulate (TSP)
EPA	Environmental Protection Agency
ERAMS	Environmental Radiation Ambient Monitoring System
F	Elemental Fluorine
Fe	Elemental Iron
ft	Foot or Feet
ft^2	Foot or Feet squared
FY	Fiscal Year
g	Gram(s)
GIS	Geographic Information Systems
GS	Gaging Station
GTS	Grimsel Test Site
GW	Groundwater

678

H	Elemental Hydrogen
ha	Hectare(s)
HEC-6T	Hydrologic Engineering Center –6T
HEPA	High Efficiency Particulate Air
HMP	Hexametaphosphate
HPGe	High Purity Germanium
HRR	Historical Release Report
HVOL	High-Volume
HYDRAQL	Chemical Reaction Model
IA	Industrial Area
IAG	Interagency Agreement
ICP/MS	Inductively Coupled Plasma/Mass Spectrometry
IHSS	Individual Hazardous Substance Site
IM/IRA	Interim Measure/Interim Remedial Action
IMP	Integrated Monitoring Plan
in	Inch(es)
ISC3	Industrial Source Complex
ISCST3	Industrial Source Complex Short-Term
K	Elemental Potassium
Ka	Arapahoe Formation geologic map unit
Kaiser-Hill	Kaiser-Hill Company, LLC
KAR	Unweathered, undifferentiated Arapahoe/Laramie Formation
K_d	Empirical distribution coefficient
kDa	Kilodalton(s)

679

kg	Kilogram(s)
KI	Laramie Formation geologic map unit
km	Kilometer(s)
K_{sp}	Solubility constant
L	Liter(s)
LANL	Los Alamos National Laboratory
LHSU	Lower Hydrostratigraphic Unit
Lower Flow System	KAR
LPS	Lipopolysaccharides
m	Meter(s)
M	Molarity, the molar concentration of a solution expressed as the number of moles of solute per liter of solution
m/s	Meter(s) per second
m/yr	Meter(s) per year
m^2	Meter(s) squared
m^3	Cubic meters
m^3/s	Meter(s) cubed per second
MBq	Mega-Becquerel
MCL	Maximum Contaminant Level
MDA	Minimum Detected Activities
MEPAS	Multimedia Environmental Contaminant Assessment System
meq/L	Milliequivalent per Liter
Mg	Elemental Magnesium
mg/L	Milligram(s) per Liter

680

mi	Mile(s)
MINEQL	An applied geochemical speciation model
MINTEQA2	An applied geochemical speciation model
mL	Milliliters or milliliter
mm	Millimeters or millimeter
Mn	Elemental Manganese
mph	Mile(s) per hour
mrem	Millirem
MSL	Mean Sea Level
mV	Millivolt(s)
N	Elemental Nitrogen
N/A	Not Applicable
NABIR	Department of Energy, Natural and Accelerated Bioremediation
NaCl	Sodium chloride
NASA	National Aeronautics and Space Administration
NCDC	National Climate Data Center
NESHAP	National Emission Standard for Hazardous Air Pollutants
NFA	No Further Action
nm	Nanometers or nanometer
NOAA	National Oceanic and Atmospheric Association
Np	Elemental Neptunium
N_s	Rate at which particles attach
N_t	Rate at which particles collide
NTA	Nitrilotriacedic Acid

681

NTS	Nevada Test Site
O	Elemental Oxygen
OPWL	Original Process Waste Lines
OU	Operable Unit
PA	Protected Area
PAC	Potential Area of Concern
pCi/L	Picocurie(s) per Liter
PCR	Polymerase Chain Reaction
PGA	γ-polyglutamic Acid
PIC	Potential Incident of Concern
PM_{10}	Particle sizes
POC	Point of Compliance
POE	Point of Evaluation
ppm	Parts per million
PPRG	Preliminary Programmatic Remediation Goals
PSA	Parameter Specific Analytical
Pu	Elemental Plutonium
Qa	Recent Alluvium
QA/QC	Quality Assurance / Quality Control
Qls	Landslide geologic map unit
Qrf	Rocky Flats Alluvium geologic map unit
Qta	Terrace Alluvium geologic map unit
R	Rejected analytical data
r	Ionic radius

682

R^2	Regression analysis residual
Ra	Elemental Radium
RAAMP	Radioactive Ambient Air Monitoring Program
RCRA	Resource Conservation and Recovery Act
RDL	Required Detection Limit
RFA	Rocky Flats Alluvium
RFCA	Rocky Flats Cleanup Agreement
RFETS	Rocky Flats Environmental Technology Site
RFI/RI	RCRA Facility Investigation/Remedial Investigation
RMRS	Rocky Mountain Remediation Services
RNA	Ribonucleic Acid
s	Solid phase
SCREEN3	Office of Air Quality Planning and Standards, Monitoring, and Analysis Division Model
SCS	Soil Conservation Service
SEP	Solar Evaporation Pond
SGW	Shallow Groundwater
Si	Elemental Silicon
SID	South Interceptor Ditch
Sill	$C_o + C$
SQL	Structured Query Language
SW	Surface water
SWD	Soil and Water Database
SWMU	Solid Waste Management Unit

683

SWWB	Site-Wide Water Balance
$t_{1/2}$	Half-life
TA	Technical Appendix
TDS	Total Dissolved Solids
TFF	Tangential-Flow Filtration
Th	Elemental Thorium
TIMS	Thermal Ionization Mass Spectrometry
TIN	Triangular Integrated Networks
TSP	Total Suspended Particulate
TSS	Total Suspended Solids
U	Elemental Uranium
UBC	Underground Building Contamination
UHSU	Upper Hydrostratigraphic Unit
Upper Flow System	RFA+VFA+COL+WCS
USDA	United States Department of Agriculture
USGS	United States Geological Survey
V	Validated data
VFA	Valley-Fill Alluvium
W	Colloid suspension stability
WATEQ3	Chemical Reaction Model
WATEQ4F	Chemical Reaction Model
WCS	Weathered Claystone of upper Arapahoe/Laramie Formations
WEPP	Water Erosion Prediction Project
WIPP	Waste Isolation Pilot Plant

684

WWE	Wright Water Engineers, Inc.
WWTP	Wastewater Treatment Plant
WY	Water Year
XANES, EXAFS	X-ray Absorption Spectroscopy, Extended X-ray Absorption Fine Structure
XPS	X-ray Photoelectron Spectroscopy
y	Year(s)
z	Formal charge
z/r	Ratio
ZTS	Zero Tension Sampler
σ_z	Gaussian distribution
σ	Standard Deviation
α	Efficiency factor
η	Collector Efficiency is the rate at which the particle/colloid collides with the surface divided by the rate at which the particle/colloid travels towards the surface
µg/L	Microgram(s) per Liter

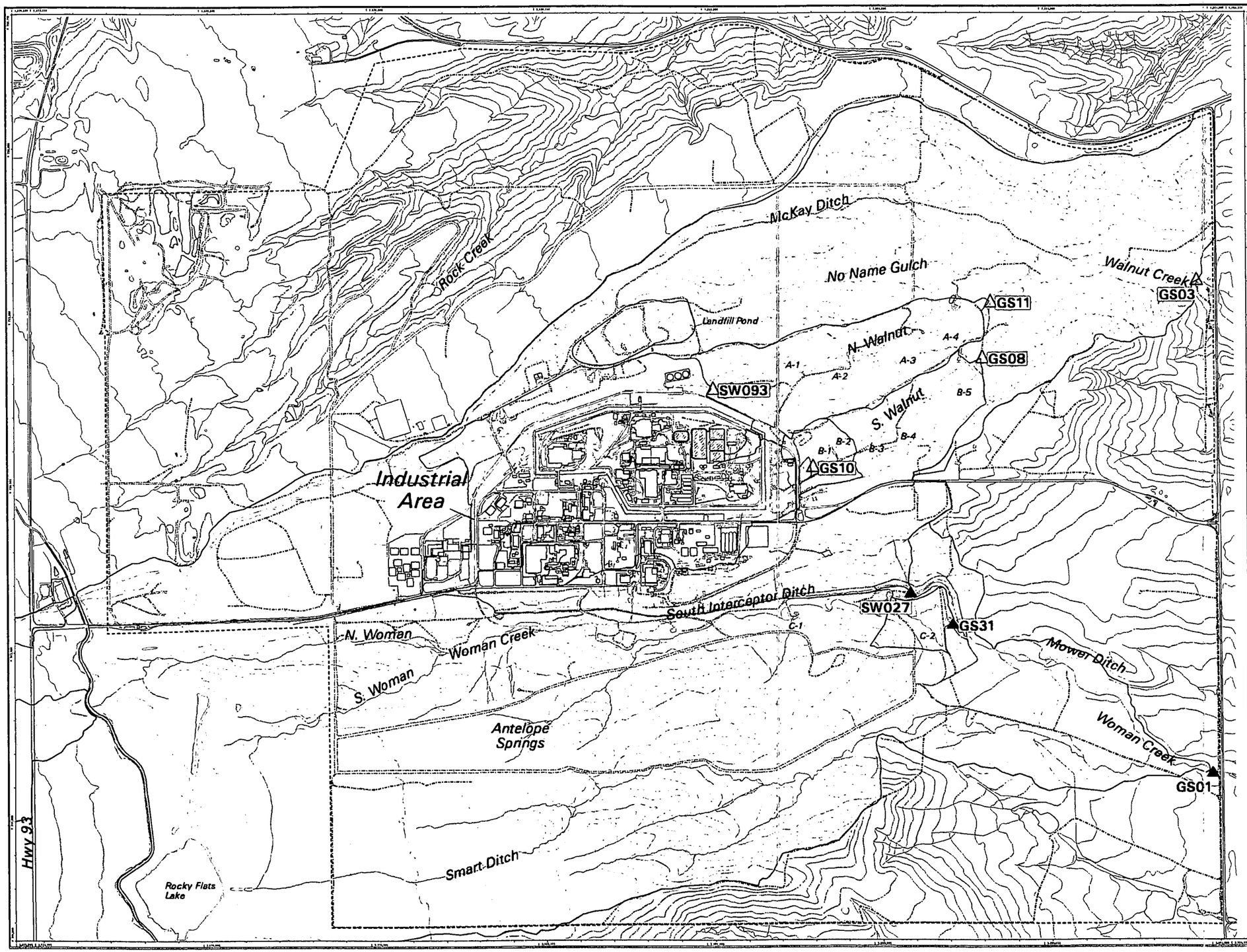

Figure TA-1-2

Actinide Migration Evaluation Pathway Report

Rocky Flats Basemap

EXPLANATION

- Walnut Creek Drainage Basin
- Woman Creek Drainage Basin
- Walnut Creek Basin Gaging Station (GS03, GS08, GS10, GS11 & SW093)
- Woman Creek Basin Gaging Station (GS01, GS31 & SW027)
- Drainage Basin Boundary
- Industrial Area Boundary

Standard Map Features

- Buildings and other structures
- Solar Evaporation Ponds (SEPs)
- Lakes and ponds
- Streams, ditches, or other drainage features
- Topographic Contour (20-Foot)
- Rocky Flats boundary
- Paved roads
- Dirt roads

DATA SOURCE BASE FEATURES:

Buildings, fences, hydrography, roads and other structures from 1994 aerial fly-over data captured by EG&G RSL, Las Vegas. Digitized from the orthophotographs. 1/95

Topographic contours were derived from digital elevation model (DEM) data by Morrison Knudson (MK) using ESRI Arc TIN and LATTICE to process the DEM data to create 5-foot contours. The DEM data was captured by the Remote Sensing Lab, Las Vegas, NV, 1994 Aerial Flyover at ~ 10 meter resolution. DEM post-processing performed by MK, Winter 1997.

Scale = 1 : 21330
1 inch represents approximately 1778 feet

250 0 500 1000 ft

State Plane Coordinate Projection
Colorado Central Zone
Datum: NAD27

U.S. Department of Energy
Rocky Flats Environmental Technology Site

GIS Dept. 303-966-7707

Prepared by: DynCorp — THE ART OF TECHNOLOGY

Prepared for: KH KAISER-HILL COMPANY

March 25, 2003

NT_Svr w:/projects/actinide_pathway_report/fy2002/misc_maps/ame_basemap_site.aml

46

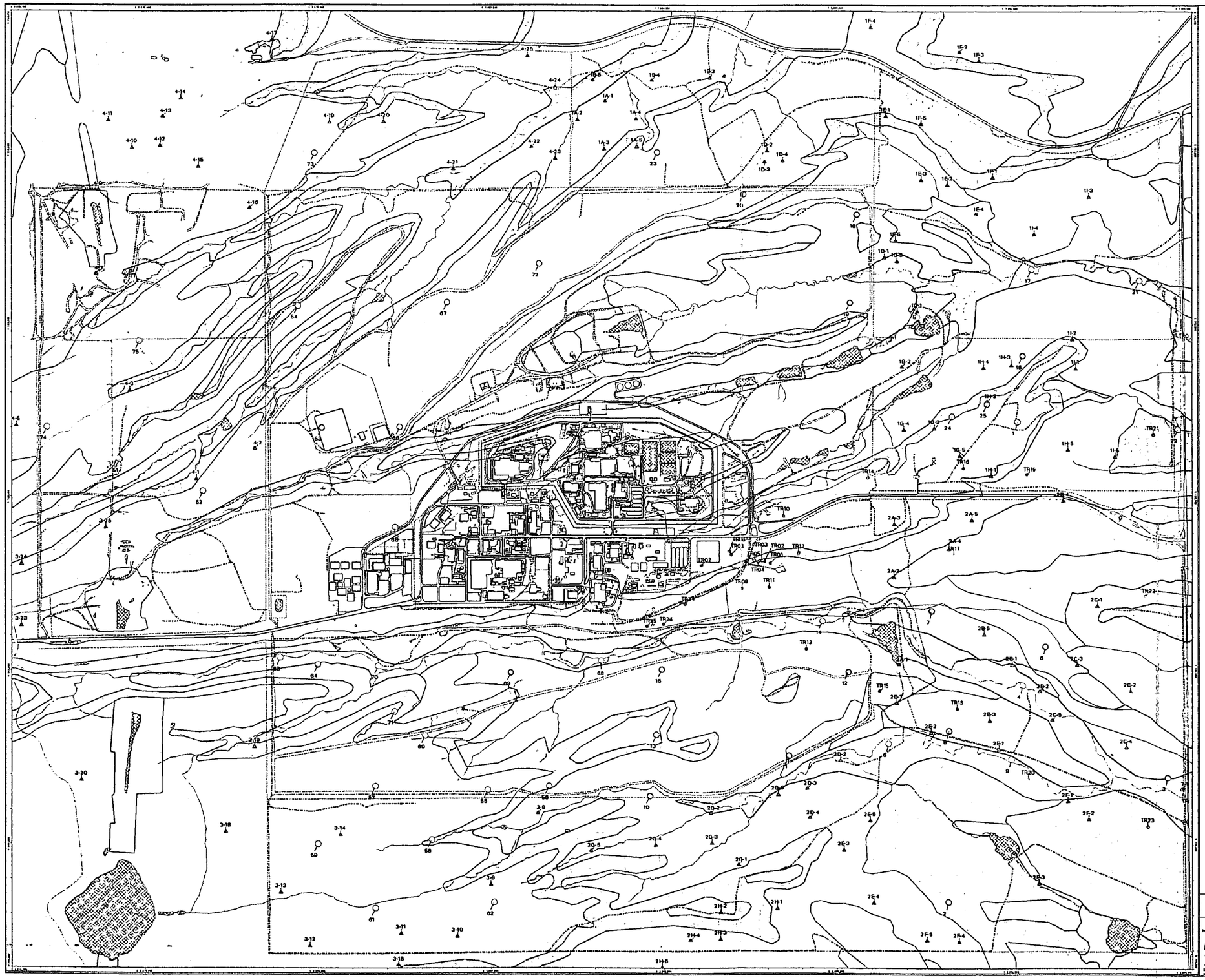

Figure TA-1-7

Actinide Migration Evaluation Pathway Report

Rocky Flats Soils Map with Hydraulic Conductivity Measurement and Soil Sampling Locations

EXPLANATION

Sampling Features

- Tension infiltrometer sampling location
- Soil Pit Location
- CDPHE Samples

Soils

- Denver clay loam, 2 - 5%
- Denver clay loam, 5 - 9%
- Denver-Kutch clay loam, 5 - 9%
- Denver-Kutch clay loam, 9 - 15%
- Denver-Kutch-Midway clay loam, 9 - 25%
- Englewood clay loam, 0 - 2%
- Englewood clay loam, 2 - 5%
- Flatirons cobbly sandy loam, 0 - 3%
- Flatirons stoney sandy loam, 0 - 5%
- Haverson loam, 0 - 3%
- Leyden-Primen-Standley cobbly clay loams, 15 - 50%
- McClave clay loam, 0 - 3%
- Midway clay loam, 9 - 30%
- Nederland very cobbly sandy loam, 15 - 50%
- Nunn clay loam, 0 - 2%
- Nunn clay loam, 2 - 5%
- Pits, gravel
- Rock outcrop, Sedimentary
- Standley-Nunn gravelly clay loam, 0 - 5%
- Valmont clay loam, 0 - 3%
- Valmont-Nederland very cobbly sandy loam, 0 - 3%
- Willowman-Leyden cobbly loam, 9 - 30%
- Yoder Fariant-Midway complex, 15 - 60%

Standard Map Features

- Buildings and other structures
- Lakes and ponds
- Streams, ditches, or other drainage features
- Fences and other barriers
- Paved roads
- Dirt roads

DATA SOURCE BASE FEATURES:
Soils data from the US Soil Conservation Service. Uncertified Golden Area Soil Survey - 1980. Buildings, fences, hydrography, roads and other structures from 1994 aerial fly-over data captured by EG&G RSL, Las Vegas. Digitized from the orthophotographs. 1/95

Scale = 1 : 20240
1 inch represents approximately 1687 feet

250 0 500 1000 ft

State Plane Coordinate Projection
Colorado Central Zone
Datum: NAD27

U.S. Department of Energy
Rocky Flats Environmental Technology Site

GIS Dept. 303-966-7767

Prepared by: DynCorp — THE ART OF TECHNOLOGY

Prepared for: KAISER-HILL

NT_Svr w:/projects/actinide_pathway_report/ly2002/misc_maps/soil_smpl.aml

49

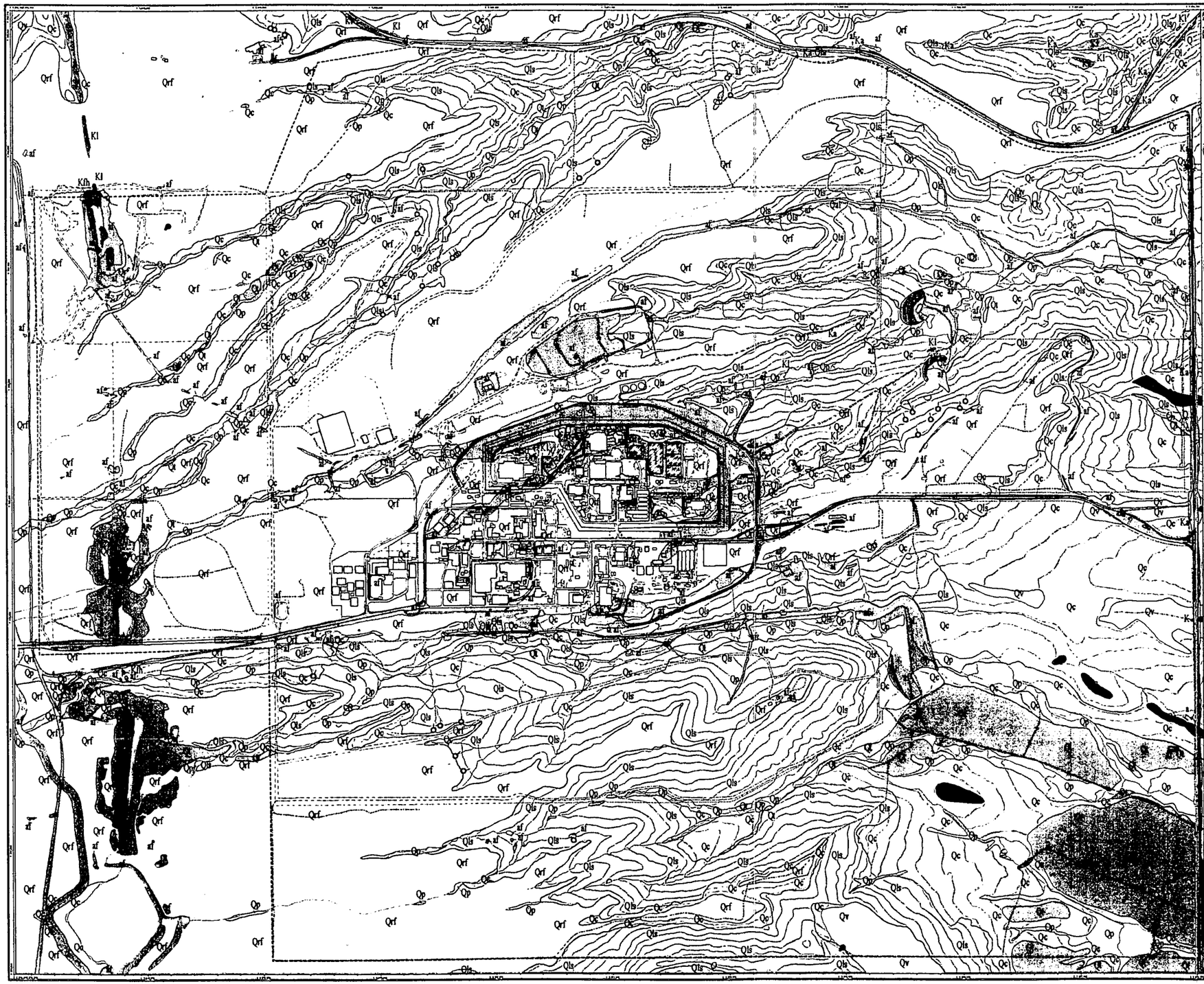

Figure TA-1-8

Actinide Migration Evaluation Pathway Report

Geologic Units at Rocky Flats Environmental Technology Site

Produced in cooperation with the U.S. Geological Survey

Geologic Map Units

af - Artificial fill
Qp - Post-Piney Creek and Piney Creek Alluvium
Qt - Terrace Alluvium
Qc - Colluvium
Qls - Landslide deposits
Qs - Slocum Alluvium
Qv - Verdos Alluvium
Qrf - Rocky Flats Alluvium
Ka - Arapahoe Formation
Kl - Laramie Formation
Kfh - Fox Hills Sandstone

Symbols

- Shallow closed depression
- Scarp of young landslide
- Areas of vegetation at and near springs
- Boundary of gravel and clay pit
- Spring
- Strike and dip of beds
- Clast identification site
- Capitol Mine (abandoned)
- Geologic Units boundaries

Standard Map Features

- Buildings and other structures
- Solar Evaporation Ponds (SEPs)
- Lakes and ponds
- Streams, ditches, or other drainage features
- Fences and other barriers
- Topographic Contour (20-Foot)
- Rocky Flats boundary
- Paved roads
- Dirt roads

DATA SOURCE BASE FEATURES:

Buildings, fences, hydrography, roads and other structures from 1994 aerial fly-over data captured by EG&G RSL, Las Vegas. Digitized from the orthophotographs. 1/95

Topographic contours were derived from digital elevation model (DEM) data by Morrison Knudson (MK) using ESRI Arc TIN and LATTICE to process the DEM data to create 5-foot contours. The DEM data was captured by the Remote Sensing Lab, Las Vegas, NV, 1994 Aerial Flyover at ~ 10 meter resolution. DEM post-processing performed by MK, Winter 1997.

Location of buildings, roads, and fences by Facilities Engr., EG&G Rocky Flats, Inc. - 1991.
Hydrology by Water Resources Division USGS - (date and author unknown)
Geologic Mapping: Shroba, R.R., and Carrara, P.E. Preliminary Surficial Geologic Map of the Rocky Flats Plant and Vicinity, Jefferson and Boulder Counties, Colorado: U.S. Geological Survey Open-File Report 94-162, Scale 1:6000
Site source of topo base; see OFR 94-162 (on map).

Subject Matter Expert:
Water Operations Manager
Stephen H Singer
RMRS T130C 107
steve.singer@rfets.gov
Phone: (303) 966-3387
Pager: (303) 212-6255

Scale = 1 : 21330
1 inch represents approximately 1778 feet
250 0 500 1000ft

State Plane Coordinate Projection
Colorado Central Zone
Datum: NAD27

U.S. Department of Energy
Rocky Flats Environmental Technology Site

Prepared for: DynCorp — THE ART OF TECHNOLOGY

Prepared by: KH Earth Sciences

CEG Dwgs. 303-966-7707

NT_Svr w:/projects/actinide_pathway_report/fy2002/misc_maps/geology90_boize.aml

50

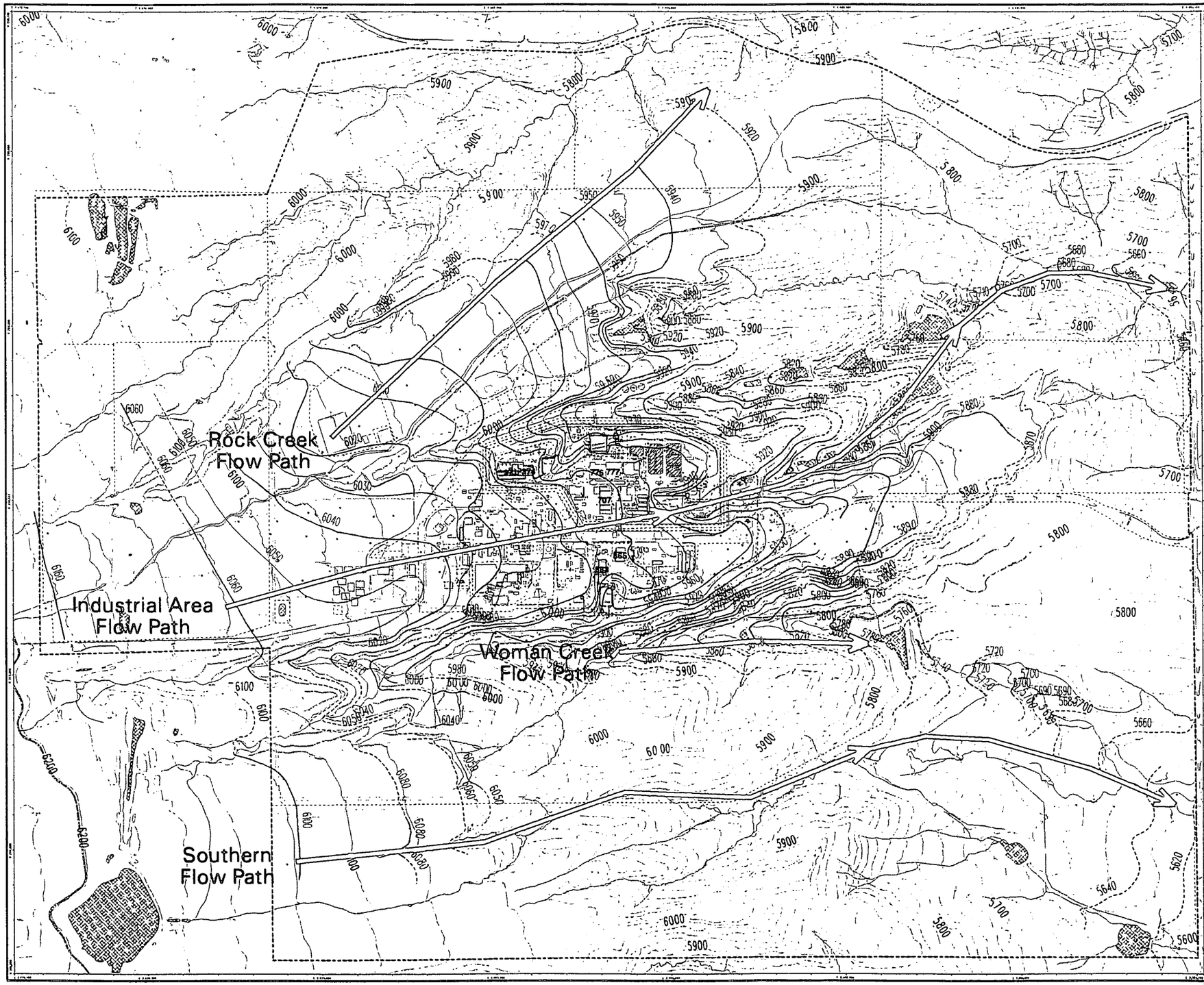

Figure TA-1-11

Actinide Migration Evaluation Pathway Report

Potentiometric Surface of Unconsolidated Surficial Deposits Second Quarter 1998

- • Groundwater Monitoring Well
- Water Level Contour
- Dashed where inferred
- Intermediate Water Level Contour
- Dashed where inferred
- Foundation Drain and Elevation
- Approximate extent of Unsaturated Area
- Area without Groundwater Elevation Data

Standard Map Features

- Buildings & other structures
- Solar evaporation ponds
- Lakes and ponds
- Streams, ditches, or other drainage features
- Fences and other barriers
- Contours (20' Intervals)
- Roads
- Rocky Flats Boundary

DATA SOURCE BASE FEATURES:
Buildings, fences, hydrography, roads and other structures from 1994 aerial fly-over data captured by EG&G RSL, Las Vegas. Digitized from the orthophotographs. 1/95

Scale = 1 : 21330
1 inch represents approximately 1778 feet
250 0 500 1000ft

State Plane Coordinate Projection
Colorado Central Zone
Datum: NAD27

U.S. Department of Energy
Rocky Flats Environmental Technology Site

GIS Dept. 303-966-7707

Prepared by: DynCorp THE ART OF TECHNOLOGY

Prepared for: KH KAISER-HILL

MAP ID: miso_maps/potent98spring_noval.aml

December 27, 2001

NT_Svr w:/projects/actinide_pathway_report/fy2002/miso_maps/potent98spring_noval.aml

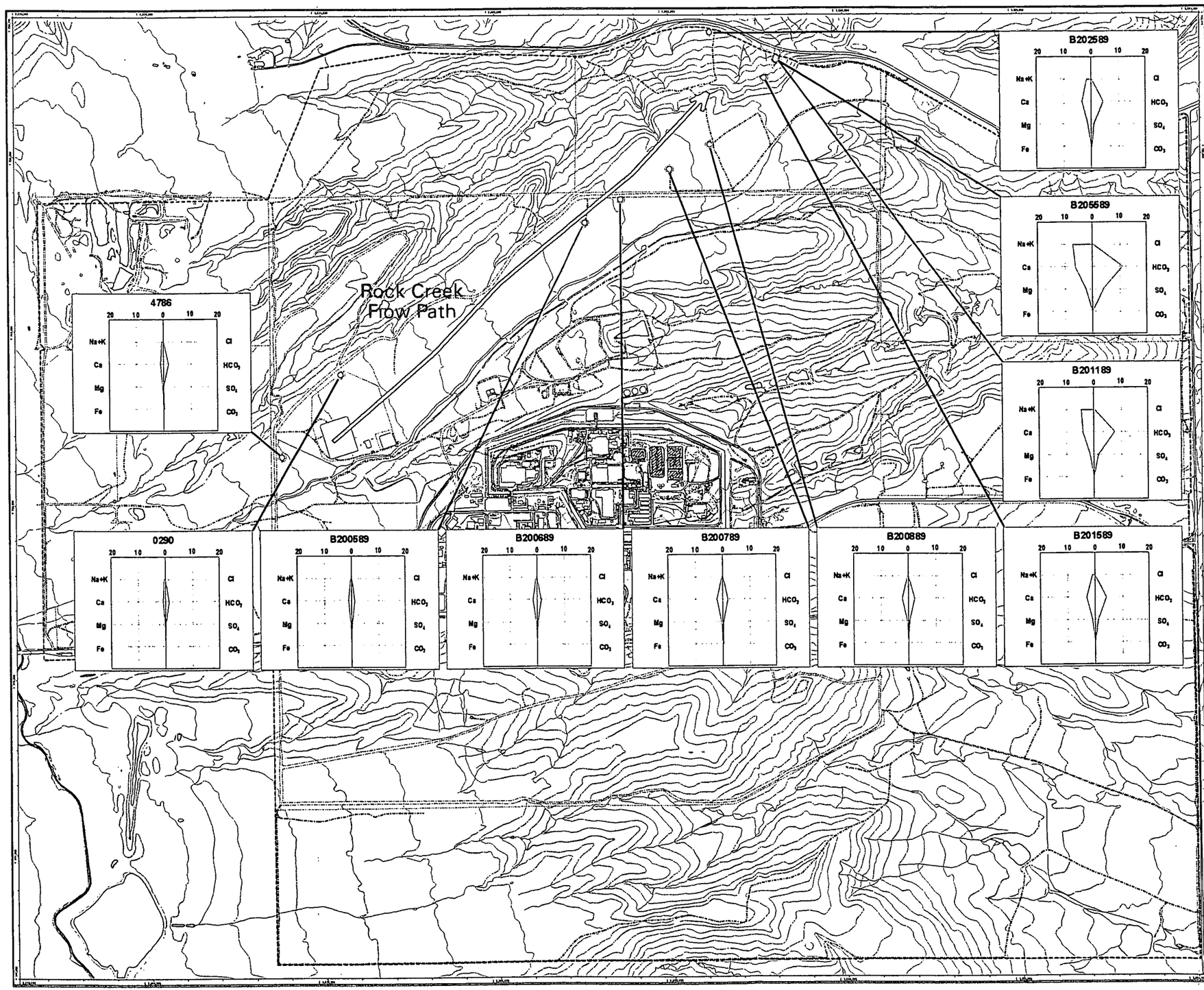

Figure TA-1-12

Actinide Migration Evaluation Pathway Report

Major Ion Concentrations in UHSU Groundwater for Rock Creek Flow Path

EXPLANATION

Diagram of dissolved major-ion concentrations ("Stiff plot") for selected wells. Concentrations are in milliequivalents per liter.

Flow Path

Upper Hydrostratigraphic Unit Monitoring Well

Standard Map Features

- Buildings and other structures
- Solar Evaporation Ponds (SEPs)
- Lakes and ponds
- Streams, ditches, or other drainage features
- Fences and other barriers
- Topographic Contour (20-Foot)
- Rocky Flats boundary
- Paved roads
- Dirt roads

DATA SOURCE BASE FEATURES:

Buildings, fences, hydrography, roads and other structures from 1994 aerial fly-over data captured by EG&G RSL, Las Vegas. Digitized from the orthophotographs. 1/95

Topographic contours were derived from digital elevation model (DEM) data by Morrison Knudson (MK) using ESRI Arc TIN and LATTICE to process the DEM data to create 5-foot contours. The DEM data was captured by the Remote Sensing Lab, Las Vegas, NV, 1994 Aerial Flyover at ~ 10 meter resolution. DEM post-processing performed by MK, Winter 1997.

Stiff Plot source:
Groundwater Geochemistry Report for the Rocky Flats Environmental Technology Site, Volume III of the Sitewide Geoscience Characterization Study, Final Report, EG&G Rocky Flats, January 1995

Scale = 1 : 21330
1 inch represents approximately 1778 feet

250 0 500 1000 ft

State Plane Coordinate Projection
Colorado Central Zone
Datum: NAD27

U.S. Department of Energy
Rocky Flats Environmental Technology Site

GIS Dept. 303-966-7707

Prepared by: DynCorp THE ART OF TECHNOLOGY

Prepared for: KAISER-HILL

NT_Svr w:/projects/actinide_pathway_report/fy2002/uhsu_ion_maps/ion_cone_rock_creek.aml

54

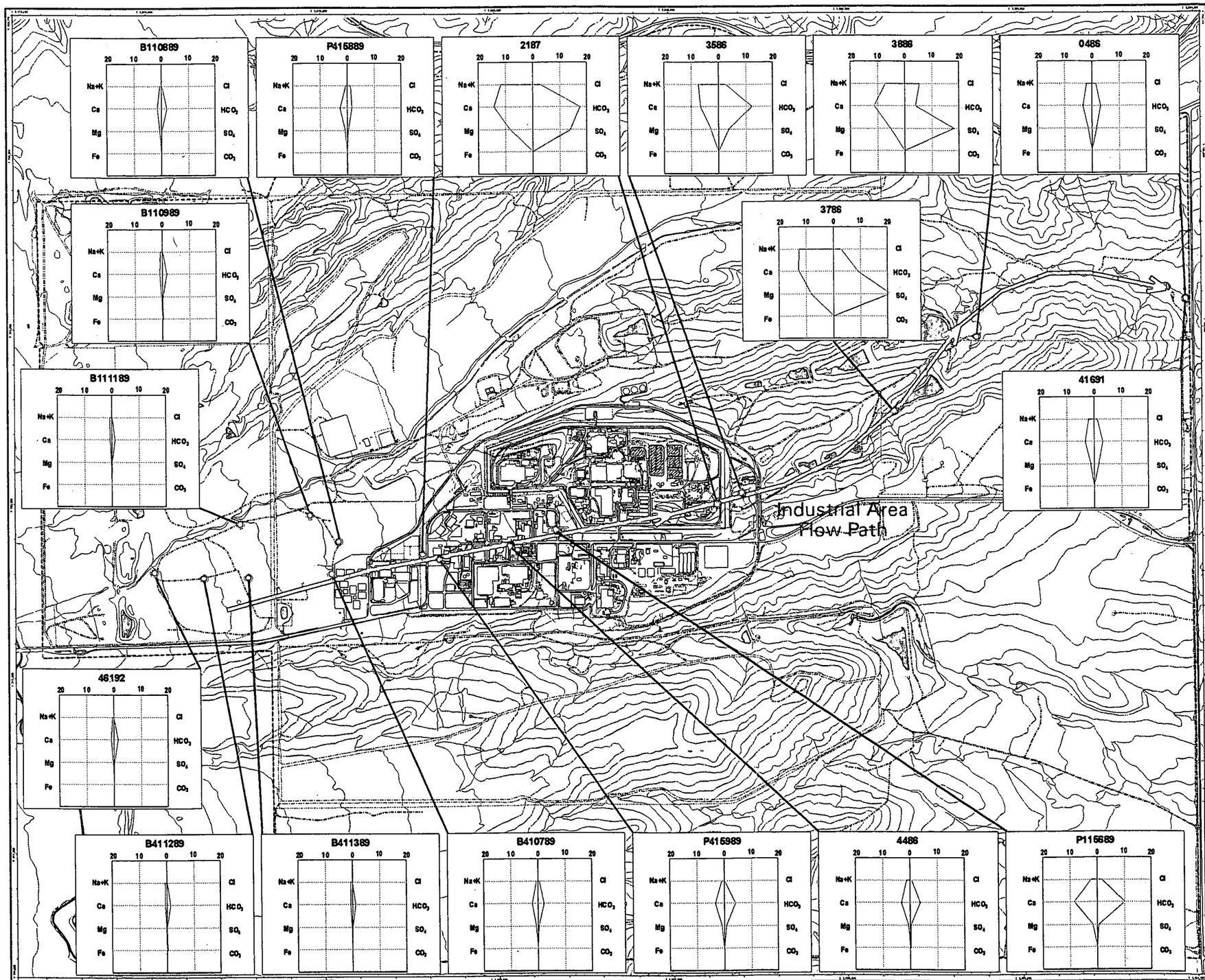

Figure TA-1-13

Actinide Migration Evaluation Pathway Report

Major Ion Concentrations in UHSU Groundwater for Industrial Area Flow Path

EXPLANATION

Diagram of dissolved major-ion concentrations ("Stiff plot") for selected wells. Concentrations are in milliequivalents per liter.

Flow Path

Upper Hydrostratigraphic Unit Monitoring Well

Standard Map Features

- Buildings and other structures
- Solar Evaporation Ponds (SEPs)
- Lakes and ponds
- Streams, ditches, or other drainage features
- Fences and other barriers
- Topographic Contour (20-Foot)
- Rocky Flats boundary
- Paved roads
- Dirt roads

DATA SOURCE BASE FEATURES:

Buildings, fences, hydrography, roads and other structures from 1994 aerial fly-over data captured by EG&G RSL, Las Vegas.
Digitized from the orthophotographs. 1/95
Topographic contours were derived from digital elevation model (DEM) data by Morrison Knudson (MK) using ESRI Arc TIN and LATTICE to process the DEM data to create 5-foot contours. The DEM data was captured by the Remote Sensing Lab, Las Vegas, NV, 1994 Aerial Flyover at ~ 10 meter resolution. DEM post-processing performed by MK, Winter 1997.

Stiff Plot source:
Groundwater Geochemistry Report for the Rocky Flats Environmental Technology Site, Volume III of the Sitewide Geoscience Characterization Study,
Final Report, EG&G Rocky Flats, January 1995

Scale = 1 : 21330
1 inch represents approximately 1778 feet

250 0 500 1000 ft

State Plane Coordinate Projection
Colorado Central Zone
Datum: NAD27

U.S. Department of Energy
Rocky Flats Environmental Technology Site

GIS Dept. 303-966-7707

Prepared by: DynCorp — THE ART OF TECHNOLOGY

Prepared for: KAISER-HILL

MAP ID: using U.S. meters

January 15, 1998

NT_Svr w:/projects/actinide_pathway_report/fy2002/uhsu_ion_maps/ion_conc_ia.aml

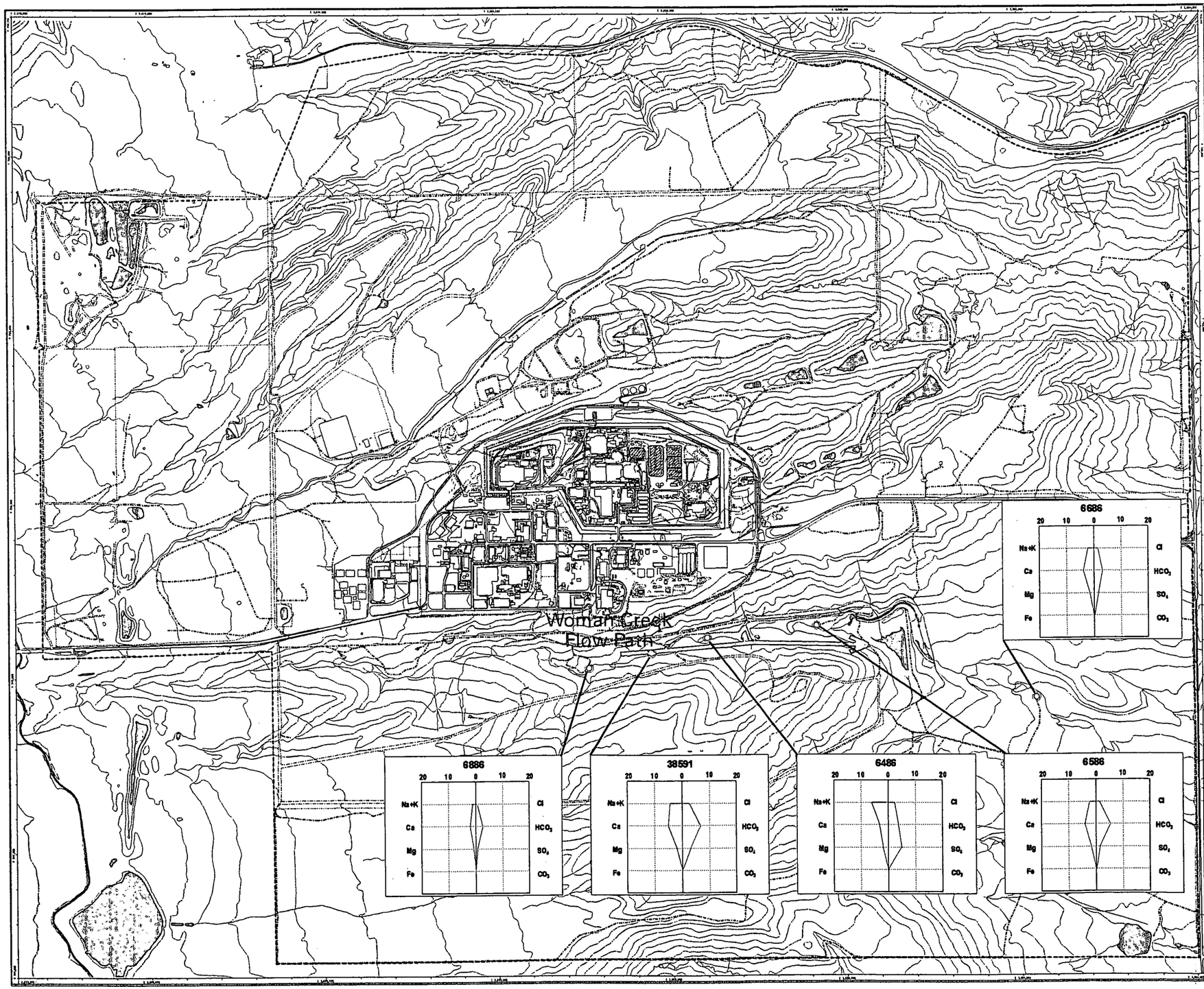

Figure TA-1-14

Actinide Migration Evaluation Pathway Report

Major Ion Concentrations in UHSU Groundwater for Woman Creek Flow Path

EXPLANATION

Diagram of dissolved major-ion concentrations ("Stiff plot") for selected wells. Concentrations are in milliequivalents per liter.

Flow Path

Upper Hydrostratigraphic Unit Monitoring Well

Standard Map Features

- Buildings and other structures
- Solar Evaporation Ponds (SEPs)
- Lakes and ponds
- Streams, ditches, or other drainage features
- Fences and other barriers
- Topographic Contour (20-Foot)
- Rocky Flats boundary
- Paved roads
- Dirt roads

DATA SOURCE BASE FEATURES:

Buildings, fences, hydrography, roads and other structures from 1994 aerial fly-over data captured by EG&G RSL, Las Vegas. Digitized from the orthophotographs. 1/95

Topographic contours were derived from digital elevation model (DEM) data by Morrison Knudson (MK) using ESRI Arc TIN and LATTICE to process the DEM data to create 5-foot contours. The DEM data was captured by the Remote Sensing Lab, Las Vegas, NV, 1994 Aerial Flyover at ~ 10 meter resolution. DEM post-processing performed by MK, Winter 1997.

Stiff Plot source:
Groundwater Geochemistry Report for the Rocky Flats Environmental Technology Site, Volume III of the Sitewide Geoscience Characterization Study, Final Report, EG&G Rocky Flats, January 1995

Scale = 1 : 21330
1 inch represents approximately 1778 feet

250 0 500 1000 ft

State Plane Coordinate Projection
Colorado Central Zone
Datum: NAD27

U.S. Department of Energy
Rocky Flats Environmental Technology Site

GIS Dept. 303-966-7797

Prepared by: DynCorp — THE ART OF TECHNOLOGY

Prepared for: KAISER-HILL COMPANY

MAP ID: uhsu_ion_maps

January 15, 1998

NT_Svr w:/projects/actinide_pathway_report/fy2002/uhsu_ion_maps/ion_conc_woman_crsek.aml

56

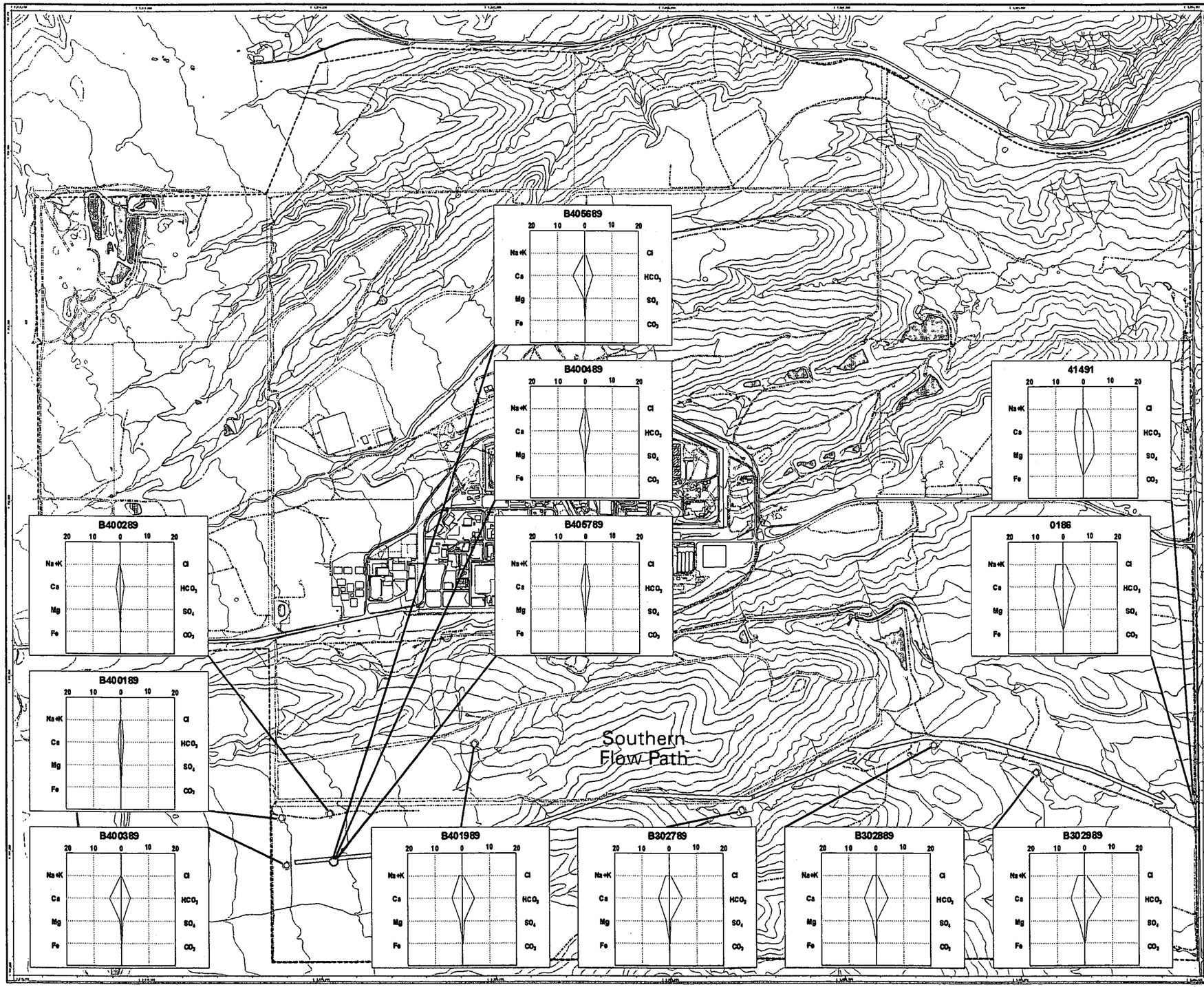

Figure TA-1-15

Actinide Migration Evaluation Pathway Report

Major Ion Concentrations in UHSU Groundwater for Southern Flow Path

EXPLANATION

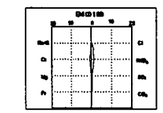

Diagram of dissolved major-ion concentrations ("Stiff plot") for selected wells. Concentrations are in milliequivalents per liter.

Flow Path

Upper Hydrostratigraphic Unit Monitoring Well

Standard Map Features

- Buildings and other structures
- Solar Evaporation Ponds (SEPs)
- Lakes and ponds
- Streams, ditches, or other drainage features
- Fences and other barriers
- Topographic Contour (20-Foot)
- Rocky Flats boundary
- Paved roads
- Dirt roads

DATA SOURCE BASE FEATURES:

Buildings, fences, hydrography, roads and other structures from 1994 aerial fly-over data captured by EG&G RSL, Las Vegas. Digitized from the orthophotographs. 1/95

Topographic contours were derived from digital elevation model (DEM) data by Morrison Knudson (MK) using ESRI Arc TIN and LATTICE to process the DEM data to create 5-foot contours. The DEM data was captured by the Remote Sensing Lab, Las Vegas, NV, 1994 Aerial Flyover at ~ 10 meter resolution. DEM post-processing performed by MK, Winter 1997.

Stiff Plot source:
Groundwater Geochemistry Report for the Rocky Flats Environmental Technology Site, Volume III of the Sitewide Geoscience Characterization Study, Final Report, EG&G Rocky Flats, January 1995

Scale = 1 : 21330
1 inch represents approximately 1778 feet

250 0 500 1000 ft

State Plane Coordinate Projection
Colorado Central Zone
Datum: NAD27

U.S. Department of Energy
Rocky Flats Environmental Technology Site

Prepared by: DynCorp THE ART OF TECHNOLOGY

Prepared for: KAISER-HILL

NT_Svr w:/projects/actinide_pathway_report/fy2002/uhsu_ion_maps/ion_conc_southern.aml

57

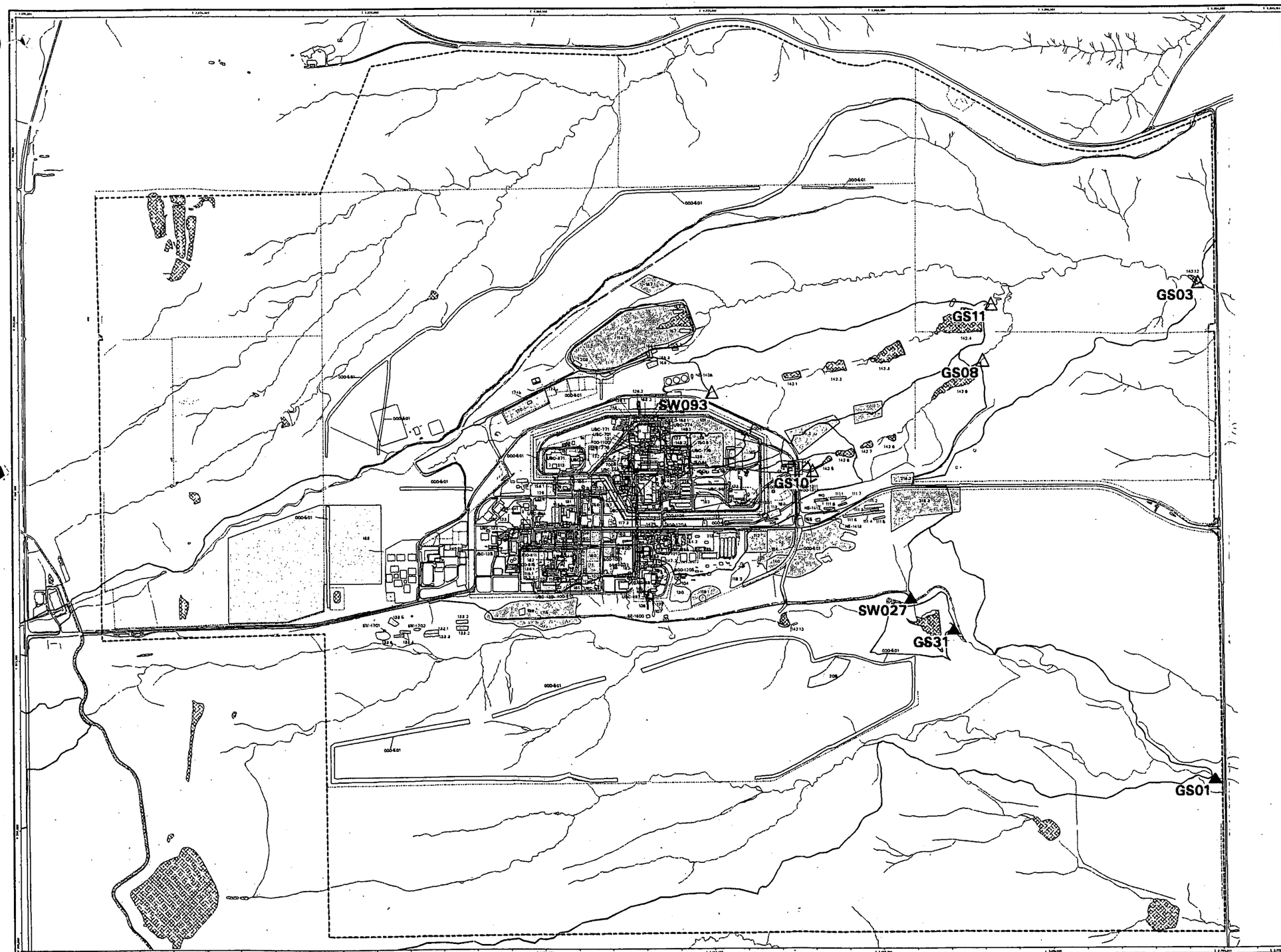

Figure TA-2-1

Actinide Migration Evaluation Pathway Report

Actinide Sources - Entire Site

Actinide Sources

- Active Actinide Site
- Original Process Waste Line (OPWL)
- Location of Original Process Waste Lines which may have been removed.
- New Process Waste Lines
- Under Building Contamination (UBC)
- Accepted as Proposed No Further Action (NFA)
- Proposed No Further Action (NFA)

Drainage Basins

- Drainage Basin Boundary
- Walnut Creek Basin Gaging Station (GS03, GS08, GS10, GS11 & SW093)
- Woman Creek Basin Gaging Station (GS01, GS31 & SW027)

Standard Map Features

- Buildings and other structures
- Lakes and ponds
- Streams, ditches, or other drainage features
- Fences and other barriers
- Rocky Flats boundary
- Paved roads

DATA SOURCE BASE FEATURES:

Buildings, fences, hydrography, roads and other structures from 1994 aerial fly-over data captured by EG&G RSL, Las Vegas. Digitized from the orthophotographs. 1/95

NOTES:

The Sanitary Sewer and Storm Drain systems at the site are included on the Active IHSS list but are not included on the map. Area investigations will be performed to determine which portions of these systems will ultimately be on the NFA list.

Scale = 1 : 21330
1 inch represents approximately 1778 feet

250 0 500 1000ft

State Plane Coordinate Projection
Colorado Central Zone
Datum: NAD27

U.S. Department of Energy
Rocky Flats Environmental Technology Site

GIS Dept. 303-966-7707

Prepared by: DynCorp THE ART OF TECHNOLOGY

Prepared for: KAISER-HILL COMPANY

NT_Svr w:/projects/actinide_pathway_report/fy2002/ihss_maps/act_sro_site_bsize.aml

151

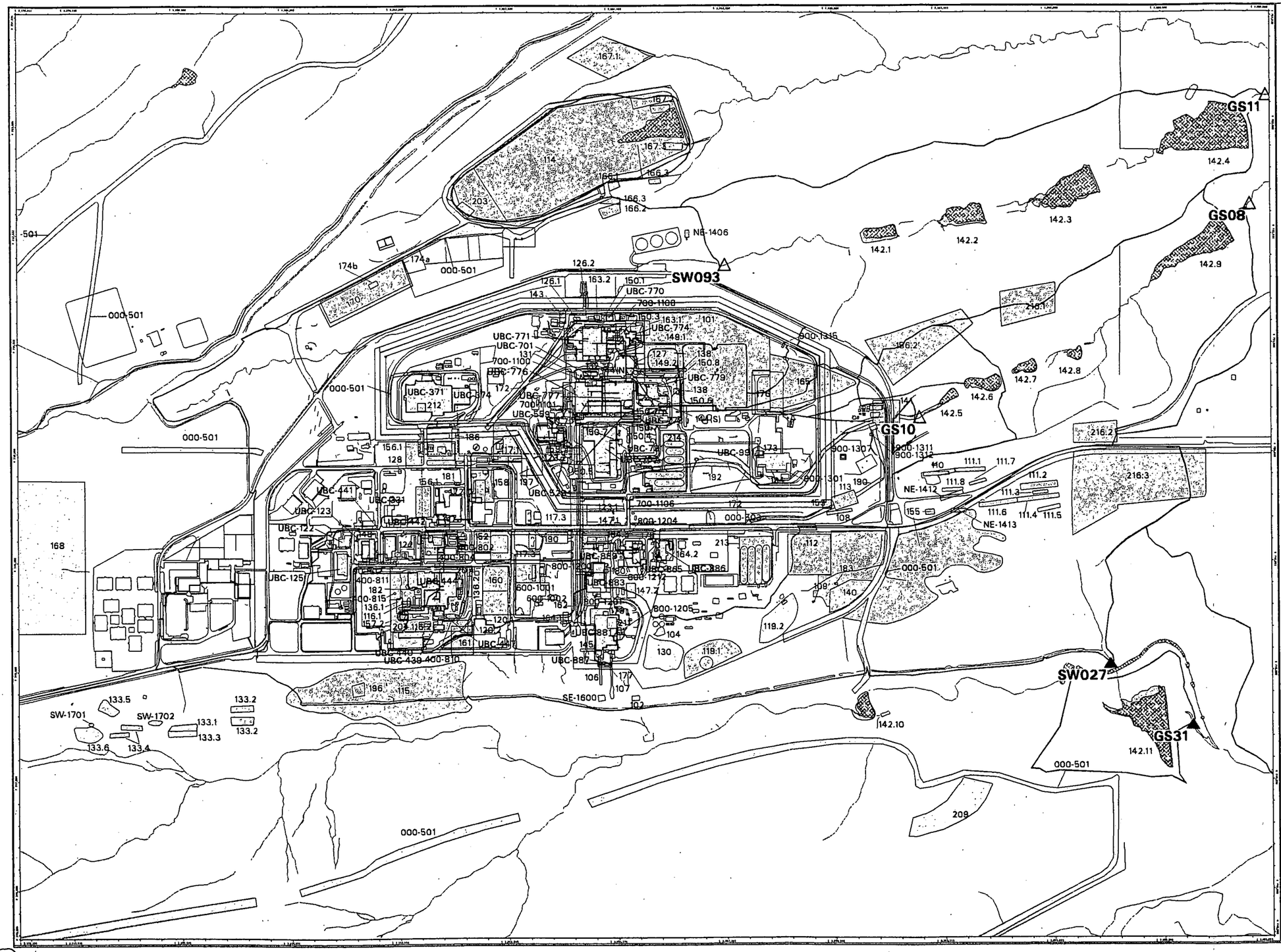

Figure TA-2-2

Actinide Migration Evaluation Pathway Report

Actinide Sources - Industrial Area

Actinide Sources

- Active Actinide Site
- Original Process Waste Line (OPWL)
- Location of Original Process Waste Lines which may have been removed.
- New Process Waste Lines
- Under Building Contamination (UBC)
- Accepted as Proposed No Further Action (NFA)
- Proposed No Further Action (NFA)

Drainage Basins

- Drainage Basin Boundary
- Walnut Creek Basin Gaging Station (GS03, GS08, GS10, GS11 & SW093)
- Woman Creek Basin Gaging Station (GS01, GS31 & SW027)

Standard Map Features

- Buildings and other structures
- Lakes and ponds
- Streams, ditches, or other drainage features
- Fences and other barriers
- Rocky Flats boundary
- Paved roads

DATA SOURCE BASE FEATURES:

Buildings, fences, hydrography, roads and other structures from 1994 aerial fly-over data captured by EG&G RSL, Las Vegas. Digitized from the orthophotographs. 1/95

NOTES:

The Sanitary Sewer and Storm Drain systems at the site are included on the Active IHSS list but are not included on the map. Area investigations will be performed to determine which portions of these systems will ultimately be on the NFA list.

Scale = 1 : 10830
1 inch represents approximately 811 feet

100 0 200 400ft

State Plane Coordinate Projection
Colorado Central Zone
Datum: NAD27

U.S. Department of Energy
Rocky Flats Environmental Technology Site

GIS Dept. 303-966-7707

Prepared by: DynCorp — THE ART OF TECHNOLOGY

Prepared for: KAISER-HILL

NT_Svr w:/projects/actinide_pathway_report/fy2002/ihss_maps/act_src_bsize.aml

December 12, 2001

152

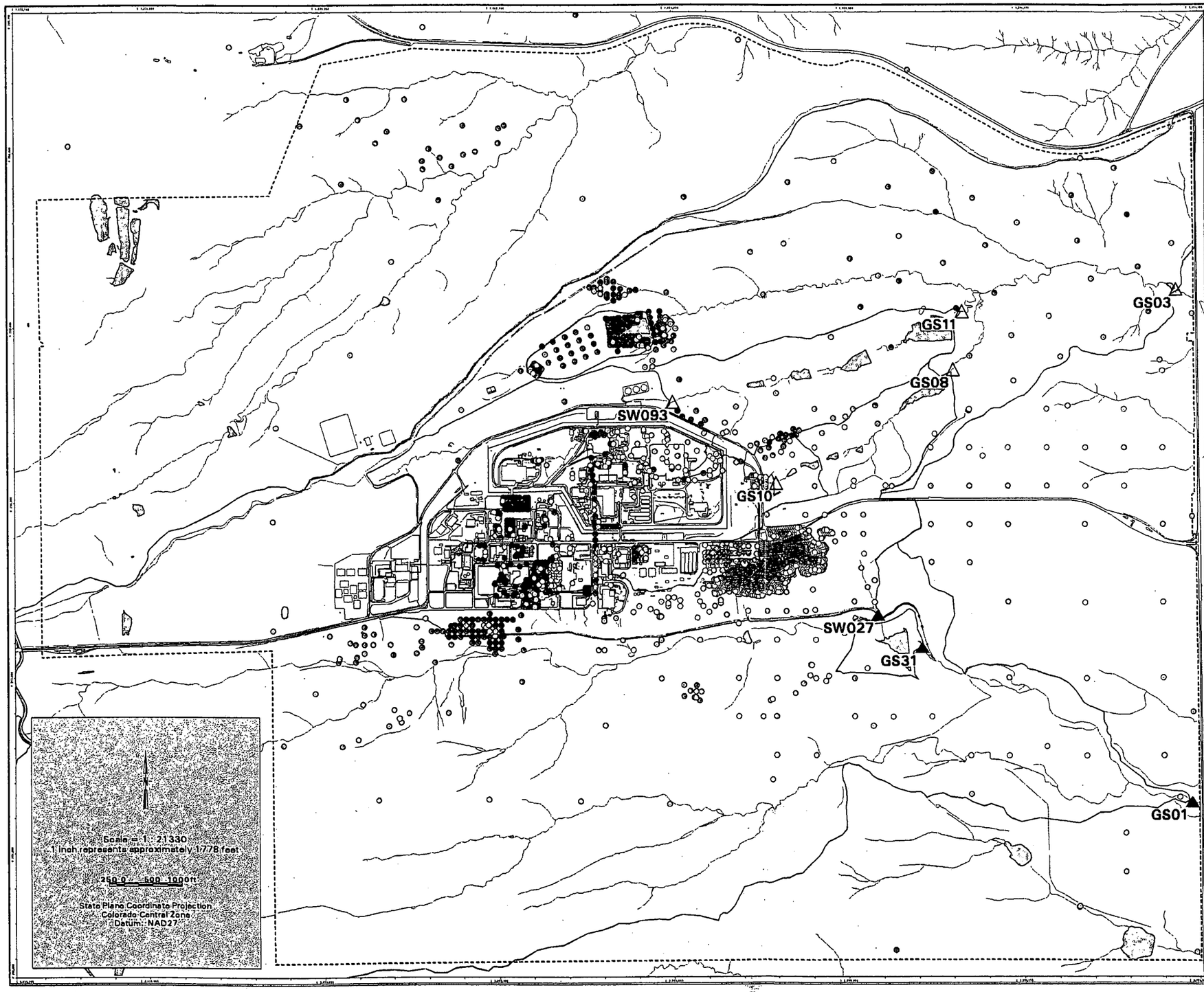

Figure TA-2-3

Actinide Migration Evaluation Pathway Report

Pu-239/240 Activity in Surface Soils

EXPLANATION

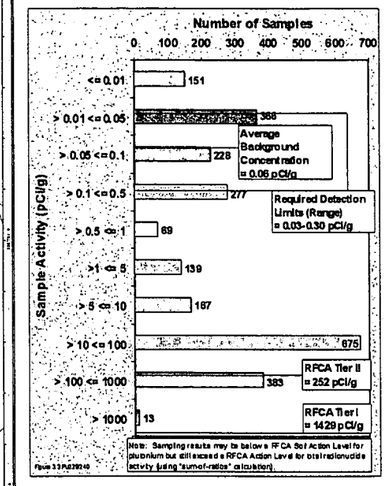

○ Value < Tier II value (Color indicates range of activity shown in the histogram above.)

▽ Tier II value < = Value < Tier I value

◇ Value > = Tier I value

N Drainage Basin Boundary

△ Walnut Creek Basin Gaging Station (GS03, GS08, GS10, GS11 & SW093)

▲ Woman Creek Basin Gaging Station (GS01, GS31 & SW027)

Standard Map Features

- Buildings and other structures
- Lakes and ponds
- Streams, ditches, or other drainage features
- Rocky Flats boundary
- Paved roads

DATA SOURCE BASE FEATURES:

Buildings, fences, hydrography, roads and other structures from 1994 aerial fly-over data captured by EG&G RSL, Las Vegas. Digitized from the orthophotographs. 1/95

Surface Soil Locations as of October 1999.

Analytical Data from SWD as of October 1999.

903 Pad data from 903 Drum Storage Area Characterization Report, September 1999.

Data Analysis performed by Wright Water Engineers (303-480-1700).

U.S. Department of Energy

Rocky Flats Environmental Technology Site

GIS Dept. 303-966-7707

Prepared by: DynCorp THE ART OF TECHNOLOGY

Prepared for: KAISER-HILL COMPANY

NT_Svr w:/projects/actinide_pathway_report/fy2002/surface_soil_maps/pu239-240.aml

153

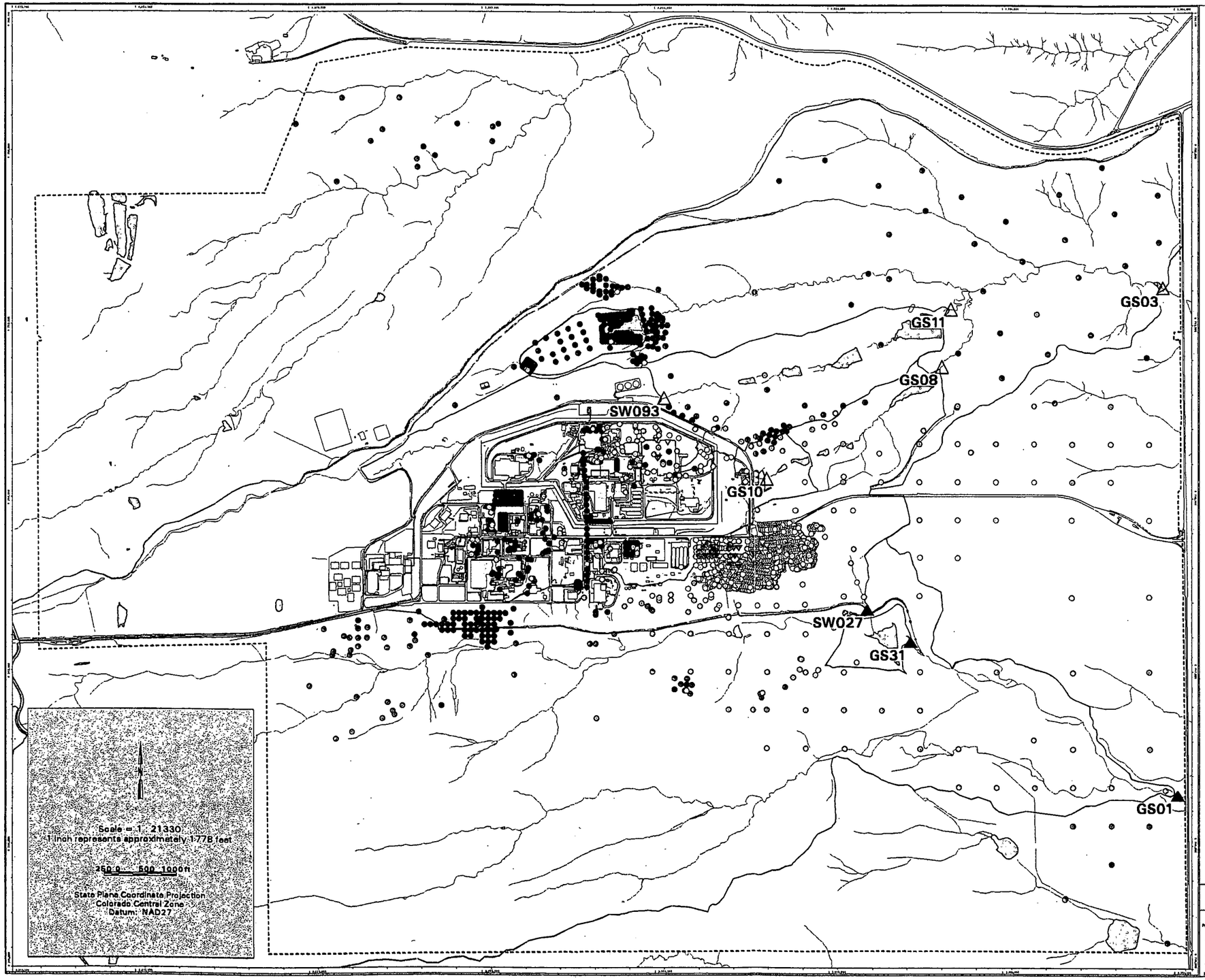

Figure TA-2-4

Actinide Migration Evaluation Pathway Report

Am-241 Activity in Surface Soils

EXPLANATION

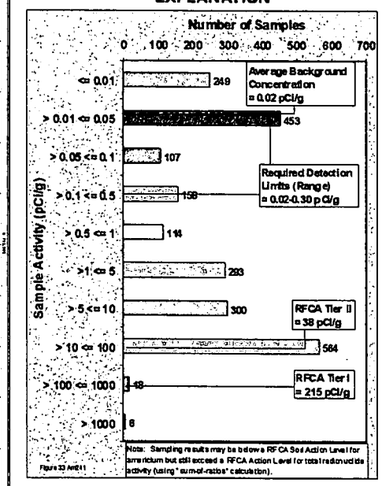

○ Value < Tier II value (Color indicates range of activity shown in the histogram above.)

▽ Tier II value < = Value < Tier I value

◇ Value > = Tier I value

N Drainage Basin Boundary

△ Walnut Creek Basin Gaging Station (GS03, GS08, GS10, GS11 & SW093)

▲ Woman Creek Basin Gaging Station (GS01, GS31 & SW027)

Standard Map Features

- Buildings and other structures
- Lakes and ponds
- Streams, ditches, or other drainage features
- Rocky Flats boundary
- Paved roads

DATA SOURCE BASE FEATURES:

Buildings, fences, hydrography, roads and other structures from 1994 aerial fly-over data captured by EG&G RSL, Las Vegas. Digitized from the orthophotographs. 1/95
Surface Soil Locations as of October 1999.

Analytical Data from SWD as of October 1999.

903 Pad data from 903 Drum Storage Area Characterization Report, September 1999.

Data Analysis performed by Wright Water Engineers (303-480-1700).

U.S. Department of Energy
Rocky Flats Environmental Technology Site

GIS Dept. 303-966-7707

Prepared for: DynCorp — THE ART OF TECHNOLOGY

Prepared for: KAISER-HILL COMPANY

NT_Svr w:/projects/actinide_pathway_report/fy2002/surface_soil_maps/am241.aml

154

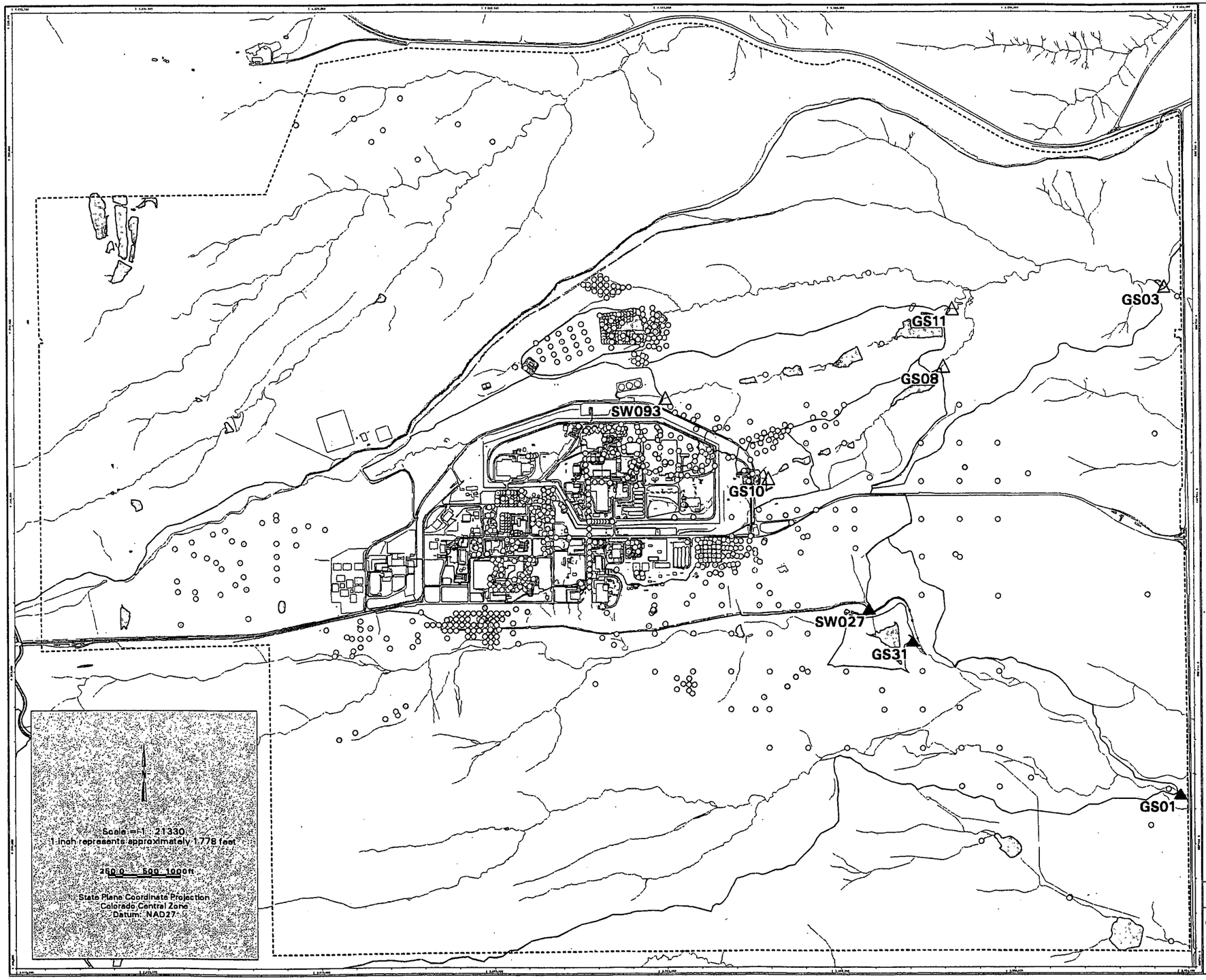

Figure TA-2-5

Actinide Migration Evaluation Pathway Report

U-233/234 Activity in Surface Soils

EXPLANATION

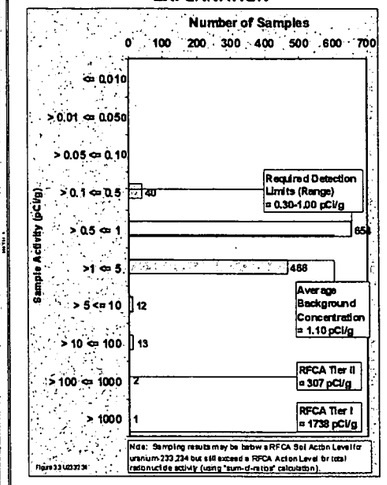

○ Value < Tier II value (Color indicates range of activity shown in the histogram above.)

▽ Tier II value < = Value < Tier I value

◇ Value > = Tier I value

N Drainage Basin Boundary

△ Walnut Creek Basin Gaging Station (GS03, GS08, GS10, GS11 & SW093)

▲ Woman Creek Basin Gaging Station (GS01, GS31 & SW027)

Standard Map Features

- Buildings and other structures
- Lakes and ponds
- Streams, ditches, or other drainage features
- Rocky Flats boundary
- Paved roads

DATA SOURCE BASE FEATURES:
Buildings, fences, hydrography, roads and other structures from 1994 aerial fly-over data captured by EG&G RSL, Las Vegas. Digitized from the orthophotographs. 1/95

Analytical Data provided by Mark Wood (KH, 303-966-6689).

Data Analysis performed by Wright Water Engineers (303-480-1700).

U.S. Department of Energy
Rocky Flats Environmental Technology Site

GIS Dept. 303-966-7707

Prepared by: DynCorp THE ART OF TECHNOLOGY

Prepared for: KAISER-HILL COMPANY

NT_Svr w:/projects/actinide_pathway_report/fy2002/surface_soil_maps/u233-234.aml

155

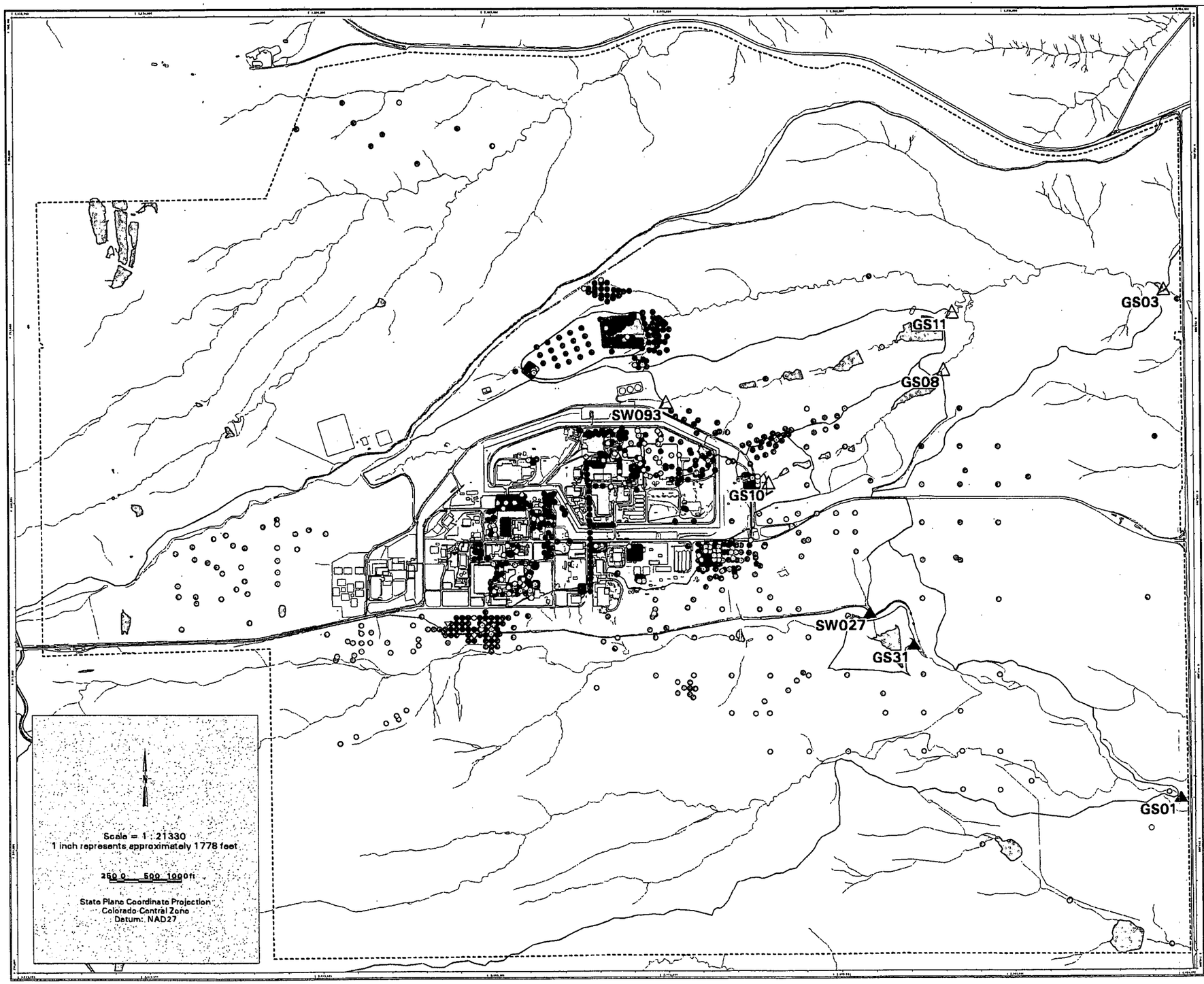

Figure TA-2-6

Actinide Migration Evaluation Pathway Report

U-235 Activity in Surface Soils

EXPLANATION

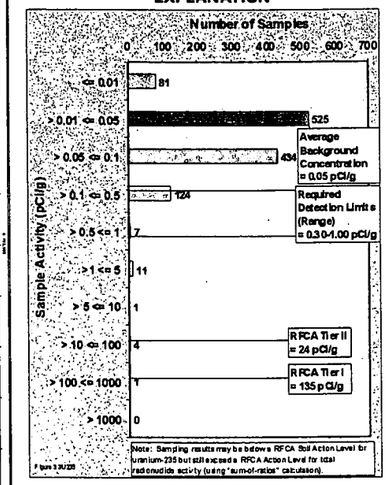

○ Value < Tier II value (Color indicates range of activity shown in the histogram above.)

▽ Tier II value < = Value < Tier I value

◇ Value > = Tier I value

N Drainage Basin Boundary

△ Walnut Creek Basin Gaging Station (GS03, GS08, GS10, GS11 & SW093)

▲ Woman Creek Basin Gaging Station (GS01, GS31 & SW027)

Standard Map Features

- Buildings and other structures
- Lakes and ponds
- Streams, ditches, or other drainage features
- Rocky Flats boundary
- Paved roads

DATA SOURCE BASE FEATURES:

Buildings, fences, hydrography, roads and other structures from 1994 aerial fly-over data captured by EG&G RSL, Las Vegas. Digitized from the orthophotographs. 1/95

Analytical Data provided by Mark Wood (KH, 303-966-6689).

Data Analysis performed by Wright Water Engineers (303-480-1700).

U.S. Department of Energy
Rocky Flats Environmental Technology Site

GIS Dept. 303-966-7707

Prepared by: DynCorp

Prepared for: KAISER-HILL

NT_Svr w:/projects/actinide_pathway_report/fy2002/surface_soil_maps/u235.aml

156

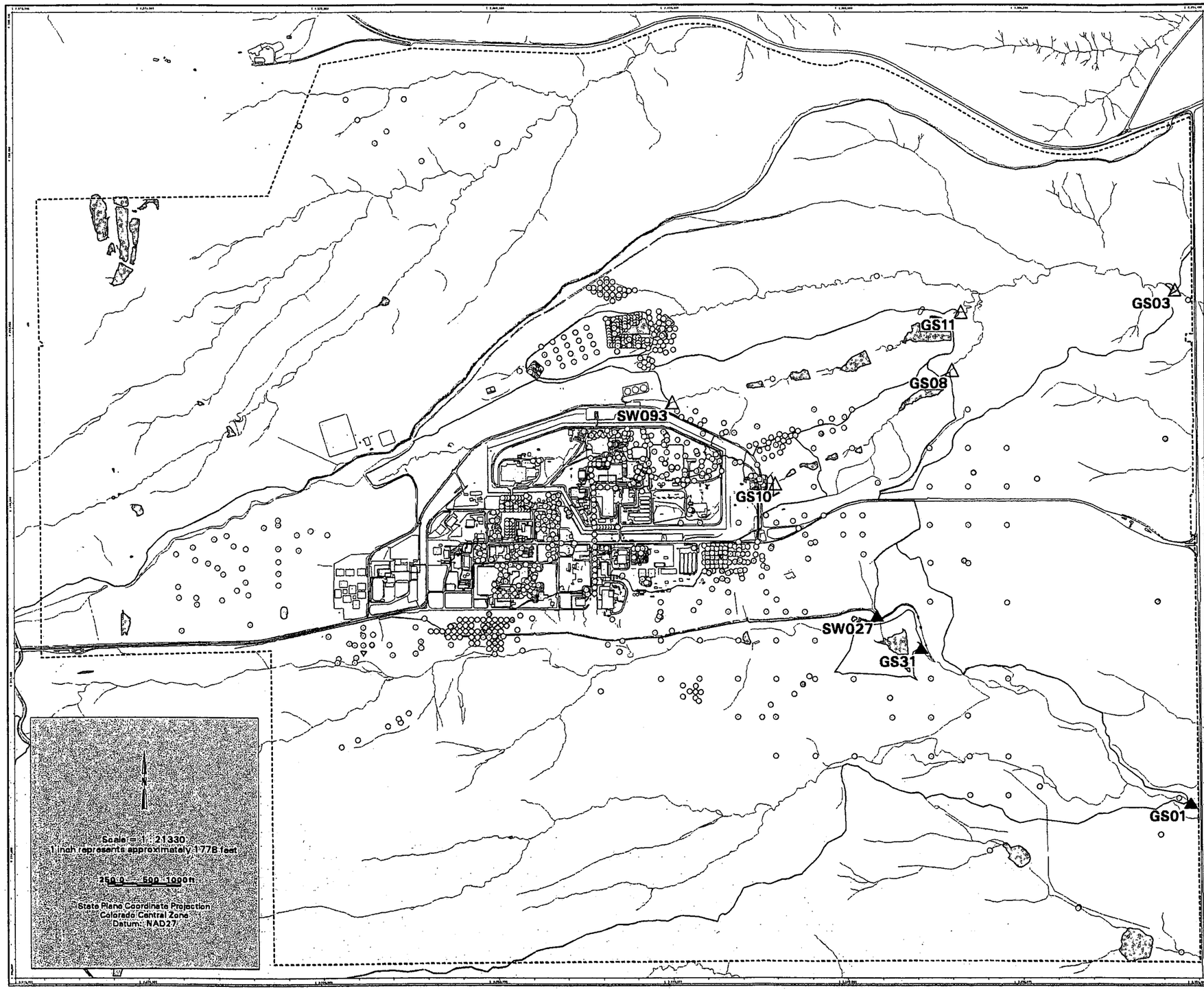

Figure TA-2-7

Actinide Migration Evaluation Pathway Report

U-238 Activity in Surface Soils

EXPLANATION

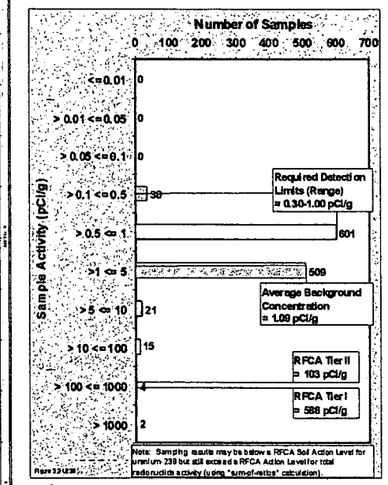

- ○ Value < Tier II value (Color indicates range of activity shown in the histogram above.)
- ▽ Tier II value < = Value < Tier I value
- ◇ Value > = Tier I value
- N Drainage Basin Boundary
- △ Walnut Creek Basin Gaging Station (GS03, GS08, GS10, GS11 & SW093)
- ▲ Woman Creek Basin Gaging Station (GS01, GS31 & SW027)

Standard Map Features

- Buildings and other structures
- Lakes and ponds
- Streams, ditches, or other drainage features
- Rocky Flats boundary
- Paved roads

DATA SOURCE BASE FEATURES:

Buildings, fences, hydrography, roads and other structures from 1994 aerial fly-over data captured by EG&G RSL: Las Vegas. Digitized from the orthophotographs. 1/95

Analytical Data provided by Mark Wood (KH, 303-966-6589).

Data Analysis performed by Wright Water Engineers (303-480-1700).

U.S. Department of Energy
Rocky Flats Environmental Technology Site
GIS Dept. 303-966-7707

Prepared for: DynCorp — THE ART OF TECHNOLOGY

Prepared for: KAISER-HILL COMPANY

NT_Svr w:/projects/actinide_pathway_report/fy2002/surface_soil_maps/u238.aml

157

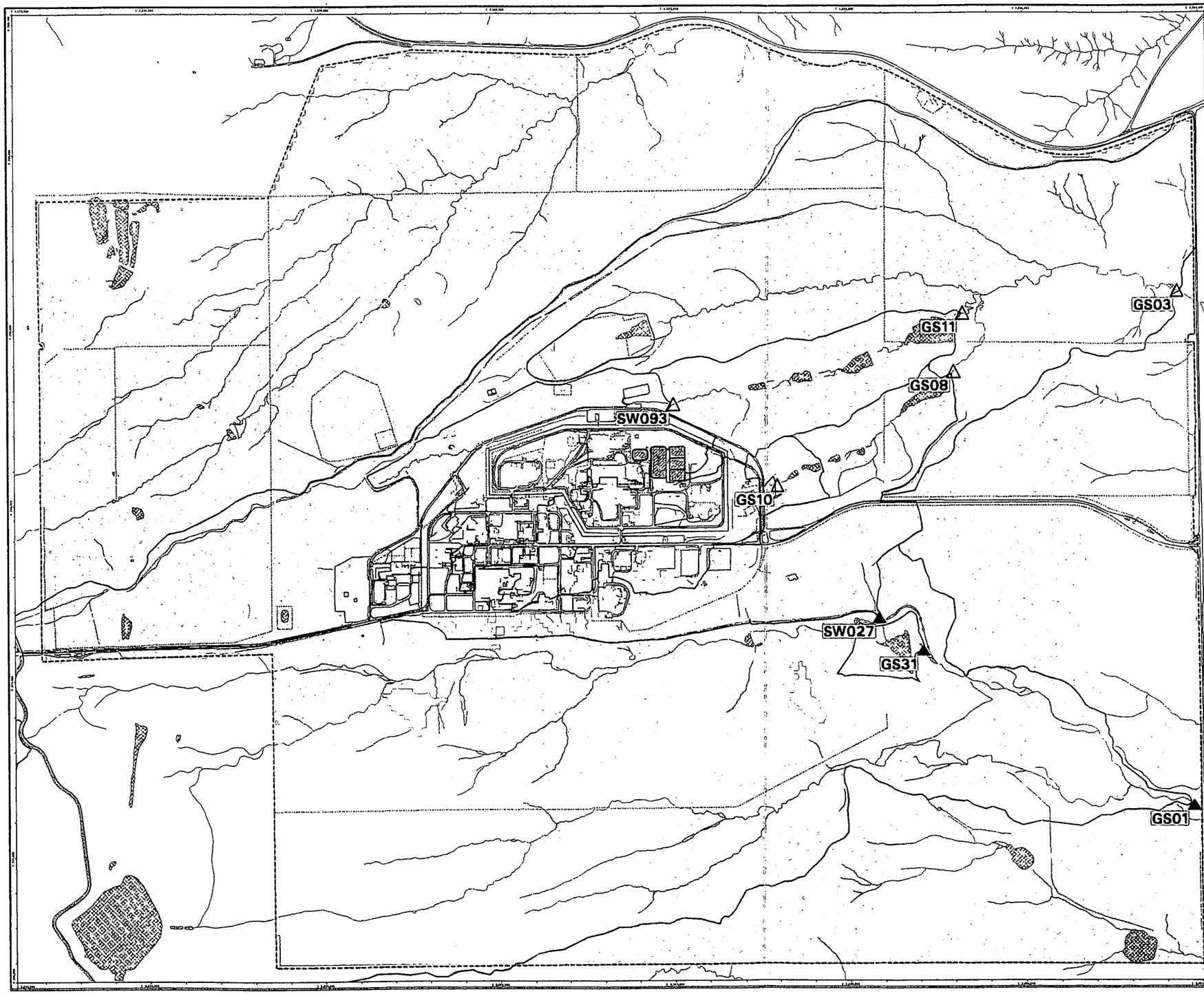

Figure TA-2-10

Actinide Migration Evaluation Pathway Report

U-233/234 Activity in Surface Soils

Kriging Analysis Isoplot (pCi/g)

EXPLANATION

- Result < = 0.01
- 0.01 < Result < = 0.05
- 0.05 < Result < = 0.1
- 0.1 < Result < = 0.5
- 0.5 < Result < = 1.0
- 1.0 < Result < = 5.0
- 5.0 < Result < = 10.0
- 10.0 < Result < = 100.0
- 100.0 < Result < = 1000.0
- Result > 1000.0
- Drainage Basin Boundary
- Walnut Creek Basin Gaging Station (GS03, GS08, GS10, GS11 & SW093)
- Woman Creek Basin Gaging Station (GS01, GS31 & SW027)

Standard Map Features

- Solar Evaporation Ponds (SEPs)
- Lakes and ponds
- Streams, ditches, or other drainage features
- Fences and other barriers
- Rocky Flats boundary
- Paved roads

DATA SOURCE BASE FEATURES:

Buildings, fences, hydrography, roads and other structures from 1994 aerial fly-over data captured by EG&G RSL, Las Vegas. Digitized from the orthophotographs. 1/95

Analytical Data provided by Mark Wood (KH, 303-966-6689).

Kriged data provided by Jeff Myers (Westinghouse-Akin, 803-502-9747).

Scale = 1 : 21330
1 inch represents approximately 1778 feet

250 0 500 1000 ft

State Plane Coordinate Projection
Colorado Central Zone
Datum: NAD27

U.S. Department of Energy
Rocky Flats Environmental Technology Site

GIS Dept. 303-966-7707

Prepared by: DynCorp — THE ART OF TECHNOLOGY

Prepared for: KH KAISER-HILL COMPANY

March 15, 2002

NT_Svr w:/projects/actinide_pathway_report/fy2002/kriged_data_maps/u233-234_grid_baize.aml

160

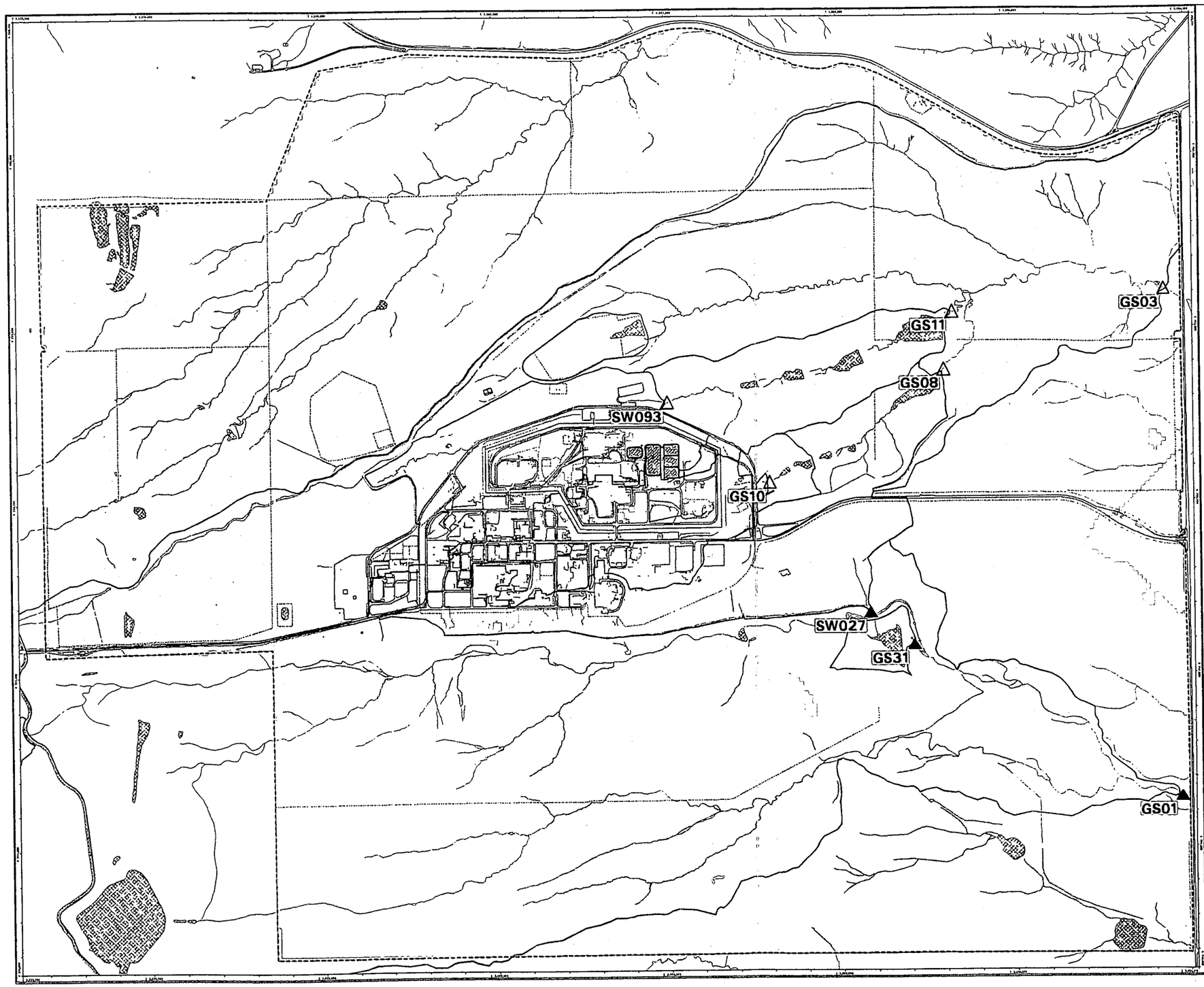

Figure TA-2-12

Actinide Migration Evaluation Pathway Report

U-238 Activity in Surface Soils Kriging Analysis Isoplot (pCi/g)

EXPLANATION

- Result < = 0.01
- 0.01 < Result < = 0.05
- 0.05 < Result < = 0.1
- 0.1 < Result < = 0.5
- 0.5 < Result < = 1.0
- 1.0 < Result < = 5.0
- 5.0 < Result < = 10.0
- 10.0 < Result < = 100.0
- 100.0 < Result < = 1000.0
- Result > 1000.0
- Drainage Basin Boundary
- Walnut Creek Basin Gaging Station (GS03, GS08, GS10, GS11 & SW093)
- Woman Creek Basin Gaging Station (GS01, GS31 & SW027)

Standard Map Features

- Solar Evaporation Ponds (SEPs)
- Lakes and ponds
- Streams, ditches, or other drainage features
- Fences and other barriers
- Rocky Flats boundary
- Paved roads

DATA SOURCE BASE FEATURES:
Buildings, fences, hydrography, roads and other structures from 1994 aerial fly-over data captured by EG&G RSL, Las Vegas. Digitized from the orthophotographs. 1/95

Analytical Data provided by Mark Wood (KH, 303-966-6689).

Kriged data provided by Jeff Myers (Westinghouse-Akin, 803-502-9747).

Scale = 1 : 21330
1 inch represents approximately 1778 feet
250 0 500 1000 ft

State Plane Coordinate Projection
Colorado Central Zone
Datum: NAD27

U.S. Department of Energy
Rocky Flats Environmental Technology Site
GIS Dept. 303-966-7707

Prepared by: DynCorp THE ART OF TECHNOLOGY

Prepared for: KAISER-HILL COMPANY

March 19, 1998

NT_Svr w:/projects/actinide_pathway_report/fy2002/kriged_data_maps/u238_grid_baize.aml

162

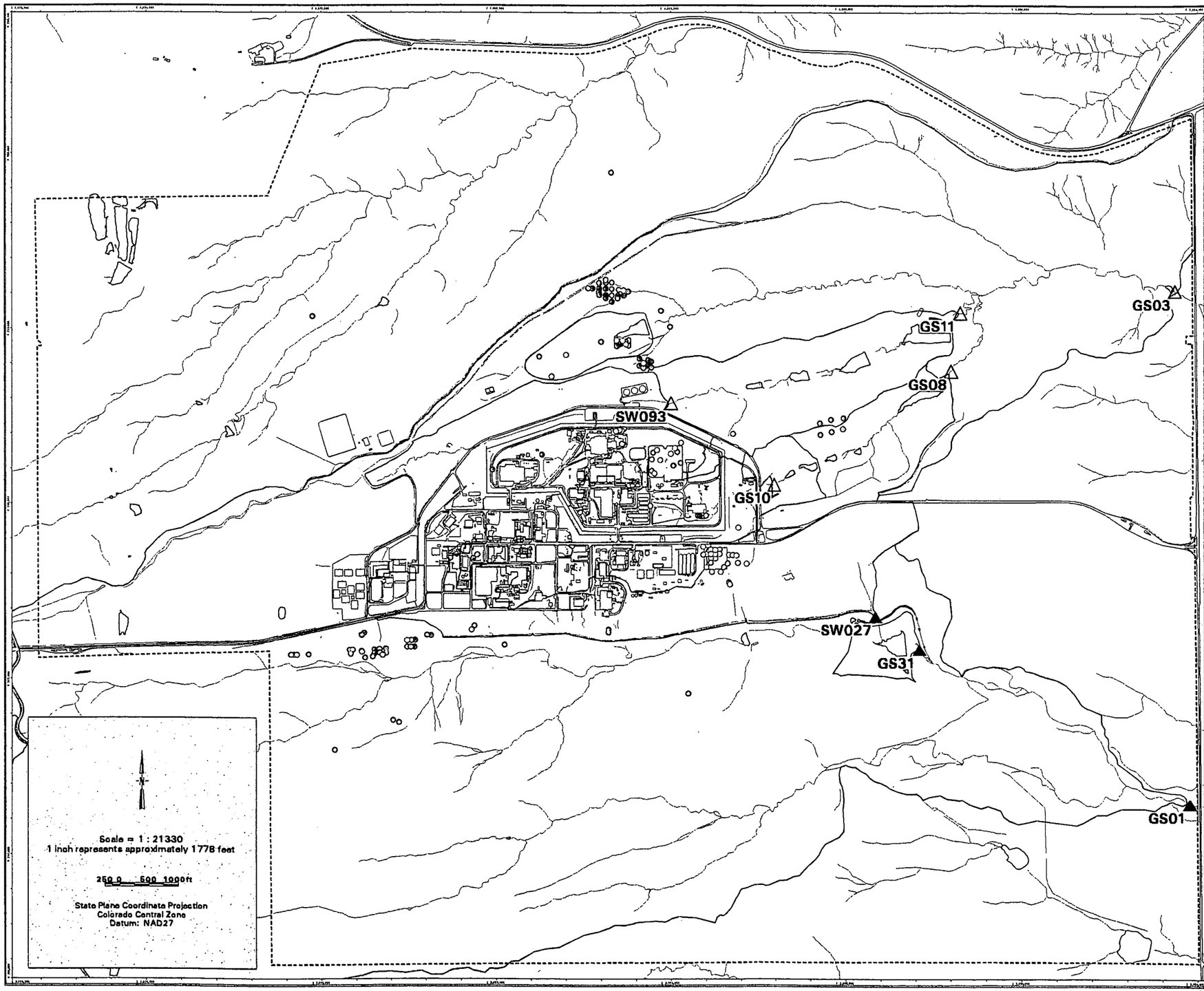

Figure TA-2-18

Actinide Migration Evaluation Pathway Report

Pu-239/240 Activity in Subsurface Soils

Depth : 0.5 - 2 ft

EXPLANATION

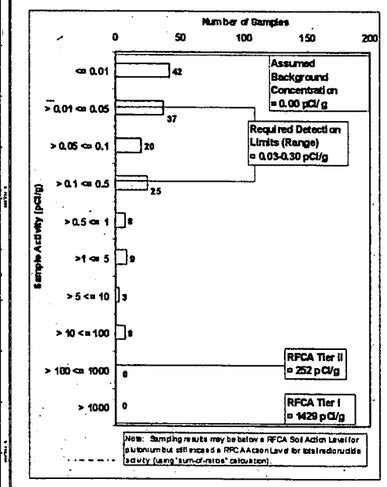

○ Value < Tier II value (Color indicates range of activity shown in the histogram above.)

▽ Tier II value < = Value < Tier I value

◇ Value > = Tier I value

N Drainage Basin Boundary

△ Walnut Creek Basin Gaging Station (GS03, GS08, GS10, GS11 & SW093)

▲ Woman Creek Basin Gaging Station (GS01, GS31 & SW027)

Standard Map Features

- Buildings and other structures
- Lakes and ponds
- Streams, ditches, or other drainage features
- Rocky Flats boundary
- Paved roads

DATA SOURCE BASE FEATURES:

Buildings, fences, hydrography, roads and other structures from 1994 aerial fly-over data captured by EG&G RSL, Las Vegas. Digitized from the orthophotographs. 1/95
Analytical Data from SWD as of October 2000.

Data Analysis performed by Wright Water engineers (303-480-1700).

U.S. Department of Energy
Rocky Flats Environmental Technology Site

GIS Dept. 303-966-7767

Prepared by: DynCorp — THE ART OF TECHNOLOGY

Prepared for: KAISER-HILL COMPANY

December 19, 2001

NT_Svr w:/projects/actinide_pathway_report/fy2002/subsurface_soil_maps/pu239-240_6in-2ft.aml

1168

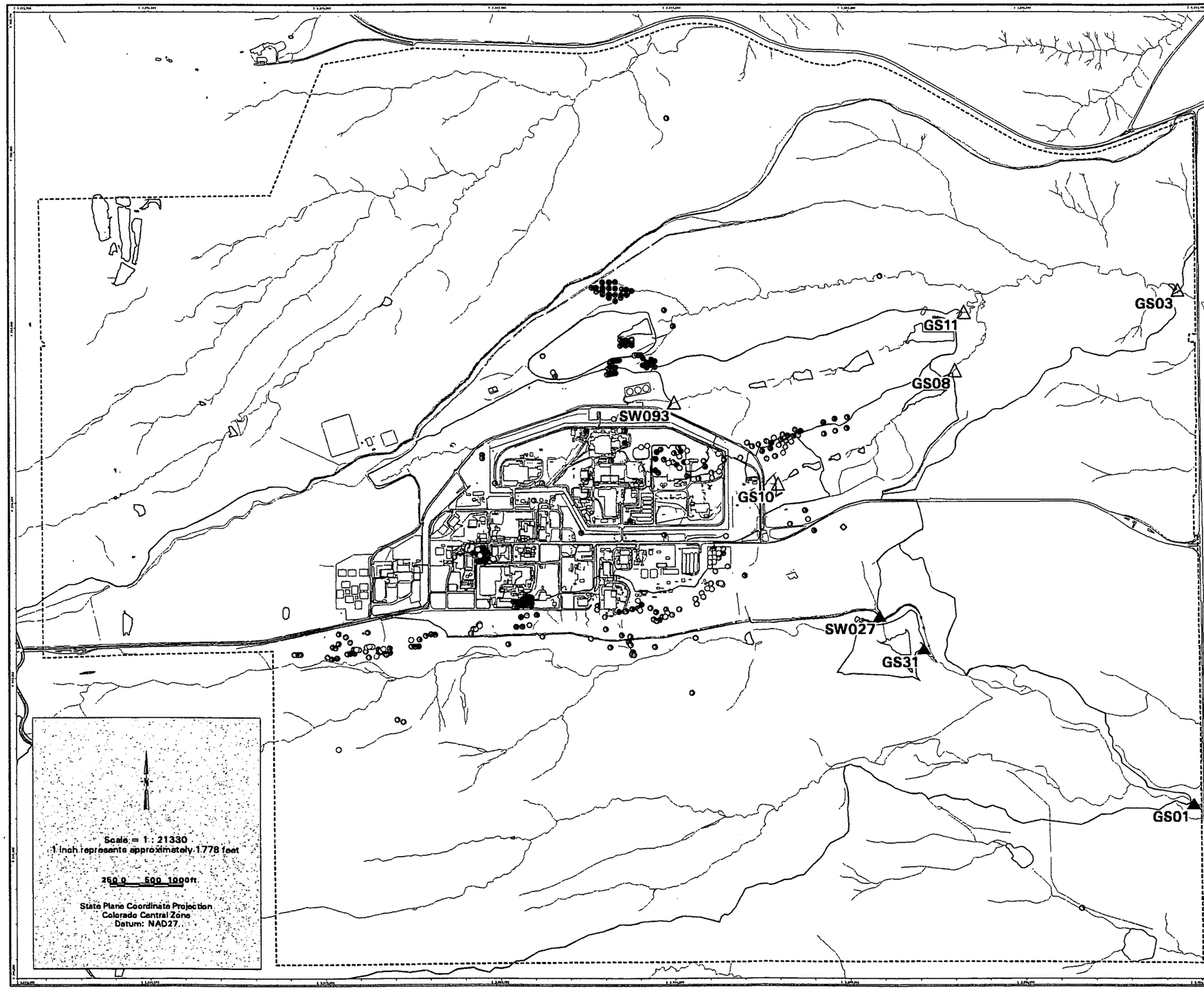

Figure TA-2-19

Actinide Migration Evaluation Pathway Report

Pu-239/240 Activity in Subsurface Soils

Depth : 2 - 4 ft

EXPLANATION

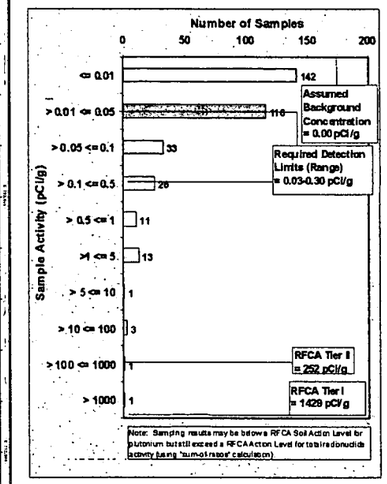

○ Value < Tier II value (Color indicates range of activity shown in the histogram above.)

▽ Tier II value < = Value < Tier I value

◇ Value > = Tier I value

N Drainage Basin Boundary

△ Walnut Creek Basin Gaging Station (GS03, GS08, GS10, GS11 & SW093)

▲ Woman Creek Basin Gaging Station (GS01, GS31 & SW027)

Standard Map Features

- Buildings and other structures
- Lakes and ponds
- Streams, ditches, or other drainage features
- Rocky Flats boundary
- Paved roads

DATA SOURCE BASE FEATURES:

Buildings, fences, hydrography, roads and other structures from 1994 aerial fly-over data captured by EG&G RSL, Las Vegas. Digitized from the orthophotographs. 1/95
Analytical Data from SWD as of October 2000.

Data Analysis performed by Wright Water engineers (303-480-1700).

U.S. Department of Energy
Rocky Flats Environmental Technology Site

GIS Dept. 303-966-7707

Prepared for: DynCorp THE ART OF TECHNOLOGY

Prepared for: KH KAISER-HILL COMPANY

NT_Svr w:/projects/actinide_pathway_report/fy2002/subsurface_soil_maps/pu239-240_2ft-4ft.aml

169

Figure TA-2-20

Actinide Migration Evaluation Pathway Report

Pu-239/240 Activity in Subsurface Soils

Depth : 4 - 6 ft

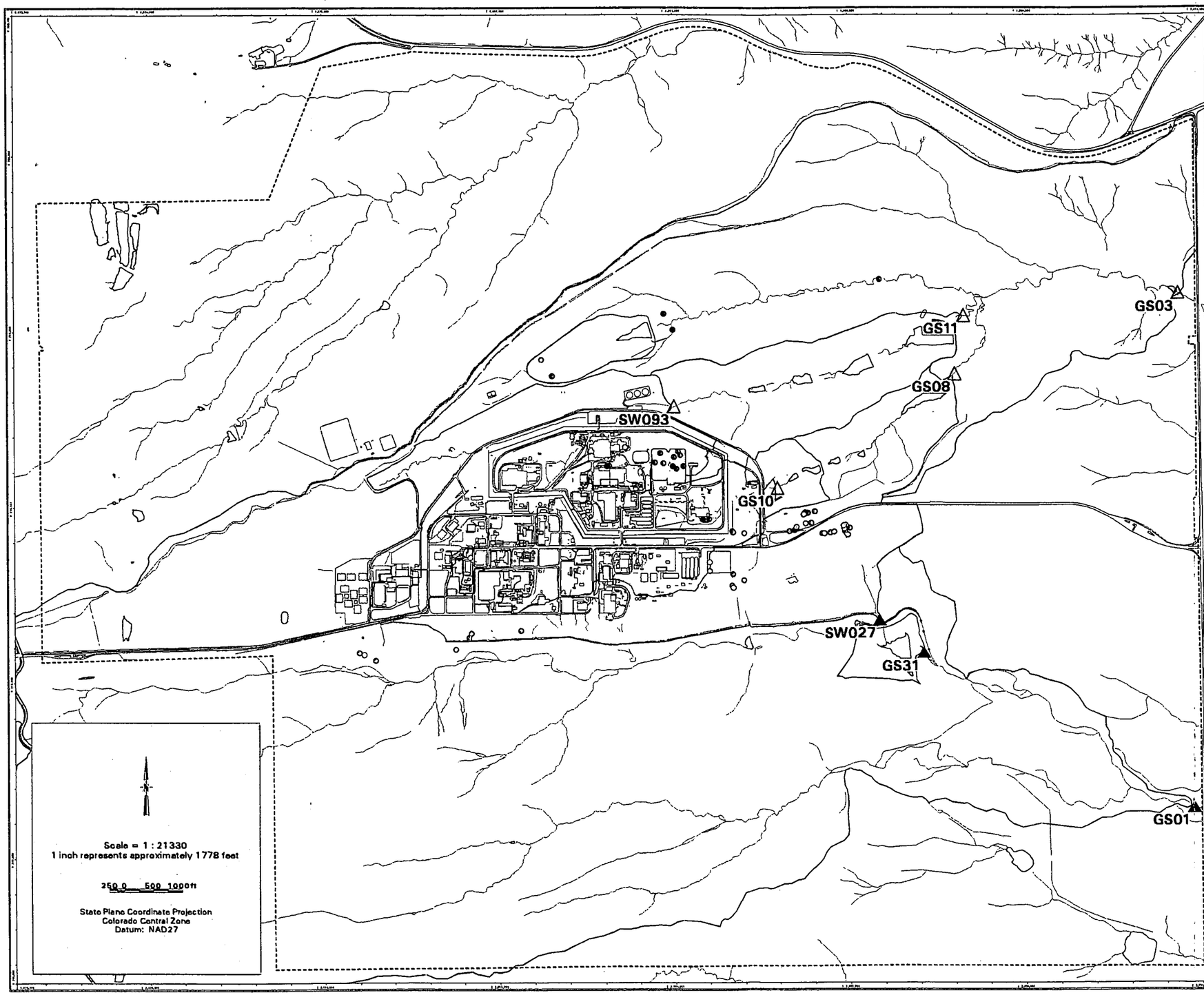

EXPLANATION

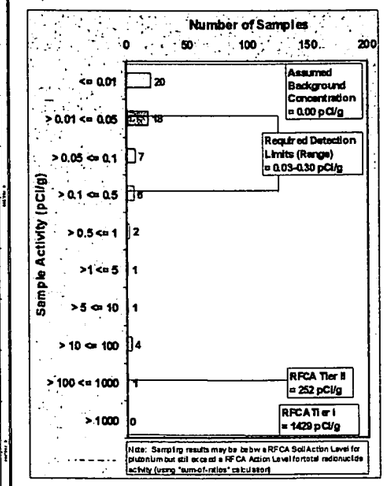

- ○ Value < Tier II value (Color indicates range of activity shown in the histogram above.)
- ▽ Tier II value < = Value < Tier I value
- ◇ Value > = Tier I value
- N Drainage Basin Boundary
- △ Walnut Creek Basin Gaging Station (GS03, GS08, GS10, GS11 & SW093)
- ▲ Woman Creek Basin Gaging Station (GS01, GS31 & SW027)

Standard Map Features

- Buildings and other structures
- Lakes and ponds
- Streams, ditches, or other drainage features
- Rocky Flats boundary
- Paved roads

DATA SOURCE BASE FEATURES:

Buildings, fences, hydrography, roads and other structures from 1994 aerial fly-over data captured by EG&G RSL, Las Vegas.
Digitized from the orthophotographs. 1/95
Analytical Data from SWD as of October 2000.

Data Analysis performed by Wright Water engineers (303-480-1700).

U.S. Department of Energy
Rocky Flats Environmental Technology Site

GIS Dept. 303-966-7707

Prepared by: DynCorp — THE ART OF TECHNOLOGY

Prepared for: KAISER-HILL COMPANY

NT_Svr w:/projects/actinide_pathway_report/fy2002/subsurface_soil_maps/pu239-240_4ft-6ft.aml

170

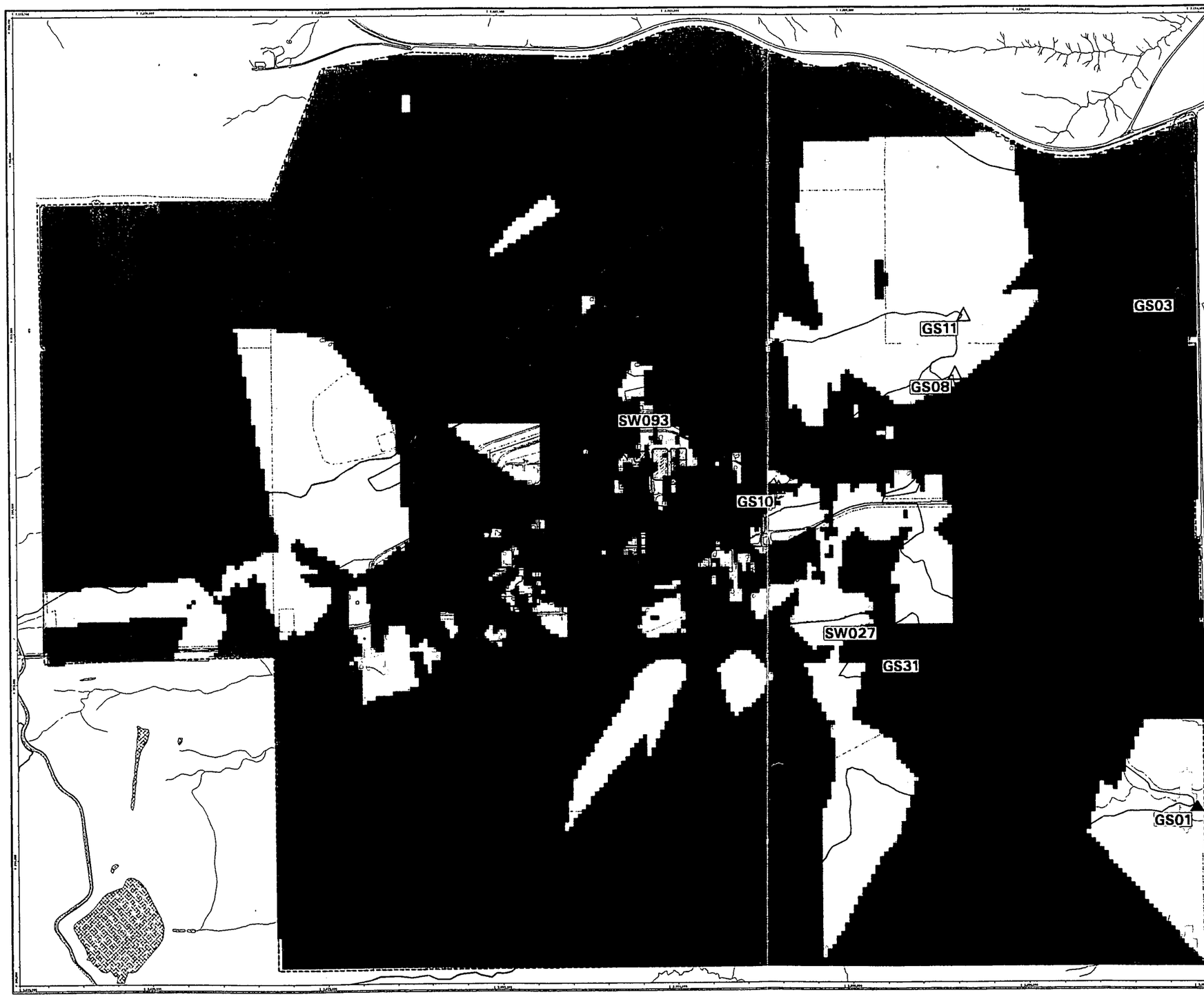

Figure TA-2-11

Actinide Migration Evaluation Pathway Report

U-235 Activity in Surface Soils

Kriging Analysis Isoplot (pCi/g)

EXPLANATION

- Result < = 0.01
- 0.01 < Result < = 0.05
- 0.05 < Result < = 0.1
- 0.1 < Result < = 0.5
- 0.5 < Result < = 1.0
- 1.0 < Result < = 5.0
- 5.0 < Result < = 10.0
- 10.0 < Result < = 100.0
- 100.0 < Result < = 1000.0
- Result > 1000.0
- Drainage Basin Boundary
- Walnut Creek Basin Gaging Station (GS03, GS08, GS10, GS11 & SW093)
- Woman Creek Basin Gaging Station (GS01, GS31 & SW027)

Standard Map Features

- Solar Evaporation Ponds (SEPs)
- Lakes and ponds
- Streams, ditches, or other drainage features
- Fences and other barriers
- Rocky Flats boundary
- Paved roads

DATA SOURCE BASE FEATURES:

Buildings, fences, hydrography, roads and other structures from 1994 aerial fly-over data captured by EG&G RSL, Las Vegas. Digitized from the orthophotographs. 1/95

Analytical Data provided by Mark Wood (KH, 303-966-6689).

Kriged data provided by Jeff Myers (Westinghouse-Akin, 803-502-9747).

Scale = 1 : 21330
1 inch represents approximately 1778 feet

250 0 500 1000 ft

State Plane Coordinate Projection
Colorado Central Zone
Datum: NAD27

U.S. Department of Energy
Rocky Flats Environmental Technology Site

GIS Dept. 303-966-7707

Prepared for: DynCorp — THE ART OF TECHNOLOGY

Prepared for: KH KAISER-HILL COMPANY

March 19, 1996

NT_Svr w:/projects/actinide_pathway_report/fy2002/kriged_data_maps/u235_grid_bsize.aml

161

Figure TA-2-9

Actinide Migration Evaluation Pathway Report

Am-241 Activity in Surface Soils

Kriging Analysis Isoplot (pCi/g)

EXPLANATION

- Result < = 0.01
- 0.01 < Result < = 0.05
- 0.05 < Result < = 0.1
- 0.1 < Result < = 0.5
- 0.5 < Result < = 1.0
- 1.0 < Result < = 5.0
- 5.0 < Result < = 10.0
- 10.0 < Result < = 100.0
- 100.0 < Result < = 1000.0
- Result > 1000.0
- Drainage Basin Boundary
- Walnut Creek Basin Gaging Station (GS03, GS08, GS10, GS11 & SW093)
- Woman Creek Basin Gaging Station (GS01, GS31 & SW027)

Standard Map Features

- Solar Evaporation Ponds (SEPs)
- Lakes and ponds
- Streams, ditches, or other drainage features
- Fences and other barriers
- Rocky Flats boundary
- Paved roads

DATA SOURCE BASE FEATURES:

Buildings, fences, hydrography, roads and other structures from 1994 aerial fly-over data captured by EG&G RSL, Las Vegas. Digitized from the orthophotographs. 1/95

Analytical Data from SWD as of October 1999.

903 Pad data from 903 Drum Storage Area Characterization Report, September 1999.

Kriged data provided by Jeff Myers (Westinghouse-Akin, 803-502-9747).

Scale = 1 : 21330
1 inch represents approximately 1778 feet

250 0 500 1000ft

State Plane Coordinate Projection
Colorado Central Zone
Datum: NAD27

U.S. Department of Energy
Rocky Flats Environmental Technology Site

GIS Dept. 303-966-7707

Prepared by: DynCorp — THE ART OF TECHNOLOGY

Prepared for: KAISER-HILL

March 19, 2002

NT_Svr w:/projects/actinide_pathway_report/fy2002/kriged_data_maps/am241_grid_baize.aml

159

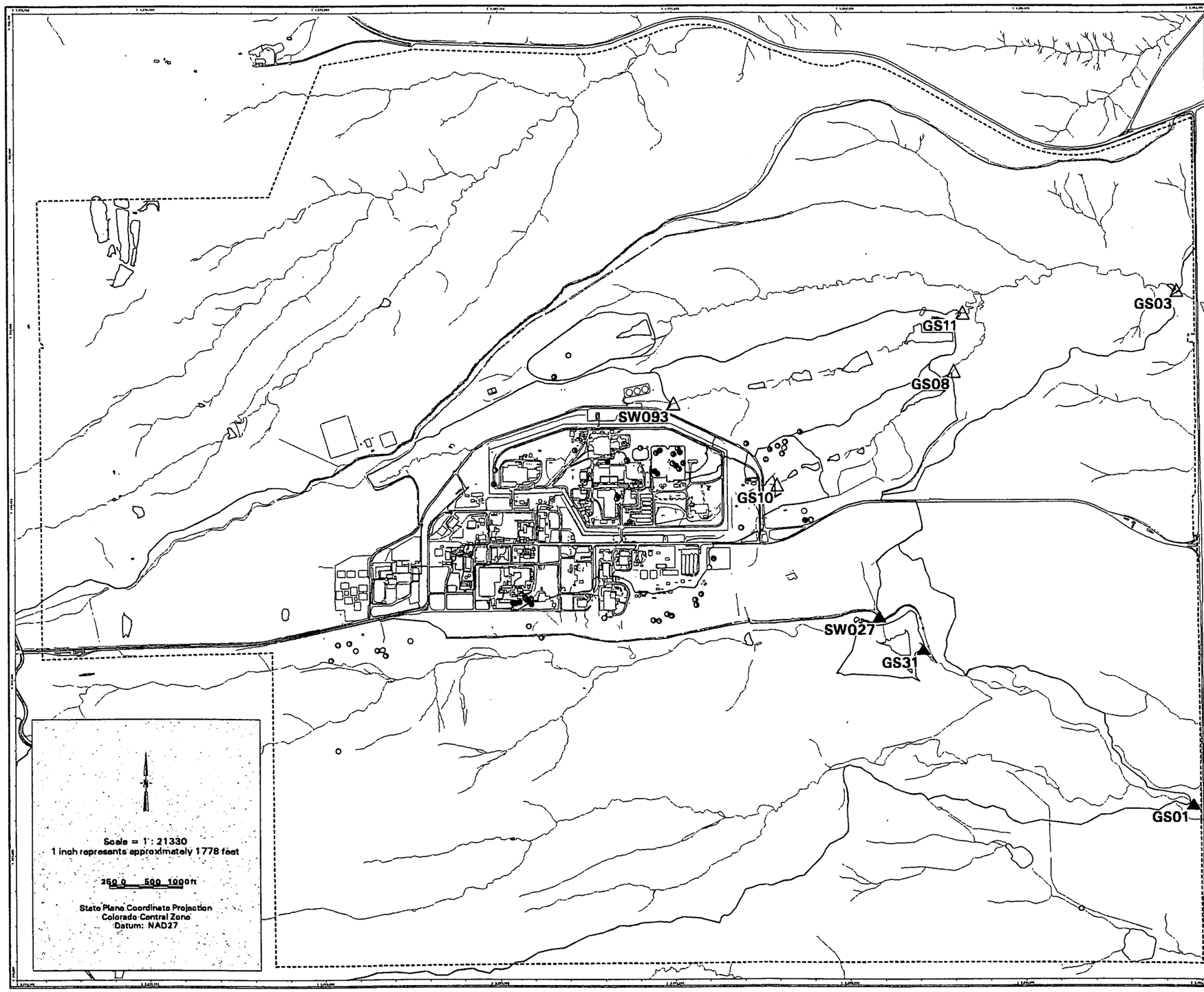

Figure TA-2-21

Actinide Migration Evaluation Pathway Report

Pu-239/240 Activity in Subsurface Soils

Depth : 6 - 8 ft

EXPLANATION

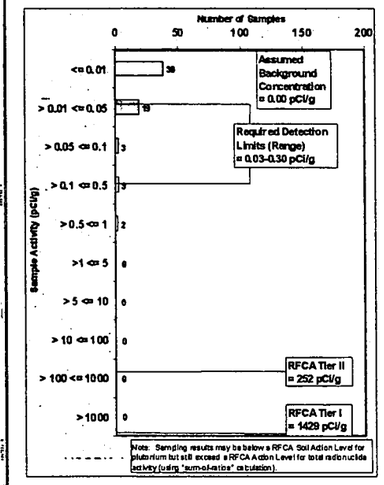

○ Value < Tier II value (Color indicates range of activity shown in the histogram above.)

▽ Tier II value < = Value < Tier I value

◇ Value > = Tier I value

Drainage Basin Boundary

△ Walnut Creek Basin Gaging Station (GS03, GS08, GS10, GS11 & SW093)

▲ Woman Creek Basin Gaging Station (GS01, GS31 & SW027)

Standard Map Features

- Buildings and other structures
- Lakes and ponds
- Streams, ditches, or other drainage features
- Rocky Flats boundary
- Paved roads

DATA SOURCE BASE FEATURES:

Buildings, fences, hydrography, roads and other structures from 1994 aerial fly-over data captured by EG&G RSL, Las Vegas. Digitized from the orthophotographs. 1/95
Analytical Data from SWD as of October 2000.

Data Analysis performed by Wright Water engineers (303-480-1700).

U.S. Department of Energy
Rocky Flats Environmental Technology Site

GIS Dept. 303-966-7707

Prepared by: DynCorp THE ART OF TECHNOLOGY

Prepared for: KH KAISER-HILL COMPANY

NT_Svr w:/projects/actinide_pathway_report/fy2002/subsurface_soil_maps/pu239-240_6ft-8ft.aml

171

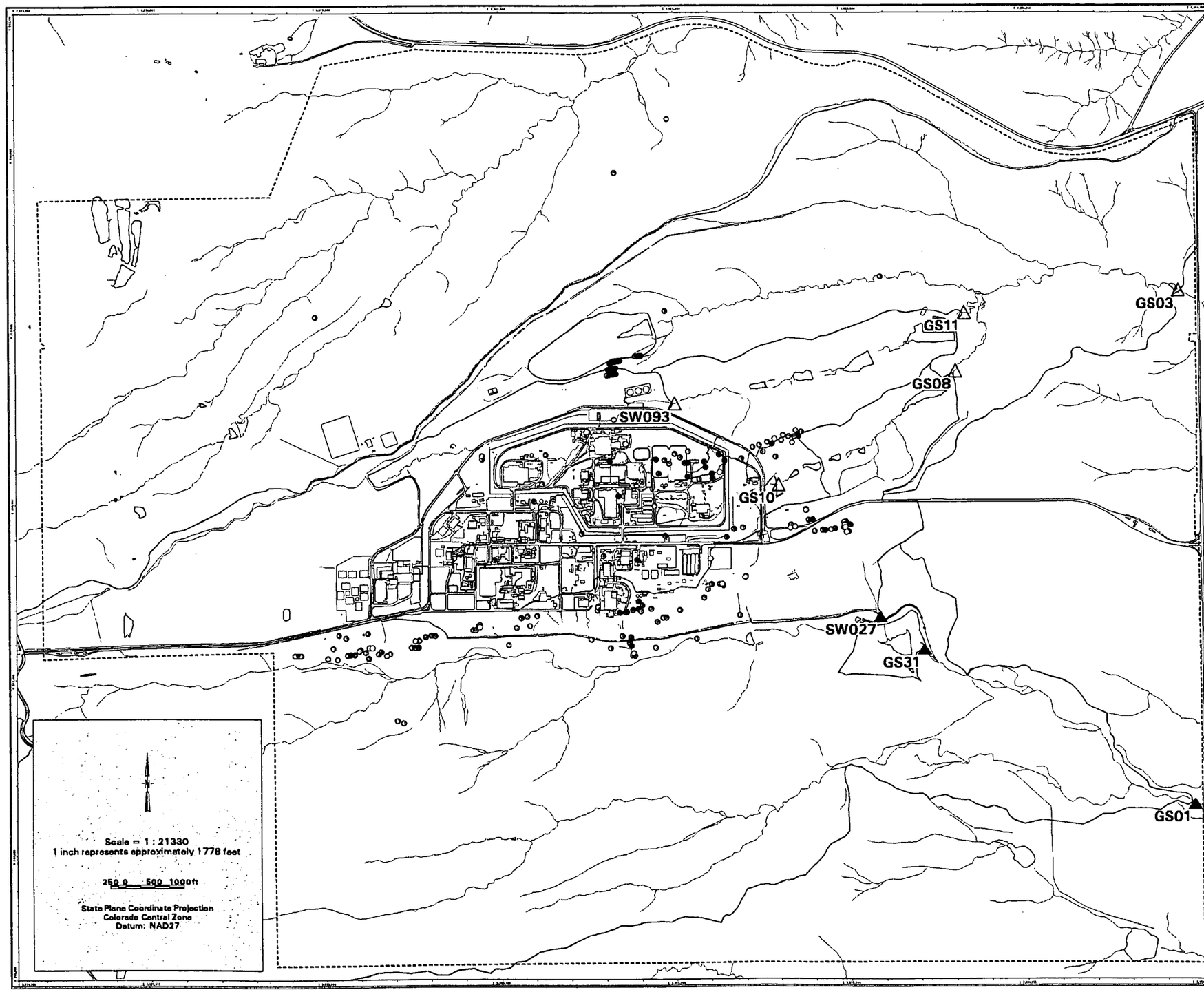

Figure TA-2-22

Actinide Migration Evaluation Pathway Report

Pu-239/240 Activity in Subsurface Soils

Depth : 8 - 10 ft

EXPLANATION

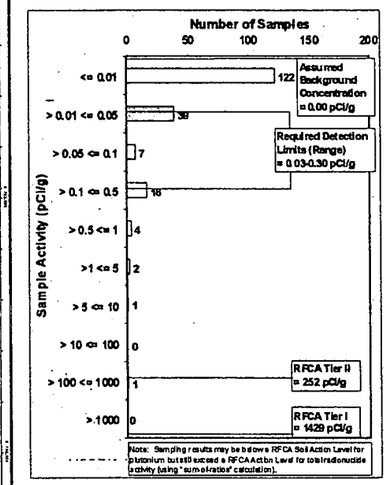

- ○ Value < Tier II value (Color indicates range of activity shown in the histogram above.)
- ▽ Tier II value < = Value < Tier I value
- ◇ Value > = Tier I value
- N Drainage Basin Boundary
- △ Walnut Creek Basin Gaging Station (GS03, GS08, GS10, GS11 & SW093)
- ▲ Woman Creek Basin Gaging Station (GS01, GS31 & SW027)

Standard Map Features

- Buildings and other structures
- Lakes and ponds
- Streams, ditches, or other drainage features
- Rocky Flats boundary
- Paved roads

DATA SOURCE BASE FEATURES:
Buildings, fences, hydrography, roads and other structures from 1994 aerial fly-over data captured by EG&G RSL, Las Vegas.
Digitized from the orthophotographs. 1/95
Analytical Data from SWD as of October 2000.

Data Analysis performed by Wright Water engineers (303-480-1700).

U.S. Department of Energy
Rocky Flats Environmental Technology Site
CES Dept. 303-966-7707

Prepared for: DynCorp — THE ART OF TECHNOLOGY

Prepared for: KAISER-HILL COMPANY

NT_Svr w:/projects/actinide_pathway_report/fy2002/subsurface_soil_maps/pu239-240_8ft-10ft.aml

172

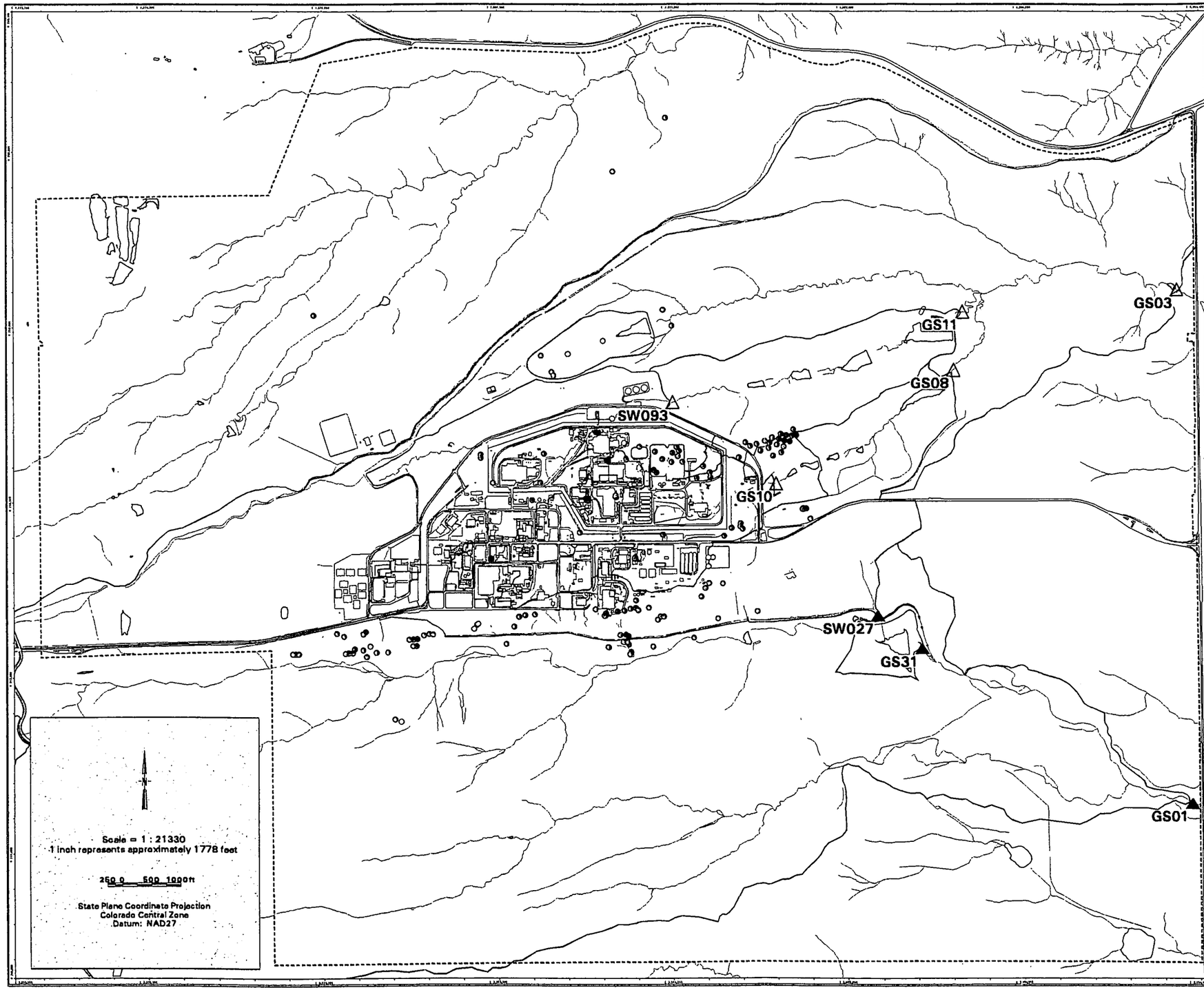

Figure TA-2-23

Actinide Migration Evaluation Pathway Report

Pu-239/240 Activity in Subsurface Soils

Depth : > 10 ft

EXPLANATION

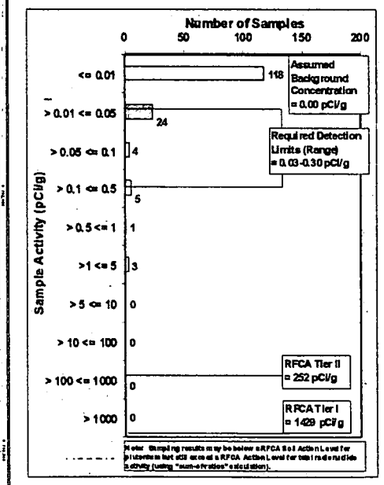

- ○ Value < Tier II value (Color indicates range of activity shown in the histogram above.)
- ▽ Tier II value < = Value < Tier I value
- ◇ Value > = Tier I value
- N Drainage Basin Boundary
- △ Walnut Creek Basin Gaging Station (GS03, GS08, GS10, GS11 & SW093)
- ▲ Woman Creek Basin Gaging Station (GS01, GS31 & SW027)

Standard Map Features

- Buildings and other structures
- Lakes and ponds
- Streams, ditches, or other drainage features
- Rocky Flats boundary
- Paved roads

DATA SOURCE BASE FEATURES:
Buildings, fences, hydrography, roads and other structures from 1994 aerial fly-over data captured by EG&G RSL, Las Vegas.
Digitized from the orthophotographs. 1/95
Analytical Data from SWD as of October 2000.

Data Analysis performed by Wright Water engineers (303-480-1700).

U.S. Department of Energy
Rocky Flats Environmental Technology Site

GIS Dept. 303-966-7707

Prepared by: DynCorp — THE ART OF TECHNOLOGY

Prepared for: KAISER-HILL COMPANY

NT_Svr w:/projects/actinide_pathway_report/fy2002/subsurface_soil_maps/pu239-240_10ft-dpr.aml

173

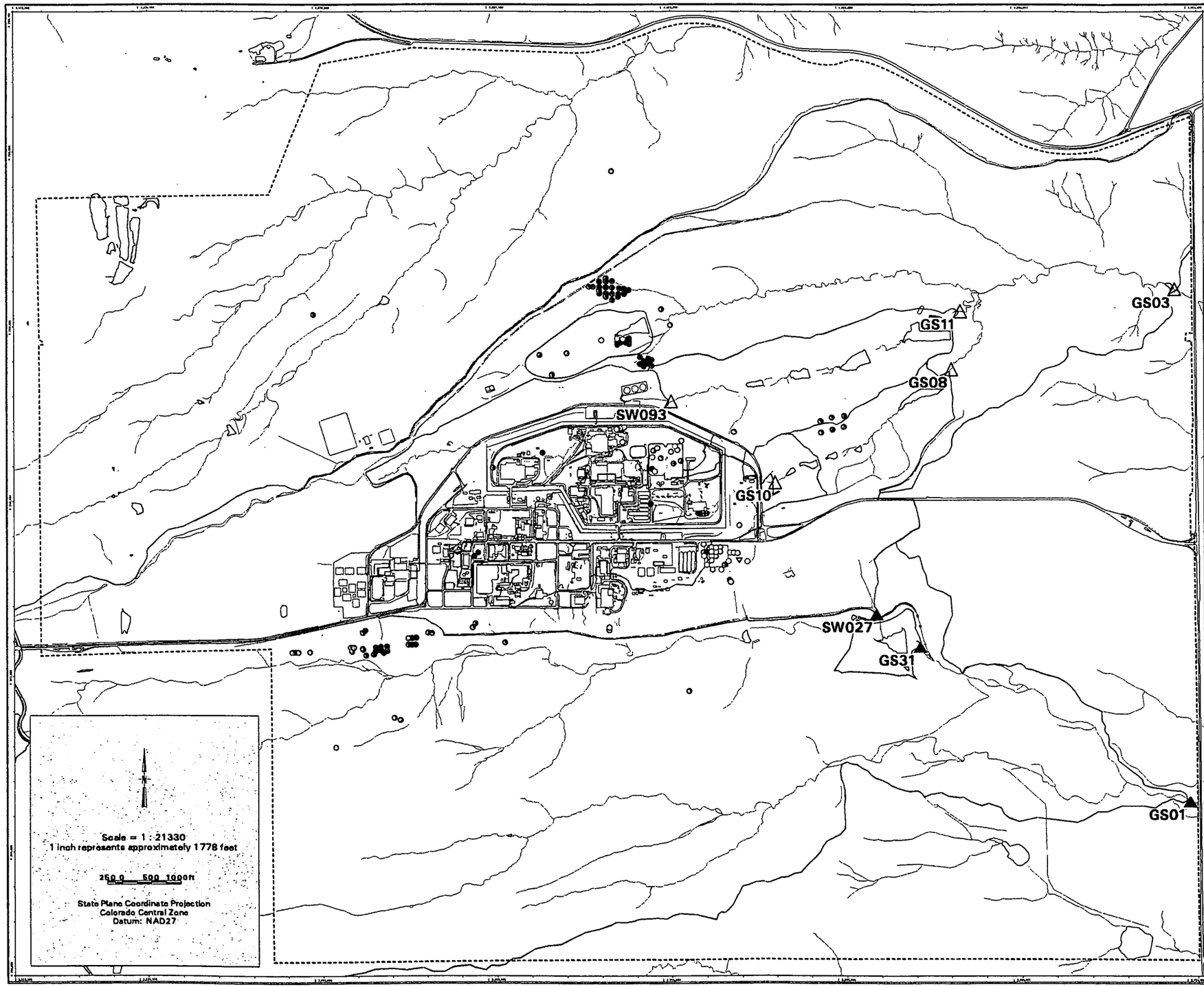

Figure TA-2-24

Actinide Migration Evaluation Pathway Report

Am-241 Activity in Subsurface Soils

Depth : 0.5 - 2 ft

EXPLANATION

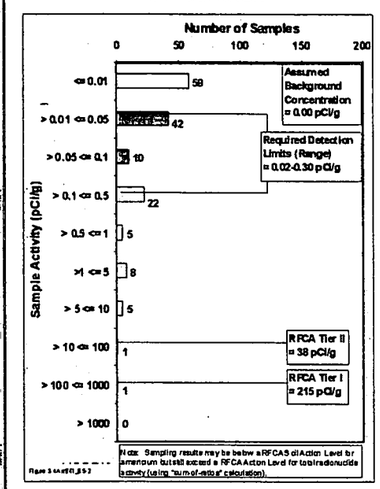

- ○ Value < Tier II value (Color indicates range of activity shown in the histogram above.)
- ▽ Tier II value < = Value < Tier I value
- ◇ Value > = Tier I value
- Drainage Basin Boundary
- △ Walnut Creek Basin Gaging Station (GS03, GS08, GS10, GS11 & SW093)
- ▲ Woman Creek Basin Gaging Station (GS01, GS31 & SW027)

Standard Map Features

- Buildings and other structures
- Lakes and ponds
- Streams, ditches, or other drainage features
- Rocky Flats boundary
- Paved roads

DATA SOURCE BASE FEATURES:

Buildings, fences, hydrography, roads and other structures from 1994 aerial fly-over data captured by EG&G RSL, Las Vegas. Digitized from the orthophotographs. 1/95
Analytical Data from SWD as of October 2000.

Data Analysis performed by Wright Water engineers (303-480-1700).

U.S. Department of Energy
Rocky Flats Environmental Technology Site

GIS Dept. 303-966-7707

Prepared by: DynCorp — THE ART OF TECHNOLOGY

Prepared for: KAISER-HILL

NT_Svr w:/projects/actinide_pathway_report/fy2002/subsurface_soil_maps/am241_6in-2ft.aml

174

Figure TA-2-25

Actinide Migration Evaluation Pathway Report

Am-241 Activity in Subsurface Soils

Depth : 2 - 4 ft

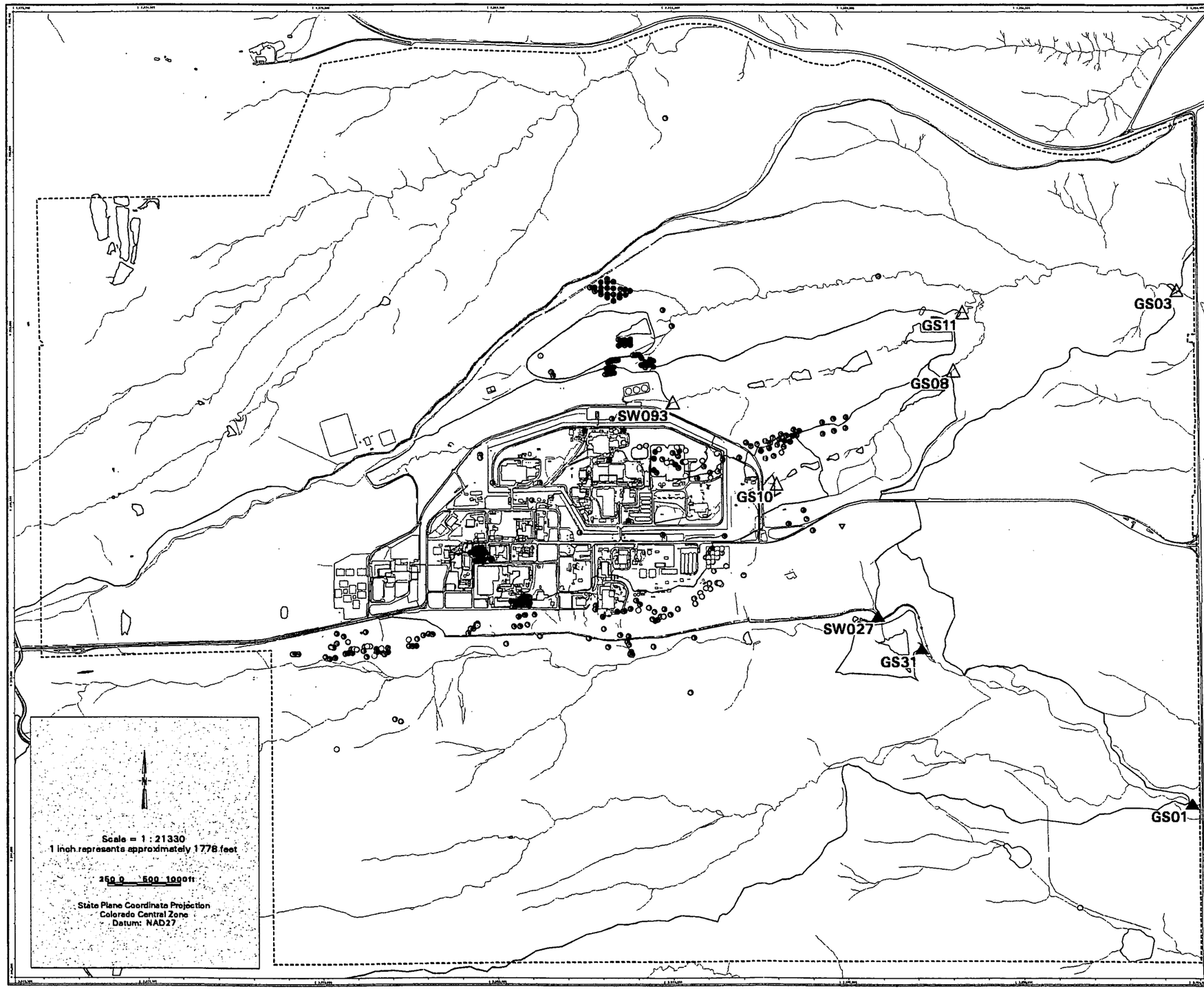

EXPLANATION

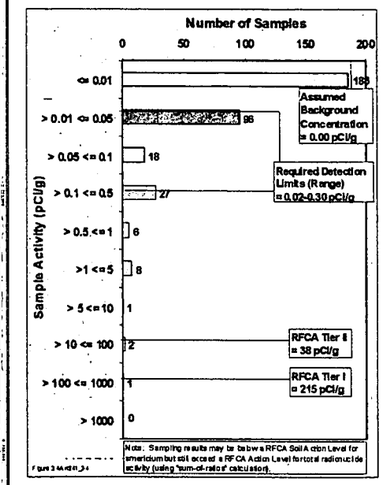

- ○ Value < Tier II value (Color indicates range of activity shown in the histogram above.)
- ▽ Tier II value < = Value < Tier I value
- ◇ Value > = Tier I value
- N Drainage Basin Boundary
- △ Walnut Creek Basin Gaging Station (GS03, GS08, GS10, GS11 & SW093)
- ▲ Woman Creek Basin Gaging Station (GS01, GS31 & SW027)

Standard Map Features

- Buildings and other structures
- Lakes and ponds
- Streams, ditches, or other drainage features
- Rocky Flats boundary
- Paved roads

DATA SOURCE BASE FEATURES:

Buildings, fences, hydrography, roads and other structures from 1994 aerial fly-over data captured by EG&G RSL, Las Vegas. Digitized from the orthophotographs. 1/95
Analytical Data from SWD as of October 2000.

Data Analysis performed by Wright Water engineers (303-480-1700).

U.S. Department of Energy
Rocky Flats Environmental Technology Site

GIS Dept. 303-966-7707

Prepared by: DynCorp — THE ART OF TECHNOLOGY

Prepared for: KH KAISER-HILL COMPANY

NT_Svr w:/projects/actinide_pathway_report/fy2002/subsurface_soil_maps/am241_2ft-4ft.aml

175

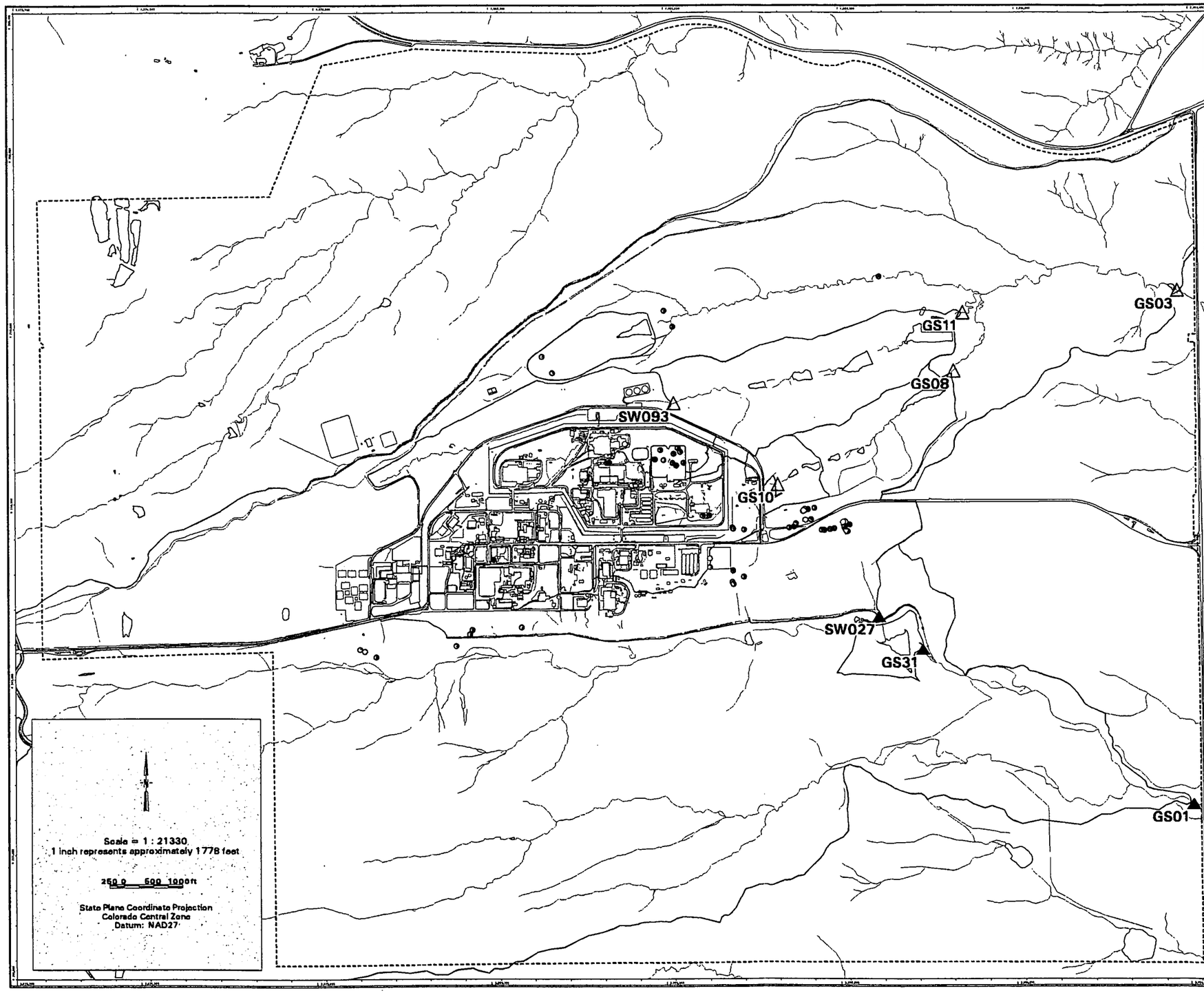

Figure TA-2-26

Actinide Migration Evaluation Pathway Report

Am-241 Activity in Subsurface Soils

Depth : 4 - 6 ft

EXPLANATION

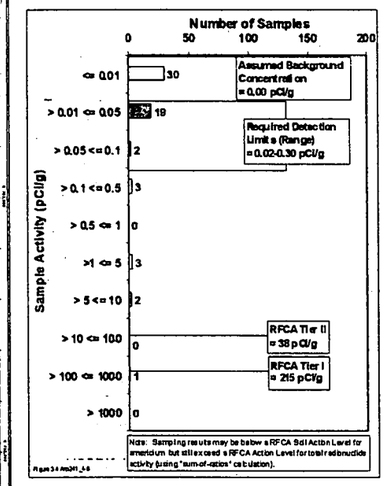

○ Value < Tier II value (Color indicates range of activity shown in the histogram above.)

▽ Tier II value < = Value < Tier I value

◇ Value > = Tier I value

N Drainage Basin Boundary

△ Walnut Creek Basin Gaging Station (GS03, GS08, GS10, GS11 & SW093)

▲ Woman Creek Basin Gaging Station (GS01, GS31 & SW027)

Standard Map Features

- Buildings and other structures
- Lakes and ponds
- Streams, ditches, or other drainage features
- Rocky Flats boundary
- Paved roads

DATA SOURCE BASE FEATURES:

Buildings, fences, hydrography, roads and other structures from 1994 aerial fly-over data captured by EG&G RSL, Las Vegas. Digitized from the orthophotographs. 1/95
Analytical Data from SWD as of October 2000.

Data Analysis performed by Wright Water engineers (303-480-1700).

U.S. Department of Energy
Rocky Flats Environmental Technology Site

GIS Dept. 303-966-7707

Prepared by: DynCorp THE ART OF TECHNOLOGY

Prepared for: KAISER-HILL COMPANY

December 18, 2001

NT_Svr w:/projects/actinide_pathway_report/fy2002/subsurface_soil_maps/am241_4ft-6ft.aml

176

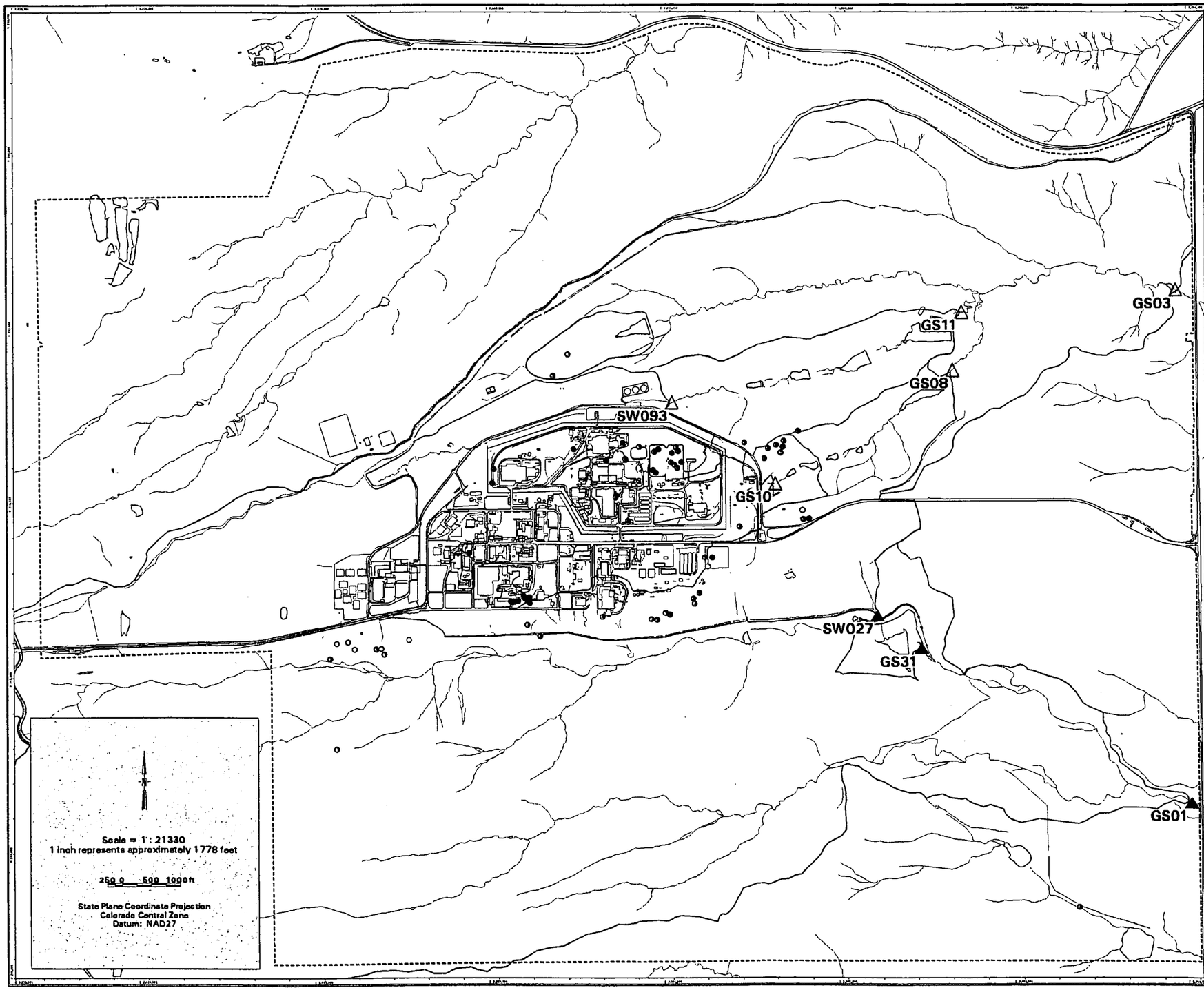

Figure TA-2-27

Actinide Migration Evaluation Pathway Report

Am-241 Activity in Subsurface Soils

Depth : 6 - 8 ft

EXPLANATION

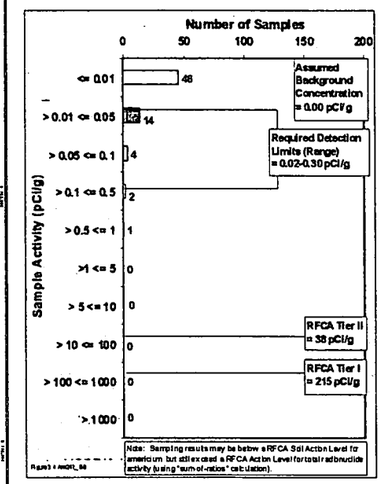

○ Value < Tier II value (Color indicates range of activity shown in the histogram above.)

▽ Tier II value < = Value < Tier I value

◇ Value > = Tier I value

N Drainage Basin Boundary

△ Walnut Creek Basin Gaging Station (GS03, GS08, GS10, GS11 & SW093)

▲ Woman Creek Basin Gaging Station (GS01, GS31 & SW027)

Standard Map Features

- Buildings and other structures
- Lakes and ponds
- Streams, ditches, or other drainage features
- Rocky Flats boundary
- Paved roads

DATA SOURCE BASE FEATURES:
Buildings, fences, hydrography, roads and other structures from 1994 aerial fly-over data captured by EG&G RSL, Las Vegas. Digitized from the orthophotographs. 1/95
Analytical Data from SWD as of October 2000.

Data Analysis performed by Wright Water engineers (303-480-1700).

U.S. Department of Energy
Rocky Flats Environmental Technology Site

GIS Dept. 303-966-7707

Prepared by: DynCorp THE ART OF TECHNOLOGY

Prepared for: KAISER-HILL COMPANY

NT_Svr w:/projects/actinide_pathway_report/fy2002/subsurface_soil_maps/am241_6ft-8ft.aml

177

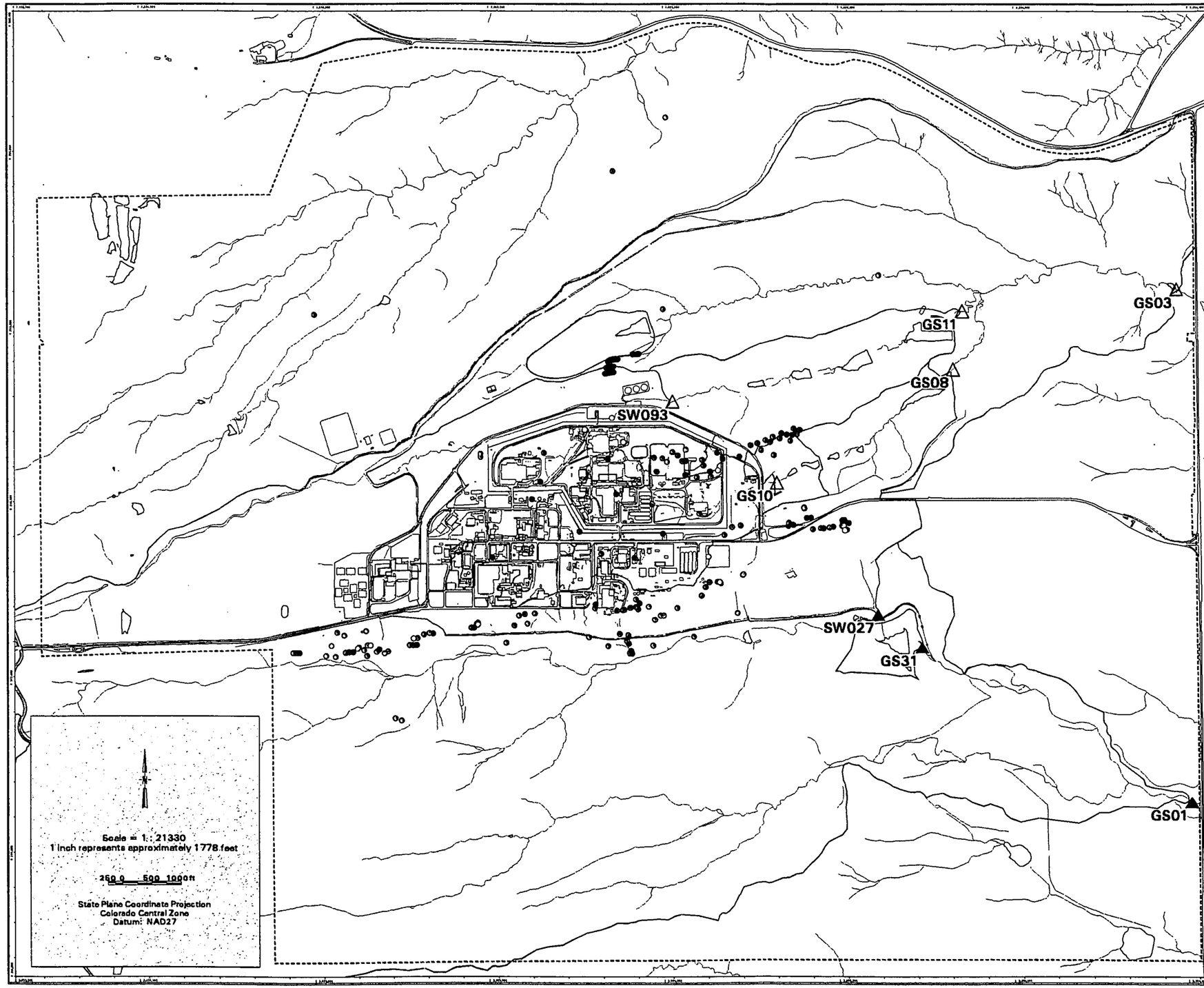

Figure TA-2-28

Actinide Migration Evaluation Pathway Report

Am-241 Activity in Subsurface Soils

Depth : 8 - 10 ft

EXPLANATION

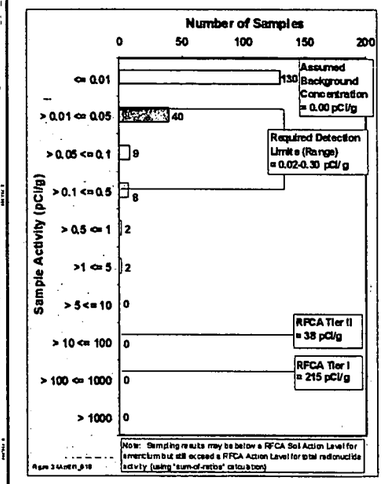

○ Value < Tier II value
(Color indicates range of activity shown in the histogram above.)

▽ Tier II value <= Value < Tier I value

◇ Value >= Tier I value

N Drainage Basin Boundary

△ Walnut Creek Basin Gaging Station (GS03, GS08, GS10, GS11 & SW093)

▲ Woman Creek Basin Gaging Station (GS01, GS31 & SW027)

Standard Map Features

- Buildings and other structures
- Lakes and ponds
- Streams, ditches, or other drainage features
- Rocky Flats boundary
- Paved roads

DATA SOURCE BASE FEATURES:

Buildings, fences, hydrography, roads and other structures from 1994 aerial fly-over data captured by EG&G RSL, Las Vegas.
Digitized from the orthophotographs. 1/95
Analytical Data from SWD as of October 2000.

Data Analysis performed by Wright Water engineers (303-480-1700).

U.S. Department of Energy
Rocky Flats Environmental Technology Site

CES Dept. 303-966-7707

Prepared by: DynCorp — THE ART OF TECHNOLOGY

Prepared for: KH KAISER-HILL COMPANY

NT_Svr w:/projects/actinide_pathway_report/fy2002/subsurface_soil_maps/am241_8ft-10ft.aml

178

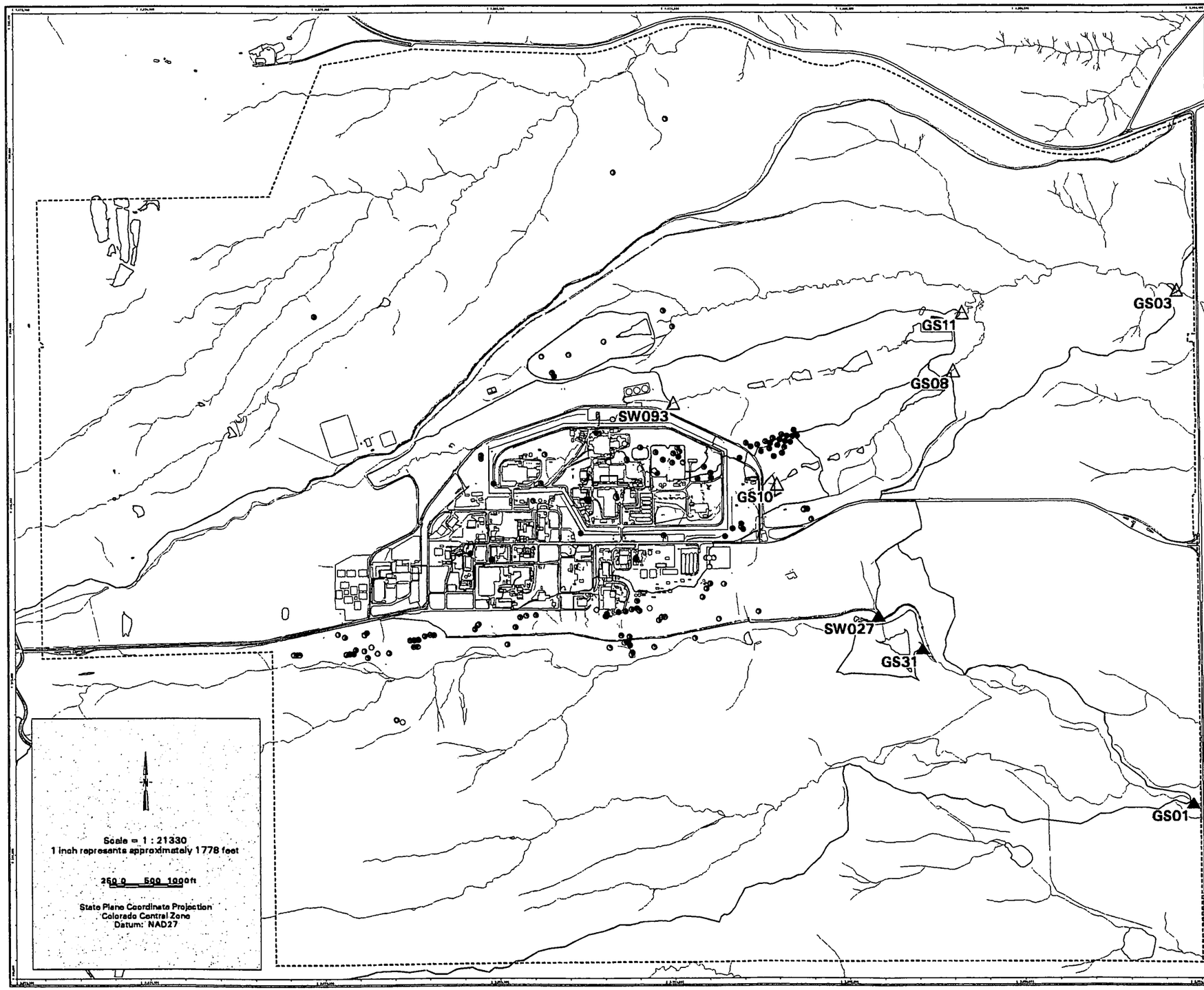

Figure TA-2-29

Actinide Migration Evaluation Pathway Report

Am-241 Activity in Subsurface Soils

Depth : > 10 ft

EXPLANATION

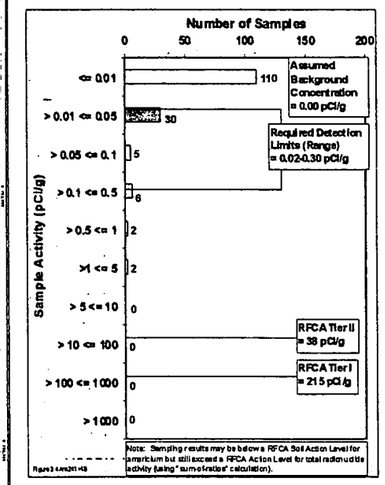

○ Value < Tier II value
(Color indicates range of activity shown in the histogram above.)

▽ Tier II value < = Value < Tier I value

◇ Value > = Tier I value

N Drainage Basin Boundary

△ Walnut Creek Basin Gaging Station (GS03, GS08, GS10, GS11 & SW093)

▲ Woman Creek Basin Gaging Station (GS01, GS31 & SW027)

Standard Map Features

- Buildings and other structures
- Lakes and ponds
- Streams, ditches, or other drainage features
- Rocky Flats boundary
- Paved roads

DATA SOURCE BASE FEATURES:
Buildings, fences, hydrography, roads and other structures from 1994 aerial fly-over data captured by EG&G RSL, Las Vegas.
Digitized from the orthophotographs. 1/95
Analytical Data from SWD as of October 2000.

Data Analysis performed by Wright Water engineers (303-480-1700).

U.S. Department of Energy
Rocky Flats Environmental Technology Site
GIS Dept. 303-966-7707

Prepared by: DynCorp — THE ART OF TECHNOLOGY

Prepared for: KAISER-HILL COMPANY

December 18, 2001

NT_Svr w:/projects/actinide_pathway_report/fy2002/subsurface_soil_maps/am241_10ft-dpr.aml

179

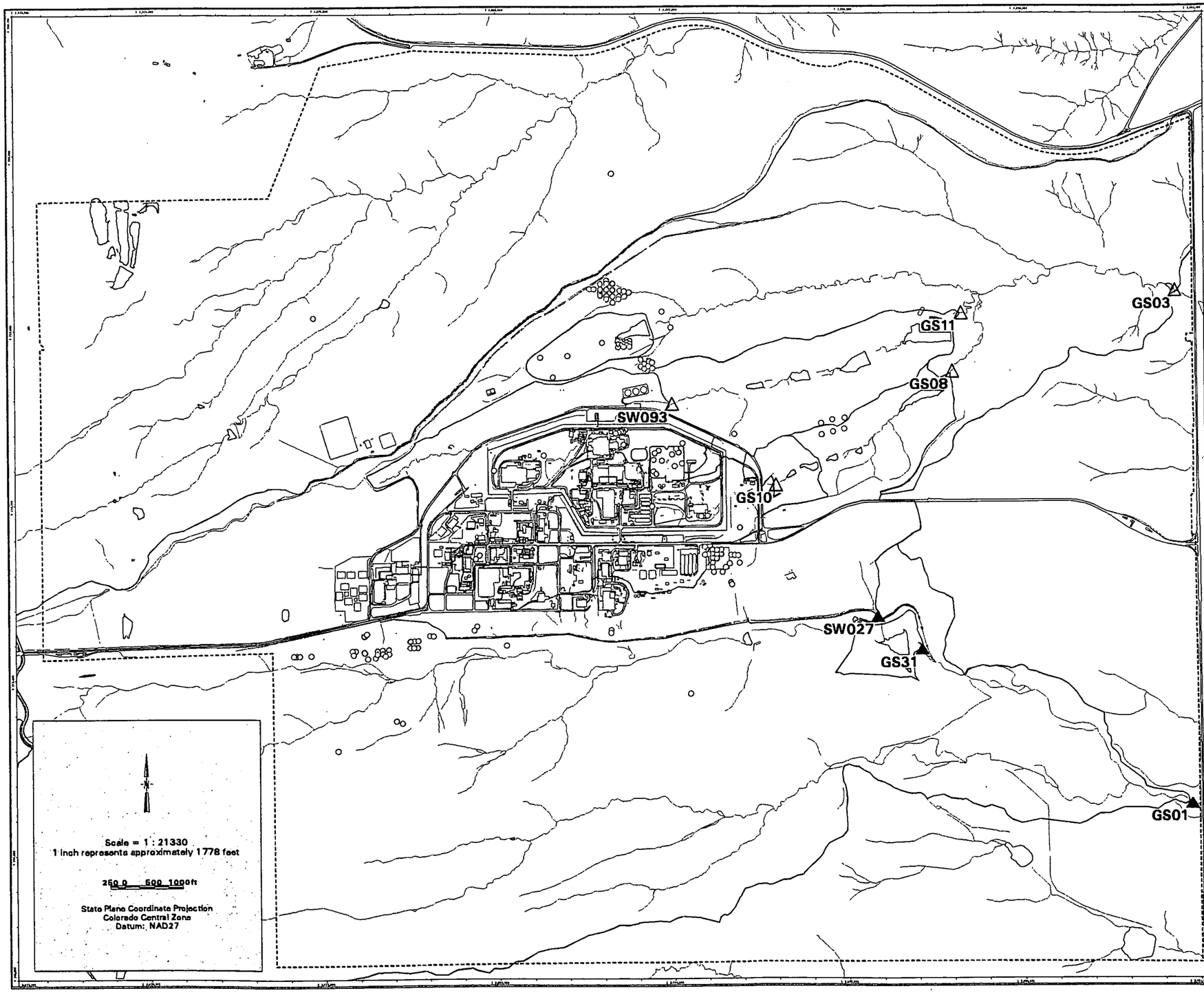

Figure TA-2-30

Actinide Migration Evaluation Pathway Report

U-233/234 Activity in Subsurface Soils

Depth : 0.5 - 2 ft

EXPLANATION

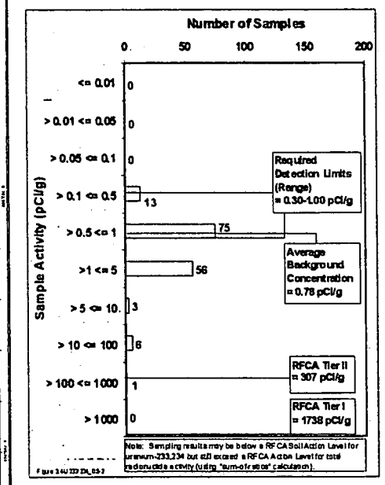

Note: Sampling results may be below a RFCA Soil Action Level for uranium-233,234 but still exceed a RFCA Action Level for total radionuclide activity (using "sum-of-ratios" calculation).

Figure 3-4U 233 234_6in-2ft

- ○ Value < Tier II value (Color indicates range of activity shown in the histogram above.)
- ▽ Tier II value < = Value < Tier I value
- ◇ Value > = Tier I value
- N Drainage Basin Boundary
- △ Walnut Creek Basin Gaging Station (GS03, GS08, GS10, GS11 & SW093)
- ▲ Woman Creek Basin Gaging Station (GS01, GS31 & SW027)

Standard Map Features

- Buildings and other structures
- Lakes and ponds
- Streams, ditches, or other drainage features
- Rocky Flats boundary
- Paved roads

DATA SOURCE BASE FEATURES:
Buildings, fences, hydrography, roads and other structures from 1994 aerial fly-over data captured by EG&G RSL, Las Vegas.
Digitized from the orthophotographs. 1/95
Analytical Data from SWD as of October 2000.

Data Analysis performed by Wright Water engineers (303-480-1700).

U.S. Department of Energy
Rocky Flats Environmental Technology Site

OIS Dept. 303-966-7767

Prepared for:
DynCorp
THE ART OF TECHNOLOGY

Prepared for:
KAISER-HILL COMPANY

December 13, 2001

NT_Svr w:/projects/actinide_pathway_report/fy2002/subsurface_soil_maps/u233-234_6in-2ft.aml

180

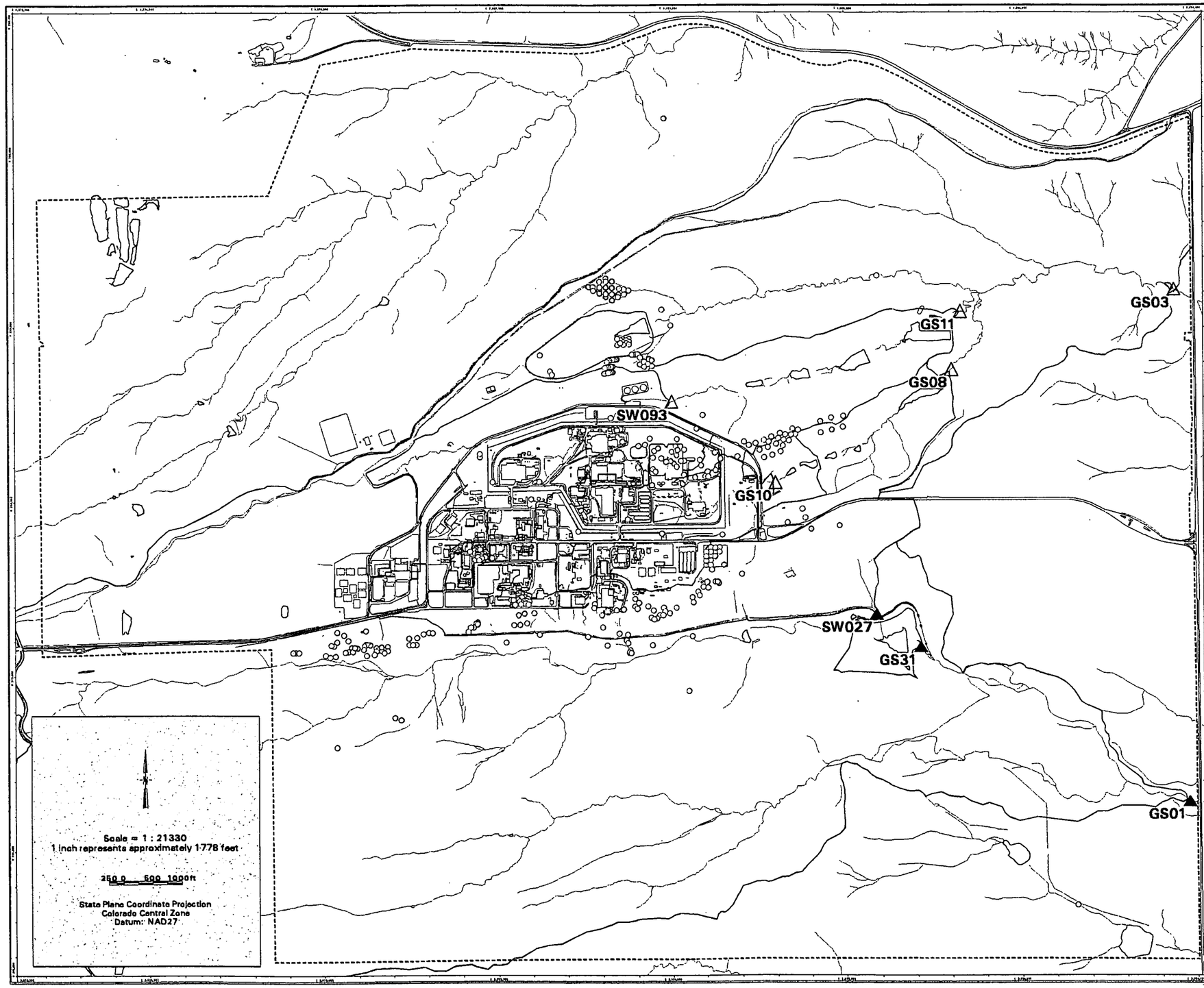

Figure TA-2-31

Actinide Migration Evaluation Pathway Report

U-233/234 Activity in Subsurface Soils

Depth : 2 - 4 ft

EXPLANATION

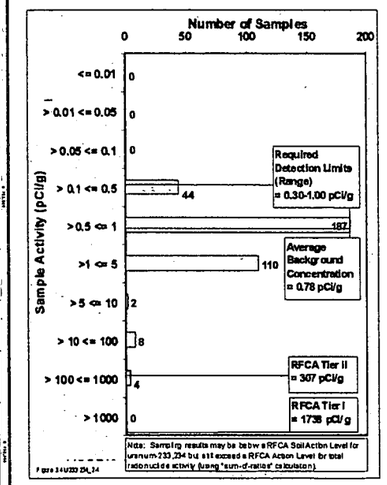

○ Value < Tier II value (Color indicates range of activity shown in the histogram above.)

▽ Tier II value < = Value < Tier I value

◇ Value > = Tier I value

N Drainage Basin Boundary

△ Walnut Creek Basin Gaging Station (GS03, GS08, GS10, GS11 & SW093)

▲ Woman Creek Basin Gaging Station (GS01, GS31 & SW027)

Standard Map Features

- Buildings and other structures
- Lakes and ponds
- Streams, ditches, or other drainage features
- Rocky Flats boundary
- Paved roads

DATA SOURCE BASE FEATURES:
Buildings, fences, hydrography, roads and other structures from 1994 aerial fly-over data captured by EG&G RSL, Las Vegas. Digitized from the orthophotographs. 1/95
Analytical Data from SWD as of October 2000.

Data Analysis performed by Wright Water engineers (303-480-1700).

U.S. Department of Energy
Rocky Flats Environmental Technology Site

GIS Dept. 303-966-7707

Prepared by: DynCorp THE ART OF TECHNOLOGY

Prepared for: KAISER-HILL COMPANY

NT_Svr w:/projects/actinide_pathway_report/fy2002/subsurface_soil_maps/u233-234_2ft-4ft.aml

181

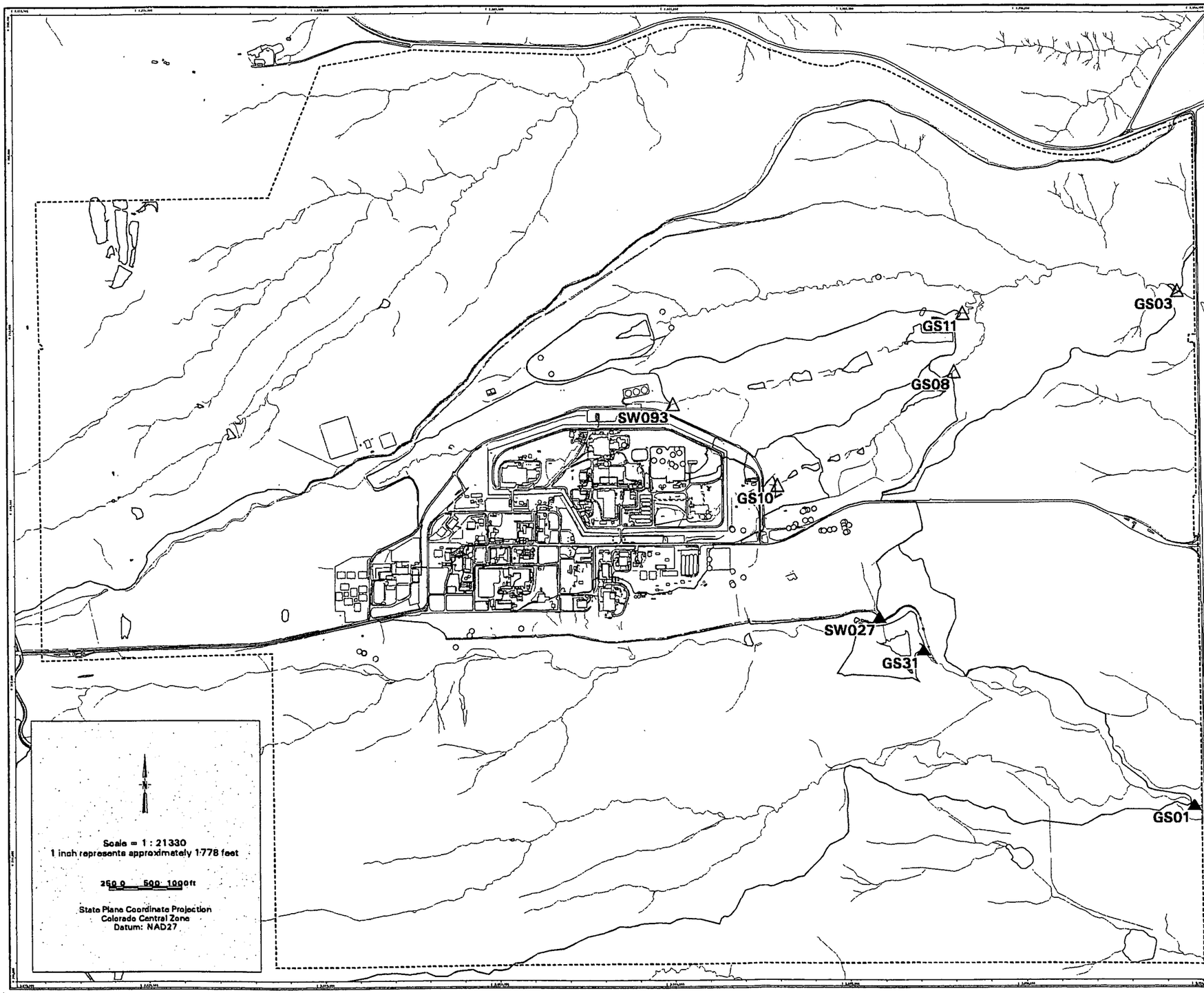

Figure TA-2-32

Actinide Migration Evaluation Pathway Report

U-233/234 Activity in Subsurface Soils

Depth : 4 - 6 ft

EXPLANATION

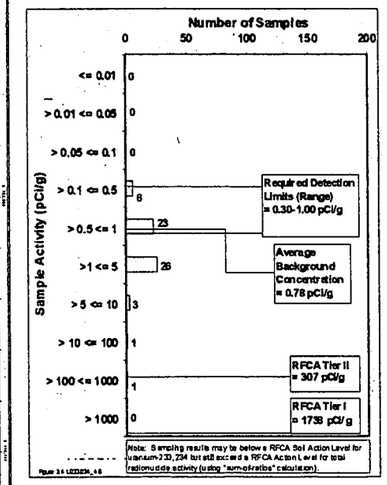

- ○ Value < Tier II value (Color indicates range of activity shown in the histogram above.)
- ▽ Tier II value < = Value < Tier I value
- ◇ Value > = Tier I value
- N Drainage Basin Boundary
- △ Walnut Creek Basin Gaging Station (GS03, GS08, GS10, GS11 & SW093)
- ▲ Woman Creek Basin Gaging Station (GS01, GS31 & SW027)

Standard Map Features

- Buildings and other structures
- Lakes and ponds
- Streams, ditches, or other drainage features
- Rocky Flats boundary
- Paved roads

DATA SOURCE BASE FEATURES:

Buildings, fences, hydrography, roads and other structures from 1994 aerial fly-over data captured by EG&G RSL, Las Vegas. Digitized from the orthophotographs. 1/95
Analytical Data from SWD as of October 2000.

Data Analysis performed by Wright Water engineers (303-480-1700).

U.S. Department of Energy
Rocky Flats Environmental Technology Site

GIS Dept. 303-966-7707

Prepared for:

DynCorp
THE ART OF TECHNOLOGY

KAISER-HILL COMPANY

NT_Svr w:/projects/actinide_pathway_report/fy2002/subsurface_soil_maps/u233-234_4ft-6ft.aml

182

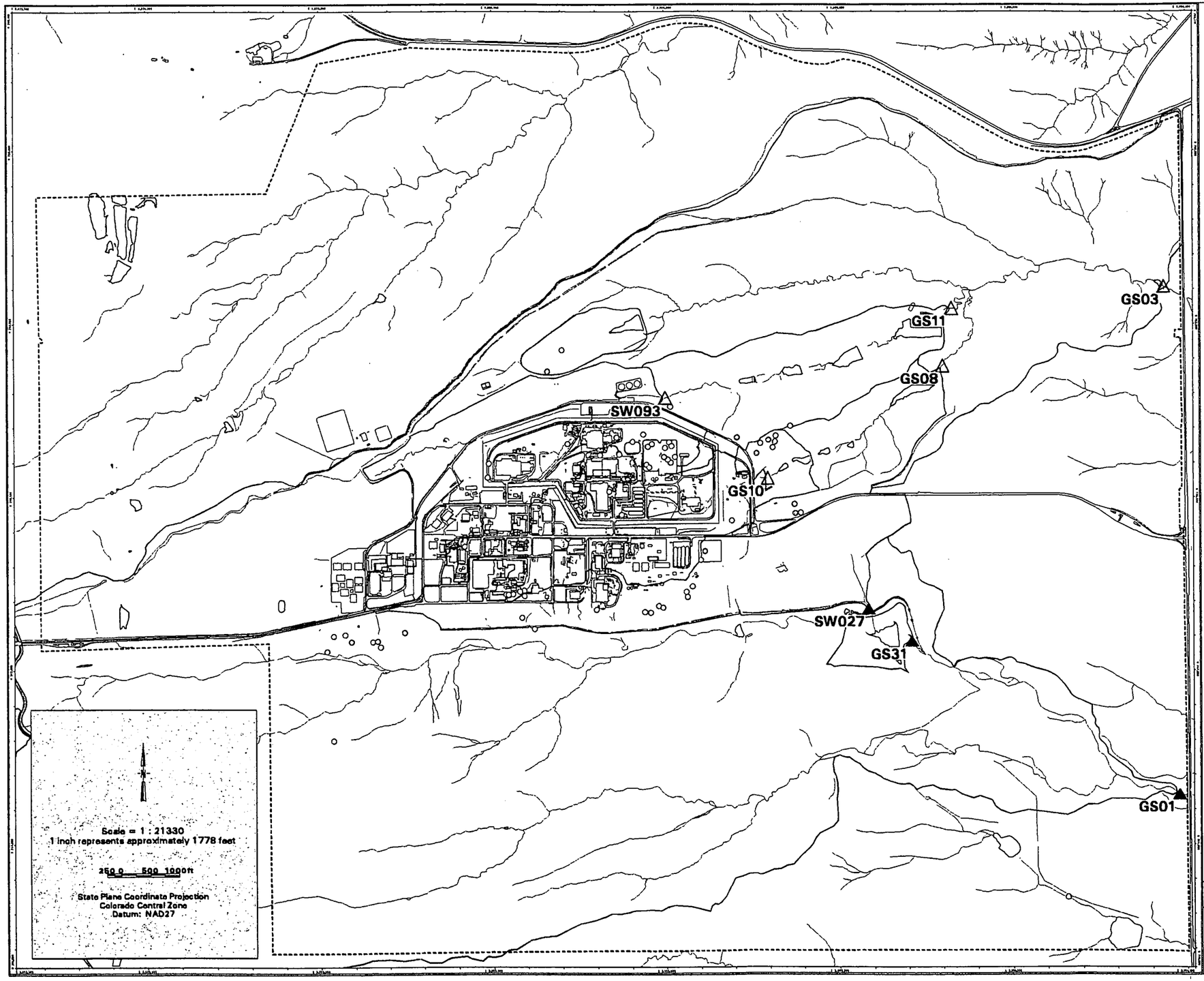

Figure TA-2-33

Actinide Migration Evaluation Pathway Report

U-233/234 Activity in Subsurface Soils

Depth : 6 - 8 ft

EXPLANATION

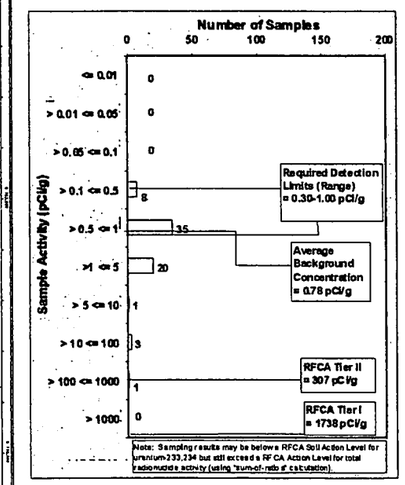

- ○ Value < Tier II value (Color indicates range of activity shown in the histogram above.)
- ▽ Tier II value < = Value < Tier I value
- ◇ Value > = Tier I value
- N Drainage Basin Boundary
- △ Walnut Creek Basin Gaging Station (GS03, GS08, GS10, GS11 & SW093)
- ▲ Woman Creek Basin Gaging Station (GS01, GS31 & SW027)

Standard Map Features

- Buildings and other structures
- Lakes and ponds
- Streams, ditches, or other drainage features
- Rocky Flats boundary
- Paved roads

DATA SOURCE BASE FEATURES:
Buildings, fences, hydrography, roads and other structures from 1994 aerial fly-over data captured by EG&G RSL, Las Vegas.
Digitized from the orthophotographs. 1/95
Analytical Data from SWD as of October 2000.

Data Analysis performed by Wright Water engineers (303-480-1700).

U.S. Department of Energy
Rocky Flats Environmental Technology Site
GIS Dept. 303-966-7707

Prepared by: DynCorp — THE ART OF TECHNOLOGY

Prepared for: KH KAISER-HILL COMPANY

NT_Svr w:/projects/actinide_pathway_report/fy2002/subsurface_soil_maps/u233-234_6ft-8ft.aml

183

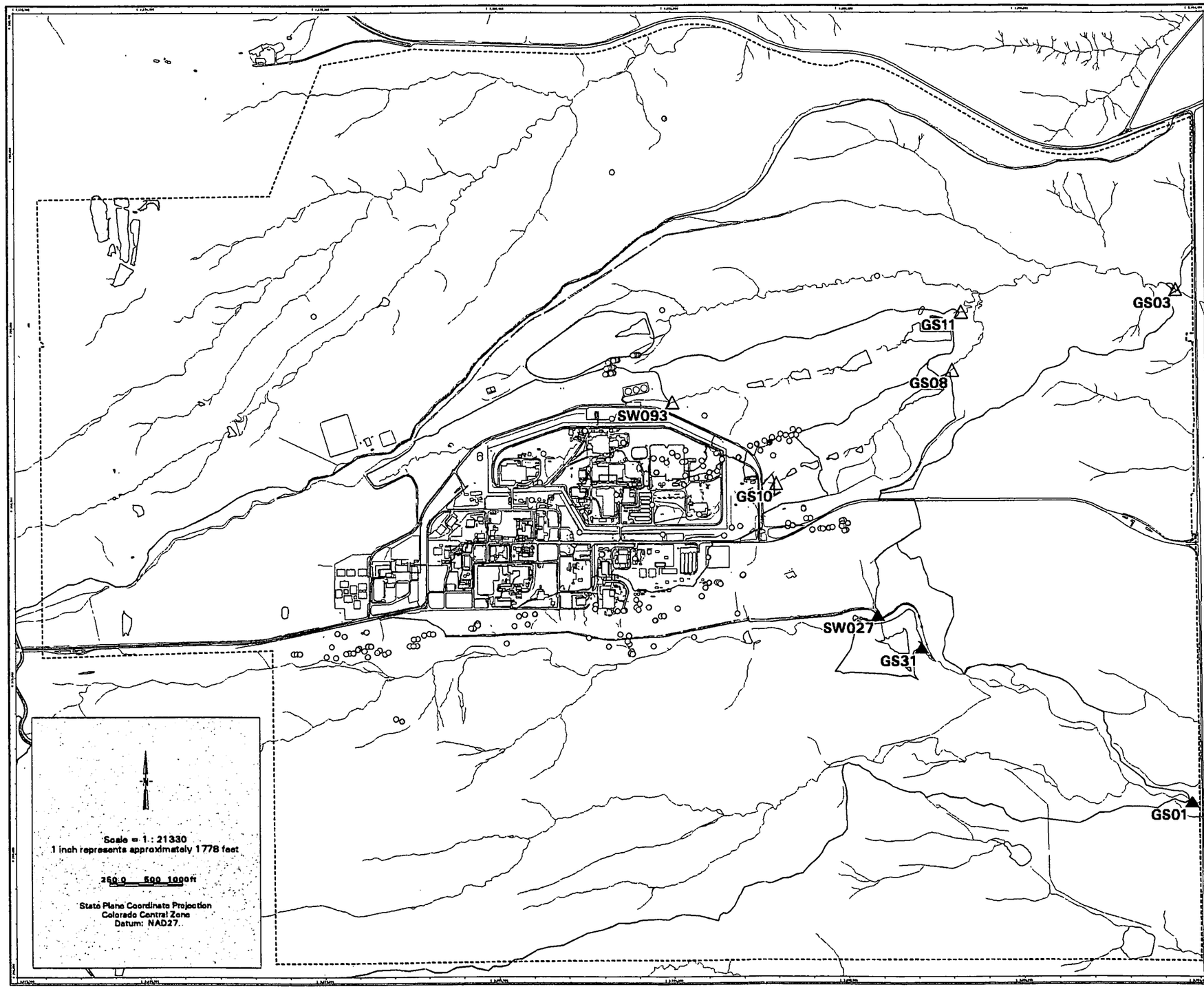

Figure TA-2-34

Actinide Migration Evaluation Pathway Report

U-233/234 Activity in Subsurface Soils

Depth : 8 - 10 ft

EXPLANATION

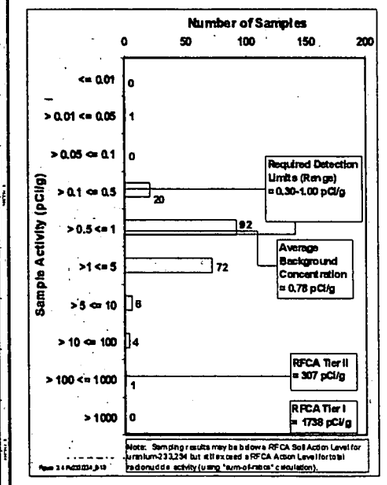

○ Value < Tier II value (Color indicates range of activity shown in the histogram above.)

▽ Tier II value < = Value < Tier I value

◇ Value > = Tier I value

N Drainage Basin Boundary

△ Walnut Creek Basin Gaging Station (GS03, GS08, GS10, GS11 & SW093)

▲ Woman Creek Basin Gaging Station (GS01, GS31 & SW027)

Standard Map Features

- Buildings and other structures
- Lakes and ponds
- Streams, ditches, or other drainage features
- Rocky Flats boundary
- Paved roads

DATA SOURCE BASE FEATURES:

Buildings, fences, hydrography, roads and other structures from 1994 aerial fly-over data captured by EG&G RSL, Las Vegas. Digitized from the orthophotographs. 1/95

Analytical Data from SWD as of October 2000.

Data Analysis performed by Wright Water engineers (303-480-1700).

U.S. Department of Energy

Rocky Flats Environmental Technology Site

OSS Dept. 303-966-7707

Prepared for: DynCorp THE ART OF TECHNOLOGY

Prepared for: KAISER-HILL COMPANY

NT_Svr w:/projects/actinide_pathway_report/fy2002/subsurface_soil_maps/u233-234_8ft-10ft.aml

184

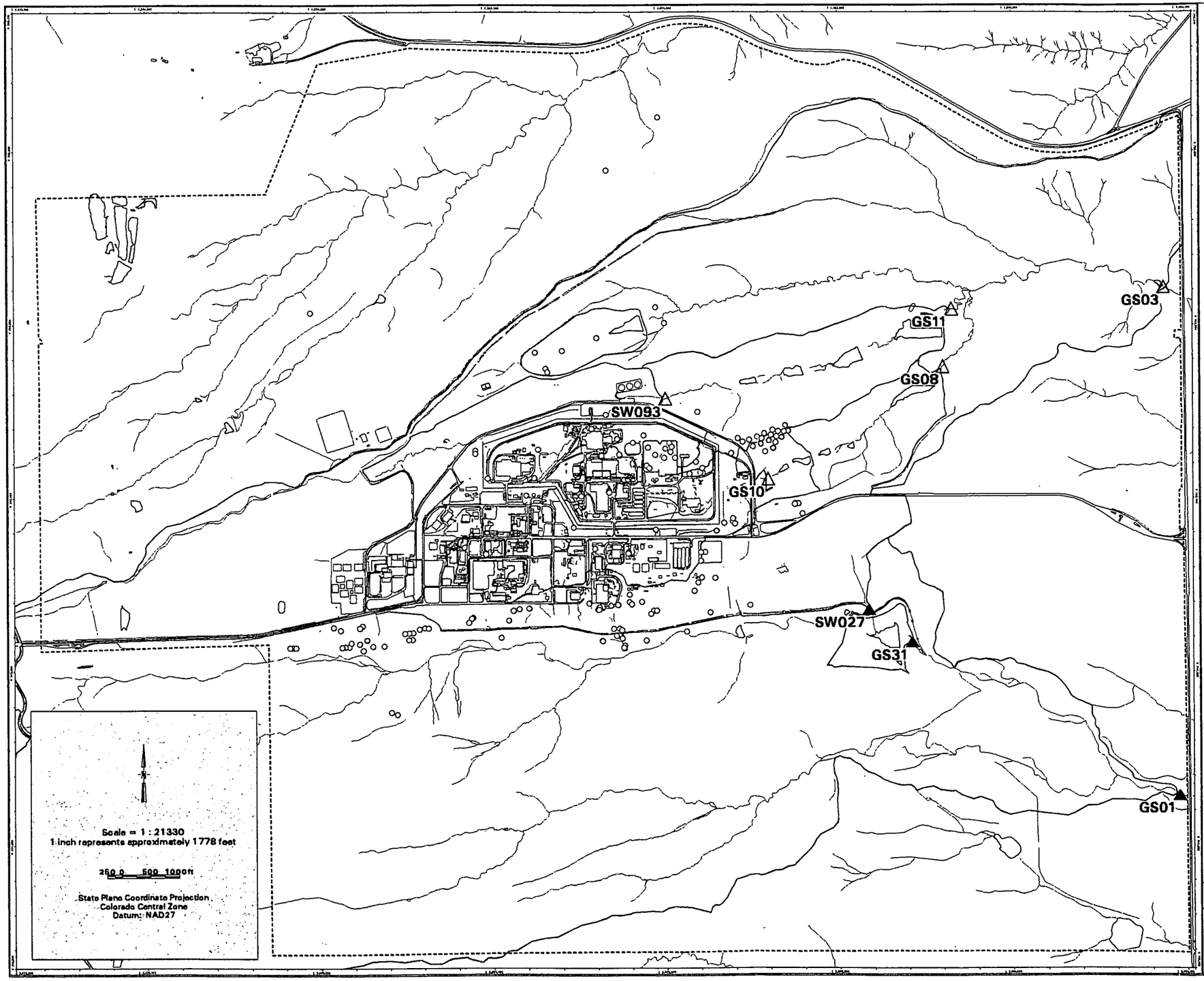

Figure TA-2-35

Actinide Migration Evaluation Pathway Report

U-233/234 Activity in Subsurface Soils

Depth : > 10 ft

EXPLANATION

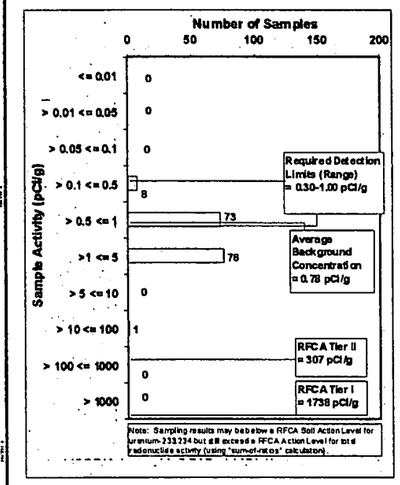

○ Value < Tier II value
(Color indicates range of activity shown in the histogram above.)

▽ Tier II value < = Value < Tier I value

◇ Value > = Tier I value

N Drainage Basin Boundary

△ Walnut Creek Basin Gaging Station (GS03, GS08, GS10, GS11 & SW093)

▲ Woman Creek Basin Gaging Station (GS01, GS31 & SW027)

Standard Map Features

- Buildings and other structures
- Lakes and ponds
- Streams, ditches, or other drainage features
- Rocky Flats boundary
- Paved roads

DATA SOURCE BASE FEATURES:
Buildings, fences, hydrography, roads and other structures from 1994 aerial fly-over data captured by EG&G RSL, Las Vegas.
Digitized from the orthophotographs. 1/95
Analytical Data from SWD as of October 2000.

Data Analysis performed by Wright Water engineers (303-480-1700).

U.S. Department of Energy
Rocky Flats Environmental Technology Site

GIS Dept. 303-966-7707

Prepared by: DynCorp — THE ART OF TECHNOLOGY

Prepared for: KH KAISER-HILL COMPANY

December 19, 2001

NT_Svr w:/projects/actinide_pathway_report/fy2002/subsurface_soil_maps/u233-234_10ft-dpr.aml

185

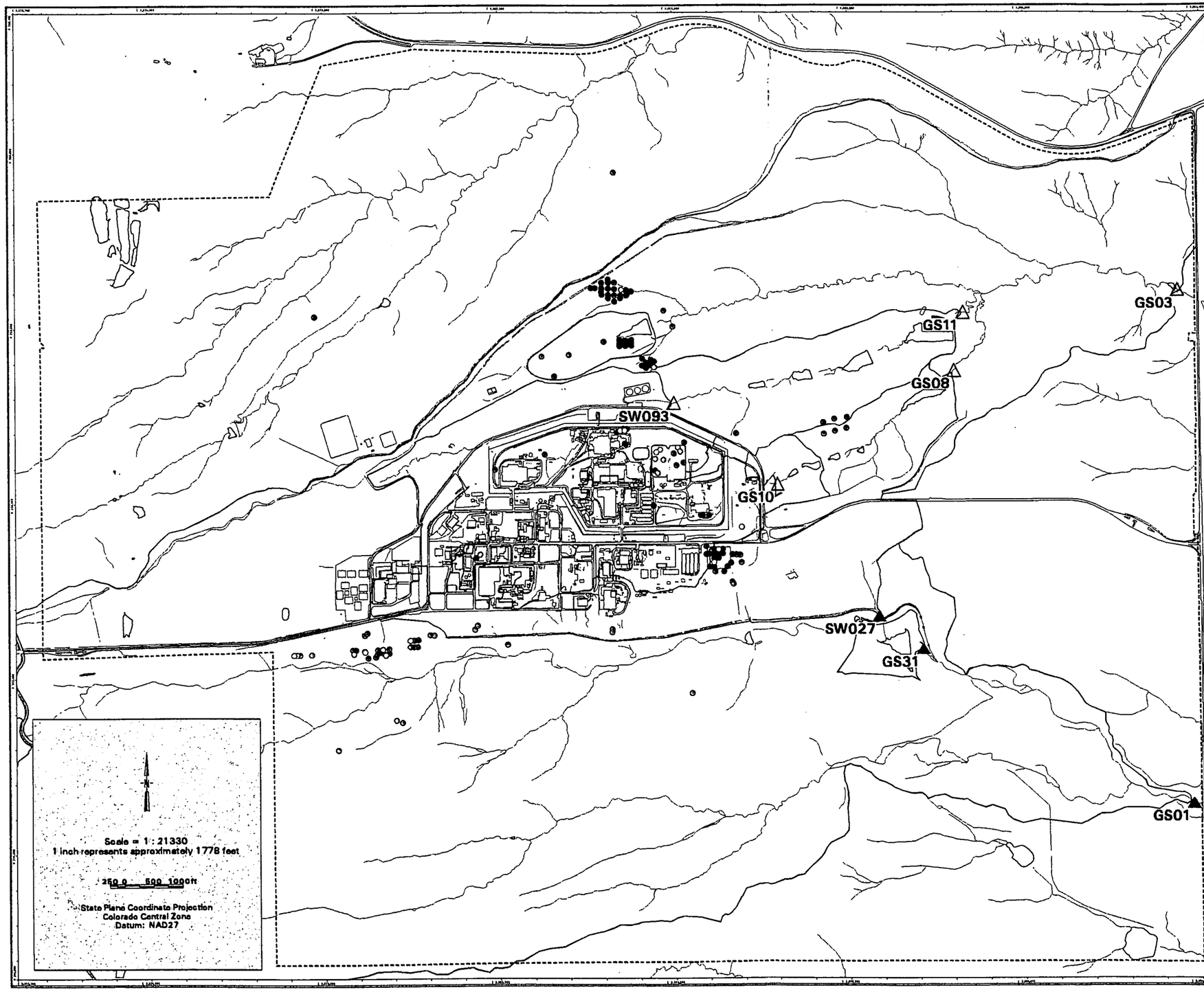

Figure TA-2-36

Actinide Migration Evaluation Pathway Report

U-235 Activity in Subsurface Soils

Depth : 0.5 - 2 ft

EXPLANATION

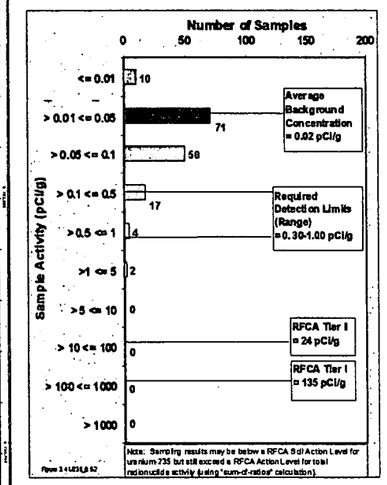

○ Value < Tier II value (Color indicates range of activity shown in the histogram above.)

▽ Tier II value < = Value < Tier I value

◇ Value > = Tier I value

N Drainage Basin Boundary

△ Walnut Creek Basin Gaging Station (GS03, GS08, GS10, GS11 & SW093)

▲ Woman Creek Basin Gaging Station (GS01, GS31 & SW027)

Standard Map Features

- Buildings and other structures
- Lakes and ponds
- Streams, ditches, or other drainage features
- Rocky Flats boundary
- Paved roads

DATA SOURCE BASE FEATURES:

Buildings, fences, hydrography, roads and other structures from 1994 aerial fly-over data captured by EG&G RSL, Las Vegas. Digitized from the orthophotographs. 1/95
Analytical Data from SWD as of October 2000.

Data Analysis performed by Wright Water engineers (303-480-1700).

U.S. Department of Energy
Rocky Flats Environmental Technology Site

GIS Dept. 303-966-7707

Prepared by: DynCorp — THE ART OF TECHNOLOGY

Prepared for: KH KAISER-HILL COMPANY

NT_Svr w:/projects/actinide_pathway_report/fy2002/subsurface_soil_maps/u235_6in-2ft.aml

186

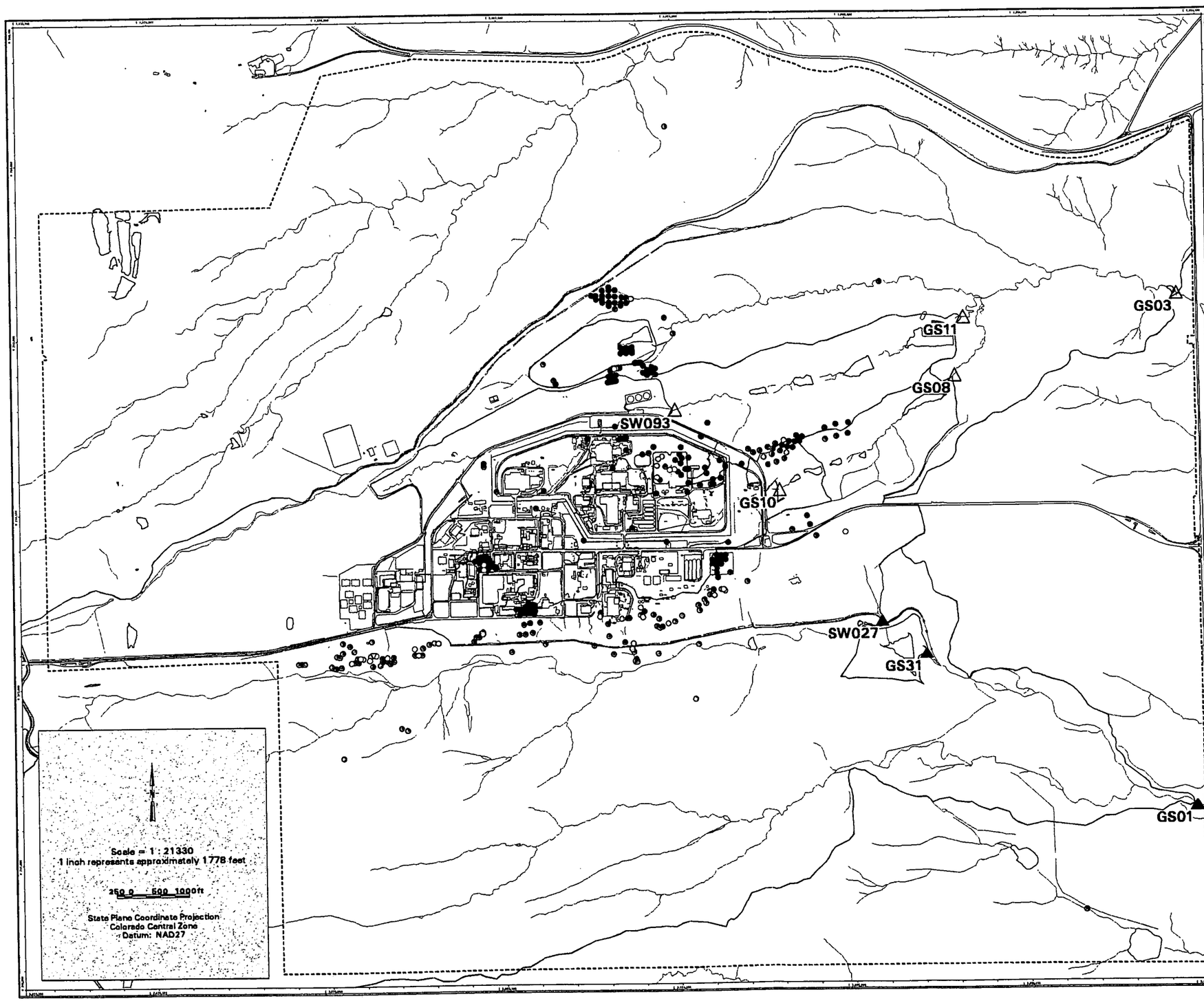

Figure TA-2-37

Actinide Migration Evaluation Pathway Report

U-235 Activity in Subsurface Soils

Depth : 2 - 4 ft

EXPLANATION

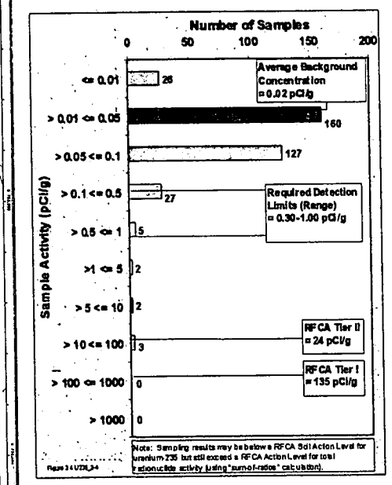

○ Value < Tier II value (Color indicates range of activity shown in the histogram above.)

▽ Tier II value < = Value < Tier I value

◇ Value > = Tier I value

N Drainage Basin Boundary

△ Walnut Creek Basin Gaging Station (GS03, GS08, GS10, GS11 & SW093)

▲ Woman Creek Basin Gaging Station (GS01, GS31 & SW027)

Standard Map Features

- Buildings and other structures
- Lakes and ponds
- Streams, ditches, or other drainage features
- Rocky Flats boundary
- Paved roads

DATA SOURCE BASE FEATURES:

Buildings, fences, hydrography, roads and other structures from 1994 aerial fly-over data captured by EG&G RSL, Las Vegas.
Digitized from the orthophotographs. 1/95
Analytical Data from SWD as of October 2000.

Data Analysis performed by Wright Water engineers (303-480-1700).

U.S. Department of Energy
Rocky Flats Environmental Technology Site

GIS Dept. 303-966-7707

Prepared by: DynCorp THE ART OF TECHNOLOGY

Prepared for: KAISER-HILL COMPANY

NT_Svr w:/projects/actinide_pathway_report/fy2002/subsurface_soil_maps/u235_2ft-4ft.aml

187

Figure TA-2-38

Actinide Migration Evaluation Pathway Report

U-235 Activity in Subsurface Soils

Depth : 4 - 6 ft

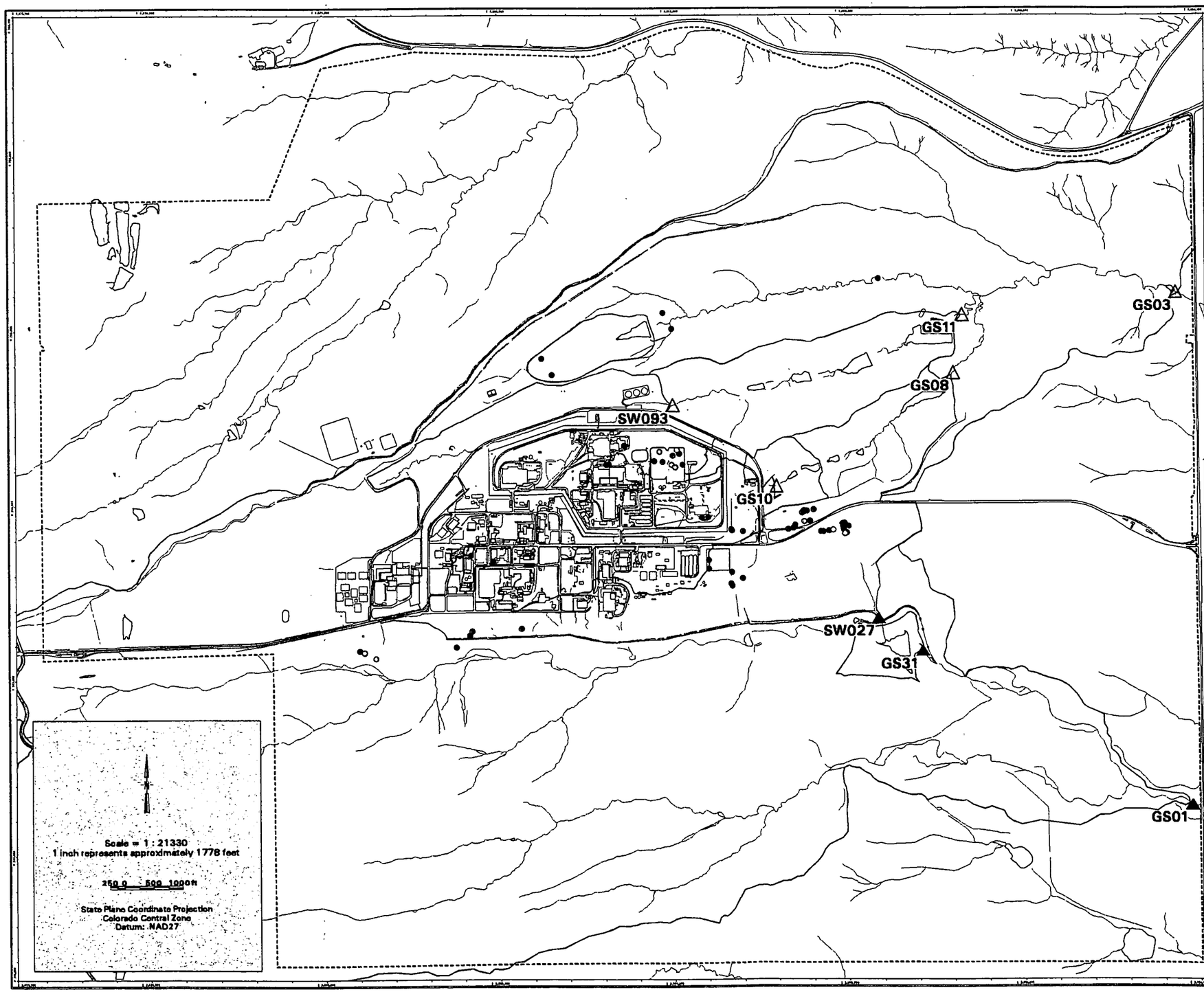

EXPLANATION

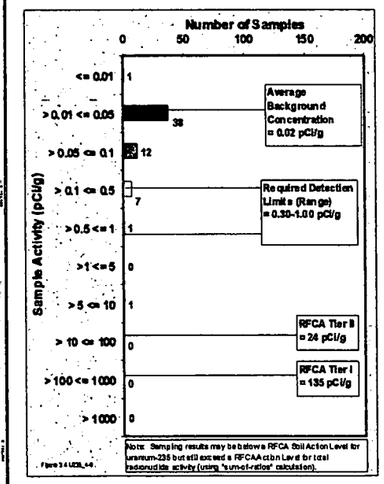

- ○ Value < Tier II value (Color indicates range of activity shown in the histogram above.)
- ▽ Tier II value < = Value < Tier I value
- ◇ Value > = Tier I value
- N Drainage Basin Boundary
- △ Walnut Creek Basin Gaging Station (GS03, GS08, GS10, GS11 & SW093)
- ▲ Woman Creek Basin Gaging Station (GS01, GS31 & SW027)

Standard Map Features

- Buildings and other structures
- Lakes and ponds
- Streams, ditches, or other drainage features
- Rocky Flats boundary
- Paved roads

DATA SOURCE BASE FEATURES:
Buildings, fences, hydrography, roads and other structures from 1994 aerial fly-over data captured by EG&G RSL, Las Vegas.
Digitized from the orthophotographs. 1/95
Analytical Data from SWD as of October 2000.

Data Analysis performed by Wright Water engineers (303-480-1700).

U.S. Department of Energy
Rocky Flats Environmental Technology Site
CBS Dept. 303-966-7707

Prepared for: DynCorp — THE ART OF TECHNOLOGY
Prepared for: KAISER-HILL COMPANY

NT_Svr w:/projects/actinide_pathway_report/fy2002/subsurface_soil_maps/u235_4ft-6ft.aml

188

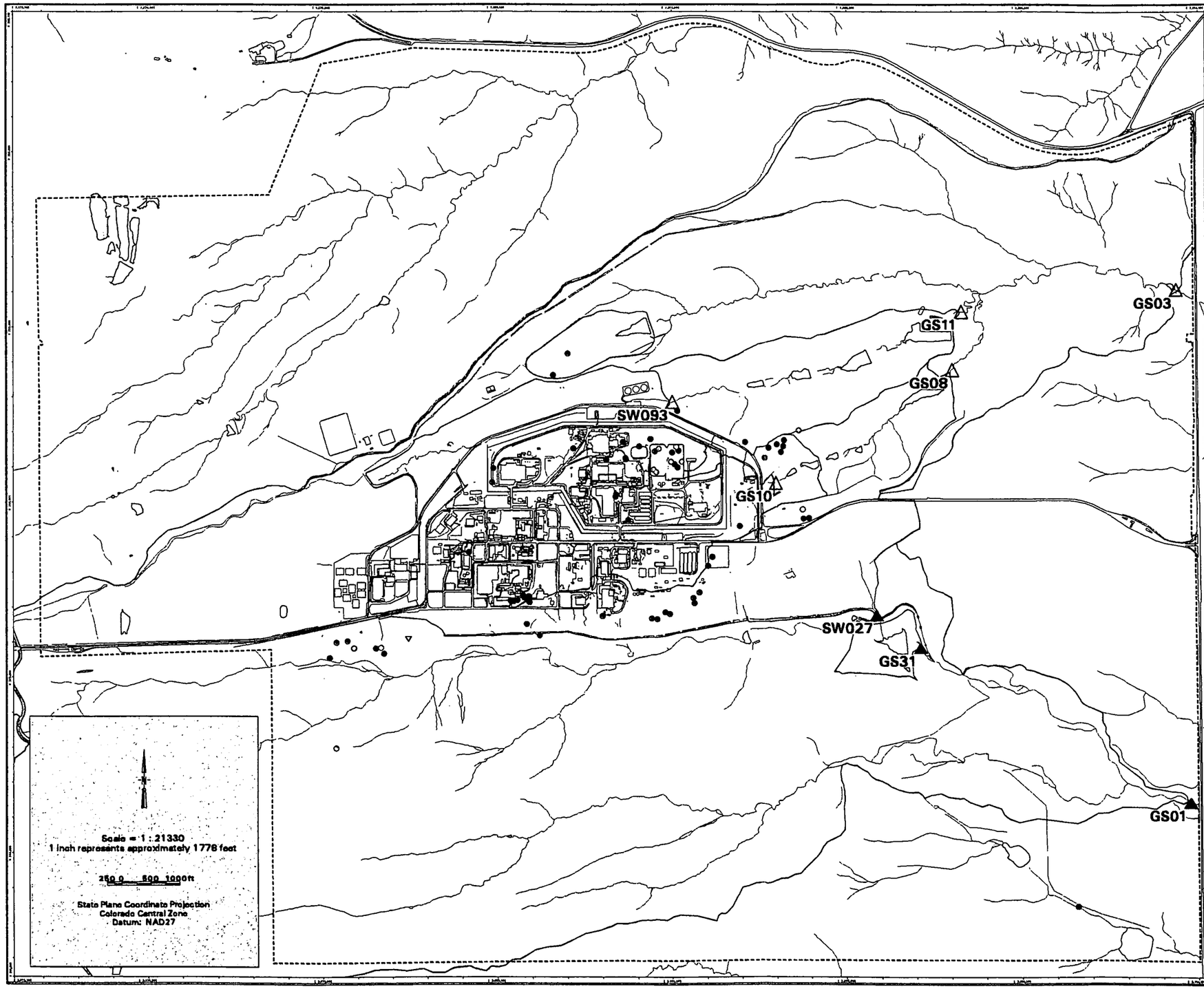

Figure TA-2-39

Actinide Migration Evaluation Pathway Report

U-235 Activity in Subsurface Soils

Depth : 6 - 8 ft

EXPLANATION

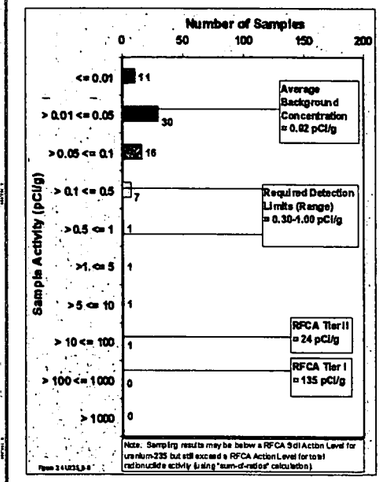

- ○ Value < Tier II value (Color indicates range of activity shown in the histogram above.)
- ▽ Tier II value < = Value < Tier I value
- ◇ Value > = Tier I value
- N Drainage Basin Boundary
- △ Walnut Creek Basin Gaging Station (GS03, GS08, GS10, GS11 & SW093)
- ▲ Woman Creek Basin Gaging Station (GS01, GS31 & SW027)

Standard Map Features

- Buildings and other structures
- Lakes and ponds
- Streams, ditches, or other drainage features
- Rocky Flats boundary
- Paved roads

DATA SOURCE BASE FEATURES:

Buildings, fences, hydrography, roads and other structures from 1994 aerial fly-over data captured by EG&G RSL, Las Vegas. Digitized from the orthophotographs. 1/95
Analytical Data from SWD as of October 2000.

Data Analysis performed by Wright Water engineers (303-480-1700).

U.S. Department of Energy
Rocky Flats Environmental Technology Site

GIS Dept. 303-966-7707

Prepared for:

DynCorp
THE ART OF TECHNOLOGY

Prepared for:

KAISER-HILL
A DYNCORP COMPANY

NT_Svr w:/projects/actinide_pathway_report/fy2002/subsurface_soil_maps/u235_6ft-8ft.aml

189

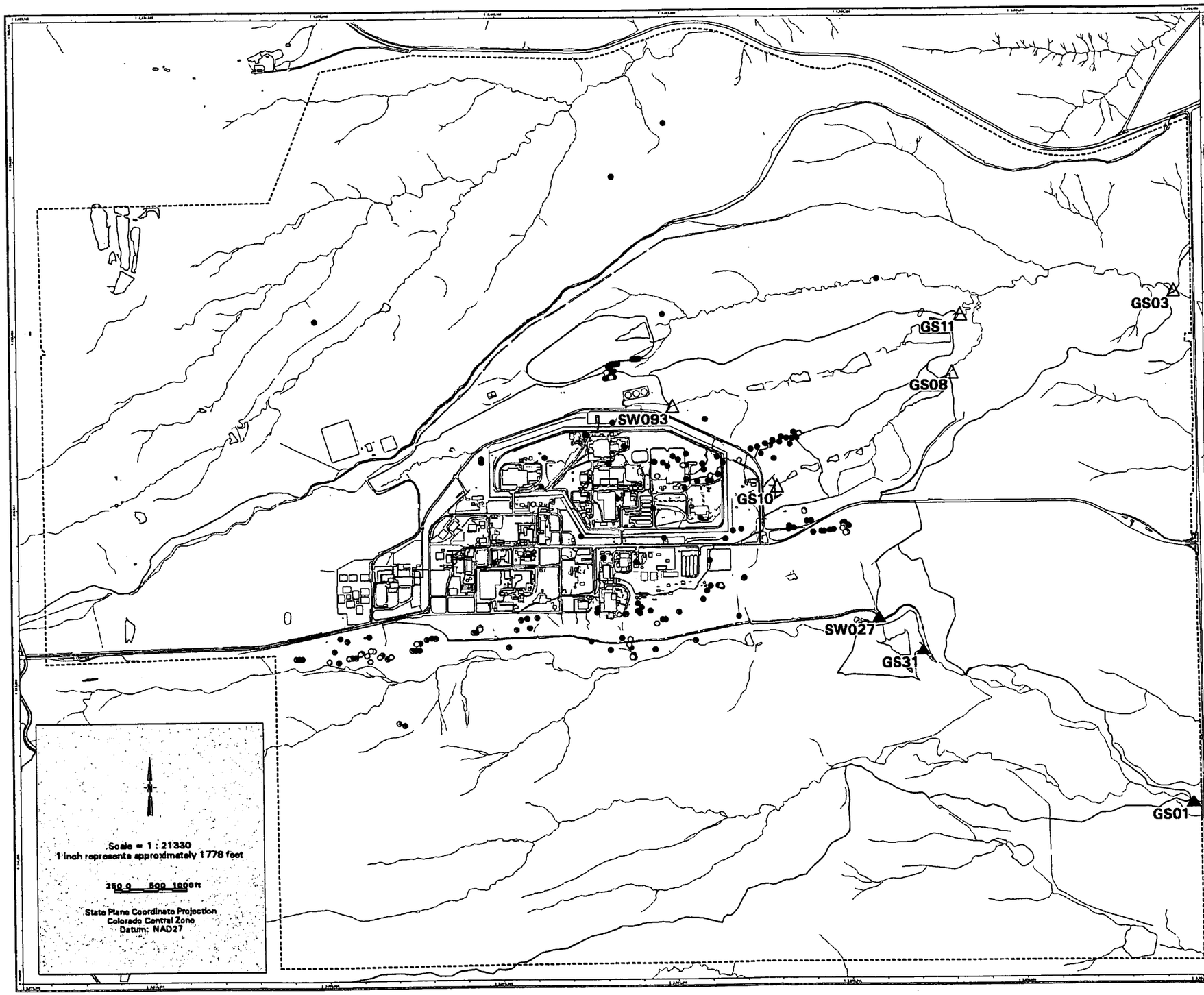

Figure TA-2-40

Actinide Migration Evaluation Pathway Report

U-235 Activity in Subsurface Soils

Depth : 8 - 10 ft

EXPLANATION

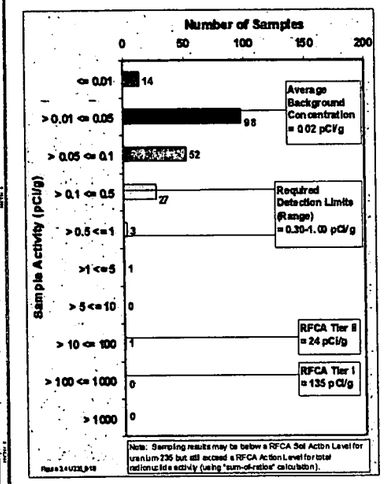

- ○ Value < Tier II value (Color indicates range of activity shown in the histogram above.)
- ▽ Tier II value < = Value < Tier I value
- ◇ Value > = Tier I value
- N Drainage Basin Boundary
- △ Walnut Creek Basin Gaging Station (GS03, GS08, GS10, GS11 & SW093)
- ▲ Woman Creek Basin Gaging Station (GS01, GS31 & SW027)

Standard Map Features

- Buildings and other structures
- Lakes and ponds
- Streams, ditches, or other drainage features
- Rocky Flats boundary
- Paved roads

DATA SOURCE BASE FEATURES:

Buildings, fences, hydrography, roads and other structures from 1994 aerial fly-over data captured by EG&G RSL, Las Vegas.
Digitized from the orthophotographs. 1/95
Analytical Data from SWD as of October 2000.

Data Analysis performed by Wright Water engineers (303-480-1700).

U.S. Department of Energy
Rocky Flats Environmental Technology Site
CBS Dept. 303-966-7707

Prepared by: DynCorp — THE ART OF TECHNOLOGY

Prepared for: KH KAISER-HILL COMPANY

NT_Svr w:/projects/actinide_pathway_report/fy2002/subsurface_soil_maps/u235_8ft-10ft.aml

190

Figure TA-2-41

Actinide Migration Evaluation Pathway Report

U-235 Activity in Subsurface Soils

Depth : > 10 ft

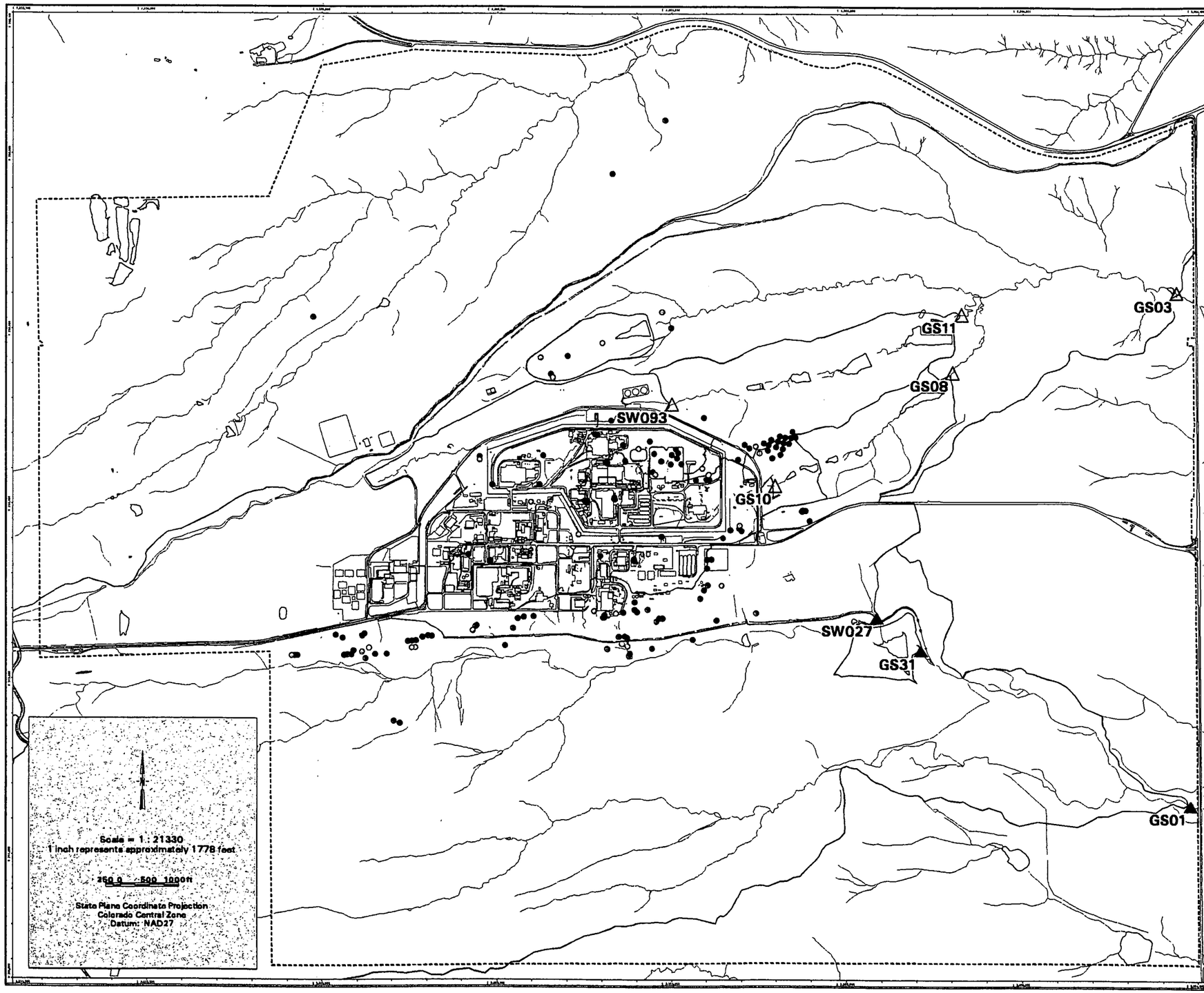

EXPLANATION

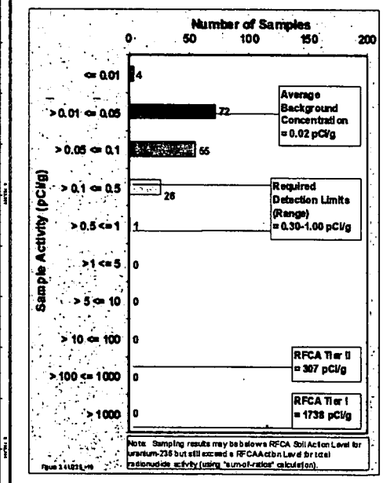

○ Value < Tier II value (Color indicates range of activity shown in the histogram above.)

▽ Tier II value < = Value < Tier I value

◇ Value > = Tier I value

N Drainage Basin Boundary

△ Walnut Creek Basin Gaging Station (GS03, GS08, GS10, GS11 & SW093)

▲ Woman Creek Basin Gaging Station (GS01, GS31 & SW027)

Standard Map Features

- Buildings and other structures
- Lakes and ponds
- Streams, ditches, or other drainage features
- Rocky Flats boundary
- Paved roads

DATA SOURCE BASE FEATURES:

Buildings, fences, hydrography, roads and other structures from 1994 aerial fly-over data captured by EG&G RSL, Las Vegas. Digitized from the orthophotographs. 1/95
Analytical Data from SWD as of October 2000.

Data Analysis performed by Wright Water engineers (303-480-1700).

U.S. Department of Energy
Rocky Flats Environmental Technology Site

GIS Dept. 303-966-7707

Prepared by: DynCorp — THE ART OF TECHNOLOGY

Prepared for: KAISER-HILL COMPANY

MAP file: actinides_soil_maps&1995_10ft-dpr.aml

December 18, 2001

NT_Svr w:/projects/actinide_pathway_report/fy2002/subsurface_soil_maps/u235_10ft-dpr.aml

191

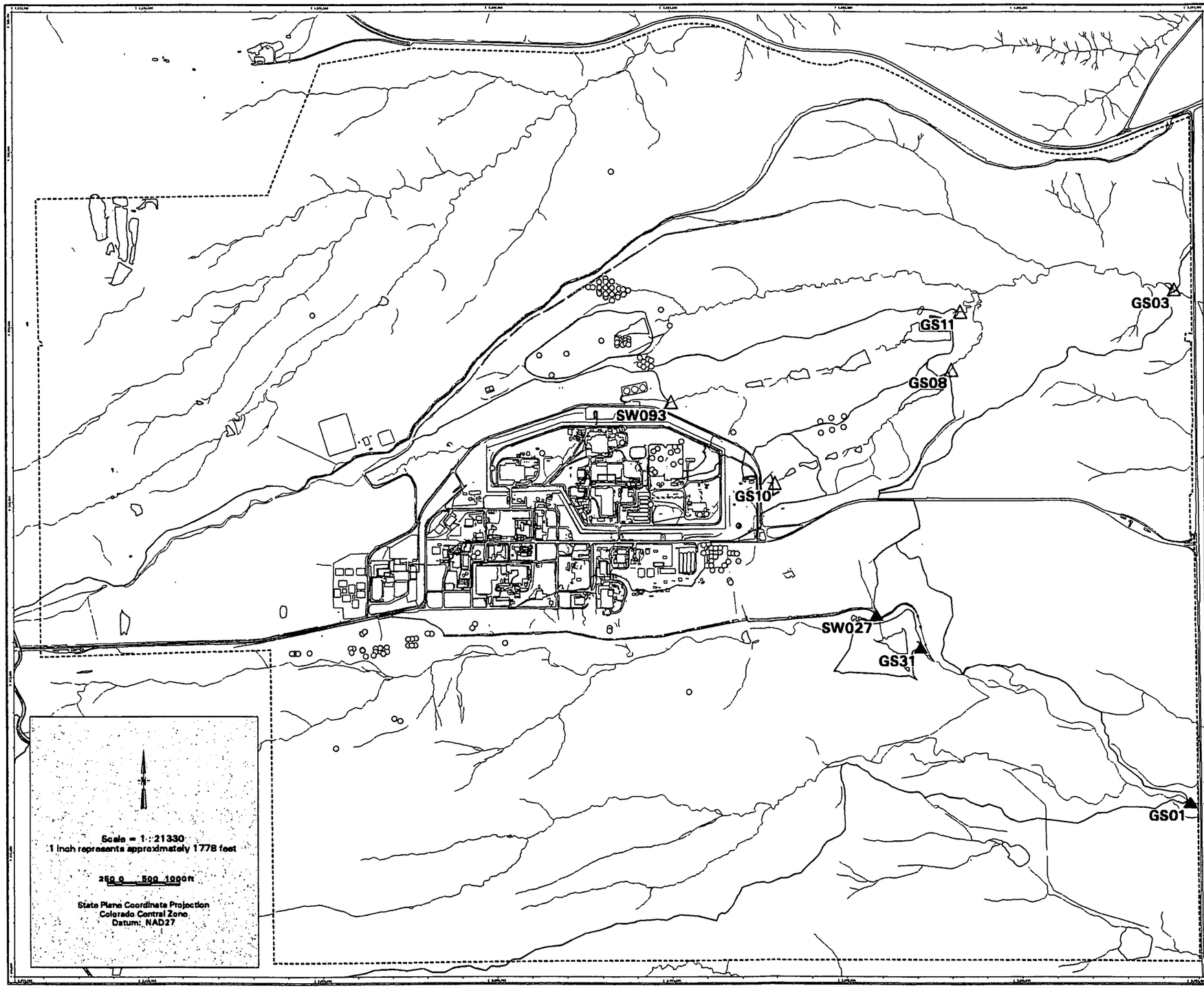

Figure TA-2-42

Actinide Migration Evaluation Pathway Report

U-238 Activity in Subsurface Soils

Depth : 0.5 - 2 ft

EXPLANATION

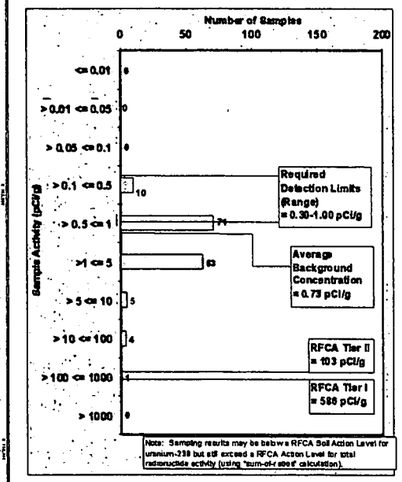

- ○ Value < Tier II value (Color indicates range of activity shown in the histogram above.)
- ▽ Tier II value < = Value < Tier I value
- ◇ Value > = Tier I value
- N Drainage Basin Boundary
- △ Walnut Creek Basin Gaging Station (GS03, GS08, GS10, GS11 & SW093)
- ▲ Woman Creek Basin Gaging Station (GS01, GS31 & SW027)

Standard Map Features

- Buildings and other structures
- Lakes and ponds
- Streams, ditches, or other drainage features
- Rocky Flats boundary
- Paved roads

DATA SOURCE BASE FEATURES:

Buildings, fences, hydrography, roads and other structures from 1994 aerial fly-over data captured by EG&G RSL, Las Vegas. Digitized from the orthophotographs. 1/95
Analytical Data from SWD as of October 2000.

Data Analysis performed by Wright Water engineers (303-480-1700).

U.S. Department of Energy
Rocky Flats Environmental Technology Site

GIS Dept. 303-966-7707

Prepared for: DynCorp — THE ART OF TECHNOLOGY

Prepared for: KH — KAISER-HILL COMPANY

NT_Svr w:/projects/actinide_pathway_report/fy2002/subsurface_soil_maps/u238_6in-2ft.aml

192

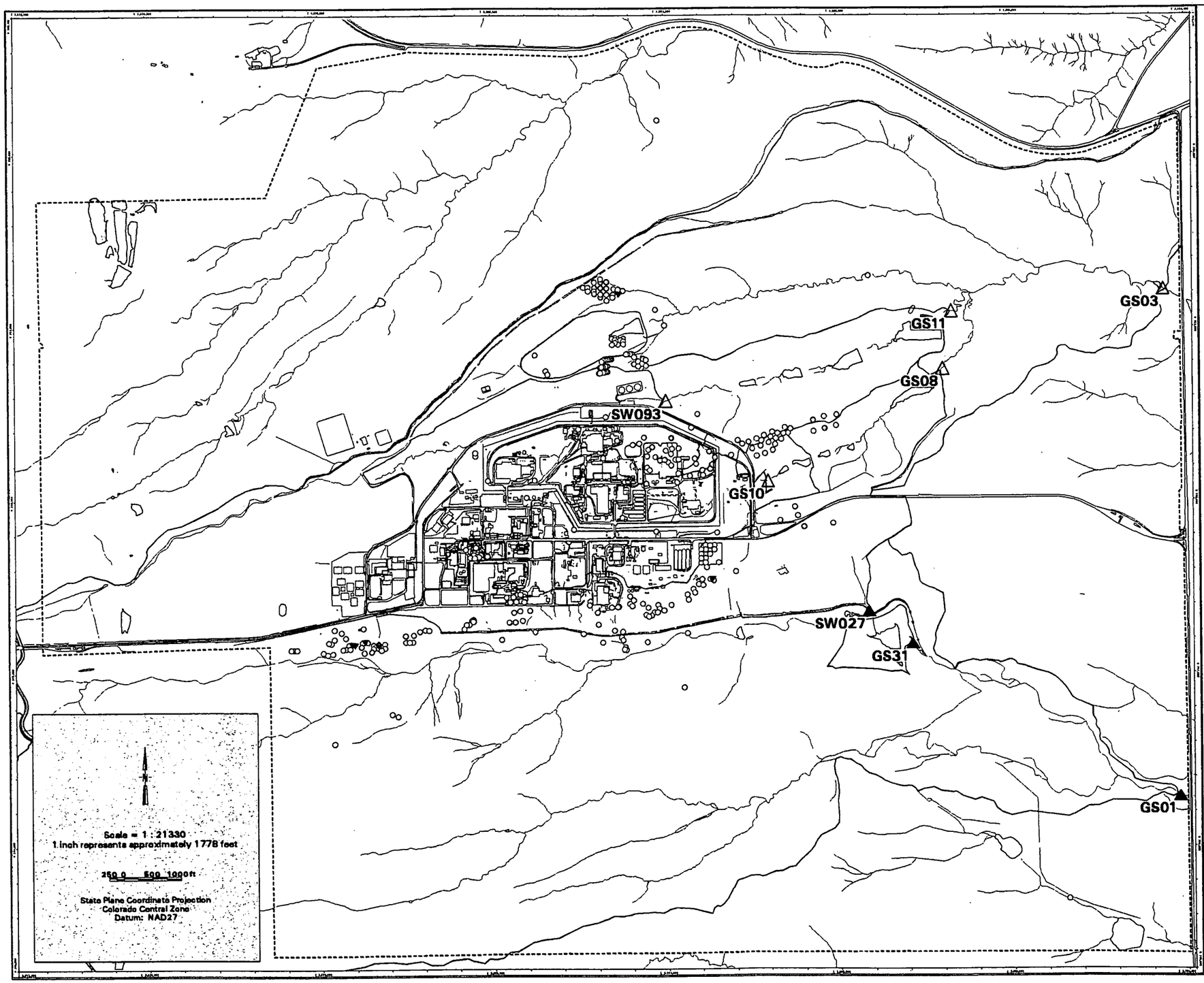

Figure TA-2-43

Actinide Migration Evaluation Pathway Report

U-238 Activity in Subsurface Soils

Depth : 2 - 4 ft

EXPLANATION

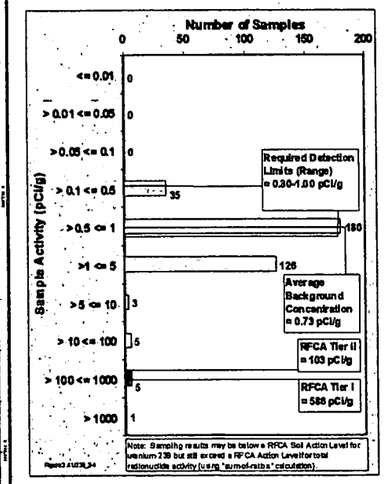

○ Value < Tier II value
(Color indicates range of activity shown in the histogram above.)

▽ Tier II value < = Value < Tier I value

◇ Value > = Tier I value

N Drainage Basin Boundary

△ Walnut Creek Basin Gaging Station (GS03, GS08, GS10, GS11 & SW093)

▲ Woman Creek Basin Gaging Station (GS01, GS31 & SW027)

Standard Map Features

- Buildings and other structures
- Lakes and ponds
- Streams, ditches, or other drainage features
- Rocky Flats boundary
- Paved roads

DATA SOURCE BASE FEATURES:
Buildings, fences, hydrography, roads and other structures from 1994 aerial fly-over data captured by EG&G RSL, Las Vegas.
Digitized from the orthophotographs. 1/95
Analytical Data from SWD as of October 2000.

Data Analysis performed by Wright Water engineers (303-480-1700).

U.S. Department of Energy
Rocky Flats Environmental Technology Site

GIS Dept. 303-966-7707

Prepared by: DynCorp — THE ART OF TECHNOLOGY

Prepared for: KH — KAISER-HILL COMPANY

NT_Svr w:/projects/actinide_pathway_report/fy2002/subsurface_soil_maps/u238_2ft-4ft.aml

193

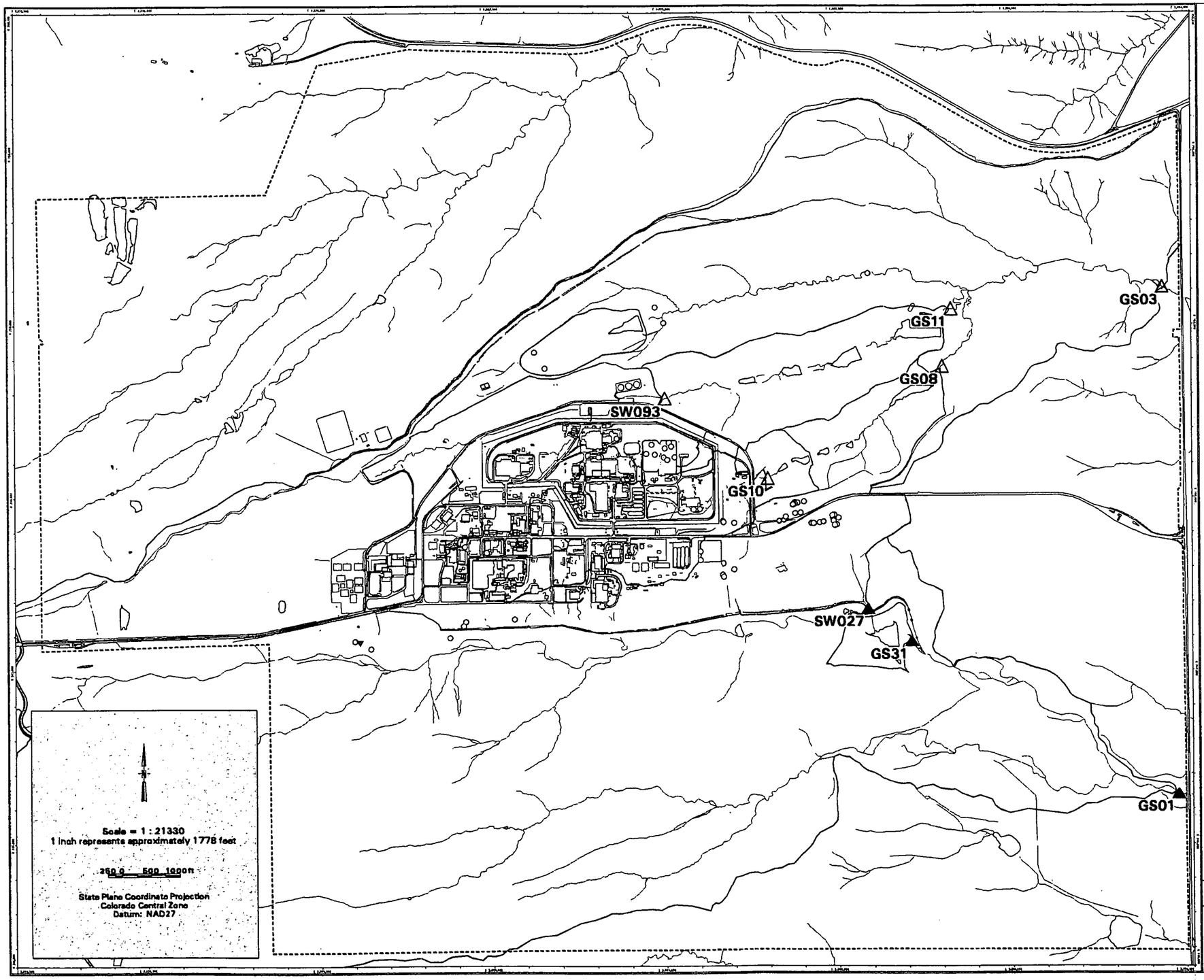

Figure TA-2-44

Actinide Migration Evaluation Pathway Report

U-238 Activity in Subsurface Soils

Depth : 4 - 6 ft

EXPLANATION

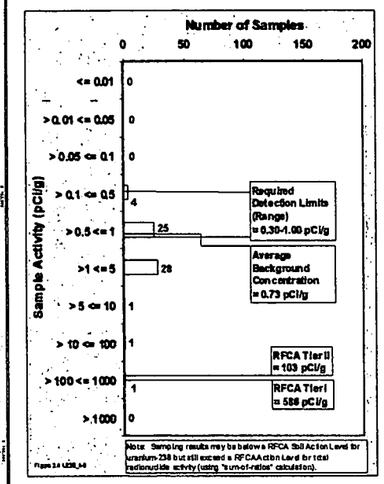

- ○ Value < Tier II value (Color indicates range of activity shown in the histogram above.)
- ▽ Tier II value < = Value < Tier I value
- ◇ Value > = Tier I value
- N Drainage Basin Boundary
- △ Walnut Creek Basin Gaging Station (GS03, GS08, GS10, GS11 & SW093)
- ▲ Woman Creek Basin Gaging Station (GS01, GS31 & SW027)

Standard Map Features

- Buildings and other structures
- Lakes and ponds
- Streams, ditches, or other drainage features
- Rocky Flats boundary
- Paved roads

DATA SOURCE BASE FEATURES:

Buildings, fences, hydrography, roads and other structures from 1994 aerial fly-over data captured by EG&G RSL, Las Vegas. Digitized from the orthophotographs. 1/95
Analytical Data from SWD as of October 2000.

Data Analysis performed by Wright Water engineers (303-480-1700).

U.S. Department of Energy
Rocky Flats Environmental Technology Site

GIS Dept. 303-966-7707

Prepared for: DynCorp — THE ART OF TECHNOLOGY

Prepared for: KAISER-HILL COMPANY

NT_Svr w:/projects/actinide_pathway_report/fy2002/subsurface_soil_maps/u238_4ft-6ft.aml

194

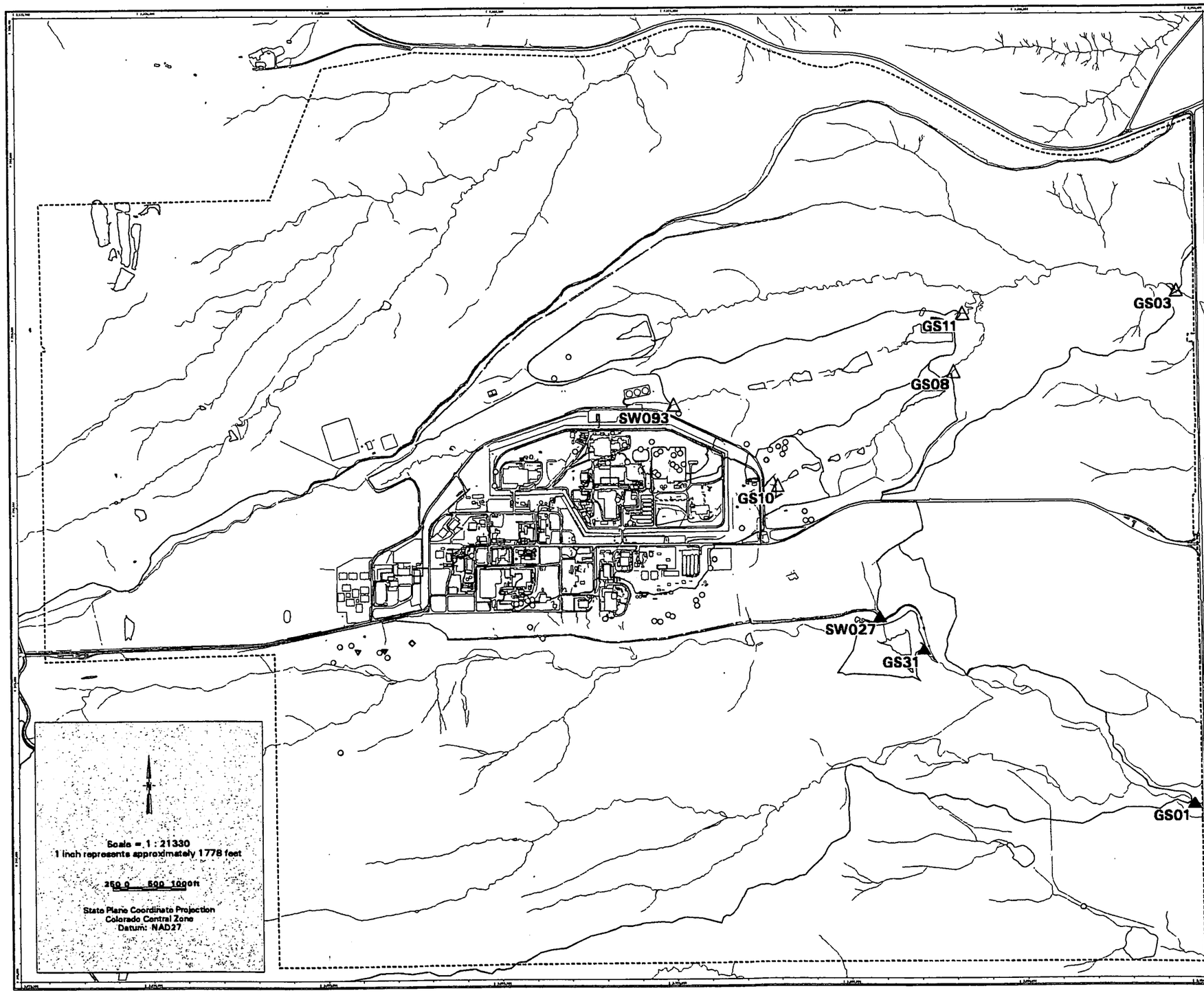

Figure TA-2-45

Actinide Migration Evaluation Pathway Report

U-238 Activity in Subsurface Soils

Depth : 6 - 8 ft

EXPLANATION

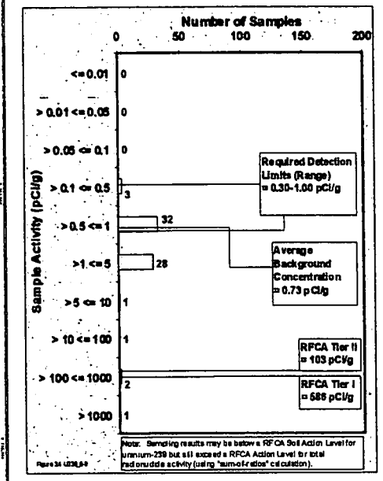

○ Value < Tier II value (Color indicates range of activity shown in the histogram above.)

▽ Tier II value < = Value < Tier I value

◇ Value > = Tier I value

N Drainage Basin Boundary

△ Walnut Creek Basin Gaging Station (GS03, GS08, GS10, GS11 & SW093)

▲ Woman Creek Basin Gaging Station (GS01, GS31 & SW027)

Standard Map Features

- Buildings and other structures
- Lakes and ponds
- Streams, ditches, or other drainage features
- Rocky Flats boundary
- Paved roads

DATA SOURCE BASE FEATURES:
Buildings, fences, hydrography, roads and other structures from 1994 aerial fly-over data captured by EG&G RSL, Las Vegas. Digitized from the orthophotographs. 1/95
Analytical Data from SWD as of October 2000.

Data Analysis performed by Wright Water engineers (303-480-1700).

U.S. Department of Energy
Rocky Flats Environmental Technology Site

GIS Dept. 303-966-7707

Prepared by: DynCorp THE ART OF TECHNOLOGY

Prepared for: KAISER-HILL COMPANY

NT_Svr w:/projects/actinide_pathway_report/fy2002/subsurface_soil_maps/u238_6ft-8ft.aml

195

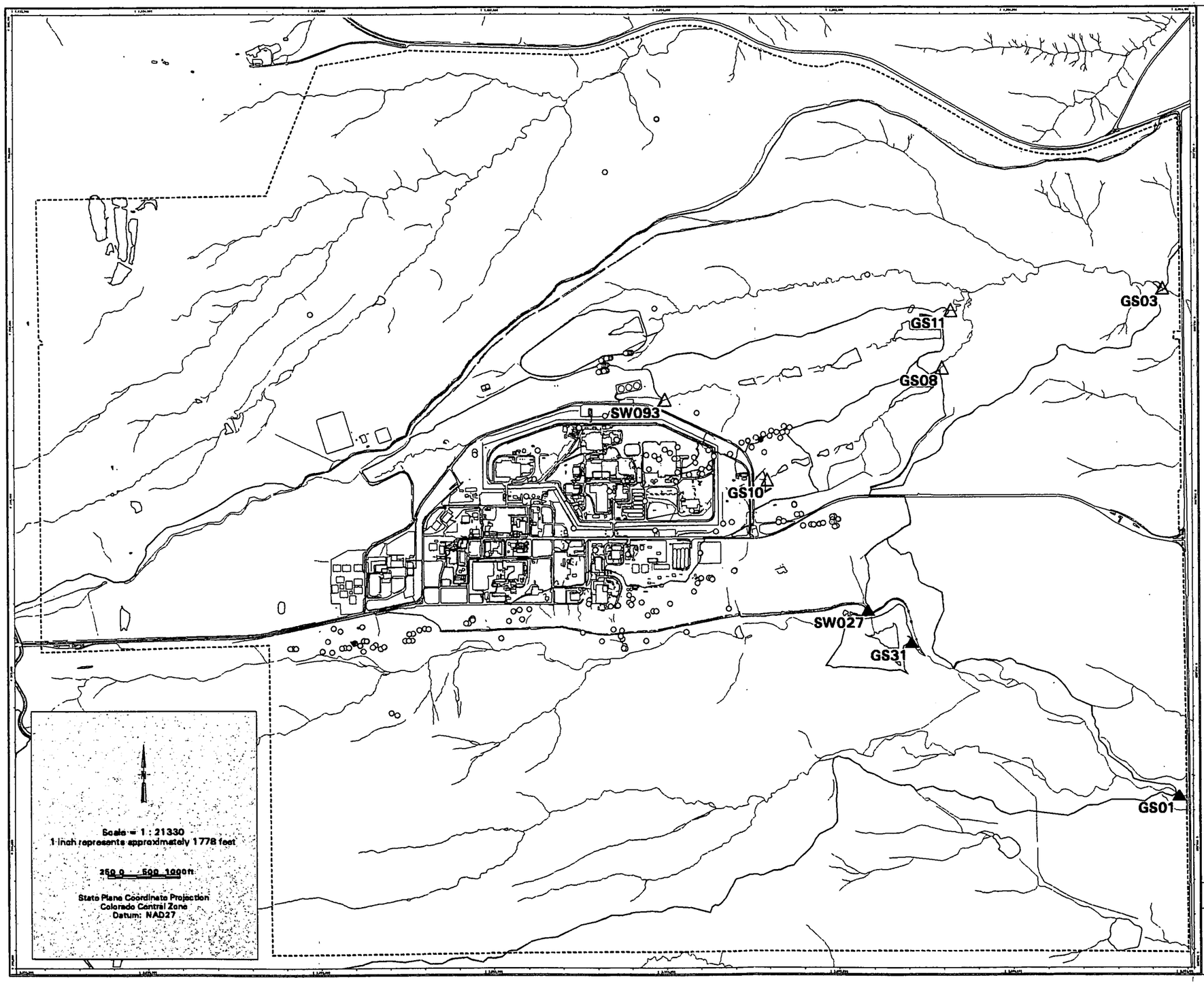

Figure TA-2-46

Actinide Migration Evaluation Pathway Report

U-238 Activity in Subsurface Soils

Depth : 8 - 10 ft

EXPLANATION

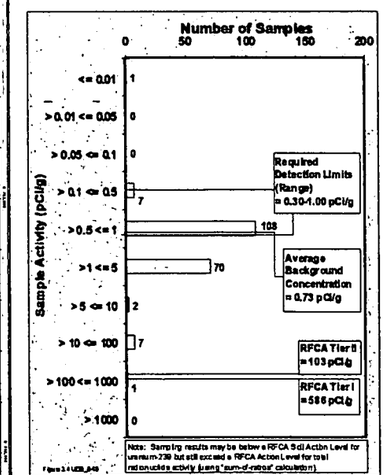

- ○ Value < Tier II value (Color indicates range of activity shown in the histogram above.)
- ▽ Tier II value < = Value < Tier I value
- ◇ Value > = Tier I value
- N Drainage Basin Boundary
- △ Walnut Creek Basin Gaging Station (GS03, GS08, GS10, GS11 & SW093)
- ▲ Woman Creek Basin Gaging Station (GS01, GS31 & SW027)

Standard Map Features

- Buildings and other structures
- Lakes and ponds
- Streams, ditches, or other drainage features
- Rocky Flats boundary
- Paved roads

DATA SOURCE BASE FEATURES:

Buildings, fences, hydrography, roads and other structures from 1994 aerial fly-over data captured by EG&G RSL, Las Vegas. Digitized from the orthophotographs. 1/95
Analytical Data from SWD as of October 2000.

Data Analysis performed by Wright Water engineers (303-480-1700).

U.S. Department of Energy
Rocky Flats Environmental Technology Site

GIS Dept. 303-966-7707

Prepared by: DynCorp — THE ART OF TECHNOLOGY

Prepared for: KH KAISER-HILL COMPANY

NT_Svr w:/projects/actinide_pathway_report/fy2002/subsurface_soil_maps/u238_8ft-10ft.aml

196

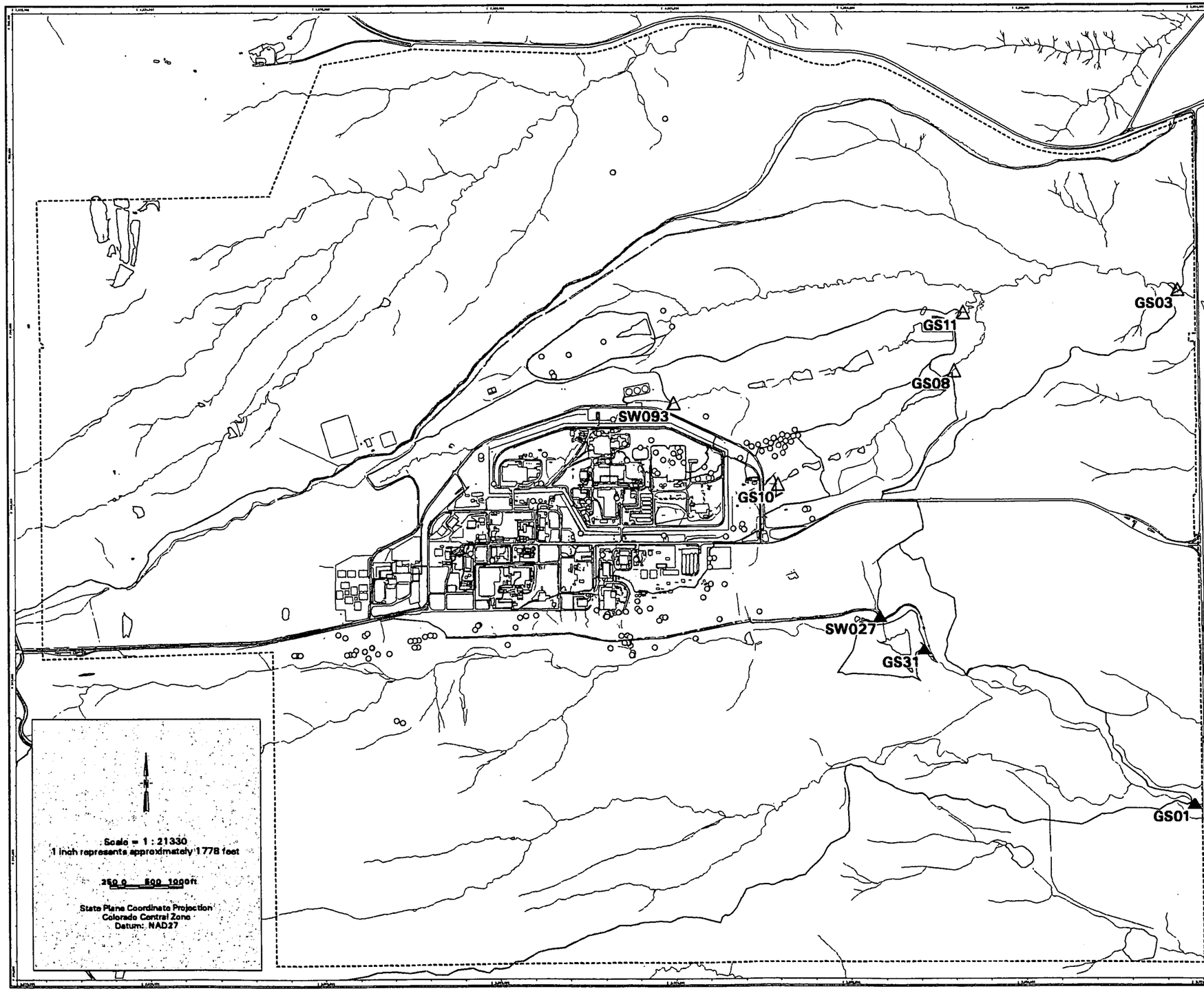

Figure TA-2-47

Actinide Migration Evaluation Pathway Report

U-238 Activity in Subsurface Soils

Depth : > 10 ft

EXPLANATION

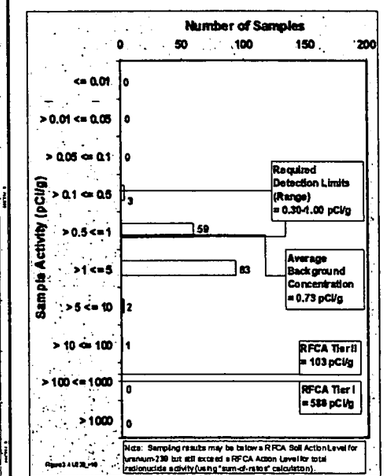

○ Value < Tier II value (Color indicates range of activity shown in the histogram above.)

▽ Tier II value < = Value < Tier I value

◇ Value > = Tier I value

N Drainage Basin Boundary

△ Walnut Creek Basin Gaging Station (GS03, GS08, GS10, GS11 & SW093)

▲ Woman Creek Basin Gaging Station (GS01, GS31 & SW027)

Standard Map Features

- Buildings and other structures
- Lakes and ponds
- Streams, ditches, or other drainage features
- Rocky Flats boundary
- Paved roads

DATA SOURCE BASE FEATURES:

Buildings, fences, hydrography, roads and other structures from 1994 aerial fly-over data captured by EG&G RSL, Las Vegas. Digitized from the orthophotographs. 1/95
Analytical Data from SWD as of October 2000.

Data Analysis performed by Wright Water engineers (303-480-1700).

U.S. Department of Energy
Rocky Flats Environmental Technology Site

GIS Dept. 303-966-7707

Prepared by: DynCorp THE ART OF TECHNOLOGY

Prepared for: KAISER-HILL COMPANY

NT_Svr w:/projects/actinide_pathway_report/fy2002/subsurface_soil_maps/u238_10ft-dpr.aml

197

Figure TA-2-48

Actinide Migration Evaluation Pathway Report

Pu-239/240 Activity in Sediments

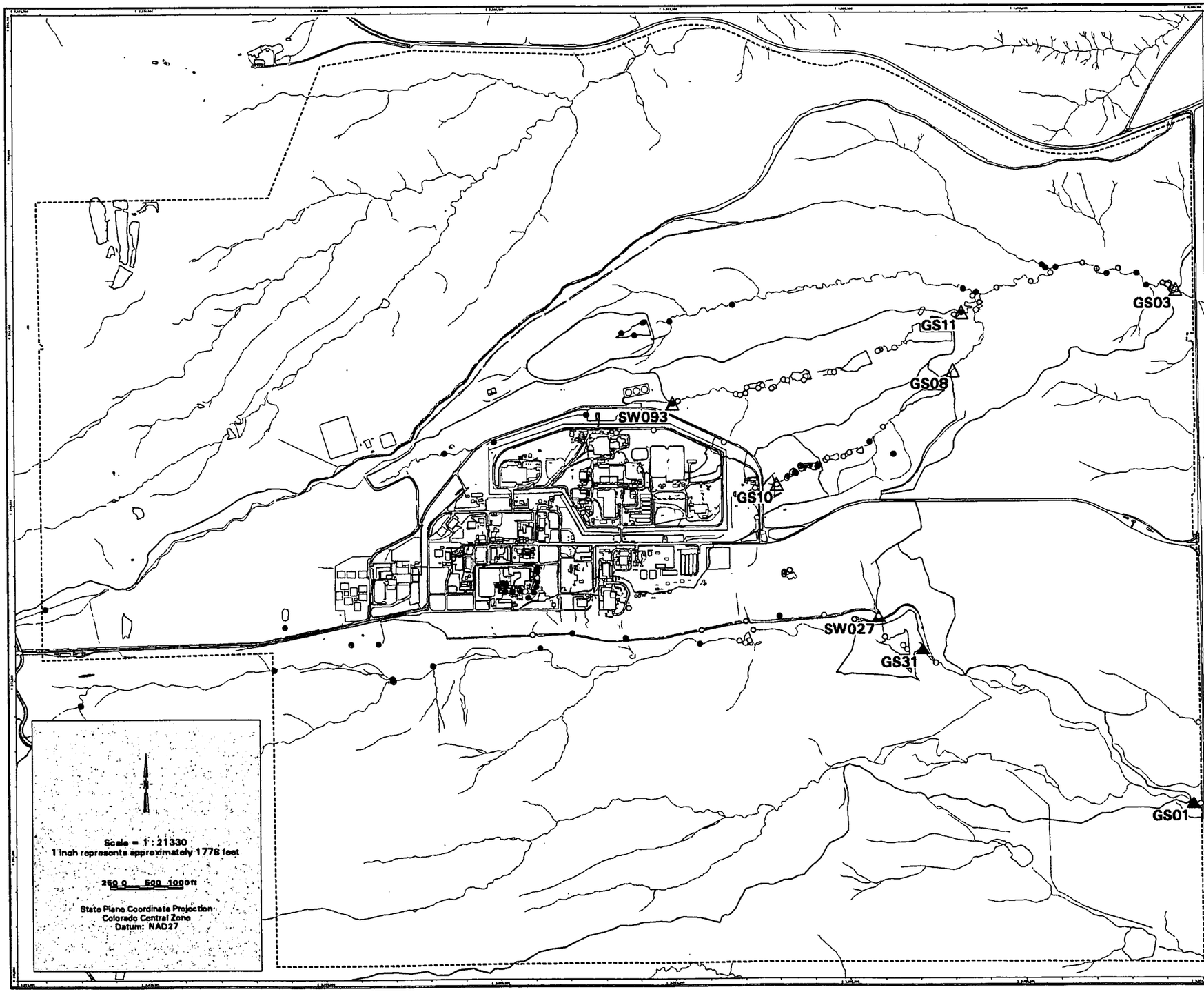

EXPLANATION

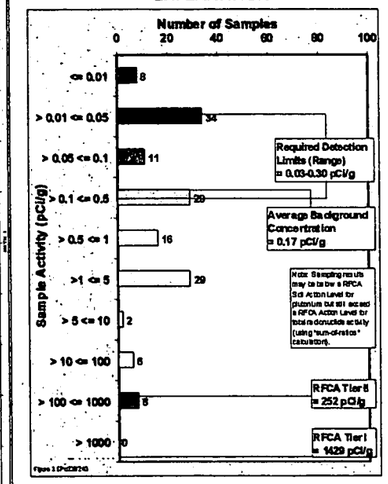

- ○ Value < Tier II value (Color indicates range of activity shown in the histogram above.)
- ▽ Tier II value < = Value < Tier I value
- ◇ Value > = Tier I value
- N Drainage Basin Boundary
- △ Walnut Creek Basin Gaging Station (GS03, GS08, GS10, GS11 & SW093)
- ▲ Woman Creek Basin Gaging Station (GS01, GS31 & SW027)

Standard Map Features

- Buildings and other structures
- Lakes and ponds
- Streams, ditches, or other drainage features
- Rocky Flats boundary
- Paved roads

DATA SOURCE BASE FEATURES:
Buildings, fences, hydrography, roads and other structures from 1994 aerial fly-over data captured by EG&G RSL, Las Vegas.
Digitized from the orthophotographs. 1/95
Analytical Data from SWD as of October 2000.

Data Analysis performed by Wright Water Engineers (303-480-1700).

U.S. Department of Energy
Rocky Flats Environmental Technology Site

GIS Dept. 303-966-7707

Prepared for: DynCorp — THE ART OF TECHNOLOGY

Prepared for: KH KAISER-HILL COMPANY

NT_Svr w:/projects/actinide_pathway_report/fy2002/sediment_maps/pu239-240_sed.aml

198

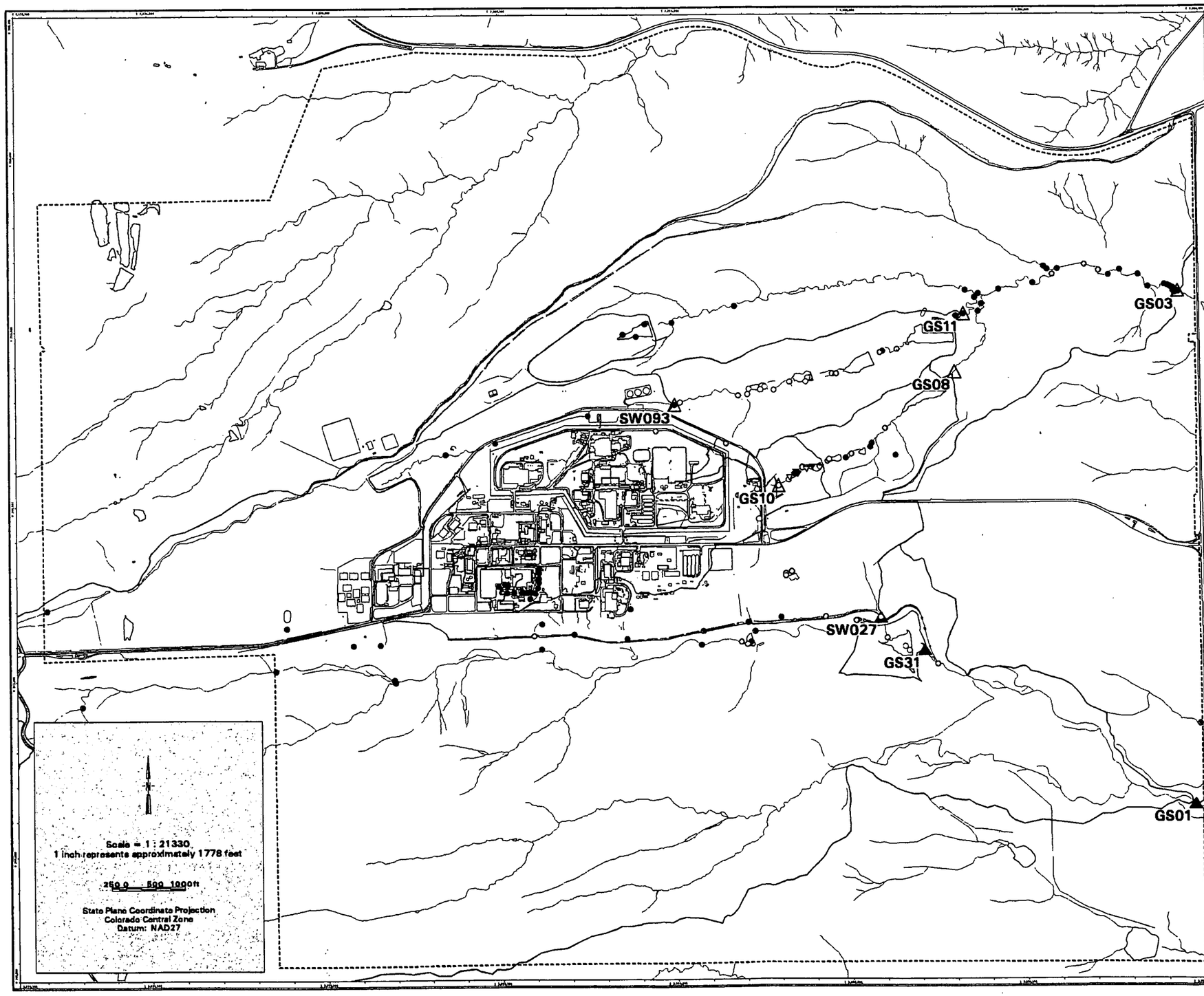

Figure TA-2-49

Actinide Migration Evaluation Pathway Report

Am-241 Activity in Sediments

EXPLANATION

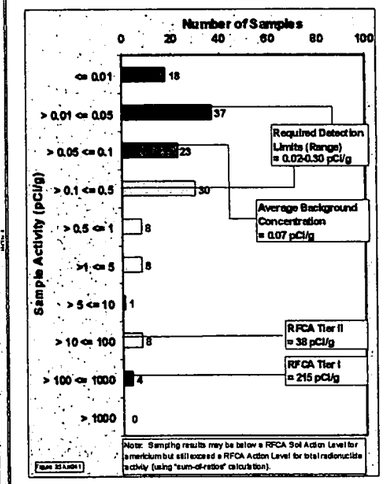

○ Value < Tier II value (Color indicates range of activity shown in the histogram above.)

▽ Tier II value < = Value < Tier I value

◇ Value > = Tier I value

Drainage Basin Boundary

△ Walnut Creek Basin Gaging Station (GS03, GS08, GS10, GS11 & SW093)

▲ Woman Creek Basin Gaging Station (GS01, GS31 & SW027)

Standard Map Features

- Buildings and other structures
- Lakes and ponds
- Streams, ditches, or other drainage features
- Rocky Flats boundary
- Paved roads

DATA SOURCE BASE FEATURES:
Buildings, fences, hydrography, roads and other structures from 1994 aerial fly-over data captured by EG&G RSL, Las Vegas.
Digitized from the orthophotographs. 1/95
Analytical Data from SWD as of October 2000.

Data Analysis performed by Wright Water Engineers (303-480-1700).

U.S. Department of Energy
Rocky Flats Environmental Technology Site

GIS Dept. 303-966-7707

Prepared for: DynCorp THE ART OF TECHNOLOGY

Prepared for: KAISER-HILL COMPANY

NT_Svr w:/projects/actinide_pathway_report/fy2002/sediment_maps/am241_sed.aml

199

Figure TA-2-50

Actinide Migration Evaluation Pathway Report

U-233/234 Activity in Sediments

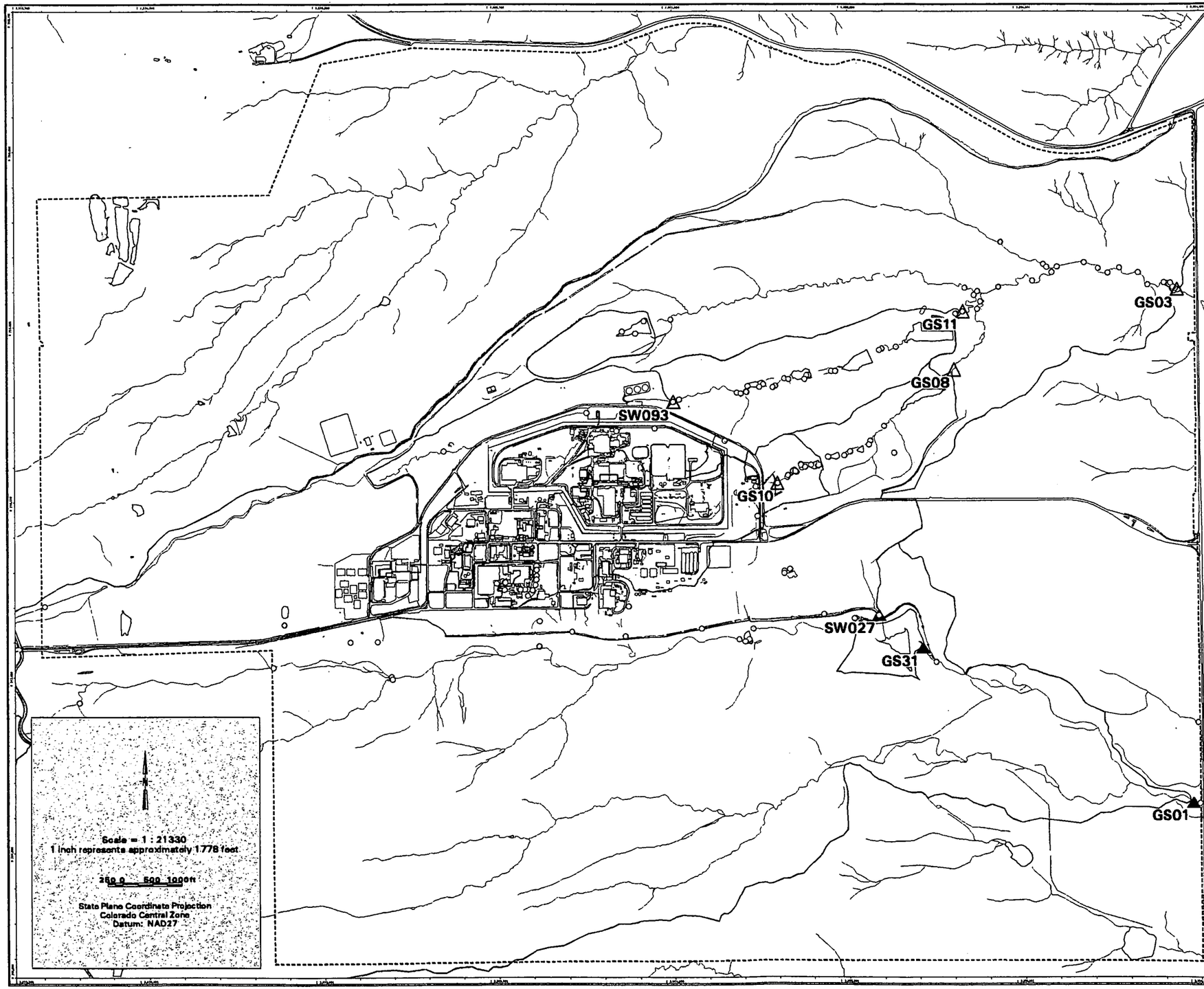

EXPLANATION

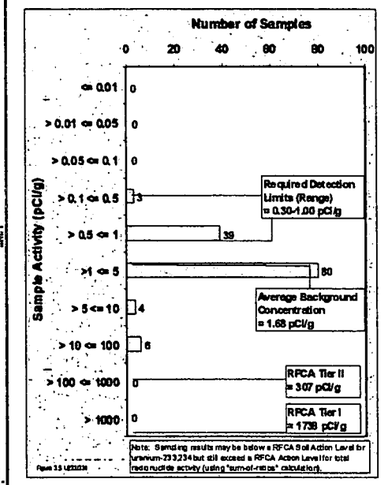

○ Value < Tier II value
(Color indicates range of activity shown in the histogram above.)

▽ Tier II value < = Value < Tier I value

◇ Value > = Tier I value

N Drainage Basin Boundary

△ Walnut Creek Basin Gaging Station (GS03, GS08, GS10, GS11 & SW093)

▲ Woman Creek Basin Gaging Station (GS01, GS31 & SW027)

Standard Map Features

- Buildings and other structures
- Lakes and ponds
- Streams, ditches, or other drainage features
- Rocky Flats boundary
- Paved roads

DATA SOURCE BASE FEATURES:

Buildings, fences, hydrography, roads and other structures from 1994 aerial fly-over data captured by EG&G RSL, Las Vegas. Digitized from the orthophotographs. 1/95
Analytical Data from SWD as of October 2000.

Data Analysis performed by Wright Water Engineers (303-480-1700).

U.S. Department of Energy
Rocky Flats Environmental Technology Site
GIS Dept. 303-966-7707

Prepared by: DynCorp — THE ART OF TECHNOLOGY
Prepared for: KH Kaiser-Hill

NT_Svr w:/projects/actinide_pathway_report/fy2002/sediment_maps/u233-234_sed.aml

200

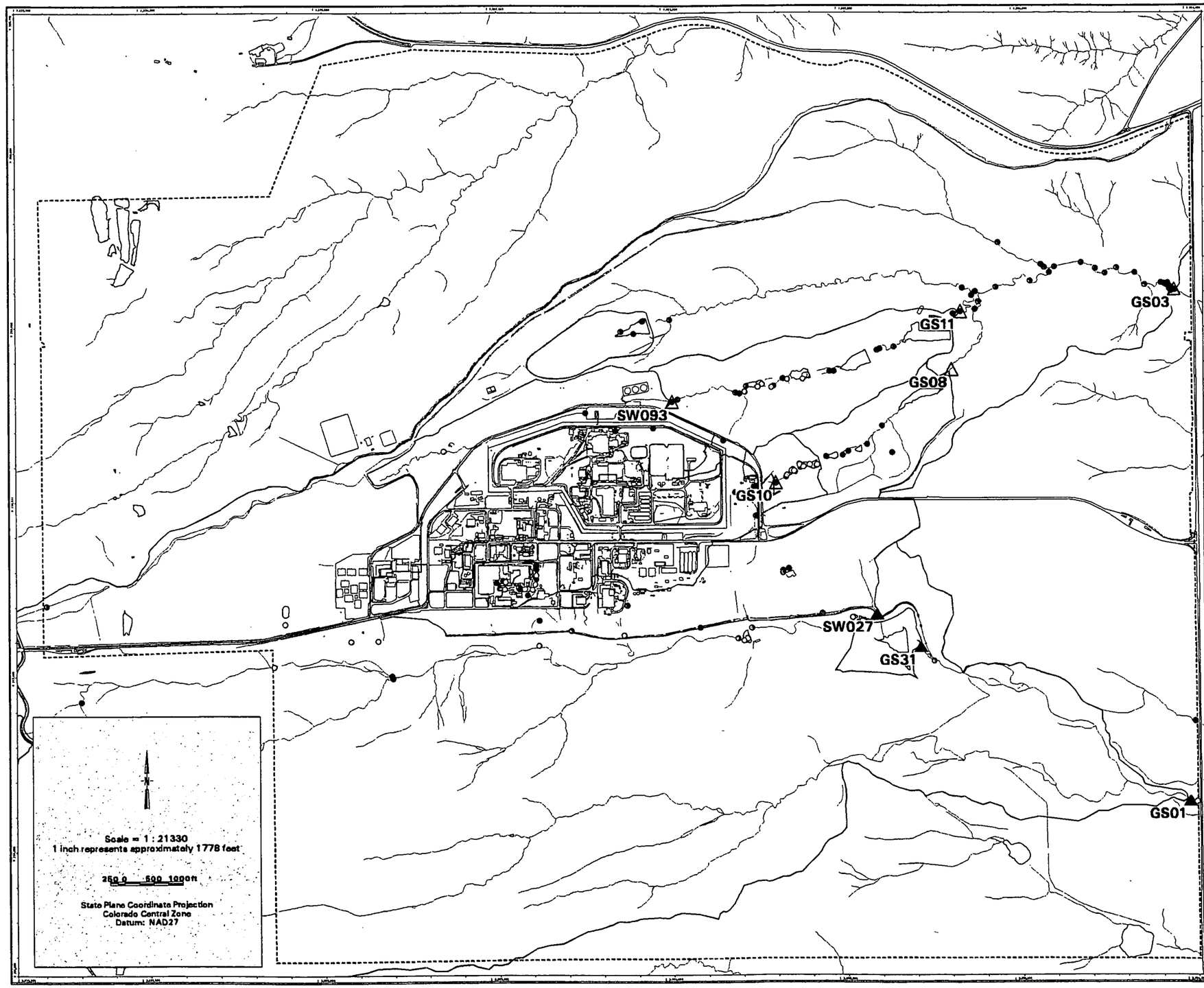

Figure TA-2-51

Actinide Migration Evaluation Pathway Report

U-235 Activity in Sediments

EXPLANATION

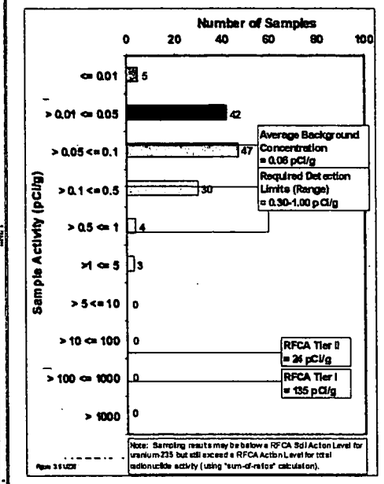

- ○ Value < Tier II value (Color indicates range of activity shown in the histogram above.)
- ▽ Tier II value < = Value < Tier I value
- ◇ Value > = Tier I value
- N Drainage Basin Boundary
- △ Walnut Creek Basin Gaging Station (GS03, GS08, GS10, GS11 & SW093)
- ▲ Woman Creek Basin Gaging Station (GS01, GS31 & SW027)

Standard Map Features

- Buildings and other structures
- Lakes and ponds
- Streams, ditches, or other drainage features
- Rocky Flats boundary
- Paved roads

DATA SOURCE BASE FEATURES:

Buildings, fences, hydrography, roads and other structures from 1994 aerial fly-over data captured by EG&G RSL, Las Vegas.
Digitized from the orthophotographs. 1/95
Analytical Data from SWD as of October 2000.

Data Analysis performed by Wright Water Engineers (303-480-1700).

U.S. Department of Energy
Rocky Flats Environmental Technology Site

GIS Dept. 303-966-7707

Prepared for: DynCorp — THE ART OF TECHNOLOGY

Prepared for: KH — KAISER-HILL COMPANY

NT_Svr w:/projects/actinide_pathway_report/fy2002/sediment_maps/u235_sed.aml

December 18, 2001

201

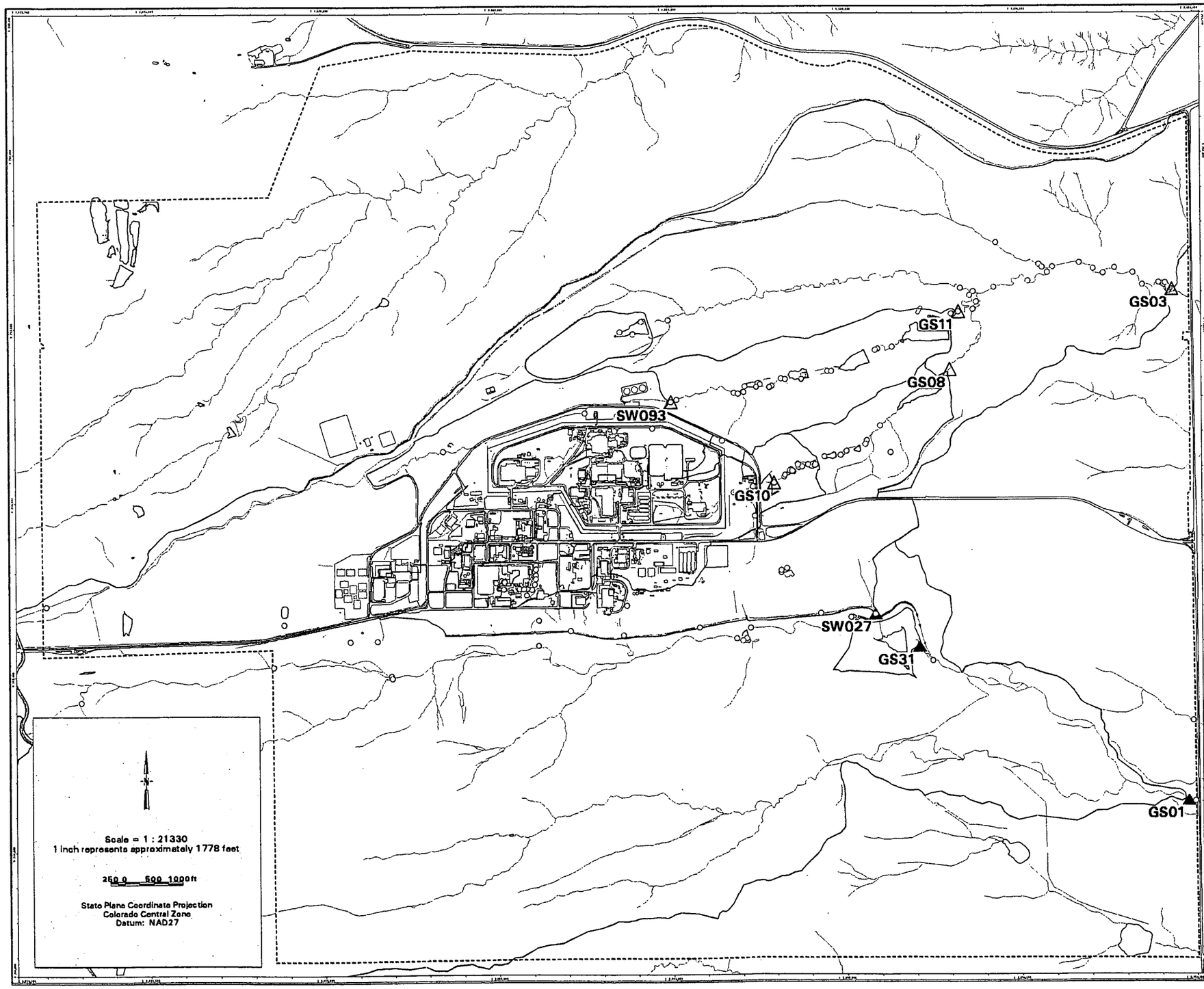

Figure TA-2-52

Actinide Migration Evaluation Pathway Report

U-238 Activity in Sediments

EXPLANATION

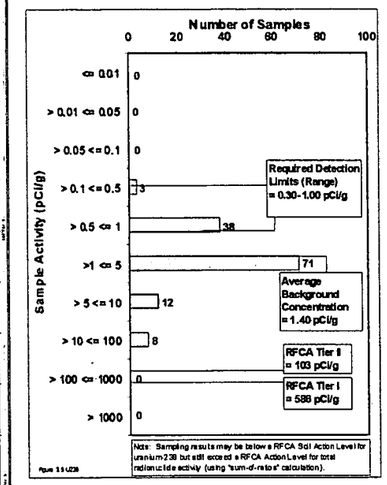

○ Value < Tier II value (Color indicates range of activity shown in the histogram above.)

▽ Tier II value <= Value < Tier I value

◇ Value >= Tier I value

Drainage Basin Boundary

△ Walnut Creek Basin Gaging Station (GS03, GS08, GS10, GS11 & SW093)

▲ Woman Creek Basin Gaging Station (GS01, GS31 & SW027)

Standard Map Features

- Buildings and other structures
- Lakes and ponds
- Streams, ditches, or other drainage features
- Rocky Flats boundary
- Paved roads

DATA SOURCE BASE FEATURES:

Buildings, fences, hydrography, roads and other structures from 1994 aerial fly-over data captured by EG&G RSL, Las Vegas. Digitized from the orthophotographs. 1/95
Analytical Data from SWD as of October 2000.

Data Analysis performed by Wright Water Engineers (303-480-1700).

U.S. Department of Energy
Rocky Flats Environmental Technology Site

GIS Dept. 303-966-7707

Prepared by: DynCorp THE ART OF TECHNOLOGY

Prepared for: KAISER-HILL COMPANY

NT_Svr w:/projects/actinide_pathway_report/fy2002/sediment_maps/u238_sed.aml

202

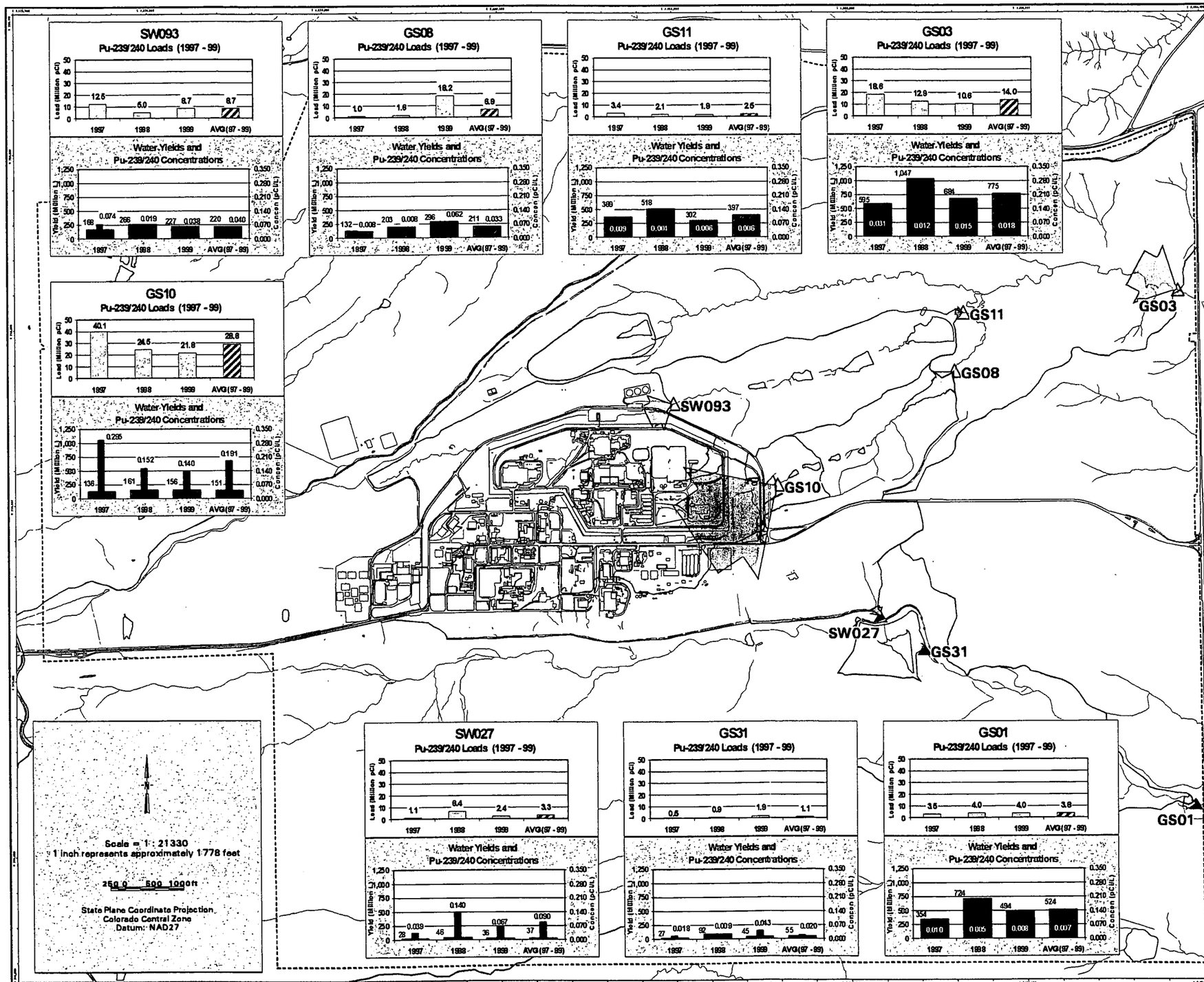

Figure TA-2-53

Actinide Migration Evaluation Pathway Report

Surface Water Actinide Load, Water Yield, and Actinide Concentration Analysis

Pu-239/240 1997-1999

EXPLANATION

Gray Arrows:

Average annual actinide load (units = pCi) from Water Year 1997 - 1999 depicted by gray arrow. Arrows sized proportionately to size of yield. Where load is very low, arrow may not be visible. Numeric value associated with each arrow is displayed in the yellow bar chart.

Upper (Yellow) Bar Chart:

Actinide load (units = pCi) for each Water Year from 1997 - 1999. Average load for the 3 years (equal to the gray arrow value) is on far right of bar chart.

Lower (Blue) Bar Chart:

Displays 2 data sets:
1) Annual water yields (units = Liters) shown as blue bars for each Water Year from 1997 - 1999. Average yield for the 3 years is rightmost bar. Vertical axis scale on left side of chart.
2) Average annual actinide concentrations (units = pCi/L) shown as green bars for each Water Year from 1997 - 1999. Average concentration for the 3 years is rightmost bar. Vertical axis scale on right side of chart.

△ Walnut Creek Basin Gaging Station (GS03, GS08, GS10, GS11 & SW093)

▲ Woman Creek Basin Gaging Station (GS01, GS31 & SW027)

N Drainage Basin Boundary

Standard Map Features

- Buildings and other structures
- Lakes and ponds
- Streams, ditches, or other drainage features
- Rocky Flats boundary
- Paved roads

DATA SOURCE BASE FEATURES:
Buildings, fences, hydrography, roads and other structures from 1994 aerial fly-over data captured by EG&G RSL, Las Vegas. Digitized from the orthophotographs. 1/95

Data Source:
Analyte data -
Approved by Greg Wetherbee (WWE, 303-966-7279 or 303-480-1700).

U.S. Department of Energy
Rocky Flats Environmental Technology Site

GIS Dept. 303-966-7707

Prepared by: DynCorp — THE ADV OF TECHNOLOGY

Prepared for: KH KAISER-HILL COMPANY

MAP ID: actinide_load_maps/pu239-240_avg3yr.aml

December 19, 2001

NT_Svr w:/projects/actinide_pathway_report/fy2002/actinide_load_maps/pu239-240_avg3yr.aml

203

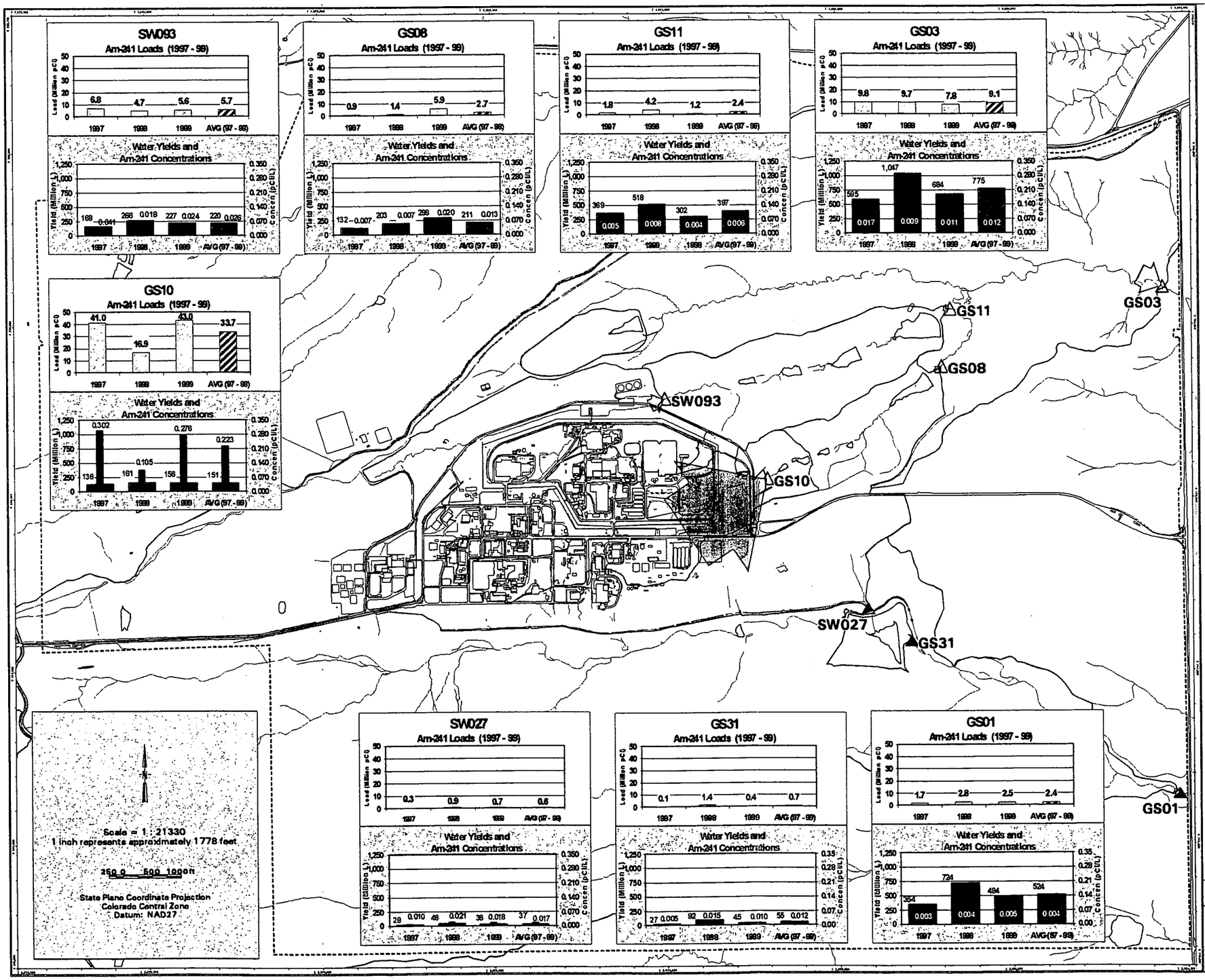

Figure TA-2-54

Actinide Migration Evaluation Pathway Report

Surface Water Actinide Load, Water Yield, and Actinide Concentration Analysis

Am-241 1997-1999

EXPLANATION

Gray Arrows:

Average annual actinide load (units = pCi) from Water Year 1997 - 1999 depicted by gray arrow. Arrows sized proportionately to size of yield. Where load is very low, arrow may not be visible. Numeric value associated with each arrow is displayed in the yellow bar chart.

Upper (Yellow) Bar Chart:

Actinide load (units = pCi) for each Water Year from 1997 - 1999. Average load for the 3 years (equal to the gray arrow value) is on far right of bar chart.

Lower (Blue) Bar Chart:

Displays 2 data sets:
1) Annual water yields (units = Liters) shown as blue bars for each Water Year from 1997 - 1999. Average yield for the 3 years is rightmost bar. Vertical axis scale on left side of chart.
2) Average annual actinide concentrations (units = pCi/L) shown as green bars for each Water Year from 1997 - 1999. Average concentration for the 3 years is rightmost bar. Vertical axis scale on right side of chart.

△ Walnut Creek Basin Gaging Station (GS03, GS08, GS10, GS11 & SW093)

▲ Woman Creek Basin Gaging Station (GS01, GS31 & SW027)

N Drainage Basin Boundary

Standard Map Features

- Buildings and other structures
- Lakes and ponds
- Streams, ditches, or other drainage features
- Rocky Flats boundary
- Paved roads

DATA SOURCE BASE FEATURES:
Buildings, fences, hydrography, roads and other structures from 1994 aerial fly-over data captured by EG&G RSL, Las Vegas. Digitized from the orthophotographs. 1/95

Data Source:
Analyte data - Approved by Greg Wetherbee (WWE, 303-966-7279 or 303-480-1700).

U.S. Department of Energy
Rocky Flats Environmental Technology Site

Prepared by: DynCorp — THE ART OF TECHNOLOGY
Prepared for: KH KAISER-HILL COMPANY

NT_Svr w:/projects/actinide_pathway_report/fy2002/actinide_load_maps/am241_avg3yr.aml

204

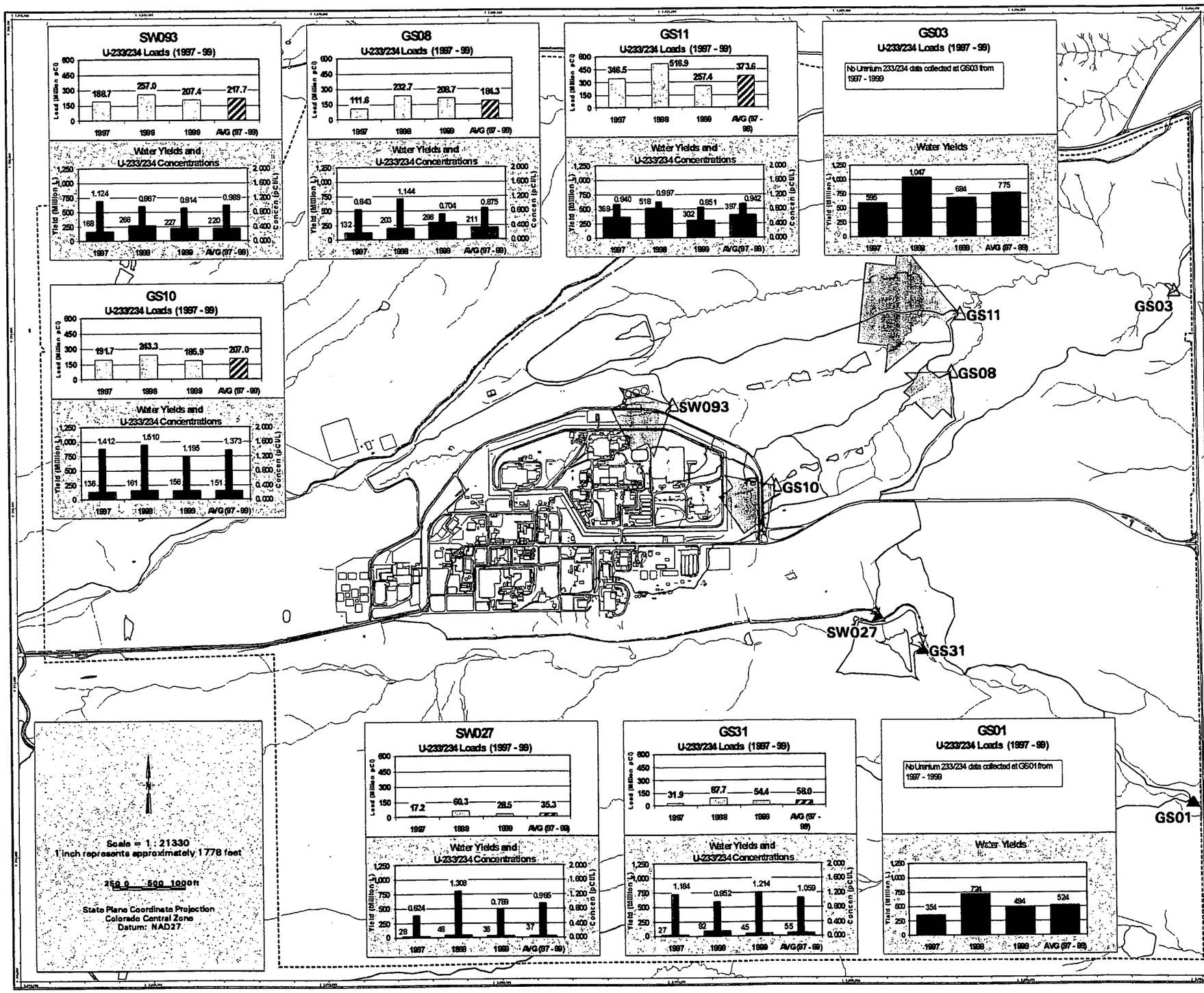

Figure TA-2-55

Actinide Migration Evaluation Pathway Report

Surface Water Actinide Load, Water Yield, and Actinide Concentration Analysis

U-233/234 1997-1999

EXPLANATION

Gray Arrows:

Average annual actinide load (units = pCi) from Water Year 1997 - 1999 depicted by gray arrow. Arrows sized proportionately to size of yield. Where load is very low, arrow may not be visible. Numeric value associated with each arrow is displayed in the yellow bar chart.

Upper (Yellow) Bar Chart:

Actinide load (units = pCi) for each Water Year from 1997 - 1999. Average load for the 3 years (equal to the gray arrow value) is on far right of bar chart.

Lower (Blue) Bar Chart:

Displays 2 data sets:
1) Annual water yields (units = Liters) shown as blue bars for each Water Year from 1997 - 1999. Average yield for the 3 years is rightmost bar. Vertical axis scale on left side of chart.
2) Average annual actinide concentrations (units = pCi/L) shown as green bars for each Water Year from 1997 - 1999. Average concentration for the 3 years is rightmost bar. Vertical axis scale on right side of chart.

Walnut Creek Basin Gaging Station (GS03, GS08, GS10, GS11 & SW093)

Woman Creek Basin Gaging Station (GS01, GS31 & SW027)

Drainage Basin Boundary

Standard Map Features

- Buildings and other structures
- Lakes and ponds
- Streams, ditches, or other drainage features
- Rocky Flats boundary
- Paved roads

DATA SOURCE BASE FEATURES:
Buildings, fences, hydrography, roads and other structures from 1994 aerial fly-over data captured by EG&G RSL, Las Vegas. Digitized from the orthophotographs. 1/95

Data Source:
Analyte data - Approved by Greg Wetherbee (WWE, 303-966-7279 or 303-480-1700).

U.S. Department of Energy
Rocky Flats Environmental Technology Site
OB Dept. 303-966-7707

Prepared for: DynCorp — THE ART OF TECHNOLOGY

Prepared for: KH KAISER-HILL COMPANY

MAP ID: y:\data\u_load_maps\u233-234_map3yr.aml

December 19, 2001

NT_Svr w:/projects/actinide_pathway_report/fy2002/actinide_load_maps/u233-234_avg3yr.aml

205

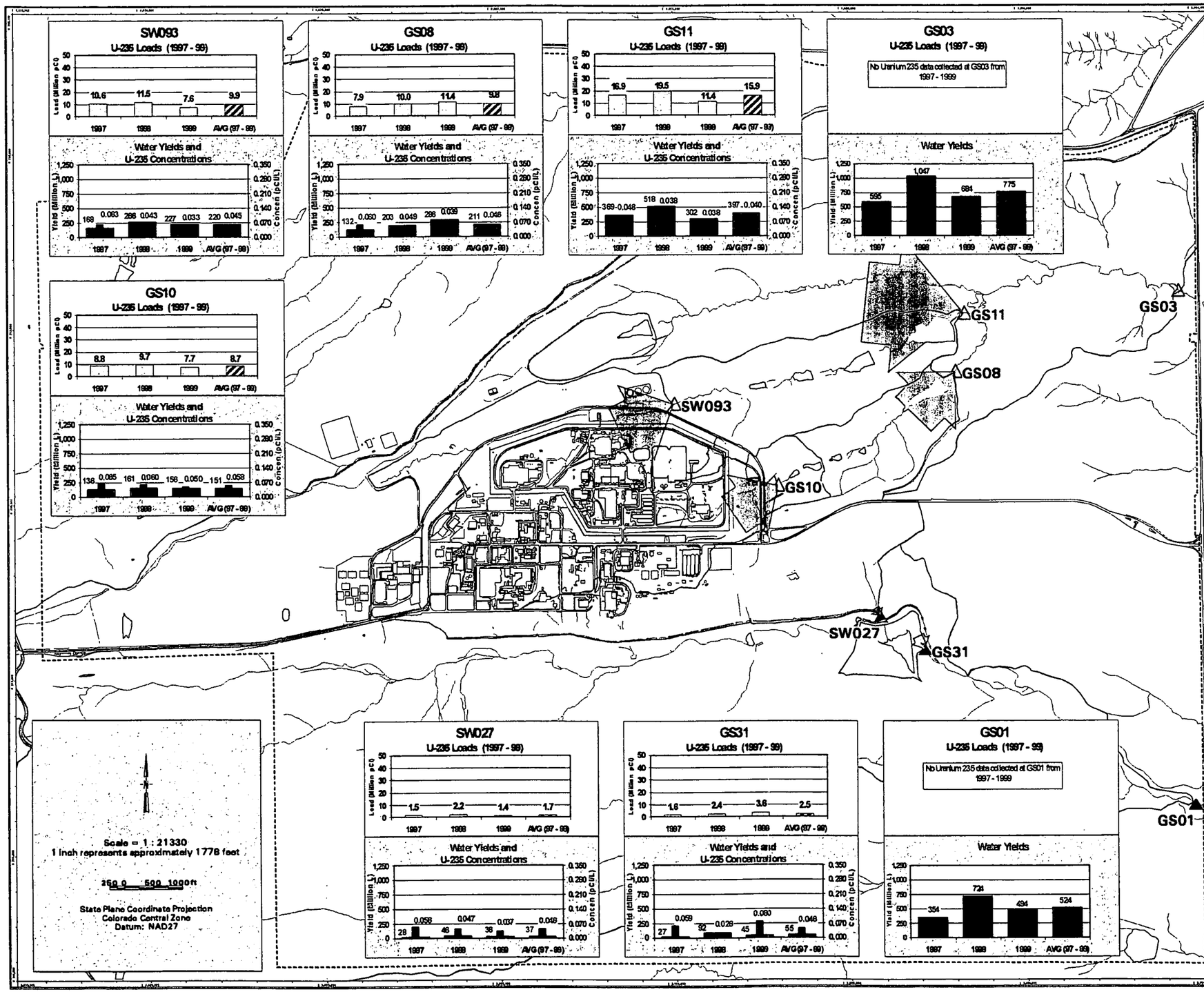

Figure TA-2-56

Actinide Migration Evaluation Pathway Report

Surface Water Actinide Load, Water Yield, and Actinide Concentration Analysis

U-235 1997-1999

EXPLANATION

Gray Arrows:

Average annual actinide load (units = pCi) from Water Year 1997 - 1999 depicted by gray arrow. Arrows sized proportionately to size of yield. Where load is very low, arrow may not be visible. Numeric value associated with each arrow is displayed in the yellow bar chart.

Upper (Yellow) Bar Chart:

Actinide load (units = pCi) for each Water Year from 1997 - 1999. Average load for the 3 years (equal to the gray arrow value) is on far right of bar chart.

Lower (Blue) Bar Chart:

Displays 2 data sets:
1) Annual water yields (units = Liters) shown as blue bars for each Water Year from 1997 - 1999. Average yield for the 3 years is rightmost bar. Vertical axis scale on left side of chart.
2) Average annual actinide concentrations (units = pCi/L) shown as green bars for each Water Year from 1997 - 1999. Average concentration for the 3 years is rightmost bar. Vertical axis scale on right side of chart.

△ Walnut Creek Basin Gaging Station (GS03, GS08, GS10, GS11 & SW093)

▲ Woman Creek Basin Gaging Station (GS01, GS31 & SW027)

N Drainage Basin Boundary

Standard Map Features

- Buildings and other structures
- Lakes and ponds
- Streams, ditches, or other drainage features
- Rocky Flats boundary
- Paved roads

DATA SOURCE BASE FEATURES:
Buildings, fences, hydrography, roads and other structures from 1994 aerial fly-over data captured by EG&G RSL, Las Vegas. Digitized from the orthophotographs. 1/95

Data Source:
Analyte data -
Approved by Greg Wetherbee (WWE, 303-966-7279 or 303-480-1700).

U.S. Department of Energy
Rocky Flats Environmental Technology Site

GIS Dept. 303-966-7707

Prepared by: DynCorp THE ART OF TECHNOLOGY

Prepared for: KH KAISER-HILL COMPANY

NT_Svr w:/projects/actinide_pathway_report/fy2002/actinide_load_maps/u235_avg3yr.aml

December 19, 2001

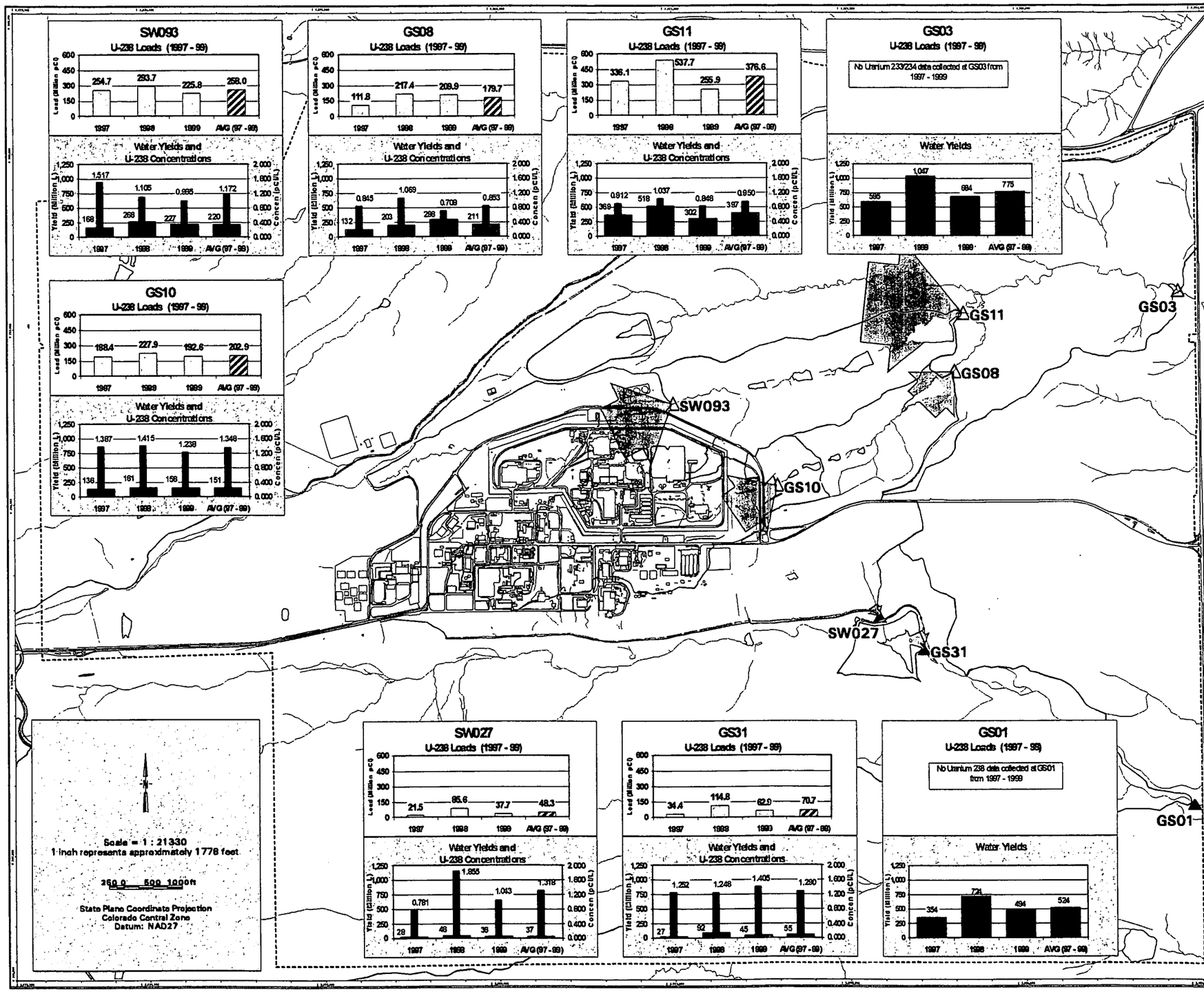

Figure TA-2-57

Actinide Migration Evaluation Pathway Report

Surface Water Actinide Load, Water Yield, and Actinide Concentration Analysis

U-238
1997-1999

EXPLANATION

Gray Arrows:

Average annual actinide load (units = pCi) from Water Year 1997 - 1999 depicted by gray arrow. Arrows sized proportionately to size of yield. Where load is very low, arrow may not be visible. Numeric value associated with each arrow is displayed in the yellow bar chart.

Upper (Yellow) Bar Chart:

Actinide load (units = pCi) for each Water Year from 1997 - 1999. Average load for the 3 years (equal to the gray arrow value) is on far right of bar chart.

Lower (Blue) Bar Chart:

Displays 2 data sets:
1) Annual water yields (units = Liters) shown as blue bars for each Water Year from 1997 - 1999. Average yield for the 3 years is rightmost bar. Vertical axis scale on left side of chart.
2) Average annual actinide concentrations (units = pCi/L) shown as green bars for each Water Year from 1997 - 1999. Average concentration for the 3 years is rightmost bar. Vertical axis scale on right side of chart.

Walnut Creek Basin Gaging Station (GS03, GS08, GS10, GS11 & SW093)

Woman Creek Basin Gaging Station (GS01, GS31 & SW027)

Drainage Basin Boundary

Standard Map Features

- Buildings and other structures
- Lakes and ponds
- Streams, ditches, or other drainage features
- Rocky Flats boundary
- Paved roads

DATA SOURCE BASE FEATURES:
Buildings, fences, hydrography, roads and other structures from 1994 aerial fly-over data captured by EG&G RSL, Las Vegas. Digitized from the orthophotographs. 1/95

Data Source:
Analyte data -
Approved by Greg Wetherbee (WWE, 303-966-7279 or 303-480-1700).

U.S. Department of Energy
Rocky Flats Environmental Technology Site

DOE Dept. 303-966-7707

Prepared for: DynCorp — THE ART OF TECHNOLOGY

Prepared for: KH — KAISER-HILL COMPANY

NT_Svr w:/projects/actinide_pathway_report/fy2002/actinide_load_maps/u238_avg3yr.aml

206

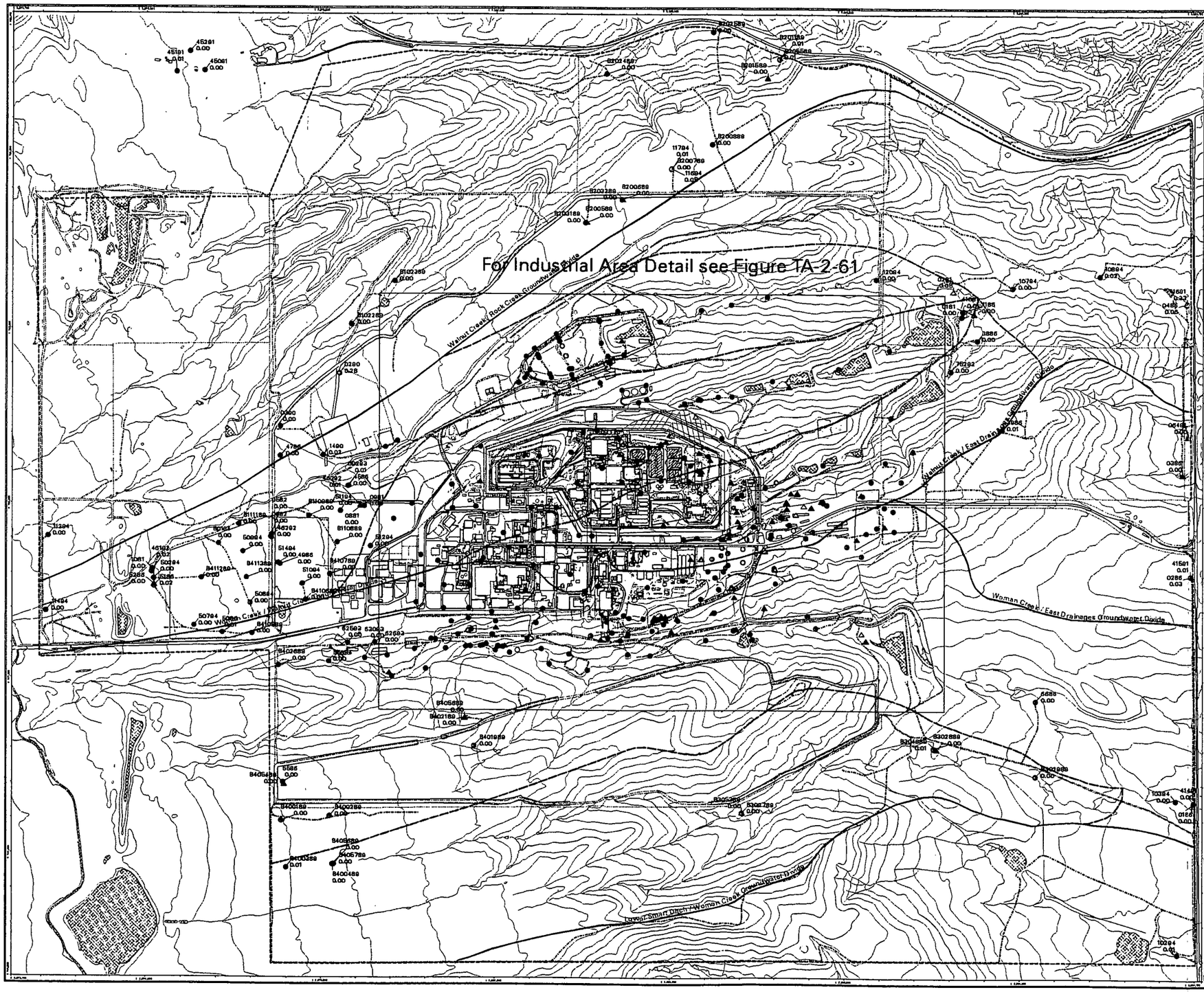

Figure TA-2-60

Actinide Migration Evaluation Pathway Report

Unfiltered UHSU Pu-239/240 in Groundwater, 1991 - 1999 (Avg.)

Pu-239/240 Activity-Concentration (pCi/L) (1991-99)

- 0 - 0.05
- 0.05 - 0.15
- 0.15 - 0.5
- 0.5 - 1.0
- > 1.0

- Alluvium Wells
- Bedrock Wells

Action Level = 0.151 pCi/L

- Groundwater Collection and Treatment Systems
- Slurry Wall
- Active Actinide Site
- Under Building Contamination (UBC)
- Accepted as Proposed No Further Action (NFA)
- Proposed No Further Action (NFA)
- Foundation Drains
- Groundwater Basin Divides
- Groundwater Sub-Basin Divides

Standard Map Features

- Buildings and other structures
- Solar Evaporation Ponds (SEPs)
- Lakes and ponds
- Streams, ditches, or other drainage features
- Fences and other barriers
- Topographic Contour (20-Foot)
- Rocky Flats boundary
- Paved roads
- Dirt roads

DATA SOURCE BASE FEATURES:

Buildings, fences, hydrography, roads and other structures from 1994 aerial fly-over data captured by EG&G RSL, Las Vegas. Digitized from the orthophotographs. 1/95

Topographic contours were derived from digital elevation model (DEM) data by Morrison Knudson (MK) using ESRI Arc TIN and LATTICE to process the DEM data to create 5-foot contours. The DEM data was captured by the Remote Sensing Lab, Las Vegas, NV, 1994 Aerial Flyover at ~ 10 meter resolution. DEM post-processing performed by MK, Winter 1997.

Scale = 1 : 21330
1 inch represents approximately 1778 feet

250 0 500 1000 ft

State Plane Coordinate Projection
Colorado Central Zone
Datum: NAD27

U.S. Department of Energy
Rocky Flats Environmental Technology Site

Prepared by: DynCorp — THE ART OF TECHNOLOGY

Prepared for: KAISER-HILL

NT_Sw w:/projects/actinide_pathway_report/fy2002/gw_uhsu_maps/pu239-240-uhsu.aml

209

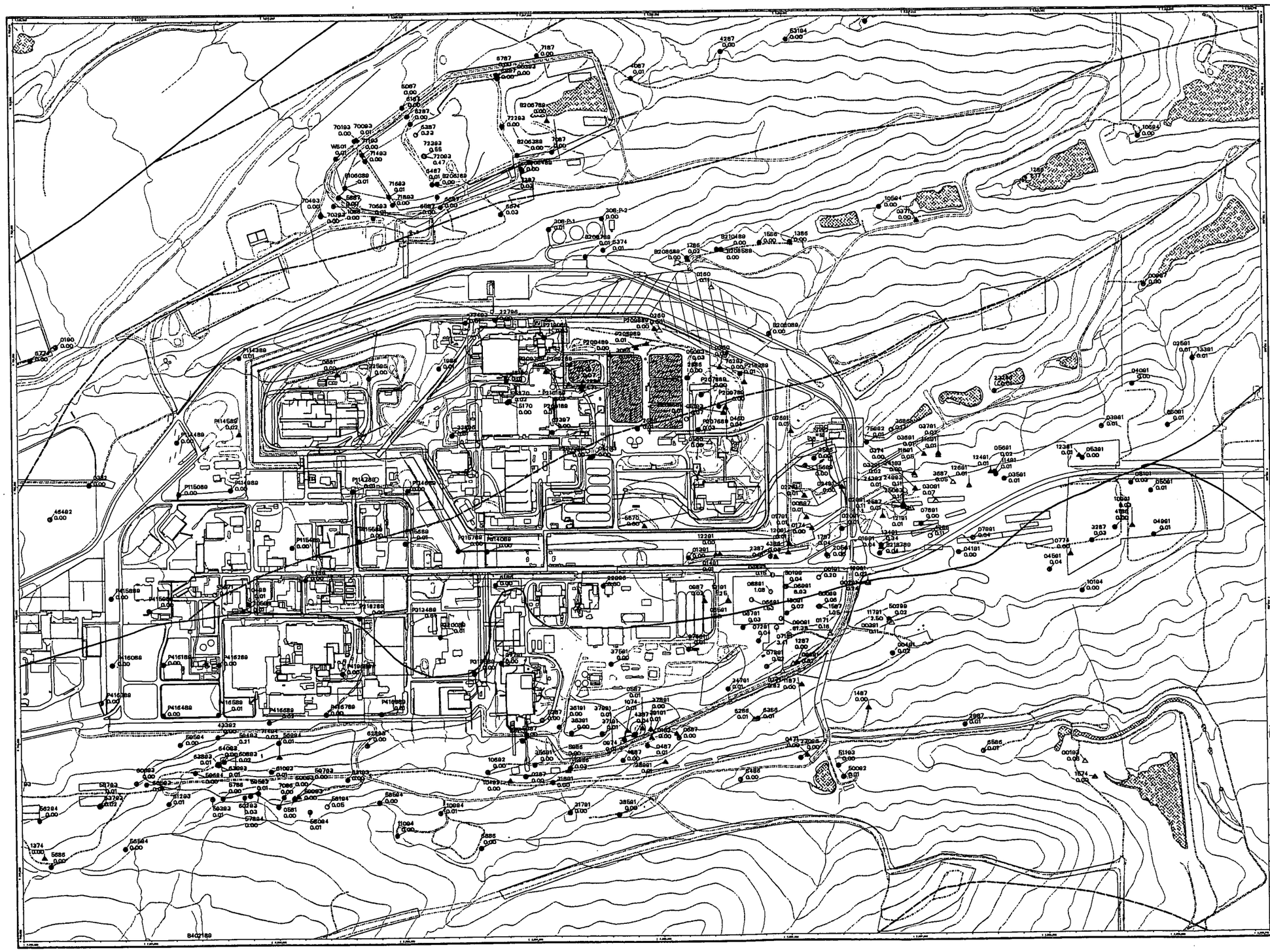

Figure TA-2-61

Actinide Migration Evaluation Pathway Report

Industrial Area

Unfiltered UHSU Pu-239/240 in Groundwater, 1991 - 1999 (Avg.)

Pu-239/240 Activity-Concentration (pCi/L) (1991-99)

- 0 - 0.05
- 0.05 - 0.15
- 0.15 - 0.5
- 0.5 - 1.0
- > 1.0

- Alluvium Wells
- Bedrock Wells

Action Level = 0.151 pCi/L

- Groundwater Collection and Treatment Systems
- Slurry Wall
- Active Actinide Site
- Under Building Contamination (UBC)
- Accepted as Proposed No Further Action (NFA)
- Proposed No Further Action (NFA)
- Foundation Drains
- Groundwater Basin Divides
- Groundwater Sub-Basin Divides

Standard Map Features

- Buildings and other structures
- Solar Evaporation Ponds (SEPs)
- Lakes and ponds
- Streams, ditches, or other drainage features
- Fences and other barriers
- Topographic Contour (20-Foot)
- Rocky Flats boundary
- Paved roads
- Dirt roads

DATA SOURCE BASE FEATURES:

Buildings, fences, hydrography, roads and other structures from 1994 aerial fly-over data captured by EG&G RSL, Las Vegas. Digitized from the orthophotographs. 1/95

Topographic contours were derived from digital elevation model (DEM) data by Morrison Knudson (MK) using ESRI Arc TIN and LATTICE to process the DEM data to create 5-foot contours. The DEM data was captured by the Remote Sensing Lab, Las Vegas, NV, 1994 Aerial Flyover at ~ 10 meter resolution. DEM post-processing performed by MK, Winter 1997.

Scale = 1 : 9220
1 inch represents approximately 768 feet

100 0 200 400ft

State Plane Coordinate Projection
Colorado Central Zone
Datum: NAD27

U.S. Department of Energy
Rocky Flats Environmental Technology Site

GIS Dept. 303-966-7707

Prepared by: DynCorp — THE ART OF TECHNOLOGY

Prepared for: KH — KAISER-HILL COMPANY

March 22, 2002

NT_Svr w:/projects/actinide_pathway_report/fy2002/gw_uhsu_maps/pu239-240-uhsu-ia.aml

210

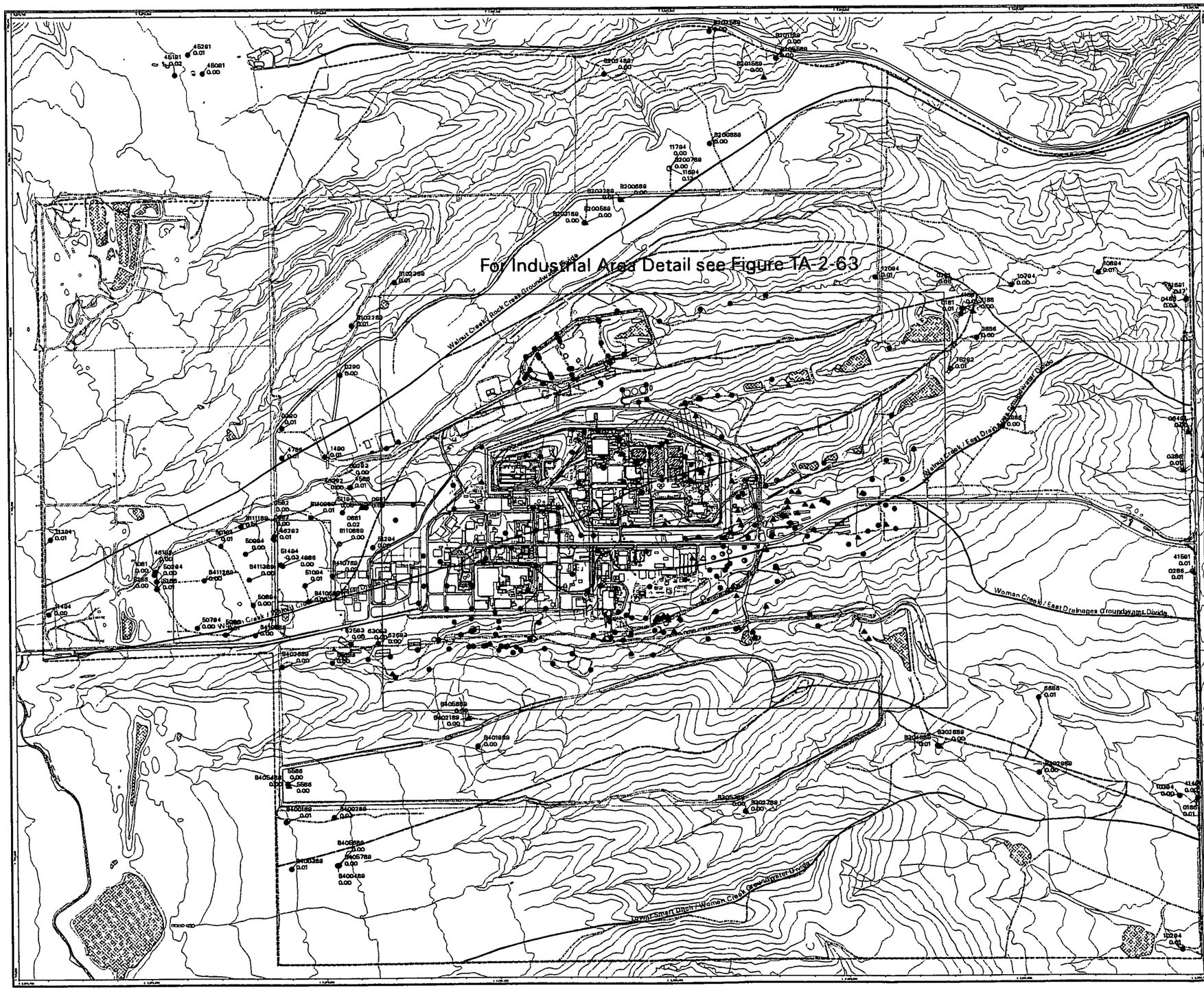

Figure TA-2-62

Actinide Migration Evaluation Pathway Report

Unfiltered UHSU Am-241 in Groundwater, 1991 - 1999 (Avg.)

Am-241 Activity-Concentration (pCi/L) (1991-99)

- 0 - 0.05
- 0.05 - 0.15
- 0.15 - 0.5
- 0.5 - 1.0
- > 1.0

- Alluvium Wells
- Bedrock Wells

Action Level = 0.145 pCi/L

- Groundwater Collection and Treatment Systems
- Slurry Wall
- Active Actinide Site
- Under Building Contamination (UBC)
- Accepted as Proposed No Further Action (NFA)
- Proposed No Further Action (NFA)
- Foundation Drains
- Groundwater Basin Divides
- Groundwater Sub-Basin Divides

Standard Map Features

- Buildings and other structures
- Solar Evaporation Ponds (SEPs)
- Lakes and ponds
- Streams, ditches, or other drainage features
- Fences and other barriers
- Topographic Contour (20-Foot)
- Rocky Flats boundary
- Paved roads
- Dirt roads

DATA SOURCE BASE FEATURES:

Buildings, fences, hydrography, roads and other structures from 1994 aerial fly-over data captured by EG&G RSL, Las Vegas. Digitized from the orthophotographs. 1/95

Topographic contours were derived from digital elevation model (DEM) data by Morrison Knudson (MK) using ESRI Arc TIN and LATTICE to process the DEM data to create 5-foot contours. The DEM data was captured by the Remote Sensing Lab, Las Vegas, NV, 1994 Aerial Flyover at ~ 10 meter resolution. DEM post-processing performed by MK, Winter 1997.

Scale = 1 : 21330
1 inch represents approximately 1778 feet

250 0 500 1000 ft

State Plane Coordinate Projection
Colorado Central Zone
Datum: NAD27

U.S. Department of Energy
Rocky Flats Environmental Technology Site

GIS Dept. 303-966-7707

Prepared by: DynCorp THE ART OF TECHNOLOGY

Prepared for: KAISER-HILL

NT_Svr w:/projects/actinide_pathway_report/fy2002/gw_uhsu_maps/am241-uhsu.aml

211

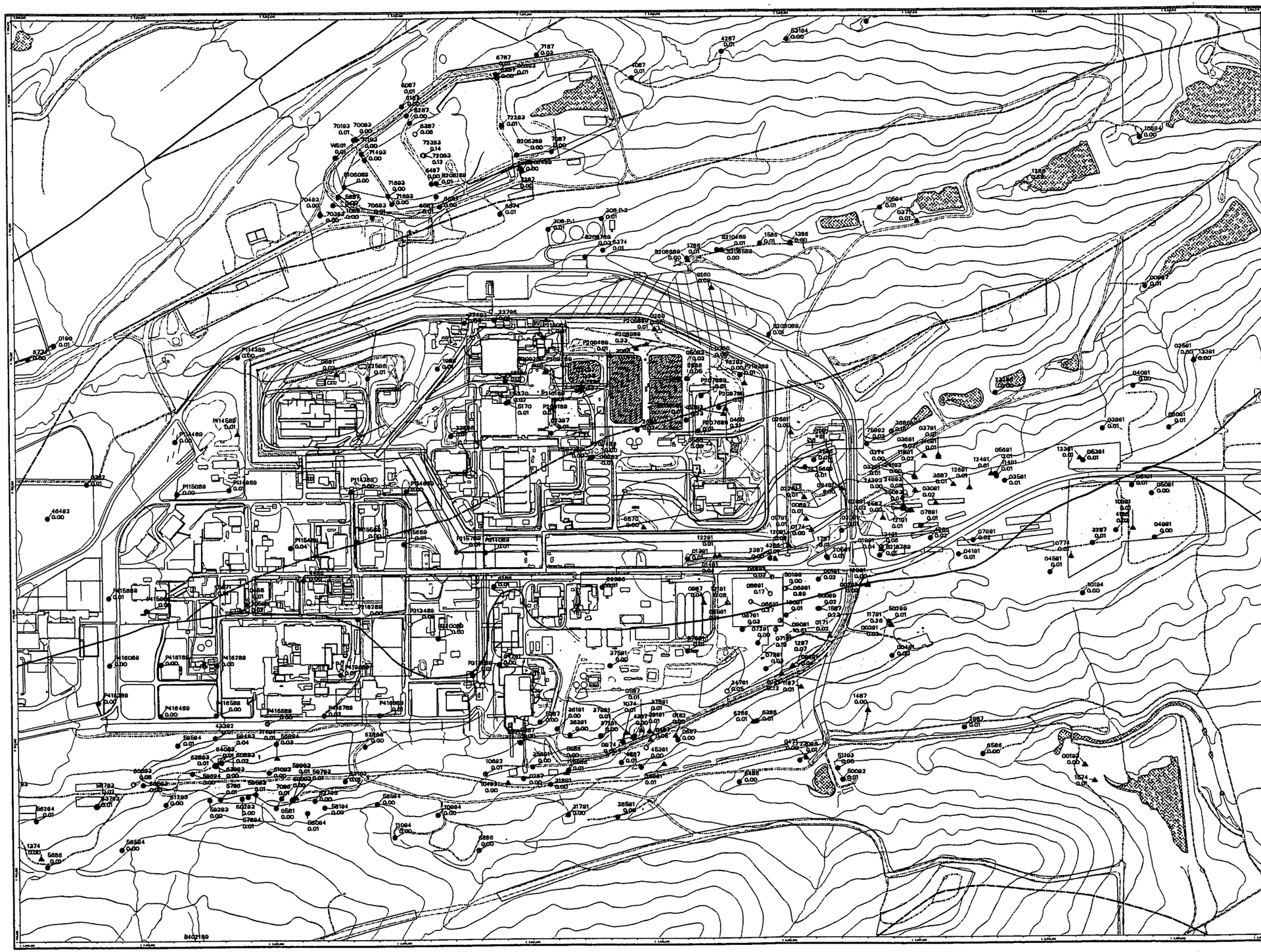

Figure TA-2-63

Actinide Migration Evaluation Pathway Report

Industrial Area

Unfiltered UHSU Am-241 in Groundwater, 1991 - 1999 (Avg.)

Am-241 Activity-Concentration (pCi/L) (1991-99)

- 0 - 0.05
- 0.05 - 0.15
- 0.15 - 0.5
- 0.5 - 1.0
- > 1.0

- Alluvium Wells
- Bedrock Wells

Action Level = 0.145 pCi/L

- Groundwater Collection and Treatment Systems
- Slurry Wall
- Active Actinide Site
- Under Building Contamination (UBC)
- Accepted as Proposed No Further Action (NFA)
- Proposed No Further Action (NFA)
- Foundation Drains
- Groundwater Basin Divides
- Groundwater Sub-Basin Divides

Standard Map Features

- Buildings and other structures
- Solar Evaporation Ponds (SEPs)
- Lakes and ponds
- Streams, ditches, or other drainage features
- Fences and other barriers
- Topographic Contour (20-Foot)
- Rocky Flats boundary
- Paved roads
- Dirt roads

DATA SOURCE BASE FEATURES:

Buildings, fences, hydrography, roads and other structures from 1994 aerial fly-over data captured by EG&G RSL, Las Vegas. Digitized from the orthophotographs. 1/95

Topographic contours were derived from digital elevation model (DEM) data by Morrison Knudson (MK) using ESRI Arc TIN and LATTICE to process the DEM data to create 5-foot contours. The DEM data was captured by the Remote Sensing Lab, Las Vegas, NV, 1994 Aerial Flyover at ~10 meter resolution. DEM post-processing performed by MK, Winter 1997.

Scale = 1 : 9220
1 inch represents approximately 768 feet

100 0 200 400 ft

State Plane Coordinate Projection
Colorado Central Zone
Datum: NAD27

U.S. Department of Energy
Rocky Flats Environmental Technology Site

Prepared by: DynCorp THE ART OF TECHNOLOGY

Prepared for: KAISER-HILL

NT_Svr w:/projects/actinide_pathway_report/fy2002/gw_uhsu_maps/am241-uhsu-ia.aml

212

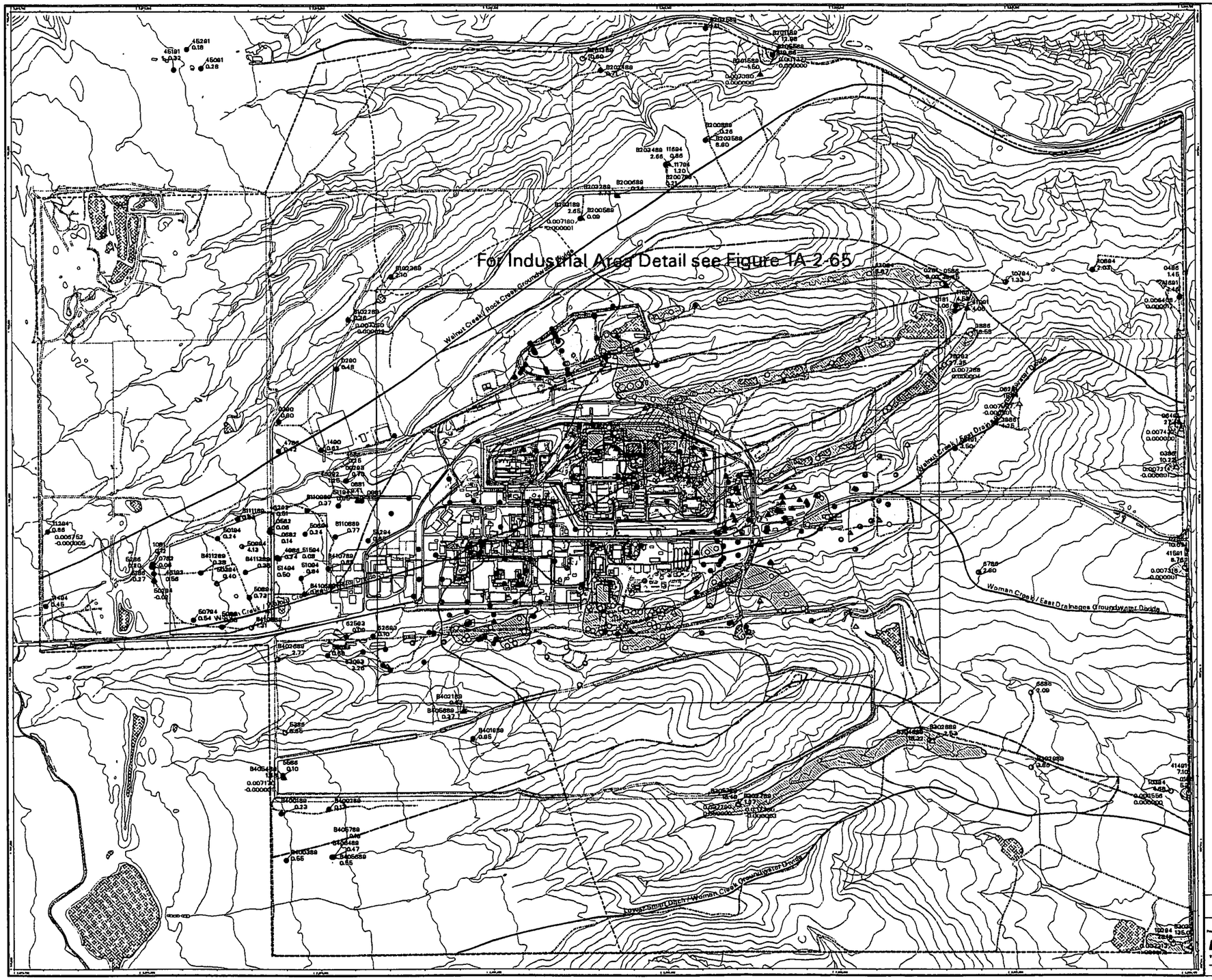

Figure TA-2-64

Actinide Migration Evaluation Pathway Report

Filtered UHSU U-233/234 in Groundwater, 1991 - 1999 (Avg.)

U-233/234 Activity-Concentration (pCi/L) (1991-99)

- 0 - 1
- 1 - 5
- 5 - 40
- 40 - 60.7
- 60.7 - 100
- > 100

- Alluvium Wells
- Bedrock Wells

Background Benchmark = 60.7 pCi/L
Action Level = 1.07 pCi/L

NOTES:
Top red value = U-235/U-238 ratio.
Bottom red value = U-236/U-238 ratio.

- Groundwater Collection and Treatment Systems
- Slurry Wall
- Active Actinide Site
- Under Building Contamination (UBC)
- Accepted as Proposed No Further Action (NFA)
- Proposed No Further Action (NFA)
- Foundation Drains
- Groundwater Basin Divides
- Groundwater Sub-Basin Divides
- U-233/234 concentration equal to or greater than 1.07 pCi/L (Action Level) (dashed where inferred)
- U-233/234 concentration equal to or greater than 5.0 pCi/L (Intermediate Level)
- U-233/234 concentration equal to or greater than 60.7 pCi/L (Background Level)

Standard Map Features

- Buildings and other structures
- Solar Evaporation Ponds (SEPs)
- Lakes and ponds
- Streams, ditches, or other drainage features
- Fences and other barriers
- Topographic Contour (20-Foot)
- Rocky Flats boundary
- Paved roads
- Dirt roads

DATA SOURCE BASE FEATURES:
Buildings, fences, hydrography, roads and other structures from 1994 aerial fly-over data captured by EG&G RSL, Las Vegas.
Digitized from the orthophotographs. 1/95
Topographic contours were derived from digital elevation model (DEM) data by Morrison Knudson (MK) using ESRI Arc TIN and LATTICE to process the DEM data to create 5-foot contours. The DEM data was captured by the Remote Sensing Lab, Las Vegas, NV, 1994 Aerial Flyover at ~ 10 meter resolution. DEM post-processing performed by MK, Winter 1997.

Scale = 1 : 21330
1 inch represents approximately 1778 feet
250 0 500 1000 ft

State Plane Coordinate Projection
Colorado Central Zone
Datum: NAD27

U.S. Department of Energy
Rocky Flats Environmental Technology Site

DOE Dept. 303-966-7707

Prepared by: DynCorp — THE ART OF TECHNOLOGY
Prepared for: KAISER-HILL COMPANY

NT_Svr w:/projects/actinide_pathway_report/hy2002/gw_uheu_maps/u233-234-uheu.aml

213

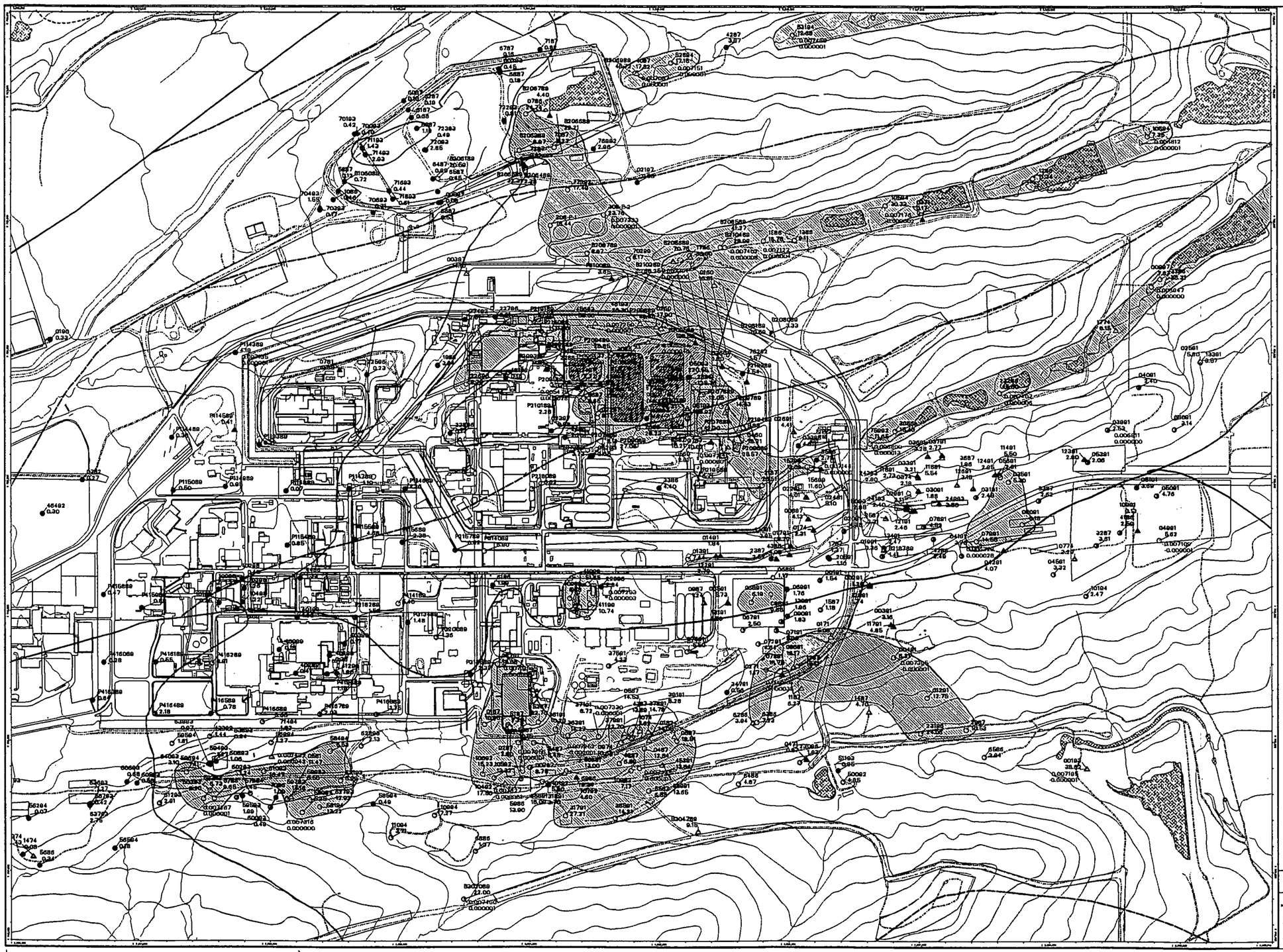

Figure TA-2-65

Actinide Migration Evaluation Pathway Report

Industrial Area

Filtered UHSU U-233/234 in Groundwater, 1991 - 1999 (Avg.)

U-233/234 Activity-Concentration (pCi/L) (1991-99)

- 0 - 1
- 1 - 5
- 5 - 40
- 40 - 60.7
- 60.7 - 100
- > 100

- Alluvium Wells
- Bedrock Wells

Background Benchmark = 60.7 pCi/L
Action Level = 1.07 pCi/L

NOTES:
Top red value = U-235/U-238 ratio.
Bottom red value = U-236/U-238 ratio.

- Groundwater Collection and Treatment Systems
- Slurry Wall
- Active Actinide Site
- Under Building Contamination (UBC)
- Accepted as Proposed No Further Action (NFA)
- Proposed No Further Action (NFA)
- Foundation Drains
- Groundwater Basin Divides
- Groundwater Sub-Basin Divides
- U-233/234 concentration equal to or greater than 1.07 pCi/L (Action Level) (dashed where inferred)
- U-233/234 concentration equal to or greater than 5.0 pCi/L (Intermediate Level)
- U-233/234 concentration equal to or greater than 60.7 pCi/L (Background Level)

Standard Map Features

- Buildings and other structures
- Solar Evaporation Ponds (SEPs)
- Lakes and ponds
- Streams, ditches, or other drainage features
- Fences and other barriers
- Topographic Contour (20-Foot)
- Rocky Flats boundary
- Paved roads
- Dirt roads

DATA SOURCE BASE FEATURES:

Buildings, fences, hydrography, roads and other structures from 1994 aerial fly-over data captured by EG&G RSL, Las Vegas. Digitized from the orthophotographs. 1/95

Topographic contours were derived from digital elevation model (DEM) data by Morrison Knudson (MK) using ESRI Arc TIN and LATTICE to process the DEM data to create 5-foot contours. The DEM data was captured by the Remote Sensing Lab, Las Vegas, NV, 1994 Aerial Flyover at ~ 10 meter resolution. DEM post-processing performed by MK, Winter 1997.

Scale = 1 : 8220
1 inch represents approximately 768 feet

100 0 200 400ft

State Plane Coordinate Projection
Colorado Central Zone
Datum: NAD27

U.S. Department of Energy
Rocky Flats Environmental Technology Site

GIS Dept. 303-966-7707

Prepared by: DynCorp — THE ART OF TECHNOLOGY

Prepared for: KAISER-HILL COMPANY

March 23, 2000

NT_Svr w:/projects/actinide_pathway_report/fy2002/gw_uhsu_maps/u233-234-uhsu-ia.aml

214

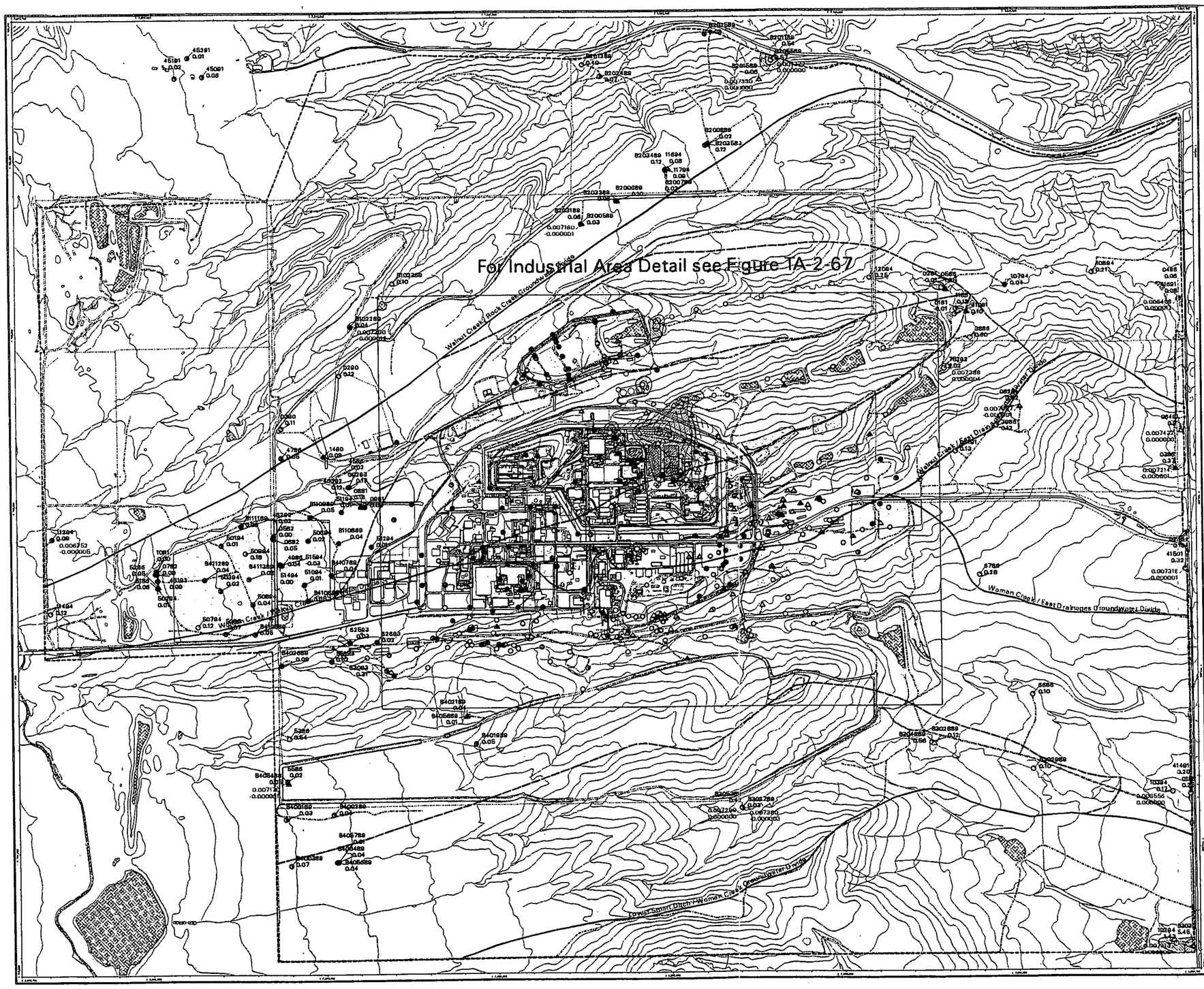

Figure TA-2-66

Actinide Migration Evaluation Pathway Report

Filtered UHSU U-235 in Groundwater, 1991 - 1999 (Avg.)

U-235 Activity-Concentration (pCi/L) (1991-99)

- 0 - 0.1
- 0.1 - 0.5
- 0.5 - 1.0
- 1.0 - 1.79
- 1.79 - 5
- > 5

- Alluvium Wells
- Bedrock Wells

Background Benchmark = 1.79 pCi/L
Action Level = 1.01 pCi/L

NOTES:
Top red value = U-235/U-238 ratio.
Bottom red value = U-236/U-238 ratio.

- Groundwater Collection and Treatment Systems
- Slurry Wall
- Active Actinide Site
- Under Building Contamination (UBC)
- Accepted as Proposed No Further Action (NFA)
- Proposed No Further Action (NFA)
- Foundation Drains
- Groundwater Basin Divides
- Groundwater Sub-Basin Divides
- U-235 concentration equal to or greater than 1.01 pCi/L (Action Level)
- U-235 concentration equal to or greater than 1.79 pCi/L (Background Level)

Standard Map Features

- Buildings and other structures
- Solar Evaporation Ponds (SEPs)
- Lakes and ponds
- Streams, ditches, or other drainage features
- Fences and other barriers
- Topographic Contour (20-Foot)
- Rocky Flats boundary
- Paved roads
- Dirt roads

DATA SOURCE BASE FEATURES:

Buildings, fences, hydrography, roads and other structures from 1994 aerial fly-over data captured by EG&G RSL, Las Vegas. Digitized from the orthophotographs. 1/95

Topographic contours were derived from digital elevation model (DEM) data by Morrison Knudson (MK) using ESRI Arc TIN and LATTICE to process the DEM data to create 5-foot contours. The DEM data was captured by the Remote Sensing Lab, Las Vegas, NV, 1994 Aerial Flyover at ~10 meter resolution. DEM post-processing performed by MK, Winter 1997.

Scale = 1 : 21330
1 inch represents approximately 1778 feet

250 0 500 1000 ft

State Plane Coordinate Projection
Colorado Central Zone
Datum: NAD27

U.S. Department of Energy
Rocky Flats Environmental Technology Site

Prepared by: DynCorp
THE ART OF TECHNOLOGY

Prepared for: KAISER-HILL

NT_Svr w:/projects/actinide_pathway_report/fy2002/gw_uhsu_maps/u235-uhsu.aml

215

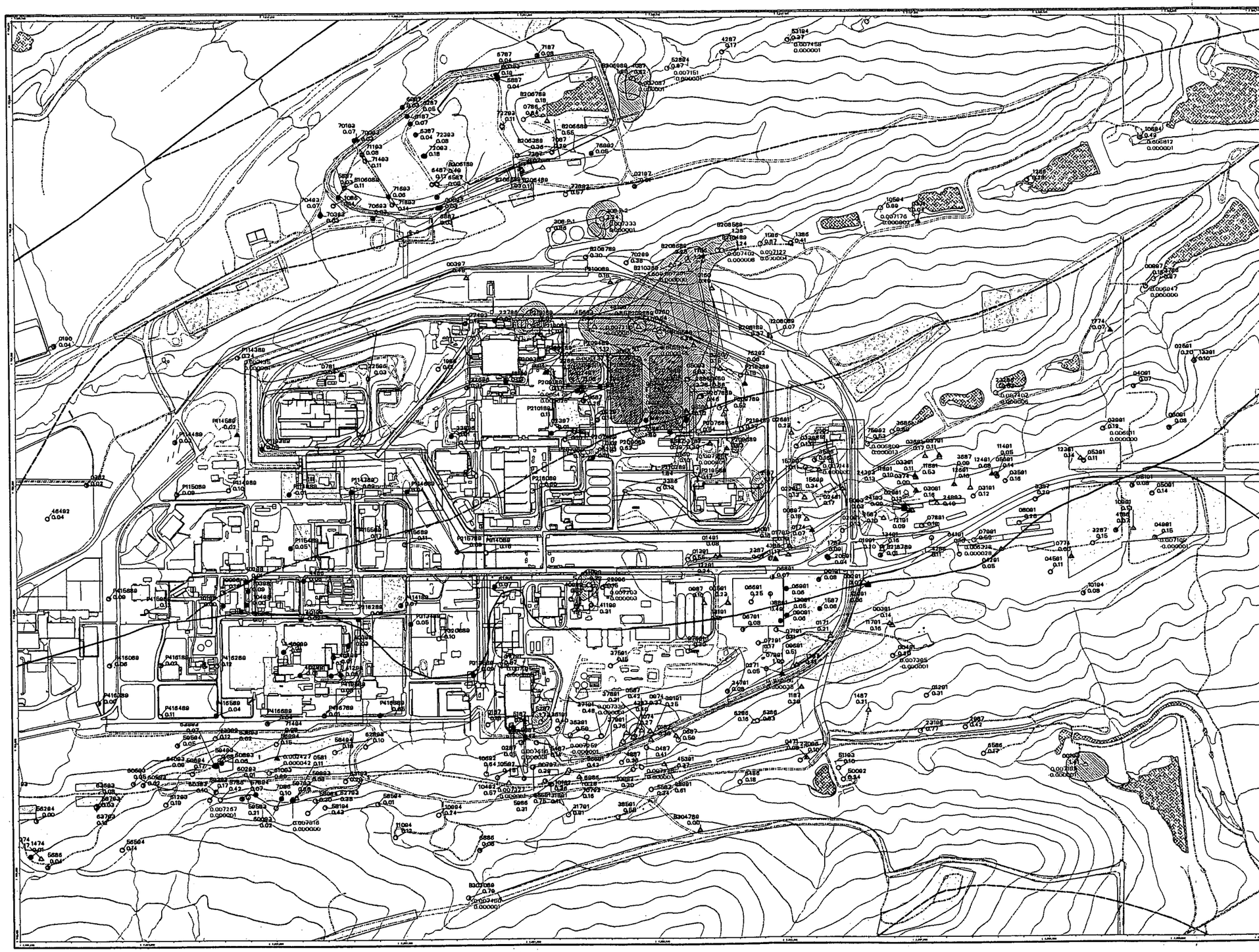

Figure TA-2-67

Actinide Migration Evaluation Pathway Report

Industrial Area

Filtered UHSU U-235 in Groundwater, 1991 - 1999 (Avg.)

U-235 Activity-Concentration (pCi/L) (1991-99)

- 0 - 0.1
- 0.1 - 0.5
- 0.5 - 1.0
- 1.0 - 1.79
- 1.79 - 5
- > 5

- Alluvium Wells
- Bedrock Wells

Background Benchmark = 1.79 pCi/L
Action Level = 1.01 pCi/L

NOTES:
Top red value = U-235/U-238 ratio.
Bottom red value = U-236/U-238 ratio.

- Groundwater Collection and Treatment Systems
- Slurry Wall
- Active Actinide Site
- Under Building Contamination (UBC)
- Accepted as Proposed No Further Action (NFA)
- Proposed No Further Action (NFA)
- Foundation Drains
- Groundwater Basin Divides
- Groundwater Sub-Basin Divides
- U-235 concentration equal to or greater than 1.01 pCi/L (Action Level)
- U-235 concentration equal to or greater than 1.79 pCi/L (Background Level)

Standard Map Features

- Buildings and other structures
- Solar Evaporation Ponds (SEPs)
- Lakes and ponds
- Streams, ditches, or other drainage features
- Fences and other barriers
- Topographic Contour (20-Foot)
- Rocky Flats boundary
- Paved roads
- Dirt roads

DATA SOURCE BASE FEATURES:
Buildings, fences, hydrography, roads and other structures from 1994 aerial fly-over data captured by EG&G RSL, Las Vegas. Digitized from the orthophotographs. 1/95 Topographic contours were derived from digital elevation model (DEM) data by Morrison Knudson (MK) using ESRI Arc TIN and LATTICE to process the DEM data to create 5-foot contours. The DEM data was captured by the Remote Sensing Lab, Las Vegas, NV, 1994 Aerial Flyover at ~ 10 meter resolution. DEM post-processing performed by MK, Winter 1997.

Scale = 1 : 9220
1 inch represents approximately 768 feet
100 0 200 400ft

State Plane Coordinate Projection
Colorado Central Zone
Datum: NAD27

U.S. Department of Energy
Rocky Flats Environmental Technology Site

GIS Dept. 303-966-7707

Prepared for: DynCorp — THE ART OF TECHNOLOGY

Prepared by: KAISER-HILL COMPANY

March 22, 2002

NT_Svr w:/projects/actinide_pathway_report/hy2002/gw_uhsu_maps/u235-uhsu-ia.aml

216

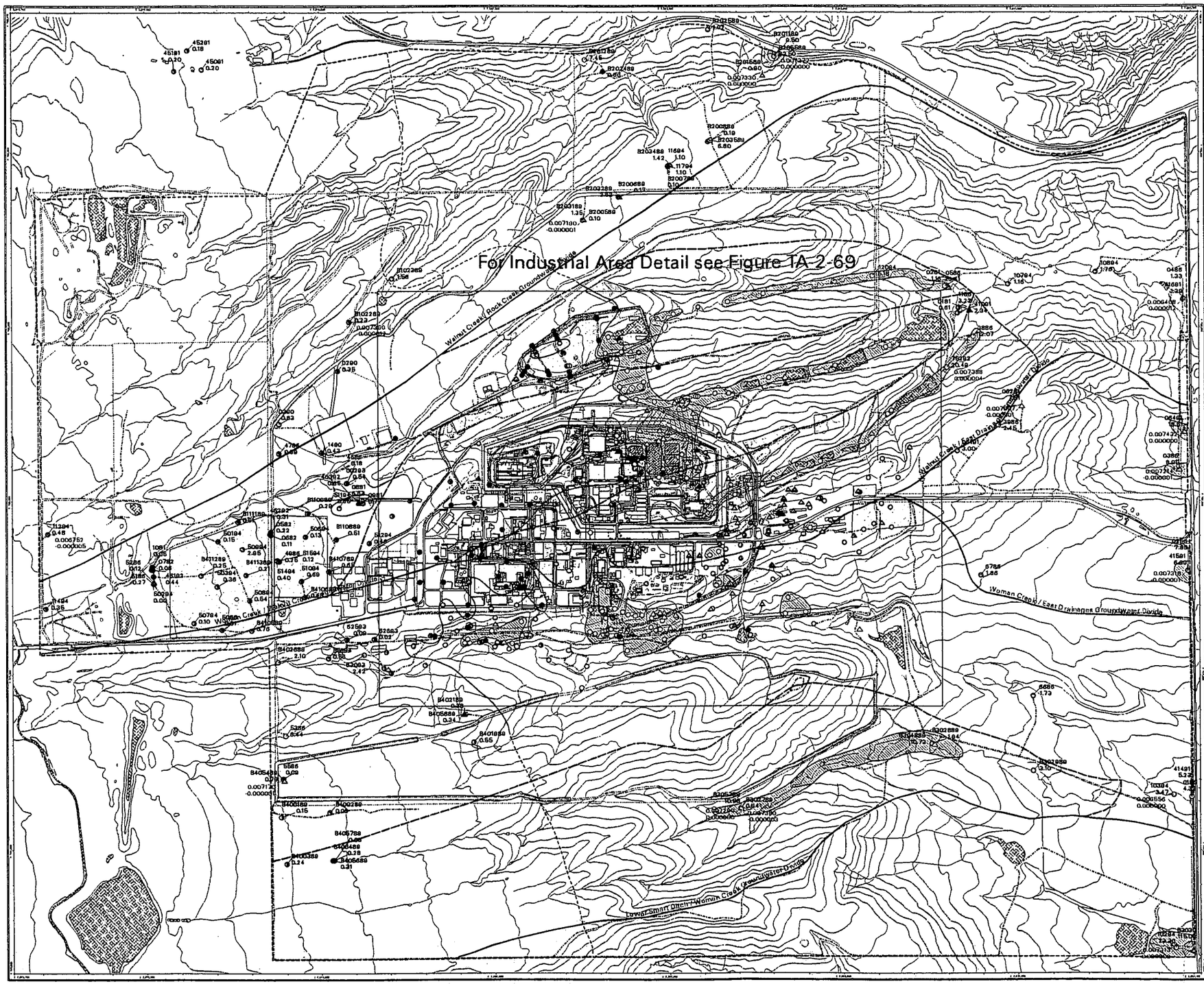

Figure TA-2-68

Actinide Migration Evaluation Pathway Report

Filtered UHSU U-238 in Groundwater, 1991 - 1999 (Avg.)

U-238 Activity-Concentration (pCi/L) (1991-99)

- 0 - 0.77
- 0.77 - 5
- 5 - 10
- 10 - 41.8
- 41.8 - 100
- > 100

- Alluvium Wells
- Bedrock Wells

Background Benchmark = 41.8 pCi/L
Action Level = 0.767 pCi/L

NOTES:
Top red value = U-235/U-238 ratio.
Bottom red value = U-236/U-238 ratio.

- Groundwater Collection and Treatment Systems
- Slurry Wall
- Active Actinide Site
- Under Building Contamination (UBC)
- Accepted as Proposed No Further Action (NFA)
- Proposed No Further Action (NFA)
- Foundation Drains
- Groundwater Basin Divides
- Groundwater Sub-Basin Divides
- U-238 concentration equal to or greater than 0.767 pCi/L (Action Level) (dashed where inferred)
- U-238 concentration equal to or greater than 5.0 pCi/L (Intermediate Level)
- U-238 concentration equal to or greater than 41.8 pCi/L (Background Level)

Standard Map Features

- Buildings and other structures
- Solar Evaporation Ponds (SEPs)
- Lakes and ponds
- Streams, ditches, or other drainage features
- Fences and other barriers
- Topographic Contour (20-Foot)
- Rocky Flats boundary
- Paved roads
- Dirt roads

DATA SOURCE BASE FEATURES:
Buildings, fences, hydrography, roads and other structures from 1994 aerial fly-over data captured by EG&G RSL, Las Vegas. Digitized from the orthophotographs. 1/95 Topographic contours were derived from digital elevation model (DEM) data by Morrison Knudson (MK) using ESRI Arc TIN and LATTICE to process the DEM data to create 5-foot contours. The DEM data was captured by the Remote Sensing Lab, Las Vegas, NV. 1994 Aerial Flyover at ~ 10 meter resolution. DEM post-processing performed by MK, Winter 1997.

Scale = 1 : 21330
1 inch represents approximately 1778 feet
250 0 500 1000 ft

State Plane Coordinate Projection
Colorado Central Zone
Datum: NAD27

U.S. Department of Energy
Rocky Flats Environmental Technology Site

DIS Dept. 303-966-7707

Prepared by DynCorp — THE ART OF TECHNOLOGY
Prepared for KAISER-HILL

NT_Svr w:/projects/actinide_pathway_report/fy2002/gw_uhsu_maps/u238-uhsu.aml

217

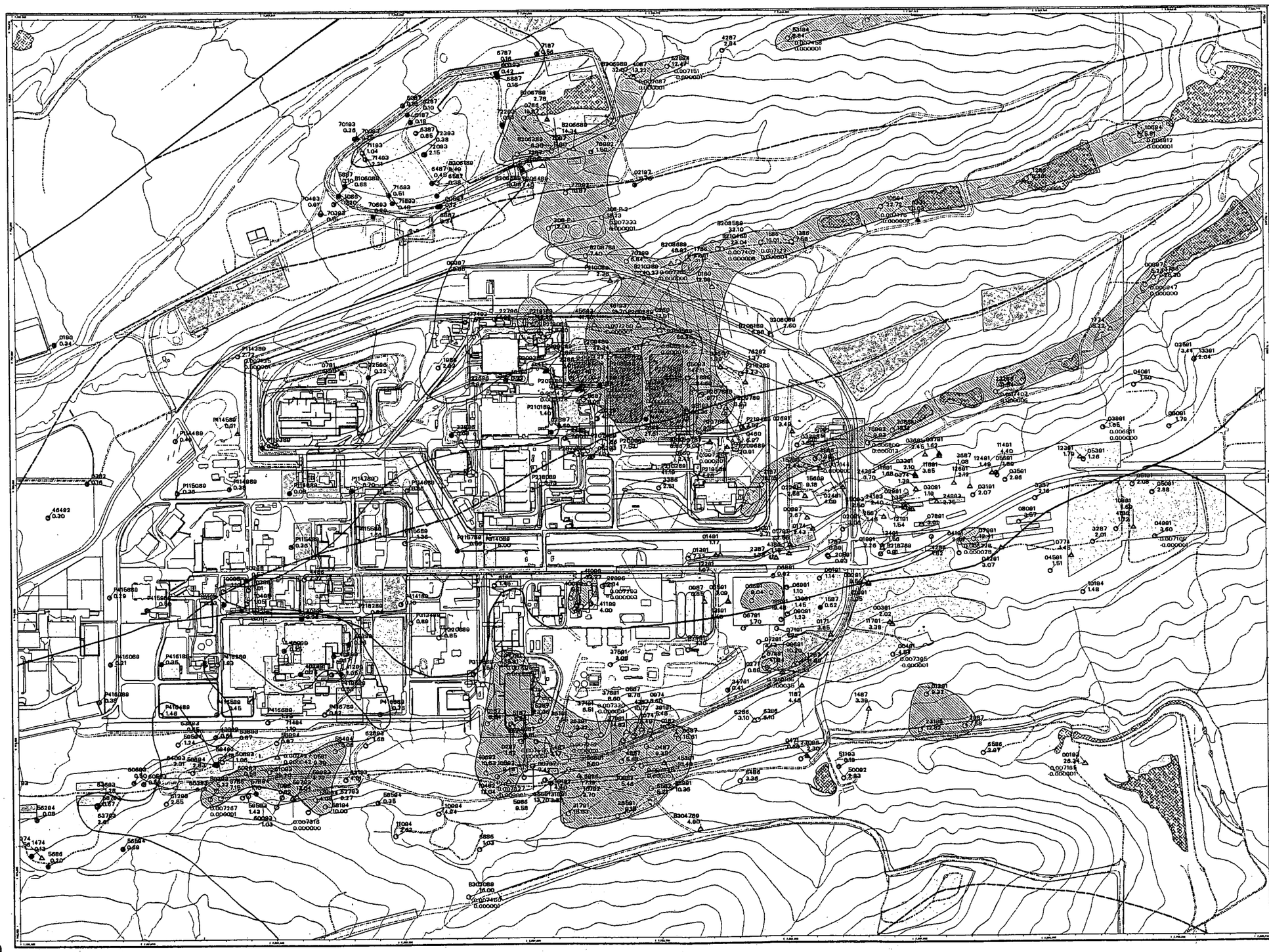

Figure TA-2-69

Actinide Migration Evaluation Pathway Report

Industrial Area

Filtered UHSU U-238 in Groundwater, 1991 - 1999 (Avg.)

U-238 Activity-Concentration (pCi/L) (1991-99)

- 0 - 0.77
- 0.77 - 5
- 5 - 10
- 10 - 41.8
- 41.8 - 100
- > 100

- Alluvium Wells
- Bedrock Wells

Background Benchmark = 41.8 pCi/L
Action Level = 0.767 pCi/L

NOTES:
Top red value = U-235/U-238 ratio.
Bottom red value = U-236/U-238 ratio.

- Groundwater Collection and Treatment Systems
- Slurry Wall
- Active Actinide Site
- Under Building Contamination (UBC)
- Accepted as Proposed No Further Action (NFA)
- Proposed No Further Action (NFA)
- Foundation Drains
- Groundwater Basin Divides
- Groundwater Sub-Basin Divides
- U-238 concentration equal to or greater than 0.767 pCi/L (Action Level) (dashed where inferred)
- U-238 concentration equal to or greater than 5.0 pCi/L (Intermediate Level)
- U-238 concentration equal to or greater than 41.8 pCi/L (Background Level)

Standard Map Features

- Buildings and other structures
- Solar Evaporation Ponds (SEPs)
- Lakes and ponds
- Streams, ditches, or other drainage features
- Fences and other barriers
- Topographic Contour (20-Foot)
- Rocky Flats boundary
- Paved roads
- Dirt roads

DATA SOURCE BASE FEATURES:
Buildings, fences, hydrography, roads and other structures from 1994 aerial fly-over data captured by EG&G RSL, Las Vegas. Digitized from the orthophotographs. 1/95 Topographic contours were derived from digital elevation model (DEM) data by Morrison Knudson (MK) using ESRI Arc TIN and LATTICE to process the DEM data to create 5-foot contours. The DEM data was captured by the Remote Sensing Lab, Las Vegas, NV, 1994 Aerial Flyover at – 10 meter resolution. DEM post-processing performed by MK, Winter 1997.

Scale = 1 : 9220
1 inch represents approximately 768 feet
100 0 200 400ft

State Plane Coordinate Projection
Colorado Central Zone
Datum: NAD27

U.S. Department of Energy
Rocky Flats Environmental Technology Site

DOE Dept. 303-966-7707

Prepared by: DynCorp — THE ART OF TECHNOLOGY

Prepared for: KAISER-HILL

March 22, 2002

NT_Svr w:/projects/actinide_pathway_report/fy2002/gw_uhsu_maps/u238-uhsu-ia.aml

218

Figure TA-2-70

Actinide Migration Evaluation Pathway Report

Unfiltered LHSU Pu-239/240 in Groundwater, 1991 - 1999 (Avg.)

Pu-239/240 Activity-Concentration (pCi/L) (1991-99)

- 0 - 0.05
- 0.05 - 0.15
- 0.15 - 0.5
- 0.5 - 1.0
- > 1.0

- Bedrock Wells
- Action Level = 0.151 pCi/L
- Active Actinide Site
- Under Building Contamination (UBC)
- Accepted as Proposed No Further Action (NFA)
- Proposed No Further Action (NFA)
- Inferred Fault

Standard Map Features

- Buildings and other structures
- Solar Evaporation Ponds (SEPs)
- Lakes and ponds
- Streams, ditches, or other drainage features
- Fences and other barriers
- Topographic Contour (20-Foot)
- Rocky Flats boundary
- Paved roads
- Dirt roads

DATA SOURCE BASE FEATURES:
Buildings, fences, hydrography, roads and other structures from 1994 aerial fly-over data captured by EG&G RSL, Las Vegas. Digitized from the orthophotographs. 1/95
Topographic contours were derived from digital elevation model (DEM) data by Morrison Knudson (MK) using ESRI Arc TIN and LATTICE to process the DEM data to create 5-foot contours. The DEM data was captured by the Remote Sensing Lab, Las Vegas, 17/, 1994 Aerial Flyover at ~ 10 meter resolution. DEM post-processing performed by MK, Winter 1997.

Scale = 1 : 21330
1 inch represents approximately 1778 feet

500 0 1000 2000ft

State Plane Coordinate Projection
Colorado Central Zone
Datum: NAD27

U.S. Department of Energy
Rocky Flats Environmental Technology Site

GIS Dept. 303-966-7707

Prepared by: DynCorp THE ART OF TECHNOLOGY

Prepared for: KAISER•HILL COMPANY

March 22, 2002

NT_Svr w:/projects/actinide_pathway_report/fy2002/gw_lhsu_maps/pu239-240-lhsu_bsize.aml

219

Figure TA-2-71

Actinide Migration Evaluation Pathway Report

Unfiltered LHSU Am-241 in Groundwater, 1991 - 1999 (Avg.)

Am-241 Activity-Concentration (pCi/L) (1991-99)

- 0 - 0.05
- 0.05 - 0.15
- 0.15 - 0.5
- 0.5 - 1.0
- > 1.0

- Bedrock Wells

Action Level = 0.145 pCi/L

- Active Actinide Site
- Under Building Contamination (UBC)
- Accepted as Proposed No Further Action (NFA)
- Proposed No Further Action (NFA)
- Inferred Fault

Standard Map Features

- Buildings and other structures
- Solar Evaporation Ponds (SEPs)
- Lakes and ponds
- Streams, ditches, or other drainage features
- Fences and other barriers
- Topographic Contour (20-Foot)
- Rocky Flats boundary
- Paved roads
- Dirt roads

DATA SOURCE BASE FEATURES:
Buildings, fences, hydrography, roads and other structures from 1994 aerial fly-over data captured by EG&G RSL, Las Vegas. Digitized from the orthophotographs. 1/95
Topographic contours were derived from digital elevation model (DEM) data by Harrison Knudsen (MK) using ESRI Arc TIN and LATTICE to process the DEM data to create 5-foot contours. The DEM data was captured by the Remote Sensing Lab, Las Vegas, NV, 1994 Aerial Flyover at ~10 meter resolution. DEM post-processing performed by MK, Winter 1997.

Scale = 1 : 21330
1 inch represents approximately 1778 feet

500 0 1000 2000 ft

State Plane Coordinate Projection
Colorado Central Zone
Datum: NAD27

U.S. Department of Energy
Rocky Flats Environmental Technology Site

GIS Dept. 303-966-7707

Prepared by: DynCorp THE ART OF TECHNOLOGY

Prepared for: KAISER•HILL COMPANY

March 22, 2002

NT_Svr w:/projects/actinide_pathway_report/fy2002/gw_lhsu_maps/am241-lhsu_bsize.aml

220

Figure TA-2-72

Actinide Migration Evaluation Pathway Report

Filtered LHSU U-233/234 in Groundwater, 1991 - 1999 (Avg.)

U-233/234 Activity-Concentration (pCi/L) (1991-99)

- 0 - 1
- 1 - 5
- 5 - 40
- 40 - 60.7
- 60.7 - 100
- > 100

Bedrock Wells

Background Benchmark = 60.7 pCi/L
Action Level = 1.07 pCi/L

Active Actinide Site

Under Building Contamination (UBC)

Accepted as Proposed No Further Action (NFA)

Proposed No Further Action (NFA)

Inferred Fault

Standard Map Features

Buildings and other structures

Solar Evaporation Ponds (SEPs)

Lakes and ponds

Streams, ditches, or other drainage features

Fences and other barriers

Topographic Contour (20-Foot)

Rocky Flats boundary

Paved roads

Dirt roads

DATA SOURCE BASE FEATURES:
Buildings, fences, hydrography, roads and other structures from 1994 aerial fly-over data captured by EG&G RSL, Las Vegas. Digitized from the orthophotographs. 1/95
Topographic contours were derived from digital elevation model (DEM) data by Morrison Knudsen (MK) using ESRI Arc TIN and LATTICE to process the DEM data to create 5-foot contours. The DEM data was captured by the Remote Sensing Lab, Las Vegas, NV, 1994 Aerial Flyover at ~ 10 meter resolution. DEM post-processing performed by MK, Winter 1997.

Scale = 1 : 21330
1 inch represents approximately 1778 feet

500 0 1000 2000ft

State Plane Coordinate Projection
Colorado Central Zone
Datum: NAD27

U.S. Department of Energy
Rocky Flats Environmental Technology Site

GIS Dept. 303-966-7707

Prepared by: DynCorp THE ART OF TECHNOLOGY

Prepared for: KAISER-HILL COMPANY

March 22, 2002

NT_Svr w:/projects/actinide_pathway_report/fy2002/gw_lhsu_maps/u233-234-lhsu_bsize.aml

221

Figure TA-2-73

Actinide Migration Evaluation Pathway Report

Filtered LHSU U-235 in Groundwater, 1991 - 1999 (Avg.)

U-235 Activity-Concentration (pCi/L) (1991-99)

- 0 - 0.1
- 0.1 - 0.5
- 0.5 - 1.0
- 1.0 - 1.79
- 1.79 - 5
- > 5

Bedrock Wells

Background Benchmark = 1.79 pCi/L
Action Level = 1.01 pCi/L

Active Actinide Site

Under Building Contamination (UBC)

Accepted as Proposed No Further Action (NFA)

Proposed No Further Action (NFA)

Inferred Fault

Standard Map Features

Buildings and other structures

Solar Evaporation Ponds (SEPs)

Lakes and ponds

Streams, ditches, or other drainage features

Fences and other barriers

Topographic Contour (20-Foot)

Rocky Flats boundary

Paved roads

Dirt roads

DATA SOURCE BASE FEATURES:
Buildings, fences, hydrography, roads and other structures from 1994 aerial fly-over data captured by EG&G RSL, Las Vegas. Digitized from the orthophotographs. 1/95
Topographic contours were derived from digital elevation model (DEM) data by Morrison Knudsen (MK) using ESRI Arc TIN and LATTICE to process the DEM data to create 5-foot contours. The DEM data was captured by the Remote Sensing Lab, Las Vegas, NV, 1994 Aerial Flyover at ~10 meter resolution. DEM post-processing performed by MK, Winter 1997.

Scale = 1 : 21330
1 inch represents approximately 1778 feet

State Plane Coordinate Projection
Colorado Central Zone
Datum: NAD27

U.S. Department of Energy
Rocky Flats Environmental Technology Site

GIS Dept. 303-966-7707

Prepared by: DynCorp THE ART OF TECHNOLOGY

Prepared for: KAISER•HILL COMPANY

March 22, 2002

NT_Svr w:/projects/actinide_pathway_report/fy2002/gw_lhsu_maps/u235-lhsu_beize.aml

222

Figure TA-2-74

Actinide Migration Evaluation Pathway Report

Filtered LHSU U-238 in Groundwater, 1991 - 1999 (Avg.)

U-238 Activity-Concentration (pCi/L) (1991-99)

- 0 - 0.77
- 0.77 - 5
- 5 - 10
- 10 - 41.8
- 41.8 - 100
- > 100

Bedrock Wells

Background Benchmark = 41.8 pCi/L
Action Level = 0.767 pCi/L

Active Actinide Site

Under Building Contamination (UBC)

Accepted as Proposed No Further Action (NFA)

Proposed No Further Action (NFA)

Inferred Fault

Standard Map Features

Buildings and other structures

Solar Evaporation Ponds (SEPs)

Lakes and ponds

Streams, ditches, or other drainage features

Fences and other barriers

Topographic Contour (20-Foot)

Rocky Flats boundary

Paved roads

Dirt roads

DATA SOURCE BASE FEATURES:
Buildings, fences, hydrography, roads and other structures from 1994 aerial fly-over data captured by EG&G RSL, Las Vegas. Digitized from the orthophotographs. 1/95
Topographic contours were derived from digital elevation model (DEM) data by Harrison Knudsen (MK) using ESRI Arc TIN and LATTICE to process the DEM data to create 5-foot contours. The DEM data was captured by the Remote Sensing Lab, Las Vegas, NV, 1994 Aerial Flyover at ~10 meter resolution. DEM post-processing performed by MK, Winter 1997.

Scale = 1 : 21330
1 inch represents approximately 1778 feet

State Plane Coordinate Projection
Colorado Central Zone
Datum: NAD27

U.S. Department of Energy
Rocky Flats Environmental Technology Site

GIS Dept. 303-966-7707

Prepared by: DynCorp THE ART OF TECHNOLOGY

Prepared for: KAISER+HILL COMPANY

March 22, 2002

NT_Svr w:/projects/actinide_pathway_report/fy2002/gw_lhsu_maps/u238-lhsu_bsize.aml

223

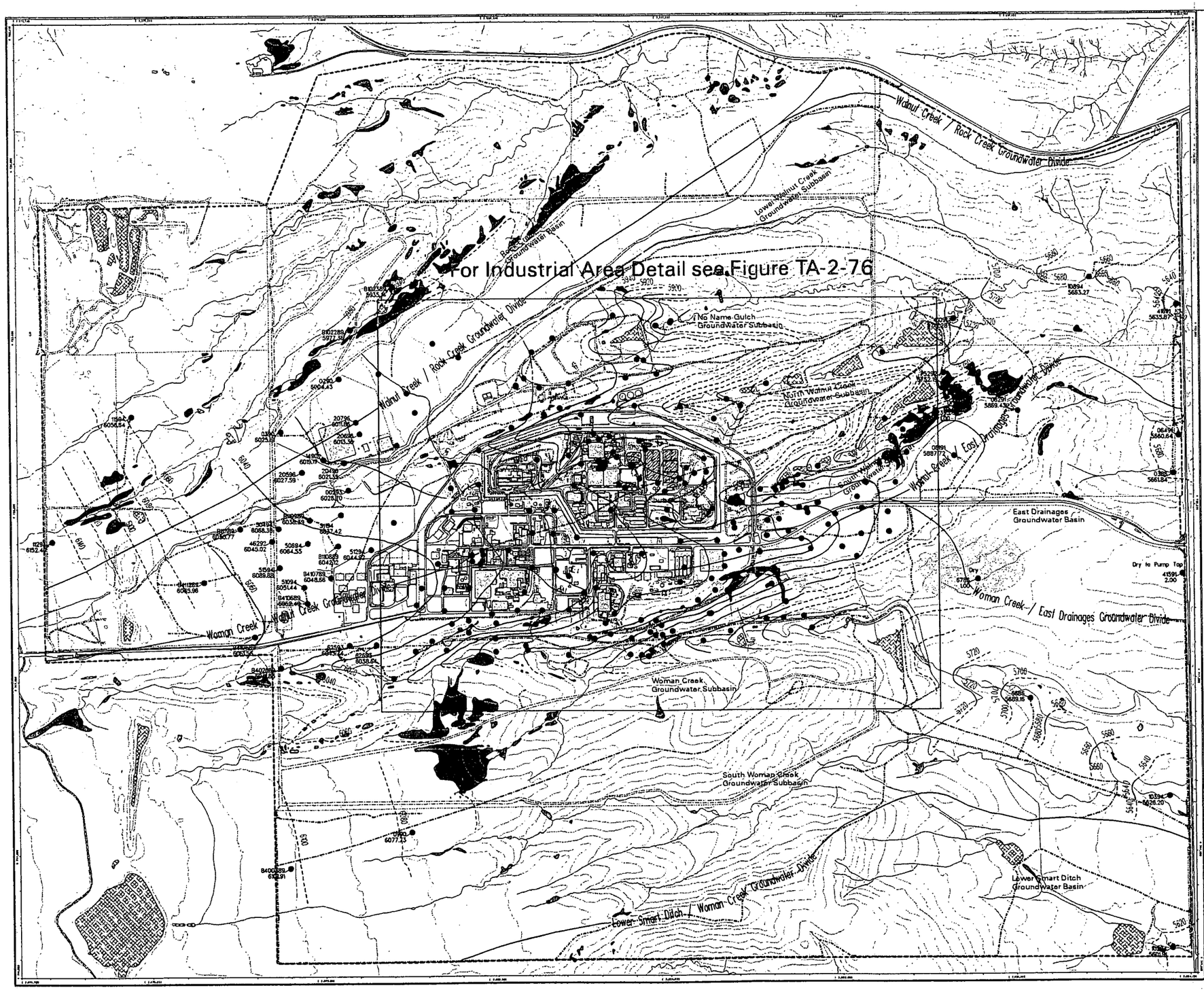

Figure TA-2-75

Actinide Migration Evaluation Pathway Report

Groundwater Basins & Divides for Permeable Units of the UHSU

- Groundwater Monitoring Well
- Water Level Contour
- Dashed where inferred
- Foundation Drain
- Approximate location of Groundwater Basin Divide
- Approximate location of Groundwater Subbasin Divide
- Approximate extent of Unsaturated Area
- Area without Groundwater Elevation Data
- Seeps

Standard Map Features

- Buildings and other structures
- Solar Evaporation Ponds (SEPs)
- Lakes and ponds
- Streams, ditches, or other drainage features
- Fences and other barriers
- Topographic Contour (20-Foot)
- Rocky Flats boundary
- Paved roads
- Dirt roads

DATA SOURCE BASE FEATURES:

Buildings, fences, hydrography, roads and other structures from 1994 aerial fly-over data captured by EG&G RSL, Las Vegas. Digitized from the orthophotographs. 1/95

Topographic contours were derived from digital elevation model (DEM) data by Morrison Knudson (MK) using ESRI Arc TIN and LATTICE to process the DEM data to create 5-foot contours. The DEM data was captured by the Remote Sensing Lab, Las Vegas, NV, 1994 Aerial Flyover at ~ 10 meter resolution. DEM post-processing performed by MK, Winter 1997.

Scale = 1 : 21330
1 inch represents approximately 1778 feet

250 0 500 1000 ft

State Plane Coordinate Projection
Colorado Central Zone
Datum: NAD27

U.S. Department of Energy
Rocky Flats Environmental Technology Site

GIS Dept. 303-966-7707

Prepared by: DynCorp — THE ART OF TECHNOLOGY

Prepared for: KAISER-HILL COMPANY

MAP ID: pot_maps

March 06, 2002

NT_Svr w:/projects/actinide_pathway_report/fy2002/pot_maps/potent99fall.aml

224

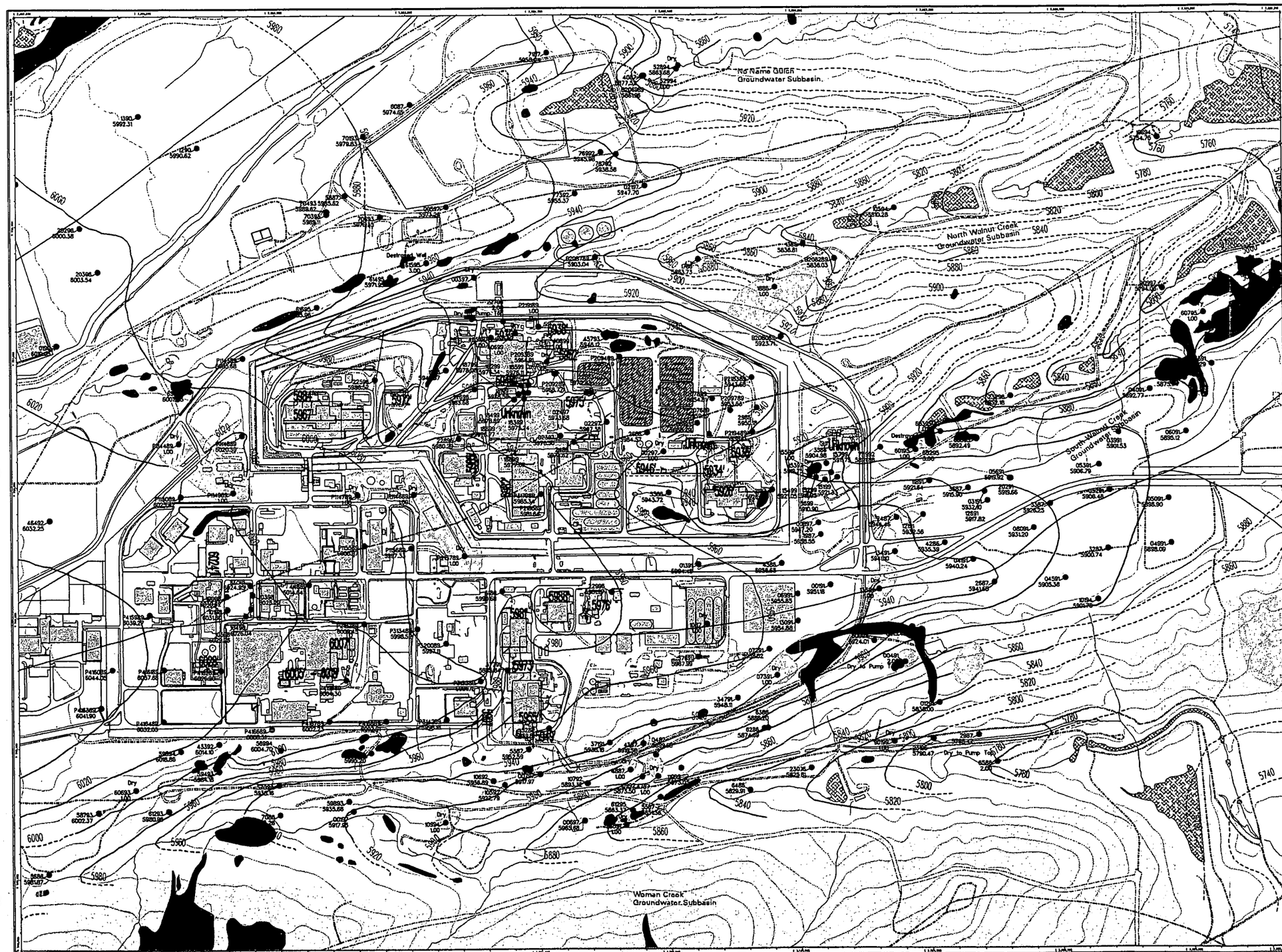

Figure TA-2-76

Actinide Migration Evaluation Pathway Report

Industrial Area

Groundwater Basins & Divides for Permeable Units of the UHSU

- Groundwater Monitoring Well
- Water Level Contour
- Dashed where inferred
- Foundation Drain
- Approximate location of Groundwater Basin Divide
- Approximate location of Groundwater Subbasin Divide
- Approximate extent of Unsaturated Area
- Area without Groundwater Elevation Data
- Seeps

Standard Map Features

- Buildings and other structures
- Solar Evaporation Ponds (SEPs)
- Lakes and ponds
- Streams, ditches, or other drainage features
- Fences and other barriers
- Topographic Contour (20-Foot)
- Rocky Flats boundary
- Paved roads
- Dirt roads

DATA SOURCE BASE FEATURES:

Buildings, fences, hydrography, roads and other structures from 1994 aerial fly-over data captured by EG&G RSL, Las Vegas. Digitized from the orthophotographs. 1/95

Topographic contours were derived from digital elevation model (DEM) data by Morrison Knudson (MK) using ESRI Arc TIN and LATTICE to process the DEM data to create 5-foot contours. The DEM data was captured by the Remote Sensing Lab, Las Vegas, NV, 1994 Aerial Flyover at ~ 10 meter resolution. DEM post-processing performed by MK, Winter 1997.

Scale = 1 : 8230
1 inch represents approximately 768 feet

100 0 200 400ft

State Plane Coordinate Projection
Colorado Central Zone
Datum: NAD27

U.S. Department of Energy
Rocky Flats Environmental Technology Site

Prepared by: DynCorp THE ART OF TECHNOLOGY

Prepared for: KAISER-HILL COMPANY

NT_Svr w:/projects/actinide_pathway_report/fy2002/pot_maps/potent99fall-ia.aml

225

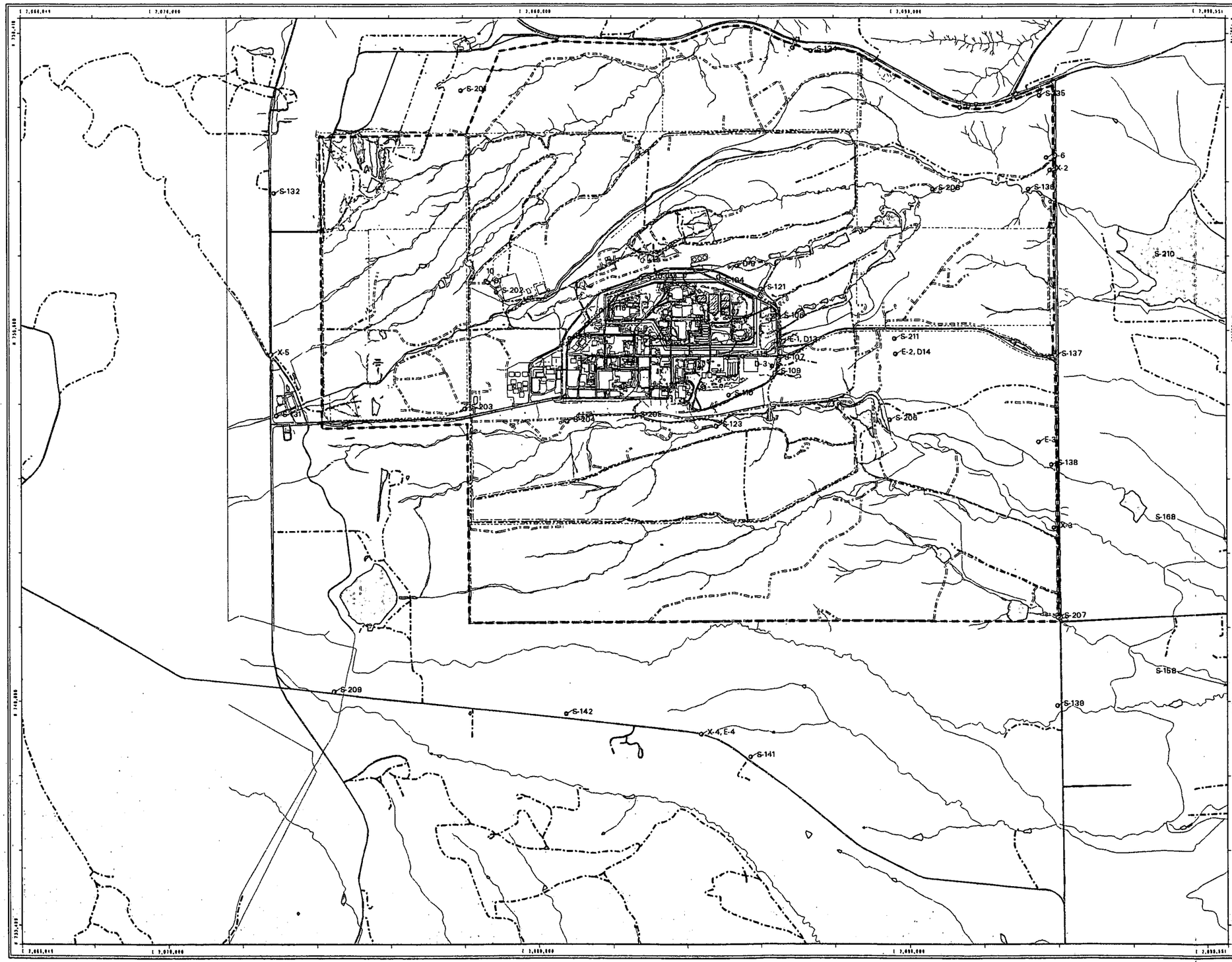

Figure TA-2-77

Actinide Migration Evaluation Pathway Report

Air Sampling Location Map

LEGEND

- Air monitoring locations

Standard Map Features

- Buildings and other structures
- Solar Evaporation Ponds (SEPs)
- Lakes and ponds
- Streams, ditches, or other drainage features
- Fences and other barriers
- Rocky Flats boundary
- Heavy duty paved roads
- Medium duty paved roads
- Light duty paved roads
- Dirt roads

DATA SOURCE BASE FEATURES:
Buildings, fences, hydrography, roads and other structures from 1994 aerial fly-over data captured by EG&G RSL, Las Vegas. Digitized from the orthophotography. 1/95

DISCLAIMER:
Neither the United States Government nor Kaiser Hill Co., nor DynCorp I&ET, nor any agency thereof, nor any of their employees, makes any warranty, express or implied, or assumes any legal liability or responsibility for the accuracy, completeness, or usefulness of any information, apparatus, product, or process disclosed, or represents that its use would not infringe privately owned rights.

Scale = 1 : 32160
1 inch represents 2680 feet

700 0 1400 2800ft

State Plane Coordinate Projection
Colorado Central Zone
Datum: NAD27

U.S. Department of Energy
Rocky Flats Environmental Technology Site

GIS Dept. 303-966-7707

Prepared by: DynCorp — THE ART OF TECHNOLOGY

Prepared for: KAISER-HILL COMPANY

MAP ID: misc_maps/air_sampling.aml

January 21, 2002

NT_Svr w:/projects/actinide_pathway_report/fy2002/misc_maps/air_sampling.aml

226

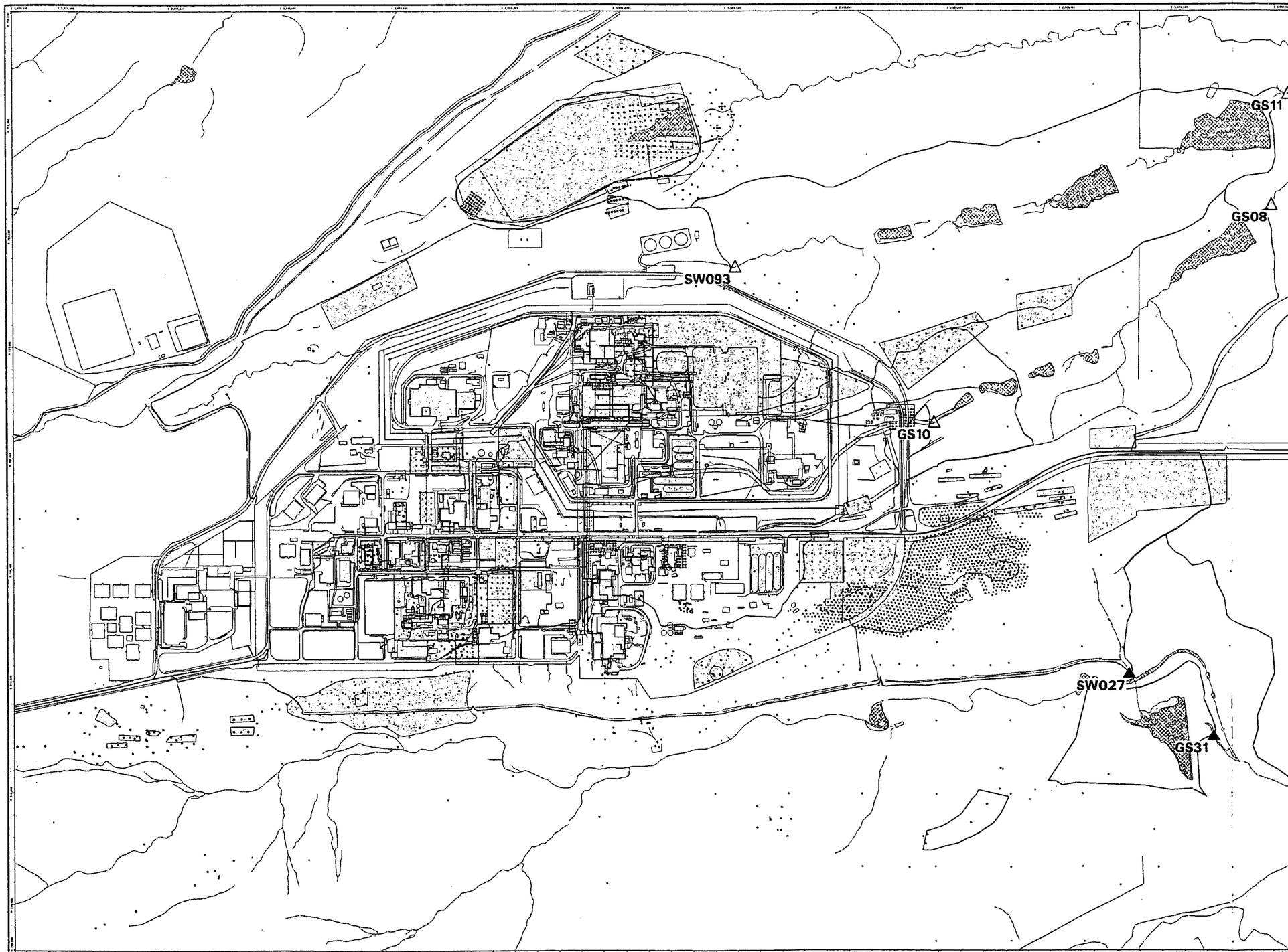

Figure TA-4-3

Actinide Migration Evaluation Pathway Report

Actinide Sources and Sample Locations

Sample Locations

- Surface Soil Sample Locations
- Sub-Surface Soil Sample Locations

Actinide Sources

- Active Actinide Site
- Original Process Waste Line (OPWL)
- Location of Original Process Waste Lines which may have been removed.
- New Process Waste Lines
- Under Building Contamination (UBC)
- Accepted as Proposed No Further Action (NFA)
- IHSS with sub-surface contamination but no validated sub-surface data

Drainage Basins

- Drainage Basin Boundary
- Walnut Creek Basin Gaging Station (GS03, GS08, GS10, GS11 & SW093)
- Woman Creek Basin Gaging Station (GS01, GS31 & SW027)

Standard Map Features

- Buildings and other structures
- Lakes and ponds
- Streams, ditches, or other drainage features
- Fences and other barriers
- Rocky Flats boundary
- Paved roads

DATA SOURCE BASE FEATURES:

Buildings, fences, hydrography, roads and other structures from 1994 aerial fly-over data captured by EG&G RSL, Las Vegas. Digitized from the orthophotographs. 1/95

NOTES:

The Sanitary Sewer and Storm Drain systems at the site are included on the Active IHSS list but are not included on the map. Area investigations will be performed to determine which portions of these systems will ultimately be on the NFA list.

Scale = 1 : 10870
1 inch represents approximately 906 feet

100 0 200 400 ft

State Plane Coordinate Projection
Colorado Central Zone
Datum: NAD27

U.S. Department of Energy
Rocky Flats Environmental Technology Site

GIS Dept. 303-966-7707

Prepared by: DynCorp THE ART OF TECHNOLOGY

Prepared for: KAISER-HILL COMPANY

NT_Svr w:/projects/actinide_pathway_report/fy2002/act_sro_samples_maps/act_sro_samples.aml

504

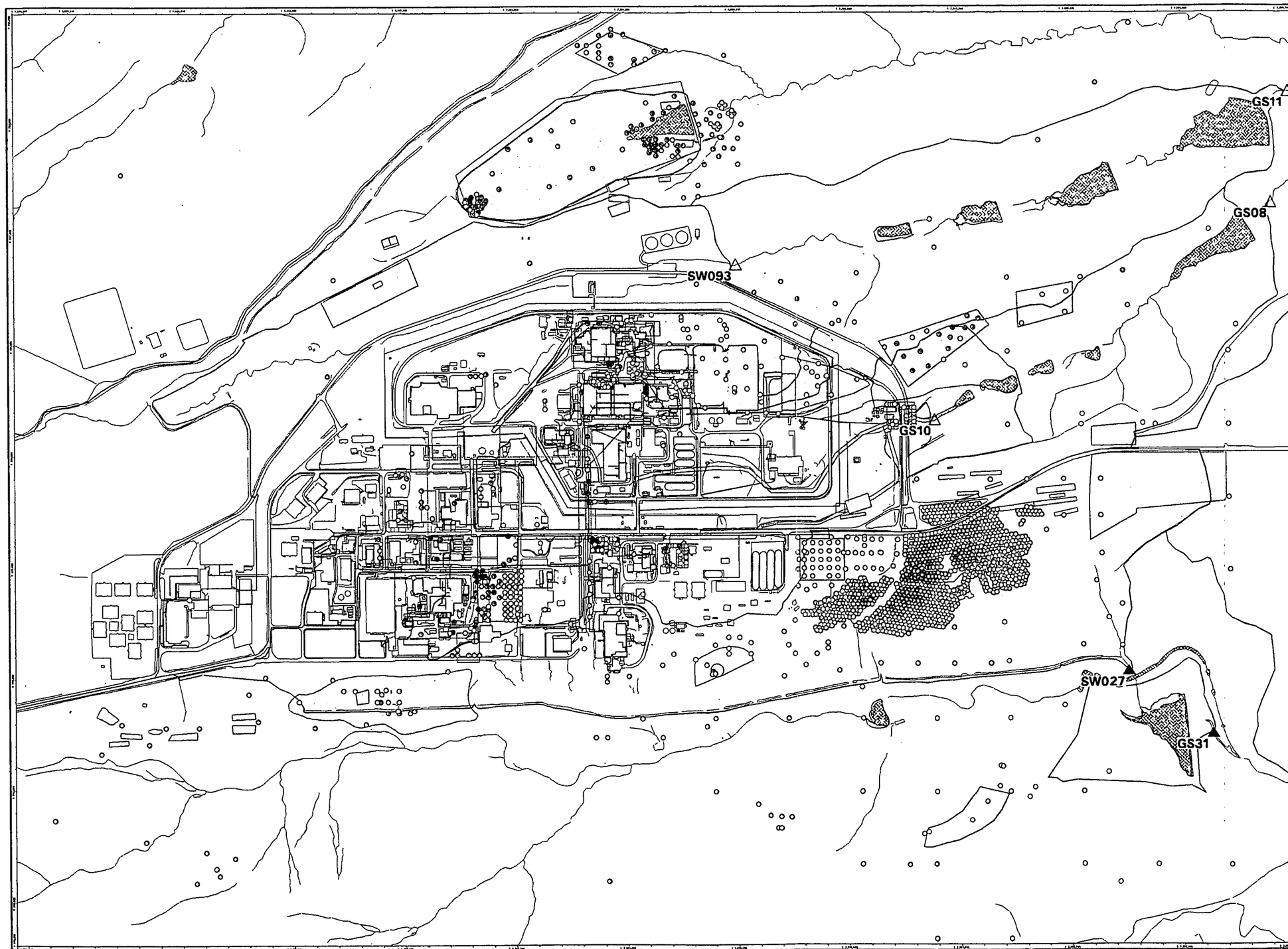

Figure TA-4-4

Actinide Migration Evaluation Pathway Report

Actinide Sources and Pu-239/240 in Surface Soils above Background (0.04 pCi/g)

EXPLANATION

Sample Locations (pCi/g)

- 0.04 < Result < = 0.05
- 0.05 < Result < = 0.1
- 0.1 < Result < = 0.5
- 0.5 < Result < = 1.0
- 1.0 < Result < = 5.0
- 5.0 < Result < = 10.0
- 10.0 < Result < = 100.0
- 100.0 < Result < = 1000.0
- Result > 1000.0

Actinide Sources

- Active Actinide Site
- Original Process Waste Line (OPWL)
- Location of Original Process Waste Lines which may have been removed.
- New Process Waste Lines
- Under Building Contamination (UBC)
- Accepted as Proposed No Further Action (NFA)
- IHSS with sub-surface contamination but no validated sub-surface data

Drainage Basins

- Drainage Basin Boundary
- Walnut Creek Basin Gaging Station (GS03, GS08, GS10, GS11 & SW093)
- Woman Creek Basin Gaging Station (GS01, GS31 & SW027)

Standard Map Features

- Buildings and other structures
- Lakes and ponds
- Streams, ditches, or other drainage features
- Rocky Flats boundary
- Paved roads

DATA & SOURCE BASE FEATURES:

Buildings, fences, hydrography, roads and other structures from 1994 aerial fly-over data captured by EG&G RSL, Las Vegas. Digitized from the orthophotographs. 1/95
Surface Soil Locations as of October 1999.

Analytical Data from SWD as of October 1999.

903 Pad data from 903 Drum Storage Area Characterization Report, September 1999.

Data Analysis performed by Wright Water Engineers (303-480-1700).

Scale = 1 : 10800
1 inch represents 900 feet

100 0 200 400 ft

State Plane Coordinate Projection
Colorado Central Zone
Datum: NAD27

U.S. Department of Energy
Rocky Flats Environmental Technology Site

GIS Dept. 303-966-7707

Prepared by: DynCorp

Prepared for: KH Kaiser-Hill

NT_Svr w:/projects/actinide_pathway_report/fy2002/act_src_samples_maps/pu239-240_bkgd.aml

February 13, 2002

505

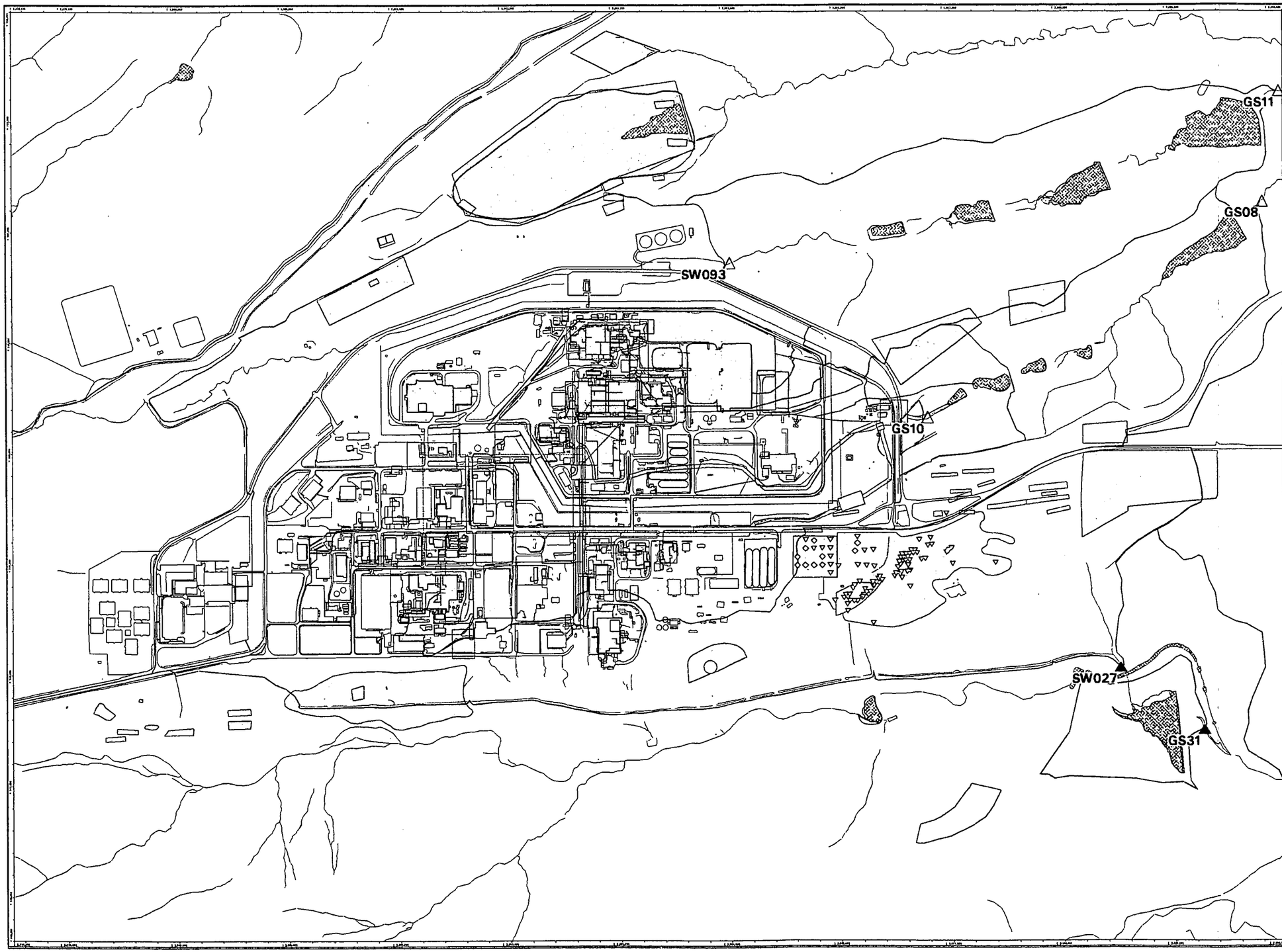

Figure TA-4-5

Actinide Migration Evaluation Pathway Report

Actinide Sources and Pu-239/240 in Surface Soils above RFCA Tier II (252.0 pCi/g)

EXPLANATION

Sample Locations (pCi/g)

- 252.0 < = Result < 1000.0
- 1000.0 < = Result < 1429.0
- Result > = 1429.0 (Tier I)

Actinide Sources

- Active Actinide Site
- Original Process Waste Line (OPWL)
- Location of Original Process Waste Lines which may have been removed.
- New Process Waste Lines
- Under Building Contamination (UBC)
- Accepted as Proposed No Further Action (NFA)
- IHSS with sub-surface contamination but no validated sub-surface data

Drainage Basins

- Drainage Basin Boundary
- Walnut Creek Basin Gaging Station (GS03, GS08, GS10, GS11 & SW093)
- Woman Creek Basin Gaging Station (GS01, GS31 & SW027)

Standard Map Features

- Buildings and other structures
- Lakes and ponds
- Streams, ditches, or other drainage features
- Rocky Flats boundary
- Paved roads

DATA SOURCE BASE FEATURES:

Buildings, fences, hydrography, roads and other structures from 1994 aerial fly-over data captured by EG&G RSL, Las Vegas. Digitized from the orthophotographs. 1/95
Surface Soil Locations as of October 1999.

Analytical Data from SWD as of October 1999.

903 Pad data from 903 Drum Storage Area Characterization Report, September 1999.

Data Analysis performed by Wright Water Engineers (303-480-1700).

Scale = 1 : 10820
1 inch represents approximately 902 feet

100 0 200 400 ft

State Plane Coordinate Projection
Colorado Central Zone
Datum: NAD27

U.S. Department of Energy
Rocky Flats Environmental Technology Site

GIS Dept. 303-966-7707

Prepared by: DynCorp — THE ART OF TECHNOLOGY

Prepared for: KAISER-HILL

NT_Svr w:/projects/actinide_pathway_report/fy2002/act_sro_samples_maps/pu239-240_tier2.aml

506

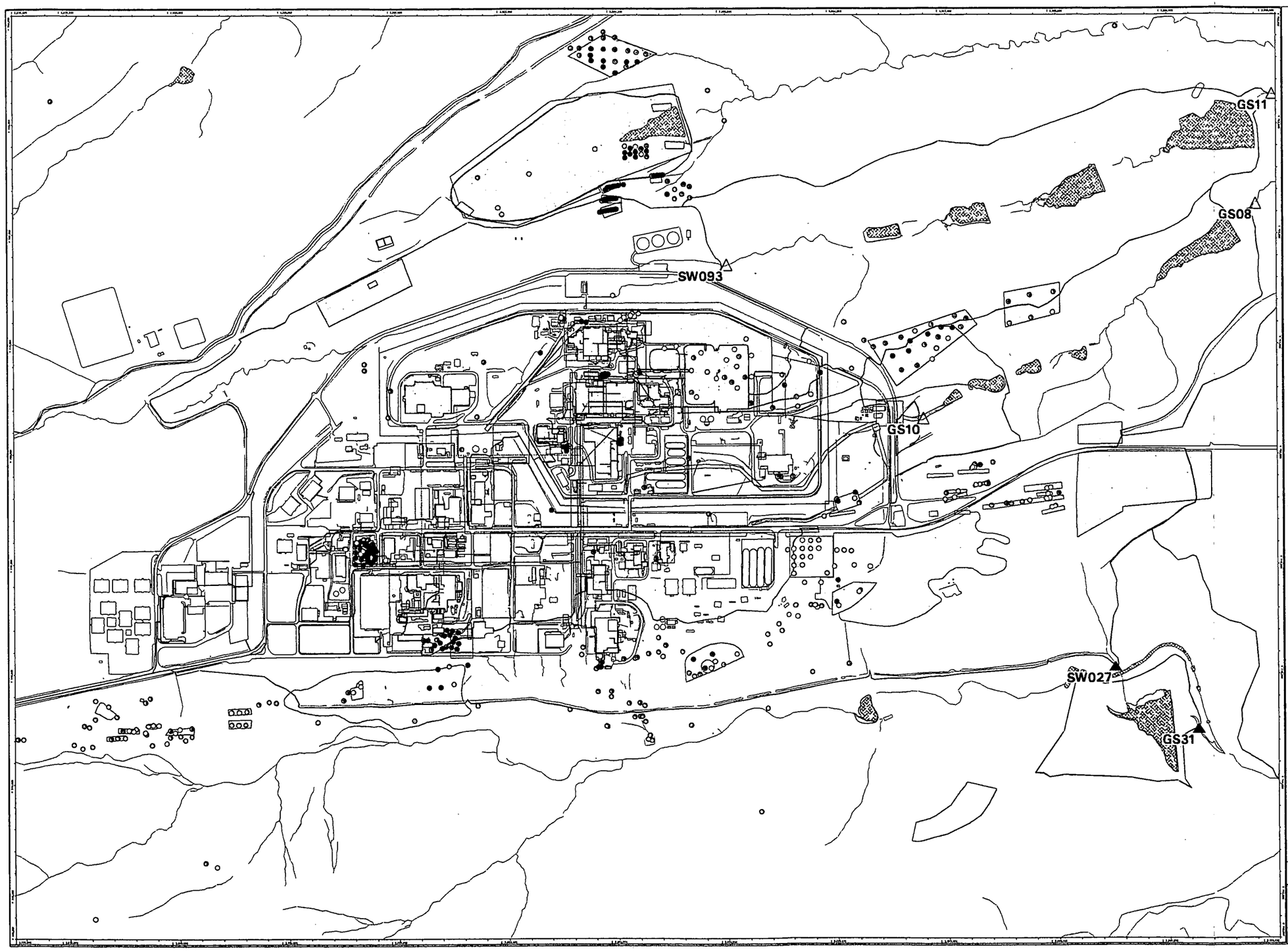

Figure TA-4-6

Actinide Migration Evaluation Pathway Report

Actinide Sources and Pu-239/240 in Sub-Surface Soils above Background (0.00 pCi/g)

EXPLANATION

Sample Locations (pCi/g)

- 0.00 < Result < = 0.01
- 0.01 < Result < = 0.05
- 0.05 < Result < = 0.1
- 0.1 < Result < = 0.5
- 0.5 < Result < = 1.0
- 1.0 < Result < = 5.0
- 5.0 < Result < = 10.0
- 10.0 < Result < = 100.0
- 100.0 < Result < = 1000.0
- Result > 1000.0

Actinide Sources

- Active Actinide Site
- Original Process Waste Line (OPWL)
- Location of Original Process Waste Lines which may have been removed.
- New Process Waste Lines
- Under Building Contamination (UBC)
- Accepted as Proposed No Further Action (NFA)
- IHSS with sub-surface contamination but no validated sub-surface data

Drainage Basins

- Drainage Basin Boundary
- Walnut Creek Basin Gaging Station (GS03, GS08, GS10, GS11 & SW093)
- Woman Creek Basin Gaging Station (GS01, GS31 & SW027)

Standard Map Features

- Buildings and other structures
- Lakes and ponds
- Streams, ditches, or other drainage features
- Rocky Flats boundary
- Paved roads

DATA SOURCE BASE FEATURES:
Buildings, fences, hydrography, roads and other structures from 1994 aerial fly-over data captured by EG&G RSL, Las Vegas.
Digitized from the orthophotographs. 1/95
Analytical Data from SWD as of October 2000.

Data Analysis performed by Wright Water engineers (303-480-1700).

Scale = 1 : 10820
1 inch represents approximately 902 feet

100 0 200 400 ft

State Plane Coordinate Projection
Colorado Central Zone
Datum: NAD27

U.S. Department of Energy
Rocky Flats Environmental Technology Site

GIS Dept. 303-966-7797

Prepared by: DynCorp — THE ART OF TECHNOLOGY

Prepared for: KH KAISER-HILL

MT_Svr w:/projects/actinide_pathway_report/fy2002/act_src_samples_maps/pu239-240_sub_surf_bkgd.aml

507

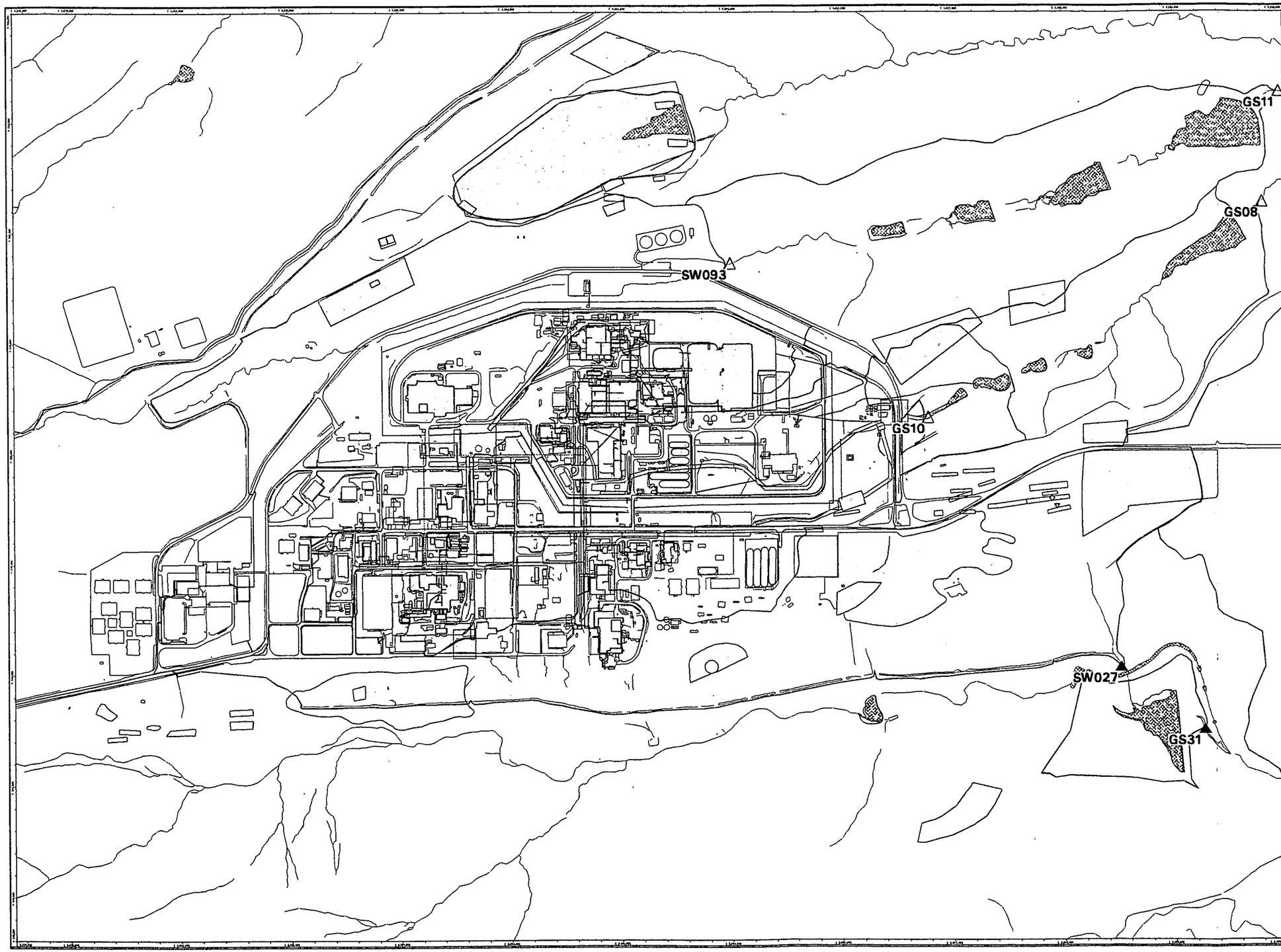

Figure TA-4-7

Actinide Migration Evaluation Pathway Report

Actinide Sources and Pu-239/240 in Sub-Surface Soils above RFCA Tier II (252.0 pCi/g)

EXPLANATION

Sample Locations (pCi/g)

- ▽ 252.0 < = Result < 1000.0
- ▽ 1000.0 < = Result < 1429.0
- ◇ Result > = 1429.0 (Tier I)

Actinide Sources

- Active Actinide Site
- Original Process Waste Line (OPWL)
- Location of Original Process Waste Lines which may have been removed.
- New Process Waste Lines
- Under Building Contamination (UBC)
- Accepted as Proposed No Further Action (NFA)
- IHSS with sub-surface contamination but no validated sub-surface data

Drainage Basins

- Drainage Basin Boundary
- Walnut Creek Basin Gaging Station (GS03, GS08, GS10, GS11 & SW093)
- Woman Creek Basin Gaging Station (GS01, GS31 & SW027)

Standard Map Features

- Buildings and other structures
- Lakes and ponds
- Streams, ditches, or other drainage features
- Rocky Flats boundary
- Paved roads

DATA SOURCE BASE FEATURES:

Buildings, fences, hydrography, roads and other structures from 1994 aerial fly-over data captured by EG&G RSL, Las Vegas. Digitized from the orthophotographs. 1/95
Analytical Data from SWD as of October 2000.

Data Analysis performed by Wright Water engineers (303-480-1700).

Scale = 1 : 10820
1 inch represents approximately 902 feet

100 0 200 400 ft

State Plane Coordinate Projection
Colorado Central Zone
Datum: NAD27

U.S. Department of Energy
Rocky Flats Environmental Technology Site

GIS Dept. 303-966-7707

Prepared by: DynCorp THE ART OF TECHNOLOGY

Prepared for: KAISER-HILL PROJECT

NT_Sw w:/projects/actinide_pathway_report/fy2002/act_sro_samples_maps/pu239-240_sub_surf_tier2.aml

508

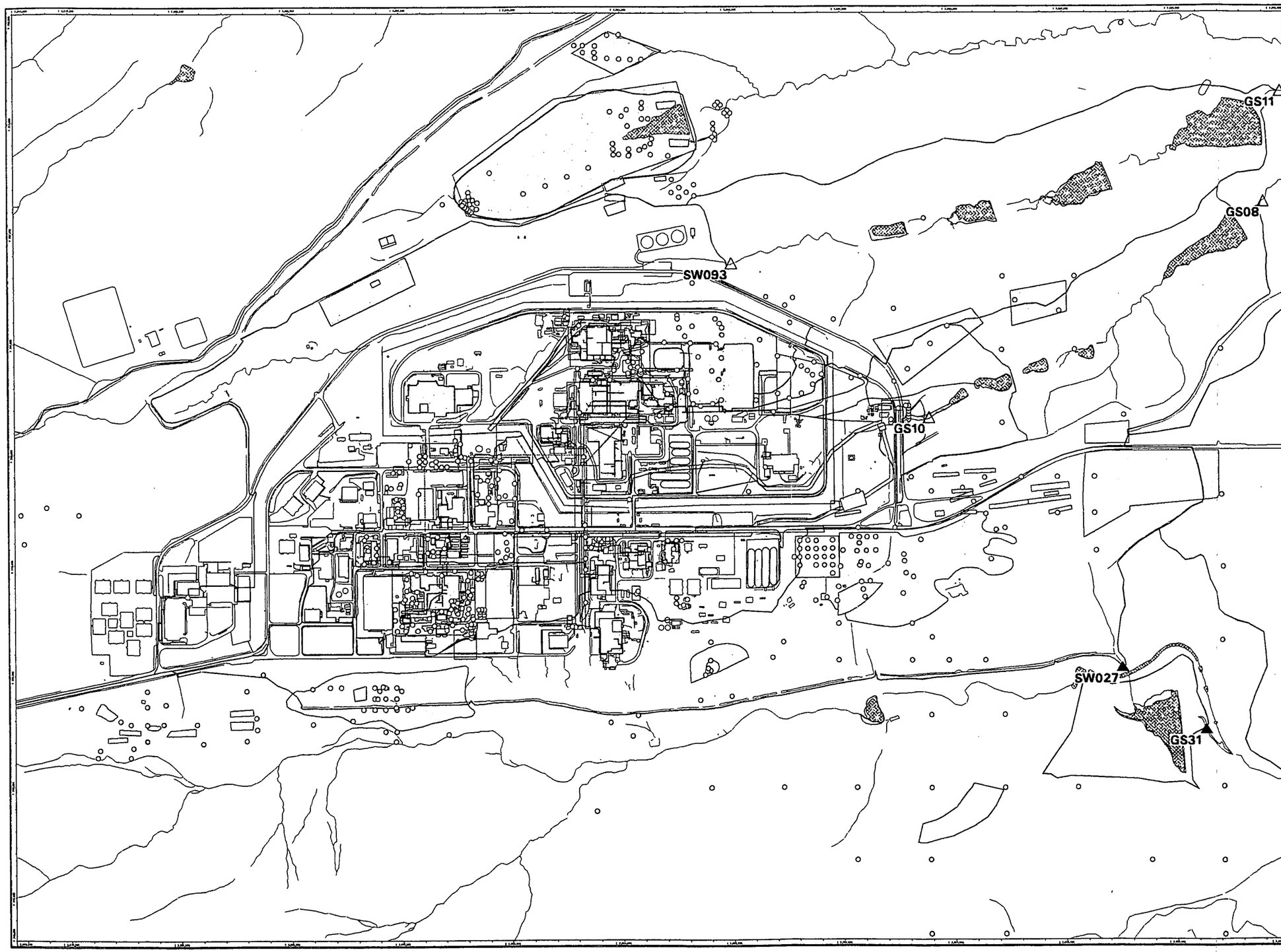

Figure TA-4-8

Actinide Migration Evaluation Pathway Report

Actinide Sources and U-238 in Surface Soils above Background (1.09 pCi/g)

EXPLANATION

Sample Locations (pCi/g)

- 1.09 < Result < = 5.0
- 5.0 < Result < = 10.0
- 10.0 < Result < = 100.0
- 100.0 < Result < = 1000.0
- Result > 1000.0

Actinide Sources

- Active Actinide Site
- Original Process Waste Line (OPWL)
- Location of Original Process Waste Lines which may have been removed.
- New Process Waste Lines
- Under Building Contamination (UBC)
- Accepted as Proposed No Further Action (NFA)
- IHSS with sub-surface contamination but no validated sub-surface data

Drainage Basins

- Drainage Basin Boundary
- Walnut Creek Basin Gaging Station (GS03, GS08, GS10, GS11 & SW093)
- Woman Creek Basin Gaging Station (GS01, GS31 & SW027)

Standard Map Features

- Buildings and other structures
- Lakes and ponds
- Streams, ditches, or other drainage features
- Rocky Flats boundary
- Paved roads

DATA SOURCE BASE FEATURES:
Buildings, fences, hydrography, roads and other structures from 1994 aerial fly-over data captured by EG&G RSL, Las Vegas. Digitized from the orthophotographs. 1/95

Analytical Data provided by Mark Wood (KH, 303-966-6689).

Data Analysis performed by Wright Water Engineers (303-480-1700).

Scale = 1 : 10800
1 inch represents 900 feet
100 0 200 400 ft

State Plane Coordinate Projection
Colorado Central Zone
Datum: NAD27

U.S. Department of Energy
Rocky Flats Environmental Technology Site

GIS Dept. 303-966-7707

Prepared by: DynCorp THE ART OF TECHNOLOGY

Prepared for: KH KAISER-HILL COMPANY

NT_Svr w:/projects/actinide_pathway_report/fy2002/act_sro_sample_maps/u238_bkgd.aml

509

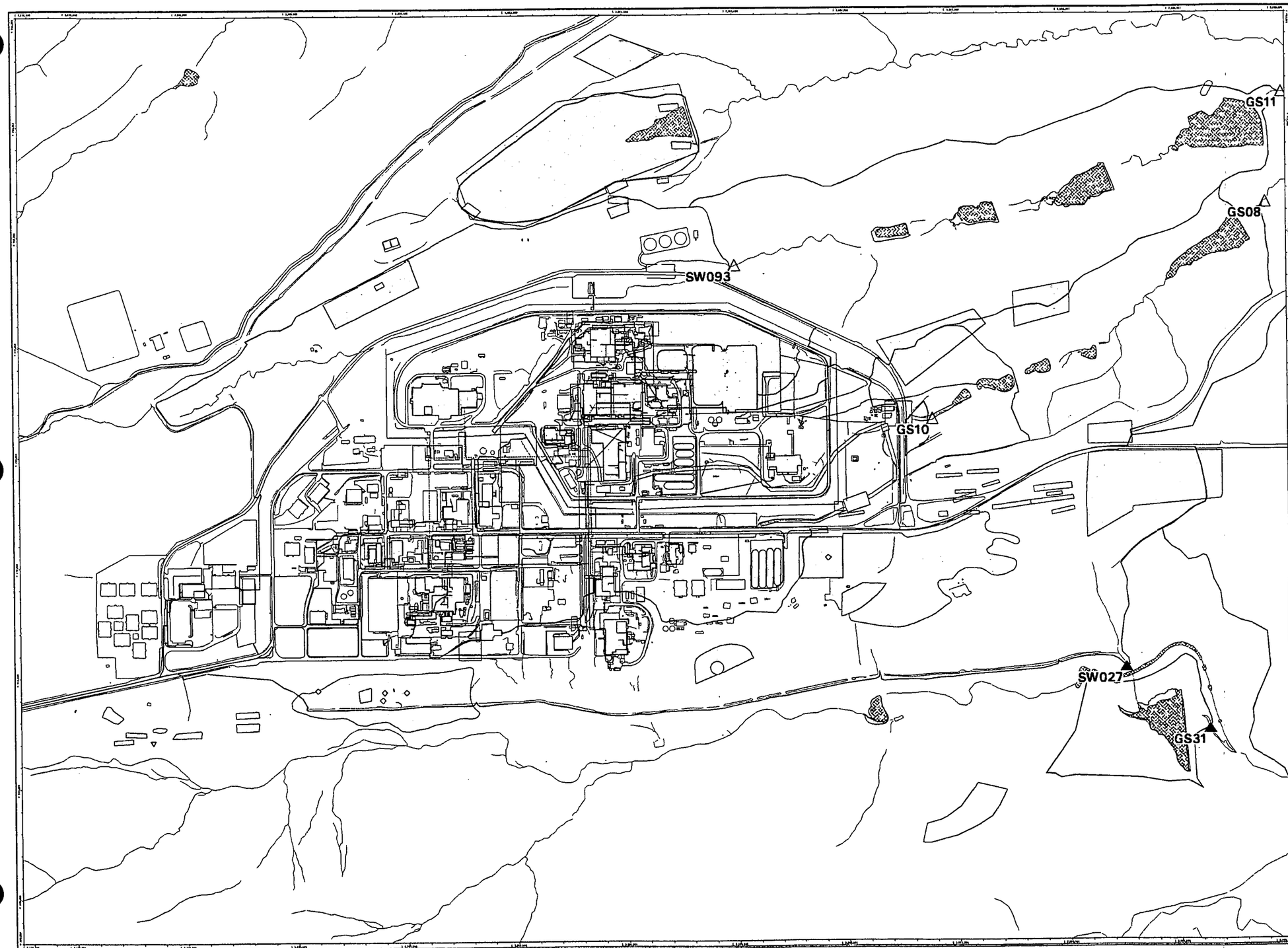

Figure TA-4-9

Actinide Migration Evaluation Pathway Report

Actinide Sources and U-238 in Surface Soils above RFCA Tier II (103.0 pCi/g)

EXPLANATION

Sample Locations (pCi/g)

- 103.0 < = Result < 586.0
- 586.0 < = Result < 1000.0 (Tier I)
- Result > = 1000.0 (Tier I)

Actinide Sources

- Active Actinide Site
- Original Process Waste Line (OPWL)
- Location of Original Process Waste Lines which may have been removed.
- New Process Waste Lines
- Under Building Contamination (UBC)
- Accepted as Proposed No Further Action (NFA)
- IHSS with sub-surface contamination but no validated sub-surface data

Drainage Basins

- Drainage Basin Boundary
- Walnut Creek Basin Gaging Station (GS03, GS08, GS10, GS11 & SW093)
- Woman Creek Basin Gaging Station (GS01, GS31 & SW027)

Standard Map Features

- Buildings and other structures
- Lakes and ponds
- Streams, ditches, or other drainage features
- Rocky Flats boundary
- Paved roads

DATA SOURCE BASE FEATURES:
Buildings, fences, hydrography, roads and other structures from 1994 aerial fly-over data captured by EG&G RSL, Las Vegas. Digitized from the orthophotographs. 1/95

Analytical Data provided by Mark Wood (KH, 303-966-6689).

Data Analysis performed by Wright Water Engineers (303-480-1700).

Scale = 1 : 10820
1 inch represents approximately 902 feet

100 0 200 400 ft

State Plane Coordinate Projection
Colorado Central Zone
Datum: NAD27

U.S. Department of Energy
Rocky Flats Environmental Technology Site

GIS Dept. 303-966-7707

Prepared by: DynCorp THE ART OF TECHNOLOGY

Prepared for: KAISER-HILL PROJECT

NT_Svr w:/projects/actinide_pathway_report/fy2002/act_sro_samples_maps/u238_tier2.aml

510

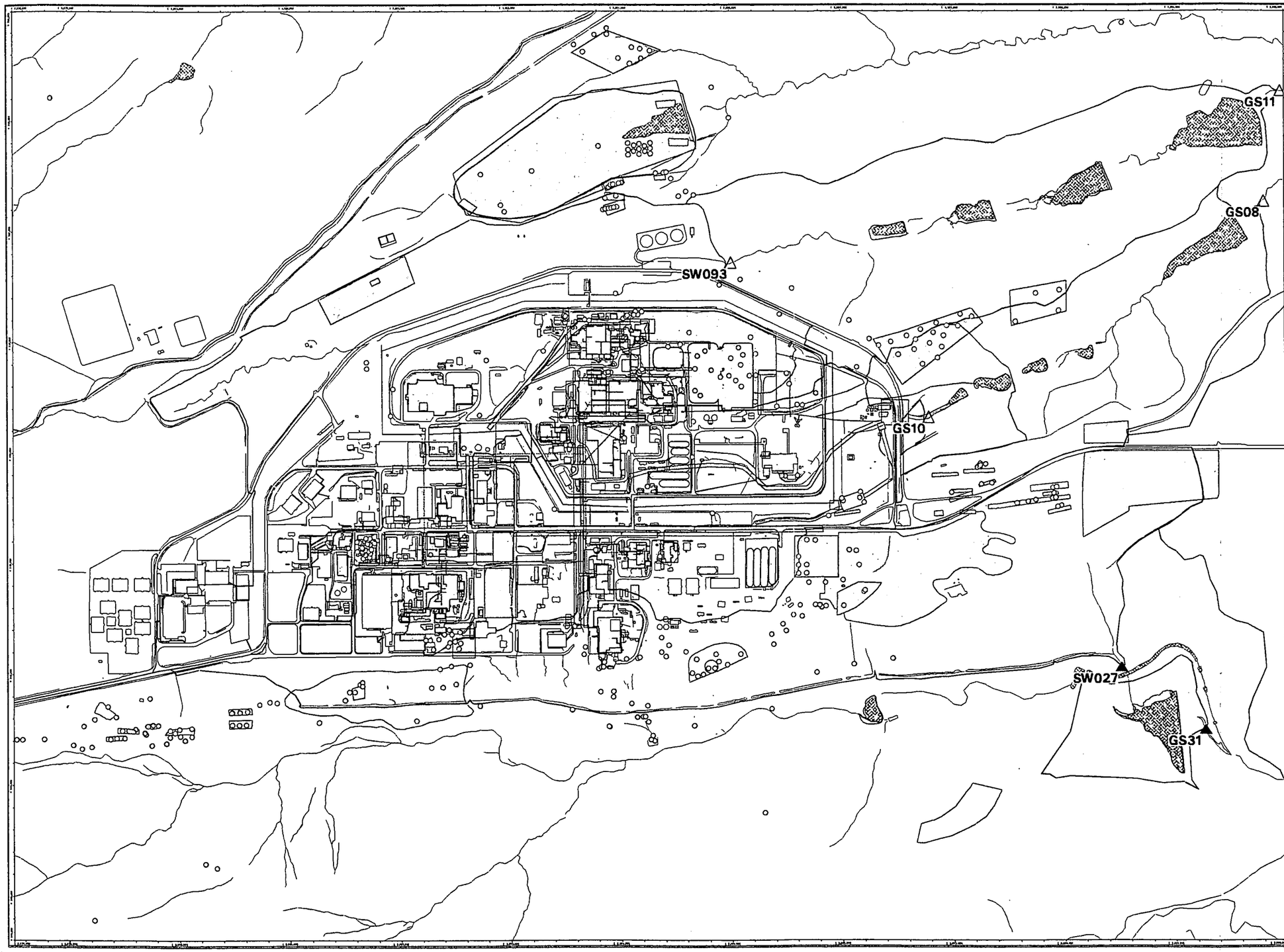

Figure TA-4-10

Actinide Migration Evaluation Pathway Report

Actinide Sources and U-238 in Sub-Surface Soils above Background (0.73 pCi/g)

EXPLANATION

Sample Locations (pCi/g)

- 0.73 < Result < = 1.0
- 1.0 < Result < = 5.0
- 5.0 < Result < = 10.0
- 10.0 < Result < = 100.0
- 100.0 < Result < = 1000.0
- Result > 1000.0

Actinide Sources

- Active Actinide Site
- Original Process Waste Line (OPWL)
- Location of Original Process Waste Lines which may have been removed.
- New Process Waste Lines
- Under Building Contamination (UBC)
- Accepted as Proposed No Further Action (NFA)
- IHSS with sub-surface contamination but no validated sub-surface data

Drainage Basins

- Drainage Basin Boundary
- Walnut Creek Basin Gaging Station (GS03, GS08, GS10, GS11 & SW093)
- Woman Creek Basin Gaging Station (GS01, GS31 & SW027)

Standard Map Features

- Buildings and other structures
- Lakes and ponds
- Streams, ditches, or other drainage features
- Rocky Flats boundary
- Paved roads

DATA SOURCE BASE FEATURES:
Buildings, fences, hydrography, roads and other structures from 1994 aerial fly-over data captured by EG&G RSL, Las Vegas.
Digitized from the orthophotographs. 1/95
Analytical Data from SWD as of October 2000.

Data Analysis performed by Wright Water engineers (303-480-1700).

Scale = 1 : 10820
1 inch represents approximately 902 feet

100 0 200 400 ft

State Plane Coordinate Projection
Colorado Central Zone
Datum: NAD27

U.S. Department of Energy
Rocky Flats Environmental Technology Site

GIS Dept. 303-966-7797

Prepared by: DynCorp THE ART OF TECHNOLOGY

Prepared for: KH KAISER-HILL COMPANY

NT_Svr w:/projects/actinide_pathway_report/fy2002/act_sro_samples_maps/u238_sub_surf_bkgd.aml

54

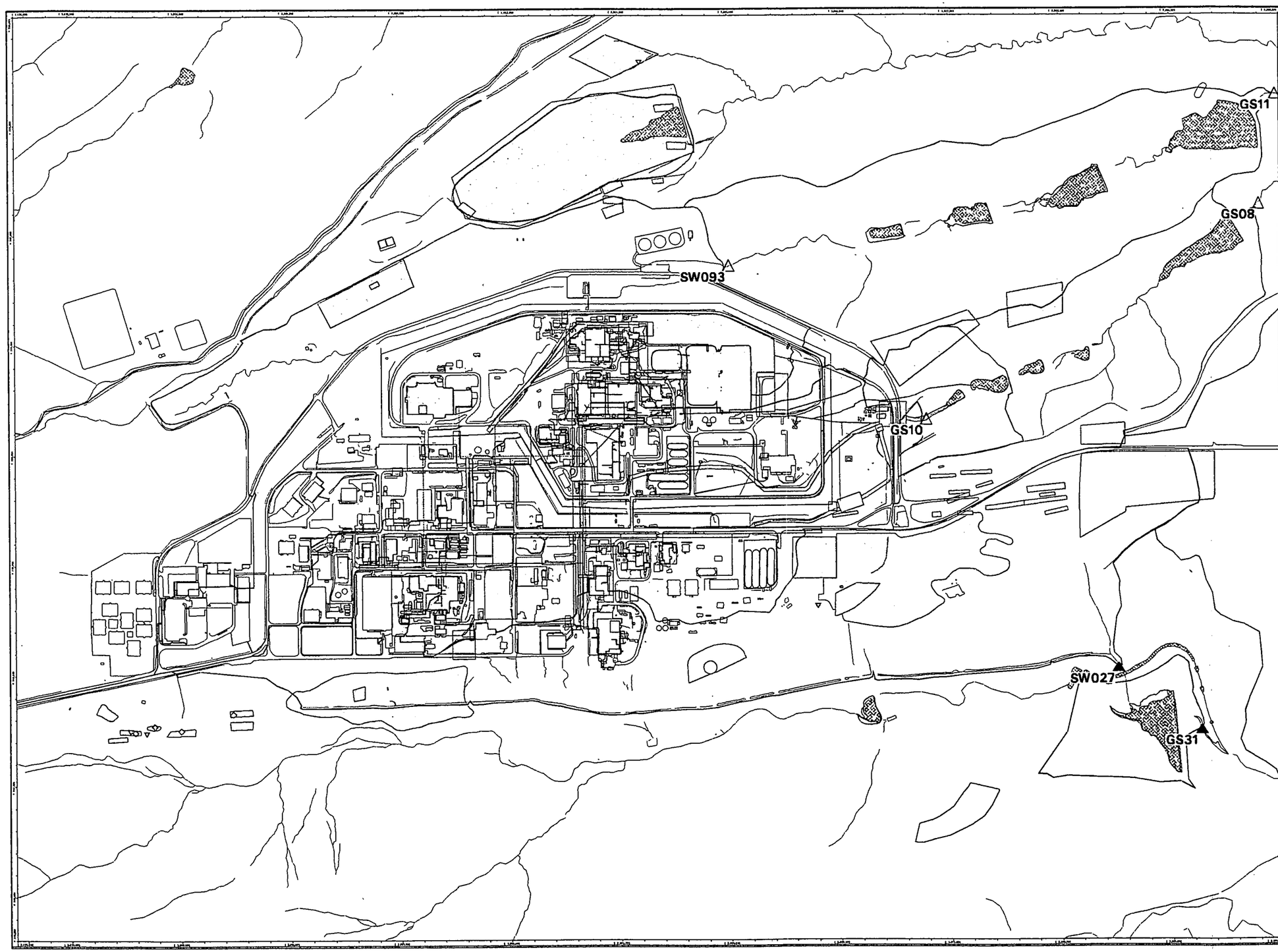

Figure TA-4-11

Actinide Migration Evaluation Pathway Report

Actinide Sources and U-238 in Sub-Surface Soils above RFCA Tier II (103.0 pCi/g)

EXPLANATION

Sample Locations (pCi/g)

- ▽ 103.0 < = Result < 586.0
- ◇ 586.0 < = Result < 1000.0 (Tier I)
- ◇ Result > = 1000.0 (Tier I)

Actinide Sources

- Active Actinide Site
- Original Process Waste Line (OPWL)
- Location of Original Process Waste Lines which may have been removed.
- New Process Waste Lines
- Under Building Contamination (UBC)
- Accepted as Proposed No Further Action (NFA)
- IHSS with sub-surface contamination but no validated sub-surface data

Drainage Basins

- Drainage Basin Boundary
- △ Walnut Creek Basin Gaging Station (GS03, GS08, GS10, GS11 & SW093)
- ▲ Woman Creek Basin Gaging Station (GS01, GS31 & SW027)

Standard Map Features

- Buildings and other structures
- Lakes and ponds
- Streams, ditches, or other drainage features
- Rocky Flats boundary
- Paved roads

DATA SOURCE BASE FEATURES:

Buildings, fences, hydrography, roads and other structures from 1994 aerial fly-over data captured by EG&G RSL, Las Vegas. Digitized from the orthophotographs. 1/95
Analytical Data from SWD as of October 2000.

Data Analysis performed by Wright Water engineers (303-480-1700).

Scale = 1 : 10820
1 inch represents approximately 902 feet

100 0 200 400 ft

State Plane Coordinate Projection
Colorado Central Zone
Datum: NAD27

U.S. Department of Energy
Rocky Flats Environmental Technology Site

GIS Dept. 303-966-7707

Prepared by: DynCorp THE ART OF TECHNOLOGY

Prepared for: KAISER-HILL

NT_Svr w:/projects/actinide_pathway_report/fy2002/act_sro_samples_maps/u238_sub_surf_tier2.aml

512

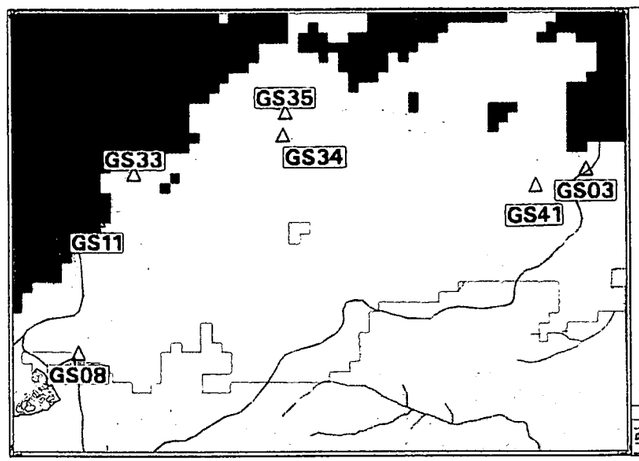

Pu-239/240 Activity in Surface Soil (Kriging Analysis)

- Result < = 0.01
- 0.01 < Result < = 0.05
- 0.05 < Result < = 0.1
- 0.1 < Result < = 0.5
- 0.5 < Result < = 1.0
- 1.0 < Result < = 5.0
- 5.0 < Result < = 10.0
- 10.0 < Result < = 100.0
- 100.0 < Result < = 1000.0
- Result > 1000.0

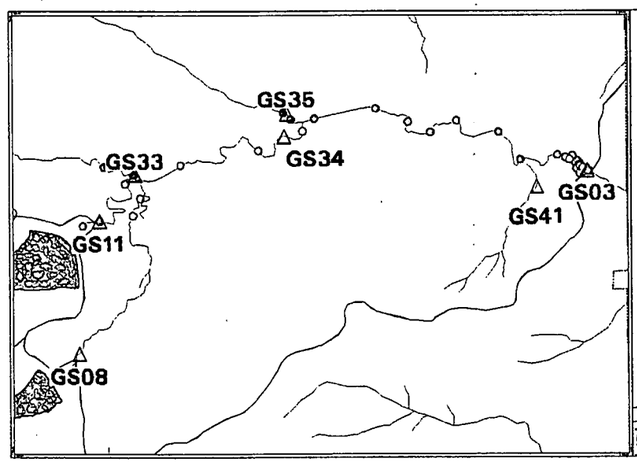

Pu-239/240 Activity in Sediments

- Result < = 0.01
- 0.01 < Result < = 0.05
- 0.05 < Result < = 0.1
- 0.1 < Result < = 0.5
- 0.5 < Result < = 1.0
- 1.0 < Result < = 5.0
- 5.0 < Result < = 10.0
- 10.0 < Result < = 100.0
- 100.0 < Result < = 1000.0
- Result > 1000.0

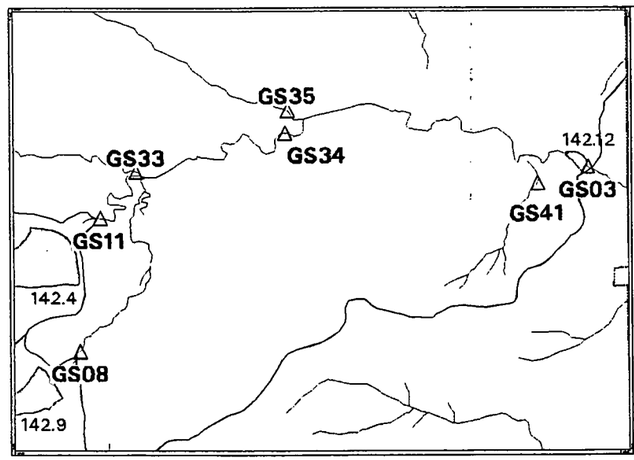

Actinide Sources

- Active Actinide Site

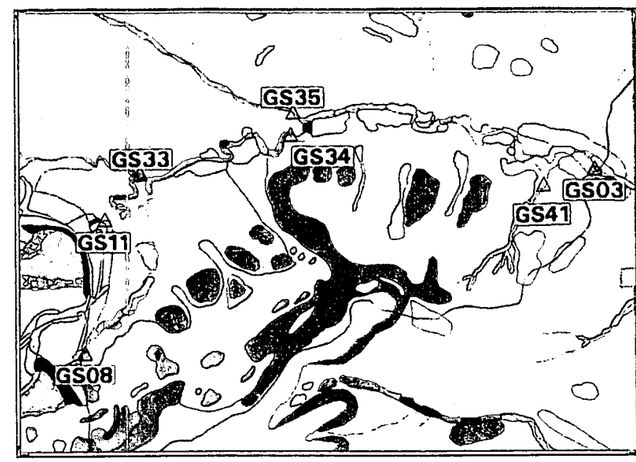

Vegetation Map

- Riparian Woodland
- Leadplant Riparian Shrubland
- Wet Meadow/Marsh Ecotone
- Short Upland Shrubland
- Willow Riparian Shrubland
- Annual Grass/Forb Community
- Xeric Tallgrass Prairie
- Ponderosa Woodland
- Reclaimed Mixed Grassland
- Mesic Mixed Grassland
- Savannah Shrubland
- Tall Upland Shrubland
- Short Marsh
- Xeric Needle and Thread Grass Prairie
- Short Grassland
- Disturbed and Developed Areas
- Open Water
- Riprap, Rock, and Gravel Piles
- Mudflats
- Tree Plantings
- Tall Marsh

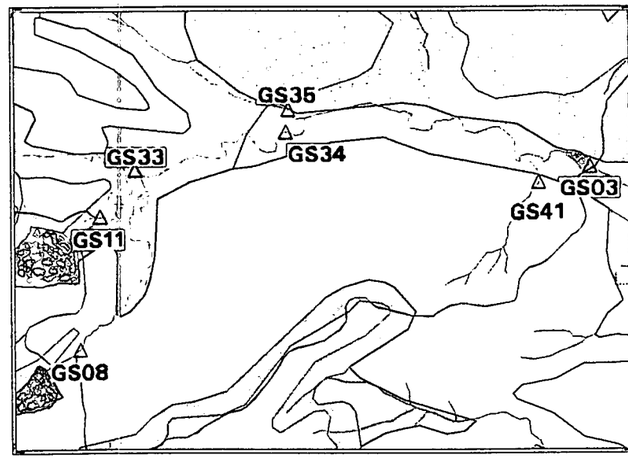

Soils Map

- Denver clay loam, 2 - 5%
- Denver-Kutch clay loam, 5 - 9%
- Denver-Kutch-Midway clay loam, 9 - 25%
- Englewood clay loam, 0 - 2%
- Englewood clay loam, 2 - 5%
- Flatirons cobbly sandy loam, 0 - 3%
- Haverson loam, 0 - 3%
- Leyden-Primen-Standley cobbly clay loams, 15 - 50%
- Midway clay loam, 9 - 30%
- Nederland very cobbly sandy loam, 15 - 50%

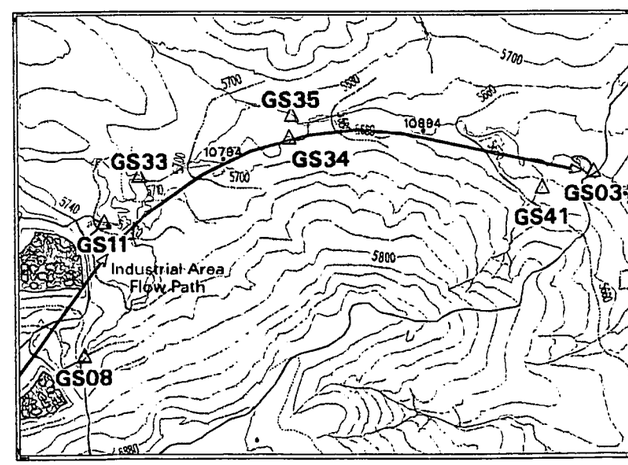

Groundwater Potentiometric Surface

- Groundwater Monitoring Well
- Water Level Contour
- Dashed where inferred
- Intermediate Water Level Contour
- Dashed where inferred
- Foundation Drain and Elevation
- Approximate extent of Unsaturated Area
- Area without Groundwater Elevation Data

Figure TA-5-3

Actinide Migration Evaluation Pathway Report

Lower Walnut Creek (Pu-239/240 Analysis)

EXPLANATION

- Walnut Creek Basin Gaging Station (GS03, GS08, GS11, GS33, GS34, GS35 & GS41)
- Drainage Basin Boundary

Standard Map Features

- Buildings and other structures
- Lakes and ponds
- Streams, ditches, or other drainage features
- Topographic Contour (20-Foot)
- Rocky Flats boundary
- Paved roads

DATA SOURCE BASE FEATURES:

Buildings, fences, hydrography, roads and other structures from 1994 aerial fly-over data captured by EG&G RSL, Las Vegas.
Digitized from the orthophotographs. 1/95

Topology (contours) were derived from digital elevation model (DEM) data by Morrison Knudson (MK) using ESRI Arc TIN and LATTICE to process the DEM data to create 5-foot contours. The DEM data was captured by the Remote Sensing Lab, Las Vegas, NV, 1994 Aerial Flyover at ~ 10 meter resolution. DEM post-processing performed by MK, Winter 1997.

Surface Soil:
Analytical Data from SWD as of October 1999.
903 Pad data from 903 Drum Storage Area Characterization Report, September 1999.
Kriged data provided by Jeff Myers (Westinghouse - Akin, 803-502-9747).

Sediment:
Analytical Data from SWD as of October 2000.
Data Analysis performed by Wright Water Engineers (303-480-1700).

Actinide Sources:
IHSS data approved by Nick Demos (SSOC, 303-966-4605).

Note: The Sanitary Sewer and Storm Drain systems at the site are included on the Active IHSS list but are not included on the map. Area investigations will be performed to determine which portions of these systems will ultimately be on the NFA list.

Vegetation:
Vegetation map data provided by PTI Environmental Services Ecology Group.

Note: This map does not show all Federally designated wetlands. See the 1995 Site wetlands map prepared by the U.S. Army Corps of Engineers for delineated wetland features.

Soils:
Soils data from the US Soil Conservation Service. Uncertified Golden Area Soil Survey - 1980.

Scale = 1 : 13536
1 Inch represents 1128 feet
250 0 500 1000 ft

State Plane Coordinate Projection
Colorado Central Zone
Datum: NAD27

DynCorp
THE ART OF TECHNOLOGY

KAISER-HILL

NT Svr w:/projects/actinide pathway report/fy2002/cross section maps/lower walnut pu239-240.aml

585

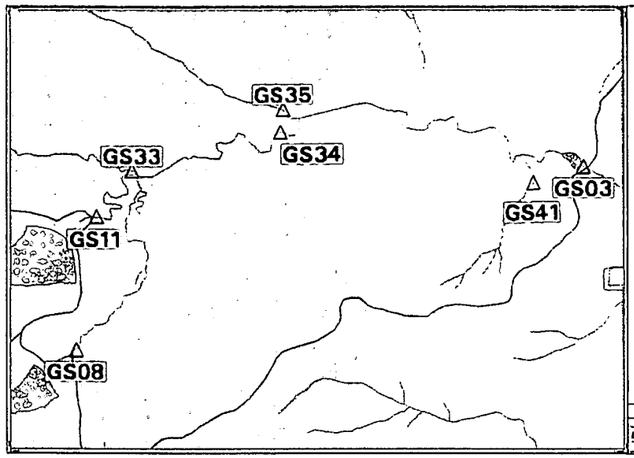

U-238 Activity in Surface Soil (Kriging Analysis)

- Result < = 0.01
- 0.01 < Result < = 0.05
- 0.05 < Result < = 0.1
- 0.1 < Result < = 0.5
- 0.5 < Result < = 1.0
- 1.0 < Result < = 5.0
- 5.0 < Result < = 10.0
- 10.0 < Result < = 100.0
- 100.0 < Result < = 1000.0
- Result > 1000.0

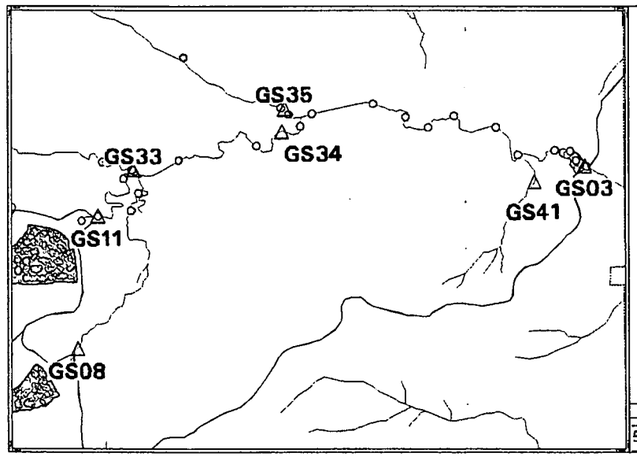

U-238 Activity in Sediments

- Result < = 0.01
- 0.01 < Result < = 0.05
- 0.05 < Result < = 0.1
- 0.1 < Result < = 0.5
- 0.5 < Result < = 1.0
- 1.0 < Result < = 5.0
- 5.0 < Result < = 10.0
- 10.0 < Result < = 100.0
- 100.0 < Result < = 1000.0
- Result > 1000.0

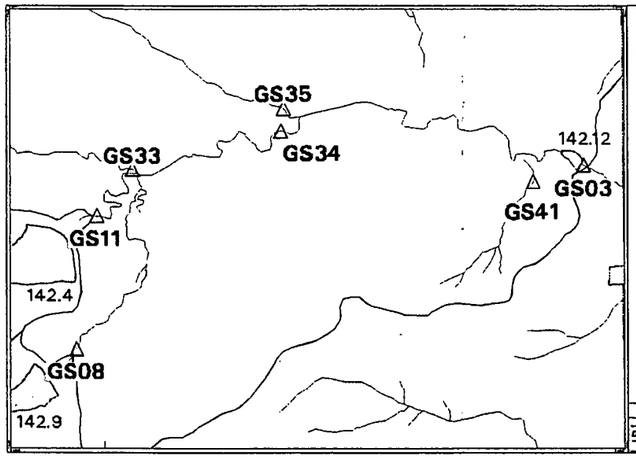

Actinide Sources

- Active Actinide Site

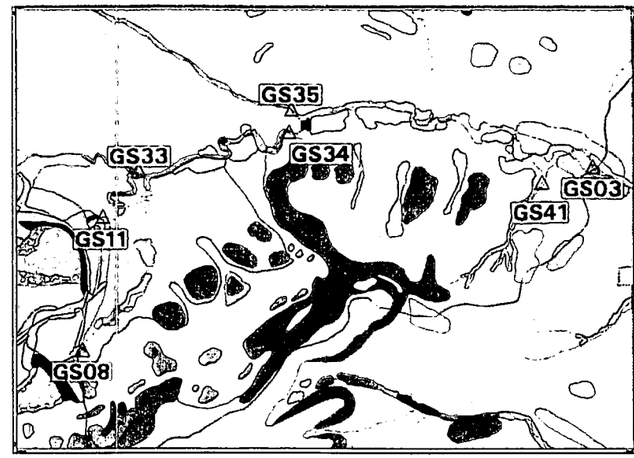

Vegetation Map

- Riparian Woodland
- Leadplant Riparian Shrubland
- Wet Meadow/Marsh Ecotone
- Short Upland Shrubland
- Willow Riparian Shrubland
- Annual Grass/Forb Community
- Xeric Tallgrass Prairie
- Ponderosa Woodland
- Reclaimed Mixed Grassland
- Mesic Mixed Grassland
- Savannah Shrubland
- Tall Upland Shrubland
- Short Marsh
- Xeric Needle and Thread Grass Prairie
- Short Grassland
- Disturbed and Developed Areas
- Open Water
- Riprap, Rock, and Gravel Piles
- Mudflats
- Tree Plantings
- Tall Marsh

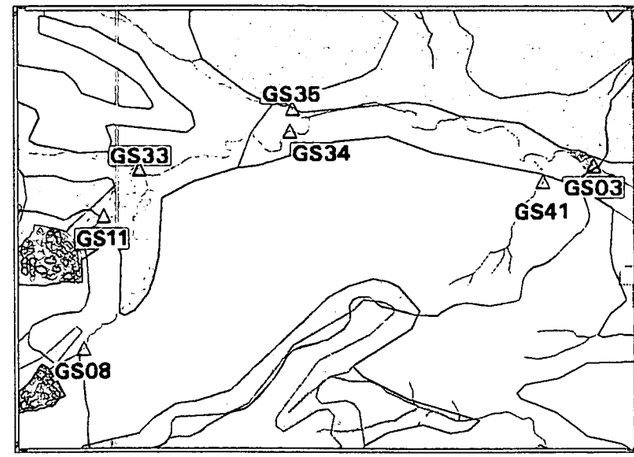

Soils Map

- Denver clay loam, 2 - 5%
- Denver-Kutch clay loam, 5 - 9%
- Denver-Kutch-Midway clay loam, 9 - 25%
- Englewood clay loam, 0 - 2%
- Englewood clay loam, 2 - 5%
- Flatirons cobbly sandy loam, 0 - 3%
- Haverson loam, 0 - 3%
- Leyden-Primen-Standley cobbly clay loams, 15 - 50%
- Midway clay loam, 9 - 30%
- Nederland very cobbly sandy loam, 15 - 50%

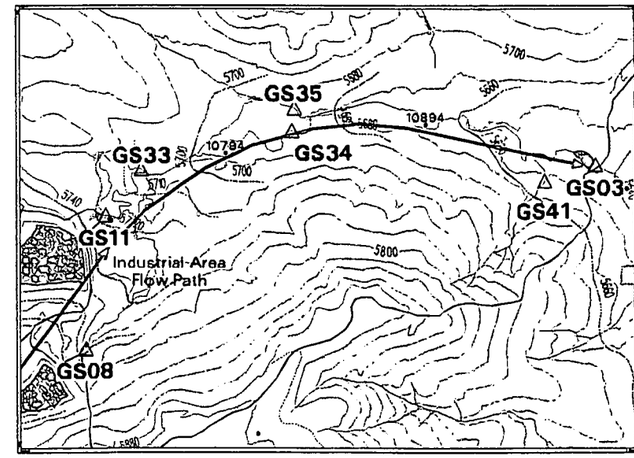

Groundwater Potentiometric Surface

- Groundwater Monitoring Well
- Water Level Contour
- Dashed where inferred
- Intermediate Water Level Contour
- Dashed where inferred
- Foundation Drain and Elevation
- Approximate extent of Unsaturated Area
- Area without Groundwater Elevation Data

Figure TA-5-6

Actinide Migration Evaluation Pathway Report

Lower Walnut Creek (U-238 Analysis)

EXPLANATION

- Walnut Creek Basin Gaging Station (GS03, GS08, GS11, GS33, GS34, GS35 & GS41)
- Drainage Basin Boundary

Standard Map Features

- Buildings and other structures
- Lakes and ponds
- Streams, ditches, or other drainage features
- Topographic Contour (20-Foot)
- Rocky Flats boundary
- Paved roads

DATA SOURCE BASE FEATURES:

Buildings, fences, hydrography, roads and other structures from 1994 aerial fly-over data captured by EG&G RSL, Las Vegas. Digitized from the orthophotographs. 1/95

Topology (contours) were derived from digital elevation model (DEM) data by Morrison Knudson (MK) using ESRI Arc TIN and LATTICE to process the DEM data to create 5-foot contours. The DEM data was captured by the Remote Sensing Lab, Las Vegas, NV, 1994 Aerial Flyover at ~ 10 meter resolution. DEM post-processing performed by MK, Winter 1997.

Surface Soil:
Analytical Data from SWD as of October 1999.
903 Pad data from 903 Drum Storage Area Characterization Report, September 1999.
Kriged data provided by Jeff Myers (Westinghouse - Akin, 803-502-9747).

Sediment:
Analytical Data from SWD as of October 2000.
Data Analysis performed by Wright Water Engineers (303-480-1700).

Actinide Sources:
IHSS data approved by Nick Demos (SSOC, 303-966-4605).

Note: The Sanitary Sewer and Storm Drain systems at the site are included on the Active IHSS list but are not included on the map. Area investigations will be performed to determine which portions of these systems will ultimately be on the NFA list.

Vegetation:
Vegetation map data provided by PTI Environmental Services Ecology Group.

Note: This map does not show all Federally designated wetlands. See the 1995 Site wetlands map prepared by the U.S. Army Corps of Engineers for delineated wetland features.

Soils:
Soils data from the US Soil Conservation Service. Uncertified Golden Area Soil Survey - 1980.

Scale = 1 : 13536
1 inch represents 1128 feet
250 0 500 1000 ft

State Plane Coordinate Projection
Colorado Central Zone
Datum: NAD27

DynCorp
THE ART OF TECHNOLOGY

KAISER-HILL COMPANY

NT Svr w:/projects/actinide pathway report/fy2002/cross section maps/lower walnut u238.aml

587

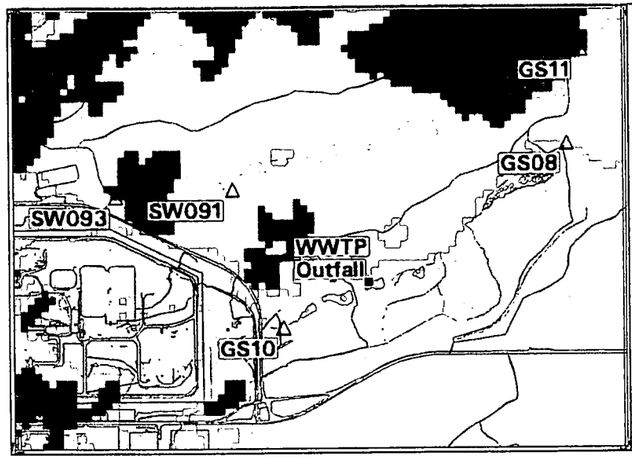

Pu-239/240 Activity in Surface Soil (Kriging Analysis)

- Result < = 0.01
- 0.01 < Result < = 0.05
- 0.05 < Result < = 0.1
- 0.1 < Result < = 0.5
- 0.5 < Result < = 1.0
- 1.0 < Result < = 5.0
- 5.0 < Result < = 10.0
- 10.0 < Result < = 100.0
- 100.0 < Result < = 1000.0
- Result > 1000.0

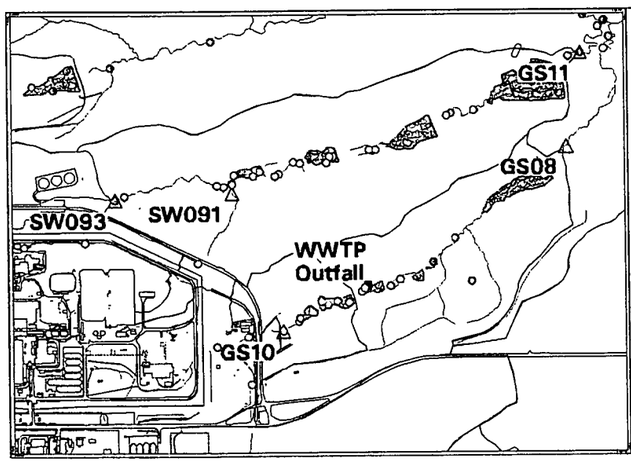

Pu-239/240 Activity in Sediments

- Result < = 0.01
- 0.01 < Result < = 0.05
- 0.05 < Result < = 0.1
- 0.1 < Result < = 0.5
- 0.5 < Result < = 1.0
- 1.0 < Result < = 5.0
- 5.0 < Result < = 10.0
- 10.0 < Result < = 100.0
- 100.0 < Result < = 1000.0
- Result > 1000.0

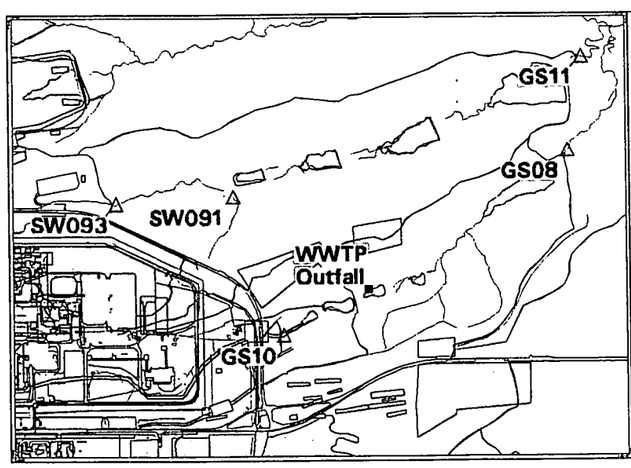

Actinide Sources

- Active Actinide Site
- Original Process Waste Line (OPWL)
- Location of Original Process Waste Lines which may have been removed.
- Under Building Contamination (UBC)
- Accepted as Proposed No Further Action (NFA)
- Proposed No Further Action (NFA)

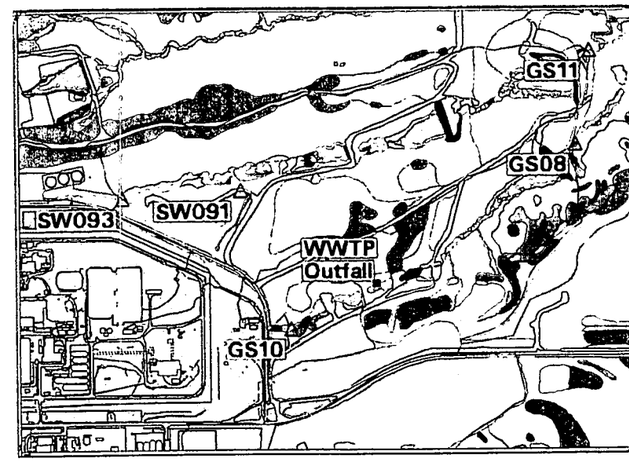

Vegetation Map

- Riparian Woodland
- Leadplant Riparian Shrubland
- Wet Meadow/Marsh Ecotone
- Short Upland Shrubland
- Willow Riparian Shrubland
- Annual Grass/Forb Community
- Xeric Tallgrass Prairie
- Ponderosa Woodland
- Reclaimed Mixed Grassland
- Mesic Mixed Grassland
- Savannah Shrubland
- Tall Upland Shrubland
- Short Marsh
- Xeric Needle and Thread Grass Prairie
- Short Grassland
- Disturbed and Developed Areas
- Open Water
- Riprap, Rock, and Gravel Piles
- Mudflats
- Tree Plantings
- Tall Marsh

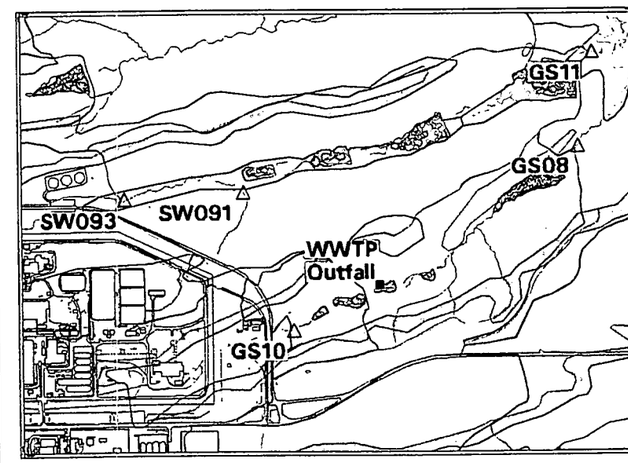

Soils Map

- Denver clay loam, 5 - 9%
- Denver-Kutch-Midway clay loam, 9 - 25%
- Englewood clay loam, 0 - 2%
- Englewood clay loam, 2 - 5%
- Flatirons cobbly sandy loam, 0 - 3%
- Haverson loam, 0 - 3%
- Leyden-Primen-Standley cobbly clay loams, 15 - 50%
- Nederland very cobbly sandy loam, 15 - 50%
- Valmont clay loam, 0 - 3%

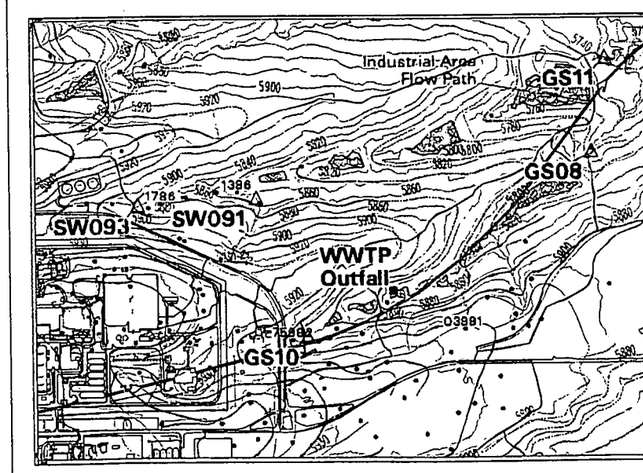

Groundwater Potentiometric Surface

- Groundwater Monitoring Well
- Water Level Contour
- Dashed where inferred
- Intermediate Water Level Contour
- Dashed where inferred
- Foundation Drain and Elevation
- Approximate extent of Unsaturated Area
- Area without Groundwater Elevation Data

Figure TA-5-9

Actinide Migration Evaluation Pathway Report

A- and B-Series Ponds (Pu-239/240 Analysis)

EXPLANATION

- Walnut Creek Basin Gaging Station (SW091, SW093, GS08, GS10 & GS11)
- WWTP Outfall
- Drainage Basin Boundary

Standard Map Features

- Buildings and other structures
- Lakes and ponds
- Streams, ditches, or other drainage features
- Topographic Contour (20-Foot)
- Rocky Flats boundary
- Paved roads

DATA SOURCE BASE FEATURES:

Buildings, fences, hydrography, roads and other structures from 1994 aerial fly-over data captured by EG&G RSL, Las Vegas. Digitized from the orthophotographs. 1/95

Topology (contours) were derived from digital elevation model (DEM) data by Morrison Knudson (MK) using ESRI Arc TIN and LATTICE to process the DEM data to create 5-foot contours. The DEM data was captured by the Remote Sensing Lab, Las Vegas, NV, 1994 Aerial Flyover at ~ 10 meter resolution. DEM post-processing performed by MK, Winter 1997.

Surface Soil:
Analytical Data from SWD as of October 1999.
903 Pad data from 903 Drum Storage Area Characterization Report, September 1999.
Kriged data provided by Jeff Myers (Westinghouse - Akin, 803-502-9747).

Sediment:
Analytical Data from SWD as of October 2000.
Data Analysis performed by Wright Water Engineers (303-480-1700).

Actinide Sources:
IHSS data approved by Nick Demos (SSOC, 303-966-4605).

Note: The Sanitary Sewer and Storm Drain systems at the site are included on the Active IHSS list but are not included on the map. Area investigations will be performed to determine which portions of these systems will ultimately be on the NFA list.

Vegetation:
Vegetation map data provided by PTI Environmental Services Ecology Group.

Note: This map does not show all Federally designated wetlands. See the 1995 Site wetlands map prepared by the U.S. Army Corps of Engineers for delineated wetland features.

Soils:
Soils data from the US Soil Conservation Service. Uncertified Golden Area Soil Survey - 1980.

Scale = 1 : 19193
1 inch represents approximately 1599 feet
250 0 500 1000 ft

State Plane Coordinate Projection
Colorado Central Zone
Datum: NAD27

Rocky Flats Environmental Restoration Site

DynCorp
THE ART OF TECHNOLOGY

KAISER-HILL

NT Svr w:/projects/actinide pathway report/fy2002/cross section maps/ab ponds pu239-240.aml

589

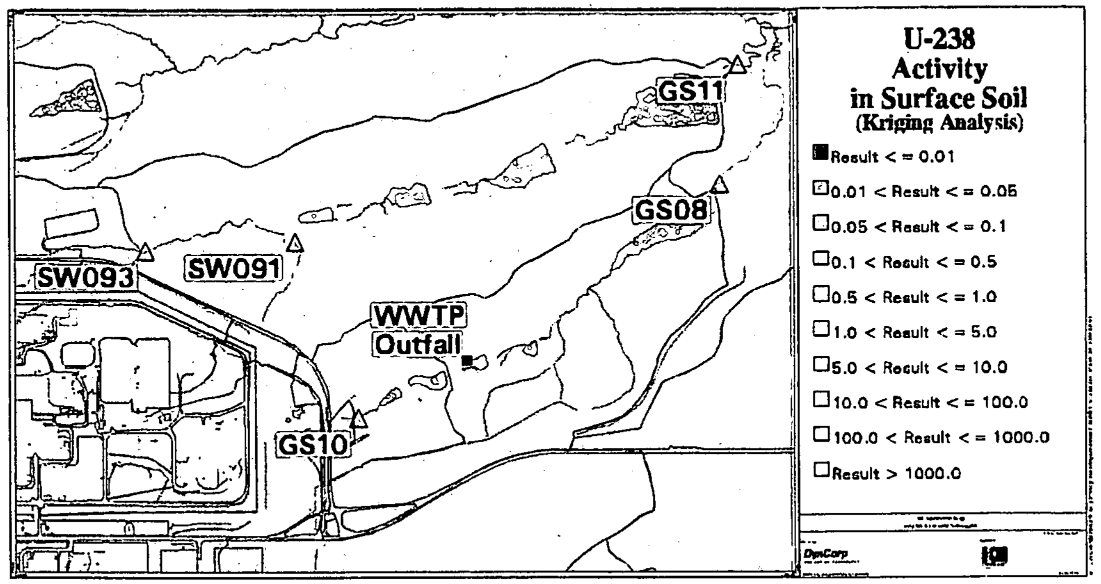

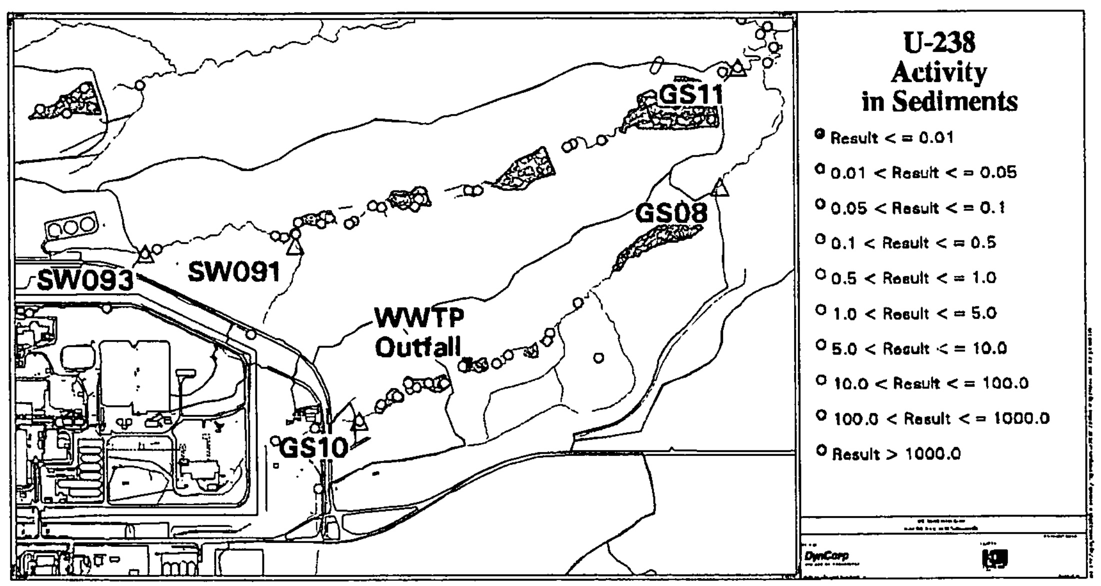

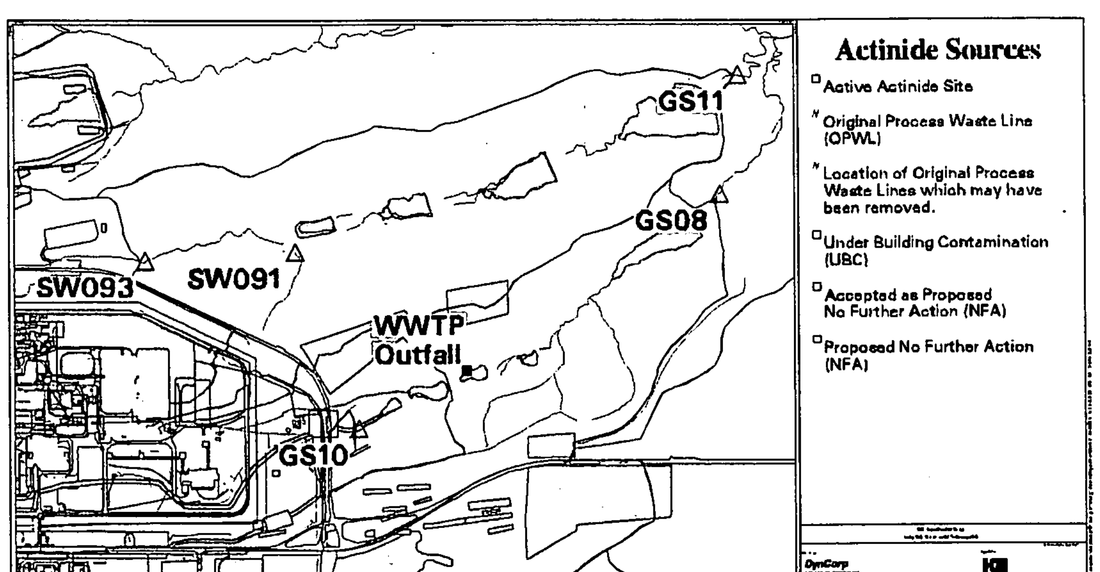

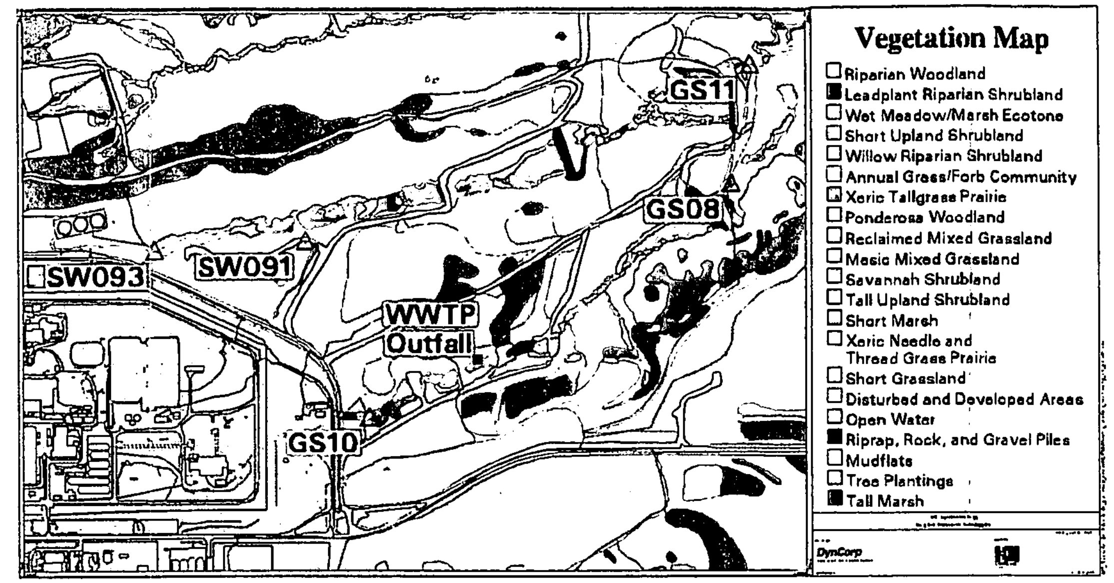

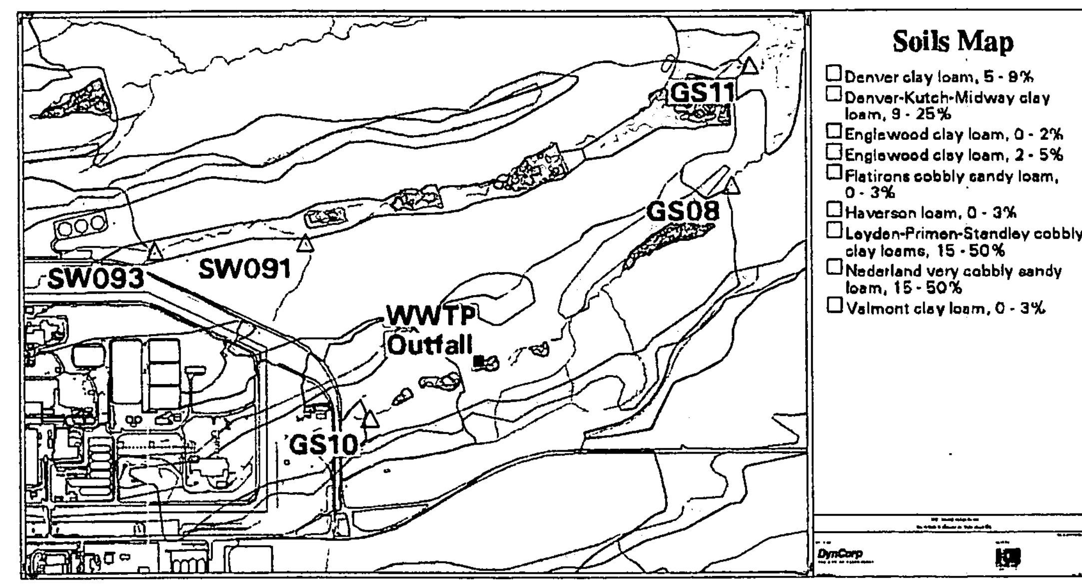

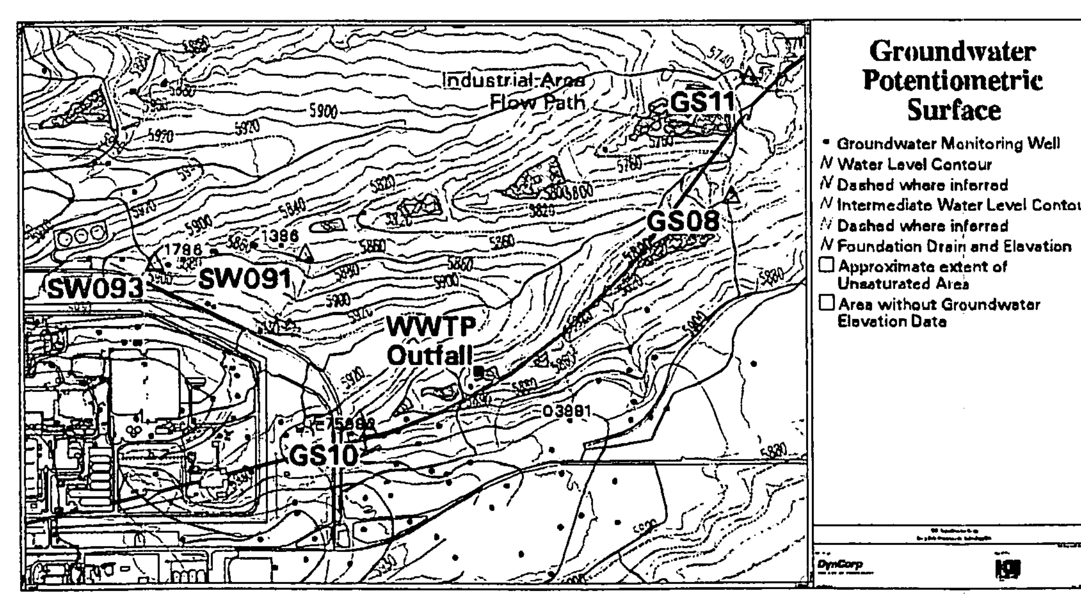

Figure TA-5-12

Actinide Migration Evaluation Pathway Report

A- and B-Series Ponds (U-238 Analysis)

EXPLANATION

△ Walnut Creek Basin Gaging Station (SW091, SW093, GS08, GS10 & GS11)

■ WWTP Outfall

Drainage Basin Boundary

Standard Map Features

- Buildings and other structures
- Lakes and ponds
- Streams, ditches, or other drainage features
- Topographic Contour (20-Foot)
- Rocky Flats boundary
- Paved roads

DATA SOURCE BASE FEATURES:

Buildings, fences, hydrography, roads and other structures from 1994 aerial fly-over data captured by EG&G RSL, Las Vegas. Digitized from the orthophotographs. 1/95

Topology (contours) were derived from digital elevation model (DEM) data by Morrison Knudson (MK) using ESRI Arc TIN and LATTICE to process the DEM data to create 5-foot contours. The DEM data was captured by the Remote Sensing Lab, Las Vegas, NV, 1994 Aerial Flyover at ~ 10 meter resolution. DEM post-processing performed by MK, Winter 1997.

Surface Soil:
Analytical Data from SWD as of October 1999. 903 Pad data from 903 Drum Storage Area Characterization Report, September 1999. Kriged data provided by Jeff Myers (Westinghouse - Akin, 803-502-9747).

Sediment:
Analytical Data from SWD as of October 2000. Data Analysis performed by Wright Water Engineers (303-480-1700).

Actinide Sources:
IHSS data approved by Nick Demos (SSOC, 303-966-4805).

Note: The Sanitary Sewer and Storm Drain systems at the site are included on the Active IHSS list but are not included on the map. Area investigations will be performed to determine which portions of these systems will ultimately be on the NFA list.

Vegetation:
Vegetation map data provided by PTI Environmental Services Ecology Group.

Note: This map does not show all Federally designated wetlands. See the 1995 Site wetlands map prepared by the U.S. Army Corps of Engineers for delineated wetland features.

Soils:
Soils data from the US Soil Conservation Service. Uncertified Golden Area Soil Survey - 1980.

Scale = 1 : 19193
1 inch represents approximately 1599 feet
250 0 500 1000 ft

State Plane Coordinate Projection
Colorado Central Zone
Datum: NAD27

DynCorp
THE ART OF TECHNOLOGY

KAISER-HILL

NT Srv w:/projects/fy2002/actinide pathway report/ab ponds u238.aml

591

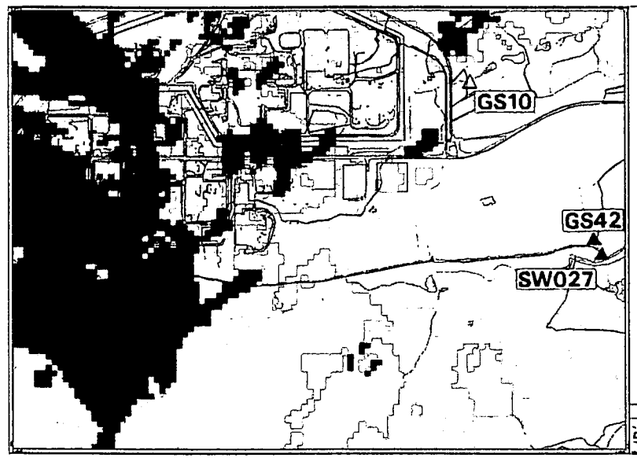

Pu-239/240 Activity in Surface Soil
(Kriging Analysis)

- Result <= 0.01
- 0.01 < Result <= 0.05
- 0.05 < Result <= 0.1
- 0.1 < Result <= 0.5
- 0.5 < Result <= 1.0
- 1.0 < Result <= 5.0
- 5.0 < Result <= 10.0
- 10.0 < Result <= 100.0
- 100.0 < Result <= 1000.0
- Result > 1000.0

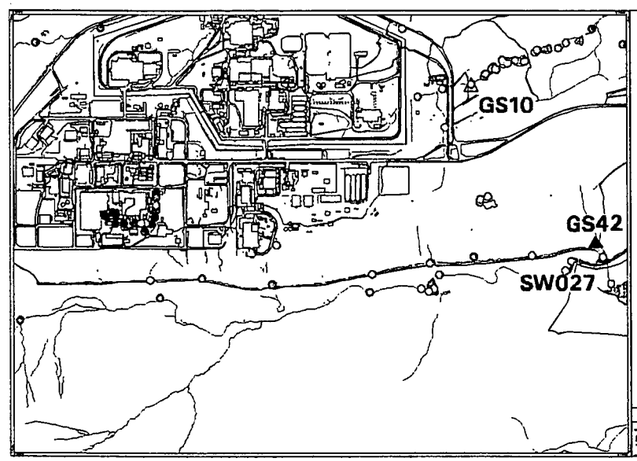

Pu-239/240 Activity in Sediments

- Result <= 0.01
- 0.01 < Result <= 0.05
- 0.05 < Result <= 0.1
- 0.1 < Result <= 0.5
- 0.5 < Result <= 1.0
- 1.0 < Result <= 5.0
- 5.0 < Result <= 10.0
- 10.0 < Result <= 100.0
- 100.0 < Result <= 1000.0
- Result > 1000.0

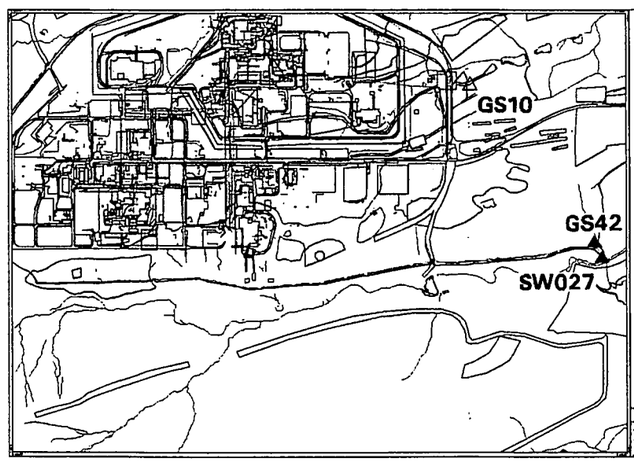

Actinide Sources

- Active Actinide Site
- Original Process Waste Line (OPWL)
- Location of Original Process Waste Lines which may have been removed.
- Under Building Contamination (UBC)
- Accepted as Proposed No Further Action (NFA)
- Proposed No Further Action (NFA)

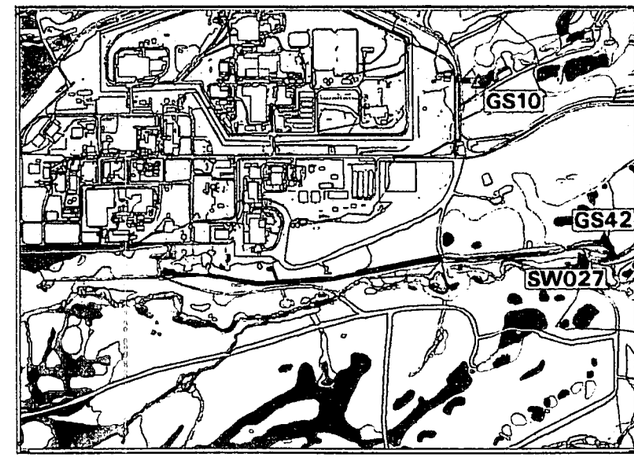

Vegetation Map

- Riparian Woodland
- Leadplant Riparian Shrubland
- Wet Meadow/Marsh Ecotone
- Short Upland Shrubland
- Willow Riparian Shrubland
- Annual Grass/Forb Community
- Xeric Tallgrass Prairie
- Ponderosa Woodland
- Reclaimed Mixed Grassland
- Mesic Mixed Grassland
- Savannah Shrubland
- Tall Upland Shrubland
- Short Marsh
- Xeric Needle and Thread Grass Prairie
- Short Grassland
- Disturbed and Developed Areas
- Open Water
- Riprap, Rock, and Gravel Piles
- Mudflats
- Tree Plantings
- Tall Marsh

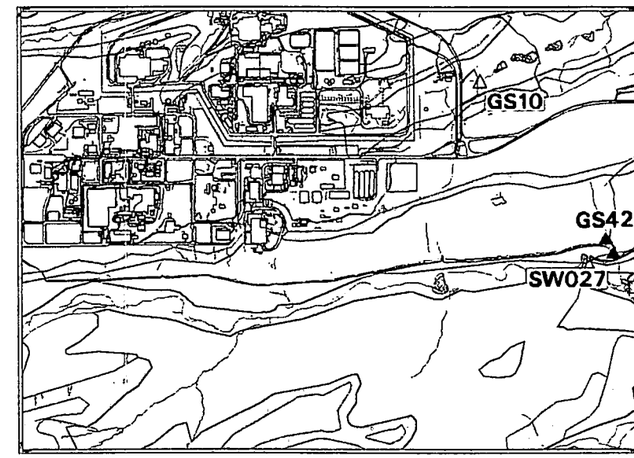

Soils Map

- Denver-Kutch clay loam, 5 - 9%
- Denver-Kutch-Midway clay loam, 9 - 25%
- Flatirons cobbly sandy loam, 0 - 3%
- Haverson loam, 0 - 3%
- Leyden-Primen-Standley cobbly clay loams, 15 - 50%
- Nederland very cobbly sandy loam, 15 - 50%
- Nunn clay loam, 0 - 2%
- Nunn clay loam, 2 - 5%
- Pits, gravel
- Valmont clay loam, 0 - 3%

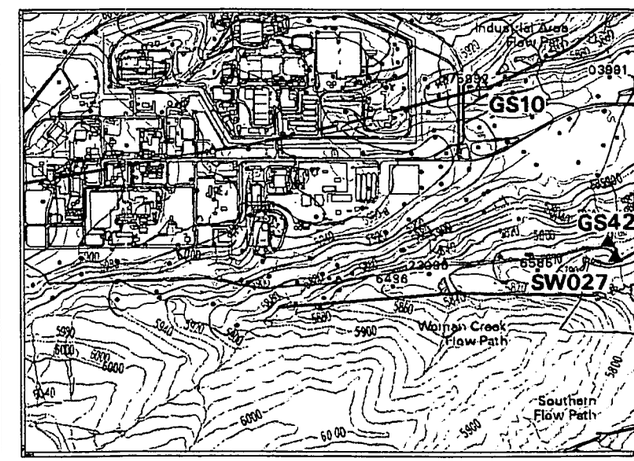

Groundwater Potentiometric Surface

- Groundwater Monitoring Well
- Water Level Contour
- Dashed where inferred
- Intermediate Water Level Contour
- Dashed where inferred
- Foundation Drain and Elevation
- Approximate extent of Unsaturated Area
- Area without Groundwater Elevation Data

Figure TA-5-15

Actinide Migration Evaluation Pathway Report

South Interceptor Ditch (Pu-239/240 Analysis)

EXPLANATION

- Walnut Creek Basin Gaging Station (GS10)
- Women Creek Basin Gaging Station (SW027, GS42)
- Drainage Basin Boundary

Standard Map Features

- Buildings and other structures
- Lakes and ponds
- Streams, ditches, or other drainage features
- Topographic Contour (20-Foot)
- Rocky Flats boundary
- Paved roads

DATA SOURCE BASE FEATURES:

Buildings, fences, hydrography, roads and other structures from 1994 aerial fly-over data captured by EG&G RSL, Las Vegas.
Digitized from the orthophotographs. 1/95
Topology (contours) were derived from digital elevation model (DEM) data by Morrison Knudson (MK) using ESRI Arc TIN and LATTICE to process the DEM data to create 5-foot contours. The DEM data was captured by the Remote Sensing Lab, Las Vegas, NV, 1994 Aerial Flyover at ~ 10 meter resolution. DEM post-processing performed by MK, Winter 1997.

Surface Soil:
Analytical Data from SWD as of October 1999.
903 Pad data from 903 Drum Storage Area Characterization Report, September 1999.
Kriged data provided by Jeff Myers (Westinghouse - Akin, 803-502-9747).

Sediment:
Analytical Data from SWD as of October 2000.
Data Analysis performed by Wright Water Engineers (303-480-1700).

Actinide Sources:
IHSS data approved by Nick Demos (SSOC, 303-966-4605).

Note: The Sanitary Sewer and Storm Drain systems at the site are included on the Active IHSS list but are not included on the map. Area investigations will be performed to determine which portions of these systems will ultimately be on the NFA list.

Vegetation:
Vegetation map data provided by PTI Environmental Services Ecology Group.

Note: This map does not show all Federally designated wetlands. See the 1995 Site wetlands map prepared by the U.S. Army Corps of Engineers for delineated wetland features.

Soils:
Soils data from the US Soil Conservation Service. Uncertified Golden Area Soil Survey - 1980.

Scale = 1 : 23671
1 inch represents approximately 1973 feet
260 0 590 1080 ft

State Plane Coordinate Projection
Colorado Central Zone
Datum: NAD27

Rocky Flats Environmental Restoration Site

DynCorp
THE ART OF TECHNOLOGY

KAISER-HILL

NT Svr w:/projects/actinide pathway report/fy2002/cross section mapsfsid pu239-240.aml

543

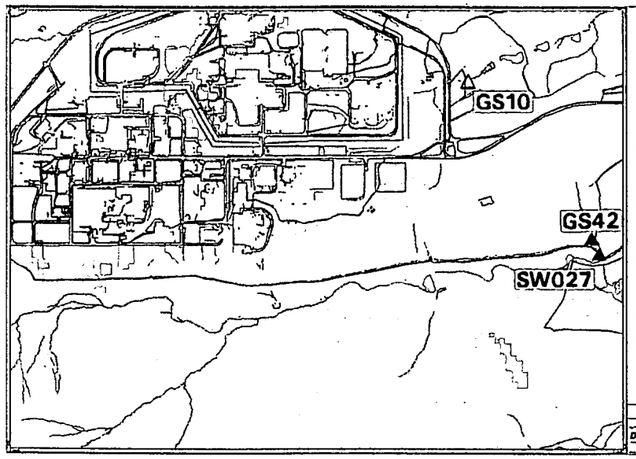

U-238 Activity in Surface Soil (Kriging Analysis)

- Result <= 0.01
- 0.01 < Result <= 0.05
- 0.05 < Result <= 0.1
- 0.1 < Result <= 0.5
- 0.5 < Result <= 1.0
- 1.0 < Result <= 5.0
- 5.0 < Result <= 10.0
- 10.0 < Result <= 100.0
- 100.0 < Result <= 1000.0
- Result > 1000.0

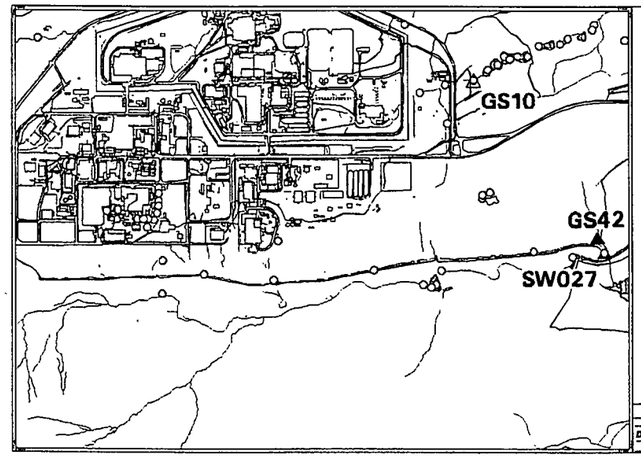

U-238 Activity in Sediments

- Result <= 0.01
- 0.01 < Result <= 0.05
- 0.05 < Result <= 0.1
- 0.1 < Result <= 0.5
- 0.5 < Result <= 1.0
- 1.0 < Result <= 5.0
- 5.0 < Result <= 10.0
- 10.0 < Result <= 100.0
- 100.0 < Result <= 1000.0
- Result > 1000.0

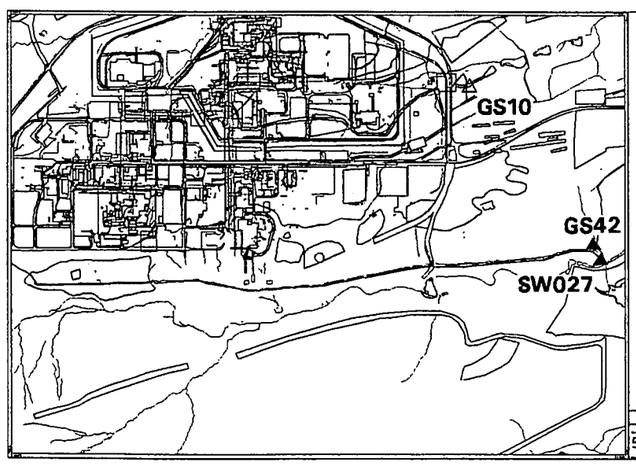

Actinide Sources

- Active Actinide Site
- Original Process Waste Line (OPWL)
- Location of Original Process Waste Lines which may have been removed.
- Under Building Contamination (UBC)
- Accepted as Proposed No Further Action (NFA)
- Proposed No Further Action (NFA)

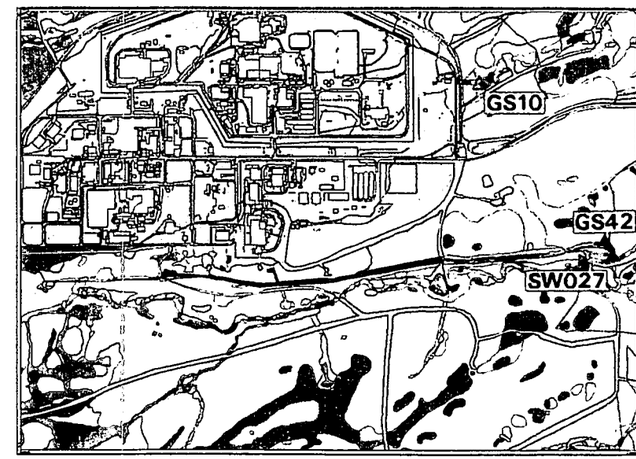

Vegetation Map

- Riparian Woodland
- Leadplant Riparian Shrubland
- Wet Meadow/Marsh Ecotone
- Short Upland Shrubland
- Willow Riparian Shrubland
- Annual Grass/Forb Community
- Xeric Tallgrass Prairie
- Ponderosa Woodland
- Reclaimed Mixed Grassland
- Mesic Mixed Grassland
- Savannah Shrubland
- Tall Upland Shrubland
- Short Marsh
- Xeric Needle and Thread Grass Prairie
- Short Grassland
- Disturbed and Developed Areas
- Open Water
- Riprap, Rock, and Gravel Piles
- Mudflats
- Tree Plantings
- Tall Marsh

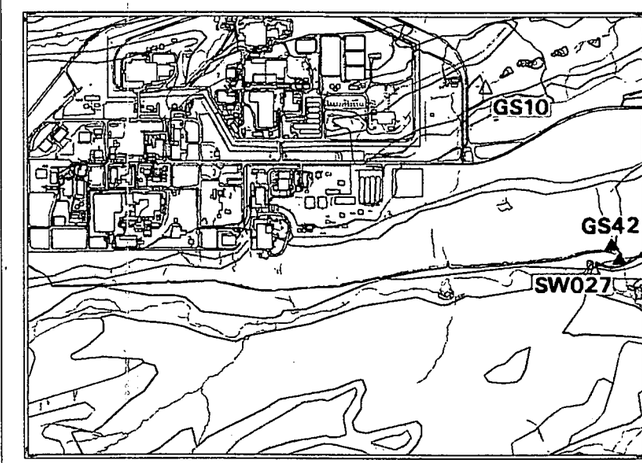

Soils Map

- Denver-Kutch clay loam, 5 - 8%
- Denver-Kutch-Midway clay loam, 8 - 25%
- Flatirons cobbly sandy loam, 0 - 3%
- Haverson loam, 0 - 3%
- Leyden-Primen-Standley cobbly clay loams, 15 - 50%
- Nederland very cobbly sandy loam, 15 - 50%
- Nunn clay loam, 0 - 2%
- Nunn clay loam, 2 - 5%
- Pite, gravel
- Valmont clay loam, 0 - 3%

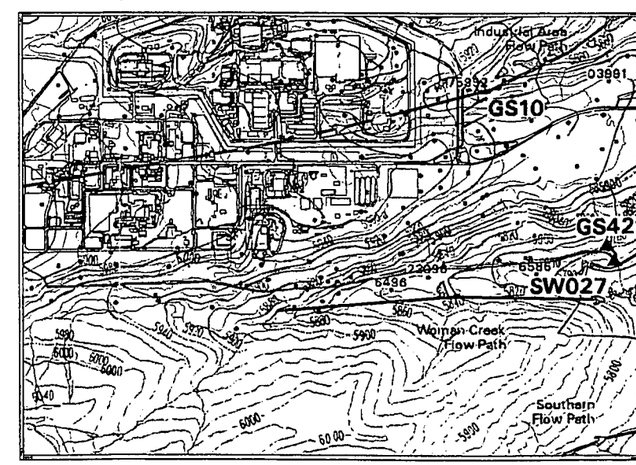

Groundwater Potentiometric Surface

- Groundwater Monitoring Well
- Water Level Contour
- Dashed where inferred
- Intermediate Water Level Contour
- Dashed where inferred
- Foundation Drain and Elevation
- Approximate extent of Unsaturated Area
- Area without Groundwater Elevation Data

Figure TA-5-18

Actinide Migration Evaluation Pathway Report

South Interceptor Ditch (U-238 Analysis)

EXPLANATION

- Walnut Creek Basin Gaging Station (GS10)
- Woman Creek Basin Gaging Station (SW027, GS42)
- Drainage Basin Boundary

Standard Map Features

- Buildings and other structures
- Lakes and ponds
- Streams, ditches, or other drainage features
- Topographic Contour (20-Foot)
- Rocky Flats boundary
- Paved roads

DATA SOURCE BASE FEATURES:

Buildings, fences, hydrography, roads and other structures from 1994 aerial fly-over data captured by EG&G RSL, Las Vegas. Digitized from the orthophotographs. 1/95

Topology (contours) were derived from digital elevation model (DEM) data by Morrison Knudson (MK) using ESRI Arc TIN and LATTICE to process the DEM data to create 5-foot contours. The DEM data was captured by the Remote Sensing Lab, Las Vegas, NV, 1994 Aerial Flyover at ~ 10 meter resolution. DEM post-processing performed by MK, Winter 1997.

Surface Soil:
Analytical Data from SWD as of October 1999.
903 Pad data from 903 Drum Storage Area Characterization Report, September 1993.
Kriged data provided by Jeff Myers (Westinghouse - Akin, 803-502-9747).

Sediment:
Analytical Data from SWD as of October 2000.
Data Analysis performed by Wright Water Engineers (303-480-1700).

Actinide Sources:
IHSS data approved by Nick Demos (SSOC, 303-966-4605).

Note: The Sanitary Sewer and Storm Drain systems at the site are included on the Active IHSS list but are not included on the map. Area investigations will be performed to determine which portions of these systems will ultimately be on the NFA list.

Vegetation:
Vegetation map data provided by PTI Environmental Services Ecology Group.

Note: This map does not show all Federally designated wetlands. See the 1995 Site wetlands map prepared by the U.S. Army Corps of Engineers for delineated wetland features.

Soils:
Soils data from the US Soil Conservation Service. Uncertified Golden Area Soil Survey - 1980.

Scale = 1 : 23671
1 inch represents approximately 1973 feet
250 0 500 1000 ft

State Plane Coordinate Projection
Colorado Central Zone
Datum: NAD27

Rocky Flats Environmental Technology Site

DynCorp
THE ART OF TECHNOLOGY

KAISER-HILL

NT Svr w:/projects/actinide pathway report/fy2002/cross section maps/sid u236.aml

595

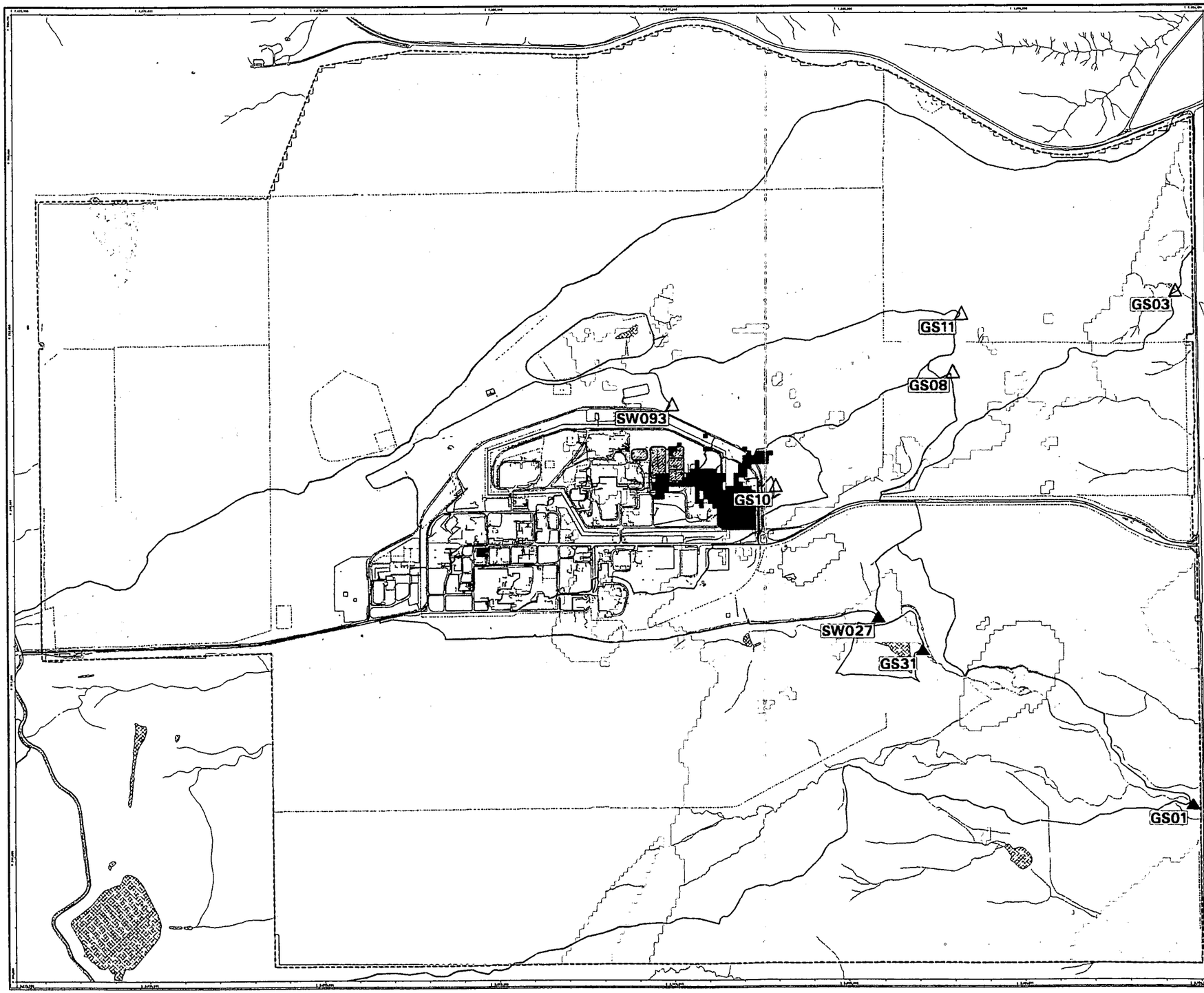

Figure TA-A-1

Actinide Migration Evaluation Pathway Report

Pu/Am Ratio for Surface Soil Samples

Pu-239/240 (pCi/g)

Am-241 (pCi/g)

Kriging Analysis Isoplot

EXPLANATION

- Ratio < 1
- 1 < = Ratio < 5
- 5 < = Ratio < 8
- 8 < = Ratio < 12
- Ratio > = 12
- Drainage Basin Boundary
- Walnut Creek Basin Gaging Station (GS03, GS08, GS10, GS11 & SW093)
- Woman Creek Basin Gaging Station (GS01, GS31 & SW027)

Standard Map Features

- Solar Evaporation Ponds (SEPs)
- Lakes and ponds
- Streams, ditches, or other drainage features
- Fences and other barriers
- Rocky Flats boundary
- Paved roads

DATA SOURCE BASE FEATURES:

Buildings, fences, hydrography, roads and other structures from 1994 aerial fly-over data captured by EG&G RSL, Las Vegas. Digitized from the orthophotographs. 1/95

Analytical Data from SWD as of October 1999.

903 Pad data from 903 Drum Storage Area Characterization Report, September 1999.

Kriged data provided by Jeff Myers (Westinghouse/803-502-9747).

Scale = 1 : 21330
1 inch represents approximately 1778 feet

250 0 500 1000 ft

State Plane Coordinate Projection
Colorado Central Zone
Datum: NAD27

U.S. Department of Energy
Rocky Flats Environmental Technology Site

GIS Dept. 303-966-7707

Prepared for:

Prepared for:

March 11, 2000

NT_Svr w:/projects/actinide_pathway_report/fy2002/kriged_data_maps/kriged_pu_am_ratio.aml

652

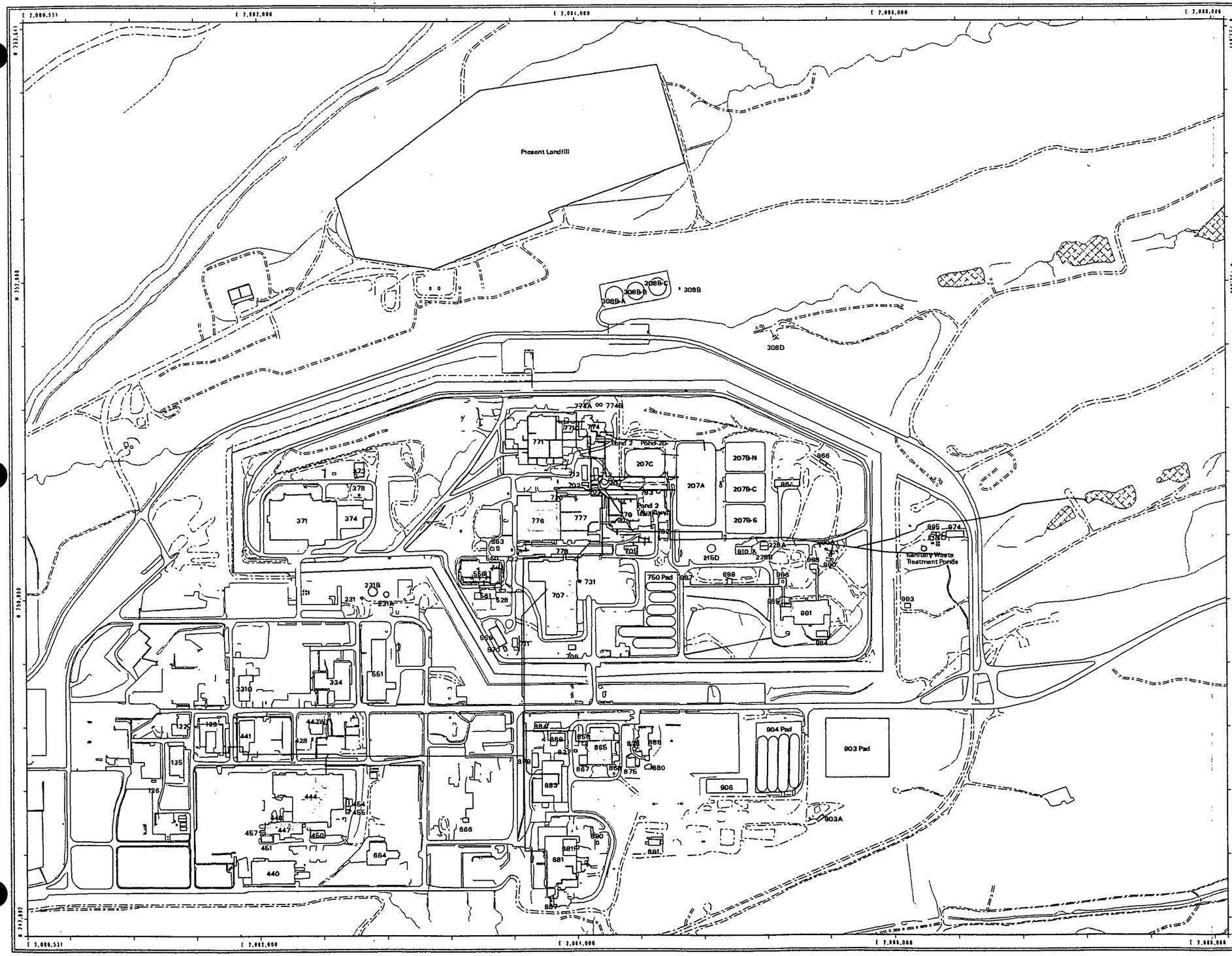

Figure TA-B-1

Actinide Migration Evaluation Pathway Report

Uranium Usage and Potential Uranium Contamination in Buildings

EXPLANATION

- U-238
- U-235 and U-238
- U-233, U-235 and U-238
- Original Process Waste Lines (OPWL)

Standard Map Features

- Lakes and ponds
- Streams, ditches, or other drainage features
- Paved roads
- Dirt roads

DATA SOURCE BASE FEATURES:
Buildings, fences, hydrographs, roads and other structures from 1994 aerial fly-over data captured by EG&G RSL, Las Vegas. Digitized from the orthophotographs. USS

N

Scale = 1 : 7420
1 inch represents approximately 618 feet

250 0 500 1000ft

State Plane Coordinate Projection
Colorado Central Zone
Datum: NAD27

U.S. Department of Energy
Rocky Flats Environmental Technology Site

GIS Dept. 303-966-7707

Prepared by:
DynCorp
THE ART OF TECHNOLOGY

Prepared for:
KAISER•HILL COMPANY

MAP ID: misc_maps/uran_bldg.aml

December 28, 2001

NT_Svr w:/projects/actinide_pathway_report/fy2002/misc_maps/uran_bldg.aml

675

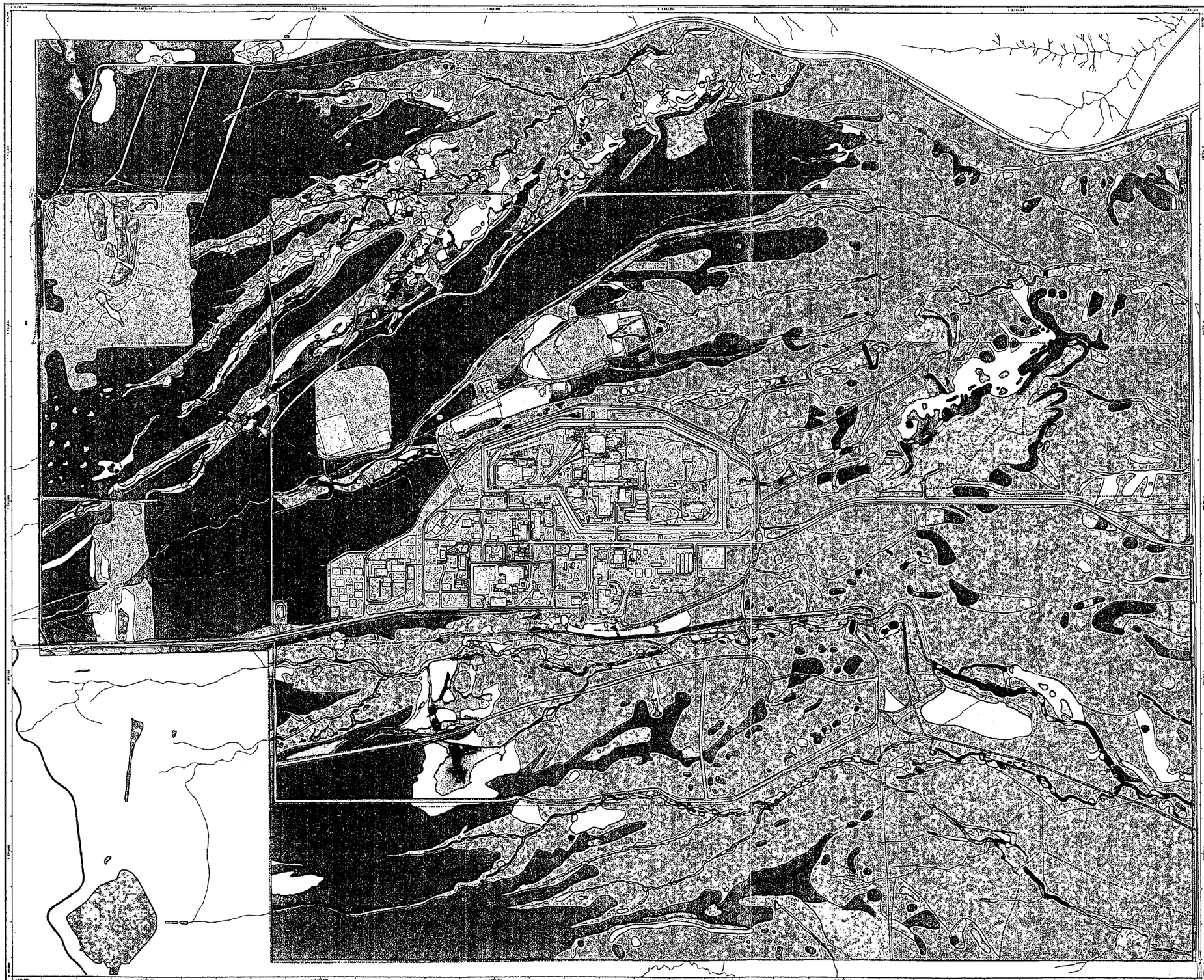

Figure TA-1-16

Actinide Migration Evaluation Pathway Report

Rocky Flats Vegetation Map

LEGEND

- Riparian Woodland
- Leadplant Riparian Shrubland
- Wet Meadow/Marsh Ecotone
- Short Upland Shrubland
- Willow Riparian Shrubland
- Annual Grass/Forb Community
- Xeric Tallgrass Prairie
- Ponderosa Woodland
- Reclaimed Mixed Grassland
- Mesic Mixed Grassland
- Savannah Shrubland
- Tall Upland Shrubland
- Short Marsh
- Xeric Needle and Thread Grass Prairie
- Short Grassland
- Disturbed and Developed Areas
- Open Water
- Riprap, Rock, and Gravel Piles
- Mudflats
- Tree Plantings
- Tall Marsh

Standard Map Features

- Buildings and other structures
- Lakes and ponds
- Streams, ditches, or other drainage features
- Fences and other barriers
- Paved roads
- Dirt roads

DATA SOURCE BASE FEATURES:

Vegetation map data provided by PTI Environmental Services Ecology Group.

Buildings, fences, hydrography, roads and other structures from 1994 aerial fly-over data captured by EG&G RSL, Las Vegas. Digitized from the orthophotographs. 1/95

NOTES:

This map does not show all Federally designated wetlands. See the 1995 Site wetlands map prepared by the U.S. Army Corps of Engineers for delineated wetland features.

Scale = 1 : 20240
1 inch represents approximately 1687 feet

250 0 500 1000ft

State Plane Coordinate Projection
Colorado Central Zone
Datum: NAD27

U.S. Department of Energy
Rocky Flats Environmental Technology Site

GIS Dept. 303-966-7707

Prepared by: DynCorp THE ART OF TECHNOLOGY

Prepared for: KAISER-HILL COMPANY

MAP ID: misc_maps/veg_site.aml

January 31, 2000

NT_Svr w:/projects/actinide_pathway_report/fy2002/misc_maps/veg_site.aml

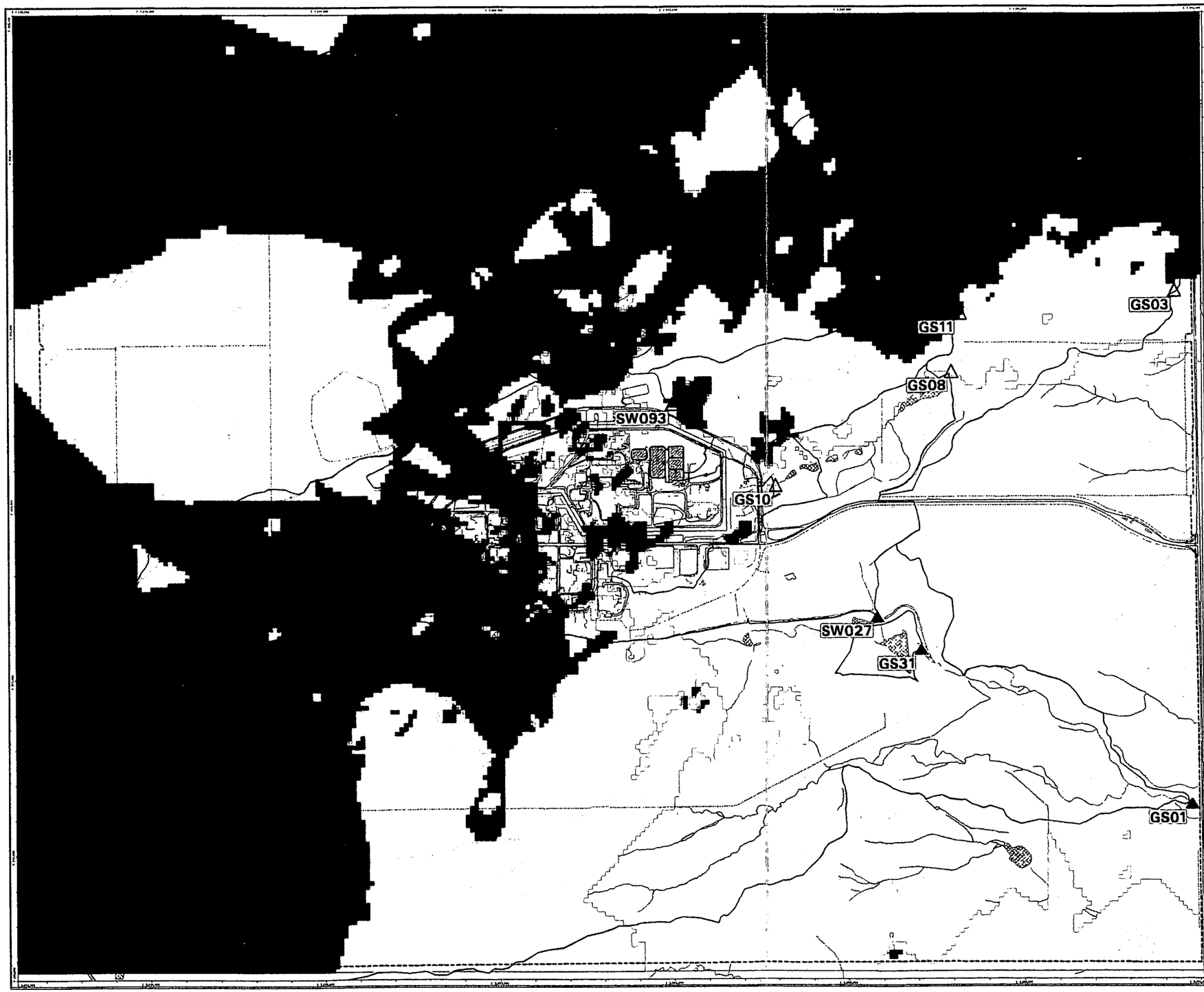

Figure TA-2-8

Actinide Migration Evaluation Pathway Report

Pu-239/240 Activity in Surface Soils

Kriging Analysis Isoplot (pCi/g)

EXPLANATION

- Result < = 0.01
- 0.01 < Result < = 0.05
- 0.05 < Result < = 0.1
- 0.1 < Result < = 0.5
- 0.5 < Result < = 1.0
- 1.0 < Result < = 5.0
- 5.0 < Result < = 10.0
- 10.0 < Result < = 100.0
- 100.0 < Result < = 1000.0
- Result > 1000.0
- Drainage Basin Boundary
- Walnut Creek Basin Gaging Station (GS03, GS08, GS10, GS11 & SW093)
- Woman Creek Basin Gaging Station (GS01, GS31 & SW027)

Standard Map Features

- Solar Evaporation Ponds (SEPs)
- Lakes and ponds
- Streams, ditches, or other drainage features
- Fences and other barriers
- Rocky Flats boundary
- Paved roads

DATA SOURCE BASE FEATURES:

Buildings, fences, hydrography, roads and other structures from 1994 aerial fly-over data captured by EG&G RSL, Las Vegas. Digitized from the orthophotographs. 1/95

Analytical Data from SWD as of October 1999.

903 Pad data from 903 Drum Storage Area Characterization Report, September 1999.

Kriged data provided by Jeff Myers (Westinghouse-Akin, 803-502-9747).

Scale = 1 : 21330
1 inch represents approximately 1778 feet

250 0 500 1000 ft

State Plane Coordinate Projection
Colorado Central Zone
Datum: NAD27

U.S. Department of Energy
Rocky Flats Environmental Technology Site

GIS Dept. 303-966-7707

Prepared by: DynCorp — THE ART OF TECHNOLOGY

Prepared for: KAISER-HILL COMPANY

March 15, 2000

NT_Svr w:/projects/actinide_pathway_report/fy2002/kriged_data_maps/pu239-240_grid_bsize.aml

158